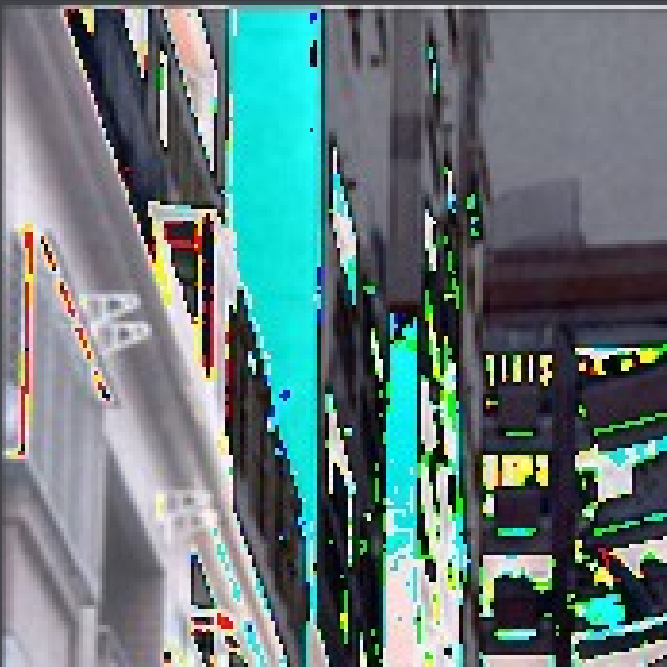


THE SEISMIC HANDBOOK

Second Edition

Farzad



THE SEISMIC DESIGN HANDBOOK

Second Edition

THE SEISMIC DESIGN HANDBOOK

Second Edition

edited by

Farzad Naeim, Ph.D., S.E.

*Vice President and Director of Research and Development
John A. Martin Associates, Inc., U.S.A.*



SPRINGER SCIENCE+BUSINESS MEDIA, LLC

Library of Congress Cataloging-in-Publication Data

The seismic design handbook / edited by Farzad Naeim.—2nd ed.
p.cm.

Includes index.

ISBN 978-1-4613-5681-3 ISBN 978-1-4615-1693-4 (eBook)

DOI 10.1007/978-1-4615-1693-4

1. Earthquake resistant design—Handbooks, manuals, etc. 2. Buildings—Earthquake effects—Handbooks, manuals, etc. I. Naeim, Farzad.

Additional material to this book can be downloaded from <http://extras.springer.com>

TA658.44 .S395 2001

624.1'762—dc21

00-054609

Copyright © 2001 by Springer Science+Business Media New York

Originally published by Kluwer Academic Publishers in 2001

Softcover reprint of the hardcover 2nd edition 2001

Second Printing 2003

All rights reserved. No part of this publication may be reproduced, stored in a retrieval system or transmitted in any form or by any means, mechanical, photocopying, recording, or otherwise, without the prior written permission of the publisher, Springer Science+Business Media, LLC.

Printed on acid-free paper.

“Among mortals second thoughts are wisest.”

Euripides,
(480-406 B.C.)

“The change of motion is proportional to the motive force impressed; and is made in the direction of the right line in which the force is impressed.”

Isaac Newton,
The Principia: Mathematical Principles of Natural Philosophy (1687 A.D.)

Contents

Contributors	ix
Acknowledgements	
Preface	
1 THE NATURE OF EARTHQUAKE GROUND MOTION BRUCE A. BOLT, D.SC.	1
2 EARTHQUAKE GROUND MOTION AND RESPONSE SPECTRA BIJAN MOHRAZ, PH.D., P.E. AND FAHIM SADEK, PH.D.	47
3 GEOTECHNICAL DESIGN CONSIDERATIONS MARSHALL LEW, PH.D., G.E.	125
4 DYNAMIC RESPONSE OF STRUCTURES JAMES C. ANDERSON, PH.D.	183
5 LINEAR STATIC SEISMIC LATERAL FORCE PROCEDURES ROGER M. DI JULIO JR., PH.D., P.E.	247
6 ARCHITECTURAL CONSIDERATIONS CHRISTOPHER ARNOLD, FAIA, RIBA	275
7 DESIGN FOR DRIFT AND LATERAL STABILITY FARZAD NAEIM, PH. D., S.E.	327
8 SEISMIC DESIGN OF FLOOR DIAPHRAGMS FARZAD NAEIM, PH.D., S.E. AND R. RAO BOPPANA, PH.D., S.E.	373

9	SEISMIC DESIGN OF STEEL STRUCTURES CHIA-MING UANG, PH.D., MICHEL BRUNEAU, PH.D., P.ENG. ANDREW S. WHITTAKER, PH.D., S.E., AND KEY-CHYUAN TSAI, PH.D., S.E.	409
10	SEISMIC DESIGN OF REINFORCED CONCRETE STRUCTURES ARNALDO T. DERECHO, PH.D. AND M. REZA KIANOUSH, PH.D.	463
11	SEISMIC DESIGN OF WOOD AND MASONRY BUILDINGS JOHN G. SHIPP, S.E., FASCE AND GARY C. HART, PH.D., P.E.	563
12	SEISMIC UPGRADING OF EXISTING STRUCTURES RONALD O. HAMBURGER, S.E. AND CRAIG A. COLE, S.E.	623
13	DESIGN OF NONSTRUCTURAL SYSTEMS AND COMPONENTS JOHN D. GILLENGERTEN, S.E.	681
14	DESIGN OF STRUCTURES WITH SEISMIC ISOLATION RONALD L MAYES, PH.D. AND FARZAD NAEIM, PH.D., S.E.	723
15	PERFORMANCE BASED SEISMIC ENGINEERING FARZAD NAEIM, PH.D., S.E., HUSSAIN BHATIA, PH.D., P.E. AND ROY M. LOBO, PH.D., P.E.	757
16	COMPUTER APPLICATIONS IN SEISMIC DESIGN FARZAD NAEIM, PH.D., S.E., ROY M. LOBO, PH.D., P.E. AND HUSSAIN BHATIA, PH.D., P.E.	793
	APPENDIX	815
	INDEX	821

Contributors

James C. Anderson, Ph.D.

Professor of Civil Engineering, University of Southern California, Los Angeles, California
(Dynamic Response of Structures)

Christopher Arnold, AIA

President, Building Systems Development, Inc., San Mateo, California
(Architectural Considerations)

Hussain Bhatia, Ph.D., P.E.

Senior Research Engineer, John A. Martin & Associates, Inc., Los Angeles, California
(Performance Based Seismic Engineering; Computer Applications in Seismic Design)

Bruce A. Bolt, Ph.D.

Professor Emeritus of Seismology, University of California, Berkeley, California
(The Nature of Earthquake Ground Motions)

Rao Boppana, Ph.D., S.E.

President, Sato and Boppana Consulting Engineers, Los Angeles, California
(Seismic Design of Floor Diaphragms)

Michel Bruneau, Ph.D., P.Eng.

Professor of Civil Engineering, State University of New York at Buffalo, New York
(Seismic Design of Steel Structures)

Craig A. Cole, S.E.

Project Manager, EQE International, Inc., Oakland, California
(Seismic Upgrading of Existing Structures)

John G. Gillengerten, S.E.

Senior Project Manager, John A. Martin & Associates, Inc., Los Angeles, California
(Design of Nonstructural Systems and Components)

Arnaldo T. Derecho, Ph.D.

Consulting Structural Engineer, Mount Prospect, Illinois
(Seismic Design of Reinforced Concrete Structures)

Roger M. Dijulio, Jr., Ph.D., P.E.

Professor of Engineering, California State University, Northridge, California
(Linear Static Lateral Force Procedures)

Ronald O. Hamburger, S.E.

Senior Vice President, EQE International, Inc., Oakland, California
(Seismic Upgrading of Existing Structures)

Gary C. Hart, Ph.D., P.E.

Professor of Civil Engineering, University of California, Los Angeles, California
(Seismic Design of Wood and Masonry Structures)

Contributors (continued)

M. Reza Kianoush, Ph.D.

Professor, Ryerson Polytechnic University, Toronto, Ontario, Canada
(Seismic Design of Reinforced Concrete Structures)

Marshall Lew, Ph.D., G.E.

Corporate Consultant, Law/Crandall, Inc., Los Angeles, California
(Geotechnical Considerations)

Roy F. Lobo, Ph.D., P.E.

Senior Research Engineer, John A. Martin & Associates, Inc., Los Angeles, California
(Performance Based Seismic Engineering; Computer Applications in Seismic Design)

Ronald M. Mayes, Ph.D.

Engineering Consultant, Berkeley, California
(Design of Structures with Seismic Isolation)

Bijan Mohraz, Ph.D.

Professor of Civil Engineering, Southern Methodist University, Dallas, Texas
(Earthquake Ground Motion and Response Spectra)

Farzad Naeim, Ph.D., S.E.

Vice President/Director of Research and Development, John A. Martin & Associates, Inc., Los Angeles, California
(Design for Drift and Lateral Stability; Seismic Design of Floor Diaphragms; Design of Structures with Seismic Isolation; Performance Based Seismic Engineering; Computer Applications in Seismic Design)

John G. Shipp, S.E., FASCE

Manager Design Services and Senior Technical Manager, EQE Engineering and Design, Costa Mesa, California
(Seismic Design of Wood and Masonry Structures)

Key-Chyuan Tsai, Ph.D., S.E.

Professor of Civil Engineering, National Taiwan University, Taipei, Taiwan
(Seismic Design of Steel Structures)

Chia-Ming Uang, Ph.D.

Professor of Structural Engineering, University of California, San Diego, California
(Seismic Design of Steel Structures)

Andrew S. Whittaker, Ph.D., S.E.

Associate Professor of Civil Engineering, State University of New York at Buffalo, New York
(Seismic Design of Steel Structures)

Acknowledgements

The editor gratefully acknowledges the efforts of contributors in preparing excellent manuscripts. Thanks are also due to the management and staff at John A. Martin and Associates, Inc., especially Jack and Trailer Martin, who have always graciously understood and accommodated my frequent shifts of emphasis from everyday office practice to writing textbooks and technical articles. If it had not been for their encouragement and support, this project would have not been completed.

The production of this edition of the handbook was made possible by the heroic efforts of two young and very talented persons. Mark Day patiently and diligently managed the digital typesetting and repeated content revisions with his usual grace, smile, and dedication. Hesaam Aslani on his short stay with our firm on his way to graduate studies at the Stanford University prepared early camera-ready versions of most of the chapters and checked mathematical expressions and numerical examples.

The International Conference of Building Officials (ICBO) and particularly Mark Johnson of that organization were a constant source of encouragement and support. It is a distinct honor to have this handbook endorsed by both ICBO and the National Council of Structural Engineers Associations.

The editor is indebted to the readers of the first edition for their very positive and encouraging feedback and for their constant reminders of their desire to see a second edition of the handbook.

Last, but not least, the editor is grateful to his life-partner and wife, Fariba, who patiently understood the need for his extended hours of work, and his children Mana and Mahan who accommodated a daddy who often could not play because he had a lot of work to do.

Preface

This handbook contains up-to-date information on planning, analysis, and design of earthquake-resistant building structures. Its intention is to provide engineers, architects, developers, and students of structural engineering and architecture with authoritative, yet practical, design information. It represents an attempt to bridge the persisting gap between advances in the theories and concepts of earthquake-resistant design and their implementation in seismic design practice.

The distinguished panel of contributors is composed of 22 experts from industry and universities, recognized for their knowledge and extensive practical experience in their fields. They have aimed to present clearly and concisely the basic principles and procedures pertinent to each subject and to illustrate with practical examples the application of these principles and procedures in seismic design practice. Where applicable, the provisions of various seismic design standards such as IBC-2000, UBC-97, FEMA-273/274 and ATC-40 are explained and their differences are highlighted.

Most of the chapters have been either totally re-written or substantially revised to reflect the recent advances in the field. In addition, a number of new chapters have been added to cover subjects such as performance based seismic engineering, seismic upgrading of

existing structures, computer applications, and seismic design of wood structures.

A new and very useful feature of this edition is the inclusion of a companion CD-ROM disc containing the complete digital version of the handbook itself and the following very important publications:

1. *UBC-IBC (1997-2000) Structural Comparisons and Cross References*, ICBO, 2000.
2. *NEHRP Guidelines for the Seismic Rehabilitation of Buildings*, FEMA-273, Federal Emergency Management Agency, 1997.
3. *NEHRP Commentary on the Guidelines for the Seismic Rehabilitation of Buildings*, FEMA-274, Federal Emergency Management Agency, 1997.
4. *NEHRP Recommended Provisions for Seismic Regulations for New Buildings and Older Structures, Part 1 – Provisions*, FEMA-302, Federal Emergency Management Agency, 1997.
5. *NEHRP Recommended Provisions for Seismic Regulations for New Buildings and Older Structures, Part 2 – Commentary*, FEMA-303, Federal Emergency Management Agency, 1997.

One should realize that seismic design is still as much an art as it is a science. Therefore,

no matter how helpful the material in this handbook might prove to be, it cannot replace or substitute sound engineering judgment. Furthermore, one must recognize that on some seismic design and detailing issues, a general consensus on the appropriate approaches does not yet exist. As an eminent engineer once said: "No two design offices completely agree on all aspects of seismic design or proper detailing." It is the editor's belief, however, that it is through the publication of books like this one, and continuation of research and development, that a general consensus of these issues will finally be reached. We have come a long way towards achieving these objectives during the last decade.

The primary purpose of this handbook is to serve practicing engineers and architects. However, its scope and its treatment of both theory and practice should also make it valuable to both teachers and students of earthquake-resistant design.

Much has been changed in seismic design practice since the first edition of this handbook was published in 1989. We have learned many lessons from world-wide damaging earthquakes during the last decade and these lessons, more or less, have been implemented in recent seismic design codes and guidelines. This is the primary reason why the volume of this edition of the handbook is roughly twice that of the first edition although its objectives have not changed.

The first edition of this handbook was received with a degree of enthusiasm that was totally above and beyond the editor's expectations. The book became the de-facto standard textbook for teaching seismic design principles at practically all major universities of the United States. UC Berkeley, Stanford, UCLA, USC, University at Buffalo, University of Illinois, Washington University at Saint Louis, University of Texas at Austin, Georgia-Tech, Cornell, and University of Michigan are among the schools that have used the first edition in this country. Overseas, it has been used at the Imperial College of London, Israel

Institute of Technology, and many other fine institutions.

The editor hopes that this second edition of the handbook will repeat the success of its predecessor and will be found as -if not more-useful to the readers. The editor welcomes any and all comments, criticisms and suggestions. Comments may be sent by e-mail to farzad@johnmartin.com. Any errata or supplementary information, if and when necessary, will be posted at <http://www.johnmartin.com/sdh>.

Farzad Naeim

October 2000

Los Angeles, California

Chapter 1

THE NATURE OF EARTHQUAKE GROUND MOTION

Bruce A. Bolt, D.Sc.

Professor Emeritus, of Seismology, University of California, Berkeley, California

Key words: Attenuation, Causes of Earthquakes, Collapse Earthquakes, Damage Mechanisms, Directivity, Earthquakes, Earthquake Faults, Earthquake Prediction, Elastic Rebound, Fault Types, Intensity Scales, Intraplate Earthquakes, Magnitude, Magnitude Scales, Magnitude Saturation, MMI, Near-Fault Effects, Plate Tectonics, Reservoir-Induced Earthquakes, Seismicity, Seismic Moment, Seismic Risk, Seismic Waves, Seismology, Source Models, Strong Ground Motion, Surface Rupture, Tectonic Earthquakes, Volcanic Earthquakes

Abstract: The aim of this chapter is to provide a basic understanding about earthquakes, their world-wide distribution, what causes them, their likely damage mechanisms, earthquake measuring scales, and current efforts on the prediction of strong seismic ground motions. This chapter, therefore, furnishes the basic information necessary for understanding the more detailed concepts that follow in the subsequent chapters of this book. The basic vocabulary of seismology is defined. The seismicity of the world is discussed first and its relationship with tectonic plates is explained. The general causes of earthquakes are discussed next where tectonic actions, dilatancy in the crustal rocks, explosions, collapses, volcanic actions, and other likely causes are introduced. Earthquake fault sources are discussed next. Various faulting mechanisms are explained followed by a brief discussion of seismic waves. Earthquake damage mechanisms are introduced and different major damage mechanisms are identified by examples. Quantification of earthquakes is of significant interest to seismic design engineers. Various earthquake intensity and magnitude scales are defined followed by a description of earthquake source models. Basic information regarding the concepts of directivity and near-fault effects are presented. Finally, the ideas behind seismic risk evaluation and earthquake prediction are discussed.

1.1 INTRODUCTION

On the average, 10,000 people die each year from earthquakes (see Figure 1-1). A UNESCO study gives damage losses amounting to \$10,000,000,000 from 1926 to 1950 from earthquakes. In Central Asia in this interval two towns and 200 villages were destroyed. Since then several towns including Ashkhabad (1948), Agadir (1960), Skopje (1963), Managua (1972), Gemona (1976), Tangshan (1976), Mexico City (1985), Spitak (1988), Kobe (1995), cities in Turkey and Taiwan (1999) and hundreds of villages have been severely damaged by ground shaking. Historical writings testify to man's long concern about earthquake hazards.

The first modern stimulus for scientific study of earthquakes came from the extensive field work of the Irish engineer, Robert Mallett, after the great Neopolitan earthquake of 1857 in southern Italy. He set out to explain the "masses of dislocated stone and mortar" in terms of

mechanical principles and in doing so established basic vocabulary such as *seismology*, *hypocenter* and *isoseismal*. Such close links between engineering and seismology have continued ever since^(1-1,1-2).

It is part of strong motion seismology to explain and predict the large amplitude-long duration shaking observed in damaging earthquakes. In the first sixty years of the century, however, the great seismological advances occurred in studying waves from distant earthquakes using very sensitive seismographs. Because the wave amplitudes in even a nearby magnitude 5 earthquake would exceed the dynamic range of the usual seismographs, not much fundamental work was done by seismologists on the rarer large earthquakes of engineering importance.

Nowadays, the situation has changed. After the 1971 San Fernando earthquake, hundreds of strong-motion records were available for this magnitude 6.5 earthquake. The 1.2g recorded at Pacoima Dam led to questions on topographic

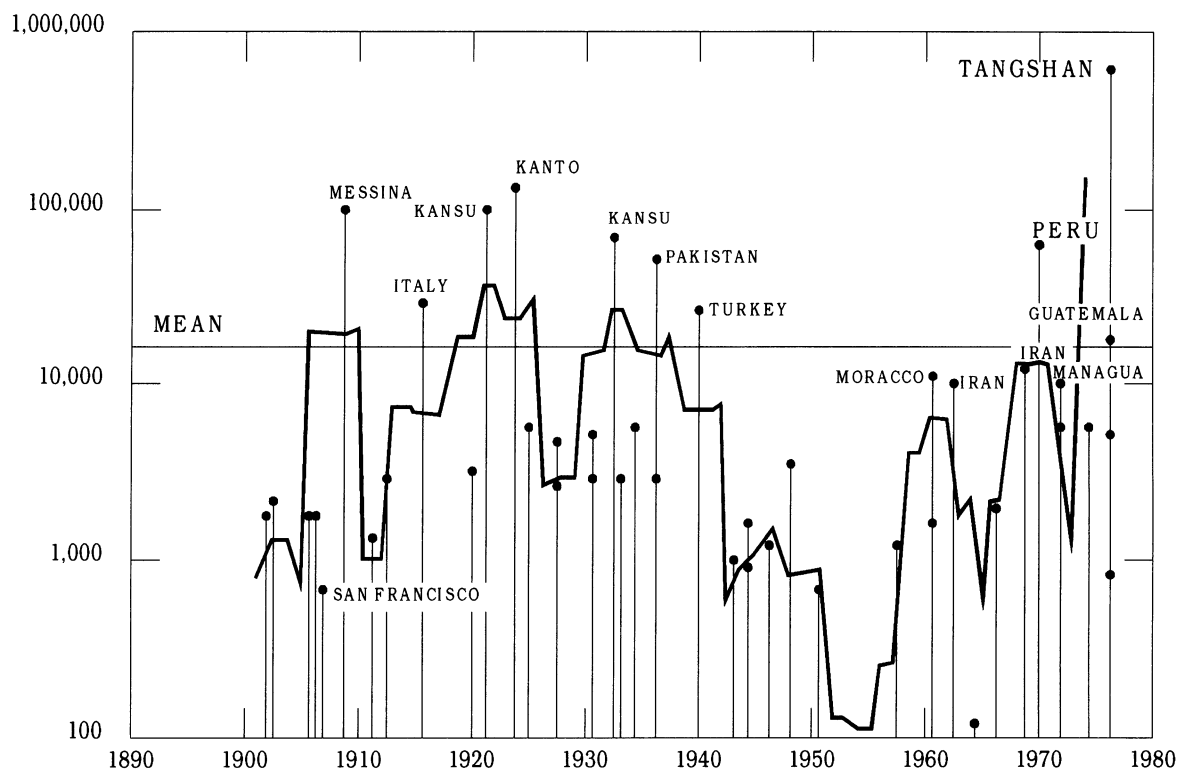


Figure 1-1. Loss of life caused by major earthquakes [After Hiroo Kanamori⁽¹⁻¹⁰⁾].

amplification and the construction of realistic models of fault-rupture and travel-path that could explain the strong motion patterns. Progress on these seismological questions followed rapidly in studies of variation in ground motions in the 1989 Loma Prieta earthquake ($M 7.0$), the 1994 Northridge earthquake ($M 6.8$) and the 1999 Chi Chi event in Taiwan ($M 7.6$). A harvest of strong motion recordings was obtained in the latter earthquake, showing numerous horizontal peak accelerations in the range $0.5g$ to $1.0g$. Digital recorders and fast computers mean that both seismologists and engineers can tackle more fundamental and realistic problems of earthquake generation and ground shaking.

Knowledge of strong ground shaking is now advancing rapidly, largely because of the growth of appropriately sited strong-motion accelerographs in seismic areas of the world. For example, in the Strong Motion Instrumentation Program in California, by the year 2000 there were 800 instruments in the free-field and 130 buildings and 45 other structures instrumented. Over 500 records had been digitized and were available for use in research or practice (see Chapter 16). In earthquake-prone regions, structural design of large or critical engineered structures such as high-rise buildings, large dams, and bridges now usually involves quantitative dynamic analysis; engineers ask penetrating questions on the likely seismic intensity for construction sites and require input motions or spectra of defining parameters. Predicted seismograms (*time-histories*) for dynamic modeling in structural design or vulnerability assessments are often needed.

The aim of this chapter is to provide a basic understanding about earthquakes, their worldwide distribution, what causes them, their likely damage mechanisms, earthquake measuring scales, and current efforts on the prediction of strong seismic ground motions. Additional helpful background on the subject may be found in References 1-2 through 1-34.

1.2 SEISMICITY OF THE WORLD

From the earthquake wave readings at different seismographic observatories, the position of the center of an earthquake can be calculated⁽¹⁻¹⁾. In this way, a uniform picture of earthquake distribution around the world has been obtained (see Figure 1-2). Definite belts of seismic activity separate large oceanic and continental regions, themselves mainly, but by no means completely, devoid of earthquake centers. Other concentrations of earthquake sources can be seen in the oceanic areas, for example, along the center of the Atlantic and Indian Oceans. These are the sites of gigantic submarine mountain ranges called mid-oceanic ridges. The geological strains that prevail throughout this global ridge system are evidenced by mountain peaks and deep rift valleys. Volcanic eruptions are frequent, and earthquakes originating along these ridges often occur in *swarms*, so that many hundreds of shocks are concentrated in a small area in a short time.

Dense concentrations of earthquake centers with some as much as 680 kilometers beneath the surface also coincide with island arcs, such as those of the Pacific and the eastern Caribbean.

On the western side of the Pacific Ocean, the whole coast of Central and South America is agitated by many earthquakes, great and small. High death tolls have ensued from the major ones. In marked contrast, the eastern part of South America is almost entirely free from earthquakes, and can be cited as an example of low seismic risk country. Other seismically quiet continental areas can be seen in Figure 1-2.

In Europe, earthquake activity is quite widespread. To the south, Turkey, Greece, Yugoslavia, Italy, Spain and Portugal suffer from it, and large numbers of people have died in disasters throughout the years. An earthquake off southwest Iberia on November 1, 1755 produced a great tsunami, which caused many of the 50,000 to 70,000 deaths occurring in

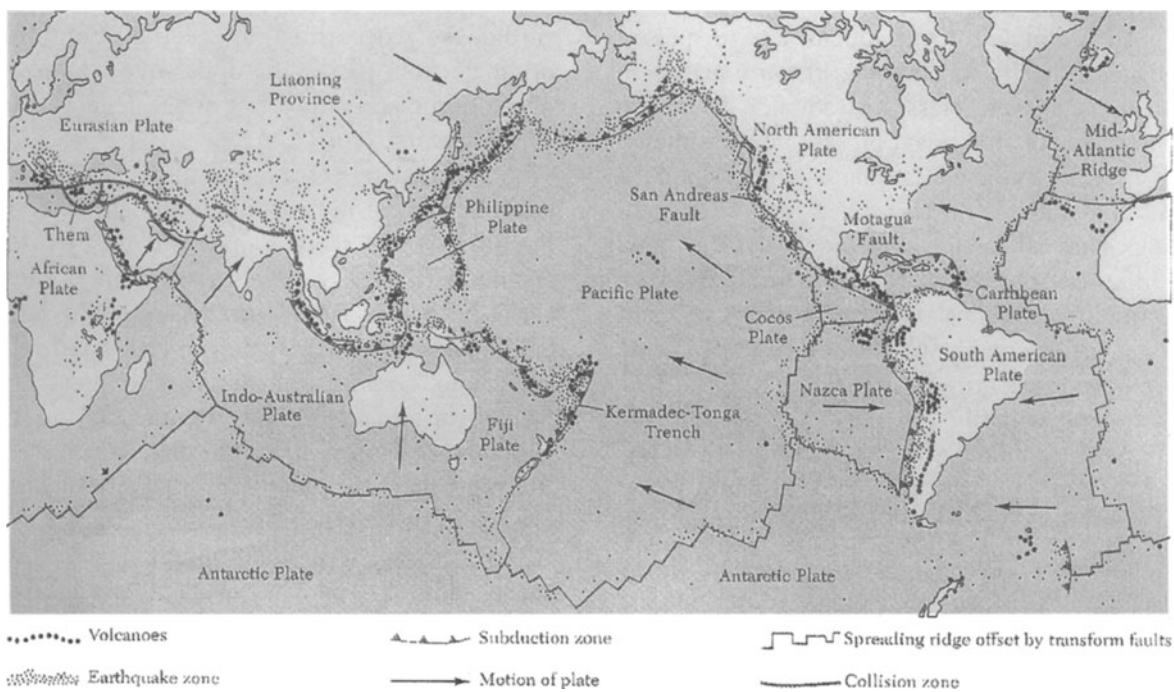


*Figure 1-2. Tectonic plates and world-wide distribution of earthquakes. (From *Earthquakes*, by Bruce A. Bolt. Copyright 1978, 1999 W. H. Freeman and Company. Used with permission.)*

Lisbon, Portugal, and surrounding areas; the shaking was felt in Germany and the Netherlands. In Alicante, Spain, on March 21, 1829, a shock killed about 840 persons and injured many hundred more. Total or partial destruction of more than 5,000 houses was reported in and near Torrevieja and Murcia. On December 28, 1908, a devastating earthquake hit Messina, Italy, causing 120,000 deaths and widespread damage. The most recent deadly one to affect that country struck on May 6, 1976, in the Friuli region near Gemona; about 965 persons were killed and 2280 injured.

On December 27, 1939, in Erzincan, Turkey, 23,000 lives were lost from a major earthquake. Similar killer earthquakes have occurred in Turkey and Iran in recent years. The Erzincan earthquake along the Anatolian fault in Turkey on March 13, 1992 caused many building collapses and the June 21, 1990 earthquake ($M 7.3$) devastated two Iranian provinces, Gilan and Zanjan. August 17, 1999 saw a 50 km rupture of the north Anatolian

fault along the Marmara Sea south of Izmit producing a magnitude 7.4 earthquake and over 16,000 deaths.

North of the Mediterranean margin, Europe is much more stable. However, destructive earthquakes do occur from time to time in Romania, Germany, Austria and Switzerland, and even in the North Sea region and Scandinavia. For example, on October 8, 1927, an earthquake occurred near Schwadorf in Austria and caused damage in an area southeast of Vienna. This earthquake was felt in Hungary, Germany, and Czechoslovakia at distances of 250 kilometers from the center of the disturbance. The seismicity in the North Sea is sufficiently significant to require attention to earthquake resistant design of oil platforms there.

In Africa, damaging earthquakes have occurred in historical times. A notable case was the magnitude 5.6 earthquake on November 14, 1981 that was felt in Aswan, Egypt. This earthquake was probably stimulated by the

impounding of water in Lake Nassar behind the high Aswan Dam.

An example of infrequent and dispersed seismicity is the occurrence of earthquakes in Australia. Nevertheless, this country does have some areas of significant present-day seismicity. Of particular interest is a damaging earthquake of moderate size that was centered near Newcastle and causing major damage and killing fourteen people. It was a surprise from a seismological point of view because no fault maps were available which showed seismogenic geological structures near Newcastle.

During an earthquake, seismic waves radiate from the earthquake source somewhere below the ground surface as opposite sides of a slipping fault rebound in opposite directions in order to decrease the strain energy in the rocks. Although in natural earthquakes this source is spread out through a volume of rock, it is often convenient to imagine a simplified earthquake source as a point from which the waves first emanate. This point is called the *earthquake focus*. The point on the ground surface directly above the focus is called the *earthquake epicenter*.

Although many foci are situated at shallow depths, in some regions they are hundreds of kilometers deep. Such regions include the South American Andes, the Tonga Islands, Samoa, the New Hebrides chain, the Japan Sea, Indonesia, and the Caribbean Antilles. On the average, the frequency of occurrence of earthquakes in these regions declines rapidly below a depth of 200 kilometers, but some foci are as deep as 680 kilometers. Rather arbitrarily, earthquakes with foci from 70 to 300 kilometers deep are called *intermediate focus* and those below this depth are termed *deep focus*. Some intermediate and deep focus earthquakes are located away from the Pacific region, in the Hindu Kush, in Romania, in the Aegean Sea and under Spain.

The shallow-focus earthquakes (focus depth less than 70 kilometers) wreak the most devastation, and they contribute about three quarters of the total energy released in earthquakes throughout the world. In California, for example, all of the known earthquakes to

date have been shallow-focus. In fact, it has been shown that the great majority of earthquakes occurring in central California originate from foci in the upper five kilometers of the Earth, and only a few are as deep as even 15 kilometers.

Most moderate to large shallow earthquakes are followed, in the ensuing hours and even in the next several months, by numerous, usually smaller earthquakes in the same vicinity. These earthquakes are called *aftershocks*, and large earthquakes are sometimes followed by incredible numbers of them. The great Rat Island earthquake in the Aleutian Island on February 4, 1965 was, within the next 24 days, followed by more than 750 aftershocks large enough to be recorded by distant seismographs. Aftershocks are sometimes energetic enough to cause additional damage to already weakened structures. This happened, for example, a week after the Northridge earthquake of January 17, 1994 in the San Fernando Valley when some weakened structures sustained additional cracking from magnitude 5.5 aftershocks. A few earthquakes are preceded by smaller *foreshocks* from the source area, and it has been suggested that these can be used to predict the main shock.

1.3 CAUSES OF EARTHQUAKES

1.3.1 Tectonic Earthquakes

In the time of the Greeks it was natural to link the Aegean volcanoes with the earthquakes of the Mediterranean. As time went on it became clear that most damaging earthquakes were in fact not caused by volcanic activity.

A coherent global geological explanation of the majority of earthquakes is in terms of what is called plate tectonics⁽¹⁻³⁾. The basic idea is that the Earth's outermost part (called the lithosphere) consists of several large and fairly stable rock slabs called plates. The ten largest plates are mapped in Figure 1-2. Each plate extends to a depth of about 80 kilometers.

Moving plates of the Earth's surface (see Figures 1-2 and 1-3) provide mechanisms for a great deal of the seismic activity of the world. Collisions between adjacent lithospheric plates, destruction of the slab-like plate as it descends or *subducts* into a dipping zone beneath island arcs (see Figure 1-4), and spreading along mid-oceanic ridges are all mechanisms that produce significant straining and fracturing of crustal rocks. Thus, the earthquakes in these tectonically active boundary regions are called *plate-edge earthquakes*. The very hazardous shallow earthquakes of Chile, Peru, the eastern Caribbean, Central America, Southern Mexico, California, Southern Alaska, the Aleutians, the Kuriles, Japan, Taiwan, the Philippines, Indonesia, New Zealand, the Alpine-Caucasian-Himalayan belt are of plate-edge type.

As the mechanics of the lithospheric plates become better understood, long-term predictions of place and size may be possible for plate-edge earthquakes. For example, many plates spread toward the subduction zones at rates of from 2 to 5 centimeters (about one to two inches) per year. Therefore in active arcs like the Aleutian and Japanese Islands and subduction zones like Chile and western Mexico, knowledge of the history of large earthquake occurrence might flag areas that currently lag in earthquake activity.

Many large earthquakes are produced by slip along faults connecting the ends of offsets in the spreading oceanic ridges and the ends of island arcs or arc-ridge chains (see Figure 1-2). In these regions, plates slide past each other along what are called *transform faults*. Considerable work has been done on the estimation of strong ground motion parameters for the design of critical structures in earthquake-prone countries with either transform faults or ocean-plate subduction tectonics, such as Japan, Alaska, Chile and Mexico. The Himalaya, the Zagros and Alpine regions are examples of mountain ranges formed by *continent-to-continent collisions*. These collision zones are regions of high present day seismic activity. The estimation of

seismic hazard along continental collision margins at tectonic plates has not as yet received detailed attention.

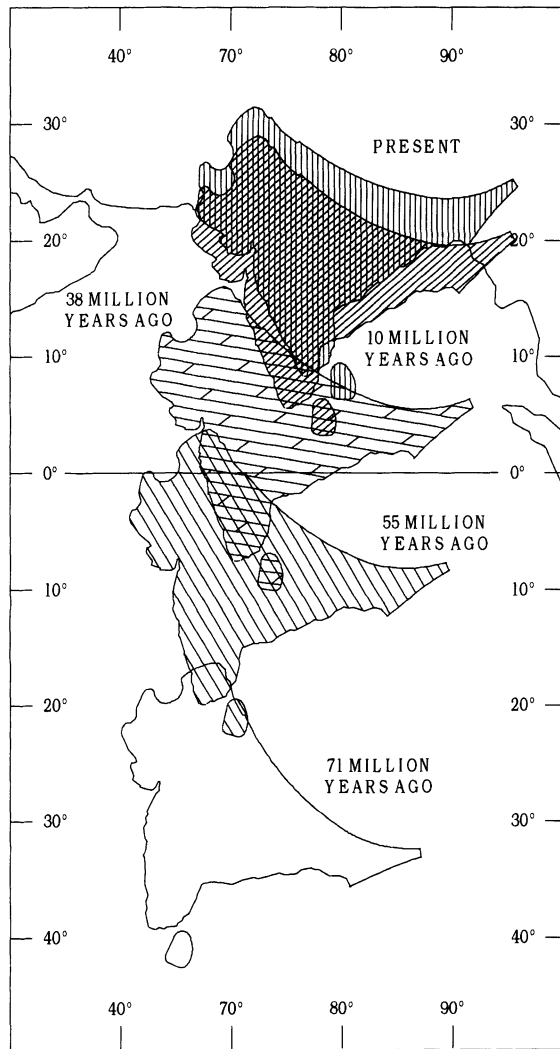


Figure 1-3. Continued drift of the Indian plate towards Asian plate causes major Himalayan earthquakes. (From *The Collision Between India and Eurasia*, by Molnar and Tapponnier. Copyright 1977 by Scientific American, Inc. All rights reserved)

While a simple plate-tectonic theory is an important one for a general understanding of earthquakes and volcanoes, it does not explain all seismicity in detail, for within continental regions, away from boundaries, large devastating earthquakes sometimes occur. These *intraplate* earthquakes can be found on nearly every continent.

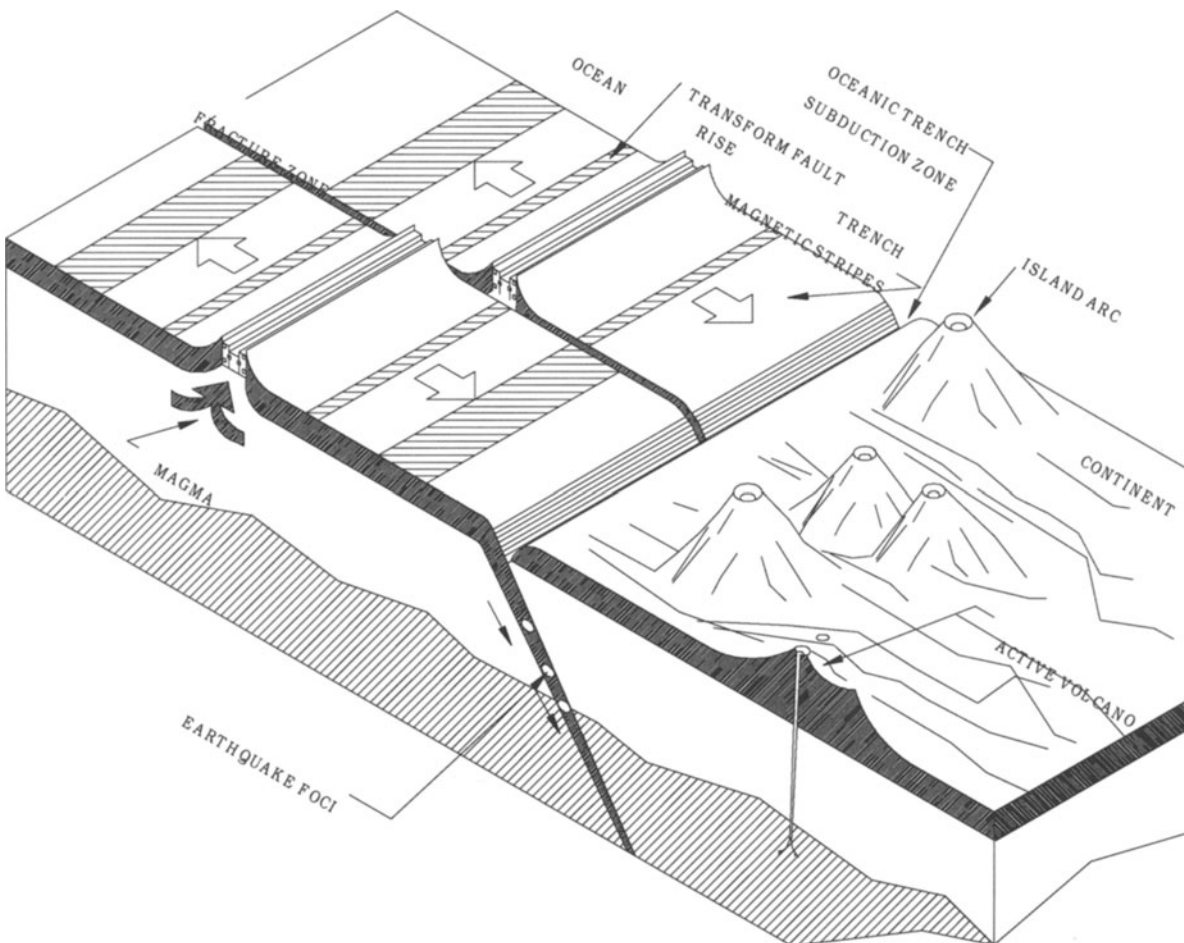


Figure 1-4. A sketch of the Earth's crust showing mid-oceanic ridges and active continental margin along a deep trench

One example of such earthquakes is the Dashte-e-Bayaz earthquake of August 31, 1968 in north-eastern Iran. In the United States, the most famous are the major earthquake series of 1811-1812 that occurred in the New Madrid area of Missouri, along the Mississippi River and the 1886 Charleston, South Carolina earthquake. One important group for example, which seems to bear no simple mechanical relation to the present plate edges, occurs in northern China.

Such major internal seismic activity indicates that lithospheric plates are not rigid or free of internal rupture. The occurrence of intraplate earthquakes makes the prediction of earthquake occurrence and size difficult in

many regions where there is a significant seismic risk.

1.3.2 Dilatancy in the Crustal Rocks

The crust of the continents is a rocky layer with average thickness of about 30 km but which can be as thick as 50 km under high mountain ranges. Under the ocean, the crustal thickness is no more than about 5 km.

At a depth in the crust of 5 kilometers or so, the lithostatic pressure (due to the weight of the overlying rocks) is already about equal to the strength of typical uncracked rock samples at the temperature (500° C) and pressure appropriate for that depth. If no other factors entered, the shearing forces required to bring

about sudden brittle failure and frictional slip along a crack would never be attained; rather, the rock would deform plastically. A way around this problem was the discovery that the presence of water provides a mechanism for sudden rupture by reduction of the effective friction along crack boundaries. Nevertheless, in a normal geological situation, such as the crust of coastal California, temperatures increase sufficiently fast so that at crustal depths greater than about 16 km the elastic rocks become viscoelastic. Strain is then relieved by slow flow or creep rather than by brittle fracture. The part of the crust above this transition point is the seismogenic zone.

Studies of the time of travel of P and S waves before the 1971 San Fernando earthquake indicated that four years before it occurred, the ratio of the velocity of the P waves to the velocity of the S waves decreased rather suddenly by 10 percent from its average value of 1.75. There was, thereafter, a steady increase in this ratio back to a more normal value. One explanation is the *dilatancy model*. This states that as the crustal rocks become strained, cracking occurs locally and the volume of rock increases or *dilates*. Cracking may occur too quickly for ground water to flow into the dilated volume to fill the spaces so the cracks become vapor-filled. The consequent fall in pore pressure leads to a reduction mainly in P wave velocities. Subsequent diffusion of ground water into the dry cracks increases the pore pressure, and provides water for lubrication along the walls of the cracks, while at the same time, the P wave velocity increases again (see Figure 1-31 in Section 1.10 below).

The full implications and relevance of the dilatancy theory of earthquake genesis are not yet clear, but the hypothesis is attractive in that it is consistent with precursory changes in ground levels, electrical conductivity and other physical properties which have been noted in the past before earthquakes. The theory has a potential for forecasting earthquakes under certain circumstances. For example, measurement of the P wave velocity in the vicinity of large reservoirs before and after

impounding of water might provide a more direct method of indicating an approaching seismic crisis near dams than is now available.

1.3.3 Explosions

Ground shaking may be produced by the underground detonation of chemicals or nuclear devices. When a nuclear device is detonated in a borehole underground, enormous nuclear energy is released. Underground nuclear explosions fired during the past several decades at a number of test sites around the world have produced substantial artificial earthquakes (up to magnitude 6.0). Resultant seismic waves have traveled throughout the Earth's interior to be recorded at distant seismographic stations.

1.3.4 Volcanic Earthquakes

As Figure 1-4 shows, volcanoes and earthquakes often occur together along the margins of plates around the world. Like earthquakes, there are also intraplate volcanic regions, such as the Hawaiian volcanoes.

Despite these tectonic connections between volcanoes and earthquakes, there is no evidence that moderate to major shallow earthquakes are not essentially all of tectonic, elastic-rebound type. Those earthquakes that can be reasonably associated with volcanoes are relatively rare and fall into three categories: (i) volcanic explosions, (ii) shallow earthquakes arising from magma movements, and (iii) sympathetic tectonic earthquakes.

Among the three categories, Category (iii), tectonically associated with volcanoes, is more difficult to tie down, as cases which may fit this category, are rare. There is no report of significantly increased volcanic activity in the great 1964 Alaska earthquake, but Puyehue Volcano in the Andes erupted 48 hours after the great 1960 Chilean earthquake. One might suppose that in a large earthquake the ground shaking would set up waves in reservoirs of magma; the general compression and dilatation of the gaseous liquid melt may trigger volcanic activity.

1.3.5 Collapse Earthquakes

Collapse earthquakes are small earthquakes occurring in regions of underground caverns and mines. The immediate cause of ground shaking is the sudden collapse of the roof of the mine or cavern. An often observed variation is the *mine burst*. This rock rupture happens when the induced stress around the mine workings causes large masses of rock to fly off the mine face explosively, producing seismic waves. Mine bursts have been observed, for example, in Canada, and are especially common in South Africa.

An intriguing variety of collapse earthquakes is sometimes produced by massive landsliding. For example, a spectacular landslide on April 25, 1974, along the Mantaro River, Peru, produced seismic waves equivalent to a magnitude 4.5 earthquake. The slide had a volume of 1.6×10^9 cubic meters and killed about 450 people.

1.3.6 Large Reservoir-Induced Earthquakes

It is not a new idea that earthquakes might be triggered by impounding surface water. In the 1870's, the U.S. Corps of Engineers rejected proposals for major water storage in the Salton Sea in southern California on the grounds that such action might cause earthquakes. The first detailed evidence of such an effect came with the filling of Lake Mead behind Hoover Dam (height 221 meters), Nevada-Arizona, beginning in 1935. Although there may have been some local seismicity before 1935, after 1936 earthquakes were much more common. Nearby seismographs subsequently showed that after 1940, the seismicity declined. The foci of hundreds of detected earthquakes cluster on steeply dipping faults on the east side of the lake and have focal depths of less than 8 kilometers.

In Koyna, India, an earthquake (magnitude 6.5) centered close to the dam (height 103

meters) caused significant damage on December 11, 1967. After impounding began in 1962, reports of local shaking became prevalent in a previously almost aseismic area. Seismographs showed that foci were concentrated at shallow depths under the lake. In 1967 a number of sizable earthquakes occurred, leading up to the principal earthquake of magnitude 6.5 on December 11. This ground motion caused significant damage to buildings nearby, killed 177 persons, and injured more than 1,500. A strong motion seismograph in the dam gallery registered a maximum acceleration of 0.63g. The series of earthquakes recorded at Koyna has a pattern that seems to follow the rhythm of the rainfall (see Figure 1-5). At least a comparison of the frequency of earthquakes and water level suggests that seismicity increases a few months after each rainy season when the reservoir level is highest. Such correlations are not so clear in some other examples quoted.

In the ensuing years, similar case histories have been accumulated for several dozen large dams, but only a few are well documented. Most of these dams are more than 100 meters high and, although the geological framework at the sites varies, the most convincing examples of reservoir induced earthquakes occur in tectonic regions with at least some history of earthquakes. Indeed, most of the thousands of large dams around the world give no sign of earthquake induction. A poll in 1976 showed that only four percent of large dams had an earthquake reported with magnitude greater than 3.0 within 16 kilometers of the dam.

Calculation shows that the stress due to the load of the water in even large reservoirs is too small to fracture competent rock. The best explanation is that the rocks in the vicinity of the reservoir are already strained from the tectonic forces so that existing faults are almost ready to slip. The reservoir either adds a stress perturbation which triggers a slip or the increased water pressure lowers the strength of the fault, or both.

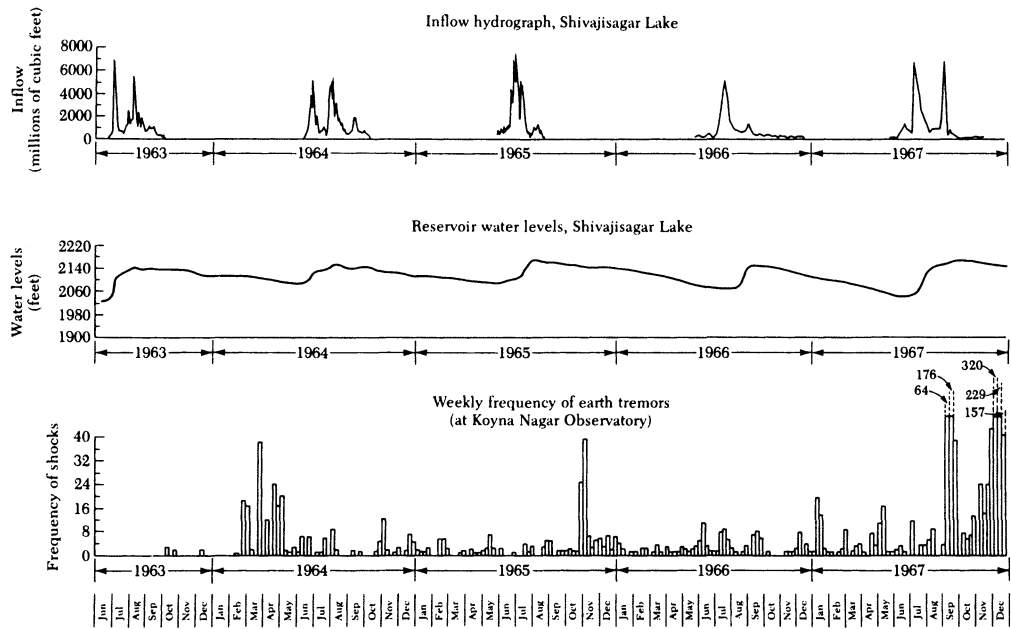


Figure 1-5. The relationship between reservoir level and local seismic activity at Koyna Dam. (From *Earthquakes*, by Bruce A. Bolt. Copyright 1978, 1999 W.H. Freeman and Company. Used with permission.)

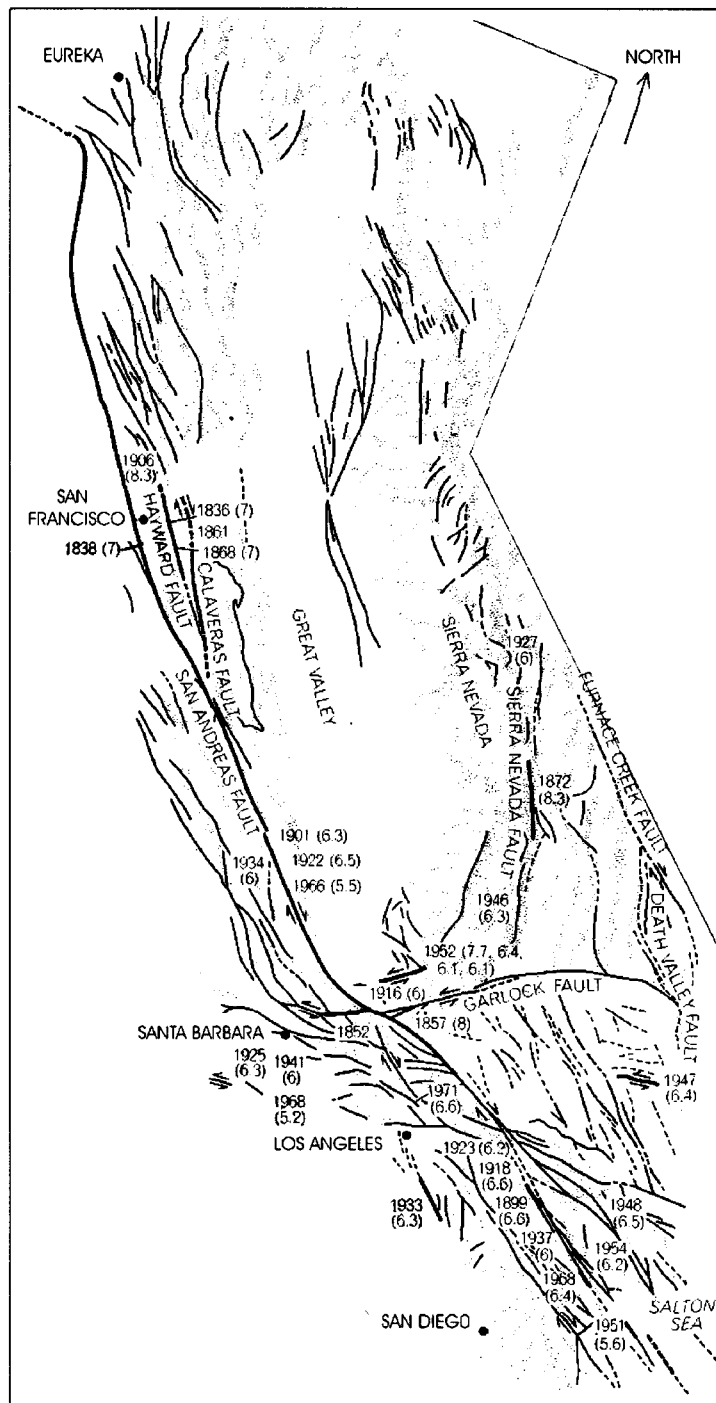


Figure 1-6. Normal fault at the Corinth Canal, Greece.
(Photo courtesy of L. Weiss.)

1.4 Earthquake fault sources

Field observations show that abrupt changes in the structure of rocks are common. In some places one type of rock can be seen butting up against rock of quite another type along a plane of contact. Such offsets of geological structure are called *faults*⁽¹⁻⁴⁾. Clear vertical offset of layers of rock along an exposed fault in the wall of the Corinth canal, Greece, can be seen in Figure 1-6.

Faults may range in length from a few meters to many kilometers and are drawn on a geological map as continuous or broken lines (see Figure 1-7). The presence of such faults indicates that, at some time in the past, movement took place along them. Such movement could have been either *slow slip*, which produces no ground shaking, or *sudden rupture* (an earthquake). Figure 1-8 shows one of the most famous examples of sudden fault rupture slips of the San Andreas fault in April 1906. In contrast, the observed surface faulting



*Figure 1-7. A simplified fault map of California. (From *The San Andreas Fault*, by Don L. Anderson. Copyright 1971 by Scientific American, Inc. All rights reserved.)*



Figure 1-8. Right-lateral horizontal movement of the San Andreas Fault in the 1906 earthquake the Old Sir Francis Highway.
(Photo by G.K Gilbert, courtesy of USGS.)

of most shallow focus earthquakes is much shorter and shows much less offset. Indeed, in the majority of earthquakes, fault rupture does not reach the surface and consequently is not directly visible. Geological mappings and geophysical work show that faults seen at the surface sometimes extend to depths of tens of kilometers in the Earth's crust.

It must be emphasized that most faults plotted on geological maps are now inactive. However, sometimes previously unrecognized active faults are discovered from fresh ground breakage during an earthquake. Thus, a fault was delineated by a line of cracks in open fields south of Oroville after the Oroville dam, California earthquake of August 1, 1975. The last displacement to occur along a typical fault may have taken place tens of thousands or even millions of years ago. The local disruptive forces in the Earth nearby may have subsided long ago and chemical processes involving water movement may have healed the ruptures,

particularly at depth. Such an inactive fault is not now the site of earthquakes and may never be again.

In seismology and earthquake engineering, the primary interest is of course in active faults, along which rock displacements can be expected to occur. Many of these faults are in well defined plate-edge regions of the Earth, such as the mid-oceanic ridges and young mountain ranges. However, sudden fault displacements can also occur away from regions of clear present tectonic activity (see Section 1.3.1).

Fault displacement in an earthquake may be almost entirely horizontal, as it was in the 1906 San Francisco earthquake along the San Andreas fault, but often large vertical motions occur, (Fig. 1-9) such as were evident in the 1992 Landers earthquake. In California in the 1971 San Fernando earthquake, an elevation change of three meters occurred across the ruptured fault in some places.



Figure 1-9. Normal fault scarp associated with the 1992 Landers, California, earthquake (Photo by Dr. Marshall Lew).

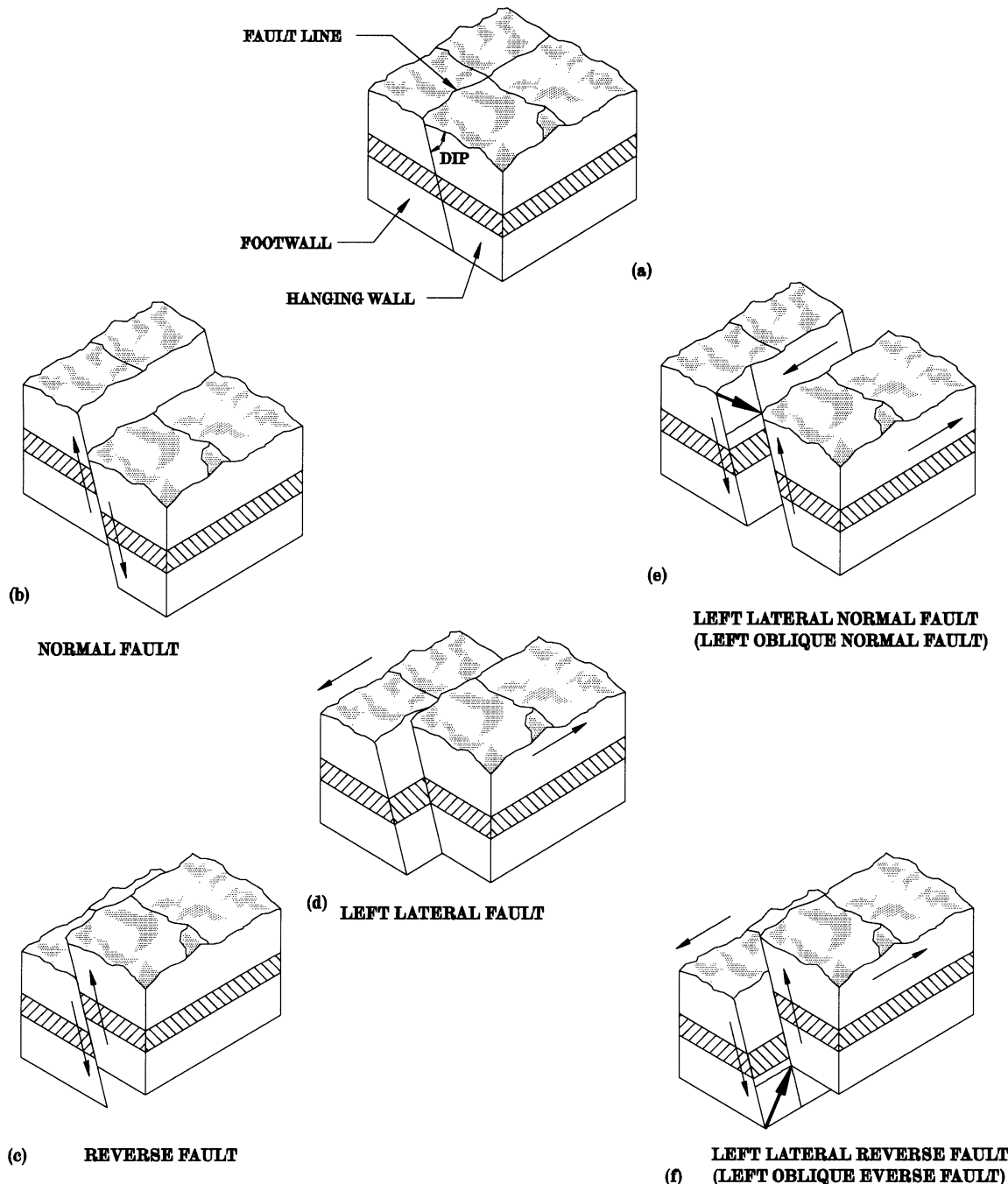


Figure 1-10. Diagrammatic sketches of fault types

The classification of faults depends only on the geometry and direction of relative slip. Various types are sketched in Figure 1-10. The *dip* of a fault is the angle that fault surface makes with a horizontal plane and the *strike* is the direction of the fault line exposed at the ground surface relative to the north.

A *strike-slip* fault, sometimes called a *transcurrent* fault, involves displacements of rock laterally, parallel to the strike. If when we stand on one side of a fault and see the motion on the other side is from left to right, the fault is *right-lateral* strike-slip. Similarly, we can identify *left-lateral* strike-slip.

A *dip-slip* fault is one in which the motion is largely parallel to the dip of the fault and thus has vertical components of displacement. A *normal* fault is one in which the rock above the inclined fault surface moves downward relative to the underlying crust. Faults with almost vertical slip are also included in this category.

A *reverse* fault is one in which the crust above the inclined fault surface moves upward relative to the block below the fault. *Thrust* faults are included in this category but are generally restricted to cases when the dip angle is small. In *blind thrust faults*, the slip surface does not penetrate to the ground surface.

In most cases, fault slip is a mixture of strike-slip and dip-slip and is called *oblique* faulting.

For over a decade it has been known that displacement in fault zones occurs not only by sudden rupture in an earthquake but also by slow differential slippage of the sides of the fault. The fault is said to be undergoing *tectonic creep*. Slippage rates range from a few millimeters to several centimeters.

The best examples of fault creep come from the San Andreas zone near Hollister, California, where a winery built straddling the fault trace is being slowly deformed; in the town, sidewalks, curbs, fences and homes are being offset. On the Hayward fault, on the east side of San Francisco Bay, many structures are being deformed and even seriously damaged by slow slip, including a large water supply tunnel, a drainage culvert and railroad tracks that intersect the zone.

Horizontal fault slippage has now also been detected on other faults around the world, including the north Anatolian fault at Ismetpasa in Turkey and along the Jordan Valley rift in Israel. Usually, such episodes of fault slip are *aseismic*-that is, they do not produce local earthquakes.

It is sometimes argued that a large damaging earthquake will not be generated along a fault that is undergoing slow fault slip, because the slippage allows the strain in the crustal rocks to be relieved periodically without sudden rupture. However, an alternative view is also plausible.

Almost all fault zones contain a plastic clay-like material called *fault gouge*. It may be that, as the elastic crystalline rocks of the deeper crust stain elastically and accumulate the energy to be released in an earthquake, the weak gouge material at the top of the fault zone is carried along by the adjacent stronger rock to the side and underneath. This would mean that the slow slip in the gouge seen at the surface is an indication that strain is being stored in the basement rocks. The implication of this view is that, on portions of the fault where slippage occurs, an earthquake at depth could result from sudden rupture, but surface offset would be reduced. On the portion where slippage is small or nonexistent, offsets would be maximum. A prediction of this kind can be checked after earthquakes occur near places where slippage is known to be taking place.

Sometimes aseismic slip is observed at the ground surface along a ruptured fault that has produced an earlier substantial earthquake. For example, along the San Andreas fault break in the 1966 earthquake on June 27 near Parkfield, California, offset of road pavement increased by a few centimeters in the days following the main earthquake. Such continued adjustment of the crustal rock after the initial major offset is probably caused partly by aftershocks and partly by the yielding of the weaker surface rocks and gouge in the fault zone as they accommodate to the new tectonic pressures in the region.

It is clear that slow slippage, when it occurs in built up areas, may have unfortunate economic consequences. This is another reason why certain types of structures should not be built across faults if at all possible. When such structures including dams and embankments must be laid across active faults, they should have jointed or flexible sections in the fault zone.

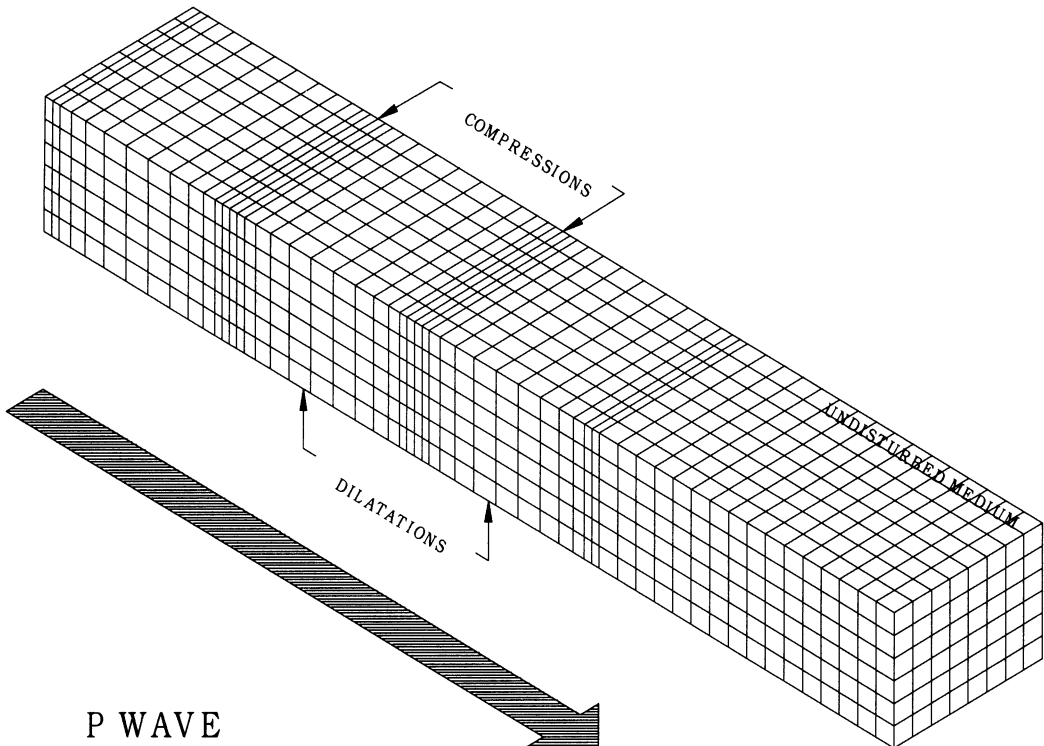


Figure 1-11. Ground Motion near the ground surface due to P waves. (From *Nuclear Explosions and Earthquakes*, by Bruce A. Bolt. Copyright 1976 W. H. Freeman and Company. Used with Permission.)

1.5 SEISMIC WAVES

Three basic types of elastic waves make up the shaking that is felt and causes damage in an earthquake⁽¹⁻¹⁾. These waves are similar in many important ways to the familiar waves in air, water, and gelatin. Of the three, only two propagate within a body of solid rock. The faster of these body waves is appropriately called the primary or *P wave*. Its motion is the same as that of a sound wave, in that, as it spreads out, it alternately pushes (compresses) and pulls (dilates) the rock (see Figure 1-11). These P waves, just like sound waves, are able to travel through both solid rock, such as granite mountains, and liquid material, such as volcanic magma or the water of the oceans.

The slower wave through the body of rock is called the secondary or *S wave*. As an S wave propagates, it shears the rocks sideways at right angles to the direction of travel (see Figure 1-12). Thus, at the ground surface S waves can

produce both vertical and horizontal motions. The S waves cannot propagate in the liquid parts of the Earth, such as the oceans and their amplitude is significantly reduced in liquefied soil.

The actual speed of P and S seismic waves depends on the density and elastic properties of the rocks and soil through which they pass. In most earthquakes, the P waves are felt first⁽¹⁻⁵⁾. The effect is similar to a sonic boom that bumps and rattles windows. Some seconds later the S waves arrive with their significant component of side-to-side motion, so that the ground shaking is both vertical and horizontal. This S wave motion is most effective in damaging structures.

The speed of P and S waves is given in terms of the density of the elastic material and the elastic moduli. We let k be the modulus of incompressibility (bulk modulus) and μ be the modulus of rigidity and ρ be the density. Then we have⁽¹⁻⁵⁾ for P waves;

$$V_p = \sqrt{\frac{k + \frac{4\mu}{3}}{\rho}} \quad (1-1)$$

for S waves;

$$V_s = \sqrt{\frac{\mu}{\rho}} \quad (1-2)$$

The third general type of earthquake wave is called a *surface wave* because its motion is restricted to near the ground surface. Such waves correspond to ripples of water that travel across a lake. Most of the wave motion is located at the outside surface itself, and as the depth below this surface increases, wave displacements become less and less.

Surface waves in earthquakes can be divided into two types. The first is called a *Love wave*. Its motion is essentially the same as that of S waves that have no vertical displacement; it moves the ground side to side in a horizontal plane parallel to the Earth's surface, but at right angles to the direction of propagation, as can be seen from the illustration in Figure 1-13. The second type of surface wave is known as a *Rayleigh wave*. Like rolling ocean waves, the pieces of rock disturbed by a Rayleigh wave move both vertically and horizontally in a vertical plane pointed in the direction in which the waves are travelling. As shown by the arrows in Figure 1-14. Each piece of rock moves in an ellipse as the wave passes.

Surface waves travel more slowly than body waves and, of the two surface waves, Love waves generally travel faster than Rayleigh waves. Thus, as the waves radiate outwards from the earthquake source into the rocks of the Earth's crust, the different types of waves separate out from one another in a predictable pattern.

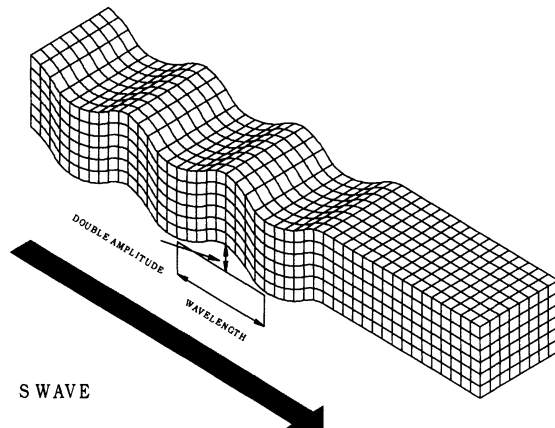


Figure 1-12. Ground motion near the ground surface due to S waves. (From *Nuclear Explosions and Earthquakes*, by Bruce A. Bolt. Copyright 1976 W. H. Freeman and Company. Used with Permission.)

An illustration of the pattern seen at a distant place is shown in Figure 1-15. In this example, the seismograph has recorded only the vertical motion of the ground, and so the seismogram contains only P, S and Rayleigh waves, because Love waves are not recorded by vertical instruments.

When the body waves (the P and S waves) move through the layers of rock in the crust they are reflected or refracted at the interfaces between rock types, as illustrated in Figure 1-16a. Also, whenever either one is reflected or refracted, some of the energy of one type is converted to waves of the other type (see Figure 1-16b).

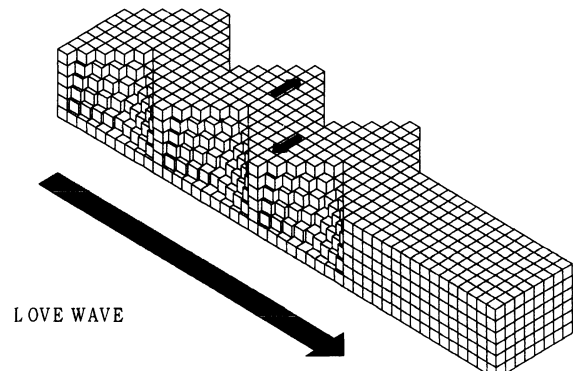


Figure 1-13. Ground motion near the ground surface due to Love waves. (From *Nuclear Explosions and Earthquakes*, by Bruce A. Bolt. Copyright 1976 W. H. Freeman and Company. Used with Permission.)

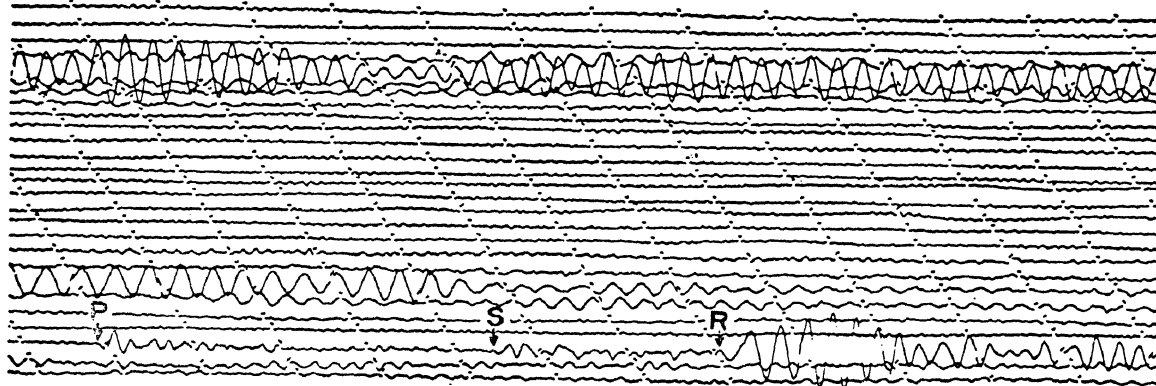


Figure 1-15. A seismograph record of the vertical component of a distant earthquake (third trace on bottom) on which the arrival of P, S and Rayleigh waves are marked. (Time increases from left to right.)

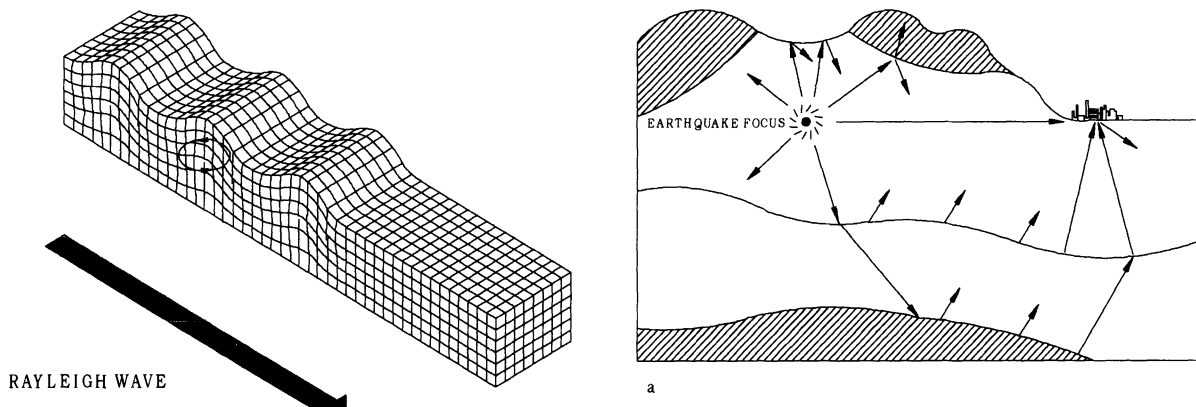


Figure 1-14. Ground motion near the ground surface due to Rayleigh waves. (From *Nuclear Explosions and Earthquakes*, by Bruce A. Bolt. Copyright 1976 W. H. Freeman and Company. Used with Permission.)

When P and S waves reach the surface of the ground, most of their energy is reflected back into the crust, so that the surface is affected almost simultaneously by upward and downward moving waves. For this reason *considerable amplification of shaking typically occurs near the surface*-sometimes doubling the amplitude of the upcoming waves.

This surface amplification enhances the shaking damage produced at the surface of the Earth. Indeed, in many earthquakes mine workers below ground report less shaking than people on the surface.

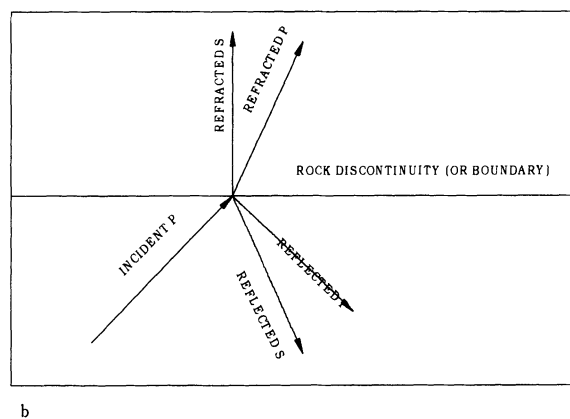


Figure 1-16. Reflection, refraction, and transformation of body waves. (From *Nuclear Explosions and Earthquakes*, by Bruce A. Bolt. Copyright 1999 W. H. Freeman and Company. Used with permission.)

Table 1-1. Magnitudes of Some Recent Damaging Earthquakes

Date	Region	Deaths	Magnitude (M_S)
December 7, 1988	Spitak, Armenia	25,000	7.0
August 1, 1989	West Iran, Kurima District	90	5.8
October 17, 1989	Santa Cruz Mountains, Loma Prieta	63	7.0
June 20, 1990	Caspian Sea, Iran	Above 40,000	7.3
March 13, 1992	Erzinean, Turkey	540	6.8
July 16, 1990	Luzon, Phillipines	1,700	7.8
July 12, 1993	Hokkaido, Japan	196	7.8
September 29, 1993	Killari, India	10,000	6.4
January 17, 1994	Northridge, California	61	6.8
January 16, 1995	Kobe, Japan	5400	6.9
August 17, 1999	Izmit, Turkey	16,000	7.4
September 21, 1999	Chi Chi, Taiwan	2,200	7.6

Another reason for modification of the incoming seismic wave amplitudes near the ground surface is the effect of layers of weathered rock and soil. When the elastic moduli have a mismatch from one layer to another, the layers act as wave filters amplifying the waves at some frequencies and deamplifying them at others. Resonance effects at certain frequencies occur.

Seismic waves of all types are progressively damped as they travel because of the non-elastic properties of the rocks and soils. The attenuation of S waves is greater than that of P waves, but for both types attenuation increases as wave frequency increases. One useful seismological quantity to measure damping is the parameter Q such that the amplitude A at a distance d of a wave frequency f (Hertz) and velocity C is given by:

$$A = A_0 e^{-(\pi f d / Q C)} \quad (1-3)$$

For P and S waves in sediments, Q is about 500 and 200, respectively.

The above physical description is approximate and while it has been verified closely for waves recorded by seismographs at a considerable distance from the wave source (*the far-field*), it is not adequate to explain important

details of the heavy shaking near the center of a large earthquake (*the near-field*). Near a fault that is suddenly rupturing, the strong ground shaking in the associated earthquake consists of a mixture of various kinds of seismic waves that have not separated very distinctly. To complicate the matter, because the source of radiating seismic energy is itself spread out across an area, the type of ground motion may be further mixed together. This complication makes identification of P, S and surface waves on strong motion records obtained near to the rupturing fault particularly difficult. However, much progress in this skill, based on intense study and theoretical modeling, has been made in recent years. This advance has made possible the computation of realistic ground motions at specified sites for engineering design purposes⁽¹⁻⁶⁾.

A final point about seismic waves is worth emphasizing here. There is considerable evidence, observational and theoretical, that earthquake waves are affected by both soil conditions and topography. For example, in weathered surface rocks, in alluvium and water-filled soil, the size of P, S and surface waves may be either increased or decreased depending on wave frequency as they pass to and along the surface from the more rigid basement rock.



Figure 1-17. Tilting of buildings due to soil liquefaction during the Niigata (Japan) earthquake of 1964

The wave patterns from earthquake sources are much affected by the three-dimensional nature of the geological structures⁽¹⁻⁶⁾. Clear evidence on this effect comes from recordings of the 1989 Loma Prieta earthquake (see Table 1-1). First, strong motion recordings show that there were reflections of high frequency S waves from the base of the Earth's crust at a depth of about 20 km, under southern San Francisco Bay. Secondly, the seismic S waves, like light waves, are polarized by horizontal layering into a horizontal component (SH type) and a vertical component (SV type). Because of large differences in the rock structure from one side of the San Andreas fault to the other, there were also *lateral* variations by refraction of SH waves across this deep crustal velocity contrast. This produced significant amplitude variations, with azimuth from the seismic source, of the strong ground shaking in a period range of about 1 to 2 seconds. In addition, there was

measurable scattering of shear waves by deep alluvial basins south of San Francisco Bay. In sum, the large wave amplitudes caused enhanced intensity in a region between San Francisco and Oakland, about 10 km wide by 15 km long.

Finally, it should be noted that seismic S waves travel through the rocks and soils of the Earth with a rotational component. Torsional components of ground motion are thought to have important effects on the response of certain types of structures. Some building codes now contain material on practices that take rotational ground motion into consideration.

1.6 EARTHQUAKE DAMAGE MECHANISMS

Earthquakes can damage structures in various ways such as:

1. by inertial forces generated by severe ground shaking.
2. by earthquake induced fires.
3. by changes in the physical properties of the foundation soils (e.g. consolidation, settling, and liquefaction).
4. by direct fault displacement at the site of a structure.
5. by landslides, or other surficial movements.
6. by seismically induced water waves such as seismic sea waves (tsunamis) or fluid motions in reservoirs and lakes (*seiches*).
7. by large-scale tectonic changes in ground elevation.

Of the above categories, by far the most serious and widespread earthquake damage and accompanying loss of life are caused by severe

ground shaking. The bulk of this handbook is devoted to design techniques and measures for reducing this type of hazard⁽¹⁻⁷⁾.

Fire hazards in earthquakes must also be emphasized. Vivid memories remain of the great conflagrations that followed the San Francisco 1906 earthquake and Tokyo's 1923 earthquake. In the 1906 San Francisco earthquake perhaps 20 percent of the total loss was due directly to ground motions. However, the fire, which in three days burned 12 square kilometers and 521 blocks of downtown San Francisco, was the major property hazard.

Soil related problems have caused major economic loss in past earthquakes. One classic example of this type of damage happened in the 1964 earthquake of Niigata, Japan. The maximum ground acceleration was

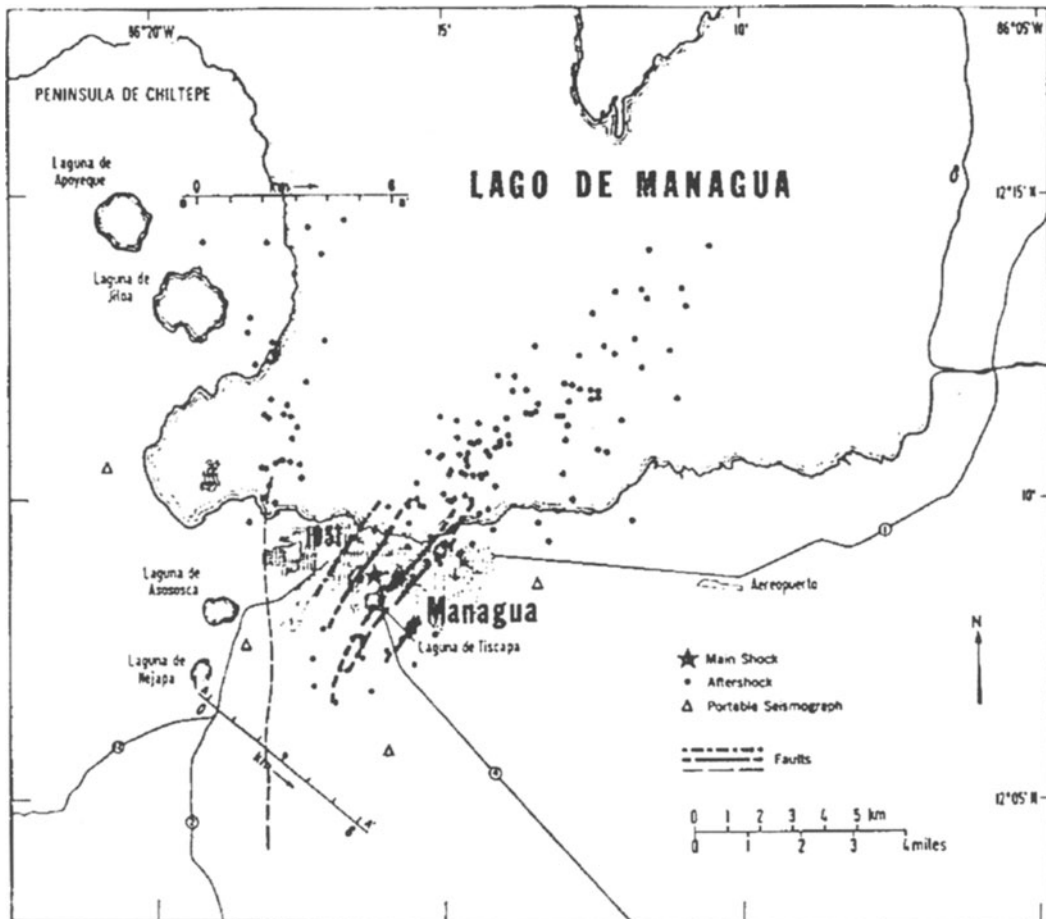


Figure 1-18. Faults rupturing under Managua (Nicaragua) during the earthquake of 1972

approximately 0.16g which considering the amount of damage, is not high. Expansion of the modern city of Niigata had involved reclamation of land along the Shinano River. In the newly deposited and reclaimed land areas many buildings tilted or subsided as a result of soil liquefaction (see Figure 1-17). 3,018 houses were destroyed and 9,750 were moderately or severely damaged in Niigata prefecture alone, most of the damage was caused by cracking and unequal settlement of the ground. About 15,000 houses in Niigata city were inundated by the collapse of a protective embankment along the Shinano River. The number of deaths was only 26. Precautionary and design measures against earthquake induced soil problems are discussed in Chapter 3.

Perhaps surface fault displacements are the most frightening aspect of earthquakes to the general public. However, although severe local damage has occurred in this way, compared with damage caused by strong ground shaking, this type of damage is rather rare. Even in very large earthquakes, the area exposed to direct surface fault displacement is much smaller than the area affected by strong ground shaking. One of the clearest examples of damage caused by direct fault displacement occurred in the Managua, Nicaragua earthquake of 1972, where four distinct faults ruptured under the city (see Figure 1-18). The total length of fault rupture within the city was about 20 kilometers, and the maximum fault displacement on two of the faults reached about 30 centimeters. Even in this case the total area damaged by direct faulting was less than one percent of the area damaged by strong ground shaking.

Earthquake-induced landslides and avalanches, although responsible for major devastation, are fortunately localized. The most pronounced example of this kind of damage occurred in Peru earthquake of May 31, 1970. This magnitude 7.75 earthquake led to the greatest seismological disaster yet experienced in the Western Hemisphere. An enormous debris avalanche from the north peak of Huascarán Mountain (see Figure 1-19) amounting to 50,000,000 or more cubic meters

of rock, snow, ice, and soil, travelled 15 kilometers from the mountain to the town of Yungay with an estimated speed of 320 kilometers per hour. At least 18,000 people were buried under this avalanche, which covered the towns of Ranrahirca and most of Yungay.

Earthquake-induced changes in ground elevations (see Figure 1-20) may not cause major injuries or loss of life. Their most important threat is the damage they can cause to structures such as bridges and dams.

Seismic sea waves, or *tsunamis*, are long water waves generated by sudden displacements under water. The most common cause of significant tsunamis is the impulsive displacement along a submerged fault, associated with a large earthquake. Because of the great earthquakes that occur around the Pacific, this ocean is particularly prone to seismic sea waves.



Figure 1-19. Aerial view of Mt. Huascarán and the debris avalanche that destroyed Yungay and Ranrahirca in May 1970 Peru earthquake. (Photo courtesy of Servicio Aerofotográfico National de Peru and L. Cluff.)

For earthquakes to generate tsunamis, dip-slip faulting (see Figure 1-10) seems to be necessary, and strike-slip faulting is almost never accompanied by damaging tsunamis. History contains many accounts of great offshore earthquakes being accompanied by destructive tsunamis. In June 15, 1896, in Honshu region of Japan a tsunami with a visual run-up height exceeding 20 meters (65 feet) drowned about 26,000 people. More recently, the Chilean earthquake of 1960 caused a tsunami with a run-up height of 10 meters at Hilo, Hawaii (see Figure 1-21). A tsunami at Crescent City, California, caused by the great Alaskan earthquake of 1964, resulted in 119 deaths and over \$104,000,000 damage.

The most important scheme to prevent loss of life in the Pacific from tsunamis is the Seismic Sea Wave Warning System. The warning system is made up of a number of

seismological observatories including Berkeley, California; Tokyo, Japan; Victoria, Canada and about 30 tide stations around the Pacific Ocean. The time of travel of a tsunami wave from Chile to the Hawaiian islands is, for example, about 10 hours and from Chile to Japan about 20 hours. Under this system, therefore, there is ample time for alerts to be followed up by local police action along coastlines so that people can be evacuated.

Apart from the tsunami warning system, the hazard can be mitigated by using adequate design of wharf, breakwater and other facilities based on techniques of coastal engineering. Often, however, zoning around coastlines is desirable to prevent building in the most low-lying areas where tsunamis are known to overwash the surface level. Sufficient information is nowadays usually available to allow local planners to make prudent decisions.



Figure. 1-20 Ground uplift along the fault in the 1999 Chi-Chi Earthquake (Photo by Dr. Farzad Naeim).



Before tsunami



After tsunami

Figure 1-21 Damage at Hilo, Hawaii, due to tsunami of May 23, 1960. (Photos courtesy of R. L. Wiegel.)

1.7 QUANTIFICATION OF EARTHQUAKES

1.7.1 Earthquake Intensity

The oldest useful yardstick of the “strength” of an earthquake is earthquake *intensity*⁽¹⁻¹⁾. Intensity is the measure of damage to works of man, to the ground surface, and of human reaction to the shaking. Because earthquake intensity assessments do not depend on instruments, but on the actual observation of effects in the meizoseismal zone, intensities can

be assigned even to historical earthquakes. In this way, the historical record becomes of utmost importance in modern estimates of seismological risk.

The first intensity scale was developed by de Rossi of Italy and Forel of Switzerland in the 1880s. This scale, with values from I to X, was used for reports of the intensity of the 1906 San Francisco earthquake, for example. A more refined scale was devised in 1902 by the Italian

volcanologist and seismologist Mercalli with a twelve-degree range from I to XII. A version is given in Table 1-2, as modified by H.O. Wood

Table 1-2. Modified Mercalli Intensity Scale (MMI) of 1931

-
- I. Not felt except by a very few under especially favorable circumstances.
 - II. Felt only by a few persons at rest, especially on upper floors of buildings. Delicately suspended objects may swing.
 - III. Felt quite noticeably indoors, especially on upper floors or buildings, but many people do not recognize it as an earthquake. Standing motor cars may rock slightly. Vibration like passing of truck. Duration estimated.
 - IV. During the day felt indoors by many, outdoors by few. At night some awakened. Dishes, windows, doors disturbed; walls make cracking sound. Sensation like heavy truck striking building. Standing motor cars rocked noticeably.
 - V. Felt by nearly everyone, many awakened. Some dishes, windows, etc., broken; a few instances of cracked plaster; unstable objects overturned. Disturbances of trees, poles, and other tall objects sometimes noticed. Pendulum clocks may stop.
 - VI. Felt by all, many frightened and run outdoors. Some heavy furniture moved; a few instances of fallen plaster or damaged chimneys. Damage slight.
 - VII. Everybody runs outdoors. Damage negligible in buildings of good design and construction; slight to moderate in well-built ordinary structures; considerable in poorly built or badly designed structures; some chimneys broken. Noticed by persons driving motor cars.
 - VIII. Damage slight in specially designed structures; considerable in ordinary substantial buildings, with partial collapse; great in poorly built structures. Panel walls thrown out of frame structures. Fall of chimneys, factory stacks, columns, monuments, walls. Heavy furniture overturned. Sand and mud ejected in small amounts. Changes in well water. Persons driving motor cars disturbed.
 - IX. Damage considerable in specially designed structures; well designed frame structures thrown out of plumb; great in substantial buildings, with partial collapse. Buildings shifted off foundations. Ground cracked conspicuously. Underground pipes broken.
 - X. Some well-built wooden structures destroyed; most masonry and frame structures destroyed with foundations; ground badly cracked. Rails bent. Landslides considerable from river banks and steep slopes. Shifted sand and mud. Water splashed (slopped) over banks.
 - XI. Few, if any, (masonry) structures remain standing. Bridges destroyed. Broad fissures in ground. Underground pipelines completely out of service. Earth slumps and land slips in soft ground. Rail bent greatly.
 - XII. Damage total. Practically all works of construction are damaged greatly or destroyed. Waves seen on ground surface. Lines of sight and level are distorted. Objects are thrown into the air.
-

Table 1-3. Japanese Seismic Intensity Scale

0. Not felt; too weak to be felt by humans; registered only by seismographs.
- I. Slight: felt only feebly by persons at rest or by those who are sensitive to an earthquake.
- II. Weak: felt by most persons, causing light shaking of windows and Japanese latticed sliding doors (*shoji*).
- III. Rather strong: shaking houses and buildings, heavy rattling of windows and Japanese latticed sliding doors, swinging of hanging objects, sometimes stopping pendulum clocks, and moving of liquids in vessels. Some persons are so frightened as to run out of doors.
- IV. Strong: resulting in strong shaking of houses and buildings. Overturning of unstable objects, spilling of liquid out of vessels.
- V. Very strong: causing cracks in brick and plaster walls, overturning of stone lanterns and grave stones, etc. and damaging of chimneys and mud and plaster warehouses. Landslides in steep mountains are observed.
- VI. Disastrous: causing demolition of more than 1% of Japanese wooden houses; landslides, fissures on flat ground accompanied sometimes by spouting of mud and water in low fields.
- VII. Ruinous: causing demolition of almost all houses: large fissures and faults are observed.

and Frank Neumann to fit conditions in California⁽¹⁻⁷⁾. The descriptions in Table 1-2 allow the damage to places affected by an earthquake to be rated numerically. These spot intensity ratings can often be separated by lines which form an isoseismal map (see Figure 1-22). Such intensity maps provide crude, but valuable information on the distribution of strong ground shaking, on the effect of surficial soil and underlying geological strata, the extent of the source, and other matters pertinent to insurance and engineering problems.

Because intensity scales are subjective and depend upon social and construction conditions of a country, they need revising from time to time. Regional effects must be accounted for. In this respect, it is interesting to compare the Japanese scale (0 to VII) summarized in Table 1-3 with the Modified Mercalli descriptions.

1.7.2 Earthquake Magnitude

If sizes of earthquakes are to be compared world-wide, a measure is needed that does not depend, as does intensity, on the density of population and type of construction. A strictly quantitative scale that can be applied to earthquakes in both inhabited and uninhabited regions was originated in 1931 by Wadati in

Japan and developed by Charles Richter in 1935 in California.

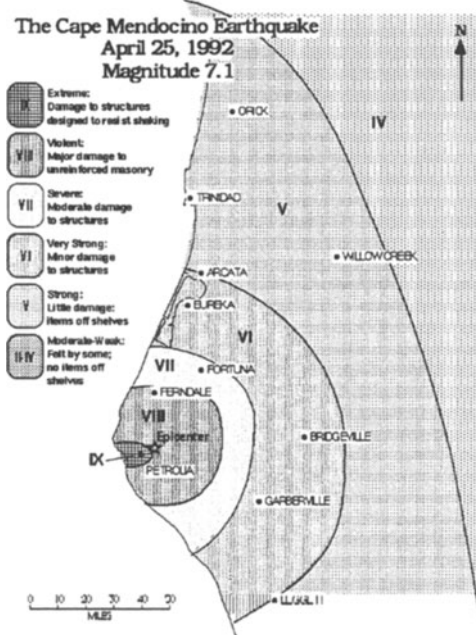


Figure 1-22. A typical isoseismal map. Similar maps are now plotted by the *Trinet* program in Southern California.

Richter⁽¹⁻⁵⁾ defined the magnitude of a local earthquake as the logarithm to base ten of the maximum seismic wave amplitude in microns (10^{-4} centimeters) recorded on a Wood-Anderson seismograph located at a distance of

100 kilometers from the earthquake epicenter (see Figure 1-23). This means that every time the magnitude goes up by one unit, the amplitude of the earthquakes waves increase 10 times. Since the fundamental period of the Wood-Anderson seismograph is 0.8 second, it selectively amplifies those seismic waves with a period ranging approximately from 0.5 to 1.5 seconds. Because the natural period of many building structures are within this range, the local Richter magnitude remains of value to engineers.

It follows from the definition of the magnitude, that it has no theoretical upper or lower limits. However, the size of an earthquake is limited at the upper end by the strength of the rocks of the Earth's crust. Since 1935, only a few earthquakes have been recorded on seismographs that have had a magnitude over 8.0. At the other extreme, highly sensitive seismographs can record earthquakes with a magnitude of less than minus two. See Table 1-4 for an average number of world-wide earthquakes of various magnitudes.

Generally speaking, shallow earthquakes have to attain Richter magnitudes of more than 5.5 before significant widespread damage occurs near the source of the waves.

At its inception, the idea behind the Richter local magnitude scale (M_L) was a modest one. It was defined for Southern California, shallow earthquakes, and epicentral distances less than about 600 kilometers. Today, the method has been extended to apply to a number of types of seismographs throughout the world (see Figure 1-24). Consequently a variety of magnitude scales based on different formulas for epicentral distance and ways of choosing an appropriate wave amplitude, have emerged:

Surface Wave Magnitude (M_s) Surface waves with a period around 20 seconds are often dominant on the seismograph records of distant earthquakes (epicentral distances of more than 2000 kilometers). To quantify these earthquakes, Gutenberg defined a magnitude scale (M_s) which is based on measuring the amplitude of surface waves with a period of 20 seconds⁽¹⁻⁸⁾.

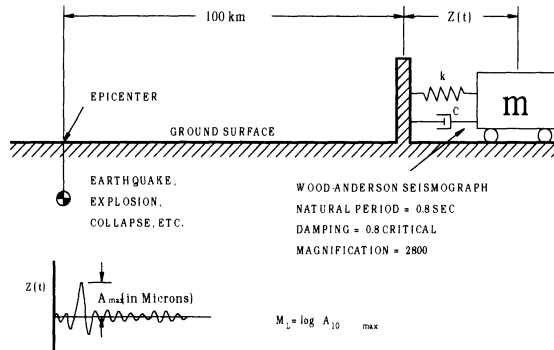


Figure 1-23. Definition of local Richter magnitude

Body Wave Magnitude (m_b) Deep focus earthquakes have only small or insignificant trains of surface waves. Hence, it has become routine in seismology to measure the amplitude of the P wave, which is not affected by the focal depth of the source, and thereby determine a P wave magnitude (m_b). This magnitude type has also been found useful in continental regions like the eastern United States where no Wood-Anderson instruments have operated historically.

Moment Magnitude (M_W) Because of significant shortcomings of M_L , m_b , and to a lesser degree M_s in distinguishing between great earthquakes, the moment magnitude scale was devised⁽¹⁻¹⁰⁾. This scale assigns a magnitude to the earthquake in accordance with its seismic moment (M_0) which is directly related to the size of the earthquake source:

$$M_W = (\log M_0)/1.5 - 10.7 \quad (1-4)$$

where M_0 is seismic moment in dyn-cm.

Magnitude Saturation As described earlier, the Richter magnitude scale (M_L) measures the seismic waves in a period range of particular importance to structural engineers (about 0.5-1.5 seconds). This range corresponds approximately to wave-lengths of 500 meters to 2 kilometers. Hence, although theoretically there is no upper bound to Richter magnitude, progressively it underestimates more seriously the strength of earthquakes produced by the longer fault rupture lengths. The saturation point for the Richter magnitude scale is about

$M_L = 7$. The body wave magnitude (m_b) saturates at about the same value.

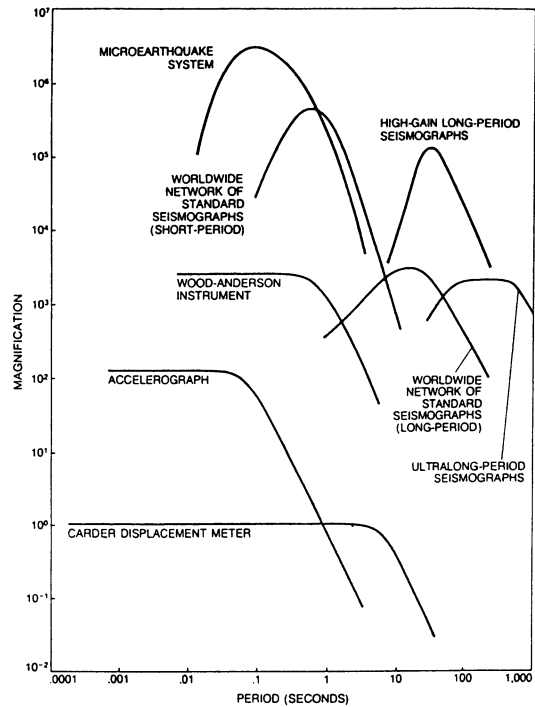


Figure 1-24. Amplification of seismic waves by various seismographs. (From *The Motion of Ground in Earthquakes*, by David M. Boore. Copyright 1977 by Scientific American, Inc. All rights reserved.)

Table 1-4. World-wide Earthquakes per Year

Magnitude M_s	Average No. $> M_s$
8	1
7	20
6	200
5	3,000
4	15,000
3	$> 100,000$

In contrast, the surface-wave magnitude (M_s) which uses the amplitude of 20 second surface waves (wave-length of about 60 kilometers) saturates at about $M_s = 8$. Its inadequacy in measuring the size of great earthquakes can be illustrated by comparing the San Francisco earthquake of 1906 and the Chilean earthquake of 1960 (see Figure 1-25). Both earthquakes had a magnitude (M_s) of 8.3. However, the area that ruptured in the San Francisco earthquake (the dashed area) was

approximately 15 kilometers deep and 400 kilometers long whereas the area that ruptured in the Chilean earthquake (the dotted area) was equal to about half of the state of California. Clearly the Chilean earthquake was a much larger event.

The moment-magnitude scale (M_W) is the only magnitude scale which does not suffer from the above mentioned saturation problem for great earthquakes. The reason is that it is directly based on the forces that work at the fault rupture to produce the earthquake and not the recorded amplitude of specific types of seismic waves. Hence, as can be expected, when moment magnitudes were assigned to the San Francisco earthquake of 1906 and the Chilean earthquake of 1960, the magnitude of the San Francisco earthquake dropped to 7.9, whereas the magnitude of the Chilean earthquake was raised to 9.5. M_s and M_W for some great earthquakes are compared in Table 1-5. Magnitudes of some recent damaging earthquakes are shown in Table 1-1.

In light of the above discussion, application of different scales have been suggested for measuring shallow earthquakes of various magnitudes:

M_D	for magnitudes less than 3
M_L or m_b	for magnitudes between 3 and 7
M_s	for magnitudes between 5 and 7.5
M_W	for all magnitudes

Table 1-5. Magnitudes of Some of the Great Earthquakes

Date	Region	M_s	M_w
January 9, 1905	Mongolia	8½	8.4
Jan. 31, 1906	Ecuador	8.6	8.8
April 18, 1906	San Francisco	8½	7.9
Jan. 3, 1911	Turkestan	8.4	7.7
Dec. 16, 1920	Kansu, China	8.5	7.8
Sept. 1, 1923	Kanto, Japan	8.2	7.9
March 2, 1933	Sanriku	8.5	8.4
May 24, 1940	Peru	8.0	8.2
April 6, 1943	Chile	7.9	8.2
Aug. 15, 1950	Assam	8.6	8.6
Nov. 4, 1952	Kamchatka	8	9.0
March 9, 1957	Aleutian Islands	8	9.1

Date	Region	M_s	M_w
Nov. 6, 1958	Kurile Islands	8.7	8.3
May 22, 1960	Chile	8.3	9.5
March 28, 1964	Alaska	8.4	9.2
Oct. 17, 1966	Peru	7.5	8.1
Aug. 11, 1969	Kurile Islands	7.8	8.2
Oct. 3, 1974	Peru	7.6	8.1
July 27, 1976	China	8.0	7.5
Aug. 16, 1976	Mindanao	8.2	8.1
March 3, 1985	Chile	7.8	7.5
Sep. 19, 1985	Mexico	8.1	8.0

1.8 EARTHQUAKE SOURCE MODELS

Field evidence in the 1906 California earthquake showed clearly that the strained rocks immediately west of the San Andreas fault had moved north-west relative to the rocks to the east. Displacements of adjacent points along the fault reached a maximum of 6 meters near Olema in the Point Reyes region.

H.F. Reid ⁽¹⁻¹¹⁾ studied the triangulation surveys made by the U.S. Coast and Geodetic Survey across the region traversed by the 1906 fault break. These surveys made in 1851-1865, 1874-1892 and just after the earthquake, showed (i) small inconsistent changes in elevation along the San Andreas fault; (ii) significant horizontal displacements parallel to the fault trace; and (iii) movement of distant points on opposite sides of the fault of 3.2 meters over the 50-year period, the west side moving north.

Based on geological evidence, geodetic surveys, and his own laboratory experiments, Reid put forth the elastic rebound theory for source mechanism that would generate seismic waves. This theory supposes that the crust of the Earth in many places is being slowly displaced by underlying forces. Differential displacements set up elastic strains that reach levels greater than can be endured by the rock. Ruptures (faults) then occur, and the strained

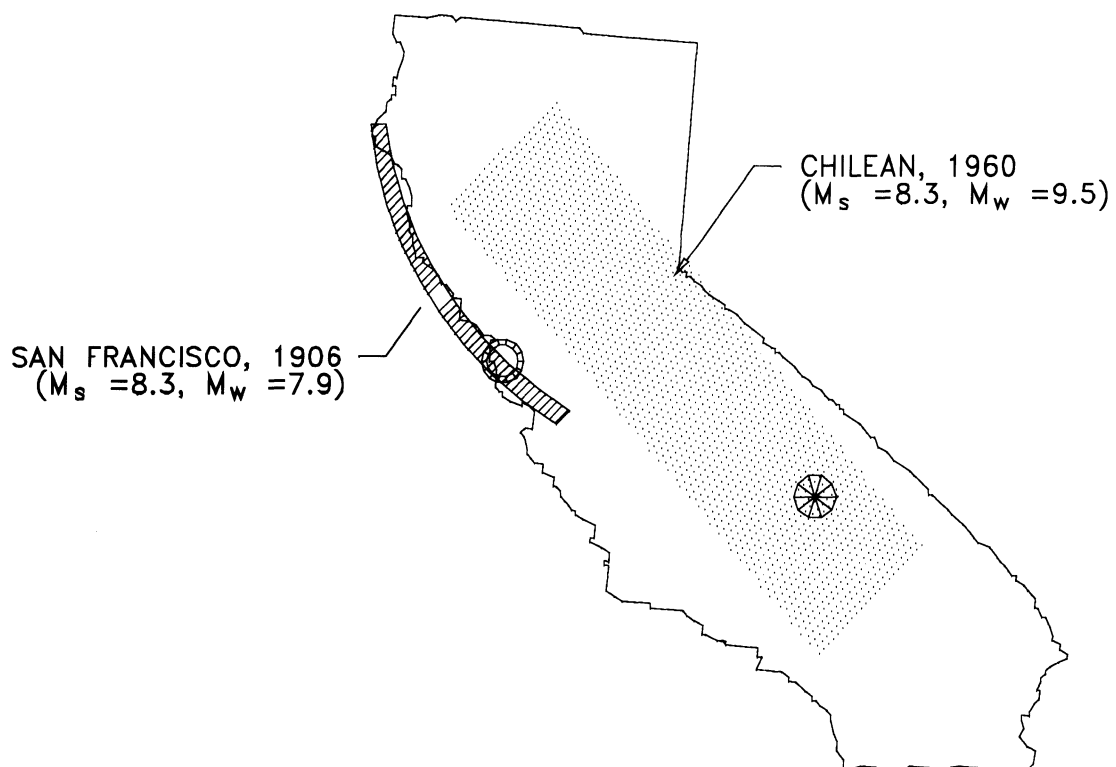
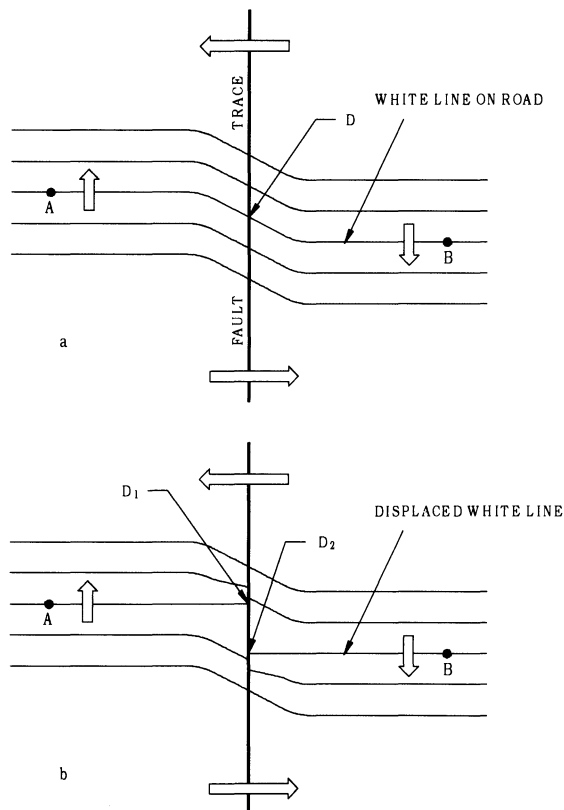


Figure 1-25. Fault rupture area for the San Francisco 1906 and Chile 1960 earthquakes. (Modified from *The Motion of Ground in Earthquakes*, By David M. Boore. Copyright 1977 by Scientific American, Inc. All rights reserved.)

rock rebounds along the fault under the elastic stresses until the strain is partly or wholly relieved (see Figures 1-26 and 1-27). This theory of earthquake mechanism has been verified under many circumstances and has required only minor modification.



*Figure 1-26. A bird's eye view of market lines drawn along a road AB, which crosses a fault trace at the ground surface. (a) Elastic strain accumulation before fault rupture. (b) Final position after the fault rupture. (From *Earthquakes*, by Bruce A. Bolt. Copyright 1999, W.H. Freeman and Company. Used with permission.)*

The strain slowly accumulating in the crust builds a reservoir of elastic energy, in the same way as a coiled spring, so that at some place, the *focus*, within the strained zone, rupture suddenly commences, and spreads in all directions along the fault surface in a series of erratic movements due to the uneven strength of the rocks along the tear. This uneven propagation of the dislocation leads to bursts of high-frequency waves, which travel into the Earth to produce the seismic shaking that

causes the damage to buildings. The fault rupture moves with a typical velocity of two to three kilometers per second and the irregular steps of rupture occur in fractions of a second. Ground shaking away from the fault consists of all types of wave vibrations with different frequencies and amplitudes.

In 1966, N. Haskell⁽¹⁻¹²⁾ developed a model "in which the fault displacement is represented by a coherent wave only over segments of the fault and the radiations from adjacent sections are assumed to be statistically independent or incoherent." The physical situation in this model is that the rupture begins suddenly and then spreads with periods of acceleration and retardation along the weakly welded fault zone. In this model, the idea of statistical randomness of fault slip or *chattering* in irregular steps along the fault plane is introduced.

More recently, Das and Aki⁽¹⁻¹³⁾ have considered a fault plane having various *barriers* distributed over it. They conceive that rupture would start near one of the barriers and then propagate over the fault plane until it is brought to rest or slowed at the next barrier. Sometimes the barriers are broken by the dislocation; sometimes the barriers remain unbroken but the dislocation reinitiates on the far side and continues; sometimes the barrier is not broken initially but, due to local repartitioning of the stresses and possible nonlinear effects, it eventually breaks, perhaps with the occurrence of aftershocks.

The elastic rebound model involving a moving dislocation along a fault plane segmented by barriers, over which roughnesses (or *asperities*) of various types are distributed stochastically, is thus the starting point for the modern interpretation of near-field records⁽¹⁻¹⁴⁾. Based on this model, there have been recently a number of attempts to compute synthetic seismograms from points near to the source and comparisons have been made with observations (see Section 1.10).

As mentioned earlier, there are different kinds of fault ruptures. Some involve purely horizontal slip (strike-slip); some involve vertical slip (dip-slip). It might be expected that

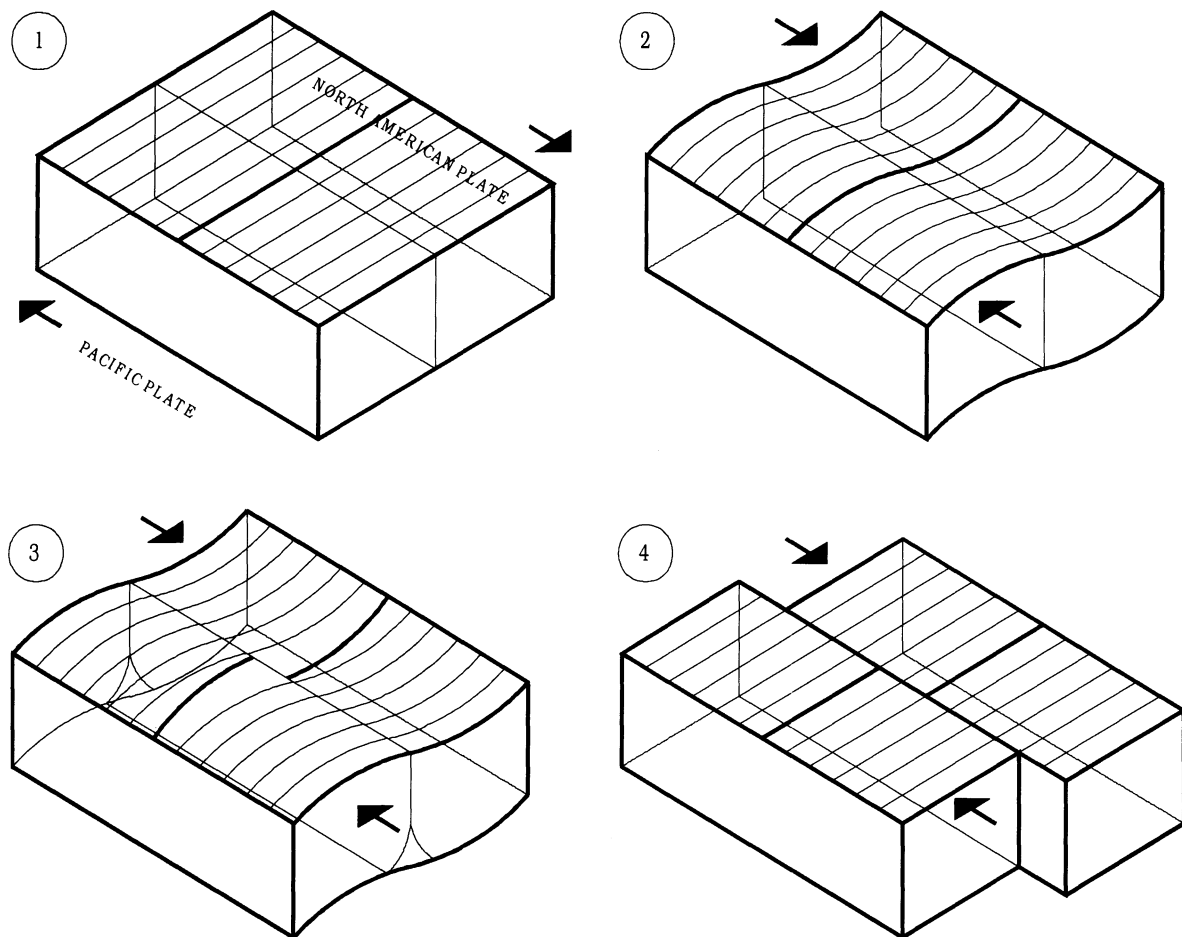


Figure 1-27. Elastic rebound model of earthquakes

the wave patterns generated by fault geometries and mechanisms of different kinds will be different to a larger or lesser extent, because of the different radiation patterns produced. These different geometries can be modeled mathematically by appropriate radiation functions.

The theory must also incorporate effects of the moving source. The Doppler-like consequences will depend on the speed of fault rupture and the directions of faulting. The physical problem is analogous (but more difficult) to the problem of sound emission from moving sources. The problem can be approached both kinematically and dynamically. The acoustic problem shows that in the far-field the pressure is the same as when the source is at rest. However, in the near-field, the time dependence of both frequency and

wave amplitude is a function of the azimuth of the site relative to the moving source (Figure 1-28).

In the case of a fault rupture toward a site at a more or less constant velocity (almost as large as the shear wave velocity), most of the seismic energy from the elastic rebound of the fault arrives in a single large pulse of motion (velocity or displacement), which occurs near the beginning of the record. This wave pulse represents the cumulative effect of almost all of the seismic radiation from the moving dislocation. In addition, the radiation pattern of the shear dislocation causes this large pulse of motion to be oriented mostly in the direction perpendicular to the fault. Coincidence of the radiation pattern maximum for tangential motion and the wave focusing due to the rupture propagation direction toward the site

produces a large displacement pulse normal to the fault strike.

The horizontal recordings of stations in the 1966 Parkfield, California and the Pacoima station in the 1971 San Fernando, California earthquake were the first to be discussed in the literature as showing characteristic velocity pulses. These cases, with maximum amplitudes of 78 and 113 cm/sec, respectively, consisted predominantly of horizontally polarized SH wave motion and were relatively long period (about 2-3 sec). The observed pulses are consistent with the elastic rebound theory of earthquake genesis propounded by H.F. Reid after the 1906 San Francisco earthquake. These velocity and displacement pulses in the horizontal direction near the source were first called the source *fling*. Additional recordings in the near field of large sources have confirmed the presence of energetic pulses of this type, and they are now included routinely in synthetic ground motions for seismic design purposes. Most recently, the availability of instrumented measured ground motion close to the sources of

the 1994 Northridge earthquake, the 1995 Kobe earthquake and the 1999 Chi-Chi earthquake provided important recordings of the “fling” or velocity pulse.

As in acoustics, the amplitude and frequency of the velocity and displacement pulses or “fling” have a geometrical focusing factor, which depends on the angle between the direction of wave propagation from the source and the direction of the source velocity. Instrumental measurements show that such directivity focusing can modify the amplitude velocity pulses by a factor of up to 10. The pulse may be single or multiple, with variations in the impetus nature of its onset and in its half-width period. A widely accepted illustration is the recorded ground displacement of the October 15, 1979 Imperial Valley, California, earthquake generated by a strike-slip fault source. The main rupture front moved toward El Centro and away from Bonds Corner.

We now summarize the main lines of approach to modeling mathematically the earthquake source. The first model is the

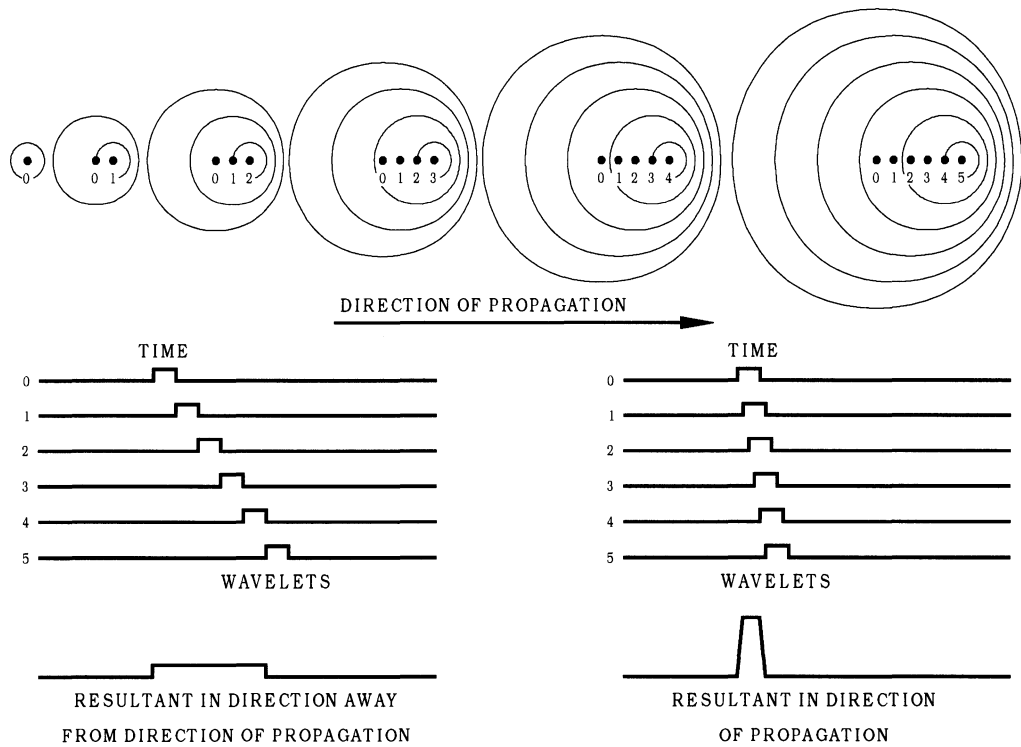


Figure 1-28. Effect of direction of fault rupture on ground motion experienced at a site. [After Benioff⁽¹⁻¹⁵⁾ and Singh⁽¹⁻¹⁶⁾]

kinematic approach in which the time history of the slip on the generating fault is given *a priori*. Several defining parameters may be specified, such as the shape, duration, and amplitude of the source (or source time function and slip), the velocity of the slip over the fault surface, and the final area of the region over which the slip occurred. Numerous theoretical papers using this approach have been published (see the various discussions in Reference 1-16). The process is a kind of complicated curve fitting whereby the parameters of the source are varied in order to estimate by inspection the closeness of fit between recorded and computed near-field or far-field seismic waves. Once the seismic source is defined by this comparison process, then the estimated source parameters can be used to extrapolate from the known ground motions near to a historical source to the future conditions required for engineering purposes.

A second approach is to use the differential equations involving the forces which produce the rupture. This dynamic procedure has received considerable emphasis lately. The basic model is a shear crack which is initiated in the pre-existing stress field and which causes stress concentrations around the tip of the crack. These concentrations, in turn, cause the crack to grow. For example, analytic expressions for particle accelerations in given directions from a uniformly growing elliptical crack are derived, but the effect of crack stoppage is not always included (this unrealistic boundary condition is included in most work of this kind).

The key to the crack problem seems to be in modeling the physical processes of the typical crack where there is interaction between the stress accumulation, rate of crack growth, and the criterion of fracture. Most studies on dynamic shear cracks are concerned primarily with the actual rupture process, and so the crack is assumed to be embedded in an infinite homogeneous medium. More realistic studies concerned with the seismic waves that are recorded in the near-field need a numerical approach, such as finite elements or finite differences, to handle geologic structural conditions.

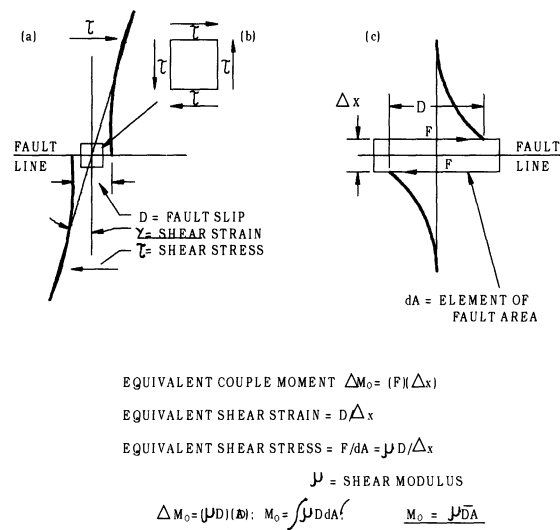


Figure 1-29. Definition of seismic moment.

The studies mentioned under kinematic and dynamic models are built around the elastic rebound theory of slip on a fault. There are, however, more general studies that take a less specific view of the earthquake source⁽¹⁻¹⁶⁾.

It should be mentioned here that the scalar seismic moment (direction of force couples along the fault ignored) is given by

$$M_0 = \mu A D \quad (1-5)$$

where μ is the rigidity of the material surrounding the fault, A is the slipped area, and D is the amount of slip (see Figure 1-29). The seismic moment is now the preferred parameter to specify quantitatively the overall size of an earthquake source.

Let us now summarize the physical model for the earthquake source generally accepted at present (see Figure 1-30). The source extends over a fault plane in the strained crustal rocks by a series of dislocations, which initiate at the focus and spread out with various rupture velocities. The dislocation front changes speed as it passes through patches on roughness (asperities on the fault).

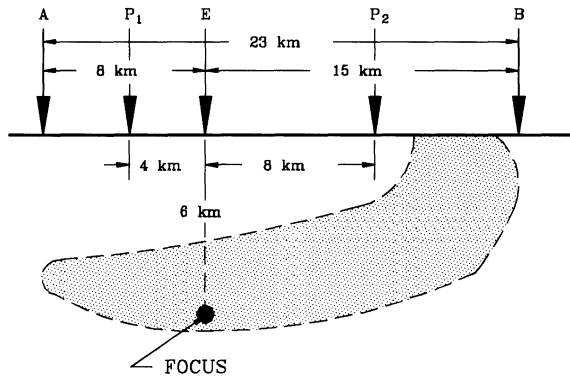


Figure 1-30. Simplified model of the vertical rupture surface for the Coyote Lake earthquake of 1979 in California

At the dislocation itself, there is a finite time for a slip to take place and the form of the slip is an elastic rebound of each side of the fault leading to a decrease of overall strain. The slip can have vertical components, as well as horizontal components, and can vary along the fault. The waves are produced near the dislocation front as a result of the release of the strain energy in the slippage⁽¹⁻⁷⁾.

This model resembles in many ways radio waves being radiated from a finite antenna. In the far-field, the theory of radio propagation gives complete solutions for the reception of radio signals through stratified media. However, when the receiver is very near to the extended antenna, the signal becomes mixed because of the finiteness of the source and interference through end effects. The main parameters in the model are:

Rupture length	L
Rupture width	W
Fault slippage (offset)	D
Rupture velocity	V
Rise time	T
Roughness (barrier) distribution density	$\phi(x)$

The main work in theoretical seismology on source properties today is to determine which of these parameters are essential, whether the set is an optimal one, and how best to estimate each parameter from both field observations and from analysis of the seismograms made in the near and the far-field.

A number of papers have now been published that demonstrate that, in certain important cases, synthetic seismograms for seismic waves near the source can be computed realistically⁽¹⁻¹⁸⁾. The synthetic motions can be compared with the three observed orthogonal components of either acceleration, velocity, or displacement at a site. There remain difficulties, however, in modeling certain observed complexities and there is a lack of uniqueness in the physical formulations which lead to acceptable fits with observations (see also Section 1.10).

1.9 SEISMIC RISK EVALUATION

Regional seismicity or risk maps recommended by seismic design codes (see Chapter 5) usually do not attempt to reflect geological conditions nor to take into account variations due to soil properties. It is necessary, therefore, for critical construction in populated regions to make special geological-engineering studies for each site, the detail and level of concern which is used depending on the density of occupancy as well as the proposed structural type. In inhabited areas, more casualties are likely to result from a failed dam or a damaged nuclear reactor, for example, than from a damaged oil pipeline.

The factors which must be considered in assessment of seismic risk of a site have been well-defined in recent times⁽¹⁻⁷⁾. Here a brief summary of these factors is listed.

Geological Input Any of the following investigations may be required.

1. Provision of a structural geologic map of the region, together with an account of recent tectonic movements.
2. Compilation of active faults in the region and the type of displacement (e.g., left-lateral, strike-slip, etc.). Fieldwork is sometimes necessary here. Of particular importance are geological criteria for fault movements in Holocene time (the past 10,000 years) such as displacements in recent soils, dating by radio-carbon methods

- of organic material in trenches across the fault, and other methods.
3. Mapping of the structural geology around the site, with attention to scarps in bedrock, effects of differential erosion and offsets in overlying sedimentary deposits. Such maps must show rock types, surface structures and local faults, and include assessments of the probable length, continuity and type of movement on such faults.
 4. In the case of through-going faults near the site, geophysical exploration to define the location of recent fault ruptures and other lineaments. Geophysical work sometimes found useful includes measurement of electrical resistivity and gravity along a profile normal to the fault. Other key geological information is evidence for segmentation of the total fault length, such as step-over of fault strands, and changes in strike.
 5. Reports of landslides, major settlements, ground warping or inundation from floods or tsunamis at the site.
 6. Checks of ground water levels in the vicinity to determine if ground water barriers are present which may be associated with faults or affect the soil response to the earthquake shaking.

Seismological Input Procedures for the estimation of ground shaking parameters for optimum engineering design are still in the early stages and many are untested. It is important, therefore, to state the uncertainties and assumptions employed in the following methods:

1. Detailed documentation of the earthquake history of the region around the site. Seismicity catalogs of historical events are needed in preparing lists of felt earthquakes. The lists should show the locations, magnitudes and maximum Modified Mercalli intensities for each earthquake. This information should be illustrated by means of regional maps.
2. Construction, where the record permits, of recurrence curves of the frequency of regional earthquakes, down to even small

magnitudes (See the Gutenberg-Richter equation, Chapter 2). Estimates of the frequency of occurrence of damaging earthquakes can then be based on these statistics.

3. A review of available historic records of ground shaking, damage, and other intensity information near the site.
4. Estimation of the maximum Modified Mercalli intensities on firm ground near the site from felt reports from each earthquake of significance.
5. Definition of the design earthquakes⁽¹⁻¹⁹⁾. The geological and seismological evidence assembled in the above sections should then be used to predict the earthquakes which would give the most severe ground shaking at the site. (Several such design earthquakes might be necessary and prudent.) Where possible, specific faults on which rupture might occur should be stated, together with the likely mechanism (strike-slip, thrust, and so on). Likely focal depth and length of rupture and estimated amount of fault displacement should be determined, with their uncertainties. These values are useful in estimating the possible magnitude of damaging earthquakes from standard curves that relate fault rupture to magnitude (see Table 1-6).

Soils Engineering Input When there is geological indication of the presence of structurally poor foundation material (such as in flood plains and filled tidelands), a field report on the surficial strata underlying the site is advisable. In addition, areas of subsidence and settlement (either natural or from groundwater withdrawal) and the stability of nearby slopes must be studied. We mention here only three factors that may require special scrutiny.

1. Study of engineering properties of foundation soils to the extent warranted for the type of building. Borings, trenchings and excavations are important for such analyses, as well as a search for the presence of sand layers which may lead to liquefaction.
2. Measurements (density, water content, shear strength, behavior under cyclic loading,

attenuation values) of the physical properties of the soil in situ or by laboratory tests of borehole core samples.

3. Determination of P and S wave speeds and Q attenuation values and in the overburden layers by geophysical prospecting methods.

Table 1-6. Earthquake Magnitude versus Fault Rupture Length

Magnitude (Richter)	Rupture (km)
5.5	5-10
6.0	10-15
6.5	15-30
7.0	30-60
7.5	60-100
8.0	100-200
8.5	200-400

1.10 EARTHQUAKE AND GROUND-MOTION PREDICTION

Aspects of earthquake prediction that tend to receive the most publicity are: prediction of the place, prediction of the size, and prediction of the time of the earthquake. For most people, prediction of earthquakes means prediction of the time of occurrence. A more important aspect for mitigation of hazard is the prediction of the strong ground motion likely at a particular site (see also Chapters 2 and 3).

First, considering the status of forecasting of the time and size of an earthquake⁽¹⁻²⁰⁾. Prediction of the region where earthquakes are likely to occur has now been largely achieved by seismicity studies using earthquake observatories. Because empirical relations between the magnitude of an earthquake and the length of observed fault rupture have also been constructed (see Table 1-6), rough limits can be placed on the size of earthquakes for a region.

Many attempts have been made to find clues for forewarning. Some physical clues for earthquake prediction are shown in Figure 1-31. In 1975, Chinese officials, using in part, increased seismicity (foreshocks) and animal restlessness, evacuated a wide area before the

damaging Haicheng earthquake. However, in the 1976 Tangshan catastrophe no forewarnings were issued. Elsewhere, emphasis has been placed on geodetic data, such as geodimeter measurements of deformation of the Californian crust along the San Andreas fault. An ex post facto premonitory change in ground level was found after the Niigata earthquake, which if it had been discovered beforehand, might have served as one indication of the coming earthquake.

Another scheme is based on detecting spatial and temporal gaps in the seismicity of a tectonic region. In 1973, a prediction was made by seismologists of the U.S. Geological Survey that an earthquake with a magnitude of 4.5 would occur along the San Andreas fault south of Hollister within the next six months. The prediction was based on four principal shocks which had occurred within 3 years on both ends of a 25-km-long stretch of the San Andreas fault, bracketing a 6-km-long section free from earthquakes in that time interval. The assumption was that the mid-section was still stressed but locked, ready to release the elastic energy in an earthquake. However, no earthquake occurred in the six months predicted. One difficulty with such methods is the assessment of a zero epoch with which to compare the average background occurrence rate.

A much publicized prediction experiment in California depended on the detection of a 22 year periodicity in moderate magnitude ($M_L = 5.5$) earthquakes centered on the San Andreas fault near Parkfield. Similar earthquakes were recorded in 1901, 1922, 1934, and 1966. Available seismograms in addition allowed quantitative comparison of the source mechanisms for the 1922, 1934, and 1966 earthquakes. Many monitoring instruments were put in place to try to detect precursors for a possible 1988 repetition. These included changes in ground water tables, radon concentration, seismicity, and fault slippage. The prediction of repetition of such a characteristic earthquake in the years 1988 ± 4 , proved to be unsuccessful.

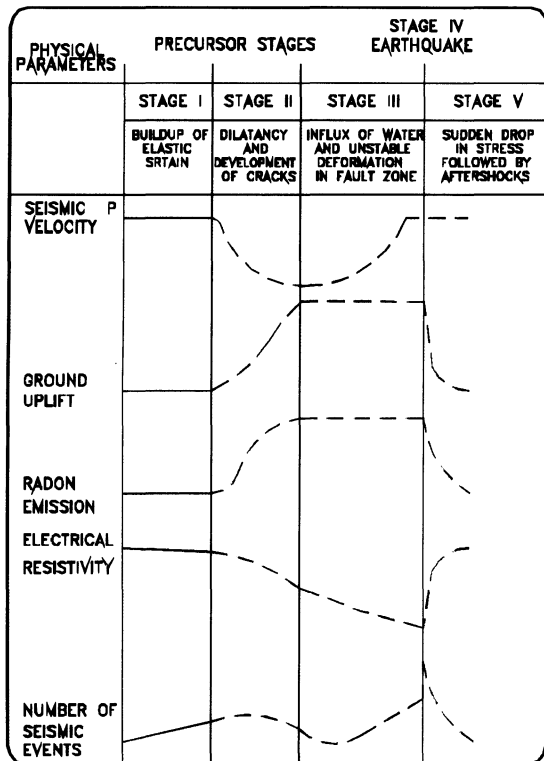


Figure 1-31 Physical clues for earthquake prediction.
[After predicting earthquakes, National Academy of Sciences. (1-1).]

It has often been pointed out that even if the ability to predict the time and size of an earthquake was achieved by seismologists, many problems remain on the hazard side. Suppose that an announcement were made that there was a chance of one in two of a destructive earthquake occurring within a month. What would be the public response? Would the major industrial and commercial work in the area cease for a time, thus dislocating large segments of the local economy? Even with shorter-term prediction, there are difficulties if work is postponed until the earthquake-warning period is over. Suppose that the predictive time came to an end and no earthquake occurred; who would take the responsibility of reopening schools and resuming other activities?

Secondly, let us consider the calculation of artificial (synthetic) seismic strong ground motions⁽¹⁻²¹⁾. The engineering demand is for the estimation of certain parameters, which will be used for design and structural checking. There

are two representations usually used. The first is the seismogram or *time history* of the ground motion at the site represented instrumentally by the seismogram or accelerogram. The second is the Fourier or response spectra for the whole motion at the site. These two representations are equivalent and are connected by appropriate transformations between the time and frequency domains.

In the simplest time-history representation, the major interest is in the peak amplitudes of acceleration, velocity, and displacement as a function of frequency of the ground motion. Another parameter of great importance is the duration of the strong ground motion, usually given in terms of the interval of time above a certain acceleration threshold (say 0.05g), in a particular frequency range. Typically, the duration of a magnitude 7 earthquake at a distance of 10 kilometers is about 25 seconds. The pattern of wave motion is also important in earthquake engineering because the nonlinear response of structures is dependent on the sequence of arrival of the various types of waves. In other words, damage would be different if the ground motion were run backwards rather than in the actual sequence of arrival. In this respect, phasing of the ground motion becomes very important and the phase spectra should be considered along with the amplitude spectrum.

The phasing of the various wave types on synthetic seismograms can be determined by estimation of times of arrival of the P, S, and surface waves. In this way, a realistic envelope of amplitudes in the time histories can be achieved.

There are two main methods for constructing synthetic ground motions. The first is the more empirical and involves maximum use of wave motion parameters from available strong ground motion records and application of general seismological theory⁽¹⁻²²⁾. The second

method entails considerable computer analysis based on models of the earthquake source and assumptions on earthquake scaling^(1-16,1-23). In the first method, the initial step is to define, from geological and seismological information, the appropriate earthquake sources for the site

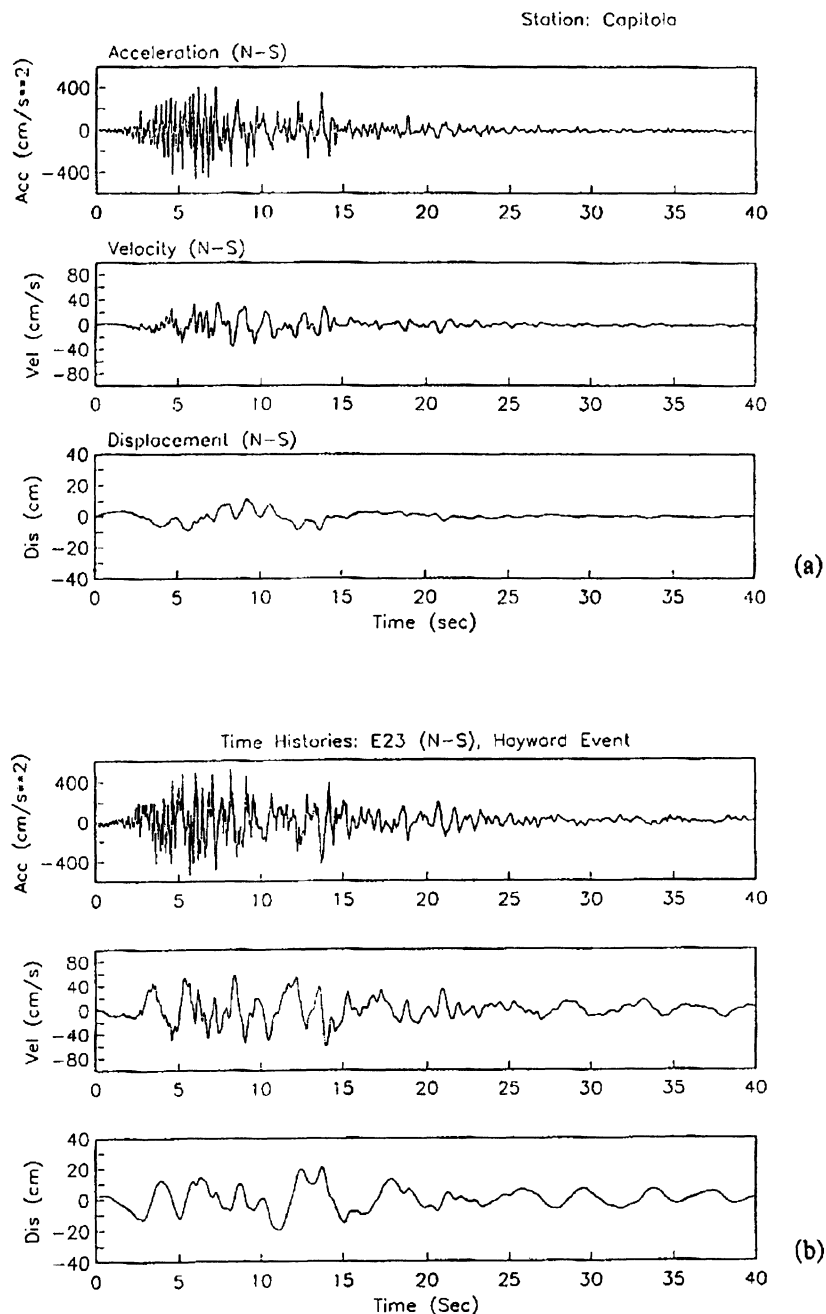


Figure 1-32. Ground motions recorded at Capitola, California in the 1989 Loma Prieta earthquake (a). The synthesized ground motions for site E23 (on rock) for a magnitude 7.2 earthquake, generated by shallow rupture 5 km away (b)

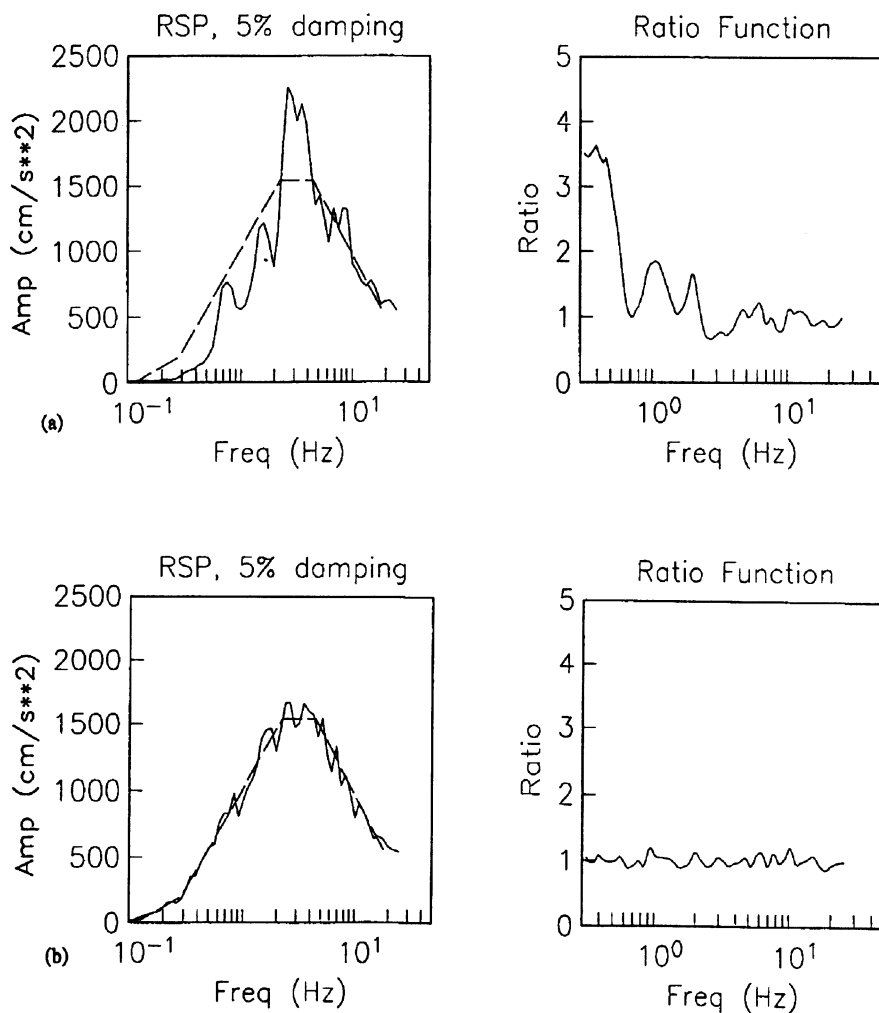


Figure 1-33. Response spectrum for the Capitola motion (Figure 1-32) compared with a target code spectrum (a). On the right, the ratio of frequency components is shown. Four iterations of the Fourier amplitude spectrum (phase fixed) of the Capitola record produced the compatibility shown (b).

of interest. The source selection may be deterministic or probabilistic and may be decided on grounds of acceptable risk. Next, specification of the propagation path distance is made, as well as the P, S and surface wave velocities along the path. These speeds allow calculation of the appropriate wave propagation delays between the source and the multi-support points of the structure and the angles of approach of the incident seismic waves.

The construction of realistic motions then proceeds as a series of iterations, starting with the most appropriate observed strong motion record available, to a set of more specific time

histories, which incorporate the seismologically defined wave patterns. The strong motion accelerograms are chosen to satisfy the seismic source type (dip-slip, etc.), and path specifications for the seismic zone in question. The frequency content is controlled by applying engineering constraints, such as a selected *response amplitude spectrum*^(1-24,1-25). The target spectra is obtained, for example, from previous data analysis, often from earthquake building codes. The fit between the final iteration and the target spectrum should fall within one standard error. Similarly, each seismogram must maintain the specified peak ground

accelerations, velocities and displacements within statistical bounds. The duration of each wave section (the P, S and surface wave portions) must satisfy prescribed source, path and site conditions. Figure 1-32 shows iterations of ground motion at site E23 for the east crossing of the San Francisco Bay Bridge for a Safety Evaluation Earthquake (SEE) of magnitude 7.2 on the nearby Hayward fault. The initial accelerogram chosen for the input motion at the pier in question is the horizontal ground motion recorded at Capitola on firm ground in the 1989 Loma Prieta earthquake. The north-south component of accelerations are shown. These records are then scaled for the required peak acceleration and then the 5% damped response spectrum is calculated. Two steps in the fitting of the response spectrum are shown in Figure 1-33. The ratio function between the calculated and target response spectrum is achieved. The process produces a realistic motion for the input site as shown in Figure 1-32. The synthetic motion has a wave pattern, including "fling", duration, amplitude and spectrum that are acceptable from both the seismological and engineering viewpoints.

At this stage, for large multi-support structures, account can be taken of the *incoherency* of ground motion. The first step is to lag, at each wave-length, the phase of the ground motion to allow for the different times of wave propagation between input points. Use must then be made of a coherency function (see Figure 1-34) that has been obtained from previous studies in similar geological regions. The process is to adjust the phase in the Fourier spectrum at each frequency so that the resulting phase spectrum for each input matches the selected coherency function.

Consider now the second method of synthesizing ground motions by computational means using a scaling relation between a small earthquake in the region and the ground motion required for engineering design or safety evaluation.

These are usually, of course, much smaller magnitude sources than required. Such smaller recorded ground motions contain essential

properties of the particular earthquake mechanism involved, however, as well as the effects of the particular geological structure between the source and the station. In terms of the theory of the response of mechanical structures, they are called *empirical Green's functions*⁽¹⁻¹⁶⁾. They can be considered as the response of the local geological system to an approximate impulse response of short duration applied at the rupturing fault. If such empirical Green's functions appropriate to the study of the site in question are not available, they must be constructed making certain mathematical assumptions and introducing appropriate tensor analysis (see Section 1.8).

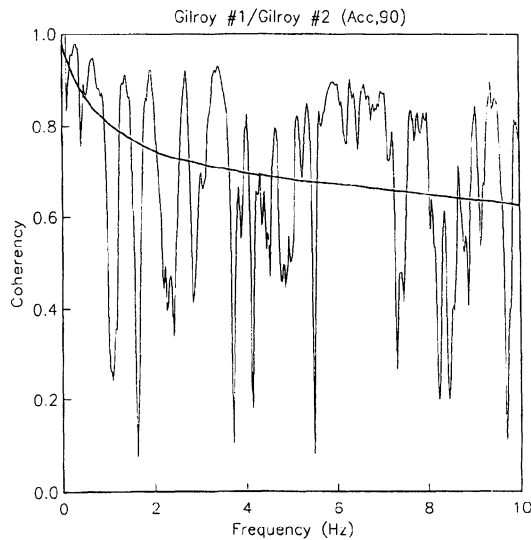


Figure 1-34. The coherency function commuted from adjacent (1750m separation) recordings of strong ground motion in the Gilroy strong ground motion array during the 1989 Loma Prieta main shock. The heavy line is a smooth representation of the coherency effect.

The size of the earthquake is then selected in terms of its seismic moment which, as was seen in Section 1.8, is given quantitatively in terms of the area of the fault slip and the amount of slip. An appropriate fault area is then mapped in terms of an elementary mesh of finite elements. The empirical Green's function mentioned above is then applied to each element of the mesh in the sequence required to achieve the appropriate rupture velocity across the whole

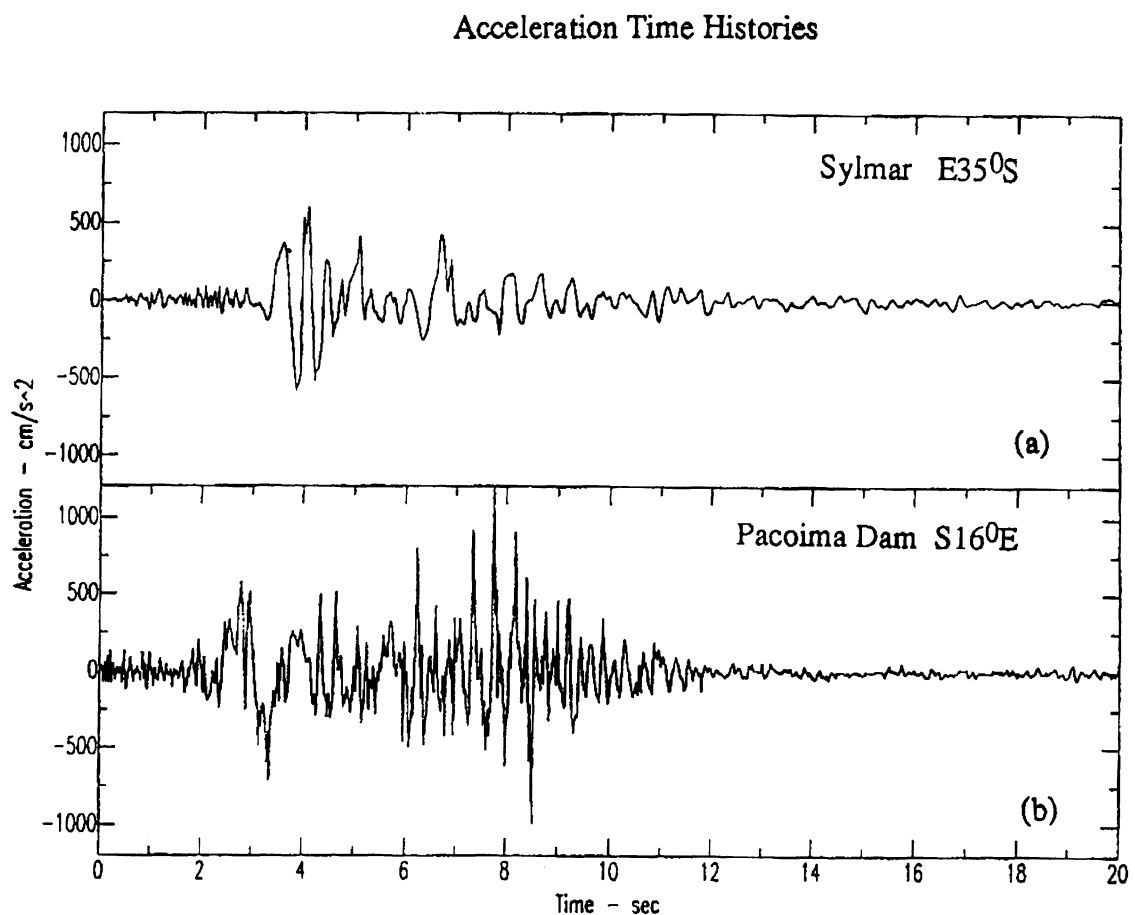


Figure 1-35. Acceleration ground motion recorded at Sylmar, California in the 1994 Northridge earthquake (a). Acceleration ground motion recorded at Pacoima Dam in the 1971 San Fernando earthquake (b).

fault surface, as well as maintain the specified overall moment for the larger earthquake. This superposition can be done in terms of amplitude and phase spectra by available computer programs and the synthetic seismogram calculated at a point on the surface in the vicinity of the original recorded empirical Green's function. Various modifications of the process described above have been explored and a number of test cases have been published.

As can be seen, the prediction of ground motions in this way involves a number of assumptions and extrapolations. A particular value of the method is to permit the exploration of the effect of changing some of the basic parameters on the expected ground motions. A major difficulty is often the lack of knowledge of the appropriate wave attenuation for the

region in question (see Section 1.5). Because of the importance of the application of attenuation factors in calculation of predicted ground motion at arbitrary distances, a great deal of work has been recently done on empirical attenuation forms^(1-26,1-27). The usual form for the peak value at distance x is given by:

$$y = \frac{ae^{bx}}{ce^{dx} + x^2}$$

Where a , b , c , and d are constants and M is the magnitude. Recent empirical fits are given in Reference 1-31.

As an example of the type of attenuation curve that is obtained from actual ground motion recordings, a relation for the peak ground displacements, D , in the 1989 Loma Prieta and 1992 Landers earthquake is given in the following equation.

$$\log D = 1.27 + 0.16 M - \log r + 0.0004 r$$

Where D (cm) is the displacement, M is the moment magnitude, and r (km) is the distance to the nearest point of energy release on the fault.

It is usual that attenuation changes significantly from one geological province to another and local regional studies need to be made to obtain the parameters involved. A discussion is given in the book by Bullen and Bolt⁽¹⁻¹²⁾ and in Reference 1-28.

The Northridge earthquake of California, January 17, 1994 allows an important comparison between the theoretical seismological expectations and actual seismic wave recordings and behavior of earthquake resistant structures. This magnitude 6.8 earthquake struck southern California at 4:31 AM local time on January 17, 1994. The earthquake rebound occurred on a southerly dipping blind-thrust fault (see Section 1.4). The rupture began at a focus about 18 km deep under the Northridge area of the San Fernando Valley. The rupture then propagated along a 45° dipping fault to within about 4 km of the surface under the Santa Susannah Mountains. No major surface fault rupture was observed although the mountainous area sustained extensional surface fracturing at various places and were uplifted by tens of centimeters. The causative fault dipped in the opposite sense to that which caused the neighboring 1971 San Fernando earthquake.

Like the 1971 earthquake, the 1994 shaking tested many types of design such as base isolation and the value of the latest Uniform Building Codes. Notable was, again, the failure of freeway bridges designed before 1971 and the satisfactory seismic resistance of Post-1989 (Loma Prieta earthquake) retrofitted freeway overpasses. The peak accelerations, recorded by many strong motion accelerometers in Los Angeles and the San Fernando Valley area, were systematically larger than average for average curves obtained from previous California earthquakes. It is notable that the

ground motions at the Olive View Hospital (see Figure 1-35) are similar to those obtained at the Pacoima Dam abutment site in the 1971 thrust earthquake⁽¹⁻²⁹⁾.

1.11 CONCLUSIONS

The state of the art in strong motion seismology is now such that prediction of key parameters, such as peak ground acceleration and duration of the significant portion of shaking at a given site, is relatively reliable. Recent earthquakes, such as Chi Chi, Taiwan 1999, have provided many recordings of the strong motion and various site conditions of rock and soil. In addition the great earthquakes of 1985 in Chile and Mexico ($M_s \approx 8$) yielded accelerograms for large- subduction-zone earthquakes. There are still, however, no clear recordings of ground motion in the near-field from earthquakes with $M_s > 7.5$ so that extrapolations to synthetic ground motions in extreme cases of wide engineering interest are not available.

To meet this need and others of engineering importance, more strong motion instruments are being placed in highly seismic areas of the world. Of special interest is the recent operation of clusters of digital instruments in urban areas. These allow the intensity of seismic waves involved in strong motion shaking in the near-field to be rapidly computed and distributed on the world wide web (see <http://www.trinet.org>).

Of special importance is the instrumentation of large structures (such as large dams and long bridges). But structural analysis requires realistic predictions of free field surface motions at all interface points on the supporting foundation under design earthquake conditions. In the past, engineers have normally carried out seismic analyses under the incorrect assumption that the motions of all support points are fully correlated, i.e. "rigid foundation" inputs are assumed⁽¹⁻³⁰⁾.

As recent strong motion data have come to hand, these observations allow the study of the effects of magnitude, epicentral distance, focal depth, etc. on such characteristics⁽¹⁻³¹⁾.

The seismological problems dealt with in this chapter will no doubt be much extended in subsequent years. First, greater sampling of strong-ground motions at all distances from fault sources of various mechanisms and magnitudes will inevitably become available. An excellent example is the wide recording of the 1999 Chi-Chi, Taiwan, earthquake⁽¹⁻³²⁾. Secondly, more realistic three dimensional numerical models will solve the problem of the sequential development of the wave mixtures as the waves pass through different geological structures. Two difficulties may persist: the lack of knowledge of the roughness distribution along the dislocated fault and, in many places, quantitative knowledge of the soil, alluvium, and crustal rock variations in the region.

REFERENCES

- 1-1 Bolt, B.A., *Earthquakes*, W.H. Freeman and Company, New York, 4th edition 1999.
- 1-2 Udias, A., 1999, *Principles of Seismology*, Cambridge University Press, Cambridge.
- 1-3 Fowler, C.M.R., *The Solid Earth*, C.V.P., Cambridge, England, 1990.
- 1-4 Yeats, R.S., Sieh, K. and Allan, C.R., 1997, *The Geology of Earthquakes*, Oxford University Press, Oxford.
- 1-5 Richter, C.F., 1958, *Elementary Seismology*, W.H. Freeman and Co., San Francisco, California.
- 1-6 Lomax, A. and Bolt, B.A., 1992, broadband waveform modelling of anomalous strong ground motion in the 1989 Loma Prieta earthquake using three-dimensional geological structures, *Geophys. Res. Letters*, 19: 1963-1966.
- 1-7 Reiter, L., 1990, *Earthquake Hazard Analysis—Issues and Insights*, Columbia University Press, New York. 254pp.
- 1-8 Gutenberg, B., and Richter, C.F., "Seismicity of the Earth and Associated Phenomena," Princeton University Press, Princeton, 1954.
- 1-9 Real, C.R., and Teng, T., "Local Richter Magnitude and Total Signal Duration in Southern California," *Bull. Seism. Soc. Am.*, Vol. 63, No. 5, October, 1973.
- 1-10 Kanamori, H., "The Energy Release in Great Earthquakes," *Jour. Geo. Res.*, 82, 20, 1977.
- 1-11 Reid, H.F., "The Elastic Respond Theory of Earthquakes," *Bull. Dept. Geol. Univ. Calif.*, 6, pp 413-444, 1911.
- 1-12 Bullen, K.E. and Bolt, B.A., *An introduction to the Theory of Seismology*, Cambridge University Press, 1985..
- 1-13 Das, S., and Aki, K., "Fault Plane with Barriers: A Versatile Earthquake Model," *J. Geophys. Res.* 82, 5658-5670, 1977.
- 1-14 Joyner, W.B. and D.M. Boore, 1988, Measurement, characterization, and prediction of strong ground motion, in Von Thun, J.L. Ed., Proceedings, Conf. On Earthq. Engrg. And soil Dynamics II, Recent Advances in Ground-Motion Evaluation, ASCE Geotechnical Special Publication No. 20. pp. 43-102.
- 1-15 Benioff, H., "Mechanism and Strain Characteristics of the White Wolf Fault as Indicated by the Aftershock Sequence, California Division of Mines and Geology, Bulletin 171, 199-202, 1955.
- 1-16 Bolt, B.A. (ed), *Seismic Strong Motion Synthetics*, Academic Press, 1987.
- 1-17 Scholtz, C.H., 1990, *The Mechanics of Earthquakes and Faulting*, Cambridge University Press, Cambridge.
- 1-18 O'Connell, D.R., 1999, Replication of apparent nonlinear seismic response with linear wave propagation model, *Science*, 293: 2045-2050.
- 1-19 Bolt, B.A., 1996, From earthquake acceleration to seismic displacement, Firth Mallet-Milne Lecture, *SECED*, London, 50 pp.
- 1-20 Rikitake, T., 1990, *Earthquake Prediction*, Amsterdam Elsevier.
- 1-21 Frankel, A.D., 1999, How does the ground shake?, *Science*, 283: 2032-2033.
- 1-22 Zeng, Y., Anderson J.G., and Yu, G., 1994, A composite source model for computing realistic synthetic strong ground motions, *Geophys. Res.*, 21, pg 725.
- 1-23 Wald, D.J. Helmberger, D.V., and Heaton, T.H., 1991, Rupture model of the 1989 Loma Prieta earthquake from the inversion of strong-motion and broadband teleseismic data, *Bull.Seism. Soc. Am.*, 81: 1540-1572.
- 1-24 Ambraseys, N.N., Simpson, K.A., and Bommer, J.J., 1996, Prediction of horizontal response spectra in Europe, *Earthq. Engrg. Struc. Dyn.*, 25: 371-400
- 1-25 Abrahamson, N.A., and Silver, W., 1997, Wmpirical reponse spectral attenuation relations for shallow crustal earthquakes, *Seism. Res. Letters*, 68: 94-127.
- 1-26 Vidale, J. and Helmberger, D.V., 1987, Path effects in strong ground motion seismology, In: *Seismic Strong Motion Synthetics*, B.A. Bolt, ed., Academic Press, New York.
- 1-27 Boore, D.M., Joyner, W., and Fumal, T., 1997, Equations for estimating horizontal response spectra and peak accelerations form western North American earthquakes: A summary of recent work, *Seism. Res. Letters*, 68: 128-153.

- 1-28 Boore, D.J. and Joyner, W., 1997, Site amplifications for generic rock sites, *Bull. Seism. Soc. Am.*, 87: 327-341.
- 1-29 Somerville, P.G., Smith, N.F. Graves, R.W., and Abrahamson, N.A., 1997, Modification of empirical strong ground motion attenuation relations to include the amplitude and duration effects of rupture directivity, *Seism. Res. Letters*, 68(1).
- 1-30 Bolt, B.A., Tsan, Y.B., Yeh, Y.T., and Hsu, M.K., 1982, Earthquake strong motions recorded by a large near-source array of digital seismographs, *Earthq. Engng Struc. Dyn.*, 10: 561-573
- 1-31 Abrahamson, N.A. and Shedlock, J.M., 1997, Overview, *Seism. Res. Letters*, 68: 9-23.
- 1-32 Shin, T.C., Kuo, K.W., Lee, W.H.K., Teng., T.L., and Tsai, Y.B., 2000, "A Preliminary Report on the 1999 Chi-Chi (Taiwan) Earthquake," *Seism. Res. Letters*, 71:23-2

Chapter 2

Earthquake Ground Motion and Response Spectra

Bijan Mohraz, Ph.D., P.E.
Southern Methodist University, Dallas, Texas

Fahim Sadek, Ph.D.
Mechanical Engineering Department, Southern Methodist University, Dallas, Texas. On assignment at the National Institute of Standards and Technology, Gaithersburg, Maryland

Key words: Earthquake Engineering, Earthquake Ground Motion, Earthquake Energy, Ground Motion Characteristics, Peak Ground Motion, Power Spectral Density, Response Modification Factors, Response Spectrum, Seismic Maps, Strong Motion Duration.

Abstract: This chapter surveys the state-of-the-art work in strong motion seismology and ground motion characterization. Methods of ground motion recording and correction are first presented, followed by a discussion of ground motion characteristics including peak ground motion, duration of strong motion, and frequency content. Factors that influence earthquake ground motion such as source distance, site geology, earthquake magnitude, source characteristics, and directivity are examined. The chapter presents probabilistic methods for evaluating seismic risk at a site and development of seismic maps used in codes and provisions. Earthquake response spectra and factors that influence their characteristics such as soil condition, magnitude, distance, and source characteristics are also presented and discussed. Earthquake design spectra proposed by several investigators and those recommended by various codes and provisions through the years to compute seismic base shears are described. The latter part of the chapter discusses inelastic earthquake spectra and response modification factors used in seismic codes to reduce the elastic design forces and account for energy absorbing capacity of structures due to inelastic action. Earthquake energy content and energy spectra are also briefly introduced. Finally, the chapter presents a brief discussion of artificially generated ground motion.

2.1 INTRODUCTION

Ground vibrations during an earthquake can severely damage structures and equipment housed in them. The ground acceleration, velocity, and displacement (referred to as ground motion) when transmitted through a structure, are in most cases amplified. This amplified motion can produce forces and displacements, which may exceed those the structure can sustain. Many factors influence ground motion and its amplification; therefore, an understanding of how these factors influence the response of structures and equipment is essential for a safe and economical design.

Earthquake ground motion is usually measured by strong motion instruments, which record the acceleration of the ground. The recorded accelerograms, after they are corrected for instrument errors and baseline (see next section), are integrated to obtain the velocity and displacement time-histories. The maximum values of ground motion (peak ground acceleration, peak ground velocity, and peak ground displacement) are of particular interest in seismic analysis and design. These parameters, however, do not by themselves describe the intensity of shaking that structures or equipment experience. Other factors, such as earthquake magnitude, distance from the fault or epicenter, duration of strong shaking, soil condition of the site, and the frequency content of the motion also influence the response of a structure. Some of these effects such as the amplitude of the motion, frequency content, and local soil conditions are best represented through a response spectrum^(2-1 to 2-4) which describes the maximum response of a damped single-degree-of-freedom (SDOF) oscillator with various frequencies or periods to ground motion. The response spectra from a number of records are often averaged and smoothed to obtain design spectra which specify the seismic design forces and displacements at a given frequency or period.

This chapter presents earthquake ground motion and response spectra, and the influence of earthquake parameters such as magnitude, duration of strong motion, soil condition, source distance, source characteristics, and directivity on ground motion and response spectra. The evaluation of seismic risk at a given site and development of seismic maps are also discussed. Earthquake design spectra proposed by several investigators and those recommended by various agencies and organizations are presented. The latter part of the chapter includes the inelastic earthquake spectra and response modification factors (R -factors) that several seismic codes and provisions recommend to account for the energy absorbing capacity of structures due to inelastic action. Earthquake energy content and energy spectra are also presented. Finally, the chapter presents a brief discussion of artificially generated ground motion.

2.2 RECORDED GROUND MOTION

Ground motion during an earthquake is measured by strong motion instruments, which record the acceleration of the ground. Three orthogonal components of ground acceleration, two in the horizontal direction and one in the vertical, are recorded by the instrument. The instruments may be located on free-field or mounted in structures. Typical strong motion accelerograms recorded on free-field and the ground floor of the Imperial County Services Building during the Imperial Valley earthquake of October 15, 1979⁽²⁻⁵⁾ are shown in Figure 2-1.

Analog accelerographs, which record ground accelerations on photographic paper or film, were used in the past. The records were then digitized manually, but later the process was automated. These instruments were triggered by the motion itself and some part of the initial motion was therefore lost, resulting in permanent displacements at the end of the record. Today, digital recording instruments

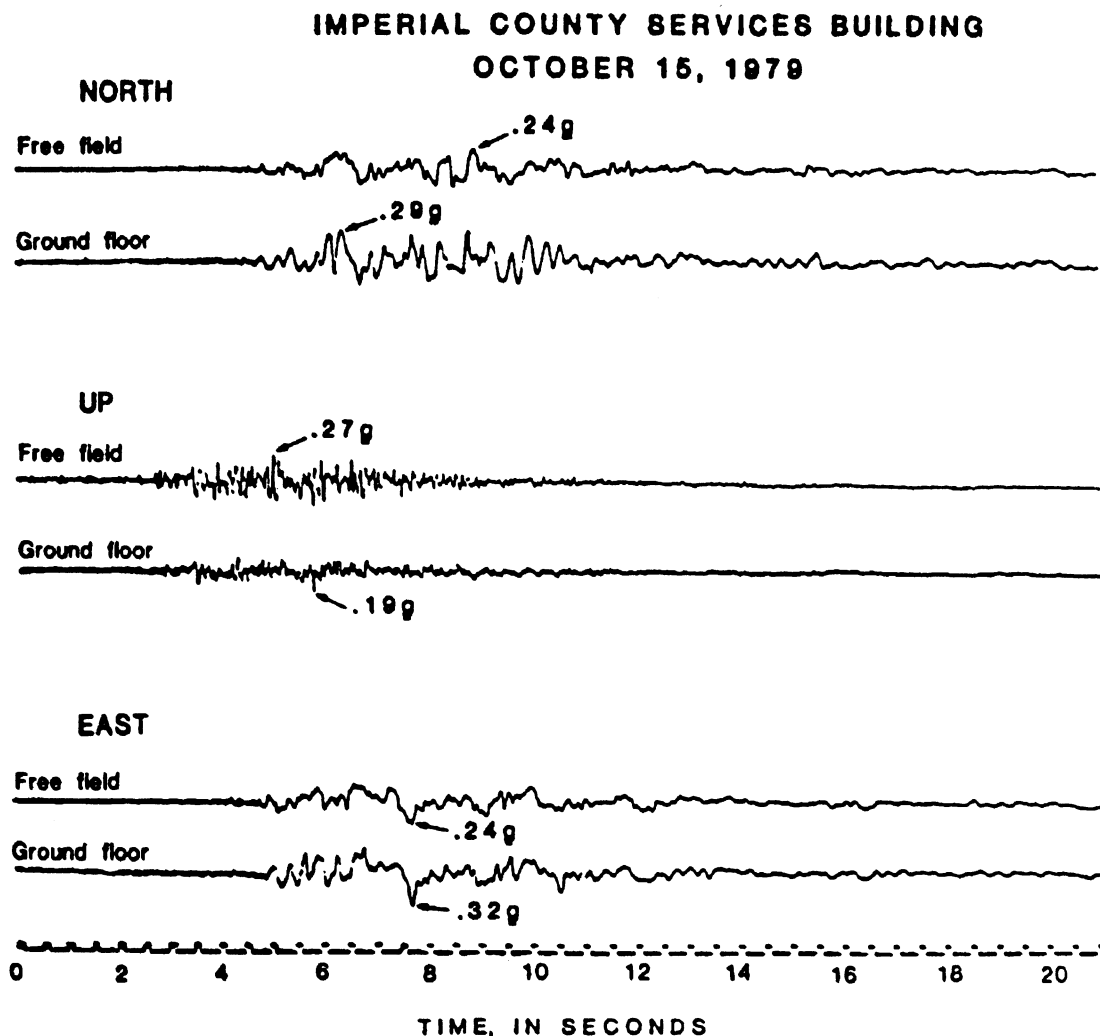


Figure 2-1. Strong motion accelerograms recorded on free field and ground floor of the Imperial County Service Building during the Imperial Valley earthquake of October 15, 1979. [After Rojahn and Mork (2-5).]

using force-balance accelerometers are finding wider application because these instruments produce the transducer output in a digital form that can be automatically disseminated via dial up modems or Internet lines. In addition to having low noise and greater ease in data processing, digital instruments eliminate the delays in recording the motion and the loss of accuracy due to digitizing traces on paper or film. They also permit recovery of the initial portion of the signal.

Accelerations recorded on accelerographs are usually corrected to remove the errors

associated with digitization (transverse play of the recording paper or film, warping of the paper, enlargement of the trace, etc.) and to establish the zero acceleration line before the velocity and displacement are computed. Small errors in establishing the zero acceleration baseline can result in appreciable errors in the computed velocity and displacement. To minimize the errors, a correction is applied by assuming linear zero acceleration and velocity baselines and then using a least square fit to determine the parameters of the lines. For a detailed description of the procedure used in

digitizing and correcting accelerograms, one should refer to Trifunac⁽²⁻⁶⁾, Hudson et al.⁽²⁻⁷⁾, and Hudson⁽²⁻⁸⁾. Another procedure which assumes a second degree polynomial for the zero acceleration baseline has also been used in the past⁽²⁻⁹⁾. The Trifunac-Hudson procedure, however, is more automated and has been used extensively to correct accelerograms. The corrected accelerograms are then integrated to obtain the velocity and displacement time-histories.

For accelerograms obtained from digital recording instruments, the initial motion is preserved, thereby simplifying the task of determining the permanent displacement. Iwan et al.⁽²⁻¹⁰⁾ proposed a method for processing digitally recorded data by computing the average ordinates of the acceleration and velocity over the final segment of the record and setting them equal to zero. A constant acceleration correction is applied to the strong shaking portion of the record which may be defined as the time segment between the first and last occurrence of accelerations of approximately 50 cm/sec². A different constant acceleration correction is applied to the remaining final segment.

In the United States, the digitization, correction, and processing of accelerograms have been carried out by the Earthquake Engineering Research Laboratory of the California Institute of Technology in the past and currently by the United States Geological Survey (USGS) and other organizations such as the California Strong Motion Instrumentation Program (CSMIP) of the California Division of Mines and Geology (CDMG). A typical corrected accelerogram and the integrated velocity and displacement for the S00E component of El Centro, the Imperial Valley earthquake of May 18, 1940 are shown in Figure 2-2.

2.3 CHARACTERISTICS OF EARTHQUAKE GROUND MOTION

The characteristics of ground motion that are important in earthquake engineering applications are:

1. Peak ground motion (peak ground acceleration, peak ground velocity, and peak ground displacement),
2. duration of strong motion, and
3. frequency content.

Each of these parameters influences the response of a structure. Peak ground motion primarily influences the vibration amplitudes. Duration of strong motion has a pronounced effect on the severity of shaking. A ground motion with a moderate peak acceleration and a long duration may cause more damage than a ground motion with a larger acceleration and a shorter duration. Frequency content strongly affects the response characteristics of a structure. In a structure, ground motion is amplified the most when the frequency content of the motion and the natural frequencies of the structure are close to each other. Each of these characteristics are briefly discussed below:

2.3.1 Peak ground motion

Table 2-1 gives the peak ground acceleration, velocity, displacement, earthquake magnitude, epicentral distance, and site description for typical records from a number of seismic events from the western United States. Some of these records are frequently used in earthquake engineering applications. Peak ground acceleration had been widely used to scale earthquake design spectra and acceleration time histories. Later studies recommended that in addition to peak ground acceleration, peak ground velocity and displacement should also be used for scaling purposes. Relationships between ground motion parameters are discussed in Section 2.6.

Table 2-1. Peak Ground Motion, Earthquake Magnitude, Epicentral Distance, and Site Description for Typical Recorded Accelerograms

Earthquake and location	Mag.	Epicentral distance (km)	Comp.	Peak Acc. (g)	Peak Vel. (in/sec)	Peak Disp. (in)	Site Description
Helena, 10/31/1935 Helena, Montana Carroll College	6.0	6.3	S00W S90W Vert	0.146 0.145 0.089	2.89 5.25 3.82	0.56 1.47 1.11	Rock
Imperial Valley, 5/18/1940 El Centro site	6.9	11.5	S00E S90W Vert	0.348 0.214 0.210	13.17 14.54 4.27	4.28 7.79 2.19	Alluvium, several 1000 ft
Western Washington, 4/13/1949 Olympia, Washington Highway Test Lab	7.1	16.9	N04W N86E Vert	0.165 0.280 0.092	8.43 6.73 2.77	3.38 4.09 1.59	Deep cohesionless soil, 420 ft
Northwest California, 10/7/1951 Ferndale City Hall	5.8	56.2	S44W N46W Vert	0.104 0.112 0.027	1.89 2.91 0.87	0.94 1.08 0.64	Deep cohesionless soil, 500 ft
Kern County, 7/21/1952 Taft Lincoln School Tunnel	7.2	41.4	N21E S69E Vert	0.156 0.179 0.105	6.19 6.97 2.63	2.64 3.60 1.98	40 ft of alluvium over poorly cemented sandstone
Eureka, 12/21/1954 Eureka Federal Building	6.5	24.0	N11W N79E Vert	0.168 0.258 0.083	12.44 11.57 3.23	4.89 5.53 1.83	Deep cohesionless soil, 250 ft deep
Eureka, 12/21/1954 Ferndale City Hall	6.5	40.0	N44W N46E Vert	0.159 0.201 0.043	14.04 10.25 2.99	5.58 3.79 1.54	Deep cohesionless soil, 500 ft deep
San Francisco, 3/22/1957 San Francisco Golden Gate Park	5.3	11.5	N10E S80E Vert	0.083 0.105 0.038	1.94 1.82 0.48	0.89 0.33 0.27	Rock
Hollister, 4/8/1961 Hollister City Hall	5.7	22.2	S01W N89W Vert	0.065 0.179 0.050	3.06 6.75 1.85	1.12 1.51 0.85	Unconsolidated alluvium over partly consolidated gravel
Parkfield, 6/27/1966 Cholame Shandon, California Array No. 5	5.6	56.1	N05W N89E Vert	0.355 0.434 0.119	9.12 10.02 2.87	2.09 2.80 1.35	Alluvium
Borrego Mountain, 4/8/1968 El Centro site	6.4	67.3	S00W S90W Vert	0.355 0.434 0.119	9.12 10.02 2.87	2.09 2.80 1.35	Alluvium
San Fernando, 2/9/1971 8244 Orion Blvd., 1 st Floor	6.4	21.1	N00W S90W Vert	0.255 0.134 0.171	11.81 9.42 12.58	5.87 5.45 5.76	Alluvium
San Fernando, 2/9/1971 Castaic Old Ridge Route	6.4	29.5	N21E N69W Vert	0.315 0.271 0.156	6.76 10.95 2.54	1.66 3.74 1.38	Sandstone
San Fernando, 2/9/1971 Pacoima Dam	6.4	7.2	S15W S74W Vert	1.170 1.075 0.709	44.58 22.73 22.96	14.83 4.26 7.61	Highly jointed diorite gneiss
San Fernando, 2/9/1971 Griffith Park Observatory	6.4	32.5	S00W S90W Vert	0.180 0.171 0.123	8.08 5.73 2.92	2.87 2.15 1.33	Granitic
Loma Prieta, 10/17/1989 Corralitos, Eureka Canyon Road	7.0	7.0	90 360 Vert	0.479 0.630 0.439	18.70 21.73 7.33	4.54 3.76 3.06	Landslide deposits
Loma Prieta, 10/17/1989 Santa Cruz – UCSC/LICK Lab	7.0	16.0	90 360 Vert	0.409 0.452 0.331	8.36 8.36 4.71	2.68 2.60 2.65	Limestone
Loma Prieta, 10/17/1989 Sunnyvale – Colton Avenue	7.0	43.0	360 270 Vert	0.219 0.215 0.103	13.16 13.42 2.91	5.45 4.98 1.21	Bay sediments/alluvium
Landers, 6/28/1992 SCE Lucerne Valley Station	7.3	1.8	350 260 Vert	0.800 0.730 0.860	12.91 58.84 16.57	28.32 107.21 17.03	Stiff alluvium overlying hard granitic rock
Northridge, 1/17/1994 Pacoima Dam	6.6	19.3	265 175 Vert	0.434 0.415 0.184	12.05 17.59 6.33	1.97 1.83 1.03	Highly jointed diorite gneiss
Northridge, 1/17/1994 Santa Monica – City Hall Ground	6.6	22.5	90 360 Vert	0.883 0.370 0.232	16.44 9.81 5.52	5.64 2.57 1.49	Alluvium
Northridge, 1/17/1994 Sylmar – County Hospital Parking Lot	6.6	15.8	90 360 Vert	0.604 0.843 0.535	30.29 50.74 7.34	5.99 12.81 2.97	Alluvium

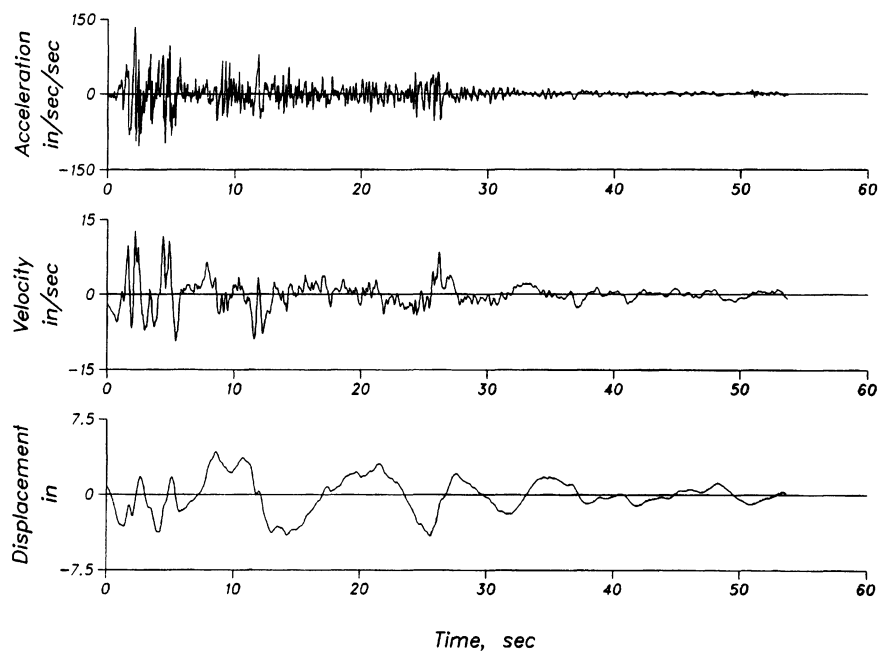


Figure 2-2. Corrected accelerogram and integrated velocity and displacement time-histories for the S00E component of El Centro, the Imperial Valley Earthquake of May 18, 1940.

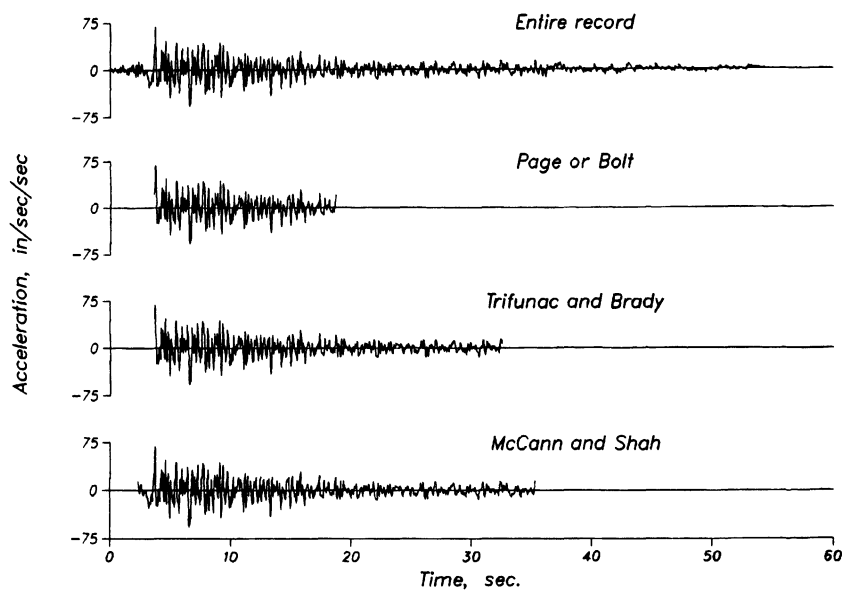


Figure 2-3. Comparison of strong motion duration for the S69E component of the Taft, California earthquake of July 21, 1982 using different procedures.

2.3.2 Duration of strong motion

Several investigators have proposed procedures for computing the strong motion duration of an accelerogram. Page et al. ⁽²⁻¹¹⁾ and Bolt ⁽²⁻¹²⁾ proposed the “bracketed duration” which is the time interval between the first and the last acceleration peaks greater than a specified value (usually 0.05g). Trifunac and Brady ⁽²⁻¹³⁾¹ defined the duration of the strong motion as the time interval in which a significant contribution to the integral of the square of acceleration ($\int a^2 dt$) referred to as the accelerogram intensity takes place. They selected the time interval between the 5% and the 95% contributions as the duration of strong motion. A third procedure suggested by McCann and Shah ⁽²⁻¹⁵⁾ is based on the average energy arrival rate. The duration is obtained by examining the cumulative root mean square acceleration (*rms*)² of the accelerogram. A search is performed on the rate of change of the cumulative *rms* to determine the two cut-off times. The final cut-off time T_2 is obtained when the rate of change of the cumulative *rms* acceleration becomes negative and remains so for the remainder of the record. The initial time T_1 is obtained in the same manner except that the search is performed starting from the “tail-end” of the record.

Figure 2-3 shows a comparison among the strong motion durations extracted from a typical record using different procedures. Table 2-2 gives the initial time T_1 , the final Time T_2 , the duration of strong motion ΔT , the *rms* acceleration, and the percent contribution to ($\int a^2 dt$) for several records. The comparisons show that these procedures result in different durations of strong motion. This is to be expected since the procedures are based on different criteria. It should be noted that since there is no standard definition of strong motion duration, the selection of a procedure for computing the duration for a certain study

depends on the purpose of the intended application. For example, it seems reasonable to use McCann and Shah’s definition, which is based on *rms* acceleration when studying the stationary characteristics of earthquake records and in computing power spectral density. On the other hand, the bracketed duration proposed by Page et al. ⁽²⁻¹¹⁾ and Bolt ⁽²⁻¹²⁾ may be more appropriate for computing elastic and inelastic response and assessing damage to structures.

Based on the work of Trifunac and Brady ⁽²⁻¹³⁾, Trifunac and Westermo ⁽²⁻¹⁶⁾ developed a frequency dependent definition of duration where the duration is considered separately in several narrow frequency bands. They define the duration as the sum of time intervals during which the integral ($\int f^2(t)dt$ -- where $f(t)$ is the ground acceleration, velocity, or displacement -- has the steepest slope and gains a significant portion (90%) of its final value. This definition considers the duration being composed of several separate segments with locations specified by the slopes of the integral. The procedure is to band-pass filter the signal $f(t)$ using two Ormsby filters in different frequency bands with specified central frequencies. The duration for each frequency band is computed as the sum of several time intervals where the smoothed integration function ($\int f^2(t)dt$) has the steepest slope. The study by Trifunac and Westermo ⁽²⁻¹⁶⁾ indicated that the duration of strong motion increases with the period of motion.

2.3.3 Frequency content

The frequency content of ground motion can be examined by transforming the motion from a time domain to a frequency domain through a Fourier transform. The Fourier amplitude spectrum and power spectral density, which are based on this transformation, may be used to characterize the frequency content. They are briefly discussed below:

¹ An earlier study by Husid et al. (2-14) used a similar definition for the duration of strong motion.

² See Section 2.3.3 for definition of *rms*

Table 2-2. Comparison of Strong Motion Duration for Eight Earthquake Records

Record	Comp.	Method*	T ₁ (sec)	T ₂ (sec)	ΔT (sec)	RMS (cm/sec ²)	∫a ² dt
El Centro, 1940	S00E	A	0.00	53.74	53.74	46.01	100
		B	0.88	26.74	25.86	65.16	97
		C	1.68	26.10	24.42	64.75	90
		D	0.88	26.32	25.44	65.60	96
	S90W	A	0.00	53.46	53.46	38.85	100
		B	1.24	26.64	25.40	54.88	95
		C	1.66	26.20	24.54	54.39	90
		D	0.80	26.62	25.82	24.73	96
Taft, 1952	N21E	A	0.00	54.34	54.34	25.03	100
		B	3.44	22.94	19.50	38.50	85
		C	3.70	34.24	30.54	31.70	90
		D	2.14	36.46	34.32	30.85	96
	S69E	A	0.00	54.38	54.38	26.10	100
		B	3.60	18.72	15.12	44.61	82
		C	3.66	32.52	28.86	33.96	90
		D	2.34	35.30	32.96	32.71	95
El Centro, 1934	S00W	A	0.00	90.28	90.28	19.48	100
		B	1.92	14.78	12.86	46.89	83
		C	2.82	23.92	21.10	38.27	90
		D	1.92	23.88	21.96	38.38	94
	S90W	A	0.00	90.22	90.22	20.76	100
		B	1.98	20.10	18.12	44.58	93
		C	2.86	23.14	20.28	41.57	90
		D	1.62	20.10	18.48	44.26	93
Olympia, 1949	N04W	A	0.00	89.06	89.06	22.98	100
		B	0.74	22.30	22.30	44.25	93
		C	1.78	25.80	25.80	40.51	90
		D	0.08	22.94	22.94	43.73	93
	N86E	A	0.00	89.02	89.02	28.10	100
		B	1.00	21.04	21.04	56.00	94
		C	4.34	18.08	18.08	59.22	90
		D	0.28	21.52	21.52	55.48	94

* A: Entire Record
 B: Page or Bolt (2-11 or 2-12)
 C: Trifunac and Brady (2-13)
 D: McCann and Shah (2-15)

Fourier amplitude spectrum. The finite Fourier transform $F(\omega)$ of an accelerogram $a(t)$ is obtained as

Where T is the duration of the accelerogram. The Fourier amplitude spectrum $FS(\omega)$ is defined as the square root of the sum of the squares of the real and imaginary parts of $F(\omega)$. Thus,

$$F(\omega) = \int_0^T a(t)e^{-i\omega t} dt, i = \sqrt{-1} \quad (2-1)$$

$$FS(\omega) = \sqrt{\left[\int_0^T a(t) \sin \omega t dt \right]^2 + \left[\int_0^T a(t) \cos \omega t dt \right]^2} \quad (2-2)$$

Since $a(t)$ has units of acceleration, $FS(\omega)$ has units of velocity. The Fourier amplitude spectrum is of interest to seismologists in characterizing ground motion. Figure 2-4 shows a typical Fourier amplitude spectrum for the S00E component of El Centro, the Imperial Valley earthquake of May 18, 1940. The figure indicates that most of the energy in the accelerogram is in the frequency range of 0.1 to 10 Hz, and that the largest amplitude is at a frequency of approximately 1.5 Hz.

It can be shown that subjecting an undamped single-degree-of-freedom (SDOF) system to a base acceleration $a(t)$, the velocity response of the system and the Fourier amplitude spectrum of the acceleration are

closely related. The equation of motion of the system can be written as

$$\ddot{x} + \omega_n^2 x = -a(t) \quad (2-3)$$

In which x and \dot{x} are the relative displacement and acceleration, and ω_n is the natural frequency of the system. Using Duhamel's integral, the steady-state response can be obtained as

$$x(t) = \frac{1}{\omega_n} \int_0^t -a(\tau) \sin \omega_n(t-\tau) d\tau \quad (2-4)$$

The relative velocity $\dot{x}(t)$ follows directly from Equation 2-4 as

$$\dot{x}(t) = \int_0^t -a(\tau) \cos \omega_n(t-\tau) d\tau \quad (2-5)$$

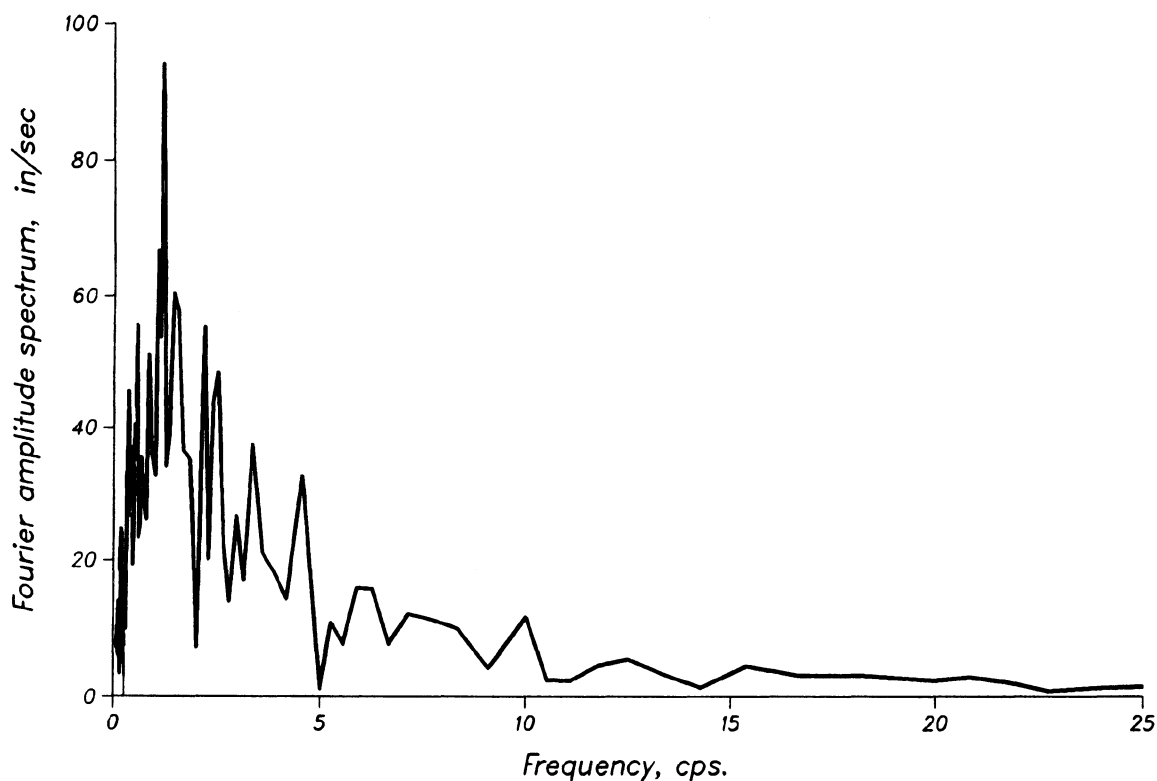


Figure 2-4. Fourier amplitude spectrum for the S00E component of El Centro, the Imperial Valley earthquake of May 18, 1940.

Equation 2-5 can be expanded as

$$\dot{x}(t) = -\left[\int_0^t a(\tau) \cos \omega_n \tau d\tau \right] \cos \omega_n t - \left[\int_0^t a(\tau) \sin \omega_n \tau d\tau \right] \sin \omega_n t \quad (2-6)$$

Denoting the maximum relative velocity (spectral velocity) of a system with frequency ω by $SV(\omega)$ and assuming that it occurs at time t_v , one can write

$$SV(\omega) = \sqrt{\left[\int_0^{t_v} a(\tau) \sin \omega \tau d\tau \right]^2 + \left[\int_0^{t_v} a(\tau) \cos \omega \tau d\tau \right]^2} \quad (2-7)$$

The pseudo-velocity $PSV(\omega)$ defined as the product of the natural frequency ω and the maximum relative displacement or the spectral displacement $SD(\omega)$ is close to the maximum relative velocity (see Section 2.7). If $SD(\omega)$

occurs at t_d then

$$PSV(\omega) = \omega SD(\omega) = \sqrt{\left[\int_0^{t_d} a(\tau) \sin \omega \tau d\tau \right]^2 + \left[\int_0^{t_d} a(\tau) \cos \omega \tau d\tau \right]^2} \quad (2-8)$$

Comparison of Equations 2-2 and 2-7 shows that for zero damping, the maximum relative velocity and the Fourier amplitude spectrum are equal when $t_v=T$. A similar comparison between Equations 2-2 and 2-8 reveals that the pseudo-velocity and the Fourier amplitude spectrum are equal if $t_d=T$. Figure 2-5 shows a comparison between $FS(\omega)$ and $SV(\omega)$ for zero damping for the S00E component of El Centro, the Imperial Valley earthquake of May 18, 1940. The figure indicates the close relationship between the two functions. It should be noted that, in general, the ordinates of the Fourier amplitude spectrum are less than those of the undamped pseudo-velocity spectrum.

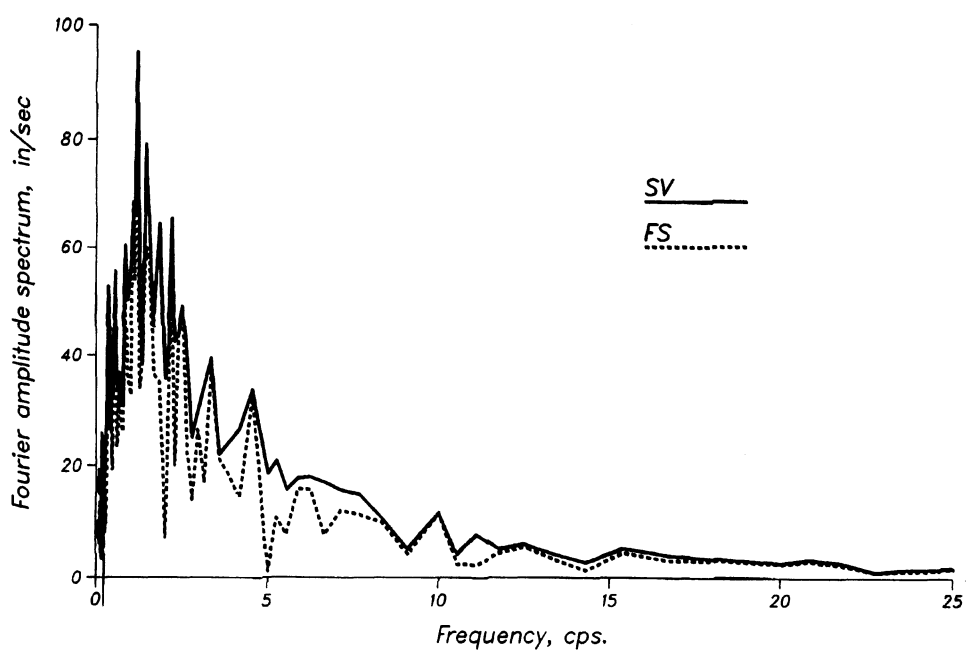


Figure 2-5. Comparison of Fourier amplitude spectrum and velocity spectrum for an undamped single-degree-of-freedom system for the S00E component of El Centro, the Imperial Valley earthquake of May 18, 1940.

Power spectral density. The inverse Fourier transform of $F(\omega)$ is

$$a(t) = \frac{1}{\pi} \int_0^{\omega_0} F(\omega) e^{i\omega t} d\omega \quad (2-9)$$

where ω_0 is the maximum frequency detected in the data (referred to as Nyquist frequency). Equations 2-1 and 2-9 are called Fourier transform pairs. As mentioned previously, the intensity of an accelerogram is defined as

$$I = \int_0^T a^2(t) dt \quad (2-10)$$

Based on Parseval's theorem, the intensity I can also be expressed in the frequency domain as

$$I = \frac{1}{\pi} \int_0^{\omega_0} |F(\omega)|^2 d\omega \quad (2-11)$$

The intensity per unit of time or the temporal mean square acceleration ψ^2 can be obtained by dividing Equation 2-10 or 2-11 by the duration T . Therefore,

$$\begin{aligned} \psi^2 &= \\ \frac{1}{T} \int_0^T a^2(t) dt &= \frac{1}{\pi T} \int_0^{\omega_0} |F(\omega)|^2 d\omega \end{aligned} \quad (2-12)$$

The temporal power spectral density is defined as

$$G(\omega) = \frac{1}{\pi T} |F(\omega)|^2 \quad (2-13)$$

Combining Equations 2-12 and 2-13, the mean square acceleration can be obtained as

$$\psi^2 = \int_0^{\omega_0} G(\omega) d\omega \quad (2-14)$$

In practice, a representative power spectral density of ground motion is computed by averaging across the temporal power spectral

densities of an ensemble of N accelerograms (see for example reference 2-17). Therefore,

$$G(\omega) = \frac{1}{N} \sum_{i=1}^N G_i(\omega) \quad (2-15)$$

where $G_i(\omega)$ is the power spectral density of the i th record. The power spectral density is frequently presented as the product of a normalized power spectral density $G^{<n>}(\omega)$ (area = 1.0) and a mean square acceleration as

$$G(\omega) = \psi^2 G^{<n>}(\omega) \quad (2-16)$$

Figure 2-6 shows a typical example of a normalized power spectral density computed for an ensemble of 161 accelerograms recorded on alluvium. Studies^(2-17, 2-18) have shown that strong motion segment of accelerograms constitutes a locally stationary random process and that the power spectral density can be presented as a time-dependent function $G(t, \omega)$ in the form:

$$G(t, \omega) = \psi^2 S(t) G^{<n>}(\omega) \quad (2-17)$$

where $S(t)$ is a slowly varying time-scale factor which accounts for the local variation of the mean square acceleration with time.

Power spectral density is useful not only as a measure of the frequency content of ground motion but also in estimating its statistical properties. Among such properties are the *rms* acceleration ψ , the central frequency ω_c , and the shape factor δ defined as

$$\psi = \sqrt{\lambda_0} \quad (2-18)$$

$$\omega_c = \sqrt{\lambda_2 / \lambda_0} \quad (2-19)$$

$$\delta = \sqrt{1 - (\lambda_1^2 / \lambda_0 \lambda_2)} \quad (2-20)$$

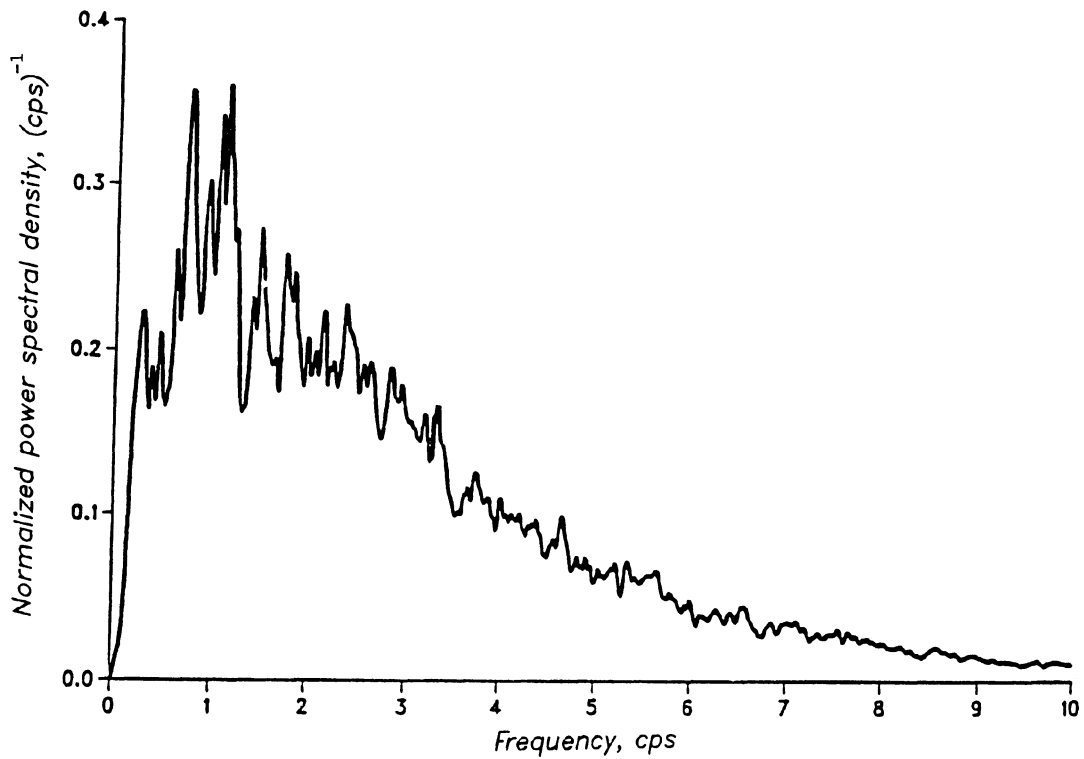


Figure 2-6. Normalized power spectral density of an ensemble of 161 horizontal components of accelerograms recorded on alluvium. [After Elghadamsi et al. (2-18).]

where λ_r is the r -th spectral moment defined as

$$\lambda_r = \int_0^{\omega_0} \omega^r G(\omega) d\omega \quad (2-21)$$

Smooth power spectral density of the ground acceleration has been commonly presented in the form proposed by Kanai (2-19) and Tajimi (2-20) as a filtered white noise ground excitation of spectral density G_0 in the form

$$G(\omega) = \frac{1 + 4\xi_g^2 (\omega / \omega_g)^2}{\left[1 - (\omega / \omega_g)^2\right]^2 + (2\xi_g \omega / \omega_g)^2} G_0 \quad (2-22)$$

The Kanai-Tajimi parameters ξ_g , ω_g , and G_0 represent ground damping, ground frequency, and ground shaking intensity. These parameters are computed by equating the *rms* acceleration, the central frequency, and the shape factor,

Equations 2-18 to 2-20, of the smooth and the raw (unsmooth) power spectral densities (2-18, 2-21). Table 2-3 gives the values of ξ_g , ω_g , and G_0 for the normalized power spectral densities on different soil conditions. Also shown are the central frequency ω_c and the shape factor δ . Using the Kanai-Tajimi parameters in Table 2-3, normalized power spectral densities for horizontal and vertical motion on various soil conditions were computed and are presented in Figures 2-7 and 2-8. The figures indicate that as the site becomes stiffer, the predominant frequency increases and the power spectral densities spread over a wider frequency range. This observation underscores the influence of site conditions on the frequency content of seismic excitations. The figures also show that the power spectral densities for horizontal motion have a sharper peak and span over a narrower frequency region than the corresponding ones for vertical motion.

Table 2-3. Central Frequency, Shape Factor, Ground Frequency, Ground Damping, and Ground Intensity for Different Soil Conditions. [After Elghadamsi et al. (2-18)]

Site Category	No. of Records	Central Frequency f_c (Hz)	Shape Factor δ	Ground Frequency f_g (Hz)	Ground Damping ξ_g	Ground Intensity G_0 (1/Hz)
Horizontal						
Alluvium	161	4.10	0.65	2.92	0.34	0.102
Alluvium on rock	60	4.58	0.59	3.64	0.30	0.078
Rock	26	5.41	0.59	4.30	0.34	0.070
Vertical						
Alluvium	78	6.27	0.63	4.17	0.46	0.080
Alluvium on rock	29	6.68	0.62	4.63	0.46	0.072
Rock	13	7.53	0.55	6.18	0.46	0.053

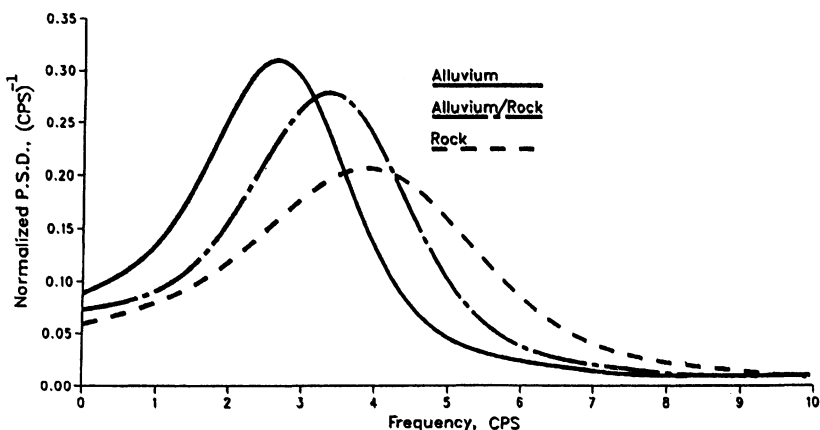


Figure 2-7. Normalized power spectral densities for horizontal motion. [After Elghadamsi et al. (2-18).]

Clough and Penzien⁽²⁻²²⁾ modified the Kanai-Tajimi power spectral density by introducing another filter to account for the numerical difficulties expected in the neighborhood of $\omega=0$. The cause of these difficulties stems from dividing Equation 2-22 by ω^2 and ω^4 , respectively, to obtain the power spectral density functions for ground velocity and displacement. The singularities close to $\omega=0$ can be removed by passing the process through another filter that attenuates the very low frequency components. The modified power spectral density takes the form

$$G(\omega) = \frac{1 + 4\xi_g^2 (\omega/\omega_g)^2}{[1 - (\omega/\omega_g)^2]^2 + (2\xi_g \omega/\omega_g)^2} \times \frac{(\omega/\omega_1)^4}{[1 - (\omega/\omega_1)^2] + 4\xi_1^2 (\omega/\omega_1)^2} (G_0) \quad (2-23)$$

Where ω_1 and ξ_1 are the frequency and damping parameters of the filter.

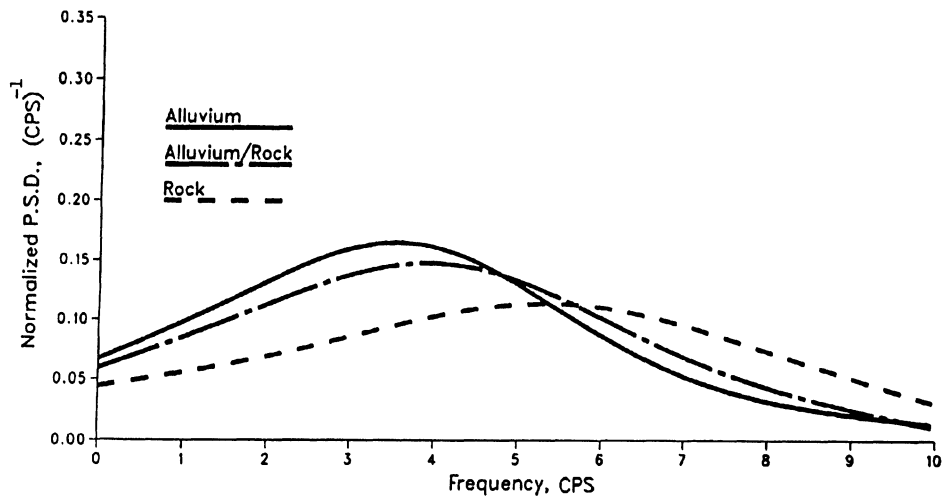


Figure 2-8. Normalized power spectral densities for vertical motion. [After Elghadamsi et al. (2-18).]

Lai⁽²⁻²¹⁾ presented empirical relationships for estimating ground frequency ω_g and central frequency ω_c for a given epicentral distance R in kilometers or local magnitude M_L . These relationships are

$$\omega_g = 27 - 0.09R \quad 10 \leq R \leq 60 \quad (2-24)$$

$$\omega_g = 65 - 7.5M_L \quad 5 \leq M_L \leq 7 \quad (2-25)$$

$$\omega_g = 1.12\omega_c - 5.15 \quad (2-26)$$

Using these relationships and the acceleration attenuation equations (see Section 2.4.1), Lai proposed a procedure for estimating a smooth power spectral density for a given strong motion duration and ground damping.

Once the power spectral density of ground motion at a site is established, random vibration methods may be used to formulate probabilistic procedures for computing the response of structures. In addition, the power spectral density of ground motion may be used for other applications such as generating artificial accelerograms as discussed in Section 2.12.

2.4 FACTORS INFLUENCING GROUND MOTION

Earthquake ground motion is influenced by a number of factors. The most important factors are: 1) earthquake magnitude, 2) distance from the source of energy release (epicentral distance or distance from the causative fault), 3) local soil conditions, 4) variation in geology and propagation velocity along the travel path, and 5) earthquake source conditions and mechanism (fault type, slip rate, stress conditions, stress drop, etc.). Past earthquake records have been used to study some of these influences. While the effect of some of these parameters such as local soil conditions and distance from the source of energy release are fairly well understood and documented, the influence of source mechanism is under investigation and the variation of geology along the travel path is complex and difficult to quantify. It should be noted that several of these influences are interrelated; consequently, it is difficult to discuss them individually without incorporating the others. Some of the influences are discussed below:

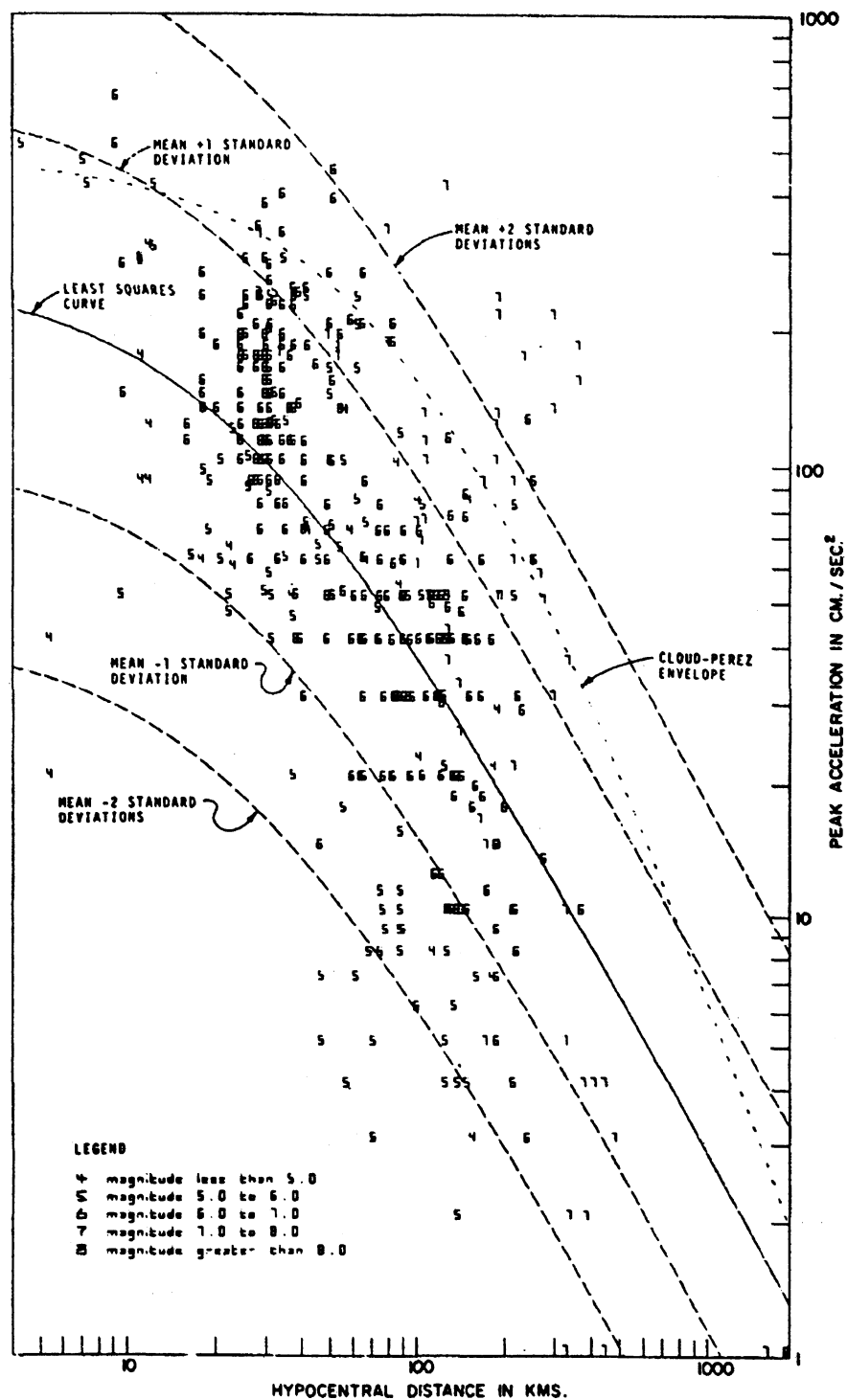


Figure 2-9. Peak ground acceleration plotted as a function of fault distance obtained from worldwide set of 515 strong motion records without normalization of magnitude. [After Donovan (2-23).]

2.4.1 Distance

The variation of ground motion with distance to the source of energy release has been studied by many investigators. In these studies, peak ground motion, usually peak ground acceleration, is plotted as a function of distance. Smooth curves based on a regression analysis are fitted to the data and the curve or its equation is used to predict the expected ground motion as a function of distance. These relationships, referred to as motion attenuation, are sometimes plotted independently of earthquake magnitude. This was the case in the earlier studies because of the lack of sufficient number of earthquake records. With the availability of a large number of records, particularly since the 1971 San Fernando earthquake, the database for attenuation studies increased and a number of investigators re-examined their earlier studies, modified their proposed relationships for estimating peak accelerations, and included earthquake magnitude as a parameter. Donovan⁽²⁻²³⁾ compiled a database of more than 500 recorded accelerations from seismic events in the United States, Japan, and elsewhere and later increased it to more than 650⁽²⁻²⁴⁾. The plot of peak ground acceleration versus fault distance for different earthquake magnitudes from his database is shown in Figure 2-9. Even though there is a considerable scatter in the data, the figure indicates that peak acceleration decreases as the distance from the source of energy release increases. Shown in the figure are the least square fit between acceleration and distance and the curves corresponding to mean plus- and mean minus- one and two standard deviations. Also presented in the figure is the envelope curve (dotted) proposed by Cloud and Perez⁽²⁻²⁵⁾.

Other investigators have also proposed attenuation relationships for peak ground acceleration, which are similar to Figure 2-9. A summary of some of the relationships, compiled by Donovan⁽²⁻²³⁾ and updated by the authors, is shown in Table 2-4. A comparison of various relationships⁽²⁻²⁴⁾ for an earthquake magnitude

of 6.5 with the data from the 1971 San Fernando earthquake is shown in Figure 2-10. This figure is significant because it shows the comparison of various attenuation relationships with data from a single earthquake. While the figure shows the differences in various attenuation relationships, it indicates that they all follow a similar trend.

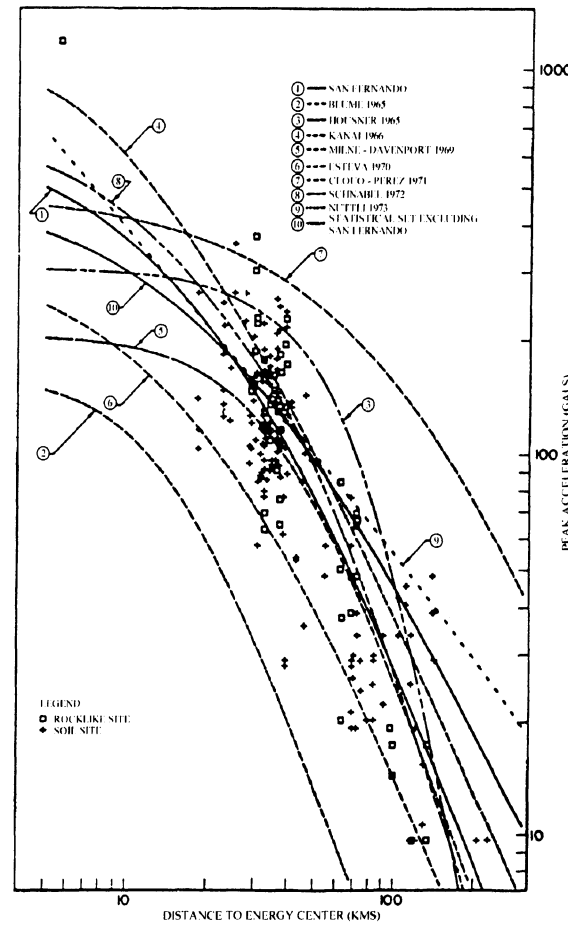


Figure 2-10. Comparison of attenuation relations with data from the San Fernando earthquake of February 9, 1971.
[After Donovan (2-24).]

Housner⁽²⁻³⁸⁾, Donovan⁽²⁻²³⁾, and Seed and Idriss⁽²⁻³⁹⁾ have reported that at farther distances from the fault or the source of energy release (far-field), earthquake magnitude influences the attenuation, whereas at distances close to the fault (near-field), the attenuation is affected by smaller but not larger earthquake magnitudes. This can be observed from the earthquake data in Figure 2-9.

Table 2-4. Typical Attenuation Relationships

Data Source	Relationship*	Reference
1. San Fernando earthquake February 9, 1971	$\log PGA = 190 / R^{1.83}$	Donovan (2-23)
2. California earthquake	$PGA = y_0 / (1 + (R' / h)^2)$ where $y_0 = -(b + 3) + 0.81M - 0.027M^2$ and b is a site factor	Blume (2-26)
3. California and Japanese earthquakes	$PGA = \frac{0.0051}{\sqrt{T_G}} 10^{(0.61M - p \log R + 0.167 - 1.83/R)}$ where $P = 1.66 + 3.60/R$ and T_G is the fundamental period of the site	Kanai (2-27)
4. Cloud (1963)	$PGA = 0.0069e^{1.64M} / (1.1e^{1.1M} + R^2)$	Milne and Davenport (2-28)
5. Cloud (1963)	$PGA = 1.254e^{0.8M} / (R + 25)^2$	Esteva (2-29)
6. U.S.C. and G.S.	$\log PGA = (6.5 - 2 \log(R' + 80)) / 981$	Cloud and Perez (2-25)
7. 303 Instrumental Values	$PGA = 1.325e^{0.67M} / (R + 25)^{1.6}$	Donovan (2-23)
8. Western U.S. records	$PGA = 0.0193e^{0.8M} / (R^2 + 400)$	Donovan (2-23)
9. U.S., Japan	$PGA = 1.35e^{0.58M} / (R + 25)^{1.52}$	Donovan (2-23)
10. Western U.S. records, USSR, and Iran	$\ln PGA = -3.99 + 1.28M - 1.75 \ln[R = 0.147e^{0.732M}]$ - M is the surface wave magnitude for M greater than or equal to 6, or it is the local magnitude for M less than 6.	Campbell (2-30)
11. Western U.S. records and worldwide	$\log PGA = -1.02 + 0.249M - \log \sqrt{R^2 + 7.3^2} - 0.00255\sqrt{R^2 + 7.3^2}$	Joyner and Boore (2-31)
12. Western U.S. records and worldwide	$\log PGA = 0.49 + 0.23(M - 6) - \log \sqrt{R^2 + 8^2} - 0.0027\sqrt{R^2 + 8^2}$	Joyner and Boore (2-32)
13. Western U.S. records	$\ln PGA = \ln \alpha(M) - \beta(M) \ln(R + 20)$ - M is the surface wave magnitude for M greater than or equal to 6, or it is the local magnitude for smaller M . - R is the closest distance to source for M greater than 6 and hypocentral distance for M smaller than 6. - $\alpha(M)$ and $\beta(M)$ are magnitude-dependent coefficients.	Idriss (2-33)
14. Italian records	$\ln PGA = -1.562 + 0.306M - \log \sqrt{R^2 + 5.8^2} + 0.169S$ - S is 1.0 for soft sites or 0.0 for rock.	Sabetta and Pugliese (2-34)
15. Western U.S. and worldwide (soil sites)	For M less than 6.5, $\ln PGA = -2.611 + 1.1M - 1.75 \ln[R + 0.822e^{0.418M}]$ For M greater than or equal to 6.5, $\ln PGA = -2.611 + 1.1M - 1.75 \ln[R + 0.316e^{0.629M}]$	Sadigh et al. (2-35)
16. Western U.S. and worldwide (rock sites)	For M less than 6.5, $\ln PGA = -1.406 + 1.1M - 2.05 \ln[R + 1.353e^{0.406M}]$ For M greater than or equal to 6.5, $\ln PGA = -1.406 + 1.1M - 2.05 \ln[R + 0.579e^{0.537M}]$	Sadigh et al. (2-35)
17. Worldwide earthquakes	$\ln PGA = -3.512 + 0.904M - 1.328 \ln \sqrt{R^2 + [0.149e^{0.647M}]^2} + [1.125 - 0.112 \ln R - 0.0957M]F + [0.440 - 0.171 \ln R]S_{sr} + [0.405 - 0.222 \ln R]S_{hr}$ - $F = 0$ for strike-slip and normal fault earthquakes and 1 for reverse, reverse-oblique, and thrust fault earthquakes. - $S_{sr} = 1$ for soft rock and 0 for hard rock and alluvium - $S_{hr} = 1$ for hard rock and 0 for soft rock and alluvium	Campbell and Bozorgnia (2-36)
18. Western North American earthquakes	$\ln PGA = b + 0.527(M - 6.0) - 0.778 \ln \sqrt{R^2 + (5.570)^2} - 0.371 \ln \frac{V_s}{1396}$ - where $b = -0.313$ for strike-slip earthquakes = -0.117 for reverse-slip earthquakes = -0.242 if mechanism is not specified - V_s is the average shear wave velocity of the soil in (m/sec) over the upper 30 meters - The equation can be used for magnitudes of 5.5 to 7.5 and for distances not greater than 80 km	Boore et al. (2-37)

* Peak ground acceleration PGA in g, source distance R in km, source distance R' in miles, local depth h in miles, and earthquake magnitude M . Refer to the relevant references for exact definitions of source distance and earthquake magnitude.

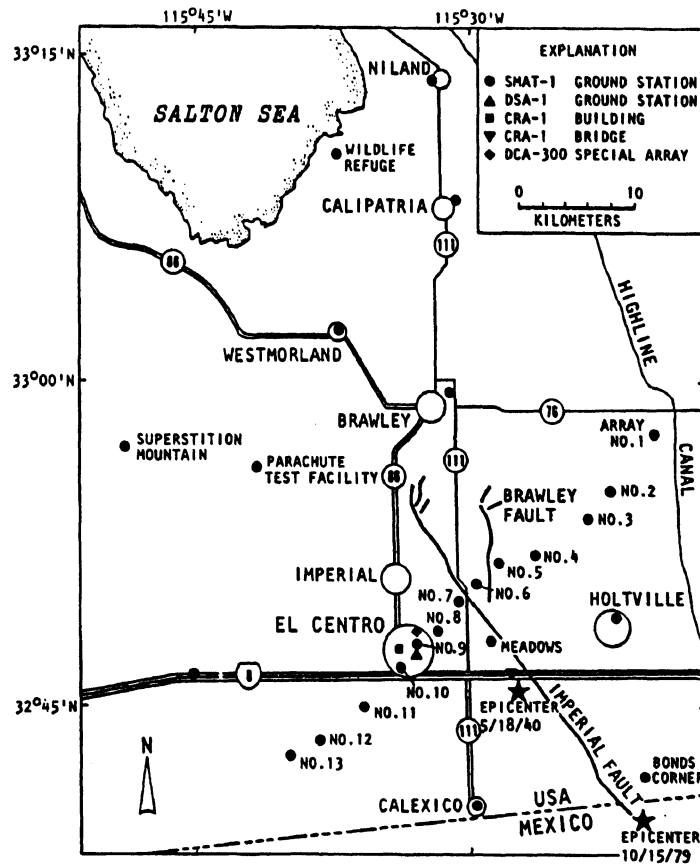


Figure 2-11. Strong motion stations in the Imperial Valley, California. [After Porcella and Matthiesen (2-40); reproduced from (2-39).]

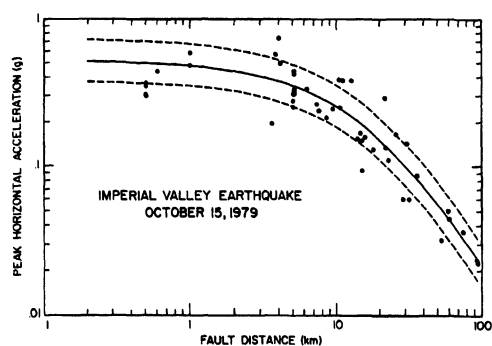


Figure 2-12. Observed and predicted mean horizontal peak accelerations for the Imperial Valley earthquake of October 15, 1979 plotted as a function of distance from the fault. The solid curve represents the median predictions based on the observed values and the dashed curves represent the standard error bounds for the regression. [After Campbell (2-30).]

The majority of attenuation relationships for predicting peak ground motion are presented in terms of earthquake magnitude. Prior to the Imperial Valley earthquake of 1979, the vast majority of available accelerograms were recorded at distances of greater than approximately 10 or 15 km from the source of energy release. An array of accelerometers placed on both sides of the Imperial Fault (2-40) prior to this earthquake (See Figure 2-11) provided excellent acceleration data for small distances from the fault. The attenuation relationship from this array presented by Campbell (2-30) is shown in Figure 2-12. The figure indicates the flat slope of the acceleration attenuation curve for distances close to the source, a phenomenon which is not observed in

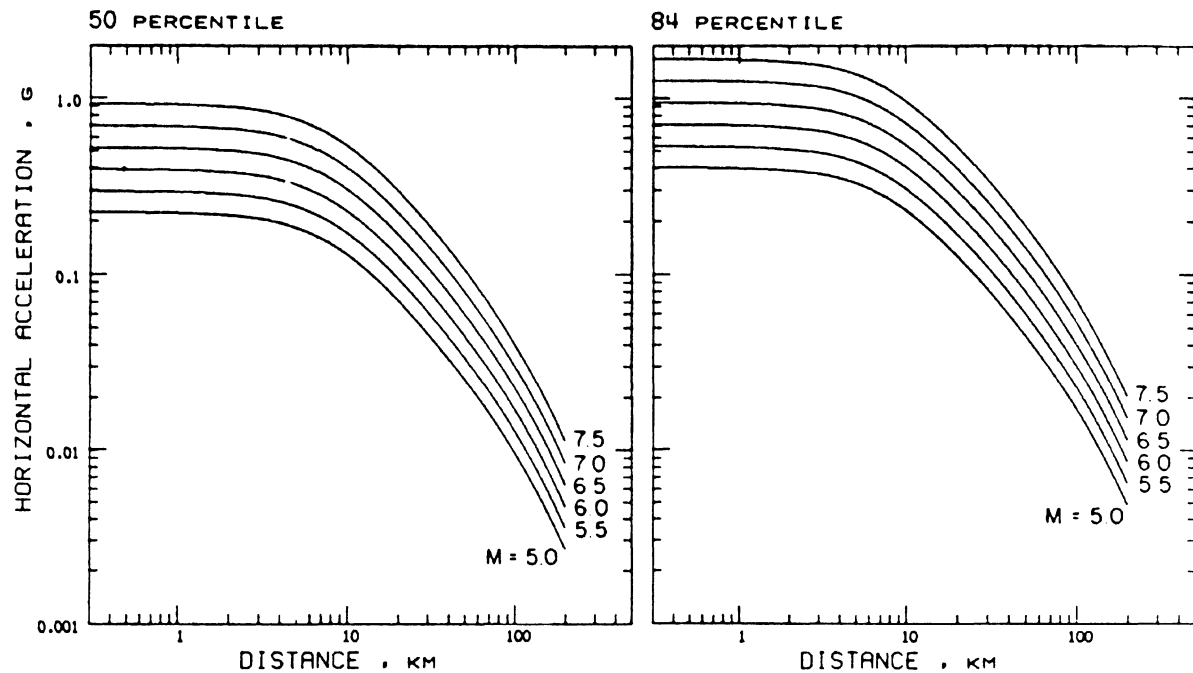


Figure 2-13. Predicted values of peak horizontal acceleration for 50 and 84 percentile as functions of distance and moment magnitude. [After Joyner and Boore (2-31).]

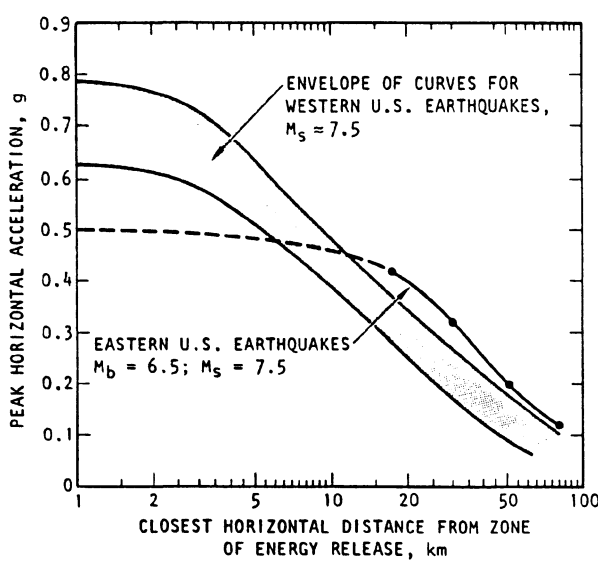


Figure 2-14. Comparison of attenuation curves for the eastern and western U.S. earthquakes. (Reproduced from 2-39.)

the attenuation curves for far-field data. Similar observations can also be made from the attenuation curves (Figure 2-13) proposed by Joyner and Boore ⁽²⁻³¹⁾. The majority of attenuation studies and the relationships presented in Table 2-4 are primarily from the data in the western United States. Several seismologists believe that ground acceleration attenuates more slowly in the eastern United States and eastern Canada, i.e. earthquakes in eastern North America are felt at much greater distances from the epicenter than western earthquakes of similar magnitude. A comparison of the attenuation curves for the western and eastern United States earthquakes recommended by Nuttli and Herrmann ⁽²⁻⁴¹⁾ is shown in Figure 2-14. Another comparison for eastern North America prepared by Milne and Davenport ⁽²⁻²⁸⁾ is presented in Figure 2-15. Both these figures reflect the slower attenuation of earthquake motions in the eastern United States and eastern Canada. According to Donovan ⁽²⁻²³⁾, a similar phenomenon also exists for Japanese earthquakes. Due to the lack of

sufficient earthquake data in the eastern United States and Canada, theoretical models which include earthquake source and wave propagation in the surrounding medium are used to study the effect of distance and other parameters on ground motion. The reader is referred to references^(2-42 to 2-44) for the detailed procedure.

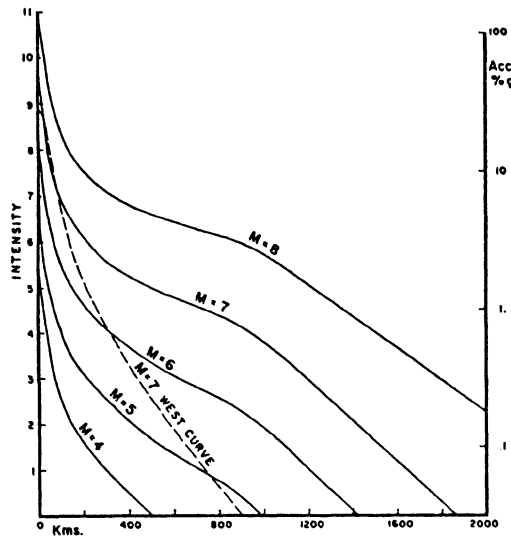


Figure 2-15. Intensity versus distance for eastern and western Canada. [After Milne and Davenport (2-28).]

In addition to source distance and earthquake magnitude, recent attenuation relationships include the effect of source characteristics (fault mechanism) and soil conditions. As an example, Campbell and Bozorgnia⁽²⁻³⁶⁾ used 645 accelerograms from 47 worldwide earthquakes of magnitude 4.7 and greater, recorded between 1957 and 1993, to develop attenuation relationship for peak horizontal ground acceleration. The data was limited to distances of 60 km or less to minimize the influence of regional differences in crustal attenuation and to avoid the complex propagation effects at farther distances observed during the 1989 Loma Prieta and other earthquakes. The peak ground acceleration was estimated using a generalized nonlinear regression analysis and given by

$$\begin{aligned} \ln(PGA) = & -3.512 + 0.904M_w \\ & -1.328 \ln \sqrt{R_s^2 + [0.149 \exp(0.647M_w)]^2} \\ & + [1.125 - 0.112 \ln R_s - 0.0957M_w]F \\ & + [0.440 - 0.171 \ln R_s]S_{sr} \\ & + [0.405 - 0.222 \ln R_s]S_{hr} + \epsilon \end{aligned} \quad (2-27)$$

where PGA is the mean of the two horizontal components of peak ground acceleration (g), M_w is the moment magnitude, R_s ³ is the closest distance to the seismogenic rupture on the fault (km), $F = 0$ for strike-slip and normal fault earthquakes and = 1 for reverse, reverse-oblique, and thrust fault earthquakes, $S_{sr} = 1$ for soft rock and = 0 for hard rock and alluvium, $S_{hr} = 1$ for hard rock and = 0 for soft rock and alluvium, and ϵ is the random error term with a zero mean and a standard deviation equal to $\ln(PGA)$ which is represented by

$$\sigma_{\ln(PGA)} = \begin{cases} 0.55 & PGA < 0.068 \\ 0.173 - 0.140 \ln(PGA) & 0.068 \leq PGA \leq 0.21 \\ 0.39 & PGA > 0.21 \end{cases} \quad (2-28)$$

with a standard error of estimate 0.021.

More recently, Boore et al.⁽²⁻³⁷⁾ used approximately 270 records to estimate the peak ground acceleration in terms of 1) the closest horizontal distance R_{jb} (km) from the recording station to a point on the earth surface that lies directly above the rupture, 2) the moment magnitude M_w , 3) the average shear wave velocity of the soil V_s (m/sec) over the upper 30 meters, and 4) the fault mechanism such that:

$$\begin{aligned} \ln(PGA) = & b + 0.527(M_w - 6.0) \\ & - 0.778 \ln \sqrt{R_{jb}^2 + (5.570)^2} - 0.371 \ln \frac{V_s}{1396} \end{aligned} \quad (2-29)$$

³ Seismogenic rupture zone was determined from the location of surface fault rupture, the spatial distribution of aftershocks, earthquake modelling studies, regional crustal velocity profiles, and geodetic and geologic data.

Where b is a parameter that depends on the fault mechanism. They recommended

$$b = \begin{cases} -0.313 & \text{for the strike - slip earthquakes} \\ -0.117 & \text{for the reverse - slip earthquakes} \\ -0.242 & \text{if the fault mechanism is not specified} \end{cases} \quad (2-30)$$

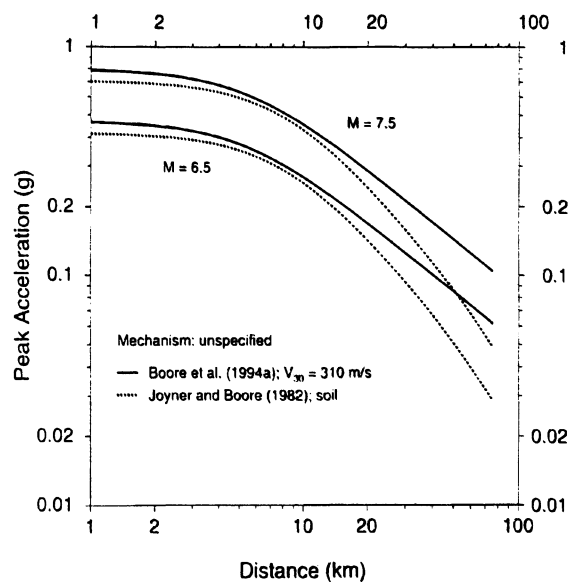


Figure 2-16. Peak ground acceleration versus distance for soil sites for earthquake magnitudes of 6.5 and 7.5. [After Boore et al. (2-37).]

Equation 2-29 is used for earthquake magnitudes of 5.5 to 7.5 and distances less than 80 km. Although Equations 2-27 and 2-29 use different definitions for the source distance, the equations indicate the decaying pattern of the peak ground acceleration with distance. Figure 2-16 shows the variation of the peak ground acceleration with distance computed from Equation 2-29 for earthquakes of magnitude 6.5 and 7.5 with an unspecified fault mechanism and for soils with a shear wave velocity of 310 m/sec. Also shown in the figure is the attenuation relationship proposed by Joyner and Boore ⁽²⁻³²⁾ (Equation 12 Table 2-4).

The variation of peak ground velocity with distance from the source of energy release (velocity attenuation) has also been studied by several investigators such as Page et al. ⁽²⁻¹¹⁾, Boore et al. ^(2-45, 2-46), Joyner and Boore ⁽²⁻³¹⁾, and Seed and Idriss ⁽²⁻³⁹⁾. Velocity attenuation curves have similar shapes and follow similar trends as the acceleration attenuation. Typical velocity attenuation curves proposed by Joyner and Boore are shown in Figure 2-17. Comparisons between Figures 2-13 and 2-17 indicate that velocity attenuates somewhat faster than acceleration.

The variation of peak ground displacement with fault distance or the distance from the

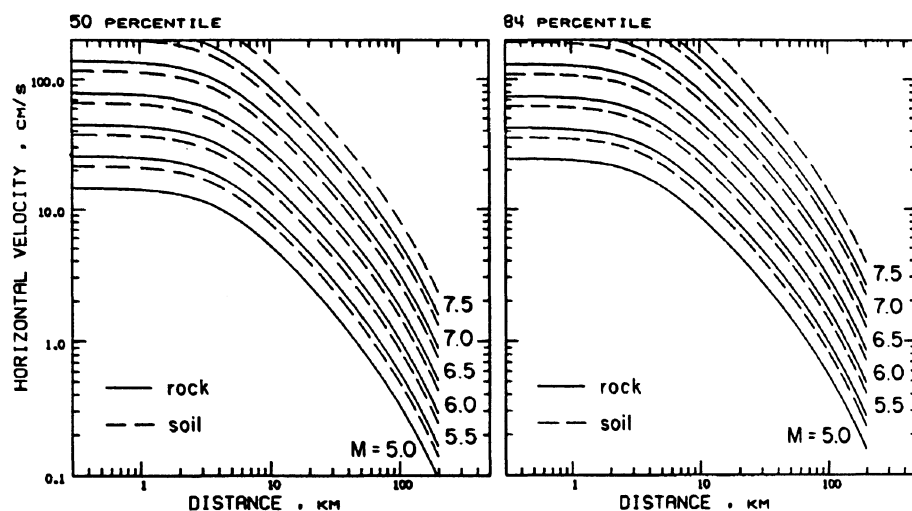


Figure 2-17. Predicted values of peak horizontal velocity for 50 and 84 percentile as functions of distance, moment magnitude, and soil condition. [After Joyner and Boore (2-31).]

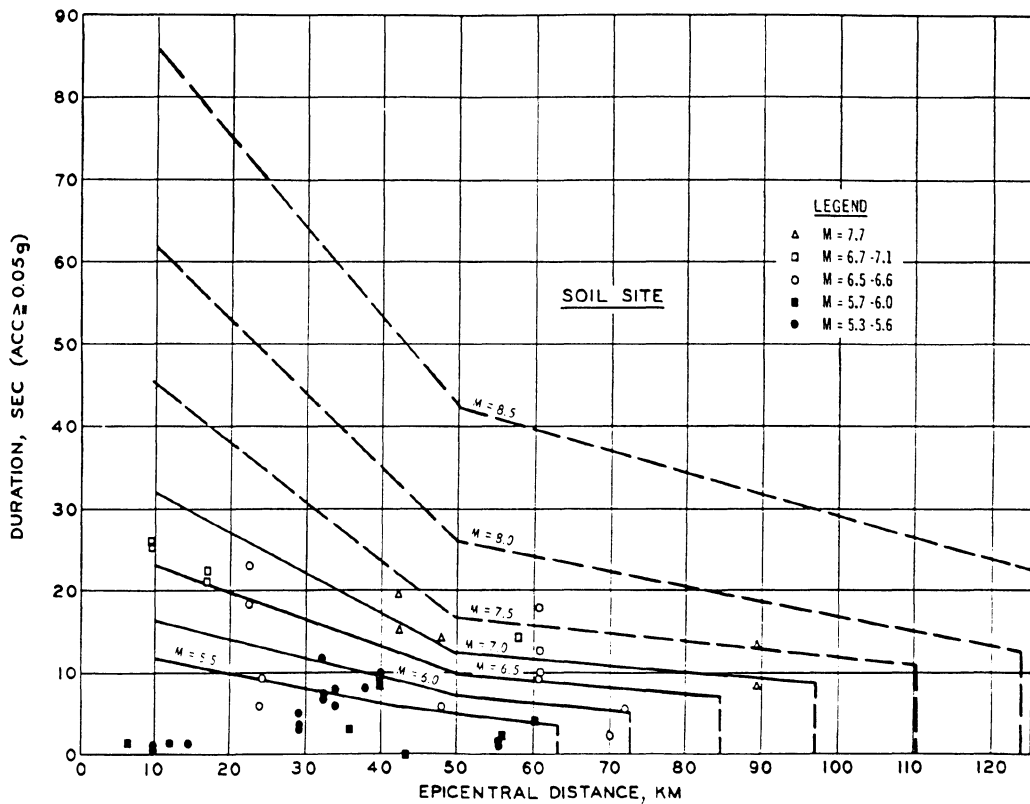


Figure 2-18. Duration versus epicentral distance and magnitude for soil. [After Chang and Krinitzsky (2-47).]

source of energy release (displacement attenuation) can also be plotted. Boore et al. (2-45, 2-46) have presented displacement attenuations for different ranges of earthquake magnitude. Only a few studies have addressed displacement attenuations probably because of their limited use and the uncertainties in computing displacements accurately.

Distance also influences the duration of strong motion. Correlations of the duration of strong motion with epicentral distance have been studied by Page et al. (2-11), Trifunac and Brady (2-13), Chang and Krinitzsky (2-47), and others. Page et al., using the bracketed duration, conclude that for a given magnitude, the duration decreases with an increase in distance from the source. Chang and Krinitzsky, also using the bracketed duration, presented the curves shown in Figures 2-18 and 2-19 for estimating durations for soil and rock as a function of distance. These figures show that

for a given magnitude, the duration of strong motion in soil is greater (approximately two times) than that in rock.

Using the 90% contribution of the acceleration intensity ($\int a^2 dt$) as a measure of duration, Trifunac and Brady (2-13) concluded that the average duration in soil is approximately 10-12 sec longer than that in rock. They also observed that the duration increases by approximately 1.0 - 1.5 sec for every 10 km increase in source distance. Although there seems to be a contradiction between their finding and those of Page et al. and Chang-Krinitzsky, the contradiction stems from using two different definitions. The bracketed duration is based on an absolute acceleration level (0.05g). At longer epicentral distances, the acceleration peaks are smaller and a shorter duration is to be expected. The acceleration intensity definition of duration is based on the relative measure of the percentile

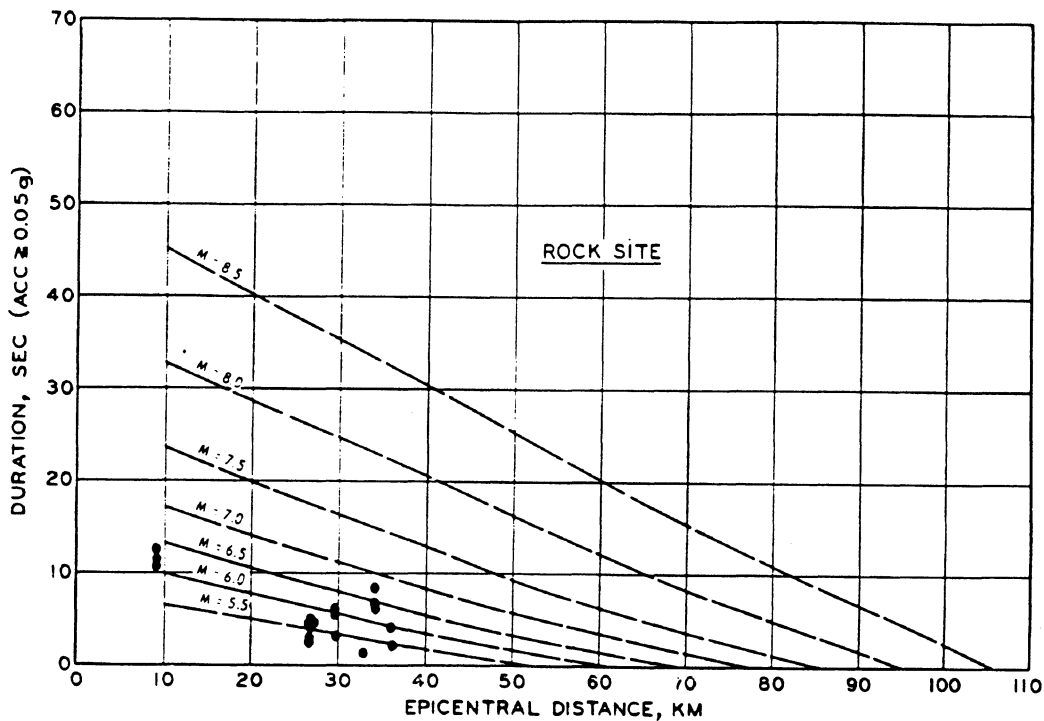


Figure 2-19. Duration versus epicentral distance and magnitude for rock. [After Chang and Krinitzky (2-47).]

contribution to the acceleration intensity. Conceivably, a more intense shaking within a shorter time may result in a shorter duration than a much less intense shaking over a longer time. According to Housner⁽²⁻³⁸⁾, at distances away from the fault, the duration of strong shaking may be longer but the shaking will be less intense than those closer to the fault.

Recently, Novikova and Trifunac⁽²⁻⁴⁸⁾ used the frequency dependent definition of duration developed by Trifunac and Westermo⁽²⁻¹⁶⁾ to study the effect of several parameters on the duration of strong motion. They employed a regression analysis on a database of 984 horizontal and 486 vertical accelerograms from 106 seismic events. Their study indicated an increase in duration by 2 sec for each 10 km of epicentral distance for low frequencies (near 0.2 Hz). At high frequencies (15 to 20 Hz), the increase in duration drops to 0.5 sec per each 10 km.

Near-Source Effects. Recent studies have indicated that near-source ground motions

contain large displacement pulses (ground displacements which are attained rapidly with a sharp peak velocity). These motions are the result of stress waves moving in the same direction as the fault rupture, thereby producing a long-duration pulse. Consequently, near source earthquakes can be destructive to structures with long periods. Hall et al.⁽²⁻⁴⁹⁾ have presented data of peak ground accelerations, velocities, and displacements from 30 records obtained within 5 km of the rupture surface. The ground accelerations varied from 0.31g to 2.0g while the ground velocities ranged from 0.31 to 1.77 m/sec. The peak ground displacements were as large as 2.55 m. Figures 2-20 and 2-21 offer two examples of near-source earthquake ground motions. The first was recorded at the LADWP Rinaldi Receiving Station during the Northridge earthquake of January 17, 1994. The distance from the recording station to the surface projection of the rupture was less than 1.0 km. The figure shows a uni-directional ground

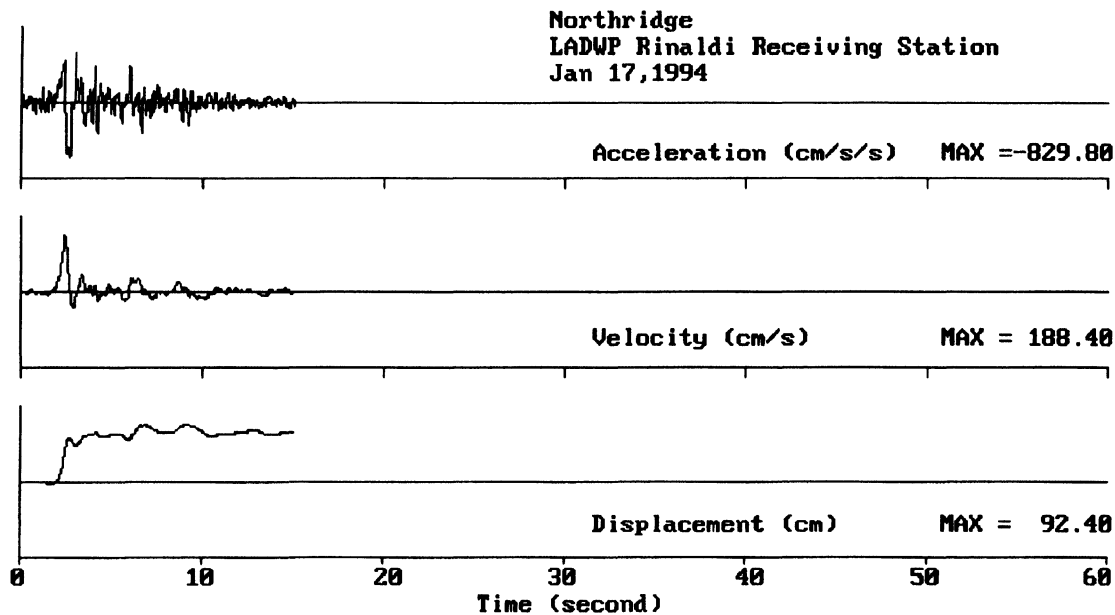


Figure 2-20. Ground acceleration, velocity, and displacement time-histories recorded at the LADWP Rinaldi Receiving Station during the Northridge earthquake of January 17, 1994.

displacement that resembles a smooth step function and a velocity pulse that resembles a finite delta function. The second example, shown in Figure 2-21, was recorded at the SCE Lucerne Valley Station during the Landers earthquake of June 28, 1992. The distance from the recording station to the surface projection of the rupture was approximately 1.8 km. A positive and negative velocity pulse that resembles a single long-period harmonic motion is reflected in the figure. Near-source ground displacements similar to that shown in Figure 2-21 have also been observed with a zero permanent displacement. The two figures clearly show the near-source ground displacements caused by sharp velocity pulses. For further details, the reader is referred to the work of Heaton and Hartzell ⁽²⁻⁵⁰⁾ and Somerville and Graves ⁽²⁻⁵¹⁾.

2.4.2 Site geology

Soil conditions influence ground motion and its attenuation. Several investigators such as Boore et al. ^(2-45 and 2-46) and Seed and Idriss ⁽²⁻³⁹⁾ have presented attenuation curves for soil and rock. According to Boore et al., peak horizontal acceleration is not appreciably affected by soil condition (peak horizontal acceleration is nearly the same for both soil and rock). Seed and Idriss compare acceleration attenuation for rock from earthquakes with magnitudes of approximately 6.6 with acceleration attenuation for alluvium from the 1979 Imperial Valley earthquake (magnitude 6.8). Their comparison shown in Figure 2-22 indicates that at a given distance from the source of energy release, peak accelerations on rock are somewhat greater than those on alluvium. Studies from other earthquakes indicate that this is generally the case for

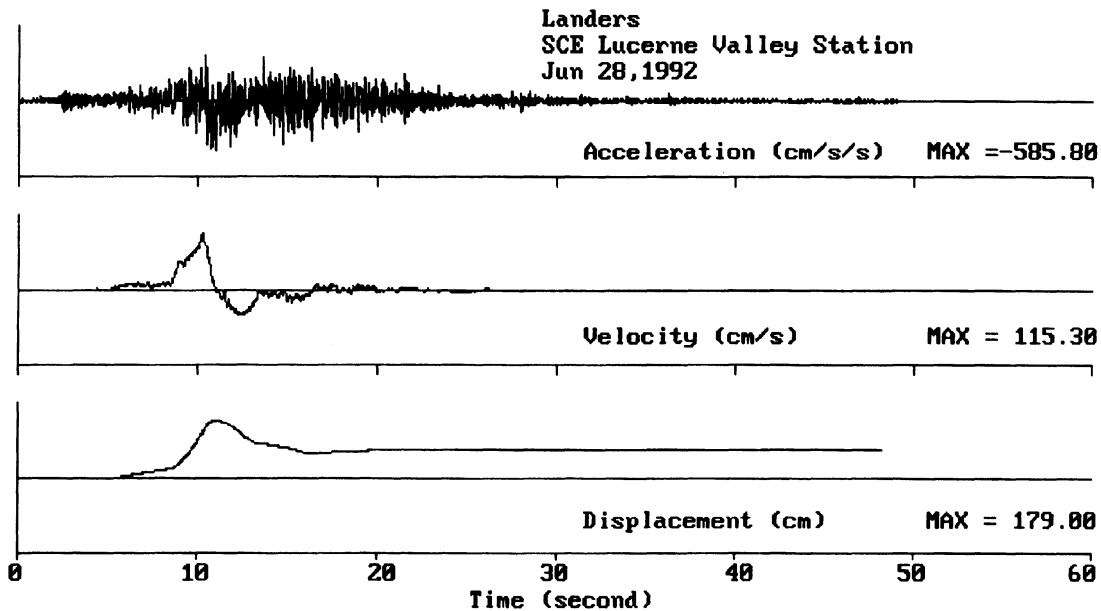


Figure 2-21. Ground acceleration, velocity, and displacement time-histories recorded at the SCE Lucerne Valley Station during the Landers earthquake of June 28, 1992.

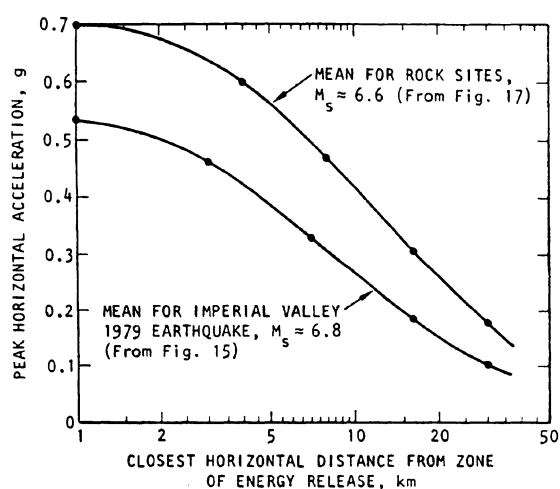


Figure 2-22. Comparison of attenuation curves for rock sites and the Imperial Valley earthquake of 1979. [After Seed and Idriss (2-39).]

acceleration levels greater than approximately 0.1g. At levels smaller than this value, accelerations on deep alluvium are slightly greater than those on rock. The effect of soil condition on peak acceleration is illustrated by

Seed and Idriss in Figure 2-23. According to this figure, the difference in acceleration on rock and on stiff soil is not that significant. Even though in specific cases, particularly soft soils, soil condition can affect peak accelerations, Seed and Idriss conclude that the influence of soil condition can generally be neglected when using acceleration attenuation curves. In a more recent study, Idriss⁽²⁻⁵²⁾, using the data from the 1985 Mexico City and the 1989 Loma Prieta earthquakes, modified the curve for soft soil sites as shown in Figure 2-24. In these two earthquakes, soft soils exhibited peak ground accelerations of almost 1.5 to 4 times those of rock for the acceleration range of 0.05g to 0.1g. For rock accelerations larger than approximately 0.1g, the acceleration ratio between soft soils and rock tends to decrease to about 1.0 for rock accelerations of 0.3g to 0.4g. The figure indicates that large rock accelerations are amplified through soft soils to a lesser degree and may even be slightly de-amplified.

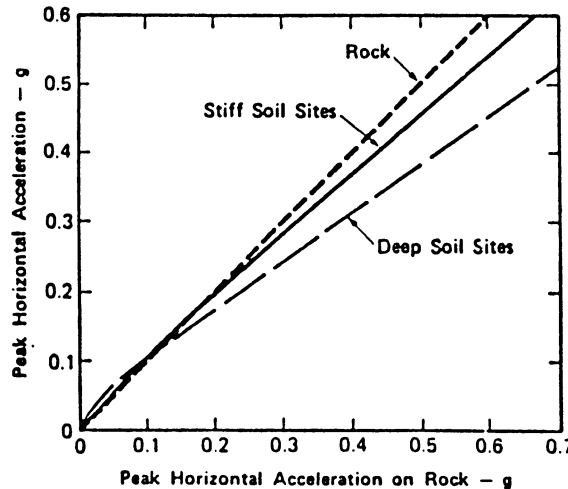


Figure 2-23. Relationship between peak accelerations on rock and soil. [After Seed and Idriss (2-39).]

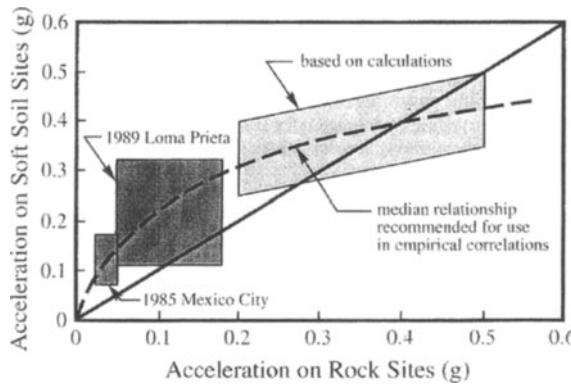


Figure 2-24. Variation of peak accelerations on soft soil compared to rock for the 1985 Mexico City and the 1989 Loma Prieta earthquakes. [After Idriss (2-52).]

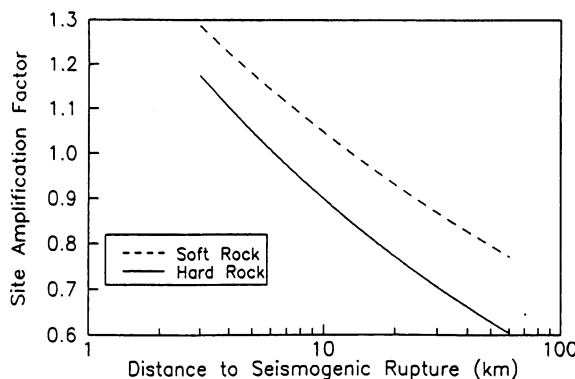


Figure 2-25. Variation of site amplification factors (ratio of peak ground acceleration on rock to that on alluvium) with distance. [After Campbell and Bozorgnia (2-36).]

The effect of site geology on peak ground acceleration can be seen in Equation 2-27 proposed by Campbell and Bozorgnia⁽²⁻³⁶⁾. The ratios of peak ground acceleration on soft rock and on hard rock to that on alluvium (defined as site amplification factors) were computed from Equation 2-27 and are shown in Figure 2-25. The figure indicates that rock sites have higher accelerations at shorter distances and lower accelerations at longer distances as compared to alluvium sites, with ground accelerations on soft rock consistently higher than those on hard rock.

Recent studies on the influence of site geology on ground motion use the average shear wave velocity to identify the soil category. Boore et al.⁽²⁻³⁷⁾ used the average shear wave velocity for the upper 30 meters of the soil layer to characterize the soil condition in the attenuation relationship in Equation 2-29. The equation indicates that for the same distance, magnitude, and fault mechanism, as the soil becomes stiffer (i.e. a higher shear wave velocity), the peak ground acceleration becomes smaller. The recent UBC code and NEHRP recommended provisions use shear wave velocities to identify the different soil profiles with a shear wave velocity of 1500 m/sec or greater defining hard rock and a shear wave velocity of 180 m/sec or smaller defining soft soil (Section 2.9).

There is a general agreement among various investigators that the soil condition has a pronounced influence on velocities and displacements. According to Boore et al.^(2-45 and 2-46), Joyner and Boore⁽²⁻³¹⁾, and Seed and Idriss⁽²⁻³⁹⁾; larger peak horizontal velocities are to be expected for soil than rock. A statistical study of earthquake ground motion and response spectra by Mohraz⁽²⁻⁵³⁾ indicated that the average velocity to acceleration ratio for records on alluvium is greater than the corresponding ratio for rock.

Using the frequency dependent definition of duration proposed by Trifunac and Westermo⁽²⁻¹⁶⁾, Novikova and Trifunac⁽²⁻⁴⁸⁾ determined that for the same epicentral distance and earthquake magnitude, the strong motion duration for

records on a sedimentary site is longer than that on a rock site by approximately 4 to 6 sec for frequencies of 0.63 Hz and by about 1 sec for frequencies of 2.5 Hz. The records on intermediate sites, furthermore, exhibited a shorter duration than those on sediments. They indicated that for frequencies of 0.63 to 21 Hz, the influence of the soil condition on the duration is noticeable.

2.4.3 Magnitude

Different earthquake magnitudes have been defined, the more common being the Richter magnitude (local magnitude) M_L , the surface wave magnitude M_S , and the moment magnitude M_W (see Chapter 1). As expected, at a given distance from the source of energy release, large earthquake magnitudes result in large peak ground accelerations, velocities, and displacements. Because of the lack of adequate data for earthquake magnitudes greater than 7.5, the influence of the magnitude on peak ground motion and duration is generally determined through extrapolation of data from earthquake magnitudes smaller than 7.5. Attenuation relationships are also presented as a function of magnitude for a given source distance as indicated in Equations 2-27 and 2-29. Both equations show that for a given distance, soil condition, and fault mechanism, the larger the earthquake magnitude, the larger is the peak ground acceleration. Figure 2-16, plotted using Equation 2-29, confirms this observation.

The influence of earthquake magnitude on the duration of strong motion has been studied by several investigators. Housner⁽²⁻³⁸⁾ and⁽²⁻⁵⁴⁾ presents values for maximum acceleration and duration of strong phase of shaking in the vicinity of a fault for different earthquake magnitudes (Table 2-5). Donovan⁽²⁻²³⁾ presents the linear relationship in Figure 2-26 for estimating duration in terms of magnitude. His estimates compare closely with those presented by Housner in Table 2-5. Using the bracketed duration (0.05g), Page et al.⁽²⁻¹¹⁾ give estimates of duration for various earthquake magnitudes near a fault (Table 2-6). Chang and Krinitzsky

⁽²⁻⁴⁷⁾ give approximate upper-bound for duration for soil and rock (Table 2-7). Their values for soil are close to those presented by Page et al., and the ones for rock are consistent with those given by Housner and by Donovan. The study by Novikova and Trifunac⁽²⁻⁴⁸⁾ which uses the frequency dependent definition of duration presents a quadratic expression for the duration in terms of earthquake magnitude. Their study indicates that the duration of strong motion does not depend on the earthquake magnitude at frequencies less than 0.25 Hz. For higher frequencies, the duration increases exponentially with magnitude.

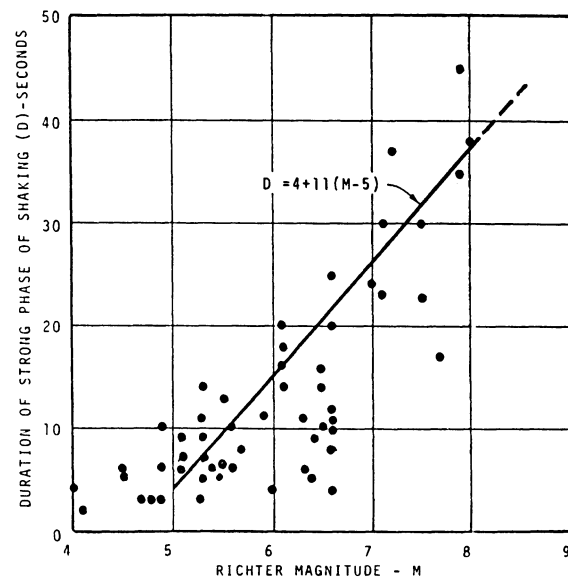


Figure 2-26. Relationship between magnitude and duration of strong phase of shaking. [After Donovan (2-23).]

Table 2-5. Maximum Ground Accelerations and Durations of Strong Phase of Shaking [after Housner (2-54)]

Magnitude	Maximum Acceleration (%g)	Duration (sec)
5.0	9	2
5.5	15	6
6.0	22	12
6.5	29	18
7.0	37	24
7.5	45	30
8.0	50	34
8.5	50	37

Table 2-6. Duration of Strong Motion Near Fault [after Page et al. (2-11)]

Magnitude	Duration (sec)
5.5	10
6.5	17
7.0	25
7.5	40
8.0	60
8.5	90

Table 2-7. Strong Motion Duration for Different Earthquake Magnitudes [after Chang and Krinitzky (2-47)]

Magnitude	Rock	Soil
5.0	4	8
5.5	6	12
6.0	8	16
6.5	11	23
7.0	16	32
7.5	22	45
8.0	31	62
8.5	43	86

2.4.4 Source characteristics

Factors such as fault mechanism, depth, and repeat time have been suggested by several investigators as being important in determining ground motion amplitudes because of their relation to the stress state at the source or to stress changes associated with the earthquake. Based on the state of stress in the vicinity of the fault, many investigators believe that large ground motions are associated with reverse and thrust faults whereas smaller ground motions are related to normal and strike-slip faults.

The above observations agree with the study by McGarr (2-55, 2-56) who concluded that ground acceleration from reverse faults should be greater than those from normal faults, with strike-slip faults having intermediate accelerations. McGarr also believes that ground motions increase with fault depth. Kanamori and Allen (2-57) presented data showing that higher ground motions are associated with faults with longer repeat times since they experience large average stress drops. Using empirical equations, Campbell (2-58) found that peak ground acceleration and velocity in reverse-slip earthquakes are larger by about 1.4 to 1.6 times than those in strike-slip

earthquakes. Joyner and Boore (2-59) believe this ratio should be 1.25.

Recent attenuation relationships include the effects of fault mechanism on ground motion as indicated in Equations 2-27 and 2-29. Equation 2-27 by Campbell and Bozorgnia (2-36) indicates that reverse, reverse-oblique, and thrust fault earthquakes result in larger ground accelerations than strike-slip and normal fault earthquakes. Figure 2-27, computed from Equation 2-27, shows the variation of peak ground acceleration with distance for earthquakes with different magnitudes and fault mechanisms on alluvium. Similar observations can also be made from Equation 2-29 by Boore et al. (2-37) where reverse earthquakes result in higher accelerations than strike-slip earthquakes.

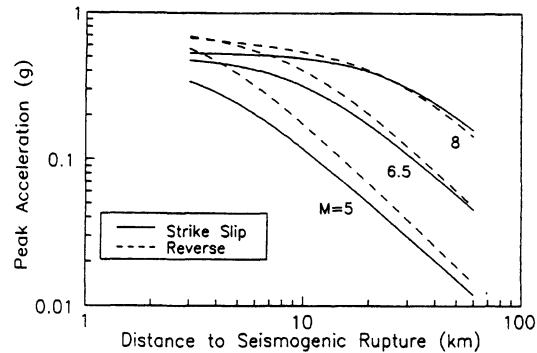


Figure 2-27. Peak ground acceleration versus distance for different magnitudes and fault mechanisms. [After Campbell and Bozorgnia (2-36).]

2.4.5 Directivity

Directivity relates to the azimuthal variation of the angle between the direction of rupture propagation (or radiated seismic energy) and source-to-site vector, and its effect on earthquake ground motion. Large ground accelerations and velocities can be associated with small angles since a significant portion of the seismic energy is channeled in the direction of rupture propagation. Consequently, when a large urban area is located within the small angle, it will experience severe damage.

According to Faccioli ⁽²⁻⁶⁰⁾, in the Northridge earthquake of January 17, 1994; the rupture propagated in the direction opposite from downtown Los Angeles and San Fernando Valley, causing moderate damage. In the Hyogoken-Nanbu (Kobe) earthquake of January 17, 1995, the rupture was directed toward the densely populated City of Kobe resulting in significant damage. The stations that lie in the direction of the earthquake rupture propagation will record shorter strong motion durations than those located opposite to the direction of propagation ⁽²⁻⁶¹⁾.

Boatwright and Boore ⁽²⁻⁶²⁾, believe that directivity can significantly affect strong ground motion by a factor of up to 10 for ground accelerations. Joyner and Boore ⁽²⁻⁵⁹⁾ indicate, however, that it is not clear how to incorporate directivity into methods for predicting ground motion in future earthquakes since the angle between the direction of rupture propagation and the source-to-recording-site vector is not known *a priori*. Moreover, for sites close to the source of a large magnitude earthquake, where a reliable estimate of ground motion is important, the angle changes during the rupture propagation. Most ground motion prediction studies do not explicitly include a variable representing directivity.

2.5 EVALUATION OF SEISMIC RISK AT A SITE

Evaluating seismic risk is based on information from three sources: 1) the recorded ground motion, 2) the history of seismic events in the vicinity of the site, and 3) the geological data and fault activities of the region. For most regions of the world this information, particularly from the first source, is limited and may not be sufficient to predict the size and recurrence intervals of future earthquakes. Nevertheless, the earthquake engineering community has relied on this limited information to establish some acceptable levels of risk.

The seismic risk analysis usually begins by developing mathematical models, which are

used to estimate the recurrence intervals of future earthquakes with certain magnitude and/or intensity. These models together with the appropriate attenuation relationships are commonly utilized to estimate ground motion parameters such as peak acceleration and velocity corresponding to a specified probability and return period. Among the earthquake recurrence models mostly used in practice is the Gutenberg-Richter relationship ^(2-63, 2-64) known as the Richter law of magnitude which states that there exists an approximate linear relationship between the logarithm of the average number of annual earthquakes and earthquake magnitude in the form

$$\log N(m) = A - Bm \quad (2-31)$$

where $N(m)$ is the average number of earthquakes per annum with a magnitude greater than or equal to m , and A and B are constants determined from a regression analysis of data from the seismological and geological studies of the region over a period of time. The Gutenberg-Richter relationship is highly sensitive to magnitude intervals and the fitting procedure used in the regression analysis ^(2-65, 2-66, 2-33). Figure 2-28 shows a typical plot of the Gutenberg-Richter relationship presented by Schwartz and Coppersmith ⁽²⁻⁶⁶⁾ for the south-central segment of the San Andreas Fault. The relationship was obtained from historical and instrumental data in the period 1900-1980 for a 40-kilometer wide strip centered on the fault. The box shown in the figure represents recurrence intervals based on geological data for earthquakes of magnitudes 7.5-8.0 ⁽²⁻⁶⁷⁾. It is apparent from the figure that the extrapolated portion of the Gutenberg-Richter equation (dashed line) underestimates the frequency of occurrence of earthquakes with large magnitudes, and therefore, the model requires modification of the B -value in Equation 2-31 for magnitudes greater than approximately 6.0 ⁽²⁻³³⁾.

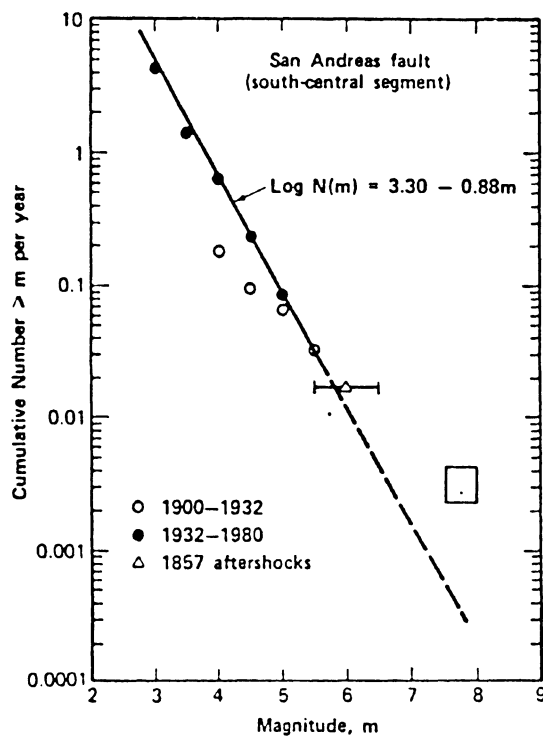


Figure 2-28. Cumulative frequency-magnitude plot. The box in the figure represents range of recurrence based on geological data for earthquake magnitudes of 7.5-8. [After Schwartz and Coppersmith (2-66); reproduced from Idriss (2-33).]

Cornell⁽²⁻⁶⁸⁾ introduced a simplified method for evaluating seismic risk. The method incorporates the influence of all potential sources of earthquakes. His procedure as described by Vanmarcke⁽²⁻⁶⁹⁾ can be summarized as follows:

1. The potential sources of seismic activity are identified and divided into smaller sub-sources (point sources).
2. The average number of earthquakes per annum $N_i(m)$ of magnitudes greater than or equal to m from the i th sub-source is determined from the Gutenberg-Richter relationship (Equation 2-31) as

$$\log N_i(m) = A_i - B_i m \quad (2-32)$$

where A_i and B_i are known constants for the i th sub-source.

3. Assuming that the design ground motion is specified in terms of the peak ground acceleration a and the epicentral distance from the i th sub-source to the site is R_i , the magnitude $m_{a,i}$ of an earthquake initiated at this sub-source may be estimated from

$$m_{a,i} = f(R_i, a) \quad (2-33)$$

where $f(R_i, a)$ is a function which can be obtained from the attenuation relationships. Substituting Equation 2-33 into Equation 2-32, one obtains

$$\log N_i(m_{a,i}) = A_i - B_i [f(R_i, a)] \quad (2-34)$$

Assuming the seismic events are independent (no overlapping), the total number of earthquakes per annum N_a which may result in a peak ground acceleration greater than or equal to a is obtained from the contribution of each sub-source as

$$N_a = \sum_{all} N_i(m_{a,i}) \quad (2-35)$$

4. The mean return period T_a in years is obtained as

$$T_a = \frac{1}{N_a} \quad (2-36)$$

In the above expression, N_a can be also interpreted as the average annual probability λ_a that the peak ground acceleration exceeds a certain acceleration a . In a typical design situation, the engineer is interested in the probability that such a peak exceeds a during the life of structure t_L . This probability can be estimated using the Poisson distribution as

$$P = 1 - e^{-\lambda_a t_L} \quad (2-37)$$

Another distribution based on a Bayesian procedure⁽²⁻⁷⁰⁾ was proposed by Donovan⁽²⁻²³⁾. The distribution is more conservative than the Poisson distribution, and therefore more appropriate when additional uncertainties such

as those associated with the long return periods of large magnitude earthquakes are encountered. It should be noted that other ground motion parameters in lieu of acceleration such as spectral ordinates may be

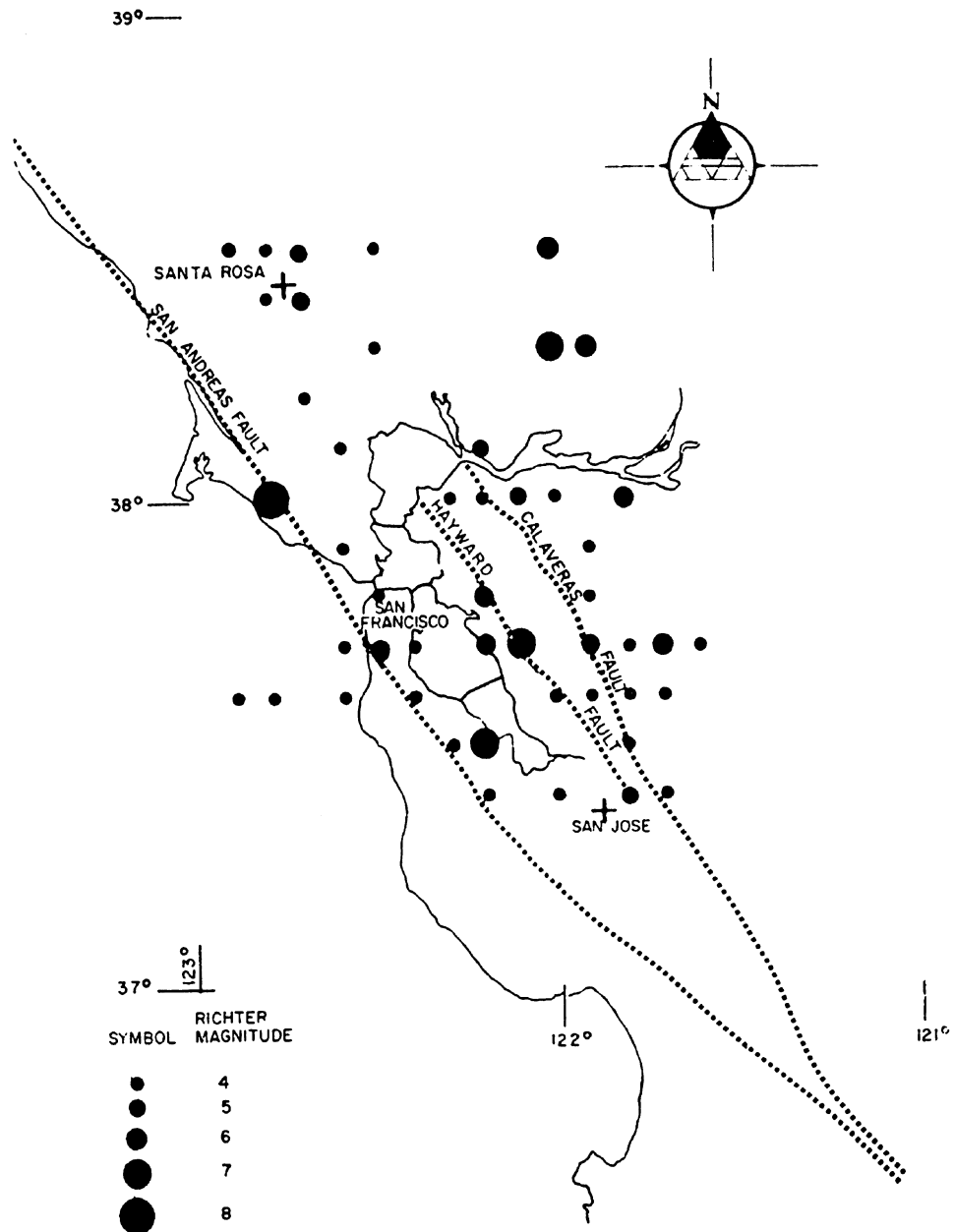


Figure 2-29. Instrumental or estimated epicentral locations within 100 kilometers of San Francisco. [After Donovan (2-23).]

used for evaluating seismic risk. Other procedures for seismic risk analysis based on more sophisticated models have also been proposed (see for example Der Kiureghian and Ang, 2-71).

The evaluation of seismic risk at a site is demonstrated by Donovan⁽²⁻²³⁾ who used as an example the downtown area of San Francisco. The epicentral data and earthquake magnitudes he considered in the evaluation were obtained over a period of 163 years and are depicted in Figure 2-29. The data is associated with three major faults, the San Andreas, Hayward, and Calaveras. Using attenuation relationships for competent soil and rock, Donovan computed the return periods for different peak accelerations (see Table 2-8). He then computed the probability of exceeding various peak ground accelerations during a fifty-year life of the structure which is shown in Figure 2-30. Plots such as those in Figure 2-30 may be used to estimate the peak acceleration for various probabilities. For example, if the structure is to be designed to resist a moderate earthquake with a probability of 0.6 and a severe earthquake with a probability of between 0.1 and 0.2 of occurring at least once during the life of the structure, the peak accelerations using Figure 2-30(b) for rock, are 0.15g and 0.4g, respectively.

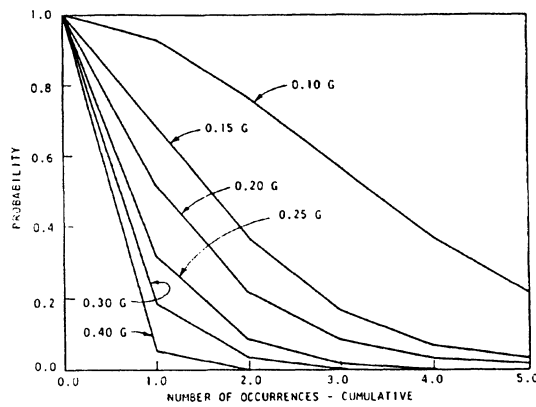
Table 2-8. Return Periods for Peak Ground Acceleration in the San Francisco Bay Area [after Donovan (2-23)]

Peak Acceleration	Return Period (years)	
	Soil	Rock
0.05	4	8
0.10	20	30
0.15	50	60
0.20	100	100
0.25	250	200
0.30	450	300
0.40	2000	700

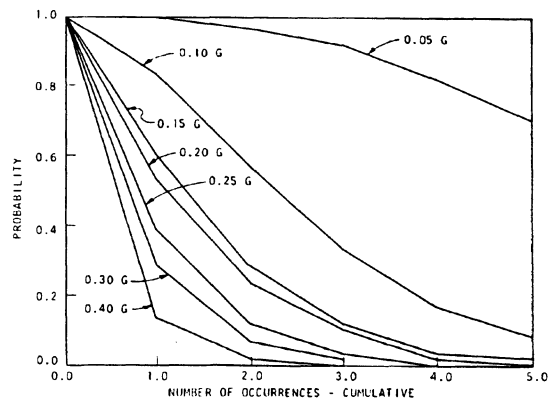
2.5.1 Development of seismic maps

Using the seismic risk principles of Cornell⁽²⁻⁶⁸⁾, Algermissen and Perkins^(2-72, 2-73) developed isoseismal maps for peak ground accelerations and velocities. Figure 2-31 is a

map, which shows contours of peak acceleration on rock having a 90% probability of not being exceeded in 50 years. The Applied Technology Council ATC⁽²⁻⁷⁴⁾ used this map to develop similar maps for effective peak acceleration (Figure 2-32) and effective peak velocity-related acceleration (Figure 2-33). The effective peak acceleration A_a and the effective peak velocity-related acceleration A_v , are defined by the Applied Technology Council⁽²⁻⁷⁴⁾ based on a study by McGuire⁽²⁻⁷⁵⁾. They are obtained by dividing the spectral accelerations between periods of 0.1 to 0.5 sec and the spectral



(a) Based on return periods using relationship 9 in Table 2-4



(b) Based on return periods using attenuation equation for rock

Figure 2-30. Estimated probabilities for a fifty year project life. [After Donovan (2-23).]

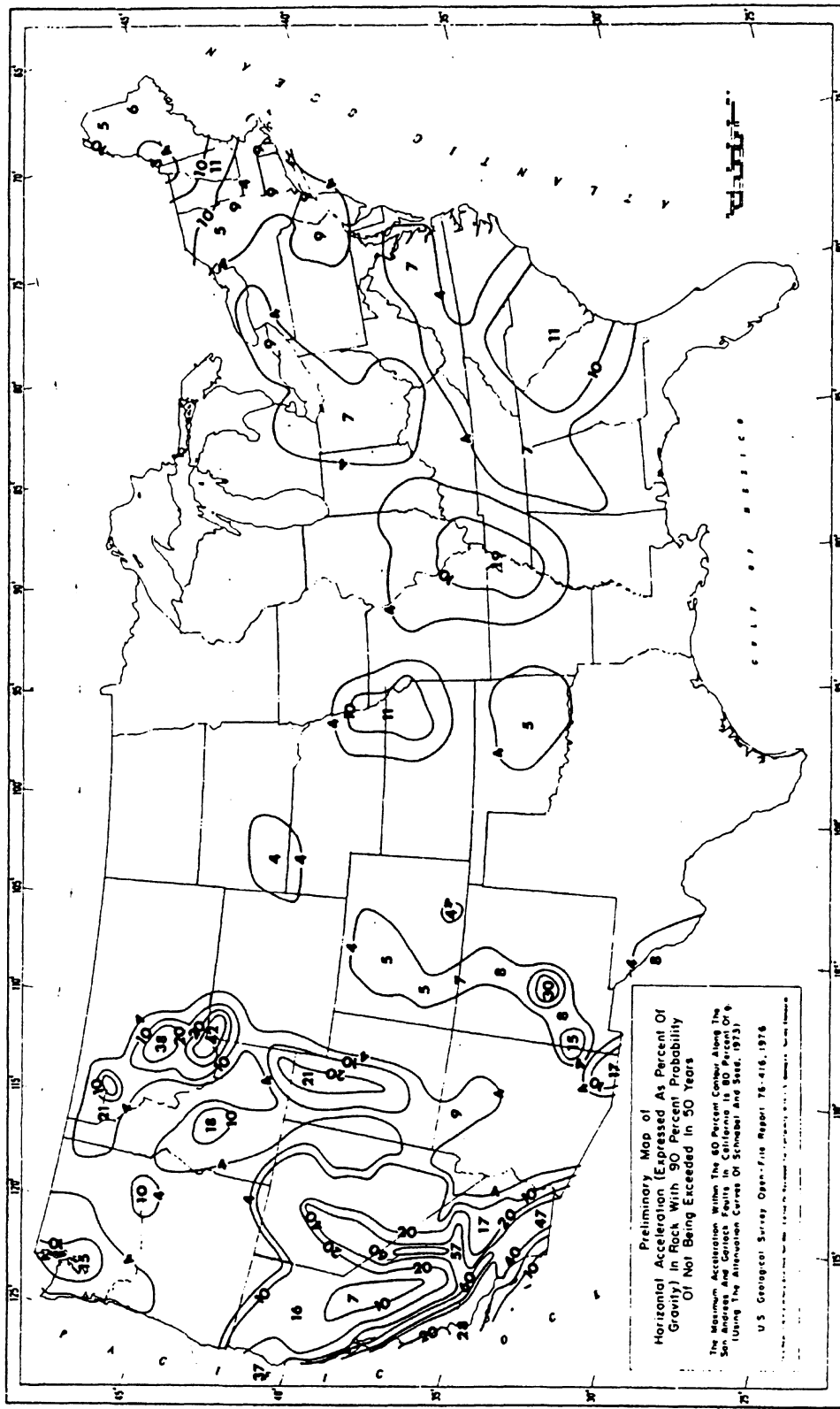


Figure 2-31. Seismic risk map developed by Algermissen and Perkins. (Reproduced from 2-74.)

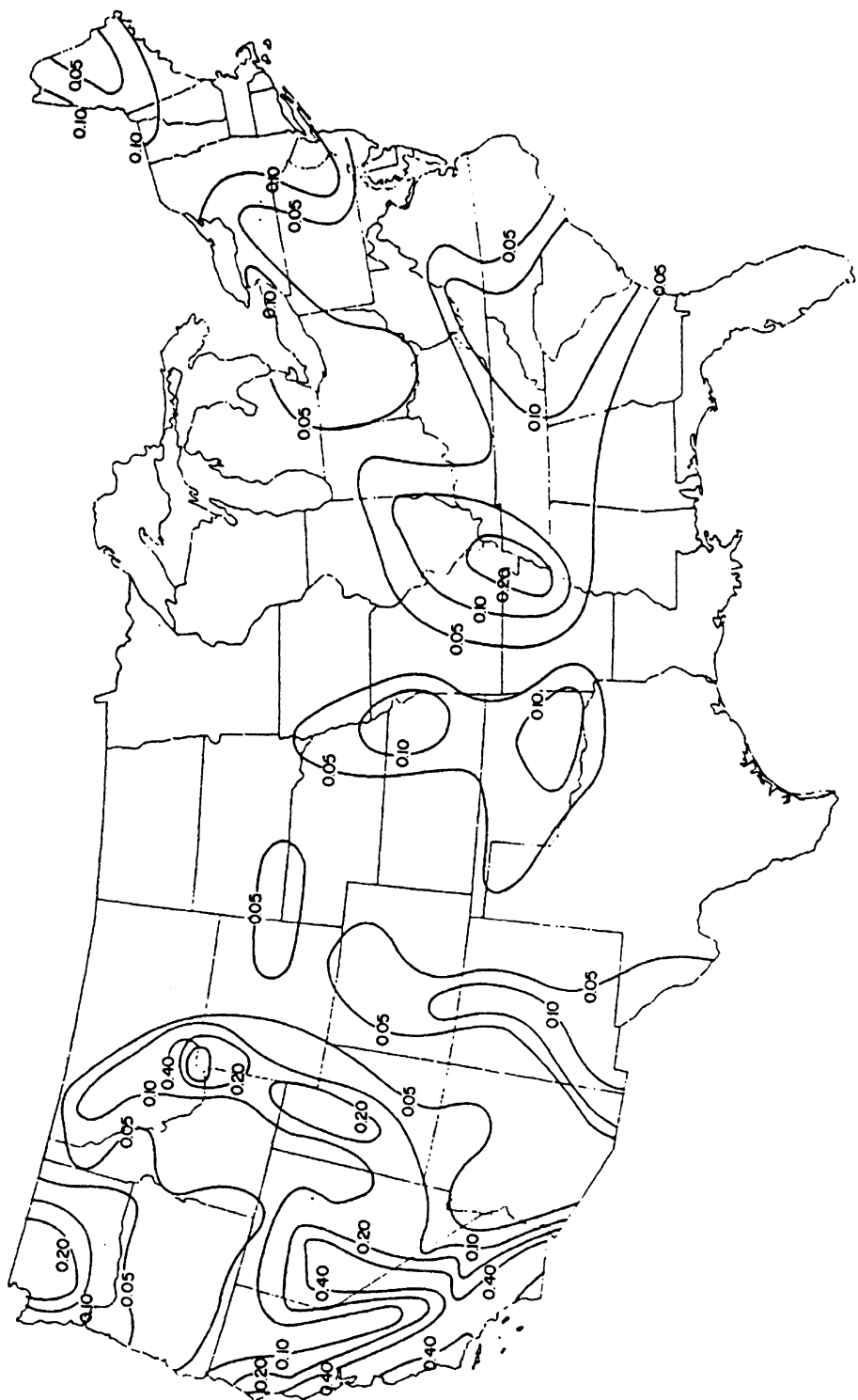
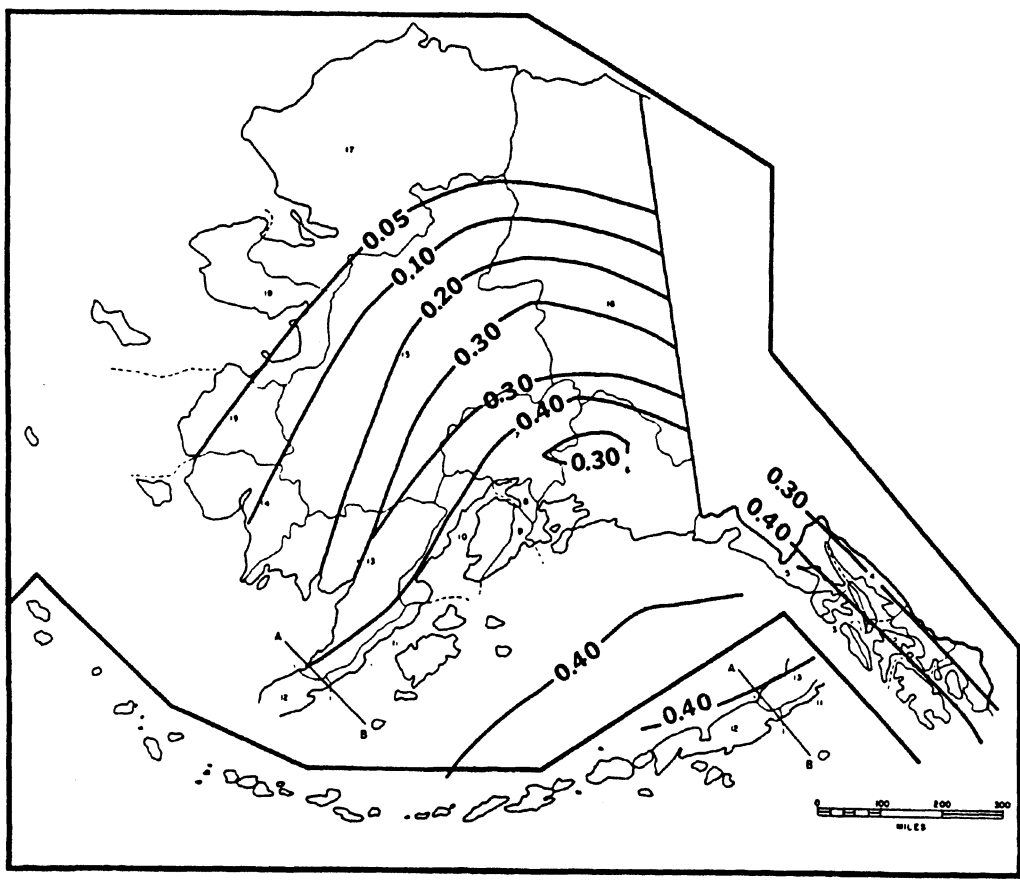
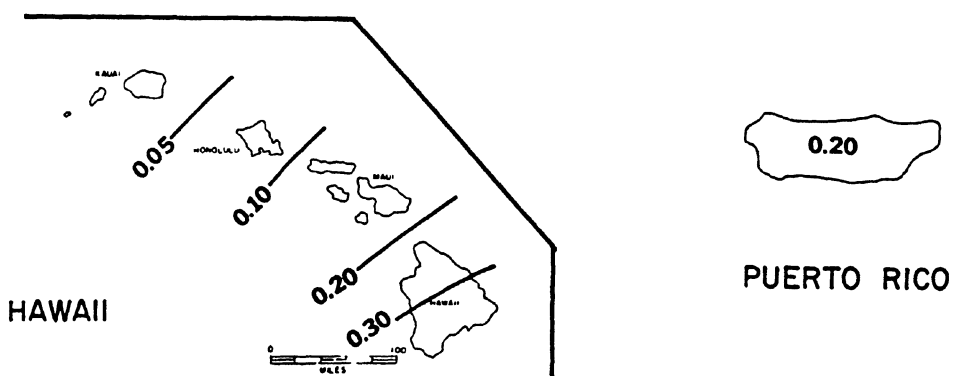


Figure 2-32. Contour map for effective peak acceleration (ATC, 2-74).



ALASKA



CONTOUR MAP FOR EFFECTIVE PEAK ACCELERATION

Figure 2-32. (continued)

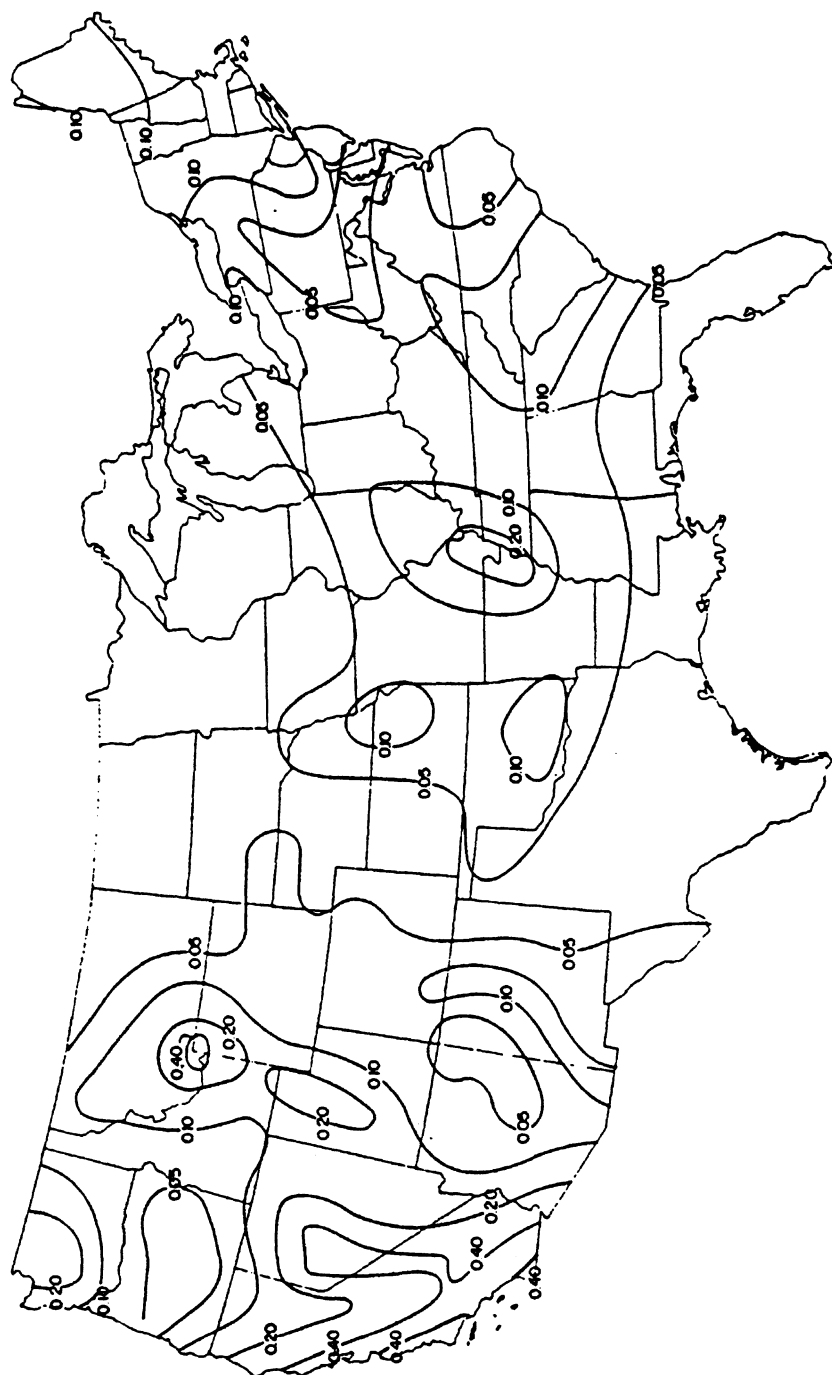
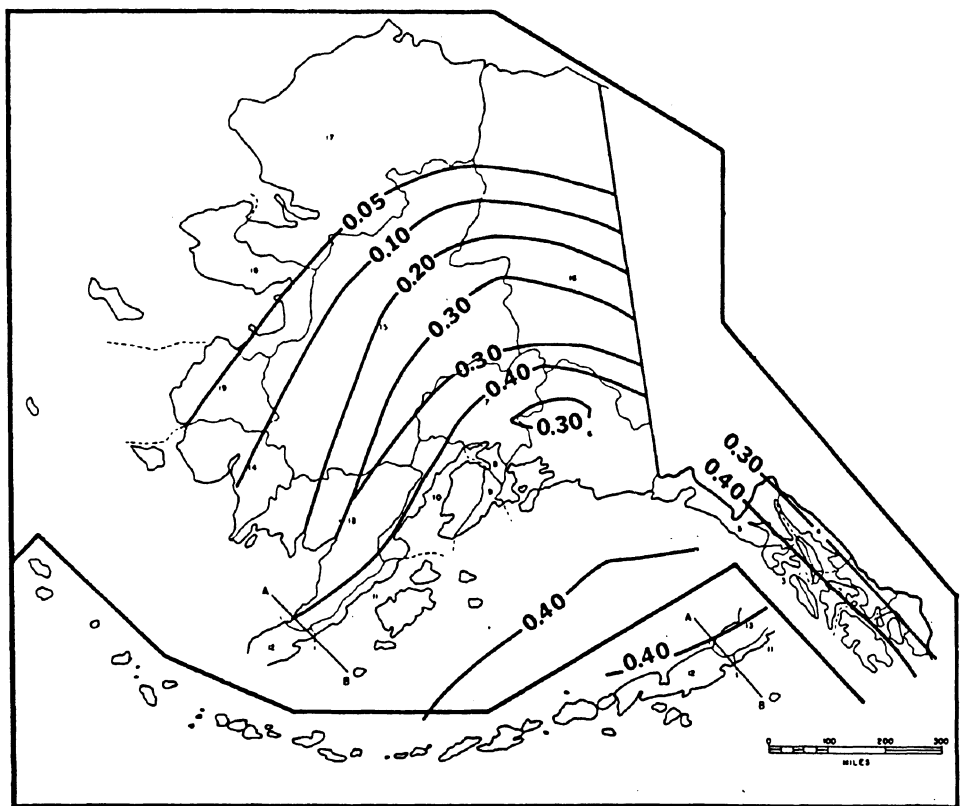
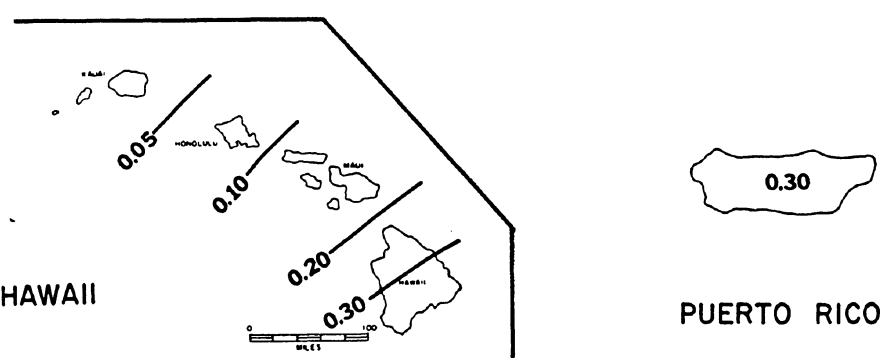


Figure 2-33. Contour map of effective peak velocity-related acceleration (ATC, 2-74).



ALASKA



**CONTOUR MAP FOR EFFECTIVE PEAK VELOCITY-RELATED
ACCELERATION COEFFICIENT**

Figure 2-33. (continued)

velocity at a period of approximately 1.0 sec by a constant amplification factor (2.5 for a 5% damped spectrum). It should be noted that the effective peak acceleration will generally be smaller than the peak acceleration while the effective peak velocity-related acceleration is generally greater than the peak velocity⁽²⁻⁷⁵⁾.

The A_a and A_v maps developed from the ATC study are in many ways similar to the Algermissen-Perkins map. The most significant difference is in the area of highest seismicity in California. Within such areas, the Algermissen-Perkins map has contours of 0.6g whereas the ATC maps have no values greater than 0.4g. This discrepancy is due to the difference between peak acceleration and effective peak acceleration and also to the decision by the participants in the ATC study to limit the design value to 0.4g based on scientific knowledge and engineering judgment. The ATC maps were also provided with the contour lines shifted to coincide with the county boundaries.

The 1985, 1988, 1991 and 1994 National Earthquake Hazard Reduction Program (NEHRP) Recommended Provisions for Seismic Regulations for New Buildings^(2-76 to 2-79) include the ATC A_a and A_v maps which correspond to a 10% probability of the ground motion being exceeded in 50 years (a return period of 475 years). The 1991 NEHRP provisions⁽²⁻⁷⁸⁾ also introduced preliminary spectral response acceleration maps developed by the United States Geological Survey (USGS) for a 10% probability of being exceeded in 50 years and a 10% probability of being exceeded in 250 years (a return period of 2,375 years). These maps, which include elastic spectral response accelerations corresponding to 0.3 and 1.0 sec periods, were introduced to present new and relevant data for estimating spectral response accelerations and reflect the variability in the attenuation of spectral acceleration and in fault rupture length⁽²⁻⁷⁸⁾.

The 1997 NEHRP recommended provisions⁽²⁻⁸⁰⁾ provide seismic maps for the spectral response accelerations at the short period range (approximately 0.2 sec) and at a

period of 1.0 sec. The maps correspond to the maximum considered earthquake, defined as the maximum level of earthquake ground shaking that is considered reasonable for design of structures. In most regions of the United States, the maximum considered earthquake is defined with a uniform probability of exceeding 2% in 50 years (a return period of approximately 2500 years). It should be noted that the use of the maximum considered earthquake was adopted to provide a uniform protection against collapse at the design ground motion. While the conventional approach in earlier editions of the provisions provided for a uniform probability that the design ground motion will not be exceeded, it did not provide for a uniform probability of failure for structures designed for that ground motion. The design ground motion in the 1997 NEHRP provisions is based on a lower bound estimate of the margin against collapse which was judged, based on experience, to be 1.5. Consequently, the design earthquake ground motion was selected at a ground shaking level that is 1/1.5 or 2/3 of the maximum considered earthquake ground motion given by the maps.

The 1997 NEHRP Guidelines for the Seismic Rehabilitation of Buildings⁽²⁻⁸¹⁾, known as FEMA-273, introduce the concept of performance-based design. For this concept, the rehabilitation objectives are statements of the desired building performance level (collapse prevention, life safety, immediate occupancy, and operational) when the building is subjected to a specified level of ground motion. Therefore, multiple levels of ground shaking need to be defined by the designer. FEMA-273 provides two sets of maps; each set includes the spectral response accelerations at short periods (0.2 sec) and at long periods (1.0 sec). One set corresponds to a 10% probability of exceedance in 50 years, known as Basic Safety Earthquake 1 (BSE-1), and the other set corresponds to a 2% probability of exceedance in 50 years, known as Basic Safety Earthquake 2 (BSE-2), which is similar to the Maximum Considered Earthquake of the 1997 NEHRP provisions⁽²⁻⁸⁰⁾. FEMA-273 also presents a method for

adjusting the mapped spectral accelerations for other probabilities of exceedance in 50 years using the spectral accelerations at 2% and 10% probabilities.

The A_a and A_v maps, developed during the ATC study, were also used, after some modifications, in the development of a single seismic map for the 1985, 1988, 1991, 1994, and 1997 editions of the Uniform Building Code^(2-82 to 2-86). The UBC map shows contours for five seismic zones designated as 1, 2A, 2B, 3, and 4. Each seismic zone is assigned a zone factor Z, which is related to the effective peak acceleration. The Z factors for the five zones are 0.075, 0.15, 0.20, 0.30, and 0.40 for zones 1, 2A, 2B, 3, and 4; respectively. The only change in the UBC seismic map occurred in the 1994 edition⁽²⁻⁸⁵⁾ reflecting new knowledge regarding the seismicity of the Pacific Northwest of the United States.

2.6 ESTIMATING GROUND MOTION

In the late sixties and early seventies, the severity of the ground motion was generally specified in terms of peak horizontal ground acceleration. Most attenuation relationships were developed for estimating the expected peak horizontal acceleration at the site. Although structural response and to some extent damage potential to structures can be related to peak ground acceleration, the use of the peak acceleration for design has been questioned by several investigators on the premise that structural response and damage may relate more appropriately to effective peak acceleration A_a and effective peak velocity-related acceleration A_v . Early Studies by Mohraz et al.⁽²⁻⁹⁾, Mohraz⁽²⁻⁵³⁾, Newmark and Hall⁽²⁻⁸⁷⁾, and Newmark et al.⁽²⁻⁸⁸⁾ recommended using ground velocity and displacement, in addition to ground acceleration, in defining spectral shapes and ordinates.

Prior to the 1971 San Fernando earthquake where only a limited number of records was available, Newmark and Hall^(2-89, 2-90)

recommended that a maximum horizontal ground velocity of 48 in/sec and a maximum horizontal ground displacement of 36 in. be used for a unit (1.0g) maximum horizontal acceleration. Newmark also recommended that the maximum vertical ground motion be taken as 2/3 of the corresponding values for the horizontal motion.

With the availability of a large number of recorded earthquake ground motion, particularly during the 1971 San Fernando earthquake, several statistical studies^(2-9, 2-91, 2-53) were carried out to determine the average peak ground velocity and displacement for a given acceleration. These studies recommended two ratios: peak velocity to peak acceleration v/a and peak acceleration-displacement product to the square of the peak velocity ad/v^2 be used in estimating ground velocities and displacements. Certain response spectrum characteristics such as the sharpness or flatness of the spectra can be related to the ad/v^2 ratio as discussed later. According to Newmark and Rosenbleuth⁽²⁻⁹²⁾, for most earthquakes of practical interest, ad/v^2 ranges from approximately 5 to 15. For harmonic oscillations, ad/v^2 is one and for steady-state square acceleration waves, the ratio is one half.

A statistical study of v/a and ad/v^2 ratios was carried out by Mohraz⁽²⁻⁵³⁾ who used a total of 162 components of 54 records from 16 earthquakes. A summary of the v/a and ad/v^2 ratios for records on alluvium, on rock, and on alluvium layers underlain by rock are given in Table 2-9. It is noted that v/a ratios for rock are substantially lower than those for alluvium with the v/a ratios for the two intermediate categories falling between alluvium and rock. Table 2-9 also shows that the v/a ratios for the vertical components are close to those for the horizontal components with the larger of the two peak accelerations. The 50 percentile v/a ratios for the larger of the two peak accelerations from Table 2-9 (24 (in/sec)/g for rock and 48 (in/sec)/g for alluvium) and those given by Seed and Idriss⁽²⁻³⁹⁾ (22 (in/sec)/g for rock and 43 (in/sec)/g for alluvium) are in close agreement. The ad/v^2 ratios in Table 2-9

Table 2-9. Summary of Ground Motion Relationships [after Mohraz (2-53)]

Soil Category	Group*	v/a (in/sec)/g	ad/v^2	d/a (in/g)	$a_{vertical}/(a_{horizontal})_L$
Rock	L	24	5.3	8	0.48
	S	27	5.2	10	
	V	28	6.1	12	
<30 ft of alluvium underlain by rock	L	30	4.5	11	0.47
	S	39	4.2	17	
	V	33	6.8	19	
30-200 ft of alluvium underlain by rock	L	30	5.1	12	0.40
	S	36	3.8	13	
	V	30	7.6	18	
Alluvium	L	48	3.9	23	0.42
	S	57	3.5	29	
	V	48	4.6	27	

* L: Horizontal components with the larger of the two peak accelerations

S: Horizontal components with the smaller of the two peak accelerations

V: Vertical components

indicate that, in general, the ratios for alluvium are smaller than those for rock and those for alluvium layers underlain by rock. The d/a ratios are also presented in Table 2-9. The values indicate that for a given acceleration, the displacements for alluvium are 2 to 3 times those for rock. The table also includes the ratio of the vertical acceleration to the larger of the two peak horizontal accelerations where it is apparent that the ratios are generally close to each other indicating that soil condition does not influence the ratios. The ratio of the vertical to horizontal acceleration of 2/3 which Newmark recommended is too conservative, but its use was justified to account for the variations greater than the median and the uncertainties in the ground motion in the vertical direction⁽²⁻⁹¹⁾.

Statistical studies of v/a and ad/v^2 ratios for the Loma Prieta earthquake of October 17, 1989 were carried out by Mohraz and Tiv⁽²⁻⁹³⁾. They used approximately the same number of horizontal components of the records on rock and alluvium that Mohraz⁽²⁻⁵³⁾ used in his earlier study. Their study indicated a mean v/a ratio of 51 and 49 (in/sec)/g and a mean ad/v^2 ratio of 2.8 and 2.6 for rock and alluvium, respectively. The differences in v/a and ad/v^2

ratios from the Loma Prieta and previous earthquakes indicate that each earthquake is different and that site condition, magnitude, epicentral distance, and duration influence the characteristics of the recorded ground motion.

2.7 EARTHQUAKE RESPONSE SPECTRA

Response spectrum is an important tool in the seismic analysis and design of structures and equipment. Unlike the power spectral density which presents information about input energy and frequency content of ground motion, the response spectrum presents the maximum response of a structure to a given earthquake ground motion. The response spectrum introduced by Biot^(2-1, 2-2) and Housner⁽²⁻³⁾ describes the maximum response of a damped single-degree-of-freedom (SDOF) oscillator at different frequencies or periods. The detailed procedure for computing and plotting the response spectrum is discussed in Chapter 3 of this handbook and in a number of publications (see for example 2-54, 2-22, 2-94, 2-95). It was customary to plot the response spectrum on a tripartite paper (four-way logarithmic paper) so that at a given frequency

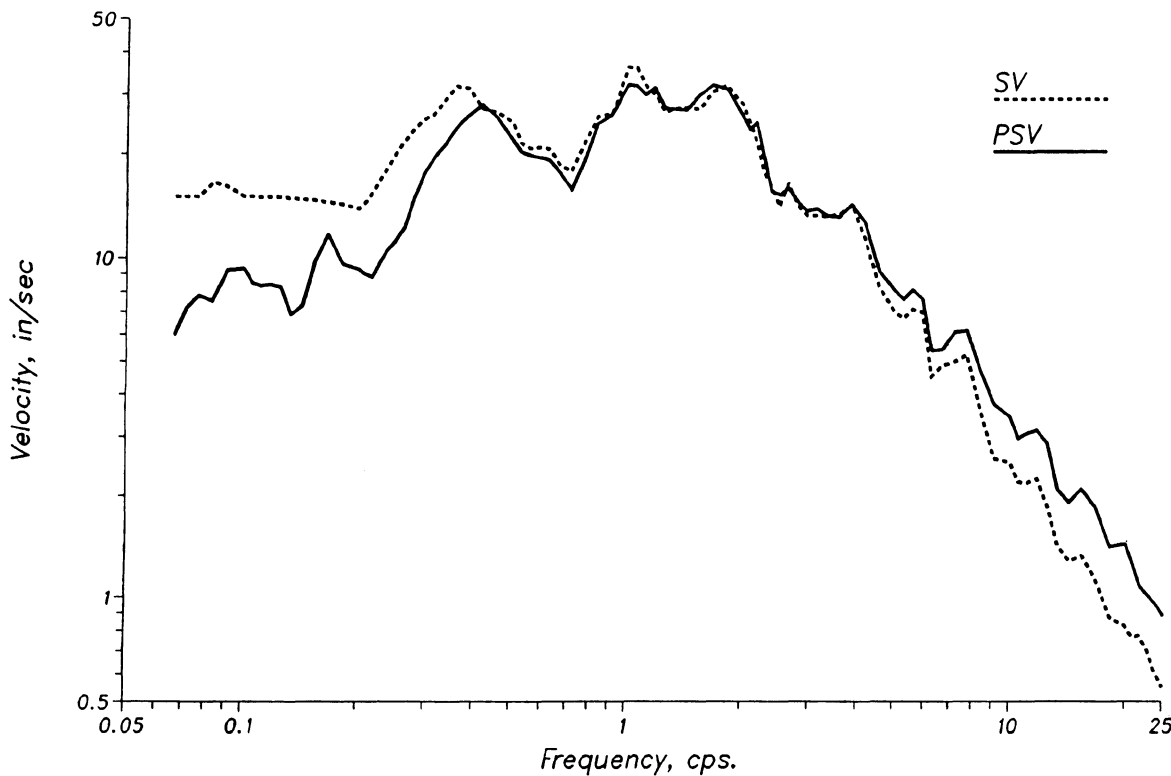


Figure 2-34. Comparison of pseudo-velocity and maximum relative velocity for 5% damping for the S00E component of El Centro, the Imperial Valley earthquake of May 18, 1940.

or period, the maximum relative displacement SD , the pseudo-velocity PSV , and the pseudo-acceleration PSA can all be read from the plot simultaneously. The parameters PSV and PSA which are expressed in terms of SD and the circular natural frequency ω as $PSV = \omega SD$ and $PSA = \omega^2 SD$ have certain characteristics that are of practical interest ⁽²⁻⁸⁷⁾. The pseudo-velocity PSV is close to the maximum relative velocity SV at high frequencies (frequencies greater than 5 Hz), approximately equal for intermediate frequencies (frequencies between 0.5 Hz and 5 Hz) but different for low frequencies (frequencies smaller than 0.5 Hz) as shown in Figure 2-34. In a recent study by Sadek et al. ⁽²⁻⁹⁶⁾, based on a statistical analysis of 40 damped SDOF structures with period range of 0.1 to 4.0 sec subjected to 72 accelerograms, it was found that the maximum relative velocity SV is equal to the pseudo-velocity PSV for periods in the neighborhood of

0.5 sec (frequency of 2 Hz). For periods shorter than 0.5 sec, SV is smaller than PSV while for periods longer than 0.5 sec, SV is larger and increases as the period and damping ratio increase. A regression analysis was used to establish the following relationship between the maximum velocity and pseudo-velocity responses:

$$\frac{SV}{PSV} = a_v T^{b_v} \quad (2-38)$$

where $a_v = 1.095 + 0.647\beta - 0.382\beta^2$, $b_v = 0.193 + 0.838\beta - 0.621\beta^2$, T is the natural period, and β is the damping ratio. The relationship between SV and PSV is presented in Figure 2-35.

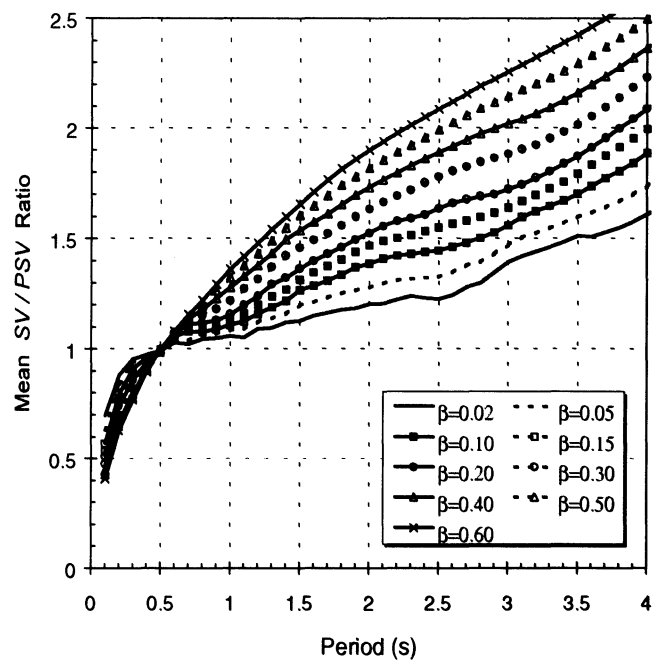


Figure 2-35. Mean ratio of maximum relative velocity to pseudo-velocity for SDOF structures with different damping ratios. [After Sadek et al. (2-96).]

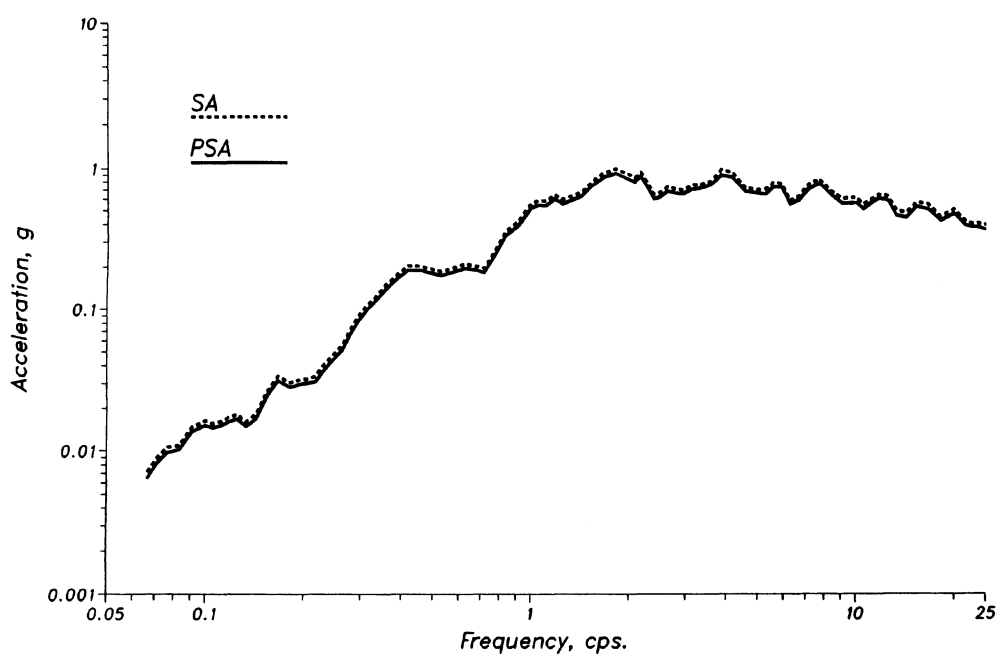


Figure 2-36. Comparison of pseudo-acceleration and maximum absolute acceleration for 5% damping for the S00E component of El Centro, the Imperial Valley earthquake of May 18, 1940.

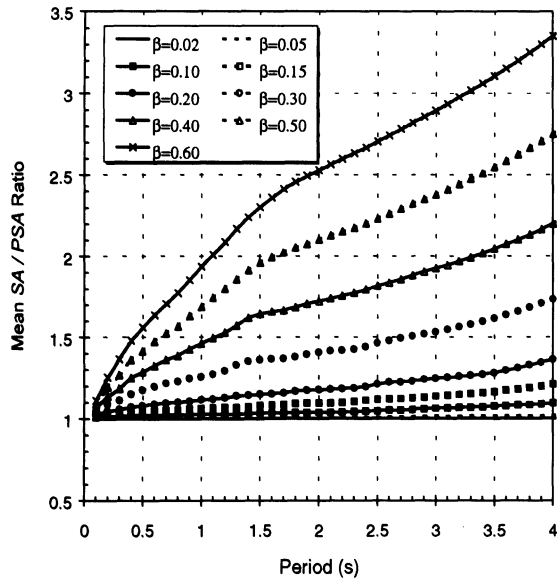


Figure 2-37. Mean ratio of maximum absolute acceleration to pseudo-acceleration for SDOF structures with different damping ratios. [After Sadek et al. (2-96).]

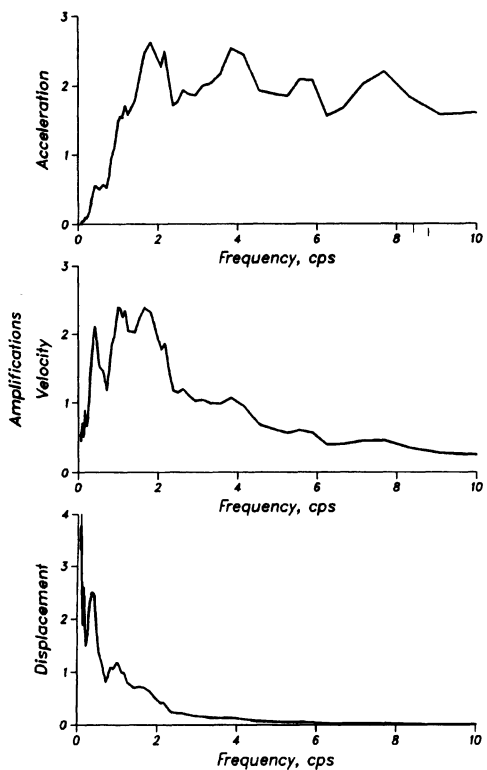


Figure 2-38. Acceleration, velocity, and displacement amplifications plotted as a function of frequency for 5% damping for the S00E component of El Centro, the Imperial Valley earthquake of May 18, 1940.

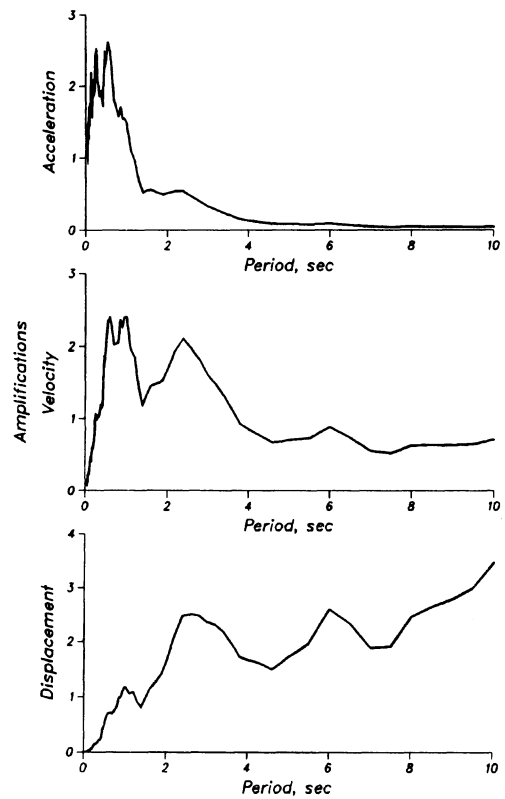


Figure 2-39. Acceleration, velocity, and displacement amplifications plotted as a function of period for 5% damping for the S00E component of El Centro, the Imperial Valley earthquake of May 18, 1940.

For zero damping, the pseudo-acceleration PSA is equal to the maximum absolute acceleration SA , but for dampings other than zero, the two are slightly different. For the inherent damping levels encountered in most engineering applications, however, the two can be considered approximately equal (see Figure 2-36). When a structure is equipped with supplemental dampers to provide large damping ratios, the difference between PSA and SA becomes significant, especially for structures with long periods. Using the results of a statistical analysis of 72 earthquake records, Sadek et al. (2-96) described the relationship between PSA and SA as:

$$\frac{SA}{PSA} = 1 + a_a T^{b_a} \quad (2-39)$$

where $a_a = 2.436\beta^{1.895}$ and $b_a = 0.628 + 0.205\beta$. The relationship between *SA* and *PSA* is presented in Figure 2-37.

Arithmetic and semi-logarithmic plots have also been used to represent response spectra. Building codes have presented design spectra in terms of acceleration amplification as a function of period on an arithmetic scale. Typical acceleration, velocity, and displacement amplifications for the S00E component of El Centro, the Imperial Valley earthquake of May 18, 1940 are shown in Figures 2-38 and 2-39 - the former plotted as a function of frequency and the latter as a function of period.

To show how ground motion is amplified in different regions of the spectrum, the peak ground displacement, velocity, and acceleration

for the S00E component of El Centro are plotted together on the response spectra, Figure 2-40. Several observations can be made from this figure. At small frequencies or long periods, the maximum relative displacement is large, whereas the pseudo-acceleration is small. At large frequencies or short periods, the relative displacement is extremely small, whereas the pseudo-acceleration is relatively large. At intermediate frequencies or periods, the pseudo-velocity is substantially larger than those at either end of the spectrum. Consequently, three regions are usually identified in a response spectrum: the low frequency or displacement region, the intermediate frequency or velocity region, and the high frequency or acceleration region. In each region, the corresponding ground motion is amplified the most. Figure 2-40 also shows

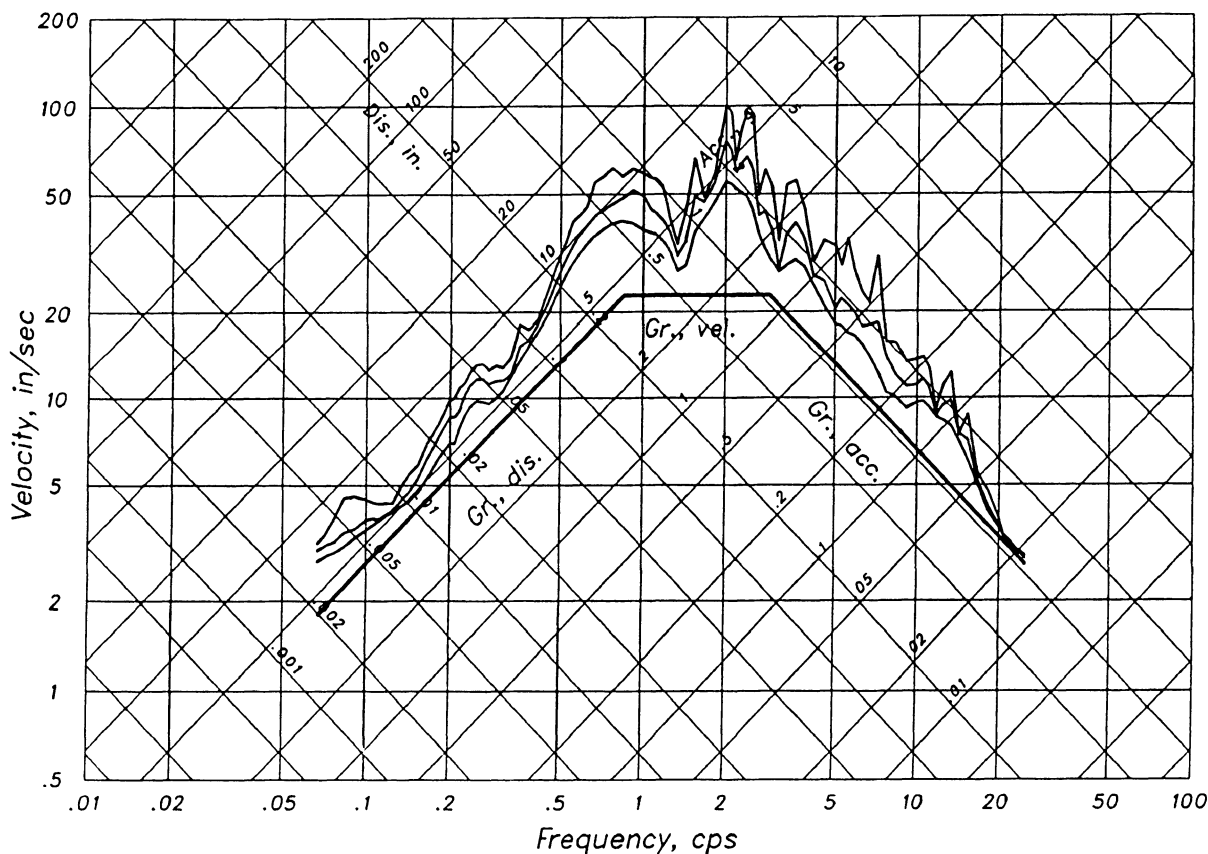


Figure 2-40. Response spectra for 2, 5, and 10% damping for the S00E component of El Centro, the Imperial Valley earthquake of May 18, 1940, together with the peak ground motions.

that at small frequencies (0.05 Hz or less), the spectral displacement approaches the peak ground displacement indicating that for very flexible systems, the maximum displacement is equal to that of the ground. At large frequencies (25-30 Hz), the pseudo-acceleration approaches the peak ground acceleration, indicating that for rigid systems, the absolute acceleration of the mass is the same as the ground. As indicated in Figure 2-40, the response spectra for a given earthquake record is quite irregular and has a number of peaks and valleys. The irregularities are sharp for small damping ratios, and become smoother as damping increases. As discussed previously, the ratio of ad/v^2 influences the shape of the spectrum. A small ad/v^2 ratio results in a pointed or sharp spectrum while a large ad/v^2 ratio results in a flat spectrum in the velocity region. Response spectra may shift toward high or low frequency regions according to the frequency content of the ground motion.

While response spectra for a specified earthquake record may be used to obtain the response of a structure to an earthquake ground motion with similar characteristics, they cannot be used for design because the response of the same structure to another earthquake record will undoubtedly be different. Nevertheless, the recorded ground motion and computed response spectra of past earthquakes exhibit certain similarities. For example, studies have shown that the response spectra from accelerograms recorded on similar soil conditions reflect similarities in shape and amplifications. For this reason, response spectra from records with common characteristics are averaged and then smoothed before they are used in design.

2.8 FACTORS INFLUENCING RESPONSE SPECTRA

Earthquake parameters such as soil condition, epicentral distance, magnitude, duration, and source characteristics influence the shape and amplitudes of response spectra. While the effects of some parameters may be studied independently, the influences of several factors are interrelated and cannot be discussed

individually. Some of these influences are discussed below:

2.8.1 Site geology

Prior to the San Fernando earthquake of 1971, accelerograms were limited in number and therefore not sufficient to determine the influence of different parameters on response spectra. Consequently, most design spectra were based on records on alluvium but they did not refer to any specific soil condition. Studies by Hayashi et al. ⁽²⁻⁹⁷⁾ and Kuribayashi et al. ⁽²⁻⁹⁸⁾ on the effects of soil conditions on Japanese earthquakes had shown that soil conditions significantly affect the spectral shapes. Other studies by Mohraz et al. ⁽²⁻⁹⁾ and Hall et al. ⁽²⁻⁹¹⁾ also referred to the influence of soil condition on spectral shapes.

The 1971 San Fernando earthquake provided a large database to study the influence of many earthquake parameters including soil condition on earthquake ground motion and response spectra. In 1976, two independent studies, one by Seed, Ugas, and Lysmer ⁽²⁻⁹⁹⁾, and the other by Mohraz ⁽²⁻⁵³⁾ considered the influence of soil condition on response spectra. The study by Seed et al. used 104 horizontal components of earthquake records from 23 earthquakes. The records were divided into four categories: rock, stiff soils less than about 150 ft deep, deep cohesionless soil with depths greater than 250 ft, and soft to medium clay and sand. The response spectra for 5% damping⁴ were normalized to the peak ground acceleration of the records and averaged at various periods. The average and the mean plus one standard deviation (84.1 percentile) spectra for the four categories from their study is presented in Figures 2-41 and 2-42. The ordinates in these plots represent the acceleration amplifications. Also shown in Figure 2-42 is the Nuclear Regulatory Commission (NRC) design spectrum proposed

⁴ they limited their study to 5% damping, although the conclusions can easily be extended to other damping coefficients.

by Newmark et al. ^(2-88, 2-100), see Section 2.9. It is seen that soil condition affects the spectra to a significant degree. The figures show that for periods greater than approximately 0.4 to 0.5 sec, the normalized spectral ordinates (amplifications) for rock are substantially lower than those for soft to medium clay and for deep cohesionless soil. This indicates that using the spectra from the latter two groups may overestimate the design amplifications for rock.

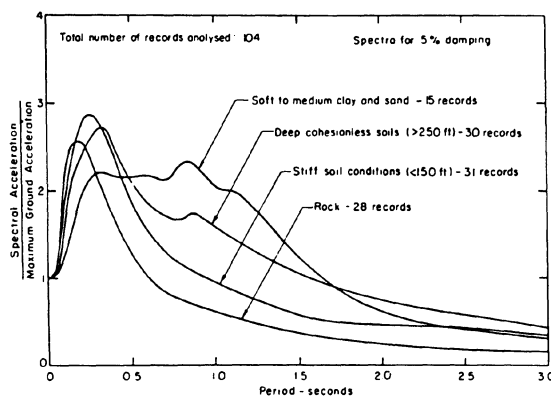


Figure 2-41. Average acceleration spectra for different soil conditions. [After Seed et al. (2-99).]

The study by Mohraz ⁽²⁻⁵³⁾ considered a total of 162 components of earthquake records divided into four soil categories: alluvium, rock, less than 30 ft of alluvium underlain by rock, and 30 - 200 ft of alluvium underlain by rock. Figure 2-43 presents the average acceleration amplifications (ratio of spectral ordinates to peak ground accelerations) for 2% damping for the horizontal components with the larger of the two peak ground accelerations. Consistent with the study by Seed et al. ⁽²⁻⁹⁹⁾, the figure shows that soil condition influences the spectral shapes to a significant degree. The acceleration amplification for alluvium extends over a larger frequency region than the amplifications for the other three soil categories. A comparison of acceleration amplifications for 5% damping from the Seed and Mohraz studies is shown in Figure 2-44. The figure indicates a remarkably close agreement even though the records used in the

two studies are somewhat different. Normalized response spectra corresponding to the mean plus one standard deviation (84.1 percentile) for the four soil categories from the Mohraz study are given in Figure 2-45. The plot indicates that for short periods (high frequencies) the spectral ordinates for alluvium are lower than the others, whereas, for intermediate and long periods they are higher.

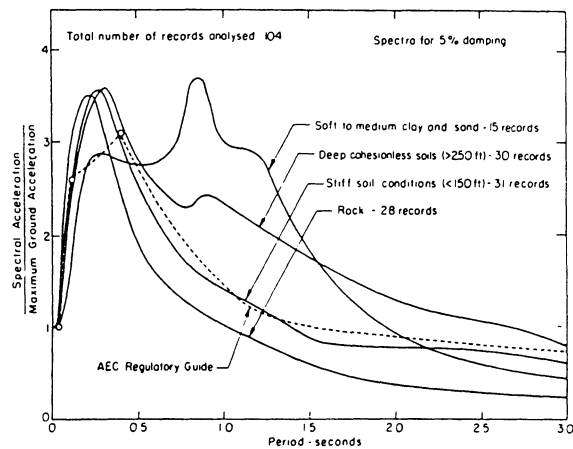


Figure 2-42. Mean plus one standard deviation acceleration spectra for different soil conditions. [After seed et al. (2-99).]

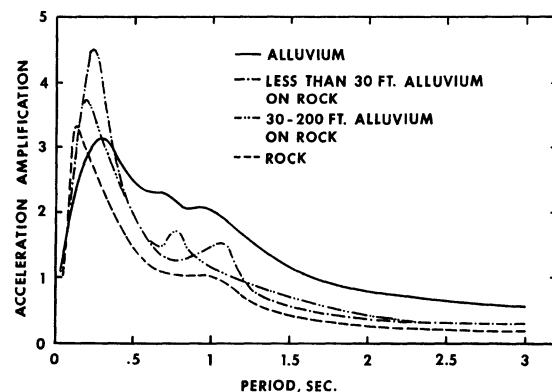


Figure 2-43. Average horizontal acceleration amplifications for 2% damping for different soil categories. [After Mohraz (2-53).]

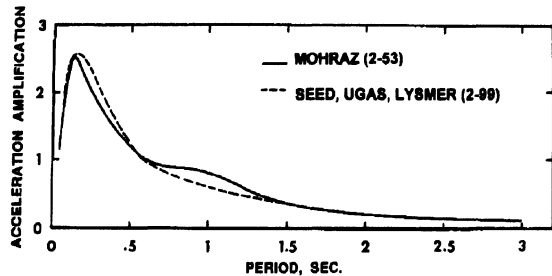


Figure 2-44. Comparison of the average horizontal acceleration amplifications for 5% damping for rock.
[After Mohraz (2-53).]

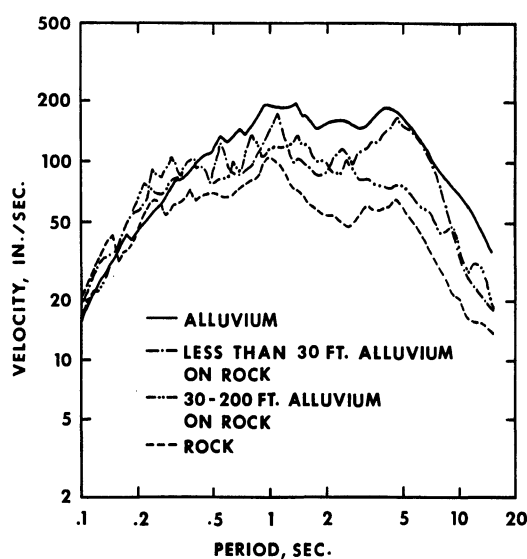


Figure 2-45. Mean plus one standard deviation response spectra for 2% damping for different soil categories, normalized to 1.0g horizontal ground acceleration. [After Mohraz (2-53).]

Recent studies indicate that the spectral shape not only depends on the three peak ground motions, but also on other parameters such as earthquake magnitude, source-to-site distance, soil condition, and source characteristics. Similar to ground motion attenuation relationships (Section 2.4), several investigators have used statistical analysis of the spectra at different periods to develop equations for computing the spectral ordinates in terms of those parameters. For example, Crouse and McGuire⁽²⁻¹⁰¹⁾ used 238 horizontal accelerograms from 16 earthquakes between 1933 and 1992 with surface wave magnitudes

greater than 6 to formulate a relationship for pseudo-velocity in terms of various earthquake parameters. The response spectra for 5% damping were computed for four site categories; rock, soft rock or stiff soil, medium stiff soil, and soft soil classified as soil class A through D, respectively. A regression analysis was performed for periods in the range of 0.1 to 4.0 sec. Their proposed equation for the pseudo-velocity (PSV) in cm/sec is given as

$$\begin{aligned} \ln(PSV) = & a + bM_s \\ & + d \ln[R + c_1 \exp(c_2 M_s)] + eF \end{aligned} \quad (2-40)$$

where M_s is the surface wave magnitude, R is the closest distance from the site to the fault rupture in km, and F is the fault type parameter which equals 1 for reverse-slip and 0 for strike-slip earthquakes. The parameters a , b , c_1 , c_2 , d and e are given in tabular form for different periods and soil categories⁽²⁻¹⁰¹⁾. Parameters b , c_1 , and c_2 are greater than zero whereas d is less than zero for all periods and different soil conditions. Figure 2-46 presents the spectral shapes for the four soil categories at a distance of 10 km from the source for a strike-slip earthquake of magnitude 7. The figure indicates higher spectral values for softer soils.

A similar study was carried out by Boore et al.⁽²⁻³⁷⁾ using the average shear wave velocity V_s (m/sec) in the upper 30 m of the surface to classify the soil condition. In their study, the pseudo-acceleration response PSA in g is given by

$$\begin{aligned} \ln(PSA) = & b_1 + b_2(M_w - 6) \\ & + b_3(M_w - 6)^2 + b_5 \ln \sqrt{R_{jb}^2 + h^2} \\ & + b_v \ln \frac{V_s}{V_A} \end{aligned} \quad (2-41)$$

where M_w and R_{jb} are the moment magnitude and distance (see section 2.4.1), respectively. The parameter b_1 is related to the fault type and is listed for different periods for strike-slip and reverse-slip earthquakes, and the case where the

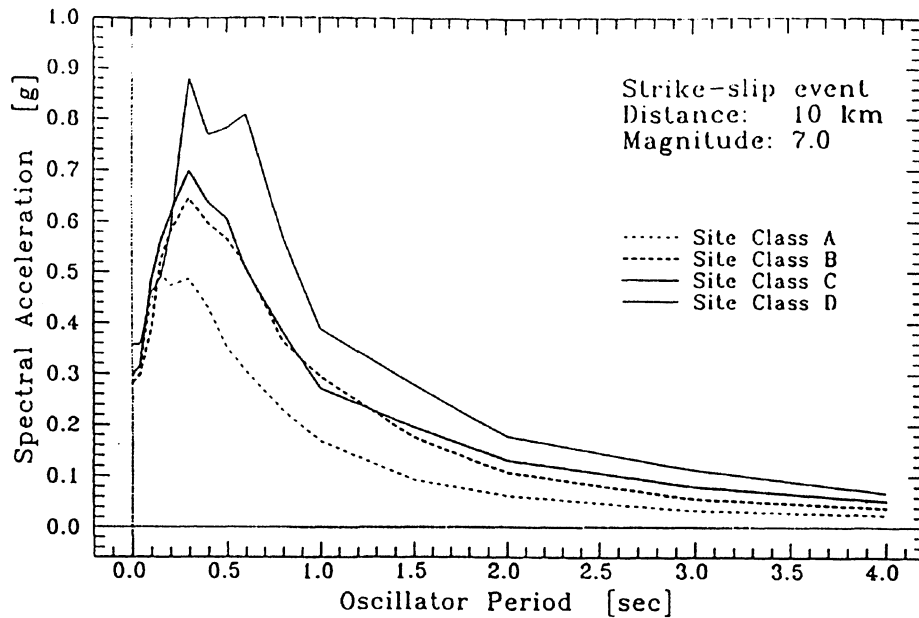


Figure 2-46. Response spectra for 5% damping for different soil conditions for a magnitude 7 strike-slip earthquake. [After Crouse and McGuire (2-101).]

fault mechanism is not specified. Factors b_2 , b_3 , b_5 , b_v , V_A , and h for different periods are also presented in tabular form⁽²⁻³⁷⁾. The parameters b_2 , V_A , and h are always positive whereas b_3 , b_5 , and b_v are always negative. Consistent with the study by Crouse and McGuire⁽²⁻¹⁰¹⁾, Equation 2-41 indicates that, for the same distance, magnitude, and fault mechanism, as the soil becomes stiffer (a higher shear wave velocity), the pseudo-acceleration becomes smaller since b_v is always negative.

2.8.2 Magnitude

In the past, the influence of earthquake magnitude on response spectra was generally taken into consideration when specifying the peak ground acceleration at a site. Consequently, the spectral shapes and amplifications in Figures 2-41 and 2-42 were obtained independent of earthquake magnitude. Earthquake magnitude does, however, influence spectral amplifications to a certain degree. A study by Mohraz⁽²⁻¹⁰²⁾ on the influence of earthquake magnitude on response

amplifications for alluvium shows larger acceleration amplifications for records with magnitudes between 6 and 7 than those with magnitudes between 5 and 6 (see Figure 2-47). While the study used a limited number of records and no specific recommendation was made, the figure indicates that earthquake magnitude can influence spectral shapes and may need to be considered when developing design spectra for a specific site.

Equations 2-40 and 2-41 in the previous section include the influence of earthquake magnitude on the pseudo-velocity and pseudo-acceleration, respectively. The equations indicate that spectral ordinates increase with an increase in earthquake magnitude. Figure 2-48 presents the spectral ordinates computed using Equation 2-41 by Boore et al.⁽²⁻³⁷⁾ for soil with a $V_s = 310$ m/sec at a zero source distance for earthquakes with magnitudes 6.5 and 7.5 and an unspecified fault mechanism. The figure indicates that the effect of magnitude is more pronounced at longer periods and it also shows a comparison with the spectra computed from an earlier study by Joyner and Boore⁽²⁻³²⁾.

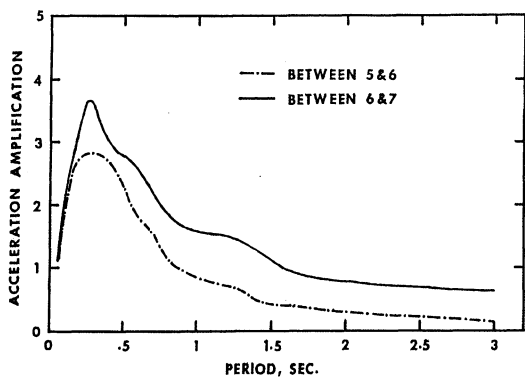


Figure 2-47. Effect of earthquake magnitude on spectral shapes. [After Mohraz (2-102).]

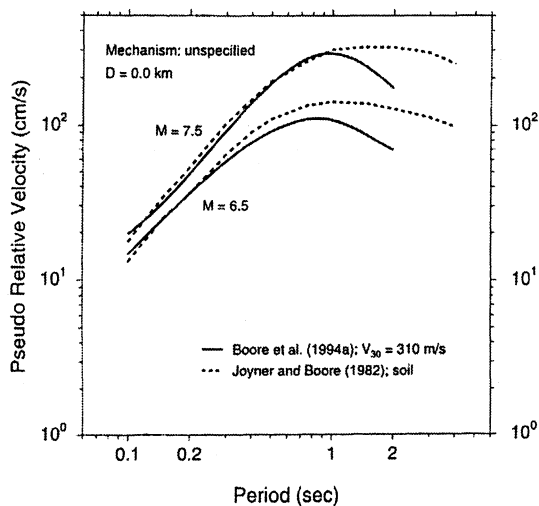


Figure 2-48. Pseudo-velocity spectra for 5% damping on soil and earthquake magnitudes 6.5 and 7.5 at a zero distance. [After Boore et al. (2-37).]

2.8.3 Distance

Recent studies have considered the effect of distance on the shape and amplitudes of the earthquake spectra. Using the data from the Loma Prieta earthquake of October 17, 1989; Mohraz⁽²⁻¹⁰³⁾ divided the records into three groups: near-field (distance less than 20 km), mid-field (distance between 20 to 50 km) and far-field (distance greater than 50 km). The average acceleration amplification (pseudo-

acceleration divided by the peak ground acceleration) for the records on rock and on alluvium for the three groups are shown in Figure 2-49. The plots indicate that for sites on rock, the amplifications for the near-field are substantially smaller than those for mid- or far-field for periods longer than 0.5 sec. For shorter periods, however, the amplifications for the near-field are larger. The effect of distance is less pronounced for records on alluvium.

Equation 2-40 proposed by Crouse and McGuire⁽²⁻¹⁰¹⁾ shows that the spectral ordinates decay with the logarithm of the distance (parameter d in the equation is always negative) for a given soil, earthquake magnitude, and source characteristics. A similar trend is also observed from Equation 2-41 by Boore et al.⁽²⁻³⁷⁾. Figure 2-50 shows the pseudo-velocity response computed using Equation 2-41 for sites on soil for a magnitude of 7.5 at various source distances for strike-slip and reverse-slip fault mechanisms. The figure indicates that the spectral ordinates decrease with distance. Since the spectral shapes are nearly parallel to each other for the distance range of 10 to 80 km, it may be concluded that distance does not significantly affect the spectral shape but influences the spectral ordinates through attenuation of ground acceleration.

2.8.4 Source characteristics

Fault mechanism may influence the spectral ordinates. Using Equation 2-40, Crouse and McGuire⁽²⁻¹⁰¹⁾, computed the ratios of the spectral ordinates for a reverse-slip fault to ordinates for strike-slip fault for two soil categories: soft rock or stiff soil (site class B) and medium stiff soil (site class C). The ratios, plotted in Figure 2-51, show that the spectral ordinates for reverse-slip faults are greater than the ordinates for strike-slip faults for short periods but not for long periods. Crouse and McGuire concluded, however, that it is difficult to attach any significance on the influence of fault mechanism on the spectral shape. Similar trends and conclusion can also be depicted from

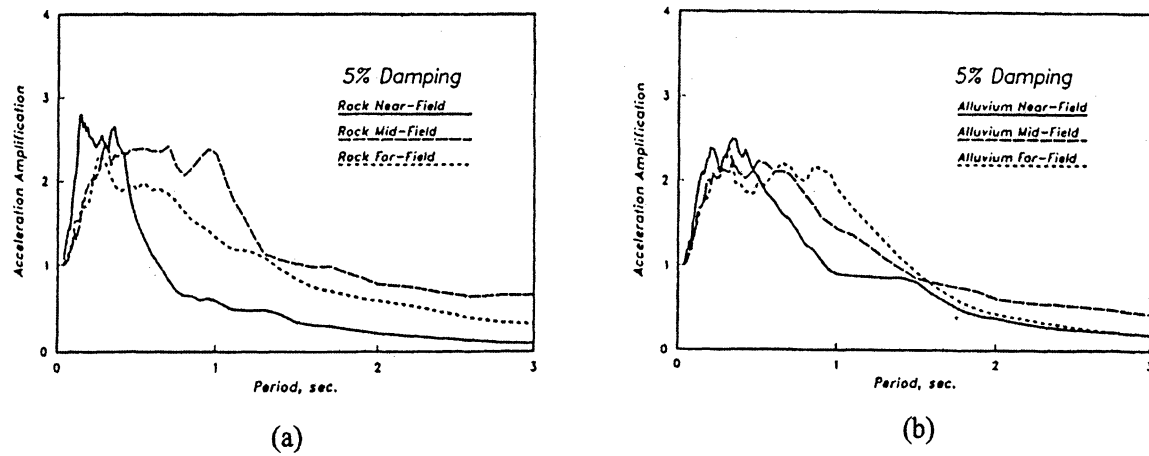


Figure 2-49. Average acceleration amplification for 5% damping for different distances from the 1989 Loma Prieta earthquake for sites on (a) rock and (b) alluvium. [After Mohraz (2-103).]

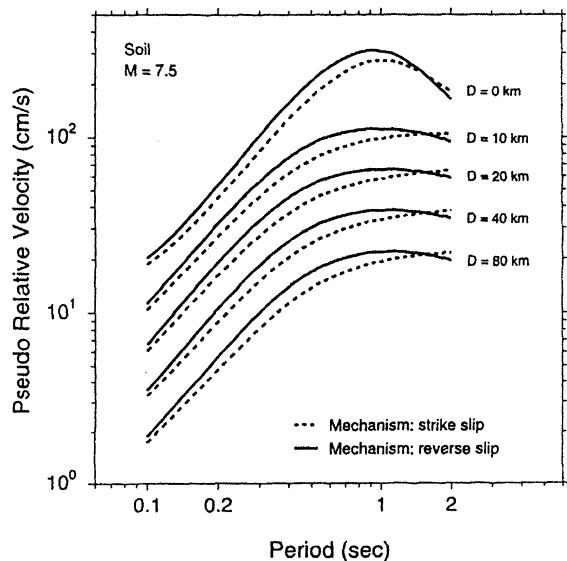


Figure 2-50. Pseudo-velocity spectra for 5% damping on soil and for earthquake magnitude 7.5 at different distances. [After Boore et al. (2-37).]

Figure 2-50 by Boore et al. ⁽²⁻³⁷⁾ where the reverse-slip faults result in a larger response for short periods and the strike-slip faults result in a larger response for long periods. The difference between the response from the two fault mechanisms, however, is not that significant.

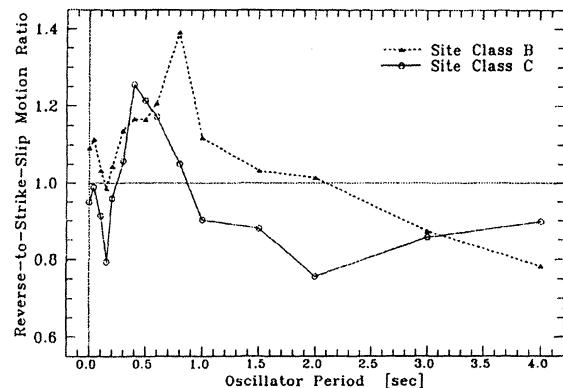


Figure 2-51. Ratio of reverse-slip to strike-slip spectral ordinates for soft rock or stiff soil referenced as site class B and medium stiff soil referenced as site class C. [After Crouse and McGuire (2-101).]

2.8.5 Duration

While earthquake response spectra provide the best quantitative description of the intensity and frequency content of ground motion, they do not provide information on the duration of strong shaking -- a parameter that many researchers and practitioners consider to be important in evaluating the damaging effects of an earthquake. The influence of the duration of

strong motion on spectral shapes has been studied by Peng et al. ⁽²⁻¹⁰⁴⁾ who used a random vibration approach to estimate site-dependent probabilistic response spectra. Their study shows that long durations of strong motion increase the response in the low and intermediate frequency regions. This is consistent with the fact that accelerograms with long durations have a greater probability of containing long-period wave components which can result in a large response in the long period or low frequency region of the spectrum.

2.9 EARTHQUAKE DESIGN SPECTRA

Because the detailed characteristics of future earthquakes are not known, the majority of earthquake design spectra are obtained by averaging a set of response spectra from records with similar characteristics such as soil condition, epicentral distance, magnitude, source mechanism, etc. For practical applications, design spectra are presented as smooth curves or straight lines. Smoothing is carried out to eliminate the peaks and valleys in the response spectra that are not desirable for design because of the difficulties encountered in determining the exact frequencies and mode shapes of structures during severe earthquakes when the structural behavior is most likely nonlinear. It should be noted that in some cases, determining the shape of the design spectra for a particular site is complicated and caution should be used in arriving at a representative set of records. For example, long period components of strong motion have a pronounced effect on the response of flexible structures. Recent strong motion data indicates that long period components are influenced by factors such as distance, source type, rupture propagation, travel path, and local soil conditions ^(2-50, 2-105, 2-106). In addition, the direction and spread of rupture propagation can affect motion in the near-field. For these reasons, the selection of an appropriate set of records in arriving at representative design spectra is important and may require selection

of different sets of records for different regions of the spectrum.

The difference between response spectra and design spectra should be kept in mind. A response spectrum is a plot of the maximum response of a damped SDOF oscillator with different frequencies or periods to a specific ground motion, whereas a smooth or a design spectrum is a specification of seismic design force or displacement of a structure having a certain frequency or period of vibration and damping ⁽²⁻¹⁰⁷⁾.

Since the peak ground acceleration, velocity, and displacement for various earthquake records differ, the computed response cannot be averaged on an absolute basis. Various procedures are used to normalize response spectra before averaging is carried out. Among these procedures, two have been most commonly used: 1) normalization according to spectrum intensity ⁽²⁻¹⁰⁸⁾ where the areas under the spectra between two given frequencies or periods are set equal to each other, and 2) normalization to peak ground motion where the spectral ordinates are divided by peak ground acceleration, velocity, or displacement for the corresponding region of the spectrum. Normalization to other parameters such as effective peak acceleration and effective peak velocity-related acceleration has also been suggested and used in development of design spectra for seismic codes.

Table 2-10. Relative Values of Spectrum Amplification Factors (after Newmark and Hall, 2-90)

Percent of Critical Damping	Amplification Factor for Displacement Velocity Acceleration		
	2.5	4.0	6.4
0	2.5	4.0	6.4
0.5	2.2	3.6	5.8
1	2.0	3.2	5.2
2	1.8	2.8	4.3
5	1.4	1.9	2.6
7	1.2	1.5	1.9
10	1.1	1.3	1.5
20	1.0	1.1	1.2

The first earthquake design spectrum was developed by Housner ^(2-109, 2-110). His design spectra shown in Figure 2-52 are based on the

characteristics of the two horizontal components of four earthquake ground motions recorded at El Centro, California in 1934 and 1940, Olympia, Washington in 1949, and Taft, California in 1952. The plots are normalized to 20% acceleration ($0.2g$) at zero period (ground acceleration). For any other acceleration, the plots or the information read from them are simply scaled up or down by multiplying them by the ratio of the desired acceleration to $0.2g$.

In the late sixties, Newmark and Hall^{(2-89, 2-}

⁹⁰⁾ recommended straight lines be used to represent earthquake design spectra. They suggested that three amplifications (acceleration, velocity, and displacement) which are constant in the high, intermediate, and low frequency regions of the spectrum (Table 2-10) together with peak ground acceleration, velocity, and displacement of $1.0g$, 48 in/sec, and 36 in. be used to construct design spectra. Their recommended ground motions and the amplifications were based on

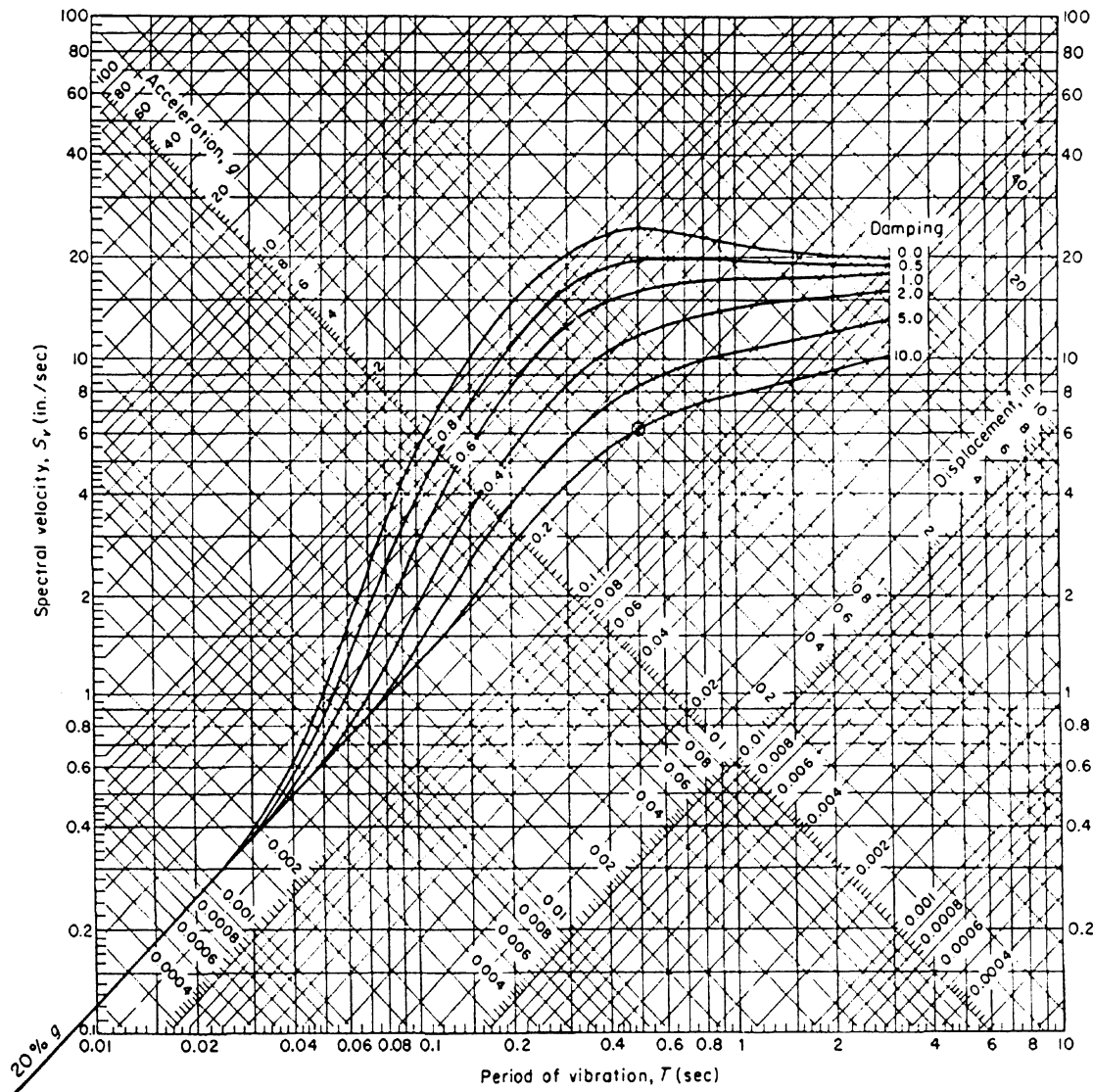


Figure 2-52. Design spectra scaled to 20% ground acceleration. [After Housner (2-110).]

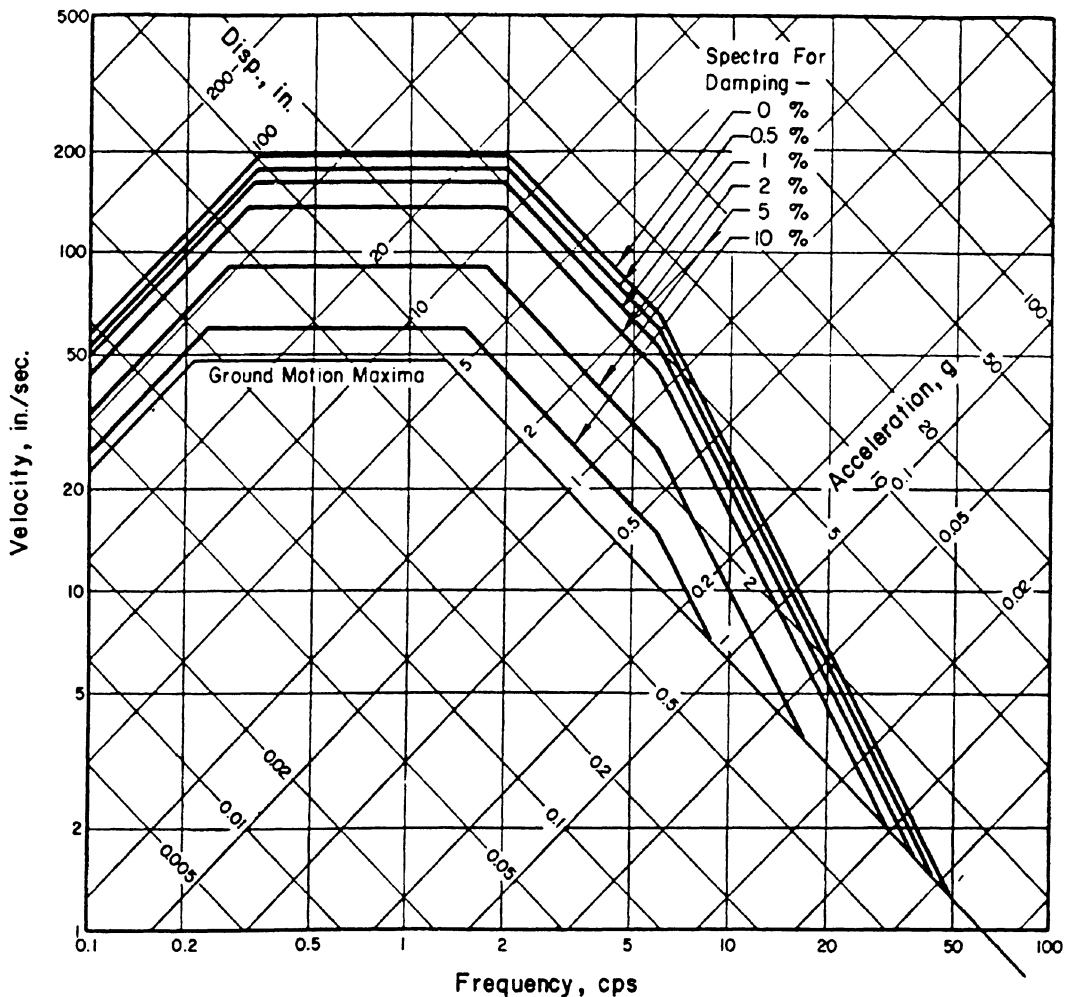


Figure 2-53. Design spectra normalized to 1.0g. [After Newmark and Hall (2-90).]

the characteristics of several earthquake records without considering soil condition. The spectral ordinates which are obtained by multiplying the three ground motions by the corresponding amplifications are plotted on a tripartite (four-way logarithmic) paper as shown in Figure 2-53. The spectral displacement, spectral velocity, and spectral acceleration are plotted parallel to maximum ground displacement, ground velocity, and ground acceleration, respectively. The frequencies at the intersections of spectral displacement and velocity, and spectral velocity and acceleration define the three amplified regions of the spectrum. At a frequency of

approximately 6 Hz, the spectral acceleration is tapered down to the maximum ground acceleration. It is assumed that the spectral acceleration for 2% damping intersects the maximum ground acceleration at a frequency of 30 Hz. The tapered spectral acceleration lines for other dampings are parallel to the one for 2%. The normalized design spectra in Figure 2-53 can be used for design by scaling the ordinates to the desired acceleration.

In the early seventies with increased activity in the design and construction of nuclear power plants in the United States, the Atomic Energy Commission AEC (later renamed the Nuclear

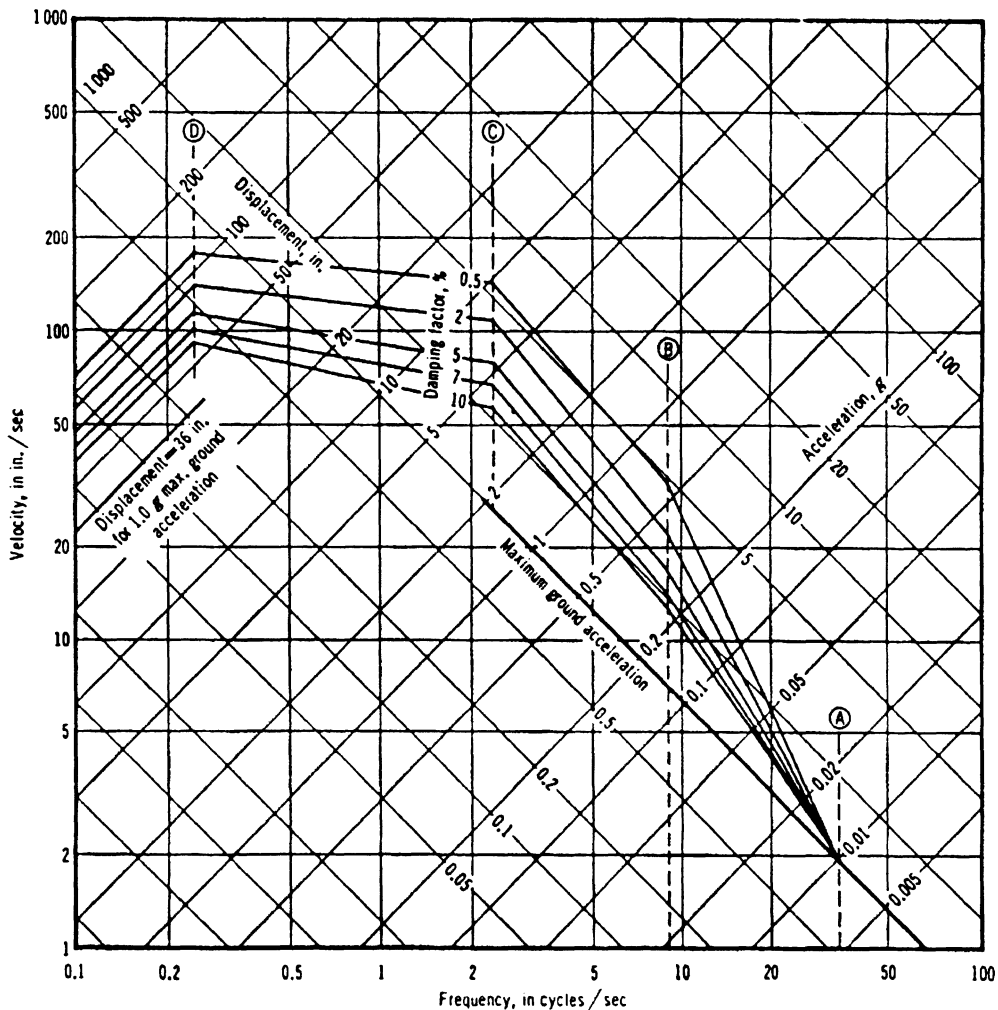


Figure 2-54. NRC horizontal design spectra scaled to 1.0g ground acceleration. A, B, C, and D are control frequencies corresponding to 33, 9, 2.5, and 0.25 HZ, respectively.

Regulatory Commission) funded two studies - one by John A. Blume and Associates⁽²⁻¹¹¹⁾ and the other by N. M. Newmark Consulting Engineering Services⁽²⁻⁹⁾ to develop recommendations for horizontal and vertical design spectra for nuclear power plants. These studies which used a statistical analysis of a number of recorded earthquake ground motions and computed response spectra were the basis for the Nuclear Regulatory Commission (NRC) Regulatory Guide 1.60^(2-88, 2-100). The studies recommended that the mean plus one standard deviation (84.1 percentile) response be used for

the design of nuclear power plants and equipment. The NRC design spectra are constructed using a set of amplifications corresponding to four control frequencies (Figure 2-54). The spectra are normalized to 1.0g horizontal ground acceleration. While the NRC spectra were developed for design of nuclear power plants, they were also used to develop and compare design spectra for other applications.

In 1978, the Applied Technology Council ATC⁽²⁻⁷⁴⁾ recommended a smooth version of the normalized spectral shapes proposed by

Seed et al. ⁽²⁻⁹⁹⁾ be used in developing earthquake design spectra for buildings. The spectral shapes in Figures 2-41 and 2-42 were smoothed using four control periods ⁽²⁻³⁹⁾. In addition, the four soil categories were reduced to three: rock and stiff soils (soil type 1), deep cohesionless or stiff clay soils (soil type 2), and soft to medium clays and sands (soil type 3). The ATC spectra which was adopted by the Seismology Committee of the Structural Engineers Association of California, SEAOC ⁽²⁻¹¹²⁾ is presented in Figure 2-55. A comparison of the spectral shapes from the study by Mohraz ⁽²⁻⁵³⁾ and those proposed by ATC is shown in Figure 2-56. The 1985, 1988, 1991, and 1994 editions of the Uniform Building Code ^(2-82 to 2-85) use the spectral shapes for the three soil conditions recommended by ATC. The design spectra for a given site is computed by multiplying the spectral shapes in Figure 2-55

by the seismic zone factor Z (or the effective peak acceleration) obtained from the seismic maps.

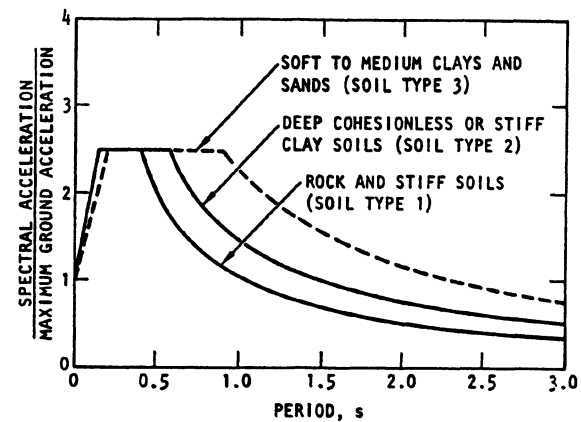


Figure 2-56. Normalized spectral curves recommended for use in building codes. (Reproduced from 2-39).

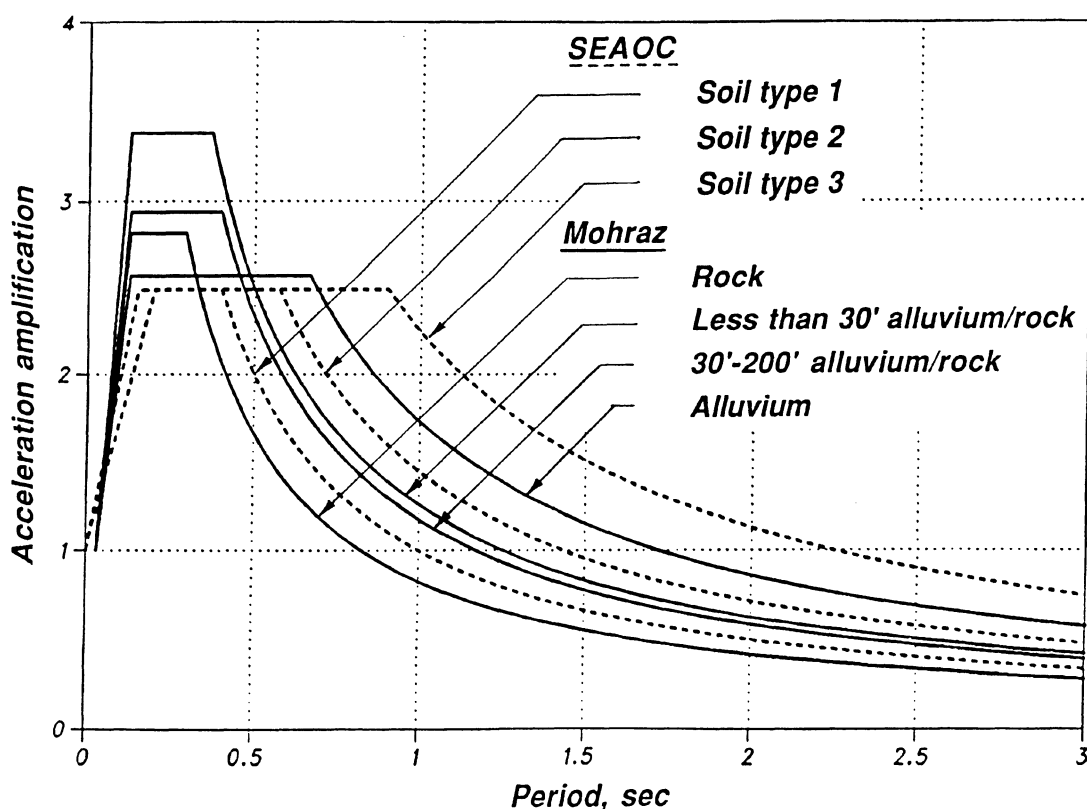


Figure 2-55. Comparison of spectral shapes for 5% damping proposed by Mohraz with those recommended by SEAOC.

The 1985, 1988, and 1991 NEHRP recommended provisions^(2-76 to 2-78) present design spectra using the effective peak acceleration A_a and the effective peak velocity-related acceleration A_v . These two factors which are obtained from seismic maps are used to define the constant acceleration and velocity segments of the design spectrum, respectively. Since A_a and A_v for the vast majority of the sites in the United States are the same, the computed spectra are similar to the UBC spectra. While the 1985 NEHRP provisions included the three soil categories defined by ATC⁽²⁻⁷⁴⁾, the 1988 NEHRP provisions⁽²⁻⁷⁷⁾ and the 1988 Uniform Building Code⁽²⁻⁸³⁾ included a fourth soil category S_4 based on the experience from the Mexico City earthquake of September 19, 1985 where most of the underlying soil is very soft⁵. Flexible structures (periods in the neighborhood of 2 sec) in that earthquake experienced large acceleration amplifications which resulted in severe and widespread damage. Consequently, it was recommended to compute the spectral shape in the velocity region from that of rock using an amplification of 2.

A new procedure for constructing design spectra and computing the base shears was recommended in the 1991 NEHRP provisions⁽²⁻⁷⁸⁾ by obtaining the spectral acceleration ordinates at periods of 0.3 and 1.0 sec from the spectral maps (see Section 2.5). The ordinate at 0.3 sec is used for the constant acceleration zone whereas the ordinate at 1.0 sec is divided by the period T for the velocity zone. The spectral ordinates from the maps are modified according to the soil category of the site. The maps in the 1991 NEHRP provisions were provided for the soil category S_2 (deep cohesionless or stiff clay soils). The provisions recommended that the spectral ordinates corresponding to the 1.0 sec period be reduced by a factor of 0.8 for soil type S_1 and amplified by factors of 1.3 and 1.7 for soil types S_3 and S_4 , respectively.

⁵ the shaking was most intense within a region underlain by an ancient dry lake bed composed of soft clay deposits.

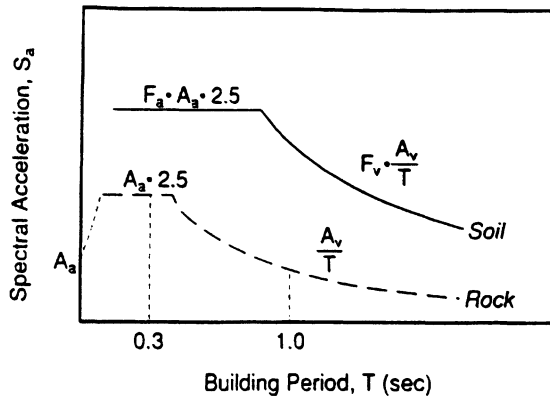


Figure 2-57. Two-factor approach for constructing site-dependent design spectra recommended by the 1994 NEHRP recommended provisions.

In 1992, a workshop on site response during earthquakes was held by the National Center for Earthquake Engineering Research (NCEER), the Structural Engineers Association of California (SEAOC), and the Building Seismic Safety Council (BSSC). The workshop⁽²⁻¹¹³⁾ recommended that the spectral amplifications at different periods should depend not only on the soil condition but also on the intensity of shaking due to soil nonlinearities. Consequently, a two-factor approach was suggested for constructing the design spectra in order to account for the dependence of the spectral shape on the shaking intensity. The two-factor approach was introduced in the 1994 NEHRP provisions⁽²⁻⁷⁹⁾, see Figure 2-57. The approach uses new seismic coefficients C_a and C_v in terms of the effective peak acceleration A_a and the effective peak velocity-related acceleration A_v such that

$$C_a = A_a F_a \text{ and } C_v = A_v F_v \quad (2-42)$$

where F_a and F_v are site amplification coefficients that vary according to soil condition and shaking intensity (seismic zone). The provisions included tables for computing coefficients F_a and F_v as well as C_a and C_v . Six soil categories, designated as A through F, were introduced in the provisions. The first five are based primarily on the average shear wave

velocity⁶ V_s (m/sec) in the upper 30 meters of the soil profile and the sixth is based on a site specific evaluation. The categories include: (A) hard rock ($V_s > 1500$), (B) rock ($760 < V_s \leq 1500$), (C) very dense soil and soft rock ($360 < V_s \leq 760$), (D) stiff soil profile ($180 < V_s \leq 360$), (E) soft soil profile ($V_s \leq 180$), and (F) soils requiring site-specific evaluations such as liquefiable and collapsible soils, sensitive clays, peats and highly organic clays, very high plasticity clays, and very thick soft/medium stiff clays.

The site coefficients F_a and F_v are based primarily on the work of Borcherdt⁽²⁻¹¹⁴⁾ who used the strong motion data from the Loma Prieta earthquake of October 17, 1989 to compute average amplification factors normalized to firm to hard rock (NEHRP site class B) for short-periods (0.1-0.5 sec), intermediate-periods (0.5-1.5 sec), mid-periods (0.4-2.0 sec), and long-periods (1.5-5.0 sec). Data for ground accelerations of approximately 0.1g were used in an empirical procedure to find amplifications F_a and F_v . Amplification factors for ground accelerations greater than 0.1g (0.2g, 0.3g, and 0.4g) were computed by extrapolation of amplification estimates at 0.1g since few strong motion records were available for ground motions greater than 0.1g for soft soil. The extrapolations were based on results from laboratory experiments and numerical modeling. The amplifications were in good agreement with those computed by Seed et al.⁽²⁻¹¹⁵⁾ based on a numerical modeling of the data from the Loma Prieta records and those by Dobry et al.⁽²⁻¹¹⁶⁾ based on a parametric study of several hundred soil profiles.

The amplifications F_a and F_v corresponding to short- and mid- periods with respect to firm to hard rock for different shaking intensities are shown in Figure 2-58. The figure indicates that site amplifications decrease with an increase in shear wave velocity and an increase in ground accelerations. Borcherdt also presented the site

amplifications in terms of the average shear wave velocity V_o in the upper 30 meters of the soil profile as:

$$\begin{aligned} F_a &= (V_o/V_s)^{m_a} \\ F_v &= (V_o/V_s)^{m_v} \end{aligned} \quad (2-43)$$

Where V_o is the average shear wave velocity for a referenced soil profile ($V_o = 1050$ m/sec for firm to hard rock). Parameters m_a and m_v represent the influence of the ground motion intensity on amplification (see Figure 2-58). Substitution for V_o results in

$$\begin{aligned} F_a &= (1050/V_s)^{m_a} \\ F_v &= (1050/V_s)^{m_v} \end{aligned} \quad (2-44)$$

The coefficients F_a and F_v recommended by Borcherdt were the basis for those presented in the 1994 NEHRP provisions by computing the coefficients for each site category by substituting the appropriate value for V_s . Borcherdt also provided values for the coefficients F_a and F_v for constructing design spectra in association with the spectral accelerations at periods of 0.3 and 1.0 sec. Since seismic maps for spectral accelerations are for deep cohesionless or stiff clay soils, the coefficients are presented with reference to soft to firm rocks and stiff clays. For this case, Equation 2-43 can be used to compute the coefficients F_a and F_v using a $V_o = 450$ m/sec.

After the Northridge earthquake of January 17, 1994, Borcherdt⁽²⁻¹¹⁷⁾ computed coefficients F_a and F_v for accelerograms recorded on different soils in the Los Angeles area. The results indicate that the coefficients are in good agreement with those suggested in his earlier study⁽²⁻¹¹⁴⁾ and also those included in the 1994 NEHRP provisions⁽²⁻⁷⁹⁾ for small shaking intensities. For large intensities, however, the coefficients computed from the Northridge data are greater than those recommended previously.

⁶ in addition to the shear wave velocity, other parameters such as average standard penetration, undrained shear strength, and plasticity index are used in the classification.

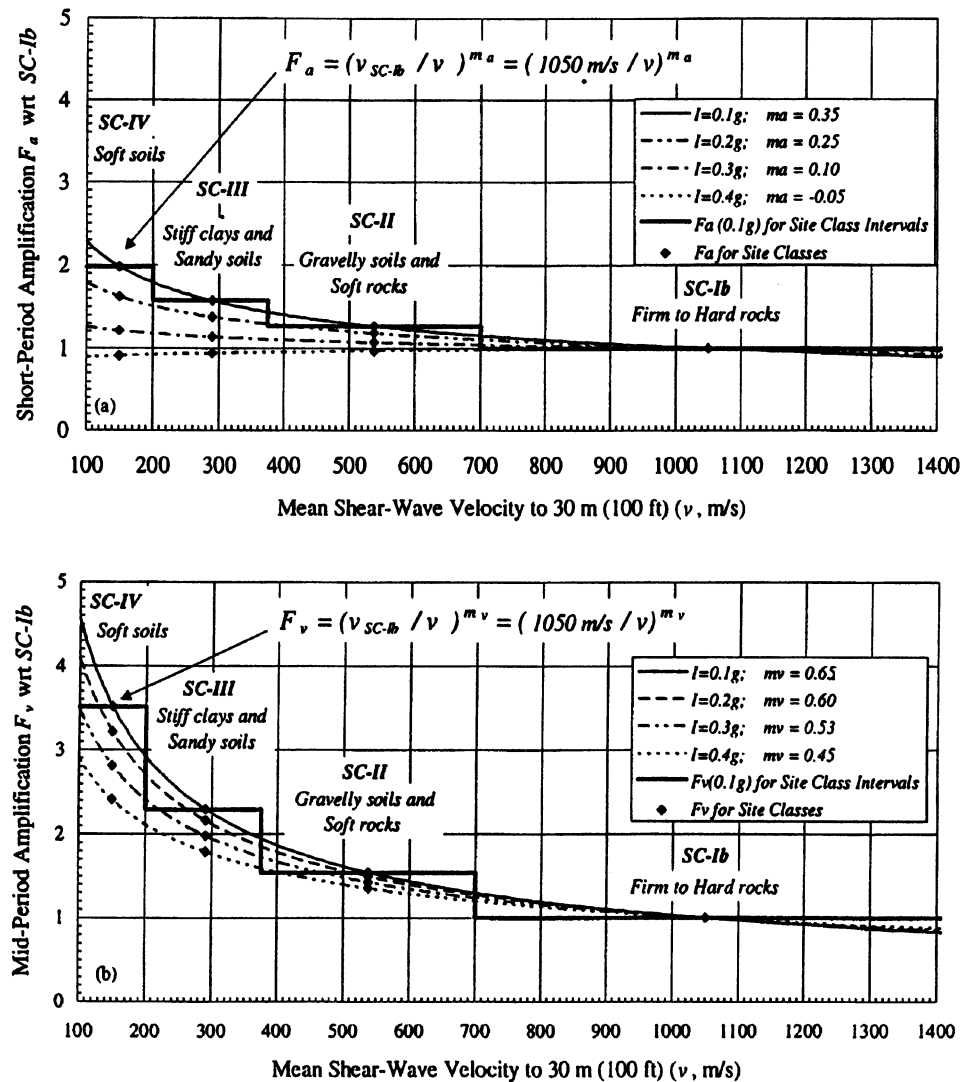


Figure 2-58. Variation of short-period F_a and long-period F_v amplification factors normalized to firm to hard rock with mean shear wave velocity. [After Borcherdt (2-114).]

The 1997 Uniform Building Code⁽²⁻⁸⁶⁾ used a method similar to that in the 1994 NEHRP provisions to construct the design spectrum. The design spectrum, Figure 2-59, is defined in terms of the seismic coefficients C_a and C_v . These coefficients are presented for the five UBC seismic zones for different soil categories, which are the same as those used in the 1994 NEHRP provisions. The only difference between the design spectra in the 1997 UBC code and the 1994 NEHRP provisions is that the former includes the near-source factors.

These factors were introduced to amplify the spectral ordinates for sites close to a seismic source in the zone with the highest seismicity (zone 4). The near-source factors depend on the distance to the closest active fault and the source type (maximum magnitude, rate of seismic activity, and slip rate).

Design spectra presented in the 1997 NEHRP recommended provisions⁽²⁻⁸⁰⁾ can be constructed from the maps of spectral response accelerations at short periods S_S (defined as 0.2 sec) and at 1.0 sec period S_1 corresponding to

the maximum considered earthquake (see Section 2.5). Since the maps are provided for rock (site class B), the spectral accelerations for other soil categories are adjusted by multiplying the spectral accelerations for rock by the site coefficients F_a and F_v in the short and the mid to long period ranges, respectively. Similar to the 1994 provisions, F_a and F_v depend on the soil category and the shaking intensity and are given in tabular form based on the study by Borcherdt⁽²⁻¹¹⁴⁾. To construct the spectra for the design earthquake, the adjusted spectral ordinates at the maximum considered earthquake are multiplied by 2/3 (see Section 2.5).

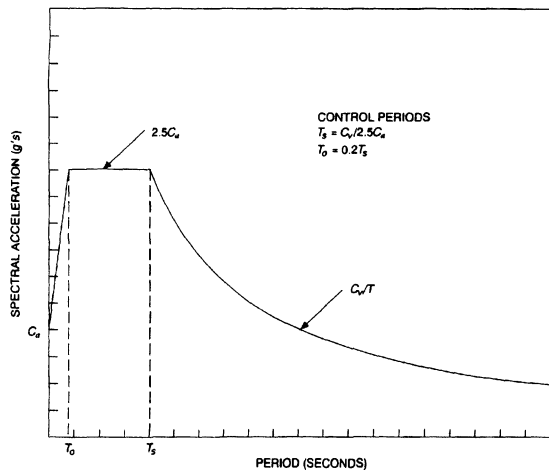


Figure 2-59. Design spectrum recommended by the 1997 Uniform Building Code (2-86).

The 1997 NEHRP Guidelines for the Seismic Rehabilitation of Buildings, FEMA-273⁽²⁻⁸¹⁾, uses a procedure similar to that of the 1997 NEHRP Provisions⁽²⁻⁸⁰⁾ to establish the 5% damped design spectra. In addition, FEMA-273 uses damping modification factors in the short- and long-period ranges to reduce the spectral ordinates for damping ratios larger than 5% due to the use of supplemental damping devices in the structure.

2.10 INELASTIC RESPONSE SPECTRA

Structures subjected to severe earthquake ground motion experience deformations beyond the elastic range. To a large extent, the inelastic deformations depend on the intensity of excitation and load-deformation characteristics of the structure and often result in stiffness deterioration. Because of the cyclic characteristics of ground motion, structures experience successive loadings and unloadings and the force-displacement or resistance-deformation relationship follows a sequence of loops known as hysteresis loops. The loops reflect a measure of a structure's capacity to dissipate energy. The shape and orientation of the hysteresis loops depend primarily on the structural stiffness and yield displacement. Factors such as structural material, structural system, and connection configuration influence the hysteretic behavior. Consequently, arriving at an appropriate mathematical model to describe the inelastic behavior of structures during earthquakes is a difficult task.

A simple model which has extensively been used to approximate the inelastic behavior of structural systems and components is the bilinear model shown in Figure 2-60. In this model, unloadings and subsequent loadings are assumed to be parallel to the original loading curve. Strain hardening takes place after yielding initiates. Elastic-plastic (elastoplastic) model is a special case of the bilinear model where the strain hardening slope is equal to zero ($\alpha = 0$). Other hysteretic models such as stiffness and strength degrading have also been suggested. The elastic-plastic model results in a more conservative response than other models. Because of its simplicity, it was widely used in the development of inelastic response spectra.

Response spectra modified to account for the inelastic behavior, commonly referred to as the inelastic spectra, have been proposed by several investigators. The use of the inelastic spectra in analysis and design, however, has been limited to structures that can be modeled

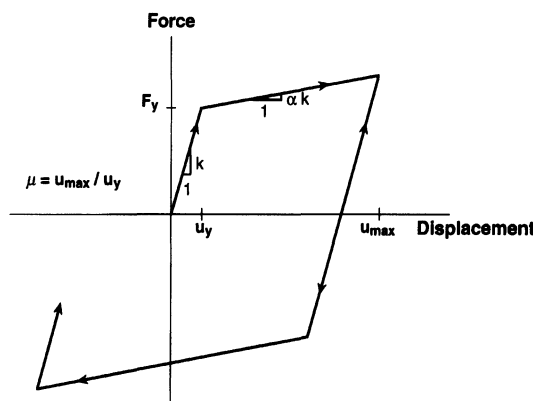


Figure 2-60. Bilinear force-displacement relationship.

as a single-degree-of-freedom. Procedures for utilizing inelastic spectra in the analysis and design of multi-degree-of-freedom systems have not yet been developed to the extent that can be implemented in design. Similar to elastic spectra, inelastic spectra were usually plotted on tripartite paper for a given damping and ductility⁷ or yield deformation. When the spectra are plotted for various ductilities, computations are repeated for several yield deformations using an iterative procedure to achieve the target ductility. Depending on the parameter plotted, different names have been used to identify the spectrum (Riddell and

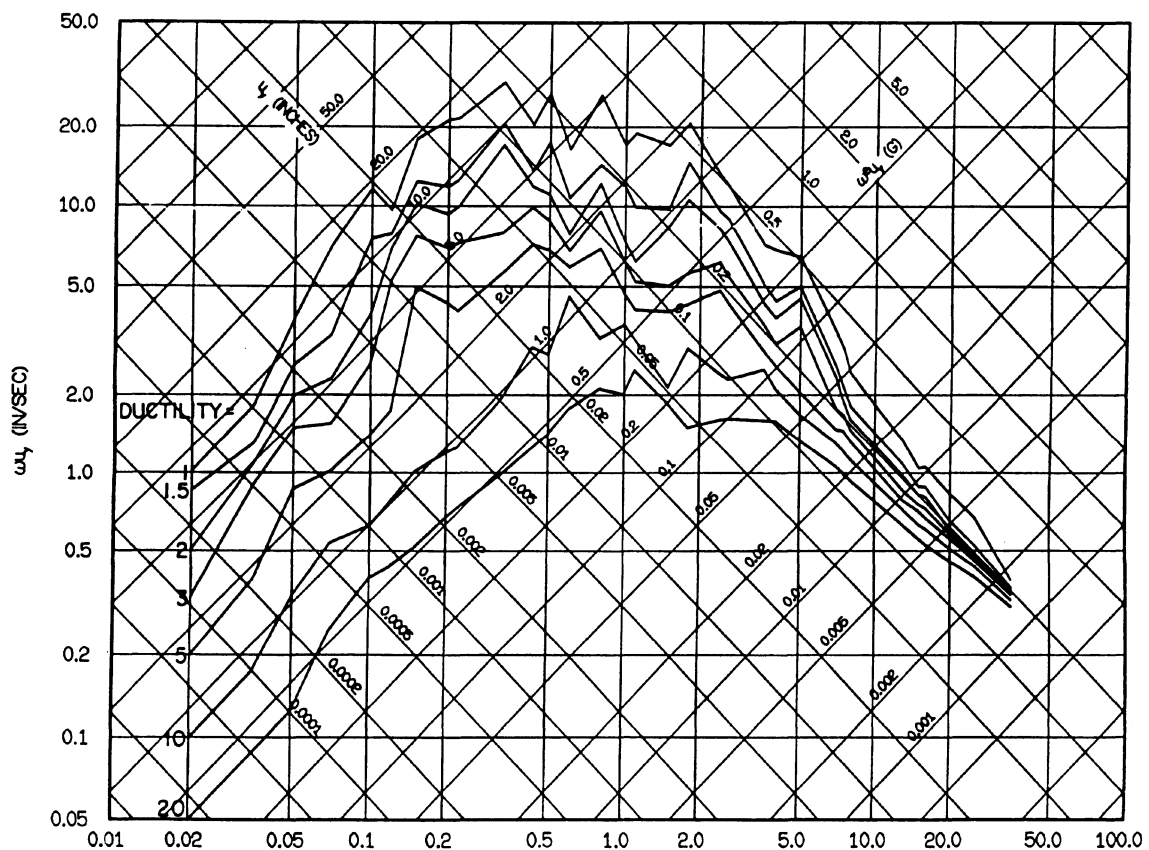


Figure 2-61. Inelastic yield spectra for the S90W component of El Centro, the Imperial Valley earthquake of May 18, 1940. Elastic-plastic systems with 5% damping. [After Riddell and Newmark (2-118).]

⁷ ratio of maximum deformation to yield deformation

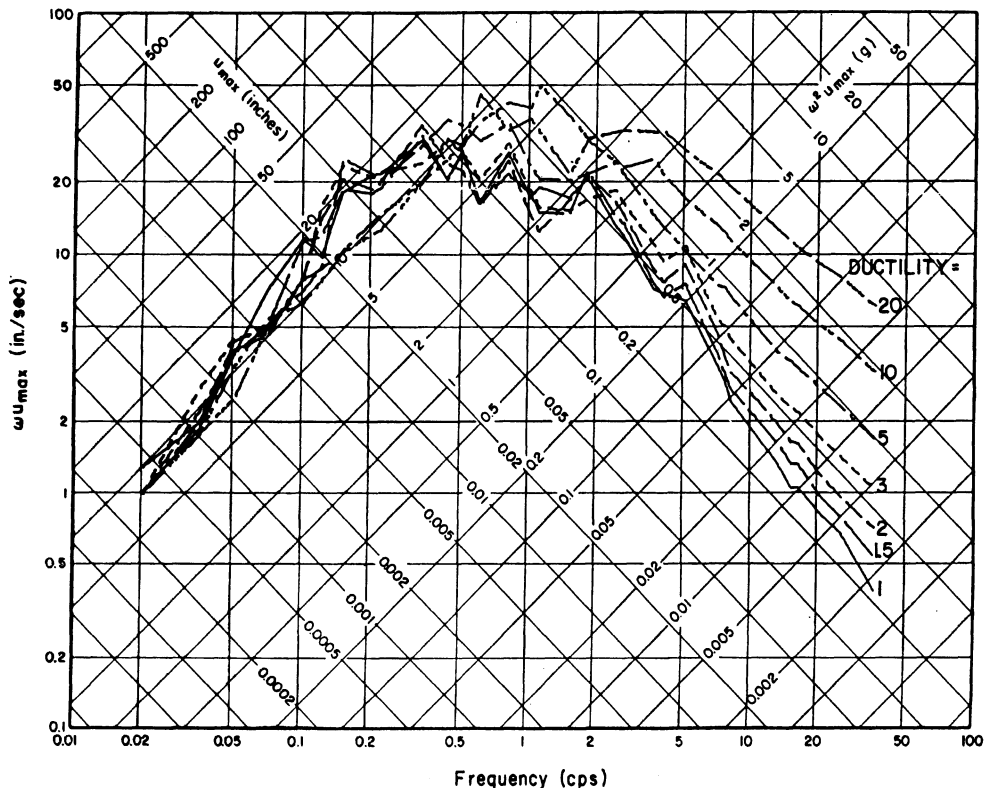


Figure 2-62. Total deformation spectra for the S90W component of El Centro, the Imperial Valley earthquake of May 18, 1940. Elastic-plastic systems with 5% damping. [After Riddell and Newmark (2-118).]

Newmark, 2-118). In the inelastic yield spectrum (IYS), the yield displacement is plotted on the displacement axis; in the inelastic acceleration spectrum (IAS), the maximum force per unit mass is plotted on the acceleration axis; and in the inelastic total displacement spectrum (ITDS), the absolute maximum total displacement is plotted on the displacement axis. For elastic-plastic behavior, the inelastic yield spectrum and the inelastic acceleration spectrum are identical. Examples of inelastic spectra for a 5% damped elastic-plastic system for the S90W component of El Centro, the Imperial Valley earthquake of May 18, 1940 are shown in Figures 2-61 and 2-62. The figures indicate that for inelastic yield and acceleration spectra, the curves for various ductilities fall below the elastic curve (ductility of one), whereas for the inelastic total deformation spectra, they primarily fall above

the elastic, particularly in the acceleration region. It should be noted that increasing the ductility ratio smoothes the spectra and minimizes the sharp peaks and valleys that are present in the plots.

A different presentation of inelastic spectra was proposed by Elghadamsi and Mohraz⁽²⁻¹¹⁹⁾. The spectrum, referred to as the yield displacement spectrum (YDS), is plotted similar to the inelastic total deformation spectrum except that it is plotted for a given yield displacement instead of a given ductility. The ductility is obtained as the ratio of the maximum displacement to the yield displacement for which the spectrum is plotted. Their procedure offers an efficient computational technique, particularly when statistical studies are used to obtain inelastic design spectra.

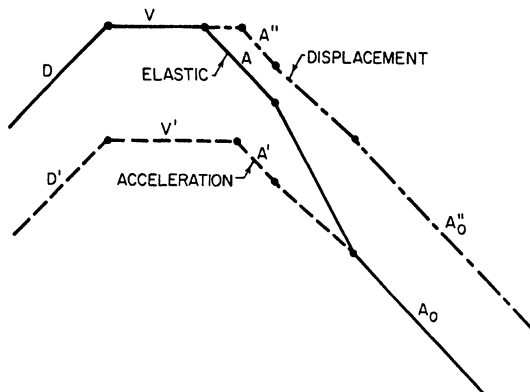


Figure 2-63. Construction of inelastic acceleration and inelastic total displacement spectra from the elastic spectrum. [After Newmark and Hall (2-89).]

Before the Riddell-Newmark study of inelastic response, the most common procedure for estimating inelastic earthquake design spectra was the one proposed by Newmark^(2-120, 2-121) and Newmark and Hall⁽²⁻⁸⁹⁾. Based on results similar to those in Figures 2-61 and 2-62, and studies by Housner⁽²⁻¹²²⁾ and Blume^(2-123 to 2-125), Newmark⁽²⁻¹²¹⁾ observed that: 1) at low frequencies, an elastic and an inelastic system have the same total displacement, 2) at intermediate frequencies, both systems absorb the same total energy, and 3) at high frequencies, they have the same force. These observations resulted in the recommendation by Newmark for constructing inelastic spectra from the elastic by dividing the ordinates of the elastic spectrum by two coefficients in terms of ductility μ . Figure 2-63 shows the construction of the inelastic spectrum from the elastic. The solid lines DVAA₀ represent the elastic response spectrum. The solid circles at the intersections of the lines correspond to frequencies which remain constant in obtaining the inelastic spectrum. The lines DV'A'A₀ represent the inelastic acceleration spectrum whereas the lines DV'A''A₀ show the total displacement spectrum. D' and V' are obtained by dividing D and V by μ . A' is obtained by dividing A by $\sqrt{(2\mu - 1)}$ (to insure that the same energy is absorbed by the elastic and the

inelastic systems). A'' and A₀ are obtained by multiplying A' and A₀ by μ .

The Riddell-Newmark study⁽²⁻¹¹⁸⁾ also considered bilinear and stiffness degrading models and concluded that using the elastic-plastic spectrum for inelastic analysis is generally on the conservative side.

2.10.1 De-amplification factors

When inelastic deformations are permitted in design, the elastic forces can be reduced if adequate ductility is provided. Riddell and Newmark⁽²⁻¹¹⁸⁾ presented a set of coefficients referred to as "de-amplification factors" by which the ordinates of the elastic design spectrum are multiplied to obtain the inelastic yield spectrum. Lai and Biggs⁽²⁻¹²⁶⁾, using artificial accelerograms with variable durations of strong motion, presented a set of coefficients referred to as "inelastic acceleration response ratios" by which the ordinates of the elastic spectrum are divided to give the inelastic yield spectrum. Since these two approaches are the inverse of one another, the reciprocal of the Lai-Biggs coefficients represent de-amplification factors. De-amplification factors can also be obtained from the Newmark-Hall⁽²⁻⁸⁹⁾ and from the Elghadamsi-Mohraz⁽²⁻¹¹⁹⁾ procedures for estimating inelastic spectra. Comparisons of the de-amplification factors from the four procedures are shown in Figure 2-64 for a 5% damping ratio and ductilities of 2 and 5. The figure indicates that the Riddell-Newmark de-amplification factors are in general the smallest (largest reduction in the elastic force) compared to the other three. Both Riddell-Newmark and Newmark-Hall de-amplification ratios remain constant over certain frequency segments, whereas those from Lai-Biggs and Elghadamsi-Mohraz follow parallel patterns. While the de-amplification ratios are affected by ductility, they are practically not influenced by damping. Since the elastic spectral ordinates decrease significantly with an increase in damping, the decrease in inelastic spectral ordinates with

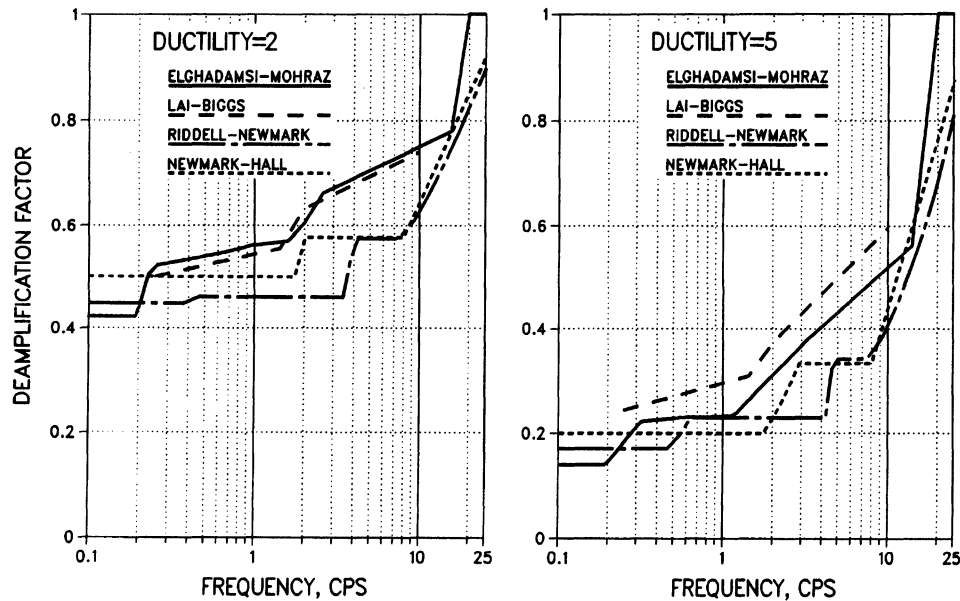


Figure 2-64. Comparison of de-amplification factors for 5% damping. [After Elghadamsi and Mohraz (2-119).]

damping stems primarily from the elastic spectral ordinates.

Elghadamsi and Mohraz⁽²⁻¹¹⁹⁾ also presented de-amplification factors for alluvium and rock. Typical de-amplification factors for alluvium and rock for 5% damping is presented in Figure 2-65. According to the figure, de-amplifications are not significantly affected by the soil condition.

The influence of the duration of strong motion on the inelastic behavior of structures has also been studied. In a non-deterministic study of nonlinear structures, Penzien and Liu⁽²⁻¹²⁷⁾ concluded that structures with elastic-plastic and stiffness degrading behavior are more sensitive to the duration of strong motion than elastic structures. Using a random vibration approach and the extreme value theory, Peng et al.⁽²⁻¹²⁸⁾ incorporated the duration of strong motion in estimating the maximum response of structures with elastic-plastic behavior. The effect of duration of strong motion on de-amplification factors from Peng's study is shown in Figure 2-66 which indicates that for a longer duration of strong motion, one should use a larger de-

amplification (smaller reduction in elastic force). It should be noted that Lai and Biggs⁽²⁻¹²⁶⁾ conclude that inelastic response spectra are not significantly affected by strong motion duration. They emphasize, however, that this conclusion is valid only when ground motion with varying strong motion durations are compatible with the same prescribed elastic response spectrum.

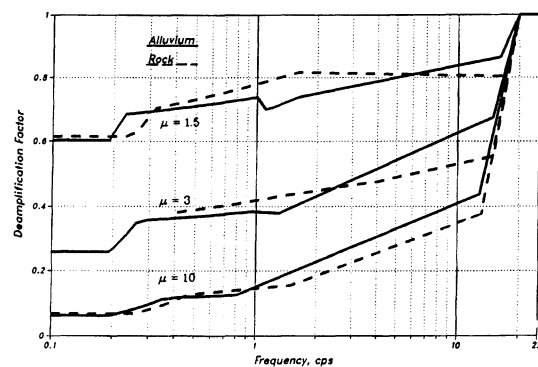


Figure 2-65. De-amplification factors for alluvium and rock for 5% damping. [After Elghadamsi and Mohraz (2-119).]

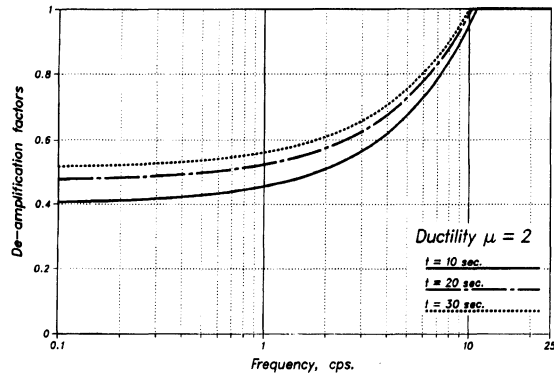


Figure 2-66. Effect of strong motion duration on de-amplification factors for systems with 2% damping. [After page et al. (1-128).]

2.10.2 Response modification factors

Current seismic codes recommend force reduction factors and displacement amplification factors to be used in design to account for the energy absorption capacity of structures through inelastic action. The force reduction factors (referred to as R -factors) are used to reduce the forces computed from the elastic design spectra. A recent study by the Applied Technology Council⁽²⁻¹²⁹⁾ proposes the following expression for computing the R -factors:

$$R = \frac{V_e}{V} = R_s R_\mu R_R \quad (2-45)$$

Where V_e is the base shear computed from the elastic response (elastic design spectrum), and V is the design base shear for the inelastic response. The response modification factor R is the product of the following terms:

1. the period-dependent strength factor R_s which accounts for the reserve strength of the structure in excess of the design strength,
2. the period-dependent ductility factor R_μ which accounts for the ductile capacity of the structure in the inelastic range, and
3. the redundancy factor R_R which accounts for the reliability of seismic framing systems

that use multiple lines of framing in each principal direction of the building.

The ductility factor R_μ is defined as the ratio of the elastic to the inelastic displacement for a system with an elastic fundamental period T and specified ductility μ such that

$$R_\mu(T, \mu) = \frac{u_y(T, \mu=1)}{u_y(T, \mu)} \quad (2-46)$$

where u_y is the yield displacement. Stated differently, R_μ is the ratio of the maximum inelastic force to the yield force required to limit the maximum inelastic response to a displacement ductility μ , or the inverse of the de-amplification factors presented in Section 2.10.1.

The relationship between displacement ductility and ductility factor has been the subject of several studies in recent years. Earlier studies by Newmark and Hall^(2-87, 2-89) provided expressions for estimating the ductility factor R_μ for elastic-plastic systems irrespective of the soil condition. The expressions are

$$R_\mu(T \leq 0.03\text{ sec}, \mu) = 1.0$$

$$R_\mu(0.12\text{ sec} \leq T \leq 0.5\text{ sec}, \mu) = \sqrt{2\mu - 1} \quad (2-47)$$

$$R_\mu(T \geq 1.0\text{ sec}, \mu) = \mu$$

A linear interpolation may be used to estimate R_μ for the intermediate periods. The expressions are plotted in Figure 2-64 for ductility ratios of 2 and 5.

Using a statistical study of 15 ground motion records from earthquakes with magnitudes 5.7 to 7.7, Krawinkler and Nassar^(2-130, 2-131) developed relationships for estimating R_μ for rock or stiff soils for 5% damping. Their proposed relationship is

$$R_\mu(T, \mu) = [c(\mu - 1) + 1]^{1/c} \quad (2-48)$$

where

$$c = \frac{T^a}{1+T^a} + \frac{b}{T} \quad (2-49)$$

and a and b are parameters that depend on the strain hardening ratio α . They recommend $a = 1.00, 1.01$, and 0.80 and $b = 0.42, 0.37$, and 0.29 for strain hardening ratios of 0% (elasto plastic system), 2% , and 10% , respectively.

Miranda and Bertero⁽²⁻¹³²⁾ using 124 accelerograms recorded on different soil conditions, developed equations for estimating R_μ for rock, alluvium, and soft soil for 5% damping. Their equation is given by

$$R_\mu(T, \mu) = \frac{\mu - 1}{\Phi} + 1 \quad (2-50)$$

where

$$\Phi(T, \mu) = 1 + \frac{1}{T(10 - \mu)} - \frac{1}{2T} \exp[-1.5(\ln T - 0.6)^2] \quad \text{for rock sites}$$

$$\Phi(T, \mu) = 1 + \frac{1}{T(12 - \mu)} - \frac{2}{5T} \exp[-2(\ln T - 0.2)^2] \quad \text{for alluvium sites}$$

$$\Phi(T, \mu) = 1 + \frac{T_g}{3T} - \frac{3T_g}{4T} \exp[-3(\ln \frac{T}{T_g} - 0.25)^2] \quad \text{for soft soil sites} \quad (2.51)$$

and T_g is the predominant period of the ground motion defined as the period at which the relative velocity of a linear system with 5% damping is maximum throughout the entire period range. A comparison of the Nassar-Krawinkler and Miranda-Bertero relationships for rock and alluvium for ductility ratios of $2, 4$, and 6 is presented in Figure 2-67. The figure

shows that the differences between these relationships are relatively small and may be ignored for engineering purposes.

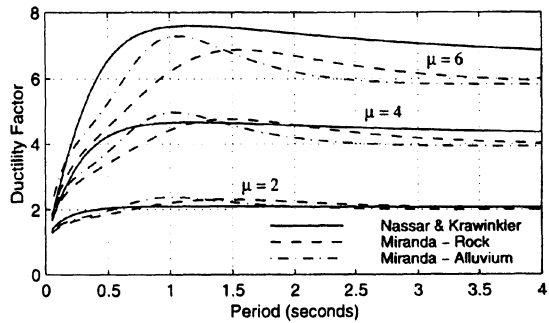


Figure 2-67. Variation of the ductility factor with period for ductility ratios of $2, 4$, and 6 . [Reproduced from ATC-19 (2-129).]

2.11 ENERGY CONTENT AND SPECTRA

While the linear and nonlinear response spectra, presented in previous sections, have been used for decades to compute design displacements and accelerations as well as base shears, they do not include the influences of strong motion duration, number of response cycles and yield excursions, stiffness and strength degradation, or damage potential to structures. There is a need to re-examine the current analysis and design procedures; especially with the use of innovative protective systems such as seismic isolation and passive energy dissipation devices. In particular, the concept of energy-based design is appealing where the focus is not so much on the lateral resistance of the structure but rather on the need to dissipate and/or reflect seismic energy imparted to the structure. In addition, energy approach is suitable for implementation within the framework of performance-based design since the premise behind the energy concept is that earthquake damage is related to the structure's ability to dissipate energy.

Housner⁽²⁻¹²²⁾ was the first to recommend energy approach for earthquake resistant design. He pointed out that ground motion

transmits energy into the structure; some of this energy is dissipated through damping and nonlinear behavior and the remainder stored in the structure in the form of kinetic and elastic strain energy. Housner approximated the input energy as one-half of the product of the mass and the square of the pseudo-velocity, $1/2 m(PSV)^2$. His study provided the impetus for later developments of energy concepts in earthquake engineering.

For a nonlinear SDOF system with pre-yield frequency and damping ratio of ω and β , respectively; subjected to ground acceleration $a(t)$ the equation of motion is given by:

$$\ddot{x} + 2\beta\omega\dot{x} + F_s[x(t)] = -a(t) \quad (2-52)$$

where $F_s[x(t)]$ is the nonlinear restoring force per unit mass. Integrating Equation (2-52) over the entire relative displacement history, results in the following energy balance equation:

$$E_I = E_K + E_D + E_S + E_H \quad (2-53)$$

where

$$E_I = \text{Input energy} = \int_0^x a(t)dx = \int_0^t a(t)\dot{x}dt \quad (2-54)$$

$$E_K = \text{Kinetic energy} = \int_0^x \dot{x}dx = \frac{\dot{x}^2}{2} \quad (2-55)$$

$$E_D = \text{Dissipative damping energy} = 2\beta\omega \int_0^x \dot{x}dx = 2\beta\omega \int_0^t \dot{x}^2 dt \quad (2-56)$$

$E_S = \text{Recoverable elastic strain energy}$

$$= \frac{F_s^2}{2\omega^2} \quad (2-57)$$

$E_H = \text{Dissipative plastic strain energy}$

$$= \int_0^x F_s dx - \frac{F_s^2}{2\omega^2} = \int_0^t F_s \dot{x} dt - \frac{F_s^2}{2\omega^2} \quad (2-58)$$

The energy terms in the above equations are given in energy per unit mass. Through the remainder of this section, the term "energy" refers to the energy per unit mass.

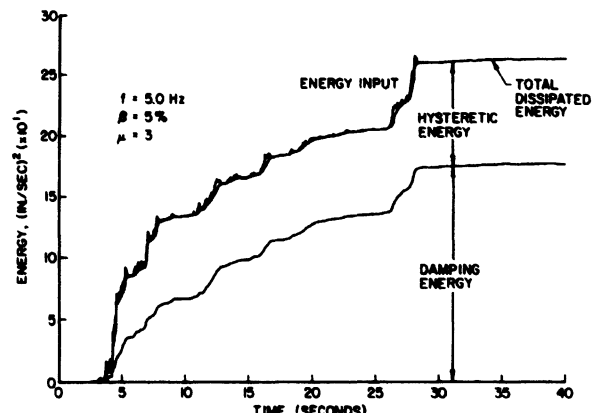
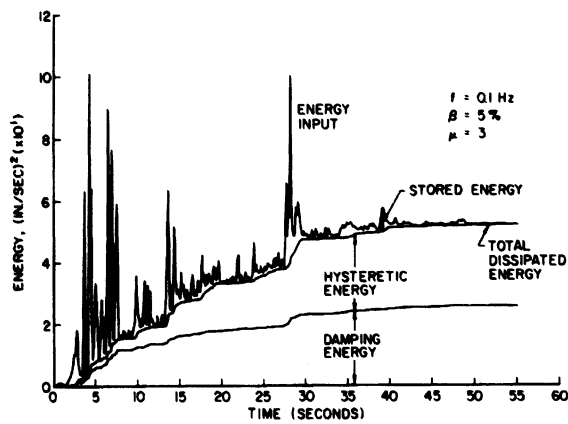
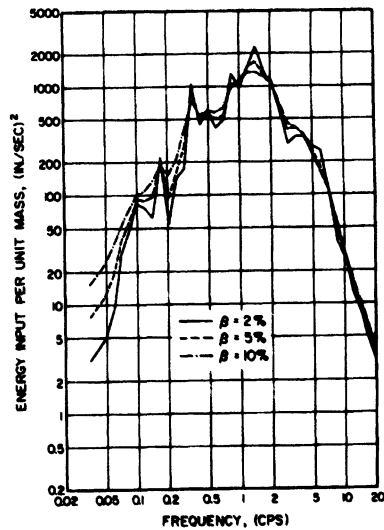


Figure 2-68. Energy time histories for a low and a high frequency, elastic-plastic structure subjected to El Centro ground motion. [After Zahrah and Hall (2-133).]

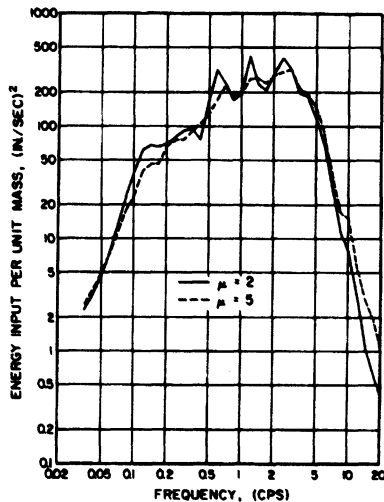
Figure 2-68 presents the energy response computed by Zahrah and Hall ⁽²⁻¹³³⁾ as a

function of time for two elastic-plastic SDOF structures; a low frequency (0.1 Hz) and a high frequency (5 Hz) structure; both with a 5% damping and a ductility of 3.0 subjected to the 1940 El-Centro ground motion. In these plots, the difference between the input energy and the dissipated energy (sum of damping and hysteretic) represents the stored energy (sum of strain and kinetic). The stored energy becomes vanishingly small at the end of motion and the energy dissipated in the structure becomes almost equal to the energy imparted to it. The larger peaks and troughs in the energy response of a low-frequency structure as compared to a high-frequency structure indicate that for low-frequency structures, a larger portion of the energy imparted to the structure is stored in the form of strain and kinetic energies.

Zahrah and Hall⁽²⁻¹³³⁾ introduced an energy spectrum as a plot of the numerical value of the input energy E_I at the end of motion as a function of period or frequency for different damping and ductility ratios. Examples of such spectra are shown in Figure 2-69 for linear structures with different damping ratios using the El-Centro record and for nonlinear structures with 2% damping and ductility ratios of 2 and 5 using Taft ground motion. Zahrah and Hall indicated that for linear structures under the same ground motion, input energy spectra are generally similar in shape to response spectra and that the quantity $1/2 m(PSV)^2$ for an undamped structure is a good estimate of the amount of input energy imparted to the structure. For damped structures, however, this quantity underestimates the input energy. They also indicated that the energy spectral shapes for nonlinear systems are similar to those of linear systems and that the amount of energy input is nearly the same for a linear and a nonlinear structure (with moderate ductility) with the same frequency.



(a)



(b)

Figure 2-69. Input energy spectra for (a) linear systems with 2, 5, and 10% damping using El Centro ground motion and (b) elstic-plastic systems with 2% damping and ductility ratios of 2 and 5 using Taft ground motion.
[After Zahrah and Hall (2-133).]

According to Uang and Bertero⁽²⁻¹³⁴⁾, the energy equations in⁽²⁻⁵³⁾ through⁽²⁻⁵⁸⁾ should be considered as "relative energy equations" since the integrations are performed for equations of motion using the relative displacements. For this system of equations, the relative input energy is defined as the work done by the static equivalent lateral force on a fixed-base system. Uang and Bertero introduced the "absolute energy equations" by integrating the equation of motion using the absolute displacements. For

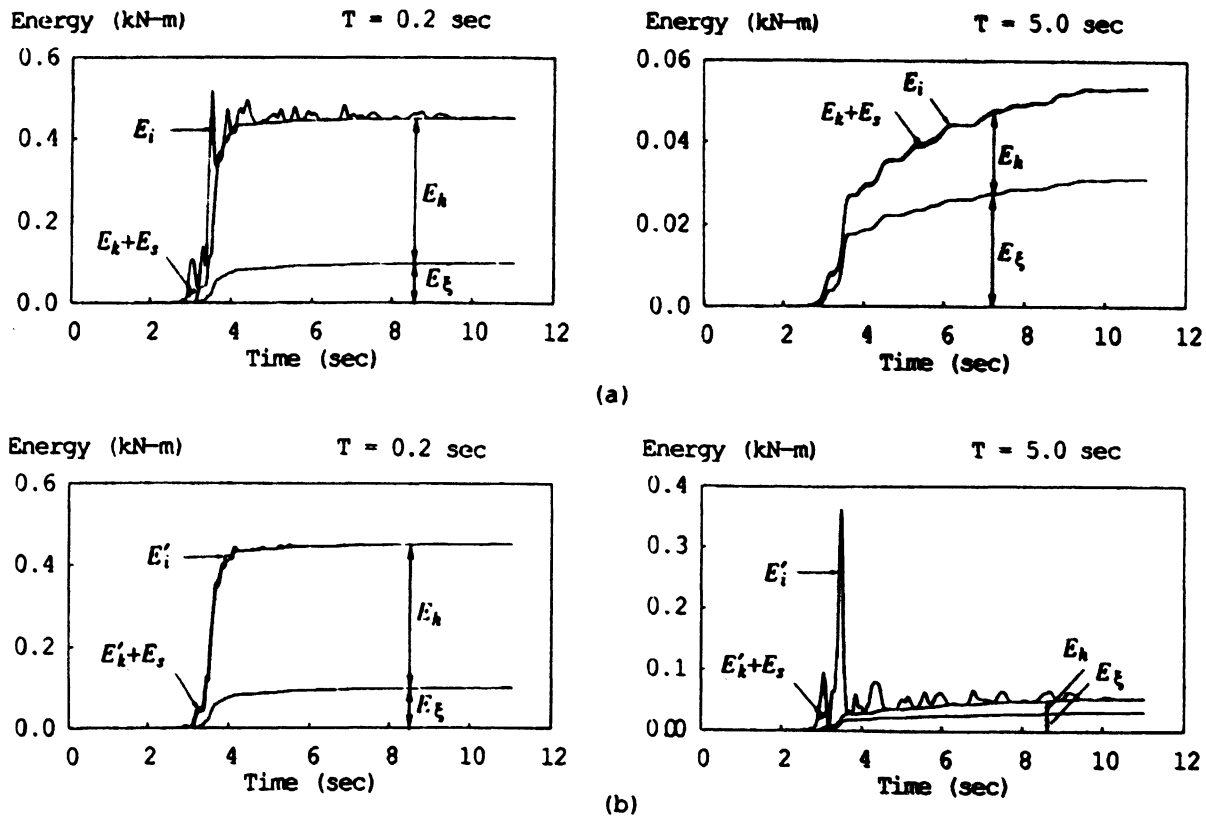


Figure 2-70. (a) Absolute and (b) relative energy time histories for elastic-plastic systems with 5% damping and ductility ratios of 5 subjected to the 1986 San Salvador earthquake. [After Uang and Bertero (2-134).]

the absolute energy terms; E_D , E_S , and E_H are the same as their relative counterparts while the absolute input energy is given as $\int \ddot{x}_t dx_g$ and the absolute kinetic energy is given as $\dot{x}_t^2 / 2$; where x_t and x_g are the absolute and ground displacement; respectively. The absolute input energy represents the work done by the total base shear on the foundation displacement. The difference between the absolute and relative, input and kinetic energies is given by:

$$\begin{aligned} E_{I,abs} - E_{I,rel} &= \\ E_{K,abs} - E_{K,rel} &= \frac{\dot{x}_g^2}{2} + \dot{x}\dot{x}_g \end{aligned} \quad (2-59)$$

Figure 2-70 shows energy time-histories for a short and a long-period elastic-plastic

structure using the relative and absolute energy terms. In addition, Uang and Bertero (2-134) converted the input energy to an equivalent velocity such that

$$V_I = \sqrt{2E_I} \quad (2-60)$$

where E_I can be the relative or absolute input energy per unit mass. Figure 2-71 presents the relative and absolute input energy equivalent velocity spectra along with the peak ground velocity for three earthquake records. As the plots indicate, the relative and absolute input energies are very close for the mid-range periods (in the vicinity of predominant periods of ground motion). For longer and shorter periods, however, the difference between relative and absolute energies is significant. The figure also shows that the absolute and relative equivalent velocities converge to the

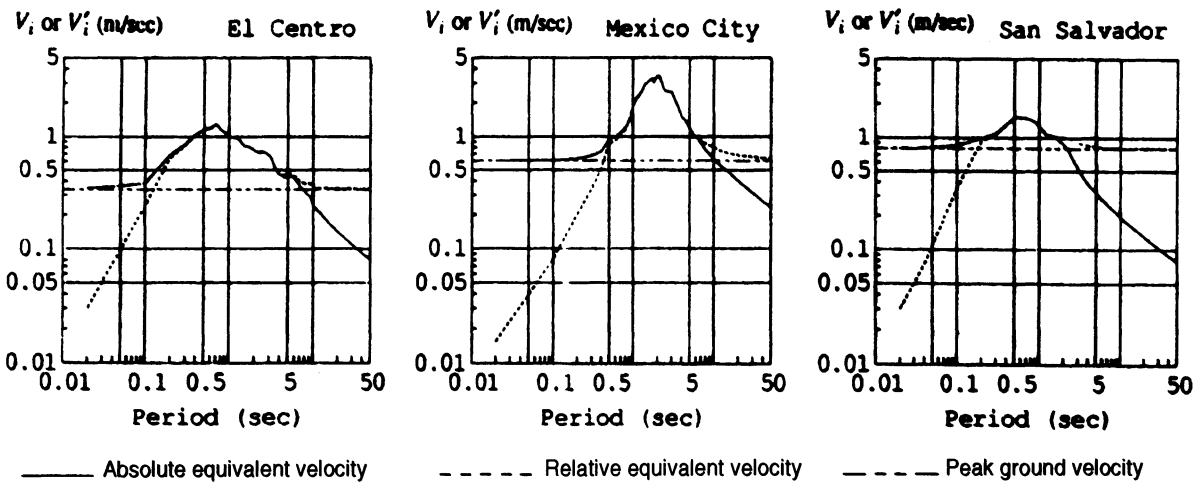


Figure 2-71. Absolute and relative input energy equivalent velocity spectra for elastic-plastic systems with 5% damping and ductility ratio of 5 using three earthquake records. [After Uang and Bertero (2-134).]

peak ground velocity at very short and very long periods, respectively. Subsequently, Uang and Bertero concluded that the absolute input energy can be used as a damage index for short-period structures, while the relative input energy is more suitable for long-period structures. Their study also showed, using energy spectra, that the input energy is insensitive to the ductility ratio. Finally, Uang and Bertero⁽²⁻¹³⁴⁾ believed that for linear structures, Housner's use of $1/2m(PSV)^2$ to estimate input energy reflects the maximum elastic energy stored in the structure without consideration of damping energy.

It should be noted that at the time of this writing, the energy concept outlined in this section does not provide the basis for seismic design, despite the body of knowledge that has been developed. Further research is required to reliably estimate both the energy demand and energy capacity of structures in order to implement energy approaches in seismic design procedures.

2.12 ARTIFICIALLY GENERATED GROUND MOTION

One major drawback in using the response spectrum method in analysis and design of structures lies in the limitation of the method to provide temporal information on structural response and behavior. Such information is sometimes necessary in arriving at a satisfactory design. For example, the response spectrum procedure can be used to estimate the maximum response in each mode of vibration, and procedures such as square root of the sum of the squares can be used to combine the modal responses. When the natural frequencies are close to each other, however, the square root of the sum of the squares can result in inaccurate estimate of the response. In such cases, the complete quadrature combination⁸ CQC, or a time-history analysis may be used. If inelastic deformation is permitted in design, the inelastic spectra and the de-amplification factors presented in the previous sections

⁸ An improved procedure for computing modal responses referred to as complete quadrature combination CQC was proposed by Der Kiureghian (see Chapter 3).

cannot be used to compute the response of structures modeled as multi-degree-of-freedom, and one therefore relies on a time-history analysis for computing the inelastic response. In many cases, structures house equipment are sensitive to floor vibrations during an earthquake. It is sometimes necessary to develop floor response spectra from the time-history response of the floor. In addition, when designing critical or major structures such as power plants, dams, and high-rise buildings, the final design is usually based on a complete time-history analysis. The problem which often arises is what representative accelerogram should be used. Artificially generated accelerograms which represent earthquake characteristics such as a given magnitude, epicentral distance, and soil condition of the site have been used for this purpose as well as in research. For example, Penzien and Liu⁽²⁻¹²⁷⁾ used artificial accelerograms to investigate the statistical characteristics of inelastic systems and Lai and Biggs⁽²⁻¹²⁶⁾ used them to obtain inelastic acceleration and displacement response ratios.

Random models have been used to simulate earthquake ground motion and generate artificial accelerograms. Both stationary and nonstationary random processes have been suggested (see for example 2-135 to 2-138). Other studies have proposed site-dependent power spectral density from recorded ground motion, which can be utilized in generating artificial accelerograms. One of the first attempts in generating artificial accelerograms was by Housner and Jennings⁽²⁻¹³⁵⁾ who modeled ground motion as a stationary Gaussian random process with a power spectral density from undamped velocity spectra of recorded accelerograms. They developed a procedure for generating a random function that has the same properties of strong earthquake ground motion and used it to generate eight artificial accelerograms of 30 sec duration which exhibit the same statistical properties of real ground motion.

The detailed description of the procedures for generating artificial accelerograms is

beyond the scope of this chapter. It may, however, be useful to briefly mention the basic elements, which are generally needed to generate an artificial accelerogram. In most cases, these elements consist of a power spectral density or a zero-damped response spectrum, a random phase angle generator, and an envelope function. The simulated motion is then obtained as a finite sum of several harmonic excitations. Usually an iterative procedure is needed to check the consistency of the artificial motion by examining its frequency content through its response spectrum or its power spectral density. A typical artificial accelerogram and integrated velocity and displacement generated from the Kanai-Tajimi^(2-19, 2-20) power spectral density for alluvium using the peak acceleration and the duration of strong motion of the S00E component of El Centro, the Imperial Valley earthquake of May 18, 1940 is shown in Figure 2-72.

2.13 SUMMARY AND CONCLUSION

The state-of-the-art in strong motion seismology and ground motion characterization has advanced significantly in the past three decades. One can now estimate, with reasonable accuracy, the design ground motion and spectral shapes at a given location. Earthquake magnitude, source distance, site geology, fault characteristics, duration of strong motion, etc. influence ground motion and spectral shapes. While building codes and seismic provisions account for some of these influences such as site geology, magnitude, and distance, others such as fault characteristics, travel path, and duration require further studies before they can be implemented.

Response spectrum is used extensively in seismic design of structures. Recent codes recommend acceleration amplifications in terms of seismic coefficients, which account for site geology, shaking intensity, and distance for constructing design spectra and computing the design lateral forces.

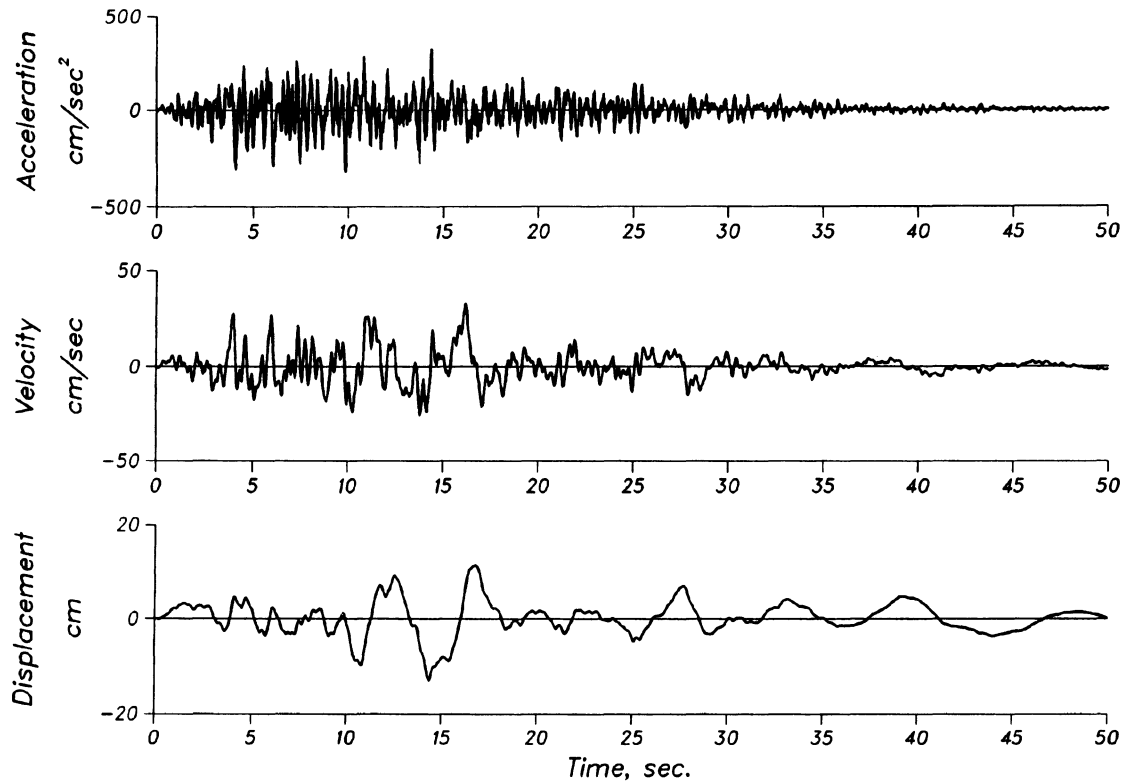


Figure 2-72. Acceleration - time history and integrated velocity and displacement generated from the Kanai-Tajimi power spectral density for alluvium using the peak ground acceleration and the duration of the S00E component of El Centro, the Imperial Valley earthquake of May 18, 1940.

In moderate and strong earthquakes, structures can experience nonlinear behavior and dissipate a portion of the seismic energy through inelastic action. To account for the energy absorption capacity of the structure, seismic codes allow the use of response modification factors, referred to as *R*-factors, to reduce the elastic design forces and amplify the elastic displacements (drifts). Although the application of inelastic spectra is limited to structures which can be modeled as single-degree-of-freedom, inelastic spectra can be used to estimate the ductility demands which are needed to compute response modification or *R*-factors.

In special cases such as design of critical or essential structures, a time-history analysis may be warranted. Determination of a representative

set of accelerograms which reflects the earthquake characteristics expected at the site is important. Artificially generated ground motion may be used to determine representative accelerograms.

In most cases, particularly for critical and essential structures, the advice of geologists, seismologists, geotechnical engineers, and structural engineers should be obtained before ground motion and spectral shape estimates are finalized for design.

ACKNOWLEDGMENT

The authors wish to thank Dr. Fawzi E. Elghadamsi who co-authored this chapter in the first edition of the handbook. His contributions, some of which are reflected in this edition, are gratefully acknowledged.

REFERENCES

- 2-1 Biot, M. A., "A Mechanical Analyzer for Prediction of Earthquake Stresses," *Bull. Seism. Soc. Am.*, Vol. 31, 151-171, 1941.
- 2-2 Biot, M. A., "Analytical and Experimental Methods in Engineering Seismology," *Proc. ASCE* 68, 49-69, 1942.
- 2-3 Housner, G. W., "An Investigation of the Effects of Earthquakes on Buildings," Ph.D. Thesis, California Institute of Technology, Pasadena, California, 1941.
- 2-4 Hudson, D. E., "Response Spectrum Techniques in Engineering Seismology," *Proc. 1st World Conf. Earthquake Eng.*, 4-1 to 4-12, Berkeley, California, 1956.
- 2-5 Rojahn, C. and Mork, P., "An Analysis of Strong Motion Data from a Severely Damaged Structure," the Imperial Services Building, El Centro, California, USGS Open File Rep. 81-194, 1981.
- 2-6 Trifunac, M. D., "Low Frequency Digitization Errors and a New Method for Zero Baseline Correction of Strong-Motion Accelerograms," Earthquake Eng. Research Laboratory, EERL 70-07, California Institute of Technology, Pasadena, California, 1970.
- 2-7 Hudson, D. E., Brady, A. G., Trifunac, M. D., and Vijayaraghavan, A., "Analysis of Strong-Motion Earthquake Accelerograms-Digitized and Plotted Data, Vol. II, Corrected Accelerograms and Integrated Ground Velocity and Displacement Curves, Parts A through Y," Earthquake Research Laboratory, California Institute of Technology, Pasadena, California, 1971-1975.
- 2-8 Hudson, D. E., "Reading and Interpreting Strong Motion Accelerograms," Earthquake Eng. Research Institute, Berkeley, California, 1979.
- 2-9 Mohraz, B., Hall, W. J., and Newmark, N. M., "A Study of Vertical and Horizontal Earthquake Spectra," Nathan M. Newmark Consulting Engineering Services, Urbana, Illinois, AEC Report WASH-1255, 1972.
- 2-10 Iwan, W. D., Moser, M. A., and Peng, C.-Y., "Some Observations on Strong-Motion Earthquake Measurements Using a Digital Accelerograph," *Bull. Seism. Soc. Am.*, Vol. 75, No. 5, 1225-1246, 1985.
- 2-11 Page, R. A., Boore, D. M., Joyner, W. B., and Caulter, H. W., "Ground Motion Values for Use in the Seismic Design of the Trans-Alaska Pipeline System," USGS Circular 672, 1972.
- 2-12 Bolt, B. A., "Duration of Strong Motion," *Proc. 4th World Conf. Earthquake Eng.*, 1304-1315, Santiago, Chile, 1969.
- 2-13 Trifunac, M. D. and Brady, A. G., "A Study of the Duration of Strong Earthquake Ground Motion," *Bull. Seism. Soc. Am.*, Vol. 65, 581-626, 1975.
- 2-14 Husid R, Median, H., and Rios, J., "Analysis de Terremotos Norteamericanos y Japoneses," *Rivista del IDIEM*, Vol. 8, No. 1, 1969.
- 2-15 McCann, W. M. and Shah, H. C., "Determining Strong-Motion Duration of Earthquakes," *Bull. Seism. Soc. Am.*, Vol. 69, No. 4, 1253-1265, 1979.
- 2-16 Trifunac, M. D. and Westermo, B. D., "Duration of Strong Earthquake Shaking," *Int. J. Soil Dynamics and Earthquake Engineering*, Vol. 1, No. 3, 117-121, 1982.
- 2-17 Moayyad, P. and Mohraz, B., "A Study of Power Spectral Density of Earthquake Accelerograms," NSF Report PFR 8004824, Civil and Mechanical Engineering Dept., Southern Methodist University, Dallas, TX, 1982.
- 2-18 Elghadamsi, F. E., Mohraz, B., Lee, C. T., and Moayyad, P., "Time-Dependent Power Spectral Density of Earthquake Ground Motion," *Int. J. Soil Dynamics and Earthquake Engineering*, Vol. 7, No. 1, 15-21, 1988.
- 2-19 Kanai, K., "Semi-Empirical Formula for the Seismic Characteristics of the Ground," Bull. Earthquake Research Institute, Vol. 35, University of Tokyo, Tokyo, Japan, 309-325, 1957.
- 2-20 Tajimi, H., "A Statistical Method of Determining the Maximum Response of a Building Structure During an Earthquake," *Proc. 2nd World Conf. Earthquake Eng.*, Vol. II, 781-797, Tokyo, Japan, 1960.
- 2-21 Lai, S. P., "Statistical Characterization of Strong Motions Using Power Spectral Density Function," *Bull. Seism. Soc. Am.*, Vol. 72, No. 1, 259-274, 1982.
- 2-22 Clough, R. W. and Penzien, J., *Dynamics of Structures*, McGraw-Hill, New York, 1993.
- 2-23 Donovan, N. C., "Earthquake Hazards for Buildings," Building Practices for Disaster Mitigation, National Bureau of Standards, U.S. Department of Commerce, Building Research Services 46, 82-111, 1973.
- 2-24 Donovan, N. C. and Bornstein, A. E., "Uncertainties in Seismic Risk Procedures," *J. Geotechnical Eng. Div.*, Vol. 104, No. GT 7, 869-887, 1978.
- 2-25 Cloud, W. K. and Perez, V., "Unusual Accelerograms Recorded at Lima, Peru," *Bull. Seism. Soc. Am.*, Vol. 61, No. 3, 633-640, 1971.
- 2-26 Blume, J. A., "Earthquake Ground Motion and Engineering Procedures for Important Installations Near Active Faults," *Proc. 3rd World Conf. Earthquake Eng.*, Vol. IV, 53-67, New Zealand, 1965.
- 2-27 Kanai, K., "Improved Empirical Formula for Characteristics of Stray Earthquake Motions,"

- Proc. Japan Earthquake Symposium*, 1-4, 1966. (In Japanese)
- 2-28 Milne, W. G. and Davenport, A. G., "Distribution of Earthquake Risk in Canada," *Bull. Seism. Soc. Am.*, Vol. 59, No. 2, 754-779, 1969.
- 2-29 Esteve, L., "Seismic Risk and Seismic Design Decisions," *Seismic Design for Nuclear Power Plants*, R. J. Hansen, Editor, MIT Press, 1970.
- 2-30 Campbell, K. W., "Near-Source Attenuation of Peak Horizontal Acceleration," *Bull. Seism. Soc. Am.*, Vol. 71, No. 6, 2039-2070, 1981.
- 2-31 Joyner, W. B. and Boore, D. M., "Peak Horizontal Acceleration and Velocity from Strong Motion Records Including Records from the 1979 Imperial Valley, California, Earthquake," *Bull. Seism. Soc. Am.*, Vol. 71, No. 6, 2011-2038, 1981.
- 2-32 Joyner, W. B. and Boore, D. M., "Prediction of Earthquake Response Spectra," *U.S. Geol. Surv. Open File Report 82-977*, 1982.
- 2-33 Idriss, I. M., "Evaluating Seismic Risk in Engineering Practice," Chapter 6, *Proc. 11th International Conf. Soil Mechanics and Foundation Eng.*, 255-320, San Francisco, 1985.
- 2-34 Sabetta, F. and Pugliese, A., "Attenuation of Peak Horizontal Acceleration and Velocity from Italian Strong-Motion Records," *Bull. Seism. Soc. Am.*, Vol. 77, No. 5, 1491-1513, 1987.
- 2-35 Sadigh, K., Egan, J., and Youngs, R., "Specification of Ground Motion for Seismic Design of Long Period Structures," *Earthquake Notes*, Vol. 57, 13, 1986.
- 2-36 Campbell, K. W. and Bozorgnia, Y., "Near-Source Attenuation of Peak Horizontal Acceleration from Worldwide Accelerograms Recorded from 1957 to 1993," *Proc. 5th U.S. National Conf. Earthquake Eng.*, Vol. 3, 283-292, Chicago, Illinois, 1994.
- 2-37 Boore, D. M., Joyner, W. B., and Fumal, T. E., "Equations for Estimating Horizontal Response Spectra and Peak Acceleration from Western North American Earthquakes: A Summary of Recent Work," *Seismological Research Letters*, Vol. 68, No. 1, 128-153, 1997.
- 2-38 Housner, G. W., "Intensity of Earthquake Ground Shaking Near the Causative Fault," *Proc. 3rd. World Conf. Earthquake Eng.*, Vol. 1, III, 94-115, New Zealand, 1965.
- 2-39 Seed, H. B. and Idriss, I. M., "Ground Motions and Soil Liquefaction During Earthquakes," Earthquake Engineering Research Institute, Berkeley, California, 1982.
- 2-40 Porcella, R. L. and Matthiesen, R. B., USGS Open-File Report 79-1654, 1979.
- 2-41 Nuttli, O. W. and Herrmann, R. B., "Consequences of Earthquakes in Mississippi Valley," ASCE Preprint 81-519, ASCE National Convention, St. Louis, 1981.
- 2-42 Hanks, T. and McGuire, R., "The Character of High-Frequency Strong Ground Motion," *Bull. Seism. Soc. Am.*, Vol. 71, 2071-2095, 1981.
- 2-43 Spudich, P. and Ascher, U., "Calculation of Complete Theoretical Seismograms in Vertically Varying Media Using Collocation Methods," *Geophys. J. R. Astron. Soc.*, Vol. 75, 101-124, 1983.
- 2-44 Atkinson, G. and Boore, D., "Ground Motion Relations for Eastern North America," *Bull. Seism. Soc. Am.*, Vol. 85, No. 1, 17-30, 1995.
- 2-45 Boore, D. M., Joyner, W. B., Oliver, A. A., and Page, R. A., "Estimation of Ground Motion Parameters," USGS, Circular 795, 1978.
- 2-46 Boore, D. M., Joyner, W. B., Oliver, A. A., and Page, R. A., "Peak Acceleration, Velocity and Displacement from Strong Motion Records," *Bull. Seism. Soc. Am.*, Vol. 70, No. 1, 305-321, 1980.
- 2-47 Chang, F. K. and Krinitzsky, E. L., "Duration, Spectral Content, and Predominant Period of Strong Motion Earthquake Records from Western United States," U.S. Army Engineer Waterways Experiment Station, Miscellaneous Paper S-73-1, Vicksburg, Mississippi, 1977.
- 2-48 Novikova E. I. and Trifunac, M. D., "Duration of Strong Motion in Terms of Earthquake Magnitude, Epicentral Distance, Site Conditions and Site Geometry," *Earthquake Engineering and Structural Dynamics*, Vol. 23, 1023-1043, 1994.
- 2-49 Hall, J. F., Heaton, T. H., Halling M. W., and Wald, D. J., "Near-Source Ground Motions and its Effects on Flexible Buildings," *Earthquake Spectra*, Vol. 11, No. 4, 569-605, 1995.
- 2-50 Heaton, T. H. and Hartzell, S. H., "Earthquake Ground Motions," *Annual Reviews of Earth and Planetary Sciences*, Vol. 16, 121-145, 1988.
- 2-51 Somerville, P. G. and Graves, R. W., "Conditions that Give Rise to Unusually Large Long Period Motions," *Structural design of Tall Buildings*, Vol. 2, 211-232, 1993.
- 2-52 Idriss, I. M., "Influence of Local Site Conditions on Earthquake Ground Motions," *Proc. 4th U.S. Nat. Conf. Earthquake Engineering*, Vol. 1, 55-57, Palm Springs, California, 1990.
- 2-53 Mohraz, B., "A Study of Earthquake Response Spectra for Different Geological Conditions," *Bull. Seism. Soc. Am.*, Vol. 66, No. 3, 915-935, 1976.
- 2-54 Housner, G. W., "Strong Ground Motion," Chapter 4 in *Earthquake Engineering*, R. L. Wiegel, Editor, Prentice-Hall, Englewood Cliffs, N.J., 1970.
- 2-55 McGarr, A., "Scaling of Ground Motion Parameters, State of Stress, and Focal Depth," *J. Geophys. Res.*, Vol. 89, 6969-6979, 1984.
- 2-56 McGarr, A., "Some Observations Indicating Complications in the Nature of Earthquake Scaling", *Earthquake Source Mechanics, Maurice*

- Ewing Ser. 6, edited by S. Das et al., 217-225, 1986.
- 2-57 Kanamori, H. and Allen, C. R., "Earthquake Repeat Time and Average Stress Drop," *Earthquake Source Mechanics, Maurice Ewing Ser. 6*, edited by S. Das et al., 227-235, 1986.
- 2-58 Campbell, K. W., "Predicting strong Ground Motion in Utah," *Evaluation of Regional and Urban Earthquake Hazards and Risks in Utah*, edited by W. W. Hays and P. L. Gori, 1988.
- 2-59 Joyner, W. B. and Boore, D. M., "Measurement, Characterization, and Prediction of Strong Ground Motion," *Proc. Earthquake engineering and Soil Dynamics II*, GT Div/ASCE, edited by J. L. Von Thun, Park City, Utah, 43-102, 1988.
- 2-60 Faccioli, E., "Estimating Ground Motions for Risk Assessment," *Proc. of the U.S.-Italian Workshop on Seismic Evaluation and Retrofit*, Edited by D. P. Abrams and G. M. Calvi, Technical Report NCEER-97-0003, National Center for Earthquake Engineering Research, Buffalo, New York, 1-16, 1997.
- 2-61 Reiter, L., *Earthquake Hazard Analysis: Issues and Insights*, Columbia University Press, New York, 1990.
- 2-62 Boatwright, J. and Boore, D. M., "Analysis of the Ground Accelerations radiated by the 1980 Livermore Valley Earthquakes for Directivity and Dynamic Source Characteristics," *Bull. Seism. Soc. Am.*, Vol. 72, 1843-1865.
- 2-63 Gutenberg, B. and Richter, C. F. "Earthquake Magnitude, Intensity, Energy, and Acceleration," *Bull. Seism. Soc. Am.*, Vol. 46, No. 2, 143-145, 1956.
- 2-64 Richter, C. F., *Elementary Seismology*, W. H. Freeman and Co., San Francisco, 1958.
- 2-65 Bender, B., "Maximum Likelihood Estimation of b Values for Magnitude Grouped Data," *Bull. Seism. Soc. Am.*, Vol. 73, No. 3, 831-851, 1983.
- 2-66 Schwartz, D. P. and Coppersmith, K. J., "Fault Behavior and Characteristic Earthquakes: Examples from the Wasatch and San Andreas Fault Zones," *J. Geophys. Res.*, Vol. 89, No. B7, 5681-5698, 1984.
- 2-67 Sieh, K. E., "Prehistoric Large Earthquakes Produced by Slip on the San Andreas Fault at Pallett Creek, California," *J. Geophys. Res.*, Vol. 83, No. B8, 3907-3939, 1978.
- 2-68 Cornell, C. A., "Engineering Seismic Risk Analysis," *Bull. Seism. Soc. Am.*, Vol. 58, No. 5, 1583-1606, 1968.
- 2-69 Vanmarcke, E. H., "Seismic Safety Assessment," *Random Excitation of Structures by Earthquakes and Atmospheric Turbulence*, edited by H. Parkus, International Center for Mechanical Sciences, Course and Lectures No. 225, Springer-Verlag, 1-76, 1977.
- 2-70 Benjamin, J. R., "Probabilistic Models for Seismic Force Design," *J. Structural Div.*, ASCE, Vol. 94, ST5, 1175-1196, 1968.
- 2-71 Der-Kiureghian, A. and Ang A. H-S., "A Fault-Rupture Model for Seismic Risk Analysis," *Bull. Seism. Soc. Am.*, Vol. 67, No. 4, 1173-1194, 1977.
- 2-72 Algermissen, S. T. and Perkins, D. M., "A Technique for Seismic Risk Zoning, General Considerations and Parameters," *Proc. Microzonation Conf.*, 865-877, Seattle, Washington, 1972.
- 2-73 Algermissen, S. T. and Perkins, D. M., "A Probabilistic Estimate of Maximum Acceleration in Rock in Contiguous United States," USGS Open File Report, 76-416, 1976.
- 2-74 Applied Technology Council, National Bureau of Standards, and National Science Foundation, "Tentative Provisions for the Development of Seismic Regulations for Buildings," ATC Publication 3-06, NBS Publication 510, NSF Publication 78-8, 1978.
- 2-75 McGuire, R. K., "Seismic Structural Response Risk Analysis, Incorporating Peak Response Progressions on Earthquake Magnitude and Distance," Report R74-51, Dept. of Civil Engineering, Mass. Inst. of Technology, Cambridge, Mass., 1975.
- 2-76 NEHRP Recommended Provisions for the Development of Seismic Regulations for New Buildings, 1985 Edition, Building Seismic Safety Council, Washington, D.C., 1985.
- 2-77 NEHRP Recommended Provisions for the Development of Seismic Regulations for New Buildings, 1988 Edition, Building Seismic Safety Council, Washington, D.C., 1988.
- 2-78 NEHRP Recommended Provisions for the Development of Seismic Regulations for New Buildings, 1991 Edition, Building Seismic Safety Council, Washington, D.C., 1991.
- 2-79 NEHRP Recommended Provisions for the Development of Seismic Regulations for New Buildings, 1994 Edition, Building Seismic Safety Council, Washington, D.C., 1994.
- 2-80 NEHRP Recommended Provisions for the Development of Seismic Regulations for New Buildings, 1997 Edition, Building Seismic Safety Council, Washington, D.C., 1997.
- 2-81 NEHRP Guidelines for the Seismic Rehabilitation of Buildings, FEMA-273, Building Seismic Safety Council, Washington, D.C., 1997.
- 2-82 Uniform Building Code, 1985 Edition, International Conference of Building Officials, Whittier, California, 1985.
- 2-83 Uniform Building Code, 1988 Edition, International Conference of Building Officials, Whittier, California, 1988.

- 2-84 Uniform Building Code, 1991 Edition, International Conference of Building Officials, Whittier, California, 1991.
- 2-85 Uniform Building Code, 1994 Edition, International Conference of Building Officials, Whittier, California, 1994.
- 2-86 Uniform Building Code, 1997 Edition, International Conference of Building Officials, Whittier, California, 1997.
- 2-87 Newmark, N. M. and Hall, W. J., "Earthquake Spectra and Design," Earthquake Engineering Research Institute, Berkeley, California, 1982.
- 2-88 Newmark, N. M., Blume, J. A., and Kapur, K. K., "Seismic Design Criteria for Nuclear Power Plants," *J. Power Div.*, ASCE, Vol. 99, No. PO2, 287-303, 1973.
- 2-89 Newmark, N. M. and Hall, W. J., "Seismic Design Criteria for Nuclear Reactor Facilities," *Proc. 4th World Conf. Earthquake Eng.*, B-4, 37-50, Santiago, Chile, 1969.
- 2-90 Newmark, N. M. and Hall, W. J., "Procedures and Criteria for Earthquake Resistant Design," Building Practices for Disaster Mitigation, National Bureau of Standards, U.S. Department of Commerce, Building Research Series 46, 209-236, 1973.
- 2-91 Hall, W. J., Mohraz B., and Newmark, N. M., "Statistical Studies of Vertical and Horizontal Earthquake Spectra," Nathan M. Newmark Consulting Engineering Services, Urbana, Illinois, 1975.
- 2-92 Newmark, N. M. and Rosenblueth, E., *Fundamentals of Earthquake Engineering*, Prentice-Hall, Englewood Cliffs, N.J., 1971.
- 2-93 Mohraz, B. and Tiv, M., "Spectral Shapes and Amplifications for the Loma Prieta Earthquake of October 17, 1989," *Proc. 3rd U.S. Conf. Lifeline Earthquake Eng.*, 562-571, Los Angeles, California, 1991.
- 2-94 Trifunac, M. D., Brady, A. G., and Hudson, D. E., "Analysis of Strong-Motion Earthquake Accelerograms, Vol. III, Response Spectra, Parts A through Y," Earthquake Eng. Research Laboratory, California Institute of Technology, Pasadena, California, 1972-1975.
- 2-95 Chopra, A. K., "Dynamics of Structures - A Primer," Earthquake Engineering Research Institute, Berkeley, California, 1981.
- 2-96 Sadek, F., Mohraz, B., and Riley, M. A., "Linear Procedures for Structures with Velocity-Dependent Dampers," *Journal of Structural Engineering*, ASCE, Vo. 128, No. 8, 887-895, 2000.
- 2-97 Hayashi, S., Tsuchida, H., and Kurata, E., "Average Response Spectra for Various Subsoil Conditions," *Third Joint Meeting, U.S. - Japan Panel on Wind and Seismic Effects*, UJNR, Tokyo, 1971.
- 2-98 Kuribayashi, E., Iwasaki, T., Iida, Y., and Tuji, K., "Effects of Seismic and Subsoil Conditions on Earthquake Response Spectra," *Proc. International Conf. Microzonation*, Seattle, Wash., 499-512, 1972.
- 2-99 Seed, H. B., Ugas, C., and Lysmer, J., "Site-Dependent Spectra for Earthquake-Resistance Design," *Bull. Seism. Soc. Am.*, Vol. 66, No. 1, 221-243, 1976.
- 2-100 Atomic Energy Commission, "Design Response Spectra for Seismic Design of Nuclear Power Plants," Regulatory Guide 1.60, Directorate of Regulatory Standards, Washington, D.C., 1973.
- 2-101 Crouse, C. B. and McGuire, J. W., "Site Response Studies for Purpose of Revising NEHRP Seismic Provisions," *Earthquake Spectra*, Vol. 12, No. 3, 407-439, 1996.
- 2-102 Mohraz, B., "Influences of the Magnitude of the Earthquake and the Duration of Strong Motion on Earthquake Response Spectra," *Proc. Central Am. Conf. on Earthquake Eng.*, San Salvador, El Salvador, 1978.
- 2-103 Mohraz, B., "Recent Studies of Earthquake Ground Motion and Amplification," *Proc. 10th World Conf. Earthquake Eng.*, Madrid, Spain, 6695-6704, 1992.
- 2-104 Peng, M. H., Elghadamsi, F. E., and Mohraz, B., "A Simplified Procedure for Constructing Probabilistic Response Spectra," *Earthquake Spectra*, Vol. 5, No. 2, 393-408, 1989.
- 2-105 Singh, J. P., "Earthquake Ground Motions: Implications for Designing Structures and Reconciling Structural Damage," *Earthquake Spectra*, Vol. 1, No. 2, 239-270, 1985.
- 2-106 "Reducing Earthquake Hazards: Lessons Learned from Earthquakes," Earthquake Engineering Research Institute, Publication No. 86-02, Berkeley, California, 1986.
- 2-107 Housner, G. W. and Jennings, P. C., "Earthquake Design Criteria," Earthquake Engineering Research Institute, Berkeley, California, 1982.
- 2-108 Housner, G. W., "Spectrum Intensities of Strong-Motion Earthquakes," *Proc. of the Symposium on Earthquakes and Blast Effects on Structures*, Earthquake Engineering Research Institute, 1952.
- 2-109 Housner, G. W., "Behavior of Structures During Earthquakes," *J. Eng. Mech. Div.*, ASCE Vol. 85, No. EM4, 109-129, 1959.
- 2-110 Housner, G. W., "Design Spectrum," Chapter 5 in Earthquake Engineering, R.L. Wiegel, Editor, Prentice-Hall, Englewood Cliffs, N.J., 1970.
- 2-111 Blume, J. A., Sharpe, R. L., and Dalal, J. S., "Recommendations for Shape of Earthquake Response Spectra," John A. Blume & Associates, San Francisco, California, AEC Report Wash-1254, 1972.

- 2-112 Seismology Committee, Structural Engineers Association of California, "Recommended Lateral Force Requirements," 1986.
- 2-113 Martin, G. M., Editor, *Proceedings of the NCEER/SEAOC/BSSC Workshop on Site Response During Earthquakes and Seismic Code Provisions*, University of Southern California, Los Angeles, 1994.
- 2-114 Borcherdt, R. D., "Estimates of Site-Dependent Response Spectra for Design (Methodology and Justification)," *Earthquake Spectra*, Vol. 10, No. 4, 617-653, 1994.
- 2-115 Seed, R. B., Dickenson, S. E., and Mok, C. M., "Recent Lessons Regarding Seismic Response Analyses of Soft and Deep Clay Sites," in *Proc. 4th Japan-U.S. Workshop on Earthquake Resistant Design of Lifeline Facilities and Countermeasures for Soil Liquefaction*, National Center for Earthquake Engineering Research, State University of New York at Buffalo, Vol. I, 131-145, 1992.
- 2-116 Dobry, R., Martin, G. M., Parra, E., and Bhattacharyya, *Study of Ratios of Response Spectra Soil/Rock and of Site Categories for Seismic Codes*, National Center for Earthquake Engineering Research, State University of New York at Buffalo, 1994.
- 2-117 Borcherdt, R. D., "Preliminary Amplification Estimates Inferred from Strong-Ground-Motion Recordings of the Northridge Earthquake of January 17, 1994," *Proc. Of the International Workshop on Site Response Subjected to Strong Earthquake Motions*, Japan Port and Harbour Research Institute, Vol. 2, 21-46, Yokosuka, Japan, 1996.
- 2-118 Riddell, R., and Newmark, N. M., "Statistical Analysis of the Response of Nonlinear Systems Subjected to Earthquakes," Civil Engineering Studies, Structural Research Series 468, Department of Civil Engineering, University of Illinois, Urbana, Illinois, 1979.
- 2-119 Elghadamsi, F. E and Mohraz, B., "Inelastic Earthquake Spectra," *J. Earthquake Engineering and Structural Dynamics*, Vol. 15, 91-104, 1987.
- 2-120 Blume, J. A., Newmark, N. M., and Corning, L. H., "Design of Multistory Reinforced Concrete Buildings for Earthquake Motions," Portland Cement Association, 1961.
- 2-121 Newmark, N. M., "Current Trends in the Seismic Analysis and Design of High-Rise Structures," Chapter 16 in *Earthquake Engineering*, R.L. Wiegel, Editor, Prentice-Hall, Englewood Cliffs, N.J., 1970.
- 2-122 Housner, G. W., "Limit Design of Structures to Resist Earthquakes," *Proc. 1st World Conf. Earthquake Engineering*, 5-1 to 5-13, Berkeley, Calif., 1956.
- 2-123 Blume, J. A., "A Reserve Energy Technique for the Earthquake Design and Rating of Structures in the Inelastic Range," *Proc. 2nd World Conf. Earthquake Engineering*, Vol. II, 1061-1084, Tokyo, Japan 1960.
- 2-124 Blume, J. A., "Structural Dynamics in Earthquake-Resistant Design," *Transactions, ASCE*, Vol. 125, 1088-1139, 1960.
- 2-125 Blume, J. A., discussion of "Electrical Analog for Earthquake Yield Spectra," *J. Engineering Mechanics Div., ASCE*, Vol. 86, No. EM3, 177-184, 1960.
- 2-126 Lai, S. P. and Biggs, J. M., "Inelastic Response Spectra for Aseismic Building Design," *J. Struct. Div., ASCE*, Vol. 106, No. ST6, 1295-1310, 1980.
- 2-127 Penzien, J. and Liu, S. C., "Nondeterministic Analysis of Nonlinear Structures Subjected to Earthquake Excitations," *Proc. 4th World Conf. Earthquake Engineering*, A-1, 114-129, Santiago, Chile, 1969.
- 2-128 Peng, M. H., Elghadamsi, F. E., and Mohraz, B., "A Stochastic Procedure for Seismic Analysis of SDOF Structures," Civil and Mechanical Engineering Dept., School of Engineering and Applied Science, Southern Methodist University, Dallas, TX, 1987.
- 2-129 Applied Technology Council ATC, *Structural Response Modification Factors*, ATC-19 Report, Redwood City, California, 1995.
- 2-130 Krawinkler, H. and Nassar, A. A., "Seismic Design Based on Ductility and Cumulative Damage Demands and Capacities," *Nonlinear Seismic Analysis and Design of Reinforced Concrete Buildings*, Edited by Fajfar and Krawinkler, Elsevier Applied Science, New York, 1992.
- 2-131 Nassar, A. A. and Krawinkler, H., *Seismic Demands for SDOF and MDOF Systems*, John A. Blume Earthquake Engineering Center, Report No. 95, Stanford University, Stanford, California, 1991.

- 2-131 Miranda, E. and Bertero, V. V., "Evaluation of Strength Reduction Factors for Earthquake-Resistant Design," *Earthquake Spectra*, Vol. 10, No. 2, 357-379, 1994.
- 2-132 Zahrah, T. F. and Hall, W. J., "Earthquake Energy Absorption in SDOF Structures," *Journal of Structural Engineering*, ASCE, Vol. 110, No. 8, 1757-1772, 1984.
- 2-133 Uang, C. M. and Bertero, V. V., "Evaluation of Seismic Energy Structures," *Earthquake Engineering and Structural Dynamics*, Vol. 19, 77-90, 1990.
- 2-134 Housner, G. W. and Jennings, P. C., "Generation of Artificial Earthquakes," *J. Engineering Mechanics Div.*, ASCE, Vol. 90, 113-150, 1964.
- 2-135 Shinozuka, M. and Salo, Y., "Simulation of Nonstationary Random Process," *J. Engineering Mechanics Div.*, ASCE, Vol. 93, 11-40, 1967.
- 2-136 Amin, M. and Ang, A. H. - S., "Nonstationary Stochastic Model of Earthquake Ground Motion," *J. Engineering Mechanics Div.*, ASCE, Vol. 74, No. EM2, 559-583, 1968.
- 2-137 Iyengar, R. N. and Iyengar, K. T. S., "A Nonstationary Random Process Model for Earthquake Accelerograms," *Bull. Seism. Soc. Am.*, Vol. 59, 1163-1188, 1969.

Chapter 3

Geotechnical Design Considerations

Marshall Lew, Ph.D., G.E.

Corporate Consultant, Law/Crandall, a division of Law Engineering and Environmental Services, Inc. (A LAWGIBB Group Member), Los Angeles

Key words: Building Code, Earthquake Ground Motion, Fault Rupture, International Building Code, Landslides, Lateral Spreading, Liquefaction Analysis, Liquefaction Mitigation, Near-Source Effects, Response Spectra, Settlement, Site Effects, Soil-Structure Interaction, Soil Profiles, Tsunamis, Uniform Building Code.

Abstract: This chapter surveys the interactions between structural and geotechnical engineering in earthquake-resistant design. The effects of the local site conditions and geology are presented as applied in the Uniform Building Code and in the new International Building Code. Methods of characterizing the site conditions, as well as consideration of near-source effects, are discussed. This chapter also addresses the issues of soil liquefaction. Methods of analysis for soil liquefaction are presented, incorporating various techniques generally accepted by the profession. The consequences resulting from liquefaction, namely liquefaction-induced settlement, lateral spreading, and loss of bearing capacity, are presented as well as methods of estimating these effects. Various methods and strategies to mitigate the effects of soil liquefaction are presented as well as the merits of each. The latter part of the chapter discusses other geologic-seismic hazards, including seismic settlement, landsliding, tsunamis, and earthquake fault rupture. There is also a discussion of soil-structure interaction and design of walls below grade for seismic earth pressures.

3.1 INTRODUCTION

Structures come in different shapes, forms, and sizes. However, all structures have at least one feature in common; they all have a foundation. A foundation is the means by which the superstructure interfaces with the underlying soil or rock. Under static conditions, generally only the vertical loads of a structure need be transferred to the supporting soil or rock. In a seismic environment, the loads imposed on a foundation from a structure under seismic excitation can greatly exceed the static vertical loads or even produce uplift; in addition, there will be horizontal forces and possibly moments at the foundation level.

Consideration must also be given to what could happen to the supporting soil or rock under seismic excitation. For example, an earthquake might cause the phenomenon of liquefaction to occur in loose sandy soils which would cause a virtually complete loss of all bearing capacity of the soil; needless to say, a structure founded on such soils would suffer great distress and upset.

This chapter will attempt to identify those phenomena that would affect the design of foundations and structures in a seismic environment. Some of these phenomena can be effectively designed for by structural detailing, but some of these phenomena are beyond the magic and wizardry of the structural engineering profession and geotechnical wizardry may also be needed. In some instances, there may not be an economical engineering solution for the problem.

This chapter will be different from other chapters in this handbook in the respect that not all of the solutions to the seismic problems will be an engineering solution. This just points out the limitations of the science and art we know as engineering. We as engineers must be able to recognize our limitations and shortcomings and realize that we cannot always be the white knight that is able to save the damsel in distress. If we can attain at least this little enlightenment, we will all be better engineers.

In a seismic environment, there may exist a potential for ground failures. It is obvious that if the ground should fail beneath a structure, the structure could be severely or totally damaged. Such an event would threaten real property and life safety. Several different ground failure mechanisms will be discussed in this chapter.

3.2 SITE AND SOIL CONDITIONS

Because a foundation must be capable of adequately supporting a structure in an economical manner, it is imperative that there be a proper geotechnical investigation. This geotechnical investigation should provide information about the soil types beneath the site and their physical characteristics (i.e., strength, compressibility, permeability, etc.). The investigation should also provide economical and feasible alternatives for the support of the structure. These recommendations should take into account the functionality and purpose of the structure. In a seismic environment, the geotechnical investigation would also need to evaluate the behavior of the supporting soils under earthquake excitation and determine or predict the impact and consequences upon the structure and the foundation types recommended.

Not only is it important to investigate the soil conditions, the general site conditions also merit deep scrutiny. This investigation should include features near the building area and also distant features. Important nearby site features would include water levels, topographic features, and the presence of other structures both above and below ground. Offsite and even distant features could have some influence upon the proposed structure, especially in a seismically active area. For example, there could be large bodies of water retained by earth dams that could fail in an earthquake; if the structure is in the path of this potential inundation, the consequences could be very grave indeed.

3.3 SITE EFFECTS

3.3.1 Effects of Soils on Earthquake Loads on Structures

It has become recognized that the local site conditions have a very important role on the response of structures. The soil and rock at a site have specific characteristics that can significantly amplify the incoming earthquake motions traveling from the earthquake source. The importance of local site conditions was recognized in the 1960s by the influence of ground motions on midheight buildings in the Caracas, Venezuela earthquake. For buildings of about the same height with similar construction, it was observed that such buildings founded on deep soils were more damaged than the similar buildings founded on rock. These observations were further confirmed with the 1985 Mexico City earthquake where ground motions in Mexico City, some several hundreds of kilometers from the fault rupture, were amplified in the deep soft lakebed deposits that underlie the city; these ground motions had a long period and affected many high-rise buildings adversely with some collapses.

3.3.2 Uniform Building Code Recognition

The Uniform Building Code (UBC) acknowledged the importance of local site effects and the concept of a "Soil Factor" was added to the lateral force design procedure in the 1976 edition of the UBC.⁽³⁻¹⁾ At that time, a Soil-Structure Resonance Factor, S, was part of the design base shear equation; the value of the "S-factor" was dependent upon the ratio of T/T_s , where T is the fundamental building period and T_s is the characteristic site period. The "S-factor" ranged from a minimum of 1.0

to a maximum of 1.5. This concept of the soil factor remained in the UBC up to the 1985 edition⁽³⁻²⁾ and was removed in the 1988 edition.⁽³⁻³⁾

In the 1985 edition, a second method of determining the Soil Factor was introduced. This method is not dependent on the ratio of T/T_s . Instead, the code defined three soil profile types, which essentially were rock, deep soil, and soft soil and the Soil Profile types were designated S_1 , S_2 , and S_3 , respectively. The values of the Soil Factor were 1.0, 1.2, and 1.5 for S_1 , S_2 , and S_3 , respectively. In response to the Mexico City earthquake, a fourth Soil Profile type, S_4 , was added in 1988 for very deep soft soils like those found in Mexico City and perhaps in some parts of the San Francisco Bay region; the S_4 factor was equal to 2.0.

Uniform Building Code, 1994 Edition

The 1994 UBC⁽³⁻⁴⁾ specifies the design base shear in a given direction to be:

$$V = \frac{ZICW}{R_w}$$

$$\text{where } C = \frac{1.25S}{T^{2/3}}$$

I = Importance Factor

Z = Seismic Zone Factor

The value of C need not exceed 2.75 and may be used for any structure without regard to soil type or structure period. The value of the Seismic Zone Factor, Z, is given in Table 3-1:

*Table 3-1. — Seismic Zone Factor
From Table 16-I of the 1994 UBC (Ref. 3-4)*

Zone	1	2A	2B	3	4
Z	0.075	0.15	0.20	0.30	0.40

The Site Coefficients, S, for the four soil types in the 1994 UBC are given in Table 3-2:

Table 3-2. — Site Coefficients, S
From Table 16-J of the 1994 UBC (Ref. 3-4)

TYPE	DESCRIPTION	S FACTOR
S ₁	A soil profile with either: (a) A rock-like material characterized by a shear-wave velocity greater than 2,500 feet per second (762 m/s) or by other suitable means of classification, or (b) Medium-dense to dense or medium-stiff to stiff soil conditions, where soil depth is less than 200 feet (60,960 mm)	1.0
S ₂	A soil profile with predominantly medium-dense to dense or medium stiff to stiff soil conditions, where the soil depth exceeds 200 feet (60,960 mm)	1.2
S ₃	A soil profile containing more than 20 feet (6,096 mm) of soft to medium-stiff clay but not more than 40 feet (12,192 mm) of soft clay	1.5
S ₄	A soil profile containing more than 40 feet (12,192 mm) of soft clay characterized by a shear wave velocity less than 500 feet per second (152.4 m/s)	2.0

The site factor is to be established from properly substantiated geotechnical data. In locations where the soil properties are not known in sufficient detail to determine the soil type, soil profile S₃ is to be used. Soil profile S₄ need not be assumed unless the building official determines that soil profile S₄ may be present at the site, or in the event that soil profile S₄ is established by geotechnical data.

Uniform Building Code, 1997 Edition

The 1997 UBC⁽³⁻⁵⁾ has some major changes from the earlier editions. The first major difference is that it is a strength-based code. From an earth science or geotechnical perspective, the 1997 UBC has tried to incorporate new understanding about ground motion amplification and attempts to account for near-source effects.

The 1997 UBC contains a number of very significant changes affecting the seismic design of buildings. The code was developed by the Seismology Committee of the Structural Engineers Association of California (SEAOC) over a period of three years and is contained in Appendix C of the 1996 Recommended Lateral Force Requirements and Commentary, also known as the SEAOC Blue Book.⁽³⁻⁶⁾ In addition to converting the code from a working stress to a strength basis, it was intended to advance the seismic provisions in several important areas. The Seismology Committee developed the proposal in coordination with a

parallel effort by the Building Seismic Safety Council (BSSC) for the 1997 NEHRP Provisions.⁽³⁻⁷⁾ (NEHRP is an acronym for the National Earthquake Hazards Reduction Program.) The NEHRP Provisions serve as the source document for other United States model building codes (BOCA and Southern Building Code). Therefore, this change is seen not only as an important advancement in seismic design requirements, but as a critical step toward the cooperative development of a single national building code for the United States by the year 2000.

The 1997 UBC code incorporates a number of important lessons from recent earthquakes and recent advances from other sources. In general it is intended to provide parity with previous requirements, except for longer period buildings in near-field locations and for structural systems with poor redundancy.

3.3.3 Overview of 1997 UBC

The following key concepts are contained in the 1997 UBC:

1. The adoption of ASCE-7 load factors for strength-based load combinations. In addition, working stress load combinations are maintained as an alternative.
2. The incorporation of a Redundancy/Reliability Factor (ρ), which is intended to encourage redundant lateral force resisting systems by penalizing non-

- redundant ones through higher lateral force requirements.
3. The incorporation of near-source factors (N_a and N_v) in Seismic Zone 4 which are intended to recognize the amplified ground motions which occur at close distances to the fault.
 4. The adoption of a new set of soil profile categories (from 1994 NEHRP) which are used in combination with Seismic Zone Factors (Z) and near-source factors, to provide site-dependent ground motion coefficients (C_a and C_v) defining ground motion response within the acceleration and velocity-controlled ranges of the spectrum. The design response spectrum differs from the spectrum in the 1994 and earlier UBC in two ways: the constant velocity portion is now defined by $1/T$, as opposed to $1/T^{2/3}$, causing it to drop more rapidly in that range, and the plateau in the constant acceleration domain varies with C_a rather than being a constant value for all soil profiles.
 5. Substantial revisions to lateral force requirements for elements of structures, nonstructural components and equipment supported by structures. These provisions more accurately represent lateral forces on elements by recognizing varying diaphragm accelerations, component amplification, component response modification, and ground motion response. Similar changes are proposed for non-building structures.
 6. A simplified design base shear calculation permitted for one- and two-story dwellings, one to three-story light frame construction and other one- and two-story buildings as permitted.
 7. The R-factor has been adjusted to provide a strength level base shear. Earlier editions of the code change proposal submitted to the International Conference of Building Officials (ICBO) contained a two-component R-factor, with values for R_0 and R_d representing overstrength and system ductility. However, it was found that the requirements for defining the plastic mechanism analysis required for the R_0

calculation could not be codified in simple language while guaranteeing accuracy, so the single R value was adopted. However, the two component R has been maintained in the SEAOC Blue Book version, essentially for its educational value.

The N_a and N_v factors represent the most significant difference between the 1997 UBC and the developing 1997 NEHRP Provisions, which will address near field effects through the use of spectral values maps which are being developed by BSSC based on new seismic risk maps developed by the United States Geological Survey (USGS). The maps represent a major research effort which was not completed (for design application) in time for use in the 1997 UBC code.

An important concept in the 1997 UBC code is the use of *elastic response parameters* to define unreduced forces and displacements ($R=1$) for calculations involving drift and deformation compatibility and in dynamic analysis. In addition, the parameter E_M has been introduced to represent the maximum earthquake force that can be developed in the structure for use in addressing non-ductile conditions, similar to the $3R_w/8$ parameter in the 1994 UBC. E_M is used to define collector strength requirements.

Near-Source Factors and Code Elastic Design Response Spectra

The design base shear, as determined in the 1994 and earlier editions of the UBC, is a function of an assumed level of ground motion. In Seismic Zone 4, this level of ground motion has been taken as being an effective peak ground acceleration (EPA) of 0.4g. While no formal relationship exists between the EPA and the peak ground acceleration (PGA), it may be taken that the EPA is about two-thirds of the PGA.

Strong motion measurements in recent large earthquakes, such as the 1994 Northridge and 1995 Kobe events, showed that ground motions are significantly greater near the earthquake source. These events had near-source ground

Table 3-3. — Soil Profile Types, 1997 UBC

From Table 16-J, 1997 UBC (Ref. 3-5)

Soil Profile Type	Soil Profile Name/Generic Description	Average Shear Wave Velocity, v_s , for upper 100 feet of soil profile, feet/second (m/s)
S_A	Hard Rock	>5,000 (1,500)
S_B	Rock	2,500 to 5,000 (760 to 1,500)
S_C	Very Dense Soil and Soft Rock	1,200 to 2,500 (360 to 760)
S_D	Stiff Soil	600 to 1,200 (180 to 360)
S_E	Soft Soil	<600 (180)
S_F	Soils Requiring Site-Specific Evaluation	

motions that greatly exceeded the EPA level for Zone 4 in the 1994 UBC codes. It has also been observed that the amplification of long-period ground motions is also greater with less competent site soil conditions.

These near-source factors apply only to Seismic Zone 4 because it is believed that the near-source effect is only significant for large earthquakes. Research of the ground motions from Northridge, Kobe, and other events have indicated that the amount of near-source effect is greater at the long periods than the short periods. Therefore, two near-source factors were introduced that result in a greater amplification of the ground motions for long periods than for those for short periods. The near-source factors were introduced in the 1997 UBC strength-based seismic code to account for this increase as a function of the earthquake potential of a known earthquake source and the distance from source to the given site.

As mentioned earlier, a new set of soil profile types has been introduced into the 1997 UBC. These soil profile types are based on the average soil properties for the upper 100 feet of the soil profile. An abbreviated description as a function of the average shear wave velocity in the upper 100 feet (approximately 30 meters) is given in Table 3-3 for five "stable" profile types, designated as S_A through S_E ; there is a sixth profile type (S_F) which require a site-

specific evaluation. The near-source factor, N_a , for short periods is shown in Table 3-4 as a function of the three seismic source types; the near-source factor, N_v , for long periods is shown in Table 3-5 for the different seismic source types.

The types of soils requiring site-specific evaluation in Soil Profile Type S_F are:

1. Soil vulnerable to potential failure or collapse under seismic loading such as liquefiable soils, quick and highly sensitive clays, collapsible weakly cemented soils.
2. Peats and/or highly organic clays [$H > 10$ feet of peat and/or highly organic clay, where H = thickness of soil].
3. Very high plasticity clays [$H > 25$ feet with Plasticity Index > 75].
4. Very thick soft/medium stiff clays [$H > 120$ feet].

The closest distance to the seismic source is to be taken as the minimum distance between the site and the area described by the vertical projection of the source on the ground surface (i.e., surface projection of the fault plane). For dipping faults, the surface projection is to include those portions of the source within 10 km of the surface as illustrated in Figure 3-1. The definitions of the seismic source types are shown in Table 3-6. For seismic sources

Table 3-4. Near-Source Factor for Short Periods, N_a
From Table 16-S, 1997 UBC (Ref. 3-5)

Seismic Source Type	Closest Distance to Known Seismic Source		
	$\leq 2 \text{ km}$	5 km	$\geq 10 \text{ km}$
A	1.5	1.2	1.0
B	1.3	1.0	1.0
C	1.0	1.0	1.0

Table 3-5. — Near-Source Factor for Long Periods, N_v
From Table 16-T, 1997 UBC (Ref. 3-5)

Seismic Source Type	Closest Distance to Known Seismic Source			
	$\leq 2 \text{ km}$	5 km	$\geq 10 \text{ km}$	$\geq 15 \text{ km}$
A	2.0	1.6	1.2	1.0
B	1.6	1.2	1.0	1.0
C	1.0	1.0	1.0	1.0

Table 3-6. — Seismic Source Type
From Table 16-U, 1997 UBC (Ref. 3-5)

Seismic Source Type	Seismic Source Description	Seismic Source Definition	
		Maximum Moment Magnitude, M	Slip Rate, SR (mm/yr)
A	Faults that are capable of producing large magnitude events and which have a high rate of seismic activity.	$M \geq 7.0$ and	$SR \geq 5$
B	All faults other than Types A or C.	$M \geq 7.0$ and $M < 7.0$ and $M \geq 6.5$ and	$SR < 5$ $SR > 2$ $SR < 2$
C	Faults which are not capable of producing large magnitude earthquakes and which have a relatively low rate of seismic activity.	$M < 6.5$ and	$SR \leq 2$

capable of larger earthquakes and having a higher seismicity or slip rate, the near-source factors are higher than for faults capable of lesser maximum earthquakes or with lower slip rates. Faults or seismic sources with lower maximum moment magnitude and low slip have N-factors with the value of unity (1.0).

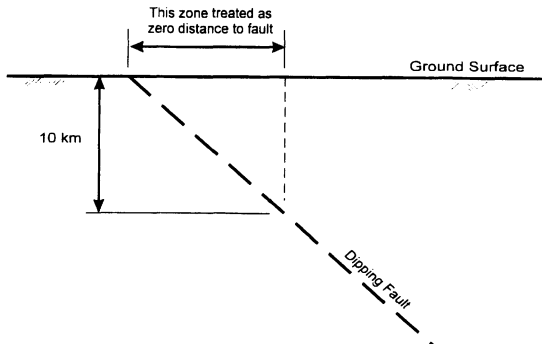


Figure 3-1. Treatment of Dipping Faults

Table 3-7. — Seismic Coefficient, C_a
From Table 16-Q, 1997 UBC (Ref. 3-5)

Soil Profile Type	Seismic Zone Factor, Z				
	Z = 0.075	Z = 0.15	Z = 0.2	Z = 0.3	Z = 0.4
S _A	0.06	0.12	0.16	0.24	0.32N _a
S _B	0.08	0.15	0.20	0.30	0.40N _a
S _C	0.09	0.18	0.24	0.33	0.40N _a
S _D	0.12	0.22	0.28	0.36	0.44N _a
S _E	0.19	0.30	0.34	0.36	0.36N _a

Table 3-8. — Seismic Coefficient, C_v
From Table 16-R, 1997 UBC (Ref. 3-5)

Soil Profile Type	Seismic Zone Factor, Z				
	Z = 0.075	Z = 0.15	Z = 0.2	Z = 0.3	Z = 0.4
S _A	0.06	0.12	0.16	0.24	0.32N _v
S _B	0.08	0.15	0.20	0.30	0.40N _v
S _C	0.13	0.25	0.32	0.45	0.56N _v
S _D	0.18	0.32	0.40	0.54	0.64N _v
S _E	0.26	0.50	0.64	0.84	0.96N _v

The Seismic Coefficients, C_a and C_v , are shown in Tables 3-7 and 3-8. As mentioned earlier, the near-source factor is only applicable in Seismic Zone 4, and only the seismic coefficients for Zone 4 are dependent on the near-source factors. The International Conference of Building Officials has published a set of maps defining the near-source zones in the state of California and adjacent portions of Nevada.⁽³⁻⁸⁾

The total design base shear, V , in a given direction is determined by the following equation:

$$V = \frac{C_v I}{R T} W$$

where I = importance factor

W = total seismic dead load

R = numerical coefficient representative of ductility and overstrength

T = fundamental period of vibration, in seconds

This formula defines the long period or constant velocity range.

For short periods (i.e., $T < C_v / 2.5C_a$), the following equation defines the constant acceleration range:

$$V = \frac{2.5C_a I}{R} W$$

In addition, for Seismic Zone 4, the total base shear is also governed by a minimum "floor" value at longer periods by the following equation:

$$V = \frac{0.8Z C_v I}{R} W$$

The elastic design response spectra, as defined by C_a and C_v , is shown in Figure 3-2. Figure 3-3 shows a comparison of the basic elastic design response spectra for UBC Seismic Zones 1, 2A, 2B, 3 and 4 for Soil Profile Type S_D; this profile type is probably the most common soil profile in most of California. For this comparison, the near-source factors have both been assumed to have a value of unity (1.0). The floor caused by the special Zone 4 restriction is misleading

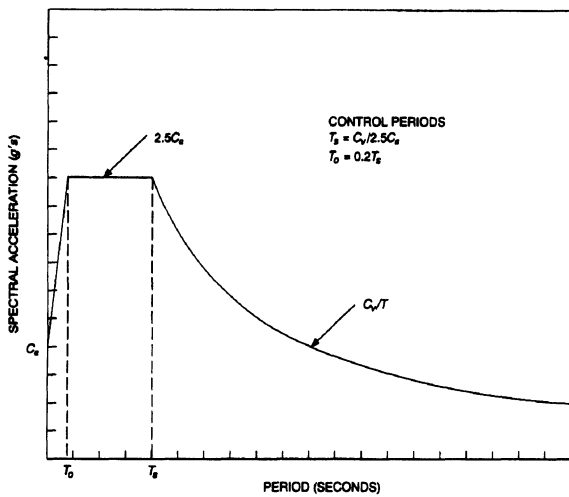


Figure 3-2. 1997 UBC Design Response Spectra. From Figure 16-3, 1997 UBC (Ref. 3-5)

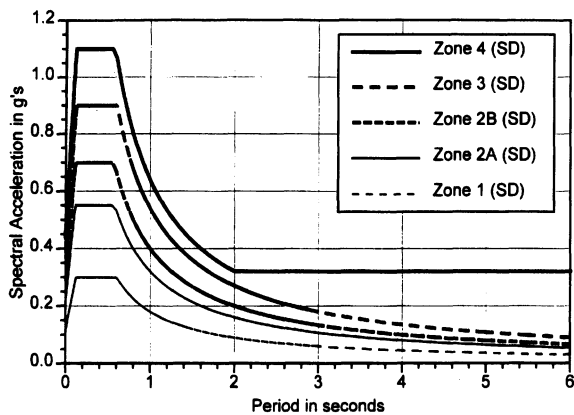


Figure 3-3. Response Spectra, UBC 1997 Edition, Soil Profile Type S_D

as the base shear computed from the design response spectrum will be greatly reduced when the "R" factor is divided through. There is another long period minimum "floor" value (that is not reduced by "R") that applies to all seismic zones that the total base shear should not be less than the following:

$$V = 0.11 C_a I W$$

With this additional minimum "floor," the differences in the base shear for longer periods between Zone 4 and the lesser zones at the longer structural periods are somewhat reduced.

Figure 3-4 shows a comparison of the elastic response spectra for the five stable soil profile types (S_A through S_E) for only Zone 4 assuming both near-source factors to be equal to unity (1.0). It is unlikely that Soil Profile Type S_A would exist in any significant metropolitan area in California. It should be noted that the spectral accelerations are larger at longer periods as the soil profile types become softer. The "floor" minimum spectral acceleration is the same regardless of soil profile type.

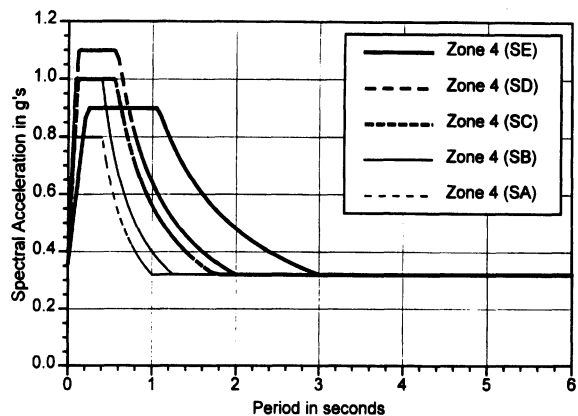


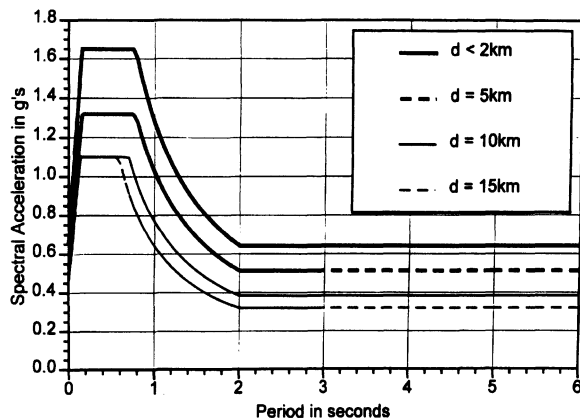
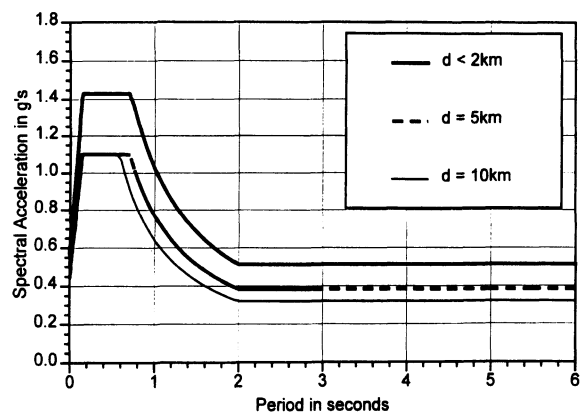
Figure 3-4. Response Spectra, Uniform Building Code 1997 Edition, Zone 4, N_a = N_v = 1.0 [After Lew and Bonneville (Ref. 3-9)]

Figure 3-5 compares the elastic response spectra in Zone 4 for a Soil Profile Type S_D for distances from a site to a Seismic Source A, the most active faults. The elastic response spectra for distances of less than 2, 5, 10, and 15 km are shown; at a distance of 15 km or greater, both N_a and N_v are equal to unity (1.0). Sites near a Seismic Source A will be subject to design base shears significantly greater than presently prescribed in the 1994 UBC. Similar plots of the elastic design response spectra for soil profile S_D near a Seismic Source Type B for distances of less than 2, 5, and 10 km are shown in Figure 3-6.

The California State Geologist has prepared near-source maps for the State of California for implementation with the adoption of the 1997 UBC. Near-source effects are only considered

Table 3-9. — Additional Definitions for Soil Profiles S_C through S_E (Ref. 3-5)

Soil Profile Type	Average Standard Penetration Blow Count	Average Undrained Shear Strength (pounds per square ft)	Average Undrained Shear Strength (kPa)
S _C	>50	>2,000	>100
S _D	15 to 50	1,000 to 2,000	50 to 100
S _E	<15	>10 feet of soft clay with PI > 20, w _{mc} > 40%, and s _u < 500 psf	>3048 mm of soft clay with PI > 20, w _{mc} > 40%, and s _u < 500 psf

Figure 3-5. Response Spectra, Uniform Building Code 1997 Edition Zone 4, Seismic Source A, and Soil Profile Type S_D [After Lew and Bonneville (Ref. 3-9)]Figure 3-6. Response Spectra, Uniform Building Code 1997 Edition Zone 4, Seismic Source B, and Soil Profile Type S_D [After Lew and Bonneville (Ref. 3-9)]

in Zone 4, thus, only parts of California, Hawaii and Alaska are affected in the United States.

Site Categorization Procedure

As mentioned in the previous section, there are six soil profile types of the 1997 UBC as given in Table 3-3. Only an abbreviated definition in terms of shear wave velocity for the soil profile types was given. The additional 1997 UBC definitions for soil profiles S_C through S_E are given below in Table 3-9.

When the soil properties are not known in sufficient detail to determine the soil profile type, the Code specifies that Type S_D be used. Soil Profile Type S_E need not be assumed unless the local building official determines that Soil Profile Type S_E may be present at the site or in the event that Type S_E is established by geotechnical data.

Determination of the Average Shear Wave Velocity

This assumes that the shear wave velocity profile will be known for the upper 100 feet (30.48 m). The average shear wave velocity, v_s , is determined by the following formula:

$$\bar{v}_s = \frac{\sum_{i=1}^n d_i}{\sum_{i=1}^n v_{si}}$$

where:

d_i = thickness of Layer i in feet (or meters)
 v_{si} = shear wave velocity in Layer i in feet/second (meters/second)

Determination of the Average Standard Penetration Resistance

The 1997 UBC defines the average field standard penetration resistance, N , and the

average standard penetration resistance for cohesionless soil layers, N_{CH} , by the following formulae:

$$\bar{N} = \frac{\sum_{i=1}^n d_i}{\sum_{i=1}^n \frac{d_i}{N_i}}$$

$$\bar{N}_{CH} = \frac{d_s}{\sum_{i=1}^n \frac{d_i}{N_i}}$$

where:

d_i = thickness of Layer i in feet (or millimeters)

d_s = the total thickness of cohesionless soil layers in the top 100 feet (30,480 millimeters)

N_i = the standard penetration resistance of soil layer in accordance with approved nationally recognized standards

Determination of Average Undrained Shear Strength.

The average undrained shear strength, S_u , is to be determined by the following equation:

$$\bar{S}_u = \frac{d_c}{\sum_{i=1}^n \frac{d_i}{S_{ui}}}$$

where:

d_c = the total thickness ($100 - d_s$) of cohesive soil layers in the top 100 feet (30,480 millimeters)

S_{ui} = the undrained shear strength in accordance with approved nationally recognized standards, not to exceed 5,000 psf (250 kPa)

3.3.4 Site Profile Examples-1994 UBC

Example 1

The soil profile at a site of a proposed hospital has been described as being interlayered beds of medium dense to dense sands and medium stiff to stiff clays. The thickness of the interlayered beds is 250 feet, at which depth, bedrock with a shear wave velocity of 2,500 feet/second is encountered. Determine the appropriate S Factor in accordance with the 1994 UBC.

Solution: Per Table 3-2 (Table 16-J, 1994 UBC), the profile type is S_2 , corresponding to an S Factor of 1.2.

Example 2

The soil profile is similar to that described in Example 1, except that the bedrock is shallower, at a depth of 127 feet. Determine the appropriate S Factor in accordance with the 1994 UBC.

Solution: Per Table 3-2, Profile Type S_1 , $S=1.0$.

Example 3

A site on reclaimed land near a river is being developed for a major commercial center. The geotechnical investigation, including a downhole seismic survey, revealed the typical shear wave velocity profile in the upper 200 feet to be:

Depth (feet)	Soil Description	Shear Wave Velocity (ft/sec)
0–15	Fill, silty sand	600
15–25	Highly plastic soft clay	300
25–50	Plastic, soft clay	450
50–75	Medium stiff clay	750
75–100	Medium stiff clay	1,000
100–150	Stiff clay	1,400
150–200	Dense sand and gravel	1,650

Determine the appropriate S Factor in accordance with the 1994 UBC.

Solution: From 15 to 50 feet, there are 35 feet of soft clays having a shear wave velocity of less than 500 feet per second; based on the description, profile is type S₃, with S=1.5.

Example 4

A site on San Francisco Bay is being considered for a major high-rise building. The geotechnical investigation has established the typical soil profile at the site to be:

Depth (feet)	Soil Description	Shear Wave Velocity (ft/sec)
0–10	Compacted fill, sandy clay	650
10–60	Young bay mud, soft	350
60–100	Older bay mud, medium stiff	1,000
100–150	Older bay mud, stiff	1,400
>150	Franciscan Formation bedrock	2,000

Determine the appropriate S Factor in accordance with the 1994 UBC.

Solution: Profile contains more than 40 feet of soft clay with shear wave velocity of less than 500 ft/sec; therefore, site profile is type S₄, and S=2.0.

3.3.5 Site Profile Examples—1997 UBC

Example 1

The soil profile at a site of an industrial facility has been investigated and the typical soil profile in the 100 feet has been determined to be:

Depth (feet)	Soil Description	Shear Wave Velocity	"N"	PI
0–30	Clay	-	-	80
30–50	Silty Sand	-	35	-
50–100	Sand and Gravel	-	50	-

Determine the appropriate soil profile type.

Solution: Based on the clay layer with a PI > 75 and H > 25 ft, this profile type is S_F, requiring site-specific evaluation.

Example 2

A site is underlain by bedrock having a measured shear wave velocity of 1,800 m/s in the upper 30 m (100 ft). Determine the appropriate soil profile type.

Solution: Soil profile type is S_A, since $v_s > 1,500 \text{ m/sec}$.

Example 3

A soil profile has the following description from the boring logs:

Depth (feet)	Soil Type	N-value
0–20	Sand	10
20–40	Sand	12
40–60	Sand	15
60–100	Sand	18

Determine the appropriate soil profile type.

Solution: Determine \bar{N} , the average field standard penetration resistance

$$\bar{N} = \frac{\sum_{i=1}^n d_i}{\sum_{i=1}^n \frac{d_i}{N_i}} = \frac{20' + 20' + 20' + 40'}{\frac{20'}{10} + \frac{20'}{12} + \frac{20'}{15} + \frac{40'}{18}}$$

$$\bar{N} = \frac{100}{2.0 + 1.67 + 1.33 + 2.22} = \frac{100}{7.22} = 13.9$$

Since \bar{N} is < 15, soil profile type is S_E.

Example 4

Given a soil profile:

Depth (feet)	Soil Type	N-value
0–10	Sand	25
10–30	Sand	40
30–75	Sand	60
75–100	Sand	70

Determine the appropriate soil profile type.

Solution:

$$\bar{N} = \frac{\sum_{i=1}^n d_i}{\sum_{i=1}^n \frac{d_i}{N_i}} = \frac{10' + 20' + 45' + 25'}{\frac{10'}{25} + \frac{20'}{40} + \frac{45'}{60} + \frac{25'}{70}}$$

$$\bar{N} = \frac{100}{0.40 + 0.50 + 0.75 + 0.36} = \frac{100}{2.01} = 49.8$$

Since $15 \leq N \leq 50$, soil profile type is S_D .

Example 5

The soil profile at a site has been determined to be:

Depth (feet)	Soil Type	N-value	Average Undrained Shear Strength (kPa)
0–10	Fill, dense sand	50	–
10–20	Clay	–	75
20–50	Clay	–	100
50–60	Clay	–	120
60–100	Clay	–	160

Determine the appropriate soil type.

Solution:

Ignore the upper 10 feet of the profile, consider just the clays.

$$\bar{s}_u = \frac{d_c}{\sum_{i=1}^n \frac{d_i}{s_{ui}}} = \frac{100 - d_s}{\sum_{i=1}^n \frac{d_i}{s_{ui}}}$$

$$= \frac{100 - 10'}{\frac{10'}{75 kPa} + \frac{30'}{100 kPa} + \frac{10'}{120 kPa} + \frac{40'}{160 kPa}}$$

$$= \frac{90}{0.13 + 0.30 + 0.08 + 0.25} = \frac{90}{0.77} = 117.4 kPa$$

Therefore, soil profile type is S_C .

3.3.6 Near-Source Factor Examples—1997 UBC

Example 1

For a building site located in the City of Palmdale, 1.1 km from the San Andreas fault, determine the Near-Source Factors, N_a and N_v . Note: the San Andreas fault has a maximum moment magnitude of about 8½ and an annual slip rate of 25 mm/yr.

Solution:

Seismic Source Type: The San Andreas fault is classified as a Type A seismic source (Table 3-6)

Per Table 3-4, Near-Source Factor, N_a , = 1.5
Per Table 3-5, Near-Source Factor, N_v , = 2.0

Example 2

For the site classified in Example 1, determine the seismic coefficients, C_a and C_v , if the soil profile is type S_D . Note: Palmdale is in Seismic Zone 4 where the Seismic Zone Factor, Z = 0.4.

Solution:

Per Table 7, C_a = 0.44 N_a = 0.44 (1.5) = 0.66
Per Table 8, C_v = 0.67 N_v = 0.67 (2.0) = 1.34

Example 3

A site is located in West Los Angeles, 7.5 km from the Newport-Inglewood fault ($M=7.0$, SR=1 mm/yr). The site profile is S_C and the site is in Seismic Zone 4. Determine the seismic coefficients, C_a and C_v .

Solution:

- The Newport-Inglewood fault is a seismic source Type B.
- Near-Source Factor, N_a = 1.0 for 7.5 km distance.
- Near-Source Factor, N_v = 1.1 for 7.5 km distance by interpolation.

For $Z = 0.4$ and S_C site,

$$C_a = 0.40 N_a = 0.40 (1.0) = 0.40$$

$$C_v = 0.56 N_v = 0.56 (1.1) = 0.616$$

Example 4

A site is located in the California desert; the closest active faults are 3.0 and 5.0 km from the site. Information on the faults are given as:

Fault	Distance (km)	Max. Magnitude	Slip Rate (mm/yr)
1	3.0	6.5	1.0
2	5.0	7.0	5.0

Determine the appropriate Near-Source Factors, N_a and N_v .

Solution:

By Table 3-6:

Fault 1 is a seismic source Type B

Fault 2 is a seismic source Type A

From Tables 3-4 and 3-5, the Near-Source Factors are:

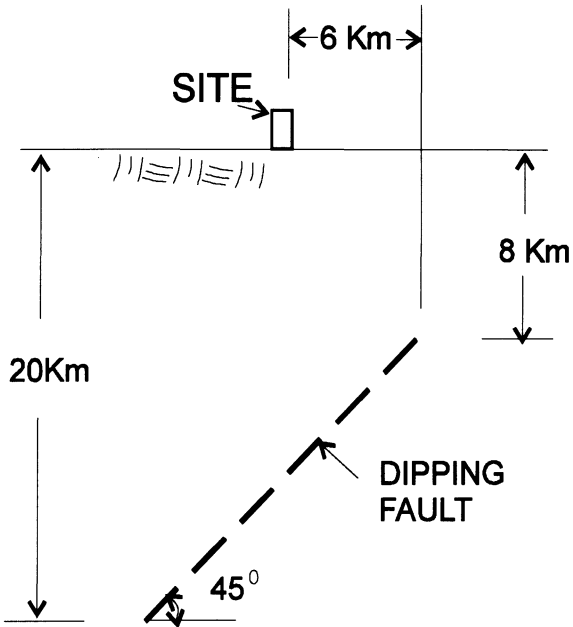
Fault	N_a	N_v
1	1.2	1.47
2	1.2	1.6

Use the maximum values; therefore, $N_a = 1.2$; $N_v = 1.6$.

Example 5

The recently discovered Bachman blind thrust fault was found to underlie the site of a new building development. Seismologists have estimated the fault properties and geometry to be:

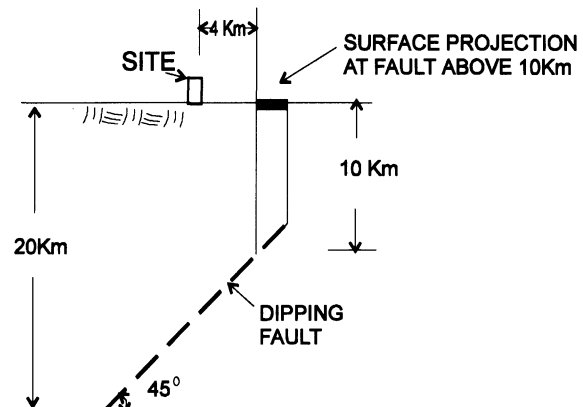
1. Buried thrust fault with a 45° dip.
2. Maximum magnitude = 7.5.
3. Maximum annual slip rate = 10 mm/yr.
4. Fault orientation relative to site is shown in the figure below.



Determine the Near-Source Factors, N_a and N_v .

Solution:

The Bachman fault, per Table 3-6, is a seismic source Type A. The surface projection of fault above a 10 km depth is shown below:



For Type A source and 4 km distance, $N_a = 1.3$ (Table 3-4) and $N_v = 1.73$ (Table 3-5)

3.3.7 NEHRP 1997 Recommended Provisions for Seismic Regulations

The NEHRP Recommended Provisions for Seismic Regulations for New Buildings and Other Structures⁽³⁻⁷⁾ present criteria for the design and construction of structures to resist earthquake ground motions. The NEHRP 1997 Provisions form the basis of the seismic provisions for the proposed unified national building code for the United States to be called the International Building Code (IBC)⁽³⁻¹⁰⁾.

3.3.8 2000 International Building Code Seismic Requirements

The International Building Code (IBC), 2000 edition⁽³⁻¹⁰⁾ has recently been published. It represents a cooperative effort to bring national uniformity to the building codes in the United States. The IBC code has been developed jointly by the International Code Council, which consists of the Building Officials and Code Administrators International, Inc. (BOCA), the International Conference of Building Officials (ICBO), and the Southern Building Code Congress International (SBCCI).

There are new earthquake definitions, assumptions, and procedures in the 2000 IBC, based on the 1997 NEHRP. The IBC specifies a procedure to establish ground motion accelerations, represented by response spectra and coefficients derived from those spectra. The design earthquake (DE) ground motions have been defined as being two-thirds of the Maximum Considered Earthquake (MCE) ground motions:

$$DE = \frac{2}{3} MCE$$

The MCE is defined as the "most severe earthquake effects" considered by the IBC, and is essentially the "worst case" earthquake, which has been used for design of special (base isolated) buildings or for collapse check of existing buildings (such as defined in FEMA 273). The DE is the "design-basis" earthquake for conventional building design, with margins

provided by the inherent conservatisms built into the NEHRP Provisions.

2000 IBC Seismic Base Shear Equation

The seismic base shear, V, in a given direction is to be determined by the following equation:

$$V = C_s W$$

Where:

C_s = seismic response coefficient

W = total dead load plus applicable portions of other loads as defined in IBC

The seismic response coefficient, C_s , is determined by the equation:

$$C_s = \frac{S_{DS}}{(R/I_E)}$$

where:

S_{DS} = the design spectral response acceleration at short periods

R = response modification factor defined in the IBC

I_E = occupancy importance factor defined in IBC and ranges from 1.0 to 1.5

The response modification factor, R , depends on the type of building system and ranges from a value of 1½ for ordinary plain masonry wall systems to values of 7 to 8 for steel eccentrically braced frame systems. The value of the seismic response coefficient C_s as shown above need not exceed the following:

$$C_s = \frac{S_{DI}}{(R/I_E)}$$

but shall not be taken less than:

$$C_s = 0.044 S_{DS} I_E$$

For buildings and structures in Seismic Design Categories E or F, and those buildings and structures for which the 1 second spectral

response, S_1 , is equal to or greater than 0.6g, the value of C_s shall not be taken as less than:

$$C_s = \frac{0.5S_1}{R/I_E}$$

where:

S_{DI} = the design spectral response acceleration at 1 second period

T = fundamental period of the building (seconds)

S_1 = maximum considered earthquake spectral response acceleration at 1 second period

Seismic Design Categories E and F are assigned to structures in mapped areas with spectral response acceleration at a period of 1 second, S_1 , exceeding 0.75g. It appears that where S_1 will be less than 0.75g in Seismic Zone 4, it will not be less than 0.60g; in this case, the structures will be assigned to Seismic Design Category D. [The seismic design categories are not discussed here, but suffice it to say that structures in Seismic Zone 4 will be either Seismic Design Category D, E, or F, which have more stringent requirements than Categories A, B, or C.]

2000 IBC Determination of Seismic Coefficient

The seismic coefficient, C_s , for the seismic base shear equation, is derived from a response spectra. This response spectra can be derived from a site-specific study or can be determined with the procedure in the 2000 IBC. In the 2000 IBC, the 5% damped response spectra is constructed from the "mapped maximum considered earthquake spectral response acceleration" at two points. One point, denoted as S_S , corresponds to short periods and the other point, denoted as S_1 , corresponds to a 1 second period. The "mapped maximum considered earthquake spectral response acceleration" corresponds to a "soft rock" (Site Class B) condition; factors are applied to account for the site conditions to develop an appropriate

response spectra. Another factor is applied to arrive at the final design response spectra.

2000 IBC Mapped Maximum Considered Earthquake Spectral Response Accelerations

The maximum considered earthquake spectral response acceleration for short period (0.2 seconds) and 1.0 second period are found on maps that are found in the 1997 NEHRP Provisions. Smaller scale versions of these maps are reproduced in the 2000 IBC. These maps were developed by the Building Seismic Safety Council (BSSC) and the United States Geological Survey (USGS) for the Federal Emergency Management Agency (FEMA). The maps are based on probabilistic seismic hazard analyses using fault source models developed by the USGS. The analyses were made for the 5% damped spectral response at 0.2- and 1.0-second periods corresponding to the ground motions having a 2 percent probability of being exceeded in 50 years; this is about a 2,500 year return period. This risk level is now referred to as the "maximum considered earthquake." Because of the tendency of probabilistic analyses to predict ground motions that greatly exceed what has been experienced, due mostly to the uncertainties in the seismic parameters and the long return period, a cap or limiting value was imposed on the spectral ordinates in the more seismically active areas of the United States, such as California. The probabilistic spectral response values were capped by the "deterministic maximum considered earthquake ground motion."

The soil class assumed in the analyses is a soil class B; the *Soil Classes* used in the IBC are the same as the *Soil Profile Types* used in the 1997 UBC. (The 1997 UBC adopted the NEHRP soil profile types.)

The deterministic maximum considered earthquake ground motion spectral response is to be calculated by taking into account the characteristic earthquake on any known fault within the region that has a slip rate exceeding 1 mm per year. The spectral response for 5% damping is to be calculated using a mean-plus-one standard deviation ground motion

Table 3-10. — Values of Site Coefficient F_a as a Function of Site Class and Mapped Spectral Response Acceleration at Short Periods, S_s (Ref. 3-10)

Site Class	Mapped Spectral Response Acceleration at Short Periods				
	$S_s \leq 0.25$	$S_s = 0.50$	$S_s = 0.75$	$S_s = 1.0$	$S_s \geq 1.25$
A	0.8	0.8	0.8	0.8	0.8
B	1.0	1.0	1.0	1.0	1.0
C	1.2	1.2	1.1	1.0	1.0
D	1.6	1.4	1.2	1.1	1.0
E	2.5	1.7	1.2	0.9	a
F	a	a	a	a	a

Note: Use straight-line interpolation for intermediate values of mapped spectral acceleration at short periods, S_s .

* Site-specific geotechnical and dynamic site response analysis should be performed to determine appropriate values.

Table 3-11. — Values of Site Coefficient F_v as a Function of Site Class and Mapped Spectral Response Acceleration at 1 Second Period, S_1 (Ref. 3-10)

Site Class	Mapped Spectral Response Acceleration at 1 Second Period				
	$S_s \leq 0.1$	$S_s = 0.2$	$S_s = 0.3$	$S_s = 0.4$	$S_s \geq 0.5$
A	0.8	0.8	0.8	0.8	0.8
B	1.0	1.0	1.0	1.0	1.0
C	1.7	1.6	1.5	1.4	1.3
D	2.4	2.0	1.8	1.6	1.5
E	3.5	3.2	2.8	2.4	a
F	a	a	a	a	a

Note: Use straight-line interpolation for intermediate values of mapped spectral acceleration at 1.0 second period, S_1 .

* Site-specific geotechnical and dynamic site response analysis should be performed to determine appropriate values.

attenuation relationship. These deterministically spectral response values are used as upper bound values in the IBC maps.

Maps for Southern California have been developed and are shown in Figures 3-7 and 3-8. From the first map, the mapped maximum considered earthquake spectral response acceleration for short period, S_s , is found based on the location of the site. The second map is used to determine the mapped maximum considered earthquake spectral response acceleration for a 1-second period, S_1 .

$$S_{MS} = F_a S_s$$

$$S_{M1} = F_v S_1$$

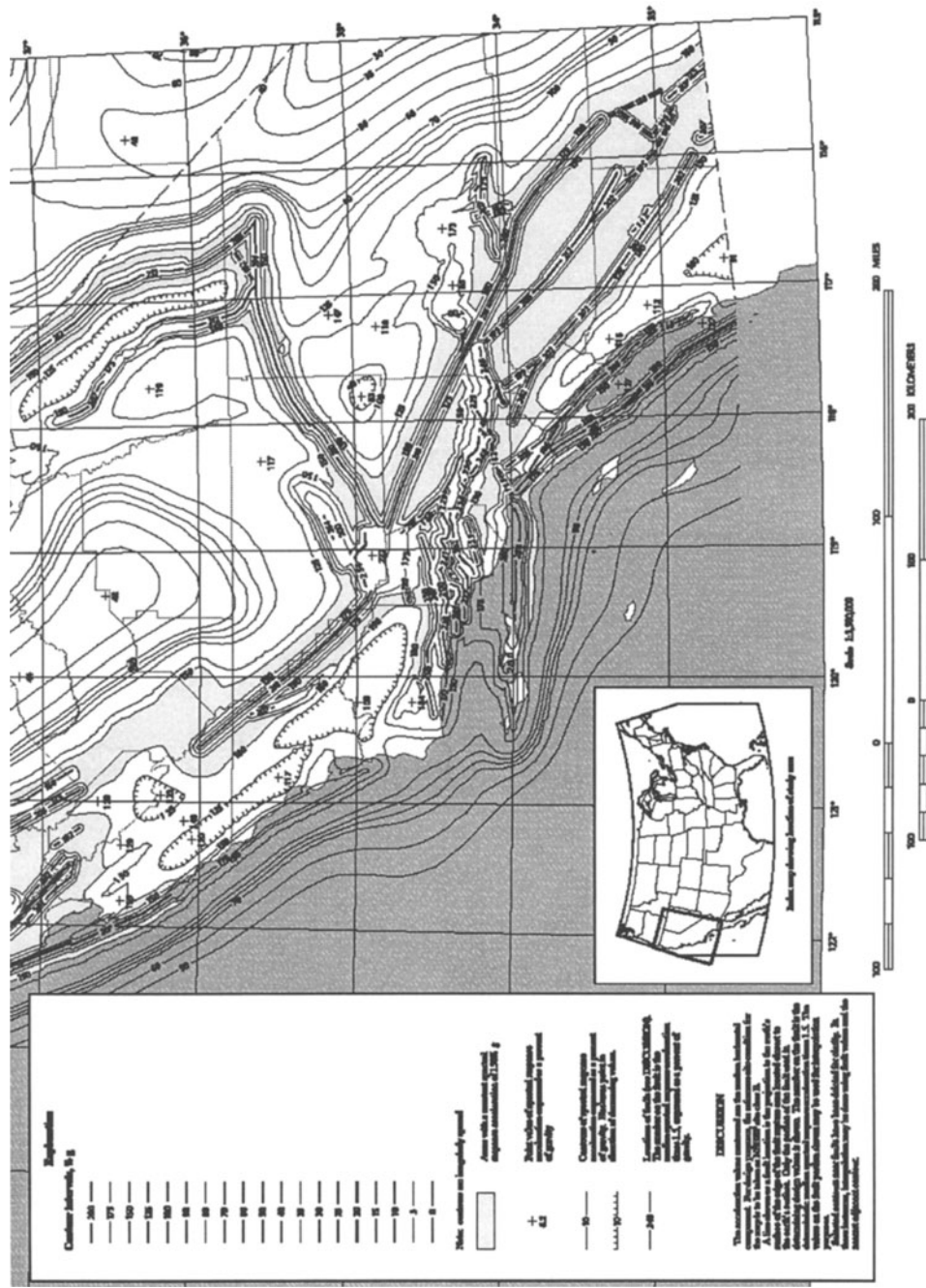
where:

F_a = site coefficient for short period response
 F_v = site coefficient for 1 second period response

The values of the site coefficients F_a and F_v are given in Tables 3-10 and 3-11.

2000 IBC Adjustments to Spectral Response for Site Class Effects

As the S_s and S_1 values correspond to a Site Class B, adjustments must be made if the site in question is other than an Site Class B profile. The S_s and S_1 values are adjusted for site effects by the following formulas:



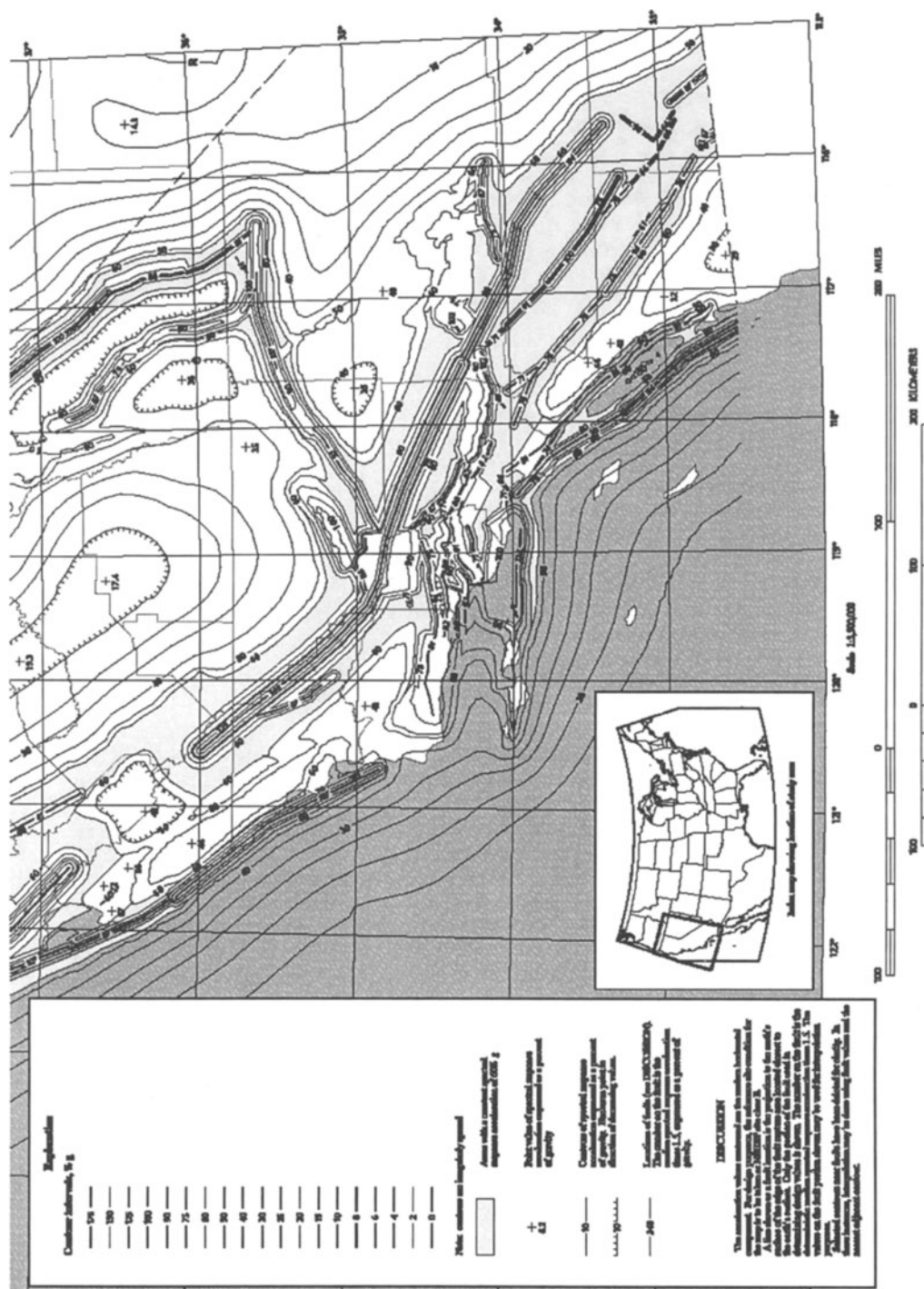


Figure 3-8. Maximum Considered Earthquake Ground Motion for Southern California: 1 Second Period Spectral Response Acceleration (%g); Site Class B [After International Code Council, 2000 (ref. 3-10)]

2000 IBC General Design Response Spectrum

To determine the general design response spectrum with 5% damping, two quantities, the 5% damped design spectral response acceleration at short periods, S_{DS} , and at 1-second period, S_{DI} , are determined by the following equations:

$$S_{DS} = \frac{2}{3} S_{MS}$$

$$S_{DI} = \frac{2}{3} S_{MI}$$

The general design response spectrum curve for 5% damping is shown in Figure 3-9 with the following additional guidelines:

1. For periods less than or equal to T_0 , the design spectral response acceleration, S_a , is given by:

$$S_a = S_{DS} (T/T_0) + 0.4 S_{DS}$$

2. For periods greater or equal to T_0 and less than or equal to T_S , the design spectral response acceleration, S_a , is given by:

$$S_a = S_{DS}$$

3. For periods greater than T_S , the design spectral acceleration, S_a , is given as:

$$S_a = \frac{S_{DI}}{T}$$

where T is the fundamental period of the structure in seconds and T_0 and T_S are given by:

$$T_0 = \frac{0.2 S_{DI}}{S_{DS}}$$

$$T_S = S_{DI}/S_{DS}$$

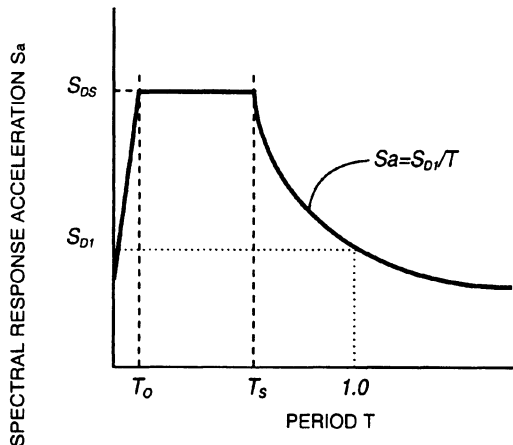


Figure 3-9. IBC Design Response Spectrum, 5% Damping
(Ref. 3-10)

2000 IBC Guidelines for Site-Specific Procedure for Determining Ground Motions

The 2000 IBC Provisions requires that the site-specific study account for: the regional seismicity and geology; the expected recurrence rates and maximum magnitudes of events on known faults and source zones; the location of the site with respect to the faults and sources; near-source effects, if any; and the characteristics of the subsurface conditions. The probabilistic “Maximum Considered Earthquake” (MCE) ground motions are those represented by a 5% damped response spectrum having a 2% probability of exceedance within a 50 year period.

Because a probabilistic hazard analysis can lead to extremely high predictions of the ground motion, the 2000 IBC provides that where the probabilistic MCE spectral response ordinates at periods of 0.2 or 1.0 seconds exceed the corresponding ordinates of the deterministic maximum considered earthquake ground motion, the MCE ground motion shall be taken as the lesser of the probabilistic or the deterministic MCE ground motion. The deterministic MCE ground motion is calculated as 150% of the median spectral response accelerations (S_{AM}) at all periods resulting from a characteristic earthquake on any known active fault within the region. The MCE ground motion has a deterministic lower limit,

however, as shown in Figure 3-10. The deterministic limit is determined by the site coefficients F_a and F_v that are determined as described earlier in Section 3.3.8.3, tables 3-10 and 3-11, and S_S is assumed to be 1.5g and S_1 is assumed to be 0.6g.

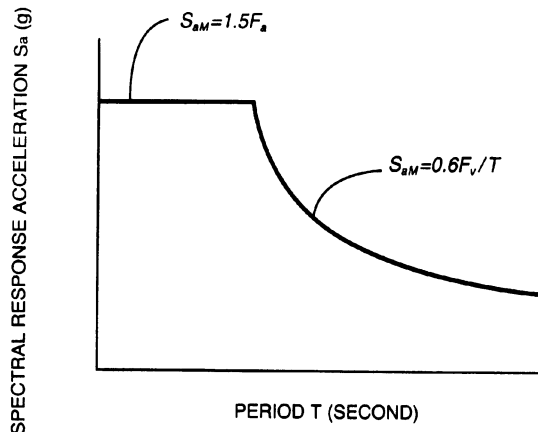


Figure 3-10. Probabilistic Ceiling on Maximum Considered Earthquake Ground Motion (Ref. 3-10)

The 2000 International Building Code has guidelines for the calculation of the deterministic MCE ground motion. The deterministic MCE ground motion is to be calculated as the spectral response accelerations (S_{aM}) at all periods resulting from a characteristic earthquake on any known fault within the region that has a slip rate exceeding 1 mm per year, using the mean-plus-one standard deviation ground motion attenuation relationship.

The design spectral response acceleration, S_a , is to be determined by:

$$S_a = \frac{2}{3} S_{aM}$$

In addition, S_a must be greater than or equal to 80 percent of the design spectral response acceleration, S_a , determined by the general response spectrum from the

The procedures in the 2000 IBC will undoubtedly be confusing until mastery of a new language and philosophy is achieved. The Near-Source factors of the 1997 UBC are replaced with a set of maps of the mapped MCE

spectral response accelerations that are based on the locations of major active earthquake sources.

3.4 SOIL LIQUEFACTION



Figure 3-11. Liquefaction-induced bearing capacity failure and settlement of a five-story building in Adapazari, Turkey, most of the ground floor is below grade. Photograph courtesy of Dr. Robert May, Gibb Ltd., Reading, U.K.

3.4.1 Causes of Liquefaction

Soil liquefaction during an earthquake is a process that leads to loss of strength or stiffness of the soil. This could result in the settlement of structures, cause landslides, precipitate failures of earth dams, or cause other types of hazards. Soil liquefaction has been observed to occur most often in loose saturated sand deposits.

During strong earthquake shaking, a loose saturated sand deposit will have a tendency to compact and, thus, have a decrease in volume. If this deposit cannot drain rapidly, there will be an increase in the pore water pressure. The effective stress in the sand deposit is equal to the difference between the overburden pressure and the pore water pressure. With increasing oscillation, the pore water pressure will increase to the point where the pore water pressure will be equal to the overburden pressure. Since the shear strength of a cohesionless soil is directly proportional to the effective stress, the sand will not have any shear strength and is now in a liquefied state. "Sand boils" appearing at the ground surface during an earthquake is evidence that liquefaction has occurred.

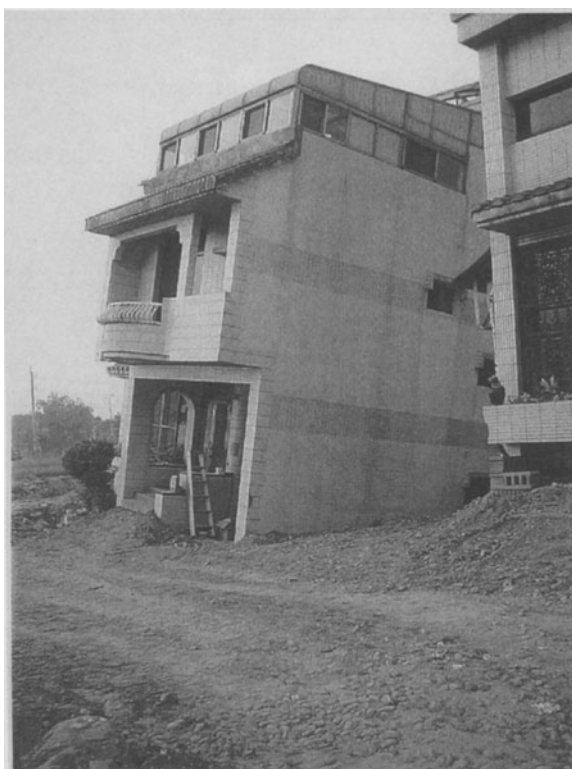


Figure 3-12. Liquefaction-induced tilting of three-story residential structure in Central Taiwan. Photograph by Dr. Farzad Naeim.

Liquefaction can have a significant and sometimes devastating effect on buildings supported on the upper soils without consideration of the consequences of

liquefaction. Figures 3-11 and 3-12 present examples of the effects of liquefaction on buildings in the 1999 Kocaeli, Turkey and Chi-Chi, Taiwan earthquakes.

3.4.2 Evaluating the Liquefaction Potential by Standard Penetration Tests

There are a number of different methods by which the potential for liquefaction of a soil can be evaluated. These methods generally compare the cyclic shear resistance of the soil with the cyclic shear stresses and strains caused by an earthquake. Simplified empirical methods have been developed that utilize case histories of past occurrences (or non-occurrences) of liquefaction during significant seismic events. Other methods use analytical techniques that incorporate dynamic analysis and laboratory testing. The most common and traditional method of analysis uses correlations between the liquefaction characteristics of soils and the Standard Penetration Test or N-value as originally described by Seed et al.⁽³⁻¹¹⁾ Since the analysis was first introduced, the methodology has been refined and various corrections are applied to account for variability in sampling and performance; a summary of recent consensus opinion on liquefaction evaluation was conducted by NCEER and has been edited by Youd and Idriss⁽³⁻¹²⁾; those consensus opinions are presented herein. Thus, for analysis, a corrected N-value is used. The value of the corrected N-value, denoted as $(N_1)_{60}$ is found by the formula:

$$(N_1)_{60} = N_m \cdot C_N C_E C_B C_R C_S$$

where N_m is the measured standard penetration resistance, C_N is a correction factor for overburden pressure, C_E is the correction factor for hammer energy ratio, C_B is a correction factor of borehole diameter, C_R is the correction factor for rod length, and C_S is the correction for samplers with or without liners.

The overburden pressure correction factor, C_N , may be calculated from the following formula:

$$C_N = (P_a / \sigma'_{vo})^{0.5}$$

where P_a is 100 kPa or approximately atmospheric pressure (2,089 pounds per square foot) and σ'_{vo} is the effective vertical overburden pressure at the depth of the standard penetration sample. Table 3-12 shows the suggested correction factors for the other corrections.

Table 3-12. Corrections to SPT (Ref. 3-12)

Factor	Equipment Variable	Term	Correction
Overburden Pressure		C_N	$(P_a/\sigma'_{vo})^{0.5}$
Energy Ratio	Safety Hammer Donut Hammer	C_E	0.60 to 1.17 0.45 to 1.00
Borehole Diameter	65 to 115 mm 150 mm 200 mm	C_B	1.0 1.05 1.15
Rod Length	3 to 4 m 4 to 6 m 6 to 10 m 10 to 30 m >30 m	C_R	0.75 0.85 0.95 1.0 <1.0
Sampling Method	Standard Sampler Sampler without liners	C_s	1.0 1.2

With respect to the energy ratio, ER, it is believed that the approximate historical average SPT energy for North American practice is 60% of the maximum theoretical energy achievable. The ER delivered by any particular SPT setup depends on the type of hammer and anvil in the drilling system and on the method of hammer release. The correction factor, C_E , normalizes the N-value to a 60% ER.

During an earthquake, the soils will be subject to cyclic shear stresses induced by the ground shaking. The average cyclic stress ratio (CSR) during an earthquake may be estimated by the following formula:

$$\text{CSR} = \tau_{av} / \sigma'_{vo} = 0.65 (a_{max} / g) \cdot (\sigma_o / \sigma'_{vo}) \cdot r_d$$

where a_{max} = maximum acceleration at the ground surface

σ_o = total overburden pressure at depth under consideration

σ'_{vo} = effective overburden pressure at depth under consideration

r_d = stress reduction coefficient

The range of values for the stress reduction, r_d , are shown in Figure 3-13.

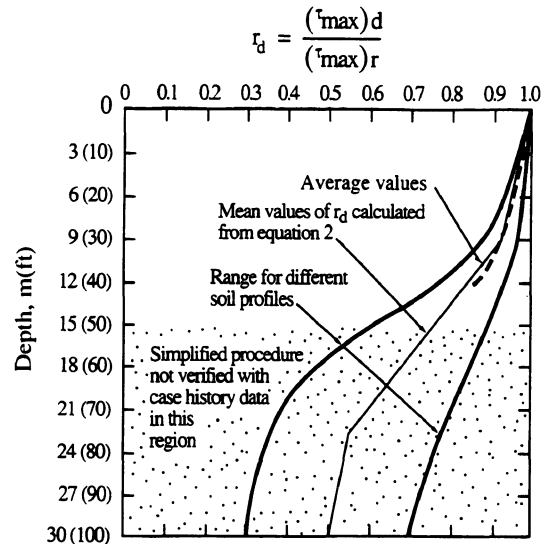


Figure 3-13. Stress Reduction Factor, r_d (Ref. 3-12)

The average value of the stress reduction coefficient, r_d , may be estimated by the following equations:

$$r_d = 1.0 - 0.00765 z \quad \text{for } z \leq 9.15 \text{ m}$$

$$r_d = 1.174 - 0.0267 z \quad \text{for } 9.15 \text{ m} < z \leq 23 \text{ m}$$

$$r_d = 0.744 - 0.008 z \quad \text{for } 23 \text{ m} < z \leq 30 \text{ m}$$

$$r_d = 0.50 \quad \text{for } z > 30 \text{ m}$$

Having estimated the average shear stress ratio, charts similar to Figure 3-14 may be used to determine the potential for liquefaction. Figure 3-14 shows the relationship between the cyclic resistance ratio (CRR) and the corrected standard penetration resistance, N_1 , for a magnitude 7.5 earthquake. The CRR is also referred to as the liquefaction resistance or liquefaction resistance ratio. If the CSR (τ_{av} / σ'_{vo}) induced by the earthquake is less than the liquefaction resistance ratio, CRR, as shown on Figure 3-14, liquefaction would not be expected to occur; similarly if the CSR exceeds the CRR, liquefaction would be expected to occur. A factor of safety against liquefaction could be determined by the ratio of the CSR divided by the CRR. For $(N_1)_{60}$ values greater than about 30, no liquefaction would be expected and the factor of safety would be great.

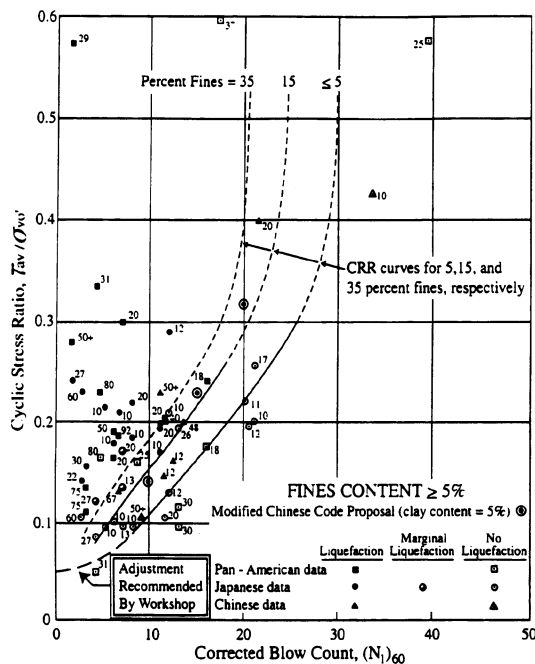


Figure 3-14. Figure 3-14. Curve Recommended for Determining CRR from SPT Data (Ref. 3-12)

The CRR base curve for clean sands (i.e., <5% fines content) may be approximated by the relationship:

$$CRR_{7.5} = \frac{a + cx + ex^2 + gx^3}{1 + bx + dx^2 + fx^3 + hx^4}$$

where:

$$\begin{aligned} a &= 0.048 \\ b &= -0.1248 \\ c &= 0.004721 \\ d &= 0.009578 \\ e &= 0.0006136 \\ f &= -0.0003285 \\ g &= -1.673 \times 10^{-5} \\ h &= 3.714 \times 10^{-6} \\ x &= (N_60) \end{aligned}$$

This equation is valid for values of (N_60) less than 30.

Figure 3-14 also shows that the influence of the fines content on the potential for liquefaction in a way that the greater the fines content, the lesser the potential for liquefaction given the same N_60 value. I.M. Idriss and R.B.

Seed have developed equations to correct the standard penetration resistance for silty sands, (N_60) , to an equivalent clean sand penetration resistance $(N_60)_{cs}$. These equations are:

$$(N_60)_{cs} = \alpha + \beta(N_60)$$

where the α and β coefficients are determined by:

$$\alpha = \exp [1.76 - (190/FC^2)]$$

$$\beta = [0.99 + (FC^{1.5}/1000)]$$

where FC is the fines content measured from laboratory gradation tests on soil samples. These equations essentially represent the CRR curves for different fines contents as shown in Figure 3-12.

As mentioned earlier, Figure 3-14 applies only for a magnitude 7.5 earthquake; to evaluate the potential for liquefaction for other magnitude events; Seed et al. (1983)⁽³⁻¹³⁾ originally determined correlation factors that allow the induced stress ratios for other magnitude events to be adjusted to correspond to a magnitude of 7.5 by dividing the stress ratios by the factors given in Table 3-13:

Table 3-13. Seed and Idriss Original Magnitude Scaling Factors (Ref. 3-13)

Earthquake Magnitude	Magnitude Scaling Factor
5.25	1.5
6	1.32
6.75	1.13
7.5	1.0
8.5	0.89

The Seed and Idriss magnitude scaling factors are based on estimates of equivalent cycles of shear stress developed during different magnitude earthquakes. However, it is generally believed now that the original Seed and Idriss magnitude scaling factors are very conservative for moderate-sized earthquakes. Idriss has proposed a new set of magnitude scaling factors after re-evaluating the data. Idriss has proposed that the magnitude scaling factor, MSF, be defined as a function of the moment magnitude, M, as given in the equation:

$$MSF = 10^{2.24} / M^{2.56}$$

Table 3-14. Magnitude Scaling Factors Defined by Various Investigators (Ref. 3-12)

Magnitude M	Seed and Idriss (original)	Idriss	Ambreseys	Arango	Andrus & Stokoe	Youd and Noble			
						P _L <20%	P _L <32%	P _L <50%	
5.5	1.43	2.20	2.86	3.00	2.20	2.80	2.86	3.42	4.44
6.0	1.32	1.76	2.20	2.00	1.65	2.10	1.93	2.35	2.92
6.5	1.19	1.44	1.69	1.60	1.40	1.60	1.34	1.66	1.99
7.0	1.08	1.19	1.30	1.25	1.10	1.25	1.00	1.2	1.39
7.5	1.00	1.00	1.00	1.00	1.00	1.00			1.00
8.0	0.94	0.84	0.67	0.75	0.85	0.8?			0.73?
8.5	0.89	0.72	0.44			0.65?			0.56?

Other researchers have also determined magnitude scaling factors; these values are shown in Table 3-14. The table also repeats the original Seed and Idriss MSF factors and also presents the new Idriss MSF factors.

There is not a concensus in the geotechnical community of which of the various sets of magnitude scaling factors to use except is it is generally accepted that the original Seed and Idriss MSF factors are conservative for magnitudes of less than 7.5. It should be noted that Arango has two sets of MSF factors. The first set was based on farthest observed liquefaction effects from the seismic energy source, estimate average peak accelerations at those distant sites, and the absorbed seismic energy required to cause liquefaction; the second set was developed from energy concepts and the relationship developed by Seed and Idriss between numbers of significant stress cycles and earthquake magnitude. The second Arango MSF factors are similar to the new Idriss MSF factors. The Youd and Noble MSF factors are found in three sets that are a function of P_L, the probability that liquefaction did not occur.

For earthquake magnitudes greater than 7.5, it recommended that the newer Idriss MSF factors be used because it is believed that the original Seed and Idriss MSF factors were not sufficiently conservative in the upper magnitude range.

Thus, the factor of safety (FS) against liquefaction may be written in terms of the CRR, CSR and MSF factors as follows:

$$FS = (CRR_{7.5}/CSR) MSF$$

where CRR_{7.5} is the cyclic resistance ratio for a magnitude 7.5 earthquake from Figure 3-14.

Example

A sand deposit has been identified beneath a site located adjacent to a river. The sand deposit is 10 feet thick and the top of the layer is 10 feet below the ground surface and overlain by a very stiff clay and is underlain by bedrock. The water level has been measured to be at a depth of 10 feet. The standard penetration resistance of the layer has been determined to be 12 blows per foot and a standard sampler was used; a drill rig with a safety hammer with an efficiency of 60% was used. The length of the drill rod is 10 meters and the borehole diameter is 5 inches (127 mm).

The design earthquake has been designated as a moment magnitude 6-3/4 event on a nearby fault and the maximum ground acceleration is expected to be 0.35 g.

The wet unit weight of the clay soils is 125 pounds per cubic foot and the wet unit weight of the sand soils is 130 pounds per cubic foot. The sands has 15% fines content according to a grain size analysis.

Compute the factor of safety against liquefaction of the sand layer.

Solution:

Step 1: Determine the effective overburden pressure at the center of the sand layer:

$$\begin{aligned}\sigma'_o &= (125 \text{ pcf}) (10 \text{ ft}) + [(130 \text{ pcf} - 62.4 \text{ pcf}) (5 \text{ ft})] \\ &= 1,588 \text{ psf}\end{aligned}$$

Step 2: Determine the total overburden pressure at the center of the sand layer:

$$\begin{aligned}\sigma_o &= (125 \text{ pcf}) (10 \text{ ft}) + (130 \text{ pcf}) (5 \text{ ft}) \\ &= 1,900 \text{ psf}\end{aligned}$$

Step 3: Determine the stress reduction factor, r_d :

$$\begin{aligned}z &= 15 \text{ ft} \times (1 \text{ meter}/3.2808 \text{ ft}) \\ &= 4.572 \text{ m}\end{aligned}$$

$$\begin{aligned}r_d &= 1 - 0.00765 z \\ &= 1 - 0.00765 (4.572) \\ &= 0.965\end{aligned}$$

Step 4: Determine the cyclic stress ratio, CSR.

$$\begin{aligned}CSR &= \tau_{av} / \sigma'_o = 0.65 (a_{max} / g)(\sigma_o / \sigma'_o) r_d \\ &= 0.65 (0.35 \text{ g/g}) (1,900 \text{ psf} / 1588 \text{ psf}) \\ &\quad (0.965) \\ &= 0.263\end{aligned}$$

Step 5: Determine correction factors to SPT blowcount:

Referring to Table 3-12, the correction factors are

Overburden pressure:

$$\begin{aligned}C_N &= (P_a / \sigma'_o)^{0.5} \\ &= (2,089 \text{ psf} / 1,588 \text{ psf})^{0.5} \\ &= 1.15\end{aligned}$$

Energy ratio:

$$C_E = 1.0, \text{ since safety hammer is } 60\% \text{ efficient}$$

Borehole diameter:

$$C_B = 1.0, \text{ since diameter is } 5 \text{ in. (127 mm)}$$

Rod length:

$$C_R = 1.0, \text{ since rod length is } 10 \text{ m}$$

Sampling method

$$C_S = 1.0, \text{ since standard sampler used}$$

$$\begin{aligned}(N_1)_{60} &= N_m \cdot C_N C_E C_B C_R C_S \\ &= (12) (1.15) (1.0) (1.0) (1.0) (1.0) \\ &= 13.8\end{aligned}$$

Step 6: Determine correction for fines content:

Since the fines content is greater than 5%, correction is needed.

$$\begin{aligned}\alpha &= \exp [1.76 - (190/FC^2)] \\ &= \exp [1.76 - (190/15^2)] \\ &= 2.50 \\ \beta &= [0.99 + (FC^{1.5}/1000)] \\ &= [0.99 + (15^{1.5}/1000)] \\ &= 1.05\end{aligned}$$

$$\begin{aligned}(N_1)_{60cs} &= \alpha + \beta(N_1)_{60} \\ &= 2.50 + 1.05 (13.8) \\ &= 17.0\end{aligned}$$

Step 7: Determine the cyclic resistance ratio, CRR_{7.5}:

Referring to Figure 3-14, for $(N_1)_{60cs} = 17.0$, the cyclic resistance ratio is

$$CRR_{7.5} = 0.185$$

Step 8: Determine the magnitude scaling factor, MSF, for magnitude 6-3/4:

Use the Idriss magnitude scaling factor,

$$\begin{aligned}MSF &= 10^{2.24} / M^{2.56} = 10^{2.24} / (6.75)^{2.56} \\ &= 1.31\end{aligned}$$

Step 9: Compute the factor of safety against liquefaction:

$$\begin{aligned} \text{FS} &= (\text{CRR}_{7.5}/\text{CSR}) \text{ MSF} \\ &= (0.185/0.263) 1.31 \\ &= 0.92 \end{aligned}$$

The factor of safety against liquefaction is less than unity (1.0), therefore, liquefaction would be expected to occur in the event of the design earthquake.

3.4.3 Evaluating the Liquefaction Potential by Cone Penetration Tests

Because of questions regarding the reliability and quality of the standard penetration resistances, and the inability to easily obtain a continuous profile of the resistances, there is more reliance now upon the cone penetration test (CPT). The CPT can provide a nearly continuous profile of penetration resistance and is generally more repeatable and consistent than other forms of penetration testing. One obvious deficiency of the CPT is the lack of a physical sample of the soil tested. A procedure similar to the simplified method for the SPT has been developed and is reported in the NCEER consensus document.⁽³⁻¹²⁾ The chart in Figure 3-15 can be used to determine the cyclic resistance ratio ($\text{CRR}_{7.5}$) for clean sands having a fines content of less than or equal to 5% from CPT data. The chart is valid only for a magnitude 7.5 earthquake and shows the calculated cyclic stress ratio (CSR) versus the corrected normalized CPT resistance denoted as q_{c1N} . Like the chart for SPT data, the CPT chart was derived from data from sites where liquefaction effects were or were not observed following past earthquakes. The CRR curve separates the region indicative of liquefaction (above the line) from the region where there was non-liquefaction (below the line).

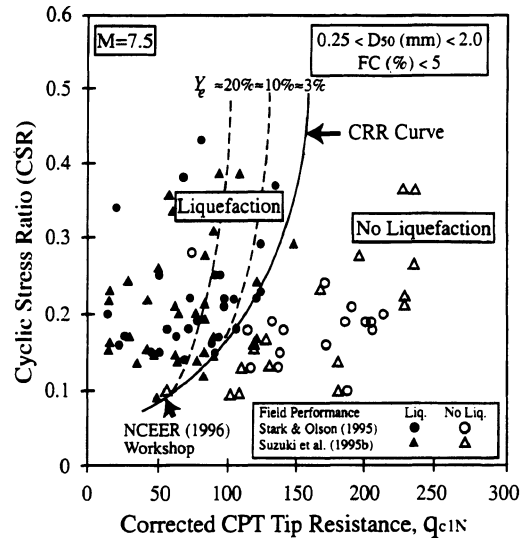


Figure 3-15. Curve Recommended for Determining CRR from CPT Data (Ref. 3-12)

The CRR curve in Figure 3-15 can be approximated by the following set of equations:

$$\text{If } (q_{c1N})_{cs} < 50$$

$$\text{CRR}_{7.5} = 0.833 [(q_{c1N})_{cs} / 1000] + 0.05$$

$$\text{If } 50 \leq (q_{c1N})_{cs} < 160$$

$$\text{CRR}_{7.5} = 93 [(q_{c1N})_{cs} / 1000]^3 + 0.08$$

where $(q_{c1N})_{cs}$ is the clean sand cone penetration resistance normalized to 100 kPa (approximately one atmosphere of pressure). The truly normalized (i.e., dimensionless) cone penetration resistance corrected for overburden stress (q_{c1N}) is given by:

$$q_{c1N} = C_Q (q_c / P_a) = q_{c1} / P_a$$

where:

$$C_Q = (P_a / \sigma'_o)^n$$

C_Q is the normalizing factor for cone penetration resistance; P_a is approximately one atmosphere of pressure given in the same units as the measured field CPT tip resistance, q_c , and calculated overburden pressure, σ'_o . C_Q is limited to a maximum value of 2 at shallow depths. The value of the exponent, n , is dependent on the grain characteristics of the soil. The value of n ranges from 0.5 for clean sands to 1.0 for clays. Discussion on the determination of the exponent n follows.

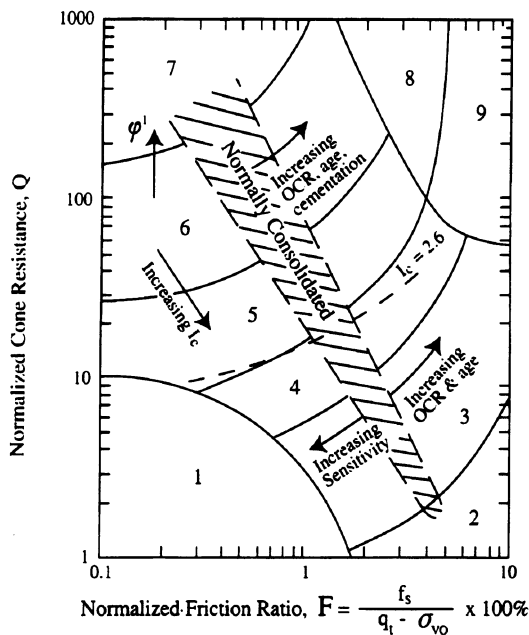


Figure 3-16. Normalized CPT Soil Behavior Type (Ref. 3-12)

Figure 3-16 can be used initially to access the soil behavior type from the CPT tests. The CPT friction ratio can be determined by taking the sleeve resistance, f_s , and dividing it by the cone tip resistance, q_c . The cone tip resistance, q_c , is determined by taking the measured tip resistance, q_t , and subtracting the total overburden pressure, σ_{vo} . The normalized cone resistance, Q , is determined by the following equation:

$$Q = [(q_c - \sigma_{vo}) / P_a] [(P_a / \sigma'_{vo})^n]$$

The normalized friction ratio, F , is determined by:

$$F = [f_s / (q_c - \sigma_{vo})] \times 100\%$$

The soil behavior type index, I_c , is determined by the following equation:

$$I_c = [(3.47 - \log Q)^2 + (1.22 + \log F)^2]^{0.5}$$

The soil behavior chart in Figure 3-16 was determined assuming an exponent, n , equal to 1.0, which is appropriate for clayey soils. To use the chart, the first step is to differentiate the soil types characterized as clays from the soil types characterized as sands and silts. The exponent n is assumed to 1.0 (characteristic of clays) and the dimensionless normalized CPT penetration resistance, Q , is:

$$Q = [(q_c - \sigma_{vo}) / \sigma'_{vo}]$$

If the calculated I_c using the computed Q is greater than 2.6, the soil is classified as clayey and may be too clay-rich or plastic to liquefy; verification by actual soil samples is highly recommended and checking with the so-called Chinese criteria, described later, should be done. However, if the computed I_c is less than 2.6, the soil is most likely to be granular and Q should be recomputed with the n exponent assumed to be 0.5. Now, C_Q should be calculated and the normalized CPT resistance, q_{c1N} , should be substituted for Q in the I_c calculation. If the I_c calculation gives a value of less than 2.6, the soil can be classified as non-plastic and granular. If the recalculated I_c gives a value of greater than 2.6, the soil is likely to be very silty and possibly plastic. If so, q_{c1N} should be recalculated with an intermediate value of 0.7 for n .

Finally, for sands with fines, the normalized penetration resistance, q_{c1N} , should be corrected to an equivalent clean sand value, $(q_{c1N})_{cs}$, with the following relationship:

$$(q_{c1N})_{cs} = K_c q_{c1N}$$

where K_c is the CPT correction factor for grain characteristics and is determined by the following equations:

$$\text{For } I_c \leq 1.64, K_c = 1.0$$

$$\text{For } I_c > 1.64, K_c = -0.403 I_c^4 + 5.581 I_c^3 - 21.63 I_c^2 + 33.75 I_c - 17.88$$

The appropriate values of the corrected tip resistance with the grain size correction, $(q_{c1N})_{cs}$, should then be used in Figure 3-15 to determine the $CRR_{7.5}$ and ultimately the factor of safety against liquefaction in the same manner as presented for SPT data.

3.4.4 Evaluating the Liquefaction Potential by Shear Wave Velocity

Simplified procedures have also been developed for the evaluation of liquefaction potential using shear wave velocities. However, there are some severe limitations when relying solely upon the shear wave velocities for liquefaction evaluation; these limitations include the fact that the shear wave velocities

are determined in situ using low strain measurement schemes, such as seismic refraction, downhole, or crosshole surveys while the liquefaction phenomena is a large strain event. Another limitation is these seismic wave techniques do not provide a means of determining the soil type classification, particularly identifying clay soils that are non-liquefiable. The use of shear wave velocities must be accompanied by soil borings that can provide visual and laboratory confirmation of soil types.

A stress-based liquefaction procedure has been developed based on information obtained from the Imperial Valley earthquake of 1979. The normalized shear wave velocity, V_{S1} , is obtained from the field measured shear wave velocity, V_S , by the equation:

$$V_{S1} = V_S (P_a / \sigma'_{vo})^{0.25}$$

where P_a again is the reference stress of 100 kPa, approximately atmospheric pressure, and σ'_{vo} is the effective overburden pressure in units of kPa. The cyclic resistance ratio, CRR, is determined by the following equation:

$$CRR_{7.5} = a(V_{S1}/100)^2 + b(V_{S1c} - V_{S1}) - b/V_{S1c}$$

where V_{S1c} is the critical value of V_{S1} which separates contractive and dilative behavior, and a and b are curve fitting parameters which have been determined to be 0.03 and 0.9, respectively, for magnitude 7.5 earthquakes. The values of V_{S1c} depend on the fines content of sand and gravel soils and are given in Table 3-15 below:

Table 3-15. Values of Critical Shear Wave Velocity, V_{S1c} (Ref. 3-12)

Fines Content in Percent	V_{S1c} (meters/second)
<5	220
about 20	210
> 35	200

The factor of safety against liquefaction can be determined by comparing the CSR with the CRR. For earthquakes with magnitudes not equal to 7.5, the magnitude scaling factors can be used to adjust the CRR accordingly.

3.4.5 Evaluating the Liquefaction Potential by Becker Penetration Tests

Evaluation of the liquefaction potential of gravelly soils is very difficult using the standard penetration test (SPT) and the cone penetration test (CPT). The coarse size of the particles, as compared with the smaller size of the SPT sampler, can lead to high N-values that are not representative. With the CPT, the same large particles interfere with the normal deformation of soil materials around the penetrometer causing an artificial increase in the penetration resistance. To overcome these difficulties, large diameter penetrometers have been tried and one of the more effective and widely used is the Becker Penetration Test (BPT). The BPT is performed by driving a 3-meter-long double-wall casing into the ground with a double-acting diesel-driven pile hammer. The hammer impacts are applied at the top of the casing and are applied continuously. The BPT resistance is defined as the number of hammer blows required to drive the casing a distance of 300 mm. It has been recommended that the casing have an outside diameter of 168 mm; the casing should be driven by an AP-1000 drill rig with a supercharged diesel hammer and the bit should be plugged. The BPT is not used directly to estimate the liquefaction potential. The corrected Becker penetration resistance has been roughly correlated with the corrected standard penetration resistance as shown in Figure 3-17. The estimated N-values are then used to determine the liquefaction potential of the gravelly soils using the procedure for the SPT.

3.4.6 Liquefaction of Clay Soils

For clayey soils, tests performed in China have shown that certain clayey materials may be vulnerable to severe strength loss due to earthquake shaking (Seed and Idriss, Ref. 3-14). A clayey soil would be considered liquefiable if all of the following criteria are met:

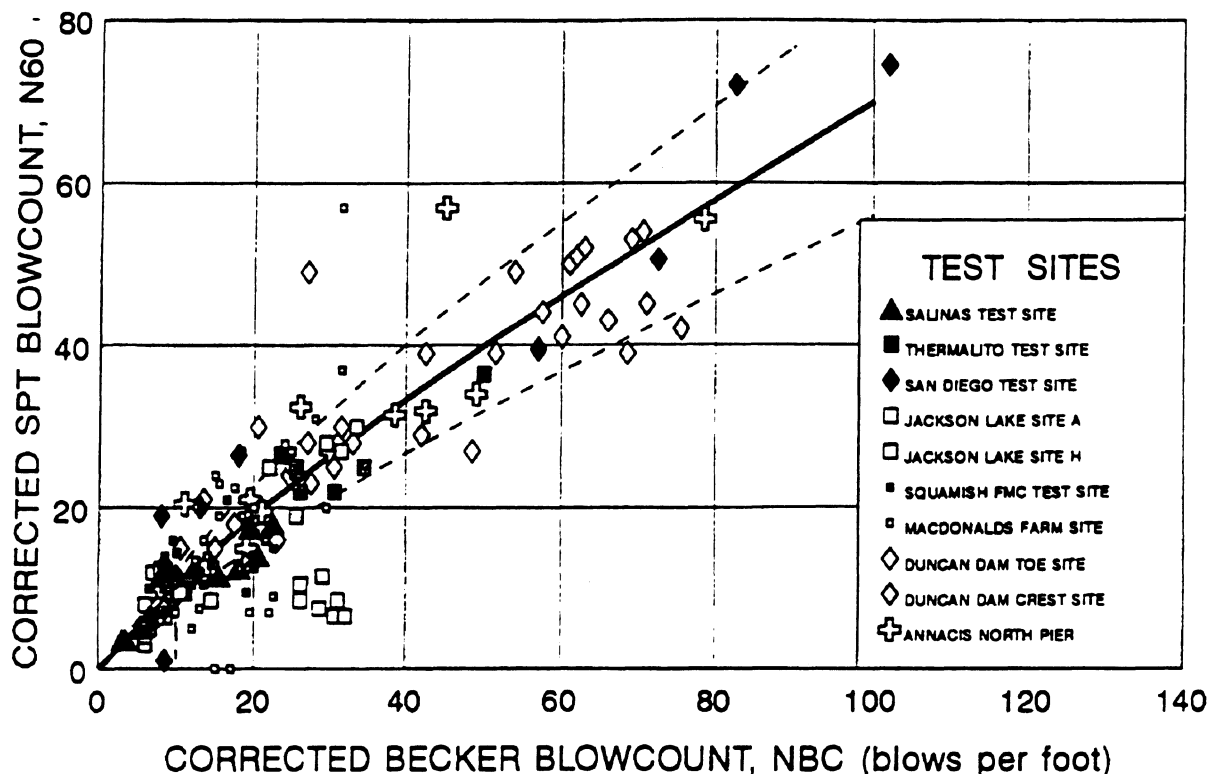


Figure 3-17. Correlation Between Corrected Becker Penetration Resistance and SPT Resistance (Ref. 3-12)

- The weight of the soil particles finer than 0.005 mm is less than 15% of the dry weight of the soil.
- The liquid limit (by Atterberg Tests) of the soil is less than 35%.
- The moisture content of the soil is less than 0.9 times the liquid limit.

Clayey soils not meeting all of these criteria may be considered to be non-liquefiable.

3.4.7 Liquefaction-Induced Settlement

When liquefaction occurs in saturated deposits, the increases in pore water pressure that cause the liquefaction to occur will eventually dissipate. This dissipation of the pore water pressure will principally be towards the ground surface; accompanying this dissipation will be some volume change of the

soil deposits which will be seen at the ground level as surface settlement. Because of the generally nonhomogeneous nature of soil, these settlements will often be nonuniform and differential settlements may affect structures and lifelines. A methodology to estimate the ground settlements resulting from liquefaction of sand deposits has been proposed by Ishihara and Yoshimine⁽³⁻¹⁵⁾. This methodology relates the factor of safety for liquefaction to the maximum shear strain developed in a deposit and a chart was developed to determine the volumetric strain as a function of the factor of safety as shown in Figure 3-18.

Knowing the strain caused by the liquefaction, the ground surface settlement may be estimated by multiplying the thickness of each layer by the strain.

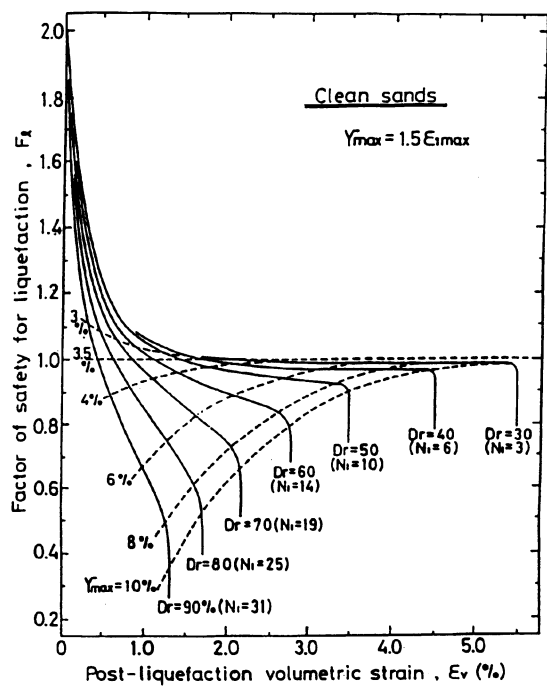


Figure 3-18. Estimation of volumetric strain based on calculated factor of safety against liquefaction as a function of relative density (Ref. 3-15)

Example

A 20 foot thick sand layer has been analyzed and found to have an induced shear stress ratio (CSR) of 0.30 while the critical shear stress ratio (CRR) was found to be 0.24. The corrected standard penetration resistance, (N_1)₆₀, was found to be 20. Estimate the liquefaction-induced settlement of the layer.

Solution:

Step 1: Calculate the factor of safety against liquefaction, FS:

$$\begin{aligned} FS &= CRR / CSR \\ &= 0.24 / 0.30 \\ &= 0.80 \end{aligned}$$

Step 2: Estimate the post-liquefaction volumetric strain:

Referring to Figure 3-18, using $FS = 0.80$ and $(N_1)_{60} = 20$,

$$\epsilon_v = 1.6\%$$

Step 3: Calculate estimated settlement:

$$\begin{aligned} \text{Settlement} &= \epsilon_v \times (\text{Layer Thickness}) \\ &= (0.016) \times (20 \text{ feet}) \\ &= 0.32 \text{ feet} \\ &= 3.84 \text{ in.} \end{aligned}$$

3.4.8 Liquefaction Induced Ground Failures and Effects on Structures

If a soil becomes liquefied and loses its shear strength, ground failures may result. If there are structures founded over or near these soil deposits, they may be damaged. Youd⁽³⁻¹⁶⁾ has classified ground failures caused by liquefaction into three categories:

- 1) lateral spreading
- 2) flow failures, and
- 3) loss of bearing capacity.

Lateral spreading is the movement of surficial soil layers in a direction parallel to the ground surface which occurs when there is a loss of shear strength in a subsurface layer due to liquefaction. Lateral spreading usually occurs on very gentle slopes with a slope of less than six percent. If there is differential lateral spreading under a structure, there could be sufficient tensile stresses developed in the structure that it could be literally torn apart. Flexible buildings have been observed to better withstand extensional displacement than more stiff or brittle buildings⁽³⁻¹⁷⁾.

Lateral spreading can have a very catastrophic impact upon long, linear buried utilities or, as some may prefer, "lifelines". During the great 1906 San Francisco earthquake, it is believed that every break in the water supply pipeline was caused by lateral spreading. This, of course, severely hampered fire-fighting efforts against the fires that were triggered by the earthquake which eventually destroyed much of San Francisco. Figure 3-19 shows the devastating effects of lateral spreading on a building during the 1989 Loma Prieta earthquake.

Flow failures occur when large zones of soil become liquefied or blocks of unliquefied soils flow over a layer of liquefied soils. Flow slides can develop where the slopes are generally greater than six percent. This phenomenon was tragically observed during the 1964 Alaska earthquake.



Figure 3-19. Damage to building at Moss Landing due to liquefaction-caused lateral spreading during the 1989 Loma Prieta earthquake (photograph courtesy of T.L. Youd)

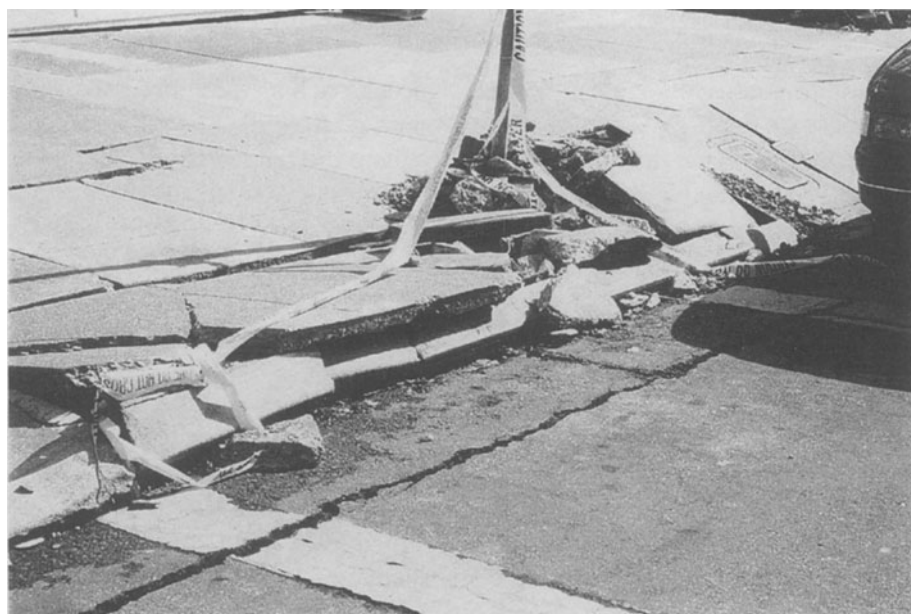


Figure 3-20. Effects of Ground Oscillation in the Marina District of San Francisco as a result of the 1989 Loma Prieta earthquake.



Figure 3-21. Liquefaction-induced loss of bearing capacity of apartment buildings during the 1964 Niigata, Japan earthquake. (Photograph by the United States Geological Survey)

On flat ground, ground oscillation can occur when liquefaction at depth decouples the overlying surface layers from the underlying liquefied soil. The decoupling causes the upper surface layers to oscillate with sometimes large displacements or visible ground waves. The observed permanent displacements are usually small and show no particular orientation. Evidence of ground oscillations in the Marina District of San Francisco due to the 1989 Loma Prieta earthquake were abundant as shown in Figure 3-20.

Liquefaction can also result in the loss of bearing capacity usually accompanied by large soil deformations. Structures supported on these soils may settle, tilt, or even overturn. Buried structures have even been observed to have "floated" out of the ground. In extreme cases, where the thickness of the liquefied soils is large, tilting or overturning failures could

occur, such as those observed in Niigata, Japan during the 1964 earthquake (Figure 3-21). Where the thickness of liquefied soil is thin, or where there is relatively thick non-liquefied soils overlying a liquefied soil deposit, severe tilting or overturning of structures might not occur, but differential vertical settlements could occur.

Buried structures, such as underground tanks, may be subject to excess buoyancy because of the increase in the pore water pressure associated with liquefaction. Retaining structures, such as retaining walls or port structures, could also be subjected to an increase in the lateral pressures should liquefaction occur in the adjacent soils. The formation of sink holes (when sand boils occur) may cause differential settlement or tilting of structures established on shallow foundations.

Of course, the degree that structures are affected directly or indirectly by liquefaction-caused failures will depend upon how extensive the liquefaction is. If the liquefaction occurs in a thick and horizontally extensive layer of sand, the effects on structures would be expected to be very great. If, in contrast, the liquefaction is isolated to very thin and non-continuous layers or lenses of soil, structures might have very minimal or even no noticeable damage.

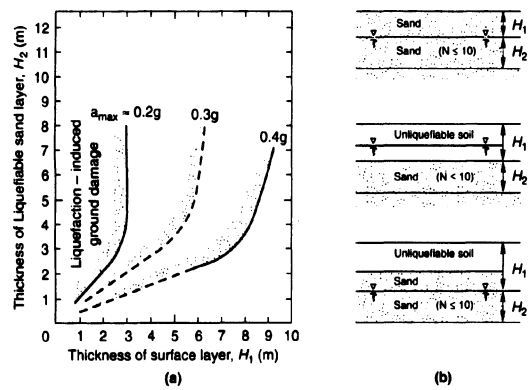


Figure 3-22. Thickness of Liquefied and Over-lying Nonliquefied Soil Layers for Determining Occurrence and Nonoccurrence of Surface Effects of Liquefaction⁽³⁻⁵⁰⁾.

Ishihara in 1985 proposed a preliminary criteria for determining the potential for disruption of the ground surface at liquefaction sites based upon empirical observations during two major Japanese earthquakes and one major Chinese earthquake.⁽³⁻¹⁸⁾ The criteria was based upon the relationship between the thickness of the liquefiable soil layers beneath a site, and the thickness of the overlying nonliquefiable soil. Ishihara's criteria was based on ground accelerations of 200 to 250 gals, approximately 0.20 to 0.25g. The Ishihara criteria is presented in Figure 3-22. Youd and Garris⁽³⁻¹⁹⁾ have looked further into the Ishihara's proposal and have determined that the criteria is generally correct in prediction of occurrence or nonoccurrence of surface liquefaction effects when there is no lateral spreading or ground oscillation. A methodology to estimate the magnitude of lateral spreading is presented in the following section. Determining whether

ground oscillation would occur will be more subjective as to estimating whether the lateral extent of liquefiable deposit is not sufficient enough to allow for decoupling of the upper nonliquefiable soils from the lower liquefiable soils.

3.4.9 Estimating Lateral Displacement Due to Liquefaction

Several methods have been developed to estimate the lateral ground displacement at liquefaction sites. These methods include analytical models [Prevost et al., 1986⁽³⁻²⁰⁾; Finn and Yogendrakumar, 1989⁽³⁻²¹⁾], physical models based upon sliding block analyses [Newmark, 1965⁽³⁻²²⁾; Byrne et al., 1992⁽³⁻²³⁾], and empirical models. One empirical model has been proposed by Bartlett and Youd (1992)⁽³⁻²⁴⁾; They collected case history data of lateral spreading from six western United States and two Japanese earthquakes. Based on their research, they proposed two statistically independent models--one for areas near steep banks with a free face, the other for ground-slope areas with gently sloping terrain. The models are expressed in the following equations:

For free-face conditions--

$$\begin{aligned} \text{Log } D_H &= -16.3658 + 1.1782 M - 0.9275 \\ \text{Log } R &- 0.0133 R + 0.6572 \text{ Log } W + 0.3483 \\ \text{Log } T_{15} &+ 4.5270 \text{ Log } (100 - F_{15}) - 0.9224 \\ D50_{15} & \end{aligned}$$

For ground slope conditions--

$$\begin{aligned} \text{Log } D_H &= -15.7870 + 1.1782 M - 0.9275 \\ \text{Log } R &- 0.0133 R + 0.4293 \text{ Log } S + 0.3483 \text{ Log } \\ T_{15} &+ 4.5270 \text{ Log } (100 - F_{15}) - 0.9224 D50_{15} \end{aligned}$$

Where:

D_H = Estimated lateral ground displacement in meters.

$D50_{15}$ = Average mean grain size in granular layers included in T_{15} , in mm.

F_{15} = Average fines content (fraction of sediment sample passing a No. 200 sieve) for granular layers included in T_{15} , in percent.

M = Moment magnitude of the earthquake.

R = Horizontal distance from the seismic energy source, in kilometers.

S = Ground slope, in percent.

T_{15} = Cumulative thickness of saturated granular layers with corrected blow counts, $(N_1)_{60}$, less than 15, in meters.

W = Ratio of the height (H) of the free face to the distance (L) from the base of the free face to the point in question, in percent.

Comparisons of the predicted displacements with the measured displacements in Bartlett and Youd's database indicates that the predicted displacements are generally valid within a factor of 2. Bartlett and Youd comment that doubling of the predicted displacement would provide an estimate with a high probability of not being exceeded.

Example - Lateral Spread Displacement Near Free Face

A building is planned adjacent to a river in a highly seismic area in a foreign country. There is a steep bank at the river's edge; the bank has a height of 3 meters. The building is planned to located a distance of 7 meters from the river at its closest point. The site has a gentle uniform slope towards the river that drops 2 meters vertically over a horizontal distance of 100 meters. The ground water is at a depth of about 3 meters and is parallel to the ground surface in the direction perpendicular to the river. The geotechnical investigation performed by a local company in the foreign country provides information about the soil conditions and the report states that there is a liquefaction potential at the site.

The design earthquake is a Moment Magnitude 7.5 on a fault located 15 km from the site. The geotechnical report identifies two granular layers as being susceptible to liquefaction. The first layer is encountered between 3 and 5 meters below the ground surface; this layer has an average mean grain size of 0.33 mm, a fines content (less than No. 200 Sieve) of 15%, and a corrected Standard Penetration Blow Count, $(N_1)_{60}$, of 10. The second layer is encountered between 8 and 10 meters below the ground surface; this layer has an average mean grain size of 0.21 mm, a fines

content of 35%, and a corrected $(N_1)_{60}$ value of 17.

Determine the estimated lateral displacement at the near edge of the building due to liquefaction.

Solution

Use the equation for free-face conditions in Section 3.4.9.

Only the upper layer needs to be included in the analysis since the $(N_1)_{60}$ value of the upper layer is less than 15 and the $(N_1)_{60}$ value of the deeper layer is greater than 15. Define parameters for analysis of the upper layer:

$$\begin{aligned} D50_{15} &= 0.33 \text{ mm} \\ F_{15} &= 15\% \\ M &= 7.5 \\ R &= 15 \text{ km} \\ T_{15} &= 5 \text{ m} - 3 \text{ m} = 2 \text{ m} \\ W &= H / L \\ &= (3 \text{ m}) / (7 \text{ m}) \\ &= 0.427 \\ &= 42.7\% \end{aligned}$$

Calculate Lateral Spread Displacement, D_H

$$\begin{aligned} \log D_H &= -16.3658 + 1.1782 M - 0.9275 \\ \log R - 0.0133 R + 0.6572 \log W \\ &\quad + 0.3483 \log T_{15} + 4.5270 \log (100 - \\ F_{15}) - 0.9224 D50_{15} \end{aligned}$$

$$\begin{aligned} &= -16.3658 + 8.8365 - 1.0908 - 0.1995 \\ &\quad + 1.0715 \\ &\quad + 0.1048 + 8.7345 - 0.3044 \\ &= 0.7868 \end{aligned}$$

Then,

$$D_H = 6.1207 \text{ m}$$

Practically speaking, the lateral displacement could range from one-half to twice this estimate. Therefore, the range is:

$$D_H = \text{about 3 to 12 m}$$

Example - Lateral Spread Displacement For A Sloping Site

A power plant is to be located in an alluvial valley which has a shallow groundwater table. The site has a gentle uniform slope which drops 0.4 meters vertically over a horizontal distance 50 meters. The ground water is at a depth of about 2 meters. The geotechnical investigation provides information about the soil conditions and the report states that there is a liquefaction potential at the site.

The design earthquake is a Moment Magnitude 6.5 on a fault located 5 km from the site. The geotechnical report identifies two granular layers as being susceptible to liquefaction. The first layer is encountered between 2 and 3 meters below the ground surface; this layer has an average mean grain size of 0.25 mm, a fines content (less than No. 200 Sieve) of 45%, and a corrected Standard Penetration Blow Count, $(N_1)_{60}$, of 6. The second layer is encountered between 5 and 10 meters below the ground surface; this layer has an average mean grain size of 0.11 mm, a fines content of 35%, and a corrected $(N_1)_{60}$ value of 10.

Determine the estimated lateral displacement at the power plant site due to liquefaction.

Solution:

Use the equation for ground slope conditions in Section 3.5.

Determine the ground slope, S

$$S = V/H = (0.4 \text{ meters}) / (50 \text{ meters}) = 0.8\%$$

Both layers need to be included in the analysis since the $(N_1)_{60}$ value of the both layers is less than 15. Define parameters for analysis:

Use weighted averages:

$$\begin{aligned} D50_{15} &= [(0.25 \text{ mm}) \times (1 \text{ m}) + (0.11 \text{ mm}) \times (5 \text{ m})] / [1 \text{ m} + 5 \text{ m}] \\ &= 0.1333 \text{ mm} \\ F_{15} &= [(45\%) \times (1 \text{ m}) + (35\%) \times (5 \text{ m})] / [1 \text{ m} + 5 \text{ m}] \\ &= 36.67\% \\ M &= 6.5 \\ R &= 5 \text{ km} \\ T_{15} &= 1 \text{ m} + 5 \text{ m} \\ &= 6 \text{ m} \end{aligned}$$

Calculate Lateral Spread Displacement, D_H

$$\begin{aligned} \log D_H &= -15.7870 + 1.1782 M - 0.9275 \log R \\ &\quad - 0.0133 R + 0.4293 \log S + 0.3483 \\ \log T_{15} &+ 4.5270 \log (100 - F_{15}) - 0.9224 D50_{15} \\ &= -15.7870 + 7.6583 - 0.6483 - 0.0665 - \\ &0.0416 \\ &\quad + 0.2710 + 8.1560 - 0.1230 \\ &= -0.5811 \end{aligned}$$

Then,

$$D_H = 0.2624 \text{ m}$$

Practically speaking, the lateral displacement could range from one-half to twice this estimate. Therefore, the range is:

$$D_H = \text{about 0.13 to 0.52 m}$$

3.4.10 Facing the Liquefaction Problem

If liquefaction is identified as a hazard that could affect a structure, there are choices that must be made. For new construction, the available choices are:

1. design for liquefaction by modifying the site soil conditions or strengthening the structure.
2. abandon or move the project, or
3. accept the risks by proceeding without designing for liquefaction.

Obviously, economics will influence the selection process in a major way. The second choice would be dependent on whether there was an alternative site without the liquefaction

problem. The third choice could invite unwanted liability exposure and problems of uninsurability or even jeopardize future property values and viability of the project. The second and third choices could be the subject of much discourse but is outside the intention and scope of this work and emphasis will be put upon designing for liquefaction.

3.4.11 Mitigation of Liquefaction Hazard by Site Modification

There are site modification methods which are intended to reduce the potential or susceptibility of the soils beneath a site to liquefy⁽³⁻²⁵⁾. These methods are summarized below:

1. Excavation and replacement of liquefiable soils
 - A. Excavation and engineered compaction of the existing soil
 - B. Excavation and engineered compaction of existing soils with additives
 - C. Excavation of existing soils and replacement with properly compacted nonliquefiable soils
2. Densification of in-situ soils
 - A. Compaction piles
 - B. Vibratory probes
 - C. Vibroflotation
 - D. Compaction grouting
 - E. Dynamic compaction or impact densification
3. In-situ improvements of soils by alteration
 - A. Mixing soils in-situ with additives
 - B. Removing in-situ soils by jetting and replacement with nonliquefiable soils
4. Grouting or chemical stabilization

Excavation and Replacement of Liquefiable Soils. The first general category of site modification methods involves the excavation of the potentially liquefiable soils. This soil may then be recompacted as an engineered fill to a higher density so that the soil will have less potential to liquefy. Alternatively, the native soils may be improved

with some additives and then properly compacted as an engineered fill. Another solution would be to waste the excavated material and replace it completely with properly compacted import material that would be nonliquefiable. As the liquefiable soils will most likely be below the water table, dewatering will be needed and excavation could be difficult due to high moisture content of the soils; these two factors may make recompaction less desirable and uneconomical.

In-Situ Densification. The second general category of site improvement methods is in-situ densification of the liquefiable soils. By densification, the soils would have less potential to liquefy because a more dense soil would not tend to have a decrease in volume when subjected to earthquake shaking; instead, a more dense soil would have a tendency to become less dense thus reducing the possibility of excess pore pressures developing.

The driving of piling into ground will produce both vibrations and displacement in the soils which would lead to densification and increased soil strength. It would be more beneficial to drive piling that would have a significant cross sectional area to maximize the lateral displacement of the soils; thus a solid pile such as a timber, concrete, or closed-end pipe pile section would be much more effective than an H-section pile. Another form of compaction piling (or displacement piles) is a sand filled steel pipe that is withdrawn after driving; the pile is pulled increments of about 6 feet and the hole is backfilled with sand. The pile is then redriven to compact the sand and this process is repeated until the steel pile is completely withdrawn; this allows the steel pile to be reused. Compaction piles have reportedly been used to stabilize hydraulic fill consisting of sand beneath a building at Treasure Island in San Francisco Bay⁽³⁻²⁶⁾; liquefaction of the treated soils did not occur in the 1989 Loma Prieta earthquake whereas liquefaction was observed in non-treated areas at other parts of Treasure Island.

Vibratory probes describes methods commonly referred to as "vibro systems or

techniques." Vibro systems are probably the most commonly used countermeasure among all of the mitigation techniques available⁽³⁻²⁷⁾. The vibrator is 12 to 18 inches in diameter and about 10 to 16 feet in length. Rotating eccentric weights mounted on a casing above the probe produce vibrations close to the tip of the probe.

Vibroflotation is one such proprietary vibro process by which a machine is lowered into the ground and compacts loose soils by simultaneous vibration and saturation⁽³⁻²⁸⁾. As the machine vibrates, water is pumped in faster than it can be absorbed by the soil. The more granular particles are vibrated in a more dense state while the excess water carries off the finer particles to the ground surface (see Figures 3-23 and 3-24). Granular soils are added from the ground surface to compensate for the loss of the finer particles and the increased density. It has been reported by Ishihara et al.⁽³⁻²⁹⁾ that oil tanks supported on sand soils compacted by the Vibroflotation technique suffered little damage and settlement in the 1978 Miyagiken-Oki earthquake in Japan, while nearby similar facilities supported on loose sand deposits that were not densified suffered considerable damage and significant settlement. Vibro compaction is a similar process although the use of water jets may not be used. Vibro compaction is generally effective in clean sand soils having less than 10% fines content (passing the No. 200 sieve). Where the fines content of sands is greater than 10%, or where there may be sands interbedded with cohesive layers, vibro replacement or "stone columns" would be viable; this method is described in more detail later in this section.

Another method of in-situ densification is compaction grouting. Grout pipes are typically installed by driving or by drilling and inserting steel pipes through which low slump, mortar-

type grout is pumped under high pressure to densify loose soils⁽³⁻²⁶⁾.

In-situ densification may also be accomplished by dynamic compaction (which is also referred to as impact densification or heavy tamping). Dynamic compaction is a method which utilizes a heavy falling weight to produce a shock wave which is propagated to some depth in the ground (Fig. 3-25).

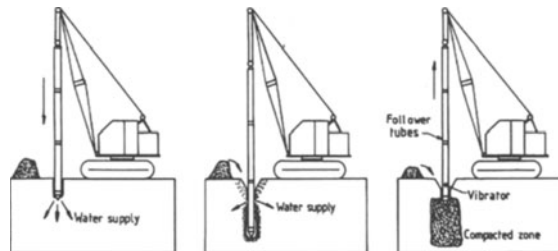


Figure 3-23. Vibroflotation technique. (Illustration courtesy of Hayward Baker, Inc.)

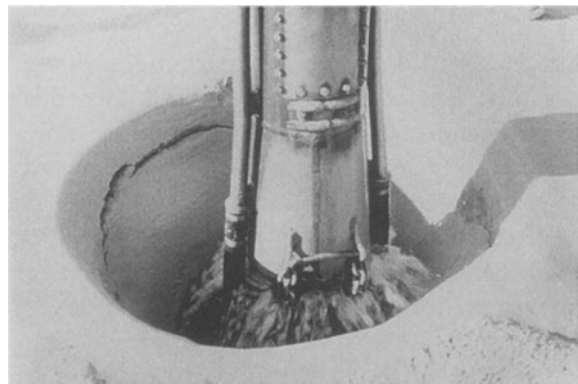


Figure 3-24. Water being pumped during vibroflotation. (Photograph courtesy of Hayward Baker, Inc.)



Figure 3-25. Dynamic Compaction technique. (Photograph courtesy of Hayward Baker, Inc.)

The effect of this compaction in granular soils is to generate high pore water pressures. As these high pore water pressures are dissipated by drainage, compaction (or more correctly, consolidation) occurs and the soils become more dense and, therefore, more resistant to liquefaction. In the United States, it is typical to use weights ranging from 10 to 35 tons that are dropped from heights of 50 to 120 feet. The energy is controlled by selection of the weight, drop height, the number of drops at each point and the spacing of the grid of drop points. The effective depth of treatment has been empirically estimated as shown in Figure 3-26; this figure shows the effective depth of treatment (in meters) as a function of the metric energy input expression of $(WH)^{0.5}$, where W is the weight to be dropped in tonnes and H is the drop height in meters⁽³⁻³⁰⁾. The effective depth of treatment has also been expressed in the form of the equation:

$$D = N (WH)^{0.5}$$

where N is a number between 0.3 and 0.7 depending on the material to be densified.

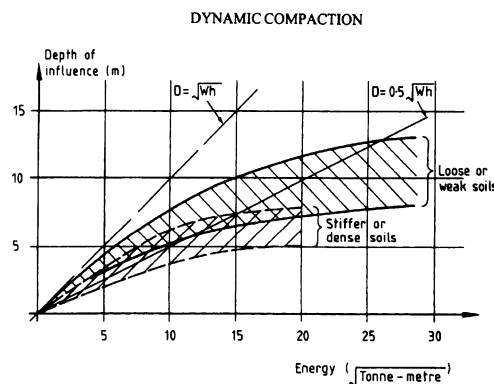


Figure 3-26. Chart to determine effective depth of treatment by Dynamic Compaction.(Ref. 3-30)

In-situ densification could also be accomplished by deep blasting. This method would use small explosive devices installed at depth to densify loose sandy materials.

Soil Alteration. The third major category of soil improvement methods is alteration of the soil to reduce the potential for liquefaction. The soil may be made more resistant by the construction of mixed-in-place solidified piles

or walls. Lime, cement, or asphalt may be mixed-in-place to create piles or walls to provide shear resistance which would confine an area of liquefiable soils to prevent flow.

Vibro-replacement is a process by which soils can be improved and is especially suitable when there are significant amounts of fine soils which do not readily respond to vibratory compaction. With vibro-replacement, a vibrator is used to penetrate the soil to a desired depth and the resulting cavity is filled with coarse-grained material which may consist of stone. This material is then compacted and forms a "stone column" (see Figure 3-27). The stone provides better transmission of the vibratory forces to the surrounding soils and therefore provides better densification. Stone columns would be installed on a pre-determined grid pattern. The stone columns would have a low compressibility and high shear strength. Because of its coarse-grained nature, excess pore pressures developed during an earthquake in the surrounding soils can be quickly dissipated.

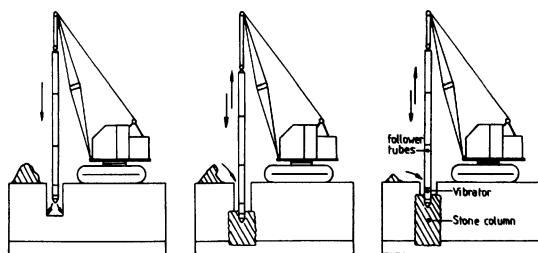


Figure 3-27. Vibro-Replacement technique. (Illustration courtesy of Hayward Baker, Inc.)

Grouting or Chemical Stabilization. The fourth category of soil improvement methods is soil grouting or chemical stabilization. These methods would improve the shear resistance of the soils by injection of particulate matter, resins, or chemicals into the voids. Common applications are jet grouting and deep soil mixing⁽³⁻²⁷⁾.

Jet grouting is a system where cylindrical or panel shapes of hardened soils are created to replace potentially liquefiable soils. A specially manufactured drill is used that has high

pressure side jetting nozzles to cut and lift the soil to the surface while simultaneously injecting grout. The resulting mixture is commonly called "soilcrete."

Deep soil mixing is a technique that uses hollow stem auger drilling equipment with paddles to mix cementitious materials into the soils to create a "soilcrete" or similar mixture⁽³⁻²⁷⁾. Gangs of 2 to 5 shafts with hollow stem augers are used. The augers could be up to 40 inches in diameter and could mix soils to depths of up to 200 feet⁽³⁻³¹⁾. Each auger is a discontinuous auger shaft that has mixing paddles. The augers drill into the soils and grout is pumped through the hollow stems and injected into the soil at the tip. Deep soil mixed walls are created with this process as the augers are used in tangent configurations. The use of deep soil mixing in liquefaction stabilization may involve the construction of a perimeter soil-cement cutoff wall installed to isolate loose cohesionless soils beneath a structure. The groundwater could be lowered to provide a dry or nonliquefiable zone beneath the structure. Reinforcement of liquefiable soils can be accomplished by the soil-cement walls in a block or lattice pattern to resist the stresses from embankments or other structures when loose cohesionless foundation materials liquefy as a result of an earthquake. This method of soil reinforcement was used to stabilize the Jackson Lake Dam in Wyoming⁽³⁻³²⁾ and a site in Kagoshima City, in western Japan for a 3-story building⁽³⁻³³⁾.

3.4.12 Mitigation of Liquefaction Hazard by Structural Design

Designing a structure to resist liquefaction must take into account the deformations of the soil that could occur in the event of liquefaction occurrence. This will greatly effect the foundation design of the building.

Designing for liquefaction may be accomplished by the use of piles or caissons which rely upon the soil or rock beneath the potentially liquefiable soil layers for support. These designs would need to account for

possible downdrag forces that would develop on the piles or caissons because of the settlement of the upper soils that could occur. Also, special design for the lateral forces or base shear may be needed because there could be a significant loss of the ability to transfer horizontal forces to the liquefied soils; this may require the use of battered piles or the design of caissons as unsupported columns through the liquefied zones. However, the use of battered piles is being discouraged because of the rigid connections the piles have with the pile caps. Under seismic excitation and liquefaction, these connections may be subjected to bending moments that could result in severe damage to the piles and/or the pile caps. Extensive damage to battered piles supporting wharf structures was observed in the Port of Oakland as a result of the 1989 Loma Prieta earthquake.

Because of the possibility of lateral spreading, the foundation system will need to be tied together quite well to act as a single unit. Floor slabs on grade could be subject to settlement or differential movement and may need to be structurally supported.

For structures of relatively low profile and relatively uniform mass distribution, a mat foundation may be feasible. The mat would be able to bridge the local areas of settlement and the structure should be able to act more or less as a rigid body. Any permanent deformations of the structure could be corrected by injection grouting or mud-jacking the structure to its proper level.

Wall structures retaining potentially liquefiable soils, such as those that might be found at port and harbor facilities, may be subjected to greater than normal lateral earth and hydrostatic pressures should liquefaction occur. Earth pressures could increase from an at-rest or active earth pressure condition to a condition where the pressure distribution could be equivalent to that imposed by a fluid having a density equal to the total unit weight of the soil.

With a structural solution to mitigate against liquefaction, there will remain a significant risk that some damage could occur to the structure

and that almost certain remedial and corrective work will be likely after the liquefaction event.

3.4.13 Mitigation of Liquefaction Hazard by Drainage

Dewatering systems may reduce the potential for liquefaction by removing the water from those layers which could liquefy. Also, the increase in effective overburden pressure will add to the resistance of the soils against liquefaction. If total dewatering of a site is not practical, providing some means of drainage may mitigate the problem. Drainage solutions to mitigate liquefaction allow for the rapid dissipation of excess pore pressures in the potentially liquefiable soil layers. If the pore pressures can be relieved quickly, the effective stresses will not decrease significantly and the soil will retain most of its shear strength not allowing liquefaction to occur. Vertical gravel drains placed in a grid pattern may be able to accomplish this. Vibro-replacement also utilizes this principle as part of its mechanism to mitigate liquefaction as the coarse-grained stone columns would be very permeable in comparison to the surrounding soils.

There are methods under development to utilize prefabricated drainage material similar to conventional vertical wick drains to control the effects of liquefaction. These drains would be of sufficient size to accommodate the large volumes of water generated during a liquefaction event without undue head loss. An integral water reservoir allows water to be stored during an earthquake; the water is gradually drained back into the surrounding soils. A water outlet would not be required for this system.

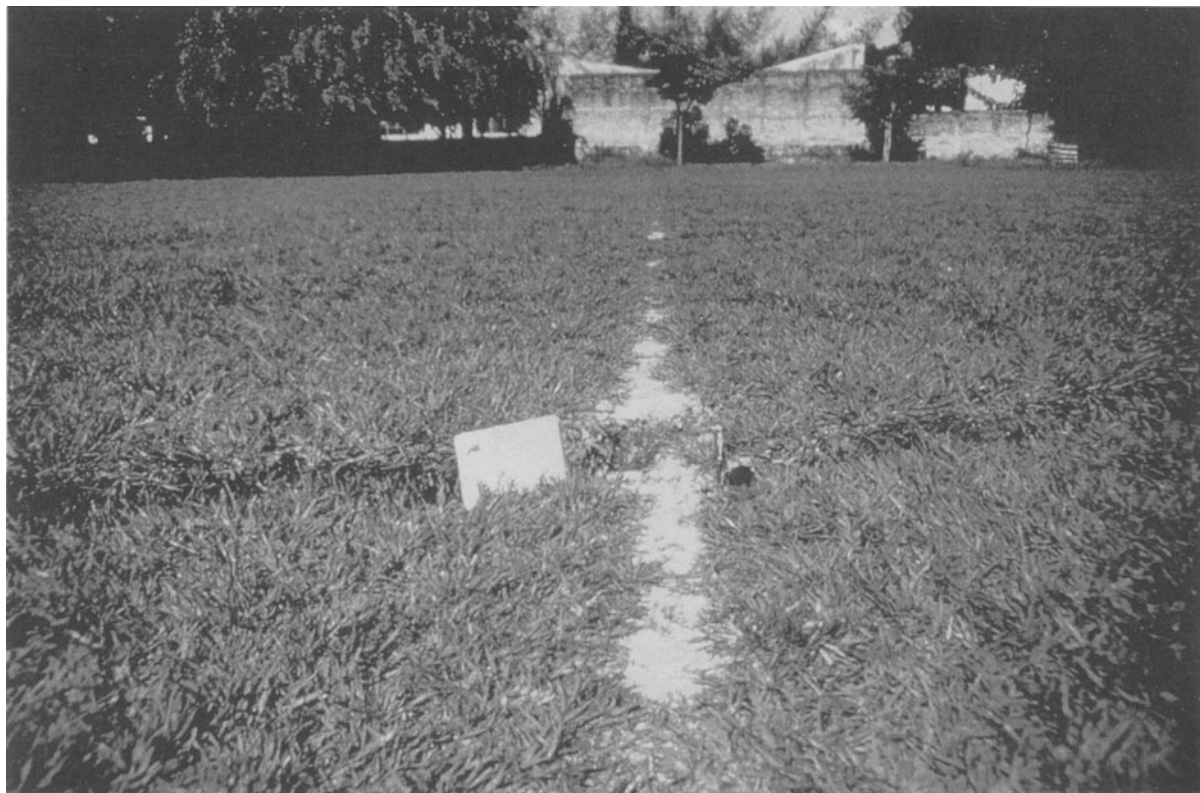


Figure 3-28. Differential compaction between an area with older natural soils and an area with loose fill soils from the 1986 San Salvador earthquake. (Photograph courtesy of Mr. Robert Chieruzzi)

3.5 SEISMIC SETTLEMENT, SUBSIDENCE AND DIFFERENTIAL COMPACTION

Seismic settlement and subsidence are two terms used to describe surface subsidence which is a result of compaction or densification of granular soils from earthquake-induced vibrations, which may occur over large areas. Although this phenomenon produces a result which is similar to what occurs from liquefaction, it occurs in dry or partially saturated soils or in saturated soils which have good drainage, that is, those soils that do not liquefy⁽³⁻³⁴⁾.

During an earthquake, a granular soil is subjected to cyclical shear from horizontal and vertical accelerations. In a strong earthquake,

the horizontal motions can cause densification because of the numerous shear cycles that occur. Whitman and DePablo have suggested that vertical accelerations greater than 1 g ($g =$ acceleration of gravity) are required to cause significant densification of granular soils.⁽³⁻³⁵⁾ However, it has been reported that over one meter (about three feet) of ground subsidence due to densification was experienced in Valdivia, Chile during the 1960 earthquake⁽³⁻³⁶⁾. It has also been reported that there was ground subsidence in the order of 5 to 7 meters over a very large area in the Mississippi Valley as a result of the New Madrid earthquakes of 1811 and 1812⁽³⁻³⁴⁾. It is difficult to determine whether some of these reported instances of subsidence were at least partially due to liquefaction or some tectonic movement, or if they were totally a result of seismic settlement.

Differential compaction occurs when there is marked difference in the density of the soils

in a horizontal sense. Such a phenomena was observed during the San Salvador Earthquake of 1986 (Figure 3-28).

Tokimatsu and Seed have proposed a simplified procedure to estimate the settlement of dry sands due to earthquake shaking without having to perform a dynamic response analysis.⁽³⁻³⁷⁾ They claim that the primary factor controlling settlements in dry sands is the cyclic shear strain induced in the soils at various depths. At any given depth, the effective shear strain, γ_{eff} , may be estimated by the relationship:

$$\gamma_{\text{eff}} = \tau_{\text{av}} / G_{\text{eff}} = [\tau_{\text{av}} / G_{\text{max}}] / [G_{\text{eff}} / G_{\text{max}}]$$

where G_{max} is the shear modulus at low strain level, G_{eff} is the effective shear modulus at the induced strain level, and τ_{av} is the average cyclic shear stress at the corresponding depth. τ_{av} may be computed by the following equation:

$$\tau_{\text{av}} = 0.65 (a_{\text{max}} / g) \cdot \sigma_0 \cdot r_d$$

Substituting this into the earlier equation and rearranging the terms, we get the following equation:

$$\gamma_{\text{eff}} [G_{\text{eff}} / G_{\text{max}}] = 0.65 (a_{\text{max}} / g) \cdot \sigma_0 r_d / G_{\text{max}}$$

The right-hand side of the equation can be evaluated for any depth. G_{max} may be evaluated by the relationship developed by Seed and Idriss⁽³⁻³⁸⁾ given below:

$$G_{\text{max}} = 1,000 \cdot (K_2)_{\text{max}} \cdot (\sigma'_m)^{1/2}$$

in units of pounds per square foot

where $(K_2)_{\text{max}}$ is approximately equal to $20(N_1)^{1/3}$ and σ'_m represents the median effective stress on the soil at the given depth. Having computed the value of $\gamma_{\text{eff}} [G_{\text{eff}} / G_{\text{max}}]$, Figure 3-29 may be used to determine the effective shear strain, γ_{eff} . Knowing the effective cyclic shear strain, the volumetric strain, ϵ_c , can be estimated by the use of Figure 3-31 which relates the strains for different N_1 values for a given 15 equivalent uniform strain cycles, which are representative of a magnitude 7.5 earthquake.

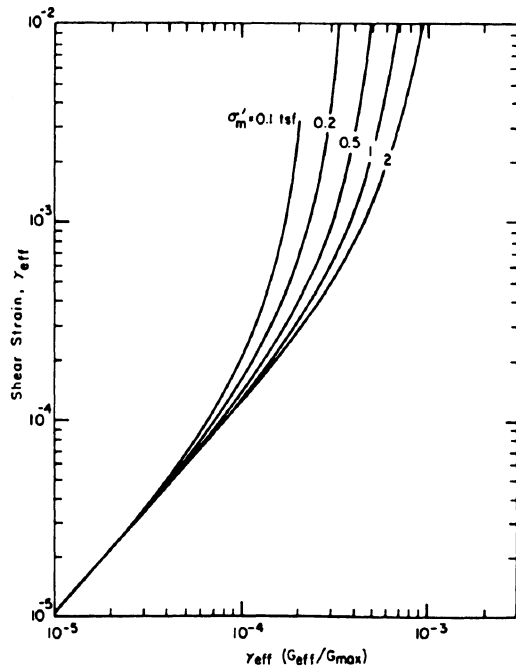


Figure 3-29. Plot for determination of induced shear strain in sand deposits (Ref. 3-37)

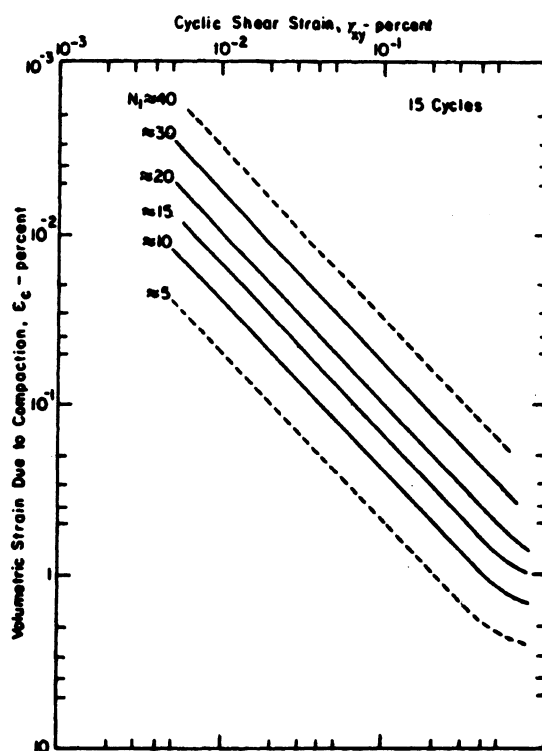


Figure 3-30. Relationship between Volumetric Strain, Shear Strain, and Penetration Resistance for dry sands (Ref. 3-37)



Figure 3-31. The Turnagain Heights landslide occurred as a result of the 1964 Great Alaska earthquake and had length of about 1.5 mi. and width from 1/4 to 1/2 mi. (Photograph by United States Geological Survey)

To account for earthquakes of different magnitudes, Seed and Tokimatsu have proposed the following Table 3-16 which relates the number of representative cycles of cyclic shear strain to different earthquake magnitudes to provide a correction factor.

Table 3-16. Correction Factors for Different Magnitude Earthquakes (Ref. 3-37)

Earthquake Magnitude	Number of representative cycles at $0.65 \tau_{max}$	Volumetric strain ratio $\epsilon_{c,N} / \epsilon_{c,N=15}$
8-1/2	26	1.25
7-1/2	15	1.0
6-3/4	10	0.85
6	5	0.6
5-1/4	2-3	0.4

Because the results in Figure 3-30 are based on tests that were performed under unidirectional simple shear conditions, Seed

and Tokimatsu recommend that the estimated volumetric strain be doubled to account for multidirectional effects of earthquake shaking. The amount of dry settlement due to earthquake shaking may then be obtained by multiplying the corrected volumetric strain by the thickness of the sand layer.

3.6 LANDSLIDING AND LURCHING

3.6.1 Landsliding

Earthquakes may trigger landslides or other forms of slope instability. Slope failures may occur as a result of the development of excess pore pressures which will reduce the shear strength of the soils or cause loss of strength along bedding or joints in rock materials. The Turnagain Heights landslide occurred as a

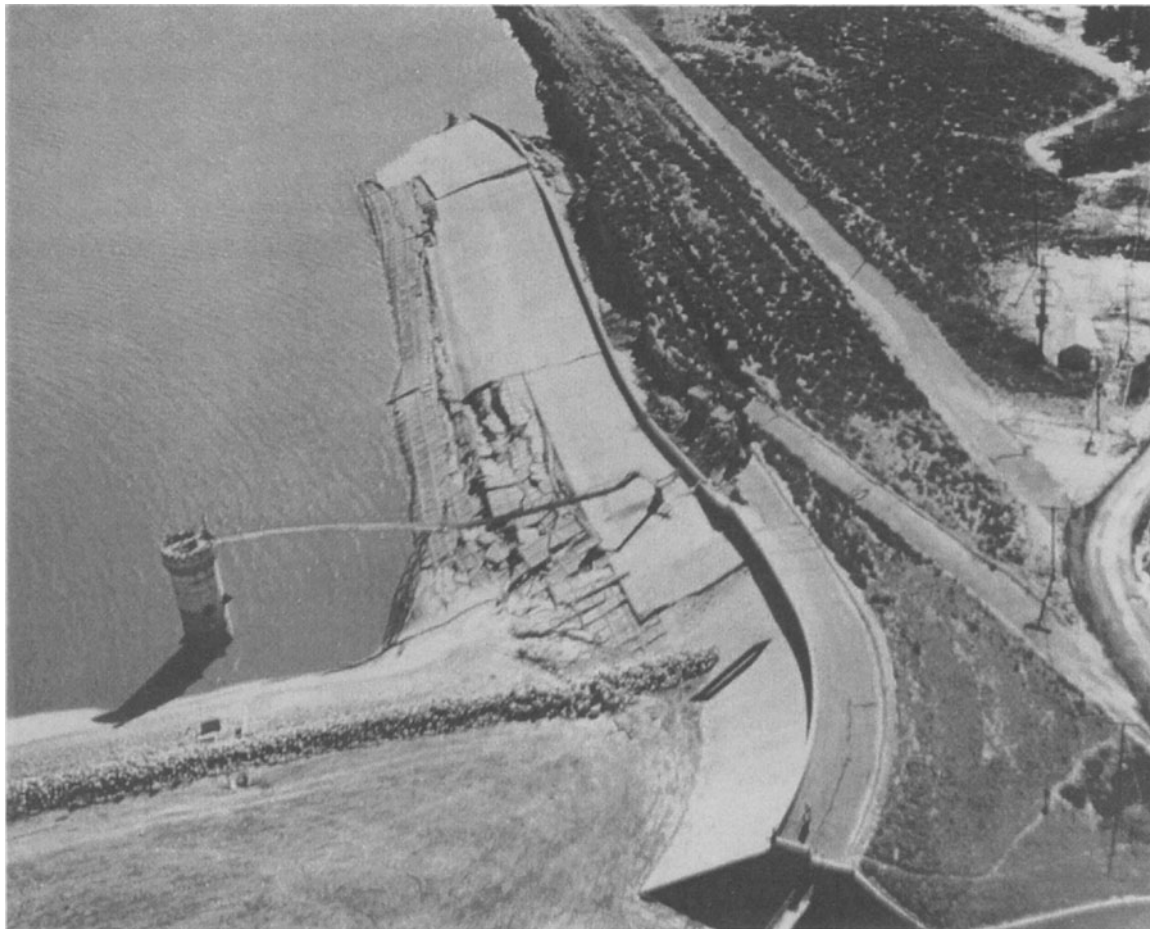


Figure 3-32. Lower Van Norman Dam after the 1971 San Fernando earthquake. (Photograph by the United States Geological Survey)

result of the 1964 Alaska earthquake (Fig. 3-31). The epicenter of the Richter magnitude 8.5 earthquake was about 130 kilometers from Anchorage but the duration of strong ground motion lasted more than three minutes. Seed and Wilson believe that the long duration of the ground motion caused the pore water pressures to continually increase causing liquefaction of silt and fine sand lenses which led to the landslide.⁽³⁻³⁹⁾ Earthquake-caused liquefaction within the Lower Van Norman Dam during the February 9, 1971 San Fernando earthquake nearly resulted in the overtopping of the dam (see Figure 3-32) which would have threatened tens or hundreds of thousands of people who lived beneath the dam in the densely populated San Fernando Valley.

Earthquakes may also cause shallow debris slides in areas with high, steep slopes. These slides could be quite minor or quite major, such as the 1970 debris avalanche triggered by the Peruvian earthquake of May 31, 1970 which buried the towns of Yungay and Ranrahirca in which 18,000 lives were lost.

Careful consideration should be given to structures that are sited in a location that could directly or indirectly be affected by some form of slope instability. A very careful geotechnical and geologic investigation would be needed to identify if such hazards exist and determine if there are any practical means of mitigation of the hazards.

3.6.2 Lurching

Lurching is a phenomena where there is movement of soil or rock masses at right angles to a cliff or steep slope. Structures founded either in part or whole on such masses may experience significant lateral and vertical deformations.

3.7 FLOODING, TSUNAMIS AND SEICHES

3.7.1 Flooding

Seismic activities may cause some calamity elsewhere which could result in flooding at the site under consideration. An important part of the site investigation should include the identification of any bodies of water or structures that contain water that are located above or upstream of the site. The consequences of failure of these bodies or structures should be evaluated to determine what are the probable flood limits and depths of inundation that could be expected. The impact of this potential flooding on structure and function could have an effect on the siting of a building. It may be practical to raise the finished floor elevation to be reasonably above the maximum expected flood elevation; if this is not possible, re-siting of the proposed building may be necessary. Otherwise, emergency procedures will need to be established in the event that the flood hazard becomes a reality.

In some regions of the United States, studies of flood hazard have been performed and flood maps are available. Some of these studies have been performed by the United States Army Corps of Engineers; others are available from the Federal Emergency Management Agency (FEMA).

3.7.2 Tsunamis

A tsunami is a long sea wave that could be generated by a rapidly occurring change in

seafloor topography caused by tectonic displacement. Such tectonic displacements may be caused by earthquakes, undersea landslides or volcanic eruptions. It is believed that strike-slip earthquakes are less likely to cause tsunamis and that a substantial vertical offset caused by a dip-slip earthquake mechanism is necessary to generate large tsunamis. A tsunami may be caused by a nearby fault rupture, or by distant earthquakes which may be thousands of miles away. In the open sea, these waves travel at great velocities, however, the amplitudes of these waves are quite small with a very long wavelength. The velocity of a tsunami water wave is approximately given by the relationship

$$v = (gD)^{0.5}$$

where g is the acceleration of gravity and D is the water depth. As the wave approaches a coastline, the shallower depth of water will cause the amplitude of the water wave to become greater. The wave may become even more accentuated where there are topographic features such as narrow bays and very shallow waters. In fact, the meaning of the word tsunami is literally "harbor wave" in the Japanese language. The wavefront may crash on shore and may extend its damaging influence inland.

Tsunamis do not occur with every earthquake with its source beneath the seafloor. Although tsunamis do not occur that often, they can cause significant damage and loss of life. Tsunamis have occurred most frequently in the Pacific Ocean. Japan has been the victim of numerous tsunamis throughout recorded history. The city of Hilo on the big island of Hawaii has been devastated several times by tsunamis; the offshore topography is conducive to channeling the destructive forces of a tsunami into waves that were estimated to be from 21 to 26 feet high in the 1946 tsunami. Great damage from tsunamis occurred as a result of the so-called Great Alaska Earthquake of March 27, 1964 (see Figures 3-33 and 3-34). Although not as frequent, tsunamis have also



Figure 3-33. Waterfront at Seward, Alaska, looking south, before the 1964 Great Alaska earthquake generated underwater landslides, surge waves, and tsunami waves that devastated the waterfront. (Photograph by United States Geological Survey)



Figure 3-34. Waterfront at Seward a few months after the earthquake, looking north. (Photograph by United States Geological Survey)

occurred in the Atlantic and Indian Oceans. Tsunamis have even been reported in the Mediterranean Sea^(3-34; 3-40).

Structural damage from tsunamis is caused by the force of the water and the impact from boats and any other objects that may be carried and propelled by the moving waters. Structures with open fronts or large areas of glass with continuous rear walls were found to have a greater potential to be damaged. Observations made after several tsunamis suggest that light frame buildings are subject to very severe damage or total destruction because of the relatively flexible type of construction. Heavy timber construction is also found to be very susceptible to damage from tsunamis. If not firmly anchored to the foundations, such structures would have a tendency to float if the water level was significant. Heavier buildings constructed of structural steel or reinforced concrete tend to be less damaged. Although structures have been observed to have withstood tsunami forces, the structural elements at the lower levels could sustain significant damage from the passage of the water and impact by objects.

It has been suggested that a structure could be designed to resist tsunami waves.⁽³⁻⁴¹⁾ Special consideration would be needed to minimize the effects of a tsunami. First, the major axis or long dimension of the building should be oriented parallel to the expected direction of the wave. A building with this orientation would have a minimal surface area that could be attacked by the on-coming waves. In addition, the building will have greater strength to resist the wave forces because of the greater amount of structural elements providing resistance along the major axis. Consideration should also be given to leaving the lower portion of the building completely open which would greatly reduce the total load applied to the structure from the tsunami wave.

The forces exerted on a structure by a tsunami are not easy to predict. The horizontal fluid pressure exerted by flowing waters, p , can be estimated by the equation

$$p = 0.5 C_D \rho V_s^2$$

where C_D is a coefficient of drag for submerged objects which is a function of the shape of the object (which may be a wall or a column), ρ is the mass density of water, and V_s is the speed of the water surge which is approximated by

$$V_s = 2(g d_s)^{0.5}$$

where g is the acceleration of gravity and d_s is the height of the water surge⁽³⁻⁴¹⁾. In addition to the dynamic fluid pressures, there could be impact loading from objects carried by the tsunamis.

3.7.3 Seiches

A seiche may occur when earthquake ground motion causes water in closed or partially closed body (such as a bay, lake, reservoir, or even a swimming pool) to oscillate from one side to the other⁽³⁻³⁴⁾. Large seiches may occur when the frequency of the in-coming earthquake waves are the same as the natural frequency of the water body and causes resonant oscillation. This oscillation could cause overtopping of dams and damage to structures located near the water, and could continue for hours.

3.8 SOIL-STRUCTURE INTERACTION

3.8.1 Conventional Structural Dynamic Analysis and Soil-Structure Interaction

In the normal dynamic analysis of a building, the usual method of dynamic analysis is to determine the free field ground motion at the site of the building, and to apply that free field ground motion at the base of the building assuming that the base is fixed. This may be

true for the case where the building is founded on rock. However, if the building is founded on soft soils, the earthquake motion at the base of the building is not likely to be identical to the free field ground motion. The presence of the structure will modify the free field motions because the soil and structure will interact to create a dynamic system quite different from just a free field condition. This "soil-structure interaction" will result in a structural response that may be quite different from the structural response computed from a fixed base building subjected to a free field ground motion.

Certainly it is a more simple problem when one can separate the determination of the design ground motion from the dynamic analysis of the building which is the case when one performs a conventional dynamic analysis. This uncoupling of the soil system from the building system may, in general, give a predicted response that could be conservative. For convenience sake, this may be a rationale to use a fixed base model over a soil-structure interaction model. Another reason for this may be that soil-structure interaction involves two distinct disciplines (as practiced in the United States), namely geotechnical and structural engineering. The use of a fixed base model may not be able to take into account all of the possible modes of response such as deformation of the base of the structure or rocking of the structure. Additionally, the periods of vibration of the structure may be longer because of the interaction. In critical structures, such as nuclear reactors, some of these other modes of response may be just as important as the primary translation modes of vibration. The change in period may also affect the response of the overall structure or its substructures or components.

It turns out that in soil-structure interaction analysis, the whole is greater than the sum of the two parts. There needs to be an understanding of both soil dynamics and structural analysis and the ability to combine these two different worlds. Because of the interaction of both the soil and the structure, both need to modeled. However, it should be

recognized that, in comparison to the structure, the soil is essentially a semi-infinite medium or unbounded domain. The soil-structure interaction model subjected to dynamic loading cannot be treated in the same way one would consider static loading. When analyzing a soil-structure system under static loading, it is sufficient to model the structure on the soil system which will have fixed or semi-fixed boundaries at a sufficient distance from the structure where these boundary conditions do not affect the static response of the structure. Under dynamic loading, the fictitious boundaries could not be sufficiently far enough away from the structure to not affect the structural response; i.e., the boundaries would reflect the traveling waves within the soil mass and not allow the energy to pass through to infinity. In an attempt to model boundaries properly, special techniques such as the boundary-element method have been developed.

3.8.2 Elements of Soil-Structure Interaction Analysis

Consider two identical structures with a rigid foundation, one founded on stiff rock and the other founded on soft soil, as shown in Figure 3-35. The soil layer overlies the rock and the distance between the two structures is small so that it may be reasonably assumed that the incident earthquake waves arriving from the earthquake source are identical for the two structures. For illustration purposes, we will consider only a vertically propagating shear wave which produces only horizontal motions. A control motion may be defined on the free ground surface of the rock, say at Point A. As the rock is stiff, it may be reasonably assumed that the motion at any point in the rock, say at Point B, is the same as the control motion at Point A.

For the structure founded on the rock, a fixed base condition would exist and the horizontal ground motion applied to the base of the structure by the earthquake would be equal

to the control motion. Rocking of the structure would not develop in a fixed base condition.

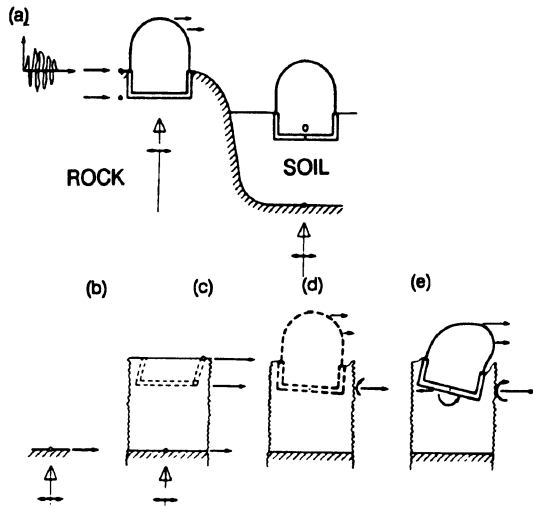


Figure 3-35. Seismic response of structure founded on rock and on soil. (a) sites; (b) outcropping rock; (c) free field; (d) kinematic interaction; (e) inertial interaction

For the structure founded on the soft soil, the earthquake motion at the base of the structure will not be the same as for the structure founded on rock and neither will the base be fixed. The motion at Point C at the top of the rock will not be as great as the motion at Point A because of the presence of the overlying soil layer. As the wave propagates upward in the soil layer, the motion may be amplified or, in some cases, deamplified; in most cases, however, amplification of the motion will occur. The frequency content of the motion will also change. The rigid base of the structure will also modify the motion. The motions will undergo a kinematic interaction which result in the base being subject to some average horizontal displacement and also some rocking. These rigid body motions in the base will apply inertial loading on the superstructure which will excite the structure. The excited structure will then cause a demand on the supporting soils to resist transverse shear and overturning moment. These demands on the soils cause what is referred to as inertial interaction and results in deformations of the soils which ultimately also cause further

modification of the motion at the base of the structure.

3.8.3 Limitations of Soil-Structure Interaction Analyses

Implicit in the formulation of present soil-structure interaction analyses is the assumption that the principle of superposition is valid. A result of this assumption is that the response that is computed is for a system that is linear in nature. However, soils are notoriously nonlinear when subjected to strong ground motions at the levels of engineering interest.⁽³⁻⁴²⁾ Although it may be possible to use material properties that are compatible with the strain levels produced during an earthquake, this is still far from a true nonlinear analysis.

Because a significant mass of soil must be modeled around the structure, there will be a large number of degrees of freedom which usually impact in computational storage and run time. This may be alleviated by substructuring the problem into two parts. The first part of the analysis is to compute the free field response of the site (without the structure present). The motions are determined at the nodes where the structure is attached. The force-displacement relationships of these nodes are also determined. The second part of the analysis is the study of the superstructure mounted on spring-dashpot systems subjected to the free field motions determined from the first part of the analysis (Fig. 3-36).

Great care must be exercised in soil-structure interaction analyses. The basic assumptions show that, although this type of analysis is more sophisticated than a conventional rigid base analysis, the current state-of-the art still falls far short of modeling reality. Such analyses should be tempered with much engineering judgment. For more detailed information on the theory of soil-structure interaction, the reader is referred to the work by Wolf⁽³⁻⁴³⁾.

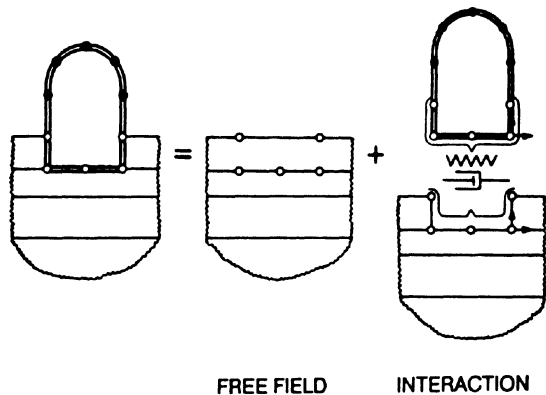


Figure 3-36. Seismic soil-structure interaction with substructure method.

3.9 FAULT RUPTURE

Fault rupture and the associated ground deformation can have extremely severe consequences to structures and systems that cross the fault plane. The fault displacements can range from a few millimeters to several meters. Figure 3-37 shows fault rupture

observed in the June 28, 1992 Landers, California earthquake (moment magnitude 7.3) which had maximum horizontal displacements of up to 6 meters across the fault. If ground surface rupture due to earthquake faulting were to occur beneath a structure, there would be substantial damage. Figure 3-38 shows the disruption of a large concrete dam in Taiwan where there was approximately 9 meters of vertical fault offset on the Chelungpu fault in the 1999 Chi-Chi earthquake in Taiwan. Figure 3-39 shows damage to a building caused by faulting, also in Taiwan. The structure would in all likelihood be a substantial, if not a total loss due to the differential ground displacement between the two sides of the fault. This displacement would be mostly lateral if the fault is a strike-slip fault or the displacement would be mostly vertical if the fault is thrust-type fault; some faults will exhibit a combination of these two types of fault movement.



Figure 3-37. Surface fault rupture (up to 6 meters horizontal movement) in the 1992 Landers earthquake.



Figure 3-38. Surface fault rupture beneath reinforced concrete dam in the 1999 Chi-Chi, Taiwan earthquake.



Figure 3-39. Building damaged by faulting during the 1999 Chi-Chi, Taiwan earthquake.

The State of California enacted legislation known as the "Alquist-Priolo Earthquake Fault Zoning Act" in 1972 shortly after the 1971 San Fernando earthquake in which extensive surface faulting damaged numerous homes, businesses and other structures. This act provides the process to mitigate the hazard of surface faulting to structures in California.⁽³⁻⁴⁴⁾ One of the specific criteria given in this legislative act provides that "No structure for human occupancy shall be permitted to be placed across the trace of an active fault." A structure for human occupancy is any structure that has an occupancy rate of 2,000 person-hours per year. For the purposes of the law, an active fault is one that has moved in Holocene time, about the last 11,000 years. The law requires that local jurisdictions must regulate new development projects within these zones determined by the State of California. The local jurisdictions must require a geologic investigation to demonstrate that proposed buildings will not be constructed across active faults. If an active fault is found, a structure for human occupancy cannot be placed over the trace of the fault and must be set back from the fault, usually a distance of at least 50 feet.

The investigation of sites for surface fault rupture hazard may not be simple task. Many active faults are complex and consist of multiple branches that may result in a zone of surface fault rupture. The evidence for identifying active fault traces may be very subtle or obscured. The distinction between recent fault activity and activity that has ceased may be difficult to ascertain. The complexity of evaluation of surface and near-surface faults and the infinite variety of site conditions makes it impossible to use a single investigative method at all sites. Investigation in heavily developed urbanized areas may be extremely difficult.

Fault investigations should first be planned to address the problem of locating existing faults and then attempting to evaluate the recency of the latest fault activity. Data can be obtained from the site and from outside of the site area. Dating of materials may be possible if

organic matter is found in the units. The most direct method of evaluating the recency of faulting is to observe, in an open trench or roadway cut, the youngest geologic unit faulted and the oldest geologic unit that is not faulted. Recent active faults may also be identified by direct observation of young, fault-related geomorphic or topographic features in the field, on aerial photographs, or on satellite images. Fault gouge materials may effectively create impermeable barriers that may cause the water level on one side of the fault to be different on the other side. Sometimes evidence of a water barrier (fault) may be seen at the ground surface. Sometimes, the drilling of borings may be needed to determine the differential water levels.

Geophysical methods are indirect methods that require a special knowledge of the geologic conditions for a reliable interpretation. Methods such as seismic refraction, seismic reflection, ground penetrating radar, electrical resistivity, gravity, magnetic intensity can provide useful information, however, they cannot prove the absence of a fault and also cannot determine the recency of activity. These methods should be used very carefully.

3.10 LATERAL SEISMIC EARTH PRESSURES

3.10.1 Active Seismic Earth Pressures

Lateral earth pressures are imposed on retaining structures. Under static conditions, flexible or yielding retaining structures would be subjected to active lateral earth pressures. These active lateral earth pressures are normally computed utilizing the classical theories developed by Coulomb and Rankine. The methodologies to determine the active lateral earth pressures on retaining walls for static conditions may be found in most geotechnical references, such as the United States Navy Design Manual DM-7-02.⁽³⁻⁴⁵⁾

When there is an earthquake, one can visualize inertial forces from the ground

shaking that would impose additional load on a retaining wall. The most commonly used formulation to calculate the seismic lateral earth pressure on a flexible or yielding retaining wall structure is the Mononobe-Okabe formulation which has been described in detail by Seed and Whitman.⁽³⁻⁴⁶⁾ This method is an extension of Coulomb earth pressure theory with the addition of horizontal and vertical forces to account for the earthquake loads. This method assumes that there is sufficient wall movement to produce the minimum wall pressures and that the backfill material consists of dry cohesionless materials. The soil wedge behind the wall is assumed to be at the point of incipient failure and the maximum shear strength is mobilized along the potential sliding surface (see Figure 3-40). The soil mass behind the wall is assumed to behave as a rigid body; therefore, the accelerations are uniform throughout the mass. The effect of the earthquake motions are then represented by inertia forces $k_h W$ and $k_v W$, where k_{hg} and k_{vg} are the horizontal and vertical components of the pseudostatic earthquake accelerations at the base of the wall.

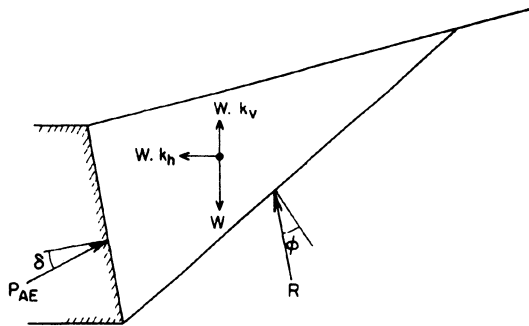


Figure 3-40. Forces acting on an active wedge in Mononobe-Okabe analysis (Ref. 3-46)

The total active thrust is given by an equation that is similar to that developed for static conditions:

$$P_{AE} = (1/2) \gamma H^2 (1 - k_v) K_{AE}$$

where K_{AE} is the dynamic active earth pressure coefficient which is defined by the following equations:

$$K_{AE} = \frac{\Im}{\Re \left[1 + \sqrt{\frac{\sin(\phi + \delta) \sin(\phi - \theta - i)}{\cos(\delta + \beta + \theta) \cos(i - \beta)}} \right]^2}$$

where

$$\Im = \cos^2(\phi - \theta - \beta) \text{ and}$$

$$\Re = \cos \theta \cos^2 \beta \cos(\delta + \beta + \theta)$$

$$\theta = \tan^{-1} [k_h / (1 - k_v)]$$

γ = moist unit weight of the soil

H = height of wall

ϕ = angle of internal friction of the soil

δ = angle of wall friction

i = angle of ground surface slope behind the wall

β = angle of slope of back of wall to vertical

k_h = pseudostatic horizontal ground acceleration/g

k_v = pseudostatic vertical ground acceleration/g

The horizontal component of the force P_{AE} may be expressed as P_{AEh} , where

$$P_{AEh} = P_{AE} \cos(\delta + \beta)$$

$$= (1/2) \gamma H^2 (1 - k_v) K_{AE} \cos(\delta + \beta)$$

For a wall with a vertical inside face ($\beta = 0$):

$$P_{AEh} = (1/2) \gamma H^2 (1 - k_v) K_{AE} \cos \delta$$

It should be remembered that the computed lateral force includes the static lateral active earth pressure and the dynamic increment of earth pressure which can be expressed as:

$$P_{AE} = P_A + \Delta P_{AE}$$

The static component, P_A , acts at a height of $H/3$ above the base of the wall. For cantilevered retaining structures, most investigators have agreed that the point of application of the resultant of the dynamic earth pressure should be at a height of $0.5H$ to $0.67H$ above the base of the wall.⁽³⁻⁴⁶⁾ Prakash has recommended that the point of application of the resultant be taken at $0.55H$ above the base of a flexible wall and at $0.45H$ above the base of a rigid wall.⁽³⁻⁴⁷⁾ Seed and Whitman recommended that the dynamic component be assumed to act at about $0.6H$ above the base of the wall.

The selection of the pseudostatic accelerations is a critical matter. If one uses anticipated peak ground accelerations, the computed lateral thrust may be very unrealistically high. As this method uses pseudostatic accelerations very much like slope stability analyses, values of the horizontal acceleration, k_h , between 0.05g and 0.15g, are commonly used, according to Whitman⁽³⁻⁴⁸⁾; these values may correspond to one-third to one-half of the peak ground accelerations. Elms and Martin⁽³⁻⁴⁹⁾ have suggested that the horizontal acceleration, k_h , be taken as one-half of the peak ground acceleration (0.5A), provided that there be an allowance for an outward displacement of 10 A inches or 250 A millimeters. The vertical acceleration, k_v , may be taken as one-half to two-thirds of k_h .

There are other methods of analyses for seismic active earth pressures on walls. Some of these methodologies are discussed in Kramer.⁽³⁻⁵⁰⁾

3.10.2 Passive Seismic Earth Pressures

As seismic activity can cause the active earth pressures to increase dramatically due to ground shaking, the same earthquake influences can cause the passive resistance of the soil to decrease. Mononobe and Okabe also formulated a theory for the seismic passive resistance of soils against a wall.

The equation for the total passive thrust on a wall retaining a dry, cohesionless backfill is given in the following equation:

$$P_{PE} = (1/2) \gamma H^2 (1 - k_v) K_{PE}$$

where the dynamic passive earth pressure coefficient, K_{PE} , is given by the following:

$$K_{PE} = \frac{\Im}{\Re} \left[1 - \left\{ \frac{\sin(\phi - \delta) \sin(\phi + i - \theta)}{\cos(i - \beta) \cos(\delta - \beta + \theta)} \right\}^{1/2} \right]^2$$

where

$$\Im = \cos^2(\phi - \theta - \beta) \text{ and}$$

$$\Re = \cos \theta \cos^2 \beta \cos(\delta - \beta + \theta)$$

The total passive thrust can also be separated into its static and dynamic components as follows:

$$P_{PE} = P_P + \Delta P_{PE}$$

It should be noted that P_{PE} will be less than P_P as the dynamic component, ΔP_{PE} , acts in an opposite direction from the static component. In other words, the Mononobe-Okabe equation predicts that the available passive resistance will be reduced during earthquake ground shaking.

3.11 CONCLUSIONS

It has been shown that the earthquake ground motions that affect structures are greatly influenced by the local site and geologic conditions. It has also been demonstrated that the ground motion response may also be influenced more greatly at different structural periods of vibration. These effects have been recognized and have been incorporated into the latest United States building codes as discussed in this chapter. Recognition of near-source effects has also been incorporated into the building codes.

Soil liquefaction is a major concern in seismically active areas that have young geologic materials with a shallow groundwater condition. Various methods of analysis have been presented that use different in-situ soil characterization technologies. The consequences of liquefaction also need to be evaluated to determine the effects on structures founded in such conditions. Methods of analysis to evaluate liquefaction-induced settlement and lateral spreading have been presented. Also presented is a discussion of the most commonly used techniques to mitigate the effects of liquefaction to allow for engineered construction to proceed.

A discussion of other geologic-seismic hazards has also been presented. These hazards include seismic settlement, fault rupture, landsliding, tsunamis, and lateral seismic pressures on buried structures. The practice of geotechnical earthquake engineering is still evolving and further advances are expected to

appear on the horizon in short order. It is expected that many of the existing technologies will be unproved or replaced with more advanced methods in the future.

REFERENCES

- 3-1. International Conference of Building Officials, *Uniform Building Code*, 1976 Edition, Whittier, California.
- 3-2. International Conference of Building Officials, *Uniform Building Code*, 1985 Edition, Whittier, California.
- 3-3. International Conference of Building Officials, *Uniform Building Code*, 1988 Edition, Whittier, California.
- 3-4. International Conference of Building Officials, *Uniform Building Code*, 1994 Edition, Whittier, California.
- 3-5. International Conference of Building Officials, *Uniform Building Code*, 1997 Edition, Whittier, California.
- 3-6. Seismology Committee, Structural Engineers Association of California, *Recommended Lateral Force Requirements and Commentary*, Sixth Edition, Sacramento, California, 1996.
- 3-7. Federal Emergency management agency, NEHRP Recommended provisions for Seismic Regulations for New Buildings and Other Structures, 1997 Edition, FEMA302, Washington, D.C.
- 3-8. International Conference of Building Officials, *Maps of Known Active Fault Nearing Source Zones in California and Adjacent Portions of Nevada*, Whittier, California, 1988.
- 3-9. Lew, Marshall and Bonneville, David, *New Building Code Requirements for the Seismic Design of Tall Buildings Near Active Faults*, Proceedings, Fourth Conference on Tall Buildings in Seismic Regions, Los Angeles, California, 1997.
- 3-10. International Code Council, *International Building Code*, 2000 Edition.
- 3-11. Seed, H.B., Tokimatsu, K., Harder, L.F., and Chung, R.M., *The Influence of SPT Procedures in Soil Liquefaction Resistance Evaluations*, University of California Berkeley, Report No. UCB/EERC-84-15, October 1984.
- 3-12. Youd, T.L. and Idriss, I.M., *Proceedings of the NCEER Workshop on Evaluation of Liquefaction Resistance of Soils*, National Center for Earthquake Engineering Research, Technical Report NCEER-97-0022, 1997.
- 3-13. Seed, H.B., Idriss, I.M., and Arango, I., "Evaluation of Liquefaction Potential Using Field Performance Data," Journal of the Geotechnical Division, ASCE, Vol. 109, No. 3, March 1983.
- 3-14. Seed, H.B., and Idriss, I.M., "Ground Motions and Soil Liquefaction During Earthquakes," Earthquake Engineering Research Institute, Berkeley, California, 1982.
- 3-15. Ishihara, K. And Yoshimine, M., *Evaluation of Settlements in Sand Deposits Following Liquefaction During Earthquakes*, Soils and Foundations, Japanese Society of Soil Mechanics and Foundation Engineering, Vol. 32, No. 1, March 1992.
- 3-16. Youd, L.T., "Major Cause of Earthquake Damage is Ground Failure," Civil Engineering, Vol. 48, No. 4, pp. 47-51, April, 1978.
- 3-17. Youd, L.T., "Ground Failure Displacement and Earthquake Damage to Buildings," Proceedings, 2nd ASCE Conference on Civil Engineering and Nuclear Power, Knoxville, Tennessee, September, 1980.
- 3-18. Ishihara, K., "Stability of Natural Deposites During Earthquakes," Proceedings of the 11th International Conference on Soil Mechanics and Foundation Engineering, San Francisco, 1985.
- 3-19. Youd, L.T., and Garris, C.T., "Liquefaction-Induced Ground Surface Disruption," Fifth United States-Japan Workshop on Earthquake Resistant Design of Lifeline Facilities and Countermeasures Against Liquefaction, National Center for Earthquake Engineering Research Technical Report, Tokyo, Japan, 1994.
- 3-20. Prevost, J.H., "DYNA-FLOW: A Nonlinear Transient Finite Element Analysis Program," Report No. 81-SM-1, Department of Civil Engineering, Princeton University, Princeton, N.J., 1981.
- 3-21. Finn, W.E.L. and Yogendrakumar, M., "TARA-3FL: Program for Analysis of Liquefaction Induced Flow Deformations," Department of Civil Engineering, University of British Columbia, Vancouver, B.C., Canada, 1989.
- 3-22. Newmark, N.M., "Effects of Earthquakes on Dams and Embankments," *Geotechnique*, Vol. 15, No. 2, 1965.
- 3-23. Byrne, P.M., Jitno, H., and Salgado, F., "Earthquake Induced Displacement of Soil-Structures Systems," Proceedings, 10th World Conference on Earthquake Engineering, Madrid, Spain, 1992.
- 3-24. Bartlett, S.F. and Youd, T.L., "Empirical Analysis of Horizontal Ground Displacement Generated by Liquefaction-Induced Lateral Spread," National Center for Earthquake Engineering Research, Technical Report NCEER-92-0021, 1992.
- 3-25. National Research Council, "Liquefaction of Soils During Earthquakes," National Academy Press, Washington, D.C., 1985.
- 3-26. Hayden, R.F., "Utilization of Liquefaction Countermeasures in North America," Fifth U.S. National Conference on Earthquake Engineering,

- Earthquake Engineering Research Institute, Chicago, July 1994.
- 3-27. Hayden, R.F. and Baez, J.I., "State of Practice for Liquefaction Mitigation in North America," Fifth United States-Japan Workshop on Earthquake Resistant Design of Lifeline Facilities and Countermeasures Against Liquefaction, National Center for Earthquake Engineering Research Technical Report, Tokyo, Japan, 1994
- 3-28. Brown, R.E., "Vibroflotation Compaction of Cohesionless Soils," Journal of Geotechnical Division, ASCE, Vol. 103, No. GT12, pp. 1437-1451, December, 1977.
- 3-29. Ishihara, K., Iwasake, Y., and Nakajima, M., "Liquefaction Characteristics of Sand Deposits at an Oil Tank Site During the 1978 Miyagiken-Oki Earthquake," Soil and Foundations, Vol. 20, No. 2, pp. 97-111, June, 1980.
- 3-30. Slocumbe, B.C., "Dynamic Compaction," Chapter 2 in *Ground Improvement*, M.P. Moseley (ed.), Blackie Academic & Professional, Bishopbriggs, Glasgow, 1993.
- 3-31. Taki, O. and Yang, D.S., "Soil-Cement Mixed Wall Technique," ASCE, Geotechnical Engineering Congress, Boulder, Colorado, 1991.
- 3-32. Pujol-Rius, A., Griffin, P., Neal, J., and Taki, O., "Foundation Stabilization of Jackson Lake Dam," 12th International Conference on Soil Mechanics and Foundation Engineering, Brazil, 1989.
- 3-33. Babasaki, R., Suzuki, K., Saitoh, S., Suzuki, Y., and Tokitoh, K., "Construction and Testing of Deep Foundation Improvement Using the Deep Cement Mixing Method," in *Deep Foundation Improvements: Design, Construction, and Testing*, ASTM STP 1089, Philadelphia, 1991.
- 3-34. Hunt, R.E., "Geotechnical Engineering Investigation Manual," McGraw-Hill Book Company, New York, 1984.
- 3-35. Whitman, R.V., and DePablo, P.O., "Densification of Sand by Vertical Vibrations," Proceedings, 4th World Conference on Earthquake Engineering, Santiago, Chile, 1980.
- 3-36. Lambe, W.T., and Whitman, R.V., "Soil Dynamics," John Wiley & Sons, New York, 1969.
- 3-37. Tokimatsu, K. and Seed, H.B., "Evaluation of Settlements in Sands due to Earthquake Shaking," Journal of Geotechnical Engineering, ASCE, Vol. 113, No. 8, August 1987.
- 3-38. Seed, H.B. and Idriss, I.M., "Simplified Procedure for Evaluating Soil Liquefaction Potential," Journal of the Soil Mechanics and Foundations Division, ASCE, Vol. 97, No. SM9, 1971.
- 3-39. Seed, H.B., and Wilson, S.D., "The Turnagain Heights Landslide, Anchorage, Alaska," Journal of the Soil Mechanics and Foundation Engineering Division, ASCE, Vol. 93, No. SM4, pp. 325-353, July, 1967.
- 3-40. Legget, R.F., and Karrow, P.F., "Handbook of Geology in Civil Engineering," McGraw-Hill Book Company, New York, 1983.
- 3-41. Wiegel, R.E. (editor), "Earthquake Engineering," Prentice Hall, Englewood Cliffs, New Jersey, 1970.
- 3-42. Seed, H. B., "Earthquake Effects on Soil-Foundation Systems," in Foundation Engineering Handbook, H.F. Winterkorn and H.Y. Fang (editors), Van Nostrand Reinhold Company, New York, 1975.
- 3-43. Wolf, J.P., "Dynamic Soil-Structure Interaction," Prentice Hall, Englewood Cliffs, New Jersey, 1985.
- 3-44. Hart, E.W., "Fault-rupture hazard zones in California," California Department of Conservation, Division of Mines and Geology, Special Publication 42, Revised 1994.
- 3-45. Naval Facilities Engineering Command, *Foundations & Earth Structures*, Design Manual 7.02, Alexandria, Virginia, 1986.
- 3-46. Seed, H.B., and Whitman, R.V., "Design of Earth Retaining Structures for Dynamic Loads," Proceedings of ASCE Specialty Conference on Lateral Stresses in the Ground and Design of Earth Retaining Structures, Ithaca, New York, pp 103-147, 1970.
- 3-47. Prakash, S., "Soil Dynamics," McGraw-Hill Book Company, New York, 1981.
- 3-48. Whitman, R.V., "Seismic design behavior of gravity retaining walls," Proceedings, ASCE Specialty Conference on Design and Performance of Earth Retaining Structures, Geotechnical Specialty Publication 25, ASCE, New York, 1990.
- 3-49. Elms, D.G. and Martin, G.R., *Factors Involved in the Seismic Design of Bridge Abutments*, Applied Technology Council Workshop on Earthquake Resistance of Highway Bridges, ATC-6-1, 1979.
- 3-50. Kramer, Steven L., *Geotechnical Earthquake Engineering*, Prentice Hall, Inc., 1996.

Chapter 4

Dynamic Response of Structures

James C. Anderson, Ph.D.

Professor of Civil Engineering, University of Southern California, Los Angeles, California

Key words: Dynamic, Buildings, Harmonic, Impulse, Single-Degree-of -Freedom, Earthquake, Generalized Coordinate, Response Spectrum, Numerical Integration, Time History, Multiple-Degree-of-Freedom, Nonlinear, Pushover, Instrumentation

Abstract: Basic principles of structural dynamics are presented with emphasis on applications to the earthquake resistant design of building structures. Dynamic characteristics of single degree of freedom systems are discussed along with their application to single story buildings. The response of these systems to harmonic and impulse loading is described and illustrated by application to simple structures. Consideration of the earthquake response of these systems leads to the concept of the elastic response spectrum and the development of design spectra. The use of procedures based on a single degree of freedom is extended to multiple degree of freedom systems through the use of the generalized coordinate approach. The determination of generalized dynamic properties is discussed and illustrated. A simple numerical integration procedure for determining the nonlinear dynamic response is presented. The application of matrix methods for the analysis of multiple degree of freedom systems is discussed and illustrated along with earthquake response analysis. A response spectrum procedure suitable for hand calculation is presented for elastic response analyses. The nonlinear static analysis for proportional loading and the nonlinear dynamic analysis for earthquake loading are discussed and illustrated with application to building structures. Finally, the use of the recorded response from buildings containing strong motion instrumentation for verification of analytical models is discussed.

4.1 Introduction

The main cause of damage to structures during an earthquake is their response to ground motions which are input at the base. In order to evaluate the behavior of the structure under this type of loading condition, the principles of structural dynamics must be applied to determine the stresses and deflections, which are developed in the structure. Structural engineers are familiar with the analysis of structures for static loads in which a load is applied to the structure and a single solution is obtained for the resulting displacements and member forces. When considering the analysis of structures for dynamic motions, the term dynamic simply means "time-varying". Hence the loading and all aspects of the response vary with time. This results in possible solutions at each instant during the time interval under consideration. From an engineering standpoint, the maximum values of the structural response are usually the ones of particular interest, specially in the case of structural design.

The purpose of this chapter is to introduce the principles of structural dynamics with emphasis on earthquake response analysis. Attention will initially be focused on the response of simple structural systems, which can be represented in terms of a single degree of freedom. The concepts developed for these systems will then be extended to include generalized single-degree-of-freedom (SDOF) systems using the generalized-coordinate approach. This development in turn leads to the consideration of the response of structures having multiple degrees of freedom. Finally, concepts and techniques used in nonlinear dynamic-response analysis will be introduced.

4.2 Dynamic Equilibrium

The basic equation of static equilibrium used in the displacement method of analysis has the form,

$$p = kv \quad (4-1)$$

where p is the applied force, k is the stiffness resistance, and v is the resulting displacement. If the statically applied force is now replaced by a dynamic or time-varying force $p(t)$, the equation of static equilibrium becomes one of dynamic equilibrium and has the form

$$p(t) = m\ddot{v}(t) + c\dot{v}(t) + kv(t) \quad (4-2)$$

where a dot represents differentiation with respect to time.

A direct comparison of these two equations indicates that two significant changes, which distinguish the static problem from the dynamic problem, were made to Equation 4-1 in order to obtain Equation 4-2. First, the applied load and the resulting response are now functions of time, and hence Equation 4-2 must be satisfied at each instant of time during the time interval under consideration. For this reason it is usually referred to as an equation of motion. Secondly, the time dependence of the displacements gives rise to two additional forces which resist the applied force and have been added to the right-hand side.

The equation of motion represents an expression of Newton's second law of motion, which states that a particle acted on by a force (torque) moves so that the time rate of change of its linear (angular) momentum is equal to the force (torque):

$$p(t) = \frac{d}{dt} (m \frac{dv}{dt}) \quad (4-3)$$

where the rate of change of the displacement with respect to time, dv/dt , is the velocity, and the momentum is given by the product of the mass and the velocity. Recall that the mass is equal to the weight divided by the acceleration of gravity. If the mass is constant, Equation 4-3 becomes

$$p(t) = m \frac{d}{dt} \left(\frac{dv}{dt} \right) = m\ddot{v}(t) \quad (4-4)$$

which states that the force is equal to the product of mass and acceleration. According to d'Alembert's principle, mass develops an inertia force, which is proportional to its acceleration and opposing it. Hence the first term on the right-hand side of Equation 4-2 is called the inertia force; it resists the acceleration of the mass.

Dissipative or damping forces are inferred from the observed fact that oscillations in a structure tend to diminish with time once the time-dependent applied force is removed. These forces are represented by viscous damping forces, that are proportional to the velocity with the constant proportionality referred to as the damping coefficient. The second term on the right-hand side of Equation 4-2 is called the damping force.

Inertia forces are the more significant of the two and are a primary distinction between static and dynamic analyses.

It must also be recognized that all structures are subjected to gravity loads such as self-weight (dead load) and occupancy load (live load) in addition to dynamic base motions. In an elastic system, the principle of superposition can be applied, so that the responses to static and dynamic loadings can be considered separately and then combined to obtain the total structural response. However, if the structural behavior becomes nonlinear, the response becomes load-path-dependent and the gravity loads must be considered concurrently with the dynamic base motions.

Under strong earthquake motions, the structure will most likely display nonlinear behavior, which can be caused by material nonlinearity and/or geometric nonlinearity. Material nonlinearity occurs when stresses at certain critical regions in the structure exceed the elastic limit of the material. The equation of dynamic equilibrium for this case has the general form

$$p(t) = m\ddot{v}(t) + c\dot{v}(t) + k(t)v(t) \quad (4-5)$$

in which the stiffness or resistance k is a function of the yield condition in the structure,

which in turn is a function of time. Geometric nonlinearity is caused by the gravity loads acting on the deformed position of the structure. If the lateral displacements are small, this effect, which is often referred to as P-delta, can be neglected. However, if the lateral displacements become large, this effect must be considered. In order to define the inertia forces completely, it would be necessary to consider the accelerations of every mass particle in the structure and the corresponding displacements. Such a solution would be prohibitively time-consuming. The analysis procedure can be greatly simplified if the mass of the structure can be concentrated (lumped) at a finite number of discrete points and the dynamic response of the structure can be represented in terms of this limited number of displacement components. The number of displacement components required to specify the position of the mass points is called the number of dynamic degrees of freedom. The number of degrees of freedom required to obtain an adequate solution will depend upon the complexity of the structural system. For some structures a single degree of freedom may be sufficient, whereas for others several hundred degrees of freedom may be required.

4.3 SINGLE-DEGREE-OF-FREEDOM SYSTEMS

4.3.1 Time-Dependent Force

The simplest structure that can be considered for dynamic analysis is an idealized, one-story structure in which the single degree of freedom is the lateral translation at the roof level as shown in Figure 4-1. In this idealization, three important assumptions are made. First, the mass is assumed to be concentrated (lumped) at the roof level. Second, the roof system is assumed to be rigid, and third, the axial deformation in the columns is neglected. From these assumptions it follows that all lateral resistance is in the resisting elements such as columns, walls, and diagonal

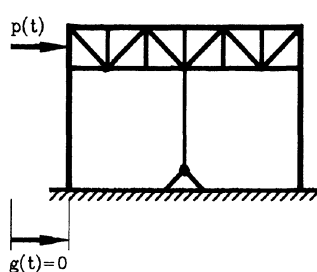
braces located between the roof and the base. Application of these assumptions results in a discretized structure that can be represented as shown in either Figure 4-1b or 4-1c with a time-dependent force applied at the roof level. The total stiffness k is simply the sum of the stiffnesses of the resisting elements in the story level.

The forces acting on the mass of the structure are shown in Figure 4-1d. Summing the forces acting on the free body results in the following equation of equilibrium, which must be satisfied at each instant of time:

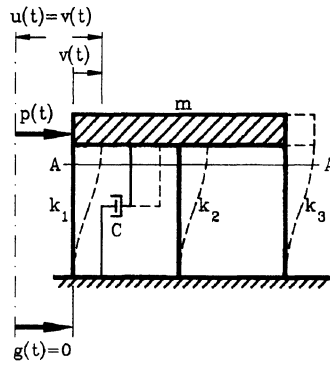
$$f_i + f_d + f_s = p(t) \quad (4-6)$$

where

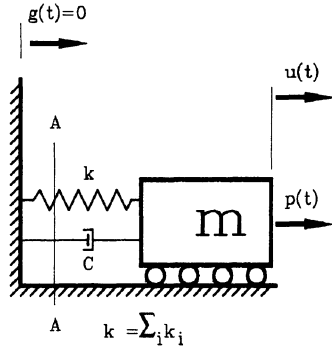
$$f_i = \text{inertia force} = m\ddot{u}$$



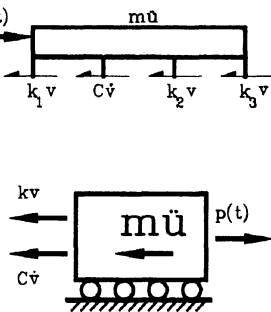
a) SINGLE STORY FRAME



b) IDEALIZED STRUCTURAL SYSTEM



c) EQUIVALENT SPRING-MASS-DAMPER SYSTEM



d) FREE BODY DIAGRAMS,
SECTION A-A

Figure 4-1. single-degree-of-freedom system subjected to time-dependent force.

$$f_d = \text{damping (dissipative) force} = cv$$

$$f_s = \text{elastic restoring force} = kv$$

$$p(t) = \text{time-dependent applied force}$$

\ddot{u} is the total acceleration of the mass, and v, v are the velocity and displacement of the mass relative to the base. Writing Equation 4-6 in terms of the physical response parameters results in

$$m\ddot{u} + cv + kv = p(t) \quad (4-7)$$

It should be noted that the forces in the damping element and in the resisting elements depend upon the relative velocity and relative displacement, respectively, across the ends of these elements, whereas the inertia force depends upon the total acceleration of the mass. The total acceleration of the mass can be

expressed as

$$\ddot{u}(t) = \ddot{g}(t) + \ddot{v}(t) \quad (4-8)$$

where

- $\ddot{v}(t)$ = acceleration of the mass relative to the base
- $\ddot{g}(t)$ = acceleration of the base

In this case, the base is assumed to be fixed with no motion, and hence $\ddot{g}(t) = 0$ and $\ddot{u}(t) = \ddot{v}(t)$. Making this substitution for the acceleration, Equation 4-7 for a time-dependent force becomes

$$m\ddot{v} + c\dot{v} + kv = p(t) \quad (4-9)$$

4.3.2 Earthquake Ground Motion

When a single-story structure, shown in Figure 4-2a, is subjected to earthquake ground motions, no external dynamic force is applied at the roof level. Instead, the system experiences an acceleration of the base. The effect of this on the idealized structure is shown in Figure 4-2b and 4-2c. Summing the forces shown in Figure 4-2d results in the following equation of dynamic equilibrium:

$$f_i + f_d + f_s = 0 \quad (4-10)$$

Substituting the physical parameters for f_i , f_d and f_s in Equation 4-10 results in an equilibrium equation of the form

$$m\ddot{u} + c\dot{v} + kv = 0 \quad (4-11)$$

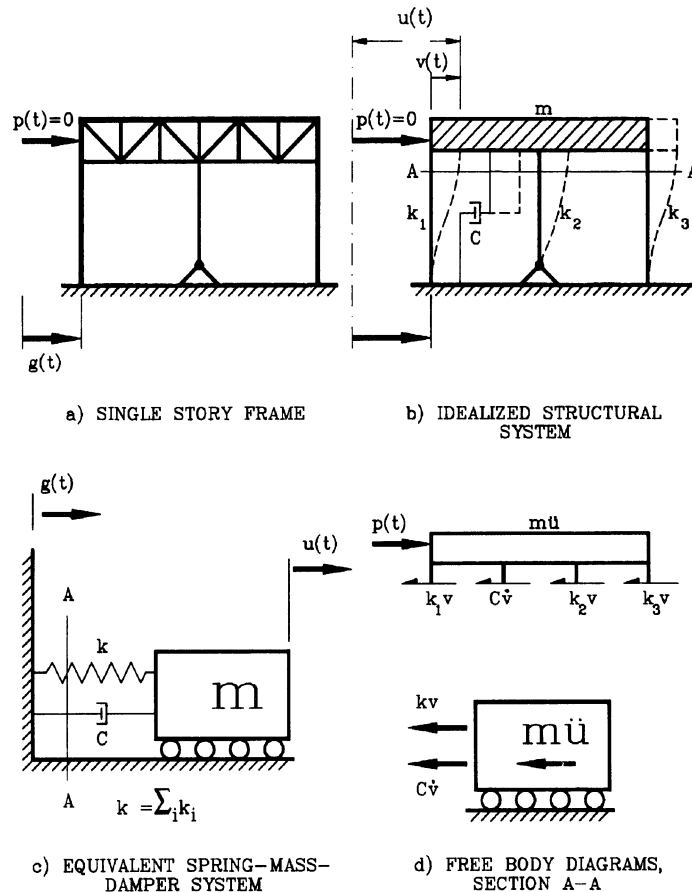


Figure 4-2. Single-degree-of-freedom system subjected to base motion.

This equation can be written in the form of Equation 4-9 by substituting Equation 4-8 into Equation 4-11 and rearranging terms to obtain

$$m\ddot{v} + c\dot{v} + kv = p_e(t) \quad (4-12)$$

where

$$\begin{aligned} p_e(t) &= \text{effective time-dependent force} \\ &= -m\ddot{g}(t) \end{aligned}$$

Hence the equation of motion for a structure subjected to a base motion is similar to that for a structure subjected to a time-dependent force if the base motion is represented as an effective time-dependent force which is equal to the product of the mass and the ground acceleration.

4.3.3 Mass and Stiffness Properties

Most SDOF models consider structures, which experience a translational displacement of the roof relative to the base. In this case the translational mass is simply the concentrated weight divided by the acceleration of gravity (32.2 ft/sec² or 386.4 in./sec²). However, cases do arise in which the rotational motion of the system is significant. An example of this might be the rotational motion of a roof slab which has unsymmetrical lateral supports. Newton's second law of motion states that the time rate of change of the angular momentum (moment of momentum) equals the torque. Considering a particle of mass rotating about an axis o , as shown in Figure 4-3, the moment of momentum can be expressed as

$$L = rm\dot{v}(t) = mr^2 \frac{d\theta}{dt} \quad (4-13)$$

The torque N is then obtained by taking the time derivative:

$$N = \frac{dL}{dt} = I\ddot{\theta} \quad (4-14)$$

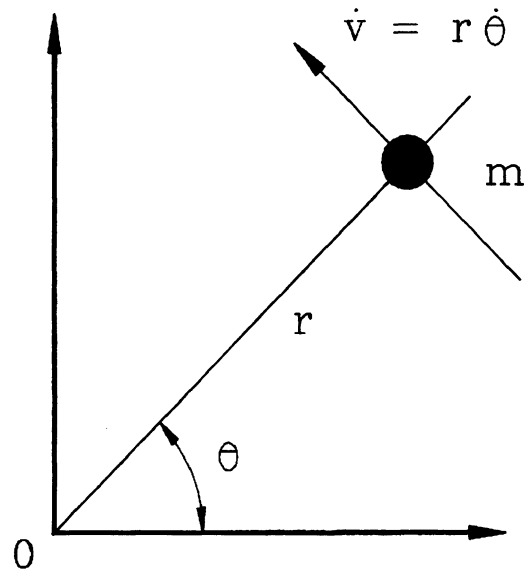


Figure 4-3. Rotating particle of mass.

where

$$I = mr^2 = \text{mass moment of inertia}$$

For a rigid body, the mass moment of inertia can be obtained by summing over all the mass particles making up the rigid body. This can be expressed in integral form as

$$I = \int \rho^2 dm \quad (4-15)$$

where ρ is the distance from the axis of rotation to the incremental mass dm . For dynamic analysis it is convenient to treat the rigid-body inertia forces as though the translational mass and the mass moment of inertia were concentrated at the center of mass. The mass and mass moment of inertia of several common rigid bodies are summarized in Figure 4-4.

Example 4-1 (Determination of Mass Properties)

Compute the mass and mass moment of inertia for the rectangular plate shown in Figure 4-5.

- Translational mass:

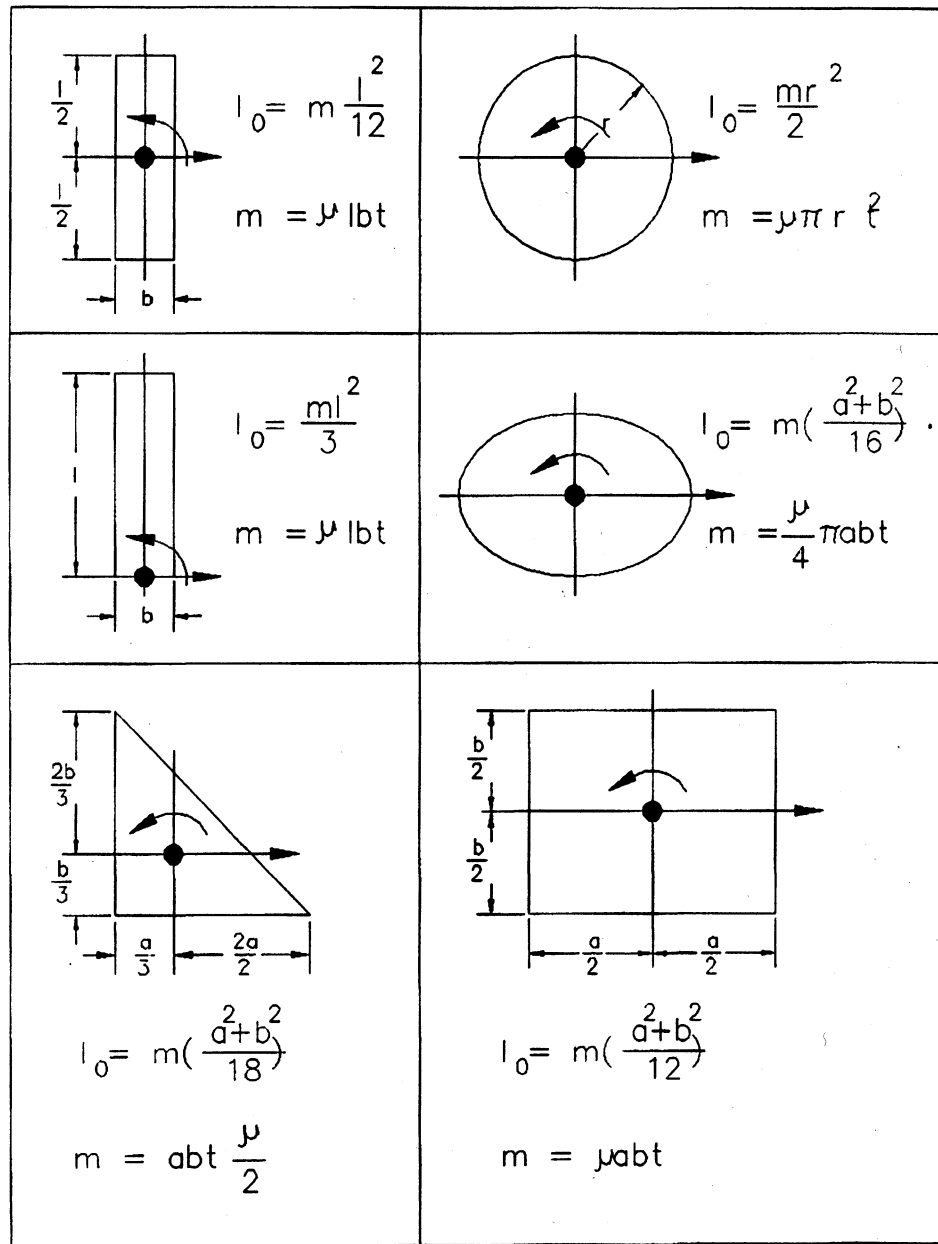


Figure 4-4. Rigid-body mass and mass moment of inertia.

$$m = \mu V = \mu abt$$

where

μ = mass density = mass per unit volume
 V = total volume

- Rotational mass moment of inertia:

$$I = \int \rho^2 dm, \quad \text{Where } \rho^2 = x^2 + y^2$$

$$dm = \mu dV = \mu t dx dy$$

$$I = \int \rho^2 dm = 4\mu t \int_0^{a/2} \int_0^{b/2} (x^2 + y^2) dx dy$$

$$I = 4\mu t \frac{b^3 a + a^3 b}{48} = \mu abt \frac{b^2 + a^2}{12}$$

$$I = m \frac{a^2 + b^2}{12}$$

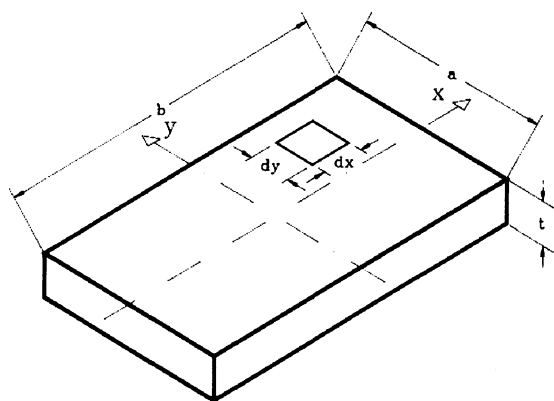


Figure 4-5. Rectangular plate of example 4-1.

In order to develop dynamic models of SDOF systems, it is necessary to review the

force—displacement (stiffness) relationships of several of the more common lateral force members used in building structures. As indicated previously, the assumptions used in developing the SDOF model restrict lateral resistance to structural members between the roof and base. These might include such members as columns, diagonal braces, and walls. Stiffness properties for these elements are summarized in Figure 4-6.

4.3.4 Free Vibration

Free vibration occurs when a structure oscillates under the action of forces that are inherent in the structure without any externally

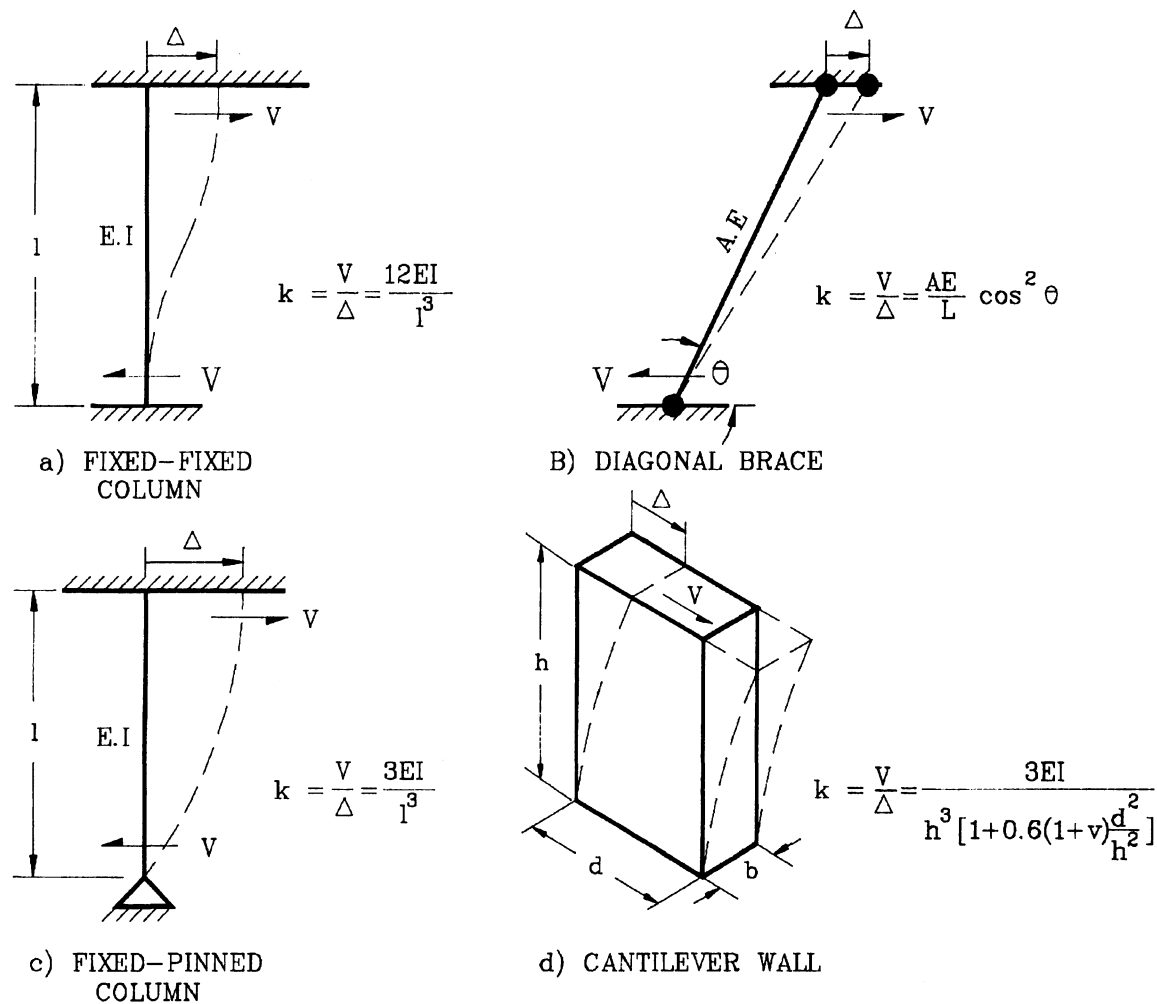


Figure 4-6. Stiffness properties of lateral force resisting elements.

applied time-dependent loads or ground motions. These inherent forces arise from the initial velocity and displacement the structure has at the beginning of the free-vibration phase.

Undamped Structures The equation of motion for an undamped SDOF system in free vibration has the form

$$m\ddot{v}(t) + kv(t) = 0 \quad (4-16)$$

which can be written as

$$\ddot{v}(t) + \omega^2 v(t) = 0 \quad (4-17)$$

where $\omega^2 = k/m$. This equation has the general solution

$$v(t) = A \sin \omega t + B \cos \omega t \quad (4-18)$$

in which the constants of integration A and B depend upon the initial velocity $\dot{v}(0)$ and initial displacement $v(0)$. Applying the initial conditions, the solution has the form

$$v(t) = \frac{\dot{v}(0)}{\omega} \sin \omega t + v(0) \cos \omega t \quad (4-19)$$

This solution in time is represented graphically in Figure 4-7.

Several important concepts of oscillatory motion can be illustrated with this result. The amplitude of vibration is constant, so that the vibration would, theoretically, continue indefinitely with time. This cannot physically be true, because free oscillations tend to diminish with time, leading to the concept of damping. The time it takes a point on the curve to make one complete cycle and return to its original position is called the period of vibration, T . The quantity ω is the circular frequency of vibration and is measured in radians per second. The cyclic frequency f is defined as the reciprocal of the period and is measured in cycles per second, or *hertz*. These three vibration properties depend only on the mass and stiffness of the structure and are related as follows:

$$T = \frac{2\pi}{\omega} = 2\pi\sqrt{\frac{m}{k}} = \frac{1}{f} \quad (4-20a)$$

The amplitude of motion is given as:

$$p = \sqrt{\left[\frac{\dot{v}(0)}{\omega} \right]^2 + [v(0)]^2} \quad (4-20b)$$

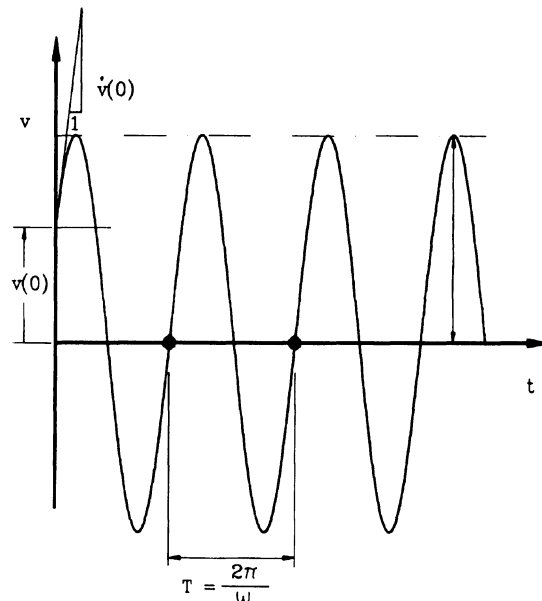


Figure 4-7. Free-vibration response of an undamped SDOF system.

It can be seen from these expressions that if two structures have the same stiffness, the one having the larger mass will have the longer period of vibration and the lower frequency. On the other hand, if two structures have the same mass, the one having the higher stiffness will have the shorter period of vibration and the higher frequency.

Example 4-2 (Period of undamped free vibration)

Construct an idealized SDOF model for the industrial building shown in Figure 4-8, and estimate the period of vibration in the two principal directions. Note that vertical cross

bracings are made of 1-inch-diameter rods, horizontal cross bracing is at the bottom chord of trusses, and all columns are W8 × 24.

- Weight determination:

Roof level:

Composition roof	9.0 psf
Lights, ceiling, mechanical	6.0 psf
Trusses	2.6 psf
Roof purlins, struts	2.0 psf
Bottom chord bracing	2.1 psf
Columns (10 ft, 9 in.)	<u>0.5 psf</u>
Total	22.2 psf

Walls:

Framing, girts, windows	4.0 psf
Metal lath and plaster	<u>6.0 psf</u>
Total	10.0 psf

Total weight and mass:

$$W = (22.2)(100)(75) + (10)(6)(200 + 150)$$

$$W = 187,500 \text{ lb} = 187.5 \text{ kips}$$

$$m = \frac{W}{g} = \frac{187.5}{386.4} = 0.485 \text{ kips-sec}^2/\text{in.}$$

- Stiffness determination:

North—south (moment frames):

$$k_i = \frac{12EI}{L^3} = \frac{(12)(29000)(82.8)}{(144)^3}$$

$$k_i = 9.6 \text{ kips/in.}$$

$$k = \sum_{i=1}^{24} k_i = 24(9.6) = 231.6 \text{ kips/in.}$$

East—west (braced frames):

$$k_i = \frac{AE}{L} \cos^2 \theta$$

$$A = \pi d^2 / 4 = 0.785$$

$$L = \sqrt{12^2 + 20^2} = 23.3 \text{ ft} = 280 \text{ in.}$$

$$\theta = \tan^{-1}(12/20) = 31^\circ, \cos(31^\circ) = 0.858$$

$$k_i = \frac{(0.785)(29000)(0.858)^2}{280} = 59.7 \text{ kips/in.}$$

$$k = \sum_{i=1}^6 k_i = 6(59.7) = 358.7 \text{ kips/in.}$$

- Period determination:

North—south:

$$\omega = \sqrt{\frac{k}{m}} = \sqrt{\frac{231.6}{0.485}} = 21.8 \text{ rad/sec}$$

$$T = \frac{2\pi}{\omega} = \frac{2\pi}{21.8} = 0.287 \text{ sec.}$$

$$f = \frac{1}{T} = 3.48 \text{ Hz}$$

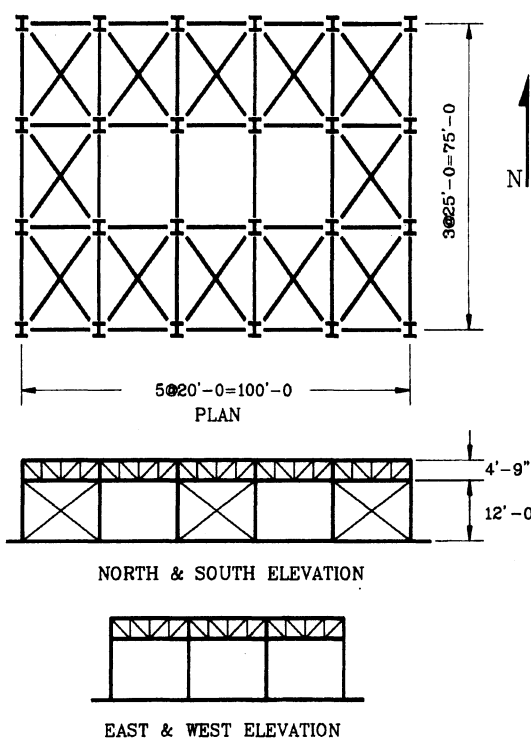


Figure 4-8. Building of Example 4-2.

East—west:

$$\omega = \sqrt{\frac{k}{m}} = \sqrt{\frac{358.7}{0.485}} = 27.2 \text{ rad/sec}$$

$$T = \frac{2\pi}{\omega} = \frac{2\pi}{27.2} = 0.23 \text{ sec.}$$

$$f = \frac{1}{T} = 4.3 \text{ HZ}$$

Damped Structures In an actual structure which is in free vibration under the action of internal forces, the amplitude of the vibration

tends to diminish with time and eventually the motion will cease. This decrease with time is due to the action of viscous damping forces which are proportional to the velocity. The equation of motion for this condition has the form

$$m\ddot{v}(t) + c\dot{v}(t) + kv(t) = 0 \quad (4-21)$$

This equation has the general solution

$$v(t) = e^{-\lambda\omega t} \left([\dot{v}(0) + v(0)\lambda\omega] \frac{\sin \omega_d t}{\omega_d} + v(0)\cos \omega_d t \right) \quad (4-22a)$$

where

$$\lambda = \frac{C}{C_{cr}} = \frac{C}{2m\omega} = \text{percentage of critical damping}$$

$$\omega_d = \omega\sqrt{1-\lambda^2} = \text{damped circular frequency}$$

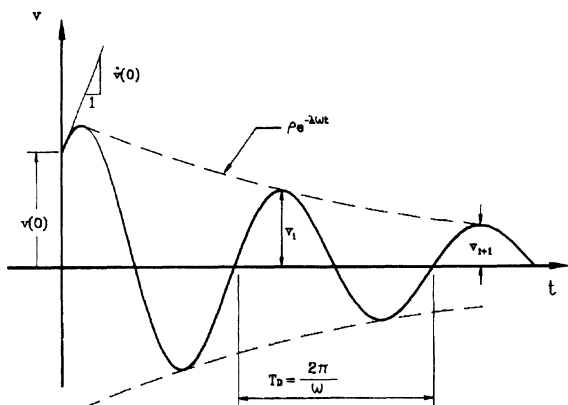


Figure 4-9. Free vibration response of a damped SDOF system.

The solution to this equation with time is shown in Figure 4-9. The damping in the oscillator is expressed in terms of a percentage of critical damping, where critical damping is

defined as $2m\omega$ and is the least amount of damping that will allow a displaced oscillator to return to its original position without oscillation. For most structures, the amount of viscous damping in the system will vary between 3% and 10% of critical. Substituting an upper value of 20% into the above expression for the damped circular frequency gives the result that $\omega_d = 0.98\omega$. Since the two values are approximately the same for values of damping found in structural systems, the undamped circular frequency is used in place of the damped circular frequency. In this case the amplitude of motion is given as:

$$p = \sqrt{\left[\frac{v(0) + v(0)\lambda\omega}{\omega_D} \right]^2 + [v(0)]^2} \quad (4-22b)$$

One of the more useful results of the free-vibration response is the estimation of the damping characteristics of a structure. If a structure is set in motion by some external force, which is then removed, the amplitude will decay exponentially with time as shown in Figure 4-9. It can further be shown that the ratio between any two successive amplitude peaks can be approximated by the expression

$$\frac{v(i)}{v(i+1)} = e^{2\pi\lambda} \quad (4-23)$$

Taking the natural logarithm of both sides results in

$$\delta = \ln \frac{v(i)}{v(i+1)} = 2\pi\lambda \quad (4-24)$$

where the parameter δ is called the *logarithmic decrement*. Solving for the percentage of critical damping, λ , gives

$$\lambda \approx \frac{\delta}{2\pi} \quad (4-25)$$

The above equation provides one of the more useful means of experimentally estimating the damping characteristics of a structure.

4.4 Response to Basic Dynamic Loading

4.4.1 Introduction

Time histories of earthquake accelerations are in general random functions of time. However, considerable insight into the response of structures can be gained by considering the response characteristics of structures to two basic dynamic loadings; harmonic loading and impulse loading. Harmonic loading idealizes the earthquake acceleration time history as a train of sinusoidal waves having a given amplitude. These might be representative of the accelerations generated by a large, distant earthquake in which the random waves generated at the source have been filtered by the soil conditions along the travel path.

Impulse loading idealizes the earthquake accelerations as a short duration impulse usually having a sinusoidal or symmetrical (isosceles) triangular shape. The idealization may be a single pulse or it may be a pulse train containing a limited number of pulses. This loading is representative of that which occurs in the near fault region.

This section will present a brief overview of the effects of harmonic loading and impulse loading on the response of building structures.

4.4.2 Harmonic Loading

For an undamped system subjected to simple harmonic loading, the equation of motion has the form

$$m\ddot{v} + kv = p_0 \sin pt \quad (3-26a)$$

where p_0 is the amplitude and p is the circular frequency of the harmonic load. For a ground acceleration, the acceleration

can be represented as $\ddot{g}_0 \sin pt$, the equivalent force amplitude as $p_{oe} = m\ddot{g}_0$ and the frequency ratio $\beta = p/\omega$. The solution for the time dependent displacement has the form

$$v(t) = \frac{m\ddot{g}_0}{k} \times \frac{1}{(1-\beta^2)} (\sin pt - \beta \sin \omega t) \quad (3-26b)$$

where

$m\ddot{g}_0 / k = p_{oe} / k$ = the static displacement

$\frac{1}{1-\beta^2}$ = dynamic amplification factor

$\sin pt$ = steady state response

$\beta \sin \omega t$ = transient response induced by the initial conditions

From equation (4-26b) it can be seen that for lightly damped systems, the peak steady state response occurs at a frequency ratio near unity when the exciting frequency of the applied load equals the natural frequency of the system. This is the condition that is called resonance. The result given in Equation (4-26b) implies that the response of the undamped system goes to infinity at resonance, however, a closer examination in the region of β equal to unity, Clough and Penzien ⁽⁴⁻⁴⁾, shows that it only tends toward infinity and that several cycles are required for the response to build up. A similar analysis for a damped system shows that at resonance, the dynamic amplification approaches a limit that is inversely proportional to the damping ratio

$$DA = \frac{1}{2\lambda} \quad (4-26c)$$

For both the undamped and the damped cases, the response builds up with the number of cycles as shown in Figure 4-10a.

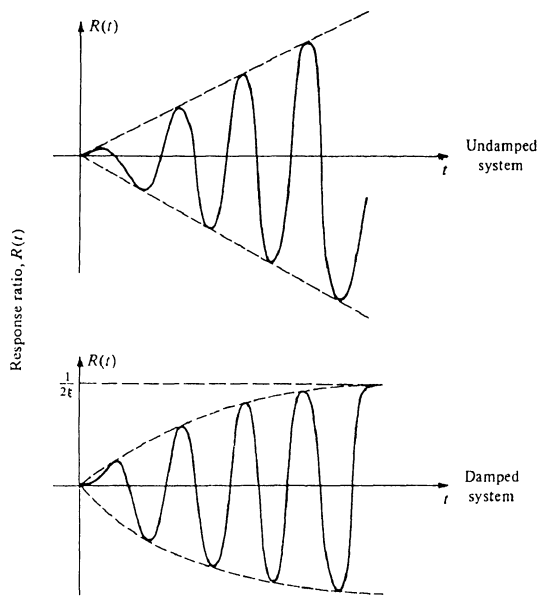


Figure 4-10a. Resonance response.

The required number of cycles for the damped case can be estimated as $1/\lambda$. The condition of resonance can occur in buildings which are subjected to base accelerations having a frequency that is close to that of the building and having a long duration. The duration of the ground shaking is an important factor in this type of response for the reasons just discussed. The Mexico City earthquakes (1957, 1979, 1985) have produced good examples of harmonic type ground motions which have a strong resonance effect on buildings. Ground motions having a period of approximately 2 seconds were recorded during the 1985 earthquake and caused several buildings to collapse in the upper floors.

It must be recognized that as the response tends to build up, the effective damping will increase and as cracking and local yielding occur the period of the structure will shift. Both of these actions in the building will tend to reduce the maximum response. Since the dynamic amplification and number of cycles to reach the maximum response are both inversely proportional to the damping, the use of supplemental damping in the building to counter this type of ground motion is attractive.

4.4.3 Impulse Motion

Much of the initial work on impulse loads was done during the period of 1950-1965 and is discussed by Norris et al.⁽⁴⁻¹⁵⁾. The force on structures generated by a blast or explosion can be idealized as a single pulse of relatively short duration. More recently it has become recognized that some earthquake motions, particularly those in the near fault region, can be idealized as either a single pulse or as a simple pulse train consisting of one to three pulses. The accelerations recorded in Bucharest, Romania during the Vrancea, Romania earthquake (1977), shown in Figure 4-10b, are a good example of this type of motion. It is of interest to note that this site is more than 100 miles from the epicenter, indicating that this type of motion is not limited to the near fault region.

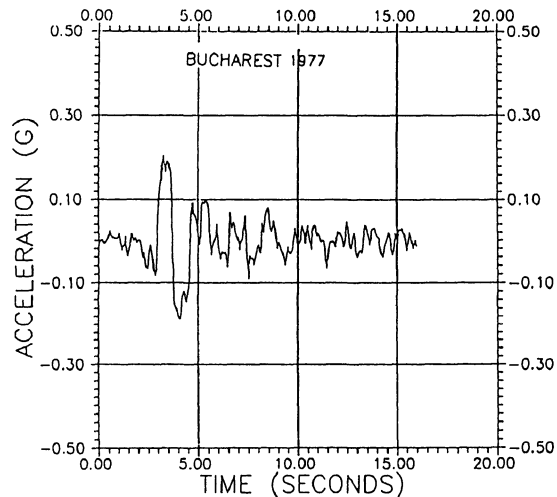


Figure 4-10b. Bucharest (1977) ground acceleration.

The maximum response to an impulse load will generally be attained on the first cycle. For this reason, the damping forces do not have time to absorb much energy from the structure. Therefore, damping has a limited effect in controlling the maximum response and is usually neglected when considering the maximum response to impulse type loads.

The rectangular pulse is a basic pulse shape. This pulse has a zero (instantaneous) rise time

and a constant amplitude, p_0 , which is applied to the structure for a finite duration t_d . During the time period when the load is on the structure ($t < t_d$) the equation of motion has the form

$$m\ddot{v} + kv = p_0 \quad (4-26d)$$

which has the general solution

$$v(t) = \frac{p_0}{k}(1 - \cos \omega t) \quad (4-26e)$$

When the impulse load is no longer acting on the structure, the system is responding in free vibration and the equation of motion becomes

$$v(t) = \frac{\dot{v}(t_d)}{\omega} \sin \omega \bar{t} + v(t_d) \cos \omega \bar{t} \quad (4-26f)$$

where

$$\bar{t} = t - t_d$$

The displacement, $v(t_d)$ and the velocity $\dot{v}(t_d)$ at the end of the loading phase become the initial conditions for the free vibration phase. It can be shown that the dynamic amplification, DA, which is defined as the ratio of the maximum dynamic displacement to the static displacement, will equal 2 if $t_d \geq T/2$ and will equal $2\sin(\pi t_d/T)$ if $t_d \leq T/2$. For elastic response, the dynamic amplification is a function of the shape of the impulse load and the duration of the load relative to the natural period of the structure as shown in Figure 4-10c.

For nonlinear behavior, the equation of motion becomes more complex, requiring the use of numerical methods for solution. Results of initial studies for basic pulse shapes were presented in the form of response charts⁽⁴⁻¹⁵⁾ such as the one shown in Figure 4-10d which can be thought of as a constant strength response spectra. For nonlinear response, the dynamic amplification factor is replaced by the

displacement ductility ratio which is defined as the ratio of the maximum displacement to the displacement at yield.

$$\mu = \frac{v_{\max}}{v_{yield}} \quad (4-26g)$$

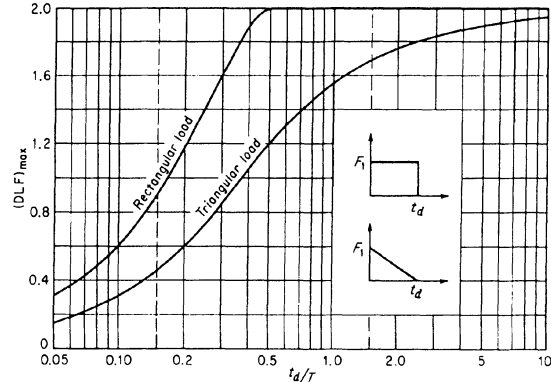


Figure 4-10c. Maximum elastic response, rectangular and triangular load pulses.[4-16]

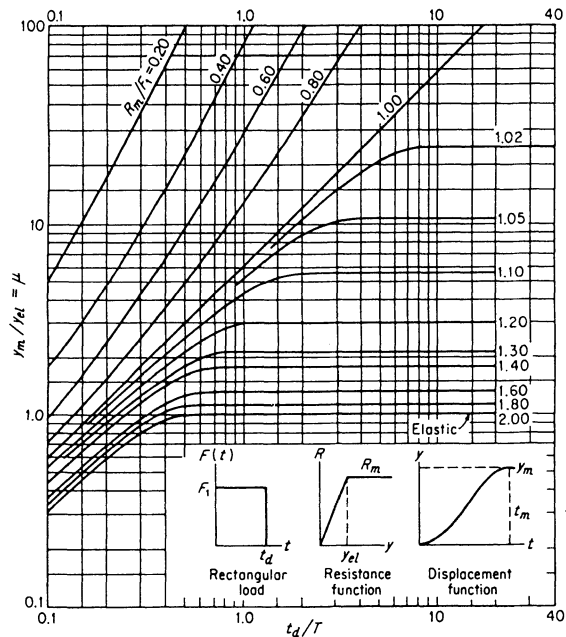


Figure 4-10d. Maximum elasto-plastic response, rectangular load pulse.[4-16]

It can also be seen that the single curve representing the elastic response becomes a family of curves for the inelastic response.

These curves depend upon the ratio of the maximum system resistance, R_m , to the maximum amplitude of the impulse load. Note that the bottom curve in Figure 4-10d which has a resistance ratio of 2 represents the elastic response curve with the ductility equal to or less than unity for all values of t_d/T . It can also be seen that as the resistance ratio decreases, the ductility demand increases.

4.4.4 Example 4-3 (Analysis for Impulse Base Acceleration)

The three bay frame shown in Figure 4-10e is assumed to be pinned at the base. It is subjected to a ground acceleration pulse which has an amplitude of $0.5g$ and a duration of 0.4 seconds. It should be noted that this acceleration pulse is similar to one recorded at the Newhall Fire Station during the Northridge earthquake (1994). The lateral resistance at ultimate load is assumed to be elasto-plastic. The columns are W10×54 with a clear height of 15 feet and the steel is A36 having a nominal yield stress of 36 ksi. Estimate the following:

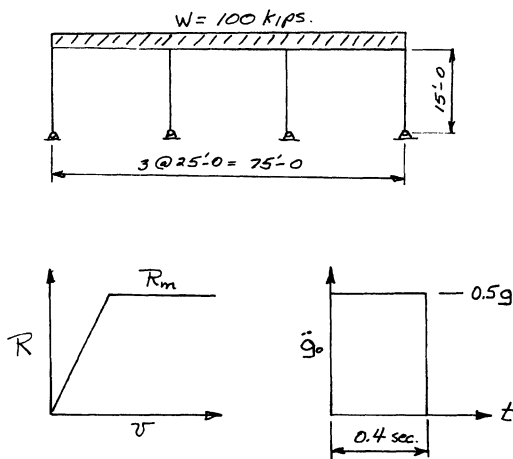


Figure 4-10e. Building elevation, resistance and loading, Example 4-3.

- (a) the displacement ductility demand, (b) the maximum displacement and (c) the residual displacement.

For a W10×54 column, $I = 303 \text{ in}^4$ and $Z = 66.6 \text{ in}^3$. The lateral stiffness of an individual column is calculated as

$$k_i = \frac{3EI}{L^3} = \frac{3(29000) \times 303}{(15 \times 12)^3} = 4.5 \frac{\text{kip}}{\text{in}}$$

and the total stiffness becomes

$$K = \sum k_i = 4 \times 4.5 = 18.0 \frac{\text{kip}}{\text{in}}$$

The mass is the weight divided by the acceleration of gravity,

$$m = \frac{W}{g} = \frac{100 \text{ kips}}{386.4 \frac{\text{in}}{\text{sec}^2}} = 0.26 \frac{\text{kips} - \text{sec}^2}{\text{in}}$$

The period of vibration of the structure can now be calculated as

$$T = 2\pi\sqrt{\frac{m}{k}} = 2\pi\sqrt{\frac{0.26}{18.0}} = 0.75 \text{ sec.}$$

and the duration ratio becomes

$$\frac{t_d}{T} = \frac{0.4}{0.75} = 0.53$$

The effective applied force, P_e is given as

$$P_e = m\ddot{g}_o = m \times 0.5g = 0.5W = 50 \text{ kips}$$

The ultimate lateral resistance of the structure occurs when plastic hinges form at the tops of the columns and a sway mechanism is formed. The nominal plastic moment capacity of a single column is

$$M_p = F_y Z = 36 \times 66.6 = 2400 \text{ in-kips}$$

and the shear resistance is

$$V_i = \frac{M_p}{h} = \frac{2400}{180} = 13.33 \text{ kips.}$$

The total lateral resistance is

$$R = 4V_i = 53.33 \text{ Kips}$$

The resistance to load ratio, is then given as

$$\frac{R}{P_{ev}} = \frac{53.3}{50} = 1.1$$

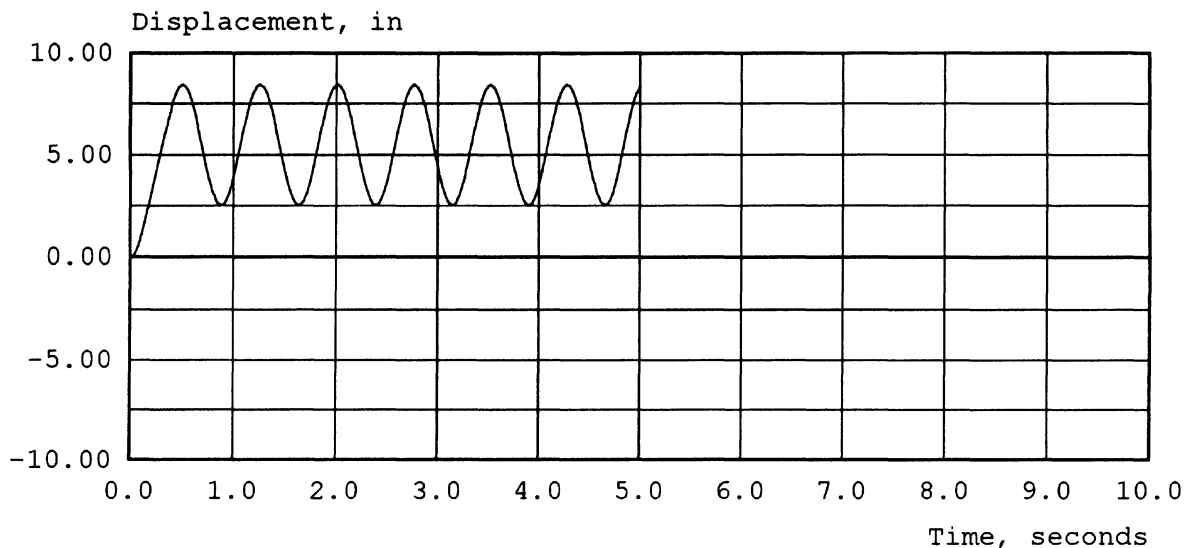


Figure 4-10f. Computed displacement time history

Using this ratio and the duration ratio, t_d/T and entering the response spectrum given in Figure 4-10d, the displacement ductility demand is found to be 2.7. The displacement at yield can be obtained as

$$v_y = \frac{R}{K} = \frac{53.3}{18} = 3.0 \text{ in.}$$

and the maximum displacement is

$$v_{\max} = \mu \times l c_y = 2.7 \times 3.0 = 8.1 \text{ in.}$$

The residual or plastic deformation is the difference between the maximum displacement and the displacement at yield.

$$v_{(\text{residual})} = v_p = 8.1 - 3.0 = 5.1 \text{ inches}$$

More recently, these calculations have been programmed for interactive computation on personal computers. The program NONLIN⁽⁴⁻¹⁴⁾ can be used to do this type of calculation and to gain additional insight through the graphics that are available. Using the program, the maximum displacement ductility is calculated to be 2.85, the maximum displacement is 8.4 inches, and the plastic displacement is 5.6 in. A plot of the calculated time history of the displacement, shown in Figure 4-10f, indicates

that structure reaches the maximum displacement on the first cycle and that from this time onward, it oscillates about a deformed position of 5.6 inches which is the plastic displacement. This can also be seen in a plot of the force versus displacement, shown in Figure 4-10g which indicates a single yield excursion followed by elastic oscillations about the residual displacement of 5.6 inches.

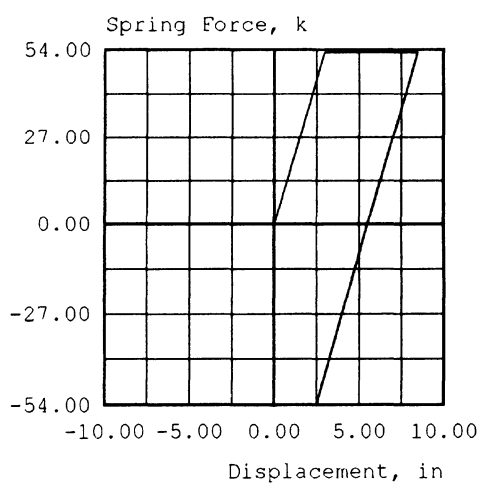


Figure 4-10g. Computed force versus displacement.

4.4.5 Approximate response to impulse loading

In order to develop a method for evaluating the response of a structural system to a general dynamic loading, it is convenient to first consider the response of a structure to a short-duration impulse load as shown in Figure 4-10h. If the duration of the applied impulse load, t , is short relative to the fundamental period of vibration of the structure, T , then the effect of the impulse can be considered as an incremental change in velocity. Using the impulse-momentum relationship, which states that the impulse is equal to the change in momentum, the following equation is obtained:

$$\dot{v}(t) = \frac{1}{m} \int_0^t p(t) dt \quad (4-26)$$

Following the application of the short-duration impulse load, the system is in free vibration and the response is given by Equation 4-19. Applying the initial conditions at the beginning of the free vibration phase,

$$\dot{v}(t_1) = \frac{1}{m} \int_0^{t_1} p(t) dt, \quad v(t_1) \text{ negligible}$$

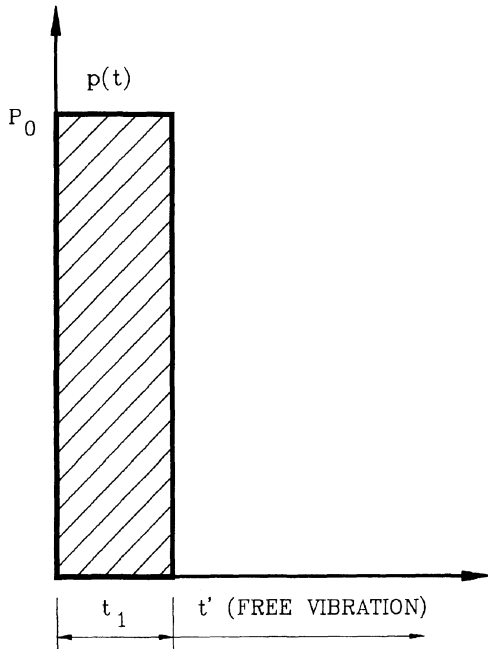


Figure 4-10h. Short duration rectangular impulse.

Equation 4-19 becomes

$$v(t - t_1) = \frac{1}{m\omega} \int_0^{t_1} p(t) dt \sin \omega(t - t_1) \quad (4-27)$$

For a damped structural system, the free-vibration response is given by Equation 4-22. Applying the above initial conditions to Equation 4-22 results in the following equation for the damped response:

$$v(t - t_1) = \frac{1}{m\omega_d} \int_0^{t_1} p(t) dt e^{-\lambda\omega(t-t_1)} \times \sin \omega_d(t - t_1) \quad (4-28)$$

4.4.6 Response to General Dynamic Loading

The above discussion of the dynamic response to a short-duration impulse load can readily be expanded to produce an analysis procedure for systems subjected to an arbitrary loading time history. Any arbitrary time history can be represented by a series of short-duration impulses as shown in Figure 4-11. Consider one of these impulses which begins at time τ after the beginning of the time history and has a duration $d\tau$. The magnitude of this differential impulse is $p(\tau) d\tau$, and it produces a differential response which is given as

$$dv(\tau) = \frac{p(\tau) \sin \omega t' d\tau}{m\omega} \quad (4-29)$$

The time variable t' represents the free-vibration phase following the differential impulse loading and can be expressed as

$$t' = t - \tau \quad (4-30)$$

Substituting this expression into Equation 4-29 results in

$$dv(\tau) = \frac{p(\tau) \sin \omega(t - \tau) d\tau}{m\omega} \quad (4-31)$$

The total response can now be obtained by superimposing the incremental responses of all the differential impulses making up the time

history. Integrating Equation 4-31, the total displacement response becomes

$$v(t) = \frac{1}{m\omega} \int_0^t p(\tau) \sin \omega(t-\tau) d\tau \quad (4-32)$$

which is known as the Duhamel integral. When considering a damped structural system, the differential response is given by Equation 4-28 and the Duhamel integral solution becomes

$$v(t) = \int_0^t \frac{p(\tau) e^{-\lambda\omega(t-\tau)} \sin \omega_d(t-\tau) d\tau}{m\omega_d} \quad (4-33)$$

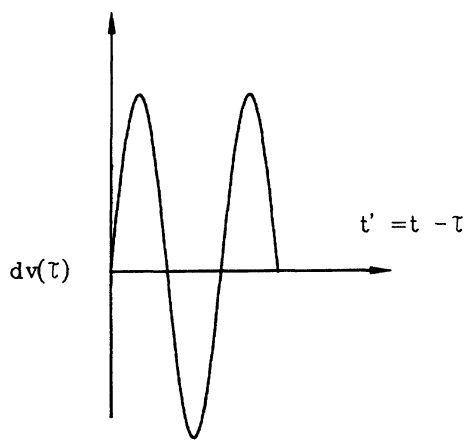
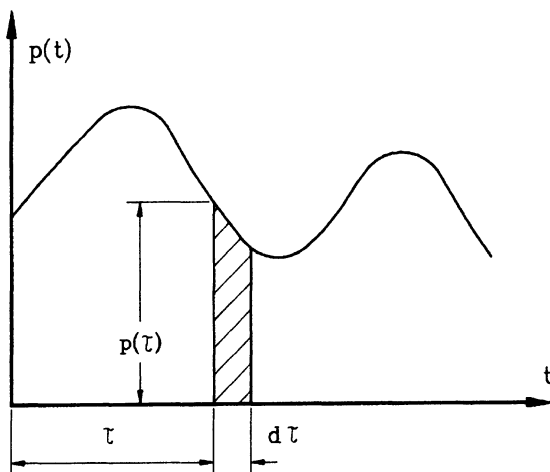


Figure 4-11. Differential impulse response.

Since the principle of superposition was used in the derivation of Equations 4-32 and 4-33, the results are only applicable to linear structural systems. Furthermore, evaluation of

the integral will require the use of numerical methods. For these two reasons, the use of a direct numerical integration procedure may be preferable for solving for the response of a dynamic system subjected to general dynamic load. This will be addressed in a later section on nonlinear response analysis. However, the Duhamel-integral result can be applied in a convenient and systematic manner to obtain a solution for the linear elastic structural response for earthquake load.

4.4.7 Earthquake Response of Elastic Structures

Time-History Response The response to earthquake loading can be obtained directly from the Duhamel integral if the time-dependent force $p(t)$ is replaced with the effective time-dependent force $P_e(t)$, which is the product of the mass and the ground acceleration. Making this substitution in Equation 4-33 results in the following expression for the displacement:

$$v(t) = \frac{V(t)}{\omega} \quad (4-34)$$

where the response parameter $V(t)$ represents the velocity and is defined as

$$V(t) = \int_0^t \ddot{g}(\tau) e^{-\lambda\omega(t-\tau)} \sin \omega_d(t-\tau) d\tau \quad (4-35)$$

The displacement of the structure at any instant of time during the entire time history of the earthquake under consideration can now be obtained using Equation 4-34. It is convenient to express the forces developed in the structure during the earthquake in terms of the effective inertia forces. The inertia force is the product of the mass and the total acceleration. Using Equation 4-11, the total acceleration can be expressed as

$$\ddot{u}(t) = -\frac{c}{m} \dot{v}(t) - \frac{k}{m} v(t) \quad (4-36)$$

If the damping term can be neglected as contributing little to the equilibrium equation, the total acceleration can be approximated as

$$\ddot{u}(t) = -\omega^2 v(t) \quad (4-37)$$

The effective earthquake force is then given as

$$Q(t) = m\omega^2 v(t) \quad (4-38)$$

The above expression gives the value of the base shear in a single-story structure at every instant of time during the earthquake time history under consideration. The overturning moment acting on the base of the structure can be determined by multiplying the inertia force by the story height:

$$M(t) = hm\omega^2 v(t) \quad (4-39)$$

Response Spectra Consideration of the displacements and forces at every instant of time during an earthquake time history can require considerable computational effort, even for simple structural systems. As mentioned previously, for many practical problems and especially for structural design, only the maximum response quantities are required. The maximum value of the displacement, as determined by Equation 4-34, will be defined as the spectral displacement

$$S_d = v(t)_{\max} \quad (4-40)$$

Substituting this result into Equations 4-38 and 4-39 results in the following expressions for the maximum base shear and maximum overturning moment in a SDOF system:

$$Q_{\max} = m\omega^2 S_d \quad (4-41)$$

$$M_{\max} = hm\omega^2 S_d \quad (4-42)$$

An examination of Equation 4-34 indicates that the maximum velocity response can be approximated by multiplying the spectral displacement by the circular frequency. This response parameter is defined as the *spectral pseudovelocity* and is expressed as

$$S_{pv} = \omega S_d \quad (4-43)$$

In a similar manner, Equation 4-37 indicates that the maximum total acceleration can be approximated as the spectral displacement multiplied by the square of the circular frequency. This product is defined as the *spectral pseudoacceleration* and is expressed as

$$S_{pa} = \omega^2 S_d \quad (4-44)$$

A plot of the spectral response parameter against frequency or period constitutes the response spectrum for that parameter. A schematic representation of the computation of the displacement spectrum for the north-south component of the motion recorded at El Centro on May 18, 1940 has been presented by Chopra⁽⁴⁻¹⁾ and is shown in Figure 4-12. Because the three response quantities are related to the circular frequency, it is convenient to plot them on a single graph with log scales on each axis. This special type of plot is called a tripartite log plot. The three response parameters for the El Centro motion are shown plotted in this manner in Figure 4-13. For a SDOF system having a given frequency (period) and given damping, the three spectral response parameters for this earthquake can be read directly from the graph.

Two types of tripartite log paper are used for plotting response spectra. Note that on the horizontal axis at the bottom of the graph in Figure 4-13, the period is increasing from left to right. For this reason, this type of tripartite log paper is often referred to as *period* paper. A similar plot of the response spectra for the El Centro N-S ground motion is shown in Figure 4-14. Here it can be seen that frequency, plotted on the horizontal axis, is increasing from left to right. This type of tripartite paper is referred to as *frequency* paper.

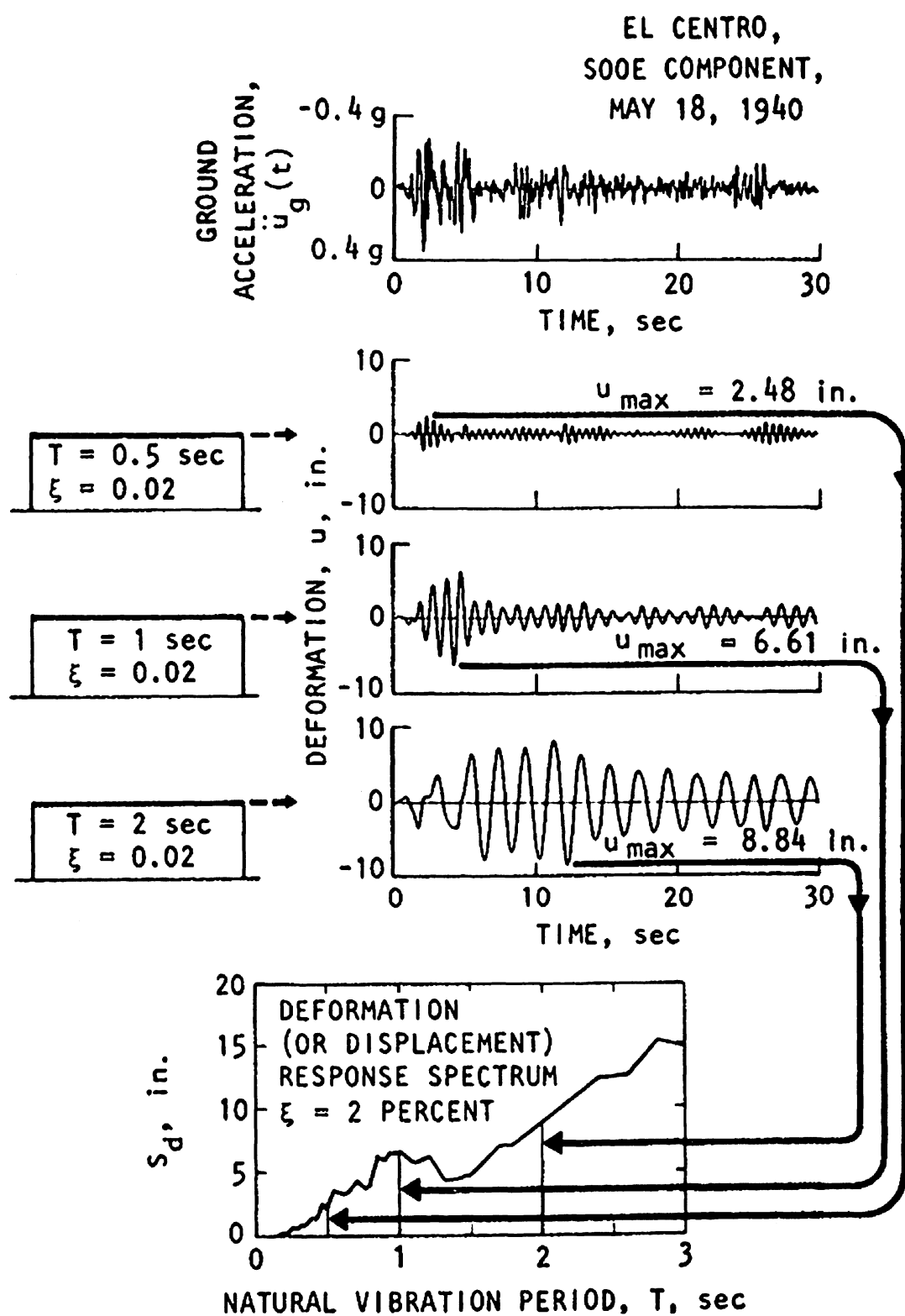


Figure 4-12. Computation of deformation (or displacement) response spectrum. [After Chopra (4-1)].

RESPONSE SPECTRUM
IMPERIAL VALLEY EARTHQUAKE
MAY 18, 1940 — 2037 PST

IIIA001 40.001.0 EL CENTRO SITE
IMPERIAL VALLEY IRRIGATION DISTRICT COMP 500E
DAMPING VALUES ARE 0, 2, 5, 10, AND 20 PERCENT OF CRITICAL

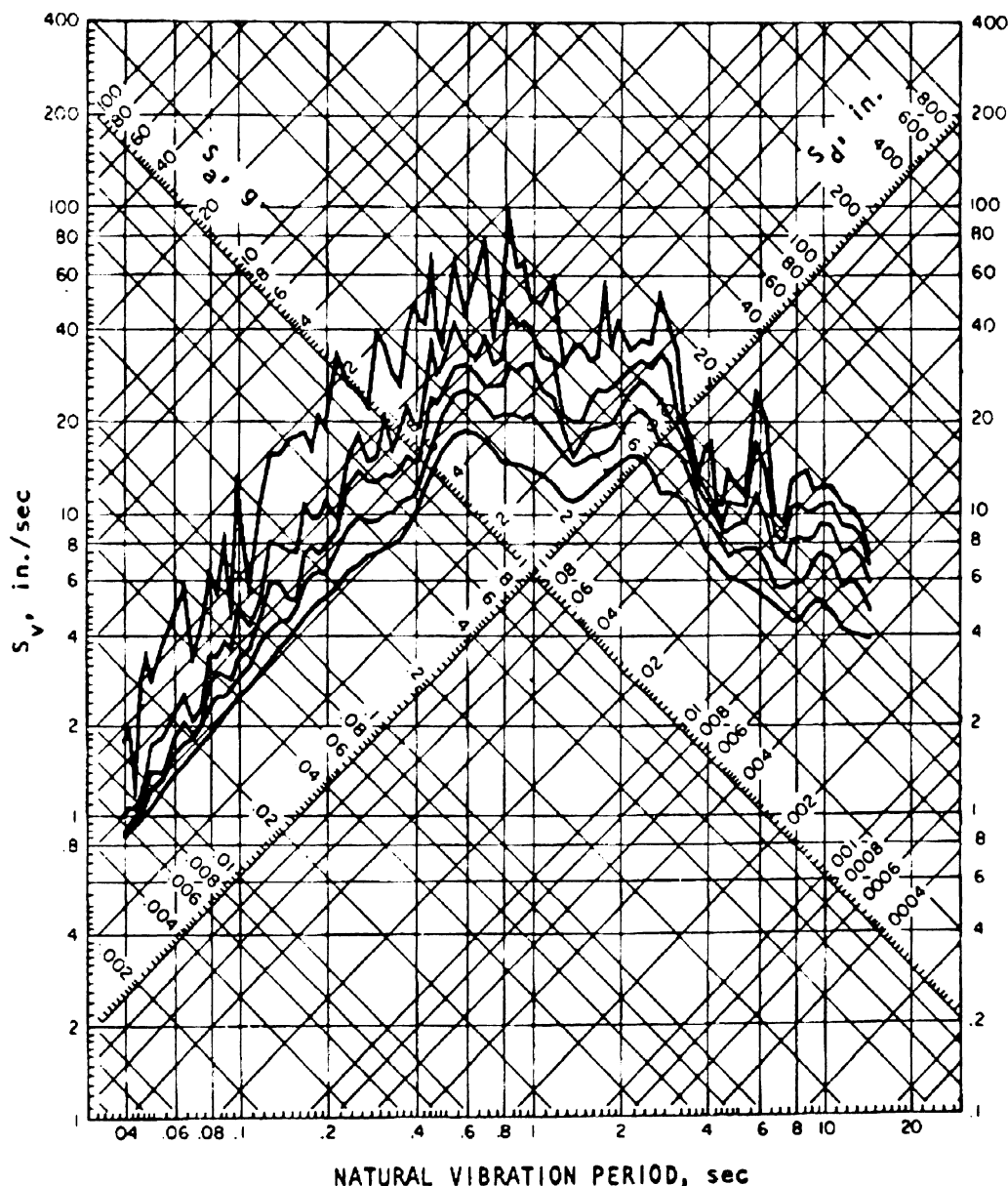


Figure 4-13. Typical tripartite response-spectra curves.

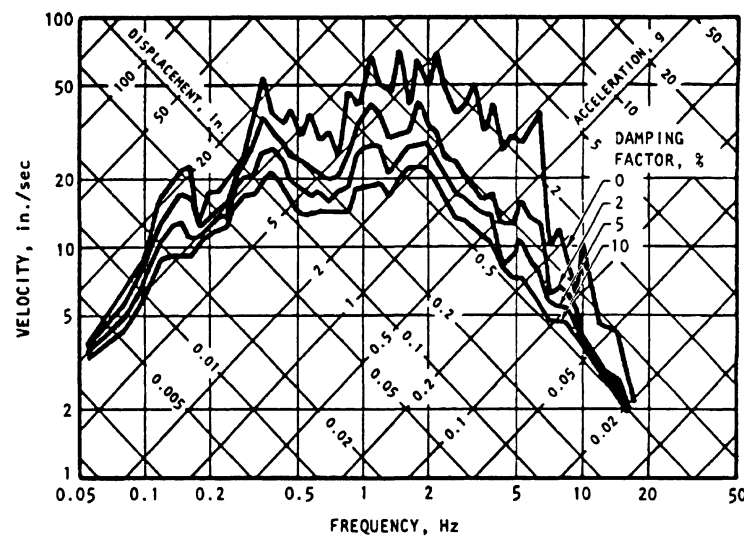


Figure 4-14. Response spectra, El Centro earthquake, May 18, 1940, north-south direction.

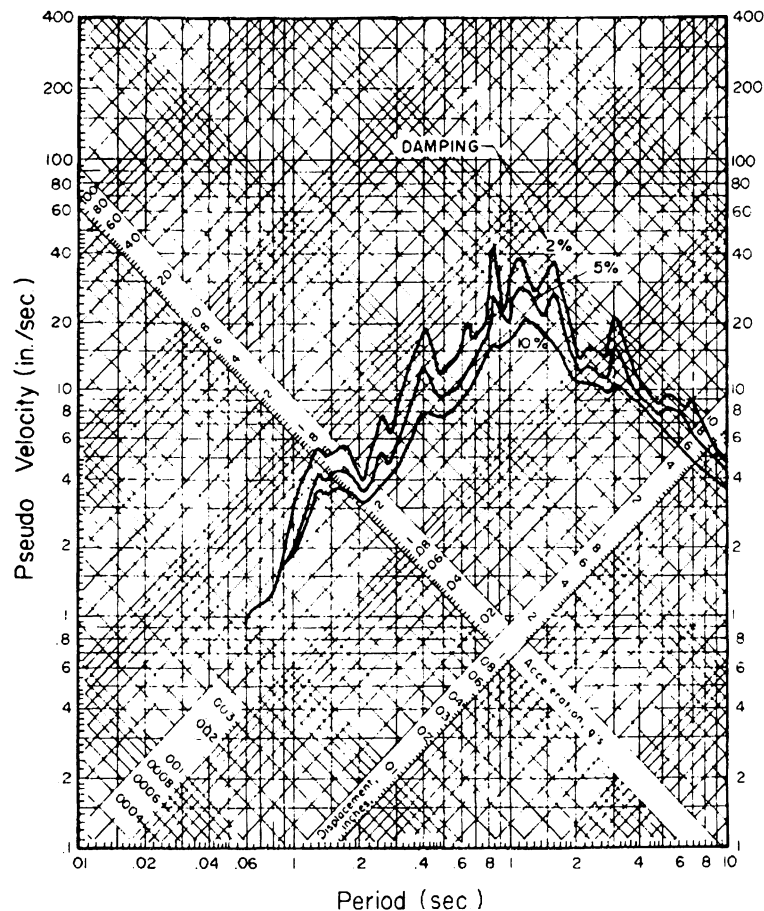


Figure 4-15. Site-specific response spectra.

4.4.8 Design Response Spectra

Use of the elastic response spectra for a single component of a single earthquake record

(Figure 4-13), while suitable for purposes of analysis, is not suitable for purposes of design. The design response spectra for a particular site should not be developed from a single

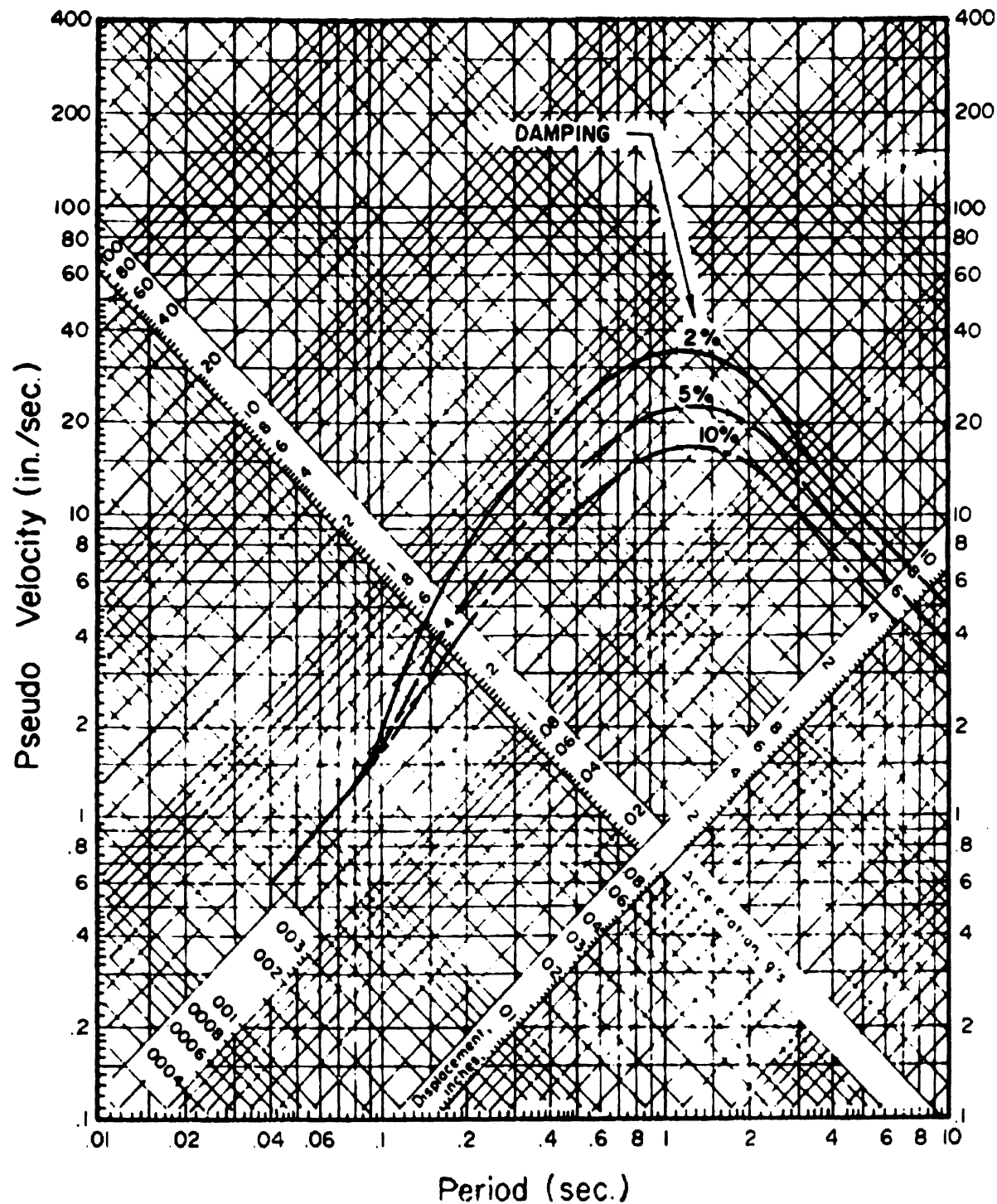


Figure 4-16. Smoothed site-specific design spectra.

acceleration time history, but rather should be obtained from the ensemble of possible earthquake motions that could be experienced at the site. This should include the effect of both near and distant earthquakes. Furthermore, a single earthquake record has a particular frequency content which gives rise to the jagged, sawtooth appearance of peaks and valleys shown in Figure 4-13. This feature is also not suitable for design, since for a given period, the structure may fall in a valley of the response spectrum and hence be underdesigned for an earthquake with slightly different response characteristics. Conversely, for a small change in period, the structure might fall on a peak and be overdesigned. To alleviate this problem the concept of the smoothed response spectrum has been introduced for design. Statistics are used to create a smoothed spectrum at some suitable design level. The mean value or median spectrum can generally be used for earthquake-resistant design of normal building structures. Use of this spectrum implies there is a 50% probability that the design level will be exceeded.

Structures that are particularly sensitive to earthquakes or that have a high risk may be designed to a higher level such as the mean plus one standard deviation, which implies that the probability of exceedance is only 15.9%. Structures having a very high risk are often designed for an enveloping spectrum which envelopes the spectra of the entire ensemble of possible site motions. Response spectra which are representative of a magnitude-6.5 earthquake at a distance of 15 miles, developed by the Applied Technology Council ⁽⁴⁻²⁾, are shown in Figure 4-15. The corresponding smoothed design spectra are shown in Figure 4-16.

Newmark and Hall ⁽⁴⁻³⁾ have proposed a method for constructing an elastic design response spectrum in which the primary input datum is the anticipated maximum ground acceleration. The corresponding values for the maximum ground velocity and the maximum ground displacement are proportioned relative to the maximum ground acceleration, which is

normalized to 1.0g. The maximum ground velocity is taken as 48 in./sec, and the maximum ground displacement is taken as 36 in. It should be noted that these values represent motions which are more intense than those normally considered for earthquake-resistant design; however, they are approximately in the correct proportion for earthquakes occurring on competent soils and can be scaled for earthquakes having lower ground acceleration.

Table 4-1. Relative values of spectrum amplification factors (4-3).

Percentage of critical Damping	Amplification factor for		
	Displacement	Velocity	Acceleration
0	2.5	4.0	6.4
0.5	2.2	3.6	5.8
1	2.0	3.2	5.2
2	1.8	2.8	4.3
5	1.4	1.9	2.6
10	1.1	1.3	1.5
20	1.0	1.1	1.2

Three principal regions of the response spectrum are identified, in which the structural response can be approximated as a constant, amplified value. Amplification factors are applied to the ground motions in these three regions to obtain the design spectrum for a SDOF elastic system. Based on a large data base of recorded earthquake motions, amplification factors which give a probability of exceedance of about 10% or less are given in Table 4-1 for various values of the structural damping. The basic shape of the Newmark—Hall design spectrum using the normalized ground motions and the amplification factors given in Table 4-1 for 5% damping is shown in Figure 4-17. The displacement region is the low-frequency region with frequencies less than 0.33 Hz (periods greater than 3.0 sec). The maximum displacement of the SDOF system is obtained by multiplying the maximum ground displacement by the displacement amplification factor given in Table 4-1. The velocity region is in the mid-frequency region between 0.33 Hz (3.0 sec) and 2.0 Hz (0.5 sec). Maximum velocities in this region are obtained by

multiplying the maximum ground velocity by the amplification factor for the velocity (Table 4-1). An amplified acceleration region lies between 2.0 Hz (0.5 sec) and 6.0 Hz (0.17 sec). The amplified response is obtained in the same manner as in the previous two cases. Structures having a frequency greater than 30 Hz (period less than 0.033 sec) are considered to be rigid and have an acceleration which is equal to the ground acceleration. In the frequency range between 6 Hz (0.17 sec) and 30 Hz (0.033 sec) there is a transition region between the ground

acceleration and the amplified acceleration region.

Similar design spectra corresponding to the postulated ground motion presented in Figures 4-15 and 4-16 are shown in Figure 4-18. In order to further define which response spectrum should be used for design, it is necessary to estimate the percentage of critical damping in the structure. A summary of recommended damping values for different types of structures and different stress conditions is given in Table 4-2 as a guideline.

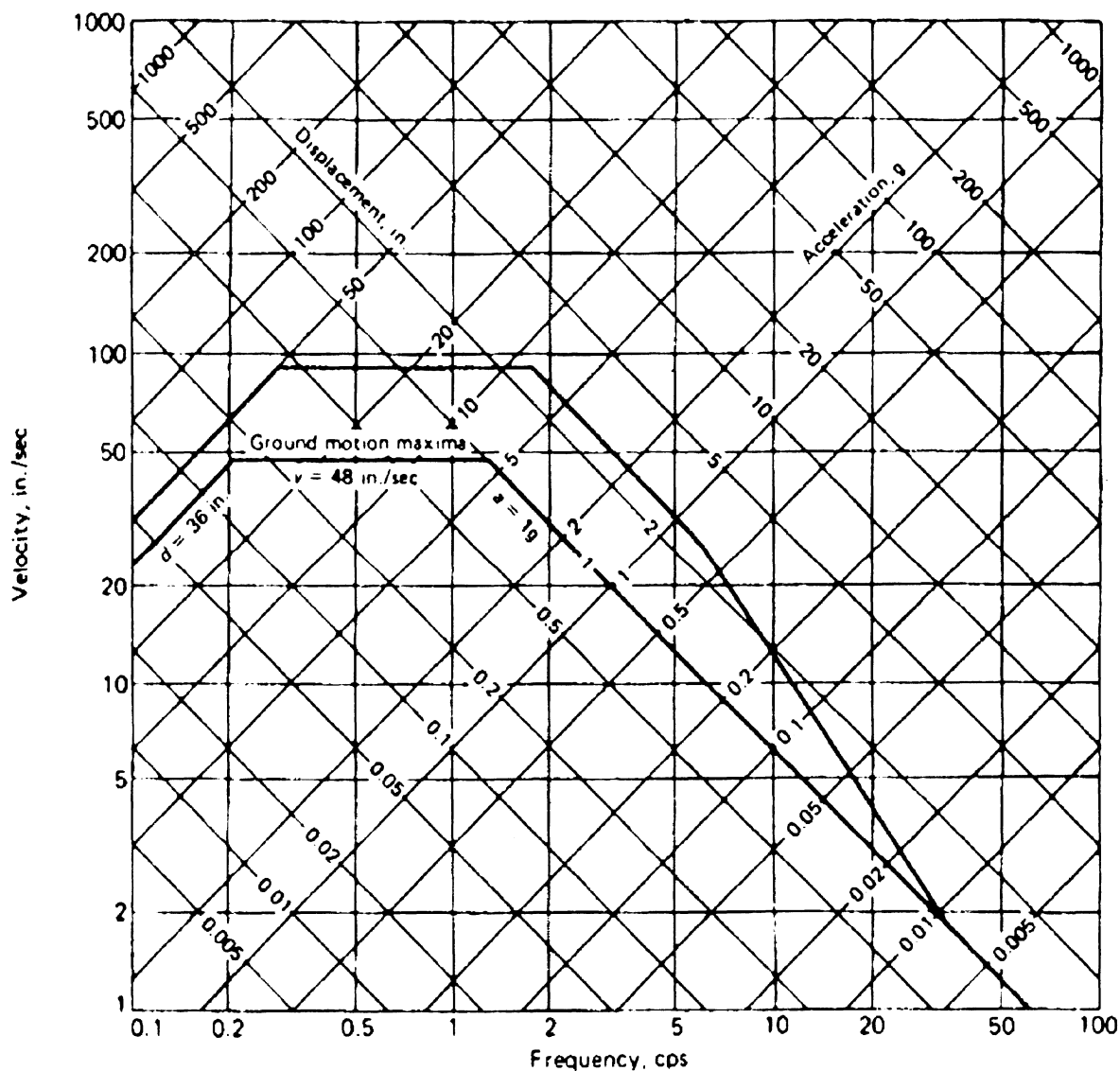


Figure 4-17. Basic Newmark-Hall design spectrum normalized to 1.0g for 5% damping (4-3).

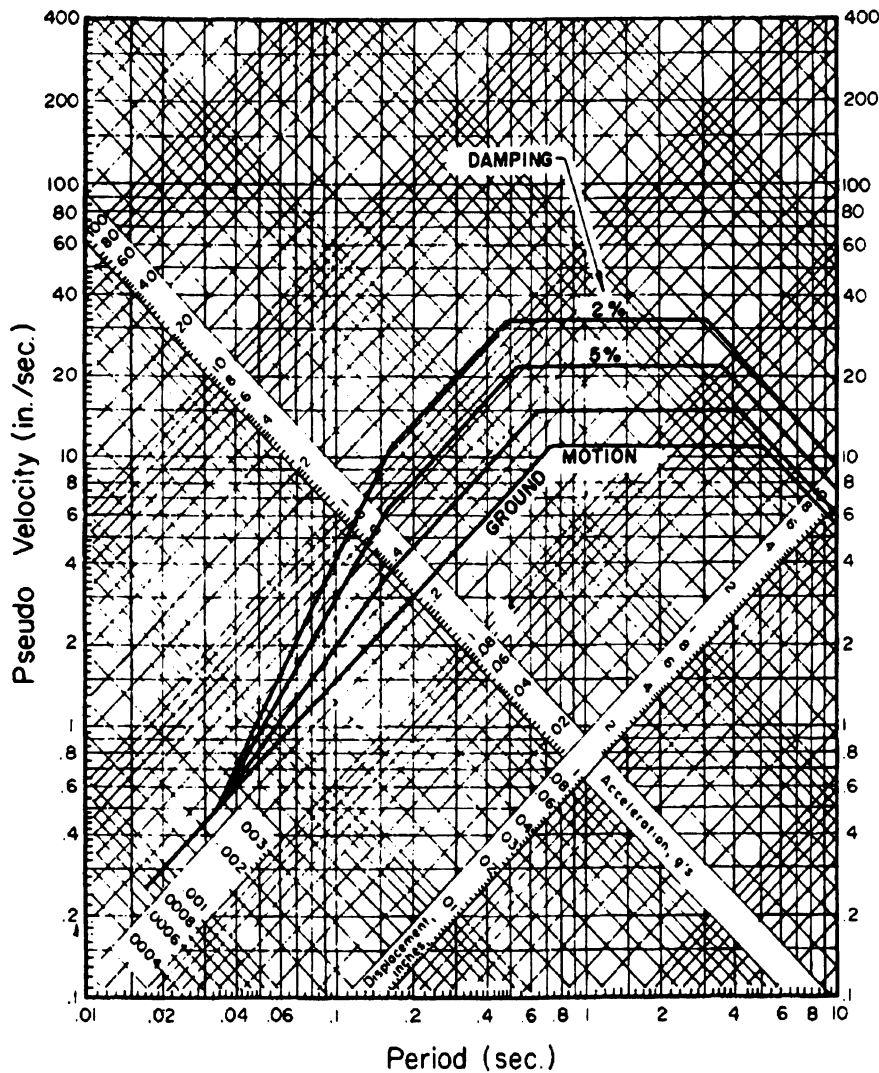


Figure 4-18. A Newmark-Hall design spectrum.

Example 4-4 (Construction of a Newmark-Hall Design Spectrum)

Construct a Newmark-Hall design spectrum for a maximum ground acceleration of 0.2g, and use it to estimate the maximum base shear for the industrial building of Example 4-1. Assume the damping is 5 percent of critical.

- Determine ground motion parameters:
ground acceleration = $(1.0)(0.2) = 0.2g$
ground velocity = $(48.0)(0.2) = 9.6 \text{ in./sec.}$
ground displacement = $(36.0)(0.2) = 7.2 \text{ in.}$
- Amplified response parameters:
acceleration = $(0.2)(2.6) = 0.52g$

$$\begin{aligned} \text{velocity} &= (9.6)(1.9) = 18.2 \text{ in./sec} \\ \text{displacement} &= (7.2)(1.4) = 10.0 \text{ in.} \end{aligned}$$

The constructed design spectrum is shown in Figure 4-19.

From Example 4-1:

N-S:

$$T = 0.287 \text{ sec.}$$

$$\omega = 21.8 \text{ rad/sec.}$$

$$f = 3.48 \text{ Hz}$$

From the design spectrum for $f = 3.48 \text{ Hz}$:

$$S_d = v(t)_{\max} = 0.42 \text{ in.}$$

Table 4-2 Recommended Damping Values (4-3)

Stress level	Type and condition of structure	Percentage of critical damping	Stress level	Type and condition of structure	Percentage of critical damping
Working stress,<1/2 yield point	Vital piping Welded steel, prestressed concrete, well-reinforced concrete(only slight cracking) Reinforced concrete with considerable cracking Bolted and / or riveted steel, wood structures with nailed or bolted joints.	1-2 2-3 3-5 5-7	At or just below yield point	Vital piping Welded steel, prestressed concrete(without complete loss in prestress) Prestressed concrete with no prestress left Bolted and / or riveted steel, wood structures with nailed or bolted joints. Wood structures with nailed joints	2-3 5-7 7-10 10-15 15-20

From Equation 4-42:

$$Q_{max} = (0.485)(21.8)^2(0.42) = 96.8 \text{ kips}$$

E-W:

$$T = 0.23 \text{ sec},$$

$$\omega = 27.2 \text{ rad/sec},$$

From the design spectrum for $f = 4.3 \text{ Hz}$:

$$S_d = 0.28 \text{ in.}$$

From Equation 4-42:

$$Q_{max} = (0.485)(21.8)^2(0.28) = 64.5 \text{ kips}$$

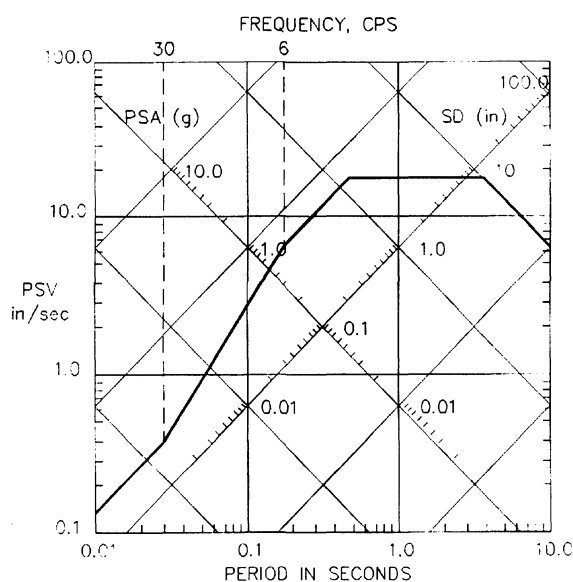


Figure 4-19. Response spectrum of Example 4-3.

4.4 GENERALIZED-COORDINATE APPROACH

Up to this point, the only structures which have been considered are single-story buildings which can be idealized as SDOF systems. The analysis of most structural systems requires a more complicated idealization even if the response can be represented in terms of a single degree of freedom. The generalized-coordinate approach provides a means of representing the response of more complex structural systems in terms of a single, time-dependent coordinate, known as the generalized coordinate.

Displacements in the structure are related to the generalized coordinate as

$$v(x, t) = \phi(x)Y(t) \quad (4-45)$$

Where $Y(t)$ is the time-dependent generalized coordinate and $\phi(x)$ is a spatial shape function which relates the structural degrees of freedom, $v(x, t)$, to the generalized coordinate. For a generalized SDOF system, it is necessary to represent the restoring forces in the damping elements and the stiffness elements in terms of the relative velocity and relative displacement between the ends of the element:

$$\Delta\dot{v}(x, t) = \Delta\phi(x)\dot{Y}(t) \quad (4-46)$$

$$\Delta v(x, t) = \Delta\phi(x)Y(t) \quad (4-47)$$

Most structures can be idealized as a vertical cantilever, which limits the number of displacement functions that can be used to represent the horizontal displacement. Once the displacement function is selected, the structure is constrained to deform in that prescribed manner. This implies that the displacement functions must be selected carefully if a good approximation of the dynamic properties and response of the system are to be obtained. This section will develop the equations for determining the generalized response parameters in terms of the spatial displacement function and the physical response parameters. Methods for determining the shape function will be discussed, and techniques for determining the more correct displacement function for a particular structure will be presented.

4.4.1 Displacement Functions and Generalized Properties

Formulation of the equation of motion in terms of a generalized coordinate will be restricted to systems which consist of an assemblage of lumped masses and discrete elements. Lateral resistance is provided by discrete elements whose restoring force is proportional to the relative displacement between the ends of the element. Damping forces are proportional to the relative velocity between the ends of the discrete damping element. Formulation of the equation of motion for systems having distributed elasticity is described by Clough and Penzien.⁽⁴⁻⁴⁾ The general equation of dynamic equilibrium is given in Equation 4-6, which represents a system of forces which are in equilibrium at any instant of time. The principle of virtual work in the form of virtual displacements states that

If a system of forces which are in equilibrium is given a virtual displacement which is consistent with the boundary conditions, the work done is zero.

Applying this principle to Equation 4-6 results in an equation of virtual work in the form

$$f_i \delta v + f_d \delta \Delta v + f_s \delta \Delta v - p(t) \delta v = 0 \quad (4-48)$$

where it is understood that $v = v(x, t)$ and that the virtual displacements applied to the damping force and the elastic restoring force are virtual relative displacements. The virtual displacement can be expressed as

$$\delta v(x, t) = \phi(x) \delta Y(t) \quad (4-49)$$

and the virtual relative displacement can be written as

$$\delta \Delta v(x, t) = \Delta\phi(x) \delta Y(t) \quad (4-50)$$

where

$$\Delta v(x, t) = \phi(x_i) Y(t) - \phi(x_j) Y(t) = \Delta\phi(x) Y(t)$$

The inertia, damping and elastic restoring forces can be expressed as

$$\begin{aligned} f_i &= m \ddot{v} = m \phi \ddot{Y} \\ f_d &= c \Delta \dot{v} = c \Delta \phi \dot{Y} \\ f_s &= k \Delta v = k \Delta \phi Y \end{aligned} \quad (4-51)$$

Substituting Equations 4-49, 4-50, and 4-51 into Equation 4-48 results in the following equation of motion in terms of the generalized coordinate:

$$m^* \ddot{Y} + c^* \dot{Y} + k^* Y = p^*(t) \quad (4-52)$$

where m^* , c^* , k^* , and p^* are referred to as the *generalized parameters* and are defined as

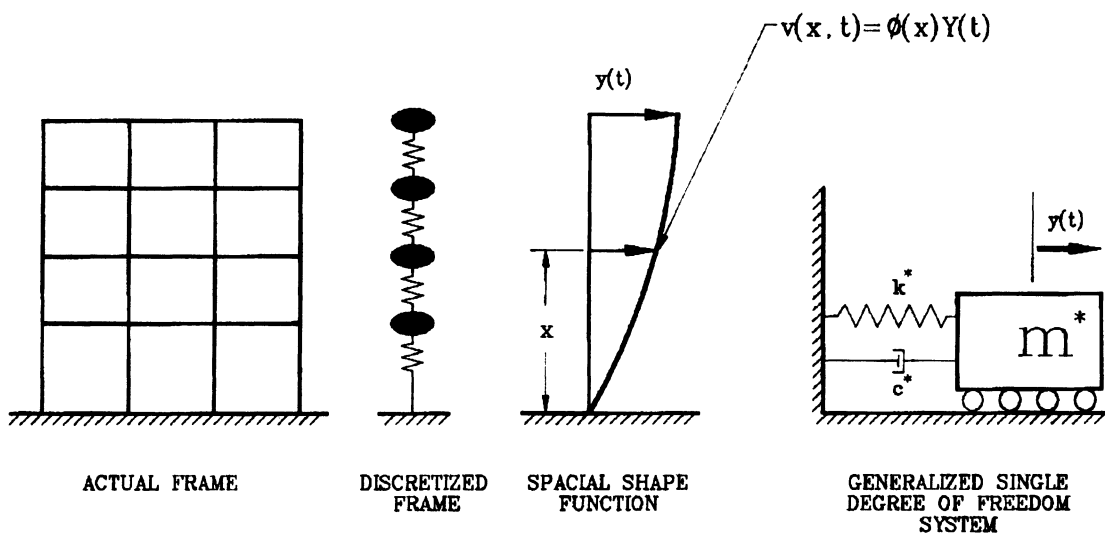


Figure 4-20. Generalized single-degree-of-freedom system.

$$\begin{aligned}
 m^* &= \sum_i m_i \phi_i^2 = \text{generalized mass} \\
 c^* &= \sum_i c_i \Delta \phi_i^2 = \text{generalized damping} \\
 k^* &= \sum_i k_i \Delta \phi_i^2 = \text{generalized stiffness} \\
 p^* &= \sum_i p_i \phi_i = \text{generalized force}
 \end{aligned} \tag{4-53}$$

For a time-dependent base acceleration the generalized force becomes

$$p^* = \ddot{g}L \tag{4-54}$$

where

$$\begin{aligned}
 L &= \sum_i m_i \phi_i \\
 &= \text{earthquake participation factor}
 \end{aligned} \tag{4-55}$$

It is also convenient to express the generalized damping in terms of the percent of critical damping in the following manner:

$$c^* = \sum_i c_i \Delta \phi_i^2 = 2\lambda m^* \omega \tag{4-56}$$

Where ω represents the circular frequency of the generalized system and is given as

$$\omega = \sqrt{\frac{k^*}{m^*}} \tag{4-57}$$

The effect of the generalized-coordinate approach is to transform a multiple-degree-of-freedom dynamic system into an equivalent single-degree-of-freedom system in terms of the generalized coordinate. This transformation is shown schematically in Figure 4-20. The degree to which the response of the transformed system represents the actual system will depend upon how well the assumed displacement shape represents the dynamic displacement of the actual structure. The displacement shape depends on the aspect ratio of the structure, which is defined as the ratio of the height to the base dimension. Possible shape functions for high-rise, mid-rise, and low-rise structures are summarized in Figure 4-21. It should be noted that most building codes use the straight-line shape function which is shown for the mid-rise system. Once the dynamic response is obtained in terms of the generalized coordinate, Equation 4-45 must be used to determine the displacements in the structure, and these in turn

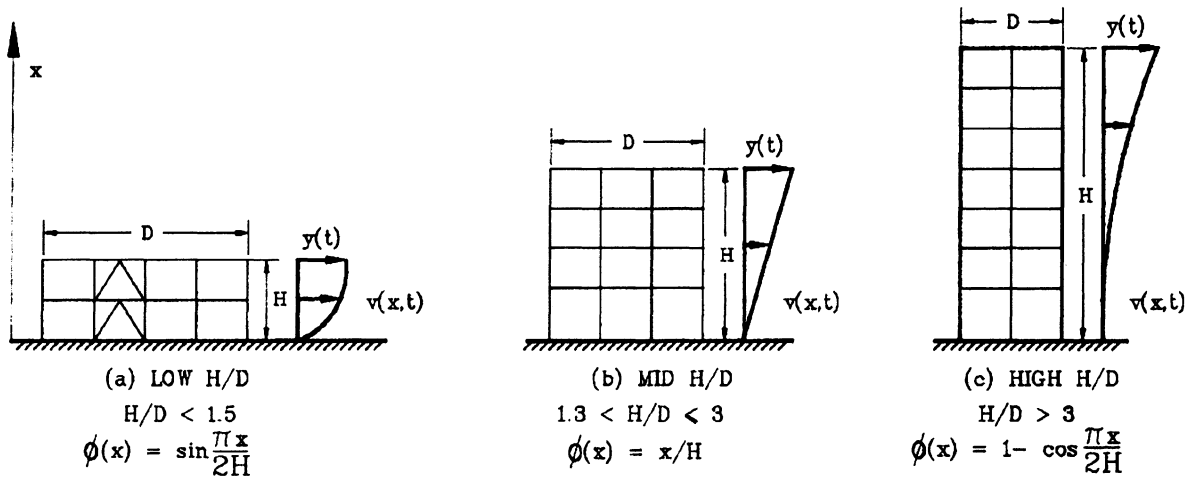


Figure 4-21. Possible shape functions based on aspect ratio.

can be used to determine the forces in the individual structural elements.

In principle, any function which represents the general deflection characteristics of the structure and satisfies the support conditions could be used. However, any shape other than the true vibration shape requires the addition of external constraints to maintain equilibrium. These extra constraints tend to stiffen the system and thereby increase the computed frequency. The true vibration shape will have no external constraints and therefore will have the lowest frequency of vibration. When choosing between several approximate deflected shapes, the one producing the lowest frequency is always the best approximation. A good approximation to the true vibration shape can be obtained by applying forces representing the inertia forces and letting the static deformation of the structure determine the spatial shape function.

Example 4-5 (Determination of generalized parameters)

Considering the four-story, reinforced-concrete moment frame building shown in Figure 4-22, determine the generalized mass, generalized stiffness, and fundamental period of vibration in the transverse direction using the following shape functions:

(a) $\phi(x) = \sin(\pi x / 2L)$ and (b) $\phi(x) = x / L$. All beams are 12 in. \times 20 in., and all columns are 14 in. \times 14 in. $f_c' = 4000$ psi, and the modulus of elasticity of concrete is 3.6×10^6 psi. Reinforcing steel is made of grade-60 bars. Floor weights (total dead load) are assumed to be 390 kips at the roof, 445 kips at the fourth and third levels, and 448 kips at the first level. Live loads are 30 psf at the roof and 80 psf per typical floor level.

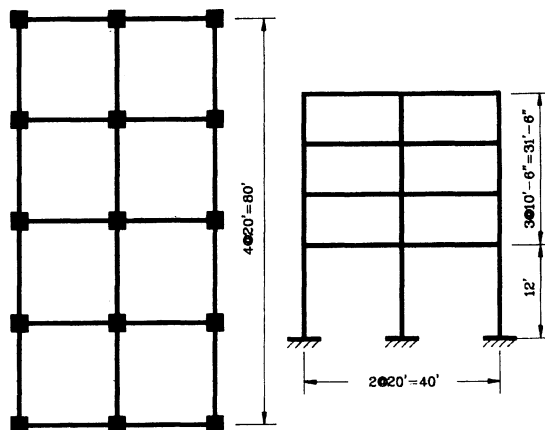


Figure 4-22. Building of Example 4-5.

Assuming beams are rigid relative to columns (Figure 4-23),

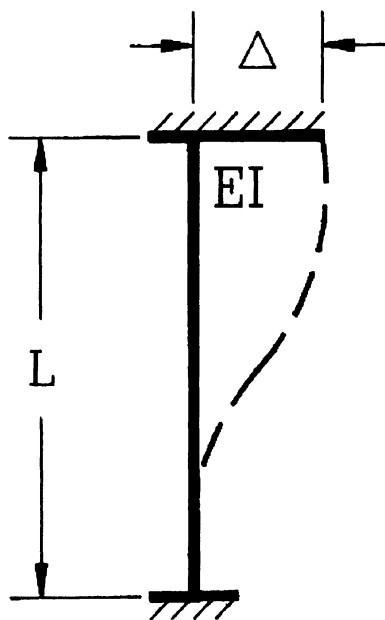


Figure 4-23. Assumed shape of column deformation.

$$V = \frac{12EI\Delta}{L^3}$$

$$K_i = \frac{V}{\Delta} = \frac{12EI}{L^3}$$

$$I_{col} = \frac{14(14)^3}{12} = 3201 \text{ in.}^4$$

$$I_{beam} = \frac{12(20)^3}{12} = 8000 \text{ in.}^4$$

$$K_{story} = \sum_{i=1}^3 K_i = 3K_i \text{ (one frame)}$$

$$K_{4,3,2} = \frac{(3)(12)(3.6 \times 10^3)(3201)}{(126)^3} = 209 \frac{\text{kips}}{\text{in.}}$$

$$K_1 = \frac{(3)(12)(3.6 \times 10^3)(3201)}{(144)^3} = 140 \frac{\text{kips}}{\text{in.}}$$

Calculating generalized properties (see Figure 4-24):

(a) Assuming $\phi(x) = \sin(\pi x / 2L)$:

Level	K	M	ϕ_i	$\Delta\phi_i$	$M\phi_i^2$	$K\Delta\phi_i^2$
4		0.252	1.000		0.252	
	209			0.071		1.054
3		0.288	0.929		0.249	
	209			0.203		8.613
2		0.288	0.726		0.152	
	209			0.306		19.570
1		0.290	0.420		0.051	
	140			0.420		24.696
					<hr/>	
					$M^* = 0.704$	$K^* = 53.933$

$$\omega = \sqrt{\frac{k^*}{m^*}} = \sqrt{\frac{53.93}{0.704}} = 8.75 \text{ rad/sec}$$

and $T_a = 0.72 \text{ sec}$

(b) Assuming $\phi(x) = x/L$

Level	K	M	ϕ_i	$\Delta\phi_i$	$M\phi_i^2$	$K\Delta\phi_i^2$
4		0.252	1.000		0.252	
	209			0.241		12.139
3		0.288	0.759		0.166	
	209			0.242		12.240
2		0.288	0.517		0.077	
	209			0.241		12.139
1		0.290	0.276		0.022	
	140			0.276		10.665
					<hr/>	
					$M^* = 0.517$	$K^* = 47.183$

$$\omega = \sqrt{\frac{k^*}{m^*}} = \sqrt{\frac{47.183}{0.517}} = 9.55 \text{ rad/sec}$$

and $T_b = 0.66 \text{ sec.}$

Since $T_a > T_b$, $\phi(x) = \sin(\pi x / 2L)$ is a better approximation to the deflected shape than $\phi(x) = x/L$.

4.4.2 Rayleigh's Method

Rayleigh's method is a procedure developed by Lord Rayleigh⁽⁴⁻⁵⁾ for analyzing vibrating systems using the law of conservation of energy. Its principal use is for determining an accurate approximation of the natural frequency of a structure. The success of

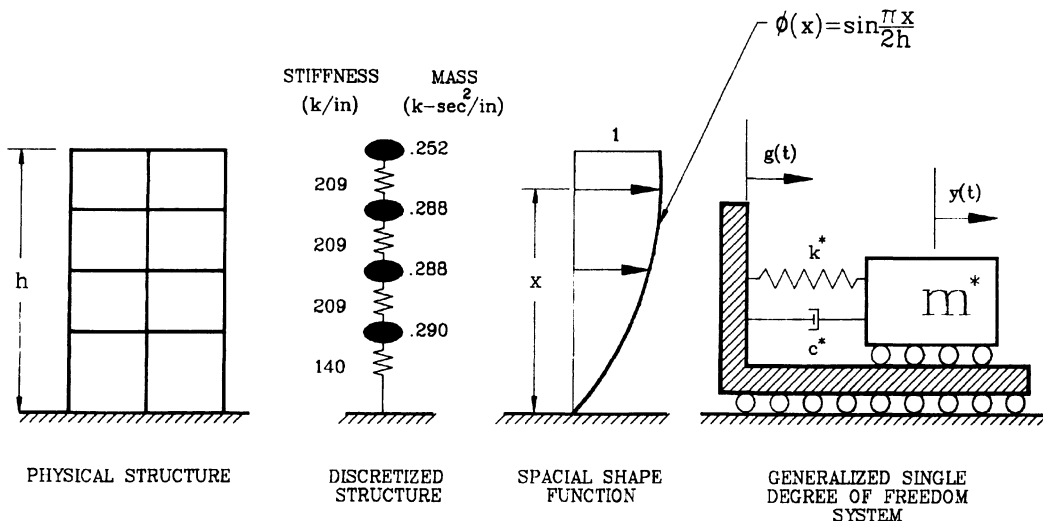


Figure 4-24. Development of a generalized SDOF model for building of Example 4-4.

the technique in accomplishing this has been recognized by most building codes, which have adopted the procedure as an alternative for estimating the fundamental period of vibration. In addition to providing an estimate of the fundamental period, the procedure can also be used to estimate the shape function $\phi(x)$.

In an undamped elastic system, the maximum potential energy can be expressed in terms of the external work done by the applied forces. In terms of a generalized coordinate this expression can be written as

$$(PE)_{\max} = \frac{Y}{2} \sum p_i \phi_i = \frac{p^* Y}{2} \quad (4-58)$$

Similarly, the maximum kinetic energy can be expressed in terms of the generalized coordinate as

$$(KE)_{\max} = \frac{\omega^2 Y^2}{2} \sum_i m_i \phi_i^2 = \frac{\omega^2 Y^2 m^*}{2} \quad (4-59)$$

According to the principle of conservation of energy for an undamped elastic system, these two quantities must be equal to each other and to the total energy of the system. Equating

Equation 4-58 to Equation 4-59 results in the following expression for the circular frequency:

$$\omega = \sqrt{\frac{p^*}{m^* Y}} \quad (4-60)$$

Substituting this result into Equation 4-20 for the period results in

$$T = 2\pi \sqrt{\frac{m^* Y}{p^*}} \quad (4-61)$$

Multiplying the numerator and denominator of the radical by Y and using Equation 4-45 results in the expression for the fundamental period:

$$T = 2\pi \sqrt{\frac{\sum_i w_i v_i^2}{8 \sum_i p_i v_i}} \quad (4-62)$$

which is the expression found in most building codes.

The forces which must be applied laterally to obtain either the shape function $\phi(x)$ or the displacement $v(x)$ represent the inertia forces, which are the product of the mass and the acceleration. If the acceleration is assumed to vary linearly over the height of a building with

uniform weight distribution, a distribution of inertia force in the form of an inverted triangle will be obtained, being maximum at the top and zero at the bottom. This is similar to the distribution of base shear used in most building codes and can be a reasonable one to use when applying the Rayleigh method. The resulting deflections can be used directly in Equation 4-62 to estimate the period of vibration or they can be normalized in terms of the generalized coordinate (maximum displacement) to obtain the spatial shape function to be used in the generalized-coordinate method.

Example 4-6 (Application of Rayleigh's Method)

Use Rayleigh's method to determine the spatial shape function and estimate the fundamental period of vibration in the transverse direction for the reinforced-concrete building given in Example 4-4.

We want to apply static lateral loads that are representative of the inertial loads on the building. Since the story weights are approximately equal, it is assumed that the accelerations and hence the inertial loads vary linearly from the base to the roof (see Figure 4-25).

Note that the magnitude of loads is irrelevant and is chosen for ease of computation. The following computations (on the bottom of this page) are a tabular solution of Equation 4-61.

$$T = 2\pi \sqrt{\frac{m^* Y}{p^*}}, \text{ or}$$

$$T = 2\pi \sqrt{\frac{(0.666)(0.3343)}{16.912}} = 0.712 \text{ sec}$$

Note that since $T = 0.721$ is greater than either of the periods calculated in Example 4-5,

Level	K	m	P	V	$\Delta = V/k$	v	ϕ	$m_i \phi_i^2$	$P_i \phi_i$
4	209	0.252	8.0	8	0.0383	0.3343	1.000	0.252	8.000
3	209	0.288	6.0	14	0.0670	0.2960	0.886	0.226	5.316
2	209	0.288	4.0	18	0.0861	0.2290	0.685	0.135	2.740
1	140	0.288	2.0	20	0.1429	0.1429	0.428	0.053	0.856
						0.000	0.000	0.666	16.912

the deflected shape given by applying the static loads is a better approximation than either of the two previous deflected shapes.

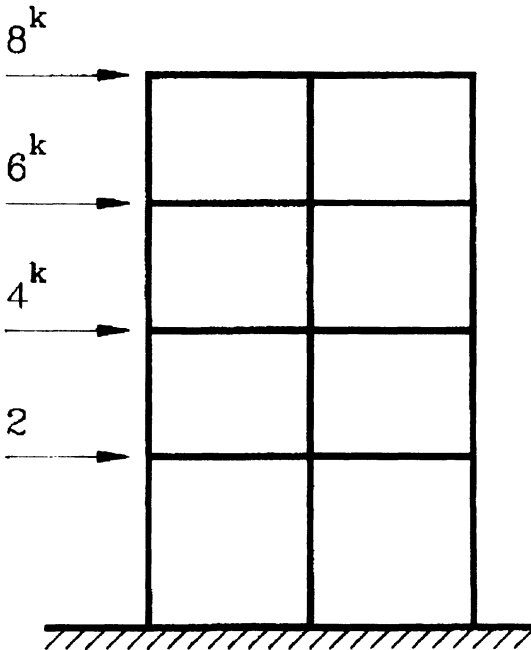


Figure 4-25. Frame of Example 4-5.

4.4.3 Earthquake Response of Elastic Structures

Time-History Analysis Substituting the generalized parameters of Equations 4-53 and 4-54 into the Duhamel-integral solution, Equation 4-33, results in the following solution for the displacement:

$$v(x, t) = \frac{\phi(x) L V(t)}{m^* \omega} \quad (4-63)$$

Using Equation 4-37, the inertia force at any position x above the base can be obtained from

$$q(x, t) = m(x)\ddot{v}(x, t) = m(x)\omega^2 v(x, t) \quad (4-64)$$

which, using Equation 4-63, becomes

$$q(x, t) = \frac{m(x)\phi(x)L\omega V(t)}{m^*} \quad (4-65)$$

The base shear is obtained by summing the distributed inertia forces over the height H of the structure:

$$Q(t) = \int q(x, t)dx = \frac{L^2}{m^*}\omega V(t) \quad (4-66)$$

The above relationships can be used to determine the displacements and forces in a generalized SDOF system at any time during the time history under consideration.

Response-Spectrum Analysis

The maximum value of the velocity given by Equation 4-35 is defined as the spectral pseudovelocity (S_{pv}), which is related to the spectral displacement (S_d) by Equation 4-43. Substituting this value into Equation 4-63 results in an expression for the maximum displacement in terms of the spectral displacement:

$$v(x)_{\max} = \frac{\phi(x)L S_d}{m^*} \quad (4-67)$$

The forces in the system can readily be determined from the inertia forces, which can be expressed as

$$q(x)_{\max} = m(x)\ddot{v}(x)_{\max} = m(x)\omega^2 v(x)_{\max} \quad (4-68)$$

Rewriting this result in terms of the spectral pseudo-acceleration (S_{pa}) results in the following:

$$q(x)_{\max} = \frac{\phi(x)m(x)L S_{pa}}{m^*} \quad (4-69)$$

Of considerable interest to structural engineers is the determination of the base shear. This is a key parameter in determining seismic design forces in most building codes. The base shear Q can be obtained from the above expression by simply summing the inertia forces and using Equation 4-55:

$$Q_{\max} = \frac{L^2 S_{pa}}{m^*} \quad (4-70)$$

It is also of interest to express the base shear in terms of the effective weight, which is defined as

$$W^* = \frac{(\sum_i w_i \phi_i)^2}{\sum_i w_i \phi_i^2} \quad (4-71)$$

The expression for the maximum base shear becomes

$$Q_{\max} = W^* S_{pa} / g \quad (4-72)$$

This form is similar to the basic base-shear equation used in the building codes. In the code equation, the effective weight is taken to be equal to the total dead weight W , plus a percentage of the live load for special occupancies. The seismic coefficient C is determined by a formula but is equivalent to the spectral pseudoacceleration in terms of g . The basic code equation for base shear has the form

$$Q_{\max} = CW \quad (4-73)$$

The effective earthquake force can also be determined by distributing the base shear over the story height. This distribution depends upon the displacement shape function and has the form

$$q_i = Q_{\max} \frac{m_i \phi_i}{L} \quad (4-74)$$

If the shape function is taken as a straight line, the code force distribution is obtained. The overturning moment at the base of the structure

can be determined by multiplying the inertia force by the corresponding story height above the base and summing over all story levels:

$$M_o = \sum_i h_i q_i \quad (4-75)$$

Example 4-7 (Spectrum Analysis of Generalized SDOF System)

Using the design spectrum given in Figure 4-26, the shape function determined in Example 4-6, and the reinforced-concrete moment frame of Example 4-5, determine the base shear in the transverse direction, the corresponding distribution of inertia forces over the height of the structure, and the resulting overturning moment about the base of the structure.

$$T = 0.721 \text{ sec.}, \quad f = 1/T = 1.39 \text{ Hz}, \\ \omega = 8.715 \text{ rad/sec.}$$

From the design spectrum $S_{pa} = 0.185g$.

Level	m_i	ϕ_i	$m_i\phi_i^2$	$m_i\phi_i$	$m_i\phi/L$	q_{max}	V_{max}
4	0.252	1.000	0.252	0.252	0.305	27.10	27.10
3	0.288	0.866	0.226	0.255	0.308	27.36	54.46
2	0.288	0.685	0.135	0.197	0.238	21.14	75.60
1	0.288	0.428	0.053	0.123	0.149	13.24	88.84
			0.666	0.827			

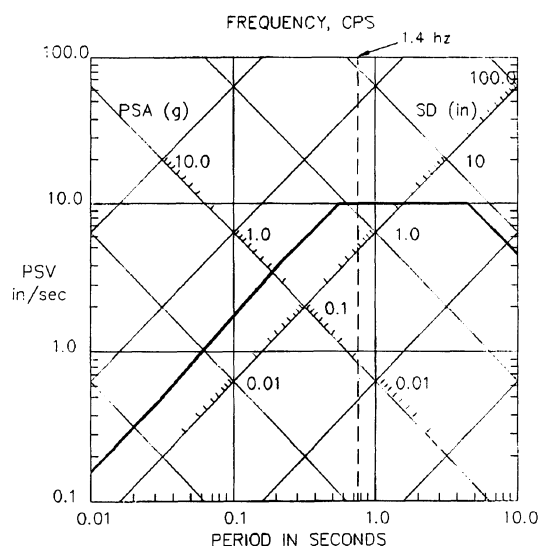
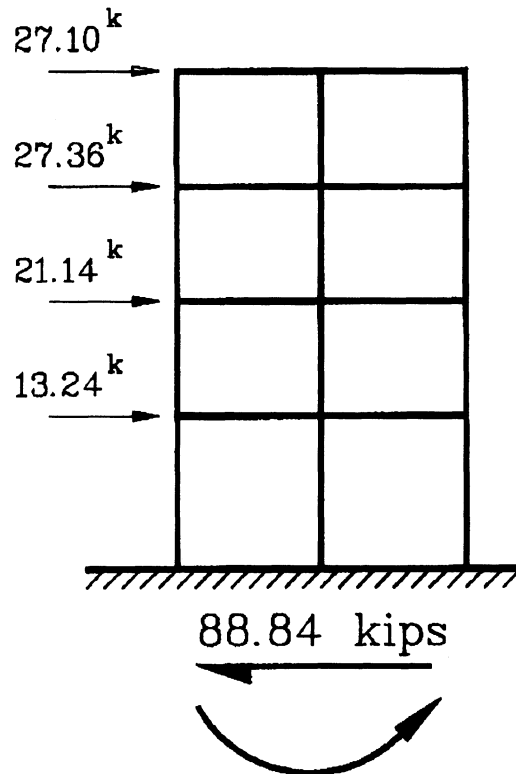


Figure 4-26. Design spectrum for Example 4-6.

From Equation 4-66,

$$Q_{max} = \frac{(0.827)^2(0.185)(386.4)}{0.666} = 88.84 \text{ kips}$$

The overturning moment is: (see Fig. 4-27)



$$M_o = 2716 \text{ ft-kips}$$

Figure 4-27. Story shears and overturning moment (Example 4-6)

$$\begin{aligned} M_o &= 27.10(43.5) + 27.36(33) + \\ &\quad 21.14(22.5) + 13.24(12) \\ &= 2716 \text{ ft-kips} \end{aligned}$$

The displacement is

$$v_{max} = \phi(\phi/m^*) S_d = \phi \alpha S_d$$

where

$$S_d = S_{pa} / \omega^2 \quad \text{and} \quad \alpha = \varphi / m^*$$

$$S_d = \frac{(0.185)(386.4)}{(8.715)^2} = 0.941$$

$$\alpha = \frac{0.827}{0.666} = 1.242$$

$$v_i = (1.242)(0.941)\phi_i = 1.168\phi_i$$

$$v_4 = 1.168 \text{ in.} \quad v_3 = 1.035 \text{ in.}$$

$$v_2 = 0.80 \text{ in.} \quad v_1 = 0.50 \text{ in.}$$

4.5 RESPONSE OF NONLINEAR SDOF SYSTEMS

In an earlier section it was shown that the response of a linear structural system could be evaluated using the Duhamel integral. The approach was limited to linear systems because the Duhamel-integral approach makes use of the principle of superposition in developing the method. In addition, evaluation of the Duhamel integral for earthquake input motions will require the use of numerical methods in evaluating the integral. For these reasons it may be more expedient to use numerical integration procedures directly for evaluating the response of linear systems to general dynamic loading. These methods have the additional advantage that with only a slight modification they can be used to evaluate the dynamic response of nonlinear systems. Many structural systems will experience nonlinear response sometime during their life. Any moderate to strong earthquake will drive a structure designed by conventional methods into the inelastic range, particularly in certain critical regions. A very useful numerical integration technique for problems of structural dynamics is the so called step-by-step integration procedure. In this procedure the time history under consideration is divided into a number of small time increments Δt . During a small time step, the behavior of the structure is assumed to be linear. As nonlinear behavior occurs, the incremental stiffness is modified. In this manner, the response of the nonlinear system is approximated by a series of linear systems having a changing stiffness. The

velocity and displacement computed at the end of one time interval become the initial conditions for the next time interval, and hence the process may be continued step by step.

4.5.1 Numerical Formulation of Equation of Motion

This section considers SDOF systems with properties m , c , $k(t)$ and $p(t)$, of which the applied force and the stiffness are functions of time. The stiffness is actually a function of the yield condition of the restoring force, and this in turn is a function of time. The damping coefficient may also be considered to be a function of time; however, general practice is to determine the damping characteristics for the elastic system and to keep these constant throughout the complete time history. In the inelastic range the principle mechanism for energy dissipation is through inelastic deformation, and this is taken into account through the hysteretic behavior of the restoring force.

The numerical equation required to evaluate the nonlinear response can be developed by first considering the equation of dynamic equilibrium given previously by Equation 4-6. It has been stated previously that this equation must be satisfied at every increment of time. Considering the time at the end of a short time step, Equation 4-6 can be written as

$$f_i(t + \Delta t) + f_d(t + \Delta t) + f_s(t + \Delta t) = p(t + \Delta t) \quad (4-76)$$

where the forces are defined as

$$f_i = m\ddot{v}(t + \Delta t)$$

$$f_d = c\dot{v}(t + \Delta t)$$

$$f_s = \sum_{i=1}^n k_i(t) \Delta v_i(t) = r_t + k(t) \Delta v(t) \quad (4-77)$$

$$\Delta v(t) = v(t + \Delta t) - v(t)$$

$$r_t = \sum_{i=1}^{n-1} k_i(t) \Delta v_i(t)$$

and in the case of ground accelerations

$$p(t + \Delta t) = p_e(t + \Delta t) = -m\ddot{g}(t + \Delta t) \quad (4-78)$$

Substituting Equations 4-77 and 4-78 into Equation 4-76 results in an equation of motion of the form

$$m\ddot{v}(t + \Delta t) + c\dot{v}(t + \Delta t) + \sum k_i \Delta v_i = -m\ddot{g}(t + \Delta t) \quad (4-79)$$

It should be noted that the incremental stiffness is generally defined by the tangent stiffness at the beginning of the time interval

$$k_i = \frac{df_s}{dv} \quad (4-80)$$

In addition, the dynamic properties given in Equations 4-77 and 4-78 can readily be exchanged for the generalized properties when considering a generalized SDOF system.

4.5.2 Numerical Integration

Many numerical integration schemes are available in the literature. The technique considered here is a step-by-step procedure in which the acceleration during a small time increment is assumed to be constant. A slight variation of this procedure, in which the acceleration is assumed to vary linearly during a small time increment, is described in detail by Clough and Penzien.⁽⁴⁻⁴⁾ Both procedures have been widely used and have been found to yield good results with minimal computational effort.

If the acceleration is assumed to be constant during the time interval, the equations for the constant variation of the acceleration, the linear variation of the velocity and the quadratic variation of the displacement are indicated in Figure 4-28. Evaluating the expression for velocity and displacement at the end of the time interval leads to the following two expressions for velocity and displacement:

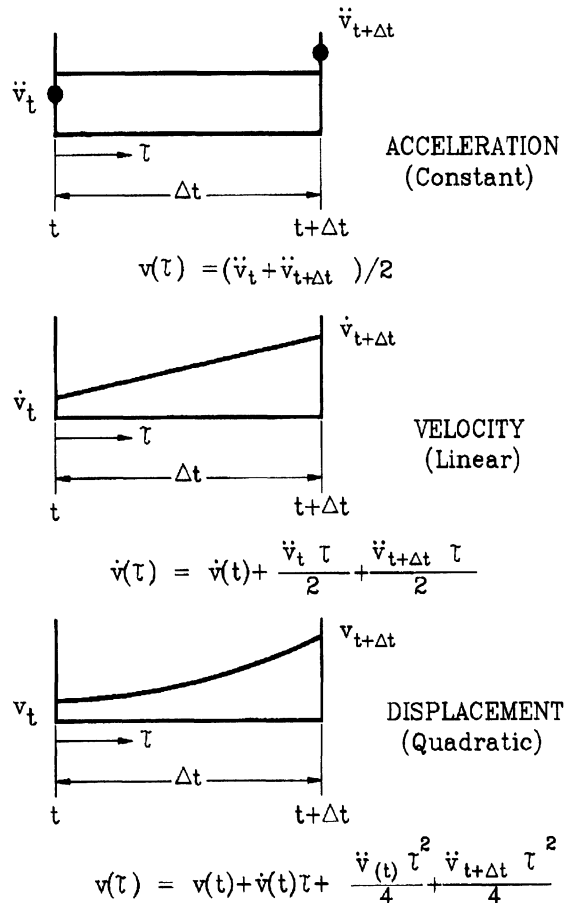


Figure 4-28. Increment motion (constant acceleration).

$$\dot{v}(t + \Delta t) = \dot{v}(t) + \ddot{v}(t + \Delta t) \frac{\Delta t}{2} + \ddot{v}(t) \frac{\Delta t}{2} \quad (4-81)$$

$$v(t + \Delta t) = v(t) + \dot{v}(t)\Delta t + \ddot{v}(t + \Delta t) \frac{\Delta t^2}{4} + \ddot{v}(t) \frac{\Delta t^2}{4} \quad (4-82)$$

Solving Equation 4-82 for the acceleration $\ddot{v}(t + \Delta t)$ gives

$$\ddot{v}(t + \Delta t) = \frac{4}{\Delta t^2} \Delta v - \frac{4}{\Delta t} \dot{v}(t) - \ddot{v}(t) \quad (4-83)$$

which can be written as

$$\ddot{v}(t + \Delta t) = \frac{4}{\Delta t^2} \Delta v + A(t) \quad (4-84)$$

where

$$\Delta v = v(t + \Delta t) - v(t)$$

$$A(t) = -\frac{4}{\Delta t} \dot{v}(t) - \ddot{v}(t)$$

Note that this equation expresses the acceleration at the end of the time interval as a function of the incremental displacement and the acceleration and velocity at the beginning of the time interval. Substituting Equation 4-83 into Equation 4-81 gives the following expression for the velocity at the end of the time increment:

$$\dot{v}(t + \Delta t) = \frac{2}{\Delta t} \Delta v - \dot{v}(t) \quad (4-85)$$

which can be written as

$$\dot{v}(t + \Delta t) = \frac{2}{\Delta t} \Delta v + B(t) \quad (4-86)$$

where

$$B(t) = -\dot{v}(t)$$

It is convenient to express the damping as a linear function of the mass:

$$c = \alpha m = \lambda C_{cr} = 2m\omega\lambda \quad (4-87)$$

Use of this equation allows the proportionality factor α to be expressed as

$$\alpha = 2\lambda\omega \quad (4-88)$$

Substituting Equations 4-85, 4-86, and 4-88 into Equation 4-79 results in the following form of the equation for dynamic equilibrium:

$$\begin{aligned} m \left[\frac{4}{\Delta t^2} \Delta v + A(t) \right] + \alpha m \left[\frac{2}{\Delta t} \Delta v + B(t) \right] + R(t) + k \Delta v \\ = m \ddot{g}(t + \Delta t) \end{aligned} \quad (4-89)$$

Moving terms containing the response conditions at the beginning of the time interval to the right-hand side of the equation results in the following so-called pseudo-static form of the equation of motion:

$$\bar{k}_t(\Delta v) = \bar{p}(t + \Delta t) \quad (4-90)$$

where

$$\bar{k}_t = \frac{4m}{\Delta t^2} + \frac{2\alpha m}{\Delta t} + k_t$$

$$\begin{aligned} \bar{p}(t + \Delta t) &= -m \ddot{g}(t + \Delta t) - R(t) \\ &\quad - m[A(t) - \alpha B(t)] \end{aligned}$$

The solution procedure for a typical time step is as follows:

1. Given the initial conditions at the beginning of the time interval, calculate the coefficients $A(t)$ and $B(t)$.
2. Calculate the effective stiffness.
3. Determine the effective force.
4. Solve for the incremental displacement

$$v = \bar{p} / \bar{k}_t \quad (4-91)$$

5. Determine the displacement, velocity and acceleration at the end of the time interval:

$$\begin{aligned} v(t + \Delta t) &= v(t) + \Delta v \\ \dot{v}(t + \Delta t) &= \frac{2}{\Delta t} + B(t) \\ \ddot{v}(t + \Delta t) &= \frac{4}{\Delta t^2} + A(t) \end{aligned} \quad (4-92)$$

6. The values given in Equation 4-92 become the initial conditions for the next time increment, and the procedure is repeated.

The above algorithm can be easily programmed on any microcomputer. If it is combined with a data base of recorded earthquake data such as EQINFOS,⁽⁴⁻⁶⁾ it can be used to gain considerable insight into the linear and nonlinear response of structures that can be modeled as either a SDOF system or as a generalized SDOF system. It also forms the background material for later developments for multiple-degree-of-freedom systems.

An important response parameter that is unique to nonlinear systems is the ductility ratio. For a SDOF system, this parameter can be defined in terms of the displacement as

$$\mu = \frac{v(\max)}{v(\text{yield})} = 1.0 + \frac{v(\text{plastic})}{v(\text{yield})} \quad (4-93)$$

As can be seen from the above equation, the ductility ratio is an indication of the amount of inelastic deformation that has occurred in the system. In the case of a SDOF system or generalized SDOF system the ductility obtained from Equation 4-93 usually represents the average ductility in the system. The ductility demand at certain critical regions, such as plastic hinges in critical members, may be considerably higher.

4.6 MULTIPLE-DEGREE-OF-FREEDOM SYSTEMS

In many structural systems it is impossible to model the dynamic response accurately in terms of a single displacement coordinate. These systems require a number of independent displacement coordinates to describe the displacement of the mass of the structure at any instant of time.

4.6.1 Mass and Stiffness Properties

In order to simplify the solution it is usually assumed for building structures that the mass of the structure is lumped at the center of mass of the individual story levels. This results in a

diagonal matrix of mass properties in which either the translational mass or the mass moment of inertia is located on the main diagonal.

$$\{f_i\} = \begin{bmatrix} m_1 & & & & & v_1 \\ & m_2 & & & & v_2 \\ & & m_3 & & & v_3 \\ & & & \ddots & & \vdots \\ & & & & \ddots & \vdots \\ & & & & & m_n \end{bmatrix} \begin{bmatrix} v_1 \\ v_2 \\ v_3 \\ \vdots \\ \vdots \\ v_n \end{bmatrix} \quad (4-94)$$

It is also convenient for building structures to develop the structural stiffness matrix in terms of the stiffness matrices of the individual story levels. The simplest idealization for a multistory building is based on the following three assumptions: (i) the floor diaphragm is rigid in its own plane; (ii) the girders are rigid relative to the columns and (iii) the columns are flexible in the horizontal directions but rigid in the vertical. If these assumptions are used, the building structure is idealized as having three dynamic degrees of freedom at each story level: a translational degree of freedom in each of two orthogonal directions, and a rotation about a vertical axis through the center of mass. If the above system is reduced to a plane frame, it will have one horizontal translational degree of freedom at each story level. The stiffness matrix for this type of structure has the tridiagonal form shown below:

For the simplest idealization, in which each story level has one translational degree of freedom, the stiffness terms k_i in the above equations represent the translational story stiffness of the i th story level. As the assumptions given above are relaxed to include axial deformations in the columns and flexural deformations in the girders, the stiffness term k_i in Equation 4-95 becomes a submatrix of stiffness terms, and the story displacement v_i

$$\{f_s\} = \begin{bmatrix} k_1 & -k_2 \\ k_2 & k_1 + k_2 & -k_3 \\ -k_3 & k_2 + k_3 & -k_4 \\ & \ddots & \ddots & \ddots \\ & & \ddots & \ddots & \ddots \\ & & & -k_n & v_{n-1} \\ -k_n & k_{n-1} + k_n & v_n \end{bmatrix} \quad (3-95)$$

becomes a subvector containing the various displacement components in the particular story level. The calculation of the stiffness coefficients for more complex structures is a standard problem of static structural analysis. For the purposes of this chapter it will be assumed that the structural stiffness matrix is known.

4.6.2 Mode Shapes and Frequencies

The equations of motion for undamped free vibration of a multiple-degree-of-freedom (MDOF) system can be written in matrix form as

$$[M]\{\ddot{v}\} + [K]\{v\} = \{0\} \quad (4-96)$$

Since the motions of a system in free vibration are simple harmonic, the displacement vector can be represented as

$$\{v\} = \{\bar{v}\} \sin \omega t \quad (4-97)$$

Differentiating twice with respect to time results in

$$\{\ddot{v}\} = -\omega^2 \{v\} \quad (4-98)$$

Substituting Equation 4-98 into Equation 4-96 results in a form of the eigenvalue equation,

$$([K] - \omega^2 [M])\{v\} = \{0\} \quad (4-99)$$

The classical solution to the above equation derives from the fact that in order for a set of homogeneous equilibrium equations to have a nontrivial solution, the determinant of the coefficient matrix must be zero:

$$\det([K] - \omega^2 [M]) = \{0\} \quad (4-100)$$

Expanding the determinant by minors results in a polynomial of degree N , which is called the frequency equation. The N roots of the polynomial represent the frequencies of the N modes of vibration. The mode having the lowest frequency (longest period) is called the first or fundamental mode. Once the frequencies are known, they can be substituted one at a time into the equilibrium Equation 4-99, which can then be solved for the relative amplitudes of motion for each of the displacement components in the particular mode of vibration. It should be noted that since the absolute amplitude of motion is indeterminate, $N-1$ of the displacement components are determined in terms of one arbitrary component.

This method can be used satisfactorily for systems having a limited number of degrees of freedom. Programmable calculators have programs for solving the polynomial equation and for doing the matrix operations required to determine the mode shapes. However, for

problems of any size, digital computer programs which use numerical techniques to solve large eigenvalue systems⁽⁴⁻⁷⁾ must be used.

Example 4-8 (Mode Shapes and Frequencies)

It is assumed that the response in the transverse direction for the reinforced-concrete moment frame of Example 4-4 can be represented in terms of four displacement degrees of freedom which represent the horizontal displacements of the four story levels. Determine the stiffness matrix and the mass matrix, assuming that the mass is lumped at the story levels. Use these properties to calculate the frequencies and mode shapes of the four-degree-of-freedom system.

•*Stiffness and mass matrices:* The stiffness coefficient κ_{ij} is defined as the force at coordinate i due to a unit displacement at coordinate j , all other displacements being zero (see Figure 4-29):

where $B = \omega^2/800$

•*Characteristic equation:*

$$|[K] - \omega^2[M]| = 0$$

$$B^4 - 6.183B^3 + 11.476B^2 - 6.430B + 0.486 = 0$$

Solution:

$$B_1 = 0.089 = \frac{\omega_1^2}{800}, \omega_1 = 8.438, T_1 = 0.744 \text{ sec}$$

$$B_2 = 0.830 = \frac{\omega_2^2}{800}, \omega_2 = 25.768, T_2 = 0.244 \text{ sec}$$

$$B_3 = 2.039 = \frac{\omega_3^2}{800}, \omega_3 = 40.388, T_3 = 0.155 \text{ sec}$$

$$B_4 = 3.225 = \frac{\omega_4^2}{800}, \omega_4 = 50.800, T_4 = 0.124 \text{ sec}$$

•*Mode shapes* (see Figure 4-29) are obtained by substituting the values of B_i , one at a time, into the equations

$$([K] - \omega^2[M])\{v\} = \{0\}$$

and determining N-1 components of the displacement vector in terms of the first component, which is set equal to unity. This results in the modal matrix

$$[\Phi] = \begin{bmatrix} 1.00 & 1.00 & 1.00 & 1.00 \\ 0.91 & 0.20 & -1.07 & -1.78 \\ 0.74 & -0.78 & -0.75 & 1.75 \\ 0.47 & -1.05 & 1.24 & -0.92 \end{bmatrix}$$

Solution of the above problem using the computer program ETABS⁽⁴⁻¹²⁾ gives the following results:

$$[K] = \begin{bmatrix} 209 & -209 & 0 & 0 \\ -209 & 418 & -209 & 0 \\ 0 & -209 & 418 & -209 \\ 0 & 0 & -209 & 349 \end{bmatrix}$$

$$[M] = \frac{1}{4} \begin{bmatrix} 1.01 & 0 & 0 & 0 \\ 0 & 1.15 & 0 & 0 \\ 0 & 0 & 1.15 & 0 \\ 0 & 0 & 0 & 1.16 \end{bmatrix}$$

$$[K] - \omega^2[M] = 200 \begin{bmatrix} 1.05 - 1.01B & -1.05 & 0 & 0 \\ -1.05 & 2.09 - 1.15B & -1.05 & 0 \\ 0 & -1.05 & 2.09 - 1.15B & -1.05 \\ 0 & 0 & -1.05 & 1.74 - 1.16B \end{bmatrix}$$

$$\{T\} = \begin{Bmatrix} 0.838 \\ 0.268 \\ 0.152 \\ 0.107 \end{Bmatrix}$$

$$[\Phi] = \begin{bmatrix} 1.00 & 1.00 & 1.00 & 1.00 \\ 0.91 & 0.20 & -1.07 & -1.78 \\ 0.74 & -0.78 & 0.75 & 1.75 \\ 0.47 & -1.05 & 1.24 & -0.92 \end{bmatrix}$$

This program assumes the floor diaphragm is rigid in its own plane but allows axial deformation in the columns and flexural deformations in the beams. Hence, with these added degrees of freedom (fewer constraints) the fundamental period increases. However, comparing the results of this example with those of Example 4-5, it can be seen that for this structure a good approximation for the first-mode response was obtained using the generalized SDOF model and the static deflected shape.

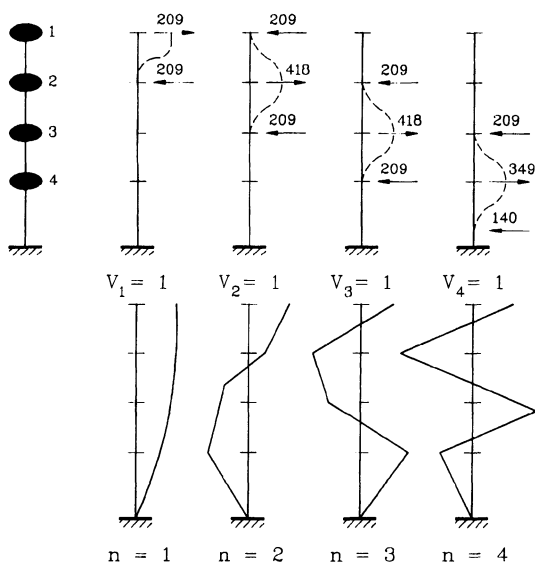


Figure 4-29. Stiffness determination and mode shape(Example 4-8).

4.6.3 Equations of Motion in Normal Coordinates

Betti's reciprocal work theorem can be used to develop two orthogonality properties of vibration mode shapes which make it possible to greatly simplify the equations of motion. The first of these states that the mode shapes are orthogonal to the mass matrix and is expressed in matrix form as

$$\{\phi_n\}^T [M] \{\phi_m\} = \{0\} \quad (m \neq n) \quad (4-101)$$

Using Equations 4-99 and 4-101, the second property can be expressed in terms of the stiffness matrix as

$$\{\phi_n\}^T [K] \{\phi_m\} = \{0\} \quad (m \neq n) \quad (4-102)$$

which states that the mode shapes are orthogonal to the stiffness matrix. It is further assumed that the mode shapes are also orthogonal to the damping matrix:

$$\{\phi_n\}^T [C] \{\phi_m\} = \{0\} \quad (m \neq n) \quad (4-103)$$

Sufficient conditions for this assumption have been discussed elsewhere.⁽⁴⁻⁸⁾ Since any MDOF system having N degrees of freedom also has N independent vibration mode shapes, it is possible to express the displaced shape of the structure in terms of the amplitudes of these shapes by treating them as generalized coordinates (sometimes called normal coordinates). Hence the displacement at a particular location, v_b can be obtained by summing the contributions from each mode as

$$v_i = \sum_{n=1}^N \phi_{in} Y_n \quad (4-104)$$

In a similar manner, the complete displacement vector can be expressed as

$$\{v\} = \sum_{n=1}^N \{\phi_n\} Y_n = [\Phi]\{Y\} \quad (4-105)$$

It is convenient to write the equations of motion for a MDOF system in matrix form as

$$[M]\{\ddot{v}\} + [C]\{\dot{v}\} + [K]\{v\} = \{P(t)\} \quad (4-106)$$

which is similar to the equation for a SDOF system, Equation 4-9. The differences arise because the mass, damping, and stiffness are now represented by matrices of coefficients representing the added degrees of freedom, and the acceleration, velocity, displacement, and applied load are represented by vectors containing the additional degrees of freedom. The equations of motion can be expressed in terms of the normal coordinates by substituting Equation 4-105 and its appropriate derivatives into Equation 4-106 to give

$$[M][\Phi]\{\ddot{Y}\} + [C][\Phi]\{\dot{Y}\} + [K][\Phi]\{Y\} = \{P(t)\} \quad (4-107)$$

Multiplying the above equation by the transpose of any modal vector $\{\phi_n\}$ results in the following:

$$\begin{aligned} & \{\phi_n\}^T [M][\Phi]\{\ddot{Y}\} + \{\phi_n\}^T [C][\Phi]\{\dot{Y}\} \\ & + \{\phi_n\}^T [K][\Phi]\{Y\} = \{\phi_n\}^T \{P(t)\} \end{aligned} \quad (4-108)$$

Using the orthogonality conditions of Equations 4-101, 4-102, and 4-103 reduces this set of equations to the equation of motion for a generalized SDOF system in terms of the generalized properties for the n th mode shape and the normal coordinate Y_n :

$$M_n^* \ddot{Y}_n + C_n^* \dot{Y}_n + K_n^* Y_n = P_n^*(t) \quad (4-109)$$

where the generalized properties for the n th mode are given as

$$M_n^* = \text{generalized mass} = \{\phi_n\}^T [M] \{\phi_n\}$$

$$C_n^* = \text{generalized damping} = \{\phi_n\}^T [C] \{\phi_n\} = 2\lambda_n \omega_n M_n^*$$

$$K_n^* = \text{generalized stiffness} = \{\phi_n\}^T [K] \{\phi_n\} = \omega_n^2 M_n^*$$

$$P_n^*(t) = \text{generalized loading} = \{\phi_n\}^T \{P(t)\} \quad (4-110)$$

The above relations can be used to further simplify the equation of motion for the n th mode to the form

$$\ddot{Y}_n + 2\lambda_n \omega_n \dot{Y}_n + \omega_n^2 Y_n = \frac{P_n^*(t)}{M_n^*} \quad (4-111)$$

The importance of the above transformations to normal coordinates has been summarized by Clough and Penzien,⁽⁴⁻⁴⁾ who state that

The use of normal coordinates serves to transform the equations of motion from a set of N simultaneous differential equations which are coupled by off diagonal terms in the mass and stiffness matrices to a set of N independent normal coordinate equations.

It should further be noted that the expressions for the generalized properties of any mode are equivalent to those defined previously for a generalized SDOF system. Hence the use of the normal modes transforms the MDOF system having N degrees of freedom into a system of N independent generalized SDOF systems. The complete solution for the system is then obtained by superimposing the independent modal solutions. For this reason this method is often referred to as the modal-superposition method. Use of this method also leads to a significant saving in computational effort, since in most cases it will not be necessary to use all N modal responses to accurately represent the response of the structure. For most structural systems the lower modes make the primary contribution to the total response. Therefore, the response can

usually be represented to sufficient accuracy in terms of a limited number of modal responses in the lower modes.

4.6.4 Earthquake-Response Analysis

Time-History Analysis As in the case of SDOF systems, for earthquake analysis the time-dependent force must be replaced with the effective loads, which are given by the product of the mass at any level, M , and the ground acceleration $\ddot{g}(t)$. The vector of effective loads is obtained as the product of the mass matrix and the ground acceleration:

$$P_e(t) = [M]\{\Gamma\}\ddot{g}(t) \quad (4-112)$$

where $\{\Gamma\}$ is a vector of influence coefficients of which component i represents the acceleration at displacement coordinate i due to a unit ground acceleration at the base. For the simple structural model in which the degrees of freedom are represented by the horizontal displacements of the story levels, the vector $\{\Gamma\}$ becomes a unity vector, $\{1\}$, since for a unit ground acceleration in the horizontal direction all degrees of freedom have a unit horizontal acceleration. Using Equation 4-108, the generalized effective load for the n th mode is given as

$$P_{en}^*(t) = L_n g(t) \quad (4-113)$$

$$\text{Where } L_n = \{\phi_n\}^T [M]\{\Gamma\}$$

Substituting Equation 4-113 into Equation 4-111 results in the following expression for the earthquake response of the n th mode of a MDOF system:

$$\ddot{Y}_n + 2\lambda_n \omega_n \dot{Y}_n + \omega_n^2 Y_n = \varphi_n \ddot{g}(t) / M_n^* \quad (4-114)$$

In a manner similar to that used for the SDOF system, the response of this mode at any

time t can be obtained by the Duhamel integral expression

$$Y_n(t) = \frac{\varphi_n V_n(t)}{M_n^* \omega_n} \quad (4-115)$$

where $V_n(t)$ represents the integral

$$V_n(t) = \int_0^t \ddot{g}(\tau) e^{-\lambda_n \omega_n (t-\tau)} \sin \omega_n (t-\tau) d\tau \quad (4-116)$$

The complete displacement of the structure at any time is then obtained by superimposing the contributions of the individual modes using Equation 4-105

$$\{v(t)\} = \sum_{n=1}^N \{\phi_n\} Y_n(t) = [\Phi]\{Y(t)\} \quad (4-117)$$

The resulting earthquake forces can be determined in terms of the effective accelerations, which for each mode are given by the product of the circular frequency and the displacement amplitude of the generalized coordinate:

$$\ddot{Y}_{ne}(t) = \omega_n^2 Y_n(t) = \frac{\varphi_n \omega_n V_n(t)}{M_n^*} \quad (4-118)$$

The corresponding acceleration in the structure due to the n th mode is given as

$$\{\ddot{v}_{ne}(t)\} = \{\phi_n\} \ddot{Y}_{ne}(t) \quad (4-119)$$

and the corresponding effective earthquake force is given as

$$\begin{aligned} \{q_n(t)\} &= [M]\{\ddot{v}_n(t)\} \\ &= [M]\{\phi_n\} \omega_n \varphi_n V_n(t) / M_n^* \end{aligned} \quad (4-120)$$

The total earthquake force is obtained by superimposing the individual modal forces to obtain

$$q(t) = \sum_{n=1}^N q_n(t) = [M][\Phi]\omega^2 Y(t) \quad (4-121)$$

The base shear can be obtained by summing the effective earthquake forces over the height of the structure:

$$\begin{aligned} Q_n(t) &= \sum_{i=1}^H q_{in}(t) = \{1\}^T \{q_n(t)\} \\ &= M_{en} \omega_n V_n(t) \end{aligned} \quad (4-122)$$

where $M_{en} = L_n^2 / M_n^*$ is the effective mass for the n th mode.

The sum of the effective masses for all of the modes is equal to the total mass of the structure. This results in a means of determining the number of modal responses necessary to accurately represent the overall structural response. If the total response is to be represented in terms of a finite number of modes and if the sum of the corresponding modal masses is greater than a predefined percentage of the total mass, the number of modes considered in the analysis is adequate. If this is not the case, additional modes need to be considered. The base shear for the n th mode, Equation 4-122, can also be expressed in terms of the effective weight, W_{en} , as

$$Q_n(t) = \frac{W_{en}}{g} \omega_n V_n(t) \quad (4-123)$$

where

$$W_{en} = \frac{\left(\sum_{i=1}^H W_i \phi_{in} \right)^2}{\sum_{i=1}^H W_i \phi_{in}^2} \quad (4-124)$$

The base shear can be distributed over the height of the building in a manner similar to Equation 4-74, with the modal earthquake forces expressed as

$$\{q_n(t)\} = \frac{[M]\{\phi_n\}Q_n(t)}{L_n} \quad (4-125)$$

4.6.5 Response-Spectrum Analysis

The above equations for the response of any mode of vibration are exactly equivalent to the expressions developed for the generalized SDOF system. Therefore, the maximum response of any mode can be obtained in a manner similar to that used for the generalized SDOF system. By analogy to Equations 4-34 and 4-43 the maximum modal displacement can be written as

$$Y_n(t)_{\max} = \frac{V_n(t)_{\max}}{\omega_n} = S_{dn} \quad (4-126)$$

Making this substitution in Equation 4-115 results in

$$Y_{n \max} = \varphi_n S_{dn} / M_n^* \quad (4-127)$$

The distribution of the modal displacements in the structure can be obtained by multiplying this expression by the modal vector

$$\{v_n\}_{\max} = \{\phi_n\} Y_{n \max} = \frac{\{\phi_n\} L_n S_{dn}}{M_n^*} \quad (4-128)$$

The maximum effective earthquake forces can be obtained from the modal accelerations as given by Equation 4-120:

$$\{q_n\}_{\max} = \frac{[M]\{\phi_n\}\varphi_n S_{pan}}{M_n^*} \quad (4-129)$$

Summing these forces over the height of the structure gives the following expression for the maximum base shear due to the n th mode:

$$Q_{n \max} = \varphi_n^2 S_{pan} / M_n^* \quad (4-130)$$

which can also be expressed in terms of the effective weight as

$$Q_{n \max} = W_{en} S_{pan} / g \quad (4-131)$$

where W_{en} is defined by Equation 4-124.

Finally, the overturning moment at the base of the building for the n th mode can be determined as

$$M_o = \langle h \rangle [M] \{ \phi_n \} \sum_n S_{pan} / M_n^* \quad (4-132)$$

where $\langle h \rangle$ is a row vector of the story heights above the base.

4.6.6 Modal Combinations

Using the response-spectrum method for MDOF systems, the maximum modal response is obtained for each mode of a set of modes, which are used to represent the response. The question then arises as to how these modal maxima should be combined in order to get the best estimate of the maximum total response. The modal-response equations such as Equations 4-117 and 4-121 provide accurate results only as long as they are evaluated concurrently in time. In going to the response-spectrum approach, time is taken out of these equations and replaced with the modal maxima. These maximum response values for the individual modes cannot possibly occur at the same time; therefore, a means must be found to combine the modal maxima in such a way as to approximate the maximum total response. One such combination that has been used is to take the sum of the absolute values (SAV) of the modal responses. This combination can be expressed as

$$r \leq \sum_{n=1}^N |r_n| \quad (4-133)$$

Since this combination assumes that the maxima occur at the same time and that they also have the same sign, it produces an upper-bound estimate for the response, which is too conservative for design application. A more reasonable estimate, which is based on probability theory, can be obtained by using the square-root-of-the-sum-of-the-squares (SRSS) method, which is expressed as

$$r \approx \sqrt{\sum_{n=1}^N r_n^2} \quad (4-134)$$

This method of combination has been shown to give a good approximation of the response for two-dimensional structural systems. For three-dimensional systems, it has been shown that the complete-quadratic-combination (CQC) method ⁽⁴⁻⁹⁾ may offer a significant improvement in estimating the response of certain structural systems. The complete quadratic combination is expressed as

$$r \approx \sqrt{\sum_{i=1}^N \sum_{j=1}^N r_i p_{ij} r_j} \quad (4-135)$$

where for constant modal damping

$$p_{ij} = \frac{8\lambda^2(1+\zeta)\zeta^{3/2}}{(1-\zeta^2)^2 + 4\lambda^2\zeta(1+\zeta)^2} \quad (4-136)$$

and

$$\zeta = \omega_j / \omega_i$$

$$\lambda = c / c_{cr}$$

Using the SRSS method for two-dimensional systems and the CQC method for either two- or three-dimensional systems will give a good approximation to the maximum earthquake response of an elastic system without requiring a complete time-history analysis. This is particularly important for purposes of design.

Table 3-3. Computation of response for model of Example 4-8

Param eter	Modal	Modal Response				SAV	SRSS	CQC
	n = 1	2	3	4				
$\omega =$	8.44	25.77	40.39	50.80				
$\alpha_n =$	1.212	-0.289	0.075	0.010				
$S_d =$	1.190	0.155	0.062	0.039				
	1.00	1.00	1.00	1.00				
	0.91	0.20	-1.07	-1.78				
Response Quantity	$\phi =$	0.74	-0.78	-0.75	1.75	Combined Response		
		0.47	-1.05	1.24	-0.92	SAV	SRSS	CQC
Displacement	n = 4	1.44	-0.045	0.019	-0.002	1.506	1.441	1.441
$v_n = \phi_n \alpha_n S_{dn}$ (Eq. 3.128)	3	1.31	-0.009	-0.020	0.003	1.342	1.310	1.310
	2	1.07	0.035	-0.014	-0.003	1.122	1.071	1.071
	1	0.68	0.047	0.023	0.001	0.751	0.682	0.682
Acceleration	n = 4	102.6	-29.9	31.0	-5.1	168.6	111.4	110.7
$\ddot{v}_n = \omega_n^2 v_n$	3	93.3	-6.0	-32.6	7.7	139.6	99.3	98.9
	2	76.2	23.2	-22.8	-7.7	129.9	83.2	83.3
	1	48.4	31.2	37.5	2.6	119.7	68.8	70.0
Inertia force	n = 4	25.91	-7.54	7.83	-1.30	42.6	28.1	27.9
$q_n = M \ddot{v}_n$	3	26.82	-1.72	-9.38	2.23	40.2	28.6	28.4
	2	21.91	6.68	-6.56	-2.23	37.4	23.9	23.9
	1	14.03	9.05	11.35	0.75	35.2	20.2	20.6
Shear	n = 4	25.91	-7.54	7.83	-1.30	42.6	28.1	28.0
$Q_n = \Sigma q_n$	3	52.73	-9.26	-1.55	0.93	64.5	53.6	53.5
	2	74.64	-2.58	-8.11	-1.30	86.6	75.1	75.1
	1	88.67	6.47	3.24	-0.55	98.9	89.0	89.0
Overturning Moment (ft-kips)	n = 4	272.1	-79.2	82.2	-13.7	447.2	295.4	293.6
	3	825.7	-176.4	65.9	-3.9	1071.9	846.9	845.3
	2	1609.4	-203.5	-19.2	-17.5	1849.6	1622.4	1621.3
	1	2673.4	-125.9	19.7	-24.1	2843.1	2676.5	2675.7

Example 4-9 (Response Spectrum Analysis)

Use the design response spectrum given in Example 4-7 and the results of Example 4-8 to perform a response-spectrum analysis of the reinforced concrete frame. Determine the modal responses of the four modes of vibration, and estimate the total response using the SAV, SRSS, and CQC methods of modal combination. Present the data in a tabular form suitable for hand calculation. Finally, compare the results with those obtained in Example 4-6 for a generalized SDOF model.

From Example 4-7,

$$[M] = \frac{1}{4} \begin{bmatrix} 1.01 & 0 & 0 & 0 \\ 0 & 1.15 & 0 & 0 \\ 0 & 0 & 1.15 & 0 \\ 0 & 0 & 0 & 1.16 \end{bmatrix}$$

$$\{\omega\} = \begin{Bmatrix} 8.44 \\ 25.77 \\ 40.39 \\ 50.80 \end{Bmatrix} \frac{r}{\text{sec}}$$

$$[\Phi] = \begin{bmatrix} 1.00 & 1.00 & 1.00 & 1.00 \\ 0.91 & 0.20 & -1.07 & -1.78 \\ 0.74 & -0.78 & -0.75 & 1.75 \\ 0.47 & -1.05 & 1.24 & -0.92 \end{bmatrix}$$

$$\{f\} = \frac{\omega}{2\pi} = \begin{bmatrix} 1.34 \\ 4.10 \\ 6.43 \\ 8.09 \end{bmatrix} \text{Hz}$$

$$S_v = \begin{bmatrix} 10.0 \\ 4.0 \\ 2.5 \\ 2.0 \end{bmatrix} \text{in./sec}$$

$$S_{dn} = S_{vn} / \omega_n$$

From Equation 4-128,

$$\{v_n\}_{\max} = \{\phi_n\}(\phi_n / M_n^*)S_{dn} = \{\phi\}\alpha S_{dn}$$

$$\{q_n\} = [M]\{\ddot{v}_n\} = [M]\omega^2\{v_n\}$$

$$Q_n = \sum_{i=1}^N q_{ni}$$

For CQC combination,

$\lambda = 0.05$ = constant for all modes

$$P_{ij} = \begin{bmatrix} 1.0000 & 0.0062 & .0025 & .0017 \\ 0.0062 & 1.0000 & 0.0452 & 0.0193 \\ 0.0025 & 0.0452 & 1.0000 & 0.1582 \\ 0.0017 & 0.0193 & 0.1582 & 1.0000 \end{bmatrix}$$

The computation of the modal and the combined response is tabulated in Table 4-3. The results are compared with those obtained for the SDOF model in Table 4-4.

Table 4-4. Comparison of results obtained from MDOF and SDOF models.

Response parameter	MDOF (Example 3-9)	SDOF (Example 3-7)
Period (sec)	0.744	0.721
Displacements(in)		
Roof	1.44	1.17
3 rd	1.31	1.04
2 nd	1.07	0.80

Response parameter	MDOF (Example 3-9)	SDOF (Example 3-7)
1 st	0.68	0.50
Inertia force (kips)		
Roof	28.1	27.1
3 rd	28.6	27.4
2 nd	23.9	21.1
1 st	20.2	13.2
Base shear (kips)	89.0	88.8
Overshooting moment (ft-kips)	2678	2716

4.7 NONLINEAR RESPONSE OF MDOF SYSTEMS

The nonlinear analysis of buildings modeled as multiple degree of freedom systems (MDOF) closely parallels the development for single degree of freedom systems presented earlier. However, the nonlinear dynamic time history analysis of MDOF systems is currently considered to be too complex for general use. Therefore, recent developments in the seismic evaluation of buildings have suggested a performance-based procedure which requires the determination of the demand and capacity. Demand is represented by the earthquake ground motion and its effect on a particular structural system. Capacity is the structure's ability to resist the seismic demand. In order to estimate the structure's capacity beyond the elastic limit, a static nonlinear (pushover) analysis is recommended ⁽⁴⁻¹⁷⁾. For more demanding investigations of building response, nonlinear dynamic analyses can be conducted.

For dynamic analysis the loading time history is divided into a number of small time increments, whereas, in the static analysis, the lateral force is divided into a number of small force increments. During a small time or force increment, the behavior of the structure is assumed to be linear elastic. As nonlinear behavior occurs, the incremental stiffness is modified for the next time (load) increment. Hence, the response of the nonlinear system is approximated by the response of a sequential series of linear systems having varying stiffnesses.

Static Nonlinear Analysis

Nonlinear static analyses are a subset of nonlinear dynamic analyses and can use the same solution procedure without the time related inertia forces and damping forces. The equations of equilibrium are similar to Equation 4-1 with the exception that they are written in matrix form for a small load increment during which the behavior is assumed to be linear elastic.

$$[K]\{\Delta v\} = \{P\} \quad (4-136a)$$

For computational purposes it is convenient to rewrite this equation in the following form

$$[K_t]\{\Delta v\} + \{R_t\} = \{P\} \quad (4-136b)$$

where K_t is the tangent stiffness matrix for the current load increment and R_t is the restoring force at the beginning of the load increment which is defined as

$$\{R_t\} = \sum_{i=1}^{n-1} [K_{ti}]\{\Delta v_i\}$$

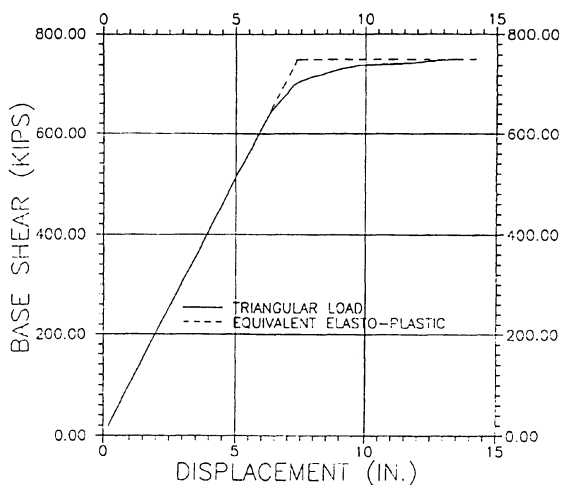


Figure 4-29a. Pushover Curve, Six Story Steel Building.

The lateral force distribution is generally based on the static equivalent lateral forces specified in building codes which tend to

approximate the first mode of vibration. These forces are increased in a proportional manner by a specified load factor. The lateral loading is increased until either the structure becomes unstable or a specified limit condition is attained. The results from this type of analysis are usually presented in the form of a graph plotting base shear versus roof displacement. The pushover curve for a six-story steel building ⁽⁴⁻¹⁸⁾ is shown in Figure 4-29a and the sequence of plastic hinging is shown in Figure 4-29b.

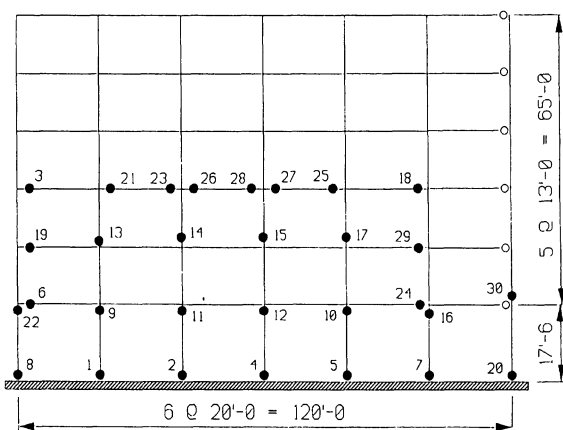


Figure 4-29b Sequence of Plastic Hinge Formation, Six Story Steel Building.

The equations of equilibrium for a multiple degree of freedom system subjected to base excitation can be written in matrix form as

$$[M]\{\ddot{v}\} + [C]\{\dot{v}\} + [K]\{v\} = -[M]\{\Gamma\}\ddot{g}(t) \quad (\text{Eq.4-137})$$

This equation is of the same form as that of Eq. 4-76 for the single degree of freedom system. The acceleration, velocity and displacement have been replaced by vectors containing the additional degrees of freedom. The mass has been replaced by the mass matrix which for a lumped mass system is a diagonal matrix with the translational mass and rotational mass terms on the main diagonal. The incremental stiffness has been replaced by the incremental stiffness matrix and the damping has been replaced by the damping matrix. This

latter term requires some additional discussion. In the mode superposition method, the damping ratio was defined for each mode of vibration. However, this is not possible for a nonlinear system because it has no true vibration modes. A useful way to define the damping matrix for a nonlinear system is to assume that it can be represented as a linear combination of the mass and stiffness matrices of the initial elastic system

$$[C] = \alpha[M] + \beta[K] \quad (\text{Eq 4-138})$$

Where α and β are scalar multipliers which may be selected so as to provide a given percentage of critical damping in any two modes of vibration of the initial elastic system. These two multipliers can be evaluated from the expression

$$\begin{Bmatrix} \alpha \\ \beta \end{Bmatrix} = 2 \begin{bmatrix} \omega_j & -\omega_i \\ -\frac{1}{\omega_j} & \frac{1}{\omega_i} \end{bmatrix} \frac{\omega_i \omega_j}{\omega_j^2 - \omega_i^2} \begin{Bmatrix} \lambda_i \\ \lambda_j \end{Bmatrix} \quad (\text{Eq.4-139})$$

where ω_i and ω_j are the percent of critical damping in the two specified modes. Once the coefficients α and β are determined, the damping in the other elastic modes is obtained from the expression

$$\lambda_k = \frac{\alpha}{2\omega_k} + \frac{\beta\omega_k}{2} \quad (\text{Eq. 4-140})$$

A typical damping function which was used for the nonlinear analysis of a reinforced concrete frame ⁽⁴⁻¹⁰⁾ is shown in Figure 4-30. Although the representation for the damping is only approximate it is justified for these types of analyses on the basis that it gives a good approximation of the damping for a range of modes of vibration and these modes can be selected to be the ones that make the major contribution to the response. Also in nonlinear dynamic analyses the dissipation of energy through inelastic deformation tends of overshadow the dissipation of energy through

viscous damping. Therefore, an exact representation of damping is not as important in a nonlinear system as it is in a linear system. One should be aware of the characteristics of the damping function to insure that important components of the response are not lost. For instance, if the coefficients are selected to give a desired percentage of critical damping in the lower modes and the response of the higher modes is important, the higher mode response may be over damped and its contribution to the total response diminished.

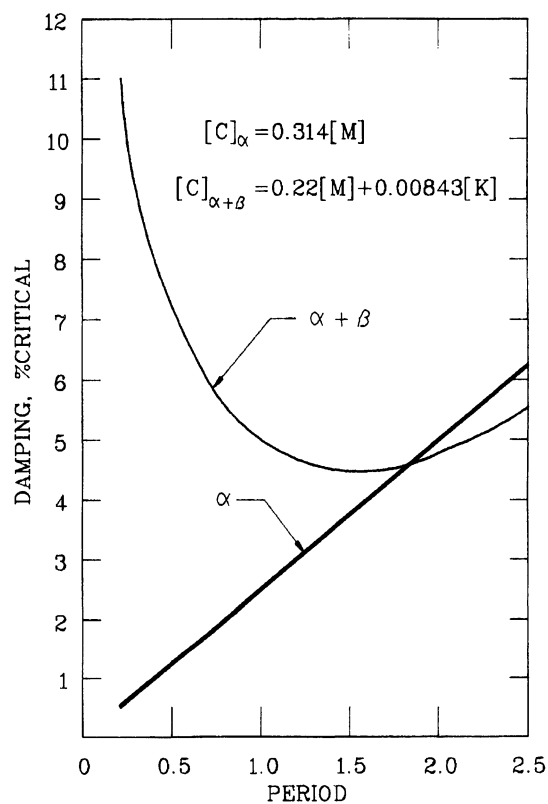


Figure 4-30. Damping functions for a framed tube.

Substituting Eq. 4-138 into Eq. 4-137 results in

$$\begin{aligned} [M]\{\ddot{v}\} + \alpha[M]\{\dot{v}\} + \beta[K_i]\{\dot{v}\} + [K]\{v\} \\ = -[M]\{\Gamma\} \ddot{g}(t) \end{aligned} \quad (\text{Eq. 4-141})$$

where K_i refers to the initial stiffness.

Representing the incremental stiffness in terms of the tangent stiffness, K_t , and rearranging some terms, results in

$$[K]\{\nu\} = [K_t]\{\Delta\nu\} = \{R_t\} + [K_t]\{\Delta\nu\} \quad (\text{Eq. 4-142})$$

where

$$\{R_t\} = \sum_{i=1}^{n-1} [K_{ti}]\{\Delta\nu_i\}$$

Using the step-by-step integration procedure in which the acceleration is assumed to be constant during a time increment, equations similar to Eqs. 4.84 and 4-86 can be developed for the multiple degree of freedom system which express the acceleration and velocity vectors at the end of the time increment in terms of the incremental displacement vector and the vectors of initial conditions at the beginning of the time increment:

$$\{\ddot{v}(t)\} = \left(\frac{4}{\Delta t^2}\right)\{\Delta\nu\} + \{A_t\} \quad (\text{Eq. 4-143})$$

$$\{\dot{v}(t)\} = \left(\frac{2}{\Delta t}\right)\{\Delta\nu\} + \{B_t\} \quad (\text{Eq. 4-144})$$

$$\{\nu(t)\} = \{\nu(t - \Delta t)\} + \{\Delta\nu\} \quad (\text{Eq. 4-144a})$$

where

$$\{A_t\} = -\frac{4}{\Delta t}\{\dot{v}(t - \Delta t)\} - \{\ddot{v}(t - \Delta t)\} \quad (\text{Eq. 4-145})$$

$$\{B_t\} = -\{\dot{v}(t - \Delta t)\} \quad (\text{Eq. 4-146})$$

Substituting Eqs. 4-142 through 4-146 into Eq. 4-141 and rearranging some terms leads to the pseudo-static form

$$[\tilde{K}]\{\Delta\nu\} = \{\tilde{P}\} \quad (\text{Eq. 4-147})$$

where

$$\begin{aligned} [\tilde{K}] &= [C_0[M] + C_1[K_t] + [K_t]] \\ \{\tilde{P}\} &= \{P(t)\} - \{R_t\} \\ &\quad - [M]\{\{A_t\} + \alpha\{B_t\}\} - \beta[K_t]\{B_t\} \\ C_0 &= \frac{4}{\Delta t^2} + \frac{2\alpha}{\Delta t} \\ C_1 &= \frac{2\beta}{\Delta t} \end{aligned}$$

The incremental displacement vector can be obtained by solving Eq. 4-147 for $\{\Delta\nu\}$. This result can then be used in Eqs. 4-143, 4-144 and 4-144a to obtain the acceleration vector, the velocity vector and the displacement vector at the end of the time interval. These vectors then become the initial conditions for the next time interval and the process is repeated.

Output from a nonlinear response analysis of a MDOF system generally includes response parameters such as the following: an envelope of the maximum story displacements, an envelope of the maximum relative story displacement divided by the story height (sometimes referred to as the interstory drift index (IDI)), an envelope of maximum ductility demand on structural members such as beams, columns, walls and bracing, an envelope of maximum rotation demand at the ends of members, an envelope of the maximum story shear, time history of base shear, moment versus rotation hysteresis plots for critical plastic hinges, time history plots of story displacements and time history plots of energy demands (input energy, hysteretic energy, kinetic energy and dissipative energy).

For multiple degree of freedom systems, the definition of ductility is not as straight-forward as it was for the single degree of freedom systems. Ductility may be expressed in terms of such parameters as displacement, relative displacement, rotation, curvature or strain.

Example 4-10. Seismic Response Analyses

The following is a representative response analysis for a six story building in which the lateral resistance is provided by moment resistant steel frames on the perimeter. The

structure has a rectangular plan with typical dimensions of 228'×84' as shown in Figure 4-31. The building was designed for the requirements of the 1979 Edition of the Uniform Building Code (UBC) with the seismic load based on the use of static equivalent lateral forces.

Elastic Analyses

As a first step in performing the analyses, the members of the perimeter frame will be stress checked for the design loading conditions and the dynamic properties of the building will be determined. This will help to insure that the analytical model of the building is correct and that the gravity loading which will be used for the nonlinear response analysis is also reasonable. This will be done using a three dimensional model of the lateral force system and the ETABS⁽⁴⁻¹¹⁾ computer program. This program is widely used on the west coast for seismic analysis and design of building systems. An isometric view of the perimeter frame including the gravity load is shown in Figure 4-32. The location of the concentrated and distributed loads depends upon the framing system shown in Figure 4-31.

Using the post-processor program STEELER⁽⁴⁻¹²⁾, the lateral force system is stress checked using the AISC-ASD criteria. The stress ratio is calculated as the ratio of the actual stress in the member to the allowable stress. Applying the gravity loads in combination with the static equivalent lateral forces in the transverse direction produces the stress ratios shown in Figure 4-33. This result includes the effect of an accidental eccentricity which is 5% of the plan dimension. The maximum stress ratio in the columns is 0.71 and the maximum in the beams is 0.92. These values are reasonable based on standard practice at the time the building was designed. Ideally, the stress ratio should be just less than one, however, this is not always possible due to the finite number of steel sections that are available.

Modal analyses indicate that the first three lateral modes of vibration in each direction

represent more than 90% of the participating mass. In the transverse direction, these modes have periods of vibration of 1.6, 0.6 and 0.35 seconds. In the longitudinal direction, the periods are slightly shorter.

Dynamic analyses are conducted using the same analytical model and considering an ensemble of five earthquake ground motions recorded during the Northridge earthquake. A representative time history of one of these motions is shown in Figure 4-34. The corresponding stress ratios in the perimeter frame are shown in Figure 4-35 for earthquake motion applied in the transverse direction. Stress ratios in the beams of the transverse frames range from 2.67 to 4.11 indicating substantial inelastic behavior. Stress ratios in excess of 1.12 are obtained in all of the columns of the transverse frames, however, it should be recalled that there is a factor of safety of approximately 1.4 on allowable stress and plastic hinging.

Nonlinear Analyses

In order to estimate the lateral resistance of the building at ultimate load, a static, nonlinear analysis (pushover) is conducted for proportional loading. The reference lateral load distribution is that specified in the 1979 UBC. This load distribution is then multiplied by a load factor to obtain the ultimate load. The nonlinear model is a two dimensional model in which the plasticity is assumed to be concentrated in plastic hinges at the ends of the members.

The results of the pushover analysis are usually represented in terms of a plot of the roof displacement versus the base shear as shown in Figure 4-36. This figure indicates that first yielding occurs at a base shear of approximately 670 kips and a roof displacement of approximately 7.25 inches. The UBC 1979 static equivalent lateral forces for this frame results in a base shear of 439 kips which implies a load factor of 1.52 on first yield. At a roof displacement of 17.5 inches, a sway mechanism forms with all girders hinged and

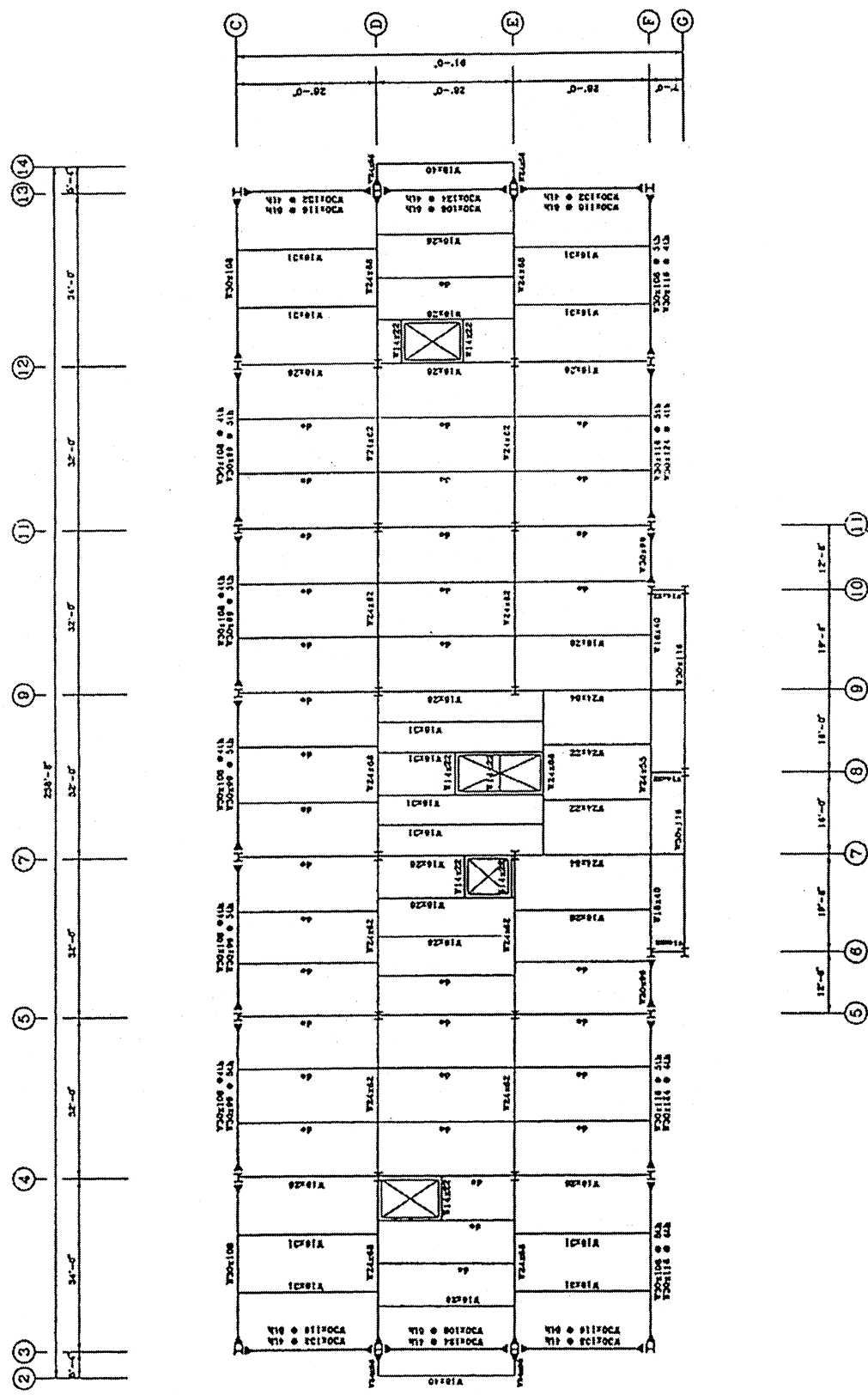


Figure 4-31 Typical floor framing plan ~ Fourth & fifth floors

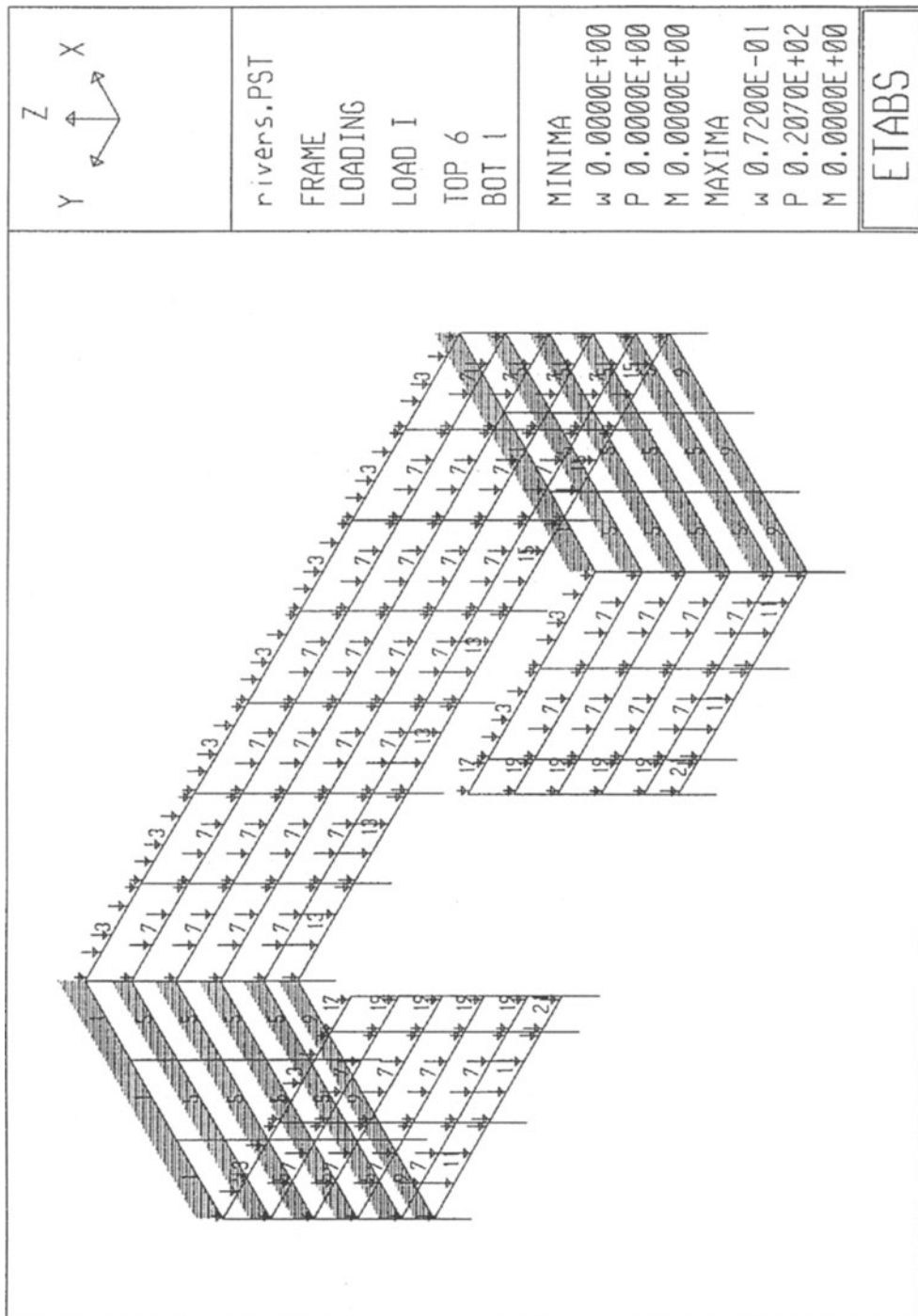


Figure 4-32. Gravity Loading Pattern, ETABS



Figure 4-33. Calculated Stress Ratios, Design Loads, ETABS

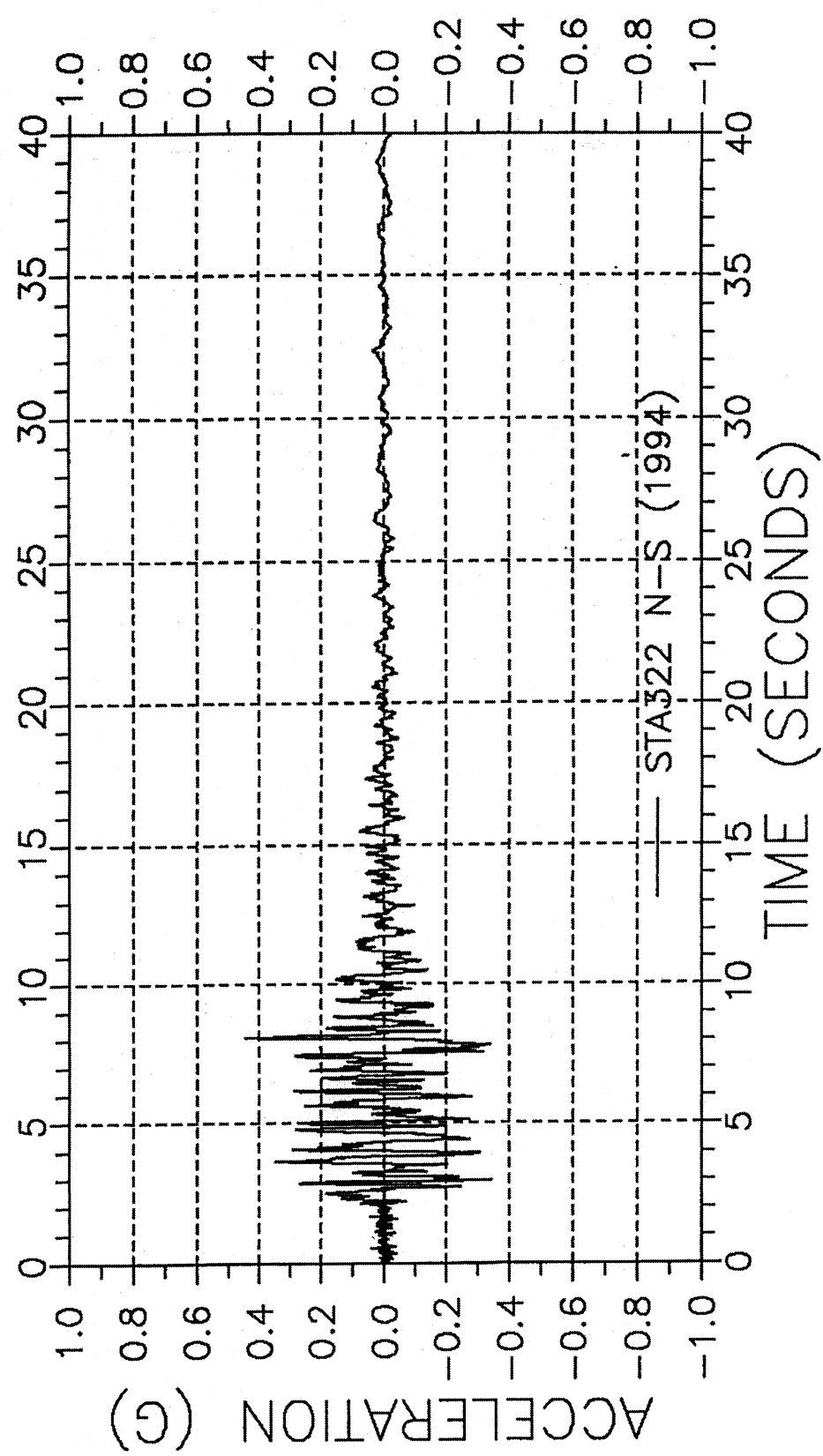


Figure 4-34. Recorded Base Acceleration, Sta. 322, N-S

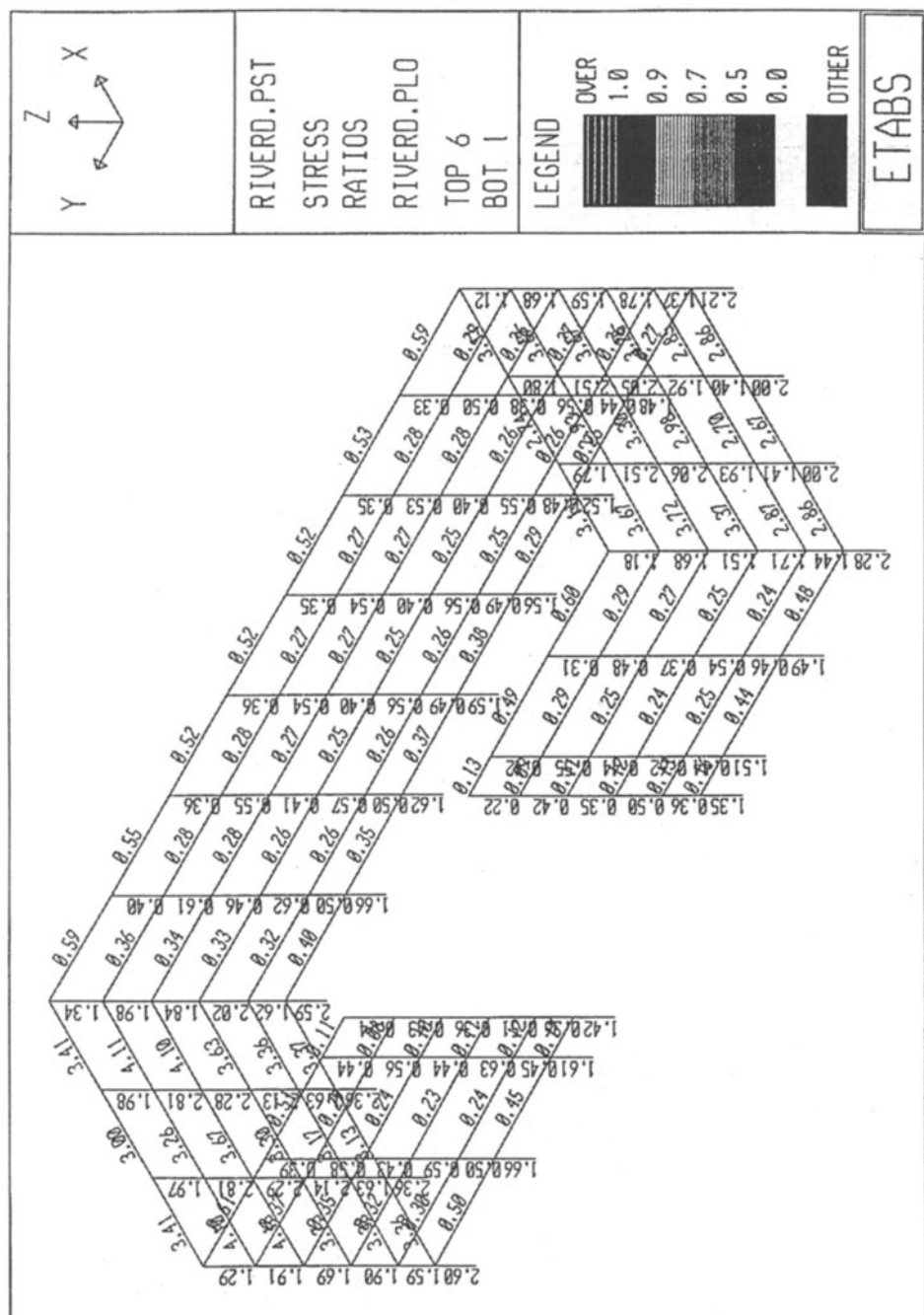


Figure 4-35. Calculated Stress Ratios, Sta. 322 Ground Motion

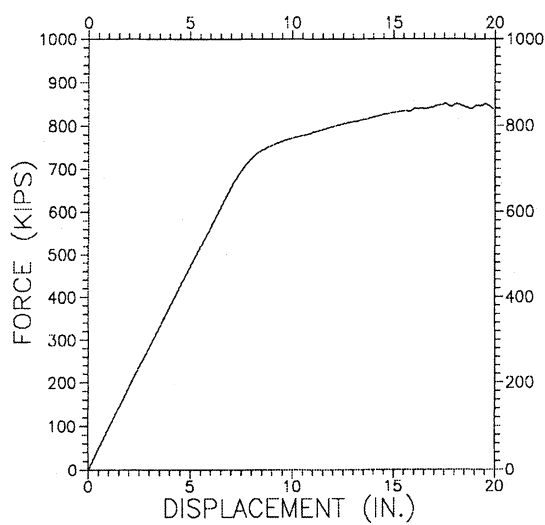


Figure 4-36. Static Pushover Curve

hinges at the base of the columns. At this displacement, the pushover curve is becoming almost horizontal indicating a loss of most of the lateral stiffness. This behavior is characterized by a large increase in displacement for a small increase in lateral load since lateral resistance is only due to strain hardening in the plastic hinges. The ultimate load is taken as 840 kips which divided by the code base shear for the frame (439 kips) results in a load factor of 1.91 on ultimate.

Note that the elastic dynamic analysis for the acceleration shown in Figure 4-34 results in a displacement at the roof of 16.7 inches. Comparing this to the pushover curve (Figure 4-36) indicates that the structure should be well into the inelastic range based on the displacement response.

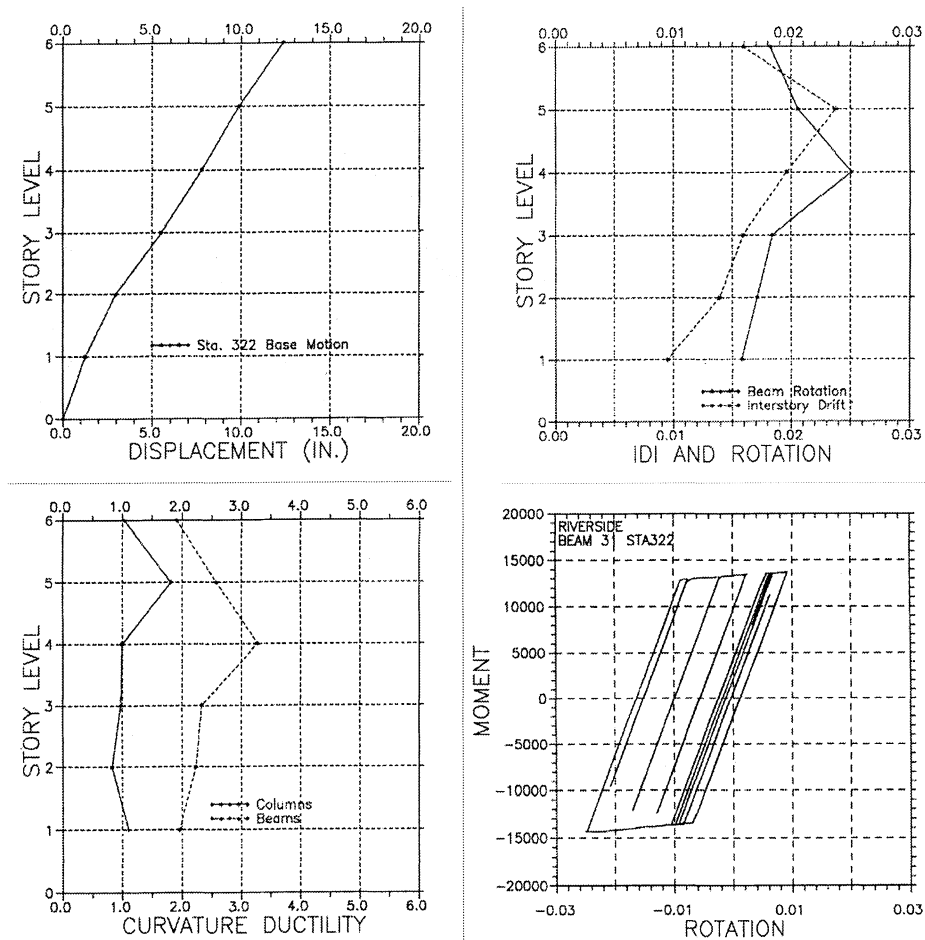


Figure 4-37. Calculated Nonlinear Dynamic Response.

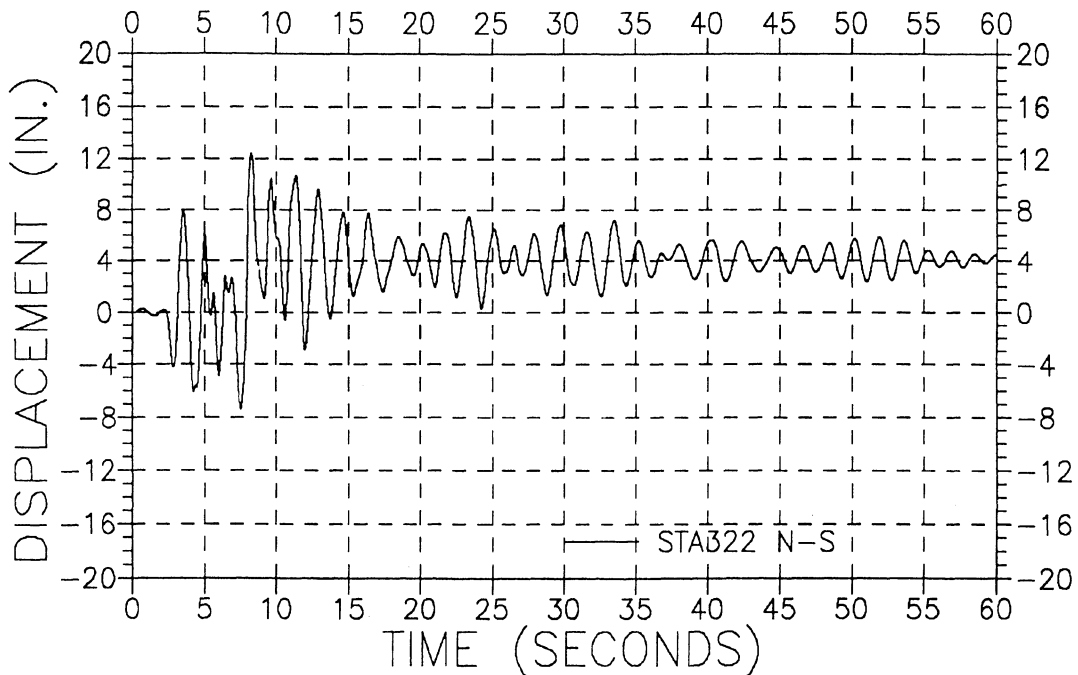


Figure 4-38. Nonlinear Displacement, Roof Level

The nonlinear dynamic response of a structure is often presented in terms of the following response parameters: (1) envelope of maximum total displacement, (2) envelope of maximum story to story displacement divided by the story height (interstory drift index), (3) maximum ductility demand for the beams and columns, (4) envelopes of maximum plastic hinge rotation, (5) moment versus rotation hysteresis curves for critical members and (6) envelopes of maximum story shear. Representative plots of four of these parameters are shown in Figure 4-37. The lateral displacement envelope (Figure 4-37a) indicates that the maximum displacement at the roof level is 12.3 inches which is less than the 16.7 inches obtained from the elastic dynamic analysis. The interstory drift and total beam rotation curves are shown in Figure 4-37b which indicates that the interstory drift ranges from 0.01 (1%) to 0.024 (2.4%). The beam rotation can be seen to range between 0.016 and 0.025. The curvature ductility demands of the beams and columns is shown in Figure 4-37c.

The maximum ductility demand for the columns is 1.8 and for the beams it is 3.3. The hysteretic behavior of a plastic hinge in a critical beam is shown in a plot of moment versus rotation in Figure 4-37d.

A final plot, Figure 4-38, shows the nonlinear displacement time history of the roof. This figure illustrates the displacement of a pulse type of input. After some lesser cycles during the first 7 seconds of the time history, the structure sustains a strong displacement at approximately 8 seconds which drives the roof to a displacement of 12 inches relative to the base. Note the acceleration pulse at this time in the acceleration time history (Figure 4-34). Following this action, the structure begins to oscillate about a new, deformed position at four inches displacement. This is a residual displacement, which the structure will have following the earthquake and is characteristic of inelastic behavior. Additional details of this analysis example can be found in the literature ⁽⁴⁻¹³⁾.

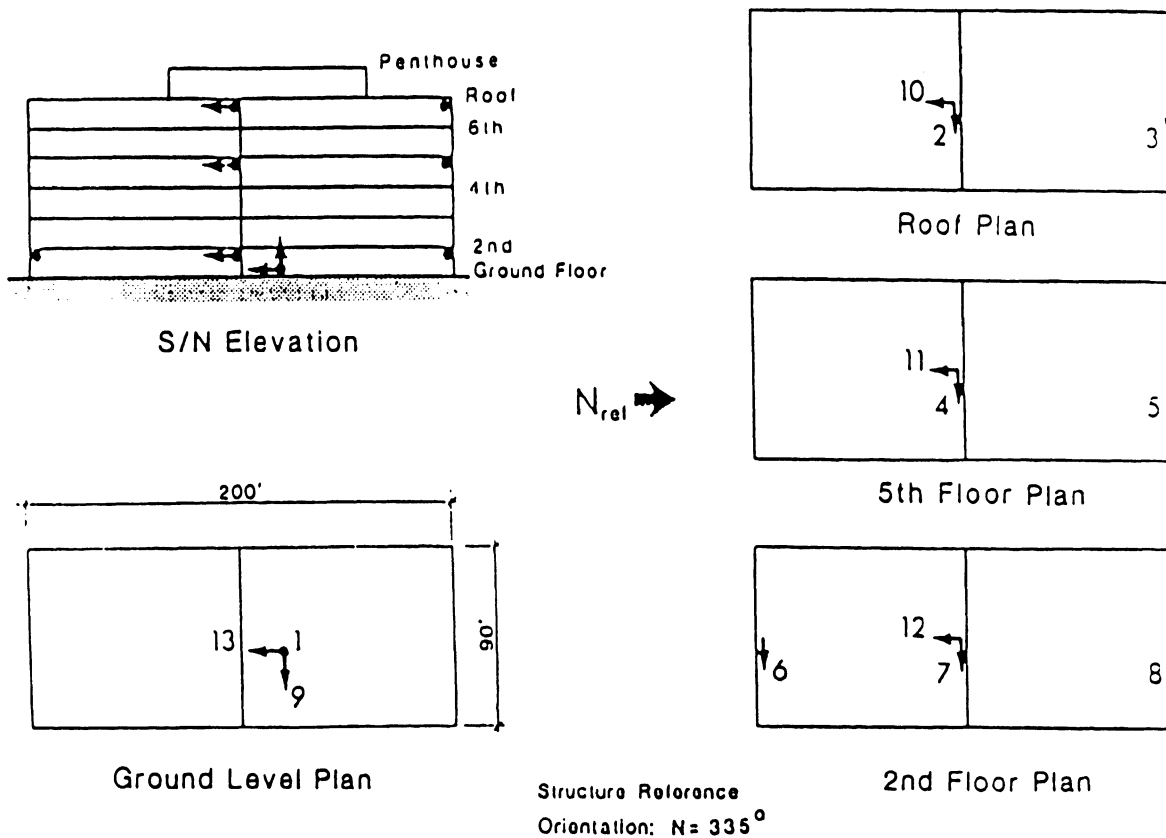


Figure 4-39. Location of Strong Motion Instrumentation

1.8 VERIFICATION OF CALCULATED RESPONSE

The dynamic response procedures discussed in the previous sections must have the ability to reliably predict the dynamic behavior of structures when they are subjected to critical seismic excitations. Hence, it is necessary to compare the results of analytical calculations with the results of large-scale experiments. The best large-scale experiment is when an earthquake occurs and properly placed instruments record the response of the building to ground motions recorded at the base. The instrumentation (accelerometers) placed in a six-story reinforced concrete building by the California Strong Motion Instrumentation Program (CSMIP) is indicated in Figure 4-39. The lateral force framing system for the

building, shown in Figure 4-40, indicates that there are three moment frames in the transverse (E-W) direction and two moment frames in the longitudinal (N-S) direction. Note that the transverse frames at the ends of the building are not continuous with the longitudinal frames. It is assumed that the floor diaphragms are rigid in their own plane. During the Loma Prieta earthquake the instrumentation recorded thirteen excellent records of building response having a duration of more than sixty seconds⁽⁴⁻¹⁹⁾. Since the response was only weakly nonlinear, the calculations can be made using the ETABS program, however, similar analyses can also be conducted with a nonlinear response program⁽⁴⁻²⁰⁾.

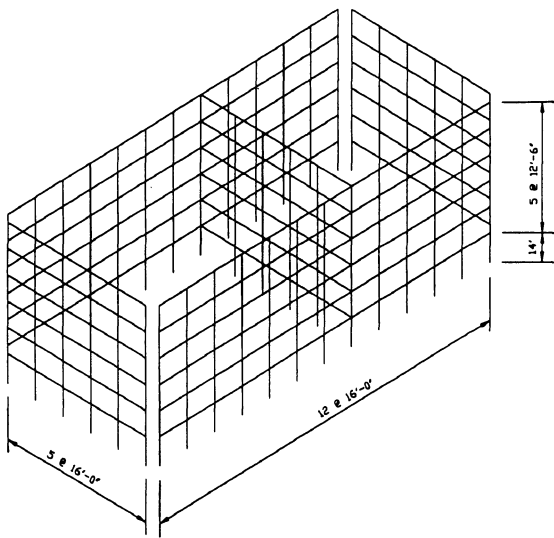
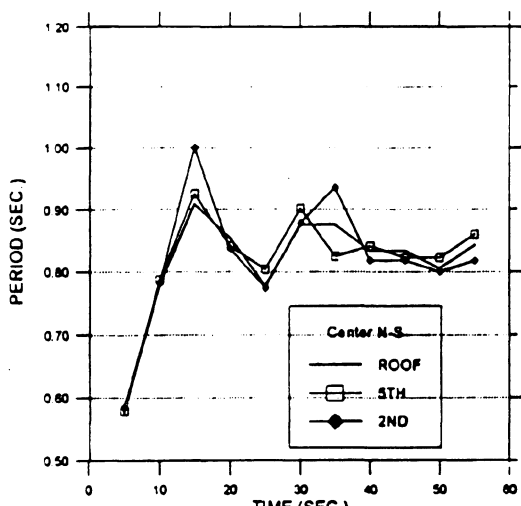


Figure 4-40. ETABS Building Model

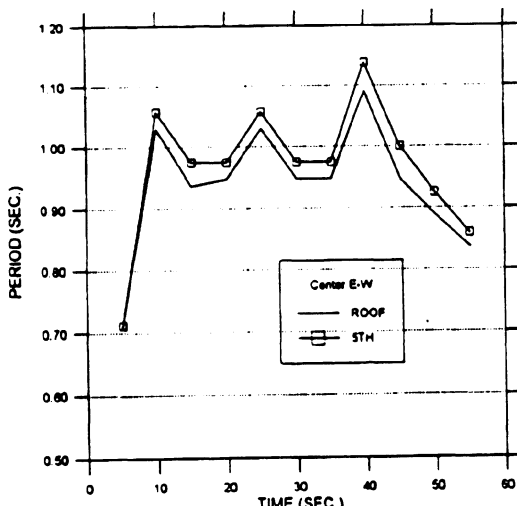
To improve the evaluation of the recorded response, spectral analyses are conducted in both the time domain (response spectra) and frequency domain (Fourier spectra). A further refinement of the Fourier analysis can be attained by calculating a Fourier amplitude spectra for a segment (window) of the recorded time history. The fixed duration window is then shifted along the time axis and the process is

repeated until the end of the time history record. This results in a “moving window Fourier amplitude spectra” (MWFAS) which indicates the changes in period of the building response during the time history as shown in Figure 4-41. In this example a ten-second window was used with a five-second shift for the first sixty seconds of the recorded response. In general, the length of the “window” should be at least 2.5 times the fundamental period of the structure.

If the connections (offsets) are assumed to be rigid, the initial stiffness of the building prior to any cracking of the concrete can be estimated using the analytical model with member properties of the gross sections. This results in a period of 0.71 seconds in the E-W direction and 0.58 seconds in the N-S direction. This condition can also be evaluated by the results obtained from the initial window of the MWFAS. An examination of Figure 4-41 indicates an initial period of 0.71 in the E-W direction and 0.58 seconds in the N-S direction. Identical results were also obtained from ambient vibration tests conducted by Marshall, et al.⁽⁴⁻²¹⁾.



(a) North-South



(b) East-West

Figure 4-41. Variation of Building Period with Time

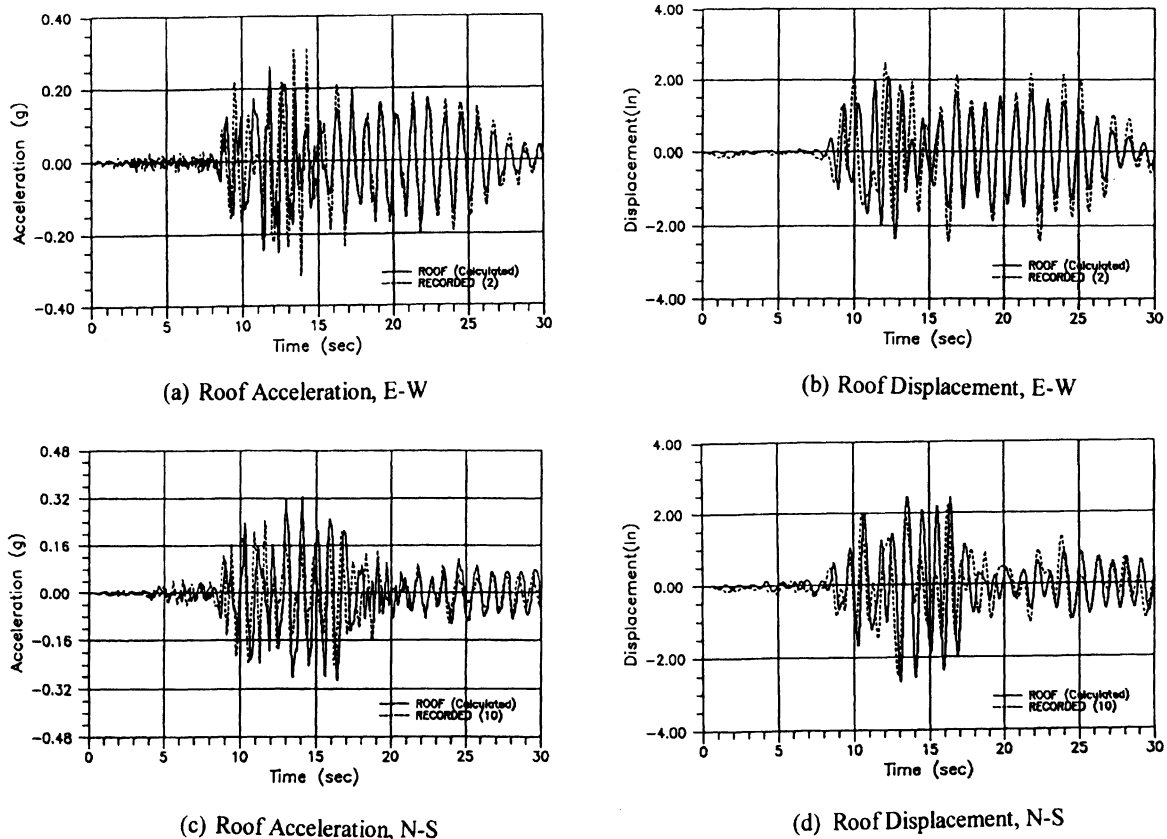


Figure 4-42. Time History Comparisons of Acceleration, Displacement

During the strong motion portion of the response, cracking in the concrete and limited yielding of the tension steel will cause the period of vibration to lengthen. In order to represent this increased flexibility in the elastic analytical model, the flexibility of the individual members can be reduced to an effective value or the rigid offsets at the connections⁽⁴⁻¹³⁾ can be reduced in length. For this example, the rigid offsets were reduced by fifty percent. This results in a period of 1.03 seconds in the E-W direction and 0.89 seconds in the N-S direction which are in the range of values obtained from the MWFAS. Considering the entire duration of the recorded response, the Fourier amplitude spectra indicates a period of 1.05 seconds in the E-W direction and 0.85 in the N-S direction. Corresponding values obtained from a response spectrum analysis

indicate 1.0 E-W and 0.90 N-S. It can be concluded that for this building, all of these values are in good agreement. The MWFAS also indicate an increase in period of approximately fifty percent in both principal directions during the earthquake. This amount of change is not unusual for a reinforced concrete building⁽⁴⁻²²⁾, however, it does indicate cracking and possible limited yielding of the reinforcement. The time histories of the acceleration and displacement at the roof level are shown in Figure 4-42. This also shows a good correlation between the measured and the calculated response.

REFERENCES

- 4-1 Chopra, A. K., *Dynamics of Structures, A Primer*, Earthquake Engineering Research institute, Berkeley, CA, 1981.
- 4-2 Applied Technology Council, *An Evaluation of a Response Spectrum Approach to Seismic Design of Buildings*, ATC-2, Applied Technology Council, Palo Alto, CA, 1974.
- 4-3 Newmark, N. M., and Hall, W. J., "Procedures and Criteria for Earthquake Resistant Design", Building Practices for Disaster Mitigation, U. S. Department of Commerce, Building Science Series 46, 1973.
- 4-4 Clough, R. W., and Penzien, J., *Structural Dynamics*, McGraw-Hill, Inc., New York, NY, 1975.
- 4-5 Rayleigh, Lord, *Theory of Sound*, Dover Publications, New York, NY, 1945.
- 4-6 Lee, V. W., and Trifunac, M. D., "Strong Earthquake Ground Motion Data in EQINFO, Part I," Report No.87-01, Department of Civil Engineering, USC, Los Angeles, CA, 1987.
- 4-7 Bathe, K. J., and Wilson, E. L., *Numerical Methods in Finite Element Analysis*, Prentice Hall, Inc., Englewood Cliffs, New Jersey, 1976.
- 4-8 Caughey, T. K., "Classical Normal Modes in Damped Linear Dynamic systems," Journal of Applied Mechanics, ASME, Paper No. 59-A-62, June, 1960.
- 4-9 Wilson, E. L., Der Kiureghian, A. and Bayo, E. P., "A Replacement for the SRSS Method in Seismic Analysis", Earthquake Engineering and Structural Dynamics, Vol. 9, 1981.
- 4-10 Anderson, J. C., and Gurfinkel, G., "Seismic Behavior of Framed Tubes," International Journal of Earthquake Engineering and Structural Dynamics, Vol. 4, No. 2, October-December, 1975.
- 4-11 Habibullah, A., "ETABS, Three Dimensional Analysis of Building Systems," User's Manual, Version 6.0, Computers & Structures, Inc. Berkeley, California, 1994.
- 4-12 Habibullah, A., "ETABS Design Postprocessors," Version 6.0, Computers & Structures, Inc. Berkeley, California, 1994.
- 4-13 Anderson, J. C., "Moment Frame Building", Buildings Case Study Project, SSC 94-06, Seismic Safety Commission, State of California, Sacramento, California, 1996.
- 4-14 Charney, F.A., NONLIN, Nonlinear Dynamic Time History Analysis of Single Degree of Freedom Systems, Advanced Structural Concepts, Golden, Colorado, 1996.
- 4-15 Norris, C.H., Hansen, R.J., Holley, M.J., Biggs, J.M., Namyat, S., and Minami, J.K., *Structural Design for Dynamic Loads*, McGraw-Hill Book Company, New York, New York, 1959.
- 4-16 U.S. Army Corps of Engineers, *Design of Structures to Resist the Effects of Atomic Weapons*, EM 1110-345-415, 1957.
- 4-17 Applied Technology Council, "Seismic Evaluation and Retrofit of Concrete Buildings", ATC-40, Applied Technology Council, Redwood City, California, 1991.
- 4-18 Anderson, J.C. and Bertero, V.V., "Seismic Performance of an Instrumented Six Story Steel Building", Report No. UCB/EERC-91/111, Earthquake Engineering Research Center, University of California at Berkeley, Berkeley, California, 1991.
- 4-19 California Division of Mines and Geology, "CSMIP Strong-Motion Records from the Santa Cruz Mountains (Loma Prieta) California Earthquake of October 17, 1989", Report OSMS 89-06.
- 4-20 Anderson, J.C. and Bertero, V.V., "Seismic Performance of an Instrumented Six Story Steel Building", Report No. UCB/EERC-93/01, Earthquake Engineering Research Center, University of California at Berkeley.
- 4-21 Marshall, R.D., Phan, L.T. and Celebi, M., "Full Scale Measurement of Building Response to Ambient Vibration and the Loma Prieta Earthquake", Proceedings, Fifth National Conference on Earthquake Engineering, Vol. II, Earthquake Engineering Research Institute, Oakland, California, 1994.
- 4-22 Anderson, J.C., Miranda, E. and Bertero, V.V., "Evaluation of the Seismic Performance of a Thirty-Story RC Building", Report No. UCB-EERC-93/01, Earthquake Engineering Research Center, University of California, Berkeley.

Chapter 5

Linear Static Seismic Lateral Force Procedures

Roger M. Di Julio Jr., Ph.D., P.E.

Professor of Engineering, California State University, Northridge

Key words: Code Philosophy, Design Base Shear, Design Story Forces, Design Drift Limitations, Equivalent Static Force Procedure, Near Fault Factors, Seismic Zone Factors, UBC-97, IBC-2000, Regular and Irregular Structures, Torsion and P-delta Effects, Site Soil Factors, Importance Factors

Abstract: The purpose of this chapter is to review and compare the sections of current seismic design provisions, which deal with the specification of seismic design forces. Emphasis will be on the equivalent static force procedures as contained in the 2000 edition of the International Building Code and the 1997 Edition of the Uniform Building Code. There are two commonly used procedures for specifying seismic design forces: The "Equivalent Static Force Procedure" and "Dynamic Analysis". In the equivalent static force procedure, the inertial forces are specified as static forces using empirical formulas. The empirical formulas do not explicitly account for the "dynamic characteristics" of the particular structure being designed or analyzed. The formulas were, however, developed to adequately represent the dynamic behavior of what are called "regular" structures, which have a reasonably uniform distribution of mass and stiffness. For such structures, the equivalent static force procedure is most often adequate. Structures that do not fit into this category are termed "irregular". Common irregularities include large floor-to-floor variation in mass or center of mass and soft stories. Such structures violate the assumptions on which the empirical formulas, used in the equivalent static force procedure, are based. Therefore, its use may lead to erroneous results. In these cases, a dynamic analysis should be used to specify and distribute the seismic design forces. Principles and procedures for dynamic analysis of structures were presented in Chapter 4.

5.1 INTRODUCTION

In order to design a structure to withstand an earthquake the forces on the structure must be specified. The exact forces that will occur during the life of the structure cannot be known. A realistic estimate is important, however, since the cost of construction, and therefore the economic viability of the project depends on a safe and cost efficient final product.

The seismic forces in a structure depend on a number of factors including the size and other characteristics of the earthquake, distance from the fault, site geology, and the type of lateral load resisting system. The use and the consequences of failure of the structure may also be of concern in the design. These factors should be included in the specification of the seismic design forces.

There are two commonly used procedures for specifying seismic design forces: The "Equivalent Static Force Procedure" and "Dynamic Analysis". In the equivalent static force procedure, the inertial forces are specified as static forces using empirical formulas. The empirical formulas do not explicitly account for the "dynamic characteristics" of the particular structure being designed or analyzed. The formulas were, however, developed to adequately represent the dynamic behavior of what are called "regular" structures, which have a reasonably uniform distribution of mass and stiffness. For such structures, the equivalent static force procedure is most often adequate.

Structures that do not fit into this category are termed "irregular". Common irregularities include large floor-to-floor variation in mass or center of mass and soft stories. Such structures violate the assumptions on which the empirical formulas, used in the equivalent static force procedure, are based. Therefore, its use may lead to erroneous results. In these cases, a dynamic analysis should be used to specify and distribute the seismic design forces.

A dynamic analysis can take a number of forms, but should account for the irregularities of the structure by modeling its "dynamic

characteristics" including natural frequencies, mode shapes and damping.

The purpose of this chapter is to review and compare the sections of current seismic design provisions, which deal with the specification of seismic design forces. Emphasis will be on, as in the documents discussed, the equivalent static force procedure.

The following seismic design provisions are included in the discussion, which follows:

1. The Uniform Building Code, Volume 2, "Structural Engineering Design Provisions" issued by the International Conference of Building Officials, 1997 edition, referred to as UBC-97.

2. "International Building Code", IBC2000 Edition, Published by the International Code Council, INC., referred to as IBC2000

IBC2000 is based on "NEHRP Recommended Provisions for Seismic Regulations for New Buildings and Other Structures, Part I Provisions, prepared by the Building Seismic Safety Council for the Federal Emergency Management Agency (FEMA), 1997 edition, referred to as FEMA-302. The commentary on this document is contained in Part 2 Commentary, designated FEMA-303.

5.2 CODE PHILOSOPHY

The philosophy of a particular document indicates the general level of protection that it can be expected to provide. Most code documents clearly state that their standards are minimum requirements that are meant to provide for life safety but not to insure against damage.

The code-specified forces are generally lower than the actual forces that would occur in a large or moderate size earthquake. This is because the structure is designed to carry the specified loads within allowable stresses and deflections, which are considerably less than the ultimate or yield capacity (when using working stress design) of the materials and system. It is assumed that the larger loads that actually occur will be accounted for by the factors of safety and by the redundancy and

ductility of the system. Life safety is thereby insured but structural damage may be sustained.

5.3 UBC-97 PROVISIONS

UBC-97, basically provides for the use of the equivalent static force procedure or a dynamic analysis for regular structures under 240 feet tall and irregular structures 65 feet or less in height. A dynamic analysis is required for regular structures over 240 feet tall, irregular structures over 65 feet tall, and buildings that are located on poor soils (type S_F) and have a period greater than 0.7 seconds.

Although UBC-97 allows for both working stress design and alternately strength or load and resistance factor design, the earthquake loads are specified for use with the latter. This is a departure from previous editions where the earthquake loads were specified at the working stress level.

5.3.1 Design Base Shear V

The design base shear is specified by the formula:

$$V = \frac{C_v I}{R T} W \quad (5-1)$$

Where, T is the fundamental period of the structure in the direction under consideration, I is the seismic importance factor, C_v is a numerical coefficient dependent on the soil conditions at the site and the seismicity of the region, W is the seismic dead load, and R is a factor which accounts for the ductility and overstrength of the structural system. Additionally the base shear is dependent on the seismic zone factor, Z. The base shear as specified by Equation 5-1 is subject to three limits:

The design base shear need not exceed:

$$V = \frac{2.5 C_a I}{R} W \quad (5-2)$$

And cannot be less than:

$$V = 0.11 C_a I W \quad (5-3)$$

Where C_a is another seismic co-efficient dependent on the soil conditions at the site and regional seismicity.

Additionally in the zone of highest seismicity (zone 4) the design base shear must be greater than:

$$V = \frac{0.8 Z N_v I}{R} W \quad (5-4)$$

Where N_v is a near-source factor that depends on the proximity to and activity of known faults near the structure. Faults are identified by seismic source type, which reflect the slip rate and potential magnitude of earthquake generated by the fault.

The near source factor N_v is also used in determining the seismic co-efficient C_v for buildings located in seismic zone 4.

5.3.2 Seismic Zone Factor Z

Five seismic zones, numbered 1 2A, 2B, 3 and 4 are defined. The zone for a particular site is determined from a seismic zone map (See Figure 5-1). The numerical values of Z are:

Zone	1	2A	2B	3	4
Z	0.075	0.15	0.2	0.3	0.4

The value of the coefficient thus normalized can be viewed as the peak ground acceleration, in percent of gravity, in each zone.

5.3.3 Seismic Importance Factor I

The importance factor I is used to increase the margin of safety for essential and hazardous facilities. For such structures I=1.25. Essential structures are those that must remain operative immediately following an earthquake such as emergency treatment areas and fire stations. Hazardous facilities include those housing toxic or explosive substances (See Table 5-1).

5.3.4 Building Period T

The building period may be determined by analysis or using empirical formulas. A single empirical formula may be used for all framing systems:

$$T = C_t h_n^{\frac{3}{4}} \quad (5-5)$$

where

$$C_t = \begin{cases} 0.035 & \text{for steel moment frames} \\ 0.030 & \text{for concrete moment frames} \\ 0.030 & \text{for eccentric braced frames} \\ 0.020 & \text{for all other buildings} \end{cases}$$

h_n = the height of the building in feet.

If the period is determined using Rayleigh's formula or another method of analysis, the value of T is limited. In Seismic Zone 4, the period cannot be over 30% greater than that determined by Equation 5-5 and in Zones 1, 2 and 3 it cannot be more than 40% greater. This provision is included to eliminate the possibility of using an excessively long period to justify an unreasonably low base shear. This limitation does not apply when checking drifts.

5.3.5 Structural System Coefficient R

The structural system coefficient, R is a measure of the ductility and overstrength of the structural system, based primarily on performance of similar systems in past earthquakes.

The values of R for various structural systems are found in Table 5-2. A higher number has the effect of reducing the design base shear. For example, for a steel special moment resisting frame the factor has value of 8.5, while an ordinary moment resisting frame the value is 4.5. This reflects the fact that a special moment resisting frame is expected to perform better during an earthquake.

5.3.6 Seismic Dead Load W

The dead load W, used to calculate the base shear, includes not only the total dead load of the structures but also partitions, 25% of the floor live load in storage and warehouse occupancies and the weight of snow when the design snow load is greater than 30 pounds per square foot. The snow load may be reduced by up to 75% if its duration is short.

The rationale for including a portion of the snow load in heavy snow areas is the fact that in these areas a significant amount of ice can build up and remain on roofs.

5.3.7 Seismic Coefficients C_v and C_a

The seismic coefficients C_v & C_a are measures of the expected ground acceleration at the site. They may be found in Tables 5-3 and 5-4.

The co-efficient, and hence the expected ground accelerations are dependent on the seismic zone and soil profile type. They therefore reflect regional seismicity and soil conditions at the site.

Additionally in seismic zone 4 they also depend on the seismic source type and near source factors N_a and N_v . These factors reflect local seismicity in the region of highest seismic activity.

5.3.8 Soil Profile Type S

The soil profile type reflects the effect of soil conditions at the site on ground motion. They are found in Table 5-5 and are labeled S_A , through S_F .

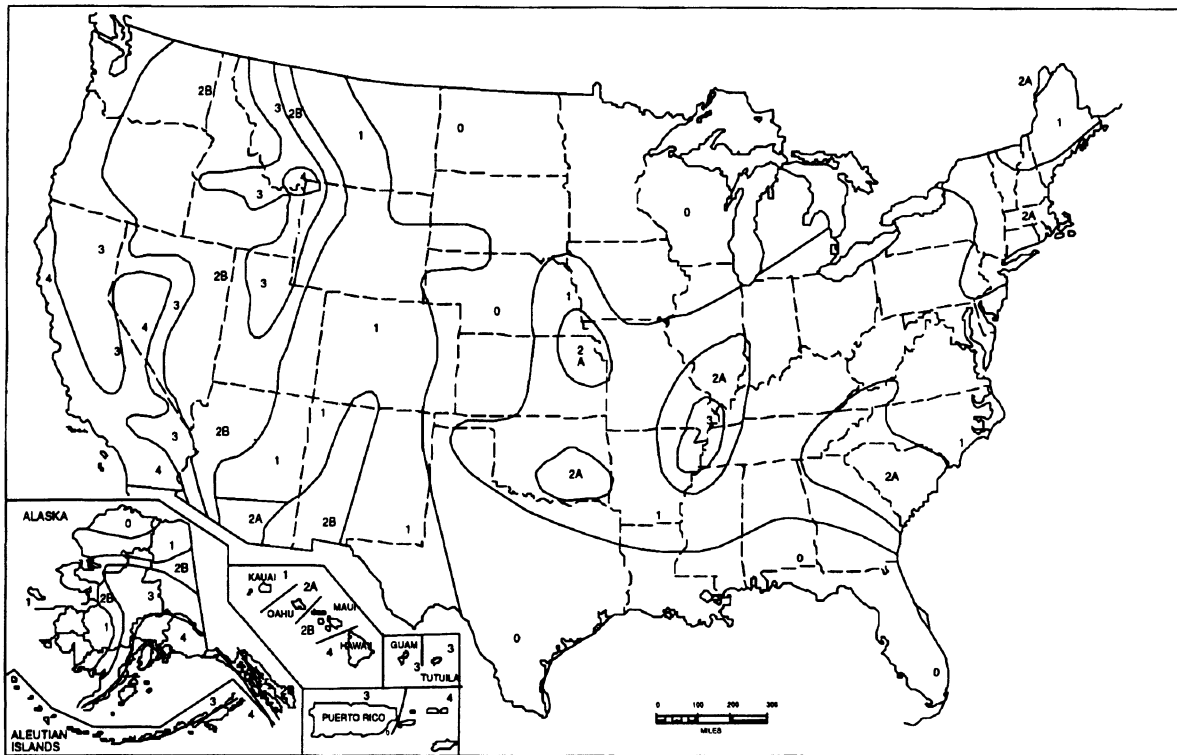


Figure 5-1. Seismic Zone Map of the United States

Table 5-1 Seismic Importance Factor

Occupancy Category	Occupancy or Functions of Structure	Seismic Importance Factor, I
1. Essential facilities	Group I, Division 1 Occupancies having surgery and emergency treatment areas. Fire and police stations. Garages and shelters for emergency vehicles and emergency aircraft. Structures and shelters in emergency-preparedness centers. Aviation control towers. Structures and equipment in government communication centers and other facilities required for emergency response. Standby power-generating equipment for Category 1 facilities. Tanks or other structures containing housing or supporting water or other fire-suppression material or equipment required for the protection of Category 1, 2 or 3 structures.	1.25
2. Hazardous facilities	Group H, Divisions 1, 2, 6 and 7 Occupancies and structures therein housing or supporting toxic or explosive chemicals or substances. Nonbuilding structures housing, supporting or containing quantities of toxic or explosive substances that, if contained within a building, would cause that building to be classified as a Group H, Division 1, 2 or 7 Occupancy.	1.25
3. Special occupancy structures	Group A, Divisions 1, 2 and 2.1 Occupancies. Buildings housing Group E, Divisions 1 and 3 Occupancies with a capacity greater than 300 students. Buildings housing Group B Occupancies used for college or adult education with a capacity greater than 500 students. Group I, Divisions 1 and 2 Occupancies with 50 or more resident incapacitated patients, but not included in Category 1. Group I, Division 3 Occupancies. All structures with an occupancy greater than 5,000 persons. Structures and equipment in power-generating stations, and other public utility facilities not included in Category 1 or Category 2 above, and required for continued operation.	1.00
4. Standard occupancy	All structures housing occupancies or having functions not listed in Category 1, 2 or 3 and Group U Occupancy towers.	1.00
5. Miscellaneous	Group U Occupancies except for towers.	1.00

Table 5-2. Structural Systems

Basic Structural System	Lateral-Force-Resisting System Description	R
1. Bearing wall system	1. Light-framed walls with shear panels a. Wood Structural panel walls for structures three stories or less b. All other light-framed walls 2. Shear walls a. Concrete b. Masonry 3. Light steel-framed bearing walls with tension only bracing 4. Braced frames where bracing carries gravity load a. Steel b. Concrete c. Heavy timber	5.5 4.5 4.5 4.5 4.5 2.8 4.4 2.8 2.8
2. Building frame system	1. Steel eccentrically braced frame (EBF) 2. Light-framed walls with shear panels a. Wood structural panel walls for structures three stories or less b. All other light-framed walls 3. Shear walls a. Concrete b. Masonry 4. Ordinary braced frames a. Steel b. Concrete c. Heavy timber 5. Special concentrically braced frames a. Steel	7.0 6.5 5.0 5.5 5.5 5.6 5.6 5.6 6.4
3. Moment-resisting frame system	1. Special moment-resisting frame (SMRF) a. Steel b. Concrete 2. Masonry moment-resisting wall frame (MMRWF) 3. Concrete intermediate moment-resisting frame (IMRF) 4. Ordinary moment-resisting frame (OMRF) a. Steel b. Concrete 5. Special truss moment frames of steel (STMF)	8.5 8.5 6.5 5.5 4.5 3.5 6.5
4. Dual systems	1. Shear walls a. Concrete with SMRF b. Concrete with steel OMRF c. Concrete with concrete IMRF d. Masonry with SMRF e. Masonry with steel OMRF f. Masonry with concrete IMRF g. Masonry with masonry MMRWF 2. Steel EBF a. With steel SMRF b. With steel OMRF 3. Ordinary braced frames a. Steel with steel SMRF b. Steel with steel OMRF c. Concrete with concrete SMRF d. Concrete with concrete IMRF 4. Special concentrically braced frames a. Steel with steel SMRF b. Steel with steel OMRF	8.5 4.2 6.5 5.5 4.2 4.2 6.0 8.5 4.2 6.5 4.2 6.5 4.2 7.5 4.2
5. Cantilevered column building systems	1. Cantilevered column elements	2.2
6. Shear wall-frame interaction systems	1. Concrete	5.5

The soil profile types are broadly defined in generic terms, for example “Hard Rock” for type S_A . They are also defined by the physical properties of the soil determined by standard tests including; shear wave velocity, standard penetration test, and undrained shear strength.

5.3.9 Seismic Source Type A, B and C

The seismic source type is used to specify the capability and activity of faults in the immediate vicinity of the structure. It is used only in seismic zone 4.

The seismic source types, labeled A, B or C, are found in Table 5-6. They are defined in terms of the slip rate of the fault and the maximum magnitude earthquake it is capable of generating. For example, the highest seismic risk is posed by seismic source type A, which is defined by a maximum moment magnitude of 7.0 or greater and a slip rate of 5mm/year or greater.

5.3.10 Near Source Factors N_a and N_v

The near source factors N_a and N_v are found in Tables 5-7 and 5-8. In seismic zone 4, they

are used in conjunction with the soil profile type to determine the seismic coefficients C_v and C_a (See Tables 5-3 and 5-4). For example, for seismic source type A at a distance to the fault of less than 2km, $N_a = 1.5$ (See Table 5-7). This is then used with Table 5-4 to determine the seismic co-efficient, C_a .

5.3.11 Distribution of Lateral Force F_x

The base shear V , as determined from Equations 5-1 through 5-4 are distributed over the height of the structure as a force at each level F_i , plus an extra force F_t at the top:

$$V = F_t + \sum_{i=1}^n F_i \quad (5-6)$$

The extra force at the top is:

$$F_t = 0.07TV \leq 0.25V \quad \text{if } T > 0.7 \text{ sec.} \quad (5-7a)$$

$$F_t = 0.0 \quad \text{if } T \leq 0.7 \text{ sec.} \quad (5-7b)$$

F_t accounts for the greater participation of higher modes in the response of longer period structures.

Table 5-3. Seismic Coefficient C_v

Soil Profile Type	Seismic Zone Factor, Z				
	Z = 0.075	Z = 0.15	Z = 0.2	Z = 0.3	Z = 0.4
S_A	0.06	0.12	0.16	0.24	$0.32N_v$
S_B	0.08	0.15	0.20	0.30	$0.40N_v$
S_C	0.13	0.25	0.32	0.45	$0.56N_v$
S_D	0.18	0.32	0.40	0.54	$0.64N_v$
S_E	0.26	0.50	0.64	0.84	$0.96N_v$
S_F	<i>Site-specific geotechnical investigation and dynamic site response analysis shall be performed.</i>				

Table 5-4. Seismic Coefficient C_a

Soil Profile Type	Seismic Zone Factor, Z				
	Z = 0.075	Z = 0.15	Z = 0.2	Z = 0.3	Z = 0.4
S_A	0.06	0.12	0.16	0.24	$0.32N_a$
S_B	0.08	0.15	0.20	0.30	$0.40N_a$
S_C	0.09	0.18	0.24	0.33	$0.40N_a$
S_D	0.12	0.22	0.28	0.36	$0.44N_a$
S_E	0.19	0.30	0.34	0.36	$0.36N_a$
S_F	<i>Site-specific geotechnical investigation and dynamic site response analysis shall be performed.</i>				

The remaining portion of the total base shear ($V - F_t$) is distributed over the height, including the top, by the formula:

$$F_x = \frac{(V - F_t)(w_x h_x)}{\sum_{i=1}^n w_i h_i} \quad (5-8)$$

Where, w is the weight at a particular level and h is the height of a particular level above the shear base. At each floor, the force is located at the center of mass.

For equal story heights and weights, Equation 5-8 distributes the force linearly, increasing towards the top. Any significant variation from this triangular distribution indicates an irregular structure.

Table 5-5. Soil Profile Types

Soil Profile Type	Soil Profile Name/Generic Description	Average Soil Properties for Top 100 Feet (30 480 mm) of Soil Profile		
		Shear Wave Velocity, feet/second (m/s)	Standard Penetration Test, (blows/foot)	Undrained Shear Strength, psf (kPa)
S_A	Hard Rock	> 5,000 (1,500)	—	—
S_B	Rock	2,500 to 5,000 (760 to 1,500)		
S_C	Very Dense Soil and Soft Rock	1,200 to 2,500 (360 to 760)	> 50	>2,000 (100)
S_D	Stiff Soil Profile	600 to 1,200 (180 to 360)	15 to 50	1,000 to 2,000 (50 to 100)
S_E	Soft Soil Profile	< 600 (180)	< 15	< 1,000 (50)
S_F	Soil Requiring Site-specific Evaluation.			

Table 5-6. Seismic Source Type

Seismic Source Type	Seismic Source Description	Seismic Source Definition	
		Maximum Moment Magnitude, M	Slip Rate, SR (mm/year)
A	Faults that are capable of producing large magnitude events and that have a high rate of seismic activity.	$M \geq 7.0$	$SR \geq 5$
B	All faults other than Types A and C.	$M \geq 7.0$ $M < 7.0$ $M \geq 6.5$	$SR < 5$ $SR > 2$ $SR < 2$
C	Faults that are not capable of producing large magnitude earthquakes and that have a relatively low rate of seismic activity.	$M < 6.5$	$SR \leq 2$

Table 5-7. Near-Source Factor N_a

Seismic Source Type	Closest Distance to Known Seismic Source		
	$\leq 2 \text{ km}$	5 km	$\geq 10 \text{ km}$
A	1.5	1.2	1.0
B	1.3	1.0	1.0
C	1.0	1.0	1.0

Table 5-8. Near-Source Factor N_V

Seismic Source Type	Closest Distance to Known Seismic Source			
	$\leq 2 \text{ km}$	5 km	10 km	$\geq 15 \text{ km}$
A	2.0	1.6	1.2	1.0
B	1.6	1.2	1.0	1.0
C	1.0	1.0	1.0	1.0

5.3.12 Story Shear and Overturning Moment V_x and M_x

The story shear at level x is the sum of all the story forces at and above that level:

$$V_x = F_t + \sum_{i=x}^n F_i \quad (5-9)$$

The overturning moment at a particular level M_x is the sum of the moments of the story forces above, about that level. Hence:

$$M_x = F_t(h_n - h_x) + \sum_{i=x}^n F_i(h_i - h_x) \quad (5-10)$$

Design must be based on the overturning moment as well as the shear at each level.

5.3.13 Torsion and P-Delta Effect

Accidental torsion, due to uncertainties in the mass and stiffness distribution, must be added to the calculated eccentricity. This is done by adding a torsional moment at each floor equal to the story shear multiplied by 5% of the floor dimension, perpendicular to the direction of the force. This procedure is equivalent to moving the center of mass by 5% of the plan dimension, in a direction perpendicular to the force.

If the deflection at either end of the building is more than 20% greater than the average deflection, it is classified as torsionally irregular and the accidental eccentricity must be amplified using the formula:

$$A_x = \left[\frac{\delta_{MAX}}{1.2\delta_{AVG}} \right]^2 \leq 3.0 \quad (5-11)$$

where

δ_{avg} = the average displacement at level x

δ_{max} = the maximum displacement at level x

P-Delta effects must be included in determining member forces and story displacements where significant.

5.3.14 Reliability / Redundancy Factor ρ

The seismic design forces and hence the base shear as determined from Equations 5-1 through 5-4, must be multiplied by a reliability/redundancy factor for the lateral load resisting system:

$$1 \leq \rho = 2 - \frac{20}{r_{max} \sqrt{A_B}} \leq 1.5 \quad (5-12)$$

Where, A_B is the ground floor area of the structure in square feet and r_{max} is the maximum element-story shear ratio.

The element story shear ratio (r_i) at a particular level is the ratio of the shear in the most heavily loaded member to the total story shear. The maximum ratio, r_{max} is defined as the largest value of r_i in the lower two-thirds of the building.

Special provisions for calculating r , for different lateral load resisting systems, are demonstrated in the examples that follow.

For special moment-resisting frames, if ρ exceeds 1.25, additional bays must be added. For the purposes of determining drift (displacement), and in seismic zones 0, 1 and 2, $\rho = 1.0$.

5.3.15 Drift Limitations

The deflections due to the design seismic forces are called the design level response displacements, Δ_s . The seismic forces used to determine Δ_s may be calculated using a reliability/redundancy factor equal to one, ignoring the limitation represented by Equation 5-3, and using an analytically determined period greater than the limits outlined in section 5.3.4.

The maximum inelastic response is defined as:

$$\Delta_M = .7R\Delta_s \quad (5-13)$$

Where, R is the structural system coefficient defined in Table 5-2.

Deflection control is specified in terms of the story drift, which is defined as the lateral displacement of one level relative to the level below. The story drift is determined from the maximum inelastic response as defined by Equation 5-13.

The displacement must include both translation and torsion. Hence, the drift must be checked in the plane of the lateral load resisting elements, generally at the ends of the building. P-Delta displacements must be included where significant.

For structures with a period less than 0.7 seconds, the maximum story drift is limited to:

$$\Delta_a \leq .025h \quad (5-14)$$

Where, h is the story height.

For structures with a period greater than 0.7 seconds:

$$\Delta_a \leq .020h \quad (5-15)$$

5.3.16 Irregular Structures

UBC-97 quantifies the notion of irregularity, which it breaks into two broad categories:

Table 5-9. Vertical Structural Irregularities

Irregularity Type and Definition	
1.	Stiffness irregularity-soft story A soft story is one in which the lateral stiffness is less than 70 percent of that in the story above or less than 80 percent of the average stiffness of the three stories above.
2.	Weight (mass) irregularity Mass irregularity shall be considered to exist where the effective mass of any story is more than 150 percent of the effective mass of an adjacent story. A roof that is lighter than the floor below need not be considered.
3.	Vertical geometric irregularity Vertical geometric irregularity shall be considered to exist where the horizontal dimension of the lateral-force-resisting system in any story is more than 130 percent of that in an adjacent story. One-story penthouses need not be considered.
4.	In-plane discontinuity in vertical lateral-force-resisting element An in-plane offset of the lateral-load-resisting elements greater than the length of those elements.
5.	Discontinuity in capacity-weak story A weak story is one in which the story strength is less than 80 percent of that in the story above. The story strength is the total strength of all seismic-resisting elements sharing the story shear for the direction under consideration.

Table 5-10. Plan Structural Irregularities

Irregularity Type and Definition	
1.	Torsional irregularity-to be considered when diaphragms are not flexible Torsional irregularity shall be considered to exist when the maximum story drift, computed including accidental torsion, at one end of the structure transverse to an axis is more than 1.2 times the average of the story drifts of the two ends of the structure.
2.	Re-entrant corners Plan configurations of a structure and its lateral-force-resisting system contain re-entrant corners, where both projections of the structure beyond a re-entrant corner are greater than 15 percent of the plan dimension of the structure in the given direction.
3.	Diaphragm discontinuity Diaphragms with abrupt discontinuities or variations in stiffness, including those having cutout or open areas greater than 50 percent of the gross enclosed area of the diaphragm, or changes in effective diaphragm stiffness of more than 50 percent from one story to the next.
4.	Out-of-plane offsets Discontinuities in a lateral force path, such as out-of-plane offsets of the vertical elements.
5.	Nonparallel systems The vertical lateral-load-resisting elements are not parallel to or symmetric about the major orthogonal axes of the lateral-force-resisting system.

vertical structural and plan structural irregularity. Vertical irregularities include soft or weak stories, large changes in mass from floor to floor and large discontinuities in the dimensions or in-plane locations of lateral load resisting elements. Plan irregular buildings include those which undergo substantial torsion when subjected to seismic loads, have re-entrant corners, discontinuities in floor diaphragms, discontinuity in the lateral force path, or lateral load resisting elements which are not parallel to each other or to the axes of the building.

The precise definitions of these irregularities are found in Tables 5-9 and 5-10. For a more detailed discussion of irregularity, see Chapter Six.

5.3.17 Dynamic Lateral Force Procedure

UBC-97 requires that, if the base shear determined by a dynamic analysis using a site-specific spectra is less than that specified by the static lateral force procedure, it must be scaled to equal that determined by the equivalent static force procedure. Similarly, if the base shear obtained from a dynamic analysis is greater than that specified by the static lateral force procedure, it may be scaled down. In this manner, the dynamic characteristics of the structure are modeled, and thus the forces are distributed properly, while the code level forces are maintained. If a site-specific spectrum is not available, the spectra provided in UBC-97 (see Figure 5-2) can be used.

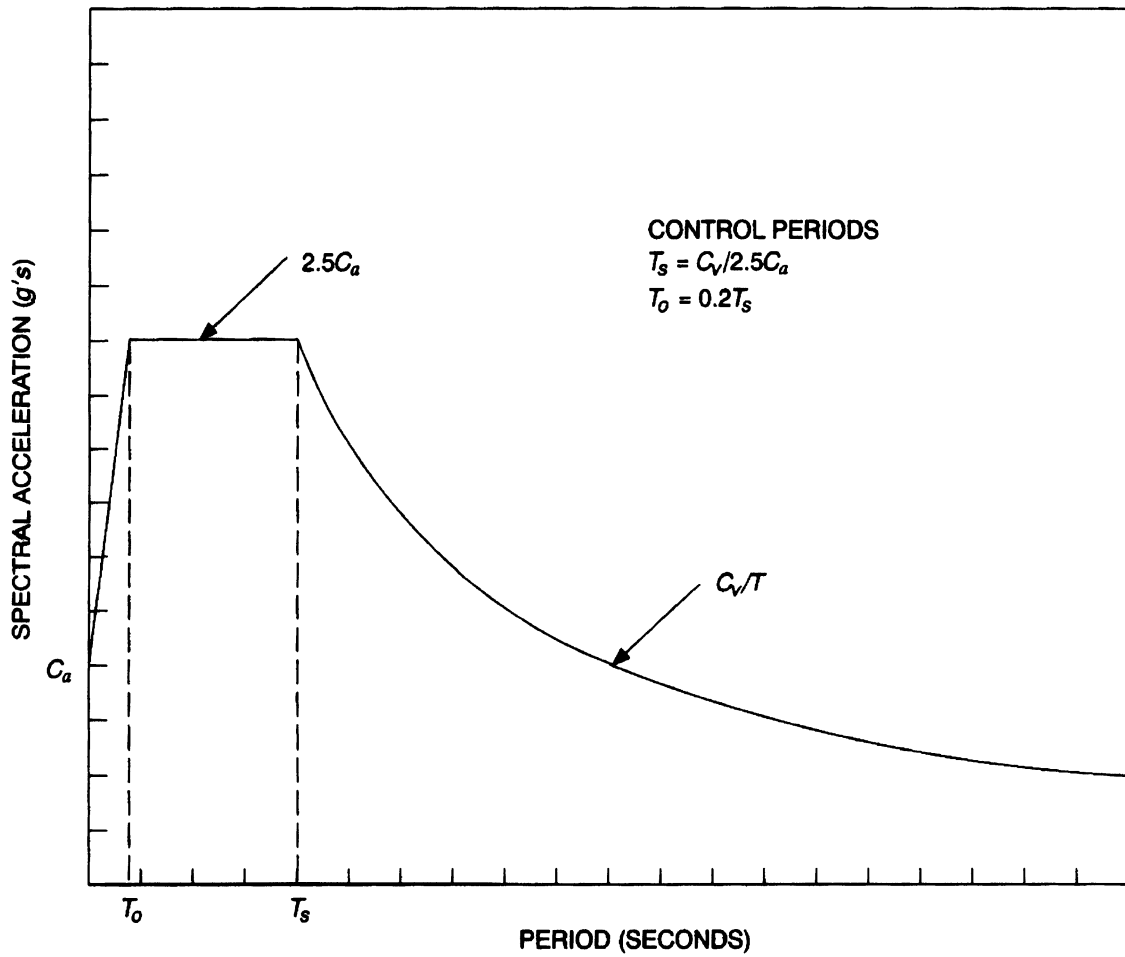


Figure 5-2. Design Response Spectra

5.3.18 Examples

Example 5-1:

Determine the UBC-97 design seismic forces for a three-story concrete shear wall office building. It is located in Southeastern California on rock with a shear wave velocity of 3000 ft/sec. The story heights are 13 feet for the first floor and 11 feet for the second and third floors. The story dead loads are 2200, 2000 and 1700 kips from the bottom up. The plan dimensions are 180 feet by 120 feet. The walls in the direction under consideration are 120 feet long and are without openings. The shear walls do not carry vertical loads. Sample calculations are presented and a complete tabulation is found in Table 5-11.

- Base Shear:

$$V = \frac{C_v IW}{RT} \quad \text{Equation 5-1}$$

I=1.0 Table 5-1

R=5.5 (Shear Walls) Table 5-2

Seismic zone 3 Figure 5-1

Z = .3 Section 5.3.2

Soil Profile Type S_B Table 5-5

C_v = .3 Table 5-3

T = .02(35)^{3/4} = .29 Seconds Equation 5-5

W = 1700 + 2000 + 2200 = 5900 k

$$V = \frac{.3(1.0)}{5.5(.29)} (5900) = 1109.2 \text{ k}$$

$$V \leq 2.5 \frac{C_a I}{R} W \quad \text{Equation 5-2}$$

Ca = .3 Table 5-4

$$V \leq \frac{2.5(.3)(1)}{5.5} (5900) = 804.5 \text{ k} < 1109.2$$

$$V \geq .11 Ca IW \quad \text{Equation 5-3}$$

$$V \geq .11 (.3) (1) (5900) = 194.7 < 804.5$$

$$V = 804.5 \text{ k}$$

- Vertical Distribution:

$$T < 0.7 \text{ sec} \quad \text{Equation 5-7b}$$

$$F_t = 0.0$$

$$F_x = (V - F_t) w_x h_x / \sum_{i=1}^n w_i h_i \quad \text{Equation 5-8}$$

$$F_3 = 804.5 (59.5) / 136.1 = 351.7 \text{ k}$$

$$F_2 = 804.5 (48) / 136.1 = 283.7 \text{ k}$$

$$F_1 = 804.5 (28.6) / 136.1 = 169.1 \text{ k}$$

- Story Shear:

$$V_x = F_t + \sum_{i=x}^n F_i \quad \text{Equation 5-9}$$

$$V_3 = 351.7 \text{ k}$$

$$V_2 = 351.7 + 283.7 = 635.4 \text{ k}$$

$$V_1 = 351.7 + 283.7 + 169.1 = 804.5 \text{ k}$$

- Overturning Moment:

$$M_x = F_t (h_n - h_x) + \sum_{i=x}^n F_i (h_i - h_x) \quad \text{Eq. 5-10}$$

$$M_3 = 351.7 (11) = 3869 \text{ ft-k}$$

$$M_2 = 351.7 (22) + 283.7 (11) = 10,858 \text{ ft-k}$$

$$M_1 = 351.7 (35) + 283.7 (24) + 169.1 (13) = 21,317$$

Table 5-11: Example 5-1

Level	h _x (ft)	w _x (k)	w _x h _x x10 ⁻³	F _t +F _t (k)	V _x (k)	M _x (ft-k)
3	35	1700.	59.5	351.7	351.7	3869.
2	24	2000.	48.0	283.7	635.4	10858
1	13	2200.	28.6	169.1	804.5	21317.
Σ		5900.	136.1	804.5		

- Allowable Inelastic Story Displacement:

$$T \leq .7 \text{ seconds}$$

$$\Delta_a \leq .025 h \quad \text{Equation 5-14}$$

2nd & 3rd Floors:

$$\Delta_a \leq .025 (11 \times 12) = 3.3 \text{ inches}$$

1st Floor:

$$\Delta_a \leq .025 (11 \times 13) = 3.56 \text{ inches}$$

- Equivalent Elastic Story Displacement:

$$\Delta \leq \frac{.025h}{.7R} = \frac{.025}{.7(5.5)}h = .0065h \quad \text{Eq. 5-13}$$

2nd & 3rd Floor:

$$\Delta \leq .0065 (11 \times 12) = .858 \text{ inches}$$

1st Floor:

$$\Delta \leq .0065 (13 \times 12) = 1.01 \text{ inches}$$

- Reliability / Redundancy Factor:

For shear walls, r_i is the maximum value of the product of the wall shear and $10/l_w$, divided by the total shear, where l_w is the length of wall in feet (120 ft).

An approximation of r_{max} can be obtained by assuming that half the story shear is carried by each wall.

$$r_{max} = \frac{(V_s/2)(10/120)}{V_s} = .04$$

$$A_B = 120 \times 180 = 21,600 \text{ ft}^2$$

$$\rho = 2 - \frac{20}{r_{max} \sqrt{A_B}} \quad \text{Equation 5-12}$$

$$\rho = 2 - 20 / .04 \sqrt{21,600} = -1.4 < \rho_{min} = 1.0$$

$$\rho = 1.0$$

Example 5-2:

Determine the UBC-97 design seismic forces for a nine story ductile moment resisting steel

frame office building located in Los Angeles, California on very dense soil and soft rock. The building is located 5km from a fault capable of large magnitude earthquakes and that has a moderate slip rate ($M>7$, $SR>2\text{mm/yr}$). The story heights are all thirteen feet. The plan area is 100 feet by 170 feet. The total dead load is 100 pounds per square foot at all levels. The moment frames consist of two four bay frames in the transverse direction and two seven bay frames in the longitudinal direction. Sample calculations are presented and a complete tabulation is found in Table 5-12.

- Base Shear:

$$V = \frac{C_v IW}{RT} \quad \text{Equation 5-1}$$

$I = 1.0$	Table 5-1
$R = 8.5$ (SMRF)	Table 5-2
Seismic Zone 4	Figure 5-1
$Z = .4$	Section 5.3.2
Soil Profile Type S _c	Table 5-5
Seismic Source Type B	Table 5-6
$N_v = 1.2$	Table 5-8
$C_v = .56 N_v = .56 (1.2) = .67$	Table 5-3

$$T = .035 (117)^{3/4} = 1.25 \text{ seconds} \quad \text{Equation 5-5}$$

$$W = .1 (170) 100 = 1700 \text{ k / floor}$$

$$W = 9 (1700) = 15,300 \text{ k}$$

$$V = \frac{(.67)(1.0)}{8.5(1.25)} W = .063 W = .063(15,300) = 964.8K$$

$$V \leq 2.5 \frac{C_a I}{R} W \quad \text{Equation 5-2}$$

$N_a = 1.0$	Table 5-7
$C_a = .4 N_a = .4 (1.0) = .4$	Table 5-4

$$V \leq 2.5 \frac{(.4)(1.0)}{8.5} (15,300) = 1800 \text{ k} > 964.8 \text{ k}$$

$$V \geq .11 C_a I W \quad \text{Equation 5-3}$$

$$V \geq .11(.4)(1.0)(15,300) = 673.2 \text{ k} < 964.8 \text{ k}$$

Since the building is in zone 4:

$$V \geq \frac{.8ZN_vI}{R}W \quad \text{Equation 5-4}$$

$$V \geq \frac{.8(.4)(1.2)(1.0)}{8.5}(15,300) = 691.2 \text{ k} < 964.8 \text{ k}$$

$$V = 964.8 \text{ k}$$

- Vertical Distribution:

$$T > .07 \text{ sec}$$

$$F_t = .07TV = .07(1.25)(964.8) = 84.4 \text{ k} \quad \text{Eq. 5-7a}$$

$$.25V = .25(964.8) = 241.2 > 84.4$$

$$F_t = 84.4 \text{ k}$$

$$(V - F_t) = 964.8 - 84.4 = 880.4$$

$$F_x = \frac{(V - F_t)(w_x h_x)}{\sum_{i=1}^n w_i h_i} \quad \text{Equation 5-8}$$

$$F_9 + F_8 = 880.4(1700)(117)/996,500 + 84.4 = 260.1 \text{ k}$$

$$F_8 = 880.4(1700)(104)/996,500 = 156.2 \text{ k}$$

(See Table 5-12)

- Story Shear:

$$V_x = F_t + \sum_{i=x}^n F_i \quad \text{Equation 5-9}$$

$$V_9 = 260.4 \text{ k}$$

$$V_8 = 260.4 + 156.2 = 416.6 \text{ k}$$

Overspinning Moment

$$M_x = F_t(h_n - h_x) + \sum_{i=x}^n F_i(h_i - h_x) \quad \text{Eq. 5-10}$$

$$M_9 = 260.1(13) = 3381 \text{ ft.-k},$$

$$M_8 = 260.1(26) + 156.2(13) = 8,793 \text{ ft-k}$$

- Allowable Inelastic Story Displacement:

$$T > 0.7 \text{ seconds}$$

Table 5-12: Example 4-2

Level	h_x (ft)	w_x (k)	$w_x h_x \times 10^{-3}$	$F_t + F_i$ (k)	V_x (k)	M_x (ft-k)
9	117	1700.	198.9	260.1	260.1	3381.
8	104	1700.	176.8	156.2	416.6	8793.
7	91	1700.	155.7	137.6	553.9	15994.
6	78	1700.	132.6	117.2	671.1	24718.
5	65	1700.	110.5	97.6	768.7	34711.
4	52	1700.	88.4	78.1	846.8	45720.
3	39	1700.	66.3	58.6	905.4	57490.
2	26	1700.	45.2	39.9	945.3	69779.
1	13	1700.	22.1	19.5	964.8	82321.
Σ		15300.	996.5	964.8		

$$\Delta_a < .02h = .02(13 \times 12) = 3.12 \text{ inches} \quad \text{Eq. 5-15}$$

- Equivalent Elastic Story Displacement:

$$\Delta_a \leq \frac{.02h}{.7R} = \frac{.02h}{.7(8.5)} = .00336h \quad \text{Eq. 5-13}$$

$$\Delta \leq .00336(13 \times 12) = .52 \text{ inches}$$

- Reliability / Redundancy Factor

For moment frames, r_i is normally 70% of the shear in two adjacent interior columns. An approximation for r_i can be obtained by assuming all interior columns carry equal shear and external columns carry half as much.

$$\rho = 2 - \frac{20}{r_{\max} \sqrt{A_B}} \quad \text{Equation 5-12}$$

$$A_B = 100 \times 170 = 17,000 \text{ ft}^2$$

Transverse Direction:

Two 4 Bay Frames

$$r_{\max} = .7(V/8 + V/8)/V = .175$$

$$\rho = 2 - \frac{20}{.175\sqrt{17,000}} = 1.12 \leq 1.25$$

$\rho_{\max} = 1.25$ for special moment frame ok.

$$\rho = 1.12$$

Longitudinal Direction:

Two 7 Bay Frames

$$r_{\max} = .7(V/14 + V/14)/V = .1$$

$$\rho = 2 - \frac{20}{.1\sqrt{17,000}} = .47 < \rho_{\min} = 1.0$$

$$\rho = 1.0$$

5.4 IBC2000 PROVISIONS

IBC2000 is broadly similar to UBC-97, but does contain significant differences. These include ground accelerations specified on a local basis by a set seismic risk maps.

The concept of a seismic use group, which is related to the importance factor in UBC-97, is introduced. In addition to defining the importance factor it is used to designate the seismic design category and to establish the allowable story drift.

The seismic design category determines the analysis procedures to be used and height and system limitations.

5.4.1 Seismic Use Group I, II, III

Each structure is assigned to a seismic use group based on the occupancy of the building and the consequences of severe earthquake damage. Three seismic hazard groups are defined:

GROUP III...."having essential facilities that are required for post-earthquake recovery and those containing substantial quantities of hazardous substances ". These facilities include fire and police stations, hospitals, medical facilities having emergency treatment facilities, emergency preparedness centers, operation centers, communication centers, utilities required for emergency backup, and structures containing significant toxic or explosive substances.

GROUP II...."have a substantial public hazard due to occupancy or use...". These include high occupancy buildings and utilities not required for emergency backup.

GROUP I -- All other buildings.

5.4.2 Occupancy Importance Factor I

An occupancy importance factor is assigned based on the seismic use group. This factor is used to increase the design base shear for structures in seismic use groups II and III.

The values of the importance occupancy factor are:

Seismic Use Group	I
I	1.0
II	1.25
III	1.50

5.4.3 Maximum Considered Earthquake Ground Motion

Regional seismicity is specified by a series of maps. The maps provide the spectral response accelerations at short periods, S_s and at a period of one second, S_1 (see Figures 5-3 and 5-4).

In areas of low seismic activity ($S_s \leq .15g$, $S_1 \leq .04g$) the acceleration need not be determined.

5.4.4 Site Class

The soil conditions at the site determine the structures "site class". These are virtually identical to the soil profile types in UBC-97 (see Table 5-5).

5.4.5 Site Coefficients F_a and F_v

The regional seismicity, as expressed by the maximum considered earthquake ground motion, S_s and S_1 , must be modified for the soil conditions at the site. These are defined by the site class. The maximum considered earthquake spectral response accelerations adjusted for site class effects, are:

$$S_{MS} = F_a S_s \quad (5-16 a)$$

$$S_{M1} = F_v S_1 \quad (5-16 b)$$

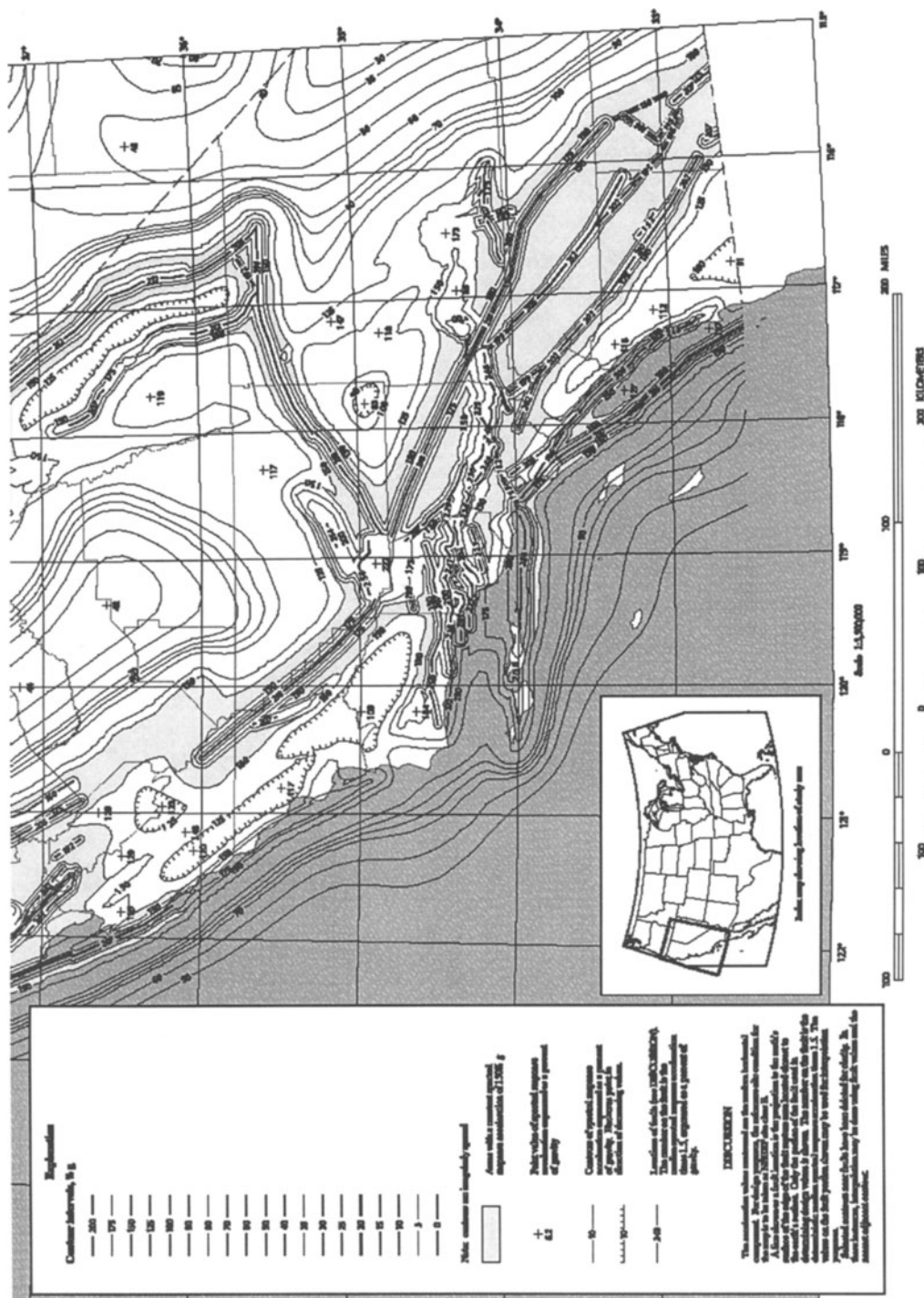


Figure 5-3. IBC 2000 Spectral Map for Short Period Range ($T=0.3$ Sec)

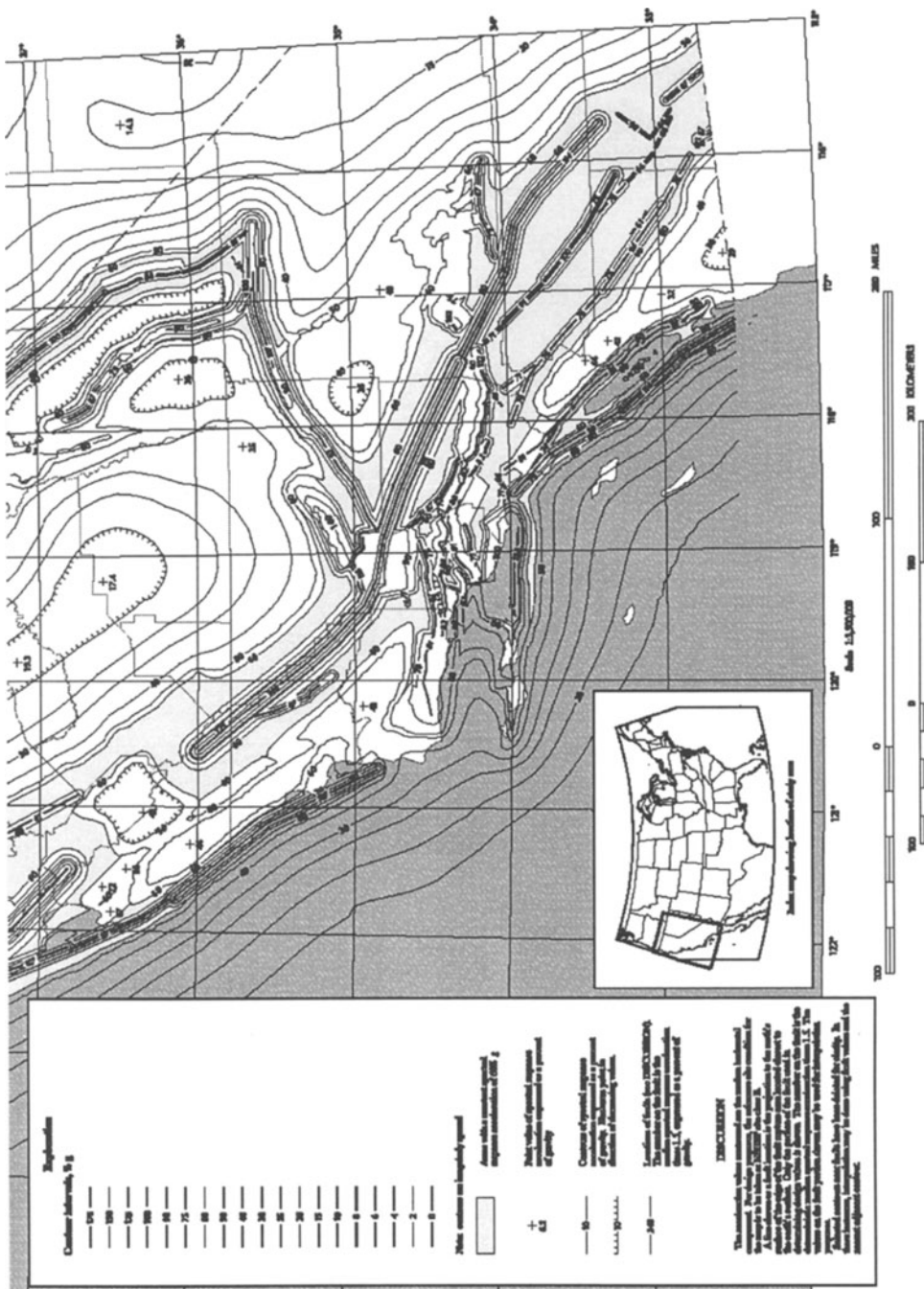


Figure 5-4. IBC 2000 Spectral Map for Intermediate Period Range ($T=1.0$ Sec).

Table 5-13. Values of F_a as a Function of Site Class and Mapped Short- Period Maximum Considered Earthquake Spectral Acceleration

Site Class	Mapped Maximum Considered Earthquake Spectral Response Acceleration at Short Periods				
	$S_s \leq 0.25$	$S_s=0.5$	$S_s=0.75$	$S_s=1.00$	$S_s \geq 1.25$
A	0.8	0.8	0.8	0.8	0.8
B	1.0	1.0	1.0	1.0	1.0
C	1.2	1.2	1.1	1.0	1.0
D	1.6	1.4	1.2	1.1	1.0
E	2.5	1.7	1.2	0.9	<i>a</i>
F	<i>a</i>	<i>a</i>	<i>a</i>	<i>a</i>	<i>a</i>

^aSite-specific geotechnical investigation and dynamic site response analyses shall be performed.

Table 5-14. Values of F_v as a Function of Site Class and Mapped 1 Second Period Maximum Considered Earthquake Spectral Acceleration

Site Class	Mapped Maximum Considered Earthquake Spectral Response Acceleration at 1 Second Period				
	$S_1 \leq 0.1$	$S_1=0.2$	$S_1=0.3$	$S_1=0.4$	$S_1 \geq 0.5$
A	0.8	0.8	0.8	0.8	0.8
B	1.0	1.0	1.0	1.0	1.0
C	1.7	1.6	1.5	1.4	1.3
D	2.4	2.0	1.8	1.6	1.5
E	3.5	3.2	2.8	2.4	<i>a</i>
F	<i>a</i>	<i>a</i>	<i>a</i>	<i>a</i>	<i>a</i>

Where, F_a and F_v are the site coefficients defined in Tables 5-13 and 5-14.

For site class F, and site class E in regions of high seismicity ($S_s > 1.25g$ or $S_1 > 5g$), a site-specific geotechnical investigation must be performed.

5.4.6 Design Spectral Response Accelerations S_{DS} and S_{D1}

The spectral accelerations for the design earthquake are:

$$S_{DS} = 2/3 S_{MS} \quad (5-17a)$$

$$S_{D1} = 2/3 S_{M1} \quad (5-17b)$$

These are the accelerations used to determine the design base shear.

5.4.7 Seismic Design Category

The structure must be assigned a seismic design category, which determines the permissible structural systems, limitations on

height and irregularity, those components of the structure that must be designed for seismic loads, and the types of analysis required.

The seismic design categories, designated A through F, are presented in Tables 5-15 and 5-16. They depend on the seismic use group and the design spectral acceleration coefficients, S_{DS} and S_{D1} . The structure is assigned the more severe of the two values taken for these tables.

5.4.8 Design Base Shear V

IBC2000 specifies the design base shear by the formula:

$$V = C_s W \quad (5-18)$$

The base shear is a percentage, C_s of the total dead load W .

5.4.9 Total Dead Load W

The seismic dead load consists of the total weight of the structure, plus partitions and permanent equipment. It also includes 25% of floor live load in areas used for storage, and the

snow load if it is greater than 30 lb/ft². The snow load may be reduced by up to 80% if its duration is short.

5.4.10 Seismic Response Coefficient C_s

The seismic response coefficient is determined from the formula:

$$C_s = \frac{S_{DS}}{R/I} \quad (5-19)$$

where

S_{DS} = the design spectral acceleration in the short period range

R = the response modification factor from Table 5-17 and defined below

I = the occupancy importance factor

The coefficient C_s, as specified by Equation 5-19, is subject to three limits.

It need not exceed:

$$C_s = \frac{S_{D1}}{TR/I} \quad (5-20)$$

It must be greater than:

$$C_s = .044 S_{DS} I \quad (5-21)$$

Additionally for structures in seismic design categories E and F, and for structures with a 1 second spectral response greater than or equal to .6g, it cannot be less than:

$$C_s = \frac{.5S_1}{R/I} \quad (5-22)$$

where

S_{D1} = the design spectral response at a 1.0 second period

T = the fundamental period of the structure

S₁ = the maximum considered earthquake spectral response acceleration at a 1 second period

5.4.11 Building Period T

The building period can be estimated using the empirical formula:

$$T_a = C_t h_n^{3/4} \quad (5-23)$$

where

Table 5-15. Seismic Design Category Based on Short Period Response Accelerations

Value of S _{DS}	Seismic Use Group		
	I	II	III
S _{DS} < 0.167g	A	A	A
0.167g ≤ S _{DS} < 0.33g	B	B	C
0.33g ≤ S _{DS} < 0.50g	C	C	D
0.50g ≤ S _{DS}	D ^a	D ^a	D ^a

^aSeismic Use Group I and II structures located on sites with mapped maximum considered earthquake spectral response acceleration at 1 second period, S₁, equal to or greater than 0.75g shall be assigned to Seismic Design Category E and Seismic Use Group III structure located on such sites shall be assigned to Seismic Design Category F.

Table 5-16. Seismic Design Category Based on 1Second Period Response Accelerations

Value of S _{DS}	Seismic Use Group		
	I	II	III
S _{D1} < 0.067g	A	A	A
0.067g ≤ S _{D1} < 0.133g	B	B	C
0.133g ≤ S _{D1} < 0.20g	C	C	D
0.20g ≤ S _{D1}	D ^a	D ^a	D ^a

$$C_t = \begin{cases} 0.035 & \text{for steel moment frames} \\ 0.030 & \text{for concrete moment frames} \\ 0.030 & \text{for eccentric braced frames} \\ 0.020 & \text{for all other buildings} \end{cases}$$

h_n = the height of the building in feet.

An alternate formula is provided for steel and concrete moment frame buildings twelve stories or less in height and with story heights ten feet or greater:

$$T_a = 0.1 N \quad (5-24)$$

where, N is the number of stories.

The period may also be determined by an analysis. The period used to determine the base shear is subject to an upper limit, which is based on the design spectral response acceleration at a period of one second, S_{D1} . The relationship between S_{D1} and the maximum

allowable period used to specify the base shear is:

S_{D1}	T_{max}/T_a
≥ 0.4	1.2
0.3	1.3
0.2	1.4
0.15	1.5
≤ 0.1	1.7

This provision insures that an excessively long analytically determined period is not used to justify an unrealistically low design base shear. When determining drifts these limits do not apply.

5.4.12 Response Modification Factor R

The response modification factor, R serves the same function as the structural system coefficient in UBC-97. It reduces the design loads to account for the damping and ductility of the structural system. An abbreviated set for values for R is found in Table 5-17.

Table 5-17 Design Coefficients and Factors for Basic Seismic-Force-Resisting Systems

Basic Seismic-Force-Resisting System	Response Modifications Coefficient, R	Deflection Amplification Factor, C_d
Bearing Wall Systems		
Special reinforced concrete shear walls	5.5	5
Ordinary reinforced concrete shear walls	4.5	4
Building Frame Systems		
Special steel concretically braced frames	6	5
Special reinforced concrete shear walls	6	5
Moment Resisting Frame Systems		
Special steel moment frames	8	5.5
Ordinary steel moment frames	4	3.5
Dual Systems with Intermediate Moment Frames Capable of Resisting at Least 25% of Prescribed Seismic Forces		
Special reinforced concrete shear walls	6	5
Ordinary reinforced concrete shear walls	5.5	4.5
Inverted Pendulum Systems and Cantilevered Column Systems		
Special steel moment frames	2.5	2.5
Ordinary steel moment frames	1.25	2.5

5.4.13 Vertical Distribution of Force F_x

The seismic force at any level is a portion of the total base shear:

$$F_x = C_{vx} V \quad (5-25)$$

where

$$C_{vx} = \frac{w_x h_x^k}{\sum_{i=1}^n w_i h_i^k} \quad (5-26)$$

where

w_i, w_x = the portion of the dead load at or assigned to level i or x
 h_i, h_x = height above the base to level i or x
 k = an exponent related to the building period as follows:

For buildings with a period of 0.5 seconds or less, $k=1.0$. If the period is 2.5 seconds or more, $k=2.0$. For buildings with a period between 0.5 and 2.5 seconds, it may be taken as 2.0 or determined by linear interpolation between 1.0 and 2.0.

For $k=1.0$ the distribution is a straight line. This is reasonable for short buildings with a regular distribution of mass and stiffness. Hence, $k=1.0$ for buildings with a period of 0.5 seconds or less.

For $k=2.0$ the distribution is a parabola with the vertex at the base. This is reasonable for tall regular buildings where the participation of higher modes is significant. Hence, $k=2.0$ for buildings with a period of 2.5 seconds or more. This effect is accounted for by the force F_t , placed at the roof in UBC-97.

5.4.14 Overturning Moment M_x

IBC2000 allows for a reduction in the design overturning moment:

$$M_x = \tau \sum_{i=x}^n F_i (h_i - h_x) \quad (5-27)$$

where

$\tau = 1.0$ for the top 10 stories

$\tau = 0.8$ for the 20th story from the top and below and is interpolated between 0.8 and 1.0 for stories in between.

Part of the reasoning behind this reduction is that the design story forces are an envelope of the maximums at each floor, and it is unlikely that they will all reach a maximum simultaneously.

5.4.15 Drift Limitations

For buildings, other than masonry, over four stories the allowable drifts are:

$$\Delta \leq \Delta_a = 0.010 h_{sx} \quad \text{Use Group III} \quad (5-28)$$

$$\Delta \leq \Delta_a = 0.015 h_{sx} \quad \text{Use Group II} \quad (5-29)$$

$$\Delta \leq \Delta_a = 0.020 h_{sx} \quad \text{Use Group I} \quad (5-30)$$

For buildings four stories or less and height, other than masonry, the allowable drifts are:

$$\Delta \leq \Delta_a = 0.015 h_{sx} \quad \text{Use Group III} \quad (5-28a)$$

$$\Delta \leq \Delta_a = 0.020 h_{sx} \quad \text{Use Group II} \quad (5-29a)$$

$$\Delta \leq \Delta_a = 0.025 h_{sx} \quad \text{Use Group I} \quad (5-30a)$$

where

Δ = the design interstory displacement

Δ_a = the allowable story displacement

h_{sx} = the height of the story below level x

The design interstory displacement Δ , is the difference in the deflections δ_x , at the top and bottom of the story under consideration. It is based on the calculated deflections and is evaluated by the formula:

$$\delta_x = \frac{C_d \delta_{xe}}{I} \quad (5-31)$$

where

C_d = the deflection amplification factor

δ_{xe} = the deflections determined by an elastic analysis.

I = the occupancy importance factor

The deflection amplification factor C_d is assigned values from 1.25 to 5.5 and accounts for the ductility of the system and the properties of the materials from which it is constructed (see Table 5-17).

In determining these deflections the period determined by an analysis may be used to calculate the base shear without considering the limitation on the period discussed in Section 5.4.11. This has the implication that lower story forces may be used to determine deflections than are used to determine member forces. A similar provision is contained in UBC-97.

Where significant, P-Delta and torsional deflections must be considered in satisfying the drift limitation. This is discussed further in the next section.

5.4.16 Torsion and P-Delta Effect

Torsion is accounted for in same manner as in UBC-97. The torsional moment resulting from the location of the center of mass plus that resulting from an assumed movement of five percent of the plan dimension must be accounted for.

For buildings with torsional irregularity, in seismic design categories C through F, the five percent accidental torsion must be amplified using Equation 5-11. For this purpose a building is irregular if the diaphragm is rigid and the maximum interstory displacement is more than 1.2 times the average.

The P-Delta effect must be included in the computation of story shears, story drifts and member forces when the value of the "stability coefficient" has a value, for any story, such that:

$$\theta = P_x \Delta / V_x h_{sx} C_d > 0.10 \quad (5-32)$$

where

Δ = the design story drift

V_x = the seismic force acting between level x and $x-1$

h_{sx} = the story height below level x

P_x = total gravity load at and above level x

C_d = the deflection amplification factor

The stability coefficient can be visualized as the ratio of the P-Delta moment ($P_x \Delta$) to the lateral force story moment ($V_x h_{sx}$). Hence if the

Table 5-18. Plan Structural Irregularities

Irregularity Type and Description	
1a	Torsional Irregularity— to be considered when diaphragms are not flexible Torsional irregularity shall be considered to exist when the maximum <i>story drift</i> , computed including accidental torsion, at one end of the <i>structure</i> transverse to an axis is more than 1.2 times the average of the <i>story drifts</i> at the two ends of the <i>structure</i> .
1b	Extreme Torsional Irregularity – to be considered when diaphragms are not flexible Extreme torsional irregularity shall be considered to exist when the maximum <i>story drift</i> , computed including accidental torsion, at one end of the <i>structure</i> transverse to an axis is more than 1.4 times the average of the <i>story drifts</i> at the two ends of the <i>structure</i> .
2	Re-entrant Corners Plan configurations of a <i>structure</i> and its lateral force-resisting system contain re-entrant corners, where both projections of the <i>structure</i> beyond a re-entrant corner are greater than 15 percent of the plan dimension of the <i>structure</i> in the given direction.
3	Diaphragm Discontinuity Diaphragms with abrupt discontinuities or variations in stiffness, including those having cutout or open areas greater than 50 percent of the gross enclosed diaphragm area, or changes in effective diaphragm stiffness of more than 50 percent from one <i>story</i> to the next.
4	Out-of-Plane Offsets Discontinuities in a lateral force resistance path, such as out-of-plane offsets of the vertical <i>elements</i> .
5	Nonparallel Systems The vertical lateral force-resisting <i>elements</i> are not parallel to or symmetric about the major orthogonal axes of the lateral force-resisting system.

Table 5-19. Vertical Structural Irregularities

Irregularity Type and Description	
1a	Stiffness Irregularity—Soft Story A soft <i>story</i> is one in which the lateral stiffness is less than 70 percent of that in the <i>story</i> above or less than 80 percent of the average stiffness of the three stories above.
1b	Stiffness Irregularity—Extreme Soft Story An extreme soft <i>story</i> is one in which the lateral stiffness is less than 60 percent of that in the <i>story</i> above or less than 70 percent of the average stiffness of the three stories above.
2	Weight (Mass) Irregularity Mass Irregularity shall be considered to exist where the effective mass of any <i>story</i> is more than 150 percent of the effective mass of an adjacent <i>story</i> . A roof that is lighter than the floor below need not be considered.
3	Vertical Geometric Irregularity Vertical geometric irregularity shall be considered to exist where the horizontal dimension of the lateral force-resisting system in any <i>story</i> is more than 130 percent of that in an adjacent <i>story</i> .
4	In-Plane Discontinuity in Vertical Lateral Force Resisting Elements An in-plane offset of the lateral force-resisting <i>elements</i> greater than the length of those <i>elements</i> or a reduction in stiffness of the resisting element in the <i>story</i> below.
5	Discontinuity in Capacity—Weak Story A weak <i>story</i> is one in which the <i>story</i> lateral strength is less than 80 percent of that in the <i>story</i> above. The <i>story</i> strength is the total strength of all seismic-resisting <i>elements</i> sharing the <i>story</i> shear for the direction under consideration.

P-Delta moment is equal to 10 percent of the story moment at any floor the P-Delta effect should be considered. The code also specifies an upper limit on the stability coefficient.

5.4.17 Irregularity

IBC2000 defines irregularity in a manner similar to UBC-97, but goes further by assigning a building to a seismic design category based on its irregularity. It distinguishes between the two broad categories of plan and vertical irregularity.

Plan irregularities include: a non-symmetrical geometric configuration, re-entrant corners, significant torsion due to eccentricity between mass and stiffness, nonparallel lateral force resisting elements, out of plane offsets and discontinuous diaphragms.

Vertical irregularities include: soft and weak stories, large changes in mass-stiffness ratios between adjacent floors, large changes in plan dimension from floor to floor and significant horizontal offsets in the lateral load system.

The definitions of plan and vertical structural irregularities and their assigned seismic design categories are found in Tables 5-18 and 5-19.

5.4.18 Reliability Factor ρ

The reliability factor ρ is identical to and serves the same function as in UBC-97 (See section 5.3.14, Equation 5-12). It is assigned a value of 1.0 for seismic design categories A, B and C. For special moment resisting frames in Seismic Design Category D, ρ cannot exceed 1.25. For special moment resisting frames in Seismic Design Categories E and F, ρ cannot exceed 1.1.

5.4.19 Analysis Procedures

The minimum level of structural analysis is dependent on the seismic design category. For buildings in category A, the design lateral force at all floors is 1 % of gravity. Buildings in categories B and C, whether regular or irregular, may be analyzed using the equivalent lateral force procedure.

The analysis procedure for buildings in categories D, E & F is specified as follows. Regular buildings up to 240 feet in height may be analyzed using the equivalent lateral force procedure. Buildings that are either over 240 feet tall, irregular, located on poor soils, or

close to known faults in areas of high seismicity require various types of dynamic analysis.

5.4.20 Dynamic Analysis

Provisions are included for a simplified two dimensional version of modal analysis which is applicable to regular structures with independent orthogonal seismic force resisting systems. For such structures the motion is predominantly planar and a two dimensional model may be appropriate.

For irregular structures or with interacting seismic force resisting systems a three dimensional model is required.

The required base shear is equal to that determined by Equation 5-18, where the period used may be 20 percent longer than the maximum period allowed in the equivalent lateral force procedure (see Section 5.4.11). The justification for this is that a modal analysis is more accurate than a static analysis. Although the total force on the building does not change appreciably its distribution over the height is more accurately modeled.

5.4.21 Examples

Example 5-3:

Rework Example 5-1 using IBC2000 and special reinforced concrete shear walls.

- Base Shear:

$$V = C_s W \quad \text{Equation 5-18}$$

seismic use group I

$I = 1.0$

$S_s = .5g$

$S_1 = .2g$

site class B

$F_a = 1.0$

$F_v = 1.0$

$S_{MS} = F_a S_s = .5g$

$S_{M1} = F_v S_1 = .2g$

$$S_{DS} = 2/3 S_{MS} = 2/3 (.5) = .333g \quad \text{Eq. 5-17a}$$

$$\begin{aligned} S_{D1} &= 2/3 S_{M1} = 2/3 (.2) = .133g && \text{Eq. 5-17b} \\ \text{seismic design cat. C} & && \text{Tables 5-15,16} \\ R = 6 \text{ (special shear walls)} & && \text{Table 5-17} \end{aligned}$$

$$C_s = \frac{S_{DS}}{R/I} = \frac{.333}{6/1} = .0555 \quad \text{Equation 5-19}$$

$$T_a = .02 h_n^{3/4} = .02(35)^{3/4} = .29 \text{ Sec} \quad \text{Eq. 5-23}$$

$$C_s \leq \frac{S_{D1}}{T(R/I)} = \frac{.133}{.29(6/1)} = .076 \quad \text{Eq. 5-20}$$

$$C_s \geq .044 S_{D1} I = .044(.333)(1) = .0147 \quad \text{Eq. 5-21}$$

$$\begin{aligned} C_s &= .0555 \\ V &= .0555 (5900) = 327.5k \end{aligned}$$

- Vertical Distribution:

$$F_x = C_{vx} V \quad \text{Equation 5-25}$$

$$C_{vx} = \frac{w_x h_x^k}{\sum_{i=1}^n w_i h_i^k} \quad \text{Equation 5-26}$$

$T < 0.5 \text{ sec}$

$k = 1.0$

Since $k=1$, the procedure is identical to Example 5-1. See Table 5-20.

- Overturning Moment:

$$M_x = \tau \sum_{i=x}^n F_i (h_i - h_x) \quad \text{Equation 5-27}$$

$\tau = 1.0$ for top ten stories

Since $\tau=1$, the procedure is the same as for Example 5-1. See Table 5-20.

Table 5-20: Example 5-3

Level	h_x (ft)	w_x (k)	$w_x h_x$ $\times 10^{-3}$	C_{vx} (k)	F_x (k)	V_x (k)	M_x (ft-k)
3	35	1700	59.5	0.44	144.1	144.1	1585
2	24	2000	48.0	0.35	114.6	258.7	4431
1	13	2200	28.6	0.21	68.8	327.5	8688
Σ		5900	136.1	1.00			

- Allowable Inelastic Story Displacements:

seismic use group I
less than four stories

$$\Delta_a = 0.025h_{sx} \quad \text{Equation 5-30a}$$

1st Floor:

$$\Delta = 0.025(13)(12) = 3.9 \text{ inches}$$

2nd and 3rd Floors:

$$\Delta = 0.025(11)(12) = 3.3 \text{ inches}$$

- Equivalent Elastic Story Displacement:

$$\delta = \frac{C_a \delta_{xe}}{I} \quad \text{Equation 5-31}$$

$$C_a = 5$$

Table 5-17

$$\delta = 5\delta_{xe}$$

1st Floor:

$$\Delta = \Delta_a / 5 = 3.9/5 = 0.78 \text{ inches}$$

2nd and 3rd Floors:

$$\Delta = \Delta_a / 5 = 3.3/5 = 0.66 \text{ inches}$$

- Reliability Factor:

seismic design category C

$$\rho = 1.0 \quad \text{Section 5.4.18}$$

Example 5-4:

Rework Example 5-2 using IBC2000.

- Base Shear:

$$V = C_s W \quad \text{Equation 5-18}$$

seismic use group I

$$I = 1.0$$

$$S_s = 2.05g$$

$$S_1 = 0.81g$$

site class C

$$F_a = 1.0$$

$$F_v = 1.3$$

$$S_{MS} = F_a S_s = 1.0 (2.05) = 2.05$$

$$S_{M1} = F_v S_1 = 1.3 (.81) = 1.05$$

$$S_{DS} = 2/3 S_{MS} = 2/3(2.05) = 1.37g$$

$$S_{D1} = 2/3 S_{M1} = 2/3 (1.05) = 0.7g$$

Section 5.4.1

Section 5.4.2

Figure 5-3

Figure 5-4

Table 5-5

Table 5-13

Table 5-14

Eq. 5-16a

Eq. 5-16b

Eq. 5-17a

Eq. 5-17b

$S_1 \geq .75g$ Tables 5-15,16; footnote a.

seismic design category E

$R = 8$ (special moment frame) Table 5-17

$$C_s = \frac{S_{DS}}{R/I} = \frac{1.37}{8/1} = .171 \quad \text{Equation 5-19}$$

$$T = .035(117)^{3/4} = 1.25 \text{ sec} \quad \text{Equation 5-23}$$

$$C_s \leq \frac{S_{D1}}{TR/I} = \frac{.7}{1.25(8/1)} = .07 \quad \text{Equation 5-20}$$

$$C_s \geq .044S_{DS}I = .044(1.37)(1) = .0603 \text{ Eq. 5-21}$$

$$C_s \geq \frac{.5S_1}{R/I} = \frac{.5(.81)}{8/1} = .051 \quad \text{Equation 5-22}$$

$$C_s = .07g$$

$$V = C_s W = .07 (15,300) = 1071 \text{ k}$$

- Vertical Distribution:

$$C_{vx} = \frac{w_x h_x^k}{\sum_{i=1}^n w_i h_i^k} \quad \text{Equation 5-26}$$

Interpolate to find k:

$$k = 1.0 + (1.25 - .5)/(2.5 - .5) = 1.375$$

$$h_9^{1.375} = 117^{1.375} = 697.8$$

$$C_{v9} = 1700(697.8)/1700(3000.9) = .233$$

$$F_9 = .233(1071) = 250 \text{ k}$$

See Table 5-21.

The story shear is determined by the same procedure as UBC-97.

- Overturning Moment:

$$M_x = \tau \sum_{i=x}^n F_i (h_i - h_x) \quad \text{Equation 5-27}$$

$\tau = 1.0$ for top ten stories

Since $\tau = 1.0$ the procedure is the same as for UBC-97. See Table 5-21.

Table 5-21: Example 5-4

Level	h_x (ft)	w_x (k)	$h_x^{1.375}$	C_{vx}	F_x (k)	V_x (k)	M_x (ft-k)
9	117	1700	697.8	.233	250	250	3250
8	104	1700	593.5	.198	212	462	9256
7	91	1700	493.9	.165	177	639	17563
6	78	1700	399.6	.133	142	781	27716
5	65	1700	311.0	.104	111	892	39312
4	52	1700	228.8	.076	81	973	51967
3	39	1700	155.1	.051	55	1028	65325
2	26	1700	88.2	.029	31	1059	79092
1	13	1700	35.0	.011	12	1071	90870
Σ		15300.	3000.9	1.0	1071		

- Allowable Inelastic Story Displacements:

seismic use group I

$$\Delta_a = 0.02h_{sx} = 0.02(13)(12) = 3.12 \text{ inches} \quad \text{Eq. 5-30}$$

- Equivalent Elastic Story Displacements:

$$C_d = 5.5$$

Table 5-17

$$\delta = C_d \delta_{xe} / I = 5.5 \delta_{xe}$$

Equation 5-31

$$\Delta \leq 2.34/5.5 = 0.567 \text{ inches}$$

- Reliability Factor:

The calculations are the same as for UBC-97
(See example 5-2):

$$\rho = 1.0 \quad \text{Longitudinal}$$

$$\rho = 1.12 \quad \text{Transverse}$$

But in seismic design category E:

$$\rho_{max} = 1.1 \quad \text{Section 5.4.18}$$

Therefore, we need more transverse bays. Note that ρ will be even higher using actual shears.

5.5 CONCLUSION

Basic linear static lateral force procedures of the 1997 UBC, the 1997 NEHRP, and the 2000 IBC codes were discussed. Numerical examples were provided to highlight practical applications of these procedures.

Chapter 6

Architectural Considerations

Christopher Arnold FAIA, RIBA

Building Systems Development Inc.

Key words: Configuration, Regular Configurations, Irregular Configurations, Proportion, Setbacks, Plan Density, Perimeter Resistance, Redundancy, Symmetry, Asymmetry, Soft-Stories, Weak Stories, Code Provisions, Plan Irregularities, Elevation Irregularities, Architectural Implications.

Abstract: While the provision of earthquake resistance is accomplished through structural means, the architectural design, and the decisions that create it, play a major role in determining the building's seismic performance. The building architecture must permit as effective a seismic design as possible: at the same time the structure must permit the functional and aesthetic aims of the building to be realized. The three categories are: (1) the building configuration, (2) structurally restrictive detailed architectural design, and (3) Hazardous nonstructural components. This chapter discusses one other issue that bears on the architectural decisions that affect seismic performance: that of the methods by which mutual architectural and engineering seismic design decisions are made during the building design and construction process. This, in turn, leads to some consideration of the architect/engineer relationship as it affects the seismic design problem.

6.1 INTRODUCTION

While the provision of earthquake resistance is accomplished through structural means, the architectural design, and the decisions that create it, play a major role in determining the building's seismic performance. The building architecture must permit as effective a seismic design as possible: at the same time the structure must permit the functional and aesthetic aims of the building to be realized.

The architectural design decisions that influence the building's seismic performance can be grouped into three categories. These categories are not exclusive, and each category of decision may influence the others, but it is useful to structure the decisions in this way because it clarifies the influences and their mutual interactions.

The three categories are:

- The building configuration: This is defined as the size, shape and proportions of the three-dimensional form of the building. The terms building concept, or conceptual design, are often also loosely used by architects to identify the configuration, although these terms also refer to architectural characteristics such as internal planning and building organization. Strictly speaking, configuration refers only to the geometrical properties of the building form.
- Structurally restrictive detailed architectural design: This refers to the architectural design of building details, such as columns or walls, that may affect the structural detailing in ways that are detrimental to good seismic design practice.
- Hazardous nonstructural components: The design of many nonstructural components is the architect's responsibility, and if inadequately designed against seismic forces, they may present a hazard to life. In addition, they may represent a major cause of property loss, and in the case of essential facilities or

other services, their damage may cause loss of building function. Engineering issues in the design of these components are dealt with in Chapter 14.

This chapter discusses one other issue that bears on the architectural decisions that affect seismic performance: that of the methods by which mutual architectural and engineering seismic design decisions are made during the building design and construction process. This, in turn, leads to some consideration of the architect/engineer relationship as it affects the seismic design problem.

6.2 CONFIGURATION CHARACTERISTICS AND THEIR EFFECTS

6.2.1 Configuration Defined

For our purposes building configuration can be defined as building size and shape: the latter includes the characteristic of proportion. In addition, our definition includes the nature, size and location of the structural elements, because these are often determined by the architectural design of the building, and are a subject of mutual agreement between architect and engineer. This extended definition of configuration is necessary because of the interaction of these elements in determining the seismic performance of the building.

In addition, architectural decisions may influence the nature, size and location of nonstructural components that may affect structural performance, either by altering the stiffness of structural members or changing the mass distribution in the building.. These elements are generally part of the initial concept of the building but they may be added later, when the building is in operation. This particularly applies to in-fill walls, which may have a dramatic effect on the effective height, stiffness, and load distribution of columns. In this chapter they are discussed later as separate

issues, apart from their relationship to configuration. These include such elements as walls, columns, service cores, and staircases, and also the quantity and type of the exterior wall elements.

6.2.2 Origins and Determinants of Configuration

The building configuration, or concept, is influenced by three main factors:

- urban design, business and real estate issues.
- planning and functional concerns.
- image and style

The selected configuration is the result of a decision process that balances these varying requirements and influences and, within a budget, resolves conflicts into an architectural concept. In very general terms three basic categories of architecture can be distinguished based on their main objective:

- **Economical containers** -the "decorated shed": warehouses, industrial plants, some department stores and commercial buildings
- **Problem/solving, functional facility** -

hospitals, educational, laboratories, residential,

- **Prestigious and/or high-style image** - corporate headquarters, some public buildings and university buildings, museums, entertainment, and some retail stores.

These categories also bear some relationship to the architects, or firms, that design them, for there is much covert specialization in architecture. This can cause client confusion: when the client who wants an economical container goes to a prestige architect, or when the client with a difficult planning problem goes to the container architect.

Building function and planning produce a demand for certain settings and kinds of space division, connected by a circulation pattern for the movement of people, supplies, and equipment. These demands ultimately lead to certain building arrangements, dimensions and determinants of configuration.

Urban design and planning requirements may affect the exterior form of the building. A height limit may set a certain maximum height; the street pattern may, particularly in a dense urban situation, determine the plan shape of the building, at least for its lower floors. City

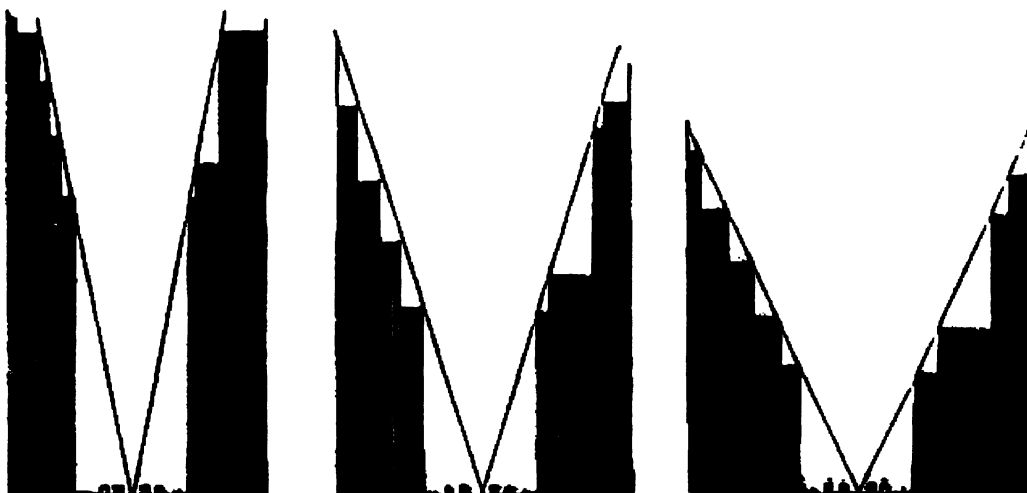


Figure 6-1. Set-back regulations, New York

planning requirements sometimes dictate the need for open first floors, for vertical setbacks, or other characteristics of architectural form. Urban design includes issues such as zoning and planning regulations, which by defining set-backs, height limits and sun-angle requirements often define the building envelope.

For example, recent studies have argued convincingly that early skyscraper form was predominantly determined by local land-use patterns, municipal codes and zoning (Figure 6-1). For example, the striking differences in form between the skyscrapers of Chicago and New York were due to the imposition of a 130 feet height limit on the former, and no limits on the latter. Zoning laws in New York, in 1916, spawned the buildings with "wedding-cake" setbacks, while a 1923 law in Chicago permitted a tower to rise above the old height limit, but restricted its total volume⁽⁶⁻¹⁾.

Engineers can accept the problems of zoning and building function in determining configuration, because they fit into the engineer's rationalist concept of the world. It is the third influence, the need for the building to present an attractive, interesting, unique, or even sensational image to the outside observer, and often the occupants, that engineers feel the trouble begins. Here is where the irrational artist takes over, and the laws of physics and economy may be violated.

It is important to understand the need for the architect sometimes to provide a distinctive image for the building. If this need did not exist the owner might go to an engineer -or contractor- to obtain a simple economical building, and indeed, many owners do so..

Up until the early years of the 20th. century for a Western architect the common acceptance required a historical style -typically mediaeval or renaissance - even when totally new building types such as railroad stations or skyscrapers were conceived. In engineering and materials terms these traditional forms were all derived from masonry structure: the need to keep the blocks of masonry in compression, and the creation of devices such as arches and vaults, to

enable the masonry to achieve larger spans than were possible by using slabs of masonry as beams or lintels. These masonry determined forms survived well into the 20th. century, even when buildings were supported by concealed steel frames, and arches had become a structural anachronism. Moreover, the prevailing historical architectural styles preferred symmetricalness, and decreed that buildings should be massive at the base, with smaller openings, and their mass should decrease with the upper floors.

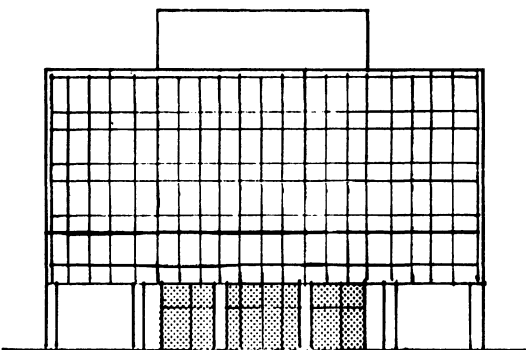


Figure 6-2. The International Style

The revolution in architectural aesthetics that began in the 1920's, and is often called the "International Style" was based on exploiting the forms that could be created by use of frame structures, combined with a desire to strip architecture of its decoration and adherence to historic styles. The International Style in architecture was not alone in extolling the virtues of unadorned structure and absence of decoration in its glorification of the beauties of Euclidean geometry. The same thing was going on in the world of painting and sculpture, and these arts were being stripped of their traditional content in favor of simplicity, geometry, and new materials.

As architects began to exploit the aesthetics of an architecture based on engineered frames, the seeds of seismic configuration problem were sown. Load-bearing masonry buildings were very limited in the extent to which configuration irregularities were possible: with short spans redundancy was always present: the

extensive use of walls, both in exteriors and interiors, meant that, even though the masonry was unreinforced, unit stresses were very low. Large cantilevers and setbacks were not possible.

But with the steel or concrete frame all these limitations were unnecessary: the building structure could be unbelievably slender (because now the columns and beams were analyzed and sized by engineers), first floor walls could be omitted, so that the building seemed to float in space. Lightness and grace were sought, rather than ornamented mass. (Figure 6-2) Buildings could even cantilever out safely so that they could become larger as they rose: the inverted pyramid could be built. These possibilities were eagerly explored by a new generation of architects: with them came other ideas: the rejection of symmetricalness of plan in favor of a more exciting and more rational disposition of elements (rational because the building elements were allowed to occur where planning function was most efficient, instead of being forced into [sometimes] inefficient symmetry).

Examples of the International Style were limited to a few avant-garde buildings in all countries before World War 2, and then bloomed in the rich economic years that began in the 50's. The United States , Western Europe, Latin America, the Soviet Union and Japan exploded in a fury of development, almost all constructed in their regional versions of the International Style. These years of intensive development saw the world's cities grow into huge metropolises: they were also years in which seismic design as it related to the new, spare, framed buildings was inadequately understood, and it took earthquakes in Latin America, Mexico and the United States (in Alaska, 1964, and San Fernando, 1971) to make engineers realize that such buildings were unforgiving and intolerant of the very irregularities that architects had embraced with such enthusiasm.

This architecture of the 50's to the 70's has left us with a legacy of poor seismic configurations that present a serious problem in

reducing the earthquake threat to our cities. The problem is exacerbated when it is allied to the engineering design problem of the use of the non-ductile reinforced concrete frame structure, which was the norm up to about 1975.

This historical discourse is relevant to seismic design, because it shows that:

- the minimalist structural frame provided the basis for an architectural aesthetic which was in tune with the spirit of the age, aesthetically, economically and politically.
- what we now call discontinuities and irregularities were critical elements of the new architectural aesthetic.
- these elements were made possible by the use of the engineered structural frame, and by a new level of architect/engineer collaboration.

It is, however, worth mentioning, that the new style originated , was promoted and developed in Western Europe, predominantly France and Germany, which, of course, are essentially non seismic zones.

A more complete discussion of the origins and influence of the International Style will be found in Reference 6-2.

6.2.3 Configuration Influences in General

Configuration largely determines the ways in which seismic forces are distributed throughout the building, and also influences the relative magnitude of those forces. For a given ground motion, the major determinant of the total inertial force in the building is , following Newton's Second Law of Motion, the building mass (approximated on the earth's surface by its weight). While the size and shape of the building (together with the choice of materials), establish its weight the building square footage and volume are determined by the building program (and the budget) : the listing of required spaces and the activities and equipment that they contain. But for any given program an almost infinite variety of

configurations can provide a solution, and it is the variables in these configurations that affect the distribution of inertial forces due to ground shaking.

Thus the discussion of configuration influence on seismic performance becomes the identification of configuration variables that affect the distribution of forces. These variables represent irregularities, or deviations from a "regular" configuration that is an optimum, or ideal, with respect to dealing with lateral forces.

6.2.4 The Optimum Seismic Configuration.

It is easiest to define a regular building by providing an example: the design discussed below represents an essentially perfectly regular building, which in turn represents an "optimum" seismic design. Its characteristics are such that deviations from the design progressively detract from its intrinsic seismic capabilities: these deviations result in "irregularities" and a familiar list of configuration irregularities can be identified. The discussion of these irregularities from an engineering and architectural viewpoint form the main body of this section..

Architecture implies occupancy: thus a solid block of concrete, which might be an optimum seismic design, is sculpture, not architecture. The great pyramid of Gizeh is architecture, and certainly approaches an optimum seismic design, but architecturally it is very uneconomic in its use of space and volume in housing only two small rooms within an enormous volume of unreinforced masonry (Figure 6-3). Our optimal seismic design is compromised by the need also to be reasonably optimal architecturally -that is, in its ability to be a functional and economically viable architectural concept.

Our design shows the three basic ways of achieving seismic resistance, and these are also part of the optimization, so the building is seismically optimized architecturally, in its configuration, and also demonstrates the best arrangement of its seismic resisting elements, in complete harmony with the architecture (Figure

6-4). For convenience, the building is arbitrarily shown as three stories: a one story building might be better seismically, all other things being equal, but with a multi-story building we can show some necessary attributes of such a building.

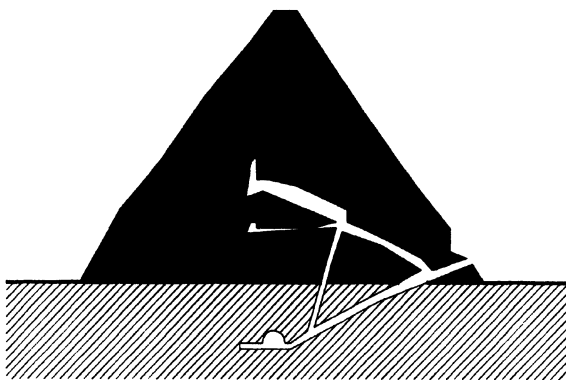


Figure 6-3. The great pyramid of Gizeh

Considered purely as architecture this little building is quite acceptable, and would be simple and economical to construct. It is also a prototypical International Style building. Depending on its exterior treatment - its materials, and the care and refinement with which they are disposed- it could range from a very economical functional building to an elegant architectural jewel; it is not complete, architecturally, of course, because stairs, elevators etc. must be added, and the building is not spatially interesting , although its interior could be configured with nonstructural components to provide almost any quality of room that was desired with the exception of interesting and/or unusual spatial volumes more than one story in height.

What are the characteristics of this design that make it regular, and also make it so good - considering only architectural configuration and the disposition of the seismic resisting elements? Any engineer will recognize them, but it is worth while listing them, because they are specific attributes whose existence or absence thereof can be quickly ascertained in any actual design. These attributes, and their effects, are:

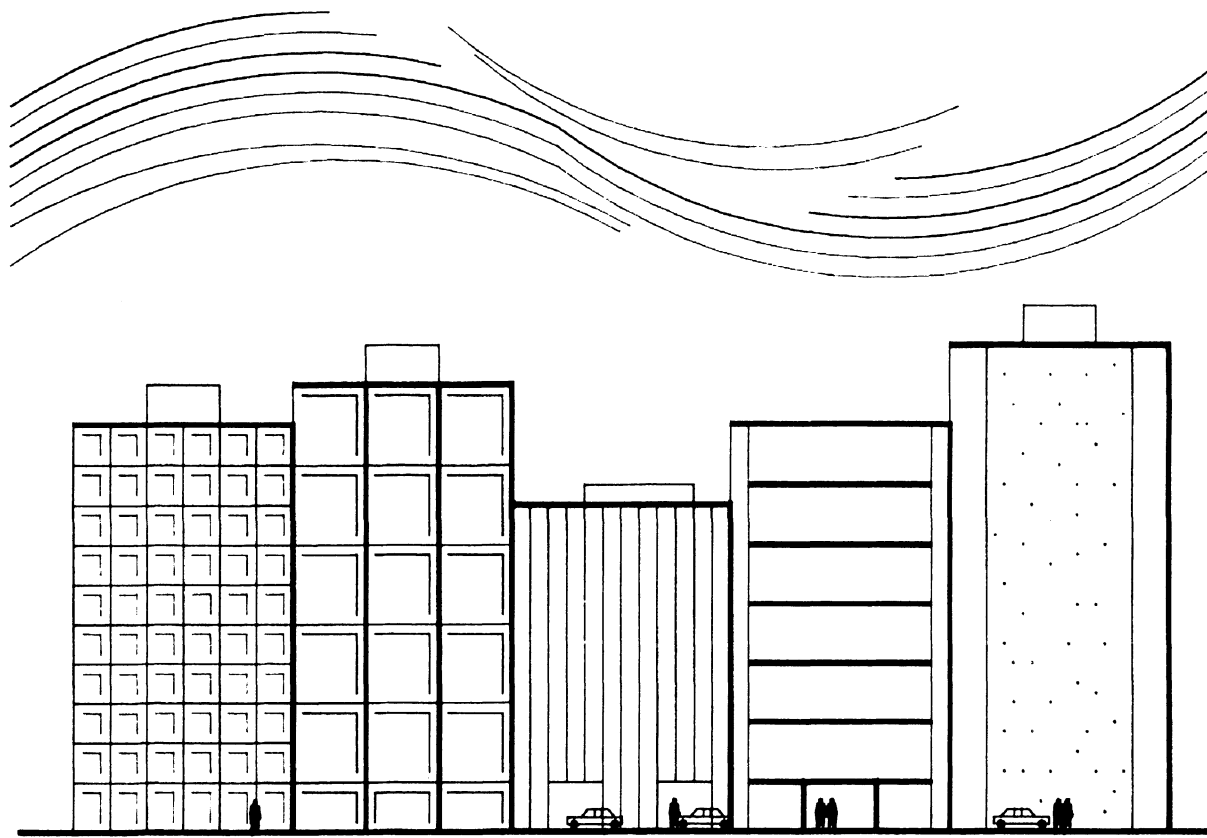


Figure 6-4. The optimal seismic design

- Low height-to base ratio
 - Minimizes tendency to overturn
- Equal floor heights
 - Equalizes column/wall stiffness
- Symmetrical plan shape
 - Reduces torsion
- Identical resistance on both axes
 - Balanced resistance in all directions
- Uniform section and elevations
 - Eliminates stress concentrations
- Maximum torsional resistance
 - Seismic resisting elements at perimeter
- Short spans
 - Low unit stress in members
- Redundancy
 - Tolerance of failure of some members
- Direct load paths, no cantilevers
 - No stress concentrations

6.3 METHODS OF ANALYSIS

6.3.1 Methods of Analysis and the Regular Building

An important aspect of a building's response to ground motion is the method of analysis used to establish the seismic forces. The estimate of total forces and their distribution is both a function of and a determinant of the lateral force-resisting system employed in the building. The great majority of designs estimate lateral forces through use of the static equivalent lateral force method (ELF) established in typical seismic codes , which involve estimating a base shear and then distributing the resulting forces through the structural elements of the building. It is

important to recognize that the forces derived from an equivalent force method used according to a typical seismic code and many other code provisions, assume a regular building, comparable to our ideal form described above. This assumption is noted in the Commentary to the 1997 NEHRP Recommended Provisions for Seismic Regulations for New Buildings⁽⁶⁻³⁾: "The *Provisions* were basically derived for buildings having regular configurations. Past earthquakes have repeatedly shown that buildings having irregular configurations suffer greater damage than buildings having regular configurations. This situation prevails even with good design and construction"

The Commentary to the 1990 Recommended Lateral Force Requirements of the Structural Engineers Association of California (Ref.6-4) discusses the design basis for regular buildings in some detail. Two important concepts apply for regular structures. First, the linearly varying lateral force distribution given by the ELF formulas are a reasonable and conservative representation of the actual response force distribution due to earthquake ground motions. Second, when the design of the elements in the lateral force resisting system is governed by the specified seismic load combinations, the cyclic inelastic deformation demands will be reasonably uniform in all elements, without large concentrations in any part of the system. The acceptable level of inelastic deformation demand for the system is therefore reasonably represented by the R_w value for the system. However, "when a structure has irregularities, then these concepts, assumptions and approximations may not be reasonable or valid, and corrective design factors and procedures are necessary to meet the design objectives".

It is safe to say, based on studies of building inventories, that over half the buildings that have been designed in the last few decades do not conform to the simple uniform building configuration upon which the code is based. For new designs, the simple equivalent lateral force

analysis of the code must often be augmented by engineering judgment based on experience.

Progressive evolution of seismic codes has resulted in increasing force levels and the consideration of additional parameters in estimating force levels, but the impact of configuration irregularity, which was first introduced into the Uniform Building Code in 1973, long remained a matter of judgment. However, starting in 1988 the UBC quantified some configuration parameters, to establish the condition of regularity or irregularity, and laid down some specific analytical requirements for irregular structures.

6.3.2 Irregular Configurations: Code Definitions and Methods of Analysis

In the Commentary to the 1980 SEAOC Recommended Lateral Force Requirements and Commentary⁽⁶⁻⁵⁾, over 20 types of "irregular structures or framing systems" were noted as examples of designs that should involve extra analysis and dynamic consideration rather than use of the normal equivalent lateral force method. These types are illustrated in Figure 6-5, which is a graphical interpretation of the SEAOC list. Scrutiny of these conditions shows that the majority of irregularities are configurational issues within the terms of our definition.

This list of irregularities defined the conditions, but provided no quantitative basis for establishing the relative significance of a given irregularity. These irregularities vary in the importance of their effects, and their influence also varies in accord with the particular geometry or dimensional basis of the condition. Thus, while in an extreme form the reentrant corner is a serious type of plan irregularity, in a lesser form it may have little significance (Figure 6-6). The determination of the point at which a given irregularity becomes serious is a matter of judgment.

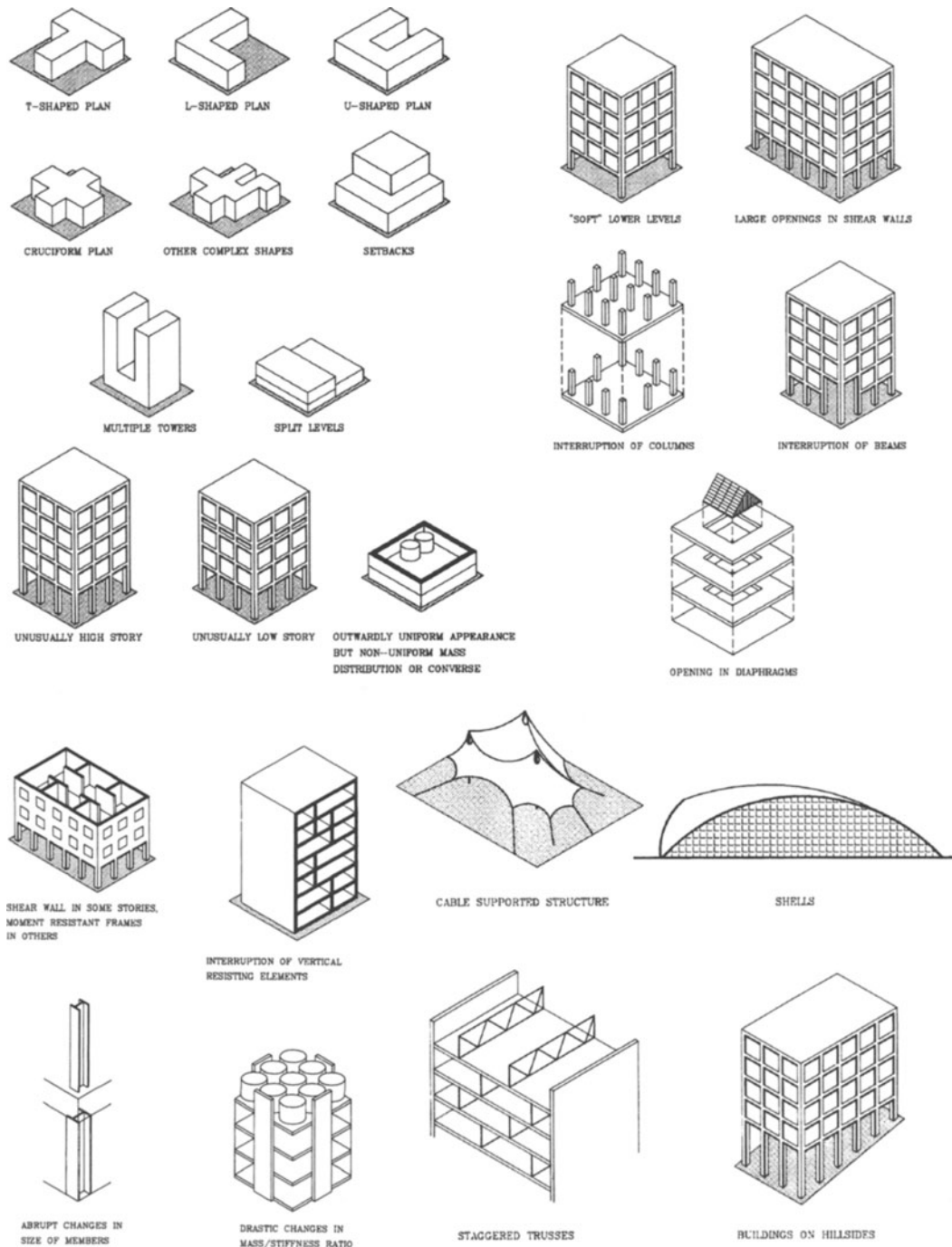


Figure 6-5. Graphic interpretation of "Irregular Structures or Framing Systems" from the commentary to the "SEAOC Recommended Lateral Force Requirements and Commentary" (a) Buildings with Irregular Configuration (b) Buildings with abrupt changes in lateral resistance (c) Buildings with abrupt changes in lateral stiffness (d) Unusual or novel structural features.

The SEAOC Commentary explained the difficulty of going beyond this basic listing as follows:

Due to the infinite variation of irregularities (in configuration) that can exist, the impracticality of establishing definite parameters and rational rules for the application of this Section are readily apparent.

However, in the most recent version of the SEAOC Requirements and Commentary, and starting in the 1988 revisions to the Uniform Building Code, (which is based on the SEAOC document), an attempt has been made to quantify some critical irregularities, and to define geometrically or by use of dimensional ratios the points at which the specific irregularity becomes an issue of such concern that remedial measures must be taken.

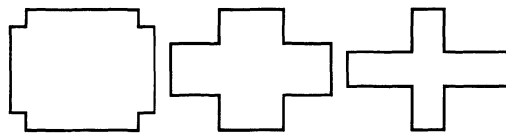


Figure 6-6. The reentrant corner plan : a range of significance

The code approach to reducing the detrimental effect of irregularity is to require more advanced methods of analysis where such conditions occur - more specifically, where the ELF analysis method must be augmented or cannot be used. While this may provide a more accurate diagnosis, and in some instances strengthening of certain members, it does not correct the condition: this must still be done by design means based on understanding of the effects of the condition on building response.

The code requirements relating to the definition of regularity and irregularity, and the determination of the analysis methods required have now become complex, and for design purposes the relevant sections of the applicable code should be referred to. The outline that follows focuses on identifying the irregular conditions for which the ELF method can be

used, must be augmented or where a more complex method is necessary. The irregularity type references are to the 1997 *NEHRP Recommended Provisions for the Development of Seismic Regulations for New Buildings* as illustrated in Figure 6-7. This figure is a graphic interpretation of Table 5.2.3.1 and Table 5.2.3.2 in the *Provisions*. The terminology and configuration requirements in the UBC and the NEHRP *Provisions* are essentially similar.

The ELF method can be used for the following irregular structural types, with the noted augmentations:

1. All structures in Seismic Design Category A (in the NEHRP *Provisions* the Seismic Design Category is a classification assigned to a structure based on its seismic use group, or occupancy, and the severity of the design earthquake ground motion at the site).
2. Structures with reentrant corners (plan irregularity type 2), diaphragm discontinuity (type 3) out-of-plane offsets (type 4), in Seismic Design Categories D, E and F, must provide for an increase in design forces of 25% for connection of diaphragms to vertical elements and to collectors, and connection of collectors to vertical elements.
3. Structures with nonparallel systems (plan irregularity type 5) in Seismic Design Category C,D,E and F, must be analyzed for seismic forces applied in the critical direction, or satisfy the following combination of loads: 100% of forces in one direction plus 30% of the forces in the perpendicular direction.
4. Structures with out-of-plane offsets (plan irregularity type 4) and in-plane discontinuity in vertical lateral force resisting elements (vertical irregularity type 4) must have the design strength to resist the maximum axial forces that can develop in accordance with specially defined load combinations.

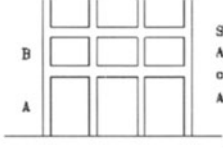
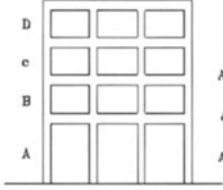
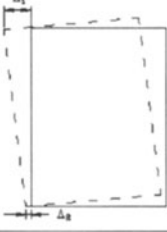
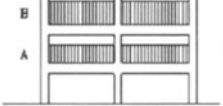
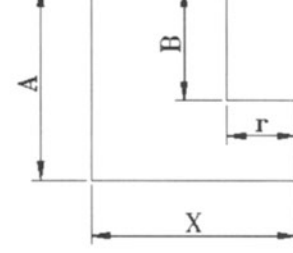
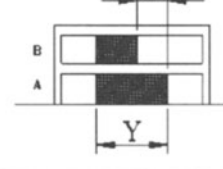
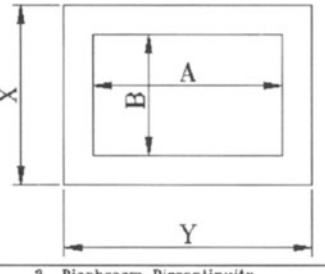
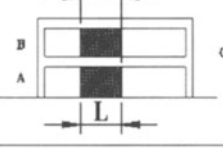
Vertical Irregularities	Plan Irregularities
 <p>STIFFNESS $A < 20\% B$ (1a) or $A < 60\% B$ (1b)</p> <p>Or</p>  <p>STIFFNESS $A < 80\% \frac{(B+C+D)}{3}$ (1a) Or $A < 70\% \frac{(B+C+D)}{3}$ (1b)</p> <p>1a Stiffness Irregularity - Soft Story and 1b Stiffness Irregularity - Extreme Soft Story</p>	 <p>$\Delta_1 > 12 \times \frac{(\Delta_1 + \Delta_2)}{2}$ (1a) or $\Delta_1 > 14 \times \frac{(\Delta_1 + \Delta_2)}{2}$ (1b)</p> <p>1a Torsional Irregularity With Stiff Diaphragm 1b Extreme Torsional Irregularity With Stiff Diaphragm</p>
 <p>MASS $B > 150\% A$</p> <p>2 Weight (mass) Irregularity</p>	 <p>Projections $Y > 15\% X$ $B > 15\% A$</p> <p>2 Reentrant Corners</p>
 <p>$X > 30\% Y$</p> <p>3 Vertical Geometric Irregularity</p>	 <p>AREA $AB > 50\% XY$</p> <p>3 Biaphragm Discontinuity</p>
 <p>Offset $L_1 > L$</p> <p>4 In-Plane Discontinuity in Vertical Lateral Force Resisting System</p>	 <p>OFFSET</p> <p>4 Out-Of-Plane Offsets</p>
 <p>Shear Strength $A < 80\% B$</p> <p>5 Discontinuity in Capacity - Weak Story</p>	 <p>5 Nonparallel Systems</p>

Figure 6-7. Irregularities defined in the 1997 NEHRP Provisions

Other buildings with plan or vertical irregularities as defined in the Tables, that are not required to use modal analysis as identified below, may use the ELF procedure with "dynamic characteristics given special consideration": the engineer must use judgment in computing forces.

Buildings with certain types of vertical irregularity may be analyzed as regular buildings in accordance with normal ELF procedures. These buildings are generally referred to as setback buildings. The following procedure may be used:

1. The base and lower portions of a building having a setback vertical configuration may be analyzed as indicated in (2) below if all of the following conditions are met:

- a. The base portion and the tower portion, considered as separate buildings, can be classified as regular and.
- b. The stiffness of the top story of the base is at least five times that of the first story of the tower.

Where these conditions are not met, the building shall be analyzed using modal analysis.

2. The base and tower portions of the building may be analyzed as separate buildings in accordance with the following:

- a. The tower may be analyzed in accordance with the usual ELF procedure with the base taken at the top of the base portion.
- b. The base portion then must be analyzed in accordance with the ELF procedure using the height of the base portion of h_n and with the gravity load and base shear of seismic forces the tower portion acting at the top level of the base portion.

Modal Analysis is required in the following instances:

1. Buildings which are in Seismic Design Category D, E or F, are over 65 feet in height, and have:

- soft stories (vertical irregularity type 1a)
- extreme soft stories (vertical irregularity type 1b)
- mass irregularities (vertical irregularity type 2)
- vertical geometrical irregularity (vertical irregularity type 3)

Exceptions: vertical structural irregularities of types 1a, 1b or 2 do not apply where no story drift ratio under design lateral load is greater than 130 percent of the story drift ratio of the next story above

2 Buildings , with torsional irregularity (plan irregularity type 1a) in Seismic Design Category D, E or F and extreme torsional irregularity ((plan irregularity type 1b) in Seismic Design Category D. In addition an increase in design forces of 25% is required for connection of diaphragms to vertical elements and to collectors, and connection of collectors to vertical elements, and a torsion amplification factor.

3. All structures over 240 feet in height.

The following irregular structures are not permitted:

Weak story structures (vertical irregularity type 5) over 2 floors or 30 feet in height with a weak story less than 65% of the strength of the story above, in Seismic Design Categories, B, C, D, E and F.

Extreme soft story structures (vertical irregularity type 1b) and extreme torsional irregularity structures (plan irregularity

type 1b) in Seismic Design categories E and F.

The Commentary to the NEHRP *Provisions* also provides a procedure which may reduce the need to perform modal analysis.

"The procedures defined in the *Provisions* include a simplified modal analysis which takes account of irregularity in mass and stiffness distribution over the height of the building. It would be adequate, in general, to use the ELF procedure for buildings whose seismic resisting system has the same configuration in all stories and all floors, and whose floor masses and cross sectional areas and moments of inertia of structural members do not differ by more than 30% in adjacent floors and in adjacent stories.

For other buildings, the following criteria should be applied to decide whether modal analysis procedures should be used:

1. The story shears should be computed using the ELF procedure.
2. On this basis, approximately dimension the structural members, and then compute the lateral displacement of the floors.
3. Replace the h_x^k term in the vertical distribution of seismic forces equation with these displacements and recompute the lateral forces to obtain new story shears.
4. If at any story the recomputed story shear differs from the corresponding value as obtained from the normal ELF procedure by more than 30%, the building should be analyzed using the modal analysis procedure. If the difference is less than this value, the building may be designed for the story shear obtained in the application of the present criterion and the modal analysis procedures are not required."

This procedure greatly reduces the likelihood that the considerably more complex modal analysis procedure will be required for the building analysis: this is of major importance because building irregularity is quite likely to be present in buildings of modest size and tight budget, and costly analysis procedures are not welcome to the owner.

In addition, the 1997 NEHRP *Provisions* make further predominantly nonquantitative comments about the use of the Equivalent Lateral Force procedure for irregular buildings:

"The ELF procedure is likely to be inadequate in the following cases:

1. Buildings with irregular mass and stiffness properties in which case the simple formulas for vertical distribution of lateral forces may lead to erroneous results;
2. Buildings (regular or irregular) in which the lateral motions in two orthogonal directions and the torsional motions are strongly coupled, and
3. Buildings with irregular distribution of story strengths leading to possible concentration of ductility demand in a few stories of the building.

In such cases, a more rigorous procedure which considers the dynamic behavior of the structure should be employed.

The *Provisions* Commentary points out that the ELF procedure, and both versions of the modal analysis procedure (a simple version and a general version with several degrees of freedom per floor which are described in the *Provisions*) are all likely to err systematically on the unsafe side if story strengths are distributed irregularly over height. This points to the importance of eliminating such irregularities if possible, but often they will be present because of detailed architectural requirements: if they cannot be eliminated, the engineer must use his judgment to assess their effects on the analysis.

Even if the modal analysis procedure is used there are limitations to the information that the analysis provides. The procedure adequately addresses vertical irregularities of stiffness, mass or geometry. Other irregularities must be carefully considered on a judgmental basis, and so the engineer must rely on his experiential and conceptual knowledge of the building's response in order to effectively accommodate all irregularities.

6.4 GENERAL BUILDING CHARACTERISTICS

6.4.1 Introduction

These are issues relating to the building configuration as a whole and apply to all configurations.

Irregularity as defined in current seismic codes , and as discussed above, covers the majority of configuration variables that have a significant effect on the seismic performance of the building. Although definitions vary, there is general agreement on those configuration irregularities that are important.

However, the code listing is not complete: issues of building proportion and size are not included, nor are issues such as the building plan density or its redundancy the subject of code provisions, although the latter is briefly mentioned.. These are discussed below. The problem of pounding, which combines the issue of drift with that of building adjacency, and as such may present an architectural problem, is discussed in Section 6.9 below.

6.4.2 Size, Proportion and Symmetry

- **Building size:**

It is possible to introduce configuration irregularities into a wood frame house that would be serious problems in a large building, and yet produce a safe structure with the inclusion of relatively inexpensive and unobtrusive provisions. This is because a small

wood frame structure is light in weight and inertial forces will be low. In addition, spans are short and relative to the floor area, there will probably be a large number of walls to share the loads.

For a larger building, the violation of basic layout and proportion principles exacts an increasingly severe cost, and as the forces become greater, good performance cannot be relied upon as in an equivalent building of better configuration.

As the absolute size of a structure increases, the number of alternatives for the arrangement of its structure decreases. A bridge span of 300ft. may be built as a beam, arch, truss, or suspension system, but a span of 3000 ft. can only be designed as a suspension structure. And as the size increases the structural discipline becomes more rigorous: architectural flourishes that are perfectly acceptable at the size of a house become physically impossible at the size of a suspension bridge.(Figure 6-8).

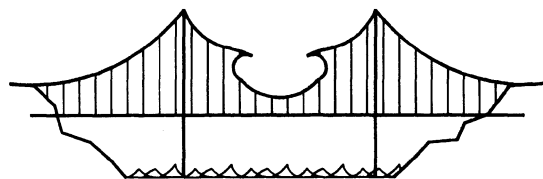


Figure 6-8. The designer's suspension bridge

In looking at the influence of building size on seismic performance, the influence of both the dynamic environment and the characteristics of ground motion result in more complexity than does the influence of size on vertical forces. Increasing the height of a building may seem equivalent to increasing the span of a cantilever beam, and so it is (all other things being equal). The problem with the analogy is that as a building grows taller its period will tend to increase, and a change in period means a change in the building response.

The effect of the building period must be considered in relation to the period of ground motion, and if amplification occurs, the effect of an increase in height may be quite disproportionate to the increase itself. Thus

doubling the building height from 6 to 10 stories may, if amplification occurs, result in a four or fivefold increase in seismic forces. The earthquake in Mexico City in 1985 resulted in major response and amplification in buildings in the 6 to 20 story range, with generally reduced response in well-built buildings below and above these heights.

Although a 100-ft. height limit throughout Japan was enforced until 1964, a 150-ft 13 story limit was the maximum in Los Angeles until 1957, and the limit was 80 ft and later 100 ft on San Francisco, height is rarely singled out as a variable to be used to reduce the building response. Two recent exceptions to this may be noted. After the Armenian earthquake of 1988, planners of the reconstruction of the city of Leninakan limited the height of new buildings to three stories, because of the ground conditions and the bad experience with taller buildings. This decision is especially interesting because it required a major shift in planning and architectural thinking: prior to this, almost all Soviet-style housing consisted of medium to high-rise blocks. After the Mexico City earthquake of 1985 a number of damaged buildings were "topped" as part of the repair strategy: a number of floors were removed, thus changing the building period to something less in tune with the long period ground motions that the city experiences.

The present approach is generally not to legislate seismic height limits (except insofar as seismic codes impose height limits relating to types of construction), but to enforce more specific seismic design and performance criteria. Generally, urban design, real-estate or programmatic factors will be more significant, and earthquake performance must be engineered with the height predetermined by these factors.

It is easy to visualize the overturning forces associated with height as a seismic problem (although the issue is more that of the aspect ratio of shear walls rather than the building as a whole), but large plan areas can be detrimental also. When the plan becomes extremely large, even if it is symmetrical and of simple shape,

the building can have trouble responding as one unit to the ground motion. Unless there are numerous interior lateral-force resisting elements, large-plan buildings impose unusually severe requirements on their diaphragms, which have large lateral spans, and can build up large forces to be resisted by shear walls or frames. The solution is to add walls or frames to reduce the span of the diaphragm, although it is recognized that this may introduce problems in the use of the building. In a very large building, seismic separations may be necessary to subdivide the building and keep the diaphragm forces within bounds, in which case the seismic separations may also act as thermal expansion joints.

An interesting example of a correct "intuitive" response to this problem is that of the design of the Imperial Hotel, Tokyo, by the architect Frank Lloyd Wright in the early 1920s. He subdivided this large complex building, with long wings and many reentrant corners, into small regular boxes, each about 35 ft. by 60 ft in plan. In doing this, he appears to have been concerned about the possibility of differential settlement caused by a travelling wave on the site. In the use of this concept, to which he attributed in large measure the success of the building in surviving the 1923 Kanto earthquake, Wright was well ahead of his time. The short-pile foundation scheme, which Wright claimed as a major invention, probably had much less to do with the building's good performance⁽⁶⁻⁶⁾.

• Building Proportion

In seismic design, the proportions of a building may be more important than its absolute size. For tall buildings, the slenderness ratio (height/least depth) of a building, calculated in the same way as for an individual member, is a more important consideration than just height alone. Dowrick⁽⁶⁻⁷⁾ suggests attempting to limit the height/depth ratio to 3 or 4, explaining:

"The more slender a building the worse the overturning effects of an earthquake and the greater the earthquake stresses in the outer columns, particularly the overturning compressive forces which can be very difficult to deal with."

As urban land becomes more expensive, there is a trend towards designing very slender "sliver" buildings which, although not necessarily very high, may have a large height/depth ratio. Nowhere is this trend more apparent than in Japanese cities, where multistory buildings may be built on sites that are of the order of 15 to 20 ft wide (Figure 6-9). However, the same economic forces often dictate that these buildings will be built very close together, so that they will tend to respond as a unit rather than as individual free-standing buildings, although more recent Japanese

buildings have incorporated relatively large separations to reduce the risk of pounding.

• Building Symmetry

The term symmetry denotes a geometrical property of building plan configuration. Structural symmetry means that the center of mass and center of resistance are located at, or close to, the same point (unless live loads affect the actual center of mass). The single admonition that appears in all codes and in textbooks that discuss configuration is that symmetrical forms are preferred to asymmetrical ones. The two basic reasons are that eccentricity between the centers of mass and resistance will produce torsion and stress concentrations.

However, a building with reentrant corners is not necessarily asymmetrical (a cruciform



Figure 6-9. Slender buildings, Tokyo, Japan

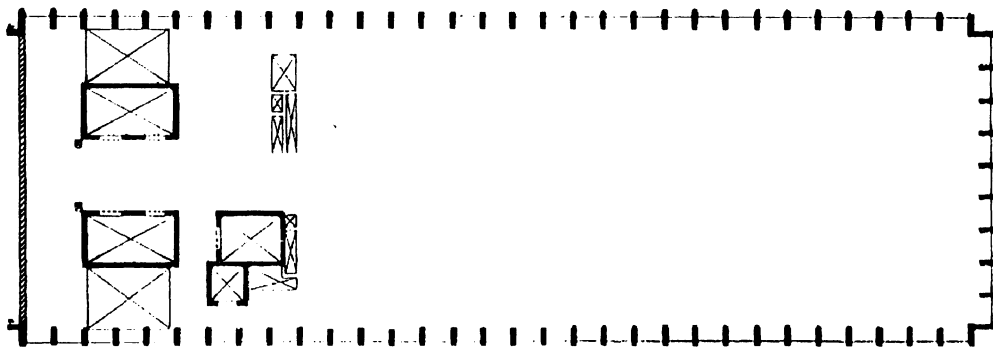


Figure 6-10. False symmetry: offset structural core

building may be symmetrical) but it is irregular, as defined, for example, in current seismic codes. Thus symmetry is not sufficient on its own, and only when it is combined with simplicity is it beneficial.

Nevertheless, it is true that as the building becomes more symmetrical, its tendency to suffer torsion and stress concentration will reduce, and performance under seismic forces will tend to be less difficult to analyze. This suggests that when good seismic performance must be achieved with maximum economy of design and construction, the symmetrical, simple shapes are much to be preferred. But these tendencies must not be mistaken for an axiom that a symmetrical building will not suffer torsion.

The effects of symmetry refer not only to the overall building shape, but to its details of design and construction. Study of building performance in past earthquakes indicates that performance is sensitive to quite small variations in symmetry within the overall form.. This is particularly true in relation to shear-wall design and where service cores are designed to act as major lateral resistant elements. It is possible to have a building which is geometrically symmetrical in exterior form, but highly asymmetrical in the arrangement of its structural systems. The most common form of this condition (sometimes termed "false symmetry") is the building with interior structural cores that, for planning reasons, are unsymmetrically arranged. This can be a major

source of undesirable torsional response. (Figure 6-10)

Experience in the Mexico City earthquake of 1985 showed that many buildings that were symmetrical and simple in overall plan suffered severely because of asymmetrical location of service cores and escape staircases. Moreover, as soon as a structure begins to suffer damage (cracking in shear walls or columns, for example), its distribution of resistance elements changes, so that even the most symmetrical of structures becomes dynamically asymmetrical and subject to torsional forces.

Finally, it must be recognized that architectural requirements will often make the symmetrical design impossible. In these circumstances, it may be necessary, depending on the size of the building and the type of asymmetry, to subdivide the building into simple elements.

There is a tendency, as noted above, for the very tall building to tend towards symmetry and simplicity. The seismic problems are most apparent in the low to medium-height building, where considerable choice exists as to plan form and the disposition of the major masses of the building.

6.4.3 Plan Density, Perimeter Resistance, and Redundancy

The size and density of structural elements in the buildings of former centuries is strikingly greater than in today's buildings. Structural

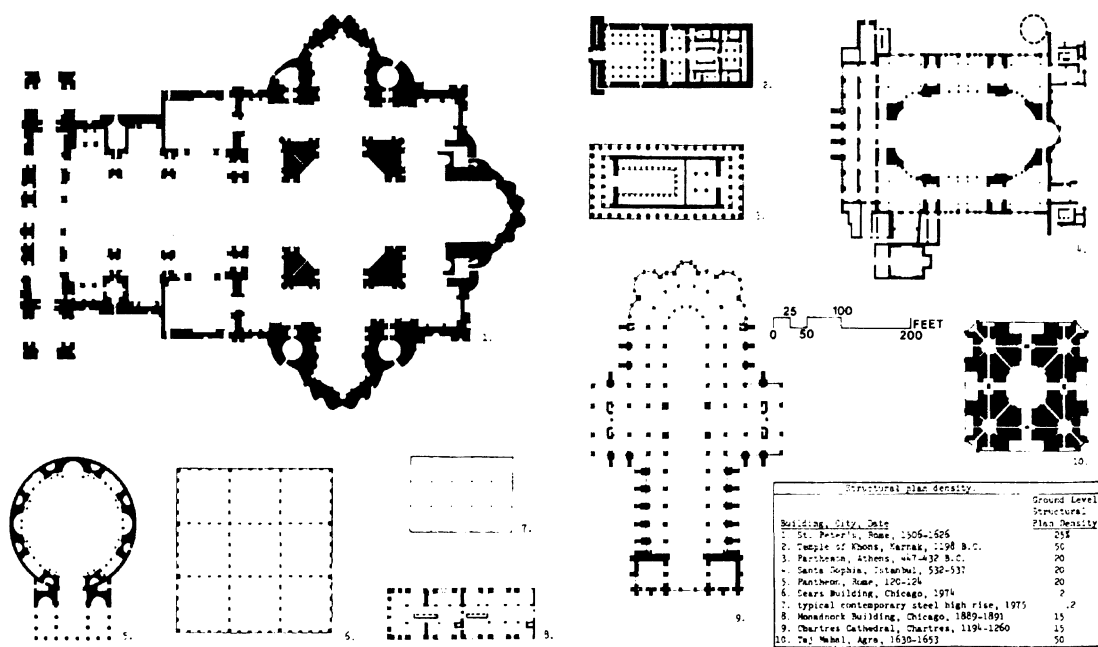


Figure 6-11. Structural plan density

technology has allowed us to push this trend continually further.

Earthquake forces are generally greater at the base of the building. The bottom story is required to carry its own lateral load in addition to the shear forces of all the stories above, which is analogous to the downward build-up of vertical gravity loads. At this same lowest level, programmatic and aesthetic criteria are often imposed on the building that demand the removal of as much solid material as possible. This requirement is the opposite of the most efficient seismic configuration, which would provide the greatest intensity of vertical resistant elements at the base, where they are most needed.

An interesting statistical measure in this regard is the ground level vertical plan density, defined as the total area of all vertical structural elements divided by the gross floor area. The most striking characteristic of the modern framed building is the tremendous reduction of structural plan density compared to historic buildings.

For instance, a typical 10- to 20-story, moment resistant steel frame building will

touch the ground with its columns over 1% or less of its plan area, and combined frame shear-wall designs will typically reach structural plan densities of only 2%. The densely filled-in "footprints" of buildings of previous eras present a striking contrast: the structural plan density can go as high as 50%, in the case of the Taj Mahal: the ratio for St. Peter's in Rome is about 25%, and for Chartres Cathedral 15%. The 16-story Monadnock Building in Chicago, which used exterior bearing walls of brick 6 ft. thick at the ground level, has a ratio of 15% (Figure 6-11).

Analogous to structural plan density is the measure of the extent of walls in a structure. Surveys of damaged buildings in Japan and Turkey have indicated a clear relationship between the length of walls in a box-type system building and the extent of damage. This relationship has been incorporated in the seismic codes of these and other countries to provide prescriptive guidance for the design of simple structures.

In Figure 6-12, although both configurations are symmetrical and contain the same amount of shear wall, the location of walls is

significantly different. The walls on the right form greater lever arms for resisting overturning and torsional moments. In resisting torsion, with the center of twist of a symmetrical building located at or near the geometrical center, the further the resisting material is placed from the center, the greater the lever arm through which it acts, and hence the greater the resisting moment that can be generated. Placing resisting members on the perimeter whenever possible is always desirable, whether the members are walls, frames, or braced frames, and whether they have to resist direct lateral forces, torsion, or both.

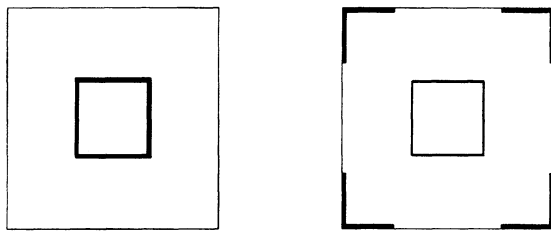


Figure 6-12. Location of lateral resistance elements

The design characteristic of redundancy plays an important role in seismic performance, and is significant in several aspects, most especially because the redundant design will almost certainly offer direct load paths and in this it tends to result in higher plan density as discussed above. In addition, historic buildings tended to be highly redundant, because short spans required many points of support, and thus each supporting member incurs much lower stresses, often even within the capability of unreinforced masonry. Thus, the very limitations of traditional materials forced the designers into good design practices such as redundancy, direct load paths and high plan density.

The detailing of connections is often cited as a key factor in seismic performance, since the more integrated and interconnected a structure is, the more load distribution possibilities there are.

6.5 SEISMIC SIGNIFICANCE OF TYPICAL CONFIGURATION IRREGULARITIES

6.5.1 Introduction

The discussion of configuration issues that follows incorporates all the code-defined issues but, in going back to our original definition of configuration, categorizes configuration problems in ways that relates the seismic implications to those of their architectural origins as decisions made at the conceptual stages of the design.

For each configuration issue, five issues are outlined: definition of the condition, its seismic effects, its architectural implications, historical performance in past earthquakes, and solutions. The notes on architectural effects discuss the origin and purpose of the condition in architectural terms: the discussion of solutions deals with conceptual design approaches, and is most relevant for the consideration of existing buildings.

6.6 PLAN CONFIGURATION PROBLEMS

6.6.1 Reentrant Corners

- Definition

The reentrant, or "inside" corner is the common characteristic of overall building configurations that, in plan, assume the shape of an L, T, H, +, or combination of these shapes.

- Seismic Effects

There are two related problems created by these shapes. The first is that they tend to produce variations of rigidity, and hence differential motions, between different parts of the building, resulting in a local stress concentration at the "notch" of the reentrant

corner. In Figure 6-13, if the ground motion occurs with a north-south emphasis at the L-shaped building shown, the wing oriented north-south will, for geometrical reasons, tend to be stiffer than the wing oriented east-west. The north-south wing, if it were a separate building, would tend to deflect less than the east-west wing, but the two wings are tied together and attempt to move differentially at their notch, pulling and pushing each other. (Figure 6-14). For ground motions along the other axis, the wings reverse roles, but the differential problem remains.

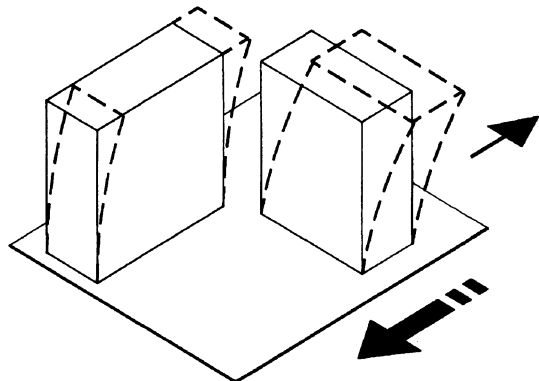


Figure 6-13. Separated buildings

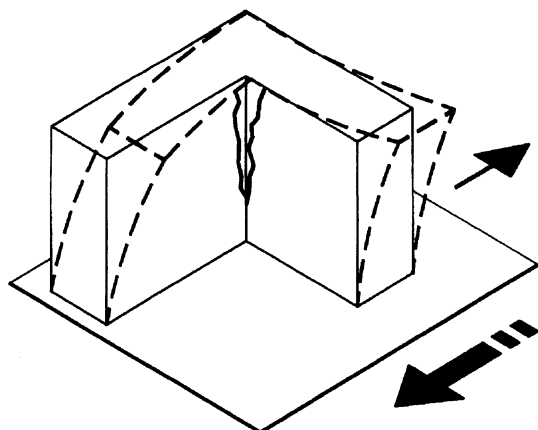


Figure 6-14. The L-shaped building

The second problem is torsion. This is because the center of mass and center of rigidity in this form cannot geometrically coincide for all possible earthquake directions.

The result is rotation, which tends to distort the form in ways that will vary in nature and magnitude depending on the nature and direction of the ground motion, and result in forces that are very difficult to analyze and predict.

The stress concentration at the notch and the torsional effects are interrelated. The magnitude of the forces and the seriousness of the problem will be dependent on:

- the mass of the building
- the structural systems
- the length of the wings and their aspect ratios
- the height of the wings and their height/depth ratios

In addition, it is not uncommon for wings of a reentrant corner building to be of different height, so that the vertical discontinuity of a setback in elevation is combined with the horizontal discontinuity of the reentrant corner, resulting in an even more serious problem.

The reentrant corner is perhaps the major irregularity that will be found in older buildings, including unreinforced masonry. In addition, in such buildings it is rare to find seismic separations at the intersections of the wings, so the prospects for torsion and stress concentration are high, when the wings are long and tall.

• Architectural Implications

Reentrant corners create a useful set of building shapes, enabling large plan areas to be accommodated in compact form, while still providing a high percentage of perimeter rooms with access to light and air. Thus such configurations are common for high-density housing and hotel projects, in which habitable rooms must be provided with windows.

Concerns for daylighting and natural ventilation that were prevalent during the energy crisis of the 1970's resulted in something of a revival of interest in the increased use of narrow buildings and the traditional set of reentrant corner

configurations. The courtyard form, most appropriate for hotels and apartment houses in tight urban sites, has always remained useful. In its contemporary form the courtyard often becomes a glass-covered atrium, but the structural form is the same.

• Historical Performance

Examples of damage to reentrant corner buildings are common, and this problem was one of the first to be identified by observers. It had been identified before the turn of the century, and by the 1920s was generally acknowledged by the experts of the day. Naito⁽⁶⁻⁸⁾ attributed significant damage in the 1923 Kanto earthquake to this factor. The same damage phenomena were reported for the 1925 Santa Barbara and 1964 Alaska earthquakes (Figure 6-15), and for the 1985 Mexico City earthquake. Large wood frame apartment houses with many reentrant corners are common in Los Angeles and suffered badly in the Northridge earthquake of 1994.

• Solutions

There are two basic alternative solutions to this problem: to separate the building structurally into simple shapes, or to tie the building together strongly at lines of stress concentration and locate resistance elements to reduce torsion.

If a decision is made to use separation joints, they must be designed and constructed correctly to achieve the intent. Structurally separated entities of a building must be fully capable of resisting vertical and lateral forces on their own. To design a separation joint, the maximum drift (or some reasonable criterion) of the two units must be calculated by the structural engineer. The worst case is when the two units would lean towards one another simultaneously, and hence the dimension of the separation space must allow for the sum of the deflections. In a tall building the relative motion between portions of the building will become very large, and create major problems of architectural detailing.



Figure 6-15. Damage concentrated at the intersection of two wings of an L-shaped school, Anchorage, Alaska, 1964

One of these is to preserve integrity against fire and smoke spread. The MGM Grand Hotel in Las Vegas is a T-shaped building in plan, with seismic joints approximately 12 in. in dimension. In the fire of 1983 these joints allowed smoke to propagate to the upper floors, resulting in many deaths.

Several considerations arise if it is decided to dispense with separation joints and tie the building together. Collectors at the intersection can transfer forces across the intersection areas, but only if the design allows for these beam like members to extend straight across without interruption. Walls in this same location are even more efficient than collectors. (Figure 6-16).

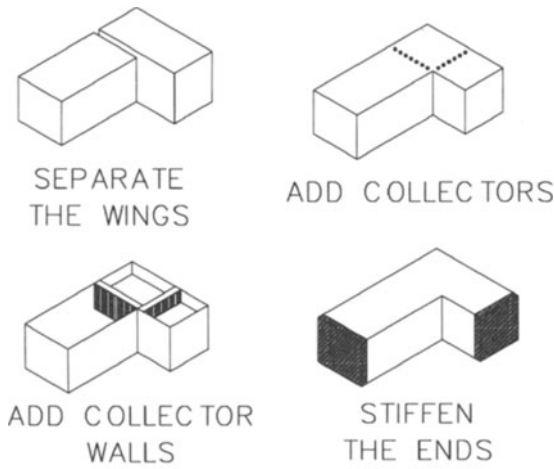


Figure 6-16. Solutions to the L-shaped building

Since the free end of the wing tends to distort most under tension, it is desirable to place resisting members at this location.

The use of splayed rather than right-angle reentrant corners lessens the stress concentration at the notch, which is analogous to the way a rounded hole in a steel beam creates less stress concentration problems than a rectangular hole, or the way a tapered cantilever beam is more desirable than one that is abruptly notched (Figure 6-17).

6.6.2 Variations in Perimeter Strength and Stiffness

• Definition

This section discusses the detrimental effects of wide variations in strength and stiffness in building elements that provide seismic resistance and are located on the building perimeter

• Seismic Effects

If arranged to provide balanced resistance perimeter resistance elements are particularly effective in reducing torsional effects because of their long lever arm relative to the center of resistance. If the resistance is not balanced, the detrimental effects can be extreme.

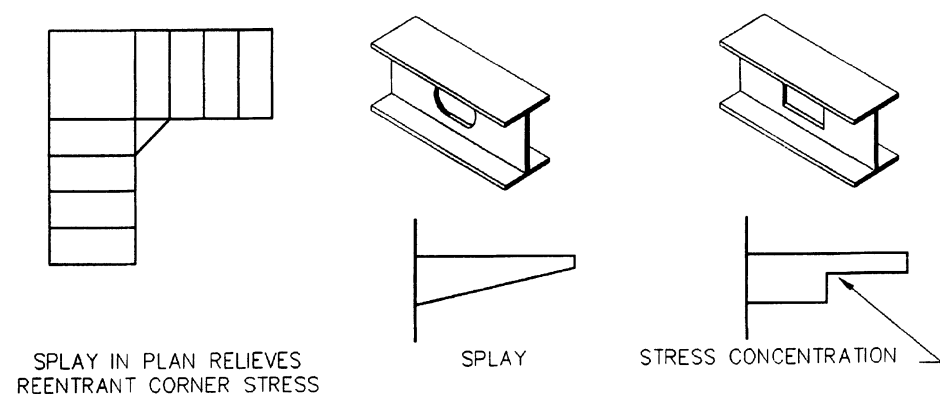


Figure 6-17. Splay in plan relieves reentrant corner problem: analogies to beam

This problem may occur in buildings whose configuration is geometrically symmetrical and simple, but nonetheless irregular for seismic design purposes. If there is wide variation in strength and stiffness around the perimeter, the centers of mass and resistance will not coincide, and torsional forces will tend to cause the building to rotate around the center of resistance. This effect is illustrated in Figure 6-18.

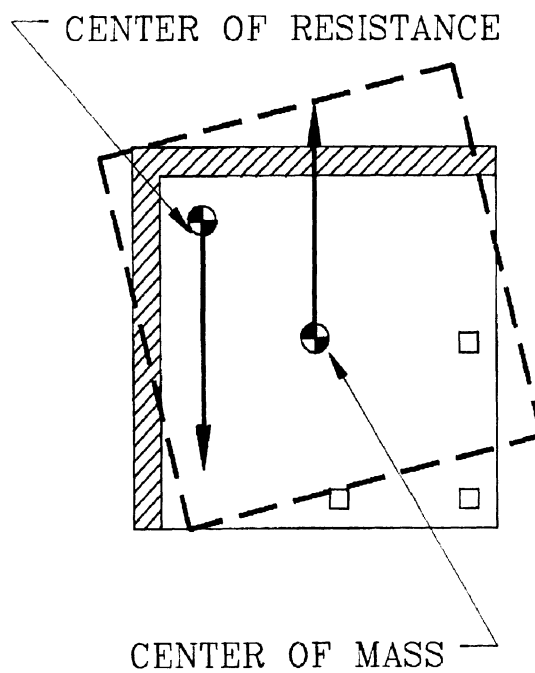


Figure 6-18. Torsional response

A common instance of this problem is that

of the open-front building. The weaknesses of open-front designs have been discussed by Degenkolb⁽⁶⁻⁹⁾:

Figure 6-19 shows the plans of three similar buildings, each with three shear walls so arranged that there is an open end and therefore major torsions in the building. If the buildings are similar, with uniform shear elements (uniform distribution of stiffness) and considering only shear deformations, it can rather simply be proved that the torsional deflection of the open end varies as the *square* of the length of the building.

• Architectural Implications

A common example of this condition occurs in store front design, particularly on corner lots, and in free-standing commercial and industrial buildings with varied openings around the perimeter. A special case is that of fire stations that require large doors for the movement of equipment. In these buildings it is particularly important to avoid major distortion of the front opening, for example if the doors jam and cannot be opened, the fire station is out of action at a time when its equipment is most needed.

Tilt-up concrete industrial and warehouse buildings, in which lateral resistance is provided by the perimeter walls, often also require a variety of openings for entrances, loading docks, and office windows, with a

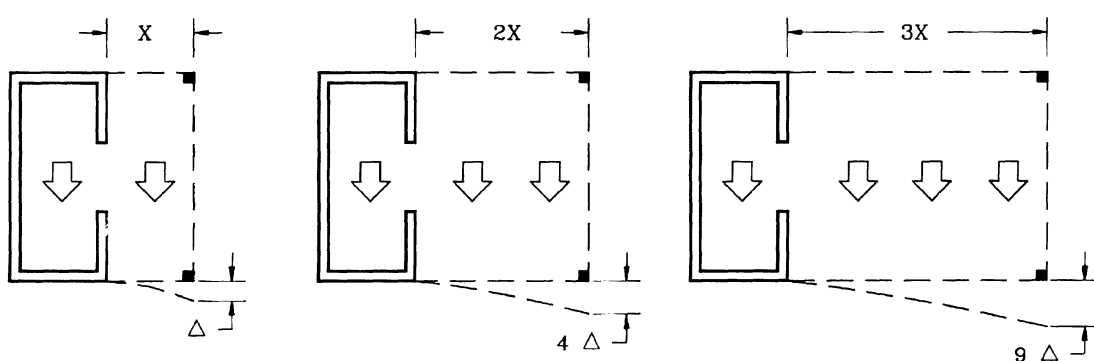


Figure 6-19. Open front design: torsional deflection varies as the square f the length

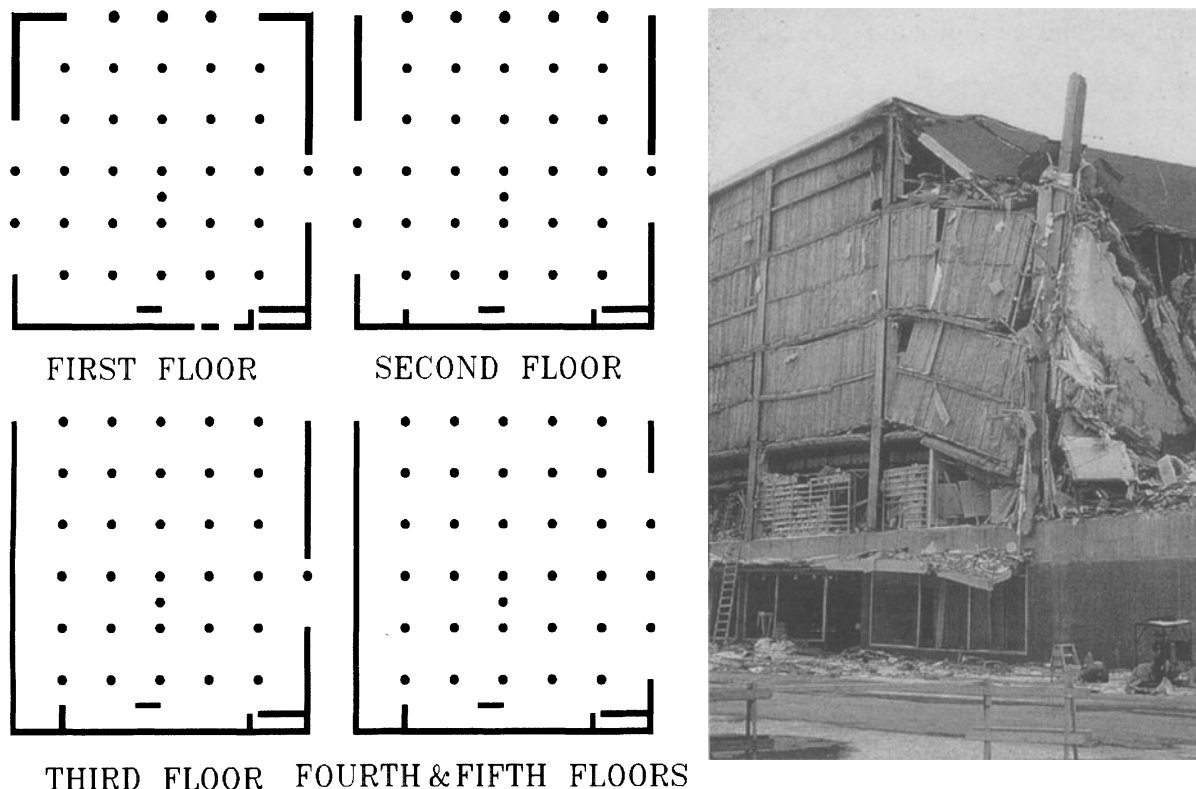


Figure 6-20. J.C.Penney department store, Anchorage, Alaska, 1964
Note: unbalanced location of perimeter walls, particularly on third, forth and fifth floors, leading to severe torsional forces and near collapse.

consequent variation in seismic resistance around the perimeter.

• Historical Performance

A classical instance of this problem occurred in the J.C.Penney Department Store in Anchorage, Alaska, in the 1964 earthquake. The building was so badly damaged that it had to be demolished. The store was a five-story building of reinforced-concrete construction. The exterior walls were a combination of poured-in-place concrete, concrete block, and precast concrete nonstructural panels which were heavy, but unable to take large stresses. The first story had shear walls on all four elevations. The upper stories, however, had a structurally open north wall, resulting in U-shaped shear wall bracing system (similar to a typical open-front store) which, when subjected to east-west lateral forces, would result in large torsional forces (Figure 6-20).

A special case is also that of apartment house and hotels that are oriented to a view, such as a beach, which implies the need for large openings on the view elevation. The El Faro building was a small apartment house located facing the beach in the Chilean resort town of Vina del Mar. In order to exploit the view, two elevations are open: the stairs and elevator shaft are concentrated to the rear of the building and their walls provide the seismic resistance. The result is a wide eccentricity between the centers of mass and resistance. In the Chilean earthquake of 1985, this building rotated and very nearly collapsed: it was subsequently demolished. (Figure 6-21)

• Solutions

The objective of any solution to this problem is to reduce the possibility of torsion, and to balance the resistance around the

perimeter. Four alternative strategies can be employed, and are shown in Figure 6-22.



Figure 6-21. El Faro apartments, Vina del Mar, Chile, 1985

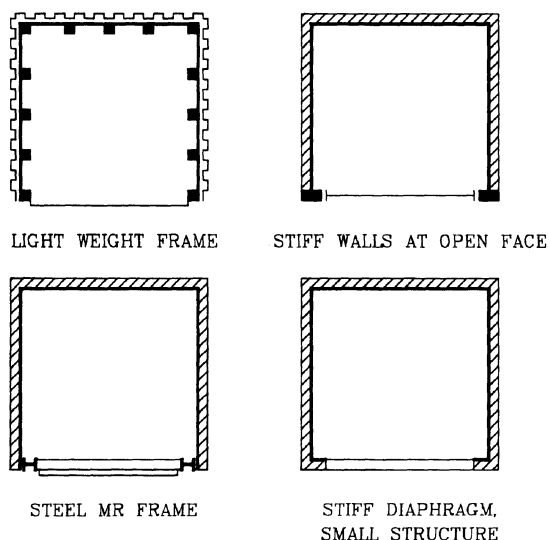


Figure 6-22. Solutions to open front buildings

The first approach is to design a frame structure with approximately equal strength and stiffness for the entire perimeter. The opaque portions of the perimeter can be constructed of nonstructural cladding material that will not affect the seismic performance of the frame. This can be done either by using lightweight cladding, or by ensuring that heavy materials (such as concrete or masonry) are isolated from the frame.

A second approach is to increase the stiffness of the open facades by adding shear walls at or near the open face. This solution is, of course, dependent on a design which permits this solution.

A third solution is to use a very strong moment-resisting or braced frame at the open front, which approaches the solid walls in stiffness. The ability to do this will be dependent on the size of the facades; a long steel frame can never approach a long concrete wall in stiffness. This is, however, a good solution for wood frame structures, such as apartment houses with a ground floor garage space, because even a rather long steel frame can be made to approach plywood walls in stiffness.

Finally, the possibility of torsion may be accepted and the structure designed to resist it. This solution will only apply to small structures with stiff diaphragms, which can be designed to act as a unit.

6.6.3 Nonparallel Systems

- **Definition**

The vertical load resisting elements are not parallel or symmetric about the major orthogonal axes of the lateral-force resisting system.

- **Seismic Effects**

This condition results in a high probability of torsional forces under a ground motion, because the centers of mass and resistance cannot coincide for all directions of ground motion. Moreover, the narrower portions of the

building will tend to be more flexible than the wider ones, which will increase the tendency to torsion.

The problem is often exacerbated by perimeters with variations of strength and stiffness (Figure 6-23). A characteristic form of this condition is the triangular or wedge-shaped building that results from street intersections at an acute angle. These forms often employ a solid, stiff party wall in combination with more open flexible facing the street. The result is a form that is very prone to torsion.

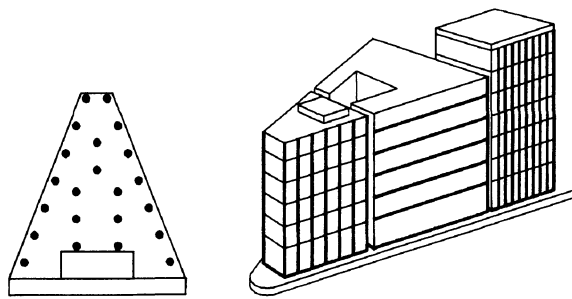


Figure 6-23. Wedge shaped plan: invitation to torsion

• Architectural Implications

Non-rectilinear forms have become increasingly fashionable in the last few years as a reaction against the rectangular "box". Forms that are triangular, polygonal, or curved have become commonplace, even in very large buildings. However, in some instances the desired forms can be achieved by nonstructural elements attached to a structure which may be essentially regular and rectilinear. (Figure 6-24) Extreme forms of non -rectilinearity are a feature of "deconstructionist" architecture, which is discussed in Section 6.11.

The traditional , trapezoidal or "flatiron" form resulting from the street-layout constraints is still common in high-density urban locations.

• Historical Performance

This form has been fairly recently identified as a problem configuration. The form was not identified as irregular in the 1890 SEAOC

Commentary , but it is identified as irregular in the 1988 UBC, the 1990 SEAOC Commentary, and subsequent codes and provisions.

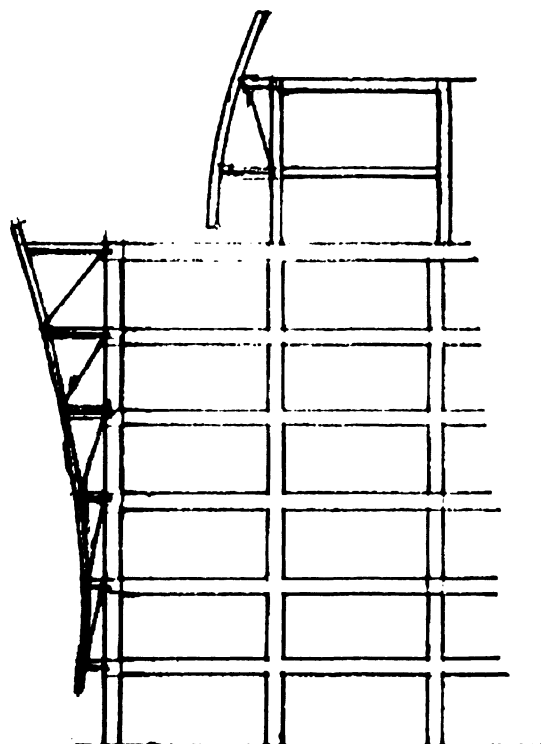


Figure 6-24. Form achieved by nonstructural attachments to main

Many buildings of this type were constructed in Mexico City, resulting from the high density and street layout of the city, and instances of poor performance were observed in the 1985 earthquake. Many buildings suffered severe distortion, particularly wedge-shaped buildings with stiff party walls opposite the apex of the triangular form (Figure 6-25). In many cases the condition was exacerbated by other irregularities such as a soft story.

• Solutions

Since 1988 the UBC and the NEHRP *Provisions* place some special requirements on the design of these types of configuration. Particular care must be exercised to reduce the effects of torsion. In general, opaque walls should be designed as frames clad in



Figure 6-25. Distortion in wedge-shaped building, Mexico City, 1985

lightweight materials, to reduce the stiffness discrepancy between these walls and the rest of the structure.

Alternatively, special design solutions may be introduced to increase the torsional resistance of the narrow parts of the building, although this may be difficult to achieve while still retaining open facades or internal areas.

6.6.4 Diaphragm Configuration

- **Definition**

The diaphragm configuration is the shape and arrangement of horizontal resistance elements that transfer forces between vertical resistance elements.

- **Seismic Effects**

Diaphragms perform a crucial role in distributing forces to the vertical seismic-resisting elements. The diaphragm acts as a horizontal beam, and its edges act as flanges. Diaphragm penetration and geometrical irregularities are analogous to such irregularities in other building elements, leading to torsion and stress concentration.

The size and location of these penetrations is critical to the effectiveness of the diaphragm. The reason for this is not hard to see when the diaphragm is visualized as a beam: it is obvious that openings cut in the tension flange of a beam will seriously weaken its load-carrying capacity. In a vertical load system, a penetration in a beam flange would occur in either a tension or a compression area; in a lateral load system, the hole will be in a region of both tension and compression, since the loading alternates in direction.

When diaphragms form part of a resistant system, they may act in either a flexible or stiff manner. This depends partly on the size of the diaphragm (its area between enclosing resistance members or stiffening beams), and also on its material. The flexibility of a diaphragm, relative to the shear walls whose forces it transmits, also has a major influence on the nature and magnitude of those forces.

• Architectural Implications

Diaphragms are generally floors or roofs, and so have major architectural functions aside from their seismic role. The shape of the diaphragm is dependent on the overall plan form of the building, and how it can be subdivided by walls or collectors.

In addition, however, architectural requirements such as staircases, elevators and duct shafts, skylights, and atria result in variety of diaphragm penetrations. In some cases, as in the need for elevators in an L-shaped building, the logical planning location for elevators (at the hinge of the L) is also the area of greatest seismic stress.

• Historical Performance

Failures specifically due to diaphragm design are difficult to identify, but there is general agreement that poor diaphragm layout is a potential contributor to failure.

• Solutions

Diaphragm penetrations are a form of irregularity specifically called out in the 1990 SEAOC Commentary that requires engineering judgment. In addition, current codes and provisions specifically define such penetrations, and impose some additional requirements on the diaphragm design in such cases.

The general approach to the design of penetrations in diaphragms is to:

- Ensure that penetrations do not interfere with diaphragm attachment to walls or frames.

- Ensure that multiple penetrations are spaced sufficiently far from one another to allow reinforcing elements to develop their required capacity
- Ensure that collectors and drag struts are uninterrupted by openings

6.7 Vertical Configuration Problems

6.7.1 Soft and Weak Stories

• Definition

A soft story is one that shows a significant decrease in lateral stiffness from that immediately above. A weak story is one in which there is a significant reduction in strength compared to that above.

• Seismic Effects

The condition may occur at any floor, but is most critical when it occurs at the first story, because the forces are generally greatest at this level.

The essential characteristics of a weak or soft first story consist of a discontinuity of strength or stiffness, which occurs at the second-story connections. This discontinuity is caused because lesser strength, or increased flexibility, in the first story structure results in extreme deflections in the first story, which, in turn, result in a concentration of forces at the second story connections.

If all the stories are approximately equal in strength and stiffness, the entire building deflection under earthquake forces is distributed approximately equally to each story. If the first story is significantly less strong or more flexible, a large portion of the total building deflection tends to concentrate there, with consequent concentration of forces at the second-story connections .(Figure 6-26)

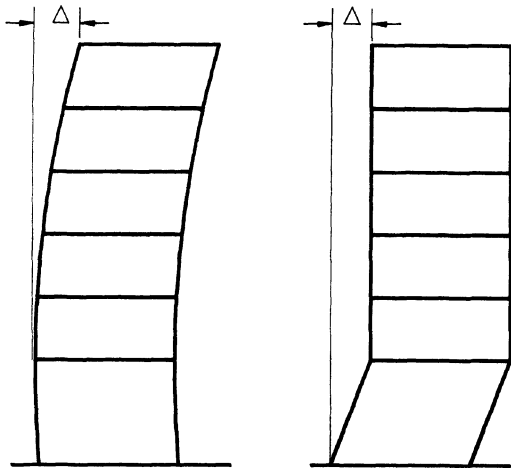


Figure 6-26. The soft-story effect

In more detail, the soft-story problem may result from four basic conditions. These are diagrammed in Figure 6-27 and are:

- A first-story structure significantly taller than upper floors, resulting in less stiffness and more deflection in the first story.
- An abrupt change of stiffness at the second story, though the story heights remain approximately equal. This is caused primarily by material choice: the use, for instance, of heavy precast concrete elements above an open first story.

- The use of a discontinuous shear wall, in which shear forces are resisted by walls that do not continue to the foundations, but stop at second floor level, thus creating a similar condition to that of the second item above.
- Discontinuous load paths, created by a change of vertical and horizontal structure at the second story.

The above characteristics, individually or in combination are readily identifiable in existing buildings provided that the building structure can be studied in its entirety, either in the field or by reference to accurate as-built construction documents.

• Architectural Implications

A taller first story often has strong programmatic justification, when large spaces, such as meeting rooms or a banking hall, must be provided at ground level. Similarly, an open ground floor often meets urban design needs by providing both real and symbolic access to a plaza or street, or by providing space at the base of a building. The changes in proportion provided by a high story, or the "floating box" concept (now somewhat outdated), are very real aesthetic tools for the architect, although engineers may find such concepts hard to rationalize in their terms.

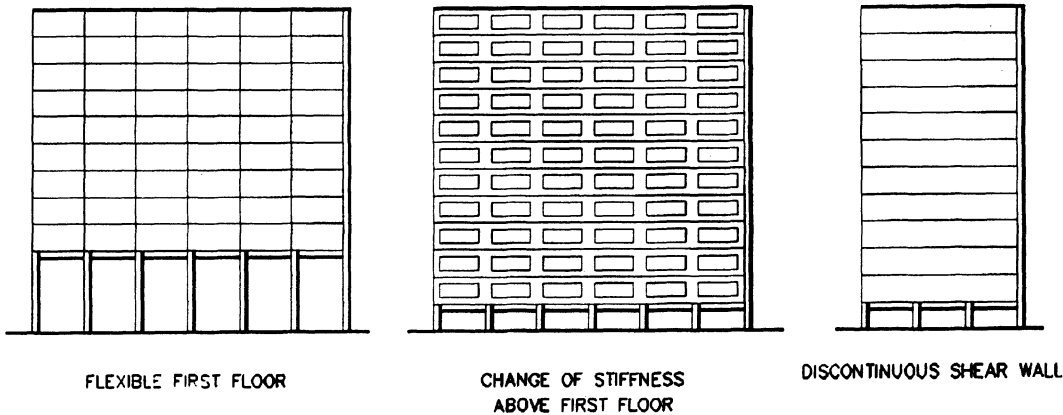


Figure 6-27. Types of soft story

Engineers must accept that some form of variation in the first story will remain a desirable architectural characteristic for the foreseeable future: whether it is "soft" or "weak" in seismic terms is a matter for the architect and engineer to resolve.

• Historical Performance

The general type of soft first story configuration was early identified as a problem. Failures in masonry buildings in the 1925 Santa Barbara earthquake were identified by Dewell and Willis⁽⁶⁻¹⁰⁾ as soft-first-story failures.

In more recent times, with extensive use of frame structures, damage to reinforced-concrete buildings in Caracas (1967) clearly identified the risk to tall buildings with this condition. In the Mexico City earthquake of 1985, researchers determined that soft first stories were a major contributor to 8% of serious failures, and the actual percentage is probably greater because many of the total collapses were precipitated by this condition.

The particular case of the discontinuous shear wall has led to clearly diagnosed failures in United States buildings. Olive View hospital, a new structure that was badly damaged in the 1971 San Fernando earthquake, represents a classic case of the problem.

The vertical configuration of the main building was a two-story layer of rigid frames on which was supported a four-story shear wall-frame structure (Figure 6-28). The second floor extended out to form a large plaza.

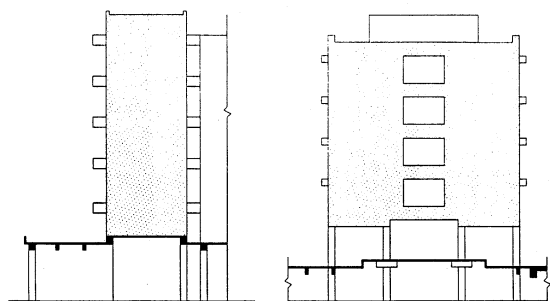


Figure 6-28. Olive View hospital, San Fernando, 1971 (a) elevation of stair towers (b) section through main building

The severe damage occurred in the soft-story portion: the upper floors moved so much as a unit that the columns at ground level could not accommodate such a huge displacement between their bases and tops and failed. The largest amount by which a column was left permanently out of plumb was 2 1/2 feet.

Though not widely identified, the stair towers at Olive View also show a clear and separate example of a discontinuous shear-wall failure. These seven-story towers were independent structures, and proved incapable of standing up on their own: three stair towers overturned completely, while the fourth leaned outwards 10 degrees. The six upper stories were rigid reinforced -concrete walls, but the bottom story was composed of six free-standing reinforced-concrete frames, which failed. The exception was the north tower, whose walls came down to the foundation directly without any discontinuity; this was the only tower to remain standing. Olive View hospital was demolished after the earthquake, and a new hospital built on the same site.

The performance of the Imperial County Services Building, El Centro, in the Imperial Valley Earthquake of 1979, provides another example of the effects of architectural characteristics on seismic resistance. The building was a reinforced-concrete structure built in 1969. In this mild earthquake the building suffered a major structural failure, resulting in column fracture and shortening (by compression) at one end—the east—of the building. (Figure 6-29). The origin of this failure lies in the discontinuous shear wall at that end of the building.

The fact that this failure originated in the configuration is made clear by the architectural difference between the east and west ends: this is an example of the large effect on seismic performance of a relatively small design variation between the two ends of the building.. The difference in location of the small ground-floor shear walls was sufficient to create a major difference in response to the rotational forces on the large end shear walls (Figure 6-30).

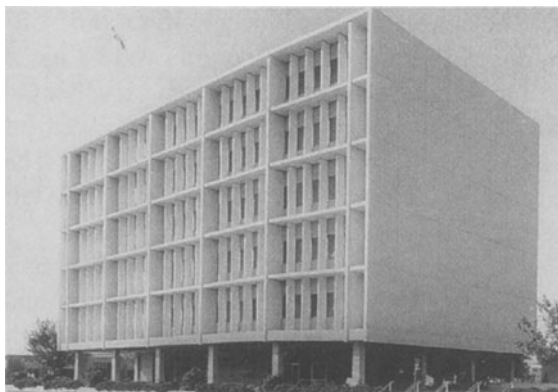


Figure 6-29. Imperial County Services Building, El Centro, California. failure of end bay at discontinuous shear wall, (Imperial valley earthquake of 1979)

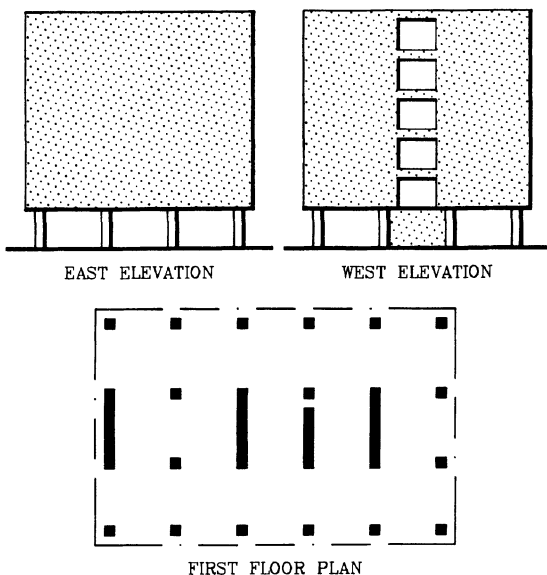


Figure 6-30. Imperial County Service Building, plan and elevations

A more recent instance is that of a medical office building in the Northridge earthquake of 1994, constructed at about the same time as the previous two buildings discussed. The simple rectangular building had discontinuous shear walls at each end. These proved inadequate to deal with the forces, with consequent severe torsional damage at each end of the building, (Figure 6-31) This building also had a structural discontinuity at the second floor that caused the "pancaking" of the second floor.

• Solutions

If a high first story is desired, either:

- Introduce bracing that stiffens the columns up to a level comparable to the superstructure.
- Add columns at the first story to increase stiffness, or
- Change the design of the first-story columns to increase stiffness.

If a large opaque wall is required in a location that could create a soft first story:

- Insure that such a wall is not part of the lateral load resisting system
- Reduce the mass of the wall by use of light material and hollow construction
- If a heavy wall is necessary, then insure that the wall is detached in such a way that the superstructure is free to deflect in a comparable way to the first floor

If the architect insists on such material and design constraints that a major discontinuous shear wall is the only solution, the engineer should refuse to do it. The liabilities involved in using such a proven failure mechanism are too great.

If the lateral resistance system is based on the use of an interior core (for a high-rise office building, for example), the perimeter columns may be tall, but there is no soft first story, provide the core is brought down to the ground. In such a building it is not difficult, if the core-plan dimensions are sufficient, to insure that the stiffness of a tall first story is adequate to prevent structural discontinuity at the second floor. One condominium building a good example of architect- engineer collaboration. That building achieved an elegant exterior appearance which appeared to be a soft first floor. However, the seismic resistance was provided by a strong interior box shear wall structure that enabled the taller first floor to be accommodated with ease. The building suffered

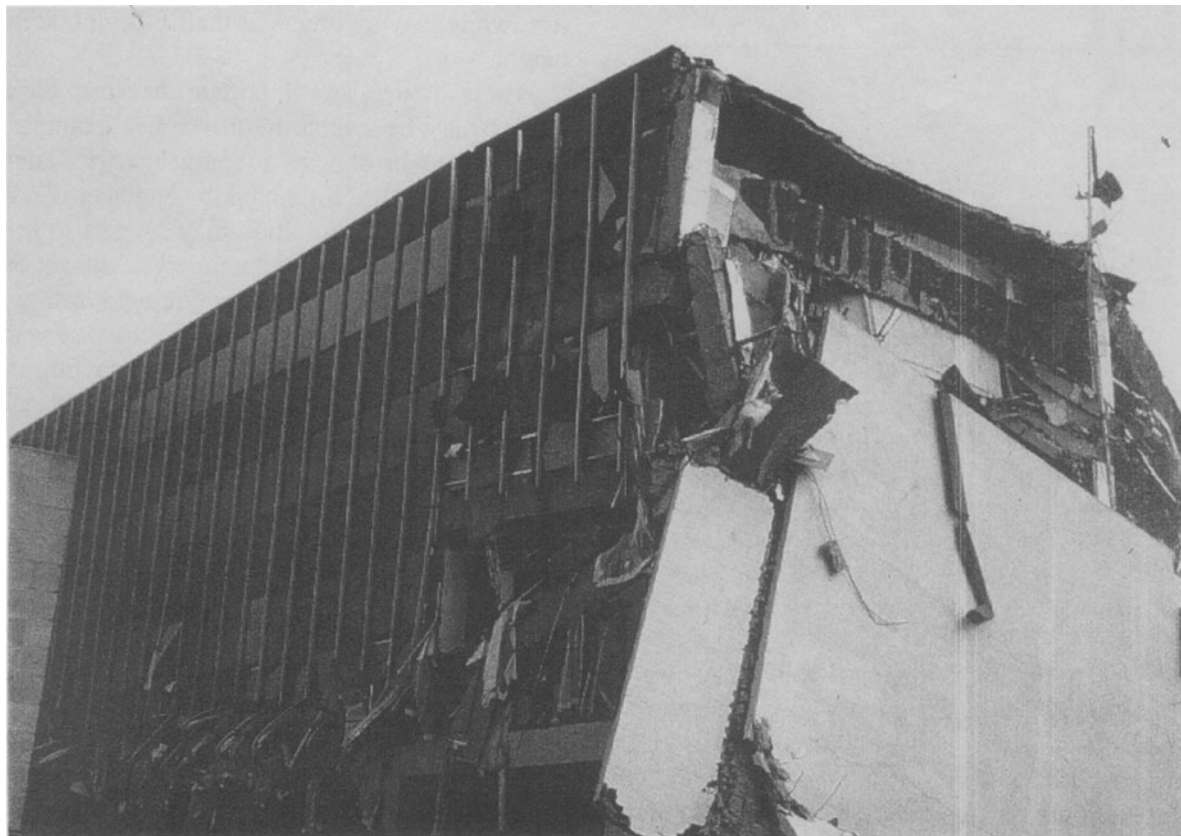


Figure 6-31. Discontinuous shear wall failure, office building, Northridge

virtually no damage in the strong Chilean earthquake of 1985.

It should be noted that in the 1997 NEHRP *Provisions* structures with a weak-story discontinuity in capacity that is less than 65% of the story above are not permitted over 2 stories or 30 feet in height in Seismic Design Categories B,C,D,E and F.

6.7.2 Columns: Variations in Stiffness, Short Columns, and Weak Column/Strong Beam.

• Definition

This section considers the use of columns of varying stiffness, by reason of either differences in length or deliberate or inadvertent bracing; the use of columns that are significantly weaker than connecting beams; and the use of columns

in one floor that are significantly shorter than those on other floors.

• Seismic Effects

Seismic forces are distributed in proportion to the stiffness of the resisting members. Hence, if the stiffness of the supporting columns (or walls) varies, those that are stiffer (usually shorter) will "attract" the most forces. The effect of this phenomenon is explained in Figure 6-32. The important point is that stiffness (and hence forces) varies approximately as the cube of the column length.

Similarly, a uniform arrangement of short columns supporting a floor will attract greater forces to that floor, with a corresponding possibility of failure. Typically such an arrangement may also involve deep and stiff spandrel beams, making the columns significantly weaker than the beams.

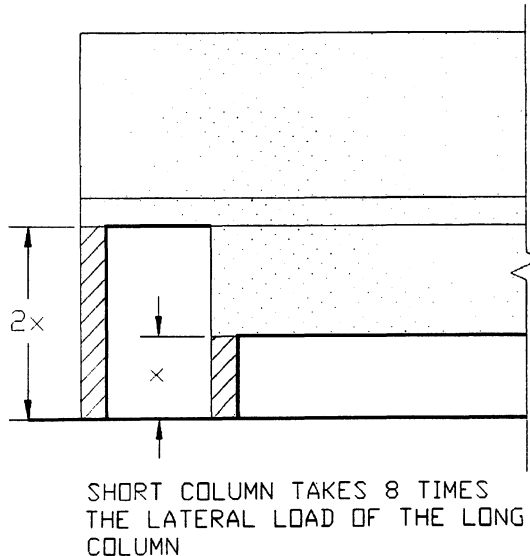


Figure 6-32. Effect of variations of column stiffness

Such a design is in conflict with a basic principle of seismic design, which is to design a structure in such a way that under severe seismic forces, *beams will deform plastically before columns*. This is based on the reasoning that as beams progress from elastic to inelastic behavior they start to deform permanently. This action will dissipate and absorb some of the seismic energy. Conversely, if the column fails first and begins to deform and buckle, major vertical compressive loads may quickly lead to total collapse.

Mixing of columns of varying stiffness on different facades may also lead to torsional effects, since the building assumes the attributes of varying perimeter resistance discussed above.

• Architectural Implications

The origin of variations in column stiffness generally lies in architectural considerations. Hillside sites, infilling of portions of frames with nonstructural but stiff material to create high strip windows, desire to raise a portion of the building off the ground on tall "pilotis", while leaving other areas on shorter columns, or stiffening some columns with a mezzanine or a

loft, while leaving others at their full, unbraced height.

These issues are important because their effects may be counterintuitive. For example, infilling may be done as a remodel activity later in the building life for which the engineer is not consulted, because intuition may suggest to the designer that he is strengthening it in the act of shortening it rather than introducing a serious stress concentration for which the structure was not designed. For vertical forces a reduction in the effective length of a column is beneficial because it reduces the likelihood of buckling, but the effect under lateral forces is quite different.

Variations in openings in different facades are often required from a daylighting or energy-conservation requirement. Where openings are created by variations in structural arrangement, rather than by variations in cladding, some of these conditions may well arise.

• Historical Performance

Significant column failures, sometimes leading to collapse, have been attributed to these conditions in a number of recent earthquakes, particularly in Japan, Latin America, and Algeria.

Many Japanese schools, employing short columns on one side of an elevation, or using a weak-column, strong-beam configuration, suffered severe damage in the Tokai-oki earthquake in 1968 and the 1978 Miyagi-ken-oki earthquake. (Figure 6-33)

In Latin America, the problem has frequently been caused by inadvertent stiffening of columns through nonstructural infill which, when combined with high glazing, creates short columns.

In the El Asnam (Algeria) earthquake of 1980, many apartment structure failures were caused by short columns used at ground level to provide a ventilated open space (called a "vide sanitaire") in a semi-basement location. The significant failure of a large condominium and hotel structure in the Guam earthquake of 1993 has been ascribed in part to the creation of a



Figure 6-33. Short column failure, school, Japan: Miyagi-ken -oki, 1978

short column condition by the introduction of nonstructural stiffening elements⁽⁶⁻¹¹⁾ (Figure 6-34)

- **Solutions**

The general solution is to match the detailed seismic design carefully to the architectural requirements. The weak-column, strong-beam condition can be avoided by insuring that deep spandrels are isolated from the columns; in the same way the lengths of columns around a facade can be kept approximately equal.

Horizontal bracing can be inserted to equalize the stiffness of a set of columns of varying height (Figure 6-35). Heavy nonstructural walls must be isolated from columns to insure that a short-column condition is not created. (Figure 6-36).

6.7.3 Vertical Setbacks

- **Definition**

A vertical setback is a horizontal, or near horizontal, offset in the plane of an exterior facade of a structure.

- **Seismic Effects**

The problem with this shape lies in the general problem of discontinuity: the abrupt change of strength and stiffness. In the case of this complex configuration, it is most likely to occur at the line of the setback, or "notch".

The seriousness of the setback effect depends on the relative proportions and absolute size of the separate parts of the building. In addition, the symmetry or

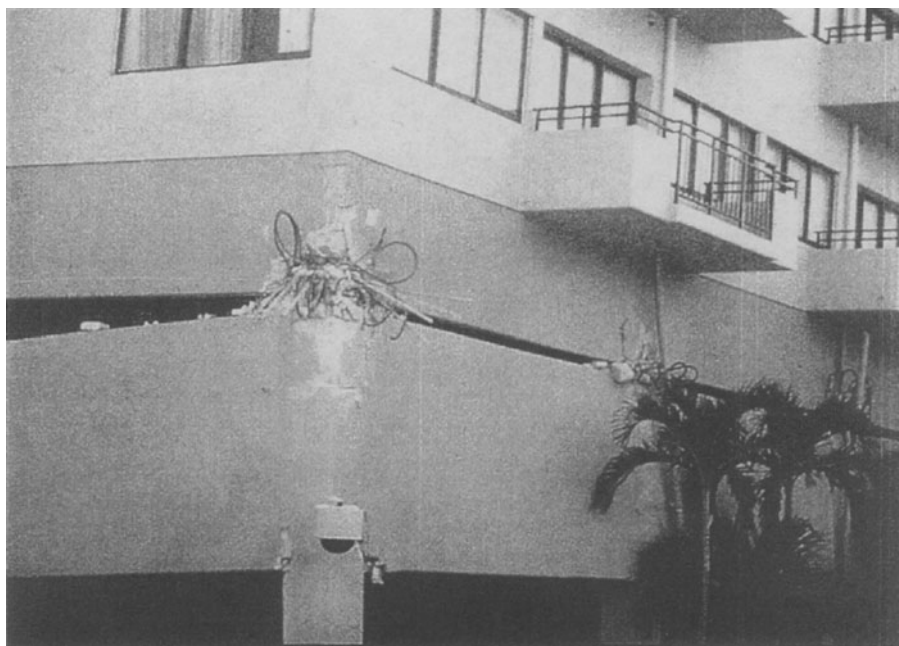


Figure 6-34. Short column failure, Guam, 1993



Figure 6-35. Horizontal bracing to stiffen a high open end entrance

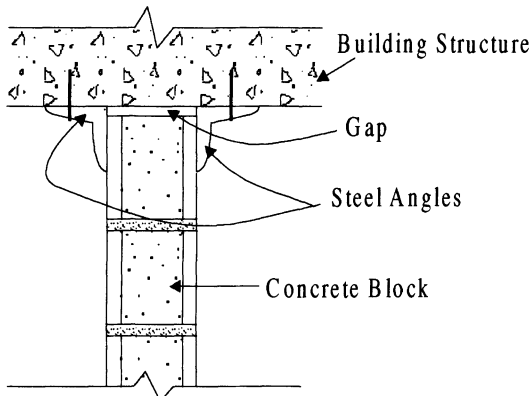


Figure 6-36. Heavy nonstructural wall isolated from structure at top and side

asymmetry in plan of the tower and base affect the nature of the forces. If the tower or base or both are dynamically asymmetrical, then torsional forces will be introduced into the structure, resulting in great complexity of analysis and behavior.

The setback configuration can also be visualized as a vertical reentrant corner. Stresses must go around a corner, because a notch has been cut out, preventing a more direct route. Hence, the smaller the steps or notches in a setback, the smaller the problem. A smooth taper avoids the notch problem altogether. A tapering beam will not experience stress concentrations, whereas a notched beam will.

Setbacks with shear walls in the tower portion that are not continued to the ground are highly undesirable. Besides the change of stiffness where the shear wall enters the base structure, the shear wall will transmit large forces to the top diaphragm of the base.

Although, typically, setbacks occur in a single building, the condition can also be created by adjoining buildings of different heights which have inadequate or nonexistent seismic separations.

• Architectural Implications

Setbacks may be introduced for several reasons. The three most common are zoning requirements that require upper floors to be set back to admit light and air to adjoining sites, program requirements that require smaller

floors at the upper levels, or stylistic requirements relating to building form.

Setbacks relating to zoning were common a few decades ago when daylighting was a major concern, and resulted in characteristic shapes of older high-rise buildings in New York and other large cities. Stylistic fashions replaced these forms with those of simple rectangular solids, made possible by advances in artificial lighting and air-conditioning. Now, there is a renewed interest in set-back shapes for stylistic reasons, while at the same time energy conservation requirements have reinstated a functional interest in setbacks for daylighting reasons.

An interesting example of this stylistic trend is that of the new planning code for San Francisco, which specifically mandates setbacks for large buildings in the downtown area. These represent relatively minor variations in the vertical plane of the facade, rather than the abrupt rising tower on a base, which is of more serious seismic consequence. The trend is, however, away from vertical structural continuity at the perimeter and thus introduces complexity and cost into the structural solution.

A type of setback configuration only made possible by modern framed construction is that of the building that grows larger with height. This type is termed *inverted setback* or *inverted pyramid* depending on its form. Its geometrical definition is the same as that of the setback, but, because of the problems of overturning, its extremes of shape are less. Nevertheless, some surprising demonstrations of this shape have appeared, and it appears to be one whose image has a powerful design appeal (Figure 6-37).

• Historical Performance

Although commonly identified as a configuration problem, severe failures of modern buildings attributed to this condition are few. While traditional towers, primarily churches, have suffered their share of failures, the number of those that have survived severe



Figure 6-37. Dallas City Hall : an inverted pyramid

damage is remarkable. An example from the Kobe earthquake of 1995 shows a failure in a setback building at the plane of weakness created by a combination of the setbacks and adjoining openings in the wall (Figure 6-38)

While there have been recorded failures of inverted-setback buildings, notably in the Agadir (Morocco) earthquake of 1960, some of the more striking examples have performed well. This is probably because the appearance of instability inherent in this form results in special attention being paid to its structural design. Typically, such buildings devote a much larger percentage of their construction cost to structure than more conventional buildings.

• Solutions

Setbacks have long been recognized as a problem, and so the Uniform Building Code has attempted to mandate special provisions for them currently, the earthquake regulations of the Code refer to setback configurations as follows:

Buildings having setbacks wherein the plan dimensions of the tower in each direction is at least 75% of the corresponding plan dimension of the lower part may be considered as uniform buildings without setbacks, provided other irregularities as defined in this section do not exist.

An appendix to the 1990 SEAOC Commentary to this section includes a lengthy discussion of the setback problem and an approach to its analysis .

In general, conceptual solutions to the setback problem are analogous to those for its horizontal counterpart, the reentrant corner plan. The first type of solution consists of a complete seismic separation in plan, so that portions of the building are free to react independently. For this solution, the guidelines for seismic separation, discussed elsewhere, should be followed.



Figure 6-38. Failure of set-back building along a plane of weakness

When the building is not separated, the analysis proposed in the appendix to the 1990 SEAOC Commentary provides the best guidelines, with some necessary interpretations to fit the particular case. Particular attention should be paid to avoiding vertical column discontinuity, so that setbacks should be arranged to coincide with normal bay sizes (which may result in a series of small bays).

Any large building with major setback conditions should be subjected to special analysis, or at least to careful investigation of probable dynamic behavior. Finally, the inverted setback configuration of any extreme form and size should be avoided in seismic areas, unless the owner is willing to assume the considerable additional structural costs that will be incurred.

The 1997 NEHRP *Provisions*, as noted earlier, permit vertical setback configurations to be analyzed using the simple ELF method if the stiffness on the top story of the base is at least

five times that of the first story of the tower. The UBC permits use of the standard ELF method for a two-stage analysis of tower and base if the average story stiffness of the base is at least 10 times greater than the average story stiffness of the tower.

6.8 STRUCTURALLY RESTRICTIVE ARCHITECTURAL DETAILING

6.8.1 Components and Connections

• Definition

By *structurally restrictive detailing* we mean detailed architectural design of a component that prevents good seismic design practice in the structural design.

• Seismic Effects

This problem represents a micro version of typical overall building configuration problems. Architectural detailing may place dimensional or location constraints on structural design resulting in weakness or eccentricity of force actions that can lead to stress concentration or local torsion. The problem is most critical at beam-column connections, which are highly stressed, but often represent a critical element in the aesthetic scheme of the building.

Structural detailing ideally provides for direct load transfer and minimum local eccentricity, with forces resolved at a point. Architectural detailing may result in inadequate size and eccentric or discontinuous load paths (Figure 6-39). The problem is particularly critical for reinforced-concrete structures, where constraints may provide inadequate room for proper placing of reinforcing.

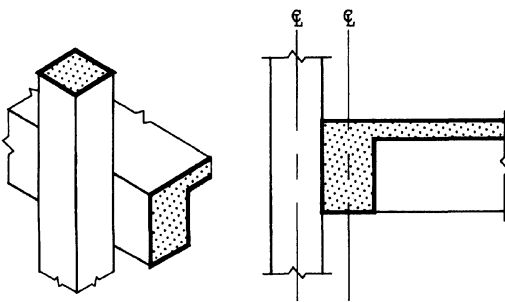


Figure 6-39. Eccentric load paths created by architectural detailing of structural connection

• Architectural Implications

Detailed design is an important element in architectural expression. As an example, the design of the perimeter beam-column connection can provide the building with a predominantly horizontal, vertical, or neutral emphasis. (Figure 6-40). But the structural implications of these variations may not be understood by the architect. Another example is the use of taper or the insertion of recesses in columns. Tapered columns may be a correct

expression of structural forces, and be easy to accommodate, or they may directly contradict structural action and lead to weakness. Recesses are often designed by architects to accentuate the line at which materials meet one another, particularly when the materials are different or meet at right angles, as in a column-slab junction.

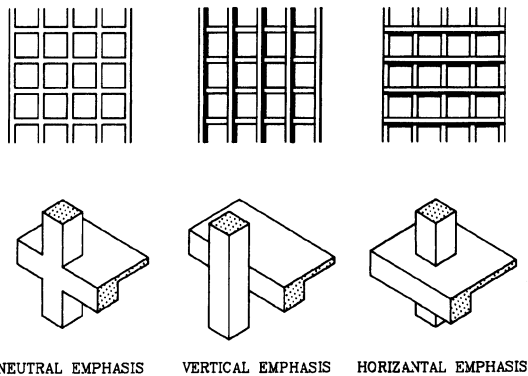


Figure 6-40. Facades: differences in architectural emphasis

• Historical Performance:

Specific performance attributable to this condition is difficult to document but the problem is generally recognized by engineers. Two well documented cases do exist where architectural detailing contributed to failure.

The first is that of the column design of the Olive View Hospital, damaged in the 1971 San Fernando earthquake (discussed previously as an example of soft-first-story failure.). A significant difference in performance was observed between corner and internal columns in this building. The twelve L-shaped corner columns were completely shattered and their load-carrying capacity reduced almost to zero. The interior columns, of square section, had spiral ties, and although they lost most of their concrete cover, they retained load-carrying capacity and probably saved the building from collapse. Because of their architectural form, it was not possible for the corner columns to use spiral ties (Figure 6-41). Higher stress and torsion in the corner columns may also have contributed to their poor performance.

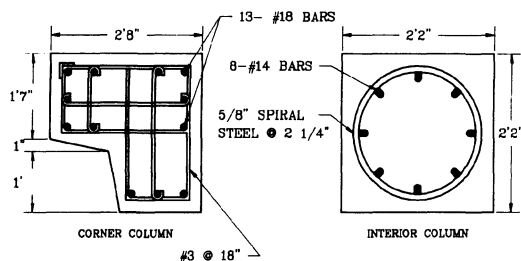


Figure 6-41. Exterior column sections at Olive View Hospital, San Fernando, California. Due to their shape, corner columns could not be spirally reinforced

The Imperial County Service Building at El Centro, California, suffered severe damage in the 1979 Imperial Valley earthquake, and four columns at one end of the building were badly shattered. Detailed study of these columns showed that an architectural recess had been placed at the line where the columns met the ground. (Figure 6-42). This recess caused a reduction in sectional area of the column and a reduction in axial load-carrying capacity. Analytical and experimental studies have shown that this change in column section accentuated the undesirable performance of these columns⁽⁶⁻⁷⁾.

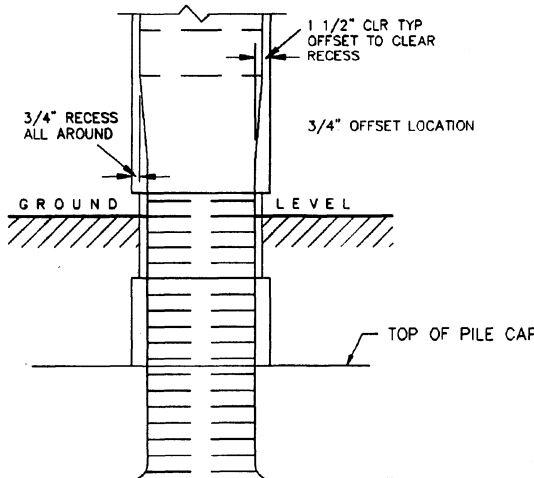


Figure 6-42. Column detail, Imperial County Services Building, El Centro, California. Note architectural recess affecting reinforcement continuity

- **Solutions:**

Close coordination between architect and engineer is necessary to insure that architectural detailing does not result in undesirable structural design constraints.

6.9 PROBLEMS OF ADJACENCY

6.9.1 Pounding

- **Definition:**

Pounding is damage caused by two buildings, or different parts of a building, hitting one another.

- **Seismic Effects:**

Pounding as characterized in Codes and Guidelines and in most analytical research studies takes the form of in plane displacements of two adjacent buildings, as in the investigation of a row of adjacent buildings by Athanassiadou et al⁽⁶⁻¹²⁾. Empirical observation shows that building separations are complex in their basic conditions and in their effects, and lack of separation is not necessarily detrimental.

Observation has shown that the end buildings of a row of adjacent buildings tend to suffer more damage than interior buildings. Analytical pounding studies consider regular buildings in elevation. In fact, the sway characteristics of buildings are much influenced by irregularities, particular that of soft first stories, that can lead to extreme displacements or even collapse. Some of these characteristics are shown in Figure 6-43. Similarly, analytical studies have always assumed regular buildings in plan. Since adjacent buildings with little or no separation will generally be found in the older sections of down town, building plans are often very irregular, leading to torsional effects under ground motion. These characteristics are shown in Figure 6-44.

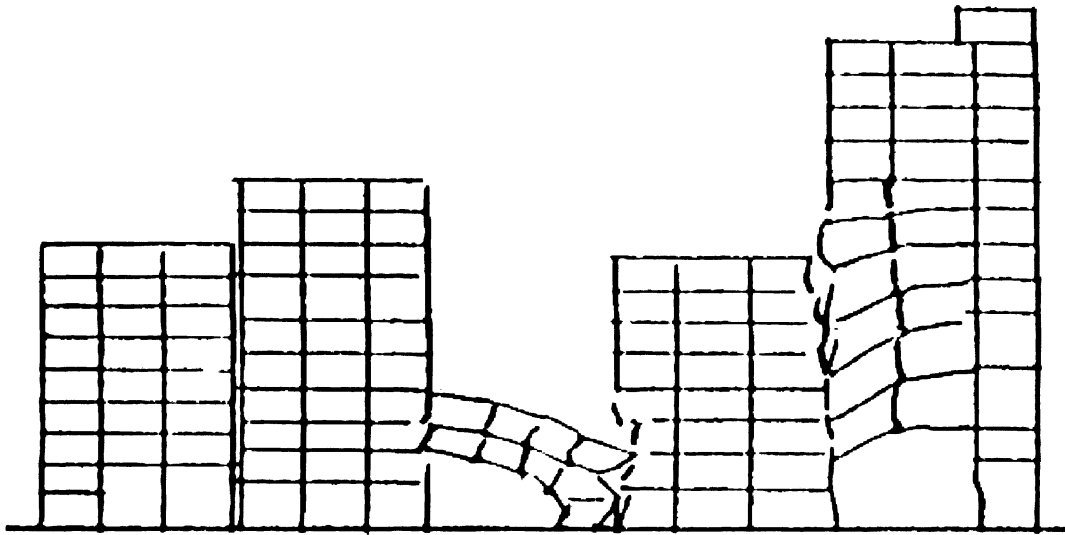


Figure 6-43. Irregularities may create extreme displacements or collapse

Study of pounding damage in Kobe in 1995 showed that very large deflections were often caused by design flaws (such as a soft first story) or near source extreme shaking velocities, or a combination of the two. In addition, many instances of large building deflections (or "leaning") related to ground/foundation failures. These effects are not accounted for in code type separation requirements, which assume a uniform deflection for the height of the building, related only to ground motion.

Observation has also shown that, in some cases, the close proximity of buildings may act as a support, particularly for buildings in mid-block, and increasing the space between buildings might serve, in some cases, to increase deflections and damage rather than reducing them. A probable instance of this was observed by the author in Mexico City, in 1985. In this instance, a tall slender building with an apparent serious soft first story problem, appeared to be restrained by low, stiff buildings on either side. (Figure 3). Several instances of this phenomenon were observed in Kobe.

This point is very difficult to assess. The response to shaking of a number of adjacent buildings with essentially no separation between them must be equivalent to the response of a large building with a variety of strengths, stiffness and other structural characteristics which would be very difficult to analyze.

The possibility of pounding is a function of the vertical deflection or drift of adjoining buildings (or parts of a building). Drift is calculated by applying the code design forces to the building and then observing the deflections that result. Since these estimated forces will be less than what we know can occur, calculated deflections must be corrected to obtain a more realistic estimate of how much the building may actually move. Alternatively, an accurate estimate of drift may be made that accounts for all foreseeable factors.

Potential pounding presents some particular problems of a socio-economic nature where existing buildings are concerned. The socio-economic problems consist of how to involve the adjoining building owner in possibly costly studies, design and construction work that the owner may not wish to participate in or may

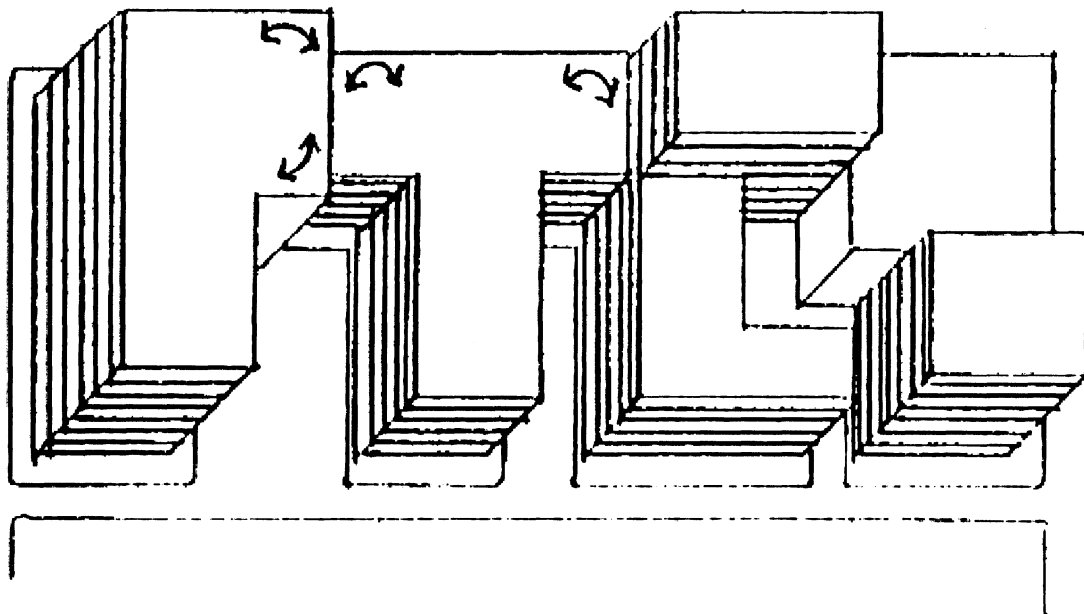


Figure 6-44. Irregularities in plan may create additional torsional effects that impact adjoining buildings

even actively oppose them. The problems are particularly critical in the case of common structure, because rehabilitation is very difficult, if not impossible, without the neighbor's involvement and probably some degree of rehabilitation to his property. In the case of falling hazards, it would be desirable for the neighbor to mitigate them, but the extent to which the federal owner can require this are not clear. The problem of pounding is traditionally dealt with by requiring a large gap between buildings. This can, in theory, be achieved without impacting the adjoining owner.

While in engineering terms it may seem obvious that it is in the adjoining owners best interest to cooperate in evaluation and mitigation, in socio-economic terms there may be many reasons, valid or otherwise, for reluctance. The owner may have real economic constraints in incurring any costs of evaluation or mitigation, and be quite ready to accept the possible risks of inaction. In addition, the owner may have short term intentions of redeveloping or selling his property, and so not wish to incur

expenses that will be of no conceivable benefit to him. Thus, the possibility of cooperative rehabilitation will be much conditioned by how the adjoining owner sees his economic future and views unsolicited action by a neighbor that might impact it.

• Architectural Implications

Pounding is included in this discussion of configuration issues because it is a matter of where buildings are located relative to other structures, which is an early architectural decision. The problem has considerable architectural implications for the construction of buildings on constricted urban sites, because to make provision for the worst case condition could result in large building separations and significant loss of usable space.

While building codes place modest limits on drift (for example, 0.005 time story height) based on static analysis, actual experience with drift and calculations of realistic figures provide some startling numbers. Freeman⁽⁶⁻¹³⁾ calculated

the actual drift on flexible buildings up to 20 stories under 0.4 g acceleration as being 0.020 - 0.055 times the story height. For a 12-story building this translates into 40-110 in. for a 14-ft story height. A separation that could accommodate two such buildings vibrating out of phase would have to be 18 ft. 4 in. wide.

Clearly compromise is necessary, but nonetheless, loss of usable space measured in lineal feet becomes serious. In addition, the idea of urban buildings with spaces of 2 - 3 feet between them suggests a very difficult maintenance problem.

• Historical Performance:

Problems of adjacency have been routinely noted by earthquake investigators over the past several decades. In the 1972 Managua earthquake, the five-story Grant Hotel suffered a complete collapse of its third floor when battered by the roof level of the adjacent two-story building.

In the 1964 Alaska earthquake, the 14-story Anchorage Westward Hotel pounded against its low rise ball room and an adjoining six-story wing, although separated by a 4-in. gap. The pounding was severe enough in the high rise to dislocate some of the metal floor decking from its steel supports.

In recent earthquakes, pounding has continued to be a serious issue. The earthquake that struck Mexico City in 1985 has revealed the fact that pounding was present in over 40% of 330 collapsed or severely damaged buildings surveyed, and in 15% of all cases it led to collapse. Many instances of pounding were observed in the Kobe earthquake of 1995.

• Solutions:

Perhaps due to the high incidence of pounding damage observed in the 1985 Mexico City earthquake a number of researchers have studied pounding problems in recent years. Two recent studies, by Jeng et al.⁽⁶⁻¹⁴⁾ and the study by Athanassiadou et al.⁽⁶⁻¹²⁾ are representative, and both contain a full set of references to other

studies of the problem. Jeng et al. present a new method for estimating the likely minimum building separation necessary to preclude seismic pounding: two 10 story concrete frame buildings are analyzed by way of example.

Athanassiadou et al. studied the seismic response of adjacent buildings in series, with similar or different dynamic characteristics, using SDOF systems subjected to base motions.

These, and other studies, confirm the results of empirical surveys, and to provide quantitative information that is necessary for code and design practice development, although as yet the quantitative data is not readily transferable to code values.

To assume that code limits on drift provide an accurate estimate of possible drift is unrealistic, but accurate estimates may provide very large worst case figures. Blume, Corning and Newmark suggest an alternative method⁽⁶⁻¹⁵⁾:

Compute the required separation as the sum of the deflections computed for each building separately on the basis of an increment in deflection for each story equal to the yield-point deflection for that story, arbitrarily increasing the yield deflections of the two lowest stories by multiplying them by a factor of 2.

An earlier edition of the Uniform Building Code contained a rule of thumb intended for the relatively stiff structures of that day⁽⁶⁻¹⁶⁾: separations should be "one inch plus one half inch for each ten feet of height above twenty feet".

It should be noted that, notwithstanding the high cost of land in Japanese cities, new structures in Kobe seem to be providing a generous allowance for differential drift.

A possible alternative approach is to place an energy-absorbing material between the buildings; this obvious simple approach seems to have been little studied.

Many buildings in Mexico City were, in fact, protected from collapse because they were erected hard up against adjoining buildings on

both sides, so that whole blocks of buildings acted as a unit, and the group was stronger than the individual structures. As evidence of this, Mexican studies showed that 42% of severely damaged buildings were corner buildings, lacking the protection of adjoining structures. This finding suggests the need for serious research on the subject of allowable drift, pounding, and the design and construction of closely spaced buildings.

6.9.2 Other Adjacency Problems

Two other problems of adjacency give cause for concern: one is that of damage caused to a building by falling portions of an adjoining building: in the 1989 Loma Prieta earthquake a death was caused in downtown Santa Cruz when a portion of unreinforced masonry wall fell through the roof of a lower adjoining building, and six deaths were caused in San Francisco when part of a masonry wall fell on some parked cars. The other adjacency problem is that created by structural elements - generally walls or columns - that are common to adjoining buildings: while instances of damage caused by this condition are not specifically identified, there is a clear problem when an owner wishes to rehabilitate a building which has structural elements common to an adjoining building that is not undergoing related rehabilitation.

6.10 THE ARCHITECT/ENGINEER RELATIONSHIP

6.10.1 Architect-Engineer Interaction

In the United States the architect/engineer relationship is delicate because typically the engineer is employed by the architect, and if he complains too much about the architect's design he may be replaced. An architect who finds his design criticized by his engineer can generally find an alternative engineer who will

accommodate him. It is extremely hard to ascertain whether this second engineer reaches this accommodation because he is more ignorant than his colleague, more of a gambler, or more inventive and clever.

There are, of course, many instances where architects and engineers have built up close relationships and communicate fruitfully, with the engineer participating at an early stage of design. However, even in these instances the pressure of business often means that, for financial reasons, the engineer is not employed until the building schematic design is complete. This applies particularly to private work, where the developer must have a design- perhaps only a three dimensional sketch -in order to procure financing, and he does not want to incur additional consultant costs until the financing is secured.

The following description is of the preliminary design process of a large U.S. architectural for a client in the Pacific Rim:

".. we developed a method whereby we would send a team of three people for a week, working in the client's office, or from a hotel room, but having client input into daily charettes, lots of alternatives in sketch form, not spending many hours of presentation, but spending the hours on design. At the end of the week we would generally have a viable concept that the client had signed off."⁽⁶⁻¹⁷⁾

Thus the schematic design for a multi-million dollar project is completed in a week: presumably the design is then brought to the engineer for him to insert a structure.

Obviously, in this instance, much depends on the knowledge and experience of this three person team to ensure that the design is structurally reasonable. More risky is when analogous processes are conducted by a single architect with a desire to produce a design that will amaze his client.

In seeking improved architect/engineer interaction a number of conditions must apply:

- The engineer must communicate directly with the architectural design person or team
- The architect must take seriously his shared responsibility with the engineer for the seismic performance of the building. Recent experiences, such as Northridge and Kobe, should encourage this attitude.
- Mutual respect and cooperation: an adversarial relationship will not be productive.
- Common language and understanding:

The architect must have some understanding of seismic engineering terms -such as acceleration, amplification, base shear, brittle failure, damping (and so on through the engineering glossary). At the same time the architect should have a general understanding of the characteristics of typical seismic structural concepts: shear walls, bracing, moment frames, diaphragms, base-isolation etc. The new concepts of performance -based seismic design should also be understood. In turn the engineer must understand the architect's functional needs and aspirations.

- Collaboration must occur at the onset of a project: before architectural concepts are developed or very early on in their conception
- Business conditions that restrict early architect/engineering interaction must be alleviated (by the use of a general consulting retainer fee, for example, recovered from those projects that are achieved).
- If the architect does not want to interact with his engineer, or if for some reason is prevented from doing so, then he should work with simple regular forms, close to the optimal seismic design

While it is reasonable for engineers to ask that architects become better informed about seismic design and the consequences of their configuration decisions, the engineer must understand that while for them seismic design is

of paramount importance, for architects and their clients it takes very low priority as far as their own interests. For the architect, seismic design and safety is taken care of by the engineer: it is no more a subject of concern than provision for vertical forces, which never comes up for discussion between owner and architect, and seldom between architect and engineer. The architect is preoccupied with issues of codes and regulations relating to planning and design far removed from seismic problems, but of great importance and interest to his client. Similarly, the architect is continuously evaluating planning options, materials issues and both functional and aesthetic concerns upon which his client is constantly questioning him. Above all, the work must be done on time and on budget, and the architect would also like the job to be profitable.

Architects vary greatly in their interests: the stereotype of the architect as an unworldly aesthete is seldom true. Some architects are brilliant salespeople and business managers: some are very close to engineers, and interested in how the building is engineered and constructed: some are excellent project managers and will ensure that budgets and schedules are kept: some are inspiring managers of people and will run an exciting and enjoyable office: some are brilliant at the design of details, the behavior of materials and the development of construction documents: and some are thoughtful and inventive designers. The large, well-run office will have a mix of the above in its staff. The small office must try and find a few people that combine the above roles. As the profession of architecture becomes more complex, specialization is becoming more common: even large firms cannot play all roles, and the small office must specialize in a limited type of design. The advent of CAD and other information systems has extended the range for the small practitioner, but these systems need large capital investments that produce their own forms of limitation.

6.11 Future Images

6.11.1 Beyond the International Style

The tenets of the International Style began to be seriously questioned in the mid-1970's, both in print by architectural critics and historians and in practice by architects beginning to bring new design approaches to the drawing board and to construction. This questioning finally bore fruit in an architectural style known broadly as "Post-modern". Although this term was criticized by critics and the architects who were seen to be designing in this style, the term became a useful mark of identity. In general, post-modernism meant:

- the revival of surface decoration on buildings
- a return to symmetry in overall form
- the use of classical forms, such as arches, decorative columns, pitched roofs, in nonstructural ways, and generally in simplified variations of the original elements.
- a revival of exterior color as an element, with a palette of characteristic colors (e.g. dark green, pink, Chinese red, bright yellow, buff etc)

Developments of post-modernism also involved both the revival of full, scholarly, classical revival as a style., and also very personal images by a few prominent architects in terms of scale and forms, which were derived from a variety of sources, such as Victorian engineering, ancient Egyptian architecture and non-Euclidean geometry.

In seismic terms, this change in stylistic acceptance was, if anything, beneficial. The return to classical forms and symmetry was helpful to the structure as a whole, and almost all of the decorative elements were nonstructural. Inspection of an early icon of post-modernism, the Portland office building designed by Michael Graves, (Figure 6-45). shows an extremely simple and ordinary structure. Indeed, the Portland building, which created a sensation when completed, has a form

that approximates our optimal structure: the sensation is all in the nonstructural surface treatments. Designed as an economical design/build project the building has recently undergone seismic retrofit unrelated to its configurational characteristics.

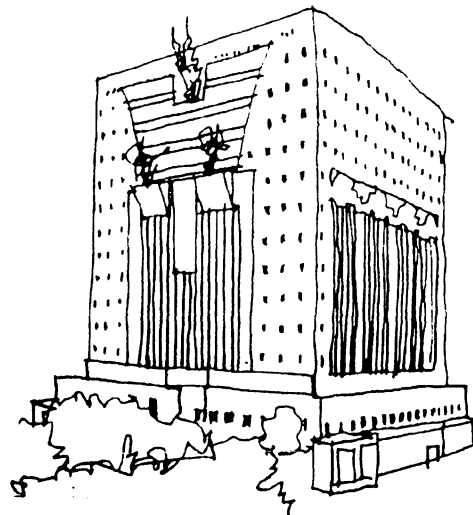


Figure 6-45. Office building, Portland, Oregon. Michael Graves, architect, 1979

It should be noted, however, that an interest in seismic design had no influence on the development of post-modernism - it is, and was a strictly aesthetic and cultural movement.

At the same time that post-modernism was making historical architectural style legitimate again, another style evolved in parallel:. This style, originally christened "hi-tech" (the term has not stuck) returned to the celebration of engineering and new industrial techniques and materials as the stuff of architecture. This style developed primarily in Europe, notably in England and France, and was exemplified in a few seminal works, such as the Pompidou Center in Paris, the Lloyds building in London, and the Hong Kong and Shanghai bank in Hong Kong. These buildings proclaimed a new version of the functionalism of the thirties, updated to provide flexibility, adaptability and advanced servicing for an uncertain future, using exposed structure with beautiful castings as connections. In truth, these buildings are as

aesthetically and stylistically conceived as any post-modern or classical revival building.

The rise of post-modernism released architects from the strait-jacketed moralities of the International Style. As a result, at present a kind of aesthetic bedlam reigns, and several competing private styles co-exist, competing for clients - and finding them. The leading exponents of the new styles form an architectural jet-set, cruising the world dropping off their stylistic gems to clients and countries that can afford them.

The importance of well-publicized designs by fashionable architects is that they create new accepted styles. Architects are very responsive to form and design and once a form gains credence practicing architects the world over begin to reproduce it. Today's New York corporate headquarters high-rise becomes tomorrow's suburban Savings and Loan Office, as became clear in the adoption of the metal and glass curtain for building exteriors. The first two highly publicized curtain walls were that of the United Nations building and the Lever Brothers building, both in New York city in the early 50's: by the mid 60's every town in America had its stock of blue-green glazed commercial buildings.

So, to predict the design vernacular of the future it is necessary to look at what is being done in high-style architecture, and in particular, to try and guess which forms seem to catching the imagination of architects and starting to be reproduced at a more modest level. Amid the bedlam of design voices, three influential trends can be discerned..

6.11.2 Influential Trends

- **The bridge building:**

The bridge building form is that of twin high-rise buildings connected at the roof with horizontal occupied space that acts as a bridge. The concept is that of a single building. The prototypical form of this, that has seized architect's imaginations, is that of the Grand Arch of the Defense (Figure 6-46), in Paris, one

of the late President Mitterand's "grand projects". This is a single office building, some 34 stories tall, designed as a cubical arch, framing the end of the Defense development on the perimeter of Paris. The arch is in line with the main axis through Paris to the Louvre, on which lies the Arch De Triomphe. The horizontal bridge structure provides exhibition and meeting spaces.

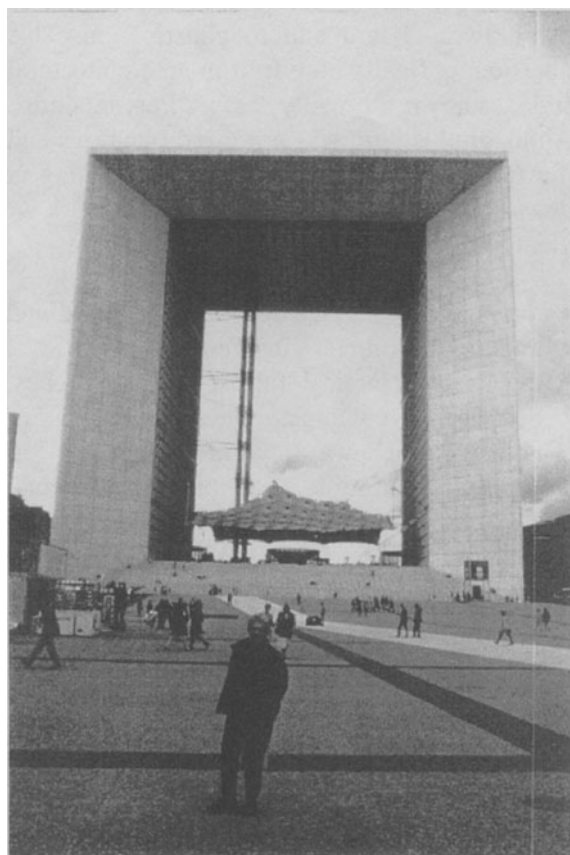


Figure 6-46. Grande Arche of the Defense, Paris, Johan Otto von Spreckelsen, architect

A similar form is that of the Umeda Sky Building (Figure 6-47) in Osaka, Japan. This building incorporates a mid-air garden , midair escalators and a mid-air bridge to connect the two parts of the building. The architect, Hiroshi Hara, sees this form as the beginning of an approach to a three-dimensional network to our congested cities. This building is in a fairly severe seismic zone and is carefully designed for earthquake resistance.



Figure 6-47. Umeda Sky building, Osaka, Japan, Hiroshi Hara, architect, 1988

The bridge or twin tower forms have immense drama and appeal, and so we can expect to see five story versions of them appearing in our shopping malls and suburban centers.

• The warped building:

A strong design trend is that of buildings that use warped forms, often combined with non vertical walls and irregular warped exterior surfaces. The most prominent exponent of these forms is the American architect Frank Gehry, who is now building these forms all over the world. His Guggenheim Museum in Bilbao, Spain, completed in 1997 is typical of his style, and has been hailed as a masterpiece by architectural critics world-wide (Figure 6-48). His tower for the Rapid Transport Headquarters

in Los Angeles, (Figure 6-49) shows his warped and non vertical forms applied to a skyscraper. Despite its flourishes, the building is essentially rectilinear with the warped elements achieved by nonstructural add-ons to the main structure.

• The Deconstructed Building

Deconstruction is a term applied to the work of a number of architects presently working around the world: the term is derived from the language and literary movement of the same name that originated in literary criticism. The principles of deconstruction were first formulated by the French philosopher and critic Jacques Derrida, in the early 1970's and have since revolutionized literary criticism and the study of language and meaning.

Because deconstructed buildings essentially ignore the limitations of constructability, few have yet been built. One of the architects most commonly associated with deconstruction is the Iraqi, Zaha Hadid, who works in London. Figure 6-50 shows her design for a normally prosaic building - a fire station completed in 1993 in Germany.

6.12 CONCLUSION

These examples of new trends in architecture have been selected because experience has shown the force of images created by architectural innovators, however strange they may at first appear. The architects illustrated are those -among many- who are having great influence in the schools of architecture and among younger professionals. Engineers may expect to be confronted by these kinds of configurations in the coming years.

Engineering rationality, and even buildability, appears to have little influence on these forms. There is controversy in the profession about this, and many critics view the new architecture as akin to theater set design, in which image is everything and its method of construction and longevity is irrelevant. Be that as it may, the zeitgeist is changing, and architects will performe have to obey it.

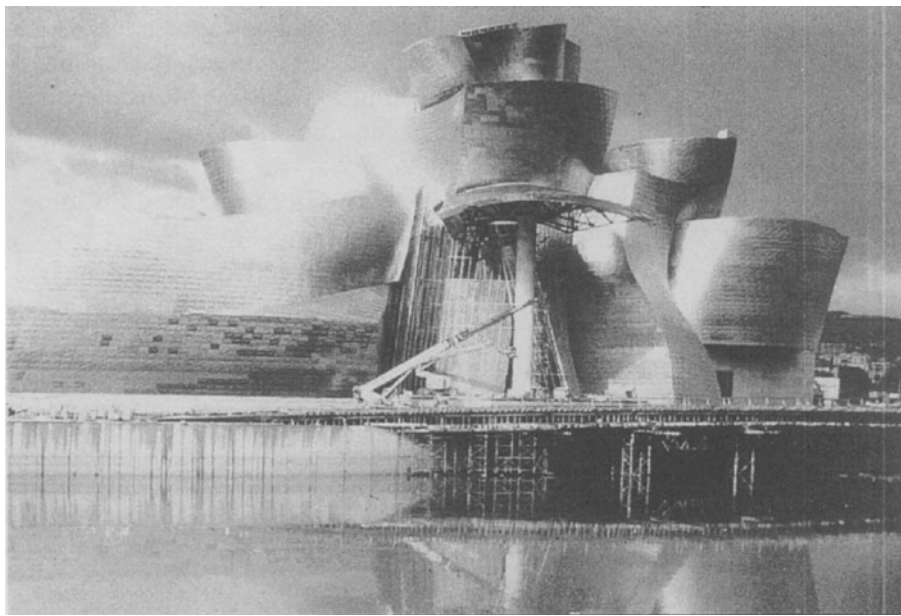


Figure 6-48. Guggenheim Museum, Bilbao, Spain, Frank Gehry, architect, 1996

Successful engineers will understand these imperatives, enjoy the experimentation that this work represents, and assist the architects in realizing their ambitions. New methods of analysis will help, but engineers must also continue to develop their own innate feeling for how buildings perform, and be able to visualize the interaction of configuration elements that are quite unfamiliar.

Meanwhile, the residue of configuration problems left by the architecture/engineering of the 50's to 70's must be dealt with. Some will disappear as aging buildings are replaced: this should be encouraged, as it is the only guaranteed way of removing the earthquake threat. For other buildings, engineers must use their ingenuity and imagination to find affordable methods of retrofit. And there need be no recriminations: these problems are the joint product of architect/engineer interaction that, in its time, was fruitful: nature always has the last word in reminding us of our collective ignorance.

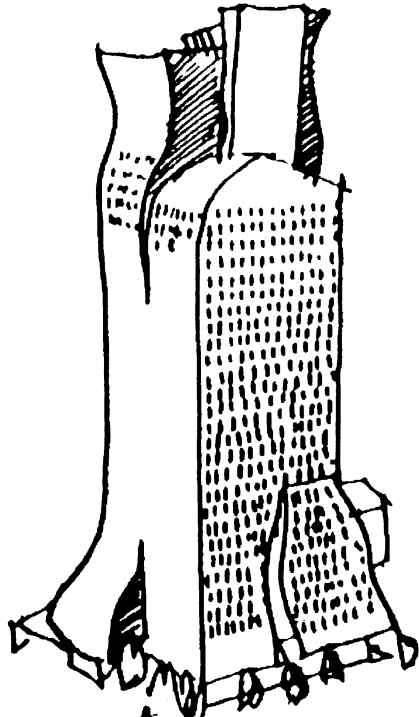


Figure 6-49. Rapid Transport District Headquarters, Los Angeles, Frank Gehry, architect, 1995

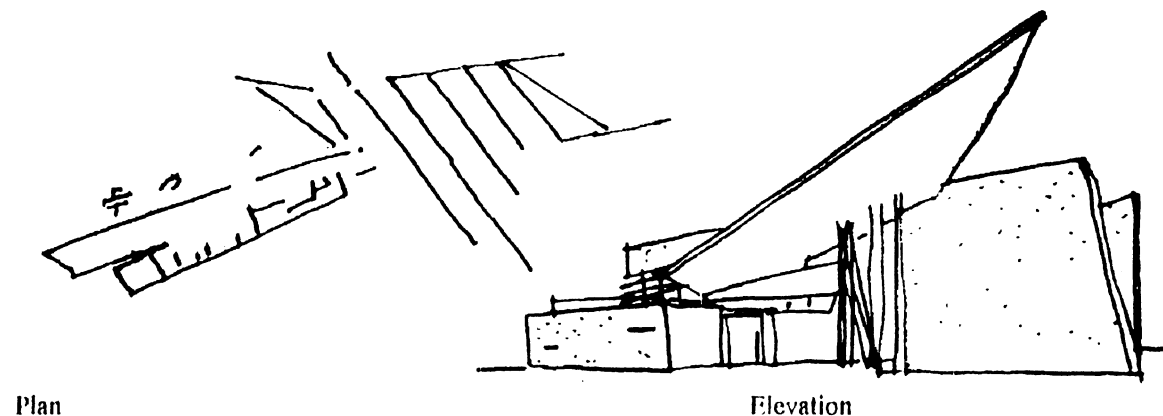


Figure 6-50. Fire Station, Vitra factory complex, Weil-am-Rhein, Germany Zaha Hadid, architect, 1995

Simple, economical buildings will continue to be built, and our optimal seismic design will continue to be viable. It may form the basis of performance based design which, if it is to be successful, will have to be free of the kinds of irregularities that make performance prediction difficult or impossible. We may expect design to develop in ways analogous to the poetry and prose of written communication. Most discourse is carried out in prose: the serviceable language of business and news reporting. At the level of literature, prose approaches an art form, in which the subtleties of language and human behavior are explored. Out in advance, often almost unintelligible, are the poets using words and language in new and unexpected ways: but over time they reveal insights in language so compelling that our speech and even our behavior is changed. Thus the language of Shakespeare shows up in the newspaper and even the office E-mail.

REFERENCES

- 6-1 Willis, C., *Form Follows Finance*, Princeton Architectural Press, New York, 1995
- 6-2 Arnold, C., "Architectural Aspects of Seismic Resistant Design" : Proceedings, Eleventh World Conference on Earthquake Engineering, Acapulco, 1996
- 6-3 Building Seismic Safety Council, *NEHRP Recommended Provisions for Seismic Regulations for New Buildings*, Building Seismic Safety Council, Washington, DC (1997)
- 6-4 Seismology Committee, Structural Engineers Association of California, *Recommended Lateral Force Requirements and Commentary*, Structural Engineers Association of California, 1990
- 6-5 Seismology Committee, Structural Engineers Association of California, *Recommended Lateral Force Requirements and Commentary*, Structural Engineers Association of California, 1980
- 6-6 Reitherman, R.K., "Frank Lloyd Wright's Imperial Hotel: a Seismic Re-evaluation" ,Proceedings, Seventh World Conference on Earthquake Engineering. Istanbul, 1980
- 6-7 Dowrick, D.J., *Earthquake Resistant Design*, John Wiley and Sons, London, 1989
- 6-8 Naito, T., "Earthquake-proof Construction", Bulletin of Seismic Society of America, Vol. 17, No. 2, June 1977.
- 6-9 Degenkolb, H.J., "Seismic Design: Structural Concepts" Summer Seismic Institute for Architectural faculty, AIA Research Corporation, Washington, DC, 1977

- 6-10 Dewell, H and Willis, B, "Earthquake Damage to Buildings," Bulletin of Seismic Society of America, Volume 15, No. 4 , Dec. 1925
- 6-11 Comartin, C.D., ed., "Guam Earthquake of August 8, 1993: Reconnaissance Report", Earthquake Spectra, 11, Supplement B, Earthquake Engineering Research Institute, Oakland, CA, 1993
- 6-12 Athanassiadou, C.J., Penelis, G.C and Kappos, A.J.: Seismic Response of Adjacent Buildings with Similar or Different Dynamic Characteristics, Earthquake Spectra, Volume 10, Number 2, Earthquake Engineering Research Institute, Oakland, CA, 1994
- 6-13 Freeman, S.A., "Drift Limits: Are They Realistic." Structural Moments, Structural Engineers Association of Northern California, Berkeley, CA 1980
- 6-14 Jeng, V, Kasai, and Maison, B.T.: A Spectral Method to Estimate Building Separations to Avoid Pounding, Earthquake Spectra, Volume 8, Number 2, Earthquake Engineering Research Institute, Oakland, CA, 1992
- 6-15 Blume, J.A, Newmark, N.M, and Corning,L.H, *Design of Multistory Concrete Buildings for Earthquake Motion*,Portland Cement Association, Skokie, IL, 1961
- 6-16 International Conference of Building Officials (ICBO), *1958 Uniform Building Code* (UBC), Whittier , CA 1958
- 6-17 Fuller, L.P. "Going Global". World Architecture, 42 , London, 1996

Chapter 7

Design for Drift and Lateral Stability

Farzad Naeim, Ph. D., S.E.

Vice President and Director of Research and Development, John A. Martin & Associates, Los Angeles, California.

Key words: Drift, P-delta, Stability, Exact methods, Approximate methods, Code provisions, UBC-97, ICBO-2000, Bent action, Chord action, Shear deformations, Moment resisting frames, Braced Frames, Shear walls, frame-wall interactions, First-order displacements, Second-order displacements.

Abstract: This chapter deals with the problems of drift and lateral stability of building structures. Design for drift and lateral stability is an issue that should be addressed in the early stages of design development. In many cases, especially in tall buildings or in cases where torsion is a major contributor to structural response, the drift criteria can become a governing factor in selection of the proper structural system. The lateral displacement or drift of a structural system under wind or earthquake forces, is important from three different perspectives: 1) structural stability; 2) architectural integrity and potential damage to various non-structural components; and 3) human comfort during, and after, the building experiences these motions. In design of building structures, different engineers attribute various meanings to the term "stability". Here, we consider only those problems related to the effects of deformation on equilibrium of the structure, as stability problems. Furthermore, we will limit the discussion to the stability of the structure as a whole. Local stability problems, such as stability of individual columns or walls, are discussed in Chapters 9, 10, and 11 of the handbook. Several practical methods for inclusion of stability effects in structural analysis as well as simplified drift design procedures are presented. These approximate methods can be valuable in evaluation of the potential drift in the early stages of design. Numerical examples are provided to aid in understanding the concepts, and to provide the reader with the "hands-on" experience needed for successful utilization of the material in everyday design practice.

7.1 INTRODUCTION

This chapter deals with the problems of drift and lateral stability of building structures. Design for drift and lateral stability is an issue which should be addressed in the early stages of design development. In many cases, especially in tall buildings or in cases where torsion is a major contributor to structural response, the drift criteria can become a governing factor in selection of the proper structural system.

In design of building structures, different engineers attribute various meanings to the term "stability"⁽⁷⁻¹⁾. Here, we consider only those problems related to the effects of deformation on equilibrium of the structure, as stability problems. Furthermore, we will limit the discussion to the stability of the structure as a whole. Local stability problems, such as stability of individual columns or walls, are discussed in Chapters 9, 10, and 11 of the handbook.

The concerns that have resulted in code requirements for limiting lateral deformation of structures are explained in Section 7.2. The concept of lateral stability, its relationship to drift and the P-Delta effect, and factors affecting lateral stability of structures are discussed in Section 7.3.

Several practical methods for inclusion of stability effects in structural analysis are presented in Section 7.4. Simplified drift design procedures are presented in Section 7.5. These approximate methods can be valuable in evaluation of the potential drift in the early stages of design.

Section 7.6 covers the drift and P-Delta analysis requirements of major United States seismic design codes.

Several numerical examples are provided to aid in understanding the concepts, and to provide the reader with the "hands-on" experience needed for successful utilization of the material in everyday design practice.

The relative lateral displacement of buildings is sometimes measured by an overall drift ratio or index, which is the ratio of maximum lateral displacement to the height of

the building. More commonly, however, an interstory drift ratio, angle, or index is used, which is defined as the ratio of the relative displacement of a particular floor to the story height at that level (see Figure 7-1). In this chapter, unless otherwise noted, the term *drift* means the relative lateral displacement between two adjacent floors, and the term *drift index*, is defined as the drift divided by the story height.

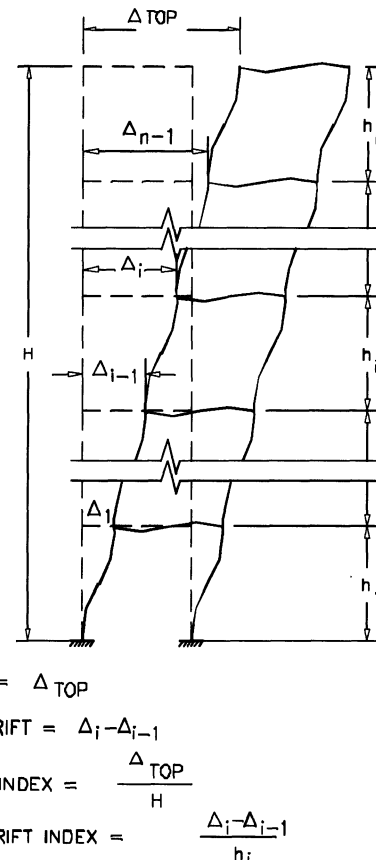


Figure 7-1. Definition of drift.

7.2 THE NEED FOR DRIFT DESIGN

The lateral displacement or drift of a structural system under wind or earthquake forces, is important from three different perspectives: 1) structural stability; 2) architectural integrity and potential damage to various non-structural components; and 3)

human comfort during, and after, the building experiences these motions.

7.2.1 Structural Stability

Excessive and uncontrolled lateral displacements can create severe structural problems. Empirical observations and theoretical dynamic response studies have indicated a strong correlation between the magnitude of interstory drift and building damage potential⁽⁷⁻²⁾. Scholl⁽⁷⁻³⁾ emphasizing the fact that the potential for drift related damage is highly variable, and is dependent on the structural and nonstructural detailing provided by the designer, has proposed the following generalization of damage potential in relationship to the interstory drift index δ :

1. at $\delta = 0.001$; nonstructural damage is probable
2. at $\delta = 0.002$; nonstructural damage is likely
3. at $\delta = 0.007$; nonstructural damage is relatively certain and structural damage is likely
4. at $\delta = 0.015$; nonstructural damage is certain and structural damage is likely

Drift control requirements are included in the design provisions of most building codes. However, in most cases, the codes are not specific about the analytical assumptions to be used in the computation of the drifts. Furthermore, most of the codes are not clear about how the magnifying effects of stability related displacements, such as P-delta deformations, are to be incorporated in evaluation of final displacements and corresponding member forces.

7.2.2 Architectural Integrity

Architectural systems and components, and a variety of other non-structural items in a building, constitute a large portion of the total investment in the project. In many cases the monetary value of these items exceeds the cost of the structural system by a large margin. In addition, these non-structural items can be potential sources of injury, and even loss of life,

for building occupants and those who are in the vicinity of the building. Past earthquakes have proven that non-structural components can also greatly influence the seismic response of the building. Chapter 13 of the handbook is devoted to this important aspect of seismic design.

7.2.3 Human Comfort

Human comfort and motion perceptibility, which are of importance in the design of structures for wind induced motions, are relatively insignificant in seismic design, where the primary objective is to limit damage and prevent loss of life. For very essential structures, where continued operation of facilities is desired during and immediately after an earthquake, a more conservative design or application of special techniques, such as seismic isolation (see Chapter 14), may be considered. However, here again, the primary goal is to keep the system operational, and to prevent damage, rather than to provide for comfort of the occupants during strong ground motion.

Some investigators have studied the behavior of building occupants during strong ground motions^(7-4, 7-5, 7-6). Such studies can provide owners, architects, and hazard mitigation authorities, with valuable guidelines for considering these human factors in planning, design, and operation of building structures.

7.3 DRIFT, P-DELTA, AND LATERAL STABILITY

7.3.1 The Concept of Lateral Stability

To illustrate the concept of stability, consider an ideal column without geometrical or material imperfections. Furthermore, assume that there are no lateral loads, and that the column remains elastic regardless of the force magnitude. If the axial force is slowly increased, the column will undergo axial

deformation, and no lateral displacements will occur. However, when the applied forces reach a certain magnitude called the critical load (P_{cr}), significant lateral displacements may be observed.

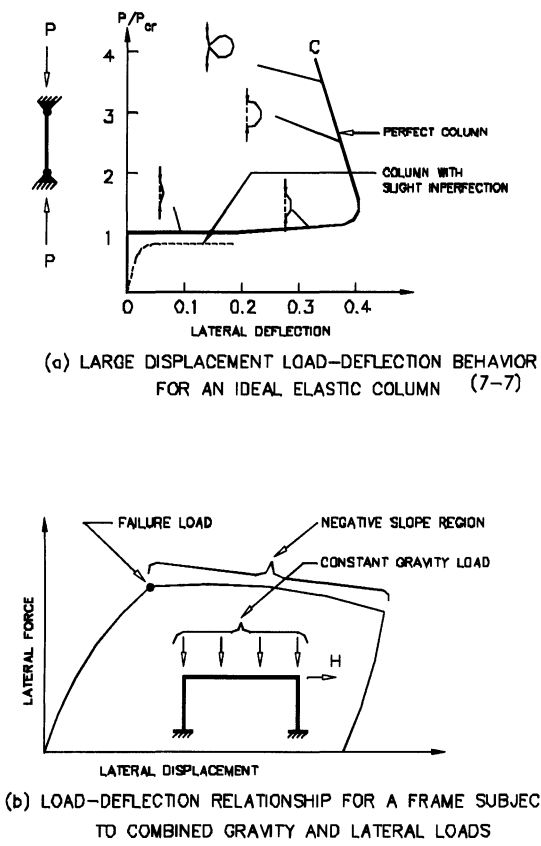


Figure 7-2. Structural stability of an idealized column and a real frame.

Figure 7-2a shows the load-deflection behavior of this ideal column. It is important to notice that when the magnitude of axial force exceeds P_{cr} , there are two possible paths of equilibrium: one along the original path, with no lateral displacements, and one with lateral displacements. However, equilibrium along the original path is not stable, and any slight disturbance can cause a change in the equilibrium position and significant lateral displacements. The force P_{cr} is called the bifurcation load or first critical load of the system. For this ideal column reaching the bifurcation point does not imply failure simply because it was assumed that it will remain

elastic regardless of the deflection magnitude. However, in a real column, such large deformations can cause yielding, stiffness reduction, and failure. In a structural system, buckling of critical members and the corresponding large lateral displacements, can cause a major redistribution of forces and overall collapse of the system.

It is important to note that the bifurcation point, exists only for perfectly symmetric members under pure axial forces. If the same ideal column is simultaneously subjected to lateral loads, or if asymmetry of material or geometric imperfections are present, as they are in any real system, lateral displacements would be observed from very early stages of loading.

When a frame under constant gravity load is subjected to slowly increasing lateral loads, the lateral displacement of the system slowly increases, until it reaches a stage that in order to maintain static equilibrium a reduction in the gravity or lateral loads is necessary (Figure 7-2b). This corresponds to the region with negative slope on the force-displacement diagram. If the loads are not reduced, the system will fail.

When the same frame is subjected to earthquake ground motion, reaching the negative slope region of the load-displacement diagram, does not necessarily imply failure of the system (see Figure 7-3). In fact, it has been shown that in the case of repeated loads with direction reversals, such as those caused by earthquake ground motion, the load capacity of the system will be significantly larger than the stability load for the same system subjected to uni-directional monotonic loads^(7-1, 7-8). Perhaps this is one reason for scarcity of stability-caused building failures during earthquakes.

Exact computation of critical loads, for real buildings, is a formidable task. This is true even in a static environment, let alone the added complexities of dynamic loading and inelastic response. Exact buckling analysis is beyond the capacity and resources of a typical design office, and beyond the usual budget and time-frame allocated for structural analysis of buildings.

In everyday structural analysis, the stability effects are accounted for either by addressing the problem at the element level (via effective length factors), or by application of one of the various P-Delta analysis methods.

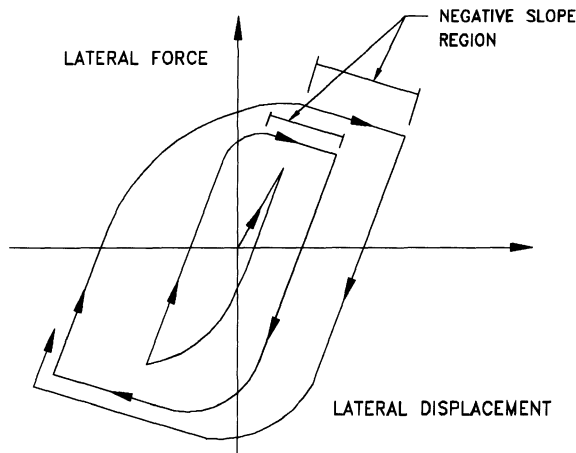


Figure 7-3. A typical load-displacement curve for a frame under constant gravity load and reversing lateral load.

The simplest way to minimize lateral stability problems is to limit the expected lateral

displacement or drift of the structure. In fact several studies^(7-9, 7-10, 7-11, 7-12) have shown that by increasing lateral stiffness, the critical load of the building will increase and the chances of stability problems are reduced. Drift limitations are imposed by seismic design codes primarily to serve this purpose.

7.3.2 P-Delta Analysis

For most practical purposes, an accurate estimate of the stability effects may be obtained by what is commonly referred to as P-delta analysis.

Overall stability failures of structures have not been common during past earthquakes. However, with the continuing trend towards lighter structural systems, and recent discoveries about the nature of near-field ground motion^(7-13, 7-14, 7-15), the second-order effects are beginning to receive more attention. It is believed that, in most cases, observance of proper drift limitations will provide the necessary safeguard against the overall lateral

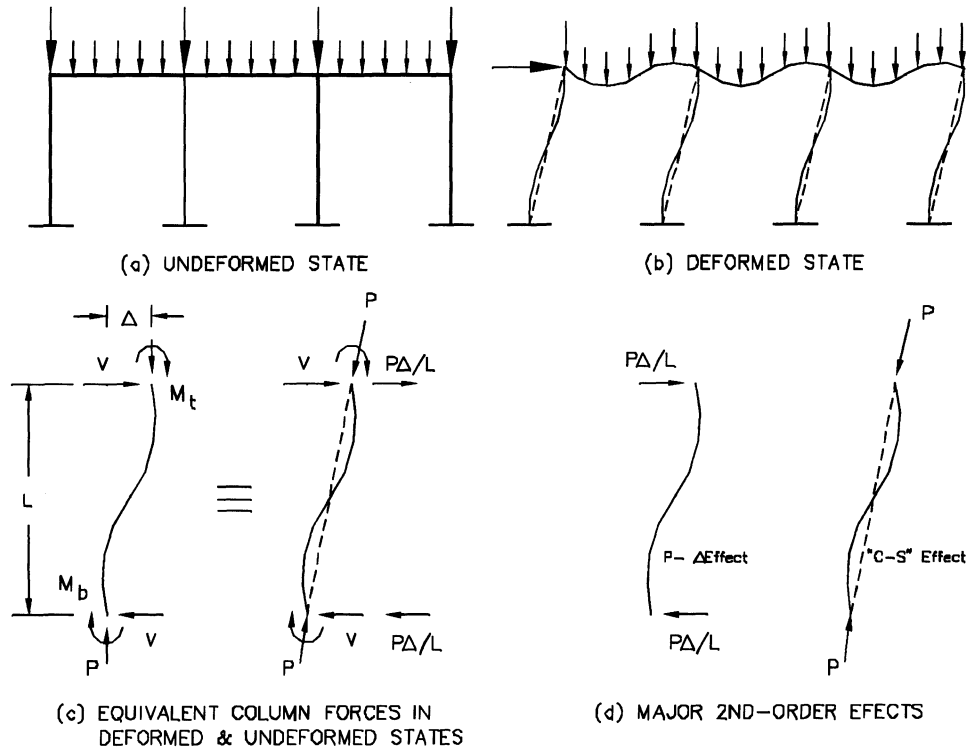


Figure 7-4. Applied loads in the undeformed and deformed states.

stability failure of the structure.

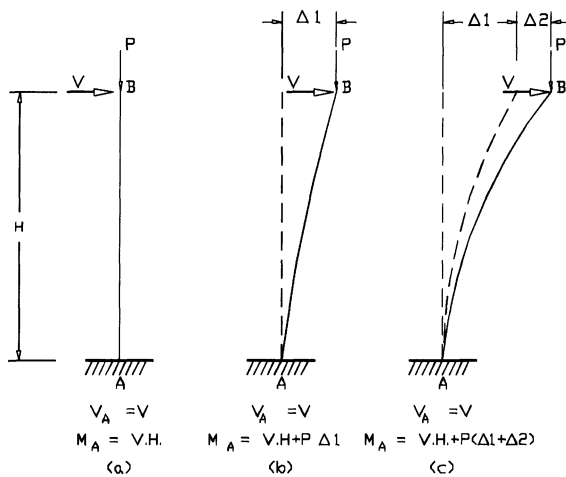


Figure 7-5. The P-delta effect. (a) Equilibrium in the undeformed state. (b) Immediate P-delta effect, (c) Accumulation of the P-delta effect.

In conventional first-order structural analysis, the equilibrium equations are formulated for the undeformed shape of the structure. However, when a structure undergoes deformation, it carries the applied loads into a deformed state along with it (Fig. 7-4). The

changes in position of the applied forces are cumulative in nature and cause additional second-order forces, moments, and displacements which are not accounted for in a first-order analysis. Studies⁽⁷⁻¹⁶⁾ have shown that the single most important second-order effect is the P-delta effect. Figure 7-5 illustrates the P-delta effect on a simple cantilever column.

In some cases, stability or second-order effects are small and can be neglected. However, in many other cases such as tall buildings, systems under significant gravity loads, soft-story buildings, or systems with significant torsional response, the second-order effects may be quite significant and hence, should be considered in the structural analysis.

Although it is true that ignoring second-order effects is not likely to result in overall stability failure of typical buildings subjected to earthquake ground motion, these effects can frequently give rise to a series of premature material failures at the level of forces, that would seem safe by a first-order analysis. Strong evidence relating excessive drift to seismic damage during earthquakes, supports this point.

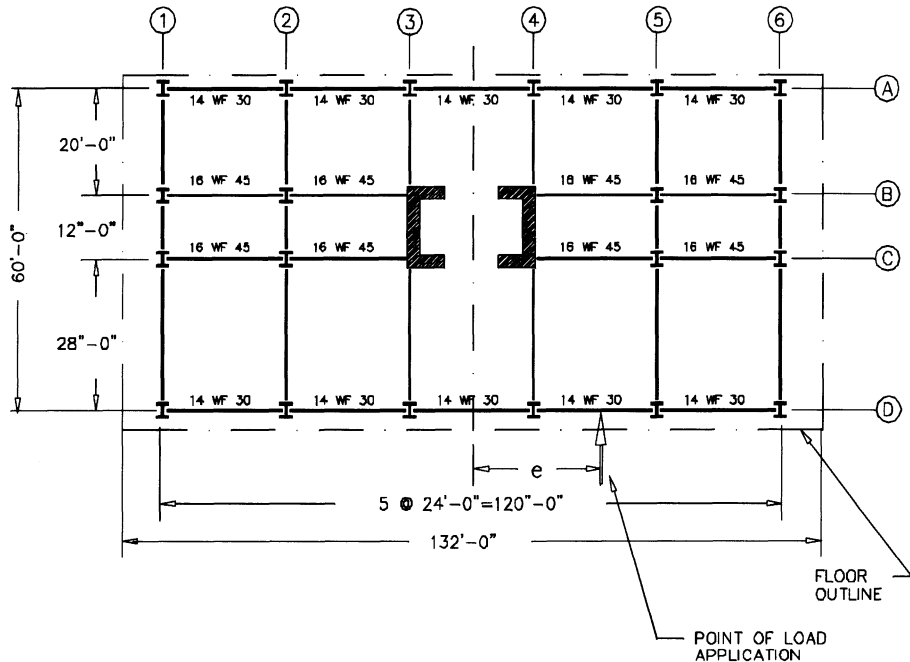


Figure 7-6. Plan of the 24 story structure (7-17).

7.3.3 Factors Affecting Lateral Stability

In general, the magnitude of the gravity loads and factors that increase lateral displacement, affect lateral stability of the structure. Chief among these factors are rotation at the base of the structure⁽⁷⁻¹²⁾, any significant rotation at any level above the base (as that caused by formation of plastic hinges in the columns or walls), and significant asymmetry or torsion in the structure.

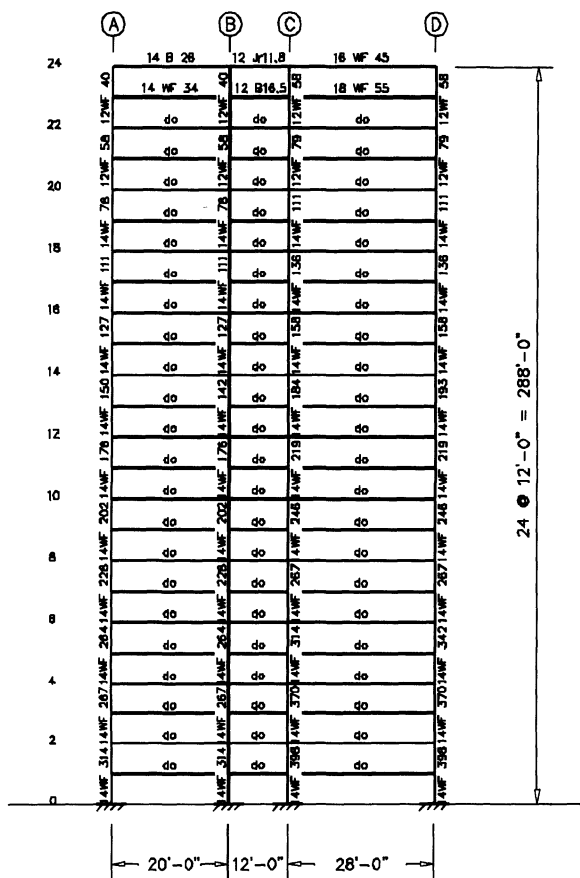


Figure 7-7. Elevation of the 24 story structure (7-17).

Wynhoven and Adams⁽⁷⁻¹⁷⁾ studied the effects of asymmetry and torsion on the ultimate load carrying capacity of a 24 story frame-shear wall building with typical plan and elevation layouts as shown in Figures 7-6 and 7-7. The behavior of individual members was idealized as elastic-perfectly plastic. To consider the influence of torsion on the load

carrying capacity of the structure, two asymmetric models were constructed by moving the shear-wall couple from grid lines three and four, to grid lines four and five in one model, and to grid lines five and six in another model. Load-displacement diagrams for the three configurations are shown in Figure 7-8, where λ is the ratio of the ultimate lateral loads to the working stress lateral loads. Gravity loads were not changed. Reduction in the ultimate lateral load carrying capacity due to induced asymmetry proved to be drastic (51% in one case and 66% in the other case).

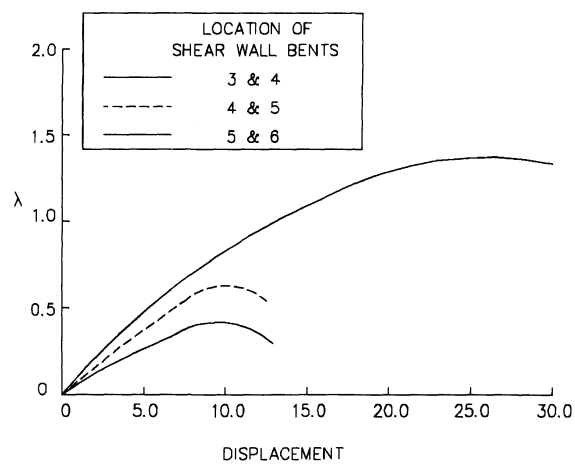


Figure 7-8. Load-displacement relationships for various configurations of the 24 story structure (7-17).

7.4 PRACTICAL SECOND-ORDER ANALYSIS TECHNIQUES

7.4.1 The Effective Length Factor Method

This method is an attempt to reduce the complex problem of overall frame stability to a relatively simple problem of elastic stability of individual columns with various end conditions. The role of the effective length factor K , is to replace an actual column of length L and complex end conditions to an equivalent column of length KL with both ends pinned, so

that the classic Euler buckling equation can be used to examine column stability. It is further assumed that if the buckling stability of each individual column has been verified by this method, then a system instability will not occur.

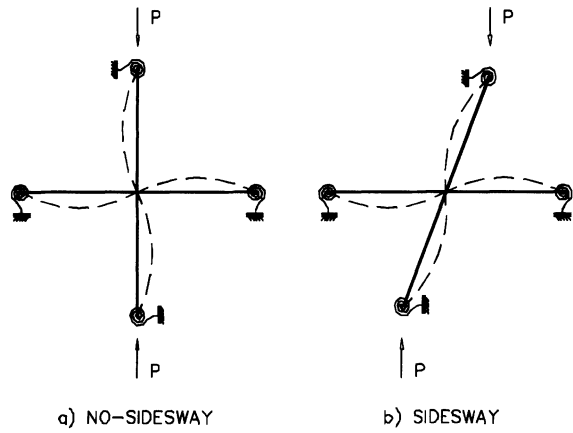


Figure 7-9. Beam-column models used in the development of the effective length factor equations.

The general equations for effective length factors are derived from the elastic stability analysis of simple beam-column models such as those shown in Figure 7-9. These equations are (7-18):

for the sidesway prevented case:

$$\frac{G_A G_B}{4} \left(\frac{\pi^2}{K^2} \right) + \left(\frac{G_A + G_B}{2} \right) \left(1 - \frac{\pi/k}{\tan \pi/k} \right) + \frac{2}{\pi/k} \tan \frac{\pi}{2K} = 1 \quad (7-1)$$

for the sidesway permitted case:

$$\left[\frac{(\pi/K)^2 G_A G_B}{36} - 1 \right] \tan \frac{\pi}{K} - \left(\frac{G_A + G_B}{6} \right) \frac{\pi}{K} = 0 \quad (7-2)$$

where G_A and G_B are the relative rotational stiffness of the beams to the columns, measured at ends A and B of the column under consideration:

$$G = \frac{\sum \frac{I_c}{L_c}}{\sum \frac{I_g}{L_g}} \quad (7-3)$$

Graphical solutions to these equations are given by the well known SSRC alignment charts⁽⁷⁻¹⁹⁾ shown in Figure 7-10. The SSRC Guide⁽⁷⁻¹⁹⁾ recommends that for pinned column bases, G be taken as 10, and for column bases rigidly attached to the foundation, the value of G be taken as unity. Furthermore, when certain conditions are known to exist at the far end of a beam, the corresponding beam stiffness term in Equation 7-3 should be multiplied by a factor. For the sidesway-prevented case, this factor is 1.5 for the far end hinged and 2.0 for the far end fixed. For the sidesway-permitted case this factor is 0.5 for the far end hinged and 0.67 for the far end fixed. Effective length factors have been incorporated in the column design interaction equations of several building design codes.

The effective-length-factor method has been subjected to serious criticism by various researchers. The main criticism is that the effective length factor method, which is based on elastic stability analysis of highly idealized cases, can not be trusted to provide reasonable estimates of the stability behavior of real structural systems. Furthermore, several studies have shown that the lateral stability of a frame, or individual story, is controlled by the collective behavior of all the columns in the story, rather than the behavior of a single column. Hence, if a stability failure is to occur, the entire story must fail as a unit⁽⁷⁻¹²⁾.

Examples and evidence of the shortcomings of the effective length factor method have been documented, among others, by MacGregor and Hage⁽⁷⁻¹⁶⁾ and Choeng-Siat-Moy^(7-20, 7-21). In spite of this evidence, the effective length factor method has continued to survive as a part of the requirements of many building codes. Recently, new editions of some building codes are moving away from this tradition.

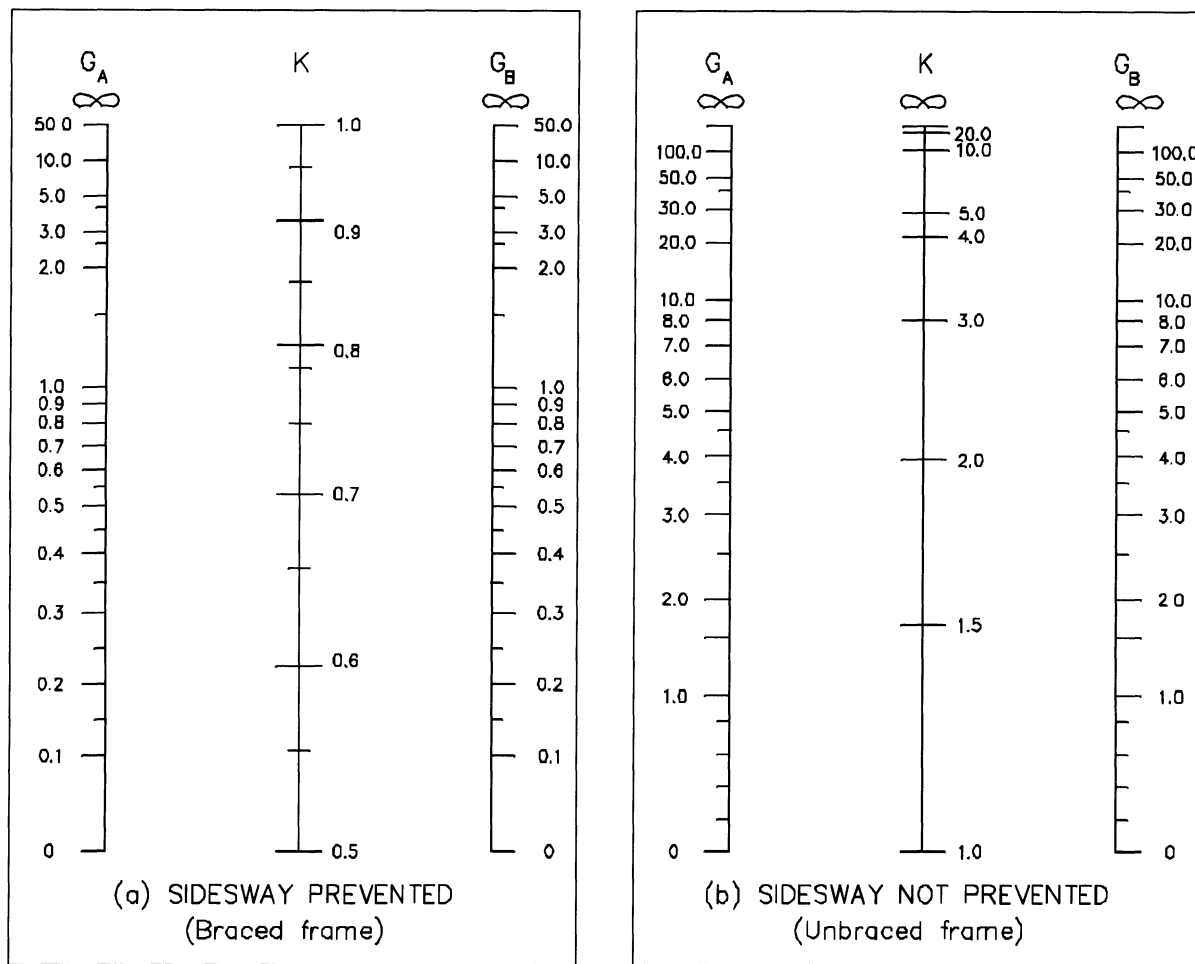


Figure 7-10. Alignment charts for determination of effective length factors⁽⁷⁻¹⁹⁾.

7.4.2 Approximate Buckling Analysis*

In approximate buckling analysis, the buckling load of a single story, or that of the structure as a whole, is estimated. A magnification factor μ , which is a function of the ratio of the actual gravity load to the buckling load, is defined, and for the design of structural members, all lateral load effects are multiplied by this magnification factor. Then, member design is performed by assuming an effective length factor of one.

Several approximate methods have been developed for estimation of critical loads of building structures^(7-10, 7-11, 7-12, 7-22). Among these, a simple method developed by Nair⁽⁷⁻²²⁾ is explained here. This method takes advantage of the fact that most multi-story buildings have lateral load-displacement characteristics that are similar to those of either a flexural cantilever or a shear cantilever.

Buildings with braced frames or shear walls, and tall buildings with unbraced frames or tubular frames, usually have lateral load deformation characteristics that approach those of a flexural cantilever. On the other hand, buildings of low or moderate height with unbraced frames (in which column axial deformations are not significant) usually have

* Parts of section 7.4.2 have been extracted from Reference 6-22 with permission from Van Nostrand Reinhold Company.

lateral load-displacement characteristics similar to those of a shear cantilever.

The above observations can be extended to the torsional behavior of structures. If in a multistory building, torsional stiffness is provided by braced frames, shear walls, or tall unbraced frames not exhibiting tube action, the torsion-rotation characteristics of the building will be similar to the lateral load-displacement characteristics of a flexural cantilever. If a building's torsional stiffness is provided by low to mid-rise unbraced frames, or by tubular frames, the building will have torsion-rotation characteristics that are similar to the lateral load-displacement characteristics of a shear cantilever.

Buildings Modeled as Flexural Cantilevers

For a flexural cantilever of height H and constant stiffness EI , the uniformly distributed vertical load, per unit height (Figure 7-11), p_{cr} , that will cause lateral buckling is given by the equation

$$p_{cr} = 7.84 EI / H^3 \quad (7-4)$$

If the stiffness varies with the equation $EI = (a/aH)EI_0$, where EI_0 is the stiffness at the base and a is the distance from the top, the critical load is given by:

$$p_{cr} = 5.78 EI_0 / H^3 \quad (7-5)$$

If the stiffness varies with the equation $EI = (a/H)^2 EI_0$, the critical load is:

$$p_{cr} = 3.67 EI_0 / H^3 \quad (\text{Eq. 7-6})$$

These solutions for critical load can be found in basic texts on elastic stability.

If a uniformly distributed lateral load of f per unit height is applied to a flexural cantilever, the lateral displacement Δ at the top is:

for a constant EI :

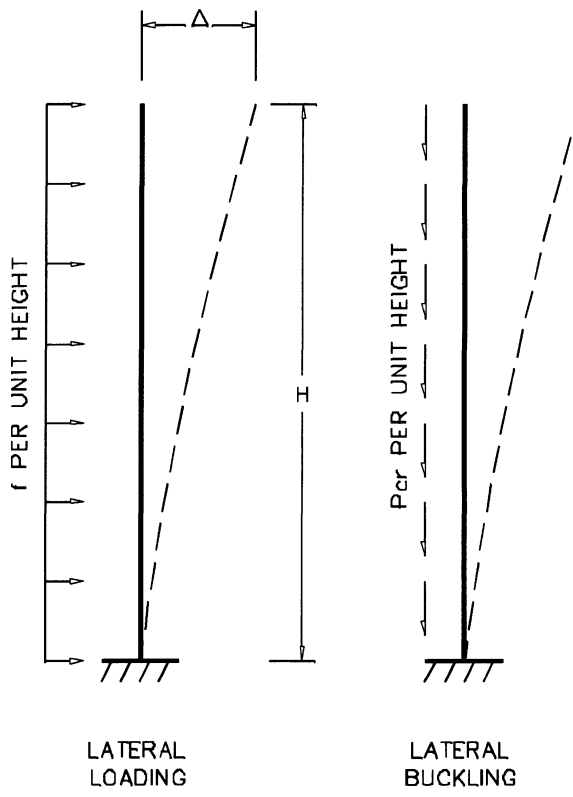
$$\Delta = 0.125 f H^4 / EI \quad (7-7)$$

for $EI = (a/H) EI_0$:

$$\Delta = 0.167 f H^4 / EI_0 \quad (7-8)$$

for $EI = (a/H)^2 EI_0$:

$$\Delta = 0.250 f H^4 / EI_0 \quad (7-9)$$



BUILDINGS MODELED AS FLEXURAL CANTILEVERS

$$P_{cr} = 0.95 f H / \Delta$$

Figure 7-11. Lateral loading and buckling of a flexural cantilever⁽⁷⁻²²⁾.

If the lateral load is not uniform, an approximate answer may be obtained by defining f as the equivalent uniform lateral load that would produce the same base moment as the lateral load used in the analysis. By combining Equations 7-4, 7-5, and 7-6 with

Equations 7-7, 7-8 and 7-9, EI can be eliminated and p_{cr} can be expressed in terms of f/Δ , as follows:

for a constant EI :

$$p_{cr} = 0.98 fH/D \quad (7-10)$$

for $EI = (a/H) EI_0$:

$$p_{cr} = 0.96 fH/D \quad (7-11)$$

for $EI = (a/H)^2 EI_0$:

$$p_{cr} = 0.92 fH/D \quad (7-12)$$

From the above equations it is obvious that the relation between p_{cr} and f/Δ is not very sensitive to stiffness variation over the height of the structure. Hence, regardless of the distribution of stiffness, the following equation is sufficiently accurate for design purposes:

$$p_{cr} = 0.95 fH/\Delta \quad (7-13)$$

The magnification factor μ , as previously defined, is given by:

$$\mu = \frac{1}{1 - \gamma p / \phi p_{cr}} \quad (7-14)$$

where p is the actual average gravity load per unit height on the building, γ is the design load factor, and ϕ is the strength reduction factor. Note that p must include the load on all vertical members, including those that are not part of the lateral-load-resisting system.

Thus, if the lateral displacement is known from a first-order analysis, the critical load and the corresponding magnification factor can be estimated using Equations 7-13 and 7-14.

For buildings whose torsional behavior approaches that of a flexural cantilever, the following formula may be used to estimate the torsional buckling load of the structure:

$$r^2 p_{cr} = 0.95 tH / \theta \quad (7-15)$$

where t is an applied torsional load, per unit height of the building, θ is the rotation at the top of the building in radians, p_{cr} is the critical vertical load for torsional buckling per unit height of the building, and r is the polar radius of gyration of the vertical loading about the vertical axis at the center of twist of the building.

For a doubly symmetric structure, uniformly distributed gravity loading, and a rectangular floor plan with dimensions a and b :

$$r^2 = \frac{a^2 + b^2}{12} \quad (7-16)$$

Buildings Modeled as Shear Cantilevers

If a portion of a vertical shear cantilever undergoes lateral deformation δ , over a height h , when subjected to a shear force V , the critical load for lateral buckling of that portion of the cantilever is given by

$$P_{cr} = Vh/\delta \quad (7-17)$$

When the above equation is applied to a single story of a building, h is the story height, δ is the story drift caused by the story shear force V , and P_{cr} is the total vertical force that would cause lateral buckling of the story (see Figure 7-12).

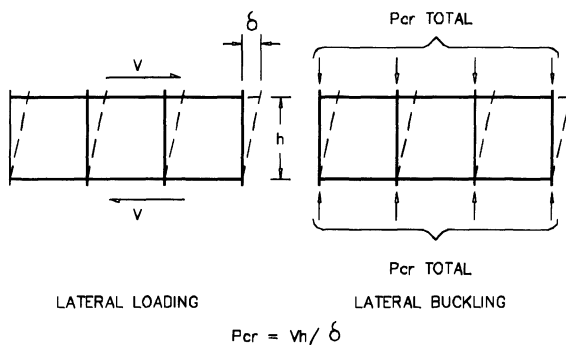


Figure 7-12. Lateral loading and buckling of a story in a shear cantilever type building⁽⁷⁻²²⁾.

The magnification factor μ , is given by

$$\mu = \frac{1}{1 - \gamma P / \phi P_{cr}} \quad (7-18)$$

where P is the total gravity force in the story, γ is the load factor, and ϕ is the strength reduction factor.

The accuracy of Equation 7-17, when applied to a single story of a framed structure, depends on the relative stiffness of the beams and columns, and on the manner in which the gravity loads are distributed among the columns. The error is greatest for stiff beams and slender columns and may be as high as 20%.

For buildings whose torsional behavior approaches that of a shear cantilever, the following equation may be used to estimate the torsional buckling load of a particular story of the building:

$$r^2 P_{cr} = T h / \theta \quad (7-19)$$

where T is an applied torsional load on the story, θ is the torsional deformation of the story (in radians) due to the torque T , h is the story height, P_{cr} is the critical load for torsional buckling of the story, and r is the polar radius of gyration of the vertical load.

Application Examples Consider the twenty story buildings shown in Figure 7-13. The buildings are analyzed using a linear elastic analysis program for a constant lateral load of 25 psf applied in the North-South direction. The East-West plan widths are 138 ft. The gravity load is assumed to be 130 psf on each floor.

For building I, the first-order displacement at the top is 0.729 ft. Using Equation 7-13:

$$H = 240 \text{ ft}$$

$$f = 0.025(138) = 3.45 \text{ kips/ft}$$

$$\Delta = 0.729 \text{ ft}$$

$$P_{cr} = 0.95(3.45)(240)/0.729 = 1079 \text{ kips/ft}$$

The estimated critical load of 1079 k/ft corresponds to 12,948 kips or 1,360 psf on each

floor. The corresponding magnification factor assuming $\gamma = \phi = 1.0$, is

$$\mu = \frac{1}{1 - 130/1360} = 1.106$$

and the magnified lateral displacement at the roof is given by:

$$\gamma\Delta = 1.106(0.729) = 0.806 \text{ ft}$$

An elastic stability analysis of this building (7-23) indicates a critical load of 1,369 psf for North-South buckling. A large-deformation analysis for combined gravity load and North-South lateral loading indicates a roof displacement of 0.805 ft.

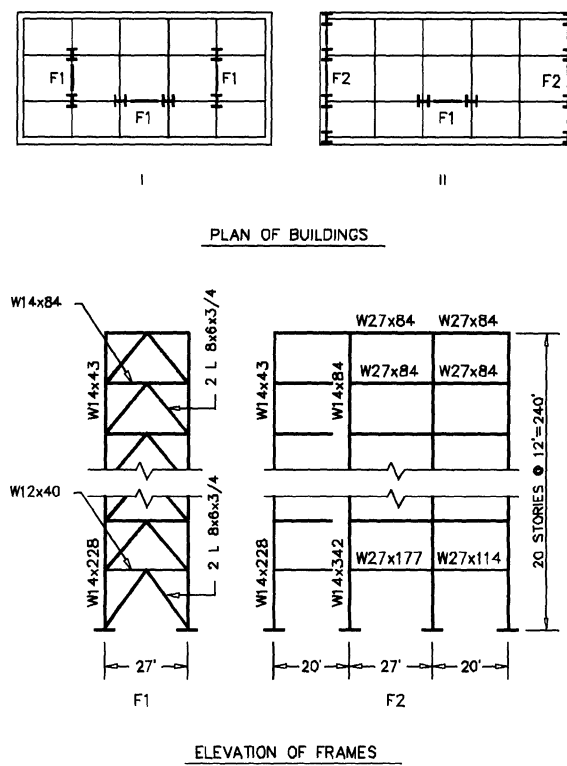


Figure 7-13. Buildings analyzed in references (7-22) and (7-23).

For building II, the computed story drifts for the 15th, 10th, and 5th levels are 0.0522 ft, 0.0609 ft, and 0.0582 ft, respectively. The corresponding story shears at these levels are 228 kips, 435 kips, and 642 kips. Using Equation 7-17:

15th story: $P_{cr} = 228(12)/0.0522 = 52,414$ kips

10th story: $P_{cr} = 435(12)/0.0609 = 85,714$ kips

5th story: $P_{cr} = 642(12)/0.0582 = 132,371$ kips

The corresponding magnification factors assuming $\gamma = \phi = 1.0$ are:

for the 15th story:

$$\mu = \frac{1}{1 - 7427/52,414} = 1.165$$

for the 10th story:

$$\mu = \frac{1}{1 - 13,616/85,714} = 1.189$$

for the 5th story:

$$\mu = \frac{1}{1 - 19,806/132,371} = 1.176$$

and the magnified story drifts are:

for the 15th story:

$$\mu \Delta = 1.165(0.0522) = 0.0608 \text{ ft}$$

for the 10th story:

$$\mu \Delta = 1.189(0.0609) = 0.0724 \text{ ft}$$

for the 5th story:

$$\mu \Delta = 1.176(0.0582) = 0.0684 \text{ ft}$$

A large-deformation analysis of this building⁽⁷⁻²³⁾ indicates story drifts of 0.0607 ft, 0.0723 ft, and 0.0686 ft for the 15th, 10th, and 5th stories, respectively.

7.4.3 Approximate P-Delta Analysis

Three methods for approximate P-delta analysis of building structures are presented in this section: the iterative P-delta method; the

direct P-delta method; and the negative bracing member method. All three methods are shown to be capable of providing accurate estimates of P-delta effects.

Iterative P-Delta Method The iterative P-delta method^(7-16, 7-24, 7-25, 7-26) is based on the simple idea of correcting first-order displacements, by adding the P-delta shears to the applied story shears. Since P-delta effects are cumulative in nature, this correction and subsequent reanalysis should be performed iteratively until convergence is achieved. At each cycle of iteration a modified set of story shears are defined as:

$$\sum V_i = \sum V_1 + (\sum P) \Delta_{i-1} / h \quad (7-20)$$

where $\sum V_i$ is the modified story shear at the end of i th cycle of iteration, $\sum V_1$ is the first-order story shear, $\sum P$ is the sum of all gravity forces acting on and above the floor level under consideration, Δ_{i-1} is the story drift as obtained from first-order analysis in the previous cycle of iteration, and h is the story height for the floor level under consideration. Iteration may be terminated when $\sum V_i \approx \sum V_{i-1}$ or $\Delta_i \approx \Delta_{i-1}$.

Generally for elastic structures of reasonable stiffness, convergence will be achieved within one or two cycles of iteration⁽⁷⁻¹⁶⁾. One should note that since the lateral forces are being modified to approximate the P-delta effect, the column shears obtained will be slightly in error⁽⁷⁻¹⁶⁾. This is true for all approximate methods which use sway forces to approximate the P-delta effect.

EXAMPLE 7-1

For the 10 story moment resistant steel frame shown in Figure 7-14, modify the first-order lateral displacements to include the P-delta effects by using the Iterative P-delta Method. The computed first-order lateral displacements and story drifts for the frame are

Table 7-1. Applied forces and computed First-Order Displacements for the 10-story frame.

Level	Story height <i>h</i> , in.	Gravity force ΣP , kips	Lateral load <i>V</i> , kips	Story shear ΣV_1 , kips	Lateral disp. <i>D</i> ₁ , in.	Story drift Δ ₁ , in.
10	144	180	30.22	30.22	7.996	0.517
9	144	396	21.94	52.17	7.479	0.736
8	144	612	19.57	71.74	6.743	0.785
7	144	828	17.20	88.93	5.958	0.907
6	144	1044	14.83	103.76	5.051	0.899
5	144	1260	12.45	116.21	4.152	0.914
4	144	1476	10.08	126.30	3.238	0.833
3	144	1692	7.71	134.01	2.400	0.867
2	144	1908	5.34	139.34	1.533	0.768
1	180	2124	2.97	142.31	0.765	0.765

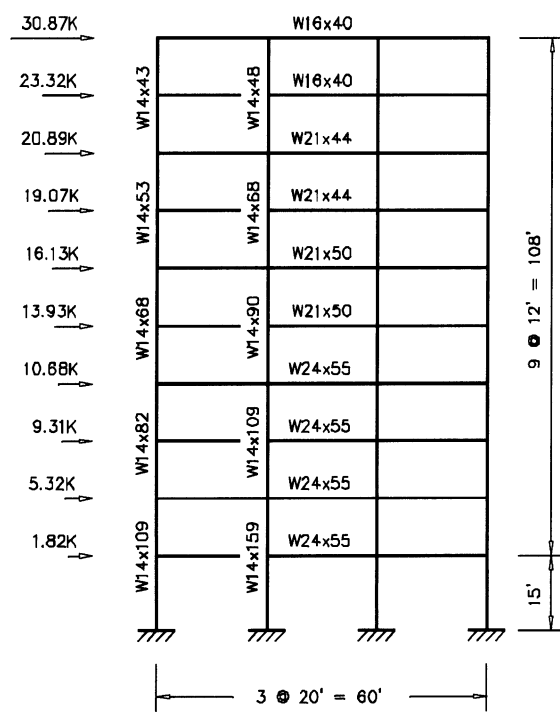


Figure 7-14. Elevation of the story moment frame used in Example 7-1.

shown in Table 7-1. The tributary width of the frame is 30 ft. The gravity load is 100 psf on the roof and 120 psf on typical floors. Use center-to-center dimensions.

The calculations for this example using the iterative P-delta method are presented in Tables 7-2 and 7-3. The convergence was achieved in two cycles of iteration. Table 7-3 also shows results obtained by an "exact" P-delta analysis.

To further explain the steps involved in the application of this method, let us consider the

bent at the 8th level of the frame. The story height (*h*) is 12 feet (144 in.), the total gravity force at this level (ΣP) is 612 kips, the story shear (ΣV) is 71.74 kips, and the first-order story drift is 0.785 inches (see Table 7-1).

The P-Delta Contribution to the story shear is:

$$\frac{(\Sigma P)\Delta_1}{h} = \frac{(612)(0.785)}{144} = 3.34 \text{ kips}$$

and the modified story shear is:

$$\begin{aligned}\Sigma V_2 &= \Sigma V_1 + (\Sigma P) \Delta_1 / h \\ &= 71.74 + 3.34 = 75.08 \text{ kips}\end{aligned}$$

Repeating this operation for all stories results in a modified set of story shears, from which a modified set of applied lateral forces is obtained (Table 7-2). A new first-order analysis of the frame subjected to these modified lateral forces results in a modified set of lateral displacements (D_2) and story drifts (Δ_2) as shown in Table 7-2. The maximum displacement obtained from the second analysis was 8.478 in., which is 9% larger than the original first-order displacement. Hence, a second iteration is necessary. Again performing the calculations for the bent at the 8th floor:

$$\frac{(\Sigma P)\Delta_2}{h} = \frac{(612)(0.823)}{144} = 3.50 \text{ kips}$$

$$\begin{aligned}\Sigma V_3 &= \Sigma V_2 + (\Sigma P) \Delta_2 / h \\ &= 71.74 + 3.50 = 75.24 \text{ kips}\end{aligned}$$

Another first-order analysis for the new set of lateral forces indicates a maximum displacement of 8.508 inches, which is less than

Table 7-2. Iterative P-delta method (First cycle of iteration)

Level	$(\Sigma P) \Delta_1 / h$, kips	$\Sigma V_1 + (\Sigma P) \Delta_1 / h$, kips	Modified lateral Force V_2 , kips	Modified lateral Disp. D_2 , in.	Modified story Drift Δ_2 , in.
10	0.65	30.87	30.87	8.478	0.533
9	2.02	54.19	23.32	7.945	0.767
8	3.34	75.08	20.89	7.178	0.823
7	5.22	94.15	19.07	6.355	0.959
6	6.52	110.28	16.13	5.396	0.955
5	8.00	124.21	13.93	4.441	0.976
4	8.59	134.89	10.68	3.465	0.897
3	10.19	144.20	9.31	2.568	0.930
2	10.18	149.52	5.32	1.638	0.823
1	9.03	151.34	1.82	0.815	0.815

Table 7-3. Iterative P-delta method (Second cycle of iteration)

Level	$(\Sigma P) \Delta_2 / h$, kips	$\Sigma V_2 + (\Sigma P) \Delta_2 / h$, kips	Modified lateral Force V_3 , kips	Modified lateral Disp. D_3 , in.	Modified story Drift Δ_3 , in.
10	0.67	30.89	30.89	8.508 (8.510)	0.534 (0.534)
9	2.11	54.28	23.39	7.975 (7.976)	0.768 (0.768)
8	3.50	75.24	20.96	7.207 (7.209)	0.825 (0.825)
7	5.51	94.44	19.20	6.382 (6.384)	0.962 (0.963)
6	6.92	110.68	16.24	5.419 (5.421)	0.959 (0.959)
5	8.54	124.75	14.07	4.461 (4.462)	0.980 (0.980)
4	9.19	135.49	10.74	3.480 (3.481)	0.900 (0.901)
3	10.93	144.94	9.45	2.580 (2.581)	0.935 (0.935)
2	10.90	150.24	5.30	1.645 (1.646)	0.827 (0.827)
1	9.62	151.93	1.69	0.818 (0.819)	0.818 (0.819)

* Values in parentheses represent results of an "exact" P-delta analysis.

1% larger than the displacements obtained in the previous iteration. Hence, the iteration was terminated at this point.

The first-order and second-order lateral displacements and story drifts are shown in Figures 7-15 and 7-16. As indicated by these figures, the results are virtually identical to the exact results.

Direct P-Delta Method The direct P-delta method⁽⁷⁻¹⁶⁾ is a simplification of the iterative method. Using this method, an estimate of final deflections is obtained directly from the first order deflections.

The simplification is based on the assumption that story drift at the i th level is proportional only to the applied story shear at that level (ΣV_i). This assumption allows the treatment of each level independent of the others.

If F is the drift caused by a unit lateral load at the i th level, then the first order drift Δ_1 is:

$$\Delta_1 = F \Sigma V_1 \quad (7-21)$$

After the first cycle of iteration,

$$\Delta_2 = F \Sigma V_2 = F(\Sigma V_1) \left(1 + (\Sigma P) \frac{F}{h} \right) \quad (7-22)$$

and after the i th cycle of iteration:

$$\begin{aligned} \Delta_{i+1} = F \Sigma V_i & \left[1 + \left((\Sigma P) \frac{F}{h} \right) + \left((\Sigma P) \frac{F}{h} \right)^2 \right. \\ & \left. + \dots + \left((\Sigma P) \frac{F}{h} \right)^i \right] \end{aligned} \quad (7-23)$$

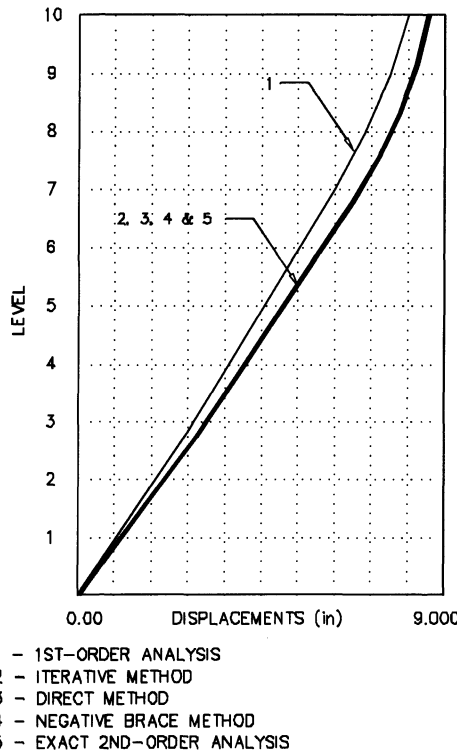


Figure 7-15. Lateral displacement of the 10-story frame as obtained by various P-delta methods.

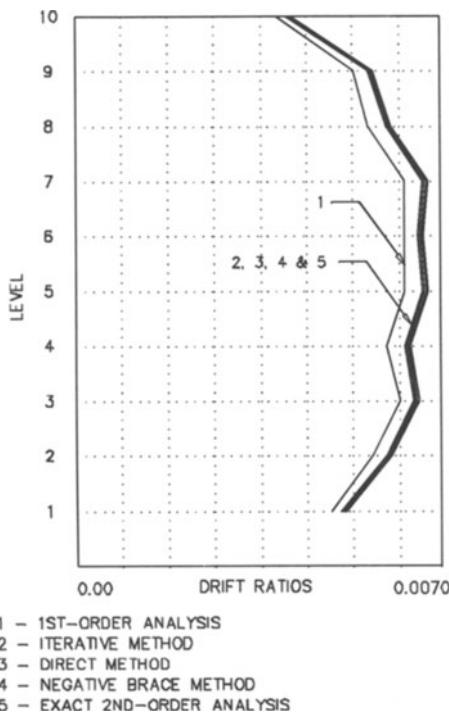


Figure 7-16. Story drift ratios of the 10 story frame as obtained by various P-delta methods.

Equation 7-23 is a geometric series that converges if $(\Sigma P) F/h < 1.0$, to

$$\Delta_{Final} = \frac{F \Sigma V_1}{1 - F_1(\Sigma P)/h} \quad (7-24)$$

But $F \Sigma V_1 = \Delta_1$. Hence, the final second-order deflection is:

$$\Delta_{Final} = \frac{\Delta_1}{1 - (\Sigma P)\Delta_1/(\Sigma V_1)h} \quad (7-25)$$

Equation 7-25 can be expressed as $\Delta_{Final} = \mu \Delta_1$, where $\mu = 1/[1 - (\Sigma P)\Delta_1/(\Sigma V_1)h]$ is a magnification factor by which the first-order effects should be multiplied to include the second-order effects. All internal forces and moments related to the lateral loads should also be magnified by μ . Member design may be carried out using an effective length factor of one.

An estimate of the critical load for an individual story, or the entire frame, can be obtained directly from Equation 7-25. Note that if $(\Sigma P)\Delta_1/(\Sigma V_1)h = 1$, the second-order displacement would go to infinity. Hence, $\Sigma P = (\Sigma V_1)h/\Delta_1$ may be considered to be the critical load of the system.

Similarly, $\Sigma(Pr^2) = \Sigma T_1 h/\theta_1$ can be viewed as the torsional critical load of the system. It is interesting to note that the critical loads and the magnification factor obtained here are in essence the same as those obtained in Section 7.4.2. by an approximate buckling analysis.

The term $(\Sigma P)\Delta_1/(\Sigma V_1)h$ is commonly referred to as the *stability index*. Similarly, a *torsional stability index* may be defined as $\Sigma(Pr^2)\theta_1/(\Sigma T_1 h)$.

It has been suggested⁽⁷⁻¹⁶⁾ that if the stability index is less than 0.0475 for all three axes of the building, the second-order effects can be ignored. For values of the stability index between 0.0475 and 0.20, the direct P-delta method can provide accurate estimates of the second-order effects. Designs for which values of the stability index exceed 0.20 should be avoided.

Table 7-4. P-delta analysis by direct P-delta method (Example 7-2)

Level	h , in	ΣV_1 , kips	ΣP , kips	Δ_1 , in.	μ	$\Delta_2 = \mu\Delta_1$, in.	2nd-Order Disp., in.
10	144	30.22	180	0.517	1.022	0.528	8.505
9	144	52.17	396	0.736	1.040	0.766	7.977
8	144	71.74	612	0.785	1.049	0.823	7.211
7	144	88.93	828	0.907	1.062	0.964	6.388
6	144	103.76	1044	0.899	1.067	0.959	5.424
5	144	116.21	1260	0.914	1.074	0.982	4.465
4	144	126.30	1476	0.838	1.073	0.899	3.483
3	144	134.01	1692	0.867	1.082	0.938	2.584
2	144	139.34	1908	0.768	1.079	0.829	1.646
1	180	142.31	2124	0.765	1.068	0.817	0.817

EXAMPLE 7-2

For the 10 story frame of Example 7-1 compute the second-order displacements and story drifts by the direct P-delta method.

The calculations using the direct P-delta method are shown in Table 7-4. For example, for the first floor which has a story height of 15 feet (180 inches), the story shear is 142.31 kips, the total gravity force is 2124 kips, and the first-order drift is 0.765 inches. The magnification factor and the second-order displacements are:

$$\mu = \frac{1}{1 - (2124)(0.765)/(142.31)(180)} = 1.068$$

$$\Delta_2 = \mu\Delta_1 = (1.068)(0.76) = 0.817 \text{ in.}$$

A comparison with the exact results (Figures 7-15 and 7-16) reveals the remarkable accuracy of this simple technique.

Negative Bracing Member Method The negative bracing member method^(7-16, 7-26, 7-27), which was first introduced by Nixon, Beaulieu and Adams⁽⁷⁻²⁷⁾, provides a direct estimate of the P-Delta effect via any standard first-order analysis program. Fictitious bracing members with negative areas are inserted (Figure 7-17) to model the stiffness reduction due to the P-delta effect.

The cross sectional area of the negative braces for each floor level can be obtained by a

simple analogy to the Hooke's law ($F = K\Delta$). The additional shear due to P-delta effect is $(\Sigma P)\Delta/h$, where ΣP is the total gravity force and h is the story height. The term $\Sigma P/h$ is a stiffness term but it is contributing to lateral displacement instead of resisting it. Hence, it can be considered as a negative stiffness. A brace with a cross sectional area A , a length L_{br} , modulus of elasticity E , making an angle α with the floor, provides a stiffness equal to $(AE\cos^2\alpha)/L_{br}$ against lateral displacement. By equating the brace stiffness to $-\Sigma P/h$, the required area of the equivalent negative brace is obtained:

$$A = -\frac{\Sigma P}{h} \frac{L_{br}}{E \cos^2 \alpha} \quad (7-26)$$

It is important to note that, due to the horizontal and vertical forces in the braces, the axial forces and shears in the columns will be slightly in error. These errors can be reduced by making the braces as long as possible (see Figure 7-17).

EXAMPLE 7-3

For the 10 story frame of Example 7-1, compute the second-order displacements and story drifts by the Negative Bracing Member Method. The modulus of elasticity of the braces is:

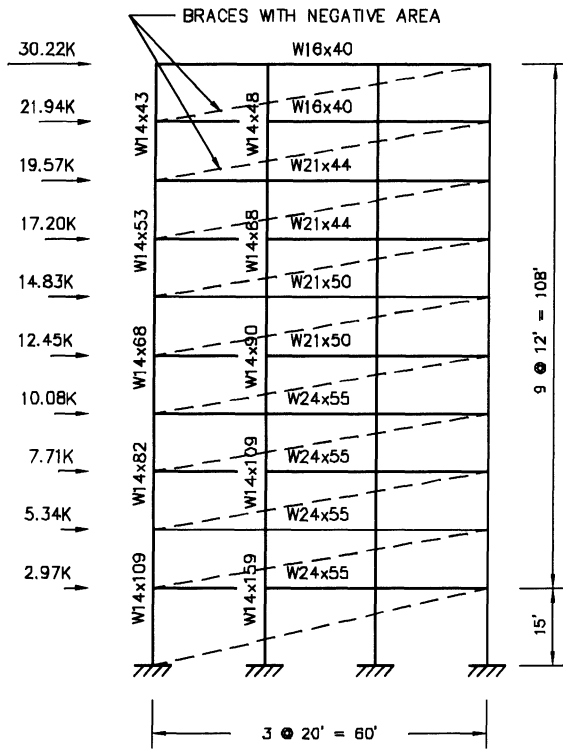


Figure 7-17. Frame modeled with negative braces.

$$E = 29,000. \text{Ksi}$$

For a typical floor,

$$L_{br} = \sqrt{(60)^2 + (15)^2} = 61.188 \text{ ft.}$$

$$\cos^2\alpha = (60/61.188)^2 = 0.9615$$

For the first floor,

$$L_{br} = \sqrt{(60)^2 + (15)^2} = 61.847 \text{ ft.}$$

$$\cos^2\alpha = (60/61.847)^2 = 0.9412$$

The negative brace area for each floor level may now be calculated using Equation 7-26. For example, for the fourth floor where the total gravity force is 1476 kips, the negative brace area is:

$$A_4 = -\frac{(1476)(734.26)}{(144)(29000)(0.9615)}$$

$$= -0.2699 \text{ in}^2$$

The brace areas, and the displacements obtained using the negative braces, are shown in Table 7-5. The very good agreement with the "exact" results (Table 7-3) is evident.

Modified Versions of Approximate P-delta Methods

The P-Delta methods presented in this chapter ignore the "C-S" effect (Figure 7-4d). For most practical problems, the C-S effects are much smaller than the P-delta effects, and can be ignored. However, if needed, the P-delta methods described in previous sections, can be simply modified to include this effect.

The modification is achieved by multiplying the member axial forces by a flexibility factor, γ . For a single column, γ is given by⁽⁷⁻²⁶⁾:

Table 7-5. P-delta analysis by negative-bracing-member method.

Level	h , in	ΣP , kips	L_{br} , in.	$E \cos^2\alpha$	A_{br} , in.	2nd-Order Disp., in.
10	144	180	734.26	27,884	-0.0329	8.458
9	144	396	734.26	27,884	-0.0724	7.929
8	144	612	734.26	27,884	-0.1120	7.168
7	144	828	734.26	27,884	-0.1514	6.350
6	144	1044	734.26	27,884	-0.1909	5.394
5	144	1260	734.26	27,884	-0.2341	4.442
4	144	1476	734.26	27,884	-0.2699	3.468
3	144	1692	734.26	27,884	-0.3094	2.572
2	144	1908	734.26	27,884	-0.3489	1.642
1	144	2124	742.16	27,295	-0.3209	0.817

$$\gamma = 1 + 0.22 \frac{4(G_A - G_B)^2 + (G_A + 3)(G_B + 2)}{[(G_A + 2)(G_B + 2) - 1]^2} \quad (7-27)$$

where G_A and G_B are the stiffness ratios as defined in Section 7.4.1. The flexibility factor γ has a rather small range of variation (from 1.0 for $G_A = G_B = \infty$, to 1.22 for $G_A = G_B = 0$). For design purposes a conservative average value of γ can be used for the entire frame. Lai and MacGregor⁽⁷⁻²⁶⁾ suggest an average value of $\gamma = 1.15$, while Stevens⁽⁷⁻¹⁰⁾ has proposed an average value of $\gamma = 1.11$.

To include the C-S effect in the previously discussed P-delta methods, it is sufficient to use $\gamma \Sigma P$ instead of ΣP wherever the term ΣP appears.

EXAMPLE 7-4

For the 10-story frame of Example 7-1, compute the second-order displacements and story drifts at the first, fifth, and the roof levels by the modified direct P-delta method. An average value of $\gamma = 1.11$ is assumed for all calculations.

Using the values listed in Table 7-4 we have:

- at the roof:

$$\frac{\gamma(\Sigma P)\Delta_1}{(\Sigma V_1)h} = \frac{(1.11)(180)(0.517)}{(30.22)(144)} = 0.024$$

$$\mu = \frac{1}{1 - 0.024} = 1.025$$

$$\Delta_2 = \mu\Delta_1 = (1.025)(0.517) = 0.530 \text{ in.}$$

- at the fifth level:

$$\frac{\gamma(\Sigma P)\Delta_1}{(\Sigma V_1)h} = \frac{(1.11)(1260)(0.914)}{(116.21)(144)} = 0.076$$

$$\mu = \frac{1}{1 - 0.076} = 1.082$$

$$\Delta_2 = \mu\Delta_1 = (1.082)(0.914) = 0.989 \text{ in.}$$

- and at the first level:

$$\frac{\gamma(\Sigma P)\Delta_1}{(\Sigma V_1)h} = \frac{(1.11)(2124)(0.765)}{(142.31)(180)} = 0.070$$

$$\mu = \frac{1}{1 - 0.070} = 1.075$$

$$\Delta_2 = \mu\Delta_1 = (1.075)(0.765) = 0.822 \text{ in.}$$

Comparison of these results with those obtained by the original method reveals an increase of less than 1% in the story drifts due to this modification.

7.4.4 "Exact" P-Delta Analysis

Construction of the geometric stiffness matrix is the backbone of any exact second-order analysis. The same matrix is also essential for any finite element buckling analysis procedure. In this section, the concept of geometric stiffness matrix is introduced, and a general approach to "exact" second-order structural analysis is discussed.

Consider the deformed column shown in Figure 7-18. For the sake of simplicity, neglect the axial deformation of the member, and the small C-S effect. The slope deflection equations for this column can be written as⁽⁷⁻¹²⁾

$$M_t = \frac{EI}{L} \left(4\theta_t + 2\theta_b - \frac{6\Delta_t}{L} + \frac{6\Delta_b}{L} \right) \quad (7-28)$$

$$M_b = \frac{EI}{L} \left(2\theta_t + 4\theta_b - \frac{6\Delta_t}{L} + \frac{6\Delta_b}{L} \right) \quad (7-29)$$

From force equilibrium:

$$F_t = -\frac{M_t + M_b}{L} - \frac{P(\Delta_t - \Delta_b)}{L} \quad (7-30)$$

$$F_b = -F_t \quad (7-31)$$

Substituting Equations 7-28 and 7-29 into Equation 7-30:

$$F_t = -\frac{6EI}{L^2}(\theta_t + \theta_b) + 12\left(\frac{EI}{L^3} - \frac{P}{L}\right)(\Delta_t - \Delta_b) \quad (7-32)$$

Now if we rewrite the above equations in a matrix form, we obtain:

$$\begin{bmatrix} M_t \\ M_b \\ F_t \\ F_b \end{bmatrix} = \begin{bmatrix} \frac{4EI}{L} & \frac{2EI}{L} & -\frac{6EI}{L^2} & \frac{6EI}{L^2} \\ \frac{2EI}{L} & \frac{4EI}{L} & -\frac{6EI}{L^2} & \frac{6EI}{L^2} \\ -\frac{6EI}{L^2} & -\frac{6EI}{L^2} & \frac{12EI}{L^3} - \frac{P}{L} & -\frac{12EI}{L^3} + \frac{P}{L} \\ \frac{6EI}{L^2} & \frac{6EI}{L^2} & -\frac{12EI}{L^3} + \frac{P}{L} & \frac{12EI}{L^3} - \frac{P}{L} \end{bmatrix} \begin{bmatrix} \theta_t \\ \theta_b \\ \Delta_t \\ \Delta_b \end{bmatrix} \quad (7-33)$$

Since we wrote the equilibrium equations for the deformed shape of the member, this is a second-order stiffness matrix. Notice that the only difference between this matrix, and a standard first-order beam stiffness matrix, is the presence of P/L or geometric terms. The stiffness matrix given by Equation 7-33 can also be written as:

$$[K] = [K_f] - [K_g] \quad (7-34)$$

where $[K_f]$ is the standard first-order stiffness matrix (material matrix) and $[K_g]$ is the geometric stiffness matrix given by:

$$\begin{bmatrix} 0 & 0 & 0 & 0 \\ 0 & 0 & 0 & 0 \\ 0 & 0 & +P/L & -P/L \\ 0 & 0 & -P/L & +P/L \end{bmatrix}$$

Inspection of the simple second-order stiffness matrix given by Equation 7-33 shows why general second-order structural analysis

has an iterative nature. The matrix includes P/L terms, but the axial force P is not known before an analysis is performed. For the first analysis cycle, P can be assumed to be zero (standard first-order analysis). In each subsequent analysis cycle, the member forces obtained from the previous cycle are used to form a new geometric stiffness matrix, and the analysis continues until convergence is achieved. If inelastic material behavior is to be considered, then the material stiffness matrix must also be revised at appropriate steps in the analysis.

Substantial research has been performed on the formulation of geometric stiffness matrices and finite element stability analysis of structures^(7-28,7-36). A complete formulation of the three-dimensional geometric stiffness matrix for wide flange beam-columns has been proposed by Yang and McGuire⁽⁷⁻³⁶⁾.

The common assumption that floor diaphragms are rigid in their own plane, allows condensation of lateral degrees of freedom into three degrees of freedom per floor level: two horizontal translations and a rotation about the vertical axis. This simplification significantly reduces the effort required for an "exact" second-order analysis. A number of schemes have been developed to permit direct and non-iterative inclusion of P-Delta effects in the analysis of rigid-diaphragm buildings^(7-37, 7-38, 7-39).

The geometric stiffness matrix for a three dimensional rigid diaphragm building is given in Figure 7-19^(7-37, 7-38). For a three-dimensional building with N floor levels, $[K_g]$ is a $3N \times 3N$ matrix. For planar frames, the matrix reduces to an $N \times N$ tridiagonal matrix. The non-zero terms of this matrix are given by:

$$\alpha_i = \frac{(\Sigma P)_i}{h_i} + \frac{(\Sigma P)_{i+1}}{h_{i+1}} \quad (7-35)$$

$$\beta_i = \frac{(\Sigma T)_i}{h_i} + \frac{(\Sigma T)_{i+1}}{h_{i+1}} \quad (7-36)$$

$$\eta_i = -\frac{(\Sigma P)_i}{h_i} \quad (7-37)$$

$$\lambda_i = -\frac{(\Sigma T)_i}{h_i} \quad (7-38)$$

Figure 7-18. Geometric stiffness matrix for three-dimensional rigid diaphragm buildings.

where h_i is the floor height for level i , P_i is weight of the i th level, T_i is the second-order story torque, and

$$(\Sigma P)_i = \sum_{j=i}^n P_j \quad (7-39)$$

$$(\Sigma T)_i = \sum_{j=i}^n T_j \quad (7-40)$$

$(\Sigma P)_i$ can also be represented in terms of story mass, m_i , and gravitational acceleration, g , as

$$(\Sigma P)_i = \left(\sum_{j=i}^n m_j \right) \times g \quad (7-41)$$

The story torque, T_i , is given by⁽⁷⁻³⁸⁾

$$T_i = \left(\sum_{j=i}^n p_j d_j^2 \right) \frac{\theta}{h_i} \quad (7-42)$$

where p_j is the vertical force carried by the j th column, d_j is the distance of j th column from the center of rotation of the floor, and θ is an

imposed unit rigid body rotation of the floor. Assuming that the dead load is evenly distributed over the floor and that a roughly uniform vertical support system is provided over the plan area of the floor, Equation 7-42 can be further simplified to

$$T_i = m_{Ri} \frac{g}{h_i} \quad (7-43)$$

where m_{Ri} is the rotational mass moment of inertia of the i th floor and g is the gravitational acceleration. The approximation involved in the derivation of Equation 7-43 is usually insignificant⁽⁷⁻³⁹⁾. Hence, for most practical problems, Equation 7-43 can be used instead of Equation 7-42, thereby allowing the direct inclusion of the P-delta effect in a three dimensional structural analysis.

7.4.5 Choice of Member Stiffnesses for Drift and P-Delta Analysis

A common difficulty in seismic analysis of reinforced concrete structures is the selection of a set of rational stiffness values to be used in force and displacement analyses. Should one use gross concrete section properties? Should one use some reduced section properties? Or should the gross concrete properties be used for one type of analysis and reduced section properties be used for another type of analysis?

The seismic design codes in the United States are not specific about this matter. Hence, the choice of section properties used in lateral analysis in general, and seismic analysis in particular, varies widely.

Contributing to the complexity of this issue, are the following factors:

1. Although elastic material behavior is usually assumed for the sake of simplicity, reinforced concrete is not a homogeneous, linearly elastic material.
2. Stiffness and idealized elastic material properties of a reinforced concrete section vary with the state of behavior of the section (e.g. uncracked, cracked and ultimate states).

3. Not all reinforced concrete members in a structure, and not all cross sections along a particular member, are in the same state of behavior at the same time.
4. For many beams and other non-symmetrically reinforced members, the stiffness properties for positive bending and negative bending are different.
5. Stiffness of reinforced concrete members and structures varies with the time, and with the history of past exposure to wind forces and earthquake ground motions.
6. Stiffness of reinforced concrete members and structures varies with the amplitude of the applied forces.

Analytical and experimental studies⁽⁷⁻⁴⁰⁾ have indicated that for motions which are within the working stress design limits of members, the measured fundamental periods of concrete structures are generally slightly less than the periods computed using gross concrete section properties. According to Reference 7-40, in the case of large amplitude motions up to the yield level, the stiffness of the building is usually somewhere between the computed values based on the gross concrete section properties and the cracked section properties. Based on this observation, the same reference suggests that for force analysis, the gross concrete section properties and the clear span dimensions be used and the effect of nonseismic structural and nonstructural elements be considered. For drift calculations, either the lateral displacements determined using the above assumptions should be doubled or the center to center dimensions along with the average of the gross section and the cracked section properties, or one half of the gross section properties should be used. Furthermore, the nonseismic structural and nonstructural elements should be neglected, if they do not create a potential torsional reaction.

Similar sets of assumptions have been proposed by research workers who have been concerned about the choice of member stiffnesses to be used in the P-delta analysis of concrete structures. For example, for second-order analysis of concrete structures subjected

to combinations of gravity and wind loads, MacGregor and Hage⁽⁷⁻¹⁶⁾ recommend using 40% of the gross section moment of inertia for beams and 80% of the gross section moment of inertia for columns. See Chapter 15 for more information on this subject.

7.5 DRIFT DESIGN PROCEDURES

7.5.1 Drift Design of Moment Frames and Framed Tubes

The lateral displacements and story drifts of moment resistant frames and symmetrical framed tubes are caused by bent action, cantilever action, the shear leak effect, and panel zone distortions. With the simplified methods presented in this section, the contribution of each of these actions to the story drift can be estimated separately. The story drifts so obtained are then added to obtain an estimate of the total story drift. Once an estimate of the drift and the extent of the contribution of each of these actions to the total drift are known, proper corrective measures can be adopted to reduce story drifts to an acceptable level.

Bent Displacements A significant portion of drift in rigid frames and framed tubes is caused by end rotations of beams and columns (Figure 7-20). This phenomenon is commonly referred to as *bent action* (also called frame action, or racking). For most typical low to mid-rise rigid frames, almost all of the drift is caused by the bent action. However, for taller frames, other actions such as axial deformation of columns (cantilever or chord action) become more significant. For extremely tall frames, the contribution of cantilever action to drift may be several times larger than that of the bent action.

In the design of framed tubes, it is usually desirable to limit the bent action drifts to 30 to 40% of the total drift. If a framed tube is also braced, the bent action drifts are usually limited to about 20 to 25% of the total drift⁽⁷⁻¹⁾. The

bent action drift Δ_{bi} for any level i of a frame, may be estimated by⁽⁷⁻⁴¹⁾:

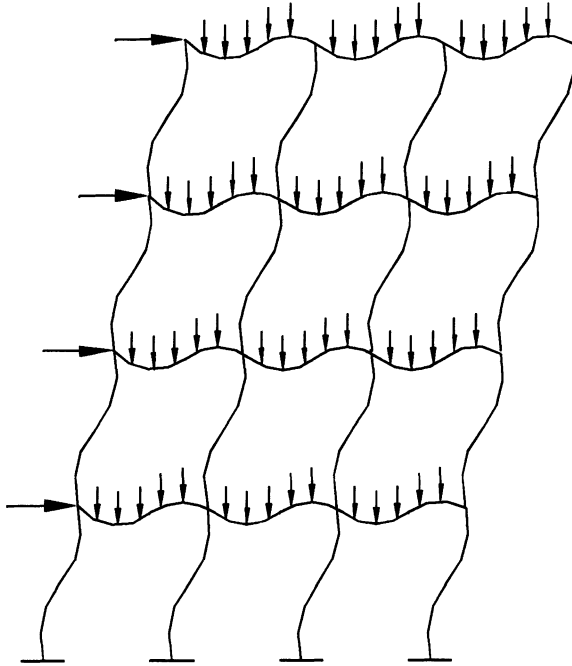


Figure 7-19. Frame deformation caused by the bent action.

$$\Delta_{bi} = \frac{(\Sigma V)_i h_i^2}{12E} \left(\frac{1}{(\Sigma K_g)_i} + \frac{1}{(\Sigma K_c)_i} \right) \quad (7-44)$$

where $(\Sigma V)_i$ is the story shear, h_i is the story height ^b, and

$(\Sigma K_g)_i$ = summation of I_{gi}/L_{gi} for all girders

$(\Sigma K_c)_i$ = summation of I_{ci}/h_i for all columns

I_{gi} = individual girder moment of inertia

L_{gi} = individual bay length

I_{ci} = individual column moment of inertia

Equation 7-44 can be derived by applying the slope deflection equations to the typical subassemblage shown in Figure 7-21. In the derivation of Equation 7-44, it is assumed that the points of contraflexure are at the mid-span of beams and columns.

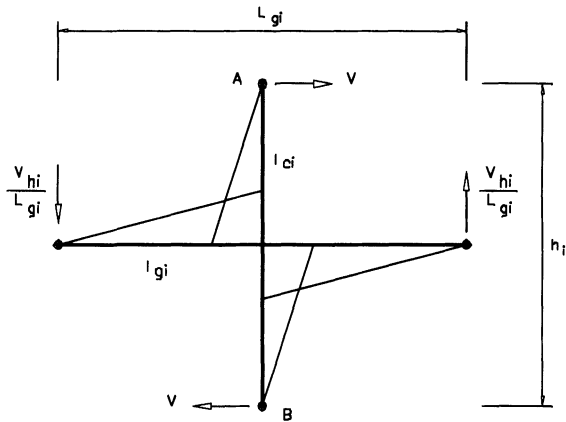


Figure 7-20. Typical subassemblage used in derivation of the bent action drift equation (7-41).

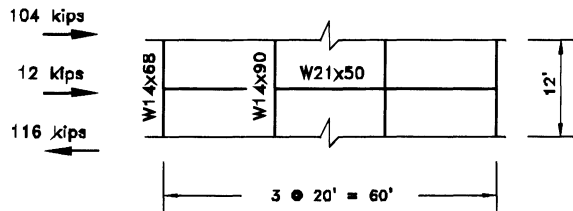


Figure 7-21. The bent at the 5th floor (Example 7-5).

Other, but similar, relationships for bent drift design have been proposed^(7-42, 7-43). Equation 7-44 can also be used to modify existing beam and column sizes to satisfy a given drift limit. Example 7-5 illustrates such an application.

EXAMPLE 7-5

For the bent at the 5th floor of the 10-story frame of Example 7-1 (Figure 7-22), estimate the story drift caused by bent action. Modify member sizes, if necessary, to limit the bent drift ratio to 0.0030. Neglect the P-delta effect.

W14x68

$I_{cl} = 723 \text{ in}^4$

W14x90

$I_{c2} = 999 \text{ in}^4$

W21x50

$I_g = 984 \text{ in}^4$

$$\sum \left(\frac{I_g}{L_g} \right) = \frac{(3)(984)}{(12)(20)} = 12.30 \text{ in}^3$$

^b Depending on the modeling assumption, center-to-center length, clear length, or something in between may be used.

$$\sum \left(\frac{I_c}{h} \right) = \frac{(2)(723+999)}{(144)} = 23.92 \text{ in.}^3$$

$$\Delta_{bi} = \frac{116(144)^2}{(12)(29000)} \left(\frac{1}{12.3} + \frac{1}{23.92} \right) = 0.85 \text{ in.}$$

$$\delta_{bi} = \frac{0.85}{144} = 0.0059 > 0.0030 \text{ N.G.}$$

1. Increasing both beam and column sizes:

$$\Delta_{\text{Limit}} = (0.0030)(144) = 0.432 \text{ in.}$$

$$\Delta_{\text{Limit}} = \frac{\Delta_{bi}}{\Phi} \text{ or } 0.432 = \frac{0.85}{\Phi} \rightarrow \Phi = 1.97$$

Select new beam and column sizes:

$$I_{c1} = (1.97)(723) = 1424 \text{ in.}^4 \rightarrow \text{use W14} \times 120 : I = 1380 \text{ in.}^4$$

$$I_{c2} = (1.97)(999) = 1968 \text{ in.}^4 \rightarrow \text{use W14} \times 176 : I = 2140 \text{ in.}^4$$

$$I_g = (1.97)(984) = 1938 \text{ in.}^4 \rightarrow \text{use W24} \times 76 : I = 2100 \text{ in.}^4$$

Check the new bent drift:

$$\sum \left(\frac{I_g}{L_g} \right) = \frac{(3)(2100)}{240} = 26.25 \text{ in.}^3$$

$$\sum \left(\frac{I_c}{h} \right) = \frac{(2)(1380+2140)}{144} = 48.89 \text{ in.}^3$$

$$\Delta_{bi} = 6.912 \left(\frac{1}{26.25} + \frac{1}{48.89} \right) = 0.405 \text{ in.} < 0.432 \text{ in. O.K.}$$

Additional member weight required for drift control:

$$W = 3(76-50)(20) + 2(176+120-68-90)(12) = 4872 \text{ lb}$$

2. Increasing beam sizes only:

$$0.432 = 6.912 \left(\frac{1}{12.3\Phi_g} + \frac{1}{23.92} \right) \rightarrow \Phi_g = 3.93 \\ I_g = (3.93)(984) = 3867 \text{ in.}^4 \rightarrow \text{use W30} \times 99 : I = 3990 \text{ in.}^4$$

Check the new bent drift:

$$\sum \left(\frac{I_g}{L_g} \right) = \frac{(3)(3990)}{240} = 49.9 \text{ in.}^3 \\ \Delta_{bi} = 6.912 \left(\frac{1}{49.9} + \frac{1}{23.92} \right) = 0.427 \text{ in.} < 0.432 \text{ in. O.K.}$$

Additional member weight required for drift control:

$$W = 3(99-50)(20) = 2940 \text{ lb}$$

3. Increasing column sizes only:

$$0.432 = 6.912 \left(\frac{1}{12.3} + \frac{1}{23.92\Phi_c} \right) \rightarrow \Phi_c < 0.$$

Therefore, bent drift control by increasing column sizes only is not feasible.

In this case, drift control by increasing beam sizes only, requires less material. However, in general, one should be careful about increasing beam sizes alone, since it can jeopardize the desirable strong column-weak girder behavior.

Cantilever Displacements In tall frames and tubes, there is significant axial deformation in the columns caused by the overturning moments. The distribution of axial forces among the columns due to the overturning moments is very similar to distribution of flexural stresses in a cantilever beam. The overturning moments cause larger axial forces and deformations on the columns which are

farther from the center line of the frame. This action, which causes a lateral deformation that closely resembles the deformation of a cantilever beam (Figure 7-23), is called the cantilever or chord action. In a properly proportioned framed tube, the cantilever deflections are significantly smaller than a similar rigid frame. As shown in Figure 7-24, this is due to the participation of some of the columns in the flange frames in resistance to cantilever deformations. The taller the framed tube, the closer the column spacings, and the stronger the spandrel girders, the more significant the tube action becomes.

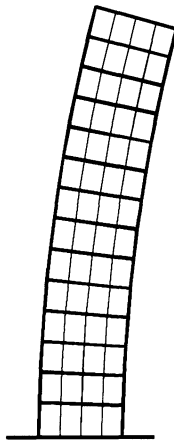


Figure 7-22. Cantilever or chord deformation.

Cantilever displacements may be estimated by simple application of the moment-area method. The moment of inertia for an equivalent cantilever beam is computed as:

$$I_{0i} = \sum (A_{ci} d_i^2) \quad (7-45)$$

where A_{ci} is cross sectional area of an individual column and d_i is its distance from the center-line of the frame. The summation is carried over all the columns of the web frames, and those columns of the flange frames which are believed to participate in resistance to cantilever deflections. The computation of cantilever displacements for each floor level can be summarized in the following steps.

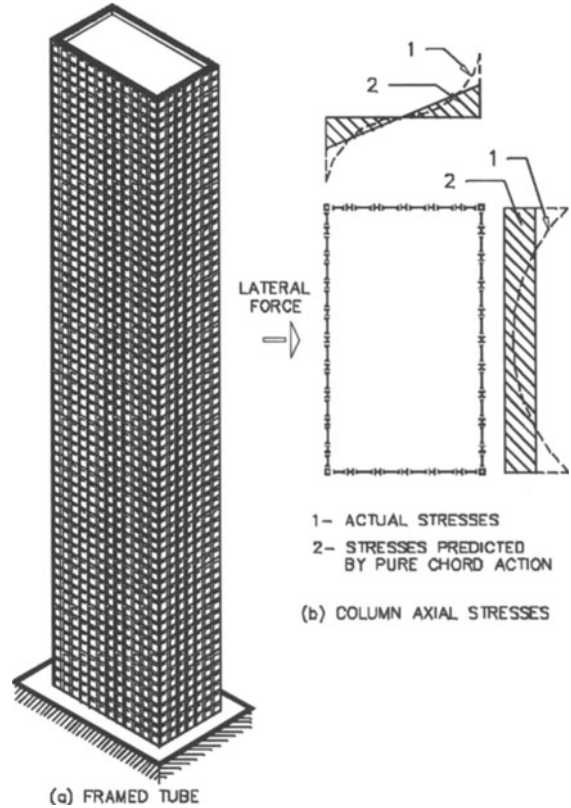


Figure 7-23. Tube action in response to lateral loads.

Step 1- Compute story moment of inertia I_{oi} using Equation 7-45.

Step 2- Compute overturning moments M_i .

Step 3- Compute Area under the M/EI_{oi} from:

$$A_i = \frac{(M_i + M_{i+1})h_i}{2EI_{0i}} \quad (7-46)$$

Step 4- Compute \bar{x}_i (see Figure 7-25) from:

$$\bar{x}_i = \frac{h_i M_i + 2M_{i+1}}{3 M_i + M_{i+1}} \quad (7-47)$$

Step 5- Compute story displacement from:

$$\Delta_{ci} = A_i(h_i - \bar{x}_i) + \sum_{j=1}^{i-1} A_j(H_i - \bar{x}_j) \quad (7-48)$$

where H_i is the total height of the i th floor measured from the base of the structure.

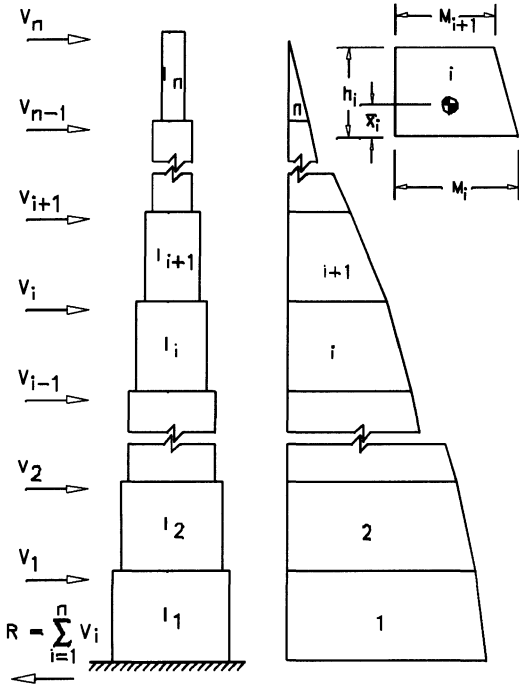


Figure 7-24. Estimating cantilever displacements by the moment-area method.

EXAMPLE 7-6

Use the moment-area method and the procedure explained in this section to compute displacements at points 1, 2 and 3 of the simple cantilever column shown in Figure 7-26. Assume $EI = 58 \times 10^6$, kips-in 2

Overshooting moments:

$$M_3 = 0.$$

$$M_2 = (100)(60) = 6000 \text{ in.-kips}$$

$$M_1 = (100)(120) = 12000 \text{ in.-kips}$$

$$M_0 = (100)(180) = 18000 \text{ in.-kips}$$

Area under M/EI curve:

$$A_0 = 0.$$

$$A_1 = \frac{(18,000 + 12,000)(60)}{(2)(58 \times 10^6)} = 0.01552$$

$$A_2 = \frac{(12,000 + 6000)(60)}{(2)(58 \times 10^6)} = 0.00931$$

$$A_3 = \frac{(6000 + 0)(60)}{(2)(58 \times 10^6)} = 0.00310$$

\bar{x}_i distances:

$$\bar{x}_0 = 0$$

$$\bar{x}_1 = \frac{(20)(18,000 + 24,000)}{18,000 + 12,000} = 28.00 \text{ in.}$$

$$\bar{x}_2 = \frac{(20)(12,000 + 12,000)}{12,000 + 6000} = 26.67 \text{ in.}$$

$$\bar{x}_3 = \frac{(20)(6000 + 0)}{6000 + 0} = 20.00 \text{ in.}$$

Displacements:

$$\Delta_1 = 0.01552(60 - 28) = 0.497 \text{ in.}$$

$$\Delta_2 = 0.01552(120 - 28) +$$

$$0.00931(60 - 26.67) = 1.738 \text{ in.}$$

$$\Delta_3 = 0.01552(180 - 28) +$$

$$0.00931(120 - 26.67) + 0.00310(60 - 20)$$

$$= 3.352 \text{ in.}$$

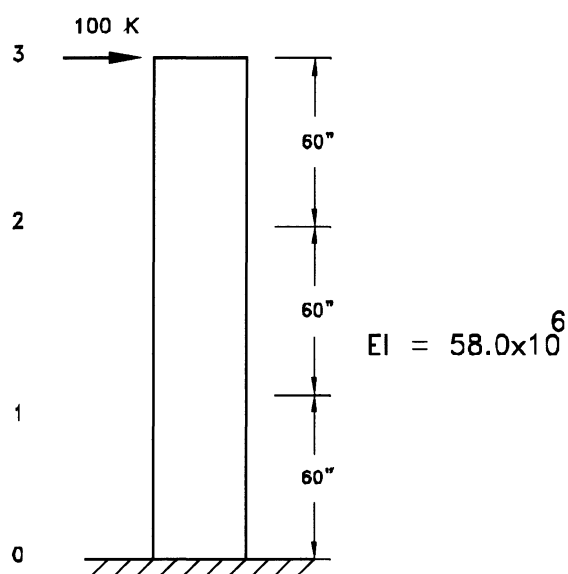


Figure 7-25. Cantilever column of example 7-6.

Shear Leak Displacements In buildings with closely spaced columns and deep girders, such as framed tubes, the contribution of shearing deformations to the lateral displacements (called the shear leak effect) may be significant. Story drifts due to the shear leak effect at level i , Δ_{shi} , may be estimated as⁽⁷⁻⁴¹⁾

$$\Delta_{shi} = \frac{\sum V_i h_i^2}{G} \left(\frac{1}{\sum A'_{gi} L_{gi}} + \frac{1}{\sum A'_{ci} h_i} \right) \quad (7-49)$$

where G is the shear modulus and A'_{gi} and A'_{ci} are the shear areas of individual girders and columns at level i .

In order to simplify the design process, an effective moment of inertia, I_{eff} , can be defined where the contributions of both flexural and shearing deformations are considered

$$I_{eff} = \frac{A'L^2 I}{24(1+\nu)I + A'L^2} \quad (7-50)$$

where A' is the shear area, L is span length, I is the moment of Inertia of the section, and ν is Poisson's ratio.

EXAMPLE 7-7

For the bent of Example 7-5, estimate the additional story drift caused by the shear leak effect.

We have

$$W14 \times 68: A' = dt_w = (14.00)(0.415) = 5.83 \text{ in.}^2$$

$$W14 \times 90: A' = dt_w = (14.02)(0.440) = 6.17 \text{ in.}^2$$

$$W21 \times 50: A' = dt_w = (20.83)(0.380) = 7.92 \text{ in.}^2$$

$$\Sigma A'_{gi} L_i = (3)(7.92)(240) = 5702.4$$

$$\Sigma A'_{ci} h_i = (2)(6.17 + 5.83)(144) = 3456.0$$

Using Equation 7-49:

$$\Delta_{shi} = \frac{116(144)^2}{11,200} \left(\frac{1}{5702.4} + \frac{1}{3456.0} \right) = 0.10 \text{ in.}$$

Panel Zone Distortions When joint shear forces are high, and the beam-column panel zones are not adequately stiffened, panel zone distortions can have a measurable impact on the story drift. The panel zone force-deformation behavior is complex and nonlinear. Currently, there is no real consensus among researchers on appropriateness of various design-oriented approaches to this problem.

Cheong-Siat-Moy⁽⁷⁻⁴⁴⁾ has recommended a simple method based on elastic theory to estimate this effect. The method assumes a linear relationship between the shearing forces

and the panel zone distortions. It also assumes a uniform distribution of shear stress throughout the panel zone.

A simple beam-column subassemblage and the corresponding force and displacement diagrams, as assumed by this method, are shown in Figure 7-27. It can be shown that the deformation angle γ and the additional lateral story drift due to panel zone distortion, Δ_p , are:

$$\gamma = \frac{2(M_c / d_g) - V}{Gtd_c} \quad (7-51)$$

$$\Delta_p = \frac{\gamma(h - d_g)}{2} \quad (7-52)$$

where M_c is the moment from one column, d_g is the girder depth, V is the column shear, G is the shear modulus, t is the panel zone thickness, d_c is the column depth, and h is the story height. Hence, $(h - d_g)$ is the clear column height.

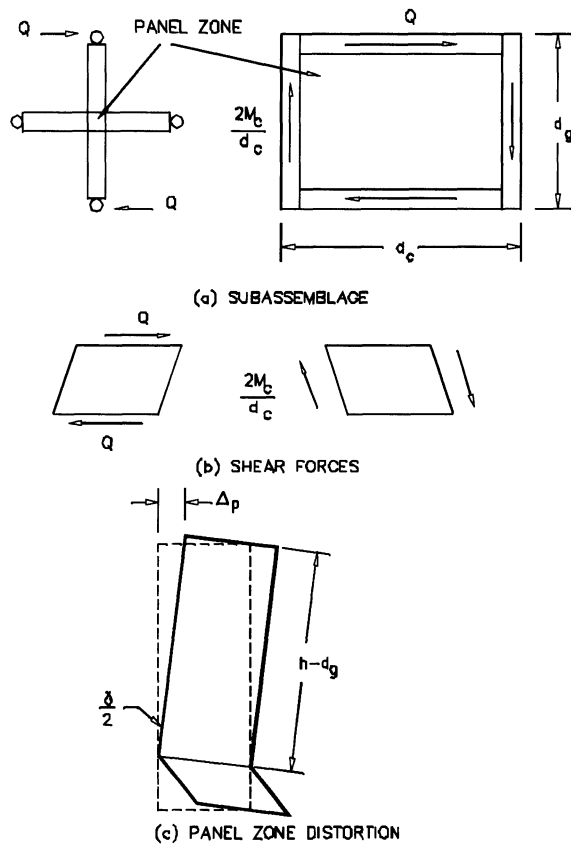


Figure 7-26. Effect of panel zone deformation⁽⁷⁻⁴⁴⁾

If the points of contraflexure are assumed to be at mid-span of the beams and columns, Equation 7-51 can be further simplified to:

$$\gamma = V \frac{(h/d_g) - 2}{Gtd_c} \quad (7-53)$$

Considering the approximate nature of the above formula, it is not necessary to apply it to each individual column. Instead, it can be used in an average sense (see Example 7-8).

A series of experimental and analytical studies on the behavior of steel beam-column panel zones have been conducted by various research institutions^(7-45,7-46,7-47,7-48). In one of these studies⁽⁷⁻⁴⁸⁾, conducted at Lehigh University, several beam-column subassemblage specimens were subjected to cyclic loads far beyond their elastic limits. Based on these tests a formula, similar to Equation 7-53, for estimation of panel zone distortions was recommended:

$$\gamma = \frac{V}{Gd_c t} \left(\frac{L_c}{d_g} - \frac{L}{h} \right) \quad (7-54)$$

where L is the beam span length, L_c is clear column length, G is the shear modulus which is taken as 11,000 ksi, and γ is the panel zone distortion in radians.

There is a serious need for further research on the seismic behavior of beam-column panel zones.

EXAMPLE 7-8

For the bent of Example 7-5, estimate the contribution of panel zone distortion to story drift assuming two conditions: a) No doubler plates, and b) $1/4$ -in. doubler plates.

$$\begin{aligned} W14 \times 68 & \quad d = 14.04 \text{ in} \quad t = 0.450 \text{ in} \\ W14 \times 90 & \quad d = 14.02 \text{ in} \quad t = 0.440 \text{ in} \\ W21 \times 50 & \quad dg = 20.83 \text{ in} \end{aligned}$$

Using Cheong-Siat Moy method (Equations 7-52 and 7-53), we have

$$\gamma = V \frac{h/d_g - 2}{Gtd_c}$$

without doubler plates:

$$\text{Average } t = 2 \frac{0.450 + 0.440}{4} = 0.445 \text{ in.}$$

$$\text{Average } V = 116/4 = 29 \text{ kips}$$

$$\gamma = 29 \frac{144/20.83 - 2}{(11200)(0.445)(14.03)} = 0.0020$$

$$\begin{aligned} \Delta_p &= \gamma \frac{h - d_g}{2} = 0.0010(144 - 20.83) \\ &= 0.123 \text{ in.} \end{aligned}$$

with doubler plates:

$$\text{Average } t = 0.445 + 0.25 = 0.695 \text{ in}$$

$$\Delta_p = 0.0013 \frac{144 - 20.83}{2} = 0.080 \text{ in.}$$

Using Lehigh's formula (Equation 7-54):

$$\gamma = \frac{V}{Gd_c t} \left(\frac{L_c}{d_g} - \frac{L}{h} \right)$$

$$L_c = 144 - 20.83 = 123.17 \text{ in}$$

$$L = 12(20) = 240 \text{ in}$$

without doubler plates:

$$t = 0.445 \text{ in}$$

$$\begin{aligned} \gamma &= \frac{(29)(123.17/20.83 - 240/144)}{(11000)(14.03)(0.445)} = \\ &0.00179 \text{ rad.} \end{aligned}$$

$$\Delta_p = (0.00179)(144 - 20.83)/2 = 0.110 \text{ in.}$$

with doubler plates:

$$t = 0.695 \text{ in.}$$

$$\gamma = \frac{(0.00179)(0.445)}{0.695} = 0.00115 \text{ rad.}$$

$$\Delta_p = (0.110)(0.00115)/(0.00179) = 0.071 \text{ in.}$$

Table 7-6. Calculation of bent-action story drifts and lateral displacements for the 10-story unbraced frame

Level	h, in.	ΣV , kips	$\Sigma(I_g/L_g)$, in. ³	$\Sigma(I_o/h)$, in. ³	Δ_{bi} , in. (Eq. 7-44)	Bent Disp., in.
10	144	30.22	6.475	12.68	0.420	6.802
9	144	52.17	6.475	12.68	0.725	6.382
8	144	71.74	10.538	17.56	0.649	5.657
7	144	88.93	10.538	17.56	0.805	5.001
6	144	103.76	12.300	23.92	0.761	4.203
5	144	116.21	12.300	23.92	0.856	3.442
4	144	126.30	16.875	29.47	0.701	2.588
3	144	134.01	16.875	29.47	0.744	1.877
2	144	139.34	16.875	43.61	0.682	1.143
1	180	142.31	16.875	52.33*	0.461	0.461

* Two-thirds of the first story height was used in calculation of the bent-action drift.

Table 7-7. Calculation of shear-leak story drifts and lateral displacements for the 10-story unbraced frame.

Level	h, in.	ΣP , kips	$\Sigma(A_g L_g)$, in. ³	$\Sigma(A_c h)$, in. ³	Δ_{sh} , in. (Eq. 7-44)	Bent Disp., In.
10	144	30.22	3516	2550	0.0379	0.8377
9	144	52.17	3516	2550	0.0653	0.7998
8	144	71.74	5206	3161	0.0675	0.7345
7	144	88.93	5206	3161	0.0837	0.6670
6	144	103.76	5999	3455	0.0893	0.5833
5	144	116.21	5999	3455	0.1000	0.4940
4	144	126.30	6703	4267	0.0897	0.3939
3	144	134.01	6703	4267	0.0951	0.3042
2	144	139.34	6703	5379	0.0864	0.2091
1	180	142.31	6703	5379	0.1226	0.1226

Drift Design of a 10 Story Moment Resistant Frame

In this subsection the approximate methods for drift and P-delta analysis which were explained previously, are put into practice by performing a complete drift design for the 10-story moment resistant steel frame introduced in Example 7-1. The goal is to achieve an economical design that meets the story drift index limitation of 0.0033.

The first step is to estimate the lateral displacements and story drifts of the structure. Calculations of story drifts and lateral displacements due to bent action, the shear leak effect, and chord action are presented in Tables 7-6, 7-7 and 7-8 respectively. It was demonstrated in Example 7-8 that the contribution of panel zone deformations to story drifts for this structure, at the level of forces considered here, is not significant.

Therefore, this effect is ignored in subsequent analyses.

The total displacements and story drifts are magnified using the direct P-delta Method. These calculations are shown in Table 7-9. Notice that in sizing the members for strength, all lateral load related forces and moments should also be multiplied by the corresponding story magnification factors (see μ in Table 7-9). Once the internal forces are thus magnified, it is rational to design the members using an equivalent length factor of one.

Figures 7-28 and 7-29 depict the contribution of each action to the total lateral displacement and story drift. The dominance of bent action in the lateral response of this frame can be clearly seen in these figures. As explained previously, if the frame was significantly taller, bent action would be

Table 7-8. Calculation of chord-action and lateral displacements for the 10-story unbraced frame

Level	h, in.	ΣV kips	M_{ov}^a , in-kips	I_{oi} , in ⁴	A,	\bar{x} in.	Chord disp. in.	Chord drift, in.
10	144	30.22	4,352	3,672,000	0.294×10^5	48.00	0.5746	0.0722
9	144	52.17	11,864	3,672,000	1.096×10^5	60.88	0.5024	0.0774
8	144	71.74	22,194	4,619,520	1.830×10^5	64.72	0.4250	0.0838
7	144	88.93	35,001	4,619,520	3.074×10^5	66.63	0.3412	0.0795
6	144	103.76	49,942	5,947,200	3.546×10^5	67.78	0.2617	0.0777
5	144	116.21	66,677	5,947,200	4.868×10^5	68.56	0.1840	0.0664
4	144	126.30	84,864	7,168,320	5.249×10^5	69.12	0.1176	0.0557
3	144	134.01	104,161	7,168,320	6.547×10^5	69.55	0.0619	0.0366
2	144	139.34	124,226	9,639,360	5.882×10^5	69.89	0.0253	0.0171
1	180	142.31	149,841	9,639,360	8.824×10^5	87.20	0.0082	0.0082

^a Overturning moment.

Table 7-9. Calculation of total first and second order story drifts and lateral displacements for the 10-story unbraced frame

Level	h, in.	ΣV , kips	ΣP , kips	Δ_1 in.	μ	$\Delta_2 = \mu \Delta_1$ in.	2nd -Order Disp.,in.
10	144	30.22	180	0.517	1.022	0.528	8.547
9	144	52.17	396	0.849	1.047	0.889	8.019
8	144	71.74	612	0.773	1.048	0.810	7.130
7	144	88.93	828	0.941	1.065	1.002	6.320
6	144	103.76	1044	0.898	1.067	0.958	5.318
5	144	116.21	1260	0.987	1.080	1.066	4.360
4	144	126.30	1476	0.833	1.073	0.894	3.294
3	144	134.01	1692	0.865	1.082	0.936	2.400
2	144	139.34	1908	0.786	1.081	0.850	1.464
1	180	142.31	2124	0.584	0.614	0.614	0.614

replaced by chord action as the dominant contributor to lateral displacement.

The results of this approximate analysis are compared to the results of an exact elastic analysis in Figures 7-30 and 7-31, where the good agreement between the two sets of results may be observed.

Given the dominance of bent action in this case, a simple drift design strategy based on reducing the bent drift is adopted. The maximum bent drift is about 80% of the maximum total drift. Hence, it would be rational to reduce the bent drift ratios to 80% of the maximum allowable value of 0.0033 (≈ 0.0026). It should be noted that increasing member sizes would further reduce the contribution of chord and shear leak actions to the drift. Assuming that the drift control is to be achieved by increasing both beam and column sizes, the average magnification factors Φ by which the moment of inertia of beams and

columns should be multiplied can be calculated as described in part 1 of Example 7-5. Based on the average values of Φ , new member sizes for beams and columns are selected. These member sizes are shown in Figure 7-32, where the computed values of Φ are shown in parenthesis.

At this stage, another round of displacement analysis, similar to that performed in Tables 7-6 to 7-9, is necessary to make sure that the new design satisfies the drift design criteria. Results of this analysis are shown in Figures 7-33 and 7-34, which indicate that the new design satisfies the design drift criteria. This was also confirmed by performing an exact structural analysis (Figures 7-35 and 7-36).

The last item on the agenda, is to check the satisfaction of the strength criteria by the new design. Codified equivalent static lateral forces, which are based on a pre-determined fundamental period for the structure, do not necessarily change with variation of stiffness.

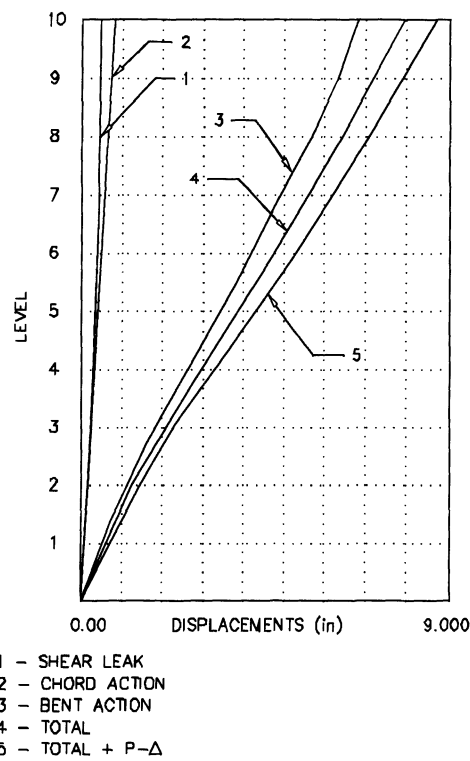


Figure 7-27. Contribution of various actions to the total lateral displacement of the 10 story frame.

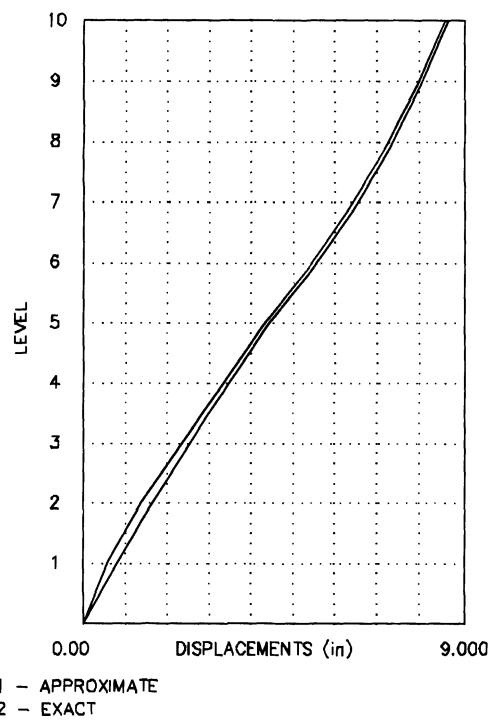


Figure 7-29. Comparison of approximate and "exact" second-order displacements.

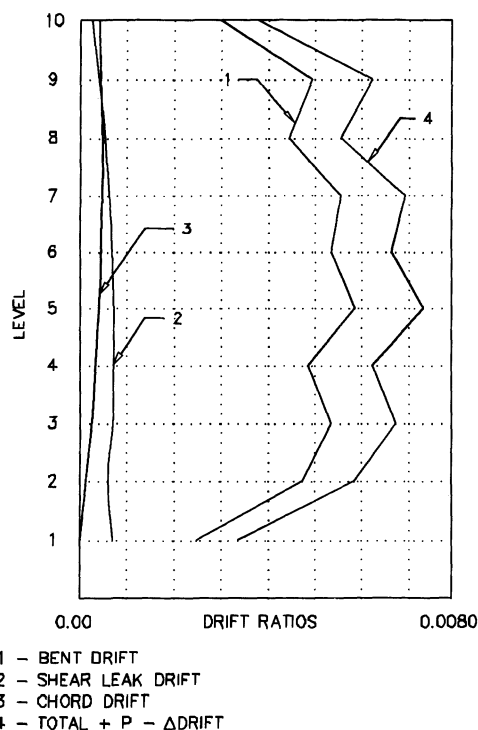


Figure 7-28. Contribution of various actions to the total interstory drift ratios of the 10 story frame.

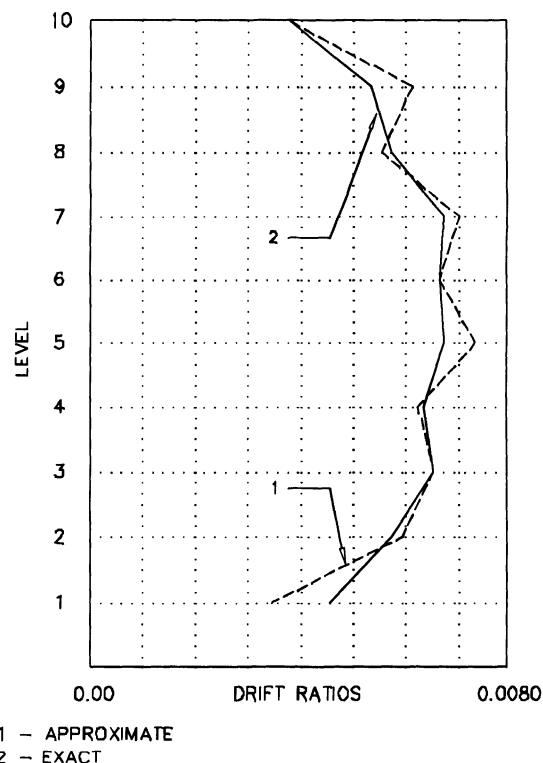


Figure 7-30. Comparison of approximate and "exact" second-order interstory drift ratios.

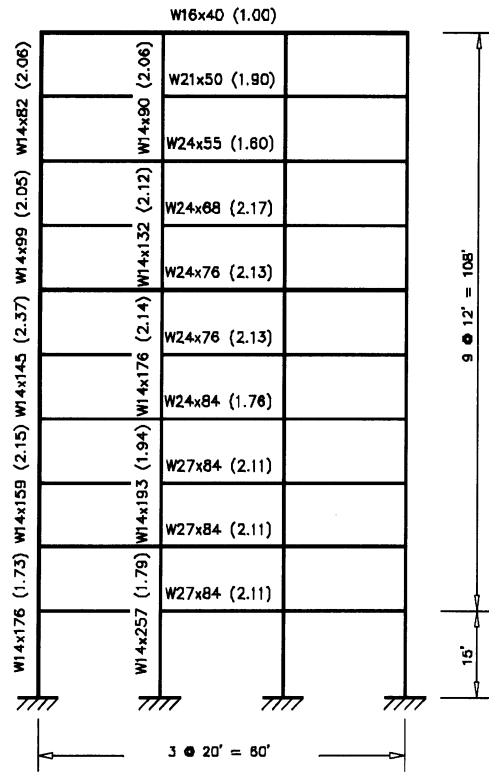


Figure 7-31. Member sections after drift design.

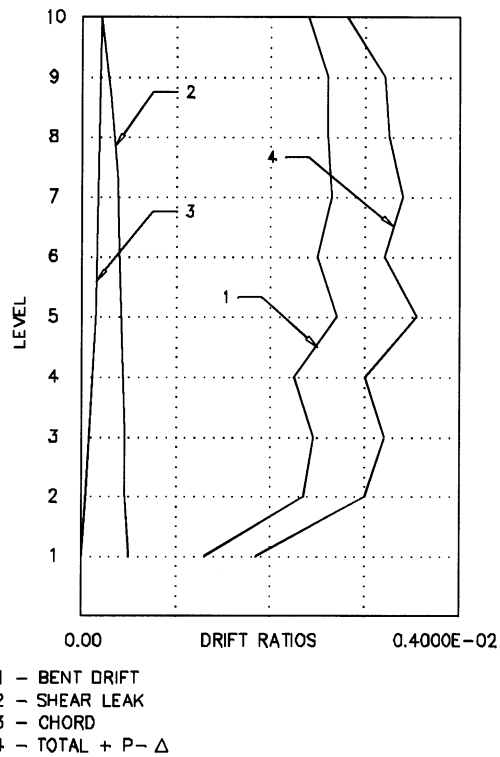


Figure 7-33. Approximate interstory drift ratios for the 10 story frame after drift design.

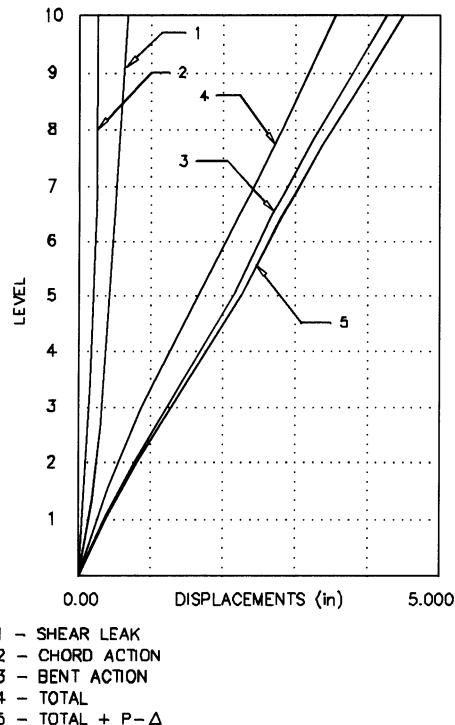


Figure 7-32. Approximate lateral displacements for the 10 story frame after drift design.

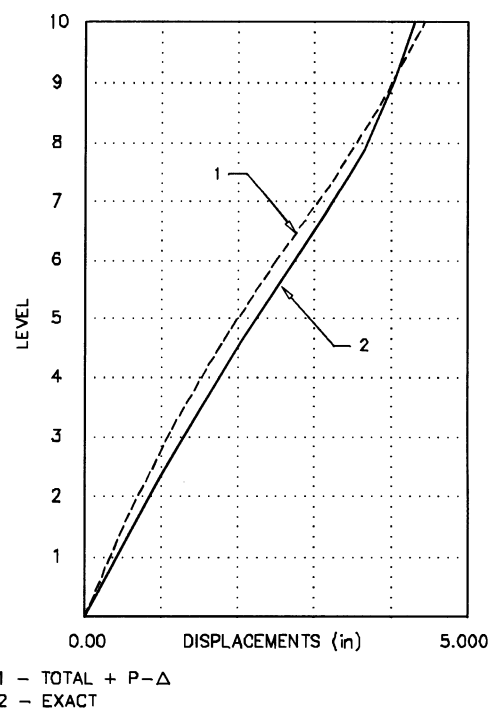


Figure 7-34. ‘Exact’ versus approximate displacements for the 10 story frame after drift design.

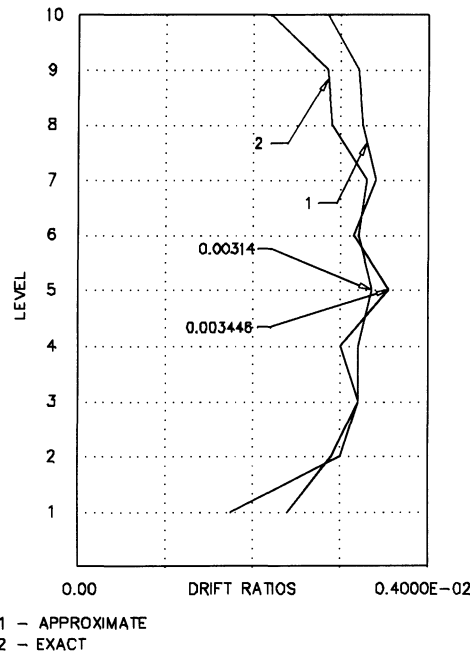


Figure 7-35. "Exact" versus approximate interstory drift ratios for the 10 story frame after drift design.

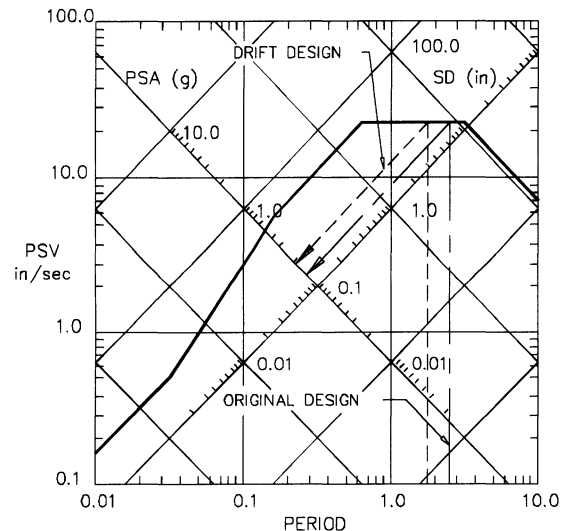


Figure 7-36. Influence of drift design on imposed inertial forces.

In reality, however, increasing member sizes for drift control, increases the stiffness of the structure and reduces its natural periods. In multistory buildings, reduction of natural periods usually implies an increase in the inertial forces exerted on the structure. Therefore, the adequacy of the modified design

to withstand increased inertial forces should be examined.

Let us assume that the design ground motion for this example is represented by the design spectrum shown in Figure 7-37. Application of the Rayleigh method, or a simple dynamic analysis, reveals that the fundamental period of the original design (Figure 7-14) is about 2.7 seconds. The fundamental period of vibration of the structure after drift design (Figure 7-32) is about 1.9 seconds. Given the design spectrum of Figure 7-37, the spectral acceleration corresponding to the first mode of vibration of the structure, is about 0.15g for the original design and 0.20g for the modified design. Hence, the modified design will be expected to withstand about 33% more inertial forces than the original one.

7.5.2 Drift Design of Braced Frames

Lateral displacements of braced frames are primarily caused by two actions: deformation of the braces, and axial deformation of the columns (chord action). Several methods are available for estimation of braced frame displacements (7-44, 7-49, 7-50). The contribution of brace deformations to story drift may be estimated by⁽⁷⁻⁴⁴⁾:

$$S_{br} = \sum \frac{A_{br} E \cos^2 \alpha}{L_{br}} \quad (7-55)$$

$$\Delta_{br} = \frac{\Sigma V}{S_{br}} \quad (7-56)$$

where Δ_{br} is story drift due to brace deformations, ΣV is the story shear, S_{br} is the sum of stiffnesses of the braces at the level under consideration, E is the modulus of elasticity of brace, A_{br} and L_{br} are the cross sectional area and the length of each brace, and α is the angle that a brace makes with the horizontal axis. The summation is carried out over all braces at the level under consideration. Equation 7-55 is valid as long as the braces do not yield or buckle.

For ordinary braced frames, the bent story stiffness is negligible in comparison with the brace stiffness. However, in cases where rigid beam-column connections are utilized (such as eccentrically braced frames) the bent stiffness can be significant. In these situations, the bent story stiffness (see Sec. 7.5.1, "Bent Displacements") should be added to the brace stiffness.

The cantilever drifts may be computed via the Moment Area Method as explained in Sec. 7.5.1, "Cantilever Displacements". Note that in ordinary braced frames, where beams and columns are not joined by moment connections, only some of the columns (those in the vicinity of braces) provide significant resistance to cantilever deflections.

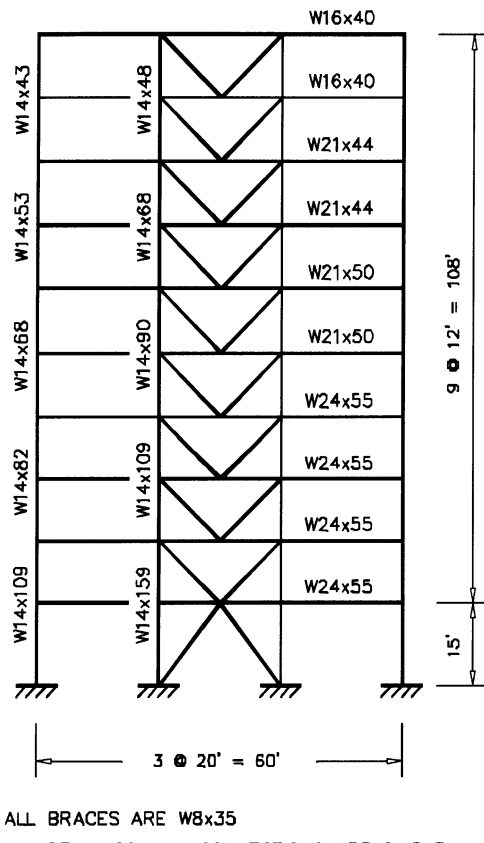


Figure 7-37. Braced frame elevation (Example 7-9).

EXAMPLE 7-9

Estimate the first and second-order lateral displacements and story drifts for the 10-story braced steel frame shown in Figure 7-38. All

beam to column connections are simple. The tributary width of the frame is 30 ft. The gravity load is 100 psf on the roof level and 120 psf on typical floors. Assume that the braces are so proportioned that none of them either yield or buckle under the given loads.

We have

$$W8 \times 35 \quad A = 10.3 \text{ in}^2$$

For braces at typical floors,

$$L_{br} = \sqrt{(10)^2 + (12)^2} = 15.62 \text{ ft.} = 187.44 \text{ in.}$$

$$\cos \alpha = 10 / 15.62 = 0.6402$$

$$S_{br} = \sum E \frac{A_{br}}{L_{br}} \cos^2 \alpha$$

$$= 2(29000)(10.3)(0.6402)^2 / 187.44$$

$$= 1306.27 \text{ kips/in.}$$

For braces at the first floor,

$$L_{br} = \sqrt{(10)^2 + (15)^2} = 18.03 \text{ ft.} = 216.33 \text{ in.}$$

$$\cos \alpha = 10 / 18.03 = 0.5547$$

$$S_{br} = \frac{2(29000)(10.3)(0.5547)^2}{216.33} = 849.67 \text{ kips/in.}$$

The brace action story drifts and lateral displacements are calculated in Table 7-10. To show the accuracy of the above simple procedure, an exact first-order elastic analysis was also performed, in which large column areas were used to eliminate axial deformation of the columns. Results of the exact and approximate analyses are compared in Figure 7-39, where good agreement can be observed.

The chord action story drifts and lateral displacements are calculated in Table 7-11. The total drifts are magnified using the direct P-delta method in Table 7-12. The extent of contribution of each action to the lateral response of the frame is shown in Figure 7-40, where the dominance of chord action is evident. The results obtained by the above simple procedure are compared with those obtained by an exact second-order analysis in Figures 7-41 and 7-42.

Table 7-10. Calculation of brace-action story drifts and lateral displacements for the 10-story braced frame of example 7-9.

Level	h, in.	ΣV , kips	S_{br} kips/in.	Δ_{br} , in.	Lat. disp. in.
10	144	30.22	1306	0.0231	0.8279
9	144	52.17	1306	0.0399	0.8048
8	144	71.74	1306	0.0549	0.7649
7	144	88.93	1306	0.0681	0.7100
6	144	103.76	1306	0.0794	0.6419
5	144	116.21	1306	0.0890	0.5625
4	144	126.30	1306	0.0967	0.4735
3	144	134.01	1306	0.1026	0.3768
2	144	139.34	1306	0.1067	0.2742
1	180	142.31	850	0.1675	0.1675

Table 7-11. Calculation of chord-action story drifts and lateral displacements for the braced frame of Example 7-9.

Level	h, in.	ΣV , kips	M_{ov} , in.-kips	I_{oi} , in. ⁴	A, in. ²	\bar{x} , in.	Chord disp., in.	Chord drift, in.
10	144	30.22	4,352	406,080	2.66×10^5	48.00	2.958	0.452
9	144	52.17	11,864	406,080	9.92×10^5	60.88	2.506	0.443
8	144	71.74	22,194	576,000	14.7×10^5	64.72	2.063	0.426
7	144	88.93	35,001	576,000	24.6×10^5	66.63	1.637	0.397
6	144	103.76	49,942	763,200	27.6×10^5	67.78	1.240	0.360
5	144	116.21	66,677	763,200	37.9×10^5	68.56	0.880	0.312
4	144	126.30	84,864	921,600	40.8×10^5	69.12	0.568	0.256
3	144	134.01	104,161	921,600	50.9×10^5	69.55	0.312	0.190
2	144	139.34	124,226	1,344,960	42.2×10^5	69.89	0.122	0.122
1	180	142.31	149,841	1,344,960	63.2×10^5	87.20	0.000	0.000

Table 7-12 Calculation of total first-order and second-order story drifts and lateral displacements for the braced frame of example 7-9.

Level	h, in.	ΣV , kips	ΣP , kips	Δ_1 , in.	μ	$\Delta_2 = \mu \Delta_1$, in.	2nd-Order Disp., in.
10	144	30.22	180	0.475	1.020	0.485	3.897
9	144	52.17	396	0.483	1.026	0.496	3.412
8	144	71.74	612	0.481	1.029	0.495	2.916
7	144	88.93	828	0.465	1.031	0.479	2.421
6	144	103.76	1044	0.439	1.032	0.453	1.942
5	144	116.21	1260	0.401	1.031	0.413	1.489
4	144	126.30	1476	0.353	1.029	0.363	1.076
3	144	134.01	1692	0.301	1.027	0.309	0.713
2	144	139.34	1908	0.229	1.022	0.234	0.404
1	180	142.31	2124	0.168	1.014	0.170	0.170

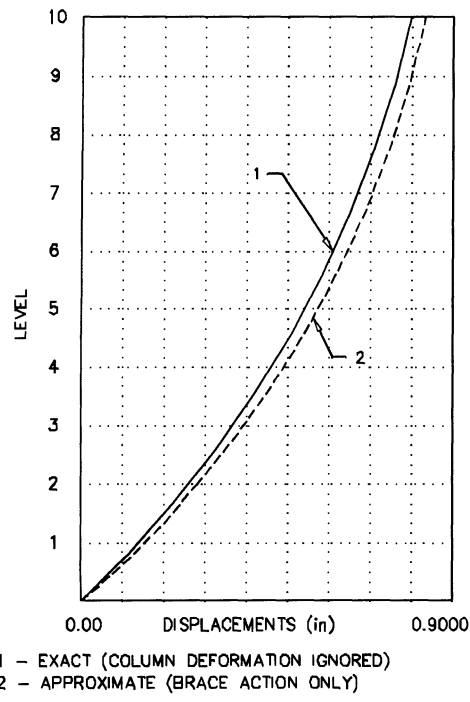


Figure 7-38. Lateral displacements caused by brace deformations.



Figure 7-40. "Exact" versus approximate lateral displacements for the braced frame of example 7-9.

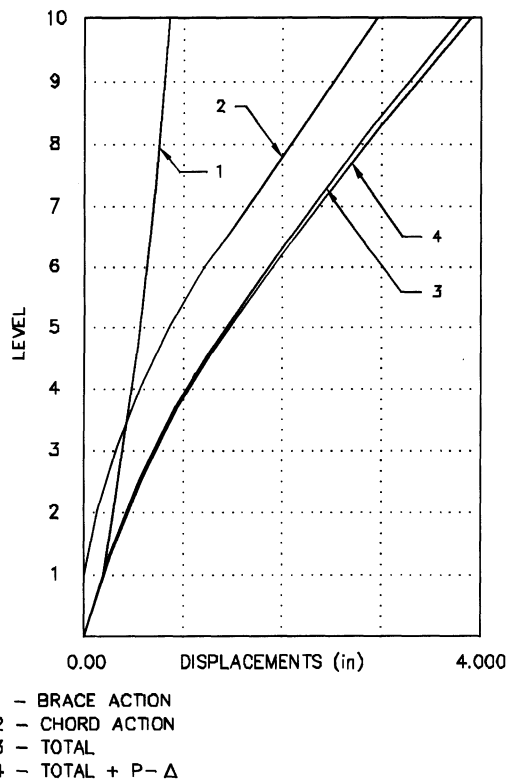


Figure 7-39. Contribution of various actions to the total lateral displacement of the braced frame of Example 7-9.

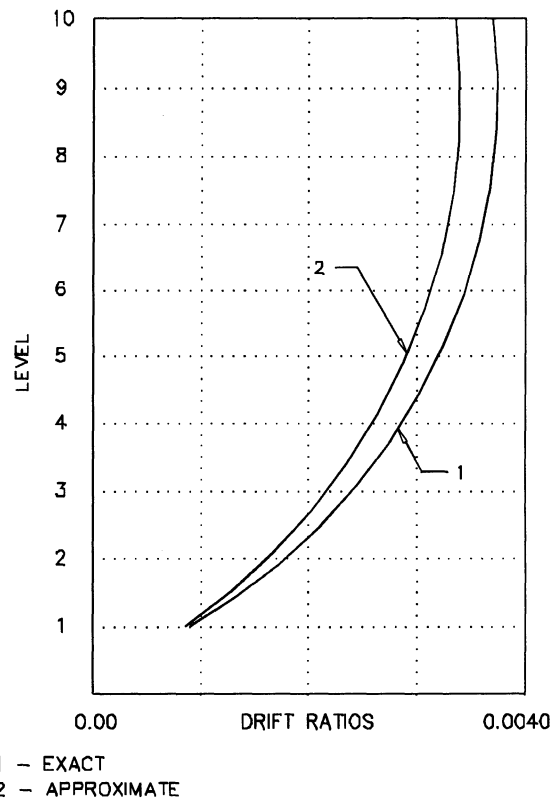


Figure 7-41. "Exact" versus approximate interstory drift ratios for the braced frame of Example 7-9.

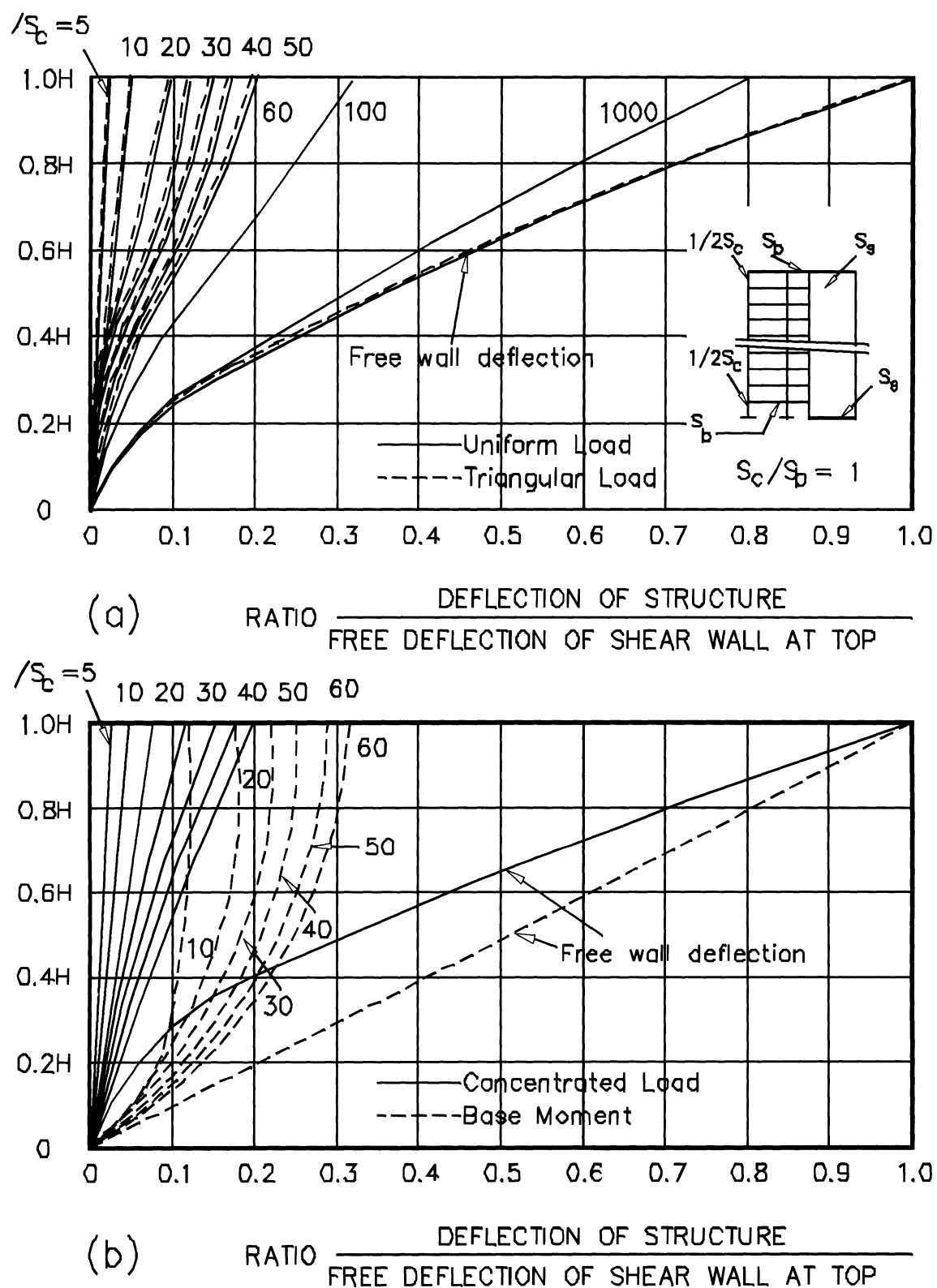


Figure 7-42. Design aid for drift design of frame-shear wall systems⁽⁷⁻⁵¹⁾ ($S_g/S_b=1$).

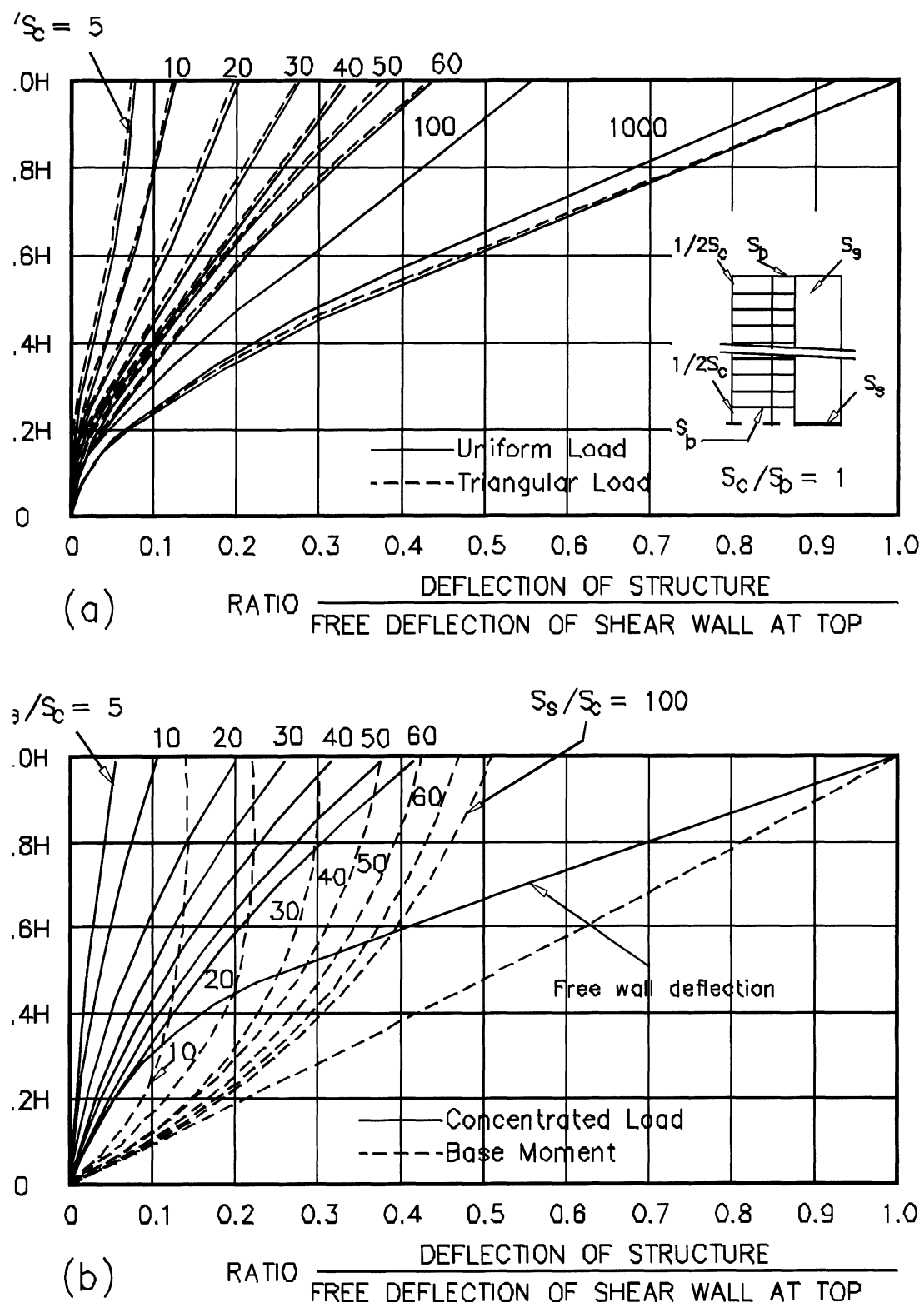


Figure 7-43. Design aid for drift design of frame-shear wall systems⁽⁷⁻⁵¹⁾ ($S_c/S_b=5$).

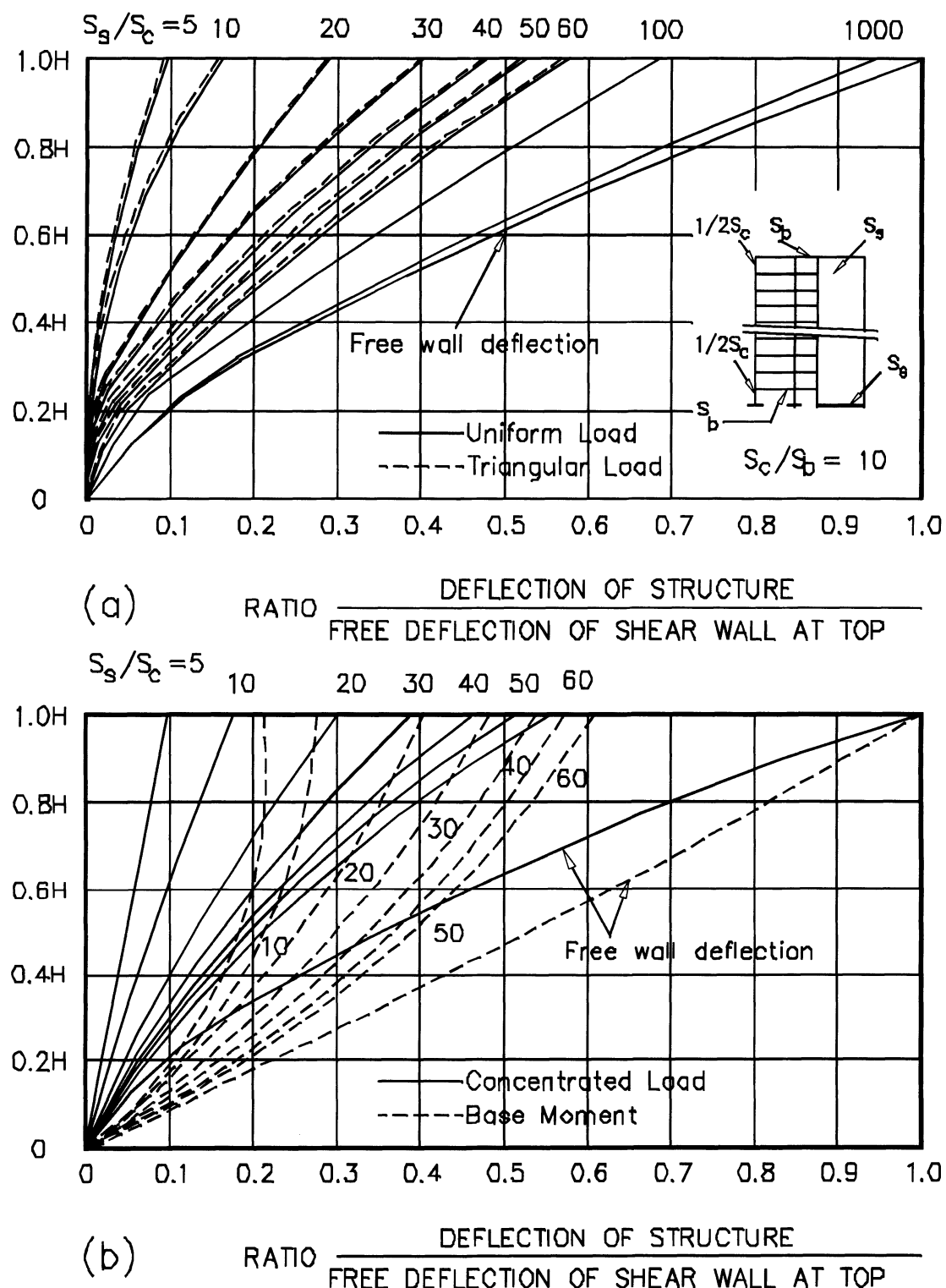


Figure 7-44. Design aid for drift design of frame-shear wall systems⁽⁷⁻⁵¹⁾ ($S_c/S_b=10$)

7.5.3 Drift Design of Frame - Shear Wall Systems

Estimates of the lateral displacements of Frame-Shear wall systems may be obtained using the charts developed by Khan and Sbarounis⁽⁷⁻⁵¹⁾. Some of these charts, for the case of constant stiffness over the height, are reproduced in Figures 7-43 to 7-45. A sample application of the charts is presented in Example 7-10. In order to utilize the charts, the sum of stiffnesses of beams (S_b), columns (S_c) and shear walls (S_s) should be computed by adding the corresponding EI/L terms.

The charts provide the ratio of the lateral deflection of the frame-shear wall system to the free deflection (at the top) of the shear wall alone. Note that the ratio of S_s/S_c should be normalized by multiplying it by $(10/N)^2$, where N is the number of stories in the structure.

Another method for estimating drift and natural periods of frame-shear wall systems, has been developed by Stafford Smith et al.^(7-52, 7-53). The method has been shown to provide accurate estimates of lateral displacements for a variety of structural systems. It can be easily adapted to programmable calculators. It is rather tedious, however, for hand calculations.

EXAMPLE 7-10

Use the Khan and Sbarounis charts to estimate the lateral displacement at the top of the 30-story frame-shear wall building shown in Figure 7-46. Assume a uniform lateral pressure of 30psf. Story heights are 12.5 feet. Use gross concrete section properties and $E = 4000$ ksi.

Column Stiffnesses:

Col. Type	b, in.	h, in.	I, ft^4	$I/L, \text{ft}^3$
C1	24	24	1.333	0.1067
C2	28	28	2.470	0.1976
C3	32	32	4.214	0.3371
C4	36	36	6.750	0.5400

$$\text{Total } I/L = 4(0.1067) + 6(0.1976)$$

$$+ 4(0.3371) + 2(0.5400)$$

$$= 4.041 \text{ ft}^3$$

Beams:

$$B1: \quad I = \frac{(14)(36)^3}{(12)^5} = 2.625 \text{ ft}^4$$

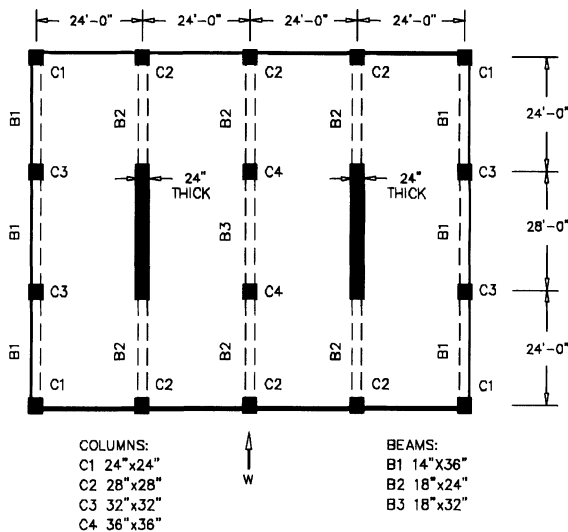


Figure 7-45. Plan of the 30 story frame-shear wall building⁽⁷⁻⁵²⁾.

$$B2: \quad I = \frac{(18)(24)^3}{(12)^5} = 1.000 \text{ ft}^4$$

$$B3: \quad I = \frac{(18)(32)^3}{(12)^5} = 2.370 \text{ ft}^4$$

$$\begin{aligned} \text{Total } I/L &= \frac{(4)(2.625)}{24} + \frac{(2)(2.625)}{28} \\ &+ \frac{(6)(1.00)}{28} + \frac{(1)(2.37)}{28} \\ &= 0.924 \text{ ft}^3 \end{aligned}$$

Walls:

$$I = \frac{(2)(28)^3}{12} = 3658.67 \text{ ft}^4$$

$$\text{Total } I/L = \frac{(2)(3658.67)}{12.5} = 585.39$$

$$\frac{S_s}{S_c} = \frac{585.39}{4.041} \left(\frac{10}{30} \right)^2 = 16.10$$

$$\frac{S_c}{S_b} = \frac{4.041}{0.924} = 4.37$$

Free deflection of the wall:

$$w = \frac{30(4)(24)}{1000} = 2.88 \text{ kips/ft}$$

$$\Delta = \frac{wl^4}{8EI} = \frac{(2.88)(375)^4}{(8)(576000)(3658.67)(2)} \\ = 1.69 \text{ ft.} = 20.28 \text{ in.}$$

Using the curve corresponding to $S_s/S_c = 20$ from Chart (a) of Figure 7-44, we have $D_{\text{top}} = (0.22)(20.28) = 4.06$ inches, which compares very well with the computed exact displacement of 4.23 inches (see Figure 7-47).

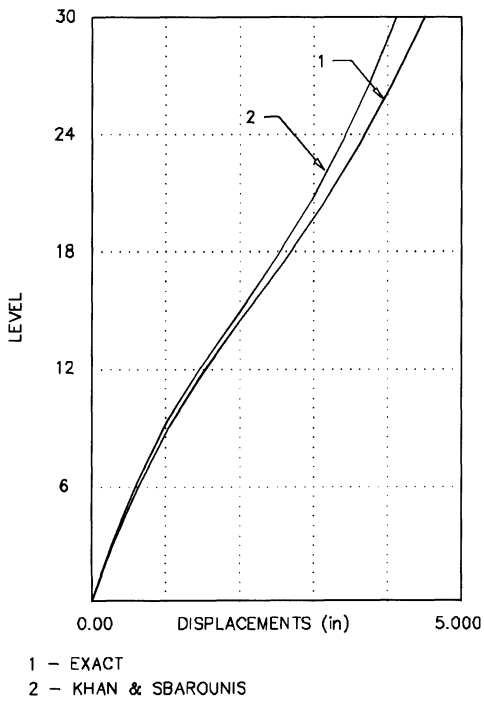


Figure 7-46. Lateral displacement of the 30 story frame-shear wall building.

7.5.4 Torsional Effects

One of the most important tasks in the process of the selection, and the subsequent proportioning, of a structural system, is the minimization of torsional response. In general, this is a rather difficult task, and its success is strongly dependent on the intuition and experience of the designer.

For buildings in which the locations and relative stiffnesses of the lateral load resisting sub-systems (e.g. frames and walls) do not vary significantly along the height, the torsional displacements may be estimated as follows:

1. For buildings which are composed of only one type of lateral load resisting system (moment frames, braced frames, or walls), the torsional rotation at the i th floor, θ_i , and the corresponding torsional drift of the j th frame at this floor, Δ_j , may be estimated as:

$$\theta_i = \frac{(\Sigma V_i) e_i^2}{J} \quad (7-57)$$

$$\Delta_j = R_j \theta_i \quad (7-58)$$

where ΣV_i is the story shear, e_i is the eccentricity of the "center of rigidity" from the center of mass, R_j is the closest distance from the j th frame to the center of rigidity, and J is the torsional story stiffness given by

$$J = \sum K_j R_j^2 \quad (7-59)$$

2. For combination systems (frame-shear wall systems, moment frame and braced frame combinations), the process is more complex:
 - The direct lateral displacements and story drifts of the structure are obtained via the Khan-Sbarounis charts or any other appropriate method.
 - The total direct story shear carried by the frames subjected to the above displacements, V_{fi} , are calculated (see Section 7.5.1, "Bent Displacements").
 - The shear V_{fi} is distributed among the various frames according to their relative stiffness in the direction of applied load.
 - The rest of the story shear ($\Sigma V_i - V_{fi}$) is distributed among the various walls (braced frames) according to their relative stiffness in the direction of applied loads.
 - The shear in each frame or wall, as calculated in the two preceding steps, is used as a measure of rigidity, and the center of rigidity of the entire system is located.

- The torsional rotation and the corresponding torsional drift of individual frames and walls are calculated using Equations 7-57 and 7-58.

It may be noticed that the concept of the "center of rigidity" is of significant use in the preliminary evaluation of the torsional response. However, the physical limitations of such a concept when applied to the seismic response of general, three dimensional, multistory structures should be clearly understood. In a three dimensional, multi-story structure, if it exhibits significant plan and elevation irregularities, the lateral resistance is provided by a combination of strongly interdependent actions, both within a single story, and among various floors. In general, for such a complex system, centers of rigidity (points of application of forces for a torsion-free response) do not exist. Furthermore, if and when they exist, they must all lie on a single vertical line⁽⁷⁻⁵⁴⁾.

7.6 SEISMIC CODE REQUIREMENTS FOR DRIFT AND P-DELTA ANALYSIS

7.6.1 UBC-97 Provisions

UBC-97⁽⁷⁻⁵⁷⁾, addresses design for drift and lateral stiffness within the framework of strength design. The reduced lateral displacement calculated by utilizing the reduction factor, R , is called Δ_s . The maximum inelastic response displacement is called Δ_M and is calculated from

$$\Delta_M = 0.7R\Delta_s \quad (7-60)$$

Alternatively, Δ_M may be computed by nonlinear time history analysis. The analysis to determine Δ_M must consider P-delta effects. P-delta effects, however, may be ignored when the ratio of secondary moments to first-order moments does not exceed 0.10. This ratio is calculated from

$$\theta = \frac{P_x \Delta_{sx}}{V_x h_{sx}} \quad (7-61)$$

where

Δ_{sx} = story drift based on Δ_s acting between levels x and $x-1$

V_x = the design seismic shear force acting between levels x and $x-1$

h_{sx} = the story height below level x

P_x = the total unfactored vertical design load at and above level x .

In seismic zones 3 and 4, P-delta effects need not be considered when the story drift index does not exceed $0.02/R$.

UBC-97 permitted drift using Δ_M is a function of the fundamental period of the structure

$$\begin{cases} \Delta_{Mx} \leq 0.025h_{sx} & \text{for } T < 0.7 \text{ sec.} \\ \Delta_{Mx} \leq 0.020h_{sx} & \text{for } T \geq 0.7 \text{ sec.} \end{cases} \quad (7-61)$$

where

Δ_{sx} = story drift based on Δ_M acting between levels x and $x-1$

The fundamental period used in drift calculations is not subject to lower-bound period formulas of the code (see Chapter 4) and may be based on the Rayleigh formula or other rational calculations such as a detailed computer model of the structure. Furthermore, UBC-97 permits these drift limits to be exceeded when the engineer can demonstrate that greater drift can be tolerated by both structural and nonstructural elements whose performance can affect the seismic safety of the structure. Therefore, if local drift is exceeded locally in an area without a serious seismic ramification, it can be tolerated and there is no need for a redesign.

7.6.2 IBC-2000 Provisions

The provisions of IBC-2000⁽⁷⁻⁵⁸⁾ embody a convergence of the efforts initiated by the Applied Technology Council's ATC 3-06⁽⁷⁻⁵⁹⁾ document published in 1978 and its successive modifications by the Federal Emergency Management Agency⁽⁷⁻⁶⁰⁾ and that of the UBC

provisions. Therefore, setting aside the difference in the language and vocabulary, IBC-2000 and UBC-97 drift and P-delta provisions are very similar⁽⁷⁻⁶⁰⁾. Quite rationally, IBC-2000 addresses seismic design for drift and lateral stiffness exclusively at the ultimate limit state of building behavior.

According to IBC-2000 provisions, the design story drift, Δ , is computed as the difference of the deflections, δ_x , at the top and bottom of the story under consideration in accordance with the following formula

$$\delta_x = \frac{C_d \delta_{xe}}{I_E} \quad (7-62)$$

where:

C_d = the deflection amplification factor as given in Table 5-17,

δ_{xe} = the deflection determined by an elastic analysis of the force-resisting system, and

I_E = the occupancy importance factor as given in Section 5.4.2.

The maximum inter-story drift index calculated using Equation 7-62 should not exceed the corresponding limits described in Section 5.4.15. Furthermore, for structures assigned to seismic design categories C, D, E, or F having plan irregularity types 1a or 1b (see Chapter 5) the design story drift is to be computed as the largest difference of the deflections along any of the edges of the structure at the top and bottom of the story under consideration.

To determine whether a P-delta analysis is required, a stability coefficient is used. This is in fact, the same as the stability index introduced previously in this Chapter. P-delta effects need not be considered when the stability coefficient, θ as determined from Equation 7-63 is less than 0.10:

$$\theta = \frac{P_x \Delta}{V_x h_{sx} C_d} \quad (7-63)$$

where

Δ = the design story drift

V_x = the seismic shear force acting between level x and $x-1$

h_{sx} = the story height below level x , and

P_x = the total unfactored vertical design load at and above level x .

The stability coefficient, θ , should not exceed an upper limit of θ_{max} given as

$$\theta_{max} = \frac{0.5}{\beta C_d} \leq 0.25 \quad (7-63)$$

where:

β = the ratio of shear demand to shear capacity for the story between level x and $x-1$. If this ratio is not calculated, a value of $\beta = 1$ should be used.

When θ is greater than 0.10 but less than θ_{max} , IBC-2000 permits direct calculation of P-delta effects in a manner very similar to the direct P-delta method discussed earlier in this Chapter. That is, the calculated first-order interstory drifts are to be multiplied by a factor of $1/(1-\theta)>1$. If, however, θ is larger than θ_{max} the structure is potentially unstable and should be redesigned.

REFERENCES

- 7-1 Council on Tall Buildings, Committee 16, "Stability," Chapter SB-4, Vol. SB of *Monograph on Planning and Design of Tall Buildings*, ASCE, New York, 1979.
- 7-2 Scholl, R.E. (ed), "Effects Prediction Guidelines for Structures Subjected to Ground Motion," Report No. JAB-99-115, URS/Blume Engineers, San Francisco, 1975.
- 7-3 Scholl, R.E., "Brace Dampers: An Alternative Structural System for Improving the Earthquake Performance of Buildings," *Proceedings of the 8th World Conference on Earthquake Engineering*, San Francisco, Vol 5., Prentice Hall, 1984.
- 7-4 Ohta, Y., and Omote, S., "An Investigation into Human Psychology and Behavior During an Earthquake," *Proceedings of the 6th World Conference on Earthquake Engineering*, India, 1977.
- 7-5 Miletic, D.S., and Nigg, J.M., "Earthquakes and Human Behavior," *Earthquake Spectra*, EERI, Vol. 1, No. 1, Feb., 1984.

- 7-6 Durkin, M.E., "Behavior of Building Occupants in Earthquakes," *Earthquake Spectra*, EERI, Vol. 1, No. 2, Feb., 1985.
- 7-7 Chen, W.F., and Lui, E.M., *Structural Stability*, Elsevier Science Publishing Company, New York, 1987.
- 7-8 Wakabayashi, M., *Design of Earthquake Resistant Buildings*, MacGraw Hill, New York, 1986.
- 7-9 Rosenblueth, E., "Slenderness Effects in Buildings," *Journal of the Structural Division*, ASCE, Vol. 91, No. ST1, Proc. Paper 4235, January, 1967, pp. 229-252.
- 7-10 Stevens, L. K., "Elastic Stability of Practical Multi-Story Frames," *Proceedings, Institution of Civil Engineers*, Vol. 36, 1967, pp. 99-117.
- 7-11 Goldberg, J. E., "Approximate Methods for Stability and Frequency Analysis of Tall Buildings," *Proceedings, Regional Conference on Tall Buildings*, Madrid, Spain, September, 1973, pp. 123-146.
- 7-12 Council on Tall Buildings, Committee 23, "Stability," Chapter CB-8, Vol. CB of *Monograph on Planning and Design of Tall Buildings*, ASCE, New York, 1978.
- 7-13 Singh, J.P., "Earthquake Ground Motions: Implications for Designing Structures and Reconciling Structural Damage," *Earthquake Spectra*, EERI, Vol. 1, No. 2, Feb., 1985.
- 7-14 Naeim, F., "On Seismic Design Implications of the 1994 Northridge Earthquake Records," *Earthquake Spectra*, EERI, Vol. 11, No. 1, Feb. 1995.
- 7-15 Anderson, J.C., and Bertero, V.V., "Uncertainties in Establishing Design Earthquakes," *Proceedings of a two-day Course from EERI on Strong Ground Motion*, San Francisco and Los Angeles, Apr., 1987.
- 7-16 MacGregor, J.G., and Hage, S.E., "Stability Analysis and Design of Concrete Frames," *Journal of the Structural Division*, ASCE, Vol. 103, No. ST10, October, 1977, pp. 1953-1970.
- 7-17 Wynhoven, J.H., and Adams, P.F., "Behavior of Structures Under Loads Causing Torsion," *Journal of the Structural Division*, ASCE, Vol. 98, No. ST7, July, 1972, pp. 1361-1376.
- 7-18 Salmon, C.G., and Johnson, J.E., *Steel Structures, Design and Behavior*, 2nd Edition, Harper and Row, 1980, pp. 843-851.
- 7-19 Johnston, B.G. (ed.), *Structural Stability Research Council, Guide to Stability Design Criteria for Metal Structures*, 3rd Edition, John Wiley and Sons, New York, 1976.
- 7-20 Cheong-Siat-Moy, F., "Frame Design Without Using Effective Column Length," *Journal of the Structural Division*, ASCE, Vol. 104, No. ST1, Jan., 1978, pp. 23-33.
- 7-21 Cheong-Siat-Moy, F., "K-Factor Paradox," *Journal of Structural Engineering*, ASCE, Vol. 112, No. 8, Aug., 1986, pp. 1747-1760.
- 7-22 Nair, R. S., "A Simple Method of Overall Stability Analysis for Multistory Buildings," *Developments in Tall Buildings - 1983*, Council on Tall Buildings and Urban Habitat, Lynn S. Beedle (Editor-in-Chief), Van Nostrand Reinhold, New York, 1983.
- 7-23 Nair, R.S., "Overall Elastic Stability of Multistory Buildings," *Journal of the Structural Division*, ASCE, Vol. 101, No. ST12, Dec., 1975, pp. 2487-2503.
- 7-24 Springfield, J., and Adams, P.F., "Aspects of Column Design in Tall Steel Buildings," *Journal of the Structural Division*, ASCE, Vol. 98, No. ST5, May, 1972, pp. 1069-1083.
- 7-25 Wood, B.R., Beaulieu, D., and Adams, P.F., "Column Design by P-Delta Method," *Journal of the Structural Division*, ASCE, Vol. 102, No. ST2, Feb., 1976, pp. 411-427.
- 7-26 Lai, S.A., and MacGregor, J.G., "Geometric Nonlinearities in Unbraced Multistory Frames," *Journal of Structural Engineering*, ASCE, Vol. 109, No. 11, Nov., 1983, pp. 2528-2545.
- 7-27 Nixon, D., Beaulieu, D., and Adams, P.F., "Simplified Second-Order Frame Analysis," *Canadian Journal of Civil Engineering*, Vol. 2, No. 4, Dec., 1975, pp. 602-605.
- 7-28 Renton, J.D., "Stability of Space Frames by Computer Analysis," *Journal of the Structural Division*, ASCE, Vol. 88, No. ST4, Aug., 1962, pp. 81-103.
- 7-29 Chu, K.H., and Rampetsreiter, R.H., "Large Deflection Buckling of Space Frames," *Journal of the Structural Division*, ASCE, Vol. 98, No. ST12, Dec., 1972, pp. 2701-2722.
- 7-30 Connor, J.J., Jr., Logcher, R.D., and Chen, S.C., "Nonlinear Analysis of Elastic Frame Structures," *Journal of the Structural Division*, ASCE, Vol. 94, No. ST6, Jun., 1968, pp. 1525-1547.
- 7-31 Zarghammee, M.S., and Shah, J.M., "Stability of Space Frames," *Journal of the Engineering Mechanics Division*, ASCE, Vol. 94, No. EM2, Apr., 1968, pp. 371-384.
- 7-32 Krajcinovic, D., "A Consistent Discrete Elements Technique for Thin-Walled Assemblages," *International Journal of Solids and Structures*, Vol. 5, 1969, pp. 639-662.
- 7-33 Barsoum, R.S., and Gallagher, R.H., "Finite Element Analysis of Torsional Flexural Stability Problems," *International Journal for Numerical Methods in Engineering*, Vol. 2, 1970, pp. 335-352.
- 7-34 Bazant, Z.P., and El Nimeiri, M., "Large-Deflection Buckling of Thin Walled Beams and Frames," *Journal of the Engineering Mechanics Division*, ASCE, Vol. 79, No. EM6, Dec., 1973, pp. 1259-1281.
- 7-35 Yoo, C.H., "Bimoment Contribution to Stability of Thin-Walled Assemblages," *Computers and Structures*, Vol. 11, 1980, pp. 465-471.

- 7-36 Yang, Y., and McGuire, W., "Stiffness Matrix for Geometric Nonlinear Analysis," *Journal of Structural Engineering*, ASCE, Vol. 112, No. 4, Apr., 1986, pp. 853-877.
- 7-37 Naeim, F., *An Automated Design Study of the Economics of Earthquake Resistant Structures*, Ph.D. Dissertation, Department of Civil Engineering, University of Southern California, Aug., 1982.
- 7-38 Neuss, C.F., Maison, B.F., and Bouwkamp, J.G., *A Study of Computer Modeling Formulation and Special Analytical Procedures for Earthquake Response of Multistory Buildings*, A Report to National Science Foundation, J.G. Bouwkamp, Inc., Berkeley, California, Jan., 1983, pp. 335-362.
- 7-39 Wilson, E.L., and Habibullah, A., "Static and Dynamic Analysis of Multi-Story Buildings Including the P-Delta Effects," *Earthquake Spectra*, EERI, Vol. 3, No. 2, May, 1987.
- 7-40 Freeman, S.A., Czarnicki, R.M., and Honda, K.K., "Significance of Stiffness Assumptions on Lateral Force Criteria," in *Reinforced Concrete Structures Subjected to Wind and Earthquake Forces*, Publication SP-63, American Concrete Institute, Detroit, Michigan, 1980.
- 7-41 Wong, C.H., El Nimeiri, M.M., and Tang, J.W., "Preliminary Analysis and Member Sizing of Tall Tubular Steel Buildings," *AISC Engineering Journal*, American Institute of Steel Construction, Second Quarter, 1981, pp. 33-47.
- 7-42 Council on Tall Buildings, Committee 14, "Elastic Analysis and Design," Chapter SB-2, Vol. SB of *Monograph on Planning and Design of Tall Buildings*, ASCE, New York, 1979.
- 7-43 Cheong-Siat-Moy, F., "Multistory Frame Design Using Story Stiffness Concept," *Journal of the Structural Division*, ASCE, Vol. 102, No. ST6, Jun., 1976, pp. 1197-1212.
- 7-44 Cheong-Siat-Moy, F., "Consideration of Secondary Effects in Frame Design," *Journal of the Structural Division*, ASCE, Vol. 103, No. ST10, Oct., 1977, pp. 2005-2019.
- 7-45 Krawinkler, H., Bertero, V.V., and Popov, E.P., *Inelastic Behavior of Steel Beam-to-Column Subassemblies*, Earthquake Engineering Research Center, University of California, Berkeley, Report No. EERC 71-7, Oct., 1971.
- 7-46 Becker, E.R., *Panel Zone Effect on the Strength and Stiffness of Rigid Steel Frames*, Structural Mechanics Laboratory Report, University of Southern California, Jun., 1971.
- 7-47 Richards, R.M., and Pettijohn, D.R., *Analytical Study of Panel Zone Behavior in Beam-Column Connections*, University of Arizona, Nov., 1981.
- 7-48 Slutter, R.G., *Tests of Panel Zone Behavior in Beam-Column Connections*, Fritz Engineering Laboratory, Lehigh University, Report No. 200-81-403-1, 1981.
- 7-49 Teal, E.J., *Practical Design of Eccentric Braced Frames to Resist Seismic Forces*, Structural Steel Educational Council.
- 7-50 White, R.N., and Salmon, C.G., (eds), *Building Structural Design Handbook*, John Wiley and Sons, New York, 1987.
- 7-51 Khan, F.R., and Sbarounis, J.A., "Interaction of Shear Walls and Frames," *Journal of the Structural Division*, ASCE, Vol. 90, No. ST3, Jun., 1964, pp. 285-335.
- 7-52 Stafford Smith, B., Kuster, M., and Hoenderkamp, J.C.D., "Generalized Method for Estimating Drift in High-Rise Structures," *Journal of Structural Engineering*, ASCE, Vol. 110, No. 7, Jul., 1984, pp. 1549-1562.
- 7-53 Stafford Smith, B., and Crowe, E., "Estimating Periods of Vibration of Tall Buildings," *Journal of Structural Engineering*, ASCE, Vol. 112, No. 5, May, 1986, pp. 1005-1018.
- 7-54 Riddell, R., and Vasques, J., "Existence of Centers of Resistance and Torsional Uncoupling of Earthquake Response of Buildings," *Proceedings of the 8th World Conference on Earthquake Engineering*, San Francisco, Vol 5., Prentice Hall, 1984.
- 7-55 International Conference of Building Officials, *Uniform Building Code -1997*, Whittier, California, 1997.
- 7-56 International Code Council, *International Building Code 2000*, Falls Church, Virginia, 2000.
- 7-57 Applied Technology Council, *Tentative Provisions for the Development of Seismic Regulations for Buildings*, Publication ATC-3-06, 1978.
- 7-58 Federal Emergency Management Agency, *1997 Edition of NEHRP Recommended Provisions for the Development of Seismic Regulations for New Buildings*, 1997.

Chapter 8

Seismic Design of Floor Diaphragms

Farzad Naeim, Ph.D.,S.E.

Vice President and Director of Research and Development, John A. Martin & Associates, Los Angeles, California.

R. Rao Boppana, Ph.D.,S.E.

President, Sato & Boppana, Los Angeles, California.

Key words: Design, Diaphragm, Earthquake, Flexible Diaphragms, IBC-2000, Reinforced Concrete, Seismic, Structural Steel, Rigid Diaphragms, Timber, UBC-97.

Abstract: This chapter surveys the seismic behavior and design of floor and roof diaphragms. Following some introductory remarks, a classification of diaphragm behavior is presented in Section 8.2, and a discussion on the determination of diaphragm rigidity in Section 8.3. Potential diaphragm problems are explained in Section 8.4 where examples are provided to clarify the subject. Provisions of major United States building codes for seismic design of diaphragms are summarized in Section 8.5. Finally, in Section 8.6, the current standard procedures for design of diaphragms are presented via their application in a number of realistic design examples

8.1 INTRODUCTION

The primary function of floor and roof systems is to support gravity loads and to transfer these loads to other structural members such as columns and walls. Furthermore, they play a central role in the distribution of wind and seismic forces to the vertical elements of the lateral load resisting system (such as frames and structural walls). The behavior of the floor/roof systems under the influence of gravity loads is well established and guidelines for use in structural design have been adopted (8-1,8-2).

In the earthquake resistant design of building structures, the building is designed and detailed to act as a single unit under the action of seismic forces. Design of a building as a single unit helps to increase the redundancy and the integrity of the building. The horizontal forces generated by earthquake excitations are transferred to the ground by the vertical systems of the building which are designed for lateral load resistance (e.g. frames, bracing, and walls). These vertical systems are generally tied together as a unit by means of the building floors and roof. In this sense, the floor/roof structural systems, used primarily to create enclosures and resist gravity (or out of plane) loads are also designed as horizontal diaphragms to resist and to transfer horizontal (or in-plane) loads to the appropriate vertical elements.

The analysis and design of a floor or roof deck under the influence of horizontal loads is performed assuming that the floor or roof deck behaves as a horizontal continuous beam supported by the vertical lateral load resisting elements (hereafter referred to as VLLR elements). The floor deck is assumed to act as the web of the continuous beam and the beams at the floor periphery are assumed to act as the flanges of the continuous beam (see Figure 8-1).

Accurate determination of the in-plane shears and bending moments acting on a floor diaphragm, and the corresponding horizontal force distribution among various VLLR

elements requires a three dimensional analysis that accounts for the relative rigidity of the various elements including the floor diaphragms. Increasingly, this type of analysis is being performed for design and rehabilitation of major buildings that feature significant plan irregularities. In general, however, some assumptions are made on the horizontal diaphragm rigidity and a relatively simple analysis is performed to determine distribution of lateral forces. Obviously, the accuracy of the results obtained depends on the validity of the assumptions made. In addition, the behavior of certain floor systems such as plywood, metal deck, and precast concrete diaphragms are difficult to model analytically due to their various attachments. In some cases testing may be required to establish the strength and stiffness properties of such systems.

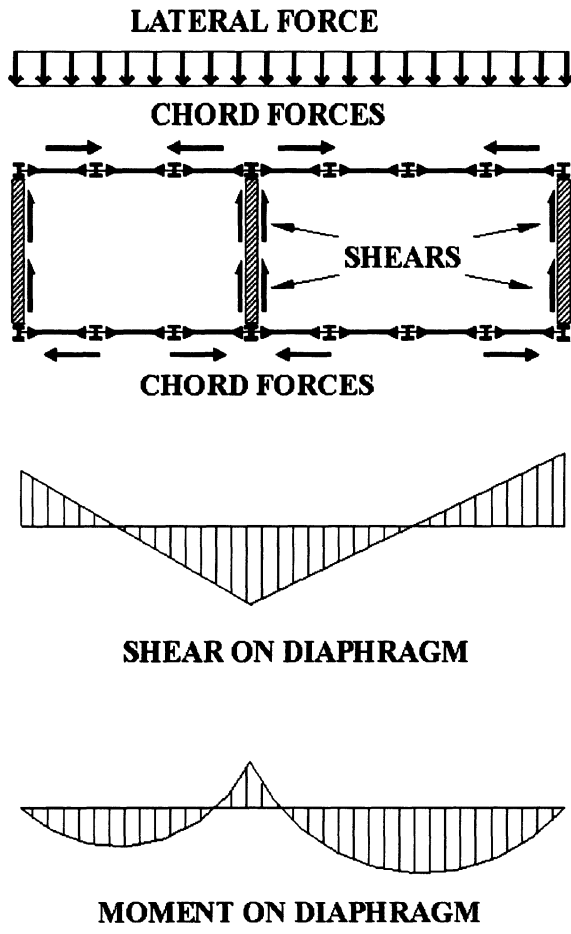


Figure 8-1. Design forces on a diaphragm

While for the great majority of structures, simplified analysis procedures result in a safe design, studies indicate that neglecting the real behavior of floor diaphragms can sometimes lead to serious errors in assessing the required lateral load resistance capacities of the VLLR elements^(8-3, 8-4, 8-5).

This chapter addresses the major issues of seismic behavior and design of diaphragms. It starts by classification of diaphragm behavior in Section 8.2, and a discussion on the determination of diaphragm rigidity in Section 8.3. Potential diaphragm problems are explained in Section 8.4 where examples are provided to clarify the subject. Provisions of major United States building codes for seismic design of diaphragms are summarized in Section 8.5. Finally, in Section 8.6, the current standard procedures for design of diaphragms are presented via their application in a number of realistic design examples.

8.2 CLASSIFICATION OF DIAPHRAGM BEHAVIOR

The distribution of horizontal forces by the horizontal diaphragm to the various VLLR elements depends on the relative rigidity of the horizontal diaphragm and the VLLR elements. Diaphragms are classified as "rigid", "flexible", and "semi-rigid" based on this relative rigidity.

A diaphragm is classified as rigid if it can distribute the horizontal forces to the VLLR elements in proportion to their relative stiffness. In the case of rigid diaphragms, the diaphragm deflection when compared to that of the VLLR elements will be insignificant. A diaphragm is called flexible if the distribution of horizontal forces to the vertical lateral load resisting elements is independent of their relative stiffness. In the case of a flexible diaphragm, the diaphragm deflection as compared to that of the VLLR elements will be significantly large. A flexible diaphragm distributes lateral loads to the VLLR elements as a series of simple beams spanning between these elements.

No diaphragm is perfectly rigid or perfectly flexible. Reasonable assumptions, however, can

be made as to a diaphragm's rigidity or flexibility in order to simplify the analysis. If the diaphragm deflection and the deflection of the VLLR elements are of the same order of magnitude, then the diaphragm can not reasonably be assumed as either rigid or flexible. Such a diaphragm is classified as semi-rigid.

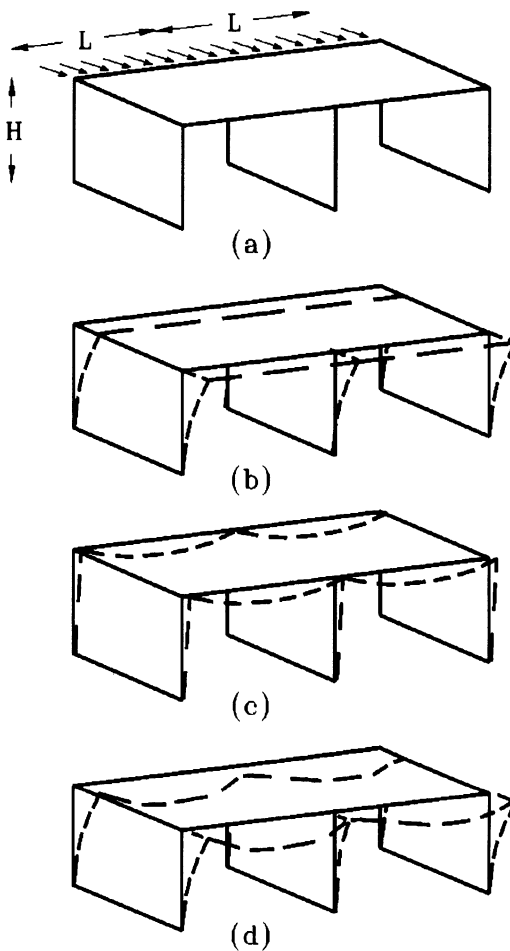


Figure 8-2. Diaphragm behavior. (a) Loading and building proportions. (b) Rigid diaphragm behavior. (c) Flexible diaphragm behavior, (d) Semi rigid diaphragm behavior

Exact analysis of structural systems containing semi-rigid diaphragms is complex, since any such analysis should account for the relative rigidity of all structural elements including the diaphragm. The horizontal load distribution of a semi-rigid diaphragm may be approximated as that of a continuous beam supported on elastic supports. In most cases consisting of semi-rigid diaphragms,

assumptions can be made to bound the exact solution without resorting to a complex analysis.

The absolute size and stiffness of a diaphragm, while important, are not the final determining factors whether or not a diaphragm will behave as rigid, flexible, or semi-rigid⁽⁸⁻³⁾. Consider the one-story concrete shear wall building shown in Figure 8-2a. Keeping the width and the thickness of walls and slabs constant, it is possible to simulate rigid, flexible and semi-rigid diaphragms as the wall heights and diaphragm spans are varied. The wall stiffness decreases with an increase in the floor height (H). Similarly, the diaphragm stiffness decreases with an increase in span (L).

The dashed line in Figure 8-2b indicates the deflection of the system under the influence of horizontal forces when the diaphragm is rigid. This can be accomplished by increasing H and decreasing L so that the stiffness of the diaphragm relative to the wall is significantly larger. In such a situation, the deflection of the diaphragm under horizontal loads is insignificant when compared to the deflections of the walls. The diaphragm will move as a rigid body and will force the walls to move together accordingly. The force distribution among the walls will depend only on the relative stiffness of the walls. In Figure 8-2b it is assumed that the applied load and the wall stiffness are symmetric. If this is not the case, in addition to the rigid body translation, the diaphragm will experience rigid body rotation.

Figure 8-2c shows the deflection of the system under the influence of horizontal forces when the diaphragm is flexible. This can be accomplished by decreasing H and increasing L such that the stiffness of the diaphragm when compared to the walls is small. In such a situation, the diaphragm segments between the walls act as a series of simply supported beams and the load distribution to the walls can be determined based on the tributary area of the diaphragm to the wall. Obviously, a flexible diaphragm can not experience the rotation or torsion that occurs due to the rigid body rotation of a rigid diaphragm.

The dashed line in Figure 8-2d indicates the deflection pattern of a semi-rigid diaphragm under the influence of lateral forces. Here the stiffness of the walls and the diaphragm are of the same order. Both wall deflections and diaphragm deflections do contribute to the total system deflection. Determination of exact load distribution among the walls requires a three dimensional analysis of the entire system (including the diaphragm).

8.3 DETERMINATION OF DIAPHRAGM RIGIDITY

In order to estimate the diaphragm rigidity, it is necessary to predict the deflection of the diaphragm under the influence of lateral loads. The various floor and roof systems that have evolved primarily for the purpose of supporting gravity loads do not lend themselves easily to analytical calculation of lateral deflections. Some of the more common floor systems in use today are: (1) cast-in-place concrete; (2) precast planks or Tees with or without concrete topping; (3) metal deck with or without concrete fill and; (4) wood framing with plywood sheathing.

With the single exception of cast-in-place concrete floor system which is a monolithic construction, all the other floor systems mentioned above consist of different units joined together with some kind of connections. In precast concrete construction, adjacent units are generally connected together by welding embedded plates or reinforcing bars. This will help the units to deflect vertically without separation while providing some diaphragm action. The strength and rigidity of such a diaphragm will depend to a great extent on the type and spacing of connections. Analytical computation of deflections and stiffness of such a diaphragm is complex. As an alternative, a bonded topping slab on precast floor or roof can be provided with sufficient reinforcement to ensure continuity and resistance for shear transfer mechanism. In floor systems consisting of metal decks, the deck is welded intermittently to the supports below. Adjacent

units of the deck are connected together by means of button punching or welding. Here again, the diaphragm stiffness is directly related to the spacing and type of connections. In the wood construction, the plywood sheathing is nailed directly to the framing members. Again, strength and stiffness depends on the spacing of the nails and whether or not the diaphragm is blocked.

It is general practice to consider the diaphragms made of cast in place concrete, precast with concrete topping, and metal deck with concrete fill as rigid while the diaphragms consisting of precast planks without concrete topping, metal deck without concrete fill, and plywood sheathing as flexible. This classification is valid for most cases. Gross errors in force distribution, however, can occur if the above assumption is used without paying attention to the relative rigidity of the VLLR elements and the diaphragm^(8-3, 8-4, 8-5).

Metal deck manufacturers have established test programs to provide strength and deflection characteristics of various metal decks and various connection patterns^(8-6, 8-7). Similarly, the Uniform Building Code provides an empirical formula to compute plywood diaphragm deflections and tables to establish the strength of such diaphragms.

8.4 SIGNIFICANT FACTORS AFFECTING DIAPHRAGM BEHAVIOR

Identifying every situation where special attention should be given to the design and detailing of floor diaphragms requires substantial experience and a good amount of engineering judgement. Certain cases, however, more often than not, require special attention and in this section guidelines for identification of such cases are provided.

In general, low-rise buildings and buildings with very stiff vertical elements such as shear walls are more susceptible to floor diaphragm flexibility problems than taller structures.

In buildings with long and narrow plans, if seismic resistance is provided either by the end walls alone, or if the shear walls are spaced far away from each other, floor diaphragms may exhibit the so-called bow action (see Figure 8-3). The bow action subjects the end walls to torsional deformation and stresses. If sufficient bond is not provided between the walls and the diaphragm, the two will be separated from each other starting at the wall corners. This separation results in a dramatic increase in the wall torsion and might lead to collapse.

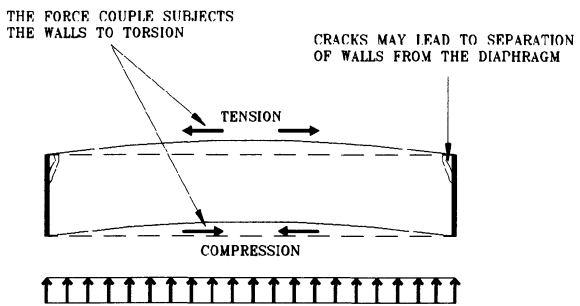


Figure 8-3 A plan showing how the so-called bow action subjects the end walls to torsion

The Arvin High School Administrative Building in California which suffered extensive damage during the Kern County earthquake of July 21, 1952 is a good example in this regard. Schematic plans and elevations of this building are shown in Figure 8-4. An analytical study of this building by Jain⁽⁸⁻⁸⁾ indicated that the two lowest natural frequencies of the building were close to the fundamental frequencies of the floor and roof diaphragms modeled as simply supported beams. When an analytical model of the building was subjected to a 0.20g constant spectral acceleration, with four translational modes considered, the two diaphragm modes represented 74 percent of the sum of the modal base shears. As documented by Steinburgge⁽⁸⁻⁹⁾ diaphragm deflections caused a separation between the roof diaphragm and the wall corners at the second story wall located at the west end of the building. This action subjected the wall to significant torsional stresses beyond its capacity.

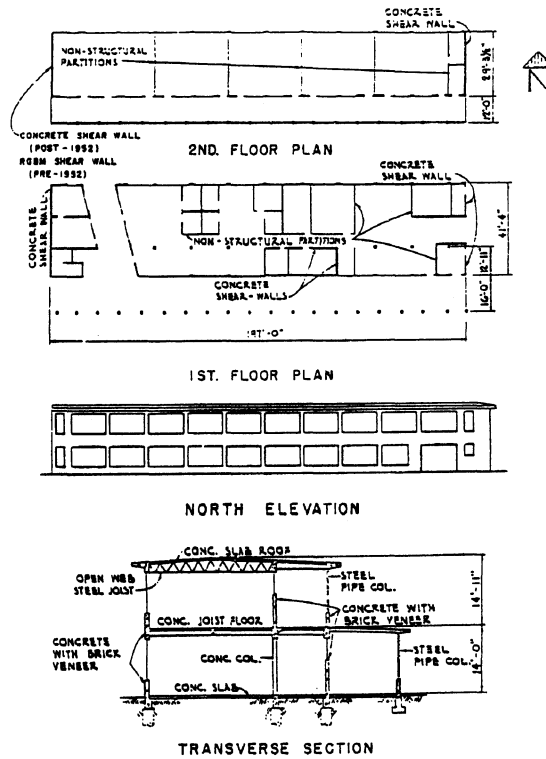


Figure 8-4. Plan and elevation of the Arvin High School Administrative Building (8-8)

Another potential problem in diaphragms can be due to any abrupt and significant changes in a wall stiffness below and above a diaphragm level, or any such changes in the relative stiffness of adjacent walls in passing through one floor level to another (Figure 8-5). This can cause high shear stresses in the floor diaphragm and/or a redistribution of shear forces among the walls.

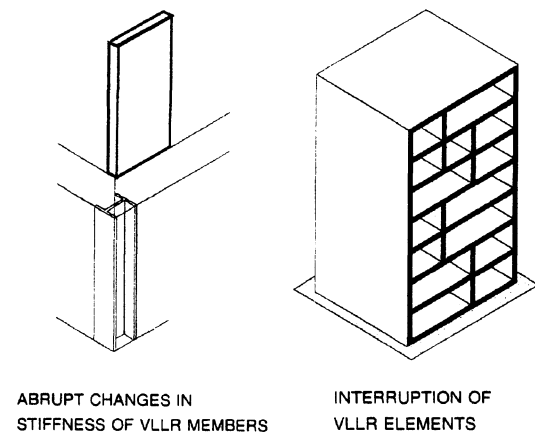


Figure 8-5. Abrupt changes in stiffness and location of VLLR elements can cause drastic redistribution of forces

As an example consider the three story concrete shear wall building shown in Figure 8-6. The concrete floor diaphragms are eight inches thick. A set of static lateral forces of 24 kips, 48 kips and 73 kips are applied at the center of mass of the first, second, and third levels, respectively. The base of the building is assumed to be fixed and the reported results are based on an elastic analysis. An analysis based on a rigid-diaphragm assumption and a finite element analysis considering the un-cracked diaphragm stiffness, yield very close results. However, if we make a simple change in the elevation of the building by moving the opening at the second level, from the wall on line A to the wall on line B (Figure 8-7), the results of the two methods will be markedly different (see Figure 8-8). For example, the rigid diaphragm assumption suggests that the shear force in wall A is reduced from 94.3 kips above the first floor diaphragm to 26 kips below this level, while the finite element model of the building, shows that such a large portion of the shear force is not transferred away from this wall by the floor diaphragm.

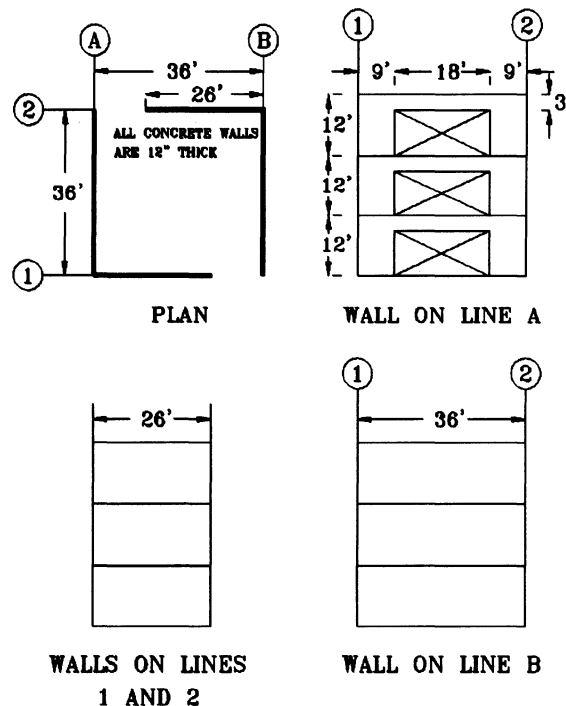


Figure 8-6. Plan and elevation of a simple three story shear wall building (Note the uniform stiffness along the height of walls on lines A and B.)

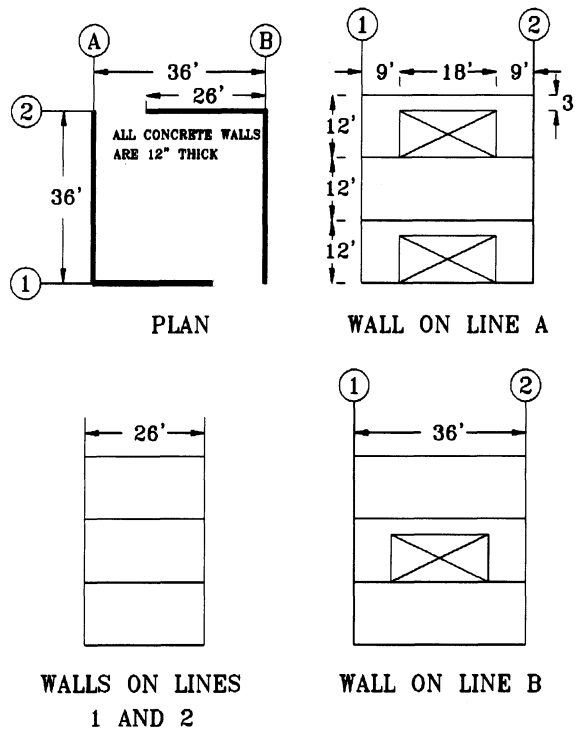


Figure 8-7. Altered plan and elevation of the three story shear wall building (Note the abrupt change of stiffness along the height of walls on lines A and B.)

In buildings with significant plan irregularities, such as multi-wing plans, L-shape, H-shape, V-shape plans, etc. (Figure 8-9) particular attention should be paid to accurately access the in-plane diaphragm stress at the joints of the wings and to design for them. In this type of buildings, the fan-like deformations in the wings of diaphragm can lead to a stress concentration at the junction of the diaphragms (see Figure 8-10). If these stress concentrations are not accounted for, serious problems can arise. For the case of reinforced concrete diaphragms, it is recommended to limit the maximum compressive stresses to $0.2f_c'$. Alternatively, special transverse reinforcement can be provided. In some cases the diaphragm stresses at the junctions may be so excessive that a feasible diaphragm thickness and reinforcement can not be accommodated. In these cases the wings should be separated by seismic joints. One example for this type of problems was provided by the West Anchorage High School Building in Anchorage, Alaska, which suffered severe damage during the

FINITE ELEMENTS ANALYSIS RIGID DIAPHRAGM ASSUMPTION

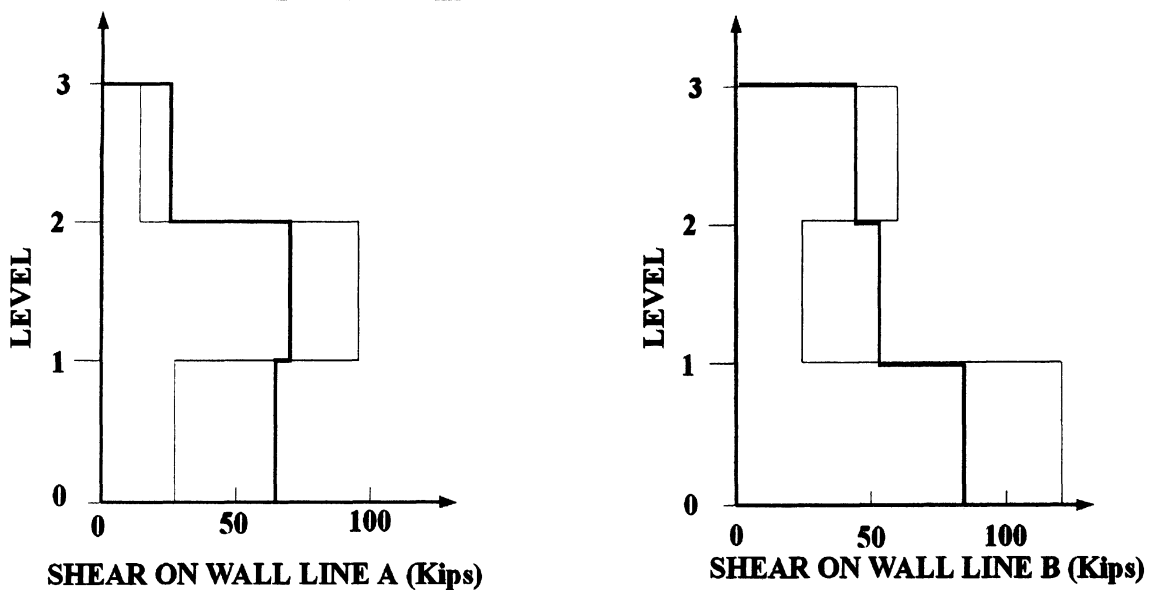


Figure 8-8. Computed shears of walls on lines A and B

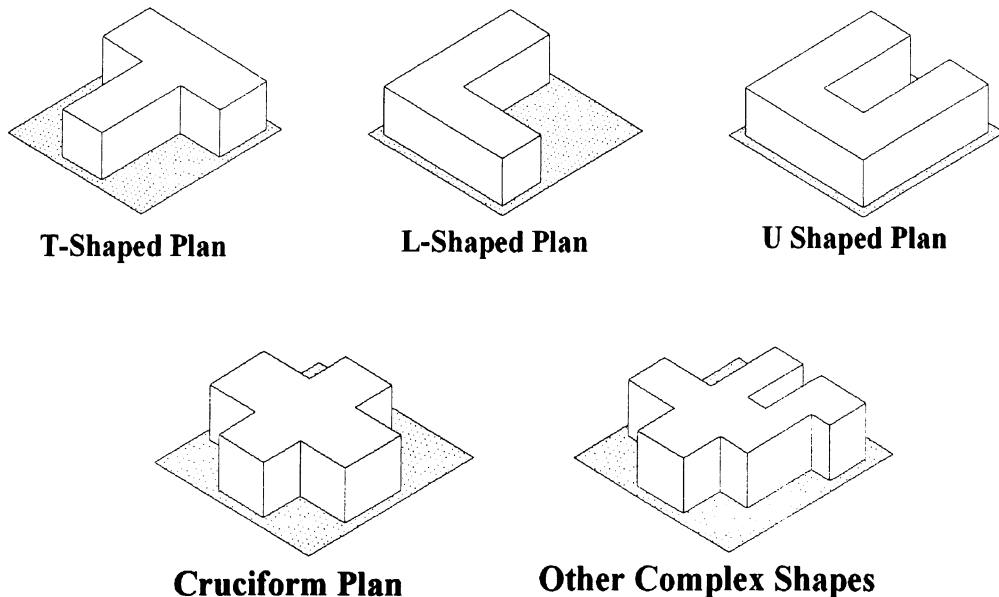


Figure 8-9. Typical plan Irregularities

Alaskan earthquake of March 27, 1964 (see Figure 6-15).

Other classes of buildings deserving special attention to diaphragm design include those with relatively large openings in one or more of the floor decks (Figure 8-11) and tall buildings resting on a significantly larger low-rise part (Figure 8-12). In the later case, the action of the low-rise portion as the shear base and the corresponding redistribution of shear forces (kick-backs) may subject the diaphragm located at the junction of the low-rise and high-rise parts (and sometimes a number of floor diaphragms above and below the junction) to some significant in-plane shear deformations.

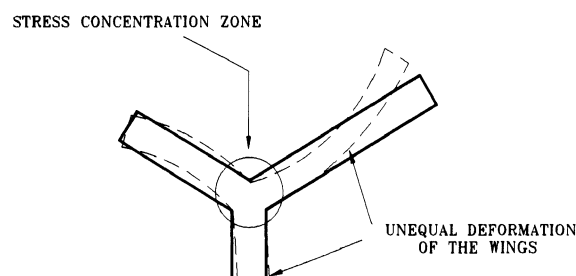


Figure 8-10. Fan-like deformation of wings causes stress concentration at the junction

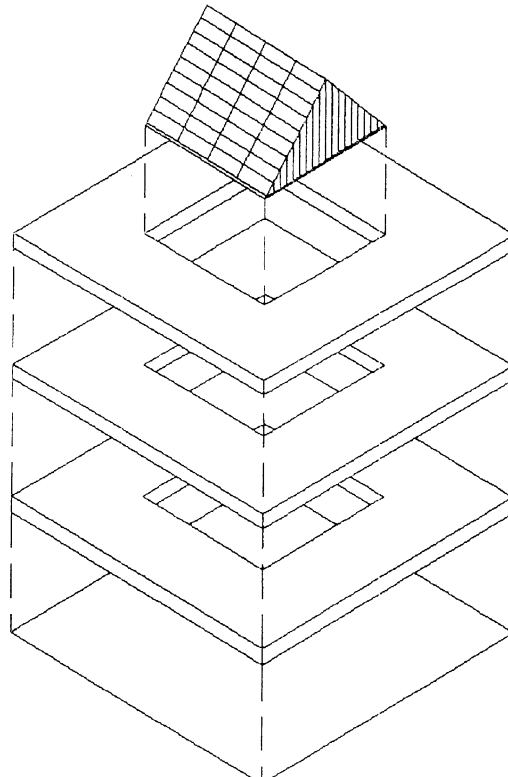


Figure 8-11. Significant floor openings are cause for concern

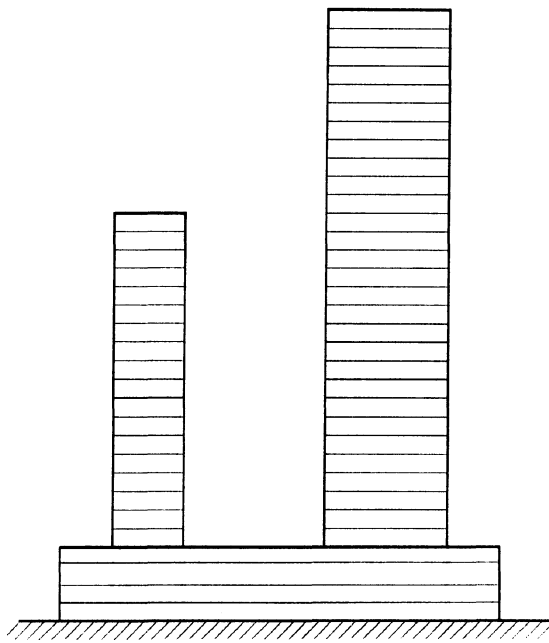


Figure 8-12. Elevation of towers on an expanded low-rise base

8.5 CODE PROVISIONS FOR DIAPHRAGM DESIGN

8.5.1 UBC-97, ASCE 7-95, and IBC-2000 Provisions

Diaphragm design provisions contained in the UBC-97, ASCE 7-95 and IBC-2000 are similar but vary in the degree of detailed information they provide. All these model codes contain a clause limiting the in-plane deflection of the floor diaphragms as follows:

The deflection in the plane of the diaphragm, as determined by engineering analysis, shall not exceed the permissible deflection of attached elements. Permissible deflection shall be that deflection which will permit the attached element to maintain its structural integrity under the individual loading and continue to support the prescribed loads.

UBC-97 requires the roof and floor diaphragms to be designed to resist the forces determined in accordance with:

$$F_{px} = \frac{F_t + \sum_{i=x}^n F_i}{\sum_{i=x}^n W_i} w_{px} \quad (8-1)$$

The minimum value of F_{px} to be used in analysis is $0.5C_a I w_{px}$. However, it need not exceed $1.0C_a I w_{px}$ where:

C_a = seismic coefficient (see section 5.3)

I = Importance factor (see Section 5.3)

i = Index identifying the i th level above the base

x = Floor level under design consideration

W = Total seismic dead load of the building

F_i = the lateral force applied to level i .

F_t = that portion of the base shear, V , considered concentrated at the top of the structure in addition to F_n

W_i = the portion of W at level i .

w_{px} = the weight of the diaphragm and the elements tributary thereto at level x , including 25% of the floor live load in storage and warehouse occupancies.

UBC-97 makes an exception for buildings of no more than three stories in height excluding basements, with light-frame construction and for other buildings not more than two stories in height excluding basements, diaphragm design forces may be estimated using a simplified procedure as follows:

$$F_{px} = \frac{3.0C_a}{R} w_{px} \quad (8-2)$$

where R is the numerical coefficient representative of the inherent overstrength and global ductility of the lateral-force-resisting system as described in Chapter 5. In the above equation, F_{px} should not be less than $0.5C_a w_{px}$ and need not exceed $C_a w_{px}$.

ASCE 7-95 requires the floor and roof diaphragms to be designed for a minimum seismic force equivalent to 50% of the seismic coefficient C_a times the weight of the

diaphragm. Diaphragm connections can be positive connections, mechanical or welded.

IBC-2000 requires the roof and floor diaphragm to be designed to resist the force F_p as follows:

$$F_p = 0.2I_E S_{DS} w_p + V_{px} \quad (8-3)$$

where:

F_p = The seismic force induced by the parts.

I_E = Occupancy importance factor (see Section 5.4.2).

S_{DS} = The short period site design spectral response acceleration coefficient (see Section 5.4.6).

w_p = The weight of the diaphragm and other elements of the structure attached to.

V_{px} = The portion of the seismic shear force at the level of diaphragm, required to be transferred to the VLLR elements because of the offsets or changes in stiffness of the VLLR elements above or below the diaphragm.

Notice that vertical distribution of lateral forces in IBC-2000 takes place in accordance with Equations 5-25 and 5-26 (see Section 5.4.13) which do not necessarily conform with the distributions obtained according to the UBC-97 formulas.

IBC-2000 provisions also require that diaphragms be designed to resist both shear and bending stresses resulting from these forces. Ties or struts should be provided to distribute the wall anchorage forces.

Obviously, the floor or roof diaphragm at every level need to be designed to span horizontally between the VLLR elements and to transfer the force F_{px} to these elements (see Figure 8-13a). All contemporary model codes require the diaphragms to be designed to transfer lateral forces from the vertical lateral load resisting elements above the diaphragm to the other VLLR elements below the diaphragm due to offsets in the placement of VLLR elements or due to changes in stiffness of these elements. For example, in Figure 8-13b, the

force P_1 has to be transferred by the diaphragm to the VLLR elements below the diaphragm since the VLLR element above the diaphragm has been discontinued at this level. In addition, the force P_2 from the other VLLR element above, has to be redistributed among the VLLR elements below the diaphragm. The diaphragm must be designed to transfer these additional loads.

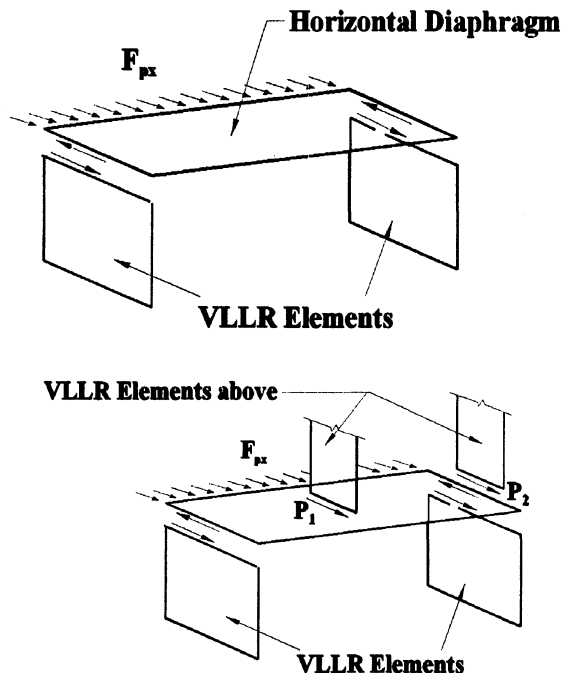


Figure 8-13. Code provisions for diaphragm design

As per UBC-97, additional requirements for the design of diaphragms are as follows:

Diaphragms supporting concrete or masonry walls should be designed with continuous ties between diaphragm chords to distribute the anchorage forces into the diaphragm. Added chords of subdiaphragms may be used to form subdiaphragms to transmit the anchorage forces to the main continuous crossties. The length to width ratio of the wood structural subdiaphragms should not exceed 2½ to 1. Diaphragm deformations should also be considered in the design of supported walls. Furthermore, in design of wood diaphragms providing lateral support for concrete or

masonry walls in seismic zones 2, 3, and 4, anchorage should not be accomplished by use of toenails or nails subjected to withdrawal. In addition, wood framing should not be used in cross-grain bending or tension.

For structures in Seismic Zones 3 and 4 having a plan irregularity of type 2 in Table 5-10, diaphragm chords and drag members should be designed considering independent movement of the projecting wings of the structure. Each of these diaphragm elements should be designed for the more severe of the following two conditions:

1. Motion of the projecting wings in the same direction; and
2. Motion of the projecting wings in opposing directions.

This requirement is considered satisfied if a three-dimensional dynamic analysis according to the code provisions is performed.

As a requirement for flexible diaphragms, the design seismic forces providing lateral support for walls or frames of masonry or concrete are to be based on Equation 8-1 and determined with the value of the response modification factor, R , not exceeding 4.0.

8.5.2 ACI 318-95 Provisions

The thickness of concrete slabs and composite topping slabs serving as structural diaphragms used to transmit earthquake forces cannot be less than 2 inches. This requirement reflects current usage in joist and waffle systems and composite topping slabs on precast floor and roof systems. Thicker slabs are required when the topping slab does not act compositely with the precast system to resist the design seismic forces.

A composite cast-in-place concrete topping slab on precast units is permitted to be used as a structural diaphragm provided the topping slab is reinforced and its connections are proportioned and detailed for complete transfer of forces to the elements of the lateral force resisting system. A bonded topping slab is required so that the floor or roof system can provide restraint against slab buckling.

Reinforcement is required to ensure the continuity of the shear transfer across precast joints. The connection requirements are to promote provisions of a complete system with necessary shear transfers. Obviously, the cast-in-place topping on a precast floor or roof system can be used without the composite action provided that the topping alone is proportioned and detailed to resist the design forces. In this case, a thicker topping slab has to be provided.

The shear strength requirements are the same as those for slender structural walls (see Chapter 10). The term A_{cv} in the equation for calculating the nominal shear strength refers to the thickness times the width of the diaphragm.

8.6 DESIGN EXAMPLES

As discussed in Chapter 6, it is desirable from the structural point of view to have regular buildings with minimal offset in the location of VLLR elements and without sudden changes in stiffness from floor to floor. Quite often, however, other requirements of the project (such as architectural considerations) control these parameters and the structural engineer is faced with buildings that are considered irregular in terms of seismic behavior and design.

Diaphragm design consists primarily of the following tasks:

1. Determining the lateral force distribution on the diaphragm and computing diaphragm shears and moments at different locations.
2. Providing adequate in-plane shear capacity in the diaphragm to transfer lateral forces to the VLLR elements.
3. Providing suitable connection between the diaphragm and the VLLR elements.
4. Design of boundary members or reinforcement to develop chord forces, and
5. Computing diaphragm deflections, when necessary, to ascertain that the diaphragm is stiff enough to support the curtain walls, etc. without excessive deflections.

In addition, the diaphragm must be designed and detailed for local effects caused by various openings such as those caused by the elevator shafts. Parking structure diaphragms with ramps are a special case of diaphragms with openings. The effect of the ramp attachment to floors above and below the ramp should be considered in lateral force distribution, especially for non-shear wall buildings.

In this section, the current design procedures for seismic design of floor diaphragms are demonstrated by means of four design examples which are worked out in detail. In the first example, a concrete floor diaphragm at the top of a parking level under a two story wood framed apartment building is designed. The second example explains diaphragm design for a four story concrete parking structure, which has setbacks in elevation of the building and the shear walls. In the third example, the metal-deck diaphragm of a three story steel framed office building is designed. Finally, the fourth example, explains the wood diaphragm design

for a typical one story neighborhood shopping center.

EXAMPLE 8-1

It is proposed to build a two story wood framed apartment building on top of one story concrete parking. The building will be located in a zone of high seismicity. The concrete floor supporting the wood construction (see Figure 8-14) will be a 14 inch thick, hard rock concrete, flat plate ($f_c' = 4000 \text{ lb/in}^2$). The lateral force resisting system for the concrete parking structure consists of concrete block masonry walls ($f_m' = 3000 \text{ lb/in}^2$). Given that the superimposed dead load from the two story wood framing above is 65 pounds per square foot, design the concrete diaphragm per typical requirements of the modern model codes. Floor to floor height is 10 feet. Assume that the structural analysis of the building has produced a seismic base shear coefficient of 0.293 for strength design purposes ($V=0.293W$).

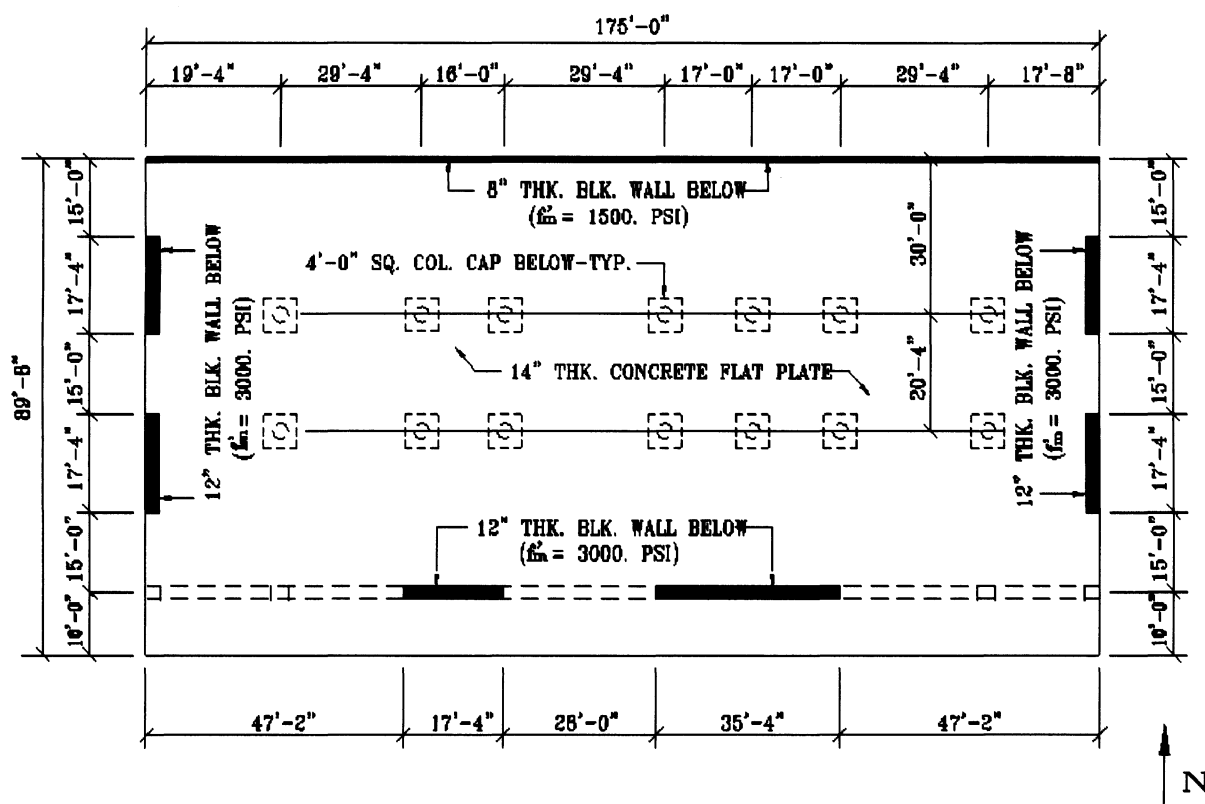


Figure 8-14. Second floor framing plan (Example 8-1)

SOLUTION

- Dead loads and seismic shears:

Superimposed dead load from wood framing above = 65 lb/ft²

Concrete slab at 150 lb/ft³ = (14/12)(150) = 175 lb/ft²

Miscellaneous (M + E + top half of column weights) = 10 lb/ft²

Total floor weight = (175)(89.66)(65+175+10) = 3922.6 kips

N-S walls:

12-in walls at 124 lb/ft² = 4(5)(17.33)(0.124) = 43 kips

E-W walls:

8" wall at 78 lb/ft² = (5)(175)(0.078) = 68.25 kips

12" walls at 124 lb/ft² = (5)(17.33+35.33)(0.124) = 32.65 kips

The weight of the walls parallel to the applied seismic force does not contribute to the diaphragm shears. However, in general, they are included conservatively in the design of concrete floor diaphragms. In this example, the weight of the walls parallel to the applied seismic force is not included in calculating diaphragm shears.

E-W weight = $W_x = 3922.6 + 43 = 3965.6$ kips

N-S weight = $W_y = 3922.6 + 68.25 + 32.65 = 4023.5$ kips

- Base shears:

$$F_{Py} = 0.293(3965.6) = 1161.9 \text{ kips (in } y \text{ direction)}$$

$$F_{Px} = 0.293(4023.5) = 1178.9 \text{ kips (in } x \text{ direction)}$$

- Center of mass (see Figure 8-15):

In computing the location of the center of mass of the walls it is generally assumed that

one half of the height of a wall above and below the diaphragm will contribute to the mass of each floor. The parameters needed for determination of the center of mass of the walls are calculated in Table 8-1. Therefore, the center of mass of the walls is located at:

$$x_1 = \frac{\sum xW}{\sum W} = \frac{12,703.0}{143.85} = 88.31 \text{ ft}$$

$$y_1 = \frac{\sum yW}{\sum W} = \frac{8,564.1}{143.85} = 59.53 \text{ ft}$$

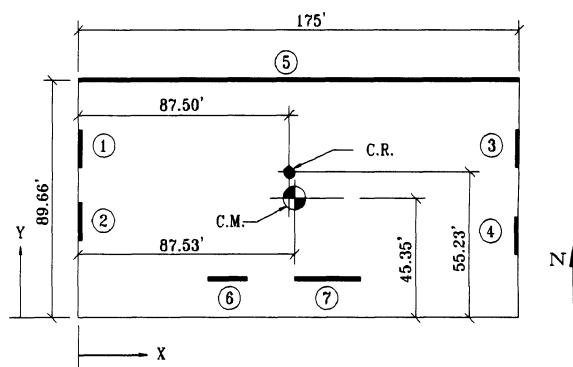


Figure 8-15. Locations of centers of mass and rigidity.

Since the slab is of uniform thickness, the center of mass of the floor coincides with its geometric centroid:

$$x_2 = 87.50 \text{ ft}$$

$$y_2 = 44.83 \text{ ft}$$

Location of the combined center of mass:

$$x_m = \frac{143.9(88.31) + 3922.6(87.5)}{143.9 + 3922.6} = 87.53 \text{ ft}$$

$$y_m = \frac{143.9(59.53) + 3922.6(44.83)}{143.9 + 3922.6} = 45.35 \text{ ft}$$

- Center of rigidity:

For a cantilever wall (see Figure 8-16):

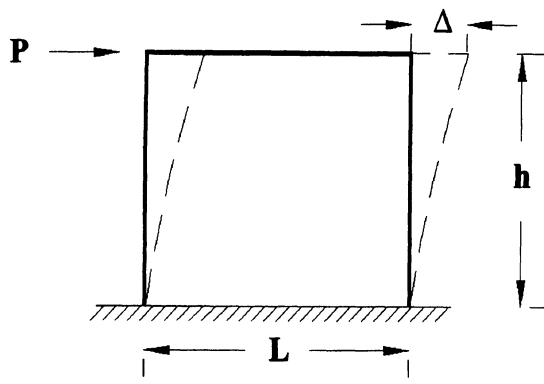


Figure 8-16. Deformation of a cantilever wall panel

$$\Delta = \frac{Ph^3}{3EI} + \frac{1.2Ph}{AG}$$

Denoting wall thickness by t and assuming $G = 0.40E$ for masonry, this relation may be rewritten as:

$$\Delta = \frac{4P(h/L)^3}{Et} + \frac{3P(h/L)}{Et}$$

The relative wall rigidities, $R = 1/D$, may be computed assuming a constant value of P , say $P=1,000,000$ pounds. Using the parameters generated in Tables 8-2 and 8-3, the location of the center of rigidity is established as:

$$x_r = \frac{\sum xR_y}{\sum R_y} = \frac{4886.0}{55.84} = 87.50 \text{ ft}$$

$$y_r = \frac{\sum yR_x}{\sum R_x} = \frac{6506.93}{117.8} = 55.23 \text{ ft}$$

- Torsional eccentricity:

$$e_x = x_r - x_m = 87.5 - 87.53 \approx 0 \text{ ft}$$

$$e_y = y_r - y_m = 55.23 - 45.35 = 9.88 \text{ ft}$$

Table 8-1 Center of Mass Calculations for Example 8-1

Wall No.	Weight, Lb/ft ²	Length, ft	Area, ft ²	Weight, Kips	Dir.	x, ft	xW, ft-kips	y, ft	yW, ft-kips
1	124	17.33	86.65	10.74	y	0.50	5.37	66.00	708.84
2	124	17.33	86.65	10.74	y	0.50	5.37	33.67	361.62
3	124	17.33	86.65	10.74	y	174.50	1,874.10	66.00	708.84
4	124	17.33	86.65	10.74	y	174.50	1,874.10	33.67	361.62
5	78	175.00	875.00	68.25	x	87.50	5,971.88	89.33	6,096.78
6	124	17.33	86.65	10.74	x	55.84	559.72	10.00	107.40
7	124	35.33	176.70	21.90	x	110.16	2,412.50	10.00	219.00
Σ			143.85				12,703.		8,564.

Table 8-2. Relative Rigidity of the Walls

Wall No.	Height, ft	Length, ft	H/L	E, lb/in ²	t, in.	Δ	R = 1/ Δ
1	10	17.33	0.5770	3,000,000	11.625	0.0716	13.96
2	10	17.33	0.5770	3,000,000	11.625	0.0716	13.96
3	10	17.33	0.5770	3,000,000	11.625	0.0716	13.96
4	10	17.33	0.5770	3,000,000	11.625	0.0716	13.96
5	10	175.00	0.0571	1,500,000	7.625	0.0150	66.67
6	10	17.33	0.5770	3,000,000	11.625	0.0716	13.96
7	10	35.33	0.2830	3,000,000	11.625	0.0269	37.17

Table 8-3. Center-of-Rigidity Calculations for Example 8-1

Wall No.	Dir.	x	y	R _x	R _y	xR _y	yR _x
1	y	0.50	----	----	13.96	6.98	----
2	y	0.50	----	----	13.96	6.98	----
3	y	174.50	----	----	13.96	2,436.02	----
4	y	174.50	----	----	13.96	2,436.02	----
5	x	----	89.33	66.67	----	----	5,995.63
6	x	----	10.00	13.96	----	----	139.60
7	x	----	10.00	37.17	----	----	371.70
Σ				117.80	55.84	4,886.00	6,506.93

Table 8-4. Wall Shear for Seismic forces in the N-S Direction

Wall No	R _x	R _y	d _x , ft	d _y , ft	Rd	Rd ²	F _v , kips	F _{t-1} , kips	F _{t-2} , kips	F _{total-1} , kips	F _{total-2} , kips	F _{design} , kips
1	0	13.96	-87.00	----	-1214.52	105,663	294.70	-20.70	20.70	274.00	315.40	315.40
2	0	13.96	-87.00	----	-1214.52	105,663	294.70	-20.70	20.70	274.00	315.40	315.40
3	0	13.96	87.00	----	1214.52	105,663	294.70	20.70	-20.70	315.40	274.00	315.40
4	0	13.96	87.00	----	1214.52	105,663	294.70	20.70	-20.70	315.40	274.00	315.40
5	66.67	0	----	34.10	2273.45	77,524	0.00	38.80	-38.80	38.80	-38.80	38.80
6	13.96	0	----	-45.23	-631.41	28,559	0.00	-10.80	10.80	-10.80	10.80	10.80
7	37.17	0	----	-45.23	-168.20	76,041	0.00	-28.70	28.70	-28.70	28.70	28.70
Σ												1179.50

Modern codes generally require shifting of the center of mass of each level of the building a minimum of 5% of the building dimension at that perpendicular to the direction of force in addition to the actual eccentricity:

$$e_x = 0.05(175) = \pm 8.75 \text{ ft}$$

$$e_y = 9.88 \pm 0.05(89.67) = 14.36 \text{ ft or } 5.4 \text{ ft}$$

- Torsional Moments:

$$T_y = F_{Py} e_x = 1178.9(\pm 8.75) = \pm 10315.4 \text{ ft-k}$$

$$T_{x+} = F_{Px} e_{y+} = 1161.9(14.36) = 16,684.9 \text{ ft-k}$$

$$T_x = F_{Px} e_y = 1161.9(5.40) = -6,274.2 \text{ ft-k}$$

In-plane forces in the walls due to direct shear are computed from

$$F_{vx} = V_x \frac{R_x}{\sum R_x}$$

$$F_{vy} = V_y \frac{R_y}{\sum R_y}$$

and the in-plane wall forces due to torsion are computed from

$$F_{tx} = T_x \frac{Rd}{\sum Rd^2}$$

$$F_{ty} = T_y \frac{Rd}{\sum Rd^2}$$

where d is the distance of each wall from the center of rigidity. Using these formulas, the wall forces for seismic force acting in the N-S and E-W directions are calculated and reported in Tables 8-4 and 8-5, respectively. Note that the contribution of torsion, if it reduces the magnitude of the design wall shears, is ignored. The design shear forces are summarized in Table 8-6.

Table 8-5. Wall Shear for Seismic forces in the E-W Direction

Wall No	R_x	R_y	d_x ft	d_y ft	Rd	Rd^2	F_v , kips	F_{t-1} , kips	F_{t-2} , kips	$F_{total-1}$, kips	$F_{total-2}$, kips	F_{design} Kips
1	0	13.96	-87.00	----	-1214.52	105,663	0.00	33.52	12.60	33.52	12.60	33.52
2	0	13.96	-87.00	----	-1214.52	105,663	0.00	33.52	12.60	33.52	12.60	33.52
3	0	13.96	87.00	----	1214.52	105,663	0.00	-33.52	-12.60	-33.52	-12.60	33.52
4	0	13.96	87.00	----	1214.52	105,663	0.00	-33.52	-12.60	-33.52	-12.60	33.52
5	66.67	0	----	34.10	2273.45	77,524	657.60	594.85	-23.60	594.85	634.00	634.00
6	13.96	0	----	-45.23	-631.41	28,559	137.70	155.10	6.60	155.10	144.30	155.10
7	37.17	0	----	-45.23	-168.20	76,041	366.60	413.00	17.50	413.00	384.10	413.00
Σ												1,162.95

or

Table 8-6. Shear Design Forces (kips)

Wall No	Wall L ft.	E-W Load	N-S Load	Max Load
1	17.33	33.52	315.40	315.40
2	17.33	33.52	315.40	315.40
3	17.33	33.52	315.40	315.40
4	17.33	33.52	315.40	315.40
5	175.00	634.00	38.80	634.00
6	17.33	155.10	10.80	155.10
7	35.33	413.00	28.70	413.00

- Diaphragm design for seismic force in the N-S direction:

The wall forces and the assumed direction of torque due to the eccentricity are shown in Figure 8-17. Using this information, the distribution of the applied force on the diaphragm may be calculated. Denoting the left and right diaphragm reactions per unit length by V_L and V_R , from force equilibrium (see Figure 8-18),

$$V_L \frac{175}{2} + V_R \frac{175}{2} = 1179.5 \text{ Kips}$$

or

$$V_L + V_R = 13.48 \quad (I)$$

from moment equilibrium:

$$\left(\frac{175}{3}\right) \frac{175}{2} V_L + 2\left(\frac{175}{3}\right) \frac{175}{2} V_R = 1179.5(96.25)$$

$$V_L + 2V_R = 22.24 \quad (II)$$

Solving equations I and II for V_L and V_R yields:

$$V_L = 4.72 \text{ k/ft, and}$$

$$V_R = 8.76 \text{ k/ft.}$$

The mid-span diaphragm moment¹ (Figure 8-18) is:

$$M = 548(87.5) - 19.4(79.66) - 4.72(87.5)(58.33)/2 - 6.74(87.5)(29.17)/2 = 25,758 \text{ ft-kips}$$

Check slab shear stress along walls 1 and 2:

$$L = 17.33 \text{ ft}, \quad t = 14 \text{ inches}$$

Slab capacity without shear reinforcement

$$\phi V_c = \phi(2) \sqrt{f'_c b t}$$

$$= \frac{0.85(2)\sqrt{4000}(14)(17.33)(12)}{1000}$$

¹ The mid-span moment has been used in this example to demonstrate the chord design procedures. This moment, however, is not necessarily the maximum moment. In a real design situation the maximum moment should be calculated and used for the chord design.

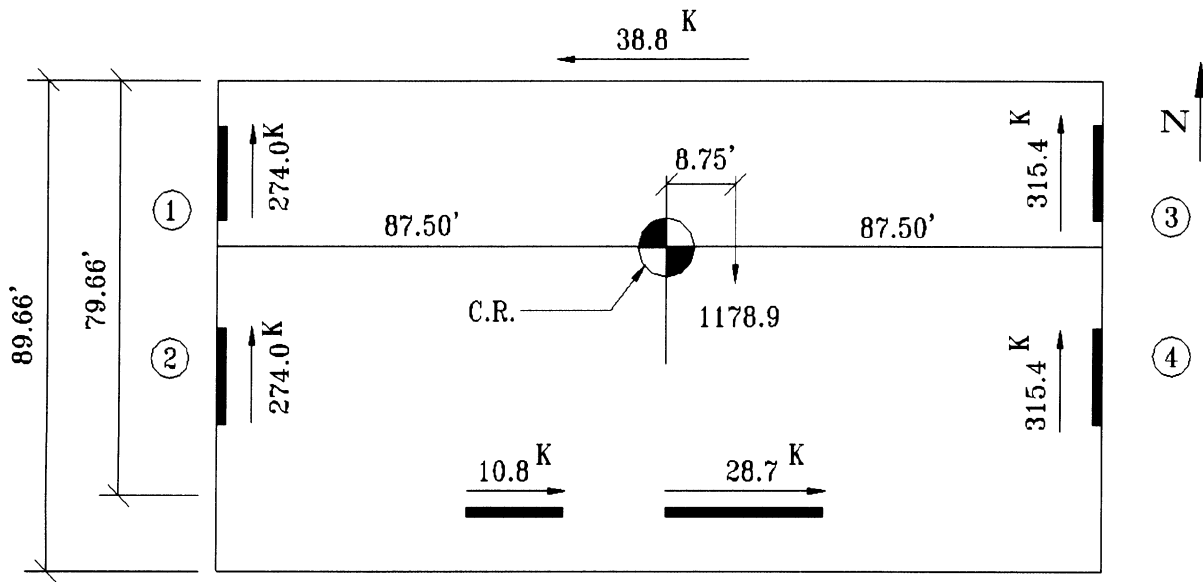


Figure 8-17. Design wall forces for seismic load in the N - S direction

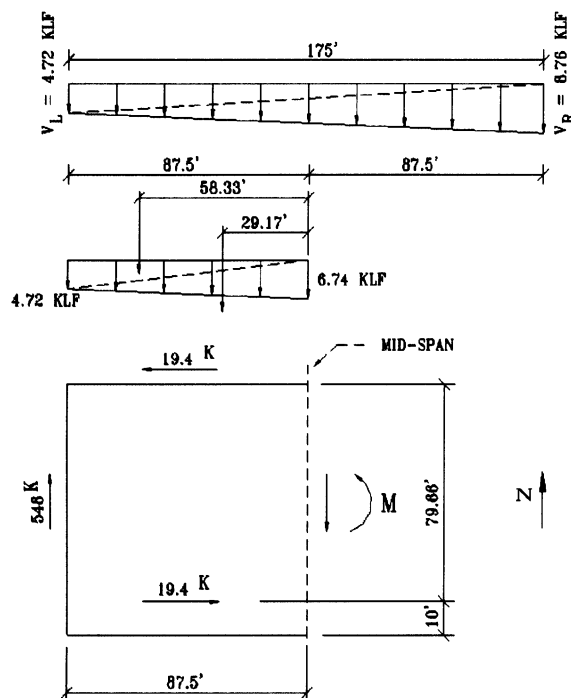


Figure 8-18 Force distribution and diaphragm moments for seismic load in the N-S direction.

$$= 313 \text{ kips} \approx 315.4 \text{ O.K.}$$

Chord Design:

$$T_u = \frac{M^1}{d} = \frac{1.0(25,758)}{(89.66 - 4.0)} = 301 \text{ kips}$$

$$A_s = \frac{T_u}{\phi f_y} = \frac{301}{0.9(60)} = 5.57 \text{ in}^2$$

Provide 6#9 chord bars ($A_s = 6.0 \text{ in}^2$) along the slab edges at the North and South sides of the building. Here, we have assumed that the chord bars will be placed over a 4 ft. strip of the slab.

- Diaphragm design for seismic force in the N-S direction:

A sketch of the wall forces indicating the assumed direction of the torque due to eccentricity is shown in Figure 8-19.

Similar to the N-S direction, the force and moment equilibrium equations may be used to obtain the distribution of lateral force on the diaphragm:

¹ Arguably, strict conformity with the UBC-97 would require this moment to be multiplied by a factor of 1.1 (UBC-97 Sec. 1612.2.1 Exception 2). No such requirement exists, however, in the IBC-2000 which replaces UBC-97.

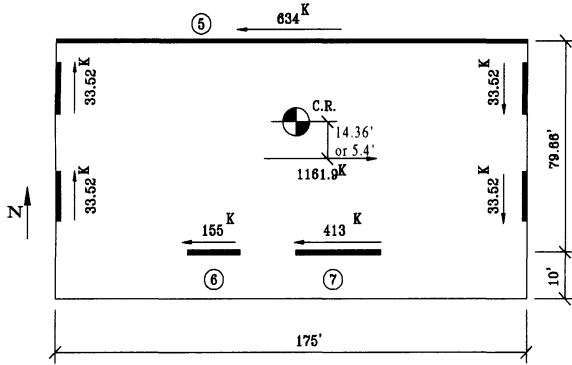


Figure 8-19. Design wall forces for seismic load in the E-W direction

$$V_L \frac{89.66}{2} + V_R \frac{89.66}{2} = 1162.95 \text{ Kips}$$

or

$$V_L + V_R = 25.95 \quad (\text{III})$$

and

$$\begin{aligned} V_L \frac{89.66}{2} (29.89) + V_R \frac{89.66}{2} (59.77) \\ = 1162.95(45.35) \end{aligned}$$

or

$$V_L + 2V_R = 39.36 \quad (\text{IV})$$

solving equations III and IV for V_L and V_R :

$$V_L = 12.54 \text{ k/ft and } V_R = 13.41 \text{ k/ft}$$

The mid-span diaphragm moment (Figure 8-20):

$$\begin{aligned} M &= 568(34.83) + 33.52(175) - \\ &12.55(44.83)(29.83)/2 - 12.98(44.83)(14.94)/2 \\ &= 12,916 \text{ ft-kips} \end{aligned}$$

Similarly, diaphragm moments at other locations, including the cantilever portion of the diaphragm can be calculated.

- Check diaphragm shear capacity:

along wall 5:

$$L = 175 \text{ ft, } t = 14 \text{ in.}$$

$$\phi V_c = \frac{0.85(2)\sqrt{4000}(14)(175)(12)}{1000}$$

$$= 3,161 \text{ kips} > 634 \text{ O.K.}$$

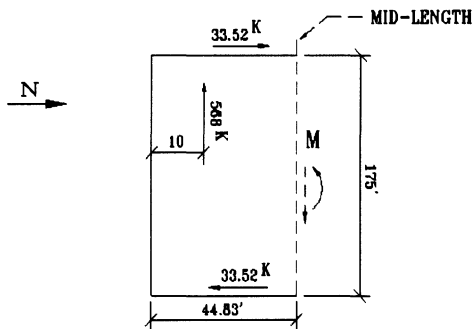
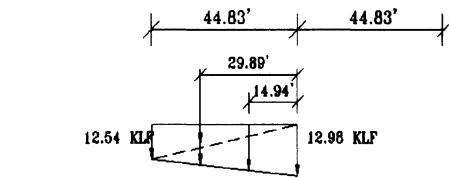
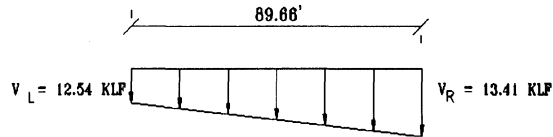


Figure 8-20. Force distribution and diaphragm moments for seismic load in the E-W direction

along wall 6:

$$L = 17.33 \text{ ft, } t = 14 \text{ in.}$$

$$\phi V_c = \frac{0.85(2)\sqrt{4000}(14)(17.3)(12)}{1000}$$

$$= 313 \text{ kips} > 155 \text{ O.K.}$$

along wall 7:

$$L = 35.33 \text{ ft, } t = 14 \text{ in.}$$

$$\phi V_c = \frac{0.85(2)\sqrt{4000}(14)(35.33)(12)}{1000}$$

$$= 638 \text{ kips} > 413 \text{ O.K.}$$

Chord Design:

$$T_u = \frac{M}{d} = \frac{12,916}{(175.0 - 1.0)} = 74.23 \text{ kips}$$

$$A_s = \frac{T_u}{\phi f_y} = \frac{74.23}{0.9(60)} = 1.37 \text{ in}^2$$

Provide 4#6 chord bars ($A_s = 1.76 \text{ in}^2$) along the slab edges at the East and West sides of the building where the maximum chord force occurs.

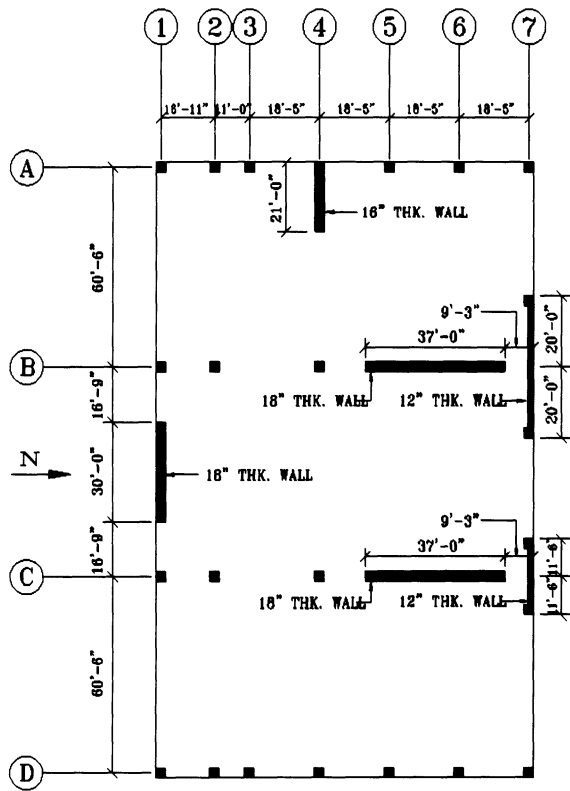


Figure 8-21. Ground floor framing plan (Example 8-2).

EXAMPLE 8-2

Perform a preliminary design the third floor diaphragm of the four story parking structure shown in Figures 8-21 through 8-25. The building is to be located in southern California (UBC seismic zone 4). Access to each floor will be provided from an adjacent parking structure that will be separated by a seismic joint. Typical floor and roof framing consists of a 5½

inches thick post-tensioned slabs spanning to 36 in. deep post-tensioned beams. Typical floor dead load for purposes of seismic design is estimated at 150 pounds per square foot. This includes contributing wall and column weights. Typical floor to floor height is 10 feet. This building is irregular and therefore needs to be analyzed using the dynamic response procedures. Furthermore, the redundancy factor for the building needs to be calculated and applied. For preliminary design purposes only, however, use the UBC-97 static lateral force procedure and ignore accidental torsion. Soil profile type is S_D , $I = 1.0$, $N_a = N_v = 1.0$. Use $f'_c = 5,000 \text{ lb/in}^2$ and $F_y = 60,000 \text{ lb/in}^2$.

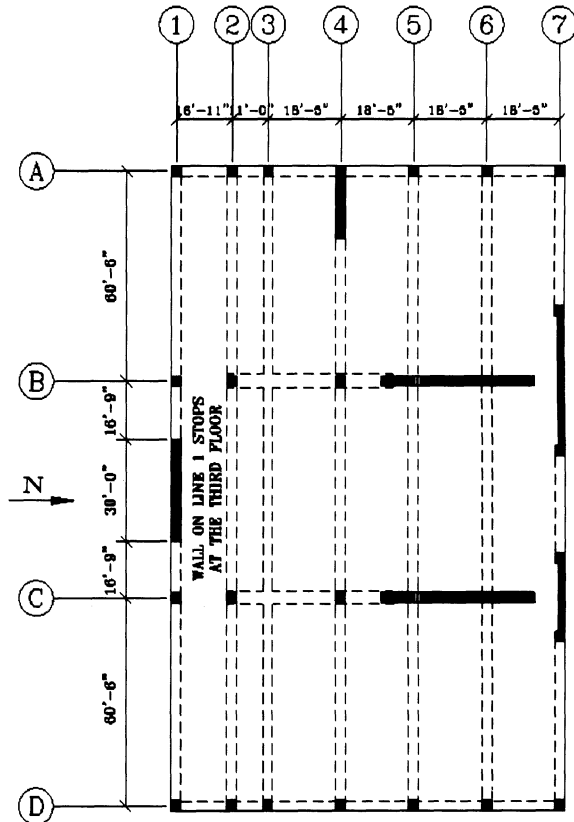


Figure 8-22. Second and third floor framing plan (Example 8-2)

SOLUTION

- Weight Computations:

$$\begin{aligned} \text{Roof Weight} &= (68')(185')(0.15 \text{ k/ft}^2) \\ &= 1887 \text{ kips} \end{aligned}$$

$$\begin{aligned}
 \text{4th Floor Weight} &= (85')(185')(0.15 \text{ k/ft}^2) \\
 &= 2359 \text{ kips} \\
 \text{3rd Floor Weight} &= (104')(185')(0.15 \text{ k/ft}^2) \\
 &= 2886 \text{ kips} \\
 \text{2nd Floor Weight} &= (104')(185')(0.15 \text{ k/ft}^2) \\
 &= 2886 \text{ kips} \\
 \text{Total Weight} &= 1887 + 2359 + 2(2886) \\
 &= 10018 \text{ kips}
 \end{aligned}$$

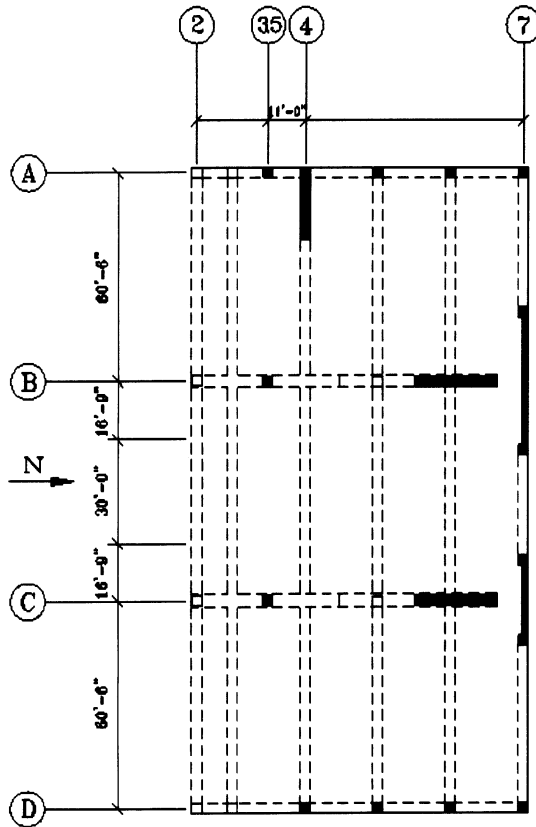


Figure 8-23. Fourth floor framing plan (Example 8-2)

- Design Lateral Forces

$$T = C_t (h_n)^{3/4}$$

Take $C_t = 0.02$

$$\therefore T = 0.02(40)^{3/4} = 0.318 \text{ Sec.}$$

$$\begin{aligned}
 \text{Base Shear } (V) &= \frac{C_a I}{R T} (W) \\
 &= \frac{0.64(1.0)}{4.5(0.318)} (W)
 \end{aligned}$$

$$\begin{aligned}
 &= 0.447(W) > (0.11C_a I)W \\
 &= 0.048W \\
 &> 0.8 \frac{Z N_v I}{R} (W) = 0.07W \\
 &> 2.5 \frac{C_a I}{R} (W) = 0.244W
 \end{aligned}$$

$$\therefore V = 0.244 W = 2444.4 \text{ kips}$$

$$F_x = (V - F_t) \frac{W_x h_x}{\sum W_x h_x}$$

$$F_{px} = \frac{F_t + \sum F_i}{\sum W_i} w_{px}$$

$$T = 0.318 \text{ Sec.} < 0.7 \text{ Sec.} \Rightarrow F_t = 0$$

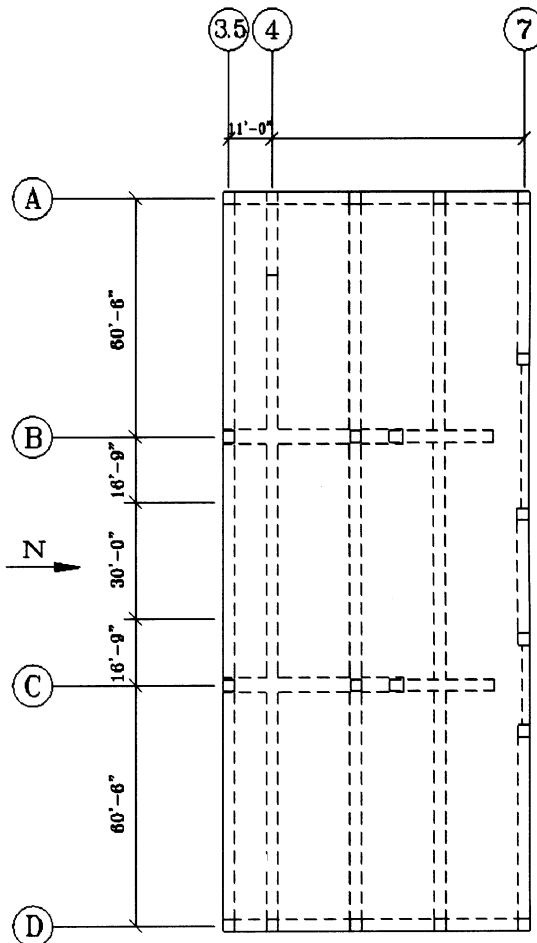


Figure 8-24. Roof framing plan (Example 8-2)

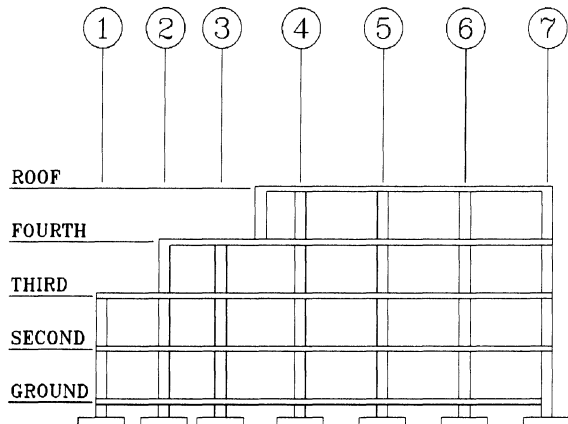


Figure 8-25. A section through the building (Example 8-2)

Values of F_{px} for various floors are calculated in Table 8-7. Concrete diaphragm is assumed to be rigid. The seismic shear forces acting on the walls were obtained by a computer analysis and are shown in Figures 8-26 and 8-27.

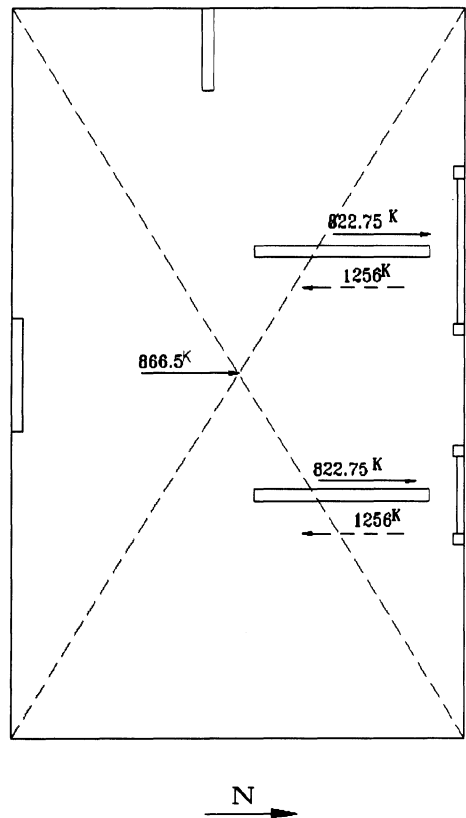


Figure 8-26. Forces on the third floor diaphragm due to N-S seismic loading (Wall shears above the diaphragm are shown with solid arrows while wall shears below the diaphragm are indicated by dashed lines.)

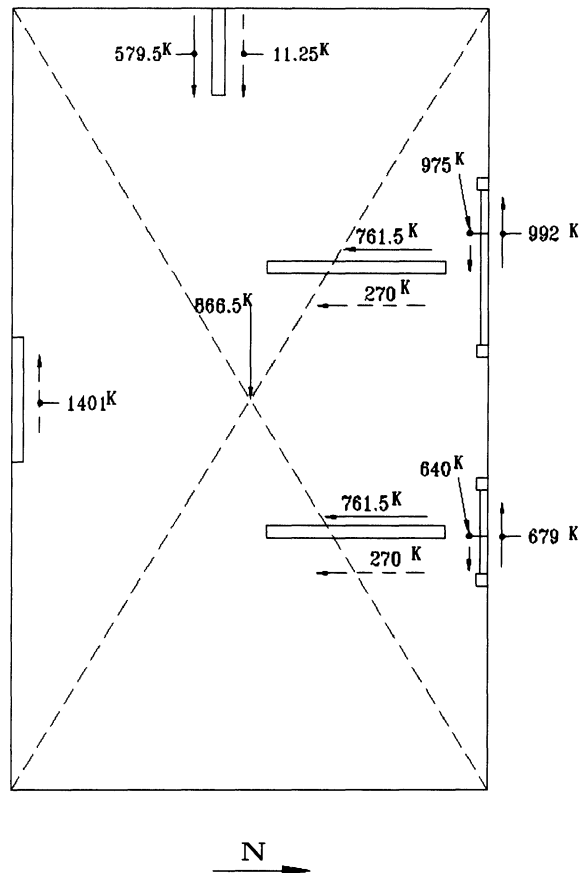


Figure 8-27. Forces on the third floor diaphragm due to E-W seismic loading (Wall shears above the diaphragm are shown with solid arrows while wall shears below the diaphragm are indicated by dashed lines.)

- Diaphragm Design in the N-S Direction:

Net shear forces acting on the walls and the corresponding diaphragm load, shear and moment diagrams are shown in Figure 8-28. Check 8" thick slab shear capacity along the walls on grid lines B and C:

Maximum slab shear = 283.75 kips

Slab capacity without shear reinforcement =

$$\phi V_c = \phi 2\sqrt{f_c} = \frac{0.85(2)\sqrt{5000}(5.5)(37)(12)}{1000}$$

$$= 294 > 283.75 \text{ kips} \quad \text{O.K.}$$

Therefore, no shear reinforcement seems to be required by the code.

Chord Design:

Table 8-7. Calculation of Diaphragm Design Forces for Example 8-2

Level	h_x , ft	W_x , Kips	$W_x \cdot h_x$	$\frac{W_x \cdot h_x}{\Sigma W_i \cdot h_i}$	F_x , Kips	ΣF_x , Kips	ΣW_i , Kips	$\frac{\Sigma F_i}{\Sigma W_i}$	F_{px} , Kips
Roof	40	1,887	75,480	0.324	792.4	792.4	1,887	0.420	792.4
4th	30	2,359	70,770	0.304	743.0	1,535.4	4,246	0.362	853.1
3rd	20	2,886	57,720	0.248	606.0	2,141.4	7,132	0.300	866.5
2nd	10	2,886	28,860	0.124	303.0	2,444.4	10,018	0.244	704.2
Σ		10,018	232,830	1.00	2444.4				

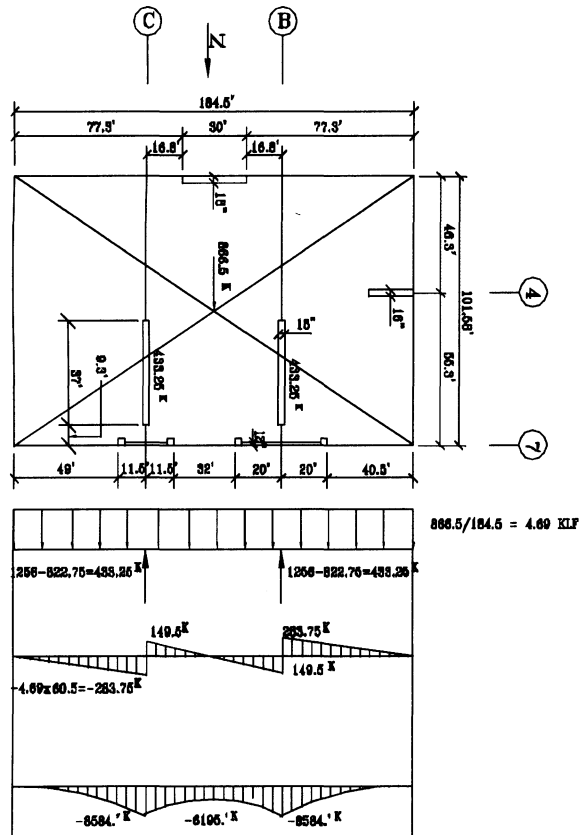


Figure 8-28. Diaphragm loading, shear, and moment diagrams for seismic load in the N-S direction

$$T_u = \frac{M}{d} = \frac{8,586}{(101.58 - 1.0)} = 85.4 \text{ kips}$$

$$A_s = \frac{T_u}{\phi f_y} = \frac{85.4}{0.9(60)} = 1.58 \text{ in}^2$$

Therefore provide 3 #7 chord bars ($A_s = 1.8 \text{ in}^2$) along slab edges on the North and South sides of the building.

- Diaphragm Design in the E-W Direction:

Net shear forces acting on the walls and the corresponding diaphragm load, shear and moment diagrams are shown in Figure 8-29.

Moment Calculations:

at Section A-A:

$$M_{A-A} = 1,401(25.4) - \frac{8.53(25.4)^2}{2}$$

$$= 32,833 \text{ ft-kips}$$

at Section B-B:

$$M_{B-B} = 1,401(50.8) - 590.6(4.5) - \frac{8.53(50.8)^2}{2}$$

$$= 57,505 \text{ ft-kips}$$

at Section C-C:

$$M_{C-C} = 56(25.4) - \frac{8.53(25.4)^2}{2}$$

$$+ \frac{16.1}{37}(1031)(63.5)$$

$$= 27,158 \text{ ft-kips}$$

∴ Estimated maximum moment¹ = 57,505 ft-k
Chord Design:

$$T_u = \frac{M}{d} = \frac{57,505}{(184.5 - 2.0)} = 315 \text{ kips}$$

¹ A more accurate value of the maximum moment may be obtained by reading the moment diagram plotted to a larger scale.

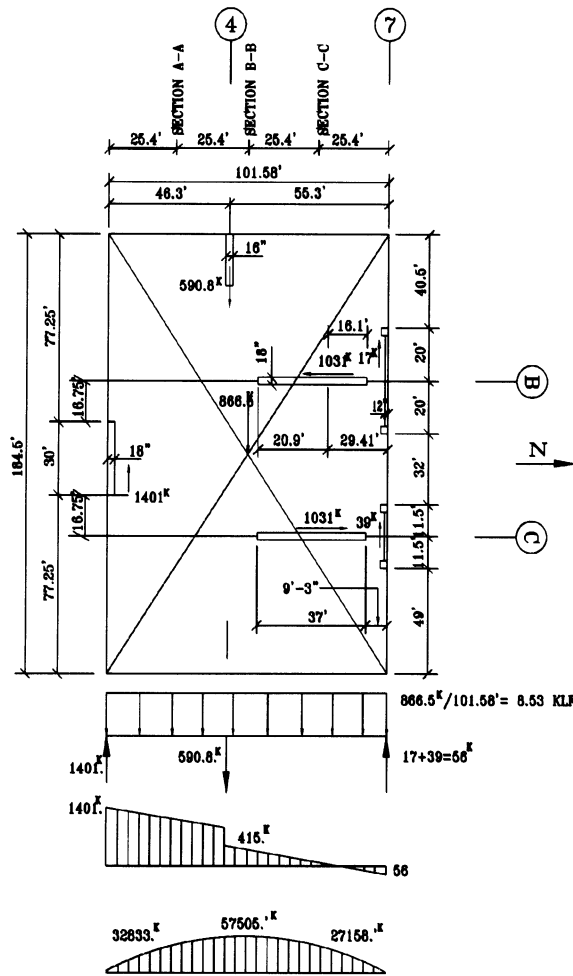


Figure 8-29. Diaphragm loading, shear, and moment diagrams for seismic load in the E-W direction

$$A_s = \frac{T_u}{\phi f_y} = \frac{315}{0.9(60)} = 5.83 \text{ in}^2$$

Therefore provide 6 #9 chord bars ($A_s = 6.0 \text{ in}^2$) along slab edges on the east and west sides of the building

$$C_u = T_u$$

Compression C_u to be resisted by edge beam and concrete slab. Check 5½-in.-thick slab shear capacity along the wall on line 1: For $L = 30 \text{ ft}$, slab capacity without shear Reinforcement is:

$$\phi V_c = \frac{0.85(2)\sqrt{5000}(5.5)(30)(12)}{1000} = 238 \text{ kips} < 1401 \text{ N.G.}$$

for $L = 184.5 \text{ ft}$, slab capacity without shear reinforcement is:

$$\phi V_c = \frac{0.85(2)\sqrt{5000}(5.5)(184.5)(12)}{1000} = 1465 \text{ kips} > 1401 \text{ O.K.}$$

Check the capacity of 30 foot long slab with #4 bars @ 18 inches, at the top and bottom of the slab:

$$\phi V_c = 238 \text{ kips}$$

$$\#4 @ 18'' A_s = 0.13 \text{ in}^2/\text{ft}$$

$$\phi V_s = (0.85)(2 \times 0.13)(60)(30 \text{ ft}) = 398 \text{ kips}$$

$$\phi V_n = 398 + 238 = 636 \text{ kips} < 1401 \text{ kips}$$

Drag struts are needed to transfer the difference ($1401 - 636 = 765 \text{ kips}$).

- Design of Drag Struts (see Figure 8-30):

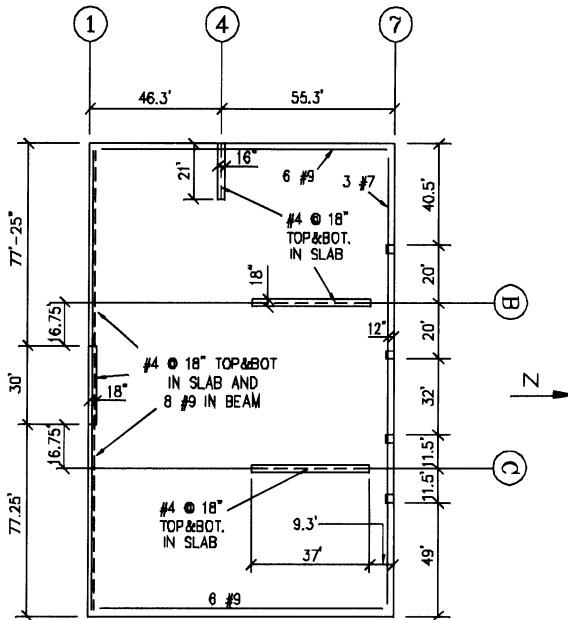


Figure 8-30. Diaphragm chord, drag, and shear reinforcement

The two beams along the Grid line 1 may be designed to transfer the slab shear into the walls:

$$A_s = \frac{\left(\frac{765}{2}\right)}{(0.9)(60)} = 7.08 \text{ in}^2$$

\therefore Provide 8 #9 bars ($A_s = 8.0 \text{ in}^2$) in the beams for seismic shear transfer.

Drag strut length provided = $2(77.3) = 154.6 \text{ ft}$

Capacity of slab along drag strut

$$= \frac{0.85(2)\sqrt{5000}(5.5)(154.6)(12)}{1000} \\ = 1228 \text{ kips} > 693 \quad \text{O.K.}$$

Check shear capacity of $5\frac{1}{2}$ -in. thick slab at the wall on grid line 4 to carry $590.8/2 = 295.4$ kips of shear (notice that slab occurs on both sides of the wall):

$$\phi V_c = \frac{0.85(2)\sqrt{5000}(5.5)(21)(12)}{1000} \\ = 167 \text{ kips} < 295.4 \quad \text{N.G.}$$

Therefore Shear reinforcement is required. Using #4 bars @ 18 inches at the top and bottom of the slab:

$$\phi V_s = (0.85)(2 \times 0.13)(60)(21) = 278 \text{ kips}$$

$$\phi V_n = 167 + 278 = 445 \text{ kips} > 295.4 \quad \text{O.K.}$$

Therefore drag struts are not required. It can be realized by observation that the slab shear capacity along the walls on the grid line 7 is sufficient. Check the shear capacity of the slab along the cross walls on grid lines *B* and *C*. Here again, slab occurs on both sides of the wall:

$$\phi V_c = \frac{0.85(2)\sqrt{5000}(5.5)(37)(12)}{1000} \\ = 294 \text{ kips} < \left(\frac{1031}{2}\right) = 515.5 \quad \text{N.G.}$$

Therefore shear Reinforcement is required. Try #4 bars @ 18 inches at the top and bottom of the slab:

$$\phi V_s = (0.85)(0.13 \times 2)(60)(37) = 490 \text{ kips}$$

$$\phi V_n = 294 + 490 = 784 \text{ kips} > 515.5$$

Therefore drag struts are not required.

EXAMPLE 8-3

Design the roof diaphragm of the three story steel framed building shown in Figure 8-31. The building is supported on the top of a one story subterranean concrete parking structure. The parking structure deck may be considered as the shear base for the steel structure. The lateral load resisting system for the steel building consists of moment resisting frames in both directions. Beams and columns which are not part of the lateral system are not shown in Figure 8-31. The floor construction consists of 3 1/4 inches of light-weight concrete on the top of a 3 inch deep, 20 gage, metal deck. The maximum spacing of floor purlins is 10 feet. Mechanical equipment is located on the roof, west of grid line D. The roof construction west of grid line D consists of 4 1/2 inches of hard rock concrete on the top of a 3 inch deep, 18 gage, metal deck. The maximum spacing of the roof purlins is 8 feet. The roof construction east of grid line D is similar to the typical floor construction.

The estimated total dead loads for seismic design are 100 psf at the typical floors, 200 psf at the mechanical areas of the roof, and 70 psf elsewhere on the roof. The building is located in area of high seismicity. A three dimensional computer analysis of the building has resulted in a working stress level (WSD) roof diaphragm design force of 364.8 kips in the N-S and E-W directions. The distribution of the roof diaphragm shear among the moment-resistant steel frames are shown in Figures 8-32 and 8-33.

SOLUTION

- Diaphragm Design in the E-W Direction

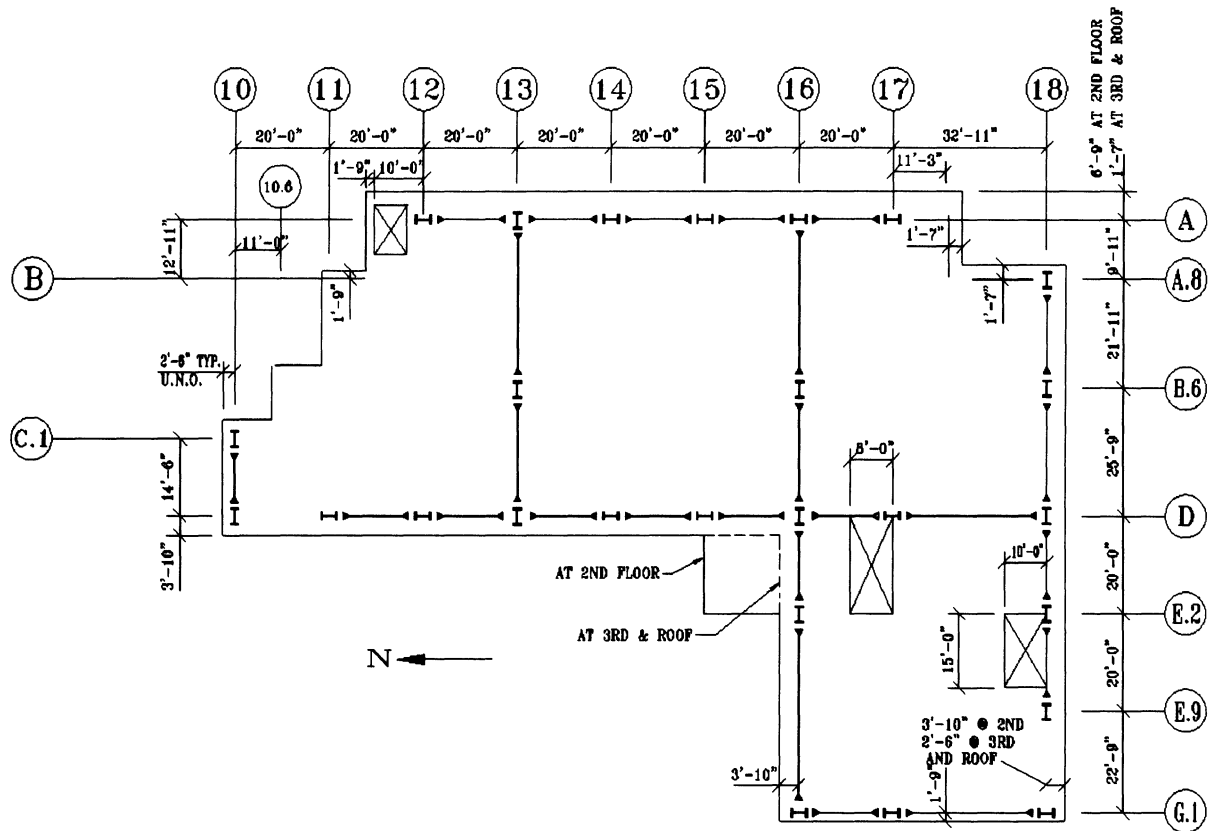


Figure 8-31. Typical floor framing plan for building of Example 8-3 (Opening shown exist on second and third floors only)

The design lateral force of 3604.8 kips is distributed along the roof in the same proportion as the mass distribution at this level. This loading pattern and the corresponding diaphragm shear diagram are shown in Figure 8-34. The maximum diaphragm shear per linear foot occurs at grid line 10 and is equal to:

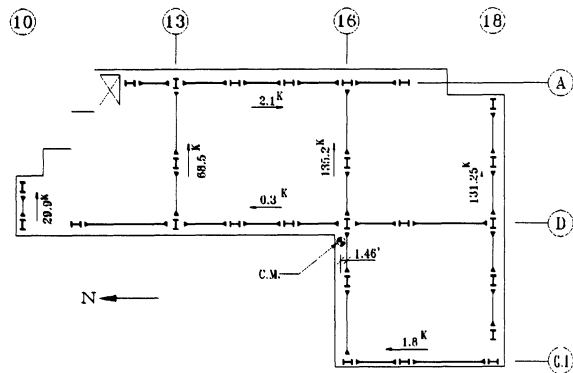


Figure 8-32. Frame shears for E-W seismic loading

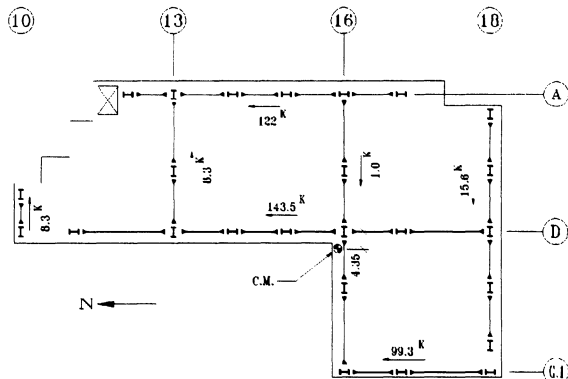
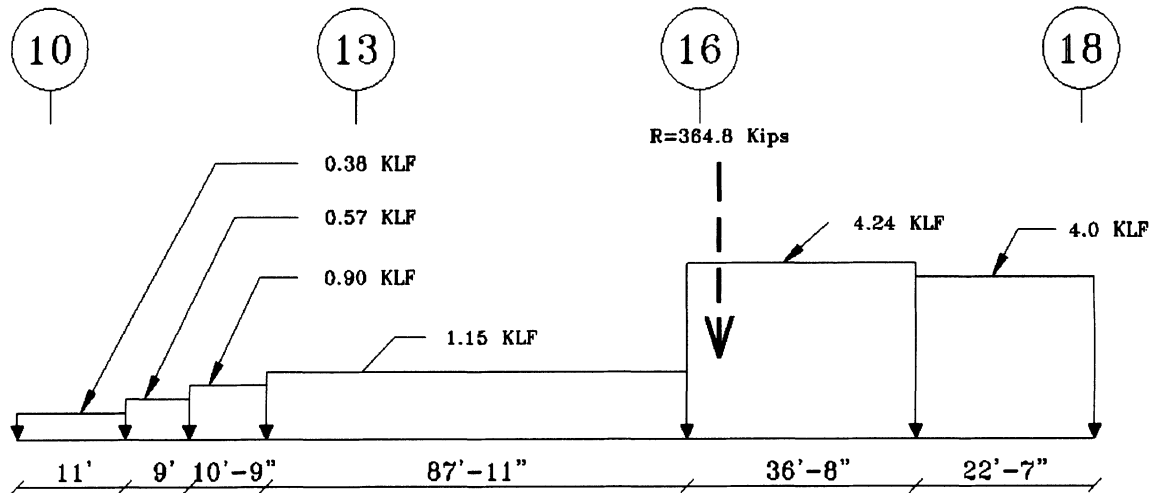


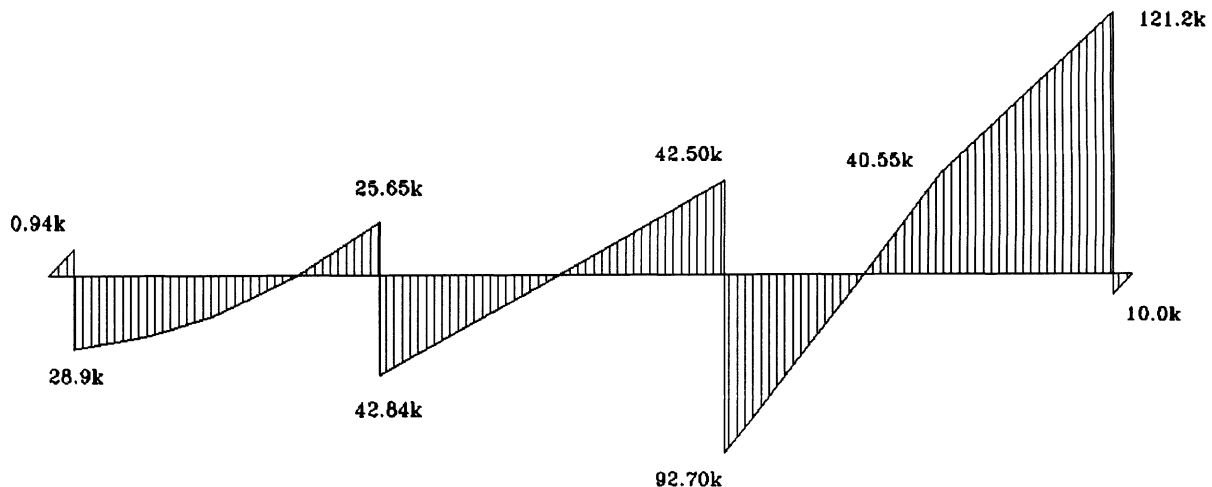
Figure 8-33. Frame shears for N-S seismic loading

$$v = \frac{29.9 \text{ kips}}{(3.8 + 14.5 + 2.5) \text{ ft}} = 1.44 \text{ k/ft}$$

This value, has to be compared with the allowable shear values supplied by the metal deck manufacturer. For example, if a Verco 20 gage, W3 Formlok deck with 3 1/4 light-weight



LOADING DIAGRAM



SHEAR DIAGRAM

Figure 8-34. Diaphragm loading and shear diagrams for the E-W seismic loading

concrete fill and puddle welds in every flute is used, the allowable shear would be 1.74 kips compared to the required value of 1.44 kips (see Figure 8-35).

Check diaphragm chord requirements:

As mentioned earlier in this Chapter, the frame beams at the perimeter of the building will act as chord members or flanges of the diaphragm. To get a handle on the magnitude of

the chord forces, diaphragm moments are computed at various sections. The transverse shear forces (in the N-S frames) are small and hence, are ignored in this analysis.

Moment at grid line 13

$$\begin{aligned}
 &= 29.9(60) - 0.38(11)(57) - 0.57(9)(47) \\
 &\quad - 0.90(10.75)(37.125) - 1.15(31.75)^2/2 \\
 &= 375.8 \text{ kips-ft}
 \end{aligned}$$

W3 FORMLOK LIGHT WEIGHT CONCRETE (110pcf)

GALVANIZED

ALLOWABLE SUPERIMPOSED LOADS (Lbs./Sq. Ft.), DIAPHRAGM SHEAR VALUES (q) (Lbs./L.F.) AND FLEXIBILITY FACTORS (F)

TOTAL SLAB DEPTH & CONCRETE WT. psf	DECK GAGE & WT. psf	NUMBER OF SPANS	SPAN														
			8'-0"	8'-6"	9'-0"	9'-6"	10'-0"	10'-6"	11'-0"	11'-6"	12'-0"	12'-6"	13'-0"	13'-6"	14'-0"	14'-6"	15'-0"
6 1/4" 43.5 2 HOUR FIRE RATING	22	1	309	238	213	191	172	155	141	128	116	106	97	88	81	74	68
		2	309	279	254	232	172	155	141	128	116	106	97	88	81	74	68
		3	309	279	254	232	213	155	141	128	116	106	97	88	81	74	68
		q	1780	1760	1740	1725	1710	1695	1680	1670	1660	1650	1640	1630	1620	1615	1610
		F	.47	.48	.48	.49	.49	.50	.50	.50	.50	.51	.52	.52	.52	.52	.52
	21	1	341	309	281	215	194	176	160	145	133	121	111	102	93	86	79
		2	341	309	281	256	235	176	160	145	133	121	111	102	93	86	79
		3	341	309	281	256	235	217	201	145	133	121	111	102	93	86	79
		q	1810	1790	1770	1750	1730	1715	1700	1685	1670	1660	1650	1640	1630	1620	1610
		F	.43	.44	.44	.45	.45	.46	.46	.47	.47	.48	.48	.48	.49	.49	.49
	20	1	357	323	294	268	205	186	169	154	141	129	118	108	100	92	84
		2	357	323	294	268	246	227	169	154	141	129	118	108	100	92	84
		3	357	323	294	268	246	227	210	195	141	129	118	108	100	92	84
		q	1830	1805	1780	1760	1740	1720	1700	1690	1680	1665	1650	1640	1630	1620	1610
		F	.42	.43	.43	.44	.44	.45	.45	.45	.45	.46	.46	.47	.47	.47	.47
	19	1	400	372	338	309	284	262	201	183	168	154	142	131	121	111	103
		2	400	372	338	309	284	262	242	225	168	154	142	131	121	111	103
		3	400	372	338	309	284	262	242	225	209	196	142	131	121	111	103
		q	1890	1860	1830	1805	1780	1760	1740	1725	1710	1695	1680	1670	1660	1645	1630
		F	.37	.38	.38	.39	.39	.40	.41	.41	.41	.42	.42	.42	.43	.43	.43
	18	1	400	400	369	338	310	286	264	241	187	172	158	146	135	125	116
		2	400	400	369	338	310	286	264	241	229	214	158	146	135	125	116
		3	400	400	369	338	310	286	264	241	229	214	200	188	176	125	116
		q	1940	1905	1870	1845	1820	1795	1770	1750	1730	1715	1700	1690	1680	1665	1650
		F	.34	.35	.35	.36	.36	.37	.37	.38	.38	.39	.39	.39	.40	.40	.40
	16	1	400	400	400	400	370	341	316	293	273	255	197	182	169	157	146
		2	400	400	400	400	370	341	316	293	273	255	239	224	211	157	146
		3	400	400	400	400	370	341	316	293	273	255	239	224	211	199	188
		q	2070	2025	1980	1945	1910	1880	1850	1830	1810	1790	1770	1750	1730	1715	1700
		F	.28	.29	.30	.31	.31	.32	.32	.32	.32	.33	.33	.34	.34	.34	.34
7 1/4" 52.7 3 HOUR FIRE RATING	22	1	315	280	250	224	202	182	165	150	136	124	113	103	94	86	79
		2	364	329	299	224	202	182	165	150	136	124	113	103	94	86	79
		3	364	329	299	273	202	182	165	150	136	124	113	103	94	86	79
		1.9	2100	2080	2060	2040	2020	2010	2000	1985	1970	1960	1950	1945	1940	1930	1920
		F	.40	.41	.41	.41	.41	.42	.42	.42	.42	.43	.43	.43	.44	.44	.44
	21	1	400	314	281	253	228	206	187	170	155	142	130	119	109	100	92
		2	400	363	330	302	228	206	187	170	155	142	130	119	109	100	92
		3	400	363	330	302	277	255	187	170	155	142	130	119	109	100	92
		2.1	2130	2125	2080	2060	2040	2025	2010	1995	1980	1970	1960	1950	1940	1935	1930
		F	.37	.38	.38	.38	.38	.39	.39	.40	.40	.40	.40	.40	.41	.41	.41
	20	1	400	380	345	268	240	218	198	180	165	150	138	126	116	107	98
		2	400	380	345	316	290	218	198	180	165	150	138	126	116	107	98
		3	400	380	345	316	290	267	247	180	165	150	138	126	116	107	98
		2.3	2150	2120	2090	2070	2050	2035	2020	2005	1990	1980	1970	1960	1950	1940	1930
		F	.35	.36	.36	.37	.37	.38	.38	.38	.38	.39	.39	.39	.39	.39	.39
	19	1	400	400	397	363	333	258	235	214	196	180	166	153	141	130	120
		2	400	400	397	363	333	307	285	214	196	180	166	153	141	130	120
		3	400	400	397	363	333	307	285	264	246	180	166	153	141	130	120
		2.7	2210	2180	2150	2125	2100	2080	2060	2040	2020	2010	2000	1985	1970	1960	1950
		F	.31	.32	.32	.33	.33	.34	.34	.34	.34	.35	.35	.35	.36	.36	.36
	18	1	400	400	400	396	364	335	260	238	218	201	185	171	158	146	135
		2	400	400	400	396	364	335	310	288	218	201	185	171	158	146	135
		3	400	400	400	396	364	335	310	288	268	251	235	171	158	146	135
		2.9	2260	2225	2190	2160	2130	2110	2090	2070	2050	2035	2020	2005	1990	1980	1970
		F	.29	.30	.30	.31	.31	.31	.32	.32	.33	.33	.33	.33	.33	.33	.33
	16	1	400	400	400	400	399	370	343	320	248	229	212	197	183	170	
		2	400	400	400	400	399	370	343	320	299	280	212	197	183	170	
		3	400	400	400	400	399	370	343	320	299	280	263	247	183	170	
		3.5	2380	2340	2300	2265	2230	2200	2170	2145	2120	2100	2080	2065	2050	2035	2020
		F	.25	.26	.26	.26	.26	.27	.27	.28	.28	.28	.28	.29	.29	.29	.29

Figure 8-35. A Verco Formlok diaphragm design table (reproduced with permission of Verco Manufacturing Company, Benicia, California)

**W3 FORMLOK NORMAL WEIGHT CONCRETE (145 psf)
GALVANIZED**

ALLOWABLE SUPERIMPOSED LOADS (Lbs./Sq. Ft.), DIAPHRAGM SHEAR VALUES (q) (Lbs./L.F.) AND FLEXIBILITY FACTORS (F)

TOTAL SLAB DEPTH & CONCRETE WT. psf	DECK GAGE & WT. psf	NUMBER OF SPANS	SPAN														
			q	8'-0"	8'-6"	9'-0"	9'-6"	10'-0"	10'-6"	11'-0"	11'-6"	12'-0"	12'-6"	13'-0"	13'-6"	14'-0"	14'-6"
6½" 60.4 1 HOUR FIRE RATING	22	1	266	235	209	186	166	149	134	120	108	97	87	79	71	64	57
		2	322	291	209	186	166	149	134	120	108	97	87	79	71	64	57
		3	322	291	265	242	166	149	134	120	108	97	87	79	71	64	57
		1.9	2430	2410	2390	2375	2360	2345	2330	2315	2300	2290	2280	2265	2270	2260	2250
		F	.34	.35	.35	.36	.36	.36	.36	.36	.36	.37	.37	.37	.37	.37	.37
	21	1	356	266	236	211	189	170	153	138	125	113	102	93	84	76	68
		2	356	322	293	211	189	170	153	138	125	113	102	93	84	76	69
		3	356	322	293	267	246	170	153	138	125	113	102	93	84	76	69
		2.1	2460	2435	2410	2390	2370	2355	2340	2330	2320	2305	2290	2280	2270	2265	2260
		F	.32	.33	.33	.33	.33	.33	.34	.34	.34	.34	.34	.34	.34	.35	.35
	20	1	373	337	250	224	201	181	163	147	133	121	110	100	90	82	74
		2	373	337	306	280	201	181	163	147	133	121	110	100	90	82	74
		3	373	337	306	280	257	181	163	147	133	121	110	100	90	82	74
		2.3	2480	2455	2430	2405	2380	2365	2350	2335	2320	2310	2300	2290	2280	2270	2260
		F	.31	.31	.31	.32	.32	.32	.32	.33	.33	.33	.33	.33	.33	.34	.34
	19	1	400	388	353	322	239	216	196	178	162	147	134	123	112	103	94
		2	400	388	353	322	296	216	196	178	162	147	134	123	112	103	94
		3	400	388	353	322	296	273	252	178	162	147	134	123	112	103	94
		2.7	2540	2510	2480	2455	2430	2410	2390	2370	2350	2340	2330	2315	2300	2290	2280
		F	.27	.28	.28	.29	.29	.29	.30	.30	.30	.30	.30	.30	.30	.30	.30
	18	1	400	400	385	352	323	241	219	199	181	166	152	139	127	117	107
		2	400	400	385	352	323	298	276	199	181	166	152	139	127	117	107
		3	400	400	385	352	323	298	276	256	238	223	152	139	127	117	107
		2.9	2590	2555	2520	2490	2460	2440	2420	2400	2380	2365	2350	2335	2320	2310	2300
		F	.25	.26	.26	.27	.27	.27	.27	.28	.28	.28	.28	.28	.29	.29	.29
	16	1	400	400	400	400	385	355	329	248	227	208	191	176	162	150	139
		2	400	400	400	400	385	355	329	305	284	266	191	176	162	150	139
		3	400	400	400	400	385	355	329	305	284	266	249	234	213	150	139
		3.5	2710	2670	2630	2595	2560	2530	2500	2475	2450	2430	2410	2395	2380	2365	2350
		F	.22	.22	.22	.23	.23	.23	.23	.24	.24	.24	.24	.25	.25	.25	.25
7½" 72.5 2 HOUR FIRE RATING	22	1	311	275	244	217	194	173	155	140	125	113	101	91	82	73	66
		2	378	275	244	217	194	173	155	140	125	113	101	91	82	73	66
		3	378	342	311	217	194	173	155	140	125	113	101	91	82	73	66
		1.9	2910	2890	2870	2850	2830	2820	2810	2795	2780	2770	2760	2755	2750	2740	2730
		F	.29	.29	.30	.30	.30	.30	.30	.30	.30	.30	.30	.30	.30	.31	.31
	21	1	350	310	276	246	221	198	178	161	145	131	119	107	97	88	79
		2	400	377	276	246	221	198	178	161	145	131	119	107	97	88	79
		3	400	377	343	313	221	198	178	161	145	131	119	107	97	88	79
		2.1	2940	2915	2890	2870	2850	2835	2820	2805	2790	2780	2770	2760	2750	2745	2740
		F	.27	.27	.27	.27	.27	.27	.28	.28	.28	.28	.28	.28	.28	.29	.29
	20	1	400	328	292	261	234	210	190	171	155	140	127	115	109	95	86
		2	400	395	359	261	234	210	190	171	155	140	127	115	105	95	86
		3	400	395	359	328	301	210	190	171	155	140	127	115	105	95	86
		2.3	2950	2925	2900	2880	2860	2845	2830	2815	2800	2790	2780	2760	2750	2740	2740
		F	.26	.26	.26	.27	.27	.27	.27	.27	.27	.27	.27	.27	.27	.28	.28
	19	1	400	400	400	310	279	252	228	207	188	171	156	142	130	119	109
		2	400	400	400	377	346	252	228	207	188	171	156	142	130	119	109
		3	400	400	400	377	346	319	295	207	188	171	156	142	130	119	109
		2.7	3020	2990	2950	2935	2910	2890	2870	2850	2830	2815	2800	2790	2780	2770	2760
		F	.23	.24	.24	.24	.24	.24	.24	.25	.25	.25	.25	.25	.25	.25	.25
	18	1	400	400	400	400	352	280	254	231	211	193	176	161	148	135	124
		2	400	400	400	400	378	348	254	231	211	193	176	161	148	135	124
		3	400	400	400	400	378	348	322	299	278	251	231	211	193	176	161
		2.9	3070	3035	3000	2970	2940	2920	2900	2880	2860	2845	2830	2815	2800	2790	2780
		F	.21	.22	.22	.22	.22	.23	.23	.23	.23	.23	.23	.23	.23	.24	.24
	16	1	400	400	400	400	400	400	363	328	263	242	222	204	188	174	160
		2	400	400	400	400	400	400	384	356	263	242	222	204	188	174	160
		3	400	400	400	400	400	400	400	400	384	356	332	310	290	204	188
		3.5	3190	3150	3110	3075	3040	3010	2980	2955	2930	2910	2890	2875	2860	2845	2830
		F	.18	.19	.19	.19	.19	.20	.20	.20	.20	.20	.20	.20	.21	.21	.21

Figure. 8-35 (continued)

Chord force at grid line 13
= 375.8/57.58 = 6.52 kips

Moment at grid line 16
= 29.9(120) - 0.38(11)(137) - 0.57(9)(107)
- 0.90(10.75)(97.125) -
1.15(87.92)(47.76) - 4.24(3.8)²/2 + 68.5(60)
= 777.2 k-ft

Chord force at grid line 16
= 777.2/57.58 = 13.5 kips

Similarly, diaphragm moments and chord forces can be computed at other locations. In design of beams and the beam-column connections, these chord forces must be considered. The metal deck-beam welds must be verified to be able to develop the chord forces in addition to their shear transfer capability.

- Diaphragm Design in the N-S Direction

Here again, the applied lateral force of 364.8 kips is distributed in proportion to the mass distribution (see Figure 8-36). Diaphragm shears and moments at any location can be computed similar to the east-west seismic analysis. For example,

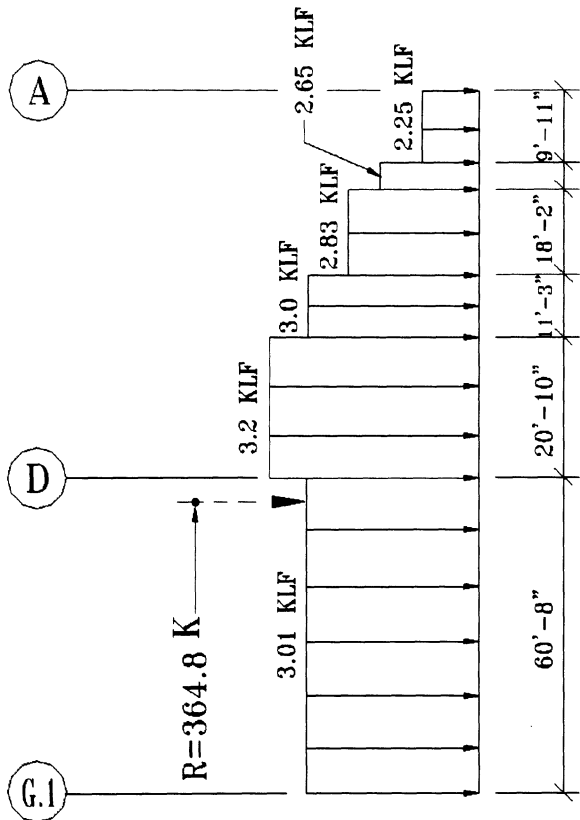


Figure 8-36. Diaphragm loading diagrams for the N-S seismic loading

diaphragm shear at grid line G.1

$$= \frac{99.3 - 3.01(1.75)}{59.25} = 1.59 \text{ kips/ft}$$

diaphragm shear at grid line D

$$= \frac{3.01(60.67) - 99.3}{59.25} = 1.40 \text{ kips/ft}$$

Both of the above computed diaphragm shears are less than the allowable shear value of 3.07 kips per linear foot for a Verco 18 gage, W3 Formlok deck with puddle welds in all flutes. As an example of diaphragm moment

calculations, we compute the diaphragm moment at grid line D:

diaphragm moment at grid line D

$$= 99.3(58.92) - \frac{3.01(60.67)^2}{2}$$

$$= 311 \text{ ft - kips}$$

Chord force at grid line D

$$= 311.05 / 52.92 = 5.87 \text{ kips}$$

To complete this design, diaphragm moments should be computed at a few other locations on the diaphragm, in order to establish the maximum moment, and the corresponding maximum chord force. The beams along grids 16 and 18, near grid line D may be designed to carry these chord forces.

EXAMPLE 8-4

The ground floor and roof plans of a one story neighborhood shopping center which is being planned for a city in a zone of high seismicity are shown in Figure 8-37. The roof framing consists of plywood panelized roof with glue laminated beams and purlins. The roof dead load for the purposes of seismic design calculations is estimated to be 16 pounds per square foot. In addition to the framing weight, this includes allowances for composition roof, insulation, acoustic tile ceiling and a miscellaneous load of 1.5 pounds per square foot. Design the roof diaphragm in accordance with the UBC-97 requirements (IBC-2000 diaphragm design process is virtually the same). Assume $Z = 0.40$, $I = 1.0$, $N_a = N_v = 1.0$, and the S_B soil type.

- Dead load and base shear in the N-S direction

$$\text{north wall at } 75 \text{ lb/ft}^2 = 75(14/2 + 2)(180)$$

$$= 121,500 \text{ lb}$$

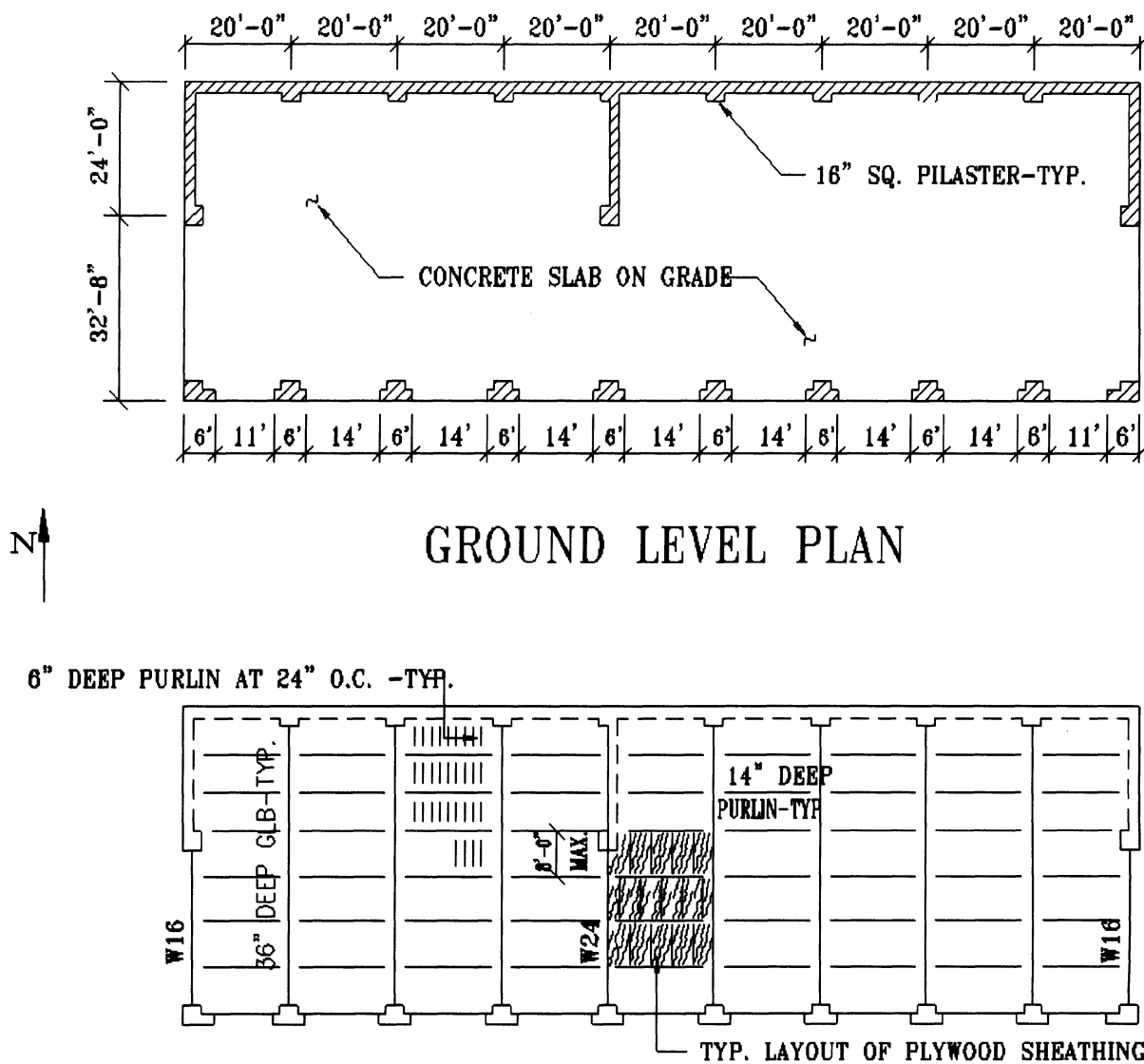


Figure 8-37. Floor plans for building of Example 8-4

$$\text{pilasters in North wall} = 75(14/2)(1.33 \times 8) \\ = 5,600 \text{ lb}$$

$$\text{roof at } 16 \text{ lb/ft}^2 = 16(180)(56.67) \\ = 163,210 \text{ lb}$$

$$\text{pilasters in South piers} = 75(14/2)(1.33 \times 10) \\ = 7,000 \text{ lb}$$

$$\text{total dead load} = 121,500 + 5,600 + 7000 + \\ 40500 + 16,200 + 163,210 = 354,010 \text{ lb}$$

$$\text{south piers at } 75 \text{ lb/ft}^2 = 75(14/2+2)(10 \times 6) \\ = 40500 \text{ lb}$$

Because this is a one story light-weight structure, we can use the simplified method according to UBC-97 section 1629.8.2. Notice that for flexible diaphragms providing lateral

$$\text{glass window at } 15 \text{ lb/ft}^2 \\ = 15(14/2 + 2)(7 \times 14 + 2 \times 11) = 16,200 \text{ lb}$$

support for masonry, an R value of 4.0 must be used (UBC-97 section 1633.2.9.3)

$$\text{Base Shear } (V) = \frac{3.0C_a}{R} W$$

$$F_{px} = \frac{3.0C_a}{R} W_{px}$$

$$F_{px} = \frac{3.0(0.4)}{4.0} W_{px} = 0.30W_{px}$$

$$= 0.30(354,010)$$

$$= 106,203 \text{ lb in N-S direction}$$

This value, however, is intended for strength design purposes. To convert it to the corresponding working stress design value, we divide it by a load factor of 1.4.

$$F_{px(WSD)} = \frac{106,203}{1.40} = 75,859 \text{ lb}$$

- Diaphragm design in the N-S direction (see Figure 8-38):

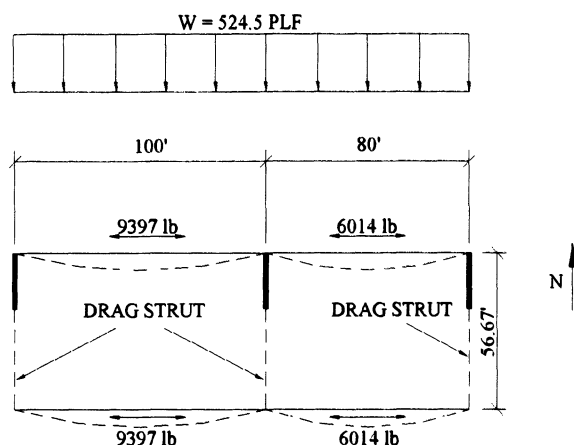


Figure 8-38. Chord forces for the N-S seismic loading based on flexible diaphragm assumption.

The diaphragm is assumed to be flexible. Therefore, in both directions, the wall loads will be based on the tributary diaphragm areas.

$$\text{N-S diaphragm load} = \frac{75,859 \text{ lb}}{180 \text{ ft}}$$

$$= 421 \text{ lb/ft}$$

East wall:

$$\text{diaphragm shear} = 421(80/2)$$

$$= 16,840 \text{ lb}$$

$$\text{diaphragm unit shear} = 16,840/56.67$$

$$= 297 \text{ lb/ft}$$

$$\text{force in the drag strut} = 297(32.67)$$

$$= 9,703 \text{ lb}$$

Center Wall:

$$\text{east side shear} = 421(80/2) = 16,840 \text{ lb}$$

$$\text{diaphragm unit shear} = 16,840/56.67$$

$$= 297 \text{ lb/ft}$$

$$\text{west side shear} = 421(100/2) = 21,050 \text{ lb}$$

$$\text{diaphragm unit shear} = 21,050/56.67$$

$$= 372 \text{ lb/ft}$$

$$\text{force in the drag strut} =$$

$$(297 + 372)(32.67) = 21,856 \text{ lb}$$

West Wall:

$$\text{diaphragm shear} = 421(100/2) = 21,050 \text{ lb}$$

$$\text{diaphragm unit shear} = 21,050/56.67$$

$$= 372 \text{ lb/ft}$$

$$\text{force in the drag strut} = 372(32.67)$$

$$= 12,153 \text{ lb}$$

Diaphragm plywood requirements: Per UBC-97 Table 23-II-H (or similarly from IBC-2000 Table 2306.3.1), use $\frac{3}{8}$ -in. Structural 1 wood panel diaphragm, blocked, 8d nails at $2\frac{1}{2}$ -in. on center at the boundaries and continuous panel edges, 8d nails at 4 in. on center at other panel edges, and 12 in. on center on intermediate framing members. Allowable diaphragm shear is $530/1.4 = 378 \text{ lb/ft}$ which is greater than the maximum demand of 372 lb/ft.

Chord Design (see Figure 8-38):

for the 100 ft span:

$$M = \frac{421(100)^2}{8} = 526,250 \text{ ft-lb}$$

$$d = 56.67 - \frac{8}{12} = 56.0 \text{ ft}$$

$$C \text{ or } T = \frac{536,250}{56.0} = 9,397 \text{ lb}$$

for the 80 ft span:

$$M = \frac{421(80)^2}{8} = 336,800 \text{ ft-lb}$$

$$d = 56.67 - \frac{8}{12} = 56.0 \text{ ft}$$

$$C \text{ or } T = \frac{336,800}{56.0} = 6,014 \text{ lb}$$

Provide horizontal reinforcement as chord reinforcement in the North wall at the roof level. The maximum required area of steel is:

$$A_s = \frac{9,397}{1.33(24,000)} = 0.30 \text{ in}^2$$

Therefore a #5 continuous horizontal bar may be used typically ($A_s = 0.31 \text{ in}^2$). A chord member is also required on the south side of the diaphragm. Alternatively, a timber chord member may be designed and used. Since the required chord area is small, one can design the edge purlin to act as a chord. Bolt purlin to the piers and provide metal strap across the beams for continuity of the chord.

Design of drag struts: The steel beams may be designed to act as drag struts to transfer the drag force from the steel beam to the block walls (see Figure 8-38). Diaphragm shear is transferred from plywood to the drag strut by means of the nailer as shown in Figure 8-39. The nailer is bolted to the drag strut. The plywood sheathing is nailed to the nailer. The drag strut force is transferred to the wall by

means of the steel angle shown in Figure 8-40. The steel angle is welded to the steel beam and bolted to the wall. A wood ledger is used to transfer the diaphragm shear from the plywood to the wall, and to attach purlins to the wall.

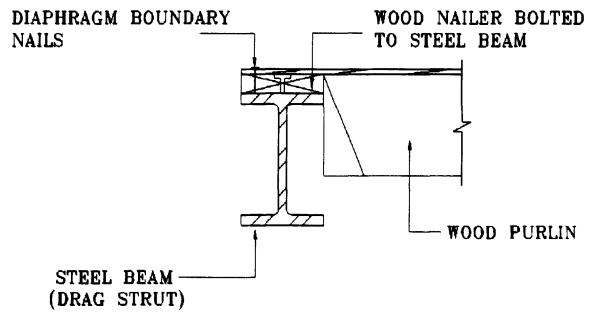


Figure 8-39. Typical detail for transfer of shear from plywood to the drag strut

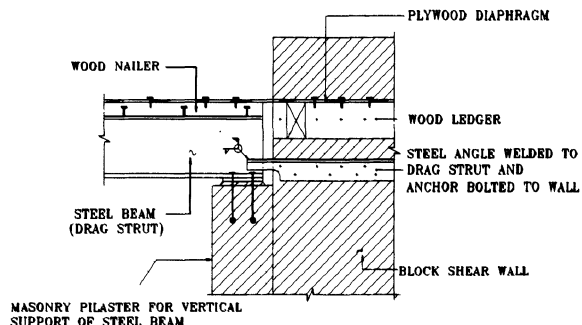


Figure 8-40. Typical detail for transfer of force from drag struts to a block shear wall

- Dead load and base shear in the E-W direction:

east and West walls at 75 psf =

$$75(14/2+2)(2)(24) + 75(14/2)(24) = 45,000 \text{ lb}$$

$$\begin{aligned} \text{pillasters at 75 psf} &= 75(14/2)(16/12)(3) \\ &= 2,100 \text{ lb} \end{aligned}$$

glass windows at 15 psf =

$$15(14/2 + 2)(32.67) = 8,821 \text{ lb}$$

roof at 16 psf = $16(180)(56.67) = 163,210 \text{ lb}$

$$\begin{aligned} \text{total dead load} &= 45,000 + 2,100 + 8,821 + \\ &163,210 = 219,131 \text{ lb} \end{aligned}$$

$$F_{px} = 0.30W_{px} = 0.3(219,131) = 65,739 \text{ lb}$$

$$F_{px(WSD)} = \frac{65,739}{1.40} = 46,957 \text{ lb}$$

- diaphragm design in the E-W direction (see Figure 8-41):

North wall:

$$\text{E-W diaphragm load} = \frac{46,957 \text{ lb}}{56.67 \text{ ft}} = 829 \text{ lb/ft}$$

$$\text{diaphragm shear} = 829 \times \frac{56.67}{2} = 23,490 \text{ lb}$$

$$\text{effective length of diaphragm} = 180 \text{ ft}$$

$$\text{diaphragm unit shear} = \frac{23,490}{180} = 131 \text{ lb/ft} < 378 \text{ lb/ft}$$

Therefore plywood requirements specified for N-S seismic is adequate along this wall.

South wall:

$$\text{diaphragm shear} = 829 \times \frac{56.67}{2} = 23,490 \text{ lb}$$

Length of diaphragm in direct contact with the wall is $10 \times 6 \text{ ft} = 60 \text{ ft}$. However, the south-side edge purlins, which were also designed and detailed as the chord for N-S seismic, will act as drag members along the south wall. Therefore, diaphragm shear = $23,490/180=131 < 378 \text{ lb/ft}$. Hence, previously specified plywood detailing will be adequate. Push or pull at the wall in a typical drag strut is

$$T = (131 \text{ lb/ft})(14/2 \text{ ft}) = 917 \text{ lb.}$$

The edge purlin and its bolting to the wall must be verified for the above force.

Chord design:

$$\text{diaphragm span} = 56.67 \text{ ft}$$

$$M = 829(56.67)^2/8 = 332,791 \text{ ft-lb}$$

$$d = 180 - 8/12 = 179.33 \text{ ft}$$

$$C \text{ or } T = 332,791/179.33 = 1,856 \text{ lb}$$

The chord force is small. Hence, the steel beam and the horizontal reinforcement in the block wall will work as chord members.

- Diaphragm deflections:

The span to width ratio of the diaphragm in both directions is less than 4. Therefore, deflection is not expected to be a problem. However, if a deflection check is necessary, a simple procedure described in the Timber Construction Manual⁽⁸⁻¹⁴⁾ or formula 23-1 of the IBC-2000 may be used to estimate diaphragm deflections.

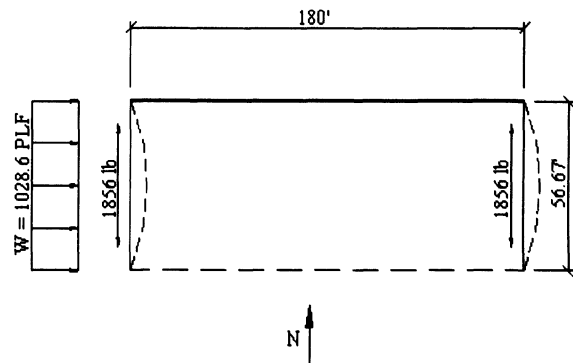


Figure 8-41. Chord forces for E-W seismic loading

REFERENCES

- 8-1 International Conference of Building Officials (1997), *The Uniform Building Code -1997 Edition*, Whittier, California.
- 8-2 International Code Council (2000), *International Building Code 2000*, Virginia.
- 8-3 Boppana, R.R., and Naeim, F., "Modeling of Floor Diaphragms in Concrete Shear Wall Buildings," *Concrete International, Design & Construction, ACI*, July, 1985.
- 8-4 Roper, S.C., and Iding, R.H., "Appropriateness of the Rigid Floor Assumption for Buildings with Irregular Features," *Proceedings of 8th World Conference on Earthquake Engineering*, San Francisco, California, 1984.
- 8-5 Mendes, S., "Wood Diaphragms: Rigid Versus Flexible Inappropriate Assumptions Can Cause Shear-Wall Failures," *Proceedings of the 56th Annual Convention, Structural Engineers Association of California*, San Diego, California, 1987.
- 8-6 S.B. Barnes and Associates, "Report on Use of H.H. Robertson Steel Roof and Floor Decks as Horizontal Diaphragms," prepared for H.H. Robertson Company by S.B. Barnes and Associates, Los Angeles, California, July, 1963.
- 8-7 American Iron and Steel Institute, "Design of Light Gage Steel Diaphragms," American Iron and Steel Institute, New York, 1982.
- 8-8 Jain, S.K., "Analytical Models for the Dynamics of Buildings," *Earthquake Engineering Research Laboratory, Report No. 83-02*, California Institute of Technology, Pasadena, May, 1983.
- 8-9 Steinburge, K.V., Manning, J.H., and Dagenkolb, H.J., "Building Damage in Anchorage," in *The Prince Williams Sound, Alaska, Earthquake of 1964, and Aftershocks*, F.J. Wood (Editor-in-Chief), U.S. Department of Commerce, Washington, D.C., 1967.
- 8-10 Buildings Officials and Code Administrators International, "The BOCA Basic Building Code," Homewood, Illinois, 1987.
- 8-11 American National Standards Institute, "American National Standards Building Code Requirements for Minimum Design Loads in Buildings and Other Structures," ANSI A58.1-1982, New York, 1982.
- 8-12 Federal Emergency Management Agency, "1997 Edition of NEHRP Recommended Provisions for the Development of Seismic Regulations for New Buildings," 1997
- 8-13 Seismology Committee of Structural Engineers Association Of California, "Tentative Lateral Force Requirements," November-December, 1986.
- 8-14 American Institute of Timber Construction, "Timber Construction Manual," 2nd edition, American Institute of Timber Construction, Englewood, Colorado, 1974.
- 8-15 American Concrete Institute (1995), *Building Code Requirements for Reinforced Concrete—ACI 318-95*, Detroit, Michigan.
- 8-16 Building Seismic Safety Council, "NEHRP Recommended Provisions for Seismic Regulations for New Buildings and other Structures, (NEHRP—National Earthquake Hazards Reduction Program), 1997 Edition, Part 1: Provisions, Part 2: Commentary, Washington, DC 20005.
- 8-17 American Society of Civil Engineers (1996), *Minimum Design Loads for Buildings and other Structures (ASCE 7-95)*, ASCE, New York, 1996

Chapter 9

Seismic Design of Steel Structures

Chia-Ming Uang, Ph.D.

Professor of Structural Engineering, University of California, San Diego

Michel Bruneau, Ph.D., P.Eng.

Professor of Civil Engineering, State University of New York at Buffalo

Andrew S. Whittaker, Ph.D., S.E.

Associate Professor of Civil Engineering, State University of New York at Buffalo

Key-Chyuan Tsai, Ph.D., S.E.

Professor of Civil Engineering, National Taiwan University

Key words: Seismic Design, Steel Structures, NEHRP Recommended Seismic Provisions, AISC Seismic Provisions, R Factor, Ductility, System Overstrength, Capacity Design, 1994 Northridge Earthquake, Moment-Resisting Frames, Brittle Fracture, Moment Connections, Concentrically Braced Frames, Buckling, Braces, Eccentrically Braced Frames, Links.

Abstract: Seismic design of steel building structures has undergone significant changes since the Northridge, California earthquake in 1994. Steel structures, thought to be ductile for earthquake resistance, experienced brittle fracture in welded moment connections. The latest AISC Seismic Provisions reflect the significant research findings that resulted from the Northridge earthquake. This chapter first starts with a description of the seismic design philosophy, the concept of system parameters (R , C_d , and Ω_o) and capacity design. Background information for the seismic requirements in the AISC Seismic Provisions of Moment Frames, Concentrically Braced Frames, and Eccentrically Braced Frames are then presented. Design examples are provided for each of the three structural systems.

9.1 Introduction

9.1.1 General

Steel is one of the most widely used materials for building construction in North America. The inherent strength and toughness of steel are characteristics that are well suited to a variety of applications, and its high ductility is ideal for seismic design. To utilize these advantages for seismic applications, the design engineer has to be familiar with the relevant steel design provisions and their intent and must ensure that the construction is properly executed. This is especially important when welding is involved.

The seismic design of building structures presented in this chapter is based on the NEHRP Recommended Provisions for the Development of Seismic Regulation for New Buildings (BSSC 1997). For seismic steel design, the NEHRP Recommended Provisions incorporate by reference the AISC Seismic Provisions for Structural Steel Buildings (1997b).

9.1.2 NEHRP Seismic Design Concept

The NEHRP Recommended Provisions are based on the *R*-factor design procedure. In this procedure, certain structural components are designated as the structural fuses and are specially detailed to respond in the inelastic range to dissipate energy during a major earthquake. Since these components are expected to experience significant damage, their locations are often selected such that the damage of these components would not impair the gravity load-carrying capacity of the system. Aside from these energy dissipating components, all other structural components including connections are then proportioned following the capacity design concept to remain in the elastic range.

Consider a structural response envelope shown in Figure 9-1, where the abscissa and ordinate represent the story drift and base shear

ratio, respectively. If the structure is designed to respond elastically during a major earthquake, the required elastic base shear ratio, C_{eu} , would be high. For economical reasons, the NEHRP Recommended Provisions take advantage of the structure's inherent energy dissipation capacity by specifying a design seismic force level, C_s , which is reduced significantly from C_{eu} by a response modification factor, R :

$$C_s = \frac{C_{eu}}{R} \quad (9-1)$$

The C_s design force level is the first significant yield level of the structure, which corresponds to the force level beyond which the structural response starts to deviate significantly from the elastic response. Idealizing the actual response envelope by a linearly elastic-perfectly plastic response shown in Figure 9-1, it can be shown that the R factor is composed of two contributing factors (Uang 1991):

$$R = R_\mu \Omega_o \quad (9-2)$$

The ductility reduction factor, R_μ , accounts for the reduction of seismic forces from C_{eu} to C_y . Such a force reduction is possible because ductility, which is measured by the ductility factor μ ($= \delta_u/\delta_y$), is provided by the energy-dissipating components in the structural system.

The system overstrength factor, Ω_o , in Eq. 9-2 accounts for the reserve strength between the force levels C_y and C_s . Several factors contribute to this overstrength factor. These include structural redundancy, story drift limits, material overstrength, member oversize, non-seismic load combinations, and so on.

The *R*-factor design approach greatly simplifies the design process because the design engineer only has to perform an elastic structural analysis even though the structure is expected to deform well into the inelastic range during a major earthquake. After the elastic story drift, δ_e , is computed from a structural analysis, the NEHRP Recommended Provisions then specify a deflection amplification factor,

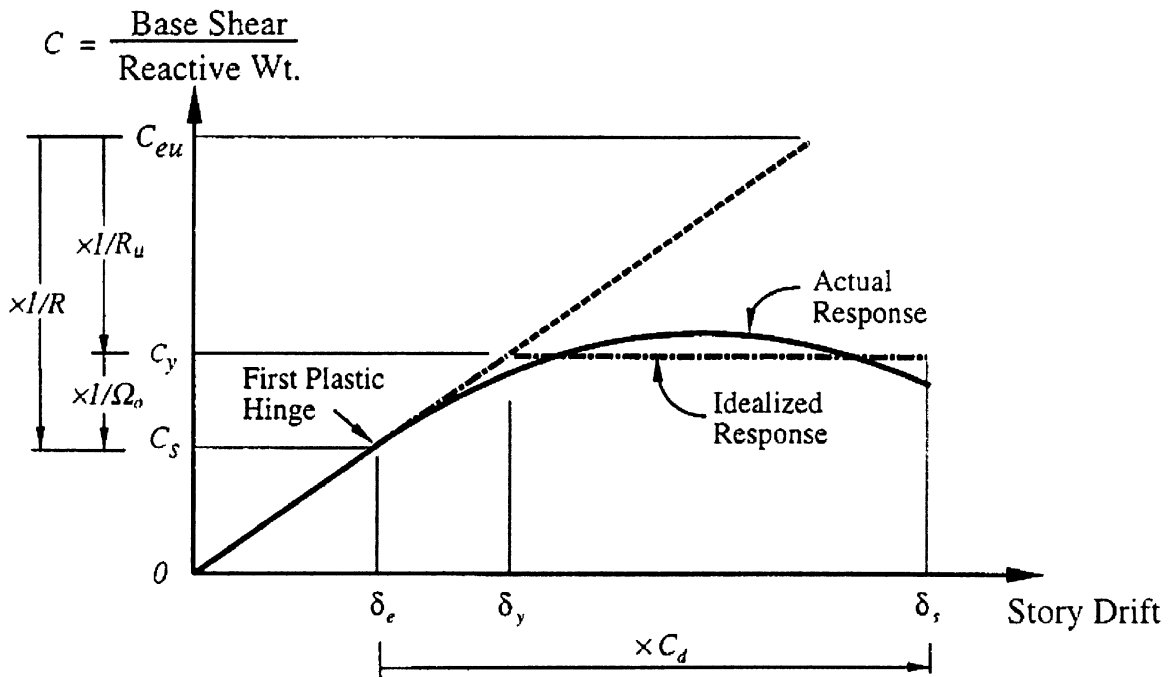


Figure 9-1. General structural response envelope

C_a , to estimate the Design Story Drift, δ_s , in Figure 9-1:

$$\delta_s = \frac{C_d \delta_e}{I} \quad (9-3)$$

where I is the Occupancy Importance Factor. The story drift thus computed cannot exceed the allowable drift specified in the NEHRP Recommended Provisions. Depending on the Seismic Use Group, the allowable drift for steel buildings varies from 1.5% to 2.5% of the story height.

Note that the ultimate strength of the structure (C_y in Figure 9-1) is not known if only an elastic analysis is performed at the C_s design force level. Nevertheless, the ultimate strength of the structure is required in capacity design to estimate, for example, the axial force in the columns when a yield mechanism forms in the structure. For this purpose, the NEHRP Recommended Provisions specify Ω_o values to simplify the design process. Therefore, in addition to the load combinations prescribed in

the AISC LRFD Specification (1993), the AISC Seismic Provisions require that the columns be checked for two additional special load combinations using the amplified horizontal earthquake load effects, $\Omega_o E$:

$$1.2D + 0.5L + 0.2S + \Omega_o E \quad (9-4)$$

$$0.9D - \Omega_o E \quad (9-5)$$

The amplified seismic load effects are to be applied without consideration of any concurrent bending moment on the columns. In addition, the required strengths determined from these two load combinations need not exceed either (1) the maximum load transferred to the column considering 1.1 R_y times the nominal strengths of the connecting beam or brace elements of the frame, or (2) the limit as determined by the resistance of the foundation to uplift. Refer to the next section for the factor R_y .

The R , C_d , and Ω_o values specified in the NEHRP Recommended Provisions for different types of steel framing systems are listed in

Table 9-1. Steel framing systems and design parameters (NEHRP 1997)

Frame System	R	Ω_0	C_d
<i>Bearing Wall Systems</i>			
Ordinary Concentrically Braced Frames (OCBFs)	4	2	3 1/2
<i>Building Frame Systems</i>			
Eccentrically Braced Frames (EBFs)			
• Moment connections at columns away from links	8	2	4
• Non-moment connections at columns away from links	7	2	4
Special Concentrically Braced Frames (SCBFs)	6	2	5
Ordinary Concentrically Braced Frames(OCBFs)	5	2	4 1/2
<i>Moment Resisting Frame Systems</i>			
Special Moment Frames (SMFs)	8	3	5 1/2
Intermediate Moment Frames (IMFs)	6	3	5
Ordinary Moment Frames (OMFs)	4	3	3 1/2
Special Truss Moment Frames (STMFs)	7	3	5 1/2
<i>Dual Systems with SMFs Capable of Resisting at Least 25% of Prescribed Seismic Forces</i>			
Eccentrically Braced Frames (EBFs)			
• Moment connections at columns away from links	8	2 1/2	4
• Non-moment connections at columns away from links	7	2 1/2	4
Special Concentrically Braced frames (SCBFs)	8	2 1/2	6 1/2
Ordinary Concentrically Braced Frames (OCBFs)	6	2 1/2	5

Table 9-1. Seismic design of three widely used systems (moment-resisting frames, concentrically braced frames, and eccentrically braced frames) that are presented later in this chapter makes use of these parameters.

9.1.3 Structural Steel Materials

The ductility of steel generally reduces with an increase of the yield stress. Therefore, the AISC Seismic Provisions permit only the following grades of steel for seismic design: ASTM A36, A53, A500 (Grades B and C), A501, A572 (Grades 42 or 50), A588, A913 (Grade 50 or 65), or A992. Further, for those structural members that are designed to yield under load combinations involving Ω_0 times the design seismic forces, the specified minimum yield strength, F_y , shall not exceed 50 ksi unless the suitability of the material is determined by testing or other rational criteria. This limitation does not apply to columns of A588 or A913

Grade 65 steel for which the only expected inelastic behavior is yielding at the column base.

The specified minimum yield strength is used to design the structural components that are expected to yield during the design earthquake. However, to estimate the force demand these components would impose on other structural components (including connections) that are expected to remain elastic, the expected yield strength, F_{ye} , of the energy dissipating components needs to be used for capacity design:

$$F_{ye} = R_y F_y \quad (9-6)$$

For rolled shapes and bars, the AISC Seismic Provisions stipulate that R_y shall be taken as 1.5 for A36 and 1.3 for A572 Grade 42. For rolled shapes and bars of other grades of steel and for plates, R_y shall be taken as 1.1 (SSPC 1995).

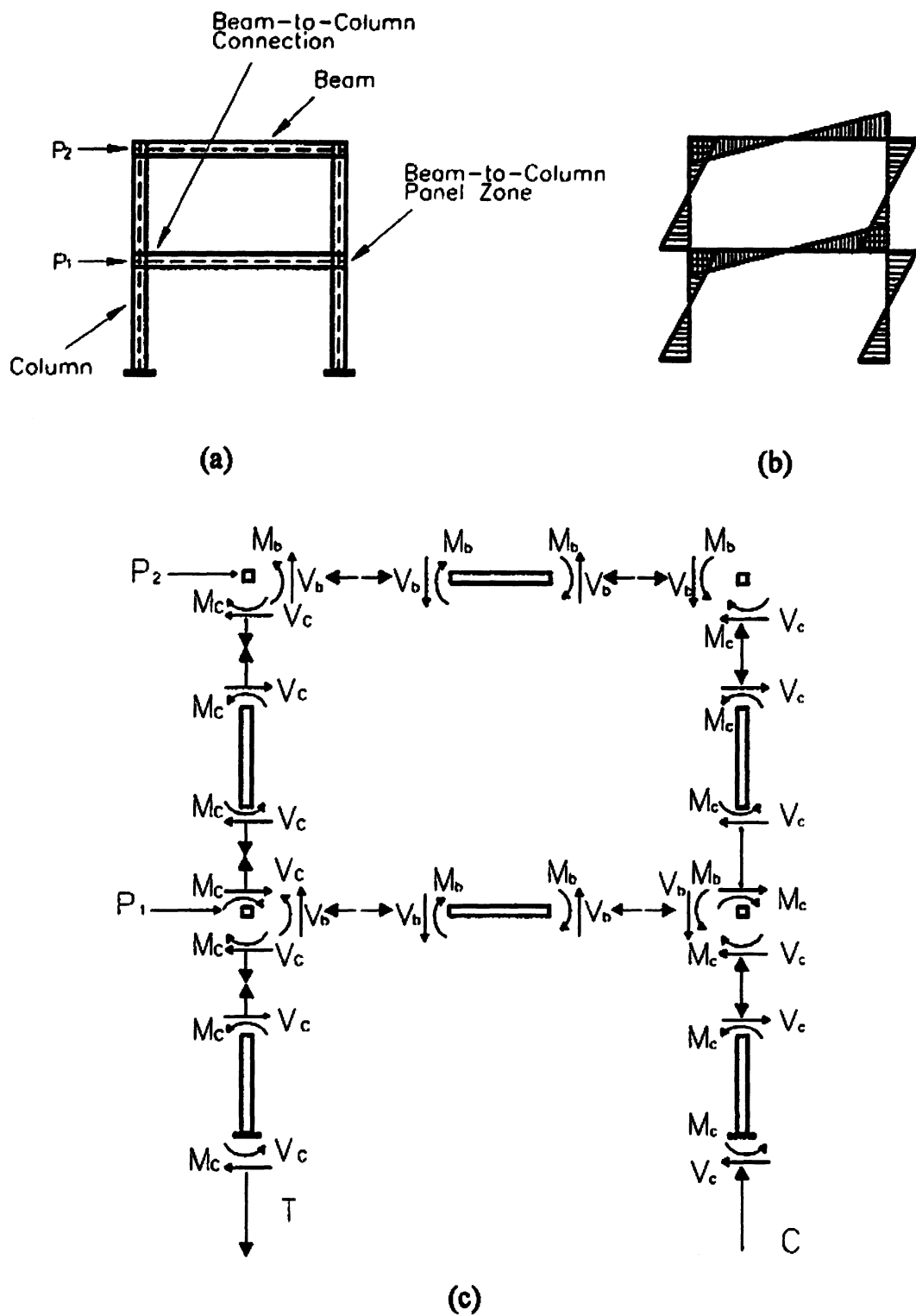


Figure 9-2. (a) Geometry considering finite dimensions of members, (b) Typical moment diagram under lateral loading, and (c) Corresponding member forces on beams, columns, and panel zones

9.2 Behavior and Design of Moment-Resisting Frames

9.2.1 Introduction

Steel moment-resisting frames (SMFs) are rectilinear assemblies of columns and beams that are typically joined by welding or high-strength bolting or both. Resistance to lateral loads is provided by flexural and shearing actions in the beams and the columns. Lateral stiffness is provided by the flexural stiffness of the beams and columns; the flexibility of the beam-column connections are often ignored although such flexibility may substantially increase deflections in a moment-resisting frame. Components of an SMF together with sample internal actions are shown in Figure 9-2.

The AISC Seismic Provisions define three types of seismic steel moment-resisting frames: Ordinary Moment Frames, Intermediate Moment Frames, and Special Moment Frames. All three framing systems are designed assuming ductile behavior of varying degrees, for earthquake forces that are reduced from the elastic forces by a response modification factor, R (see Table 9-1 for values of R).

SMFs are considered to be the most ductile of the three types of moment frames considered by AISC. For this reason, and due to their architectural versatility, SMFs have been the most popular seismic framing system in high seismic regions in the United States. SMFs are designed for earthquake loads calculated using a value of R equal to 8. Stringent requirements are placed on the design of beams, columns, beam-to-column connections, and panel zones. Beam-to-column connections in SMFs are required to have a minimum inelastic rotation capacity of 0.03 radian.

Intermediate Moment Frames (IMFs) are assumed to be less ductile than SMFs but are expected to withstand moderate inelastic deformations in the design earthquake. IMFs are designed using a value of R equal to 6; fully restrained (FR) or partially restrained (PR)

connections can be used in such frames. Beam-to-column connections in IMFs are required to have an inelastic rotation capacity of 0.02 radian. Other requirements are listed in the AISC Seismic Provisions (1997b).

Ordinary moment frames (OMFs) are less ductile than IMFs, and are expected to sustain only limited inelastic deformations in their components and connections in the design earthquake. Beam-to-column connections in OMFs are required to have an inelastic rotation capacity of 0.01 radian. FR and PR connections can be used in OMFs. Because OMFs are less ductile than IMFs, an OMF must be designed for higher seismic forces than an IMF; an OMF is designed for earthquake loads calculated using a value of R equal to 4.

The remainder of this section addresses issues associated with the design, detailing, and testing of special moment frames and components. The design philosophy for such frames is to dissipate earthquake-induced energy in plastic hinging zones that typically form in the beams and panel zones of the frame. Columns and beam-to-column connections are typically designed to remain elastic using capacity design procedures.

9.2.2 Analysis and Detailing of Special Moment Frames

Because the SMF is a flexible framing system, beam and column sizes in SMFs are often selected to satisfy story drift requirements. As such, the nominal structural strength of an SMF can substantially exceed the minimum base shear force required by the NEHRP Recommended Provisions. When analyzing SMFs, all sources of deformation should be considered in the mathematical model. NEHRP stipulates that panel zone deformations must be included in the calculation of story drift.

The AISC Seismic Provisions prescribe general requirements for materials and connections that are particularly relevant to SMF construction:

1. Steel in SMF construction must comply with the requirements described in Section 9.1.3. In addition, a minimum Charpy V-notch toughness of 20 ft-lbs at 70°F is required for thick materials in SMFs: ASTM A6 Group 3 shapes with flanges 1½ inches or thicker, ASTM A6 Groups 4 and 5 shapes, and plates that are 1½ inches or greater in thickness in built-up members.
2. Calculation of maximum component strengths (e.g., for strong column-weak beam calculations) for capacity design must be based on the expected yield strength, F_{ye} (see Eq. 9-6).
3. To prevent brittle fractures at the welds, AISC prescribes that welded joints be performed in accordance with an approved Welding Procedure Specifications and that all welds used in primary members and connections in the seismic force resisting system be made with a filler metal that has a minimum Charpy V-notch toughness of 20 ft-lbs at minus 20°F.

9.2.3 Beam Design

A beam in a steel SMF is assumed to be able to develop its full plastic moment (M_p) calculated as

$$M_p = Z_b F_y \quad (9-7)$$

where Z_b is the plastic section modulus. In order to prevent premature beam flange or web local buckling, and to maintain this moment for large plastic deformations, the width-thickness ratios of the web and flange elements should be limited to the values of λ_{ps} given in Table 9-2. (The λ_p values are for non-seismic design.) In addition, both flanges of the beam must be laterally braced near potential plastic hinges; the unbraced length of the beam must not exceed $2500 r_y / F_y$, where r_y is the radius of

gyration about the weak axis for out-of-plane buckling.

9.2.4 Beam-to-Column Connections

Introduction

For discussion purposes, a beam-to-column connection includes the beam-column panel zone and the beam-to-column joints. Connections in an SMF need to satisfy three criteria: (1) a sufficient strength to develop the full plastic moment of the beam, (2) a sufficient stiffness to satisfy the assumption of a fully rigid (FR) connection, and (3) a large post-yield deformation capacity without significant loss of strength. Prior to the 1994 Northridge, California earthquake, the welded flange-bolted web steel moment connections were assumed by design professionals to easily satisfy all three criteria. Unfortunately, many moment-resisting connections suffered extensive damage during this earthquake. In addition to brittle fracture in the groove welded connections (mostly in the beam bottom flange), other types of fracture that were seldom observed in laboratory testing prior to the Northridge earthquake were also reported. Figure 9-3a shows cracks extending into the column panel zone, and Figure 9-3b presents a “divot” pullout from the column flange. The causes of failure are discussed in Bruneau et al. (1997).

The poor performance of welded moment-frame connections in more than 200 multistory buildings in the Northridge earthquake led to the development of a national program, funded by the Federal Emergency Management Agency (FEMA), to investigate the causes of failure and to develop alternative connections for repair, rehabilitation, and new construction. Part of the FEMA program involved full-scale testing of large-size steel beam-column connections (SAC 1996). The laboratory testing of the pre-Northridge prequalified welded flange-bolted web connection replicated many of the failure modes observed in the field after the earthquake. The mean value of beam plastic

Table 9-2. Limiting width-thickness ratios

Description of Element	Width-Thickness Ratio	λ_p	λ_{ps}
Flanges of I-shaped beams and channels in flexure	b/t	$65/\sqrt{F_y}$	$52/\sqrt{F_y}$
Webs of I-shaped beams in combined flexure and axial compression	h/t_w	for $P_u/\phi_b P_y \leq 0.125$: $\frac{640}{\sqrt{F_y}} \left(1 - \frac{2.75P_u}{\phi_b P_y}\right)$ for $P_u/\phi_b P_y > 0.125$: $\frac{191}{\sqrt{F_y}} \left(2.33 - \frac{P_u}{\phi_b P_y}\right) \geq \frac{253}{\sqrt{F_y}}$	for $P_u/\phi_b P_y \leq 0.125$: $\frac{520}{\sqrt{F_y}} \left(1 - \frac{1.54P_u}{\phi_b P_y}\right)$ for $P_u/\phi_b P_y > 0.125$: $\frac{191}{\sqrt{F_y}} \left(2.33 - \frac{P_u}{\phi_b P_y}\right) \geq \frac{253}{\sqrt{F_y}}$
Round HHS in axial compression or flexure	D/t	$\frac{2070}{F_y}$	$\frac{1300}{F_y}$
Rectangular HHS in axial compression or flexure	b/t	$\frac{190}{\sqrt{F_y}}$	$\frac{110}{\sqrt{F_y}}$

rotation capacity from all of the tests of the pre-Northridge connection detail was 0.004 radian (Whittaker et al. 1998), which was significantly less than the target value of 0.03 radian. In response to these findings, the 1997 AISC Seismic Provisions require that (1) the design of beam-to-column joints and connections in SMFs must be based on qualifying tests of at least two specimens, and (2) each connection must develop a plastic rotation of 0.03 radian.

Beam-to-Column Connection Details

Shortly after the 1994 earthquake, the prequalified welded flange-bolted web connection was deleted from most building codes and replaced by general provisions that required the design professional to demonstrate the adequacy of the connection by either full-scale testing or calculations supported by test data. In response to this action, design professionals have proposed new types of moment-resisting connections for steel buildings. Some of these proposals are discussed below. In all cases, the proposed connection details relocate the beam plastic hinge away from the face of the column. Only

welded connections are considered in this section.

These connection details fall in one of the two categories: weakening the beam cross-section away from the face of the column, or reinforcing the beam cross-section at the column face. Only non-proprietary moment connections are discussed.

Reinforced Connections

A variety of reinforced connections have been developed since the Northridge earthquake. Some reinforced connection details are shown in Figure. 9-4: cover plates, welded flange plates, triangular haunches, straight haunches, and vertical plate ribs. Note that these connection details would not only increase the beam plastic hinge rotation demand but also increase the maximum moment demand at the face of the column, which could require a stronger panel zone or a larger section for the column to maintain the strong column-weak beam system (SAC 1995). Typical design practice for reinforced connections is to keep the reinforced component in the elastic range for moments associated with substantial strain

hardening in the beam beyond the reinforcement. Although it may be tempting to assume a linear distribution of bending moment along the length of the beam to size the reinforcement, the effects of gravity load on the beam bending moment diagram, if significant, must be carefully considered. For all of the connection details described below, notch-toughness rated weld filler metal, qualified welders, and high quality inspection should be specified.

Immediately after the Northridge earthquake, cover plates (see Figure 9-4a) have been one of the more popular strategies for reinforcing beam-to-column connections. Testing has been completed at a number of laboratories and significant data are available (e.g., Engelhardt and Sabol 1996, and SAC 1996). In most cases, the bottom cover plate is rectangular and wider than the beam bottom flange, and the top cover plate is tapered and narrower than the beam top flange. This configuration permits the bottom cover plate to be used as an erection seat, and facilitates down-hand welding in the field. Welded, not bolted, web connections are recommended as an effective way of reducing the thickness of the cover plates. Although a significant number of cover plated connection specimens have achieved beam plastic rotations exceeding 0.03 radian, Hamburger (1996) reported a failure rate of approximately 20 percent for cover-plated connections in laboratory tests. Another concern with the cover-plate connection is that the seam between the flange cover plate and the beam flange acts as a notch at the column face that may lead to cracks propagating into the column flange and beyond. Further information is available in SAC (1997).

The welded flange-plate connection (see Figure 9-4b) is closely related to the cover-plate connection, with the major difference being that only the flange plates are groove welded to the column (Jokerst and Soyer 1996, Noel and Uang 1996). As such, flange plates of the welded flange-plate connection are thicker than the comparable cover plates shown in Figure 9-4a. There is no notch effect associated with the

welded flange-plate connection because the beam flanges are not welded to the column flange. The bottom welded flange plate can be shop welded to the column, thereby eliminating one field groove weld, and providing an erection seat for the beam.

Welded triangular and straight haunch reinforced connections (see Figures 9-4c and d) underwent extensive laboratory testing following the Northridge earthquake (e.g., SAC 1996, Gross et al. 1998) because both reinforcements could be used for seismic repair and retrofit. Most of the haunch connection tests conducted to date incorporated a haunch to the bottom flange, although the addition of haunches to both the top and bottom flanges was also considered. Of the different types of haunch details tested to date, the triangular T-shaped haunches appear to be the most effective (Yu et al. 2000). Large plastic rotations were achieved with this type of connection. Vertical rib plates (see Figure 9-4e) can also be used to reduce the stress demand in the welded joint (Chi and Uang 2000).

Reduced Beam Sections

An alternative to relocating the plastic hinge away from the face of the column is to reduce the plastic moment of the beam at a short distance from the column face. Beam sections can be reduced by tapering the flanges, or by radius-cutting the flanges as shown in Figure 9-5. The latter approach appears to be the most promising because the re-entrant corners of the tapered flange profile tend to promote premature fracture in the beam flanges.

Originally proposed and tested by Plumier (1990), the use of the reduced beam section (RBS), also termed the *dogbone* by many design professionals, has seen broad support from engineers, steel producers, and fabricators. Both reduced-beam-section profiles have achieved plastic rotations in excess of 0.03 radian. Additional information is provided in Iwankiw and Carter (1996), Chen et al. (1996), Engelhardt et al. (1996), and Zekioglu et al. (1996).



(a) Beam bottom flange weld fracture propagating through column flange and web



(b) Beam bottom flange weld fracture causing a column divot fracture

Figure 9-3. Examples of brittle fracture of steel moment frame connections (courtesy of David P. O'sullivan, EQE International, San Francisco)

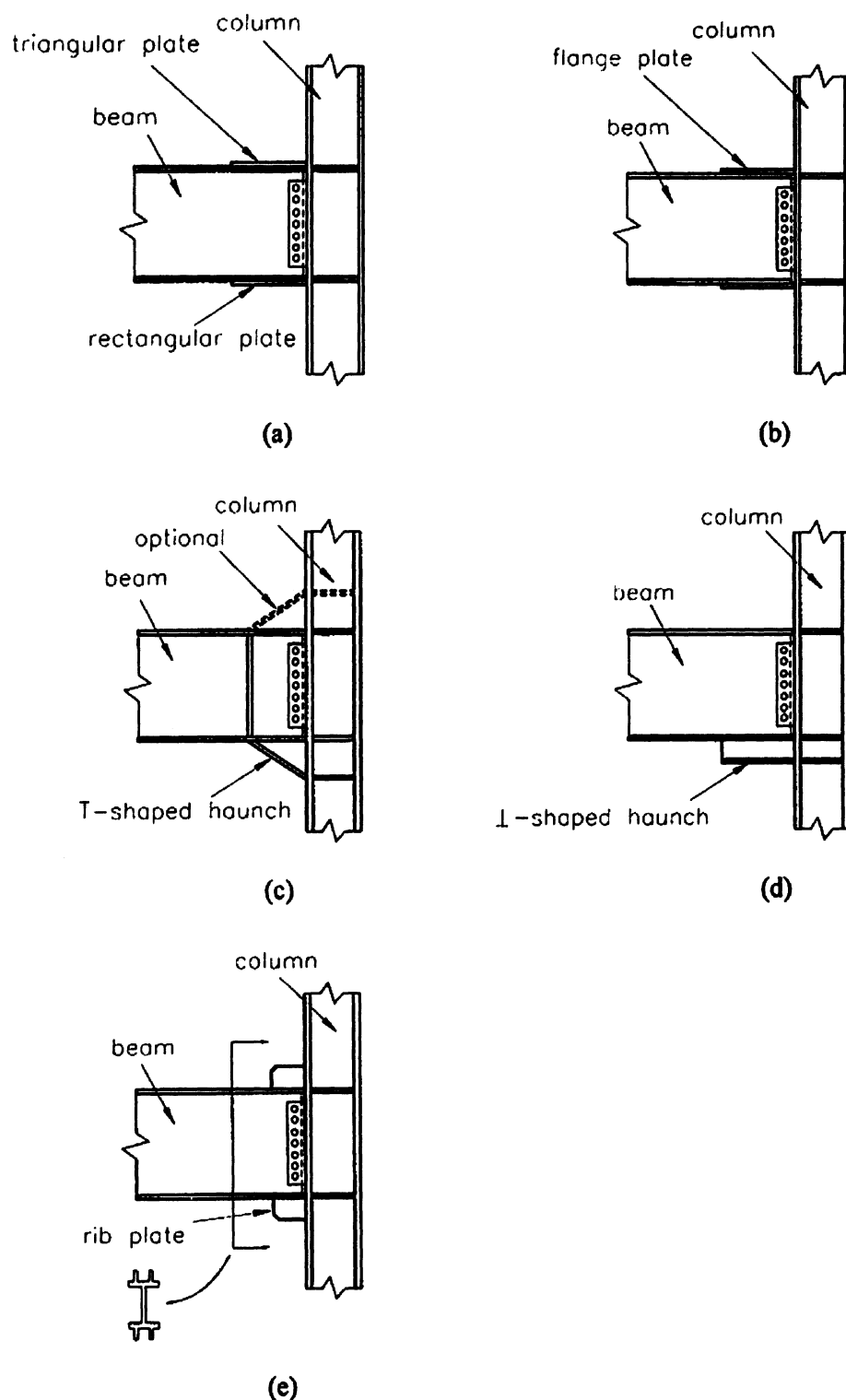


Figure 9-4. Reinforced moment connections: (a) cover plates, (b) welded flange plates, (c) triangular haunches, (d) straight haunch, (e) rib plates

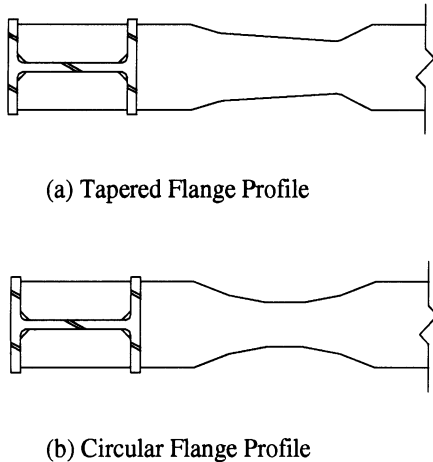


Figure 9-5. Moment connection with reduced beam section

Reducing the width of the beam flange serves to delay flange local buckling but increases the likelihood of web local buckling and lateral-torsional buckling because the in-plane stiffness of the flanges is significantly reduced. The reduced beam section usually experiences web local buckling first, followed by lateral-torsional buckling and flange local buckling.

The stability of RBS beams was studied as part of the SAC Joint Venture (Uang and Fan 2000). It was found from a statistical study that web local buckling is the governing mode of buckling. While the λ_{ps} values presented in Section 9.2.3 for flange local buckling and lateral-torsional buckling still can be used for RBS design, the λ_{ps} value for web local buckling needs to be reduced from $520/\sqrt{F_y}$ to $418/\sqrt{F_y}$ (SAC 2000). The study also showed that additional lateral bracing near the RBS is generally unnecessary.

Design engineers frequently use deep columns in a moment frame to control drift. When the deep section wide-flange columns are used, however, an experimental study showed that significant torsion leading to the twisting of the column could result (Gilton et al. 2000). Two factors contribute to the column twisting.

First, the lateral-torsional buckling amplitude of the beam tends to be larger when the RBS is used. Second, the stress in the column produced by warping torsion is highly dependent on the ratio $(d_c - t_{cf})/t_{cf}^3$. For example, this ratio is equal to $0.671/\text{in}^2$ for a W14x398 section ($I_x = 6000 \text{ in}^4$). If the designer chooses a deep section W27x161 for a comparable moment of inertia ($I_x = 6280 \text{ in}^4$) to control drift, the ratio is drastically increased to $21.04/\text{in}^2$, implying that this section is susceptible to column twisting. Lateral bracing near the RBS region then may be required to minimize the twisting. A procedure to check if column twisting is a concern has been developed (Gilton et al. 2000).

9.2.5 Beam-to-Column Panel Zones

Introduction

A beam-to-column panel zone is a flexible component of a steel moment-resisting frame that is geometrically defined by the flanges of the column and the beam (see Figure 9-6).

Although seismic building codes require the consideration of panel zone deformations in the story drift computations, panel zones are rarely modelled explicitly in mathematical models of steel moment-resisting frames. Mathematical representations of moment-resisting frames are generally composed of beams and columns modelled as line elements spanning between the beam-column intersection points. Such a representation will underestimate the elastic flexibility of a moment-resisting frame. An approximate analysis procedure that includes the flexibility of panel zones for drift computations have been proposed (Tsai and Popov 1990). This procedure will be demonstrated in an SMF design in Section 9.5.2.

Typical internal forces on a panel zone are shown in Figure 9-6a; axial, shearing, and flexural forces are typically present in a panel zone. In this figure, continuity plates are shown in the column at the level of the beam flanges and the moments M_1 and M_2 represent

earthquake actions. Assuming that the flanges resist 100 percent of the moment and that the distance between the centroids of the flanges is 95 percent of the beam depth, compression and tension flange forces as shown in Figure 9-6b can replace the beam moments.

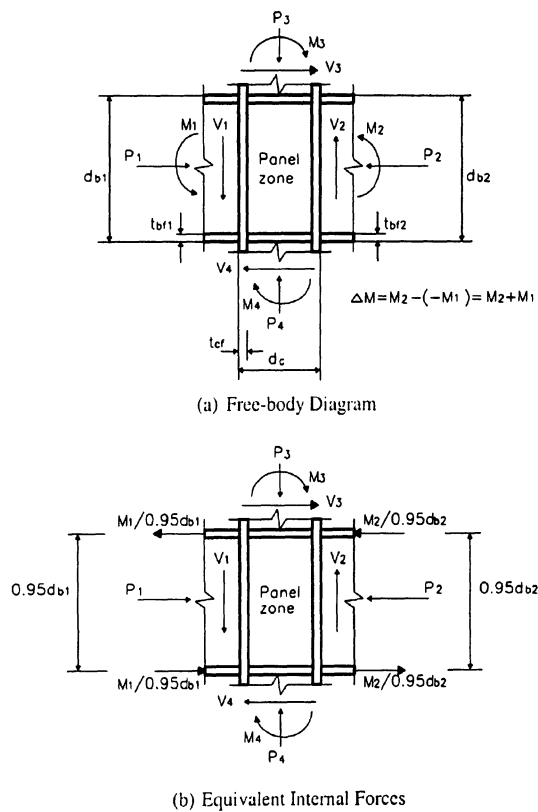


Figure 9-6. Internal forces acting on a panel zone of a moment-resisting frame subjected to lateral loading

The continuity plates shown in Figure 9-6 serve to prevent column flange distortion and column web yielding and crippling. If such plates are not provided in a column with thin flanges, and the beam flange imposes a tensile force on the column flange, inelastic strains across the groove weld of the beam flange are much higher opposite the column web than they are at the flange tips. Thus, weld cracks and fractures may result. Because the design of beam-to-column joints and connections is based upon qualifying cyclic tests, AISC (1997) requires that continuity plates of the size used in the qualifying tests be provided in the connection. However, welding of the highly

restrained joints, such as continuity plates, induces residual stress in steel members. In addition to the normal variation of material properties in the column, the process of mill rotary straightening of the W-shaped member alters the mechanical properties by cold working in the "k" area. (The "k" area is defined by AISC as the region extending from about the midpoint of the radius of the fillet into the web approximately 1 to 1.5 in. beyond the point of tangency between the fillet and web.) As a result, a reduction in ductility and toughness in the "k" area may occur. In some cases, values of Charpy V-notch toughness less than 5 ft-lb at 70° F have been reported. Since welding in the "k" area may increase the likelihood of fracture, a recent AISC Advisory (1997a) has suggested that welds for the continuity plates be stopped short of the "k" area. Fillet welds and/or partial joint penetration welds, proportioned to transfer the calculated forces, are preferred to complete joint penetration welds.

Required Shear Strength

Using the information presented in Figure 9-6b, and taking a free-body diagram immediately below the upper continuity plate, the horizontal shearing force in the panel zone (V_{pz}) can be calculated as

$$V_{pz} = \frac{M_1}{0.95d_{b1}} + \frac{M_2}{0.95d_{b2}} - V_c \quad (9-8)$$

where all terms are defined above and in the figure, and V_c is the shearing force in the column immediately above the panel zone. Because V_c reduces the shearing force in the panel zone, and its magnitude is substantially smaller than the first two terms on the right hand side of this equation, V_c can be ignored conservatively in the calculation of the maximum shearing force. Therefore, for beams of equal depth,

$$V_{pz} \approx \frac{\Delta M}{d_b} \quad (9-9)$$

where $\Delta M = (M_1 + M_2)$ is the unbalanced beam moment.

Prior to the publication of the 1988 Uniform Building Code (ICBO 1988), panel zones were designed to remain elastic for $M_1 = M_2 = M_p$, where M_p is the nominal plastic moment of the beam under consideration. The strength of the panel zone at first yield was computed as $0.55F_{yc}A_{wc}$, where F_{yc} is the nominal yield strength of the column and A_{wc} is the area of the column web ($=d_c t_{cw}$). This design procedure was intended to produce *strong panel zones* such that yielding in the moment-resisting frame was minimized in the panel zone region.

Both the 1988 Uniform Building Code and the 1992 AISC Seismic Provisions relaxed the design provisions for panel zone regions and permitted *intermediate strength panel zones* and *minimum strength panel zones*. Previous studies by Krawinkler et al. (1975) had shown that panel zone yielding could dissipate a large amount of energy in a stable manner. Intermediate and minimum strength panel zones were introduced to encourage panel zone yielding. According to the 1992 AISC Seismic Provisions, intermediate strength panel zones were designed for

$$\Delta M = \sum M_p - 2M_g \quad (9-10)$$

where M_g is the gravity moment for one beam. If the gravity moment is taken to be 20 percent of the plastic moment, the above equation gives $\Delta M = 0.8\sum M_p$. Minimum strength panel zones were allowed for a value of $\Delta M = \sum M_E \leq 0.8\sum M_p$, where the unbalanced beam moment produced by the prescribed design seismic forces is $\sum M_E = (M_{E1} + M_{E2})$. It has been shown (Tsai and Popov 1988) that steel moment frames with intermediate- or minimum-strength panel zones are likely to have a substantially smaller overstrength factor, Ω_o , than those with strong panel zones. In addition, the lateral stiffness of

an intermediate- or minimum-strength panel-zone frame can be significantly smaller than that computed using a mathematical model based on centerline dimensions.

Current AISC provisions (AISC 1997) require the use of Ω_o equal to 3.0 (see Table 9-1) for beam moments induced by the design earthquake loads. It also replaces the nominal plastic moment by the expected plastic moment and prescribes that the required strength of a panel zone need not exceed the shear force determined from $0.8\sum M_{pb}^*$, where $\sum M_{pb}^*$ is the sum of the beam moment(s) at the intersection of the beam and column centrelines. ($\sum M_{pb}^*$ is determined by summing the projections of the expected beam flexural strength(s) at the plastic hinge location(s) to the column centreline.) That is, the panel zone shall be designed for the following unbalanced moment:

$$\Delta M = \Omega_o \sum M_E \leq 0.8 \sum M_{pb}^* \quad (9-11)$$

Substituting Eq. (9-11) into Eq. (9-9) would give the required shear strength in the panel zone.

Post-Yield Strength and Detailing Requirements

The 1992 AISC equation for calculating the design shear strength of a panel zone ($\phi_v V_n$, where $\phi_v = 0.75$) was based on the work of Krawinkler et al. (1975):

$$\phi_v V_n = \phi_v \left[0.60 F_{yc} d_c t_p \left(1 + \frac{3b_{cf} t_{cf}^2}{d_b d_c t_p} \right) \right] \quad (9-12)$$

where d_c is the depth of the column, t_p is the total thickness of the panel zone, including doubler plates ($t_p = t_{cw}$ if no doubler plates are present), b_{cf} is the width of the column flange, t_{cf} is the thickness of the column flange, and d_b is the depth of the column. The second term

in the parentheses represents the contribution of column flanges (assumed to be linearly elastic) to the shear strength of the panel zone. The equation used to calculate V_n assumes a level of shear strain of $4\gamma_y$ in the panel zone, where γ_y is the yield shearing strain.

A panel zone must also be checked for a minimum thickness (t) to prevent premature local buckling under large inelastic shear deformations:

$$t = \frac{(d_z + w_z)}{90} \quad (9-13)$$

In this empirical equation, d_z is the depth of the panel zone between the continuity plates, and w_z is the width of the panel zone between the column flanges. If doubler plates are used to satisfy this equation for t , the plates must be plug welded to the column web such that the plates do not buckle independently of the web.

If used, doubler plates must be welded to the column flanges using either a complete joint penetration groove weld or a fillet weld that develops the design shear strength of the full doubler plate thickness. When such plates are welded directly to the column web and extend beyond the panel zone, minimum weld size can be used to connect the top and bottom edges to the column web. However, because of the cold working due to the rotary straightening practice and the resulting variations of material properties exhibited in the column "k" areas, the AISC Advisory (1997) suggested that, as an interim measure, the design engineer increase the column size to avoid the use of doubler plates.

9.2.6 Column Design

The column of an SMF must be designed per the LRFD Specifications (1997) as a beam-column to avoid axial yielding, buckling, and flexural yielding. Columns are routinely spliced by groove welding. Such connections are required to have sufficient strength to resist the imposed axial, shearing, and flexural forces

calculated using the specified load combinations. In addition, the column axial strength should be sufficient to resist the axial forces produced by the special load combinations of Eqs. 9-4 and 9-5. Additional strength is required if either the welds are partial penetration groove welds or the welds are subjected to net tension forces. Column splices using fillet welds or partial joint penetration groove welds shall not be located within 4 feet or one-half the column clear height of beam-to-column connections, which is less.

Special moment frames are designed using the strong column-weak beam philosophy because such an approach improves the energy dissipation capacity of the frame, promotes plastic hinge formation in the beams, increases the seismic resistance of the frame, and ostensibly prevents the formation of a soft story mechanism. Seismic regulations seek to achieve a strong column-weak beam system by ensuring that, at a beam-to-column connection, the sum of the column plastic moments exceeds the sum of the beam plastic moments. With few exceptions, AISC (1997) requires that:

$$\frac{\sum M_{pc}^*}{\sum M_{pb}^*} > 1.0 \quad (9-14)$$

where $\sum M_{pc}^*$ is the sum of the moment capacities in the columns above and below the joint at the intersection of the beam and column centerlines, and $\sum M_{pb}^*$ is the sum of the moment demands in the beams at the intersection of the beam and column centerlines.

The value of $\sum M_{pc}^*$ is determined by summing the projections of the *nominal* flexural strength of the columns above and below the connection to the beam centerline, with a reduction for the axial force in the column. $\sum M_{pc}^*$ can be conservatively approximated as $\sum Z_c(F_{yc} - P_{uc}/A_g)$, where A_g is the gross area of the column, P_{uc} is the

required column compressive strength, Z_c is the plastic section modulus of the column, and F_{yc} is the minimum specified yield strength of column. The value of $\sum M_{pb}^*$ is calculated by summing the projection of the expected beam flexural strengths at the plastic hinge locations to the column. $\sum M_{pb}^*$ can be approximated as $\sum (1.1R_y F_y Z + M_v)$, where Z is the plastic modulus of the beam section at the potential plastic hinge location, and M_v accounts for the additional moment due to shear amplification from the location of the plastic hinge to the column centerline. As illustrated in Figure 9-7, for reinforced connections using haunches or vertical ribs, SAC (1996) suggests that plastic hinges be assumed to be located at a distance $s_h = d/3$ from the toe of haunch or ribs. For cover plated connections, SAC recommends that the plastic hinge be located at a distance $s_h = d/4$ beyond the end of cover plate. When the ratio in Eq. 9-14 is no greater than 1.25, the width-

to-thickness ratios of the flange and web elements of the column section shall be limited to the λ_{ps} values in Table 9-2 because plastic hinge formation in the column may occur due to the shift of inflection point during an earthquake. Otherwise, columns shall comply with the limiting values of λ_p in the same table.

9.3 Behavior and Design of Concentrically Braced Frames

9.3.1 Design Philosophy

Concentrically braced frames are frequently used to provide lateral strength and stiffness to low- and mid-rise buildings to resist wind and earthquake forces. Although some architects favor the less intrusive moment frames, others have found architectural expression in exposing braced frames which the public intuitively associates with seismic safety in some

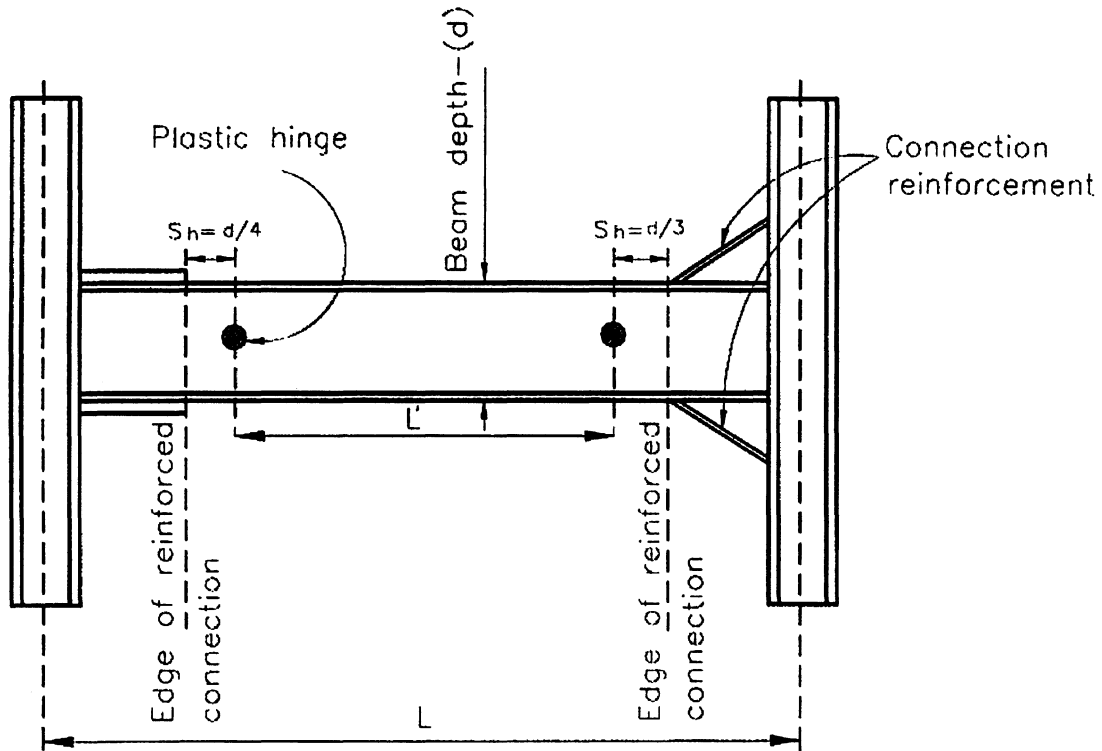


Figure 9-7. Assumed beam plastic hinge locations (Adapted from Interim Guidelines Advisory No. 1, SAC 1997)

earthquake-prone regions. However, for those frames to provide adequate earthquake resistance, they must be designed for appropriate strength and ductility. This is possible for many of the concentrically braced frame (CBF) configurations shown in Figure 9-8, but not all, as described in this section.

In a manner consistent with the earthquake-resistant design philosophy presented elsewhere in this chapter, modern concentrically braced frames are expected to undergo inelastic response during infrequent, yet large earthquakes. Specially designed diagonal braces in these frames can sustain plastic deformations and dissipate hysteretic energy in a stable manner through successive cycles of buckling in compression and yielding in tension. The preferred design strategy is, therefore, to ensure that plastic deformations only occur in the braces, leaving the columns, beams, and connections undamaged, thus allowing the

structure to survive strong earthquakes without losing gravity-load resistance.

Past earthquakes have demonstrated that this idealized behavior may not be realized if the braced frame and its connections are not properly designed. Numerous examples of poor seismic performance have been reported (Tremblay et al. 1995, 1996; AIJ 1995). As shown in Figure 9-9, braces with bolted connections have fractured through their net section at bolt holes, beams and columns have suffered damage, and welded and bolted connections have fractured. Collapses have occurred as a consequence of such uncontrolled inelastic behavior.

The design requirements necessary to achieve adequate strength and ductility in concentrically braced frames are presented in this section. Two types of systems are permitted by the AISC Seismic Provisions: Special Concentrically Braced Frames (SCBs) and

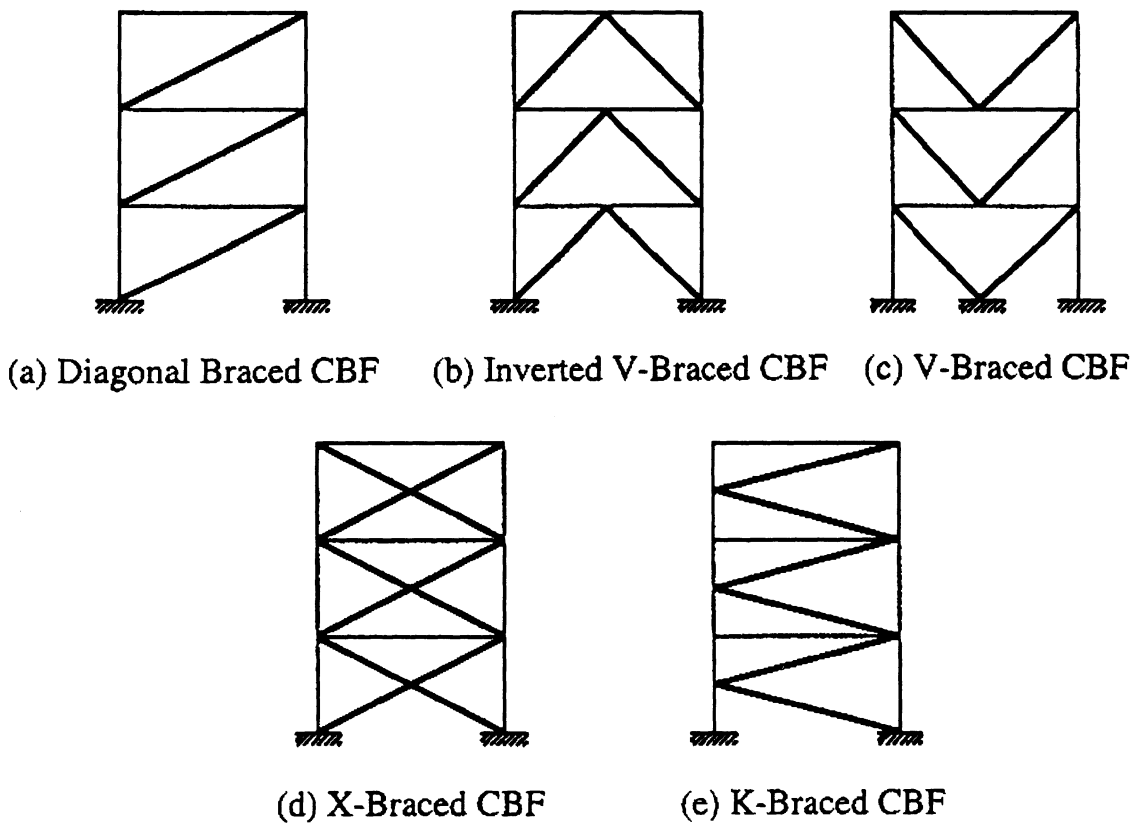


Figure 9-8. Typical brace configuration

Ordinary Concentrically Braced Frames (OCBFs). The emphasis herein is on the SCBF, which is designed for stable inelastic performance using a response modification factor, R , of 6. Some of the more stringent ductile detailing requirements are relaxed for the OCBFs because it is assumed that these frames will be subjected to smaller inelastic deformation demands due to the use of a smaller response modification factor. However, if an earthquake greater than that considered for design occurs, SCBFs are expected to perform better than OCBFs because of their substantially improved deformation capacity.

9.3.2 Hysteretic Energy Dissipation Capacity of Braces

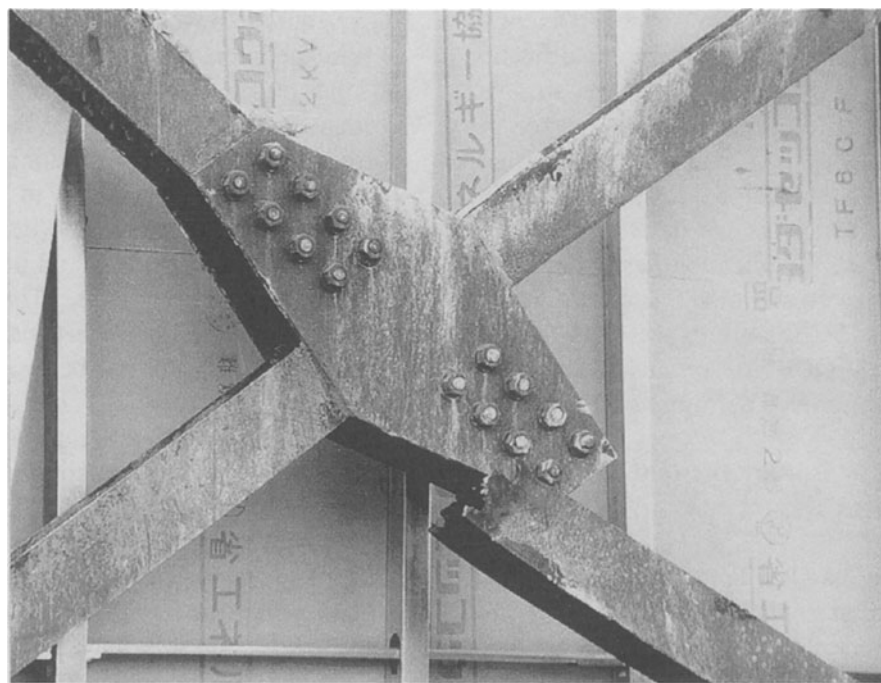
Given that diagonal braces are the structural members chosen to plastically dissipate seismic energy, an examination of the physical behavior of a single brace subjected to axial load reversal is useful. It is customary to express the inelastic behavior of axially loaded members in terms of the axial force, P , versus the axial elongation, δ . According to convention, tension forces and elongations are expressed with positive values. A schematic representation of such a hysteretic curve is shown in Figure 9-10. Note that the transverse member deflection at mid-span is represented by Δ .

A full cycle of inelastic deformations can be described as follows. Starting from an initially unloaded condition (point O in Figure 9-10), the member is first compressed axially in an elastic manner. Buckling occurs at point A. Slender members will experience elastic buckling along plateau AB, for which the applied axial force can be sustained while the member deflects laterally. Up to that point, the brace behavior has remained elastic and unloading would proceed along the line BAO if the axial compressive was removed.

During buckling, flexural moments develop along the member, equal to the product of the axial force and lateral deflection, with the largest value reached at the point of maximum deflection, Δ , at mid-span. Eventually, the

plastic moment of the member, reduced by the axial load, is reached at mid-span, and a plastic hinge starts to develop there (point B in Figure 9-10). The interaction of flexure and axial force on the plastic moment must be taken into account to determine the actual value of Δ corresponding to point B. Along segment BC, further increases in Δ result in greater plastic hinge rotations at mid-span (i.e., the member develops a “plastic kink”) and a corresponding drop in axial resistance. The relationship between P and δ is nonlinear, partly as a result of the plastic interaction between flexure and axial force.

Upon unloading (starting at point C in Figure 9-10), the applied compression force is removed in an elastic manner. After unloading, the member retains a large residual axial deformation as well as a large lateral deflection. When loading the member in tension, behavior is first elastic, up to point D. Then, at point D, the product of the axial force, P , and the mid-span transverse deformation, Δ , equals the member reduced plastic moment and a plastic hinge forms at mid-span. However, this time, along segment DE, plastic hinge rotations act in the reverse sense to those along segment BC, and the transverse deflection reduces. As a result, progressively larger axial forces can be applied. The bracing member cannot be brought back to a perfectly straight position before the member yields in tension. Consequently, when unloaded and reloaded in compression, the brace behaves as a member with an initial deformation and its buckling capacity, P'_{cr} , is typically lower than the corresponding buckling capacity upon first loading, P_{cr} . Upon further cycles of loading, the value of P'_{cr} rapidly stabilizes to a relatively constant value. Typically, the ratio of P'_{cr}/P_{cr} depends on the member slenderness ratio, KL/r , and expressions have been proposed to capture this relationship (Bruneau et al. 1997). For simplicity, a constant value of $P'_{cr} = 0.8P_{cr}$ is specified in the AISC Seismic Provisions (1992) and must be considered whenever it gives a more critical design condition.

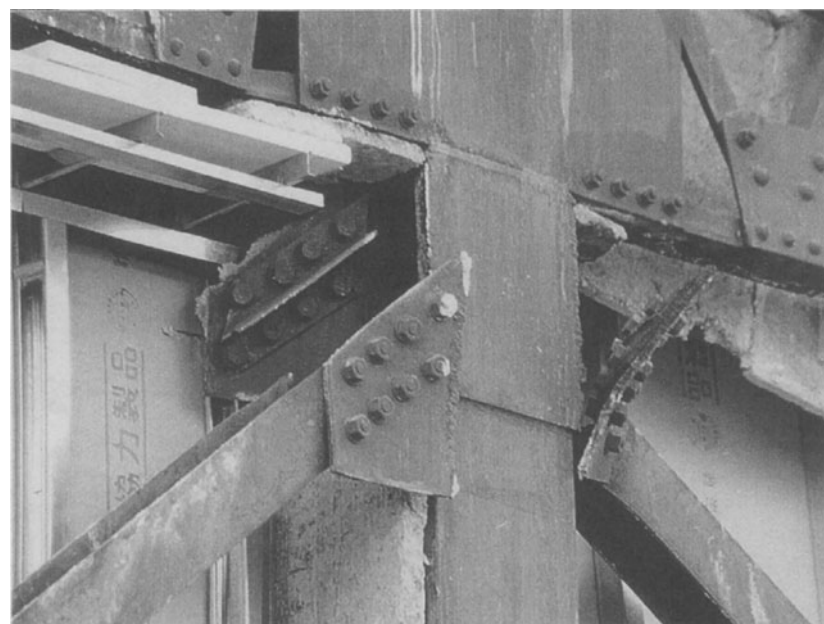


(a) Net section fracture at bolt holes



(b) Severe distortion of beam without lateral support at location of chevron braces

Figure 9-9. Examples of damage to non-ductile braced frames



(c) Fracture of welded connection and web tear-out in brace



(d) Weld fracture

Figure 9-9 Examples of damage to Non-Ductile braced frames (continued)

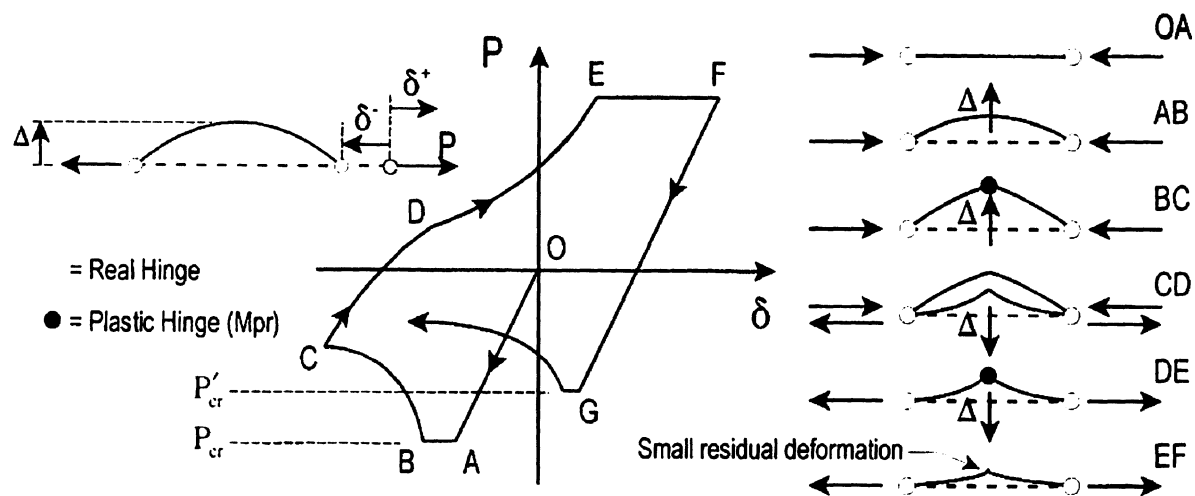


Figure 9-10. Hysteresis of a brace under cyclic axial loading

Beyond this difference, the hysteretic curve repeats itself in each subsequent cycle of axial loading and inelastic deformations, with a shape similar to the OABCDEF of Figure 9-10.

9.3.3 Design Requirements

Concentrically braced frames exhibit their best seismic performance when both yielding in tension and inelastic buckling in compression of their diagonal members contribute significantly to the total hysteretic energy

dissipation. The energy absorption capability of a brace in compression depends on its slenderness ratio (KL/r) and its resistance to local buckling during repeated cycles of inelastic deformation.

Limits on Effective Slenderness Ratio

As can be deduced from Figure 9-10, slenderness has a major impact on the ability of a brace to dissipate hysteretic energy. For a very slender brace, segment OA is short while

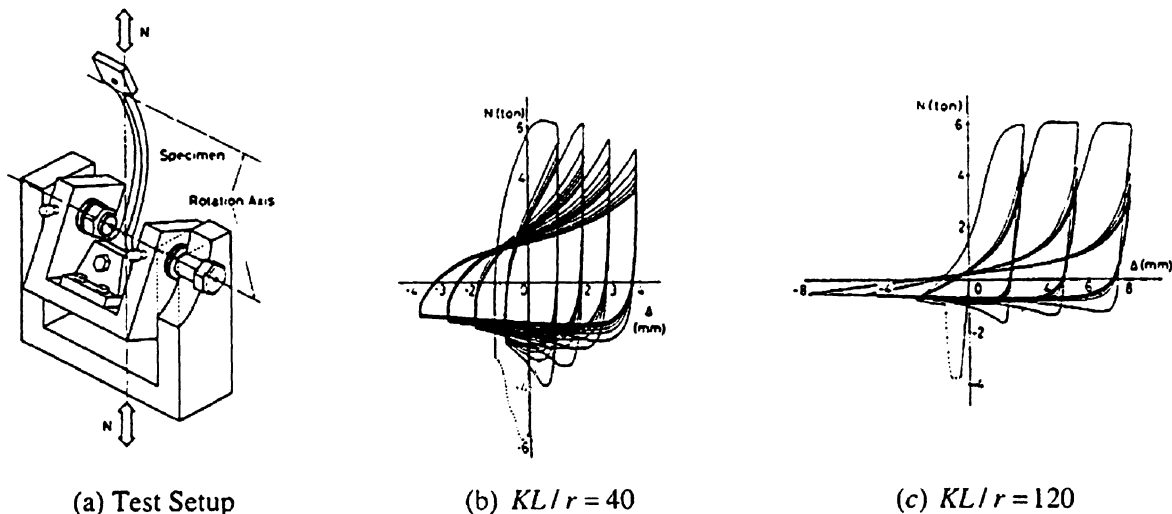


Figure 9-11. Brace Hysteresis loops by experimentation. (Nakashima and Wakabayashi 1992, referring to a figure by Shibata et al. 1973, with permission from CRC Press, Boca Raton, Florida)

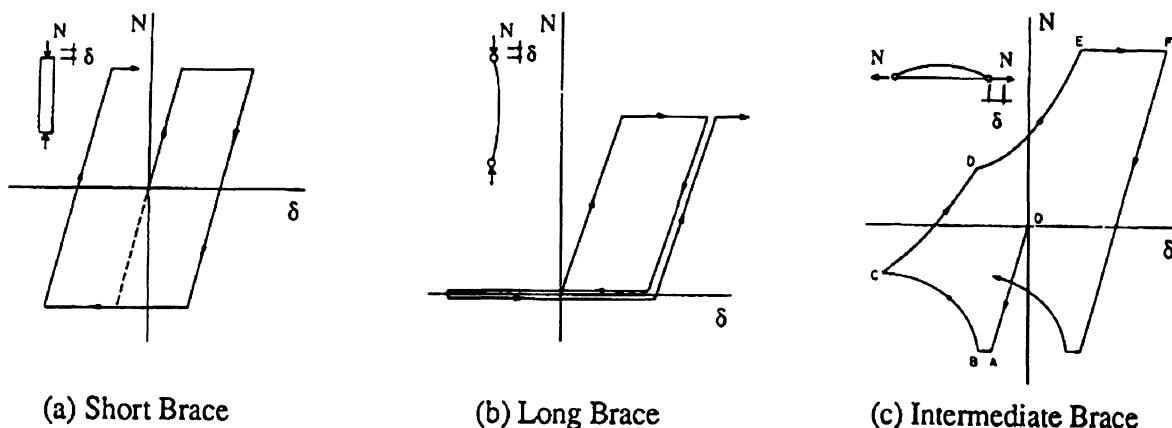


Figure 9-12. Schematic hysteretic behavior of braces of short, long, and intermediate slenderness (Nakashima and Wakabayashi 1992, with permission from CRC Press, Boca Raton, Florida).

segment AB is long, resulting in poor energy dissipation capacity in compression. For stocky braces, the reverse is true, and segment AB (i.e., elastic buckling) may not exist. Slenderness has no impact on the energy dissipation capability of braces in tension.

Typical hysteretic loops obtained experimentally for axially loaded members of intermediate and large slenderness ratios are shown in Figure 9-11, where the parameter λ ($= \kappa l / (\pi \sqrt{r_y E})$) is a non-dimensional slenderness ratio (Nakashima and Wakabayashi 1992). Schematic illustrations of simplified hysteresis loops for short, intermediate and long braces are shown in Figure 9-12.

Very slender brace members (such as bars or plates) can result from a practice called tension-only design, often used prior to the promulgation of modern seismic provisions for steel buildings, and still used in non-seismic regions. In that design approach, the tension brace is sized to resist all the lateral loads, and the contribution of the buckled compression brace is ignored. While tension-only design may be acceptable for wind resistance, it is not permissible for earthquake resistance. As shown in Figure 9-13, braced frames with very slender members must progressively drift

further and further to be able to dissipate the same amount of energy at each cycle, perhaps leading to collapse due to second-order effects.

Seismic detailing provisions typically limit brace slenderness to prevent the above problem and to ensure good energy dissipation capacity. Many seismic codes require:

$$\frac{KL}{r} \leq \frac{720}{\sqrt{F_y}} \quad (9-15)$$

where F_y is in ksi. For ASTM A992 or A572 Grade 50 steel, this corresponds to an effective slenderness ratio of 102. Recently, the AIS C Seismic Provisions (1997) have relaxed this limit to:

$$\frac{KL}{r} \leq \frac{1000}{\sqrt{F_y}} \quad (9-16)$$

for bracing members in SCBFs, but kept the more stringent limit of Eq. 9-15 for OCBFs. Nevertheless, the authors recommend the use of Eq. 9-15 for both SCBFs and OCBFs.

Limits on Width-to-Thickness Ratio

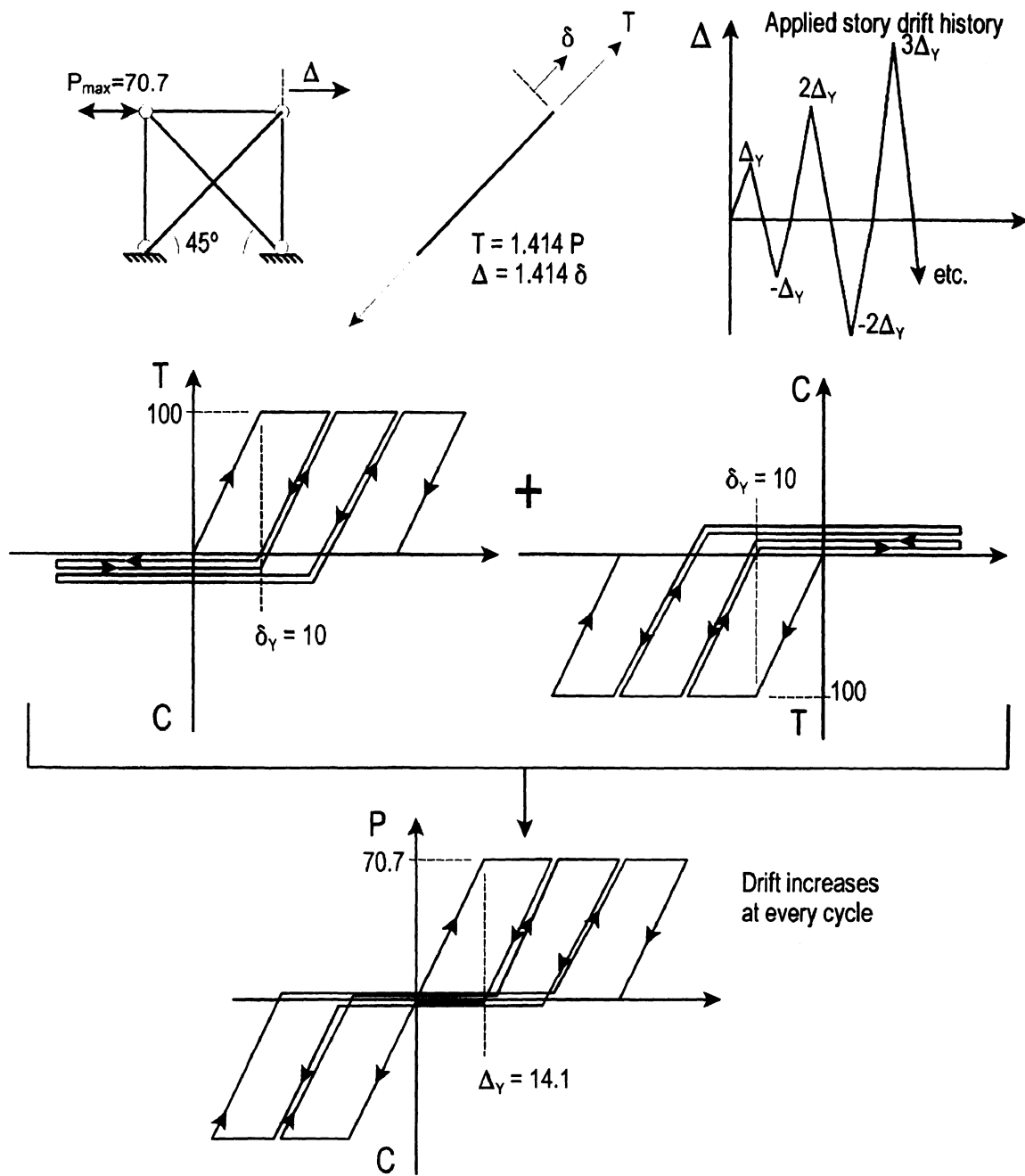


Figure 9-13. Hysteretic Behavior of Single-Story braced frame having very slender braces

The plastic hinge that forms at mid-span of a buckled brace may develop large plastic rotations that could lead to local buckling and rapid loss of compressive capacity and energy dissipation during repeated cycles of inelastic deformations. Past earthquakes and tests have shown that locally buckled braces can also

suffer low-cycle fatigue and fracture after a few cycles of severe inelastic deformations (especially when braces are cold-formed rectangular hollow sections). For these reasons, braces in SCBFs must satisfy the width-to-thickness ratio limits for compact sections. For OCBFs, braces can be compact or non-

compact, but not slender, i.e., $b/t \leq \lambda_r$, per LRFD Specification. Based on experimental evidence, more stringent limits are specified for some types of structural shapes. In particular, the width-to-thickness ratio of angles (b/t), the outside diameter to wall thickness ratio of unstiffened circular hollow sections (D/t), and the outside width to wall thickness ratio of unstiffened rectangular sections must not exceed $52/\sqrt{F_y}$, $1300/F_y$, and $110/\sqrt{F_y}$, respectively (see Table 9-2). Note that the AISC Seismic Provisions (1997) define b for rectangular hollow sections as the "out-to-out width", not the flat-width ($= b - 3t$) as defined in the AISC Specifications (AISC 1994).

Redundancy

Energy dissipation by tension yielding of braces is more reliable than buckling of braces in compression. To provide structural redundancy and a good balance of energy dissipation between compression and tension members, structural configurations that depend predominantly on the compression resistance of braces should be avoided. Examples of poor braced frames layout are shown in Figure 9-14, together with recommended alternatives. Four braces in compression and only one brace in tension resist the load applied on the 5-bay braced frame shown in Figure 9-14a. All braces in the braced-core of Figure 9-14c are in compression to resist the torsional moment resulting from seismically-induced inertial force acting at the center of mass. (For simplicity, columns resisting only gravity loads are not shown in that figure.) Better designs are shown in Figures 9-14b and 9-14d for each of these cases, respectively.

Seismic design codes attempt to prevent the use of non-redundant structural systems by requiring that braces in a given line be deployed such that at least 30% of the total lateral horizontal force acting along that line is resisted by tension braces, and at least 30% by compression braces. Although the wording of such clauses does not cover the case shown in

Figure 9-14c, the intent does. Codes generally waive this requirement if nearly elastic response is expected during earthquakes, something achieved in the AISC Seismic Provisions by the special load conditions described in Section 9.1. Note that in calculating the strength of an OCBF, the AISC Seismic Provisions also require that $\phi_c P_{cr}$ ($= 0.9\phi_c P_{cr}$) be used instead of $\phi_c P_{cr}$, for the reasons described in the previous section. There is no such requirement for SCBFs, but the authors prefer to observe this requirement for both OCBFs and SCBFs, recognizing, however, that the tension brace may have sufficient strength to accommodate the strength degradation of the compression brace upon repeated cycling, and that such a force redistribution may be considered when calculating the strength of the braced panel using $\phi_c P_{cr}$. This approach is not recommended for V- and inverted-V-types of OCBF.

9.3.4 Bracing Connections Design Requirements

When a brace is in tension, net section fracture and block shear rupture at the end of the brace must be avoided. Likewise, the brace connections to beams and columns must be stronger than the braces themselves. Using capacity design, calculation of brace strength must recognize that the expected yield strength of the brace, F_{ye} , will typically exceed its specified minimum yield strength, F_y (see Eq. 9-6). Thus, connections must be designed to resist an axial force equal to $R_y F_y A_g$. However, when plastic analysis is used to demonstrate that braces are unlikely to yield, connections may be designed for the maximum force obtained from such an analysis.

Connections must also be able to resist the forces due to buckling of the brace. If strong connections permit the development of a plastic hinge at each end of a brace, they should be designed to resist a moment equal to $1.1R_y M_p$ of the brace in the direction of buckling. Otherwise, the connecting elements will themselves yield in flexure (such as gussets out

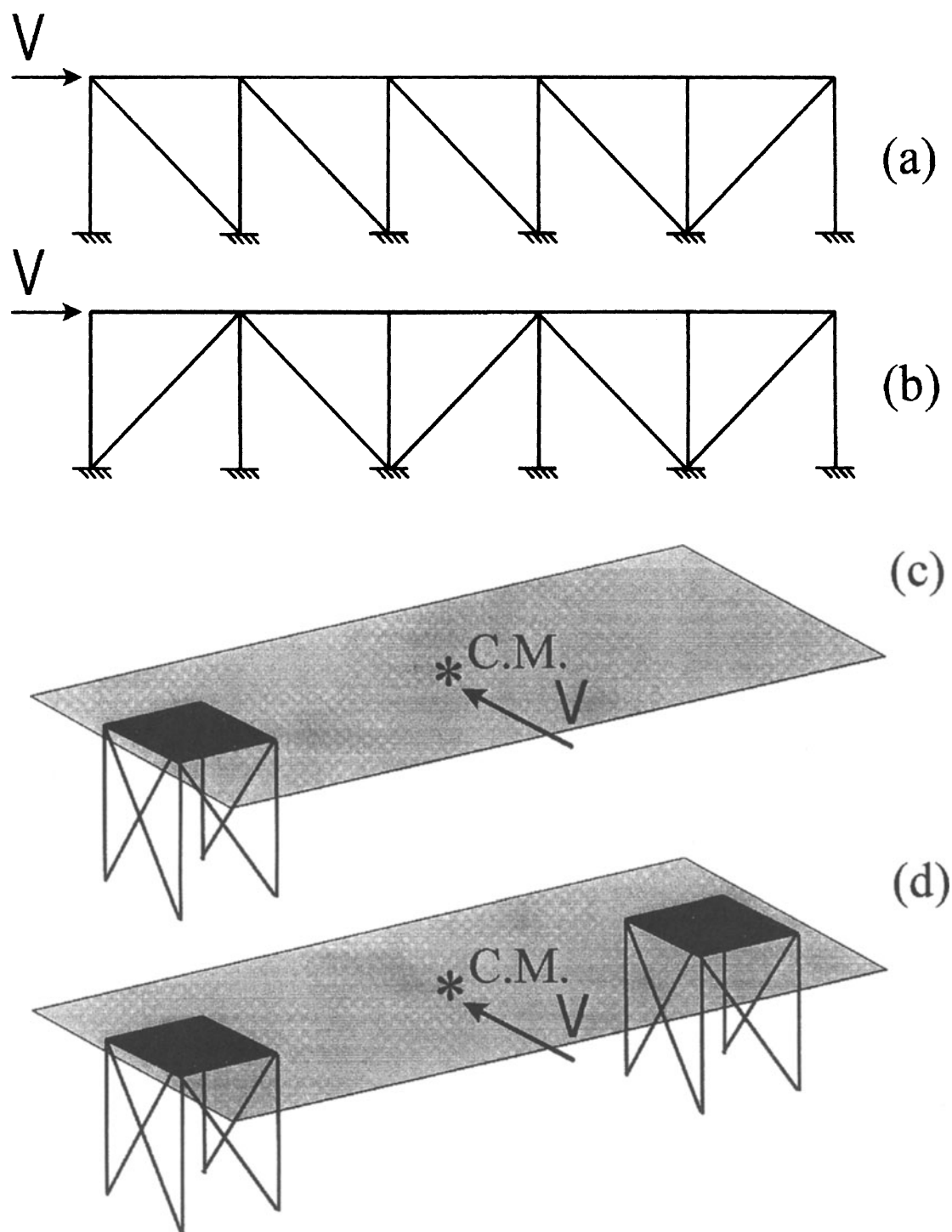


Figure 9-14. Brace configurations to ensure structural redundancy and balanced energy dissipation between compression and tension members: (a and c) poor configurations; (b and d) acceptable configurations

of their plane); these must then be designed to resist the maximum brace compression force in a stable manner while undergoing the large plastic rotations that result from brace buckling. Astaneh-Asl et al. (1986) suggested providing a clear distance of twice the plate thickness between the end of the brace and the assumed line of restraint for the gusset plate to permit plastic rotations and to preclude plate buckling (see Figure 9-15).

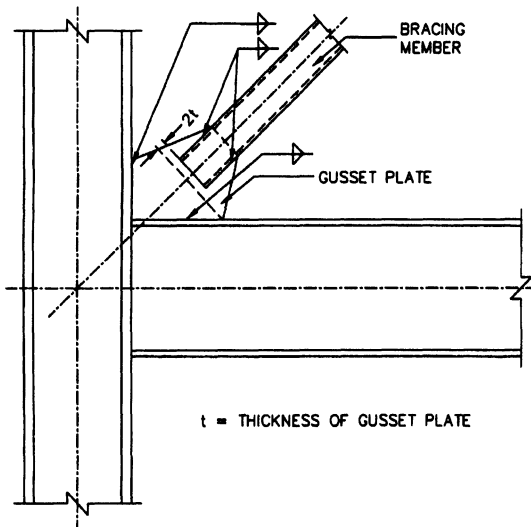


Figure 9-15. Brace-to-gusset connection detail to permit ductile out-of-plane brace buckling (AISC 1997, with permission from American Institute of Steel Construction, Chicago, Illinois)

9.3.5 Columns and Beams

Beams and columns in braced frames must be designed to remain elastic when all braces have reached their maximum tension or compression capacity ($1.1R_y$ times the nominal strength) to eliminate inelastic response in all components except for the braces. This requirement could be too severe for columns, however, as the braces along the height of a multistory frame do not necessarily reach their capacity simultaneously during an earthquake. Statistical approaches have been proposed to evaluate the maximum likely column load (Redwood and Channagiri 1991). The AISC Seismic Provisions address this issue using special load conditions described in Section 9.1,

with the further specification that the maximum axial tension forces in columns need not be taken larger than the value corresponding to foundation uplift. For SCBFs, the Provisions also require that columns satisfy the same width-to-thickness ratio limits as braces (i.e., λ_{ps} in Table 9-2).

Partial penetration groove welds in column splices have been observed to fail in a brittle manner (Bruneau and Mahin 1990). When a welded column splice is expected to be in tension under the loading combination shown in Eq. 9-5, the AISC Seismic Provisions mandate that the partial joint penetration groove welded joints in SCBFs be designed to resist 200% of the strength required by elastic analysis using code-specified forces. Column splices also need to be designed to develop at least the nominal shear strength of the smaller connected member and 50% of the nominal flexural strength of the smaller connected section.

9.3.6 Special Bracing Configuration Requirements

Special requirements apply to the design of V-type and inverted V-type braced frames (also known as chevron braced frames). Because braces meet at the mid-span of beams in these frames, the vertical force resulting from the unequal compression and tension strengths of these braces can have a considerable impact on the cyclic behavior of the frame. That vertical force introduces flexure in the beam, and possibly a plastic hinge in the beam, producing the plastic collapse mechanism shown in Figure 9-16. Therefore, it is imperative that beams in chevron braced frames be continuous between columns. It has also been observed that once a yielding mechanism develops in a chevron-type brace at a particular story, damage tends to concentrate at that story. A comprehensive discussion of the seismic behavior of chevron braced frames under seismic loading is beyond the scope of this chapter, and is presented elsewhere (Bruneau et al. 1997).

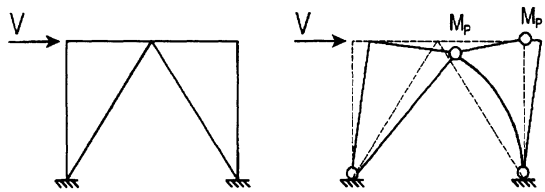


Figure 9-16. Plastic collapse mechanism of chevron braced frame having plastic hinge in beam

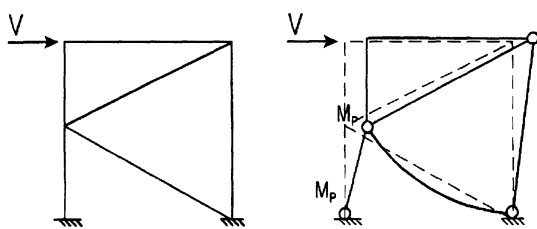


Figure 9-17. Plastic collapse mechanism of K-Braced frame with plastic hinge in column

Seismic provisions usually require that beams in chevron braced frames be capable of resisting their tributary gravity loads neglecting the presence of the braces. The AISC Seismic Provisions also require that each beam in an SCBF be designed to resist a maximum unbalanced vertical load calculated using full yield strength for the brace in tension, and 30% of the brace buckling strength in compression. In OCBFs, this latter provision need not be considered. However, braces in OCBFs must be designed to have 1.5 times the strength required by load combinations that include seismic forces, which is equivalent to designing chevron braced frames for a smaller value of R to compensate for their smaller ductility.

Finally, to prevent instability of a beam bottom flange at the intersection point of the braces in a chevron braced frame, in a manner similar to that shown in Figure 9-9b, the top and bottom flanges of beams in SCBFs and OCBFs must be designed to resist a lateral force equal to 2% of the nominal beam flange strength (i.e., $0.02A_fF_y$). This requirement is best met by the addition of a beam perpendicular to the chevron braced frame.

The above concepts also explain why a number of braced frame configurations are undesirable in seismic regions. For example, in

a K-type braced frame (see Figure 9-17), the unequal buckling and tension-yielding strengths of the braces would create an unbalanced horizontal load at the mid-height of the columns, jeopardizing the ability of the column to carry gravity loads if a plastic hinge forms at the mid-height of the column.

9.4 Behavior and Design of Eccentrically Braced Frames

9.4.1 Introduction

While a properly designed and constructed steel moment frame can behave in a very ductile manner, moment frames are very flexible and their design is usually dictated by the drift limitations. Concentrically braced frames, on the other hand, have a large lateral stiffness, but their energy dissipation capacity is affected by brace buckling. In the early 1970s, an innovative steel system called the Eccentrically Braced Frame (EBF) that combines the advantages of both the steel moment frame and braced frame was proposed in Japan (Fujimoto et al. 1972, Tanabashi et al. 1974). The EBF dissipates energy by controlled yielding of shear or moment links. In the United States, the EBF system was first studied by Roeder and Popov (1978). This attractive system rapidly gained acceptance by the design profession (Teal 1979, Libby 1981, Merovich et al. 1982), some being constructed well before detailed design provisions were developed in the United States. In the 1980s, numerous studies on link behavior provided insight into the cyclic response of EBFs (Manheim and Popov 1983, Hjelmstad and Popov 1983, 1984, Malley and Popov 1984, Kasai and Popov 1986a and 1986b, Ricles and Popov 1989, Engelhardt and Popov 1989). EBF design provisions were first promulgated in the 1988 Uniform Building Code. Experimental verifications of EBF response at the system level were also conducted in the mid- to late-1980s (Yang 1985, Roeder et al. 1987, Whittaker et al. 1989).

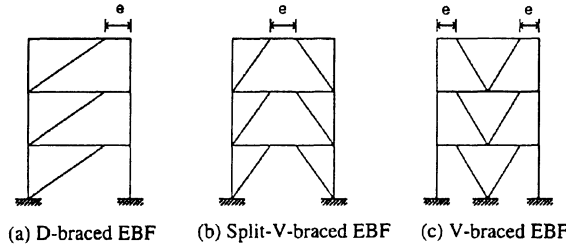


Figure 9-18. Typical EBF configurations

9.4.2 Basic Concept and EBF Behavior

An eccentrically braced frame is a framing system in which the axial force induced in the braces are transferred either to a column or another brace through shear and bending in a small segment of the beam. Typical EBF geometries are shown in Figure 9-18. The critical beam segment is called a “link” and is designated by its length, e . Links in EBFs act as structural fuses to dissipate the earthquake induced energy in a building in a stable manner. To serve its intended purpose, a link needs to be properly detailed to have adequate strength and stable energy dissipation. All the other structural components (beam segments outside of the link, braces, columns, and connections)

are proportioned following capacity design provisions to remain essentially elastic during the design earthquake.

Elastic Stiffness

The variations of the lateral stiffness of a simple EBF with respect to the link length is shown in Figure 9-19 (Hjelmstad and Popov 1984). Note that e/L ratios of 0.0 and 1.0 correspond to a concentrically braced frame and a moment frame, respectively. The figure clearly shows the advantage of using a short link for drift control.

Link Deformation

Consider the idealized split V-type EBF in Figure 9-18b. Once the links have yielded in shear, the plastic mechanism shown in Figure 9-20a will form. Applying simple plastic theory, the kinematics of the plastic mechanism require that:

$$\gamma_p = \frac{L}{e} \theta_p \quad (9-17)$$

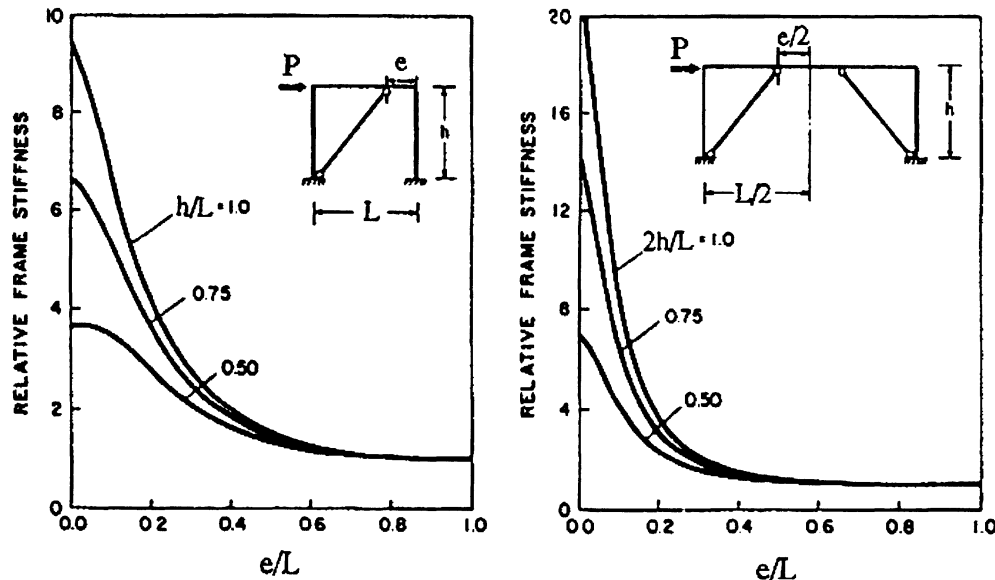
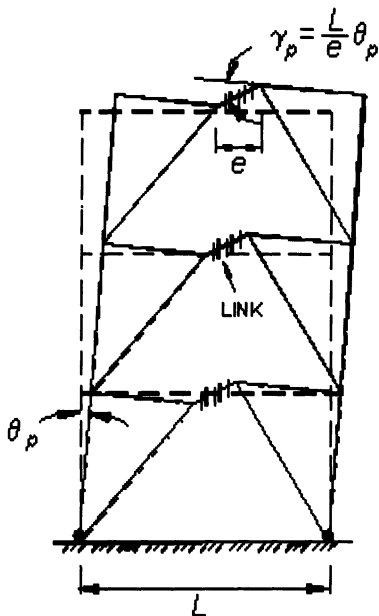
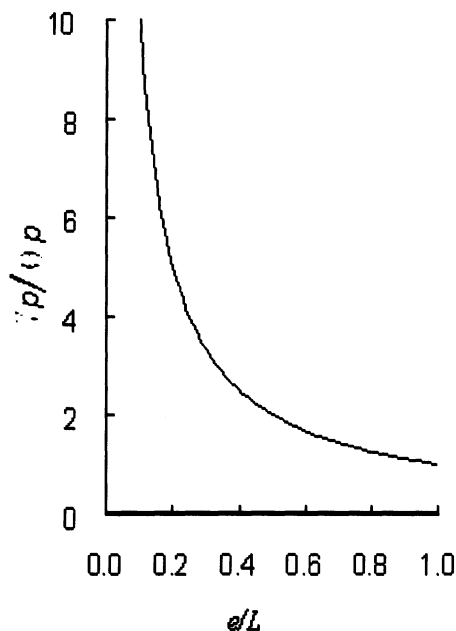


Figure 9-19. Variations of lateral stiffness with respect to link length (Hjelmstad and Popov 1994)



(a) Kinematic Mechanism



(b) Variation of Link Angle with e/L

Figure 9-20. Kinematic mechanism and link plastic angle of a K-type EBF

where θ_p is the plastic drift angle (or plastic story drift ratio), and γ_p is the plastic deformation of the link. Based on Eq. 9-17, the variation of γ_p with respect to the link length is shown in Figure 9-20b. Because the elastic component of the total drift angle is generally small, the plastic story drift angle, θ_p , can be conservatively estimated as the total story drift divided by the story height, h :

$$\theta_p \approx \frac{\Delta_s}{h} = \frac{C_d \Delta_e}{h} \quad (9-18)$$

where Δ_e is the story drift produced by the prescribed design earthquake force, and C_d (= 4) is the deflection amplification factor. To ensure that the deformation capacity of the link is not exceeded, it is obvious from Eq. 9-17 that the link length cannot be too short. Note that the kink that forms between the link and the beam outside the link also implies damage of the concrete slab at the ends of the link.

Ultimate Strength

Unless architectural considerations dictate otherwise, a short link is usually used so that the link will yield primarily in shear. The lateral strength of such an EBF can then be calculated conveniently using simple plastic theory. Assuming that the link behaves in an elastic-perfectly plastic manner, the lateral strength, P_u , of the simple one-story split V-shaped EBF frame can be computed by equating the external work to the internal work:

$$\text{External work} = P_u (h\theta_p) \quad (9-19a)$$

$$\text{Internal work} = \int_0^e V_p \gamma_p dx = e V_p \gamma_p \quad (9-19b)$$

where V_p is the shear strength of the link. Substituting Eq. 9-17 into Eq. 9-19b, the resulting ultimate strength of the EBF frame is

$$P_u = \frac{V_p L}{h} \quad (9-20)$$

As long as the link yields in shear, the above equation shows that the ultimate strength is independent of the link length. This simple plastic theory can also be applied to multistory frames (Kasai and Popov 1985).

Once the link length exceeds a threshold value, flexure and shear dominates the link strength. The ultimate strength of the frame then decreases with an increase in link length. Figure 9-21 illustrates the strength variations. This figure also indicates that the ultimate strength of an EBF with short links is significantly larger than that of a moment frame (i.e., $e/L = 1.0$).

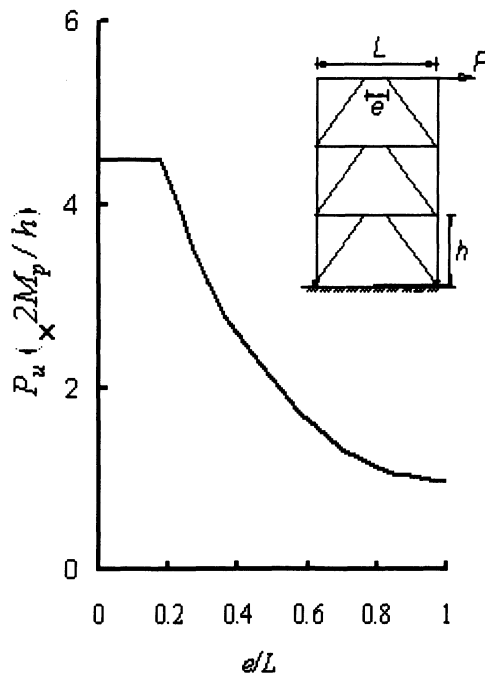


Figure 9-21. Variations of EBF ultimate strength with e/L (Kasai and Popov 1985)

9.4.3 Link Behavior

Critical Length for Shear Link

Figure 9-22 shows the free-body diagram of a link. Ignoring the effects of axial force and the interaction between moment and shear in the link, flexural hinges form at two ends of the link when both M_A and M_B reach the plastic

moment, M_p . A shear hinge is said to form when the shear reaches V_p . The plastic moment and shear capacities are respectively computed as follows:

$$M_p = F_y Z \quad (9-21a)$$

$$V_p = 0.6F_y(d - 2t_f)t_w \quad (9-21b)$$

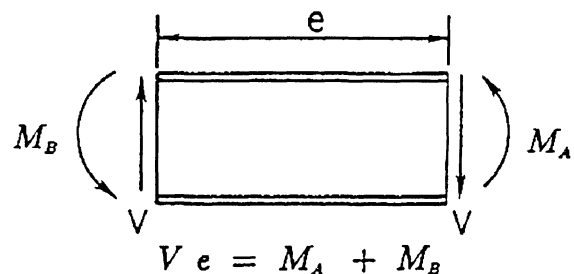


Figure 9-22. Link deformation and free-body diagram

A balanced yielding condition corresponds to the simultaneous formation of flexural hinges and a shear hinge. The corresponding link length is

$$e_0 = \frac{2M_p}{V_p} \quad (9-22)$$

In a short link ($e \leq e_0$), a shear hinge will form. When $e > e_0$, a flexural (or moment) hinge forms at both ends of the link, and the corresponding shear force is:

$$V = \frac{2M_p}{e} \quad (9-23)$$

Based on plastic theory, Eq. 9-22 can be modified slightly to include the effect of interaction between M and V . Nevertheless, experimental results indicated that the interaction is weak and that such interaction can be ignored (Kasai and Popov 196b). Test results also showed that a properly stiffened short link can strain harden and develop a shear strength equal to $1.5V_p$. The end moments of a link that has yielded in shear can continue to increase

due to strain hardening and, therefore, flexural hinges can develop. To avoid low-cycle fatigue failure of the link flanges due to high strains, these end moments are limited to $1.2M_p$, and the maximum length (e_0 in Eq. 9-22) for a shear link was modified as follows (Kasai and Popov 1986b):

$$e_0 = \frac{2(1.2M_p)}{1.5V_p} = \frac{1.6M_p}{V_p} \quad (9-24)$$

Longer Links

Experimental results have shown that the inelastic deformation capacity of an EBF can be greatly reduced when long links ($e > e_0$) are used. Following the above logic, it can be shown that flexural hinges dominate the link response when e is larger than $2.6M_p/V_p$. In the transition region where $1.6M_p/V_p < e < 2.6M_p/V_p$, the link undergoes simultaneous shear and flexural yielding (Engelhardt and Popov 1989). Figure 9-23 classifies links in EBFs. Note that when longer links are used in the D-type or V-type EBF (see Figure 9-18), the welded connection between the link and the column is subjected to high moments and it could be vulnerable to brittle fracture if detailed similar to the connections that failed during the Northridge earthquake (see Section 9.2).

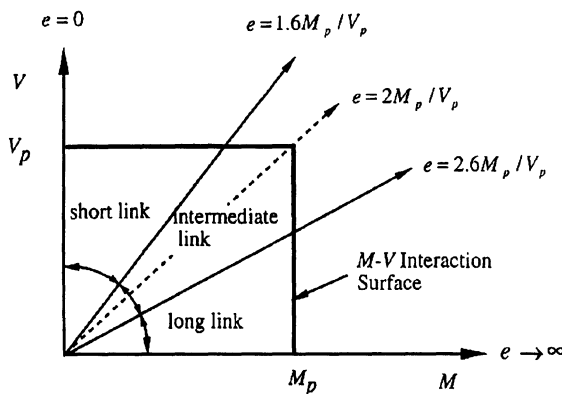


Figure 9-23. Classification of links

Based on experimental results, the link deformation capacity, γ_a , as given by the AISC Seismic Provisions is shown in Figure 9-24. The calculated rotation angle, γ_p , cannot exceed γ_a .

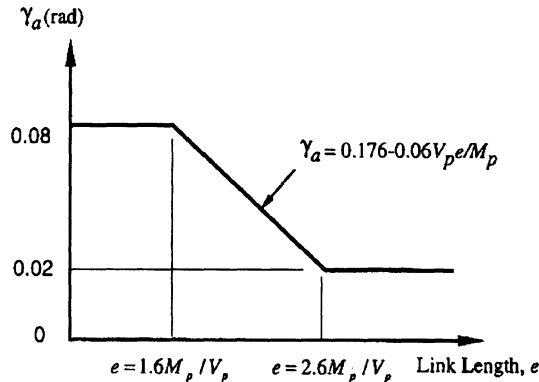


Figure 9-24. Allowable link angles per AISC Seismic Provisions (1997)

Effect of Axial Force

The presence of an axial force in a link reduces not only the flexural and shear capacities but also its inelastic deformation capacity (Kasai and Popov 1986b). When the axial force, P_u , exceeds 15% of the yield force, $P_y (= A_g F_y)$, the P - M interaction formula for plastic design (AISC 1989) can be used to compute the reduced plastic moment, M_{pa} :

$$M_{pa} = 1.18M_p \left(1 - \frac{P_u}{P_y} \right) \quad (9-25)$$

The reduced shear capacity is (Manheim and Popov 1983):

$$V_{pa} = V_p \sqrt{1 - (P_u / P_y)^2} \quad (9-26)$$

Replacing M_p and V_p in Eq. 9-24 by M_{pa} and V_{pa} , the reduced value of e_0 when $\rho A_w / A_g \geq 0.3$ can be approximated as follows (Kasai and Popov 1986b):

$$e_0 = \left(1.15 - 0.5\rho' \frac{A_w}{A_g} \right) \frac{1.6M_p}{V_p} \quad (9-27)$$

where $\rho' = P/V$, and $A_w = (d - 2t_f)t_w$. The correction is unnecessary if $\rho A_w / A_g < 0.3$, in which case the AISC Seismic Provisions (1997) require that the link length shall not exceed that given by Eq. 9-24.

Effect of Concrete Slab

Research conducted on composite links showed that composite action can significantly increase the link shear capacity during the first cycles of large inelastic deformations. However, composite action deteriorates rapidly in subsequent cycles due to local concrete floor damage at both ends of the link (Ricles and Popov 1989). For design purposes, it is conservative to ignore the contribution of composite action for calculating the link shear strength. But the overstrength produced by the composite slab effect needs to be considered when estimating the maximum forces that the shear link imposes to other structural components (Whittaker et al. 1989).

Link Detailing

Full-depth web stiffeners must be placed symmetrically on both sides of the link web at the diagonal brace ends of the link. These end stiffeners are required to have a combined width not less than $(b_f - 2t_w)$ and a thickness not less than $0.75t_w$ nor 3/8 inch, whichever is larger.

The link section needs to satisfy the same compactness requirement as the beam section for special moment frames. Further, the link needs to be stiffened in order to delay the onset of web buckling and to prevent flange local buckling. The stiffening requirement is dependent on the length of link (see Figure 9-23). For a shear link with $e \leq 1.6M_p/V_p$, a relationship among the link web deformation angle, the web panel aspect ratio as well as the beam web slenderness ratio was developed

(Kasai and Popov 1986a). A conservative approximation of the relationship follows:

$$a = C_B t_w - \frac{d}{5} \quad (9-28)$$

where a = stiffener spacing, d = link depth, t_w = link web thickness, and $C_B = 56, 38$, and 29 for $\gamma_p = 0.03, 0.06$, and 0.09 radian, respectively. These C_B values are slightly modified and are adopted in the AISC Seismic Provisions (1997) as follows:

(1) When $e \leq 1.6M_p/V_p$, intermediate stiffeners are needed per Eq. 9-28, but the coefficient C_B is a function of the deformation demand; the relationship between C_B and γ_p implied by the AISC Seismic Provisions is shown in Figure 9-25.

(2) When $1.6M_p/V_p \leq e \leq 5M_p/V_p$, intermediate stiffeners shall be provided at a distance $1.5b_f$ from each end of the link to control flange local buckling.

(3) When $5M_p/V_p \leq e \leq 2.6M_p/V_p$, intermediate stiffeners satisfying the requirements of both Cases 1 and 2 are needed.

(4) When $e > 2.6M_p/V_p$, intermediate stiffeners are not required.

Intermediate link web stiffeners must be full depth. While two-sided stiffeners are required at the end of the link where the diagonal brace intersects the link, intermediate stiffeners placed on one side of the link web are sufficient for links less than 25 inches in depth. Fillet welds connecting a link stiffener

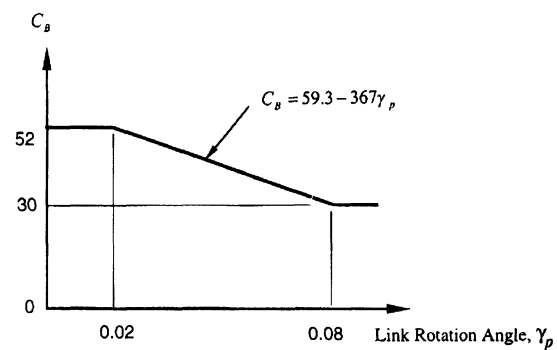


Figure 9-25. Variation of C_B

to the link web shall have a design strength to resist a force of $A_{st}F_y$, where A_{st} is the stiffener area. The design strength of fillet welds fastening the stiffener to the flanges shall be adequate to resist a force of $A_{st}F_y/4$.

Lateral Bracing of Link

To ensure stable hysteresis, a link must be laterally braced at each end to avoid out-of-plane twisting. Lateral bracing also stabilizes the eccentric bracing and the beam segment outside the link. The concrete slab alone cannot be relied upon to provide lateral bracing. Therefore, both top and bottom flanges of the link beam must be braced. The bracing should be designed for 6 percent of the expected link flange strength, $R_yF_yb_f t_f$.

9.4.4 Capacity Design of Other Structural Components

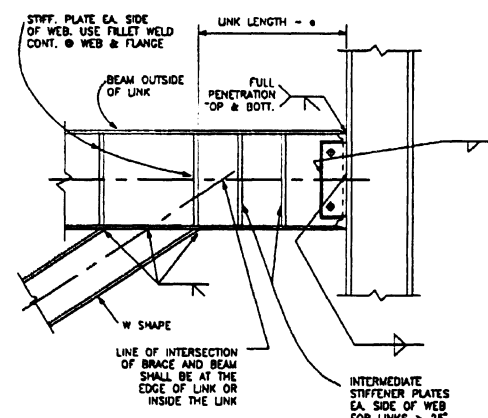
Links in an EBF are designated as structural fuses and are sized for code-specified design seismic forces. All other elements (beam segments outside the link, braces, columns, and connections) are then designed for the forces generated by the actual (or expected) capacity of the links rather than the code-specified design seismic forces. The capacity design concept thus requires that the computation of the link strength not only be based on the expected yield strength of the steel but also includes the consideration of strain-hardening and overstrength due to composite action of the slab.

Diagonal Brace

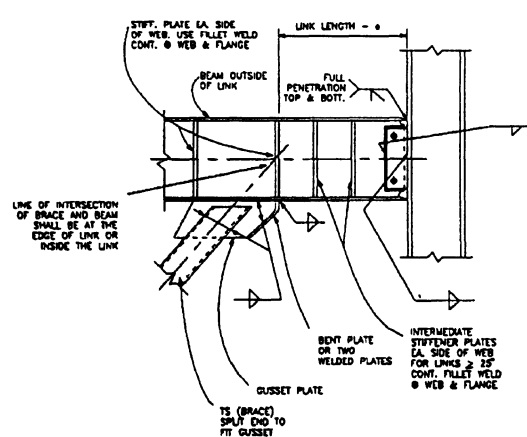
The required axial and flexural strength of the diagonal brace shall be those generated by the expected shear strength of the link R_yV_n increased by 125 percent to account for strain-hardening. The nominal shear capacity, V_n , is the lesser of V_p or $2M_p/e$. Although braces are not expected to experience buckling, the AISC Seismic Provisions take a conservative approach by requiring that a compact section ($\lambda < \lambda_p$) be used for the brace.

At the connection between the diagonal brace and the beam, the intersection of the brace and beam centerlines shall be at the end of the link or within the length of the link (see Figure 9-26a). If the intersection point lies outside the link length, the eccentricity together with the brace axial force produces additional moments in the beam and brace.

The diagonal brace-to-beam connection at the link end of the brace shall also be designed to develop the expected strength of the brace. No part of this connection shall extend over the link length to reduce the link length, e . If the connection is designed as a pin (see Figure 9-26b), the gusset plate needs to be properly stiffened at the free edge to avoid local buckling (Roeder et al. 1989).



(a) Diagonal Brace Fully Connected to Link



(b) Diagonal Brace Pin-Connected to Link

Figure 9-26. EBF link and connection details (AISC 1997)

Link-to-Column Connections

Of the common EBF configurations shown in Figure 9-18, it is highly desirable to use the split V-braced EBF in order to avoid the moment connection between the link and column. Prior to the 1994 Northridge earthquake, test results showed that the fully restrained welded connection between the column and the link (especially longer links) is vulnerable to brittle fracture similar to those found in the beam-to-column moment connections after the Northridge earthquake. Therefore, the AISC Seismic Provisions (1997) require that the deformation capacity of the link-to-column connections be verified by qualifying cyclic tests. Test results shall demonstrate that the link inelastic rotation capacity is at least 20 percent greater than that calculated by Eq. 9-17.

When reinforcements like cover plates are used to reinforce the link-to-column connection, the link over the reinforced length may not yield. Under such circumstances, the link is defined as the segment between the end of the reinforcement and the brace connection. Cyclic testing is not needed when (1) the shortened link length does not exceed e_o in Eq. 9-24, and (2) the design strength of the reinforced connection is equal to or greater than the force produced by a shear force of $1.25 R_y V_n$ in the link.

Tests also demonstrated that the welded connections of links to the weak-axis of a column were vulnerable to brittle fracture (Engelhardt and Popov 1989); this type of connection should be avoided.

Beam-to-Column Connection

For the preferred EBF configuration where the link is not adjacent to a column, a simple framing connection between the beam and the column is considered adequate if it provides some restraint against torsion in the beam. The AISC Seismic Provisions stipulate that the magnitude of this torsion be calculated by

considering perpendicular forces equal to 2 percent of the beam flange nominal strength, $F_y b_f t_f$, applied in opposite directions on each flange.

Beam Outside of Link

The link end moment is distributed between the brace and the beam outside of the link according to their relative stiffness. In preliminary design, it is conservative to assume that all the link end moment is resisted by the beam. The link end moment shall be calculated using 1.1 times the expected nominal shear strength ($R_y V_n$) of the link. Because a continuous member is generally used for both the link and the beam outside the link, it is too conservative to use the expected yield strength ($R_y F_y$) for estimating the force demand produced by the link while the beam strength is based on the nominal yield strength (F_y). Therefore, the AISC Seismic Provisions allow designers to increase the design strength of the beam by a factor R_y .

The horizontal component of the brace produces a significant axial force in the beam, particularly if the angle between the diagonal brace and the beam is small. Therefore, the beam outside the link needs to be designed as a beam-column. When lateral bracing is used to increase the capacity of the beam-column, this bracing must be designed to resist 2 percent of the beam flange nominal strength, $F_y b_f t_f$.

Column

Using a capacity design approach, columns in braced bays shall have a sufficient strength to resist the sum of gravity-load actions and the moments and axial forces generated by 1.1 times the expected nominal strength ($R_y V_n$) of the link. This procedure assumes that all links will yield and reach their maximum strengths simultaneously. Nevertheless, available multistory EBF test results showed that this preferred yielding mechanism is difficult to develop. For example, shaking table testing of a 6-story reduced scale EBF model showed that

links in the bottom two stories dissipated most of the energy (Whittaker et al. 1989). Therefore, this design procedure may be appropriate for low-rise buildings and the upper stories of medium- and high-rise buildings but may be too conservative in other instances.

The alternative design procedure permitted by the AISC Seismic Provisions is to amplify the design seismic axial forces and moments in columns by the overstrength factor, Ω_o ($= 2.0$, see Table 9-1). See Eqs. 9-4 and 9-5 for the load combinations. The computed column

forces need not exceed those computed by the first procedure. Therefore, the first design procedure will generally produce a more conservative design for columns.

9.5 Design Examples

9.5.1 General

A six-story office building having the floor plan shown in Figure 9-27 is used to

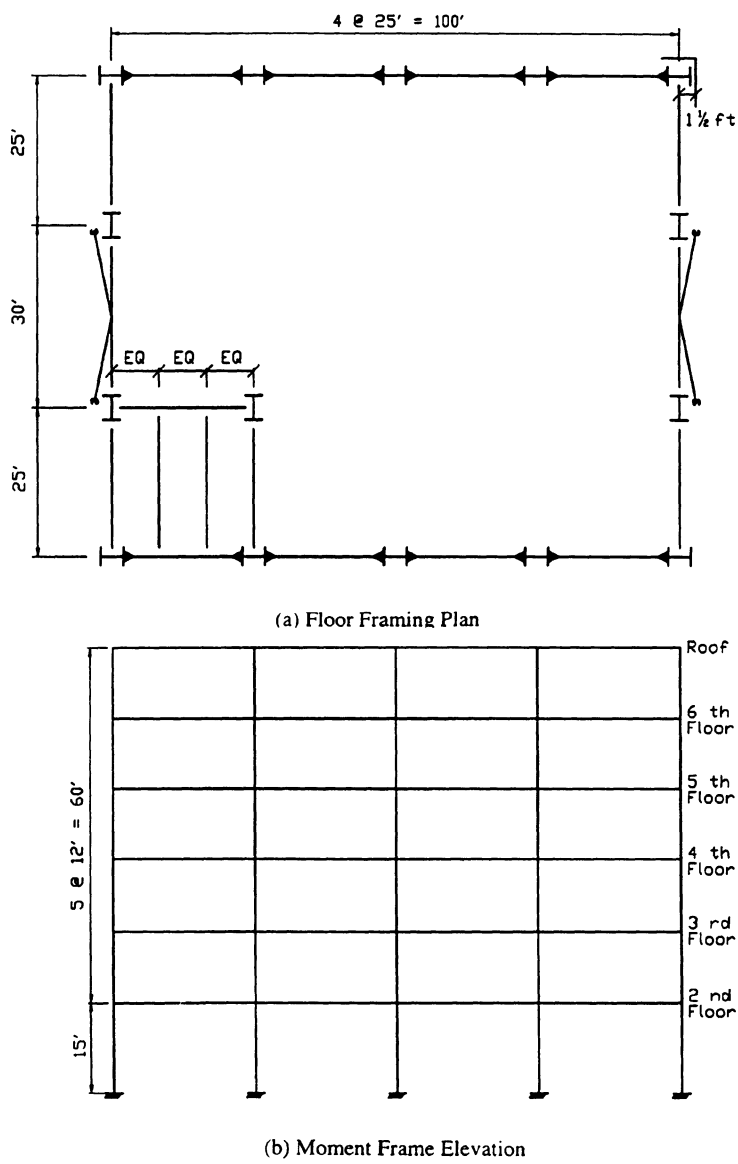


Figure 9-27. A six-story office building

demonstrate the seismic design procedures. The design follows the AISC Seismic Provisions (1997) and the Load and Resistance Factor Design Specification for Structural Steel Buildings (1993). Special Moment-Resisting Frames (SMFs) are used in the E-W direction, and their design is presented in Section 9.5.2. Braced frames provide lateral load-resistance in the N-S direction; these are designed as Special Concentrically Braced Frames (SCBFs) in Section 9.5.3 and Eccentrically Braced Frames (EBFs) in Section 9.5.4, respectively.

The design gravity loads are listed in Table 9-3. The NEHRP Recommended Provisions (1997) are the basis for computing the design seismic forces. It is assumed that the building is located in a high seismic region with the following design parameters:

$$S_S = 1.5 \text{ g}$$

$$S_1 = 0.6 \text{ g}$$

Site Class = B

$I = 1.0$ (Seismic User Group I)

Seismic Design Category = D

The design response spectrum is shown in Figure 9-28.

The design follows the Equivalent Lateral Force Procedure of the NEHRP Recommended Provisions. The design base shear ratio, C_s , is computed as follows:

$$C_s = \frac{S_{D1}}{T(R/I)} \leq \frac{S_{DS}}{(R/I)} \quad (9-29)$$

where S_{D1} ($= 0.4 \text{ g}$) and S_{DS} ($= 1.0 \text{ g}$) are the design spectral response accelerations at a period of 1.0 second and in the short period range, respectively. The values of R for the three framing systems considered in this example are listed in Table 9-4. The NEHRP empirical period formula is used to compute the approximate fundamental period, T_a :

$$T_a = C_T h_n^{3/4} \quad (9-30)$$

where h_n (ft) is the building height, and the coefficient C_T is equal to 0.035, 0.030, and 0.02 for SMFs, EBFs, and SCBFs, respectively. Alternatively, the value of T obtained from a dynamic analysis can be used in design, but the period thus obtained cannot be taken larger than $C_u T_a$ for the calculation of required structural strengths, where $C_u = 1.2$.

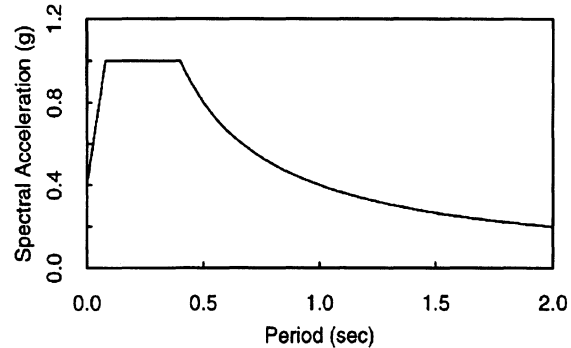


Figure 9-28. Elastic design response spectrum

for this design example. To establish seismic forces for story drift computations, however, this upper limit is waived by the NEHRP Recommended Provisions. Recognizing that the analytically predicted period of a multistory SMF is generally larger than $C_u T_a$, this upper bound value is used to compute the design base shear ratio for preliminary design. Based on Eq. 9-1, the design base shear ratios for the three types of frames are listed in Table 9-4.

The following two load combinations are to be considered:

$$1.2D + 0.5L + 1.0E \quad (9-31)$$

$$0.9D - 1.0E \quad (9-32)$$

where $E = \rho Q_E + 0.2 S_{DS} D$. The Redundancy Factor, ρ , is

$$\rho = 2 - \frac{20}{r_{\max} \sqrt{A}} = 2 - \frac{20}{0.25 \sqrt{8549}} = 1.13 \quad (9-33)$$

(See the NEHRP Recommended Provisions on ρ .) Therefore, the above two load combinations can be expressed as

Table 9-3. Design gravity loads

Load	Dead Load (psf)	Live Load +(psf)
Roof	70	20
Floor	90*	50
Cladding	20	-

*80 psf for computing reactive weight.

+ Use $L = L_0(0.25 + 15/\sqrt{A_t})$ for live load reduction (ASCE 1998)

Table 9-4. System parameters and design base shears

Framing System	R	Ω_o	C_d	T_a (sec)	C_s	V_B^* (kip)	k
SMF	8	3	5 ½	1.07	0.047	111	1.285
SCBF	6	2	5	0.51	0.131	305	1.0
EBF	8	2	4	0.76	0.066	156	1.13

*Values have been increased by 5% to account for accidental eccentricity.

$$\begin{aligned} & 1.2D + 0.5L + 1.0(\rho Q_E + 0.2D) \\ &= 1.4D + 0.5L + \rho Q_E \end{aligned} \quad (9-34)$$

$$0.9D - 1.0(\rho Q_E + 0.2D) = 0.7D - \rho Q_E \quad (9-35)$$

The design base shear, V_B ($= C_s W$, where W = building reactive weight), for computing the seismic effect (Q_E) is distributed to each floor level as follows:

$$F_x = \frac{W_x h_x^k}{\sum W_i h_i^k} V_B \quad (9-36)$$

where the values of k listed in Table 9-4 are used to consider the higher-mode effect. Based on Eq. 9-36, the design story shears for each example frame are summarized in Table 9-5.

9.5.2 Special Moment Frames (SMF)

Story Shear Distribution

The story shear distribution of the SMF listed in Table 9-5 is for strength computations. To compute story drift, however, it is permissible to use the actual fundamental period, T , of the structure. The actual period of this 6-story SMF is expected to be larger than

the approximate period, T_a ($= 1.07$ seconds), determined from Eq. 9-30. There exists many approaches to the preliminary design of SMF. The one followed in this section has been proposed by Becker (1997). First, the fundamental period can be estimated using a simplified Rayleigh method (Teal 1975):

$$T = 0.25 \sqrt{\frac{\Delta_r}{C_1}} \quad (9-37)$$

where

T = fundamental period,

Δ_r = lateral deflection at the top of the building under the lateral load V ,

$C_1 = V/W$,

V = lateral force producing deflection, and

W = building reactive weight.

The story drift requirement is:

$$\delta_x = \frac{C_d \Delta}{I} < 0.02H,$$

$$\Delta_r < \frac{0.02HI}{C_d} = \frac{0.02 \times 75 \times 12}{5.5} = 3.27 \text{ in}$$

Assuming conservatively that the total deflection is about 60% of the allowable value,

$$\Delta_r = 0.60(3.27) = 1.96 \text{ in}$$

Table 9-5. Design story shears

Floor	W_i (kips)	h_i (ft)	Story Shear* (kips)		
			SMF	SCBF	EBF
R	322	75	34	84	45
6	387	63	67	168	90
5	387	51	92	236	125
4	387	39	109	288	150
3	387	27	120	324	167
2	392	15	125	345	176

* $\rho (= 1.13)$ is included.

$$C_1 = 1.05\rho(C_s) = 1.05(1.13) \frac{0.4}{T(R/I)} = \frac{0.059}{T}$$

(where 1.05 accounts for torsion)

$$T = 0.25 \sqrt{\frac{1.96}{0.059/T}} = 1.44\sqrt{T}$$

Solving the above equation gives a value of T equal to 2.0 seconds. For this value, however,

$$\begin{aligned} C_s &= \frac{S_{D1}}{T(R/I)} = \frac{0.4}{2(8/1.0)}, \\ &= 0.025 < 0.044 S_{DS} \end{aligned}$$

and $C_s = 0.044$ controls. That is, the minimum seismic base shear for drift computations is

$$V = 1.05 \times \rho \times 0.044 W = 0.052 W$$

Since the base shear ratios for strength and drift designs are 0.047 and 0.044, respectively, a scaling factor of 0.94 ($= 0.044/0.047$) can be used to reduce the story shears listed in Table 9-5 for drift computations.

Member Proportions

For brevity in this design example, detailed calculations are presented only for the beams on the fourth floor and the columns above and below that floor (see Figure 9-29). The portal method is used for preliminary design. Assuming that the point of inflection occurs at the mid-length of each member:

$$2F_1 + 3F_2 = 0.94(109) = 102.5 \text{ kips}$$

$$F_1 = F_2/2, \quad F_2 = 25.6 \text{ kips}$$

Consider the interior beam-column assembly shown in Figure 9-29. Summing the moments at the point of inflection at point P, the beam shear, F_3 , is calculated to be:

$$12F_2 = 25F_3, \quad F_3 = 12.3 \text{ kips}$$

The story drift due to column and girder deformations is:

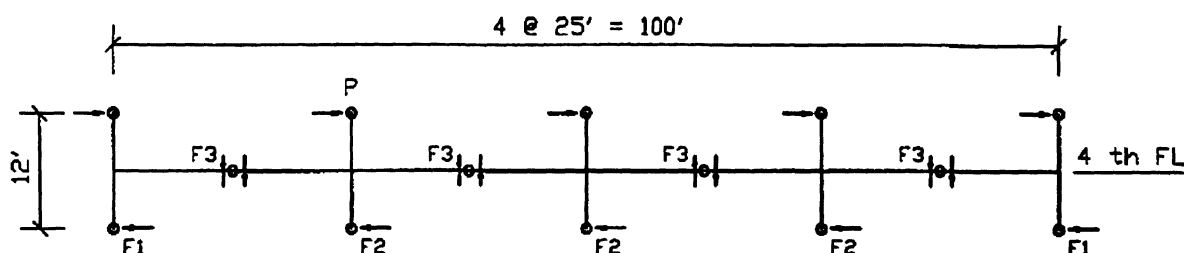


Figure 9-29. Typical shear force distributions in beams and columns

$$\Delta = \Delta_c + \Delta_g = \frac{F_2 h^3}{12EI_c} + \frac{F_2 L h^2}{12EI_g} \quad (9-38)$$

where

Δ = story drift,

Δ_c = drift produced by column deformation,

Δ_g = drift produced by beam deformations,

F_2 = column shear,

h = story height,

L = beam length between points of inflection,

I_c = moment of inertia of column, and

I_g = moment of inertia of beam.

Eq. 9-38 uses centerline dimensions and ignores the shear and axial deformations of the beams and column. In equating Eq. 9-38 to the allowable drift, it is assumed that the panel zone deformation will contribute 15% to the story drift; the actual contribution of the panel zone deformation will be verified later.

$$\delta_x = \frac{C_d \Delta}{I} \leq (0.85)0.02h,$$

$$\Delta \leq 0.0031h = 0.45 \text{ in}$$

$$\frac{F_2 h^2}{12E} \left(\frac{h}{I_c} + \frac{L}{I_g} \right) \leq 0.45 \quad (9-39)$$

The above relationship dictates the stiffness required for both the beams and columns in order to meet the story drift requirement. By setting $I = I_c = I_g$ as a first attempt, Eq. 9-39 gives a required $I = 1532 \text{ in}^4$. Using A992 steel for both the columns and the beams, it is possible to select W14×132 columns ($I_c = 1530 \text{ in}^4$) and W24×62 beams ($I_g = 1532 \text{ in}^4$).

In addition to satisfying the story drift requirements, the strength of the columns and beams also need to be checked for the forces produced by the normal seismic load combinations (Eqs. 9-34 and 9-35). However, beam and column sizes of this 6-story SMF are generally governed by the story drift and strong-column weak-girder requirements. Therefore, the strength evaluations of these members are not presented here.

A formal check of the strong column-weak beam requirement will be performed later. A

quick check of this requirement for the flexural strength of both the beams and columns is worthwhile before the moment connections are designed. It is assumed that the column axial stress (P_u / A_g) is equal to $0.15F_y$. Beams are designed using the reduced beam section strategy in this example. Assuming that (1) the reduced beam plastic sectional modulus (Z_{RBS}) is 70% of the beam plastic sectional modulus (Z_{BM}), and (2) the moment gradient (M_v) from the plastic hinge location to the column centerline is 15% of the design plastic moment at the plastic hinge location:

$$\sum M_{pc}^* = 2[Z_c(F_y - P_u/A_g)] \approx 2(0.85Z_c F_y)$$

$$Z_{RBS} \approx 0.7Z_{BM}, M_v \approx 0.15(1.1R_y Z_{RBS} F_y)$$

$$\begin{aligned} \sum M_{pb}^* &= 2[1.1R_y Z_{RBS} F_y + M_v] \\ &\approx 2(1.1R_y Z_{RBS} F_y \times 1.15) \\ &\approx 2(1.1 \times 1.1 \times 0.7 \times 1.15 Z_{BM} F_y) \\ &= 2(0.97)Z_{BM} F_y \end{aligned}$$

To satisfy Eq. 9-14:

$$\frac{\sum M_{pc}^*}{\sum M_b^*} = \frac{2(0.85Z_c)}{2(0.97Z_{BM})} \geq 1.0$$

$$\frac{Z_c}{Z_{BM}} \geq 1.15$$

For the beam and column sizes selected:

$$\frac{Z_c}{Z_{BM}} = \frac{234}{153} = 1.53 \geq 1.15 \quad (\text{OK})$$

Both W14×132 and W24×62 satisfy the λ_{ps} requirements given in Table 9-2. Since the RBS is to be used, additional check of the beam web compactness is required:

$$\frac{h}{t_w} = 50.1 < \frac{418}{\sqrt{F_y}} = 59.1 \quad (\text{OK})$$

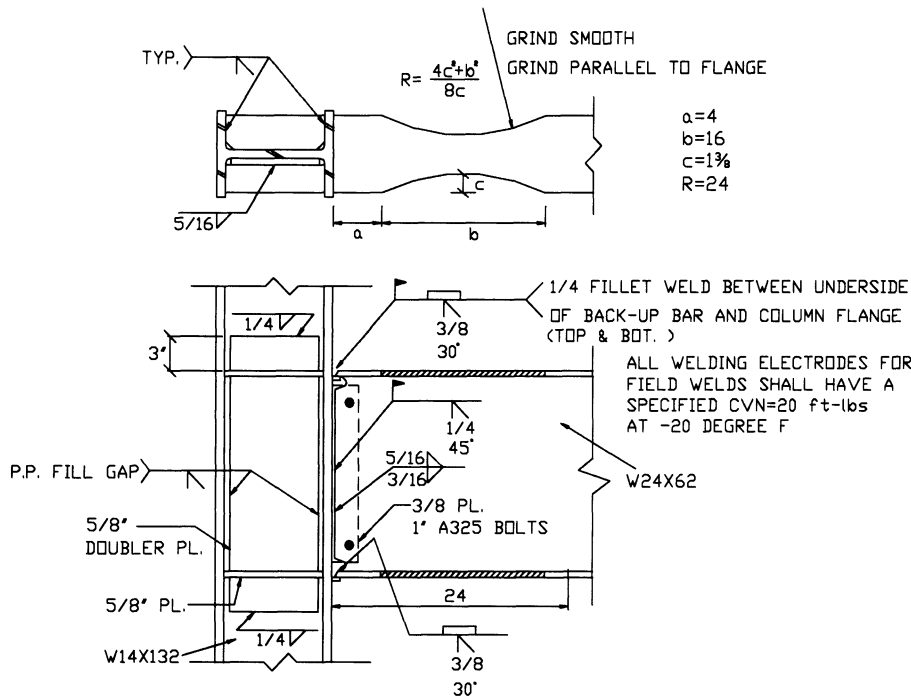


Figure 9-30. Reduced beam section and the welded beam-column connection details.

Beam-to-Column Connection Design

Reduced beam section details employing radius-cut (Figure 9-30) is the most promising beam-to-column connection detail. The key dimensions of the radius cut include the distance from the face of the column (dimension a), the length of the cut (dimension b), and the depth of the cut (dimension c). To minimize the moment gradient between the narrowest section and the face of column, the dimensions a and b should be kept small. However, making these dimensions too short may result in high strains either at the face of column or within the reduced beam sections. It has been recommended that (Engelhardt et al. 1996):

$$a \approx (0.5 \text{ to } 0.75)b_f$$

$$b \approx (0.65 \text{ to } 0.85)d$$

$$c \geq \frac{Z}{2t_f(d-t_f)} \left[1 - \frac{\alpha(L-a-0.5b)}{1.1L} \right] \leq 0.25b_f$$

where L ($= 142.7$ in) is the distance from the face of the column to the point of inflection in the beam, b_f , t_f and d are flange width, flange thickness and beam depth, respectively. To determine the maximum cut dimension, c , it is assumed that the strain-hardened plastic moment developed at the narrowest beam section is equal to 1.1 times the plastic moment of the reduced section ($Z_{RBS}F_{ye}$). The factor 1.1 accounts for strain hardening. The factor α limits the beam moment (αM_p) developed at the face of column. The maximum value of α should range between 0.85 and 1.0. Based on an α equal to 0.90,

$$a = 4.0 \text{ in} = 0.57b_f$$

$$b = 16 \text{ in} = 0.67d$$

$$c = 1.375 \text{ in} \approx 0.20b_f$$

$$R = \frac{4c^2 + b^2}{8c} = 24 \text{ in}$$

Following the SAC Interim Guidelines (SAC 1997), other features of the connection include the use of notch-toughness weld metal, the use of a welded web connection, and the use of continuity plates. Lateral supports capable of resisting a minimum of 2% of the unreduced flange force should be provided such that the unbraced length is no larger than the following (see Figure 9-31):

$$L_b = \frac{2500}{F_y} r_y = \frac{2500}{50} (1.38) = 69 \text{ in} = 5.75 \text{ ft}$$

Additional bracing near the RBS is unnecessary because deep section is not used for the column.

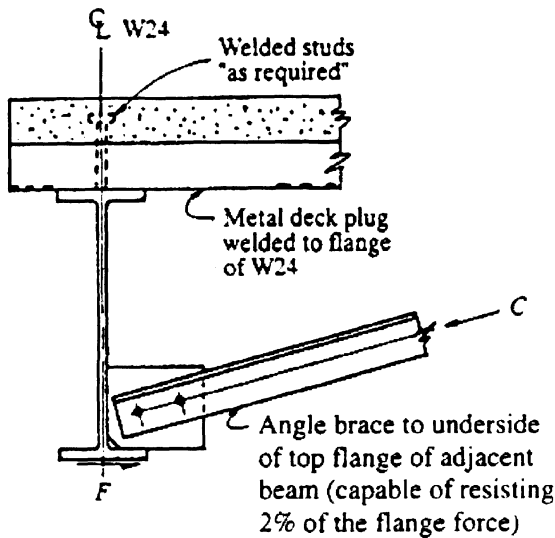


Figure 9-31. Lateral support for the beam

Strong Column-Weak Beam Criterion

The axial force in interior columns in a moment frame, produced by seismic loading, can be ignored generally. The axial force due to dead load on the upper floors, roof, and cladding is:

$$P_D = \text{roof} + (4 \text{ to } 6) \text{ floors} + \text{cladding}$$

$$= (25 \times 14)(0.07) + 3(25 \times 14)(0.09)$$

$$+(25 \times 12)(0.02) = 125 \text{ kips}$$

and the live load axial force, including live load reduction, is

$$L = L_D \left(0.25 + \frac{15}{\sqrt{4(4)(25 \times 14)}} \right) = 22.5 \text{ psf}$$

$$P_L = 3(25 \times 14)(0.0225) + (25 \times 14)(0.02 \times 0.45)$$

$$= 26.8 \text{ kips}$$

Therefore, the factored axial load is

$$P_u = 1.4(125) + 0.5(26.8) = 188 \text{ kips}$$

The column moment capacity is

$$\sum M_{pc}^* = \sum Z_c (F_{yc} - P_{uc}/A_g)$$

$$= 2(234)(50 - 188/38.8)$$

$$= 21132 \text{ kip-in}$$

The plastic sectional modulus of the RBS is

$$Z_{RBS} = Z_{BM} - 2ct_f(d - t_f)$$

$$= 153 - 2(1.375)(23.74 - 0.59) = 115 \text{ in}^4$$

The design plastic moment capacity of the reduced beam section is

$$M_{pd} = 1.1R_y Z_{RBS} F_y$$

$$= 1.1 \times 1.1 \times 115 \times 50 = 6958 \text{ kip-in}$$

and the corresponding beam shear is

$$V_{pd} = \frac{1.1R_y Z_{RBS} F_y}{[0.5(25 \times 12) - d_c/2 - a - b/2]}$$

$$= 53 \text{ kips}$$

After extrapolating the beam moment at the plastic hinge location to the column center-line, the beam moment demand is

$$\sum M_{pb}^* = \sum (M_{pd} + M_v)$$

$$= \sum [M_{pd} + V_{pd}(d_c/2 + a + b/2)]$$

$$= 2 \left[26958 + 53 \left(\frac{14.66}{2} + 4 + 8 \right) \right]$$

$$= 15965 \text{ kip-in}$$

$$\frac{\sum M_{pc}^*}{\sum M_{pb}^*} = 1.32 > 1.0 \quad (\text{OK})$$

Therefore, the strong column-weak beam condition is satisfied.

Panel Zone Design

The unbalanced beam moment, ΔM , for the panel zone design is determined from the special load combination in Eq. 9-4, where the beam moment at the column face produced by $\Omega_o(\rho Q_E)$ is

$$\begin{aligned} M_1 = M_2 &= \Omega_o(F_3/0.94)L \\ &= 3.0(12.3/0.94)142.7 = 5602 \text{ kip-in} \end{aligned}$$

$$\Delta M = M_1 + M_2 = 11204 \text{ kip-in}$$

But the above moment need not be greater than $0.8 \sum M_{pb}^*$. Extrapolating the beam moment at the plastic hinge location to the column face, M_{pb}^* is computed as follows:

$$\begin{aligned} M_{pd}^* &= M_{pd} + V_{pd} \left(a + \frac{b}{2} \right) \\ &= 6958 + 53(4.0 + 8.0) = 7594 \text{ kip-in} \\ 0.8 \sum M_{pb}^* &= 0.8(2)(7594) = 12150 \text{ kip-in} \end{aligned}$$

Therefore, the shear in the panel zone is

$$V_u = \frac{\Delta M}{0.95d_b} - \frac{\Delta M}{h} = 497 - 78 = 419 \text{ kips}$$

The shear capacity of the panel zone is

$$\begin{aligned} \phi V_n &= 0.75(0.6)(50.0)(14.66)t_p \\ &\times \left[1 + \frac{3(14.725)(1.03)^2}{(23.74)(14.66)t_p} \right] \end{aligned}$$

Equating V_u and ϕV_n to solve for the required panel zone thickness gives $t_p = 1.14$ in. Since the column web thickness is 0.645 in, use a 1/2 in thick doubler plate. (The column size needs to be increased if the designer prefers not to use doubler plates.) Check Eq. 9-13 for local buckling of the doubler plate:

$$t_{(req'd)} = \frac{d_z + w_z}{90} = 0.39 \text{ in}$$

Since both the thicknesses of column web and doubler plate are larger than the required thickness, plug welds are not required to connect the doubler plate to the column web. See Figure 9.30 for the connection details.

The component of story drift produced by the panel zone deformation is computed as follows (Tsai and Popov 1990):

$$\begin{aligned} \gamma_p &= \frac{V}{d_c t_p G} \\ &= \frac{419 \times 0.94 / \Omega_o}{14.66(0.645 + 0.50)29000 / 2.6} \\ &= 0.00070 \text{ rad} \end{aligned}$$

where G is the shear modulus. The story drift due to the panel zone deformation, Δ_p , is:

$$\Delta_p = 0.00070 \times 12 \times 12 = 0.10 \text{ in}$$

The total story drift produced by the column, beam, and panel zone deformations is:

$$\begin{aligned} \Delta_c + \Delta_g + \Delta_p &= \frac{F_2 h(h-d_b)^2}{12EI_c} \\ &\quad + \frac{F_2 h^2(L-d_c)}{12EI_g} + \Delta_p \end{aligned}$$

$$= 0.10 + 0.281 + 0.10 = 0.48 < 0.52 \text{ in } (\text{OK})$$

Note that the clear lengths are used to compute the deformations of the beams and column in the above equation.

9.5.3 Special Concentrically Braced Frames (SCBFs)

The six-story inverted-V braced frame shown in Figure 9-32 is analyzed for the loads specified earlier. The service dead load, live load, and seismic member forces, calculated taking into account load-paths and live load reduction, and maximum forces resulting from the critical load combination, are presented in Tables 9-6 and 9-7, where the axial forces and moments are expressed in kips and kip-ft,

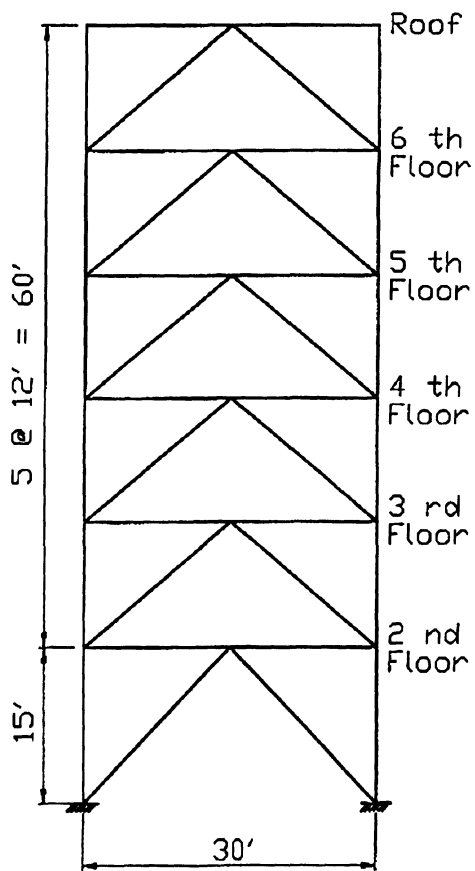


Figure 9-32. Concentrically braced frame elevation

respectively. Cladding panels are assumed connected at the columns. Note that the load combination $1.2D+0.5L+1.0E$ governs for the design of all members.

In the first phase of design (called “strength design” hereafter), members are sized without attention paid to special seismic detailing requirements, as normally done in non-seismic applications, and results are also presented in Tables 9-6 and 9-7. Members are selected per a minimum weight criterion, with beams and braces constrained to be wide-flanges sections of same width, and columns constrained to be W14 shapes continuous over two stories. ASTM A992 steel is used for all members, and the effective length factors, K , of 1.0 were respectively used in calculating the in-plane and out-of-plane buckling strength of braces. Additional information on the effects of end-fixity on the inelastic non-linear behavior of

braces is presented elsewhere (Bruneau et al. 1997). Note that this frame geometry leads to substantial foundation uplift forces. Although not done here, increasing the number of braced bays will reduce the uplift forces.

In the second phase of design, (hereafter called “ductile design”), the seismic requirements are checked, and design is modified as necessary. The special ductile detailing requirements of braces are first checked. Here, all braces are found to have a slenderness ratio in excess of the permissible limit (Eq. 9-15), and some also violate the specified flange width-to-thickness ratio limit. For example, for the fifth story braces (W8×31), the slenderness ratio is:

$$(KL/r)_y = (1.0)(19.21)(12)/2.02$$

$$= 114.1 > 720/\sqrt{50} = 102 \quad (\text{NG})$$

Table 9-6. Strength design results for columns and W-shape braces (axial force in kips)

Story	P_D	P_L	P_{Lr}	P_{Q_E} or T_{Q_E}	P_u^a	T_u^b	Member	$\phi_c P_n$	KL/r	$b_f/2t_f$	h/t_w
Columns											
6	26.6	-	4.20	0	37	-	W14x30	190	96.6	8.7	45.4
5	66.7	10.5	4.86	29.8	132	-	W14x30	190	96.6	8.7	45.4
4	108	18.9	4.86	89	261	25	W14x53	439	75.0	6.1	30.8
3	149	26.2	4.86	172	416	90	W14x53	439	75.0	6.1	30.8
2	191	33.0	4.86	275	593	177	W14x90	1008	38.9	10.2	25.9
1	232	39.6	4.86	388	783	276	W14x90	947	48.6	10.2	25.9
Braces											
6	5.9	-	1.7	48	62	49.6	W8x24	73.7	143.2	8.1	25.8
5	7.7	4.2	-	95	120	102	W8x31	149	114.1	9.2	22.2
4	7.7	4.2	-	133	163	145	W8x35	170	113.6	8.1	20.4
3	7.7	4.2	-	164	198	180	W8x48	244	110.8	5.9	15.8
2	7.7	4.2	-	182	218	200	W8x48	244	110.8	5.9	15.8
1	6.9	3.8	-	218	257	240	W8x67	292	120.1	4.4	11.1

^a from load combination $1.2D + 0.5L + 1.0E$ (see Eq. 9-34), where $E = \rho Q_E$.^b from load combination $0.9D - 1.0E$ (see Eq. 9-35).

Table 9-7. Strength design results for beams (axial force in kips, moment in kip-in)

Level	P_D	M_D	P_L	M_L	P_{Lr}	M_{Lr}	$P_{Q_E}^b$	P_u^a	M_u^a	Section	$\phi_c P_n$	$\phi_b M_n$	KL/r	$b_f/2t_f$	h/t_w
Roof	-	11.1	-	-	-	2.0	37.2	42	16.5	W8X21	64.4	76.5	142.9	6.6	27.5
6	4.6	14.7	-	5.0	0.8	-	74.2	81	30.3	W8X24	120	87.0	111.8	8.1	25.8
5	6.0	14.8	2.1	3.3	-	-	104	113	30.4	W8X31	217	114	89.1	9.2	22.2
4	6.0	15.2	1.4	3.1	-	-	128	141	31	W8X31	217	114	89.1	9.2	22.2
3	6.1	14.9	1.2	2.9	-	-	142	156	30.6	W8X31	217	114	89.1	9.2	22.2
2	5.9	15.6	1.2	2.9	-	-	154	170	31.7	W8X31	217	114	89.1	9.2	22.2

^a from load combination $1.2D + 0.5L + 1.0E$ (see Eq. 9-34), where $E = \rho Q_E$.^b $M_E = 0$.

and the width-to-thickness ratio is:

$$b/t = b_f/2t_f = 9.2 > 52/\sqrt{50} = 7.35 \quad (\text{NG})$$

These braces, therefore, have insufficient capacity to dissipate seismic energy through repeated cycles of yielding and inelastic buckling. Cold-formed square structural tubes with a specified yield strength of 46 ksi under ASTM A500 Grade B are first selected to replace the wide-flange brace sections. As shown in Table 9-8, a strength design using such hollow shapes effectively reduces brace slenderness, but does not necessarily satisfy the stringent width-to-thickness ratio limits prescribed for seismic design.

For example, for the first story braces (TS10x10x1/4), the width-to-thickness ratio is:

$$b/t = 10/0.25 = 40 > 110/\sqrt{46} = 16.22 \quad (\text{NG})$$

Consequently, new brace sections are selected to comply with both the width-to-thickness and member slenderness ratio limits. These are presented in Table 9-9.

At each story, the reduced compression strength $0.8(\phi_c P_n)$ is then considered. Here, the tension brace at each level has sufficient reserve strength to compensate for the loss in compression resistance upon repeated cyclic loading, and the chosen braces are thus adequate. For example, for the TS6x6x5/8 braces at the third story,

Factored design forces: $P_u = 198 \text{ kips}$
 $T_u = 180 \text{ kips}$

Table 9-8. Strength design results for TS-shape braces (axial force in kips)

Story	P_u^a	T_u^b	Member	$\phi_c P_n$	KL/r	b/t
6	62	49.6	TS6X6X3/16	88	97.7	32.0
5	120	102	TS8X8X3/16	157	72.5	42.7
4	163	145	TS9X9X3/16	178	64.2	48.0
3	198	180	TS8X8X1/4	207	73.2	32.0
2	218	200	TS9X9X1/4	253	64.8	36.0
1	257	240	TS10X10X1/4	284	64.3	40.0

^a from load combination $1.2D + 0.5L + 1.0E$ (see Eq. 9-34), where $E = \rho Q_E$.^b from load combination $0.9D - 1.0E$ (see Eq. 9-35).

Table 9-9. Ductility design results for TS-shape braces (axial force in kips)

Story	P_u^a	T_u^b	Member	$\phi_c P_n$	KL/r	b/t
6	62	49.6	TS6X6X3/8	157	101	16.0
5	120	102	TS6X6X3/8	157	101	16.0
4	163	145	TS6X6X1/2	196	104	10.0
3	198	180	TS6X6X5/8	224	107	9.6
2	218	200	TS7X7X1/2	288	88	14.0
1	257	240	TS8X8X1/2	351	84	16.0

^a from load combination $1.2D + 0.5L + 1.0E$ (see Eq. 9-34), where $E = \rho Q_E$.^b from load combination $0.9D - 1.0E$ (see Eq. 9-35).

Design strengths:

$$\phi_c P_n = 224 \text{ kips}, \phi_t T_n = \phi_t A_g F_y = 513 \text{ kips}$$

Reduced compression design strength:

$$0.8(\phi_c P_n) = 0.8(224) = 179 \text{ kips} < P_u = 198 \text{ kips}$$

Therefore, the redistributed force demand in the tension brace is:

$$T'_u = T_u + (\phi_c P_n - 0.8\phi_c P_n) = 180 + (224 - 179) \\ = 225 \text{ kips} < \phi_c T_n = 513 \text{ kips} \quad (\text{OK})$$

Finally, the redundancy requirement is satisfied by checking that members in tension carry at least 30% but no more than 70% of the story shear. Note that for bays with the same number of compression and tension braces, satisfying the above member slenderness limits, this is usually not a concern. For example, check the first story brace as follows:

$$\frac{T_u / \cos \theta}{V_B} = \frac{240 / 0.707}{305} = 0.56$$

which is between 0.3 and 0.7.

Design Forces in Connections

Connections are designed to resist their expected brace tension yield force of $R_y A_g F_y$. For example, for the braces in the first story, this would correspond to a force of $(1.1)(14.4)(46) = 729$ kips. The brace gusset used with tubular braces usually permits out-of-plane buckling and needs to be detailed per Figure 9-15 to resist the applied axial force while undergoing large plastic rotation.

Design Forces in Columns

When $P_u / \phi_c P_n$ in columns is greater than 0.4 (as is the case here), the AISC Seismic Provisions require that columns also be designed to resist forces calculated according to the special load combinations in Eqs. 9-4 and 9-5. However, these forces need not exceed those calculated considering $1.1R_y T_n$ and $1.1R_y P_n$ of the braces. Members designed to satisfy this requirement are presented in Table 9-10.

Table 9-10. Ductility design results for columns (axial force in kips)

Story	P_u^a	T_u^b	$\sum P_n^c$	$\sum T_n^d$	Member	$\phi_c P_n$
6	34	-	34	-	W14X30	190
5	146	-	225	221	W14X30	190
4	314	80	420	465	W14X61	591
3	538	211	647	790	W14X61	591
2	796	378	886	1150	W14X109	1220
1	1078	568	1196	1543	W14X109	1147

^a from load combination $1.2D + 0.5L \pm \Omega_o Q_E$ (see Eq. 9-4), where $\Omega_o = 2.0$.^b from load combination $0.9D \pm \Omega_o Q_E$ (see Eq. 9-5).^c $1.2D + 0.5L + \Sigma(1.1R_y P_n)$, where P_n is the brace nominal compressive strength.^d $1.2D + 0.5L + \Sigma(1.1R_y T_n)$, where T_n is the brace nominal tensile strength.

Cases b and d are used to check column splices and foundation uplift.

Table 9-11. Ductility design results for beams^a (force in kips, moment in kip-in)

Level	T_n	$0.3\phi_c P_n$	Unbalanced Force		M_{ux}	P_u	Section	$\phi_b M_{nx}$	$\phi_c P_n$	Ratio
			Vertical	Horizontal						
6	372	47.3	203	1522	127	254	W30X148	1789	1172	0.90
5	372	47.3	203	1522	127	254	W30X148	1789	1172	0.90
4	479	58.7	263	1973	164	328	W30X173	2164	1765	0.96
3	524	63.0	288	2160	180	360	W30X191	2398	1956	0.94
2	570	86.4	302	2265	189	378	W30X191	2398	1956	0.99

^a Ductility design not required at top story of a chevron braced frame per AISC Seismic provisions.

Note that columns splices would have to be designed to resist the significant uplift forces shown in this table, although the AISC Seismic Provisions indicate that the tension forces calculated in Table 9-10 need not exceed the value corresponding the uplift resistance of the foundation.

Design Forces in Beams

Finally, beams are checked for compliance with the special requirements presented in Section 9.3. Here, all beams are continuous between columns, and are braced laterally at the ends and mid-span. W30 shapes were chosen to limit beam depth.

Beams are, therefore, redesigned to resist the unbalanced vertical force induced when the compression braces are buckled and the tension braces are yielded. In this example, this substantial force governs the design. The corresponding moments and axial forces acting on the beams are shown in Table 9-11, along with the resulting new beam sizes. Note that the

adequacy of these beams is checked using the AISC (1993) beam-column interaction equations.

For example, for the W30x191 beam on the second floor:

$$\frac{P_u}{2\phi_c P_n} + \left(\frac{M_{ux}}{\phi_b M_{nx}} \right) = \frac{189}{2(1956)} + \left(\frac{2265}{2398} \right) = 0.05 + 0.94 = 0.99 < 1.0 \quad (\text{OK})$$

Incidentally, note that this section is a compact section.

9.5.4 Eccentrically Braced Frames (EBFs)

The configuration of the split-V-braced EBF is shown in Figure 9-33, and the design seismic forces are listed in Table 9-5. The geometry is chosen such that the link length is about 10% of the bay width, and the inclined angle of the braces is between 35 to 60 degrees:

$$e = 0.1L = 3 \text{ ft} = 36 \text{ in}$$

$$\theta = \tan^{-1}(15/13.5) = 48^\circ \quad (\text{first story})$$

$$\theta = \tan^{-1}(12/13.5) = 42^\circ \quad (\text{other stories})$$

In this example, detailed design calculations are only presented for members at the first story to illustrate the procedure. Unless indicated otherwise, ASTM A992 steel is used.

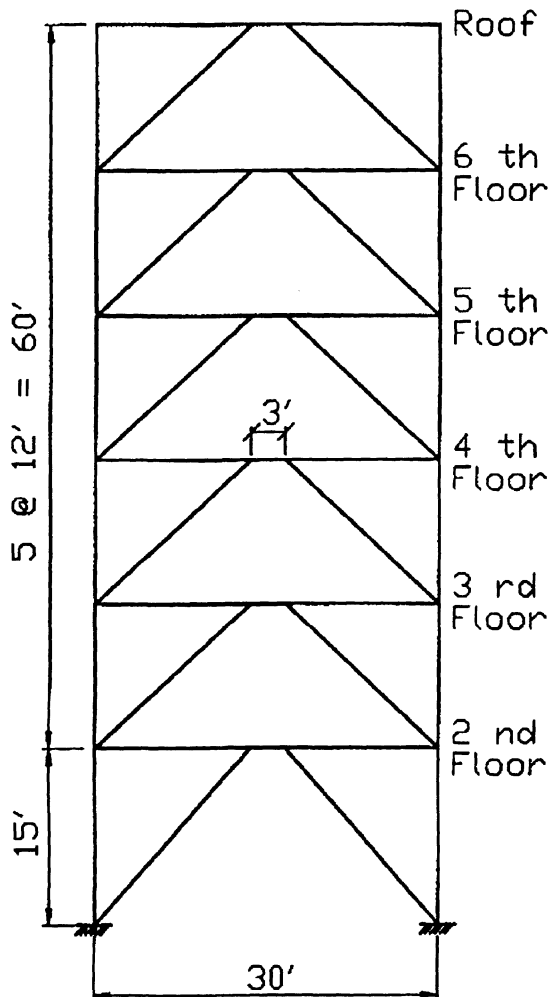


Figure 9-33. Eccentrically braced frame elevation

Link Design

Shear links with $e \leq 1.6 M_p/V_p$ are used to achieve higher structural stiffness and strength. The AISC Seismic Provisions stipulate that the beam outside the link shall be able to resist the forces generated by at least 1.1 times the expected nominal shear strength of the link.

Assuming that the braces are rigidly connected to the link, that the beam can resist 95% of the link end moment, and that the beam flexural capacity is reduced by 30% due to the presence of an axial force:

$$(0.7)R_y(\phi_b M_p) \geq 0.85(1.1)R_y V_n(e/2)$$

or

$$1.35M_p/V_n \geq e$$

For shear links, the above requirement for the maximum link length is more stringent than $1.6M_p/V_p$. The required strengths for the link on the second floor are

$$\begin{aligned} V_u &= 1.4D + 0.5L + E \\ &= 1.4(1.1) + 0.5(0.4) + 98.0 = 100 \text{ kips} \\ M_u &= 1.4D + 0.5L + E \\ &= 1.4(8.0) + 0.5(3.0) + 98(3.0/2) = 160 \text{ kip-ft} \end{aligned}$$

Note that there is no axial force acting on the shear links (i.e., $P_u = 0$ kip). Illustrating this procedure for the shear link on the second floor:

$$\begin{aligned} 1.35M_p/V_p &\geq 36 \text{ in} \Rightarrow M_p/V_p \geq 26.7 \text{ in} \\ V_u &= 100 \text{ kips} \leq \phi V_n = \phi V_p \\ &= 0.9(0.6)(50)t_w(d - 2t_f) \\ &\Rightarrow t_w(d - 2t_f) \geq 3.70 \text{ in}^2 \\ V_u &= 100 \text{ kips} \leq \phi V_n = \phi(2M_p/e) \\ &= 2(0.9)(50Z_x)/36 \Rightarrow Z_x \geq 40.0 \text{ in}^3 \end{aligned}$$

Based on the above three requirements, select a W12×45 section for the link:

$$Z_x = 64.7 \text{ in}^3 > 40.0 \text{ in}^3 \quad (\text{OK})$$

$$t_w(d - 2t_f) = 3.87 \text{ in}^2 > 3.70 \text{ in}^2 \quad (\text{OK})$$

$$\frac{M_p}{V_p} = \frac{Z_x}{0.6(d - 2t_f)t_w} = 27.9 \text{ in} > 26.7 \text{ in} \quad (\text{OK})$$

$$\frac{b_f}{2t_f} = 7.0 < \frac{52}{\sqrt{F_y}} = 7.4 \quad (\text{OK})$$

$$\frac{h}{t_w} = 29.0 < \frac{520}{\sqrt{F_y}} = 73.5 \quad (\text{OK})$$

$$\begin{aligned} V_n &= \min \{V_p, 2M_p/e\} \\ &= \min \{116, 180\} = 116 \text{ kips} \end{aligned} \quad (\text{OK})$$

Beam Outside of Link

The moment at both ends of the link is:

$$\begin{aligned} M_u &= 1.1(R_y V_n e / 2) \\ &= 1.1(1.1 \times 116 \times 3.0 / 2) = 211 \text{ kip-in} \end{aligned}$$

This moment is resisted by both the rigidly connected brace and the beam outside the link. Assuming that the beam resists 85% of the link moment, the beam end moment including the gravity load effect ($M_D = 8$ kip-ft, $M_L = 3$ kip-ft) is

$$\begin{aligned} M_u &= 0.85(211) + 1.2(8.0) \\ &+ 0.5(3.0) = 190 \text{ kip-ft} \end{aligned}$$

The axial force ratio in the beam is

$$\frac{P_u}{\phi_b P_y} = \frac{126}{0.9 A_g F_y} = 0.212 > 0.125$$

Checking the beam web local buckling (see Table 9-2):

$$\begin{aligned} \lambda_{ps} &= \frac{191}{\sqrt{F_y}} \left(2.33 - \frac{P_u}{\phi_b P_y} \right) \geq \frac{253}{\sqrt{F_y}} \\ &= 57.2 \end{aligned}$$

$$\lambda = \frac{h}{t_w} = 16.7 < \lambda_{ps} \quad (\text{OK})$$

Checking the strength of the beam segment as a beam-column:

$$[L_p = 6.9 \text{ ft}] < [L_b = 13.5 \text{ ft}] < [L_r = 20.3 \text{ ft}]$$

$$\phi_b M_p = 243, \quad BF = 5.07, \quad C_b \approx 1.67$$

$$\begin{aligned} \phi_b M_n &= C_b [\phi_b M_p - BF(L_b - L_p)] \\ &= 350 \geq \phi_b M_p \end{aligned}$$

Use $\phi_b M_n = 243$ kip-ft

$$P_{el} = \frac{\pi^2 EI_x}{(KL_x)^2} = 3817 \text{ kips}$$

$$C_m = 0.85$$

$$B_1 = \frac{C_m}{\frac{P_u}{P_e}} = \frac{0.85}{1 - \frac{126}{3817}} = 0.88 < 1.0$$

Use $B_1 = 1.0$

$$(KL)_y = 13.5 \text{ ft}, \quad \phi_c P_n = 337 \text{ kips}$$

$$\frac{P_u}{R_y(\phi_c P_n)} + \frac{8}{9} \frac{B_1 M_u}{R_y(\phi_b M_n)} = 0.34 + 0.63$$

$$= 0.97 < 1.0 \quad (\text{OK})$$

Diagonal Brace

To compute the beam shear, V_b , assume the beam moment at the column end is zero.

$$1.25 R_y V_b = 160 \text{ kips}$$

$$1.25 R_y V_b (e/2) = 240 \text{ kip-ft}$$

$$V_b = \frac{1.25 R_y V_b (e/2)}{L_b} = 18 \text{ kips}$$

Therefore, the brace force including the gravity load effect ($V_D = 5.7$ kips, $V_L = 2.2$ kips) is

$$\begin{aligned} P_u &= (1.25 R_y V_b + V_b + 1.2 V_D + 0.5 V_L) / \sin(\theta) \\ &= 250 \text{ kips} \end{aligned}$$

The brace length is 20.2 ft. Selecting a square tubular section TS8×8×1/2 (A500 Grade B steel):

$$\phi_c P_n = 366 \text{ kips} > 250 \text{ kips} \quad (\text{OK})$$

$$b/t = 6.5/0.5 = 13 < \lambda_p = 190/\sqrt{F_y} = 28 \quad (\text{OK})$$

Once the brace size is determined, it is possible to determine the link end moment based on the relative stiffness (I/L) of the brace and the beam segment outside the link. The moment distribution factor is

$$(DF)_{br} = \frac{I_{br}/L_{br}}{I_{br}/L_{br} + I_b/L_b} = 0.20$$

Therefore, the moment at the end of brace is

$$M_u = 240 \times (DF)_{br} = 48 \text{ kip-ft}$$

The brace capacity is checked as a beam-column:

$$\phi_b M_n = \phi_b (Z_x F_y) = 137 \text{ kip-ft}$$

$$\begin{aligned} \frac{P_u}{\phi_c P_n} + \frac{8}{9} \frac{M_u}{\phi_b M_n} &= 0.68 + 0.31 \\ &= 0.99 < 1 \end{aligned} \quad (\text{OK})$$

Link Rotation

The axial force produced by the design seismic force in the first story is

$$P = 88/\cos(\theta) = 132 \text{ kips}$$

The axial deformation of the brace is

$$\Delta = \frac{PL}{EA} = \frac{132(20.2 \times 12)}{29000(14.4)} = 0.077 \text{ in}$$

The elastic story drift is

$$\delta_e = \frac{\Delta}{\cos(\theta)} = 0.115 \text{ in}$$

and the design story drift is

$$\delta_s = C_d \delta_e / I = 4.0(0.115) / 1.0 = 0.46 \text{ in}$$

Therefore, the link rotation is

$$\gamma_p = \frac{L}{e} \left(\frac{\delta_s}{h} \right) = \frac{30.0}{3.0} \left(\frac{0.46}{15 \times 12} \right) = 0.026 \text{ rad}$$

The link rotation capacity is 0.08 rad because the link length (= 36 in) is smaller than $1.6 M_p/V_p$ (= 44.6 in). Thus, the link deformation capacity is sufficient.

Lateral Bracing

Full-depth stiffeners of A36 steel are to be used in pairs at each end of the links. The required thickness of these stiffeners is

$$t = \max \{0.75t_w, 3/8\} = 3/8 \text{ in}$$

Lateral bracing similar to that shown in Figure 9-31 is needed for the links, except that the bracing needs to be designed for 6% of the expected link flange force, $R_y F_y b f_f$.

Link Stiffeners

One-sided intermediate stiffeners are permitted because the link depth is less than 25 inches. The required thickness is

$$t = \max \{t_w, 3/8\} = 3/8 \text{ in}$$

The required stiffener spacing, a , is based on Eq. 9-28, where C_B is (see Figure 9-25):

$$C_B = 59.3 - 367\gamma_p = 50.1$$

$$a = C_B t_w - \frac{d}{5} = 14.4 \text{ in}$$

Therefore, three intermediate stiffeners are provided.

The weld between the stiffener and the link web should be designed to resist the following force:

$$F = A_{st} F_y = (3.75)(0.375)(36) = 51 \text{ kips}$$

The required total design force between the stiffener and the flanges is

$$F = A_{st} F_y / 4 = 12.8 \text{ kips}$$

A minimum fillet weld size of $\frac{1}{4}$ in. satisfies the above force requirement.

Columns

Table 9-12. Summary of member sizes and column axial loads

Floor Level	Link Size	$\Sigma 1.1R_yV_n$ (kips)	ΣP_D (kips)	ΣP_L (kips)	Column Size	Brace Size
R	W10×45	113	30	5	W12×40	TS8×8×½
6	W10×45	226	71	14	W12×40	TS8×8×½
5	W10×45	339	112	22	W12×72	TS8×8×½
4	W10×45	452	153	29	W12×72	TS8×8×½
3	W12×45	592	194	35	W12×106	TS8×8×½
2	W12×45	732	235	42	W12×106	TS8×8×½

Columns must be designed to satisfy the special load combination presented in Eq. 9-4, where $\Omega_o E$ is replaced by the seismic force generated by 1.1 times the expected nominal strength ($R_y V_n$) of the links. The column axial load produced by both gravity loads and seismic forces are listed in Table 9-12. The required axial compressive strength is

$$P_u = 1.2(235) + 0.5(42) + 732 = 1035 \text{ kips}$$

A W12×106 column, with a design axial load capacity of 1040 kips, is chosen for the lowest two stories. The column splice must be designed for the tensile force determined from the load combination in Eq. 8.5:

$$P_u = 0.9D - \Omega_o Q_E = 0.9(235) - 732$$

$$= -521 \text{ kips}$$

As stated in the SCBF design example, using more than one braced bay in the bottom stories may reduce the tensile force in the columns and increase the overturning resistance of the building.

REFERENCES

- 9-1 AIJ, *Performance of Steel Buildings during the 1995 Hyogoken-Nanbu Earthquake* (in Japanese with English summary), Architectural Inst. of Japan, Tokyo, Japan, 1995.
- 9-2 AISC, *Load and Resistance Factor Design Specification for Structural Steel Buildings*, AISC, Chicago, IL, 1993.
- 9-3 AISC, *Specifications for Structural Steel Buildings*, AISC, Chicago, IL, 1989.
- 9-4 AISC, *Near the Fillet of Wide Flange Shapes and Interim Recommendations*, Advisory Statement on Mechanical Properties, AISC, Chicago, IL, 1997a.
- 9-5 AISC, *Seismic Provisions for Structural Steel Buildings*, with Supplement No. 1 (1999), AISC, Chicago, IL, 1992 and 1997b.
- 9-6 ASCE, *Minimum Design Loads for Buildings and Other Structures*, ASCE Standard 7-98, ASCE, New York, NY, 1998.
- 9-7 Astaneh-Asl, A., Goel, S.C., Hanson, R.D., "Earthquake-resistant Design of Double Angle Bracings," *Engrg. J.*, Vol. 23, No. 4, pp. 133-147, AISC, 1981.
- 9-8 Becker, R., "Seismic Design of Steel Buildings Using LRFD," in *Steel Design Handbook* (editor: A. R. Tamboli), McGraw-Hill, 1997.
- 9-9 Bruneau, M., Mahin, S.A., "Ultimate Behavior of Heavy Steel Section Welded Splices and Design Implications," *J. Struct. Engrg.*, Vol. 116, No. 8, pp. 2214-2235, ASCE, 1990.
- 9-10 Bruneau, M., Uang, C.M., Whittaker, A., *Ductile Design of Steel Structures*, McGraw Hill, New York, NY, 1997.
- 9-11 BSSC, *NEHRP Recommended Provisions for the Development of Seismic Regulations for New Buildings*, Federal Emergency Management Agency, Washington, DC, 1997.
- 9-12 Chen, S.J., Yeh, C.H. and Chu, J.M., "Ductile Steel Beam-Column Connections for Seismic Resistance," *J. Struct. Engrg.*, Vol. 122, No. 11, pp. 1292-1299, ASCE, 1996.
- 9-13 Chi, B. and Uang, C.M., "Seismic Retrofit Study on Steel Moment Connections for the Los Angeles Department of Public Works Headquarters Building," *Report No. TR-2000/14*, Department of Structural Engineering, University of California, San Diego, La Jolla, CA, 2000.
- 9-14 Engelhardt, M. D. and Popov, E. P., "On Design of Eccentrically Braced Frames," *Earthquake Spectra*, Vol. 5, No. 3, pp. 495-511, EERI, 1989.
- 9-15 Engelhardt, M.D. and Sabol, T., "Reinforcing of Steel Moment Connections with Cover Plates: Benefits and Limitations," *Engrg. J.*, Vol. 20, Nos. 4-6, pp. 510-520, 1998.
- 9-16 Engelhardt, M.D., Winneburger, T., Zekany, A.J., and Potyraj, T.J., "The Dogbone Connection: Part II," *Modern Steel Construct.*, Vol. 36, No. 8, pp. 46-55, AISC, 1996.
- 9-17 Fujimoto, M., Aoyagi, T., Ukai, K., Wada, A., and K. Saito, "Structural Characteristics of Eccentric K-Braced Frames," *Trans.*, No. 195, pp. 39-49, AIJ, May 1972.
- 9-18 Gilton, C., Chi, B., and Uang, C.-M., "Cyclic Response of RBS Moment Connections: Weak-Axis Configuration and Deep Column Effects," *Report No. SSRP-2000/03*, Department of Structural Engineering, University of California, San Diego, La Jolla, CA, 2000.
- 9-19 Gross, J. L., Engelhardt, M. D., Uang, C.-M., Kasai, K., and N. Iwankiw, *Modification of Existing Welded Steel Moment Frame Connections for Seismic Resistance*, Steel Design Guide Series 12, AISC and NIST, 1998.
- 9-20 Hamburger, R. "More on Welded Connections," *SEAONC News*, Structural Engineers Association of Northern California, San Francisco, CA, April, 1996.
- 9-21 Hjelmstad, K. D. and Popov, E. P., "Characteristics of Eccentrically Braced Frames," *J. Struct. Engrg.*, Vol. 110, No. 2, pp. 340-353, ASCE, 1984.
- 9-22 Hjelmstad, K. D. and Popov, E. P., "Cyclic Behavior and Design of Link Beams," *J. Struct. Engrg.*, Vol. 109, No. 10, pp. 2387-2403, ASCE, 1983.
- 9-23 ICBO, *Uniform Building Code*, Int. Conf. of Building Officials, Whittier, CA, 1988.
- 9-24 Iwankiw, R.N. and Carter, C.J., "The Dogbone: A New Idea to Chew On," *Modern Steel Construct.*, Vol. 36, No. 4, pp. 18-23, AISC, Chicago IL, 1996.
- 9-25 Jokerst, M. S. and Soyer, C., "San Francisco Civic Center Complex: Performance Based Design with Passive Dampers and Welded Steel Frames," *Proc.*, 65th Annual Convention, pp. 119-134, SEAOC, 1996.
- 9-26 Kasai, K. and Popov, E. P., "On Seismic Design of Eccentrically Braced Frames," *Proc.*, 8th World Conf. Earthquake Engrg., Vol. V, pp. 387-394, IAEE, San Francisco, 1985.
- 9-27 Kasai, K. and Popov, E. P., "Cyclic Web Buckling Control for Shear Link Beams," *J. Struct. Engrg.*, Vol. 112, No. 3, pp. 505-523, ASCE, 1986a.
- 9-28 Kasai, K. and Popov, E. P., "General Behavior of WF Steel Shear Link Beams," *J. Struct. Engrg.*, Vol. 112, No. 2, pp. 362-382, ASCE, 1986b.
- 9-29 Krawinkler, H., Bertero, V.V., and Popov, E.P., "Inelastic Behavior of Steel Beam-Column Subassemblages," *Report No. UCB/EERC-71/7*, Univ. of Calif., Berkeley, Berkeley, CA, 1971.
- 9-30 Krawinkler, H., Bertero, V.V., and Popov, E.P., "Shear Behavior of Steel Frame Joints," *J. Struct. Div.*, Vol. 101, ST11, pp. 2317-2338. ASCE, 1975.

- 9-31 Libby, J. R., "Eccentrically Braced Frame Construction—A Case Study," *Engrg. J.*, Vol. 18, No. 4, pp. 149-153, AISC, 1981.
- 9-32 Malley, J. O. and Popov, E. P., "Shear Links in Eccentrically Braced Frames," *J. Struct. Engrg.*, Vol. 110, No. 9, pp. 2275-2295, ASCE, 1984.
- 9-33 Manheim, D. N. and Popov, E. P., "Plastic Shear Hinges in Steel Frames," *J. Struct. Engrg.*, Vol. 109, No. 10, pp. 2404-2419, ASCE, 1983.
- 9-34 Merovich, A., Nicoletti, J. P., and Hartle, E., "Eccentric Bracing in Tall Buildings," *J. Struct. Div.*, Vol. 108, No. ST9, pp. 2066-2080, ASCE, 1982.
- 9-35 Nakashima, M. And Wakabayashi, M., "Analysis and Design of Steel Braces and Braced Frames," in *Stability and Ductility of Steel Structures under Cyclic Loading*, pp. 309-322, CRC Press, 1992.
- 9-36 Noel, S. and Uang, C.-M., "Cyclic Testing of Steel Moment Connections for the San Francisco Civic Center Complex," *Report No. TR-96/07*, Univ. of California, San Diego, La Jolla, CA, 1996.
- 9-37 Plumier, A., "New Idea for Safe Structures in Seismic Zones," *Proc., Symposium of Mixed Structures Including New Materials*, pp. 431-436, IABSE, Brussels, Belgium, 1990.
- 9-38 Redwood, R.G., and Channagiri, V.S., "Earthquake-Resistant Design of Concentrically Braced Steel Frames," *Canadian J. Civil Engrg.*, Vol. 18, No. 5, pp. 839-850, 1991.
- 9-39 Ricles, J. M. and Popov, E. P., "Composite Action in Eccentrically Braced Frames," *J. Struct. Engrg.*, Vol. 115, No. 8, pp. 2046-2065, ASCE, 1989.
- 9-40 Roeder, C. W. and Popov, E. P., "Eccentrically Braced Steel Frames For Earthquakes," *J. Struct. Div.*, Vol. 104, No. ST3, pp. 391-411, ASCE, 1978.
- 9-41 Roeder, C. W., Foutch, D. A., and Goel, S. C., "Seismic Testing of Full-Scale Steel Building—Part II," *J. Struct. Engrg.*, Vol. 113, No. 11, pp. 2130-2145, ASCE, 1987.
- 9-42 SAC, "Interim Guidelines: Evaluation, Repair, Modification, and Design of Welded Steel Moment Frame Structures," *Report FEMA No. 267/SAC-95-02*, SAC Joint Venture, Sacramento, CA, 1995.
- 9-43 SAC, "Interim Guidelines Advisory No. 1, Supplement to FEMA 267," *Report No. FEMA 267A/SAC-96-03*, SAC Joint Venture, Sacramento, CA, 1997.
- 9-44 SAC, "Technical Report: Experimental Investigations of Beam-Column Subassemblages, Parts 1 and 2," *Report No. SAC-96-01*, SAC Joint Venture, Sacramento, CA, 1996.
- 9-45 SAC, "Recommended Seismic Design Criteria for New Moment-Resisting Steel Frame Structures," *Report No. FEMA 350*, SAC Joint Venture, Sacramento, CA, 2000.
- 9-46 Shibata, M., Nakamura T., Yoshida, N., Morino, S., Nonaka, T., and Wakabayashi, M., "Elastic-Plastic Behavior of Steel Braces under Repeated Axial Loading," *Proc., 5th World Conf. Earthquake Engrg.*, Vol. 1, pp. 845-848, IAEE, Rome, Italy, 1973.
- 9-47 SSPC, *Statistical Analysis of Tensile Data for Wide-Flange Structural Shapes*, Chaparral Steel Co., Midlothian, TX, 1994.
- 9-48 Tanabashi, R., Naneta, K., and Ishida, T., "On the Rigidity and Ductility of Steel Bracing Assemblage," *Proc., 5th World Conf. Earthquake Engrg.*, Vol. 1, pp. 834-840, IAEE, Rome, Italy, 1974.
- 9-49 Teal, E. J., "Seismic Drift Control Criteria," *Engrg. J.*, Vol. 12, No. 2, pp. 56-67, AISC, 1975.
- 9-50 Teal, E., *Practical Design of Eccentric Braced Frames to Resist Seismic Forces*, Struct. Steel Res. Council, CA, 1979.
- 9-51 Tremblay, R., Bruneau, M., Nakashima, M., Prion, H.G.L., Filiatrault, M., DeVall, R., "Seismic Design of Steel Buildings: Lessons from the 1995 Hyogoken Nanbu Earthquake," *Canadian J. Civil Engrg.*, Vol. 23, No. 3, pp. 757-770, 1996.
- 9-52 Tremblay, R., Timler, P., Bruneau, M., Filiatrault, A., "Performance of Steel Structures during the January 17, 1994, Northridge Earthquake," *Canadian J. Civil Engrg.*, Vol. 22, No. 2, pp. 338-360, 1995.
- 9-53 Tsai, K.-C., and Popov, E.P., "Seismic Panel Zone Design Effects on Elastic Story Drift of Steel Frames," *J. Struct. Engrg.*, Vol. 116, No. 12, pp. 3285-3301, ASCE, 1990.
- 9-54 Tsai, K.-C., and Popov, E.P., "Steel Beam-Column Joints in Seismic Moment-Resisting Frames," *Report No. UCB/EERC-88/19*, Univ. of Calif., Berkeley, 1988.
- 9-55 Yu, Q.S., Uang, C.M., and Gross, J., "Seismic Rehabilitation Design of Steel Moment Connection with Welded Haunch," *Journal of Structural Engineering*, Vol. 126, No. 1, pp. 69-78, ASCE, 2000.
- 9-56 Uang, C.-M. "Establishing R (or R_w) and C_d Factors for Building Seismic Provisions," *J. Struct. Engrg.*, Vol. 117, No. 1, pp. 19-28, ASCE, 1991.
- 9-57 Uang, C.-M. and Noel, S., "Cyclic Testing of Strong- and Weak-Axis Steel Moment Connection with Reduced Beam Flanges," *Report No. TR-96/01*, Univ. of Calif., San Diego, CA, 1996.
- 9-58 Uang, C.-M and Fan, C.C, "Cyclic Stability of Moment Connections with Reduced Beam Section," *Report No. SSRP-99/21*, Department of Structural Engineering, University of California, San Diego, La Jolla, CA, 1999.
- 9-59 Whittaker, A. S., Uang, C.-M., and Bertero, V. V., "Seismic Testing of Eccentrically Braced Dual Steel Frames," *Earthquake Spectra*, Vol. 5, No. 2, pp. 429-449, EERI, 1989.
- 9-60 Whittaker, A.S. and Gilani, A., "Cyclic Testing of Steel Beam-Column Connections," *Report No. EERC-STI/96-04*, Univ. of Calif., Berkeley, 1996.
- 9-61 Whittaker, A.S., Bertero V.V., and Gilani, A.S. "Evaluation of Pre-Northridge Steel Moment-

- Resisting Joints." *Struct. Design of Tall Buildings*. Vol. 7, No. 4, pp. 263-283, 1998.
- 9-62 Yang, M.-S., "Shaking Table Studies of an Eccentrically Braced Steel Structure," *Proc.*, 8th World Conf. Earthquake Engrg., Vol. IV, pp. 257-264, IAE, San Francisco, CA, 1985.
- 9-63 Zekioglu, A., Mozaffarian, H., Chang, K.L., Uang, C.-M., and Noel, S., "Designing after Northridge", *Modern Steel Construct.*, Vol. 37, No. 3, pp. 36-42, AISC, 1997.

Chapter 10

Seismic Design of Reinforced Concrete Structures

Arnaldo T. Derecho, Ph.D.

Consulting Structural Engineer, Mount Prospect, Illinois

M. Reza Kianoush, Ph.D.

Professor, Ryerson Polytechnic University, Toronto, Ontario, Canada

Key words: Seismic, Reinforced Concrete, Earthquake, Design, Flexure, Shear, Torsion, Wall, Frame, Wall-Frame, Building, Hi-Rise, Demand, Capacity, Detailing, Code Provisions, IBC-2000, UBC-97, ACI-318

Abstract: This chapter covers various aspects of seismic design of reinforced concrete structures with an emphasis on design for regions of high seismicity. Because the requirement for greater ductility in earthquake-resistant buildings represents the principal departure from the conventional design for gravity and wind loading, the major part of the discussion in this chapter will be devoted to considerations associated with providing ductility in members and structures. The discussion in this chapter will be confined to monolithically cast reinforced-concrete buildings. The concepts of seismic demand and capacity are introduced and elaborated on. Specific provisions for design of seismic resistant reinforced concrete members and systems are presented in detail. Appropriate seismic detailing considerations are discussed. Finally, a numerical example is presented where these principles are applied. Provisions of ACI-318/95 and IBC-2000 codes are identified and commented on throughout the chapter.

10.1 INTRODUCTION

10.1.1 The Basic Problem

The problem of designing earthquake-resistant reinforced concrete buildings, like the design of structures (whether of concrete, steel, or other material) for other loading conditions, is basically one of defining the anticipated forces and/or deformations in a preliminary design and providing for these by proper proportioning and detailing of members and their connections. Designing a structure to resist the expected loading(s) is generally aimed at satisfying established or prescribed safety and serviceability criteria. This is the general approach to engineering design. The process thus consists of determining the expected *demands* and providing the necessary *capacity* to meet these demands for a specific structure. Adjustments to the preliminary design may likely be indicated on the basis of results of the analysis-design-evaluation sequence characterizing the iterative process that eventually converges to the final design. Successful experience with similar structures should increase the efficiency of the design process.

In earthquake-resistant design, the problem is complicated somewhat by the greater uncertainty surrounding the estimation of the appropriate design loads as well as the capacities of structural elements and connections. However, information accumulated during the last three decades from analytical and experimental studies, as well as evaluations of structural behavior during recent earthquakes, has provided a strong basis for dealing with this particular problem in a more rational manner. As with other developing fields of knowledge, refinements in design approach can be expected as more information is accumulated on earthquakes and on the response of particular structural configurations to earthquake-type loadings.

As in design for other loading conditions, attention in design is generally focused on those areas in a structure which analysis and

experience indicate are or will likely be subjected to the most severe demands. Special emphasis is placed on those regions whose failure can affect the integrity and stability of a significant portion of the structure.

10.1.2 Design for Inertial Effects

Earthquake-resistant design of buildings is intended primarily to provide for the inertial effects associated with the waves of distortion that characterize dynamic response to ground shaking. These effects account for most of the damage resulting from earthquakes. In a few cases, significant damage has resulted from conditions where inertial effects in the structure were negligible. Examples of these latter cases occurred in the excessive tilting of several multistory buildings in Niigata, Japan, during the earthquake of June 16, 1964, as a result of the liquefaction of the sand on which the buildings were founded, and the loss of a number of residences due to large landslides in the Turnagain Heights area in Anchorage, Alaska, during the March 28, 1964 earthquake. Both of the above effects, which result from ground motions due to the passage of seismic waves, are usually referred to as secondary effects. They are distinguished from so-called primary effects, which are due directly to the causative process, such as faulting (or volcanic action, in the case of earthquakes of volcanic origin).

10.1.3 Estimates of Demand

Estimates of force and deformation demands in critical regions of structures have been based on dynamic analyses—first, of simple systems, and second, on inelastic analyses of more complex structural configurations. The latter approach has allowed estimation of force and deformation demands in local regions of specific structural models. Dynamic inelastic analyses of models of representative structures have been used to generate information on the variation of demand with major structural as well as ground-motion parameters. Such an effort involves consideration of the practical

range of values of the principal structural parameters as well as the expected range of variation of the ground-motion parameters. Structural parameters include the structure fundamental period, principal member yield levels, and force—displacement characteristics; input motions of reasonable duration and varying intensity and frequency characteristics normally have to be considered.

A major source of uncertainty in the process of estimating demands is the characterization of the design earthquake in terms of intensity, frequency characteristics, and duration of large-amplitude pulses. Estimates of the intensity of ground shaking that can be expected at particular sites have generally been based on historical records. Variations in frequency characteristics and duration can be included in an analysis by considering an ensemble of representative input motions.

Useful information on demands has also been obtained from tests on specimens subjected to simulated earthquake motions using shaking tables and, the pseudo-dynamic method of testing. The latter method is a combination of the so-called quasi-static, or slowly reversed, loading test and the dynamic shaking-table test. In this method, the specimen is subjected to essentially statically applied increments of deformation at discrete points, the magnitudes of which are calculated on the basis of predetermined earthquake input and the measured stiffness and estimated damping of the structure. Each increment of load after the initial increment is based on the measured stiffness of the structure during its response to the imposed loading of the preceding increment.

10.1.4 Estimates of Capacity

Proportioning and detailing of critical regions in earthquake-resistant structures have mainly been based on results of tests on laboratory specimens tested by the quasi-static method, i.e., under slowly reversed cycles of loading. Data from shaking-table tests and from pseudo-dynamic tests have also contributed to the general understanding of structural behavior

under earthquake-type loading. Design and detailing practice, as it has evolved over the last two or three decades, has also benefited from observations of the performance of structures subjected to actual destructive earthquakes.

Earthquake-resistant design has tended to be viewed as a special field of study, not only because many engineers do not have to be concerned with it, but also because it involves additional requirements not normally dealt with in designing for wind. Thus, while it is generally sufficient to provide adequate stiffness and strength in designing buildings for wind, in the case of earthquake-resistant design, a third basic requirement, that of ductility or inelastic deformation capacity, must be considered. This third requirement arises because it is generally uneconomical to design most buildings to respond elastically to moderate-to-strong earthquakes. To survive such earthquakes, codes require that structures possess adequate ductility to allow them to dissipate most of the energy from the ground motions through inelastic deformations. However, deformations in the seismic force resisting system must be controlled to protect elements of the structure that are not part of the lateral force resisting system. The fact is that many elements of the structure that are not intended as a part of the lateral force resisting system and are not detailed for ductility will participate in the lateral force resistant mechanism and can become severely damaged as a result. In the case of wind, structures are generally expected to respond to the design wind within their "elastic" range of stresses. When wind loading governs the design (drift or strength), the structure still should comply with the appropriate seismic detailing requirements. This is required in order to provide a ductile system to resist earthquake forces. Figure 10-1 attempts to depict the interrelationships between the various considerations involved in earthquake-resistant design.

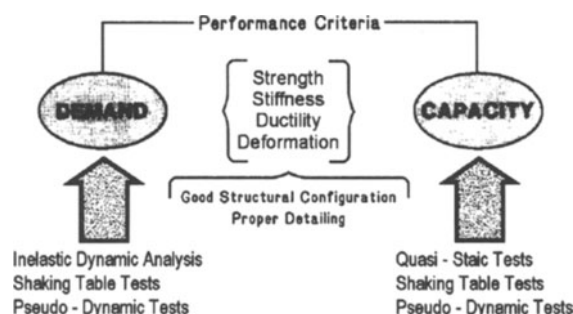


Figure 10-1. Components of and considerations in earthquake-resistant building design

10.1.5 The Need for a Good Design Concept and Proper Detailing

Because of the appreciable forces and deformations that can be expected in critical regions of structures subjected to strong ground motions and a basic uncertainty concerning the intensity and character of the ground motions at a particular site, a good design concept is essential at the start. A good design concept implies a structure with a configuration that behaves well under earthquake excitation and designed in a manner that allows it to respond to strong ground motions according to a predetermined pattern or sequence of yielding. The need to start with a sound structural configuration that minimizes "incidental" and often substantial increases in member forces resulting from torsion due to asymmetry or force concentrations associated with discontinuities cannot be overemphasized. Although this idea may not be met with favor by some architects, clear (mainly economic) benefits can be derived from structural configurations emphasizing symmetry, regularity, and the avoidance of severe discontinuities in mass, geometry, stiffness, or strength. A direct path for the lateral (inertial) forces from the superstructure to an appropriately designed foundation is very desirable. On numerous occasions, failure to take account of the increase in forces and deformations in certain elements due to torsion or discontinuities has led to severe structural

distress and even collapse. The provision of relative strengths in the various types of elements making up a structure with the aim of controlling the sequence of yielding in such elements has been recognized as desirable from the standpoint of structural safety as well as minimizing post-earthquake repair work.

An important characteristic of a good design concept and one intimately tied to the idea of ductility is structural redundancy. Since yielding at critically stressed regions and subsequent redistribution of forces to less stressed regions is central to the ductile performance of a structure, good practice suggests providing as much redundancy as possible in a structure. In monolithically cast reinforced concrete structures, redundancy is normally achieved by continuity between moment-resisting elements. In addition to continuity, redundancy or the provision of multiple load paths may also be accomplished by using several types of lateral-load-resisting systems in a building so that a "backup system" can absorb some of the load from a primary lateral-load-resisting system in the event of a partial loss of capacity in the latter.

Just as important as a good design concept is the proper detailing of members and their connections to achieve the requisite strength and ductility. Such detailing should aim at preventing nonductile failures, such as those associated with shear and with bond anchorage. In addition, a deliberate effort should be made to securely tie all parts of a structure that are intended to act as a unit together. Because dynamic response to strong earthquakes, characterized by repeated and reversed cycles of large-amplitude deformations in critical elements, tends to concentrate deformation demands in highly stressed portions of yielding members, the importance of proper detailing of potential hinging regions should command as much attention as the development of a good design concept. As with most designs but more so in design for earthquake resistance, where the relatively large repeated deformations tend to "seek and expose," in a manner of speaking, weaknesses in a structure—the proper field implementation of engineering drawings

ultimately determines how well a structure performs under the design loading.

Experience and observation have shown that properly designed, detailed, and constructed reinforced-concrete buildings can provide the necessary strength, stiffness, and inelastic deformation capacity to perform satisfactorily under severe earthquake loading.

10.1.6 Accent on Design for Strong Earthquakes

The focus in the following discussion will be on the design of buildings for moderate-to-strong earthquake motions. These cases correspond roughly to buildings located in seismic zones 2, 3 and 4 as defined in the Uniform Building Code (UBC-97).⁽¹⁰⁻¹⁾ By emphasizing design for strong ground motions, it is hoped that the reader will gain an appreciation of the special considerations involved in this most important loading case. Adjustments for buildings located in regions of lesser seismic risk will generally involve relaxation of some of the requirements associated with highly seismic areas.

Because the requirement for greater ductility in earthquake-resistant buildings represents the principal departure from the conventional design for gravity and wind loading, the major part of the discussion in this chapter will be devoted to considerations associated with providing ductility in members and structures.

The discussion in this chapter will be confined to monolithically cast reinforced-concrete buildings.

10.2 DUCTILITY IN EARTHQUAKE-RESISTANT DESIGN

10.2.1 Design Objective

In general, the design of economical earthquake resistant structures should aim at providing the appropriate dynamic and structural characteristics so that acceptable

levels of response result under the design earthquake. The magnitude of the maximum acceptable deformation will vary depending upon the type of structure and/or its function.

In some structures, such as slender, free-standing towers or smokestacks or suspension-type buildings consisting of a centrally located corewall from which floor slabs are suspended by means of peripheral hangers, the stability of the structure is dependent on the stiffness and integrity of the single major element making up the structure. For such cases, significant yielding in the principal element cannot be tolerated and the design has to be based on an essentially elastic response.

For most buildings, however, and particularly those consisting of rigidly connected frame members and other multiply redundant structures, economy is achieved by allowing yielding to take place in some critically stressed elements under moderate-to-strong earthquakes. This means designing a building for force levels significantly lower than would be required to ensure a linearly elastic response. Analysis and experience have shown that structures having adequate structural redundancy can be designed safely to withstand strong ground motions even if yielding is allowed to take place in some elements. As a consequence of allowing inelastic deformations to take place under strong earthquakes in structures designed to such reduced force levels, an additional requirement has resulted and this is the need to insure that yielding elements be capable of sustaining adequate inelastic deformations without significant loss of strength, i.e., they must possess sufficient ductility. Thus, where the strength (or yield level) of a structure is less than that which would insure a linearly elastic response, sufficient ductility has to be built in.

10.2.2 Ductility vs. Yield Level

As a general observation, it can be stated that for a given earthquake intensity and structure period, the ductility demand increases as the strength or yield level of a structure decreases. To illustrate this point, consider two

vertical cantilever walls having the same initial fundamental period. For the same mass and mass distribution, this would imply the same stiffness properties. This is shown in Figure 10-2, where idealized force-deformation curves for the two structures are marked (1) and (2). Analyses^(10-2, 10-3) have shown that the maximum lateral displacements of structures with the same initial fundamental period and reasonable properties are approximately the same when subjected to the same input motion. This phenomenon is largely attributable to the reduction in local accelerations, and hence displacements, associated with reductions in stiffness due to yielding in critically stressed portions of a structure. Since in a vertical cantilever the rotation at the base determines to a large extent the displacements of points above the base, the same observation concerning approximate equality of maximum lateral displacements can be made with respect to maximum rotations in the hinging region at the bases of the walls. This can be seen in Figure 10-3, from Reference 10-3, which shows results of dynamic analysis of isolated structural walls having the same fundamental period ($T_1 = 1.4$ sec) but different yield levels M_y . The structures were subjected to the first 10 sec of the east-west component of the 1940 El Centro record with intensity normalized to 1.5 times that of the north-south component of the same

record. It is seen in Figure 10-3a that, except for the structure with a very low yield level ($M_y = 500,000$ in.-kips), the maximum displacements for the different structures are about the same. The corresponding ductility demands, expressed as the ratio of the maximum hinge rotations, θ_{\max} to the corresponding rotations at first yield, θ_y , are shown in Figure 10-3b. The increase in ductility demand with decreasing yield level is apparent in the figure.

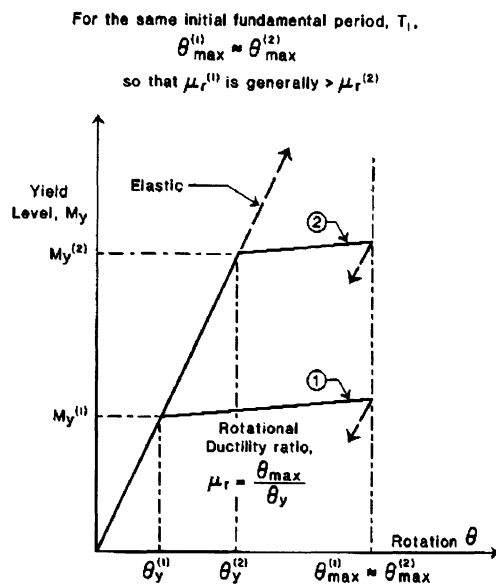


Figure 10-2. Decrease in ductility ratio demand with increase in yield level or strength of a structure.

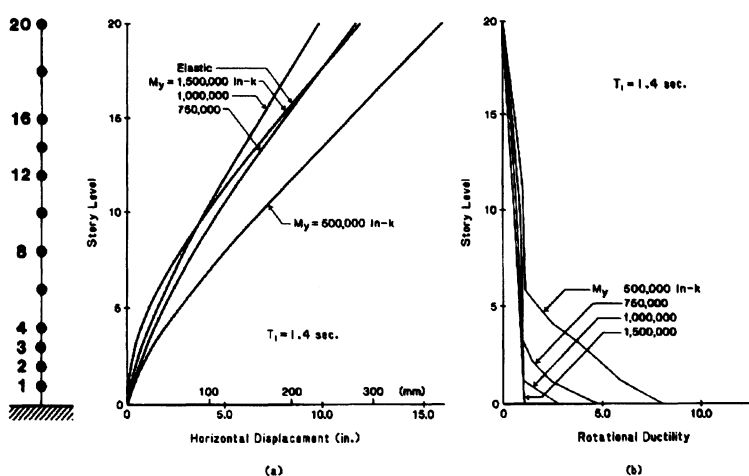


Figure 10-3. Effect of yield level on ductility demand. Note approximately equal maximum displacements for structures with reasonable yield levels. (From Ref. 10-3.)

A plot showing the variation of rotational ductility demand at the base of an isolated structural wall with both the flexural yield level and the initial fundamental period is shown in Figure 10-4.⁽¹⁰⁻⁴⁾ The results shown in Figure 10-4 were obtained from dynamic inelastic analysis of models representing 20-story isolated structural walls subjected to six input motions of 10-sec duration having different frequency characteristics and an intensity normalized to 1.5 times that of the north-south component of the 1940 El Centro record. Again, note the increase in ductility demand with decreasing yield level; also the decrease in ductility demand with increasing fundamental period of the structure.

The above-noted relationship between strength or yield level and ductility is the basis for code provisions requiring greater strength (by specifying higher design lateral forces) for materials or systems that are deemed to have less available ductility.

10.2.3 Some Remarks about Ductility

One should note the distinction between inelastic deformation demand expressed as a *ductility ratio*, μ (as it usually is) on one hand, and in terms of absolute rotation on the other. An observation made with respect to one quantity may not apply to the other. As an example, Figure 10-5, from Reference 10-3,

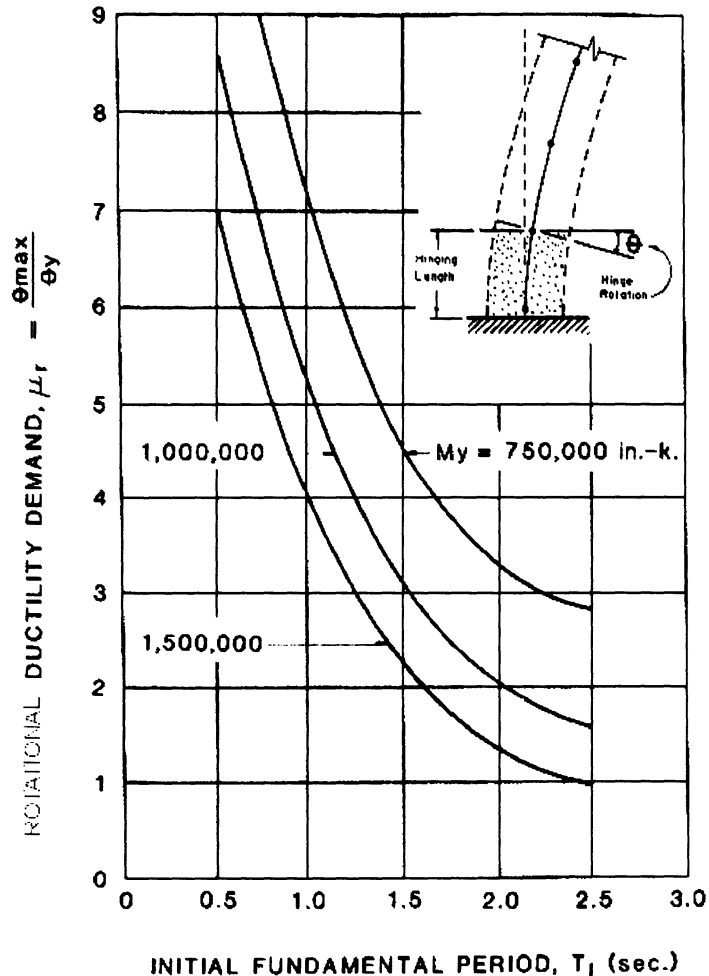


Figure 10-4. Rotational ductility demand as a function of initial fundamental period and yield level of 20-story structural walls. (From Ref. 10-4.)

shows results of dynamic analysis of two isolated structural walls having the same yield level ($M_y = 500,000$ in.-kips) but different stiffnesses, as reflected in the lower initial fundamental period T_1 of the stiffer structure. Both structures were subjected to the E-W component of the 1940 El Centro record. Even though the maximum rotation for the flexible structure (with $T_1 = 2.0$ sec) is 3.3 times that of the stiff structure, the ductility ratio for the stiff structure is 1.5 times that of the flexible structure. The latter result is, of course, partly due to the lower yield rotation of the stiffer structure.

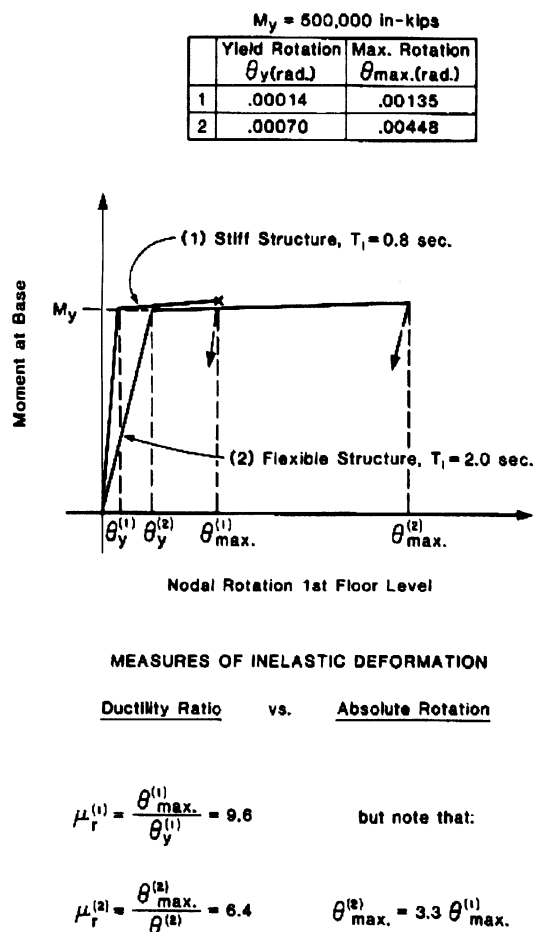


Figure 10-5. Rotational ductility ratio versus maximum absolute rotation as measures of inelastic deformation.

The term "curvature ductility" is also a commonly used term which is defined as

rotation per unit length. This is discussed in detail later in this Chapter.

Another important distinction worth noting with respect to ductility is the difference between displacement ductility and rotational ductility. The term *displacement ductility* refers to the ratio of the maximum horizontal (or transverse) displacement of a structure to the corresponding displacement at first yield. In a rigid frame or even a single cantilever structure responding inelastically to earthquake excitation, the lateral displacement of the structure is achieved by flexural yielding at local critically stressed regions. Because of this, it is reasonable to expect—and results of analyses bear this out^(10-2, 10-3, 10-5)—that rotational ductilities at these critical regions are generally higher than the associated displacement ductility. Thus, overall displacement ductility ratios of 3 to 6 may imply local rotational ductility demands of 6 to 12 or more in the critically stressed regions of a structure.

10.2.4 Results of a Recent Study on Cantilever Walls

In a recent study by Priestley and Kowalsky⁽¹⁰⁻⁶⁾ on isolated cantilever walls, it has been shown that the yield curvature is not directly proportional to the yield moment; this is in contrast to that shown in Figure 10-2 which in their opinions leads to significant errors. In fact, they have shown that yield curvature is a function of the wall length alone, for a given steel yield stress as indicated in Figure 10-6. The strength and stiffness of the wall vary proportionally as the strength of the section is changed by varying the amount of flexural reinforcement and/or the level of axial load. This implies that the yield curvature, not the section stiffness, should be considered the fundamental section property. Since wall yield curvature is inversely proportional to wall length, structures containing walls of different length cannot be designed such that they yield simultaneously. In addition, it is stated that wall design should be proportioned to the square of

wall length, L^2 , rather than the current design assumption, which is based on L^3 .

It should be noted that the above findings apply to cantilever walls only. Further research in this area in various aspects is currently underway at several institutions.

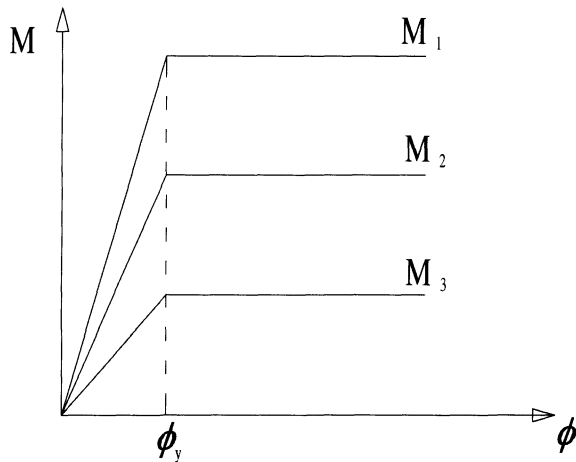


Figure 10-6. Influence of strength on moment-curvature relationship (From Ref. 10-6).

10.3 BEHAVIOR OF CONCRETE MEMBERS UNDER EARTHQUAKE-TYPE LOADING

10.3.1 General Objectives of Member Design

A general objective in the design of reinforced concrete members is to so proportion such elements that they not only possess adequate stiffness and strength but so that the strength is, to the extent possible, governed by flexure rather than by shear or bond/anchorage. Code design requirements are framed with the intent of allowing members to develop their flexural or axial load capacity before shear or bond/anchorage failure occurs. This desirable feature in conventional reinforced concrete design becomes imperative in design for earthquake motions where significant ductility is required.

In certain members, such as conventionally reinforced short walls—with height-to-width ratios of 2 to 3 or less—the very nature of the principal resisting mechanism would make a shear-type failure difficult to avoid. Diagonal reinforcement, in conjunction with horizontal and vertical reinforcement, has been shown to improve the performance of such members⁽¹⁰⁻⁷⁾.

10.3.2 Types of Loading Used in Experiments

The bulk of information on behavior of reinforced-concrete members under load has ‘generally been obtained from tests of full-size or near-full-size specimens. The loadings used in these tests fall under four broad categories, namely:

1. *Static monotonic loading*—where load in one direction only is applied in increments until failure or excessive deformation occurs. Data which form the basis for the design of reinforced concrete members under gravity and wind loading have been obtained mainly from this type of test. Results of this test can serve as bases for comparison with results obtained from other types of test that are more representative of earthquake loading.

2. *Slowly reversed cyclic (“quasistatic”) loading*—where the specimen is subjected to (force or deformation) loading cycles of predetermined amplitude. In most cases, the load amplitude is progressively increased until failure occurs. This is shown schematically in Figure 10-7a. As mentioned earlier, much of the data upon which current design procedures for earthquake resistance are based have been obtained from tests of this type. In a few cases, a loading program patterned after analytically determined dynamic response⁽¹⁰⁻⁸⁾ has been used. The latter, which is depicted in Figure 10-7b, is usually characterized by large-amplitude load cycles early in the test, which can produce early deterioration of the strength of a specimen.⁽¹⁰⁻⁹⁾ In both of the above cases, the load application points are fixed so that the moments and shears are always in phase—a condition, incidentally, that does not always occur in dynamic response.

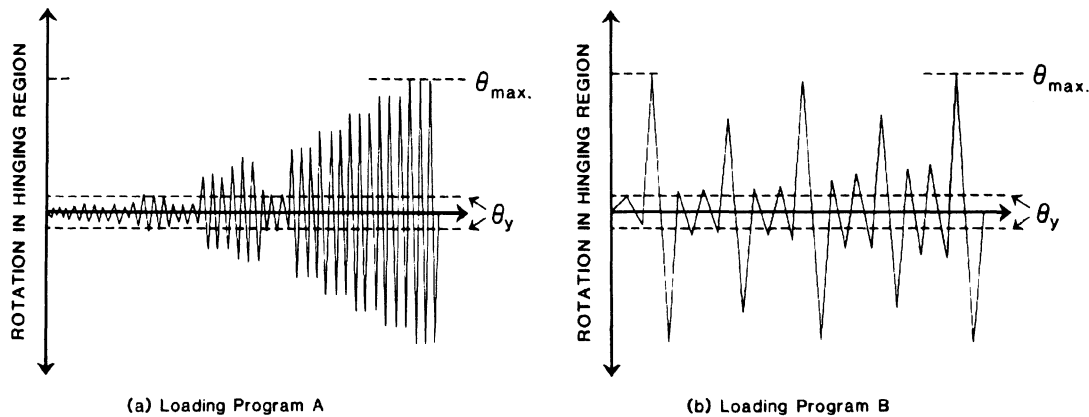


Figure 10-7. Two types of loading program used in quasi-static tests.

This type of test provides the reversing character of the loading that distinguishes dynamic response from response to unidirectional static loading. In addition, the relatively slow application of the load allows close observation of the specimen as the test progresses. However, questions concerning the effects of the sequence of loading as well as the phase relationship between moment and shear associated with this type of test as it is normally conducted need to be explored further.

3. Pseudo-dynamic tests. In this type of test, the specimen base is fixed to the test floor while time-varying displacements determined by an on-line computer are applied to selected points on the structure. By coupling loading rams with a computer that carries out an incremental dynamic analysis of the specimen response to a preselected input motion, using measured stiffness data from the preceding loading increment and prescribed data on specimen mass and damping, a more realistic distribution of horizontal displacements in the test structure is achieved. The relatively slow rate at which the loading is imposed allows convenient inspection of the condition of the structure during the progress of the test.

This type of test, which has been used mainly for testing structures, rather than members or structural elements, requires a fairly large reaction block to take the thrust from the many loading rams normally used.

4. Dynamic tests using shaking tables (earthquake simulators). The most realistic test conditions are achieved in this setup, where a specimen is subjected to a properly scaled input motion while fastened to a test bed impelled by computer-controlled actuators. Most current earthquake simulators are capable of imparting controlled motions in one horizontal direction and in the vertical direction.

The relatively rapid rate at which the loading is imposed in a typical dynamic test generally does not allow close inspection of the specimen while the test is in progress, although photographic records can be viewed after the test. Most currently available earthquake simulators are limited in their capacity to small-scale models of multistory structures or near-full-scale models of segments of a structure of two or three stories. The difficulty of viewing the progress of damage in a specimen as the loading is applied and the limited capacity of available (and costly) earthquake simulators has tended to favor the recently developed pseudo-dynamic test as a basic research tool for testing structural systems.

The effect of progressively increasing lateral displacements on actual structures has been studied in a few isolated cases by means of forced-vibration testing. These tests have usually been carried out on buildings or portions of buildings intended for demolition.

10.3.3 Effects of Different Variables on the Ductility of Reinforced Concrete Members

Figure 10-8 shows typical stress-strain curves of concrete having different compressive strengths. The steeper downward slope beyond the point of maximum stress of curves corresponding to the higher strength concrete is worth noting. The greater ductility of the lower-strength concrete is apparent in the figure. Typical stress-strain curves for the commonly available grades of reinforcing steel, with nominal yield strengths of 60 ksi and 40 ksi, are shown in Figure 10-9. Note in the figure that the ultimate stress is significantly higher than the yield stress. Since strains well into the strain-hardening range can occur in hinging regions of flexural members, stresses in excess of the nominal yield stress (normally used in conventional design as the limiting stress in steel) can develop in the reinforcement at these locations.

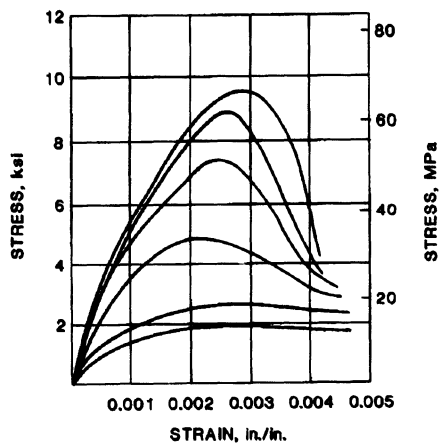


Figure 10-8. Typical stress-strain curves for concrete of varying compressive strengths.

Rate of Loading An increase in the strain rate of loading is generally accompanied by an increase in the strength of concrete or the yield stress of steel. The greater rate of loading associated with earthquake response, as compared with static loading, results in a slight increase in the strength of reinforced concrete members, due primarily to the increase in the

yield strength of the reinforcement. The calculation of the strength of reinforced concrete members in earthquake-resistant structures on the basis of material properties obtained by static tests (i.e., normal strain rates of loading) is thus reasonable and conservative.

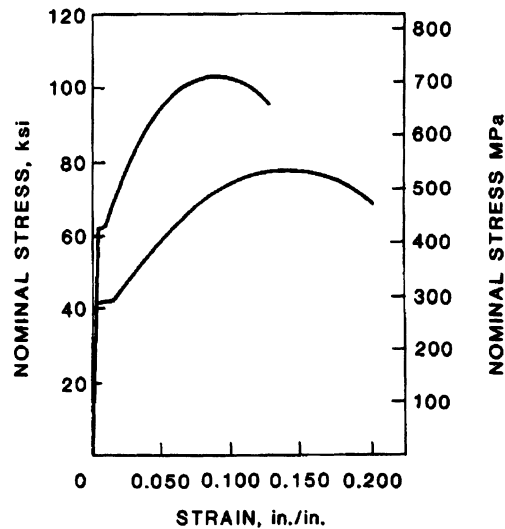


Figure 10-9. Typical stress-strain curves for ordinary reinforcing steel.

Confinement Reinforcement The American Concrete Institute *Building Code Requirements for Reinforced Concrete*, ACI 318-95⁽¹⁰⁻¹⁰⁾ (hereafter referred to as the ACI Code), specifies a maximum usable compressive strain in concrete, ϵ_{cu} of 0.003. Lateral confinement, whether from active forces such as transverse compressive loads, or passive restraints from other framing members or lateral reinforcement, tends to increase the value of ϵ_{cu} . Tests have shown that ϵ_{cu} can range from 0.0025 for unconfined concrete to about 0.01 for concrete confined by lateral reinforcement subjected to predominantly axial (concentric) load. Under eccentric loading, values of ϵ_{cu} for confined concrete of 0.05 and more have been observed.^(10-11, 10-12, 10-13)

Effective lateral confinement of concrete increases its compressive strength and deformation capacity in the longitudinal direction, whether such longitudinal stress represents a purely axial load or the compressive component of a bending couple.

In reinforced concrete members, the confinement commonly takes the form of lateral ties or spiral reinforcement covered by a thin shell of concrete. The passive confining effect of the lateral reinforcement is not mobilized until the concrete undergoes sufficient lateral expansion under the action of compressive forces in the longitudinal direction. At this stage, the outer shell of concrete usually has reached its useful load limit and starts to spall. Because of this, the net increase in strength of the section due to the confined core may not amount to much in view of the loss in capacity of the spalled concrete cover. In many cases, the total strength of the confined core may be slightly less than that of the original section. The increase in ductility due to effective confining reinforcement, however, is significant.

The confining action of rectangular hoops mainly involves reactive forces at the corners, with only minor restraint provided along the straight unsupported sides. Because of this, rectangular hoops are generally not as effective as circular spiral reinforcement in confining the concrete core of members subjected to compressive loads. However, confinement in rectangular sections can be improved using additional transverse ties. Square spirals, because of their continuity, are slightly better

than separate rectangular hoops.

The stress-strain characteristics of concrete, as represented by the maximum usable compressive strain ϵ_{cu} is important in designing for ductility of reinforced concrete members. However, other factors also influence the ductility of a section: factors which may increase or diminish the effect of confinement on the ductility of concrete. Note the distinction between the ductility of concrete as affected by confinement and the ductility of a reinforced concrete section (i.e., sectional ductility) as influenced by the ductility of the concrete as well as other factors.

Sectional Ductility A convenient measure of the ductility of a section subjected to flexure or combined flexure and axial load is the ratio μ of the ultimate curvature attainable without significant loss of strength, ϕ_u , to the curvature corresponding to first yield of the tension reinforcement, ϕ_y . Thus

$$\text{Sectional ductility, } \mu = \frac{\phi_u}{\phi_y}$$

Figure 10-10, which shows the strains and resultant forces on a typical reinforced concrete section under flexure, corresponds to the condition when the maximum usable compressive strain in concrete, ϵ_{cu} is reached. The corresponding curvature is denoted as the

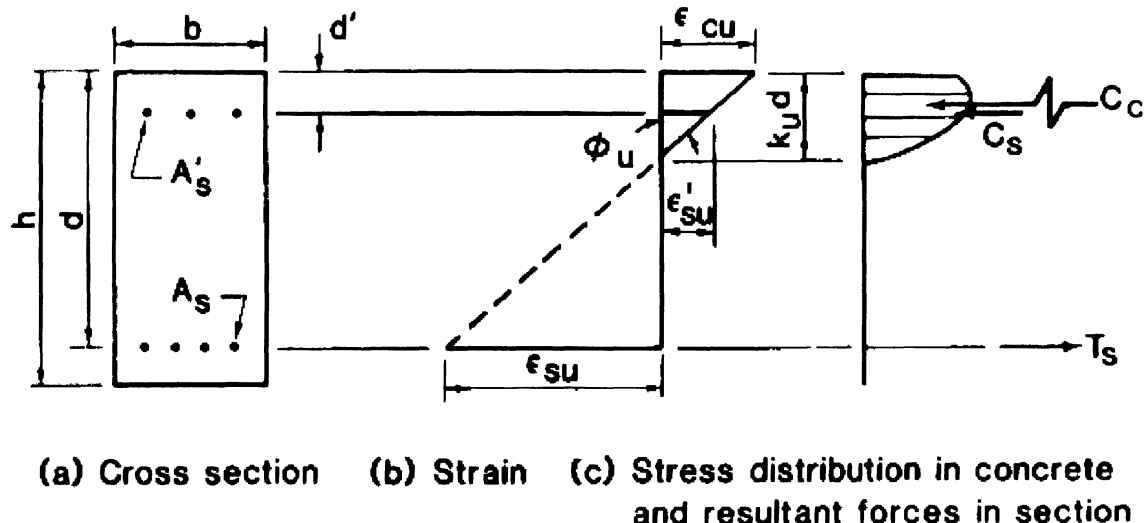


Figure 10-10. Strains and stresses in a typical reinforced concrete section under flexure at ultimate condition.

ultimate curvature, ϕ_u . It will be seen in the figure that

$$\phi_u = \frac{\epsilon_{cu}}{k_u d}$$

where $k_u d$ is the distance from the extreme compression fiber to the neutral axis.

The variables affecting sectional ductility may be classified under three groups, namely: (i) material variables, such as the maximum usable compressive strain in concrete, particularly as this is affected by confinement, and grade of reinforcement; (ii) geometric variables, such as the amount of tension and compression reinforcement, and the shape of the section; (iii) loading variables, such as the level of the axial load and accompanying shear.

As is apparent from the above expression for ultimate curvature, factors that tend to increase ϵ_{cu} or decrease $k_u d$ tend to increase sectional ductility. As mentioned earlier, a major factor affecting the value of ϵ_{cu} is lateral confinement. Tests have also indicated that ϵ_{cu} increases as the distance to the neutral axis decreases, that is, as the strain gradient across the section increases^(10-14, 10-15) and as the moment gradient along the span of the member increases or as the shear span decreases.^(10-16, 10-17)

(For a given maximum moment, the moment gradient increases as the distance from the point of zero moment to the section considered decreases.)

The presence of compressive reinforcement and the use of concrete with a high compressive strength,^a as well as the use of flanged sections, tend to reduce the required depth of the compressive block, $k_u d$, and hence to increase the ultimate curvature ϕ_u . In addition, the compressive reinforcement also helps confine the concrete compression zone and, in combination with adequate transverse reinforcement, allows the spread of the inelastic action in a hinging region over a longer length than would otherwise occur, thus improving the

ductility of the member.⁽¹⁰⁻¹⁹⁾ On the other hand, compressive axial loads and large amounts of tensile reinforcement, especially tensile reinforcement with a high yield stress, tend to increase the required $k_u d$ and thus decrease the ultimate curvature ϕ_u .

Figure 10-11 shows axial-load—moment-strength interaction curves for a reinforced-concrete section subjected to a compressive axial load and bending about the horizontal axis. Both confined and unconfined conditions are assumed. The interaction curve provides a convenient way of displaying the combinations of bending moment M and axial load P which a given section can carry. A point on the interaction curve is obtained by calculating the forces M and P associated with an assumed linear strain distribution across the section, account being taken of the appropriate stress-strain relationships for concrete and steel. For an ultimate load curve, the concrete strain at the extreme compressive fiber, ϵ_c is assumed to be at the maximum usable strain, ϵ_{cu} while the strain in the tensile reinforcement, ϵ_s , varies. A loading combination represented by a point on or inside the interaction curve can be safely resisted by the section. The balance point in the interaction curve corresponds to the condition in which the tensile reinforcement is stressed to its yield point at the same time that the extreme concrete fiber reaches its useful limit of compressive strain. Points on the interaction curve above the balance point represent conditions in which the strain in the tensile reinforcement is less than its yield strain ϵ_y , so that the strength of the section in this range is governed by failure of the concrete compressive zone. For those points on the curve below the balance point, $\epsilon_s > \epsilon_y$. Hence, the strength of the section in this range is governed by rupture of the tensile reinforcement.

Figure 10-11 also shows the variation of the ultimate curvature ϕ_u (in units of $1/h$) with the axial load P . It is important to note the greater ultimate curvature (being a measure of sectional ductility) associated with values of P less than that corresponding to the balance condition, for both unconfined and confined cases. The significant increase in ultimate curvature

^a The lower ductility of the higher-strength ($f'_c > 5000$ psi), however, has been shown to result in a decrease in sectional ductility, particularly for sections with low reinforcement indexes.⁽¹⁰⁻¹⁸⁾

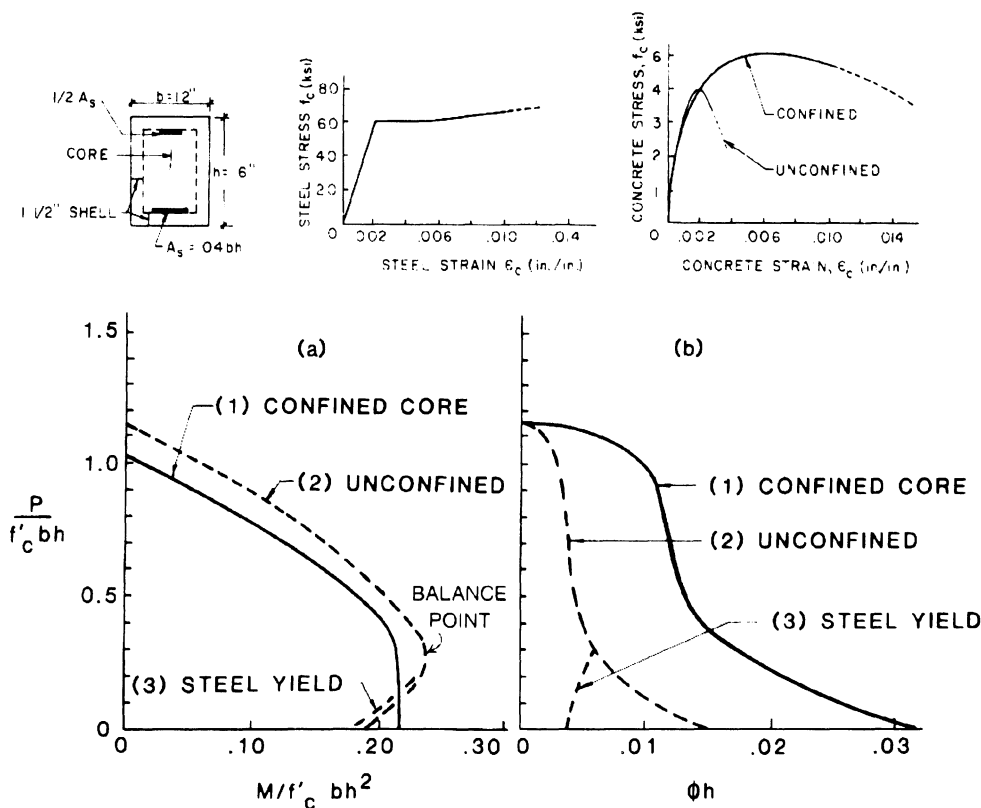


Figure 10-11. Axial load-moment interaction and load-curvature curves for a typical reinforced concrete section with unconfined and confined cores.

resulting from confinement is also worth noting in Figure 10-11b.

In the preceding, the flexural deformation capacity of the hinging region in members was examined in terms of the curvature at a section, ϕ , and hence the sectional or curvature ductility. Using this simple model, it was possible to arrive at important conclusions concerning the effects of various parameters on the ductility of reinforced concrete members. In the hinging region of members, however, the curvature can vary widely in value over the length of the "plastic hinge." Because of this, the total rotation over the plastic hinge, θ , provides a more meaningful measure of the inelastic flexural deformation in the hinging regions of members and one that can be related directly to experimental measurements. (One can, of course, speak of average curvature over the hinging region, i.e., total rotation divided by length of the plastic hinge.)

Shear The level of shear present can have a major effect on the ductility of flexural hinging regions. To study the effect of this variable, controlled tests of laboratory specimens have been conducted. This will be discussed further in the following section.

10.3.4 Some Results of Experimental and Analytical Studies on the Behavior of Reinforced Concrete Members under Earthquake-Type Loading and Related Code Provisions

Experimental studies of the behavior of structural elements under earthquake-type loading have been concerned mainly with identifying and/or quantifying the effects of variables that influence the ability of critically stressed regions in such specimens to perform properly. Proper performance means primarily possessing adequate ductility. In terms of the

quasistatic test that has been the most widely used for this purpose, proper performance would logically require that these critical regions be capable of sustaining a minimum number of deformation cycles of specified amplitude without significant loss of strength.

In the United States, there is at present no standard set of performance requirements corresponding to designated areas of seismic risk that can be used in connection with the quasi-static test. Such requirements would have to specify not only the minimum amplitude (i.e., ductility ratio) and number of deformation cycles, but also the sequence of application of the large-amplitude cycles in relation to any small-amplitude cycles and the permissible reduction in strength at the end of the loading.

As mentioned earlier, the bulk of experimental information on the behavior of elements under earthquake-type loading has been obtained by quasi-static tests using loading cycles of progressively increasing amplitude, such as is shown schematically in Figure 10-7a. Adequacy with respect to ductility for regions of high seismicity has usually been inferred when displacement ductility ratios of anywhere from 4 to 6 or greater were achieved without appreciable loss of strength. In New Zealand,⁽¹⁰⁻²⁰⁾ moment resisting frames are designed for a maximum ductility, μ , of 6 and shear walls are designed for a maximum ductility of between 2.5 to 5. Adequate ductile capacity is considered to be present if all primary that are required to resist earthquake-induced forces are accordingly designed and detailed.

In the following, some results of tests and analyses of typical reinforced-concrete members will be briefly reviewed. Where appropriate, related code provisions, mainly those in Chapter 21 of the ACI Code⁽¹⁰⁻¹⁰⁾ are also discussed.

Beams Under earthquake loading, beams will generally be most critically stressed at and near their intersections with the supporting columns. An exception may be where a heavy concentrated load is carried at some intermediate point on the span. As a result, the focus of attention in the design of beams is on

these critical regions where plastic hinging can take place.

At potential hinging regions, the need to develop and maintain the strength and ductility of the member through a number of cycles of reversed inelastic deformation calls for special attention in design. This special attention relates mainly to the lateral reinforcement, which takes the form of closed hoops or spirals. As might be expected, the requirements governing the design of lateral reinforcement for potential hinging regions are more stringent than those for members designed for gravity and wind loads, or the less critically stressed parts of members in earthquake-resistant structures. The lateral reinforcement in hinging regions of beams is designed to provide (i) confinement of the concrete core, (ii) support for the longitudinal compressive reinforcement against inelastic buckling, and (iii) resistance, in conjunction with the confined concrete, against transverse shear.

In addition to confirming the results of sectional analyses regarding the influence of such variables as concrete strength, confinement of concrete, and amounts and yield strengths of tensile and compressive reinforcement and compression flanges mentioned earlier, tests, both monotonic and reversed cyclic, have shown that the flexural ductility of hinging regions in beams is significantly affected by the level of shear present. A review of test results by Bertero⁽¹⁰⁻²¹⁾ indicates that when the nominal shear stress exceeds about $3\sqrt{f'_c}$, members designed according to the present seismic codes can expect to suffer some reduction in ductility as well as stiffness when subjected to loading associated with strong earthquake response. When the shear accompanying flexural hinging is of the order of $5\sqrt{f'_c}$ or higher, very significant strength and stiffness degradation has been observed to occur under cyclic reversed loading.

The behavior of a segment at the support region of a typical reinforced-concrete beam subjected to reversed cycles of inelastic deformation in the presence of high shear⁽¹⁰⁻²²⁾,

¹⁰⁻²³⁾ is shown schematically in Figure 10-12. In Figure 10-12a, yielding of the top longitudinal steel under a downward movement of the beam end causes flexure—shear cracks to form at the top. A reversal of the load and subsequent yielding of the bottom longitudinal steel is also accompanied by cracking at the bottom of the beam (see Figure 10-12b). If the area of the bottom steel is at least equal to that of the top steel, the top cracks remain open during the early stages of the load reversal until the top steel yields in compression, allowing the top crack to close and the concrete to carry some compression. Otherwise, as in the more typical case where the top steel has greater area than the bottom steel, the top steel does not yield in compression (and we assume it does not buckle), so that the top crack remains open during the reversal of the load (directed upward). Even in the former case, complete closure of the crack at the top may be prevented by loose particles of concrete that may fall into the open cracks. With a crack traversing the entire depth of the beam, the resisting flexural couple consists of the forces in the tensile and compressive steel areas, while the shear along the through-depth crack is resisted primarily by dowel action of the longitudinal steel. With subsequent reversals of the load and progressive deterioration of the concrete in the hinging region (Figure 10-12c), the through-depth crack widens. The resulting increase in total length of the member due to the opening of through-depth cracks under repeated load reversals is sometimes referred to as *growth* of the member.

Where the shear accompanying the moment is high, sliding along the through-depth crack(s) can occur. This sliding shear displacement, which is resisted mainly by dowel action of the longitudinal reinforcement, is reflected in a *pinching* of the associated load—deflection curve near the origin, as indicated in Figure 10-13. Since the area under the load—deflection curve is a measure of the energy-dissipation capacity of the member, the pinching in this curve due to sliding shear represents a degradation not only of the strength but also the energy-dissipation capacity of the hinging

region. Where the longitudinal steel is not adequately restrained by lateral reinforcement, inelastic buckling of the compressive reinforcement followed by a rapid loss of flexural strength can occur.

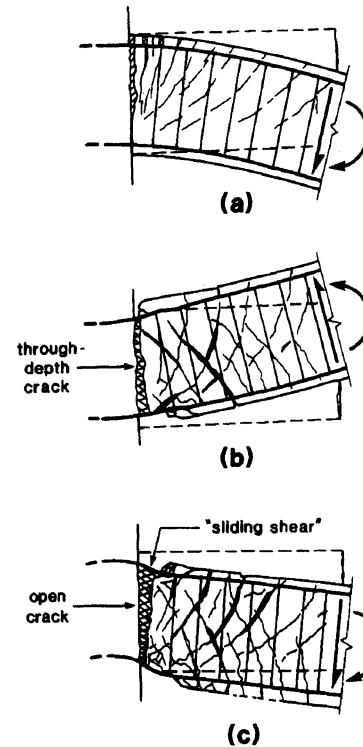


Figure 10-12. Plastic hinging in beam under high shear.
(Adapted from Ref. 10-31.)

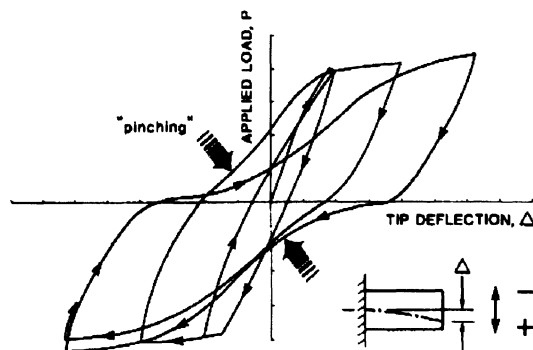


Figure 10-13. Pinching in load-displacement hysteresis loop due to mainly to sliding shear

Because of the significant effect that shear can have on the ductility of hinging regions, it has been suggested⁽¹⁰⁻²⁴⁾ that when two or more load reversals at a displacement ductility of 4 or more are expected, the nominal shear stress in critical regions reinforced according to normal

U.S. code requirements for earthquake-resistant design should be limited to $6\sqrt{f'_c}$. Results of tests reported in Reference 10-24 have shown that the use of crossing diagonal or inclined web reinforcement, in combination with vertical ties, as shown in Figure 10-14, can effectively minimize the degradation of stiffness associated with sliding shear. Relatively stable hysteretic force-displacement loops, with minimal or no pinching, were observed. Tests reported in Reference 10-25 also indicate the effectiveness of intermediate longitudinal shear reinforcement, shown in Figure 10-15, in reducing pinching of the force-displacement loops of specimens subjected to moderate levels of shear stresses, i.e., between $3\sqrt{f'_c}$ and $6\sqrt{f'_c}$.

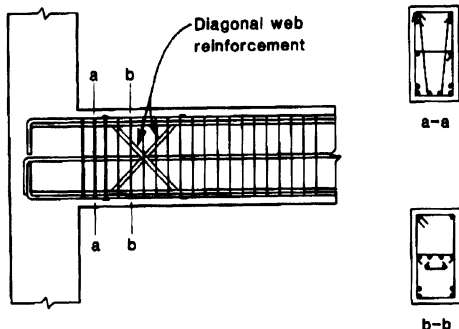


Figure 10-14. Crossing diagonal web reinforcement in combination with vertical web steel for hinging regions under high shear. (Adapted from Ref. 10-24)

As mentioned earlier, a major objective in the design of reinforced concrete members is to have the strength controlled by flexure rather than shear or other less ductile failure mechanisms. To insure that beams develop their full strength in flexure before failing in shear, ACI Chapter 21 requires that the design for shear in beams be based not on the factored shears obtained from a lateral-load analysis but rather on the shears corresponding to the maximum probable flexural strength, M_{pr} , that can be developed at the beam ends. Such a probable flexural strength is calculated by assuming the stress in the tensile reinforcement

to be equal to $1.25f_y$ and using a strength reduction factor ϕ equal to 1.0 (instead of 0.9). This is illustrated in Figure 10-16 for the case of uniformly distributed beam. The use of the factor 1.25 to be applied to f_y is intended to take account of the likelihood of the actual yield stress in the steel being greater (tests indicate it to be commonly 10 to 25% greater) than the specified nominal yield stress, and also in recognition of the strong possibility of strain hardening developing in the reinforcement when plastic hinging occurs at the beam ends.

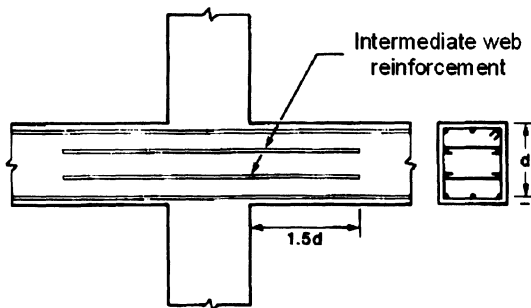


Figure 10-15. Intermediate longitudinal web reinforcement for hinging regions under moderate levels of shear.

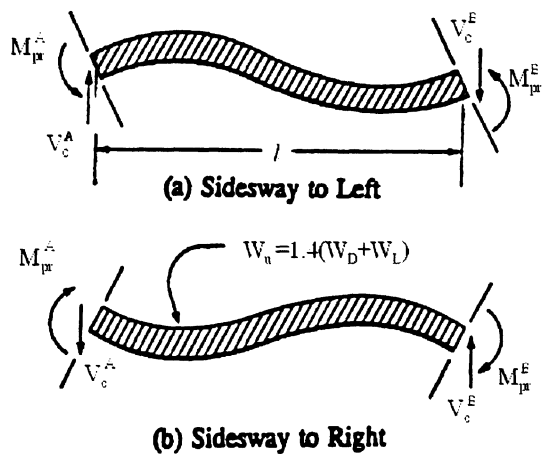


Figure 10-16. Loading cases for shear design of beams uniformly distributed gravity loads

$$V_c^A = \frac{M_{pr}^A + M_{pr}^B}{l} + \frac{W_u l}{2}$$

$$V_c^B = \frac{M_{pr}^A + M_{pr}^B}{l} - \frac{W_u l}{2}$$

M_{pr} based on $f_s = 1.25 f_y$ and $\phi = 1.0$

ACI Chapter 21 requires that when the earthquake-induced shear force calculated on the basis of the maximum probable flexural strength at the beam ends is equal to or more than one-half the total design shear, the contribution of the concrete in resisting shear, V_c , be neglected if the factored axial compressive force including earthquake effects is less than $A_g f'_c / 20$, where A_g is the gross area of the member cross-section. In the 1995 New Zealand Code,⁽¹⁰⁻²⁶⁾ the concrete contribution is to be entirely neglected and web reinforcement provided to carry the total shear force in plastic-hinging regions. It should be pointed out that the New Zealand seismic design code appears to be generally more conservative than comparable U.S. codes. This will be discussed further in subsequent sections.

Columns The current approach to the design of earthquake-resistant reinforced concrete rigid (i.e., moment-resisting) frames is to have most of the significant inelastic action or plastic hinging occur in the beams rather than in the columns. This is referred to as the "strong column-weak beam" concept and is intended to help insure the stability of the frame while undergoing large lateral displacements under earthquake excitation. Plastic hinging at both ends of most of the columns in a story can precipitate a story-sidesway mechanism leading to collapse of the structure at and above the story.

ACI Chapter 21 requires that the sum of the flexural strengths of the columns meeting at a joint, under the most unfavorable axial load, be at least equal to 1.2 times the sum of the design flexural strengths of the girders in the same plane framing into the joint. The most unfavorable axial load is the factored axial force resulting in the lowest corresponding flexural strength in the column and which is consistent with the direction of the lateral forces considered. Where this requirement is satisfied, closely spaced transverse reinforcement need be provided only over a short distance near the ends of the columns where potential hinging can occur. Otherwise, closely spaced transverse reinforcement is required over the full height of the columns.

The requirements associated with the strong column-weak beam concept, however, do not insure that plastic hinging will not occur in the columns. As pointed out in Reference 10-5, a bending-moment distribution among frame members such as is shown in Figure 10-17, characterized by points of inflection located away from the mid-height of columns, is not uncommon. This condition, which has been observed even under static lateral loading, occurs when the flexural mode of deformation (as contrasted with the shear-beam component of deformation) in tall frame structures becomes significant and may also arise as a result of higher-mode response under dynamic loading. As Figure 10-17 shows, a major portion of the girder moments at a joint is resisted (assuming the columns remain elastic) by one column segment, rather than being shared about equally (as when the points of inflection are located at mid-height of the columns) by the column sections above and below a joint. In extreme cases, such as might result from substantial differences in the stiffnesses of adjoining column segments in a column stack, the point of contraflexure can be outside the column height. In such cases, the moment resisted by a column segment may exceed the sum of the girder moments. In recognition of this, and the likelihood of the hinging region spreading over a longer length than would normally occur, most building codes require confinement reinforcement to be provided over the full height of the column.

Tests on beam-column specimens incorporating slabs,^(10-27, 10-28) as in normal monolithic construction, have shown that slabs significantly increase the effective flexural strength of the beams and hence reduce the column-to-beam flexural strength ratio, if the beam strength is based on the bare beam section. Reference 10-27 recommends consideration of the slab reinforcement over a width equal to at least the width of the beam on each side of the member when calculating the flexural strength of the beam.

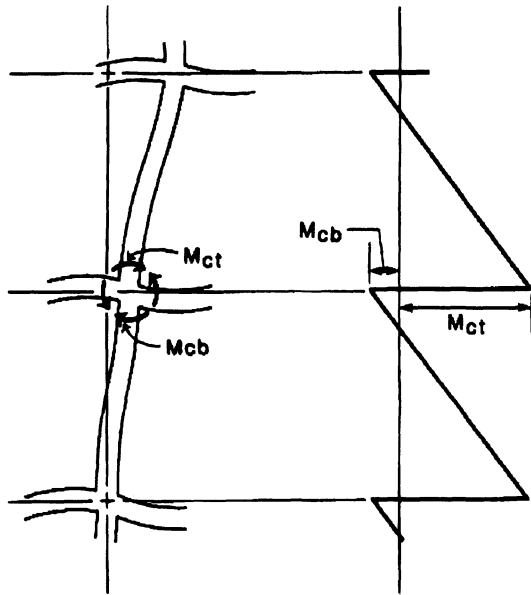


Figure 10-17. Distribution of bending moments in columns at a joint when the point of inflection is located away from mid-height.

Another phenomenon that may lead to plastic hinging in the columns occurs in two-way (three-dimensional rigid) frames subjected to ground motions along a direction inclined with respect to the principal axes of the structure. In such cases, the resultant moment from girders lying in perpendicular planes framing into a column will generally be greater than that corresponding to either girder considered separately.⁽¹⁰⁻⁵⁾ (except for certain categories of structures and those with certain irregularities, codes allow consideration of design earthquake loads along each principal axes of a structure separately, as non-concurrent loadings.) Furthermore, the biaxial moment capacity of a reinforced-concrete column under skew bending will generally be less than the larger uniaxial moment capacity. Tests reported in Reference 10-28 indicate that where bi-directional loading occurs in rectangular columns, the decrease in strength of the column due to spalling of concrete cover, and bond deterioration along the column longitudinal bars at and near the corner can be large enough to shift the hinging from the beams to the columns. Thus, under concurrent bi-directional loading, columns in two-way frames designed according to the strong column-weak beam

concept mentioned above can either yield before the framing girders or start yielding immediately following yielding of the girders.

It is worth noting that the 1985 report of ACI-ASCE Committee 352 on beam-column joints in monolithic reinforced concrete structures⁽¹⁰⁻²⁹⁾ recommends a minimum overstrength factor of 1.4, instead of the 1.2 given in ACI 318-95, for the flexural strength of columns relative to that of beams meeting at a joint when the beam strength is based only on the bare beam section (excluding slab). A design procedure (*capacity design*), based on the work of Paulay,^(10-13,10-30) that attempts to minimize the possibility of yielding in the columns of a typical frame due to the factors described in the preceding paragraph has been adopted in New Zealand.⁽¹⁰⁻²⁶⁾ The avowed purpose of capacity design is to limit inelastic action, as well as the formation of plastic hinges, to selected elements of the primary lateral-force-resisting system. In the case of frames, the ideal location for plastic hinges would be the beams and the bases of the first or lowest story columns. Other elements, such as columns, are intended to remain essentially elastic under the design earthquake by designing them with sufficient overstrength relative to the yielding members. Thus elements intended to remain elastic are designed to have strengths in the plastic hinges. For all elements, and particularly regions designed to develop plastic hinges, undesirable modes of failure, such as shear or bond/anchorage failures, are precluded by proper design/detailing. The general philosophy of capacity design is no different from that underlying the current approach to earthquake-resistant design found in ACI Chapter 21, UBC-97 and IBC-2000. The principle difference lies in the details of implementation and particularly in the recommended overstrength factors. For example, the procedure prescribes overstrength factors of 1.5 or greater^(10-13,10-32) for determining the flexural strength of columns relative to beams. This compares with the 1.2 factor specified in ACI Chapter 21. In capacity design, the flexural strength of T or inverted-L beams is to be determined by considering the

slab reinforcement over the specified width (depending upon column location) beyond the column faces as effective in resisting negative moments. It is clear from the above that the New Zealand capacity design requirements call for greater relative column strength than is currently required in U.S. practice. A similar approach has also been adopted in the Canadian Concrete Code of Practice, CSA Standard A23.3-94.⁽¹⁰⁻³³⁾ Reference 10-13 gives detailed recommendations, including worked out examples, relating to the application of capacity design to both frames and structural wall systems.

To safeguard against strength degradation due to hinging in the columns of a frame, codes generally require lateral reinforcement for both confinement and shear in regions of potential plastic hinging. As in potential hinging regions of beams, the closely spaced transverse reinforcement in critically stressed regions of columns is intended to provide confinement for the concrete core, lateral support of the longitudinal column reinforcement against buckling and resistance (in conjunction with the confined core) against transverse shear. The transverse reinforcement can take the form of spirals, circular hoops, or rectangular hoops, the last with crossties as needed.

Early tests⁽¹⁰⁻³⁴⁾ of reinforced concrete columns subjected to large shear reversals had indicated the need to provide adequate transverse reinforcement not only to confine the concrete but also to carry most, if not all, of the shear in the hinging regions of columns. The beneficial effect of axial load—a maximum axial load of one-half the balance load was used in the tests—in delaying the degradation of shear strength in the hinging region was also noted in these tests. An increase in column strength due to improved confinement by longitudinal reinforcement uniformly distributed along the periphery of the column section was noted in tests reported in Reference 10-35. Tests cited in Reference 10-32 have indicated that under high axial load, the plastic hinging region in columns with confinement reinforcement provided over the usually assumed hinging length (i.e., the longer section

dimension in rectangular columns or the diameter in circular columns) tends to spread beyond the confined region. To prevent flexural failure in the less heavily confined regions of columns, the New Zealand Code⁽¹⁰⁻²⁰⁾ requires that confining steel be extended to 2 to 3 times the usual assumed plastic-hinge length when the axial load exceeds $0.25\phi f'_c A_g$, where $\phi = 0.85$ and A_g is the gross area of the column section.

The basic intent of the ACI Code provisions relating to confinement reinforcement in potential hinging regions of columns is to preserve the axial-load-carrying capacity of the column after spalling of the cover concrete has occurred. This is similar to the intent underlying the column design provisions for gravity and wind loading. The amount of confinement reinforcement required by these provisions is independent of the level of axial load. Design for shear is to be based on the largest nominal moment strengths at the column ends consistent with the factored design axial compressive load. Some investigators,⁽¹⁰⁻⁵⁾ however, have suggested that an approach that recognizes the potential for hinging in critically stressed regions of columns should aim primarily at achieving a minimum ductility in these regions. Studies by Park and associates, based on sectional analyses⁽¹⁰⁻³²⁾ as well as tests,^(10-36, 10-37) indicate that although the ACI Code provisions based on maintaining the load-carrying capacity of a column after spalling of the cover concrete has occurred are conservative for low axial loads, they can be unconservative for high axial loads, with particular regard to attaining adequate ductility. Results of these studies indicate the desirability of varying the confinement requirements for the hinging regions in columns according to the magnitude of the axial load, more confinement being called for in the case of high axial loads.

ACI Chapter 21 limits the spacing of confinement reinforcement to 1/4 the minimum member dimension or 4 in., with no limitation related to the longitudinal bar diameter. The New Zealand Code requires that the maximum spacing of transverse reinforcement in the potential plastic hinge regions not exceed the

least of 1/4 the minimum column dimension or 6 times the diameter of the longitudinal reinforcement. The second limitation is intended to relate the maximum allowable spacing to the need to prevent premature buckling of the longitudinal reinforcement. In terms of shear reinforcement, ACI Chapter 21 requires that the design shear force be based on the maximum flexural strength, M_{pr} , at each end of the column associated with the range of factored axial loads. However, at each column end, the moments to be used in calculating the design shear will be limited by the probable moment strengths of the beams (the negative moment strength on one side and the positive moment strength on the other side of a joint) framing into the column. The larger amount of transverse reinforcement required for either confinement or shear is to be used.

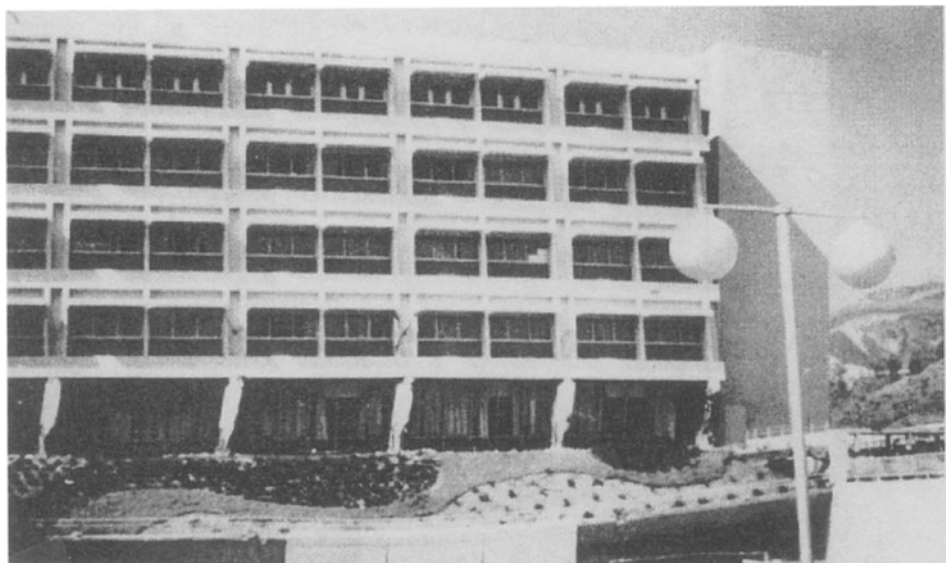
One should note the significant economy, particularly with respect to volume of lateral reinforcement, to be derived from the use of spirally reinforced columns.⁽¹⁰⁻³²⁾ The saving in the required amount of lateral reinforcement, relative to a tied column of the same nominal capacity, which has also been observed in designs for gravity and wind loading, acquires greater importance in earthquake-resistant design in view of the superior ductile performance of the spirally reinforced column. Figure 10-18b, from Reference 10-38, shows one of the spirally reinforced columns in the first story of the Olive View Hospital building in California following the February 9, 1971 San Fernando earthquake. A tied corner column in the first story of the same building is shown in Figure 10-18c. The upper floors in the four-story building, which were stiffened by shear walls that were discontinued below the second-floor level, shifted approximately 2 ft. horizontally relative to the base of the first-story columns, as indicated in Figure 10-18a.

Beam—Column Joints Beam-column joints are critical elements in frame structures. These elements can be subjected to high shear and bond-slip deformations under earthquake loading. Beam-column joints have to be

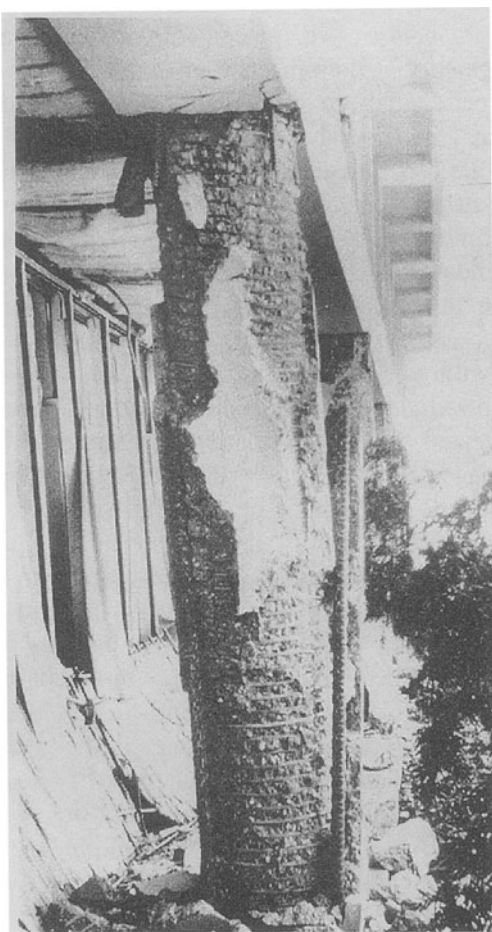
designed so that the connected elements can perform properly. This requires that the joints be proportioned and detailed to allow the columns and beams framing into them to develop and maintain their strength as well as stiffness while undergoing large inelastic deformations. A loss in strength or stiffness in a frame resulting from deterioration in the joints can lead to a substantial increase in lateral displacements of the frame, including possible instability due to P-delta effects.

The design of beam-column joints is primarily aimed at (i) preserving the integrity of the joint so that the strength and deformation capacity of the connected beams and columns can be developed and substantially maintained, and (ii) preventing significant degradation of the joint stiffness due to cracking of the joint and loss of bond between concrete and the longitudinal column and beam reinforcement or anchorage failure of beam reinforcement. Of major concern here is the disruption of the joint core as a result of high shear reversals. As in the hinging regions of beams and columns, measures aimed at insuring proper performance of beam-column joints have focused on providing adequate confinement as well as shear resistance to the joint.

The forces acting on a typical interior beam-column joint in a frame undergoing lateral displacement are shown in Figure 10-19a. It is worth noting in Figure 10-19a that each of the longitudinal beam and column bars is subjected to a pull on one side and a push on the other side of the joint. This combination of forces tends to push the bars through the joint, a condition that leads to slippage of the bars and even a complete pull through in some test specimens. Slippage resulting from bond degradation under repeated yielding of the beam reinforcement is reflected in a reduction in the beam-end fixity and thus increased beam rotations at the column faces. This loss in beam stiffness can lead to increased lateral displacements of the frame and potential instability.



(a)



(b)



(c)

Figure 10-18. Damage to columns of the 4-story Olive View Hospital building during the February 9, 1971 San Fernando, California, earthquake. (From Ref. 10-38.) (a) A wing of the building showing approximately 2 ft drift in its first story. (b) Spirally reinforced concrete column in first story. (c) Tied rectangular corner column in first story.

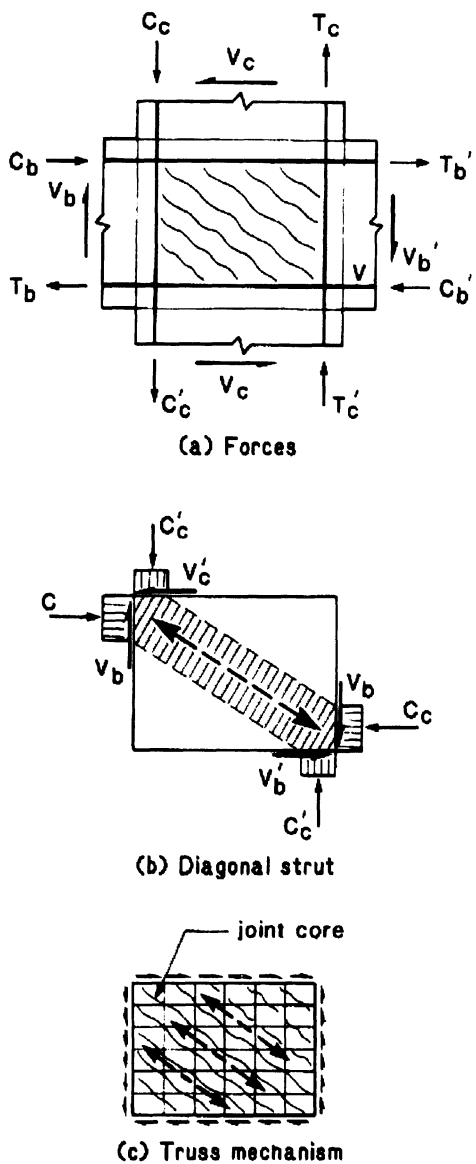


Figure 10-19. Forces and postulated shear-resisting mechanisms in a typical interior beam-column joint. (Adapted from Ref. 10-32.) (a) Forces acting on beam-column joint. (b) Diagonal strut mechanism. (c) Truss mechanism.

Two basic mechanisms have been postulated as contributing to the shear resistance of beam—column joints. These are the diagonal strut and the joint truss (or diagonal compression field) mechanisms, shown in Figure 10-19b and c, respectively. After several cycles of inelastic deformation in the beams framing into a joint, the effectiveness of the diagonal strut mechanism tends to diminish as through-depth cracks start to open

between the faces of the column and the framing beams and as yielding in the beam bars penetrates into the joint core. The joint truss mechanism develops as a result of the interaction between confining horizontal and vertical reinforcement and a diagonal compression field acting on the elements of the confined concrete core between diagonal cracks. Ideally, truss action to resist horizontal and vertical shears would require both horizontal confining steel and intermediate vertical column bars (between column corner bars). Tests cited in Reference 10-39 indicate that where no intermediate vertical bars are provided, the performance of the joint is worse than where such bars are provided.

Tests of beam-column joints^(10-27,10-40,10-41) in which the framing beams were subjected to large inelastic displacement cycles have indicated that the presence of transverse beams (perpendicular to the plane of the loaded beams) considerably improves joint behavior. Results reported in Reference 10-27 show that the effect of an increase in joint lateral reinforcement becomes more pronounced in the absence of transverse beams. However, the same tests indicated that slippage of column reinforcement through the joint occurred with or without transverse beams. The use of smaller-diameter longitudinal bars has been suggested⁽¹⁰⁻³⁹⁾ as a means of minimizing bar slippage. Another suggestion has been to force the plastic hinge in the beam to form away from the column face, thus preventing high longitudinal steel strains from developing in the immediate vicinity of the joint. This can be accomplished by suitably strengthening the segment of beam close to the column (usually a distance equal to the total depth of the beam) using appropriate details. Some of the details proposed include a combination of heavy vertical reinforcement with cross-ties (see Figure 10-14), intermediate longitudinal shear reinforcement (see Figure 10-15),⁽¹⁰⁻⁴²⁾ and supplementary flexural reinforcement and haunches, as shown in Figure 10-20.⁽¹⁰⁻³²⁾

The current approach to beam—column joint design in the United States, as contained in ACI Chapter 21, is based on providing

sufficient horizontal joint cross-sectional area that is adequately confined to resist the shear stresses in the joint. The approach is based mainly on results of a study by Meinheit and Jirsa⁽¹⁰⁻⁴¹⁾ and subsequent studies by Jirsa and associates. The parametric study reported in Reference 10-41 identified the horizontal cross-sectional area of the joint as the most significant variable affecting the shear strength of beam—column connections. Although recognizing the role of the diagonal strut and joint truss mechanisms, the current approach defines the shear strength of a joint simply in terms of its horizontal cross-sectional area. The approach presumes the provision of confinement reinforcement in the joint. In the ACI Chapter 21 method, shear resistance calculated as a function of the horizontal cross-sectional area at mid-height of the joint is compared with the total horizontal shear across the same mid-height section. Figure 10-21 shows the forces involved in calculating the shear at mid-height of a typical joint. Note that the stress in the yielded longitudinal beam bars is to be taken equal to 1.25 times the specified nominal yield strength f_y of the reinforcement.

The ACI-ASCE Committee 352 Recommendations⁽¹⁰⁻²⁹⁾ have added a requirement relating to the uniform distribution of the longitudinal column reinforcement around the perimeter of the column core, with a maximum spacing between perimeter bars of 8 in. or one-third the column diameter or the cross-section dimension. The lateral confinement, whether from steel hoops or beams, and the distributed vertical column reinforcement, in conjunction with the confined concrete core, provide the necessary elements for the development of an effective truss mechanism to resist the horizontal and vertical shears acting on a beam—column joint. Results of recent tests on bi-directionally loaded beam—column joint specimens⁽¹⁰⁻²⁸⁾ confirm the strong correlation between joint shear strength and the horizontal cross-sectional area noted by Meinheit and Jirsa.⁽¹⁰⁻⁴¹⁾

Some investigators^(10-13, 10-32, 10-39) have suggested that the ACI Chapter 21 approach does not fully reflect the effect of the different

variables influencing the mechanisms of resistance operating in a beam-column joint and have proposed alternative expressions based on idealizations of the strut and joint truss mechanisms.

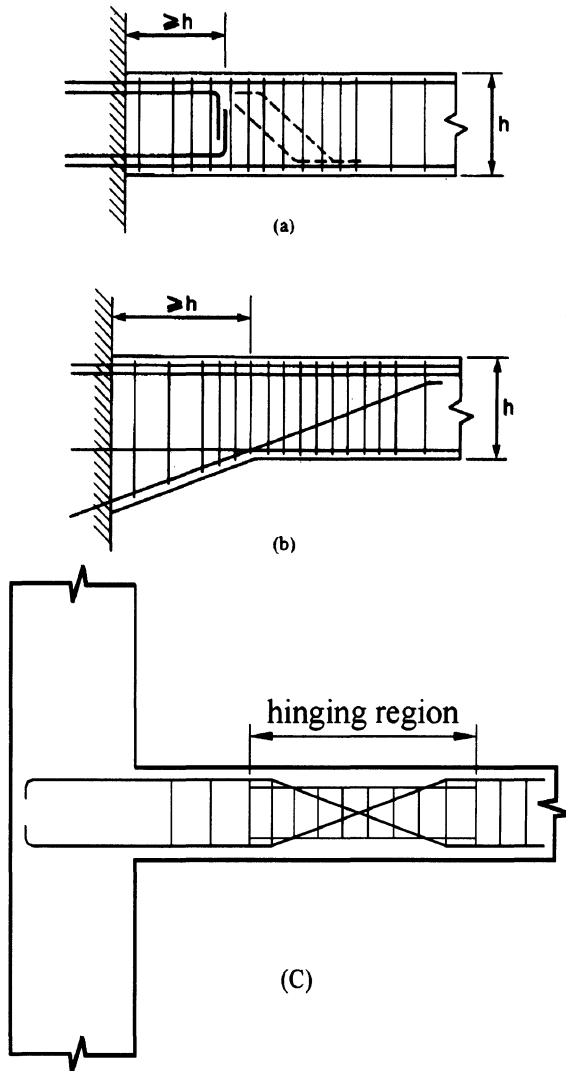


Figure 10-20. Proposed details for forcing beam hinging away from column face⁽¹⁰⁻²⁶⁾. See also Fig. 10-15. (a) Supplementary flexural reinforcement. (b) Haunch. (c) Special reinforcement detail.

To limit slippage of beam bars through interior beam-column joints, the ACI-ASCE Committee 352 Recommendations call for a minimum column dimension equal to 20 times the diameter of beam bars passing through the joint. For exterior joints, where beam bars terminate in the joint, the maximum size of beam bar allowed is a No. 11 bar.

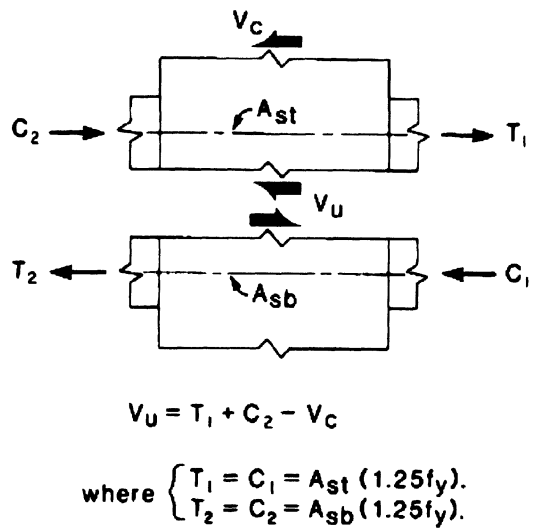


Figure 10-21. Shear force at mid-height of beam-column joint- ACI Chapter 21 design practice.

When the depth of an exterior column is not sufficient to accommodate the required development length for beam bars, a beam stub at the far (exterior) side of the column,⁽¹⁰⁻³²⁾ such as is shown in Figure 10-22, can be used. Embedding the 90° beam bar hooks outside of the heavily stressed joint region reduces the stiffness degradation due to slippage and improves the overall performance of the connection.

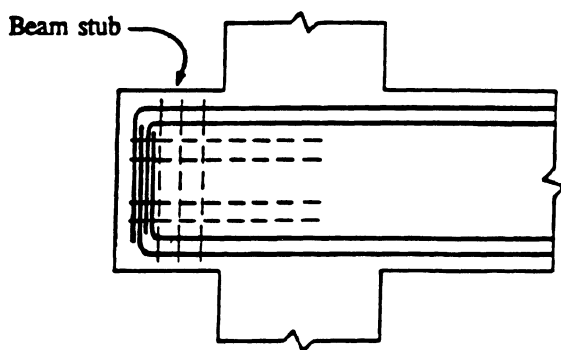


Figure 10-22. Exterior beam stub for anchoring beam bars

Slab—Column Connections By omitting consideration of the reinforced concrete flat plate in its provisions governing the design of structures in high-seismic-risk areas, ACI Chapter 21 essentially excludes the use of such a system as part of a ductile frame resisting

seismic loads in such areas. Two-way slabs without beams, i.e., flat plates, are, however, allowed in areas of moderate seismic risk.

The flat plate structure is an economical and widely used form of construction in non-seismic areas, especially for multistory residential construction. Its weakest feature, as is well known, is its vulnerability to a punching shear failure at the slab-column junctions. The collapse of a number of buildings using such a system during the 1964 Anchorage, Alaska and the 1967 Caracas, Venezuela earthquakes, as well as several buildings using waffle slabs during the September 1985 Mexican earthquake,^(10-43, 10-44) clearly dramatized this vulnerability. Although a flat plate may be designed to carry vertical loads only, with structural walls taking the lateral loads, significant shears may still be induced at the slab-column junctions as the structure displaces laterally during earthquake response.

Tests on slab—column connections subjected to reversed cyclic loading^(10-45, 10-46) indicate that the ductility of flat-slab—column connections can be significantly increased through the use of stirrups enclosing bands of flexural slab reinforcement passing through the columns. Such shear-reinforced bands essentially function as shallow beams connecting the columns.

Structural Walls Reinforced concrete structural walls (commonly referred to as shear walls), when properly designed, represent economical and effective lateral stiffening elements that can be used to reduce potentially damaging interstory displacements in multistory structures during strong earthquakes. The structural wall, like the vertical steel truss in steel buildings, has had a long history of use for stiffening buildings laterally against wind forces. The effectiveness of properly designed structural walls in reducing earthquake damage in multistory buildings has been well demonstrated in a number of recent earthquakes.

In earthquake-resistant design, the appreciable lateral stiffness of structural walls can be particularly well utilized in combination with properly proportioned coupling beams in

coupled wall systems. Such systems allow considerable inelastic energy dissipation to take place in the coupling beams (which are relatively easy to repair) at critical levels, sometimes even before yielding occurs at the bases of the walls.

Attention in the following discussion will be focused on slender structural walls, i.e., walls with a height-to-width ratio greater than about 2.0, such as are used in multistory buildings. These walls generally behave like vertical cantilever beams. Short or squat walls, on the other hand, resist horizontal forces in their plane by a predominantly truss-type mechanism, with the concrete providing the diagonal compressive strut(s) and the steel reinforcement the equilibrating vertical and horizontal ties. Tests on low-rise walls subjected to slowly reversed horizontal loading⁽¹⁰⁻⁴⁷⁾ indicate that for walls with height-to-width ratios of about 1.0, horizontal and vertical reinforcement are equally effective. As the height-to-width ratio of a wall becomes smaller, the vertical reinforcement becomes more effective in resisting shear than the horizontal steel.⁽¹⁰⁻⁴⁸⁾

In the following discussion, it will be assumed that the isolated structural wall is loaded by a resultant horizontal force acting at some distance above the base. Under such a loading, flexural hinging will occur at the base of the wall. Where the wall is designed and loaded so that it yields in flexure at the base, as might be expected under strong earthquakes, its behavior becomes a function primarily of the magnitude of the shear force that accompanies such flexural hinging as well as the reinforcement details used in the hinging region near the base. Thus, if the horizontal force acts high above the base (long shear arm), it will take a lesser magnitude of the force to produce flexural hinging at the base than when the point of application of the load is close to the base (short shear arm). For the same value of the base yield moment, the moment-to-shear ratio in the former case is high and the magnitude of the applied force (or shear) is low, while in the latter case the moment-to-shear ratio is low and the applied shear is high. In both cases, the

magnitude of the applied shear is limited by the flexural yield strength at the base of the wall.

In this connection, it is of interest to note that dynamic inelastic analyses of isolated walls⁽¹⁰⁻⁴⁾ covering a wide range of structural and ground motion parameters have indicated that the maximum calculated shear at the base of walls can be from 1.5 to 3.5 times greater than the shear necessary to produce flexural yielding at the base, when such shear is distributed in a triangular manner over the height of the wall, as is prescribed for design in most codes. This is shown in Figure 10-23, which gives the ratio of the calculated maximum dynamic shear, V_{dyn}^{max} , to the resultant of the triangularly distributed shear necessary to produce flexural yielding at the base, V_T , as a function of the fundamental period T_1 and the available rotational ductility μ_r^a . The input accelerograms used in the analyses had different frequency characteristics and were normalized with respect to intensity so that their spectrum intensity (i.e., the area under the corresponding 5%-damped velocity response spectrum, between periods 0.1 and 3.0 sec) was 1.5 times that of the N-S component of the 1940 El Centro record. The results shown in Figure 10-23 indicate that a resultant shear force equal to the calculated maximum dynamic shear need not be applied as high as two-thirds the height of the wall above the base to produce yielding at the base. Figure 10-24, also from Reference 10-4, shows the distance (expressed as the ratio M_y / V_{max}^{dyn}) from the base at which the resultant dynamic force would have to act to produce yielding at the base, as a function of the fundamental period and the available rotational ductility of the wall. The ordinate on the right side of the figure gives the distance above the base as a fraction of the wall height. Note that for all cases, the resultant dynamic force lies below the approximate two-thirds point associated with the triangular loading specified in codes.

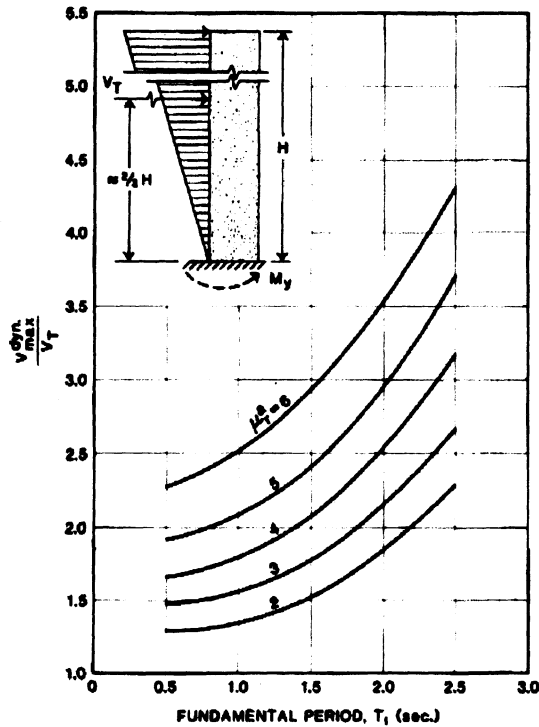


Figure 10-23. Ratio $V_{\max}^{\text{dyn}} / V_T$ as a function of T_1 and μ_r^a . -20 story isolated structural walls. (From Ref. 10-4.)

These analytical results suggest not only that under strong earthquakes the maximum dynamic shear can be substantially greater than that associated with the lateral loads used to design the flexural strength of the base of the wall, but also, as a corollary, that the moment-to-shear ratio obtained under dynamic conditions is significantly less than that implied by the code-specified distribution of design lateral loads. These results are important because unlike beams in frames, where the design shear can be based on the maximum probable flexural strengths at the ends of the member as required by statics (see Figure 10-16), in cantilever walls it is not possible to determine a similar design shear as a function of the flexural strength at the base of the wall using statics alone, unless an assumption is made concerning the height of the applied resultant horizontal force. In the capacity design method adopted in New Zealand as applied to structural walls,^(10-13,10-49) the design base shear at the base of a wall is obtained by multiplying the shear at the base corresponding to the code-

specified forces by a flexural overstrength factor and a "dynamic shear magnification factor". The flexural overstrength factor in this case represents the ratio of flexural overstrength (accounting for upward deviations from the nominal strength of materials and other factors) to the moment due to the code-specified forces, with a typical value of about 1.39 or higher. Recommended values for the dynamic shear magnification factor range from 1.0 for a one-story high wall to a maximum of 1.8 for walls 6-stories or more in height.

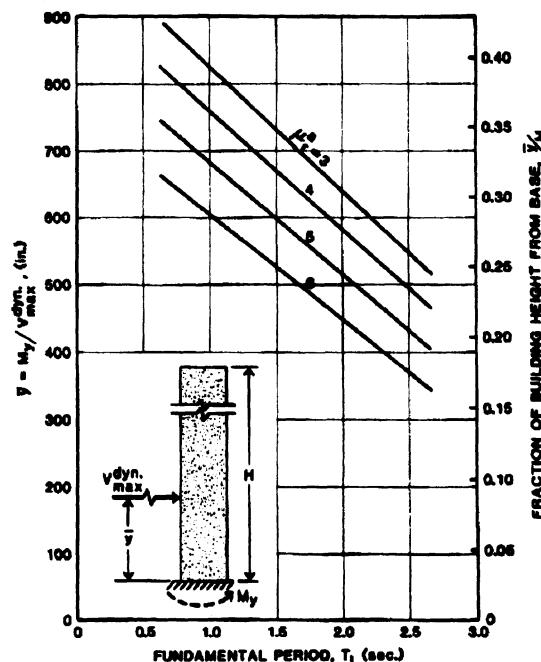


Figure 10-24. Ratio $Y = M_y / V_{\max}^{\text{dyn}}$ as a function of T_1 and μ_r^a . -20 story isolated structural walls. (From Ref. 10-4.)

Tests on isolated structural walls^(10-50,10-51) have shown that the hinging region, i.e., the region where most of the inelastic deformation occurs, extends a distance above the base roughly equal to the width of the wall. The ductility of the hinging region at the base of a wall, like the hinging region in beams and columns, is heavily dependent on the reinforcing details used to prevent early disruption of critically stressed areas within the region. As observed in beams and columns, tests of structural walls have confirmed the

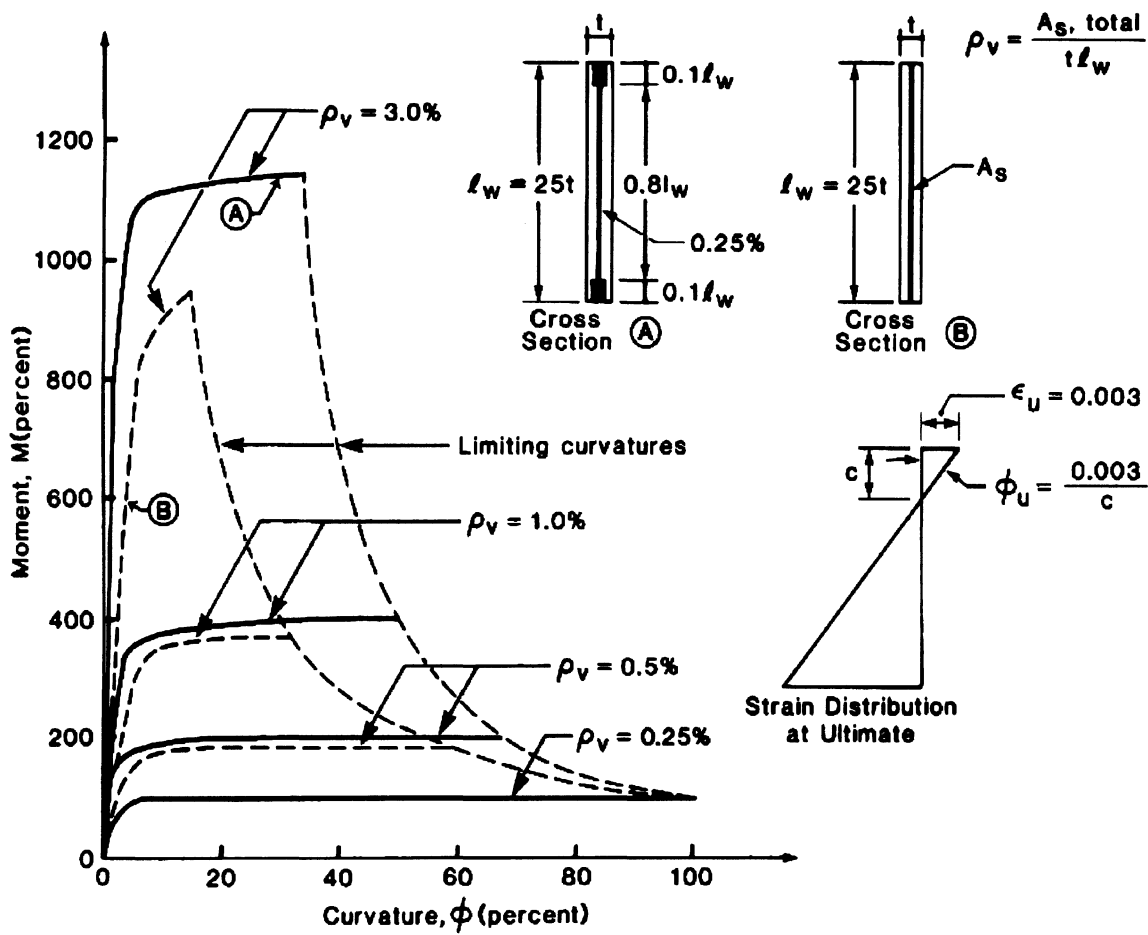


Figure 10-25. Moment-curvature curves for statically loaded rectangular walls as a function of reinforcement distribution.⁽¹⁰⁻⁵²⁾

effectiveness of adequate confinement in maintaining the strength of the hinging region through cycles of reversed inelastic deformation. The adverse effects of high shears, acting simultaneously with the yield moment, on the deformation capacity of the hinging region of walls has also been noted in tests.

Early tests of slender structural walls under static monotonic loading⁽¹⁰⁻⁵²⁾ have indicated that the concentration of well-confined longitudinal reinforcement at the ends of the wall section can significantly increase the ductility of the wall. This is shown in Figure 10-25 from Reference 10-52. This improvement in behavior resulting from a concentration of well-confined longitudinal reinforcement at the ends of a wall section has also been observed in

tests of isolated walls under cyclic reversed loading.^(10-50, 10-51) Plain rectangular walls, not having relatively stiff confined boundary elements, are prone to lateral buckling of the compression edge under large horizontal displacements.^(10-50, 10-52)

Figure 10-26 shows a sketch of the region at the base of a wall with boundary elements after a few cycles of lateral loading. Several modes of failure have been observed in the laboratory. Failure of the section can occur in flexure by rupture of the longitudinal reinforcement or by a combination of crushing and sliding in a weakened compression flange. Alternatively, failure, i.e., loss of lateral-load-resisting capacity, can occur by sliding along a near-horizontal plane near the base (in rectangular-

section walls especially) or by crushing of the web concrete at the junction of the diagonal struts and the compression flange (in walls with thin webs and/or heavy boundary elements).

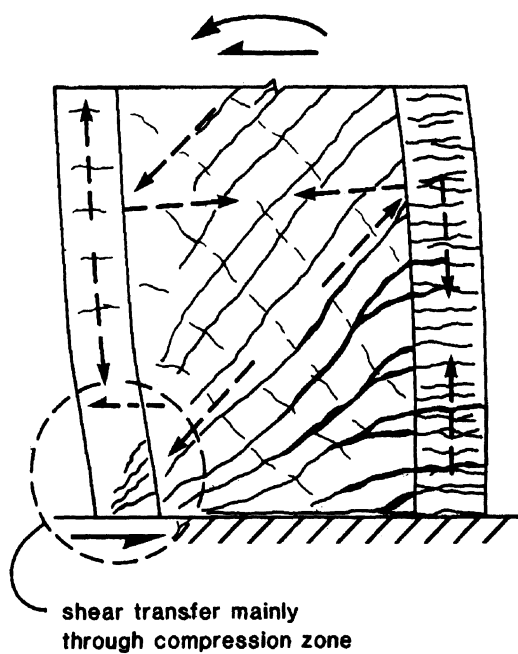


Figure 10-26. Moment-curvature curves for statically loaded rectangular walls as a function of reinforcement distribution.⁽¹⁰⁻⁵⁴⁾

Since walls are generally designed to be under-reinforced, crushing in the usual sense associated with monotonic loading does not occur. However, when the flanges are inadequately confined, i.e., with the longitudinal and lateral reinforcement spaced far apart, concrete fragments within the cores of the flanges that had cracked in flexure under earlier cycles of loading can be lost in subsequent loading cycles. The longitudinal bars can buckle under compression and when subsequently stretched on reversal of the loading can rupture in low-cycle fatigue. It is also worth noting that because of the Bauschinger effect (i.e., the early yielding, reflected in the rounding of the stress-strain curve of steel, that occurs during load reversals in the inelastic range and the consequent reduction in the tangent modulus of the steel reinforcement at relatively low compressive

stresses), the compression steel in members subjected to reversed cycles of inelastic loading tends to buckle earlier than in comparable monotonically loaded specimens.

As in beams and columns, degradation of strength and ductility of the hinging region of walls is strongly influenced by the magnitude of the shear that accompanies flexural yielding. High shears ($> 6\sqrt{f_c}$), when acting on a web area traversed by crisscrossing diagonal cracks, can precipitate failure of the wall by crushing of the diagonal web struts or a combined compression-sliding failure of the compression flange near the base. Shear in the hinging region is resisted by several mechanisms, namely, shear-friction along a near-horizontal plane across the width of the wall, dowel action of the tensile reinforcement and to a major extent (as in beams) by shear across the compression flange. After several cycles of load reversals and for moderate moment-to-shear ratios, the flexural cracks become wide enough to reduce the amount of shear carried by shear friction. As suggested by Figure 10-26, the truss action that develops in the hinging region involves a horizontal (shear) component of the diagonal strut that acts on the segment of the compression flange close to the base. If the compression flange is relatively slender and inadequately confined, the loss of core concrete under load reversals results in a loss of stiffness of this segment of the compression flange. The loss of stiffness and strength in the compression flange or its inability to support the combined horizontal (shear) component of the diagonal strut and the flexural compressive force can lead to failure of the wall.

Thus confinement of the flanges of walls, and especially those in the hinging region, is necessary not only to increase the compressive strain capacity of the core concrete but also to delay inelastic bar buckling and, together with the longitudinal reinforcement, prevent loss of the core concrete during load reversals (the so-called "basket effect"). By maintaining the strength and stiffness of the flanges, confinement reinforcement improves the shear transfer capacity of the hinging region through

the so-called "dowel action" of the compression flange, in addition to serving as shear reinforcement. As in beams, the diagonal tension cracking that occurs in walls and the associated truss action that develops induces tensile stresses in the horizontal web reinforcement. This suggests the need for proper anchorage of the horizontal reinforcement in the flanges.

Where high shears are involved, properly anchored crossing diagonal reinforcement in the hinging regions of walls, just as in beams, provides an efficient means of resisting shear and particularly the tendency toward sliding along cracked and weakened planes.

A series of tests of isolated structural wall specimens at the Portland Cement Association^(10-50, 10-51) have provided some indication of the effect of several important variables on the behavior of walls subjected to slowly reversed cycles of inelastic deformations. Some results of this investigation have already been mentioned in the preceding. Three different wall cross-sections were considered in the study, namely, plain rectangular sections, barbell sections with heavy flanges (columns) at the ends, and flanged sections with the flanges having about the same thickness as the web. In the following, results for some of the parameters considered will be presented briefly.

1. *Monotonic vs. reversed cyclic loading.* In an initial set of two nominally identical specimens designed to explore the effect of load reversals, a 15% decrease in flexural strength was observed for a specimen loaded by cycles of progressively increasing amplitude of displacement when compared with a specimen that was loaded monotonically. Figures 10-27a and 10-28a show the corresponding load-deflection curves for the specimens. A comparison of these figures shows not only a reduction in strength but also that the maximum deflection of the wall subjected to reversed loading was only 8 in., compared to about 12 in. for the monotonically load specimen, indicating a reduction in deflection capacity of about 30%. Figure 10-28b, when compared

with Figure 10-27b, shows the more severe cracking that results from load reversals.

2. *Level of shear stress.* Figure 10-29 shows a plot of the variation of the maximum rotational ductility with the maximum nominal shear stress in isolated structural wall specimens reported in References 10-50 and 10-51. The decrease in rotational ductility with increasing values of the maximum shear stress will be noted. The maximum rotation used in determining ductility was taken as that for the last cycle in which at least 80% of the previous maximum observed load was sustained throughout the cycle. The yield rotation was defined as the rotation associated with the yielding of all of the tensile reinforcement in one of the boundary elements.

The presence of axial loads—of the order of 10% of the compressive strength of the walls—increased the ductility of specimens subjected to high shears. In Figure 10-29, the specimens subjected to axial loads are denoted by open symbols. The principal effect of the axial load was to reduce the shear distortions and hence increase the shear stiffness of the hinging region. It may be of interest to note that for walls loaded monotonically,⁽¹⁰⁻⁵²⁾ axial compressive stress was observed to increase moment capacity and reduce ultimate curvature, results consistent with analytical results from sectional analysis.

3. *Section shape.* As mentioned earlier, the use of wall sections having stiff and well-confined flanges or boundary elements, as against plain rectangular walls, not only allows development of substantial flexural capacity (in addition to being less susceptible to lateral buckling), but also improves the shear resistance and ductility of the wall. In walls with relatively stiff and well-confined boundary elements, some amount of web crushing can occur without necessarily limiting the flexural capacity of the wall. Corley et al.⁽¹⁰⁻⁵³⁾ point out that trying to avoid shear failure in walls, particularly walls with stiff and well-confined boundary elements, may be a questionable design objective.

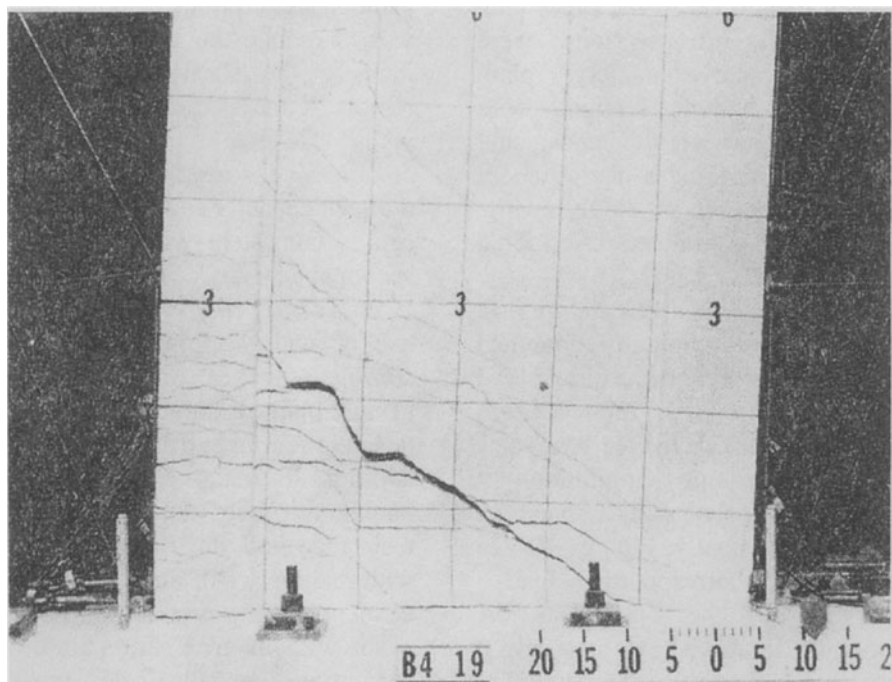
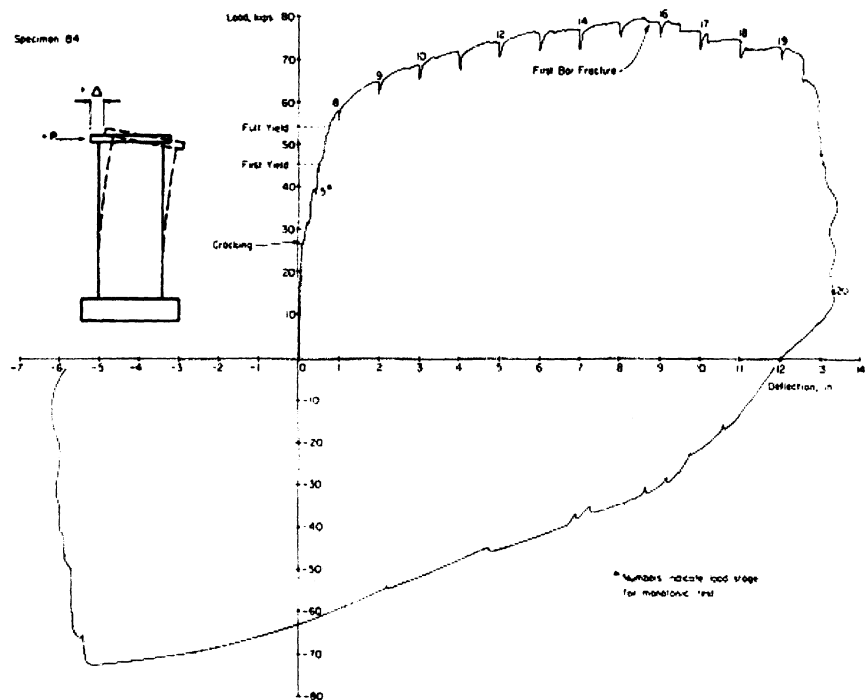


Figure 10-27. (a) Load-deflection curve of monotonically loaded specimen. (b) view of specimen at +12 in. top deflection.⁽¹⁰⁻⁵³⁾

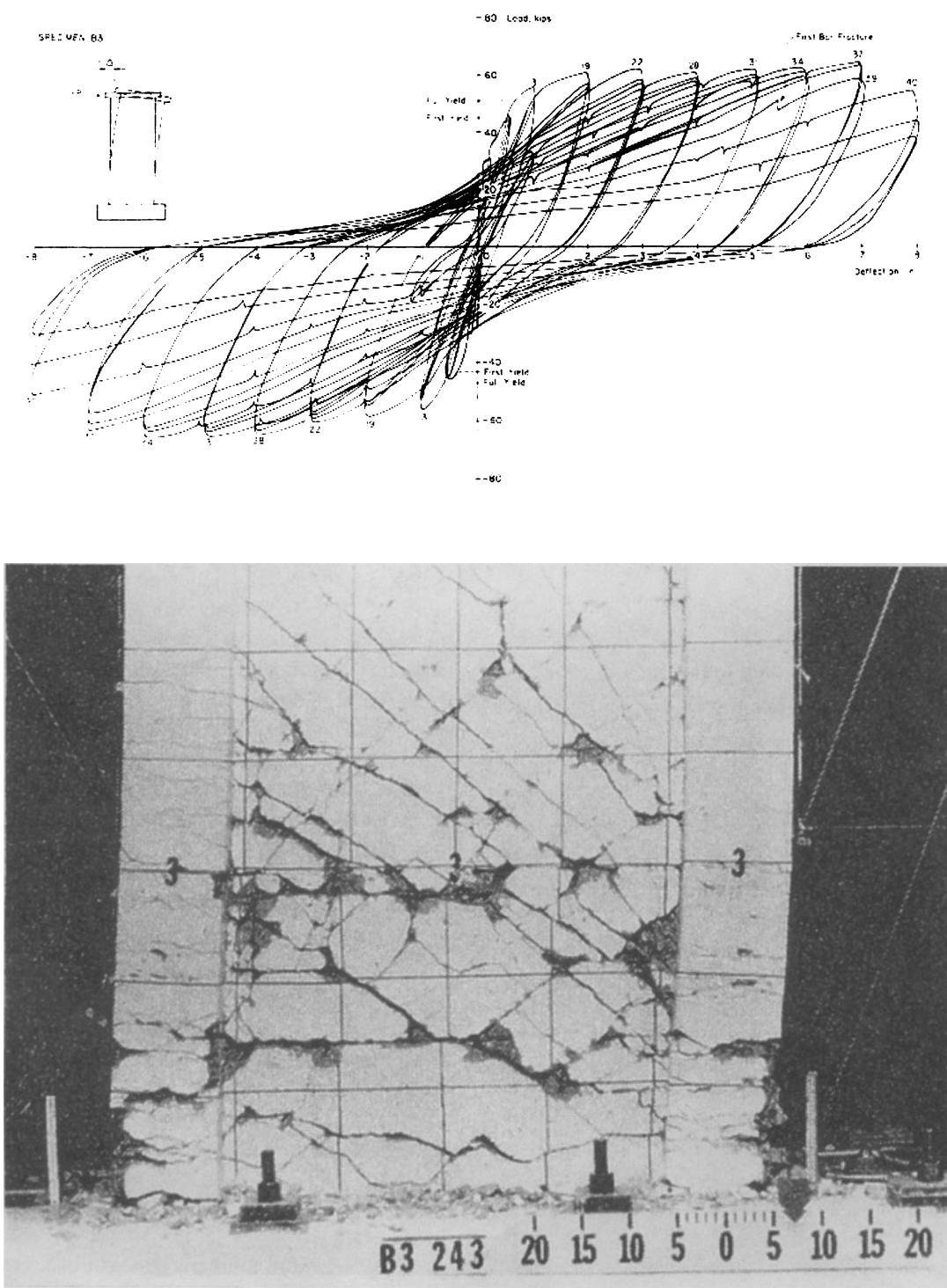


Figure 10-28. (a) Load-deflection curve of specimen subjected to load cycles of progressively increasing amplitude. (b) View of specimen at +8 in. top deflection.⁽¹⁰⁻⁵³⁾

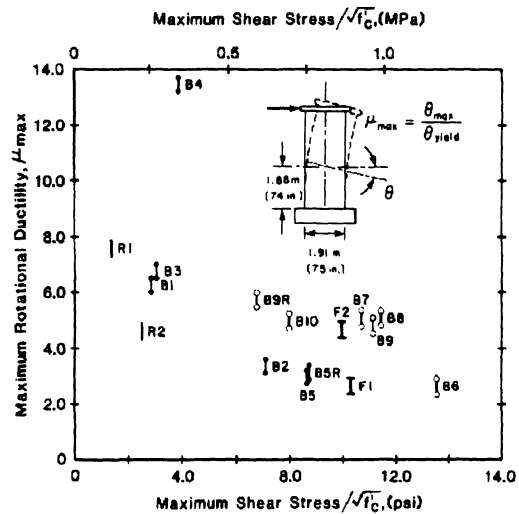


Figure 10-29. Variation of rotational ductility with maximum average shear stress in PCA isolated wall tests⁽¹⁰⁻⁵¹⁾.

Thus, although ACI Chapter 21 limits the maximum average shear stress in walls to $10\sqrt{f'_c}$ (a value based on monotonic tests) with the intent of preventing web crushing, web crushing occurred in some specimens subjected to shear stresses only slightly greater than $7\sqrt{f'_c}$. However, those specimens where web-crushing failure occurred were able to develop deformations well beyond the yield deformation prior to loss of capacity.

4. Sequence of large-amplitude load cycles. Dynamic inelastic analyses of isolated walls⁽¹⁰⁻⁸⁾ have indicated that in a majority of cases, the maximum or a near-maximum response to earthquakes occurs early, with perhaps only one elastic response cycle preceding it. This contrasts with the loading program commonly used in quasi-static tests, which consists of load cycles of progressively increasing amplitude. To examine the effect of imposing large-amplitude load cycles early in the test, two nominally identical isolated wall specimens were tested. One specimen was subjected to load cycles of progressively increasing amplitude, as were most of the specimens in this series. Figure 10-30a indicates that specimen B7 was able to sustain a rotational ductility of slightly greater than 5 through three

repeated loading cycles. The second specimen (B9) was tested using a modified loading program similar to that shown in Figure 10-7b, in which the maximum load amplitude was imposed on the specimen after only one elastic load cycle. The maximum load amplitude corresponded to a rotational ductility of 5. As indicated in Figure 10-30b, the specimen failed before completing the second load cycle. Although results from this pair of specimens cannot be considered conclusive, they suggest that tests using load cycles of progressively increasing amplitude may overestimate the ductility that can be developed under what may be considered more realistic earthquake response conditions. The results do tend to confirm the reasonable expectation that an extensively cracked and "softened" specimen subjected to several previous load cycles of lesser amplitude can better accommodate large reversed lateral deflections than a virtually uncracked specimen that is loaded to near-capacity early in the test. From this standpoint, the greater severity of the modified loading program, compared to the commonly used progressively increasing-amplitude loading program, appears obvious.

5. Reinforcement detailing. On the basis of the tests on isolated walls reported in References 10-50 and 10-51, Oesterle et al.⁽¹⁰⁻⁵⁴⁾ proposed the following detailing requirements for the hinging regions of walls:

- The maximum spacing of transverse reinforcement in boundary elements should be $5d_b$, where d_b is the diameter of the longitudinal reinforcement.
- Transverse reinforcement in the boundary element should be designed for a shear

$$V_{nb} = M_{nb}/1.5 l_b,$$

where

M_{nb} = nominal moment strength of boundary element

l_b = width of boundary element (in the plane of the wall)

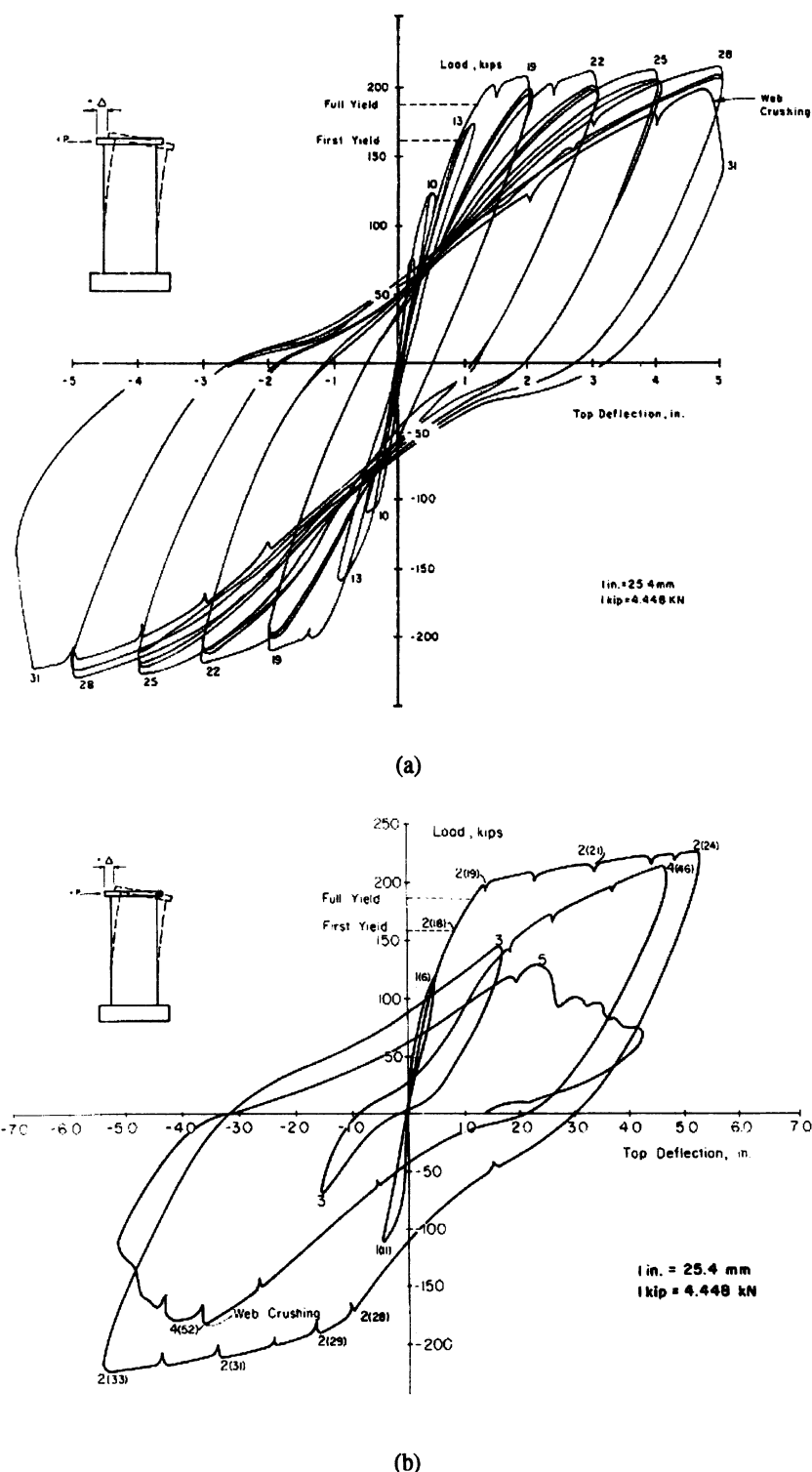


Figure 10-30. Comparison of behavior of isolated walls subjected to different loading histories. (10-53)
 (a) specimen subjected to progressively increasing load amplitudes (see Fig. 10-7a). (b) Specimen subjected to loading history characterized by large-amplitude cycles early in loading (see Fig. 10-7b).

- No lap splices should be used for cross-ties in segments of boundary elements within the hinging region.
- A recommendation on anchoring horizontal web reinforcement in the boundary elements, such as is shown in Figure 10-31a, has been adopted by ACI Chapter 21. For levels of shear in the range of $5\sqrt{f'_c}$ to $10\sqrt{f'_c}$, the study indicates that alternate 90° and 135° hooks, as shown in Figure 10-31b, can be used.

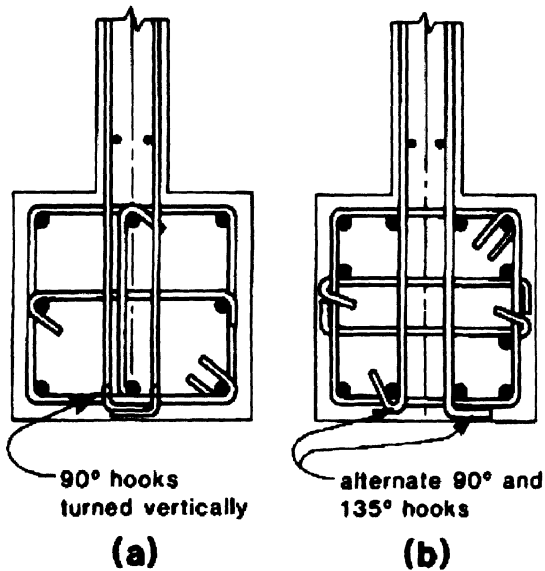


Figure 10-31. Alternative details for anchorage of horizontal web reinforcement in boundary elements.⁽¹⁰⁻⁵⁴⁾ (a) detail for walls subjected to low-to-moderate stress levels. (b) Detail for walls subjected to high shear stress levels.

The specimens tested in this series had special confinement reinforcement only over a length near the base equal to the width of the wall, i.e., the approximate length of the hinging region. Strain readings as well as observations of the general condition of the walls after failure showed that significant inelasticity and damage were generally confined to the hinging region. In view of this, it has been suggested that special confinement reinforcement for boundary elements need be provided only over the lengths of potential hinging regions. These are most likely to occur at the base and at points

along the height of the wall where discontinuities, associated with abrupt and significant changes in geometry, strength, or stiffness, occur.

Coupled Walls As mentioned earlier, a desirable characteristic in an earthquake-resistant structure is the ability to respond to strong ground motion by progressively mobilizing the energy-dissipative capacities of an ascending hierarchy of elements making up the structure.

In terms of their importance to the general stability and safety of a building, the components of a structure may be grouped into primary and secondary elements. *Primary elements* are those upon the integrity of which depend the stability and safety of the entire structure or a major part of it. In this category fall most of the vertical or near-vertical elements supporting gravity loads, such as columns and structural walls, as well as long-span horizontal elements. *Secondary elements* are those components whose failure would affect only limited areas or portions of a structure.

The strong column-weak beam design concept discussed earlier in relation to moment-resisting frames is an example of an attempt to control the sequence of yielding in a structure. The "capacity design" approach adopted in New Zealand which, by using even greater conservatism in the design of columns relative to beams, seeks to insure that no yielding occurs in the columns (except at their bases)—is yet another effort to achieve a controlled response in relation to inelastic action. By deliberately building in greater flexural strength in the primary elements (the columns), these design approaches force yielding and inelastic energy dissipation to take place in the secondary elements (the beams).

When properly proportioned, the coupled-wall system can be viewed as a further extension of the above design concept. By combining the considerable lateral stiffness of structural walls with properly proportioned coupling beams that can provide most of the energy-dissipative mechanism during response

to strong ground motions, a better-performing structural system is obtained. The stiffness of the structural wall makes it a desirable primary element from the standpoint of damage control (by restricting interstory distortions), while the more conveniently repairable coupling beams provide the energy-dissipating secondary elements. Figure 10-32a shows a two-wall coupled-wall system and the forces acting at the base and on a typical coupling beam. The total overturning moment at the base of the coupled wall = $M_1 + M_2 + TL$. A typical distribution of the elastic shear force in the coupling beams along the height of the structure due to a statically applied lateral load is shown in Figure 10-32b. Note that the accumulated shears at each end of the coupling beams, summed over the height of the structure, are each equal to the axial force (T) at the base of the corresponding wall. The height to the most critically stressed coupling beam tends to move downward as the coupling-beam stiffness (i.e., the degree of coupling between the two walls) increases.

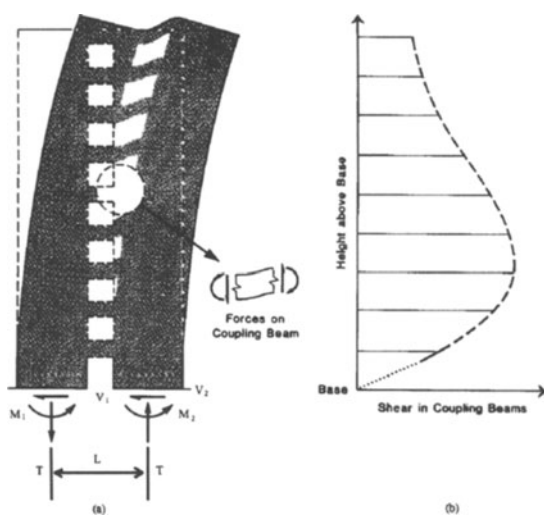


Figure 10-32. Laterally loaded coupled wall system. (a) Forces on walls at base. (b) Typical distribution of shears in coupling beams over height of structure.

In a properly designed earthquake-resistant coupled-wall system, the critically stressed coupling beams should yield first—before the bases of the walls. In addition, they must be capable of dissipating a significant amount of

energy through inelastic action. These requirements call for fairly stiff and strong beams. Furthermore, the desire for greater lateral-load-resisting efficiency in the system would favor stiff and strong coupling beams. However, the beams should not be so stiff or strong flexurally that they induce appreciable tension in the walls, since a net tension would reduce not only the yield moment but also the shear resistance of the wall (recall that a moderate amount of compression improves the shear resistance and ductility of isolated walls). This in turn can lead to early flexural yielding and shear-related inelastic action at the base of the tension wall. Dynamic inelastic analyses of coupled-wall systems⁽¹⁰⁻⁵⁶⁾ have shown, and tests on coupled-wall systems under cyclic reversed loading⁽¹⁰⁻⁵⁷⁾ have indicated, that when the coupling beams have appreciable stiffness and strength, so that significant net tension is induced in the “tension wall”, a major part of the total base shear is resisted by the “compression wall” (i.e., the wall subjected to axial compression for the direction of loading considered), a situation not unlike that which occurs in a beam.

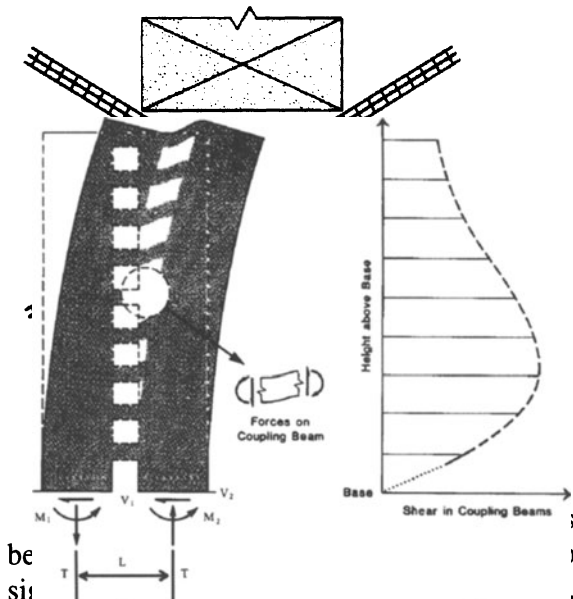
The design of a coupled-wall system would then involve adjusting the wall-to-coupling beam strength and stiffness ratios so as to strike a balance between these conflicting requirements. A basis for choosing an appropriate beam-to-wall strength ratio, developed from dynamic inelastic response data on coupled-wall systems, is indicated in Reference 10-58. The Canadian Code for Concrete, CSA Standard A23.3-94⁽¹⁰⁻⁵⁸⁾, recommends that in order to classify as a fully effective coupled wall system, the ratio

$$\frac{TL}{M_1 + M_2 + TL}$$

must be greater than 2/3. Those

with lower ratios are classified as partially coupled wall system in which the coupled wall system are to be designed for higher seismic design forces (14% greater) due to their lower amount of energy dissipation capacity due to reduced coupling action. Once the appropriate relative strengths and stiffness have been established, details to insure adequate ductility in potential hinging regions can be addressed.

Because of the relatively large shears that develop in deep coupling beams and the likelihood of sliding shear failures under reversed loading, the use of diagonal reinforcement in such elements has been suggested (see Figure 10-33). Tests by Paulay and Binney⁽¹⁰⁻⁵⁹⁾ on diagonally reinforced coupling beams having span-to-depth ratios in the range of 1 to 1½ have shown that this arrangement of reinforcement is very effective in resisting reversed cycles of high shear. The specimens exhibited very stable force-deflection hysteresis loops with significantly higher cumulative ductility than comparable conventionally reinforced beams. Tests by Barney et al.⁽¹⁰⁻⁶⁰⁾ on diagonally reinforced beams with span-to-depth ratios in the range of 2.5 to 5.0 also indicated that diagonal reinforcement can be effective even for these larger span-to-depth ratios.



The diagonal bars are designed to resist both shear and bending and assumed to function at their yield stress in both tension and compression. To prevent early buckling of the diagonal bars, Paulay and Binney recommend the use of closely spaced ties or spiral binding to confine the concrete within each bundle of diagonal bars. A minimum amount of "basketing reinforcement," consisting of two layers of small-diameter horizontal and vertical

bars, is recommended. The grid should provide a reinforcement ratio of at least 0.0025 in each direction, with a maximum spacing of 12 in. between bars.

10.4 CODE PROVISIONS FOR EARTHQUAKE-RESISTANT DESIGN

10.4.1 Performance Criteria

In recent years, the performance criteria reflected in some building code provisions such as IBC-2000⁽¹⁰⁻⁶¹⁾ have become more explicit than before. Although these provisions explicitly require design for only a single level of ground motion, it is expected that buildings designed and constructed in accordance with these requirements will generally be able to meet a number of performance criteria, when subjected to earthquake ground motions of differing severity. The major framework of the performance criteria is discussed in the report by the Structural Association of California Vision 2000 (SEAOC, 1995).⁽¹⁰⁻⁶²⁾ In this report, four performance levels are defined and each performance level is expressed as the desired maximum level of damage to a building when subjected to a specific seismic ground motion. Categories of performance are defined as follows:

1. fully operational
2. operational
3. life-safe
4. near collapse

For each of the performance levels, there is a range of damage that corresponds to the building's functional status following a specified earthquake design level. These earthquake design levels represent a range of earthquake excitation that have defined probabilities of occurrence over the life of the building. SEAOC Vision 2000 performance level definition includes descriptions of structural and non-structural damage, egress systems and overall building state. Also included in the performance level descriptions

is the level of both transient and permanent drift in the structure. Drift is defined as the ratio of interstory deflection to the story height.

The fully operational level represents the least level of damage to the building. Except for very low levels of ground motion, it is generally not practical to design buildings to meet this performance level.

Operational performance level is one in which overall building damage is light. Negligible damage to vertical load carrying elements as well as light damage to the lateral load carrying element is expected. The lateral

groups are categorized based on the type of occupancy and importance of the building. For example, buildings such as hospitals, power plants and fire stations are considered as essential facilities also known as post-disaster buildings and are assigned as seismic use group III. These provisions specify progressively more conservative strength, drift control, system selection, and detailing requirements for buildings contained in the three groups, in order to attain minimum levels of earthquake performance suitable to the individual occupancies.

the structure and the maximum base shear that can be developed. Pushover analysis, which is relatively a new technology, should be carried out with caution. For example, when the response of a structure is dominated by modes other than the first mode, the results may not represent the actual behavior.

For the design of most buildings, reliance will usually have to be placed on the simplified prescriptions found in most codes⁽¹⁰⁻¹⁾. Although necessarily approximate in character in view of the need for simplicity and ease of application—the provisions of such codes and the philosophy behind them gain in reliability as design guides with continued application and modification to reflect the latest research findings and lessons derived from observations of structural behavior during earthquakes. Code provisions must, however, be viewed in the proper perspective, that is, as minimum requirements covering a broad class of structures of more or less conventional configuration. Unusual structures must still be designed with special care and may call for procedures beyond those normally required by codes.

The basic form of modern code provisions on earthquake-resistant design has evolved from rather simplified concepts of the dynamic behavior of structures and has been greatly influenced by observations of the performance of structures subjected to actual earthquakes.⁽¹⁰⁻⁶⁹⁾ It has been noted, for instance, that many structures built in the 1930s and designed on the basis of more or less arbitrarily chosen lateral forces have successfully withstood severe earthquakes. The satisfactory performance of such structures has been attributed to one or more of the following^{(10-70), (10-71)}: (i) yielding in critical sections of members (yielding not only may have increased the period of vibration of such structures to values beyond the damaging range of the ground motions, but may have allowed them to dissipate a sizable portion of the input energy from an earthquake); (ii) the greater actual strength of such structures resulting from so-called nonstructural elements which are generally ignored in analysis, and the significant energy-dissipation capacity that

cracking in such elements represented; and (iii) the reduced response of the structure due to yielding of the foundation.

The distribution of the code-specified design lateral forces along the height of a structure is generally similar to that indicated by the envelope of maximum horizontal forces obtained by elastic dynamic analysis. These forces are considered *service loads*, i.e., to be resisted within a structure's elastic range of stresses. However, the magnitudes of these code forces are substantially smaller than those which would be developed in a structure subjected to an earthquake of moderate-to-strong intensity, such as that recorded at El Centro in 1940, if the structure were to respond elastically to such ground excitation. Thus, buildings designed under the present codes would be expected to undergo fairly large deformations (four to six times the lateral displacements resulting from the code-specified forces) when subjected to an earthquake with the intensity of the 1940 El Centro.⁽¹⁰⁻²⁾ These large deformations will be accompanied by yielding in many members of the structure, and, in fact, such is the intent of the codes. The acceptance of the fact that it is economically unwarranted to design buildings to resist major earthquakes elastically, and the recognition of the capacity of structures possessing adequate strength and ductility to withstand major earthquakes by responding inelastically to them, lies behind the relatively low forces specified by the codes. These reduced forces are coupled with detailing requirements designed to insure adequate inelastic deformation capacity, i.e., ductility. The capacity of an indeterminate structure to deform in a ductile manner, that is to deform well beyond the yield limit without significant loss of strength, allows such a structure to dissipate a major portion of the energy from an earthquake without serious damage.

10.4.3 Principal Earthquake-Design Provisions of ASCE 7-95, IBC-2000, UBC-97, and ACI Chapter 21 Relating to Reinforced Concrete

The principal steps involved in the design of earthquake-resistant cast-in-place reinforced concrete buildings, with particular reference to the application of the provisions of nationally accepted model codes or standards, will be discussed below. The minimum design loads specified in ASCE 7-95, *Minimum design Loads for Buildings and Other Structures*⁽¹⁰⁻⁷²⁾ and the design and detailing provisions contained in Chapter 21 of ACI 318-95, *Building Code Requirements for Reinforced Concrete*,⁽¹⁰⁻¹⁰⁾ will be used as bases for the discussion. Emphasis will be placed on those provisions relating to the proportioning and detailing of reinforced concrete elements, the subject of the determination of earthquake design forces having been treated in Chapters 4 and 5. Where appropriate, reference will be made to differences between the provisions of these model codes and those of related codes. Among the more important of these is the IBC-2000⁽¹⁰⁻⁶¹⁾ which is primarily a descendant of ATC 3-06⁽¹⁰⁻⁷³⁾ and the latest edition of the *Recommended Lateral Force Requirements* of the Structural Engineers Association of California (SEAOC-96).⁽¹⁰⁻⁷⁴⁾

The ASCE 7-95 provisions relating to earthquake design loads are basically similar to those found in the 1997 Edition of the Uniform Building Code (UBC-97)⁽¹⁰⁻¹⁾. The current UBC-97 earthquake design load requirements are based on the 1996 SEAOC Recommendations (SEAOC-96). Except for minor modifications, the design and detailing requirements for reinforced concrete members found in UBC-97 (SEAOC-96) and IBC-2000 are essentially those of ACI Chapter 21.

Although the various code-formulating bodies in the United States tend to differ in what they consider the most appropriate form in which to cast specific provisions and in their judgment of the adequacy of certain design requirements, there has been a tendency for the different codes and model codes to gradually

take certain common general features. And while many questions await answers, it can generally be said that the main features of the earthquake-resistant design provisions in most current regional and national codes have good basis in theoretical and experimental studies as well as field observations. As such, they should provide reasonable assurance of attainment of the stated objectives of earthquake-resistant design. The continual refinement and updating of provisions in the major codes to reflect the latest findings of research and field observations⁽¹⁰⁻⁷⁵⁾ should inspire increasing confidence in the soundness of their recommendations.

The following discussion will focus on the provisions of ASCE 7-95 and ACI Chapter 21, with occasional references to parallel provisions of IBC-2000 and UBC-97 (SEAOC-96).

The design earthquake forces specified in ASCE 7-95 is intended as equivalent static loads. As its title indicates, ASCE 7-95 is primarily a load standard, defining minimum loads for structures but otherwise leaving out material and member detailing requirements. ACI Chapter 21 on the other hand, does not specify the manner in which earthquake loads are to be determined, but sets down the requirements by which to proportion and detail monolithic cast-in-place reinforced concrete members in structures that are expected to undergo inelastic deformations during earthquakes.

Principal Design Steps Design of a reinforced concrete building in accordance with the equivalent static force procedure found in current U.S. seismic codes involves the following principal steps:

1. Determination of design "earthquake" forces:
 - Calculation of base shear corresponding to the computed or estimated fundamental period of vibration of the structure. (A preliminary design of the structure is assumed here.)
 - Distribution of the base shear over the height of the building.

2. Analysis of the structure under the (static) lateral forces calculated in step (1), as well as under gravity and wind loads, to obtain member design forces and story drift ratios. The lateral load analysis, of course, can be carried out most conveniently by using a computer program for analysis.

For certain class of structures having plan or vertical irregularities, or structure over 240 feet in height, most building codes require dynamic analysis to be performed. In this case, ASCE 7-95 and IBC-2000 require that the design parameters including story shears, moments, drifts and deflections determined from dynamic analysis to be adjusted. Where the design value for base shear obtained from dynamic analysis (V_d) is less than the calculated base shear (V) determined using the step 1 above, these design parameters is to be increased by a factor of V/V_d .

3. Designing members and joints for the most unfavorable combination of gravity and lateral loads. The emphasis here is on the design and detailing of members and their connections to insure their ductile behavior.

The above steps are to be carried out in each principal (plan) direction of the building. Most building codes allow the design of a structure in each principal direction independently of the other direction on the assumption that the design lateral forces act non-concurrently in each principal direction. However, for certain building categories which may be sensitive to torsional oscillations or characterized by significant irregularities and for columns forming part of two or more intersecting lateral-force-resisting systems, orthogonal effects need to be considered. For these cases, the codes consider the orthogonal effects requirement satisfied if the design is based on the more severe combination of 100 percent of the prescribed seismic forces in one direction plus 30 percent of the forces in the perpendicular direction.

Changes in section dimensions of some members may be indicated in the design phase under step (3) above. However, unless the required changes in dimensions are such as to

materially affect the overall distribution of forces in the structure, a reanalysis of the structure using the new member dimensions need not be undertaken. Uncertainties in the actual magnitude and distribution of the seismic forces as well as the effects of yielding in redistributing forces in the structure would make such refinement unwarranted. It is, however, most important to design and detail the reinforcement in members and their connections to insure their ductile behavior and thus allow the structure to sustain without collapse the severe distortions that may occur during a major earthquake. The code provisions intended to insure adequate ductility in structural elements represent the major difference between the design requirements for conventional, non-earthquake-resistant structures and those located in regions of high earthquake risk.

Load Factors, Strength Reduction Factors, and Loading Combinations Used as Bases for Design Codes generally require that the strength or load-resisting capacity of a structure and its component elements be at least equal to or greater than the forces due to any of a number of loading combinations that may reasonably be expected to act on it during its life. In the United States, concrete structures are commonly designed using the ultimate-strength^b method. In this approach, structures are proportioned so that their (ultimate) capacity is equal to or greater than the required (ultimate) strength. The required strength is based on the most critical combination of factored loads, that is, specified service loads multiplied by appropriate *load factors*. The capacity of an element, on the other hand, is obtained by applying a *strength-reduction factor* ϕ to the nominal resistance of the element as determined by code-prescribed expressions or procedures or from basic mechanics.

Load factors are intended to take account of the variability in the magnitude of the specified

^b Since ACI 318-71, the term "ultimate" has been dropped, so that what used to be referred to as "ultimate-strength design" is now simply called "strength design."

loads, lower load factors being used for types of loads that are less likely to vary significantly from the specified values. To allow for the lesser likelihood of certain types of loads occurring simultaneously, reduced load factors are specified for some loads when considered in combination with other loads.

ACI 318-95 requires that structures, their components, and their foundations be designed to have strengths not less than the most severe of the following combinations of loads:

$$U = \begin{cases} 1.4D + 1.7L \\ 0.75[1.4D + 1.7L \pm (1.7W \text{ or } 1.87E)] \\ 0.9D \pm (1.3W \text{ or } 1.43E) \\ 1.4D + 1.7L + (1.7H \text{ or } 1.4F) \\ 0.9D + (1.7H \text{ or } 1.4F) \\ 0.75(1.4D + 1.7L + 1.4T) \end{cases} \quad (10-1)$$

where

U = required strength to resist the factored loads

D = dead load

L = live load

W = wind load

E = earthquake load

F = load due to fluids with and maximum heights well-defined pressures

H = load due to soil pressure

T = load due to effects of temperature, shrinkage, expansion of shrinkage compensating concrete, creep, differential settlement, or combinations thereof.

ASCE 7-95 specifies slightly different load factors for some load combinations, as follows:

$$U = \begin{cases} 1.4D \\ 1.2(D + F + T) + 1.6(L + H) + 0.5(L_r \text{ or } S \text{ or } R) \\ 1.2D + 1.6(L_r \text{ or } S \text{ or } R) + (0.5L \text{ or } 0.8W) \\ 1.2D + 1.3W + 0.5L + 0.5(L_r \text{ or } S \text{ or } R) \\ 1.2D + 1.0E + 0.5L + 0.2S \\ 0.9D + (1.3W \text{ or } 1.0E) \end{cases} \quad (10-2)$$

where

L_r = roof live load

S = snow load

R = rain load

For garages, places of public assembly, and all areas where the live load is greater than 100 lb/ft², the load factor on L in the third, fourth, and fifth combinations in Equation 10-2 is to be taken equal to 1.0.

For the design of earthquake-resistant structures, UBC-97 uses basically the same load combinations specified by ASCE 7-95 as shown in Equation 10-2.

IBC-2000 requires that the load combinations to be the same as those specified by ASCE 7-95 as shown in Equation 10-2. However, the effect of seismic load, E, is defined as follows:

$$\begin{aligned} E &= \rho Q_E + 0.2 S_{DS} D \\ E &= \rho Q_E - 0.2 S_{DS} D \end{aligned} \quad (10-3)$$

where

E = the effect of horizontal and vertical earthquake-induced forces,

S_{DS} = the design spectral response acceleration at short periods

D = the effect of dead load

ρ = the reliability factor

Q_E = the effect of horizontal seismic forces

To consider the extent of structural redundancy inherent in the lateral-force-resisting system, the reliability factor, ρ , is introduced for buildings located in areas of moderate to high seismicity. This is basically a penalty factor for buildings in which the lateral resistance is limited to only few members in the structure. The maximum value of ρ is limited to 1.5.

The factor 0.2 S_{DS} in Equation (10-3) is placed on the dead load to account for the effects of vertical acceleration.

For situations where failure of an isolated, individual, brittle element can result in the loss of a complete lateral-force-resisting system or in instability and collapse, IBC-2000 has a specific requirement to determine the seismic design forces. These elements are referred to as collector elements. Columns supporting

discontinuous lateral-load-resisting elements such as walls also fall under this category. The seismic loads are as follows:

$$\begin{aligned} E &= \Omega_o Q_E + 0.2 S_{DS} D \\ E &= \Omega_o Q_E - 0.2 S_{DS} D \end{aligned} \quad (10-4)$$

where Ω_o is the system overstrength factor which is defined as the ratio of the ultimate lateral force the structure is capable of resisting to the design strength. The value of Ω_o varies between 2 to 3 depending on the type of lateral force resisting system.

As mentioned earlier, the capacity of a structural element is calculated by applying a strength reduction factor ϕ to the nominal strength of the element. The factor ϕ is intended to take account of variations in material strength and uncertainties in the estimation of the nominal member strength, the nature of the expected failure mode, and the importance of a member to the overall safety of the structure. For conventional reinforced concrete structures, ACI 318-95 specifies the following values of the strength reduction factor ϕ :

- 0.90 for flexure, with or without axial tension
- 0.90 for axial tension
- 0.75 for spirally reinforced members subjected to axial compression, with or without flexure
- 0.70 for other reinforced members (tied columns) subjected to axial compression, with or without flexure (an increase in the ϕ value for members subjected to combined axial load and flexure is allowed as the loading condition approaches the case of pure flexure)
- 0.85 for shear and torsion
- 0.70 for bearing on concrete

ACI Chapter 21 specifies the following exception to the above values of the strength-

reduction factor as given in the main body of the ACI Code:

For structural members other than joints, a value $\phi = 0.60$ is to be used for shear when the nominal shear strength of a member is less than the shear corresponding to the development of the nominal flexural strength of the member. For shear in joints, $\phi = 0.85$.

The above exception applies mainly to low-rise walls or portions of walls between openings.

Code Provisions Designed to Insure Ductility in Reinforced Concrete Members

The principal provisions of ACI Chapter 21 will be discussed below. As indicated earlier, the requirements for proportioning and detailing reinforced concrete members found in UBC-97 (SEAOC-96) and IBC-2000 are essentially those of ACI Chapter 21. Modifications to the ACI Chapter 21 provisions found in UBC-97 and IBC-2000 will be referred to where appropriate.

Special provisions governing the design of earthquake-resistant structures first appeared in the 1971 edition of the ACI Code. The provisions Chapter 21 supplement or supersede those in the earlier chapters of the code and deal with the design of ductile moment-resisting space frames and shear walls of cast-in-place reinforced concrete.

ACI 318-95 does not specify the magnitude of the earthquake forces to be used in design. The Commentary to Chapter 21 states that the provisions are intended to result in structures capable of sustaining a series of oscillations in the inelastic range without critical loss in strength. It is generally accepted that the intensity of shaking envisioned by the provisions of the first seven sections of ACI Chapter 21 correspond to those of UBC seismic zones 3 and 4. In the 1983 edition of the ACI Code, a section (Section A.9; now section 21.8) was added to cover the design of frames located in areas of moderate seismic risk, roughly corresponding to UBC seismic zone 2. For structures located in areas of low seismic risk (corresponding to UBC seismic zones 0 and 1)

and designed for the specified earthquake forces, very little inelastic deformation may be expected. In these cases, the ductility provided by designing to the provisions contained in the first 20 Chapters of the code will generally be sufficient.

A major objective of the design provisions in ACI Chapter 21, as well as in the earlier chapters of the code, is to have the strength of a structure governed by a ductile type of flexural failure mechanism. Stated another way, the provisions are aimed at preventing the brittle or abrupt types of failure associated with inadequately reinforced and over-reinforced members failing in flexure, as well as with shear (i.e., diagonal tension) and anchorage or bond failures. The main difference between Chapter 21 and the earlier chapters of the ACI Code lies in the greater range of deformation, with yielding actually expected at critical locations, and hence the greater ductility required in designs for resistance to major earthquakes. The need for greater ductility follows from the design philosophy that uses reduced forces in proportioning members and provides for the inelastic deformations that are expected under severe earthquakes by special ductility requirements.

A provision unique to earthquake-resistant design of frames is the so-called strong column-weak beam requirement. As discussed in Section 10.3.4 under "Beam—Column Joints," this requirement calls for the sum of the flexural strengths of columns meeting at a frame joint to be at least 1.2 times that of the beams framing into the joint. This is intended to force yielding in such frames to occur in the beams rather than in the columns and thus preclude possible instability due to plastic hinges forming in the columns. As pointed out earlier, this requirement may not guarantee non-development of plastic hinges in the columns. The strong column-weak beam requirement often results in column sizes that are larger than would otherwise be required, particularly in the upper floors of multistory buildings with appreciable beam spans.

1. Limitations on material strengths. ACI Chapter 21 requires a minimum specified concrete strength f'_c of 3000 lb/in.² and a maximum specified yield strength of reinforcement, f_y of 60,000 lb/in.². These limits are imposed with a view to restricting the unfavorable effects that material properties beyond these limits can have on the sectional ductility of members. ACI Chapter 21 requires that reinforcement for resisting flexure and axial forces in frame members and wall boundary elements be ASTM 706 grade 60 low-alloy steel intended for applications where welding or bending, or both, are important. However, ASTM 615 billet steel bars of grade 40 or 60 may be used provided the following two conditions are satisfied:

$$(actual f_y) \leq (specified f_y) \pm 18,000 \text{ lb/in.}^2$$

$$\frac{\text{actual ultimate tensile stress}}{\text{actual } f_y} \geq 1.25$$

The first requirement helps to limit the increase in magnitude of the actual shears that can develop in a flexural member beyond that computed on the basis of the specified yield stress when plastic hinges form at the ends of a beam. The second requirement is intended to insure reinforcement with a sufficiently long yield plateau.

In the "strong column-weak beam" frame intended by the code, the relationship between the moment capacities of columns and beams may be upset if the beams turn out to have much greater moment capacity than intended by the designer. Thus, the substitution of 60-ksi steel of the same area for specified 40-ksi steel in beams can be detrimental. The shear strength of beams and columns, which is generally based on the condition of plastic hinges forming (i.e., M_y acting) at the member ends, may become inadequate if the actual moment capacities at the member ends are greater than intended as a result of the steel having a substantially greater yield strength than specified.

2. Flexural members (beams). These include members having a clear span greater than four times the effective depth that are subject to a factored axial compressive force not exceeding $A_g f'_c / 10$, where A_g is the gross cross-sectional area. Significant provisions relating to flexural members of structures in regions of high seismic risk are discussed below.

(a) Limitations on section dimensions

$$\text{width}/\text{depth} \geq 0.3$$

$$\text{width} \begin{cases} \geq 10 \text{ in.} \\ \leq \text{width of supporting column} + 1.5 \times (\text{depth of beam}) \end{cases}$$

(b) Limitations on flexural reinforcement ratio (see also Figure 10-34):

$$\rho_{\min} = \begin{cases} 200/f_y \\ \text{two continuous bars at both top and bottom of member} \\ \frac{3\sqrt{f_c}}{f_y} \end{cases}$$

$$\rho_{\max} = 0.025$$

The minimum steel required can be waived if the area of tensile reinforcement at every section is at least one-third greater than required by analysis.

(c) Moment capacity requirements:

At beam ends

$$M_y^+ \geq 0.5M_y^-$$

At any section in beam span

$$M_y^+ \text{ or } M_y^- \geq 0.25 (M_y^{\max} \text{ at beam ends})$$

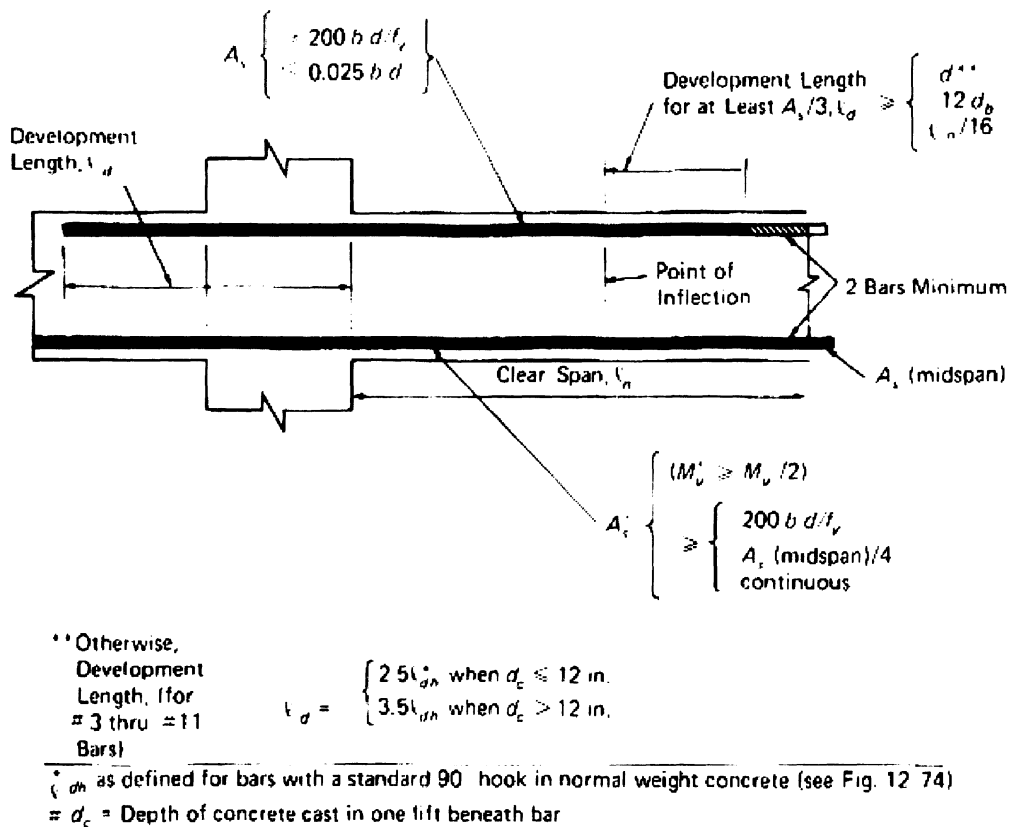


Figure 10-34. Longitudinal reinforcement requirements for flexural members

(d) Restrictions on lap splices: Lap splices shall not be used

- (1) within joints,
- (2) within $2h$ from face of support, where h is total depth of beam,
- (3) at locations of potential plastic hinging. Lap splices, where used, are to be confined by hoops or spiral reinforcement with a maximum spacing or pitch of $d/4$ or 4 in.

(e) Restrictions on welding of longitudinal reinforcement: Welded splices and mechanical connectors may be used provided:

- (1) they are used only on alternate bars in each layer at any section;
- (2) the distance between splices of adjacent bars is ≥ 24 in.
- (3) Except as noted above, welding of reinforcement required to resist load combinations including earthquake effects is not permitted. Also, the welding of stirrups, ties, inserts, or other similar elements to longitudinal bars is prohibited

(f) Development length requirements for longitudinal bars in tension:

- (1) For bar sizes 3 through 11 with a standard 90° hook (as shown in Figure 10-35) in normal weight concrete, the development length

$$l_{dh} \geq \begin{cases} \frac{f_y d_b}{65\sqrt{f_c}}, \\ 8d_b, \\ 6 \text{ in.} \end{cases}$$

$(d_b$ is bar diameter).

- (2) When bars are embedded in lightweight-aggregate concrete, the development length is to be at least equal to the greater of $10d_b$, 7.5 in. or 1.25 times the values indicated above.

- (3) The 90° hook shall be located within the confined core of a column or boundary element.

- (4) For straight bars of sizes 3 through 11, the development length,

$l_d \geq 2.5 \times (l_{dh}$ for bars with 90° hooks), when the depth of concrete cast in one lift beneath the bar is ≤ 12 in., or $l_d \geq 3.5 \times (l_{dh}$ for bars with 90° hooks) if the above mentioned depth is > 12 in.

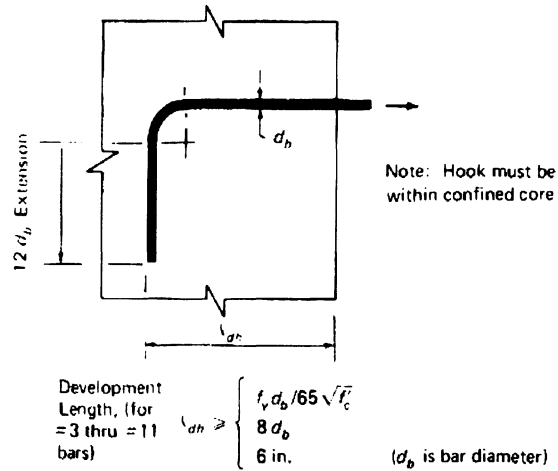


Figure 10-35. Development length for beam bars with 90° hooks.

- (5) If a bar is not anchored by means of a 90° hook within the confined column core, the portion of the required straight development length not located within the confined core shall be increased by a factor of 1.6.
- (6) When epoxy-coated bars are used, the development lengths calculated above to be increased by a factor of 1.2. However, for straight bars, with covers less than $3d_b$ or clear spacing less than $6d_b$, a factor of 1.5 to be used.

(g) Transverse reinforcement requirements for confinement and shear: Transverse reinforcement in beams must satisfy requirements associated with their dual function as confinement reinforcement and shear reinforcement (see Figure 10-36).

- (1) Confinement reinforcement in the form of hoops is required:

- (i) over a distance $2d$ from faces of support (where d is the effective depth of the member);
 - (ii) over distances $2d$ on both sides of sections within the span where flexural yielding may occur due to earthquake loading.
- (2) Hoop spacing:
- (iii) First hoop at 2 in. from face of support.
 - (iv) Maximum spacing

$$\leq \begin{cases} d/4 \\ 8 \times (\text{diameter of smallest longitudinal bar}) \\ 24 \times (\text{diameter of hoop bars}) \\ 12 \text{ in.} \end{cases}$$

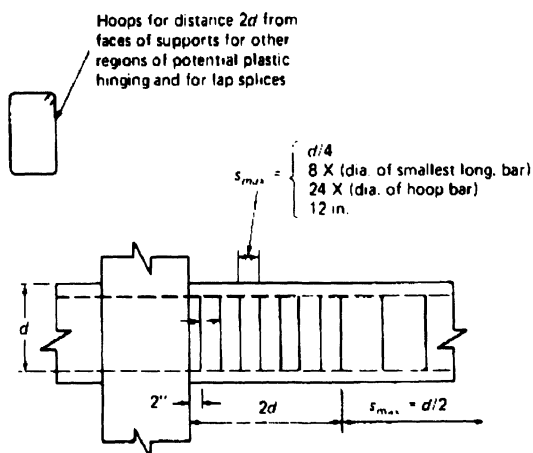


Figure 10-36. Transverse reinforcement limitations for flexural members. Minimum bar size- #3

- (3) Lateral support for perimeter longitudinal bars where hoops are required: Every corner and alternate longitudinal bar shall be supported by the corner of a hoop with an included angle 135° , with no longitudinal bar farther than 6 in. along the tie from such a laterally supported bar. Where the longitudinal perimeter bars are arranged in a circle, a circular hoop may be used.

- (4) Where hoops are not required, stirrups with seismic hooks at both ends with a spacing of not more than $d/2$ to be provided throughout the length of the member.
- (5) Shear reinforcement—to be provided so as to preclude shear failure prior to development of plastic hinges at beam ends. Design shears for determining shear reinforcement are to be based on a condition where plastic hinges occur at beam ends due to the combined effects of lateral displacement and factored gravity loads (see Figure 10-16). The *probable flexural strength*, M_{pr} associated with a plastic hinge is to be computed using a strength reduction factor $\phi = 1.0$ and assuming a stress in the tensile reinforcement $f_s = 1.25f_y$.
- (6) In determining the required shear reinforcement, the contribution of the concrete, V_c , is to be neglected if the shear associated with the probable flexural strengths at the beam ends is equal to or greater than one-half the total design shear and the factored axial compressive force including earthquake effects is less than $A_g f'_c / 20$.
- (7) The transverse reinforcement provided must satisfy the requirements for confinement or shear, whichever is more stringent.

Discussion:

- (a) Limitations on section dimensions: These limitations have been guided by experience with test specimens subjected to cyclic inelastic loading.
- (b) Flexural reinforcement limitations: Because the ductility of a member decreases with increasing tensile reinforcement ratio, ACI Chapter 21 limits the maximum reinforcement ratio to 0.025. The use of a limiting ratio based on the "balanced condition" as given in the earlier chapters of the code, while applicable to members loaded monotonically, fails to describe conditions in flexural members subjected to

reversals of inelastic deformation. The limiting ratio of 0.025 is based mainly on considerations of steel congestion and also on limiting shear stresses in beams of typical proportions. From a practical standpoint, low steel ratios should be used whenever possible. The requirements of at least two continuous bars top and bottom, refers to construction rather than behavioral requirements.

The selection of the size, number, and arrangement of flexural reinforcement should be made with full consideration of construction requirements. This is particularly important in relation to beam-column connections, where construction difficulties can arise as a result of reinforcement congestion. The preparation of large-scale drawings of the connections, showing all beam, column, and joint reinforcements, will help eliminate unanticipated problems in the field. Such large-scale drawings will pay dividends in terms of lower bid prices and a smooth-running construction job. Reference 10-76 provides further recommendations on reinforcement detailing.

- (c) Positive moment capacity at beam ends: To allow for the possibility of the positive moment at the end of a beam due to earthquake-induced lateral displacements exceeding the negative moment due to the gravity loads, the code requires a minimum positive moment capacity at beam ends equal to 50% of the corresponding negative moment capacity.
- (d) Lap splices: Lap splices of flexural reinforcement are not allowed in regions of potential plastic hinging since such splices are not considered to be reliable under reversed inelastic cycles of deformation. Hoops are mandatory for confinement of lap splices at any location because of the likelihood of loss of the concrete cover.
- (e) Welded splices and mechanical connectors: Welded splices and mechanical connectors are to conform to the requirements given in Chapter 12 of the ACI 318-95. A major requirement is that the splices develop at

least 125% of the specified yield strength of the bar.

As mentioned earlier, the welding of stirrups, ties, inserts, or other similar elements to longitudinal bars is not permitted.

- (f) Development length: The expression for l_{dh} given above already includes the coefficients 0.7 (for concrete cover) and 0.80 (for ties) that are normally applied to the basic development length, l_{db} . This is so because ACI Chapter 21 requires that hooks be embedded in the confined core of a column or boundary element. The expression for l_{dh} also includes a factor of about 1.4, representing an increase over the development length required for conventional structures, to provide for the effect of load reversals.

Except in very large columns, it is usually not possible to develop the yield strength of a reinforcing bar from the framing beam within the width of a column unless a hook is used. Where beam reinforcement can extend through a column, its capacity is developed by embedment in the column and within the compression zone of the beam on the far side of the connection (see Figure 10-34). Where no beam is present on the opposite side of a column, such as in exterior columns, the flexural reinforcement in a framing beam has to be developed within the confined region of the column. This is usually done by means of a standard 90° hook plus whatever extension is necessary to develop the bar, the development length being measured from the near face of the column, as indicated in Figure 10-35. The use of a beam stub at the far (exterior) side of a column may also be considered (see Figure 10-22). ACI Chapter 21 makes no provision for the use of size 14 and 18 bars because of lack of sufficient information on the behavior at anchorage locations of such bars when subjected to load reversals simulating earthquake effects.

- (g) Transverse reinforcement: Because the ductile behavior of earthquake-resistant

frames designed to current codes is premised on the ability of the beams to develop plastic hinges with adequate rotational capacity, it is essential to insure that shear failure does not occur before the flexural capacity of the beams has been developed. Transverse reinforcement is required for two related functions: (i) to provide sufficient shear strength so that the full flexural capacity of the member can be developed, and (ii) to insure adequate rotation capacity in plastic-hinging regions by confining the concrete in the compression zones and by providing lateral support to the compression steel. To be equally effective with respect to both functions under load reversals, the transverse reinforcement should be placed perpendicular to the longitudinal reinforcement.

Shear reinforcement in the form of stirrups or stirrup ties is to be designed for the shear due to factored gravity loads and the shear corresponding to plastic hinges forming at both ends of a beam. Plastic end moments associated with lateral displacement in either direction should be considered (Figure 10-16). It is important to note that the required shear strength in beams (as in columns) is determined by the flexural strength of the frame member (as well as the factored loads acting on the member), rather than by the factored shear force calculated from a lateral load analysis. The use of the factor 1.25 on f_y for calculating the probable moment strength is intended to allow for the actual steel strength exceeding the specified minimum and also recognizes that the strain in reinforcement of sections undergoing large rotations can enter the strain-hardening range.

To allow for load combinations not accounted for in design, a minimum amount of web reinforcement is required throughout the length of all flexural members. Within regions of potential hinging, stirrup ties or hoops are required.

A hoop may be made of two pieces of reinforcement: a stirrup having 135° hooks with 6-diameter extensions anchored in the confined core and a crosstie to close the hoop (see Figure 10-37). Consecutive ties are to have their 90° hooks on opposite sides of the flexural member.

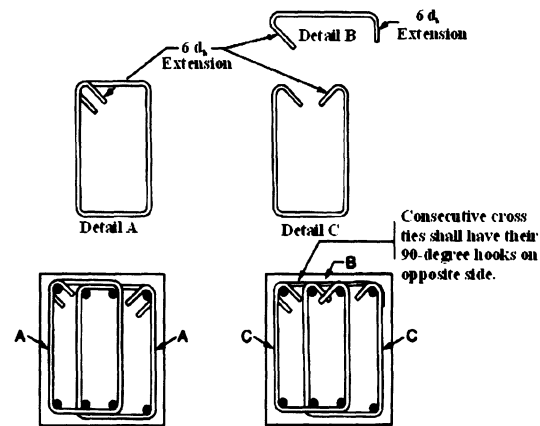


Figure 10-37. Single and two-piece hoops

3. Frame members subjected to axial load and bending. ACI Chapter 21 makes the distinction between columns or beam—columns and flexural members on the basis of the magnitude of the factored axial load acting on the member. Thus, if the factored axial load does not exceed $A_g f'_c / 10$, the member falls under the category of flexural members, the principal design requirements for which were discussed in the preceding section. When the factored axial force on a member exceeds $A_g f'_c / 10$, the member is considered a beam—column. Major requirements governing the design of such members in structures located in areas of high seismic risk are given below.

- (a) Limitations on section dimensions: shortest cross-sectional dimension ≥ 12 in. (measured on line passing through geometric centroid);

$$\frac{\text{shortest dimension}}{\text{perpendicular dimension}} \geq 0.4$$

(b) Limitations on longitudinal reinforcement:

$$\rho_{\min} = 0.01, \quad \rho_{\max} = 0.06$$

(c) Flexural strength of columns relative to beams framing into a joint (the so-called "strong column-weak beam" provision):

$$\sum M_e \geq \frac{6}{5} \sum M_g \quad (10-5)$$

where

$\sum M_e$ = sum of the design flexural strengths of the columns framing into joint. Column flexural strength to be calculated for the factored axial force, consistent with the direction of the lateral loading considered, that results in the lowest flexural strength

$\sum M_g$ = sum of design flexural strengths of beams framing into joint

The lateral strength and stiffness of columns not satisfying the above requirement are to be ignored in determining the lateral strength and stiffness of the structure. Such columns have to be designed in accordance with the provisions governing members not proportioned to resist earthquake-induced forces, as contained in the ACI section 21.7. However, as the commentary to the Code cautions, any negative effect on the building behavior of such non-conforming columns should not be ignored. The potential increase in the base shear or of torsional effects due to the stiffness of such columns should be allowed for.

(d) Restriction on use of lap splices: Lap splices are to be used only within the middle half of the column height and are to be designed as tension splices.

(e) Welded splices or mechanical connectors for longitudinal reinforcement: Welded splices or mechanical connectors may be used at any section of a column, provided that:

(1) they are used only on alternate longitudinal bars at a section;

(2) the distance between splices along the longitudinal axis of the reinforcement is ≥ 24 in.

(f) Transverse reinforcement for confinement and shear: As in beams, transverse reinforcement in columns must provide confinement to the concrete core and lateral support for the longitudinal bars as well as shear resistance. In columns, however, the transverse reinforcement must all be in the form of closed hoops or continuous spiral reinforcement. Sufficient reinforcement should be provided to satisfy the requirements for confinement or shear, whichever is larger.

(1) Confinement requirements (see Figure 10-38):

- Volumetric ratio of spiral or circular hoop reinforcement:

$$\rho_s \geq \begin{cases} 0.12 \frac{f_c'}{f_{yh}} \\ 0.45 \left(\frac{A_g}{A_{ch}} - 1 \right) \frac{f_c'}{f_{yh}} \end{cases} \quad (10-6)$$

f_{yh} = specified yield strength of transverse reinforcement, in lb/in.²

A_{ch} = core area of column section, measured to the outside of transverse reinforcement, in in.²

- Rectangular hoop reinforcement, total cross-sectional area, within spacings:

$$A_{sh} \geq \begin{cases} 0.09 s h_c \frac{f_c'}{f_{yh}} \\ 0.3 s h_c \left(\frac{A_g}{A_{ch}} - 1 \right) \frac{f_c'}{f_{yh}} \end{cases} \quad (10-7)$$

where

h_c = cross-sectional dimension of column core, measured center-to-center of confining reinforcement

s = spacing of transverse reinforcement

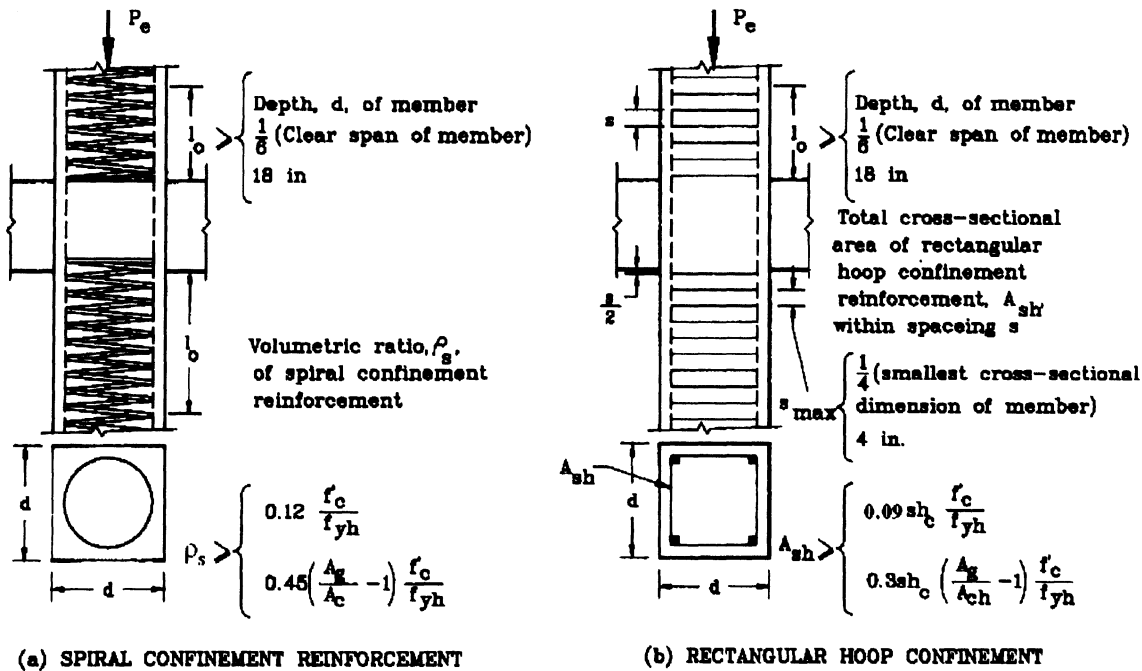


Figure 10-38. Confinement requirements for column ends.

measured along axis of member, in in.
 $s_{max} = \min \left\{ \frac{1}{4}(\text{smallest cross-sectional dimension of member}), 4 \text{ in.} \right\}$

maximum permissible spacing in plane of cross-section between legs of overlapping hoops or cross ties is 14 in.

- (2) Confinement reinforcement is to be provided over a length l_0 from each joint face or over distances l_0 on both sides of any section where flexural yielding may occur in connection with lateral displacements of the frame, where

$$l_0 \geq \begin{cases} \text{depth } d \text{ of member} \\ 1/6(\text{clear span of member}) \\ 18 \text{ in.} \end{cases}$$

UBC-97 further requires that confinement reinforcement be provided at any section of a column where the nominal axial strength, ϕP_n is less than the sum of the shears corresponding to

the probable flexural strengths of the beams (i.e., based on $f_s = 1.25f_y$ and $\phi = 1.0$) framing into the column above the level considered.

- (3) over segments of a column not provided with transverse reinforcement in accordance with Eqs. (10-6) and (10-7) and the related requirements described above, spiral or hoop reinforcement is to be provided, with spacing not exceeding $6 \times (\text{diameter of longitudinal column bars})$ or 6 in., whichever is less.
- (4) Transverse reinforcement for shear in columns is to be based on the shear associated with the maximum probable moment strength, M_{pr} , at the column ends (using $f_s = 1.25 f_y$ and $\phi = 1.0$) corresponding to the range of factored axial forces acting on the column. The calculated end moments of columns meeting at a joint need not exceed the sum of the probable moment strengths of the girders framing into the joint. However, in no case should the design

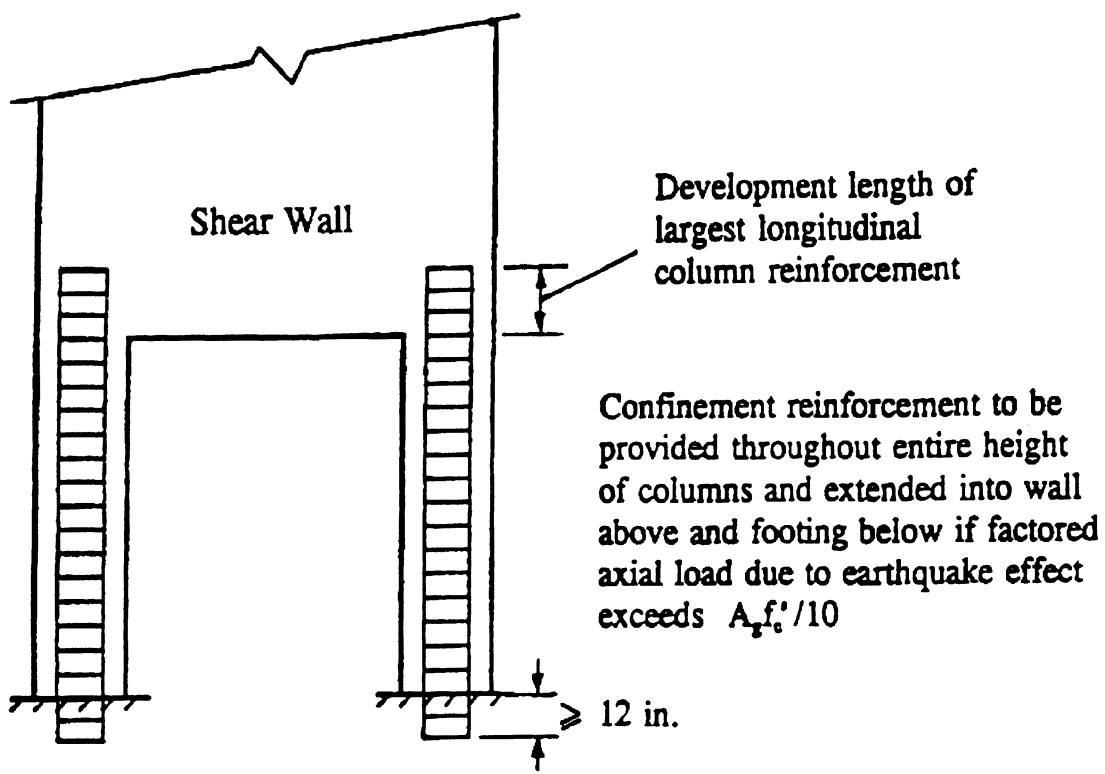


Figure 10-39. Columns supporting discontinued wall.

shear be less than the factored shear determined by analysis of the structure.

- (g) Column supporting discontinued walls: Columns supporting discontinued shear walls or similar stiff elements are to be provided with transverse reinforcement over their full height below the discontinuity (see Figure 10-39) when the axial compressive force due to earthquake effects exceeds $A_g f'_c / 10$.

The transverse reinforcement in columns supporting discontinued walls be extended above the discontinuity by at least the development length of the largest vertical bar and below the base by the same amount where the column rests on a wall. Where the column terminates in a footing or mat, the transverse reinforcement is to be extended below the top of the footing or mat a distance of at least 12 in.

Discussion:

(b) Reinforcement ratio limitation: ACI Chapter 21 specifies a reduced upper limit for the reinforcement ratio in columns from the 8% of Chapter 10 of the code to 6%. However, construction considerations will in most cases place the practical upper limit on the reinforcement ratio ρ near 4%. Convenience in detailing and placing reinforcement in beam-column connections makes it desirable to keep the column reinforcement low.

The minimum reinforcement ratio is intended to provide for the effects of time-dependent deformations in concrete under axial loads as well as maintain a sizable difference between cracking and yield moments.

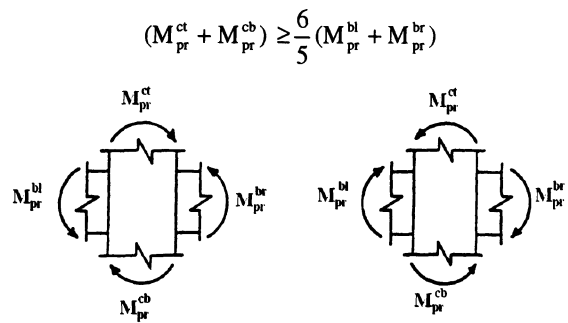


Figure 10-40. Strong column-weak beam frame requirements.

(c) Relative column-to-beam flexural strength requirement: To insure the stability of a frame and maintain its vertical-load-carrying capacity while undergoing large lateral displacements, ACI Chapter 21 requires that inelastic deformations be generally restricted to the beams. This is the intent of Equation 10-5 (see Figure 10-40). As mentioned, formation of plastic hinges at both ends of most columns in a story can precipitate a sidesway mechanism leading to collapse of the story and the structure above it. Also, as pointed out in Section 10.3.4 under "Beam—Column Joints," compliance with this provision does not insure that plastic hinging will not occur in the columns.

If Equation 10-5 is not satisfied at a joint, columns supporting reactions from such a joint are to be provided with transverse reinforcement over their full height. Columns not satisfying Equation 10-5 are to be ignored in calculating the strength and stiffness of the structure. However, since such columns contribute to the stiffness of the structure before they suffer severe loss of strength due to plastic hinging, they should not be ignored if neglecting them results in unconservative estimates of design forces. This may occur in determining the design base shear or in calculating the effects of torsion in a structure. Columns not satisfying Equation 10-5 should satisfy the minimum requirements for members not

proportioned to resist earthquake-induced forces, discussed under item 6 below.

(f) Transverse reinforcement for confinement and shear: Sufficient transverse reinforcement in the form of rectangular hoops or spirals should be provided to satisfy the larger requirement for either confinement or shear.

Circular spirals represent the most efficient form of confinement reinforcement. The extension of such spirals into the beam—column joint, however, may cause some construction difficulties.

Rectangular hoops, when used in place of spirals, are less effective with respect to confinement of the concrete core. Their effectiveness may be increased, however, with the use of supplementary cross-ties. The cross-ties have to be of the same size and spacing as the hoops and have to engage a peripheral longitudinal bar at each end. Consecutive cross-ties are to be alternated end for end along the longitudinal reinforcement and are to be spaced no further than 14 in. in the plane of the column cross-section (see Figure 10-41). The requirement of having the cross-ties engage a longitudinal bar at each end would almost preclude placing them before the longitudinal bars are threaded through.

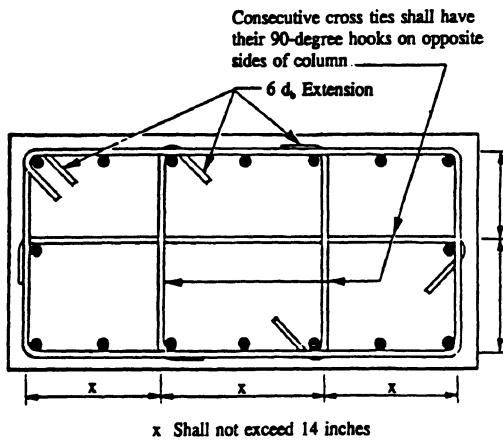
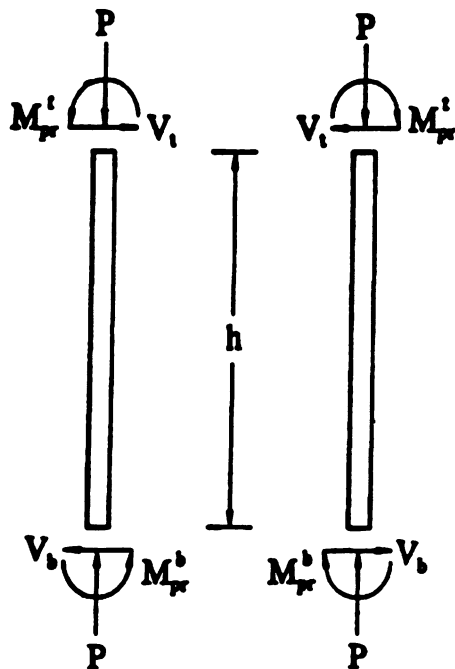
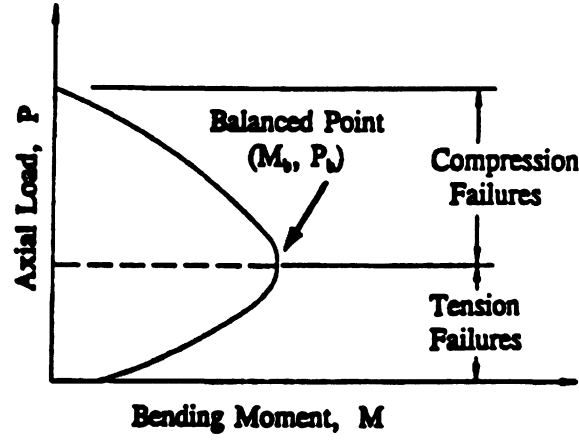


Figure 10-41. Rectangular transverse reinforcement in columns.

$$V_t = V_b = \frac{M_{pr}^t + M_{pr}^b}{h}$$



(a) Sidesway to Right (b) Sidesway to Left



Typical Interaction Diagram

Figure 10-42. Loading cases for design of shear reinforcement for columns.

In addition to confinement requirements, the transverse reinforcement in columns must resist the maximum shear associated with the formation of plastic hinges at the column ends. Although the strong column-weak beam provision governing relative moment strengths of beams and columns meeting at a joint is intended to have most of the inelastic deformation occur in the beams of a frame, the code recognizes that hinging can occur in the columns. Thus, the shear reinforcement in columns is to be based on the shear corresponding to the development of the probable moment strengths at the ends of the columns, i.e., using $f_s = 1.25 f_y$ and $\phi = 1.0$. The values of these end moments —obtained from the P - M interaction diagram for the particular column section considered—are to be the

maximum consistent with the range of possible factored axial forces on the column. Moments associated with lateral displacements of the frame in both directions, as indicated in Figure 10-42, should be considered. The axial load corresponding to the maximum moment capacity should then be used in computing the permissible shear in concrete, V_c .

- (g) Columns supporting discontinued walls: Columns supporting discontinued shear walls tend to be subjected to large shears and compressive forces, and can be expected to develop large inelastic deformations during strong earthquakes; hence the requirement for transverse reinforcement throughout the height of such columns according to equations (10-6) and (10-7) if the factored axial force exceeds $A_g f'_c / 10$

4. Beam-column connections.

In conventional reinforced-concrete buildings, the beam-column connections usually are not designed by the structural engineer. Detailing of reinforcement within the joints is normally relegated to a draftsman or detailer. In earthquake resistant frames, however, the design of beam-column connections requires as much attention as the design of the members themselves, since the integrity of the frame may well depend on the proper performance of such connections. Because of the congestion that may result from too many bars converging within the limited space of the joint, the requirements for the beam—column connections have to be considered when proportioning the columns of a frame. To minimize placement difficulties, an effort should be made to keep the amount of longitudinal reinforcement in the frame members on the low side of the permissible range.

The provisions of ACI Chapter 21 dealing with beam-column joints relate mainly to:

- (a) Transverse reinforcement for confinement: Minimum confinement reinforcement, as required for potential hinging regions in columns and defined by Equations 10-6 and 10-7, must be provided in beam-column joints. For joints confined on all four sides by framing beams, a 50% reduction in the required amount of confinement reinforcement is allowed, the required amount to be placed within the depth of the shallowest framing member. In this case, the reinforcement spacing is not to exceed one-quarter of the minimum member dimension nor 6 in. (instead of 4 in. for non-confined joints). A framing beam is considered to provide confinement to a joint if it has a width equal to at least three-quarters of the width of the column into which it frames.
- (b) Transverse reinforcement for shear: The horizontal shear force in a joint is to be calculated by assuming the stress in the tensile reinforcement of framing beams equal to $1.25f_y$ (see Figure 10-21). The

shear strength of the connection is to be computed (for normal-weight concrete) as

$$\phi V_c = \begin{cases} \phi 20\sqrt{f_c} A_j & \text{for joints confined on all four sides} \\ \phi 15\sqrt{f_c} A_j & \text{for joints confined on three sides or} \\ & \text{on two opposite sides} \\ \phi 12\sqrt{f_c} A_j & \text{for all other cases} \end{cases}$$

where

$\phi = 0.85$ (for shear)

A_j = effective (horizontal) cross-sectional area of joint in a plane parallel to the beam reinforcement generating the shear forces (see Figure 10-43)

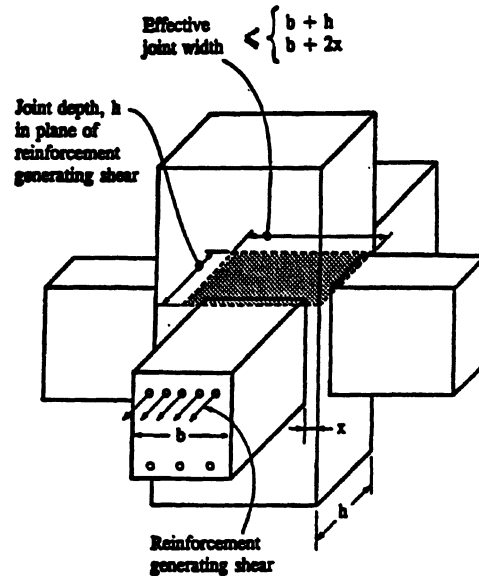


Figure 10-43. Beam-column panel zone.

As illustrated in Fig. 10-43, the effective area, A_j , is the product of the joint depth and the effective width of the joint. The joint depth is taken as the overall depth of the column (parallel to the direction of the shear considered), while the effective width of the joint is to be taken equal to the width of the

column if the beam and the column are of the same width, or, where the column is wider than the framing beam, is not to exceed the smaller of:

- beam width plus the joint depth, and
- beam width plus twice the least column projection beyond the beam side, i.e. the distance x in Fig. 10-43.

For lightweight concrete, V_c is to be taken as three-fourths the value given above for normal-weight concrete.

(c) Anchorage of longitudinal beam reinforcement terminated in a column must be extended to the far face of the confined column core and anchored in accordance with the requirements given earlier for development lengths of longitudinal bars in tension and according to the relevant ACI Chapter 12 requirements for bars in compression.

Where longitudinal beam bars extend through a joint ACI Chapter 21 requires that the column depth in the direction of loading be not less than 20 times the diameter of the largest longitudinal beam bar. For lightweight concrete, the dimension shall be not less than 26 times the bar diameter.

Discussion:

(a) Transverse reinforcement for confinement: The transverse reinforcement in a beam-column connection helps maintain the vertical-load-carrying capacity of the joint even after spalling of the outer shell. It also helps resist the shear force transmitted by the framing members and improves the bond between steel and concrete within the joint.

The minimum amount of transverse reinforcement, as given by Equations 10-6 and 10-7, must be provided through the joint regardless of the magnitude of the calculated shear force in the joint. The 50% reduction in the amount of confinement reinforcement allowed for joints having beams framing into all four sides recognizes the beneficial confining effect provided by these members.

(b) Results of tests reported in Reference 10-41 indicate that the shear strength of joints is not too sensitive to the amount of transverse (shear) reinforcement. Based on these results, ACI Chapter 21 defines the shear strength of beam-column connections as a function only of the cross-sectional area of the joint, (A_j) and f'_c (see Section 10.3.4 under "Beam-Column Joints").

When the design shear in the joint exceeds the shear strength of the concrete, the designer may either increase the column size or increase the depth of the beams. The former will increase the shear capacity of the joint section, while the latter will tend to reduce the required amount of flexural reinforcement in the beams, with accompanying decrease in the shear transmitted to the joint. Yet another alternative is to keep the longitudinal beam bars from yielding at the faces of the columns by detailing the beams so that plastic hinging occurs away from the column faces.

(c) The anchorage or development-length requirements for longitudinal beam reinforcement in tension have been discussed earlier under flexural members. Note that lap splicing of main flexural reinforcement is not permitted within the joint.

5. *Shear Walls.* When properly proportioned so that they possess adequate lateral stiffness to reduce inter-story distortions due to earthquake-induced motions, shear walls or structural walls reduce the likelihood of damage to the non-structural elements of a building. When used with rigid frames, walls form a system that combines the gravity-load-carrying efficiency of the rigid frame with the lateral-load-resisting efficiency of the structural wall. In the form of coupled walls linked by appropriately proportioned coupling beams (see Section 10.3.4 under "Coupled Walls"), alone or in combination with rigid frames, structural walls provide a laterally stiff structural system that allows significant energy dissipation to take place

in the more easily repairable coupling beams.

Observations of the comparative performance of rigid-frame buildings and buildings stiffened by structural walls during earthquakes⁽¹⁰⁻⁷⁷⁾ have pointed to the consistently better performance of the latter. The performance of buildings stiffened by properly designed structural walls has been better with respect to both life safety and damage control. The need to insure that critical facilities remain operational after a major tremor and the need to reduce economic losses from structural and nonstructural damage, in addition to the primary requirement of life safety (i.e., no collapse), has focused attention on the desirability of introducing greater lateral stiffness in earthquake-resistant multistory buildings. Where acceleration-sensitive equipment is to be housed in a structure, the greater horizontal accelerations that may be expected in laterally stiffer structures should be allowed or provided for.

The principal provisions of ACI Chapter 21 relating to structural walls and diaphragms are as follows (see Figure 10-44):

- (a) Walls (and diaphragms) are to be provided with shear reinforcement in two orthogonal directions in the plane of the wall. The minimum reinforcement ratio for both longitudinal and transverse directions is

$$\rho_v = \frac{A_{sv}}{A_{cv}} = \rho_n \geq 0.0025$$

where the reinforcement is to be continuous and distributed uniformly across the shear area, and

A_{cv} = net area of concrete section, i.e., product of thickness and width of wall section

A_{sv} = projection on A_{cv} of area of shear reinforcement crossing the plane of A_{cv}

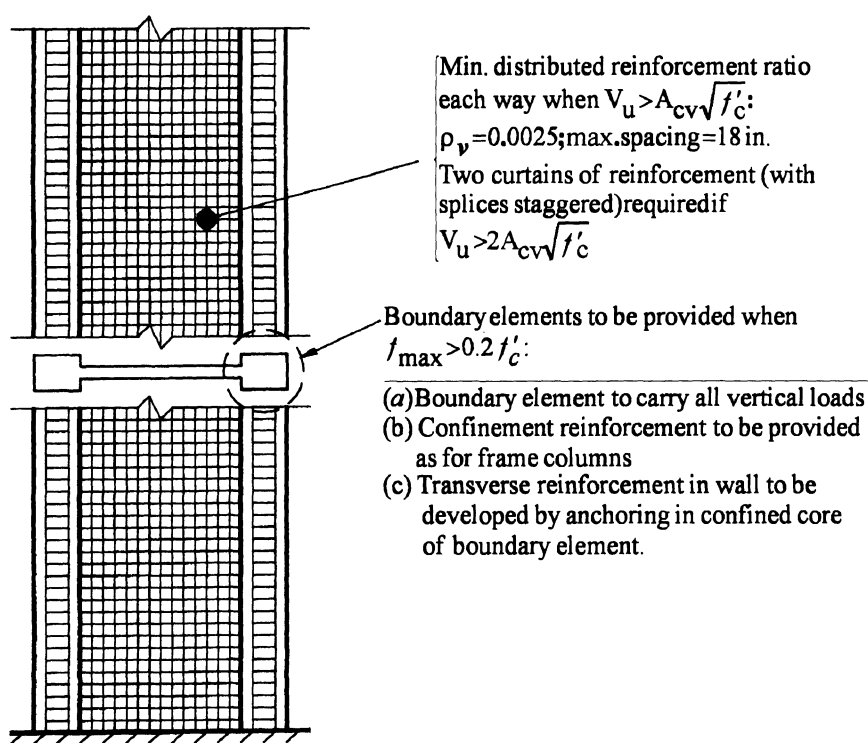


Figure 10-44. Structural wall design requirements.

ρ_n = reinforcement ratio corresponding to plane perpendicular to plane of A_{cv}

The maximum spacing of reinforcement is 18 in. At least two curtains of reinforcement, each having bars running in the longitudinal and transverse directions, are to be provided if the in-plane factored shear force assigned to the wall exceeds $2A_{cv}\sqrt{f'_c}$. If the (factored) design shear force does not exceed $A_{cv}\sqrt{f'_c}$, the shear reinforcement may be proportioned in accordance with the minimum reinforcement provisions of ACI Chapter 14.

(b) Boundary elements: Boundary elements are to be provided, both along the vertical boundaries of walls and around the edges of openings, if any, when the maximum extreme-fiber stress in the wall due to factored forces including earthquake effects exceeds $0.2\sqrt{f'_c}$. The boundary members may be discontinued when the calculated compressive stress becomes less than $0.15\sqrt{f'_c}$. Boundary elements need not be provided if the entire wall is reinforced in accordance with the provisions governing transverse reinforcement for members subjected to axial load and bending, as given by Equations 10-6 and 10-7.

Boundary elements of structural walls are to be designed to carry all the factored vertical loads on the wall, including self-weight and gravity loads tributary to the wall, as well as the vertical forces required to resist the overturning moment due to factored earthquake loads. Such boundary elements are to be provided with confinement reinforcement in accordance with Equations 10-6 and 10-7.

Welded splices and mechanical connections of longitudinal reinforcement of boundary elements are allowed provided that:

- 1) they are used only on alternate longitudinal bars at a section;

- 2) the distance between splices along the longitudinal axis of the reinforcement is ≥ 24 in.

The requirements for boundary elements in UBC-97 and IBC-2000 provisions which are essentially similar are much more elaborate and detailed in comparison with ACI-95. In these two provisions, the determination of boundary zones may be based on the level of axial, shear, and flexural wall capacity as well as wall geometry. Alternatively, if such conditions are not met, it may be based on the limitations on wall curvature ductility determined based on inelastic displacement at the top of the wall. Using such a procedure, the analysis should be based on cracked shear area and moment of inertia properties and considering the response modification effects of possible non-linear behavior of building. The requirements of boundary elements using these provisions are discussed in detail under item (f) below.

(c) Shear strength of walls (and diaphragms):

For walls with a height-to-width ratio $h_w/l_w \geq 2.0$, the shear strength is to be determined using the expression:

$$\phi V_n = \phi A_{cv} (2\sqrt{f'_c} + \rho_n f_y)$$

where

$\phi = 0.60$, unless the nominal shear strength provided exceeds the shear corresponding to development of nominal flexural capacity of the wall

A_{cv} = net area as defined earlier

h_w = height of entire wall or of segment of wall considered

l_w = width of wall (or segment of wall) in direction of shear force

For walls with $h_w/l_w < 2.0$, the shear may be determined from

$$\phi V_n = \phi A_{cv} (\alpha_c \sqrt{f'_c} + \rho_n f_y)$$

where the coefficient α_c varies linearly from a value of 3.0 for $h_w/l_w = 1.5$ to 2.0 for h_w/l_w

= 2.0. Where the ratio $h_w/l_w < 2.0$, ρ_v can not be less than ρ_n .

Where a wall is divided into several segments by openings, the value of the ratio h_w/l_w to be used in calculating V_n for any segment is not to be less than the corresponding ratio for the entire wall.

The nominal shear strength V_n of all wall segments or piers resisting a common lateral force is not to exceed $8A_{cv}\sqrt{f'_c}$ where A_{cv} is the total cross-sectional area of the walls. The nominal shear strength of any individual segment of wall or pier is not to exceed $10A_{cp}\sqrt{f'_c}$ where A_{cp} is the cross-sectional area of the pier considered.

(d) Development length and splices: All continuous reinforcement is to be anchored or spliced in accordance with provisions governing reinforcement in tension, as discussed for flexural members.

Where boundary elements are present, the transverse reinforcement in walls is to be anchored within the confined core of the boundary element to develop the yield stress in tension of the transverse reinforcement. For shear walls without boundary elements, the transverse reinforcement terminating at the edges of the walls are to be provided with standard hooks engaging the edge (vertical) reinforcement. Otherwise the edge reinforcement is to be enclosed in U-stirrups having the same size and spacing as, and spliced to, the transverse reinforcement. An exception to this requirement is when V_u in the plane of the wall is less than $A_{cv}\sqrt{f'_c}$.

(e) Coupling beams: UBC-97 and IBC-2000 provide similar guidelines for coupling beams in coupled wall structures. For coupling beams with $l_n/d \geq 4$, where l_n = clear length of coupling beam and d = effective depth of the beam, conventional reinforcement in the form of top and bottom reinforcement can be used. However, for coupling beams with $l_n/d < 4$, and factored shear stress exceeding $4\sqrt{f'_c}$, reinforcement in the form of two intersecting groups of symmetrical diagonal bars to be

provided. The design shear stress in coupling beams should be limited to $10\phi\sqrt{f'_c}$ where $\phi = 0.85$.

(f) Provisions of IBC-2000 and UBC-97 related to structural walls: These provisions treat shear walls as regular members subjected to combined flexure and axial load. Since the proportions of such walls are generally such that they function as regular vertical cantilever beams, the strains across the depth of such members (in the plane of the wall) are to be assumed to vary linearly, just as in regular flexural members, i.e., the nonlinear strain distribution associated with deep beams does not apply. The effective flange width to be assumed in designing I-, L-, C- or T-shaped shear wall sections, i.e., sections formed by intersecting connected walls, measured from the face of the web, shall not be greater than (a) one-half the distance to the adjacent shear wall web, or (b) 15 percent of the total wall height for the flange in compression or 30 percent of the total wall height for the flange in tension, not to exceed the total projection of the flange.

Walls or portions of walls subject to an axial load $P_u > 0.35 P_0$ shall not be considered as contributing to the earthquake resistance of a structure. This follows from the significantly reduced rotational ductility of sections subjected to high compressive loads (see Fig. 10-11(b)).

When the shear V_u in the plane of the wall exceeds $A_{cv}\sqrt{f'_c}$, the need to develop the yield strength in tension of the transverse reinforcement is expressed in the requirement to have horizontal reinforcement terminating at the edges of shear walls, with or without boundary elements, anchored using standard hooks engaging the (vertical) edge reinforcement or alternatively, having the vertical edge reinforcement enclosed in "U" stirrups of the same size and spacing as, and spliced to, the horizontal reinforcement.

Shear Wall Boundary Zones - The detailing requirements for boundary zones, to be described subsequently, need not be satisfied in walls or portions of walls where

$$P_u \leq \begin{cases} 0.10 A_g f_c & \text{for geometrically} \\ & \text{symmetrical wall sections} \\ 0.05 A_g f_c & \text{otherwise} \end{cases}$$

and either

$$\frac{M_u}{V_u l_u} \leq 1.0 \quad \text{or} \quad V_u \leq 3l_w h_w \sqrt{f_c}$$

where l_w is the length of the entire wall in the direction of the shear force, and h_w is the height of the wall.

Shear walls or portions of shear walls not meeting the above conditions and having $P_u < 0.35 P_o$ (so that they can be considered as contributing to the earthquake resistance of the structure) are to be provided with boundary zones at each end having a length varying linearly from $0.25l_w$ for $P_u = 0.35P_o$ to $0.15l_w$ for $P_u = 0.15P_o$, with a minimum of $0.15l_w$ and are to be detailed as will be described.

Alternatively, the requirements of boundary zones not meeting the above conditions may be based on the determination of the compressive strain levels at wall edges using cracked section properties. Boundary zone detailing, however, is to be provided over the portions of the wall where compressive strains exceed 0.003. It is important to note that compressive strains are not allowed to exceed 0.015.

For shear walls in which the flexural limit state response is governed by yielding at the base of the wall, the total curvature demand (ϕ_t) can be obtained from:

$$\phi_t = \frac{\Delta_i}{(h_w - l_p/2)l_p} + \phi_y$$

where

Δ_i = inelastic deflection at the top of the wall

$$= (\Delta_t - \Delta_y)$$

Δ_t = total deflection at the top of the wall equal Δ_M , using cracked section properties, or may be taken as $2\Delta_M$, using gross section properties.

Δ_y = displacement at the top of wall corresponding to yielding of the tension reinforcement at critical section, or may be taken as

$$(M'_n/M_E) \Delta_E,$$

where M_E equals unfactored moment at critical section when top of wall is displaced Δ_E . M'_n is nominal flexural strength of critical section at P'_u .

h_w = height of the wall

l_p = height of the plastic hinge above critical section and which shall be established on the basis of substantiated test data or may be alternatively taken at $0.5l_w$

ϕ_y = yield curvature which may be estimated at $0.003/l_w$

If ϕ_t is less than or equal to $0.003/c'_u$, boundary zone details as defined below are not required. c'_u is the neutral axis depth at P'_u and M'_n . If ϕ_t exceeds $0.003/c'_u$, the compressive strains may be assumed to vary linearly over the depth c'_u , and have maximum value equal to the product of c'_u and ϕ_t .

The use of the above procedure is further discussed with the aid of the design example at the end of this Chapter.

Shear wall boundary zone detailing requirements. When required as discussed above, the boundary zones in shear walls are to be detailed in accordance with the following requirements:

(1) *Dimensional requirements:*

- (a) The minimum section dimension of the boundary zone shall be $l_w/16$.
- (b) Boundary zones shall extend above the elevation where they are required a distance equal to the development length of the largest vertical bar in the boundary zone. Extensions of the boundary zone lateral reinforcement below its base shall conform to the same requirements as for columns terminating

on a mat or footing. However, the transverse boundary zone reinforcement need not extend above the base of the boundary zone a distance greater than the larger of l_w or $M_u/4V_u$.

- (c) Boundary zones shall have a minimum length of 18 inches (measured along the length) at each end of the wall or portion of wall.
- (d) In I-, L-, C- or T-section walls, the boundary zone at each end shall include the effective flange width and shall extend at least 12 in. into the web.

(2) Confinement Reinforcement:

- (a) All vertical reinforcement within the boundary zone shall be confined by hoops or cross-ties having a steel cross-sectional area

$$A_{sh} > 0.09 h f_c' / f_{yh}$$

- (b) Hoops and cross-ties shall have a vertical spacing,

$$S_{max} < \begin{cases} 6 \text{ in.} \\ 6 \times (\text{diameter of largest vertical bar within boundary zone}) \end{cases}$$

- (c) The length-to-width ratio of the hoops shall not exceed 3; and all adjacent hoops shall be overlapping.
- (d) Cross-ties or legs of overlapping hoops shall not be spaced farther apart than 12 in. along the wall.
- (e) Alternate vertical bars shall be confined by the corner of a hoop or cross-tie.

(3) Horizontal reinforcement:

- (a) All horizontal reinforcement terminating within a boundary zone shall be anchored as described earlier, i.e., when $V_u > A_{cv} \sqrt{f'_c}$, horizontal reinforcement are to be provided with standard hooks or be enclosed in U-stirrups having the same size and spacing as, and spliced to, the horizontal bars.

(b) Horizontal reinforcement shall not be lap spliced within the boundary zone.

(4) Vertical reinforcement:

- (a) Vertical reinforcement shall be provided to satisfy all tension and compression requirements indicated by analysis. (Note again that, in contrast to earlier editions of the code, there is no longer the stipulation of rather arbitrary forces that "boundary elements", and hence the vertical steel reinforcement in these, are to be designed for.)

- (b) Area of vertical reinforcement,

$$A_v > \begin{cases} 0.005 \times (\text{area of boundary zone}) \\ \text{Two No. 5 bars at each edge of the boundary zone} \end{cases}$$

- (c) Lap splices of vertical reinforcement within the boundary zone shall be confined by hoops and crossties. The spacing of hoops and crossties confining lap-spliced vertical reinforcement shall not exceed 4 in.

Discussion:

- (a) The use of two curtains of reinforcement in walls subjected to significant shear (i.e., $> 2A_{cv} f_c'$) serves to reduce fragmentation and premature deterioration of the concrete under load reversals into the inelastic range. Distributing the reinforcement uniformly across the height and width of the wall helps control the width of inclined cracks.
- (b) ACI Chapter 21 allows calculation of the shear strength of structural walls using a coefficient $\alpha_c = 2.0$. However, advantage can be taken of the greater observed shear strength of walls with low height-to-width ratios h_w/l_w by using an α_c value of up to 3.0 for walls with $h_w/l_w = 1.5$ or less.

The upper bound on the average nominal shear stress that may be developed in any individual segment of wall ($10\sqrt{f'_c}$) is intended to limit the degree of shear redistribution among several connected wall segments. A wall segment refers to a part of a wall bounded by openings or by an opening and an edge.

It is important to note that ACI Chapter 21 requires the use of a strength-reduction factor ϕ for shear of 0.6 for all members (except joints) where the nominal shear strength is less than the shear corresponding to the development of the nominal flexural strength of the member. In the case of beams, the design shears are obtained by assuming plastic end moments corresponding to a tensile steel stress of $1.25f_y$ (see Figure 10-16). Similarly, for a column the design shears are determined not by applying load factors to shears obtained from a lateral load analysis, but from consideration of the maximum probable moment strengths at the column ends consistent with the axial force on the column. This approach to shear design is intended to insure that even when flexural hinging occurs at member ends due to earthquake-induced deformations, no shear failure would develop. Under the above conditions, ACI Chapter 21 allows the use of the normal strength-reduction factor for shear of 0.85. When design shears are not based on the condition of flexural strength being developed at member ends, the code requires the use of a lower shear strength-reduction factor to achieve the same result, that is, prevention of premature shear failure.

As pointed out earlier, in the case of multistory structural walls, a condition similar to that used for the shear design of beams and columns is not so readily established. This is so primarily because the magnitude of the shear at the base of a (vertical cantilever) wall, or at any level above, is influenced significantly by the forces and deformations beyond the particular level considered. Unlike the

flexural behavior of beams and columns in a frame, which can be considered as close-coupled systems (i.e., with the forces in the members determined by the forces and displacements within and at the ends of the member), the state of flexural deformation at any section of a structural wall (a far-coupled system) is influenced significantly by the displacements of points far removed from the section considered. Results of dynamic inelastic analyses of isolated structural walls under earthquake excitation⁽¹⁰⁻³⁾ also indicate that the base shear in such walls is strongly influenced by the higher modes of response.

A distribution of static lateral forces along the height of the wall essentially corresponding to the fundamental mode response, such as is assumed by most codes,⁽¹⁰⁻¹⁾ will produce flexural yielding at the base if the section at the base is designed for such a set of forces. Other distributions of lateral forces, with a resultant acting closer to the base of the wall, can produce yielding at the base only if the magnitude of the resultant horizontal force, and hence the base shear, is increased. Results of the study of isolated walls referred to above,⁽¹⁰⁻³⁾ which would also apply to frame—shear-wall systems in which the frame is flexible relative to the wall, in fact indicate that for a wide range of wall properties and input motion characteristics, the resultant of the dynamic horizontal forces producing yielding at the base of the wall generally occurs well below the two-thirds-of-total-height level associated with the fundamental-mode response (see Figure 10-24). This would imply significantly larger base shears than those due to lateral forces distributed according to the fundamental mode response. The study of isolated walls mentioned above indicates ratios of maximum dynamic shears to “fundamental-mode shears” (i.e., shears associated with horizontal forces distributed according to the fundamental-mode response, as used in codes) ranging from 1.3 to 4.0, the value of the ratio increases with

- increasing fundamental period (see Figure 10-23).
- (c) Since multistory structural walls behave essentially as vertical cantilever beams, the horizontal transverse reinforcement is called upon to act as web reinforcement. As such, these bars have to be fully anchored in the boundary elements, using standard 90° hooks whenever possible.
- (d) ACI Chapter 21 uses an extreme-fiber compressive stress of $0.2f'_c$, calculated using a linearly elastic model based on gross sections of structural members and factored forces, as indicative of significant compression. Structural walls subjected to compressive stresses exceeding this value are generally required to have boundary elements.

Figure 10-45 illustrates the condition assumed as basis for requiring that boundary elements of walls be designed for all the gravity loads (W) as well as the vertical forces associated with overturning of the wall due to earthquake forces (H). This requirement assumes that the boundary element alone may have to carry all the vertical (compressive) forces at the critical wall section when the maximum horizontal earthquake force acts on the wall. Under load reversals, such a loading condition imposes severe demands on the concrete in the boundary elements; hence the requirement for confinement reinforcement similar to those for frame members subjected to axial load and bending. Diaphragms of reinforced concrete, such as floor slabs, that are called upon to transmit horizontal forces through bending and shear in their own plane, are treated in much the same manner as structural walls.

- 6. Frame members not forming part of lateral-force-resisting system.** Frame members that are not relied on to resist earthquake-induced forces need not satisfy the stringent requirements governing lateral-load-resisting elements. These relate particularly to the transverse reinforcement requirements for confinement and shear. Non-lateral-load-resisting elements,

whose primary function is the transmission of vertical loads to the foundation, need comply only with the reinforcement requirements of ACI Chapter 21, in addition to those found in the main body of the code.

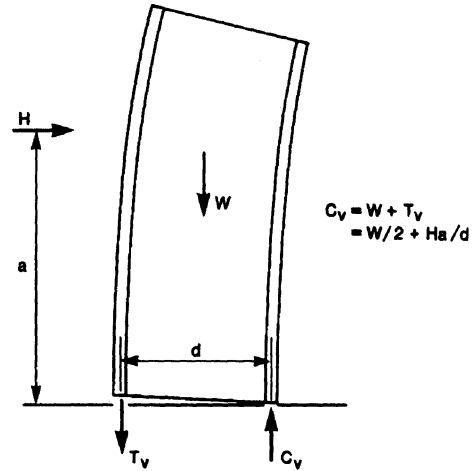


Figure 10-45. Loading condition assumed for design of boundary elements of structural walls.

The 1994 Northridge earthquake caused the collapse or partial collapse of at least two parking structures that could be attributed primarily to the failure of interior columns designed to gravity loads only. Following the experience, the requirements for frame members not proportioned to resist forces induced by earthquake motions have been extensively rewritten for the ACI 95 code. A flow chart is provided in Figure 10-46 for ease in understanding the new provisions. The requirements are as follows:

A special requirement for non-lateral-load-resisting elements is that they be checked for adequacy with respect to a lateral displacement representing the expected actual displacement of the structure under the design earthquake. For the purpose of this check, ACI Chapter 21 uses a value of twice the displacement calculated under the factored lateral loads, or $2 \times 1.7 = 3.4$ times the displacement due to the code-specified loads. This effect is combined with the effects of dead or dead and live load whichever is critical. If M_u and V_u for an element of gravity system are less than the

corresponding nominal values, that element is going to remain elastic under the design earthquake displacements. If such an element is a beam ($P_u \leq A_g f_c' / 10$), it must conform to section 2 described earlier for minimum longitudinal reinforcement requirements. In addition, stirrups spaced at no more than $d/2$ must be provided throughout the length of the member. If such an element is a column, it must conform to some of the requirements listed under sections 2 and 3 for longitudinal and shear reinforcement. In addition, similar requirements for cross-ties under section 3(f), discussion, must be met. Also ties at a maximum spacing of s_o must not exceed six times the smallest longitudinal bar diameter, nor 6 in. Further, if $P_u > 0.35 P_o$, the amount of transverse reinforcement provided must be no less than one-half that required by 3(f).

If M_u and V_u for an element of gravity system exceeds the corresponding nominal values, then it is likely to become inelastic under the design earthquake displacements. Also if deformation compatibility is not checked, this condition will be assumed to be the case. In that case, the structural material must satisfy the requirements described in section 1 and splices of reinforcement must satisfy section 2(e). If such an element is a beam ($P_u \leq A_g f_c' / 10$), it must conform to sections 2(b), and 2(g)-(5) and (6). In addition, the stirrups at no more than $d/2$ must be provided throughout the length of the member. If it is a column, it must be provided with full ductile detailing in accordance with section 3(f), 3(g), and 4(a) as well as sections 2(g)-(5) and (6).

7. Frames in regions of moderate seismic risk. Although ACI Chapter 21 does not define "moderate seismic risk" in terms of a commonly accepted quantitative measure, it assumes that the probable ground-motion intensity in such regions would be a fraction of that expected in a high-seismic-risk zone, to which the major part of Chapter 21 is addressed. By the above description, an area of moderate seismic risk would correspond roughly to zone 2 as defined in UBC-97⁽¹⁰⁻¹⁾ and

ASCE 7-95.⁽¹⁰⁻⁷²⁾ For regions of moderate seismic risk, the provisions for the design of structural walls given in the main body of the ACI Code are considered sufficient to provide the necessary ductility. The requirements in ACI Chapter 21 for structures in moderate-risk areas relate mainly to frames and are contained in the last section, section 21.8.

The same axial compressive force ($A_g f_c' / 10$) used to distinguish flexural members from columns in high-seismic-risk areas also applies in regions of moderate seismicity.

(a) Shear design of beams, columns, or two-way slabs resisting earthquake effects: The magnitude of the design shear is not to be less than either of the following:

(1) The sum of the shear associated with the development of the nominal moment strength at each restrained end and that due to factored gravity loads, if any, acting on the member. This is similar to the corresponding requirement for high-risk zones and illustrated in Figure 10-16, except that the stress in the flexural tensile reinforcement is taken as f_y rather than $1.25f_y$.

(2) The maximum factored shear corresponding to the design gravity and earthquake forces, but with the earthquake forces taken as twice the value normally specified by codes. Thus, if the critical load combination consists of dead load (D) + live load (L) + earthquake effects (E), then the design shear is to be computed from

$$U = 0.75[1.4D + 1.7L + 2(1.87E)]$$

(b) Detailing requirements for beams: The positive moment strength at the face of a joint must be at least one-third the negative moment capacity at the same section. (This compares with one-half for high-seismic-risk areas.) The moment strength—positive or negative—at any section is to be no less than one-fifth the maximum moment strength at either end of a member. Stirrup spacing requirements are identical to those for beams in high-seismic-risk areas.

However, closed hoops are not required within regions of potential plastic hinging. It should be noted that lateral reinforcement for flexural framing members subjected to stress reversals at supports to consist of closed ties, closed stirrups, or spirals extending around the flexural reinforcement as required according to chapter 7 of ACI 318-95.

- (c) Detailing requirements for columns: The same region of potential plastic hinging (l_o) as at the ends of columns in a region of high seismicity is defined at each end of a column. The spacing of ties within the region of potential plastic hinging must not exceed the smallest of 8 times the diameter of the smallest longitudinal bar enclosed; 24 times the diameter of the tie bar; or One-half the smallest cross-sectional dimension of the column, and 12 in. Outside the region of potential plastic hinging, the spacing must not exceed twice the above value. The first tie must be located at no more than half the above spacing from the joint face.
- (e) Detailing requirements for two-way slabs without beams: As mentioned earlier, requirements for flat plates in ACI Chapter 21 appear only in the section relating to areas of moderate seismic risk. This suggests that ACI Chapter 21 considers the use of flat plates as acceptable components of the lateral-load-resisting system only for areas of moderate seismicity.

Specific requirements relating to flat-plate and flat-slab reinforcement for frames in moderate-risk zones are given in ACI Chapter 21 and illustrated in the corresponding Commentary.

10.5 DESIGN EXAMPLES — REPRESENTATIVE ELEMENTS OF A 12-STORY FRAME - SHEAR WALL BUILDING

10.5.1 Preliminaries

A significant part of the damage observed in engineered buildings during earthquakes has resulted from the effects of major structural discontinuities that were inadequately provided for. The message here is clear. Unless proper provision is made for the effects of major discontinuities in geometry, mass, stiffness, or strength, it would be prudent on the part of the engineer to avoid such conditions, which are associated with force concentrations and large ductility demands in localized areas of the structure. Where such discontinuities are unavoidable or desirable from the architectural standpoint, an analysis to obtain estimates of the forces associated with the discontinuity is recommended. IBC-2000⁽¹⁰⁻⁶¹⁾ provides guidelines for estimating design forces in structures with various types of vertical and plan irregularities.

In addition to discontinuities, major asymmetry, with particular regard to the disposition in plan of the lateral-load-resisting elements, should be avoided whenever possible. Such asymmetry, which can result in a significant eccentricity between the center of stiffness and the center of mass (and hence of the resultant inertial force), can produce appreciable torsional forces in the structure. Torsional effects can be critical for corner columns or end walls, i.e., elements located far from the center of stiffness.

Another important point to consider in the preliminary design of a structure relates to the effectiveness of the various lateral-load-resisting components, particularly where these differ significantly in deformation capacity. Efficient use of structural components would suggest that the useful range of deformation of

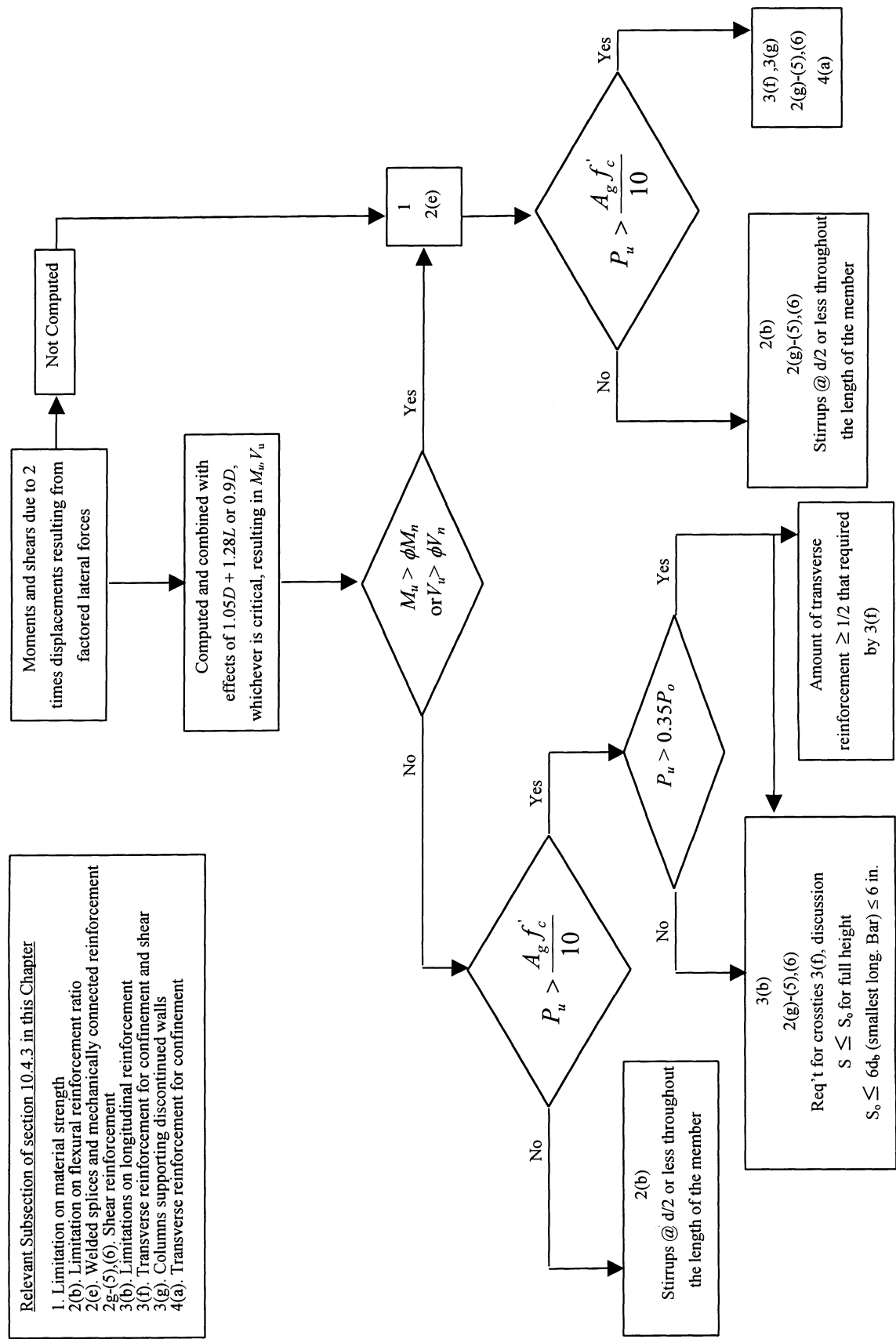


Figure 10-46. Requirements for frame members not proportioned to resist forces induced by earthquake motions.

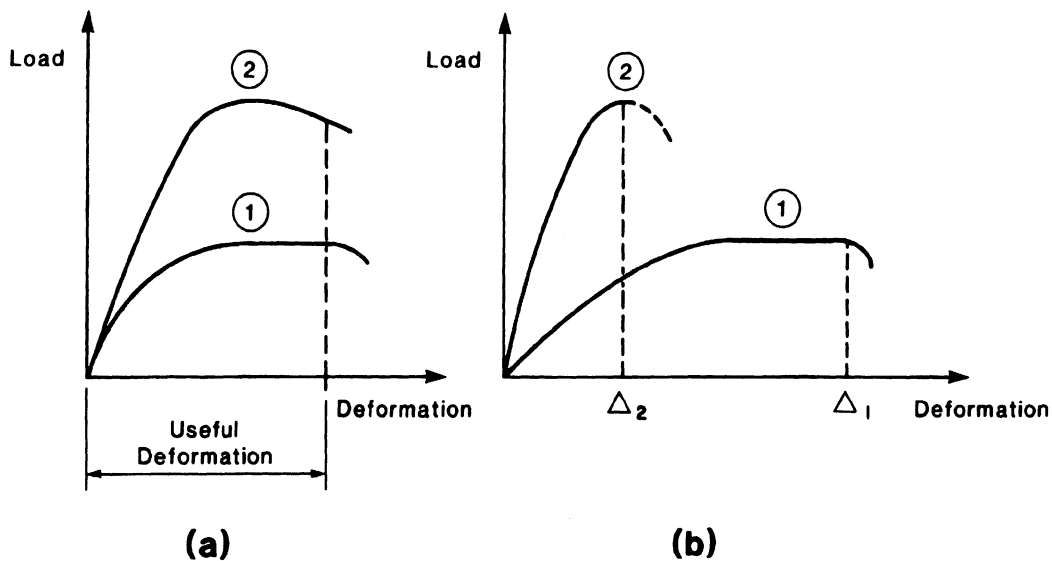


Figure 10-47. Relative deformation capacity in lateral-load-resisting elements in structure

the principal lateral-load-resisting elements in a structure be of about the same magnitude whenever practicable. This is illustrated in Figure 10-47a, which shows load—deformation curves of representative elements (1) and (2) in a structure. Such a design allows all the resisting elements to participate in carrying the induced forces over the entire range of deformation. In Figure 10-47b, the resisting elements (1) and (2) not only possess different initial stiffnesses but, more importantly, exhibit different ductilities (not *ductility ratios*) or deformation capacities. In such a case, which is typical of a frame—shear-wall structure, the design should be aimed at insuring that the maximum probable deformation or lateral displacement under dynamic conditions does not exceed the deformation capacity Δ_2 of element (2); or, if the maximum expected deformation could exceed Δ_2 , then element (1) should be so designed that it can support the additional load that may come upon it when element (2) loses a considerable part of its load-carrying capacity. It is worth noting that, generally, the lateral displacements associated with full mobilization of the ductility of rigid (open) frames are such that significant nonstructural damage can be expected. For this

reason, the building codes limit the amount of deformation that can be tolerated in the structure.

The need to tie together all the elements making up a structure or a portion of it that is intended to act as a unit cannot be overemphasized. This applies to the superstructure as well as foundation elements. Where a structure is divided into different parts by expansion joints, as when the various parts differ considerably in height, plan size, shape, or orientation, a sufficient gap should be provided between adjacent parts to prevent their pounding against each other. To avoid pounding between adjacent buildings or parts of the same building when vibrating out of phase with each other, a gap equal to the square root of the sum of the squares (SRSS) of the maximum lateral deflections (considering the deflection amplification factors specified in building codes) of the two structures under the design (code-specified) lateral forces, or the SRSS of the maximum deflections of the two structures as indicated by a dynamic analysis, would be desirable.

A good basis for the preliminary design of an earthquake-resistant building is a structure proportioned to satisfy the requirements for

gravity and wind loads. The planning and layout of the structure, however, must be undertaken with due consideration of the special requirements for earthquake-resistant design. Thus, modifications in both configuration and proportions to anticipate earthquake-related requirements should be incorporated at the outset into the basic design for gravity and wind. Essential to the finished design is particular attention to details that can often mean the difference between a severely damaged structure and one with only minor, repairable damage.

10.5.2 Example Designs of Elements of a 12-Story Frame-Shear Wall Building

The application of the earthquake-resistant design provisions of IBC-2000 with respect to design loads and those of ACI 318-95⁽¹⁰⁻¹⁰⁾ relating to proportioning and detailing of members will be illustrated for representative elements of a 12-story frame—shear wall building located in seismic zone 4. The use of the seismic design load provisions in IBC-2000, is based on the fact that it represents the more advanced version, in the sense of incorporating the latest revisions reflecting current thinking in the earthquake engineering profession.

The typical framing plan and section of the structure considered are shown in Figure 10-48a^c and b, respectively. The columns and structural walls have constant cross-sections throughout the height of the building. The floor beams and slabs also have the same dimensions at all floor levels. Although the dimensions of the structural elements in this example are within the practical range, the structure itself is hypothetical and has been chosen mainly for illustrative purposes. Other pertinent design data are as follows:

Service loads — vertical:

- Live load:

Basic, 50 lb/ft².

Additional average uniform load to allow for heavier basic load on corridors, 25 lb/ft².

Total average live load, 75 lb/ft².

Roof live load = 20 lb/ft²

- Superimposed dead load:

Average for partitions 20 lb/ft².

Ceiling and mechanical 10 lb/ft².

Total average superimposed dead load, 30 lb/ft².

Material properties:

- Concrete:
 $f'_c = 4000 \text{ lb/in.}^2$ $w_c = 145 \text{ lb/ft}^3$.
- Reinforcement:
 $f_y = 60 \text{ ksi}$.

Determination of design lateral forces

On the basis of the given data and the dimensions shown in Figure 10-48, the weights that may be considered lumped at a floor level (including that of all elements located between two imaginary parallel planes passing through mid-height of the columns above and below the floor considered) and the roof were estimated and are listed in Tables 10-1 and 10-2. The calculation of base shear V , as explained in Chapter 5, for the transverse and longitudinal direction is shown at the bottom of Tables 10-1 and 10-2. For this example, it is assumed that the building is located in Southern California with values of S_s and S_l of 1.5 and 0.6 respectively. The site is assumed to be class B (Rock) and the corresponding values of F_a and F_b are 1.0. On this basis, the design spectral response acceleration parameters S_{DS} and S_{MI} are 1.0 and 0.4 respectively. At this level of design parameters, the building is classified as Seismic Group D according to IBC-2000. The building consists of moment resisting frame in the longitudinal direction, and dual system consisting of wall and moment resisting frame in the transverse direction. Accordingly, the response modification factor, R , to be used is 8.0 in both directions.

^c Reproduced, with modifications, from Reference 10-78, with permission from Van Nostrand Reinhold Company.

Calculation of the undamped (elastic) natural periods of vibration of the structure in the transverse direction (N-S)

As shown in Figure 10-49 using the story weights listed in Table 10-1 and member stiffnesses based on gross concrete sections, yielded a value for the fundamental period of 1.17 seconds. The mode shapes and the corresponding periods of the first five modes of vibration of the structure in the transverse direction are shown in Figure 10-49. The fundamental period in the longitudinal (E-W) direction was 1.73 seconds. The mode shapes were calculated using the Computer Program ETABS⁽¹⁰⁻⁶⁶⁾, based on three dimensional analysis. In the computer model, the floors were assumed to be rigid. Rigid end offsets were assumed at the end of the members to reflect the actual behavior of the structure. The portions of the slab on each side of the beams were considered in the analysis based on the ACI 318-95 provisions. The structure was assumed to be fixed at the base. The two interior walls were modeled as panel elements with end piers (26x26 in.). The corresponding values of the fundamental period determined based on the approximate formula given in IBC-2000 were 0.85 and 1.27 seconds in the N-S and the E-W directions respectively. However, these values can be increased by 20% provided that they do not exceed those determined from analysis. On this basis, the value of T used to calculate the base shears were 1.02 and 1.52 seconds in the N-S and the E-W directions respectively.

The lateral seismic design forces acting at the floor levels, resulting from the distribution of the base shear in each principal direction are also listed in Tables 10-1 and 10-2.

For comparison, the wind forces and story shears corresponding to a basic wind speed of 85 mi/h and Exposure B (urban and suburban areas), computed as prescribed in ASCE 7-95, are shown for each direction in Tables 10-1 and 10-2.

Lateral load analysis of the structure along each principal direction, under the respective seismic and wind loads, based on three

dimensional analysis were carried out assuming no torsional effects.

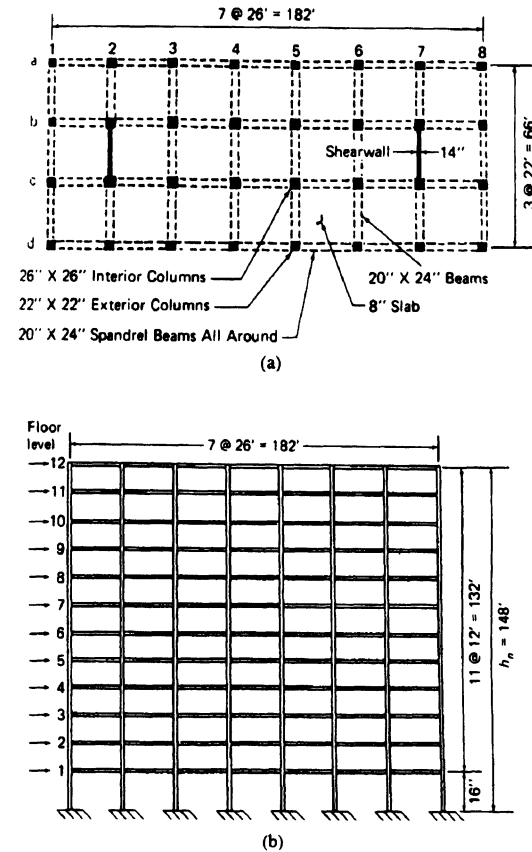


Figure 10-48. Structure considered in design example. (a) Typical floor framing plan. (b) Longitudinal section

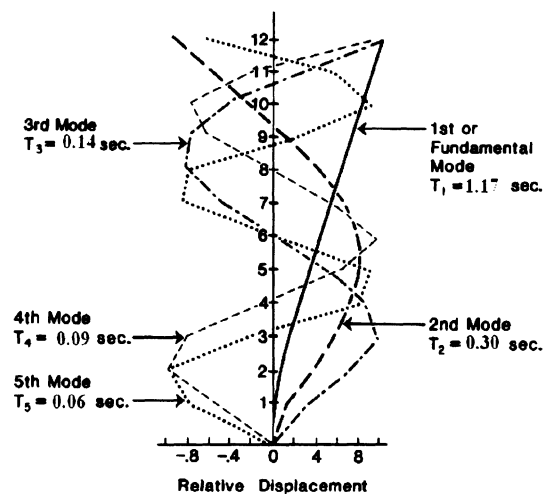


Figure 10-49. Undamped natural modes and periods of vibration of structure in transverse direction

Table 10-1. Design Lateral Forces in Transverse (Short) Direction (Corresponding to Entire Structure).

Floor Level	Height, h_x , ft	h_x^k $k=1.26$	story	Seismic forces				Wind forces		
			weight, w_x , kips $\times 10^3$	$w_x h_x^k$ ft-kips	C_{vx}	Lateral force, F_x kips	Story shear ΣF_x , kips	wind pressure lbs/ ft^2	lateral force H_x , kips	Story shear ΣH_x , kips
Roof	148	543	2100	1140	0.162	208.8	208.8	21.1	23.0	23.0
11	136	488	2200	1073	0.152	196.0	404.8	20.9	45.6	68.9
10	124	434	2200	955	0.135	174.0	578.8	20.5	44.8	113.4
9	112	382	2200	840	0.120	154.7	733.5	20.2	44.1	157.5
8	100	331	2200	728	0.103	132.8	866.3	19.8	43.2	200.7
7	88	282	2200	620	0.088	113.4	979.7	19.4	42.4	243.1
6	76	234	2200	515	0.073	94.1	1073.8	18.9	41.3	284.4
5	64	189	2200	415	0.059	76.1	1149.9	18.4	40.2	324.6
4	52	145	2200	320	0.045	58.0	1207.9	17.8	38.9	363.5
3	40	104	2200	230	0.033	42.5	1250.4	17.1	37.3	400.8
2	28	67	2200	147	0.021	27.1	1277.5	16.2	35.4	436.2
1	16	33	2200	72	0.010	12.9	1290.4	14.9	38.0	474.2
Total		-	26,300	7055	-	1290.4	-	-	474.2	-

Calculation of Design Base Shear in Transverse (Short) Direction

$$\text{Base shear, } V = C_S W \text{ where } 0.1 S_{D1} I < C_S = \frac{S_{DS}}{R/I} < \frac{S_{D1}}{T(R/I)}$$

$S_{DS} = 2/3 S_{MS}$, where $S_{MS} = F_a S_S = 1.0 \times 1.5 = 1.5$ and $S_{D1} = 2/3 S_{MI}$

where $S_{MI} = F_v S_1 = 1.0 \times 0.6 = 0.6$; $S_{DS} = 1.0$, $S_{D1} = 0.4$; $R=8$; $I=1.0$; $T=C_T h_n^{3/4} = 0.02 \times (148)^{3/4} = 0.849$ sec; T can be increased by a factor of 1.2 but should be less than the calculated value (i.e. 1.17 sec). $\therefore T = 0.849 \times 1.2 = 1.018 < 1.17$

$$0.1 \times 0.4 < C_S = \frac{1.0}{8/1} < \frac{0.4}{1.018(8/1)}$$

$$0.04 < C_S = 0.125 < 0.0491 \therefore \text{use } C_S = 0.0491$$

$$V = 0.0491 \times 26,300 = 1290.4 \text{ kips}$$

Table 10-2. Design Lateral Forces in Longitudinal Direction (Corresponding to Entire Structure).

Floor Leve l	Height, h_x , ft	h_x^k $k=1.51$	story weight, w_x , kips	Seismic forces				Wind forces		
				$w_x h_x^k \text{ ft-kips } \times 10^3$	C_{vx}	Lateral force, F_x , kips	Story shear ΣF_x , kips	wind pressure lbs/ ft^2	lateral force H_x , kips	Story shear ΣH_x , kips
Roof	148	1893	2100	3975	0.178	154.5	154.5	17.2	6.8	6.8
11	136	1666	2200	3665	0.164	142.4	296.9	17.0	13.5	20.3
10	124	1449	2200	3188	0.142	123.3	420.2	16.6	13.1	33.4
9	112	1243	2200	2734	0.122	105.9	526.1	16.3	12.9	46.3
8	100	1047	2200	2304	0.103	89.4	615.5	15.9	12.6	58.9
7	88	863	2200	1899	0.085	73.8	689.3	15.5	12.3	71.2
6	76	692	2200	1522	0.068	59.0	748.3	15.0	12.0	83.2
5	64	534	2200	1174	0.052	45.1	793.4	14.5	11.5	94.7
4	52	390	2200	858	0.038	33.0	826.4	13.9	11.0	105.7
3	40	263	2200	578	0.026	22.6	849.0	13.2	10.5	116.2
2	28	153	2200	337	0.015	13.0	862.0	12.3	9.7	125.9
1	16	66	2200	145	0.006	5.2	867.2	11.0	10.2	136.1
Total		-	26,300	22,379	-	867.2	-	-	136.1	-

In longitudinal direction, C_t (for reinforced concrete moment resisting frames) = 0.03;

$T = C_t (h_n)^{3/4} = (0.03) (148)^{3/4} = 1.27$; T can be increased by a factor of 1.2,

$$\therefore T = 1.2 \times 1.27 = 1.524 < 1.73$$

$$0.1 \times 0.4 < C_s = \frac{1.0}{8/1} < \frac{0.4}{1.524(8/1)}$$

$$0.04 < C_s = 0.125 < 0.0329 \therefore \text{use } C_s = 0.0329$$

$$V = 0.033 \times 26,300 = 867.2 \text{ kips}$$

(a) Lateral displacements due to seismic and wind effects: The lateral displacements due to both seismic and wind forces listed in Tables 10-1 and 10-2 are shown in Figure 10-50. Although the seismic forces used to obtain the curves of Figure 10-50 are approximate, the results shown still serve to draw the distinction between wind and seismic forces, that is, the fact that the former are external forces the magnitudes of which are proportional to the exposed surface, while the latter represent inertial forces depending primarily on the mass and stiffness properties of the structure. Thus, while the ratio of the total wind force in the transverse direction to that in the longitudinal direction (see Tables 10-1 and 10-2) is about 3.5, the corresponding ratio

for the seismic forces is only 1.5. As a result of this and the smaller lateral stiffness of the structure in the longitudinal direction, the displacement due to seismic forces in the longitudinal direction is significantly greater than that in the transverse direction. By comparison, the displacements due to wind are about the same for both directions. The typical deflected shapes associated with predominantly cantilever or flexure structures (as in the transverse direction) and shear (open-frame) buildings (as in the longitudinal direction) are evident in Figure 10-50. The average deflection indices, that is, the ratios of the lateral displacement at the top to the total height of the structure, are 1/5220 for wind and 1/730 for seismic

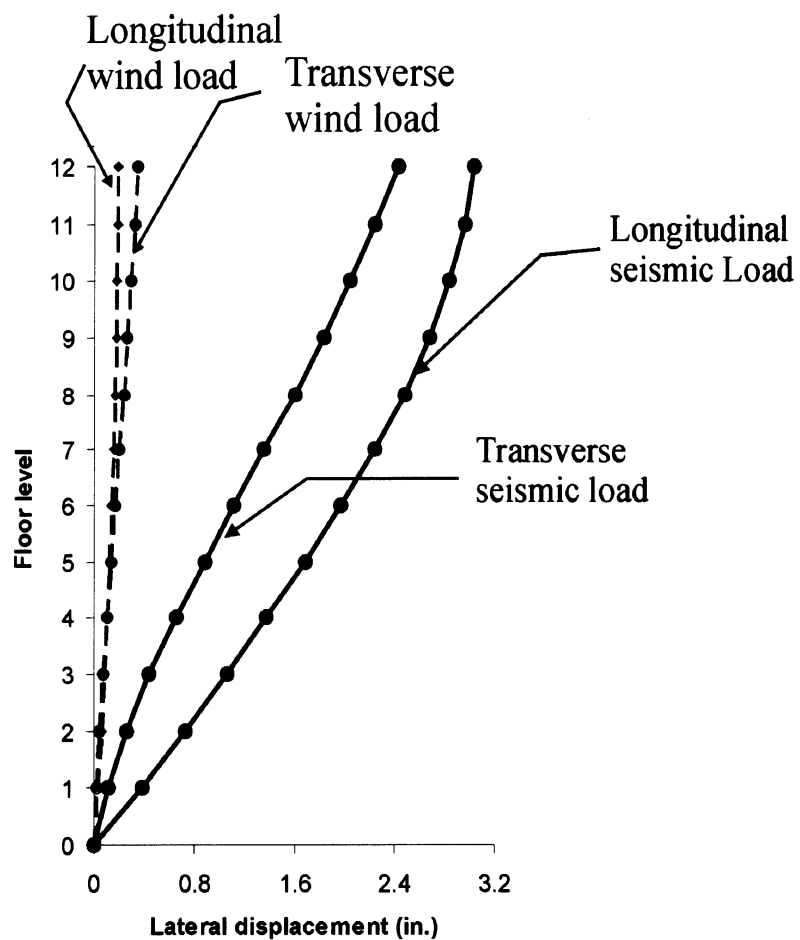


Figure 10-50. Lateral displacements under seismic and wind loads.

loads in the transverse direction. The corresponding values in the longitudinal direction are 1/9350 for wind and 1/590 for seismic loads. It should be noted that the analysis for wind was based on uncracked sections whereas that for seismic was based on cracked sections. The use of cracked section moment of inertia is a requirement by IBC-2000 for calculation of drift due to earthquake loading. However, under wind loading, the stresses within the structure in this particular example are within the elastic range as can also be observed from the amount of lateral deflections. As a result, the amount of cracking within the members is expected to be insignificant. However, for the case of seismic loading, the members are expected to deform well into inelastic range of response under the design base shear. To consider the effects of cracked sections due to seismic loads, the moments of inertia of beams, columns and walls were assumed to be 0.5, 0.7 and 0.5 of the gross concrete sections respectively.

- (b) Drift requirements: IBC-2000 requires that the design story drift shall not exceed the allowable limits. In calculating the drift limits, the effect of accidental torsion was considered in the analysis. On this basis, the mass at each floor level was assumed to displace from the calculated center of mass a distance equal to 5% of the building dimension in each direction. Table 10-3 shows the calculated displacements and the corresponding story drifts in both E-W and N-S directions. To determine the actual story drift, the calculated drifts were amplified using the C_d factor of 6.5 according to IBC-2000. These increased drifts account for the total anticipated drifts including the inelastic effects. The allowable drift limit based on IBC-2000 is 0.025 times the story height which corresponds to 3.6 in. and 4.8 in. at a typical floor and first floor respectively. The calculated values of drift are less than these limiting values. It is to be noted that using IBC-2000 provisions, it is permissible

to use the computed fundamental period of the structure without the upper bound limitation when determining the story drifts limits. However, the drift values shown are based on the calculated values of the fundamental period based on the code limits. Since the calculated drifts are less than the allowable values, further analysis based on the adjusted value of period was not necessary. In addition, the P-Δ effect need not to be considered in the analysis when the stability coefficient as defined by IBC-2000 is less than a limiting value. For the 12-story structure, the effect of P-Δ was found to be insignificant.

- (c) Load Combinations: For design and detailing of structural components, IBC-2000 requires that the effect of seismic loads to be combined with dead and live loads. The loading combinations to be used are those prescribed in ASCE-95 as illustrated in Equation (10-2) except that the effect of seismic loads are according to IBC-2000 as defined in Equation (10-3).

To consider the extent of structural redundancy inherent in the lateral-force-resisting system, the reliability factor, ρ , is defined as follows for structures in seismic design category D as defined by IBC-2000:

$$\rho = 2 - \frac{20}{r_{\max} \sqrt{A_x}}$$

where

r_{\max} = the ratio of the design story shear resisted by the single element carrying the most shear force in the story to the total story shear, for a given direction of loading. For shear walls, r_{\max} is defined as the shear in the most heavily loaded wall multiplied by $10/l_w$, divided by the story shear (l_w is the wall length)

A_x = the floor area in square feet of the diaphragm level immediately above the story

Table 10-3. Lateral displacements and Interstory drifts Due to Seismic Loads (in.).

Story Level	E-W Direction			N-S Direction		
	displacement	drift	drift × C _d *	displacement	drift	drift × C _d *
Roof	3.03	0.07	0.45	2.43	0.19	1.24
11	2.96	0.12	0.78	2.24	0.20	1.30
10	2.84	0.16	1.04	2.04	0.21	1.37
9	2.68	0.20	1.30	1.83	0.23	1.50
8	2.48	0.24	1.56	1.60	0.24	1.56
7	2.24	0.27	1.76	1.36	0.24	1.56
6	1.97	0.28	1.82	1.12	0.23	1.50
5	1.69	0.31	2.02	0.89	0.23	1.50
4	1.38	0.32	2.08	0.66	0.22	1.43
3	1.06	0.33	2.15	0.44	0.18	1.17
2	0.73	0.34	2.21	0.26	0.15	0.98
1	0.39	0.39	2.54	0.11	0.11	0.72

* C_d = 6.5

When calculating the reliability factor for dual systems such as the frame wall structure in the N-S direction, it can be reduced to 80 percent of the calculated value determined as above. However, this value can not be less than 1.0.

In the N-S direction, the most heavily single element for shear is the shear wall. Table 10-4 shows the calculated values for r over the 2/3 height of the structure. The maximum value of r occurs at the base of the structure where the shear walls carry most of the shear in the N-S direction. On this basis, the maximum value of ρ determined was 1.0.

The load combinations used for the design based on $\rho = 1.0$ and S_{DS} = 1.0 by combining

Table 10-4. Element story shear ratios for redundancy factor in N-S direction.

Story Level	V _i = shear force in wall	V _i x 10/L _w	story shear	r _i
8	189	78	886	0.09
7	234	97	980	0.10
6	275	114	1074	0.11
5	317	131	1150	0.11
4	359	149	1208	0.12
3	408	169	1250	0.14
2	448	185	1278	0.15
1	570	236	1290	0.18

$$\rho = 2 - \frac{20}{r_{\max} \sqrt{A_x}}$$

$$\rho = 2 - \frac{20}{0.18 \times \sqrt{66 \times 182}} = 0.99 \quad \text{but} \quad \rho_{\min} = 1.0$$

equations (10-2) and (10-3) are as follows:

$$U = \begin{cases} 1.2D + 1.6L + 0.5L_r \\ 1.4D \pm 1.0Q_E + 0.5L \\ 0.7D \pm 1.0Q_E \end{cases} \quad (10-8)$$

The 3-D structure was analyzed using the above load combinations. The dead and live loads were applied to the beams based on tributary areas as shown in Figure 10-51. The effect of accidental torsion was also considered in the analysis.

To protect the building against collapse, IBC-2000 requires that in dual systems, the moment resisting frames be capable to resist at least 25% of prescribed seismic forces. For this reason, the building in the N-S direction was also subjected to 25% of the lateral forces described above without including the shear

walls.

An idea of the distribution of lateral loads among the different frames making up the structure in the transverse direction may be obtained from Table 10-5, which lists the portion of the total story shear at each level resisted by each of the three groups of frames. The four interior frames along lines 3, 4, 5, and 6 are referred to as Frame T-1, while the Frame T-2 represents the two exterior frames along lines 1 and 8. The third frame, T-3 represents the two identical frame-shear-wall systems along lines 2 and 7. Note that at the top (12th floor level), the lumped frame T-1 takes 126% of the total story shear. This reflects the fact that in frame-shear-wall systems of average proportions, interaction between frame and wall under lateral loads results in the frame "supporting" the wall at the top, while at the base most of the horizontal shear is resisted by

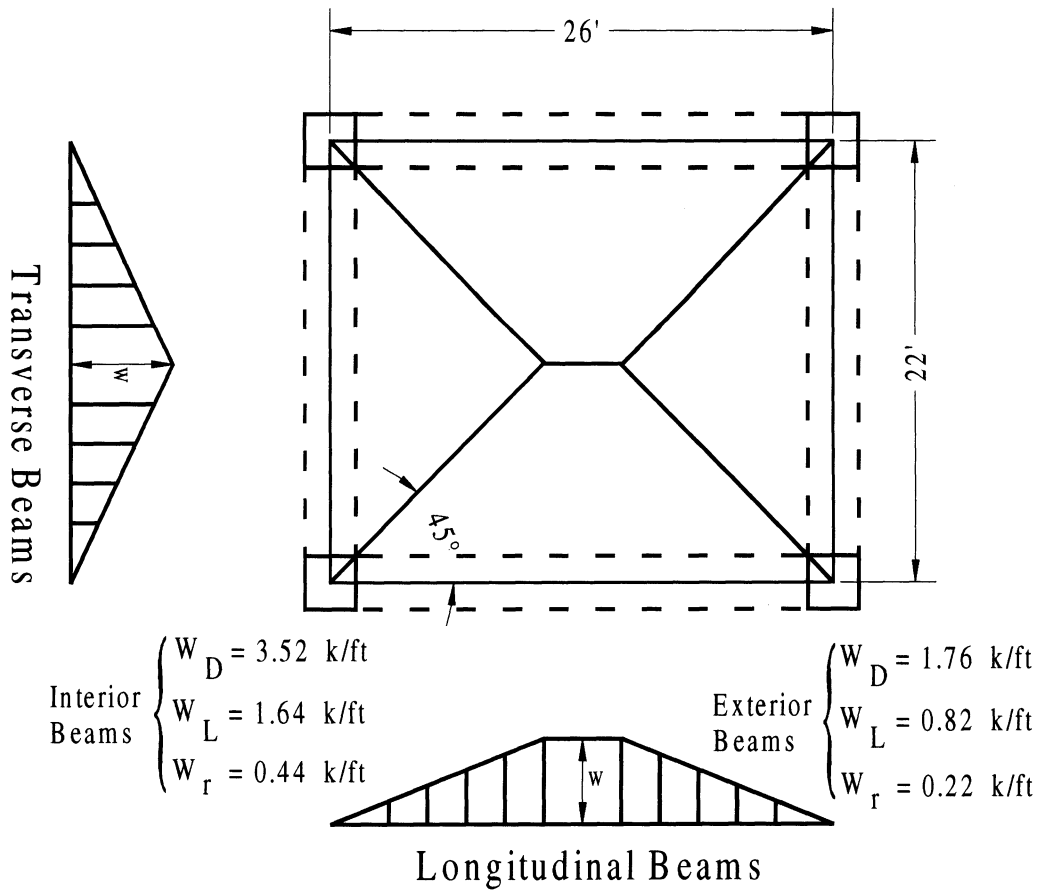


Figure 10-51. Tributary area for beam loading.

Table 10-5. Distribution of Horizontal Seismic Story Shears among the Three Transverse Frames.

Story Level	Frame T-1 (4 interior frames)		Frame T-2 (2 exterior frames)		Frame T-3 (2 interior frames with shear walls)		Total story shear, kips
	Story shear	% of total	Story shear	% of total	Story shear	% of Total	
Roof	263.6	126	102.1	49	-156.9	-75	208.8
11	228.5	56	90.3	22	86.0	21	404.8
10	259.9	45	101.9	18	216.8	37	578.8
9	282.5	39	110.4	15	340.6	46	733.5
8	303.6	35	117.3	14	445.4	51	866.3
7	317.3	32	123.6	13	538.8	55	979.7
6	324.0	30	125.6	12	624.2	58	1073.8
5	320.0	28	124.0	11	705.9	61	1149.9
4	303.2	25	117.9	10	786.8	65	1207.9
3	269.6	22	104.4	8	876.4	70	1250.4
2	225.1	18	86.4	7	966.0	75	1277.5
1	96.0	7	34.8	3	1159.6	90	1290.4

the wall. Table 10-5 indicates that for the structure considered, the two frames with walls take 90% of the shear at the base in the transverse direction.

To illustrate the design of two typical beams on the sixth floor of an interior frame, the results of the analysis in the transverse direction under seismic loads have been combined, using Equation 10-8, with results from a gravity-load analysis. The results are listed in Table 10-6. Similar values for typical exterior and interior columns on the second floor of the same interior frame are shown in Table 10-7. Corresponding design values for the structural wall section at the first floor of frame on line 3 (see Figure 10-48) are listed in Table 10-8. The

last column in Table 10-8 lists the axial load on the boundary elements (the 26 × 26-in, columns forming the flanges of the structural walls) calculated according to the ACI requirement that these be designed to carry all factored loads on the walls, including self-weight, gravity loads, and vertical forces due to earthquake-induced overturning moments. The loading condition associated with this requirement is illustrated in Figure 10-45. In both Tables 10-7 and 10-8, the additional forces due to the effects of horizontal torsional moments corresponding to the minimum IBC-2000 -prescribed eccentricity of 5% of the building dimension perpendicular to the direction of the applied forces have been included.

Table 10-6. Summary of design moments for typical beams on sixth floor of interior transverse frames along lines 3 through 6 (Figure 10-48a).

$$U = \begin{cases} 1.2D + 1.6L + 0.5L_r & (9-8a) \\ 1.4D + 0.5L \pm 1.0Q_E & (9-8b) \\ 0.7D \pm 1.0Q_E & (9-8c) \end{cases}$$

<u>BEAM AB</u>		Design moment, ft-kips		
		A	Midspan of AB	B
9-8 a		-76	+100	-202
9-8 b	Sides way to right	+91	+83	-326
	Sides way to left	-213	+85	-19
9-8 c	Sides way to right	+127	+35	-229
	Sides way to left	-177	+37	+79
<u>BEAM BC</u>		Design moment, ft-kips		
		B	Midspan of BC	C
9-8 a		-144	+92	-144
9-8 b	Sides way to right	-41	+77	-282
	Sides way to left	-282	+77	-41
9-8 c	Sides way to right	+110	+33	-213
	Sides way to left	-213	+33	+110

Table 10-7. Summary of design moments and axial loads for typical columns on second floor of interior transverse frames along lines 3 through 6 (Figure 10-48a).

$$U = \begin{cases} 1.2D + 1.6L + 0.5L_r & (9-8a) \\ 1.4D + 0.5L \pm 1.0Q_E & (9-8b) \\ 0.7D \pm 1.0Q_E & (9-8c) \end{cases}$$

		Exterior Column A			Interior Column B		
		Axial load, kips	Moment, ft-kips		Axial load, kips	Moment, ft-kips	
			Top	Kips		Top	Bottom
9-8 a		-1076	-84	+94	-1907	+6	-12
9-8 b	Sides way to right	-806	-33	+25	-1630	+73	-108
	Sides way to left	-1070	-110	+134	-1693	-94	+119
9-8 c	Sides way to right	-280	+8	-20	-698	+79	-111
	Sides way to left	-544	-69	+88	-760	-88	+116

It is pointed out that for buildings located in seismic zones 3 and 4 (i.e., high-seismic-risk areas), the detailing requirements for ductility prescribed in ACI Chapter 21 have to be met even when the design of a member is governed by wind loading rather than seismic loads.

2. Design of flexural member AB. The aim is to determine the flexural and shear reinforcement for the beam *AB* on the sixth floor of a typical interior transverse frame. The critical design (factored) moments are shown circled in Table 10-6. The beam has dimensions *b* = 20 in. and *d* = 21.5 in. The slab is 8 in. thick, $f'_c = 4000 \text{ lb/in.}^2$ and $f_y = 60,000 \text{ lb/in.}^2$.

In the following solution, the boxed-in section numbers at the right-hand margin correspond to those in ACI 318-95.

- (a) Check satisfaction of limitations on section dimensions:

$$\frac{\text{width}}{\text{depth}} = \frac{20}{21.5}$$

$$= 0.93 > 0.3 \text{ O.K. } [21.3.1.3]$$

21.3.1.4

$$\begin{aligned} \text{width} = 20 \text{ in.} & \begin{cases} \geq 10 \text{ in.} & \text{O.K.} \\ \leq (\text{width of supporting column} \\ + 1.5 \times \text{depth of beam}) \\ = 26 + 1.5(21.5) = 58.25 \text{ in.} & \text{O.K.} \end{cases} \end{aligned}$$

Table 10-8. Summary of design loads on structural wall section at first floor level of transverse frame along line 2 (or 7) (Figure 10-48a).

$$U = \begin{cases} 1.2D + 1.6L + 0.5L_r & (9-8a) \\ 1.4D + 0.5L \pm 1.0Q_E & (9-8b) \\ 0.7D \pm 1.0Q_E & (9-8c) \end{cases}$$

	Design forces acting on entire structural wall			Axial load [#] on boundary element, kips
	Axial Load, kips	Bending (overturning) Moment, ft-kips	Horizontal shear, kips	
9-8 a	-5767	Nominal	Nominal	-2884
9-8 b	-5157	30469	651	-3963
9-8 c	-2293	30469	651	-2531

[#] Based on loading condition illustrated in Figure 10-45 @ bending moment at base of wall

(b) Determine required flexural reinforcement:

(1) Negative moment reinforcement at support *B*: Since the negative flexural reinforcement for both beams *AB* and *BC* at joint *B* will be provided by the same continuous bars, the larger negative moment at joint *B* will be used. In the following calculations, the effect of any compressive reinforcement will be neglected. From $C = 0.85f_c'ba = T = A_s f_y$,

$$a = \frac{A_s}{0.85f_c'b} = \frac{60A_s}{(0.85)(4)(20)} = 0.882A_s$$

$$M_u \leq \phi M_n = \phi A_s f_y (d - a/2)$$

$$-(326)(12) = (0.90)(60)A_s \times [21.5 - (0.5)(0.882A_s)]$$

$$A_s^2 - 48.76A_s + 164.3 = 0$$

or

$$A_s = 3.64 \text{ in.}^2$$

Alternatively, convenient use may be made of design charts for singly reinforced flexural members with rectangular cross-sections, given in

standard references.⁽¹⁰⁻⁷⁹⁾ Use five No. 8 bars, $A_s = 3.95 \text{ in.}^2$. This gives a negative moment capacity at support *B* of $\phi M_n = 351 \text{ ft-kips}$.

Check satisfaction of limitations on reinforcement ratio:

$$\rho = \frac{A_s}{bd} = \frac{3.95}{(20)(21.5)} = 0.0092$$

$$> \rho_{\min} = \frac{200}{f_y} = 0.0033$$

$$> \rho_{\min} = \frac{3\sqrt{f_c'}}{f_y} = \frac{3\sqrt{4000}}{60,000} = 0.0032$$

and $< \rho_{\max} = 0.025$ O.K.

(2) Negative moment reinforcement at support *A*:

$$M_u = 213 \text{ ft-kips}$$

As at support *B*, $a = 0.882A_s$.

Substitution into

$$M_u = \phi A_s f_y (d - a/2)$$

yields $A_s = 2.31 \text{ in.}^2$. Use three No. 8 bars, $A_s = 2.37 \text{ in.}^2$. This gives a negative moment capacity at support *A* of $\phi M_n = 218 \text{ ft-kips}$.

(3) Positive moment reinforcement at supports: A positive moment capacity at the supports equal to at least 50% of the corresponding negative moment capacity is required, i.e., 21.3.2.2

$$\min M_u \text{ (at support A)} = \frac{218}{2} = 109 \text{ ft-kips}$$

which is less than $M^+_{\max} = 127$ ft-kips at A (see Table 10-6), but greater than the required M_u^+ near midspan of AB ($= 100$ ft-kips).

$$\min M_u^+ \text{ (at support B for both spans AB and BC)} = \frac{351}{2} = 176 \text{ ft-kips}$$

Note that the above required capacity is greater than the design positive moments near the mid-spans of both beams AB and BC.

Minimum positive/negative moment capacity at any section along beam AB or BC $= 351/4 = 87.8$ ft-kips.

- (4) Positive moment reinforcement at mid-span of beam AB- to be made continuous to supports: (with an effective T-beam section flange width = 52 in.)

$$a = \frac{A_s f_y}{0.85 f_c' b} = \frac{60 A_s}{(0.85)(4)(52)} = 0.339 A_s$$

Substituting into

$$M_u = (127)(12) = \phi A_s f_y \left(d - \frac{a}{2} \right)$$

yields A_s (required) $= 1.35$ in.². Similarly, corresponding to the required capacity at support B, $M_u^+ = 163$ ft-kips, we have A_s (required) $= 1.74$ in.². Use three No. 7 bars continuous through both spans. $A_s = 1.80$ in.². This provides a positive moment capacity of 172 ft-kips.

Check:

$$\rho = \frac{1.8}{(20)(21.5)} = 0.0042$$

$$> \rho_{\min} = \frac{200}{f_y} = 0.0033 \quad \text{O.K.} \quad \boxed{10.5.1}$$

$$> \rho_{\min} = \frac{3\sqrt{f'_c}}{f_y} = \frac{3\sqrt{4000}}{60,000}$$

- (c) Calculate required length of anchorage of flexural reinforcement in exterior column:

$$\text{Development length } l_{dh} \geq \begin{cases} f_y d_b / 65\sqrt{f'_c} \\ 8d_b \\ 6 \text{ in.} \end{cases} \quad \boxed{21.5.4.1}$$

(plus standard 90° hook located in confined region of column). For the No. 8 (top) bars (bend radius, measured on inside of bar, $\geq 3d_b = 3.0$ in.),

$$l_{dh} \geq \begin{cases} \frac{(60,000)(1.0)}{65\sqrt{4000}} = 15 \text{ in.} \\ (8)(1.0) = 8.0 \text{ in.} \\ 6 \text{ in.} \end{cases}$$

For the No. 7 bottom bars (bend radius $\geq 3d_b = 2.7$ in.), $l_{dh} = 13$ in.

Figure 10-52 shows the detail of flexural reinforcement anchorage in the exterior column. Note that the development length l_{dh} is measured from the near face of the column to the far edge of the vertical 12-bar-diameter extension (see Figure 10-35).

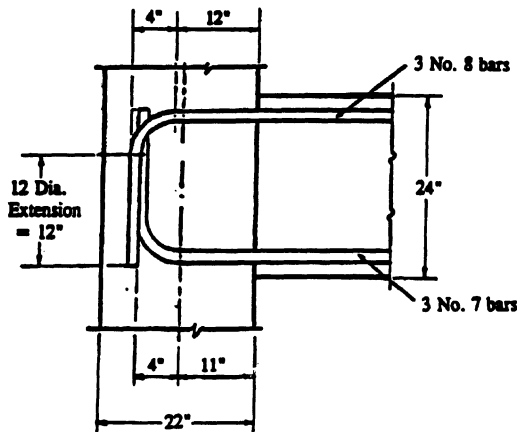


Figure 10-52. Detail of anchorage of flexural reinforcement in exterior column

(d) Determine shear-reinforcement requirements: Design for shears corresponding to end moments obtained by assuming the stress in the tensile flexural reinforcement equal to $1.25f_y$ and a strength reduction factor $\phi = 1.0$, plus factored gravity loads (see Figure 10-16). Table 10-9 shows values of design end shears corresponding to the two loading cases to be considered. In the table,

$$W_u = 1.2 W_D + 1.6 W_L = 1.2 \times 3.52 + 1.6 \times 1.64 = 6.85 \text{ kips/ft}$$

ACI Chapter 21 requires that the contribution of concrete to shear resistance, V_c , be neglected if the earthquake-induced shear force (corresponding to the probable flexural strengths at beam ends calculated using $1.25f_y$ instead of f_y and $\phi = 1.0$) is greater than one-half the total design shear and the axial compressive force including earthquake effects is less than $A_g f'_c / 20$.

21.3.4.2

For sidesway to the right, the shear at end B due to the plastic end moments in the beam (see Table 10-9) is

$$V_b = \frac{230 + 477}{20} = 35.4 \text{ kips.}$$

which is approximately 50% of the total design shear, $V_u = 69.6$ kips. Therefore, the contribution of concrete to shear resistance can be considered in determining shear reinforcement requirements.

At right end B, $V_u = 69.6$ kips. Using

$$V_c = 2\sqrt{f'_c b_w d} = \frac{2\sqrt{4000}(20)(21.5)}{1000} = 54.4 \text{ kips}$$

we have

$$\begin{aligned} \phi V_s &= V_u - \phi V_c = 69.6 - 0.85 \times 54.4 \\ &= 23.4 \text{ kips} \end{aligned} \quad [11.1.1]$$

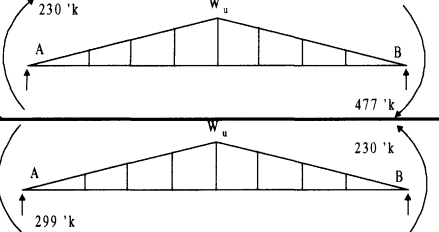
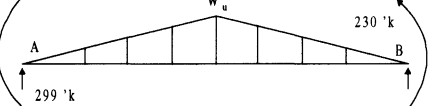
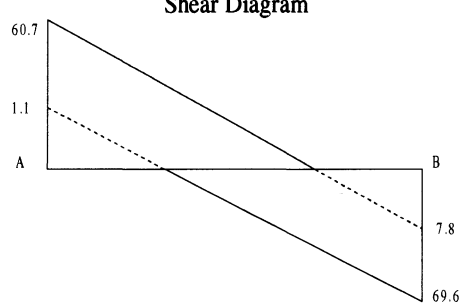
$$V_s = 27.5 \text{ kips}$$

Required spacing of No. 3 closed stirrups (hoops), since A_v (2 legs) = 0.22 in.²:

$$\begin{aligned} s &= \frac{A_v f_y d}{V_s} = \frac{(0.22)(60)(21.5)}{27.5} \\ &= 10.3 \text{ in.} \end{aligned} \quad [11.5.6.2]$$

Maximum allowable hoop spacing within distance $2d = 2(21.5) = 43$ in. from faces of supports:

Table 10-9. Determination of Design Shears for Beam AB.

Loading	$V_u = \frac{M_{pr}^A + M_{pr}^B}{l} \pm \frac{w_u l}{2}, (\text{kips})$	
	A	B
	1.1	69.6
	60.7	7.8
Shear Diagram		
		

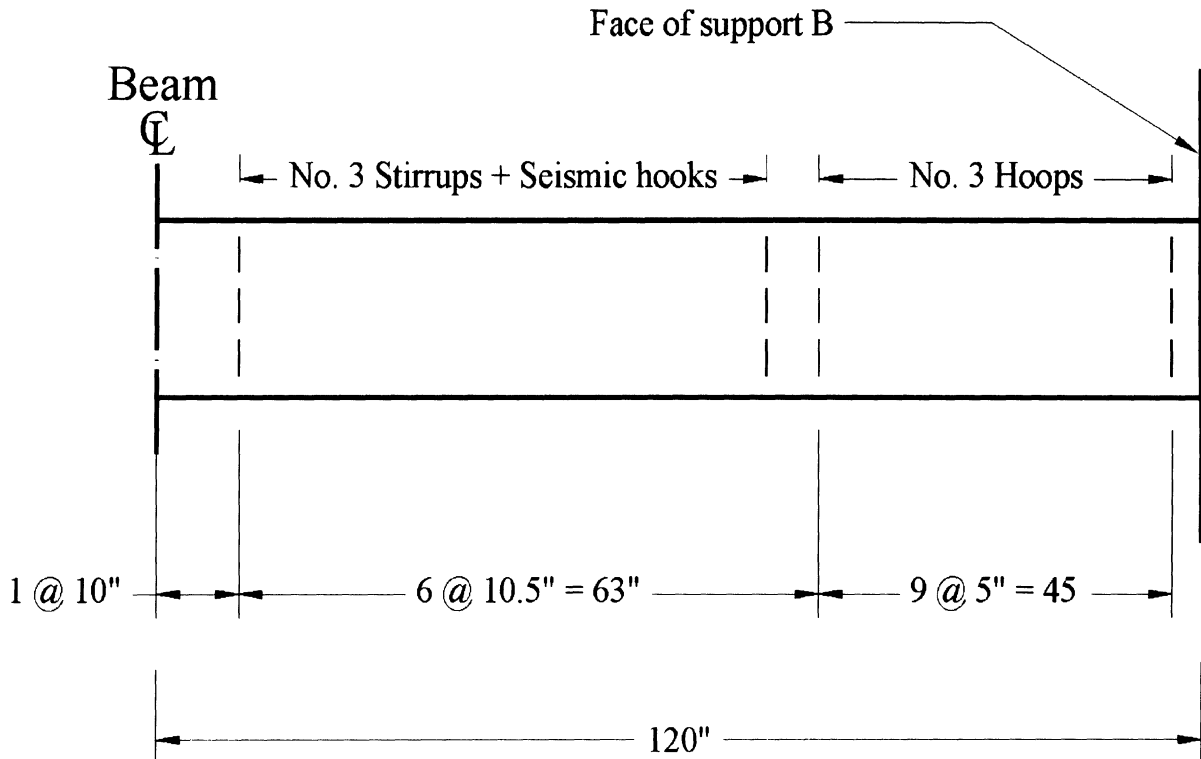


Figure 10-53. Spacing of hoops and stirrups in right half of beam AB

$$s_{\max} = \begin{cases} d/4 = 21.5/4 = 5.4 \text{ in.} \\ 8 \times (\text{dia. of smallest long. bar}) \\ = 8(0.875) = 7 \text{ in.} \\ 24 \times (\text{dia. of hoop bars}) = 24(0.375) = 9 \text{ in.} \\ 12 \text{ in.} \end{cases}$$

21.3.3.2

Beyond distance $2d$ from the supports, maximum spacing of stirrups:

$$s_{\max} = d/2 = 10.75 \text{ in.}$$

21.3.3.4

Use No. 3 hoops/stirrups spaced as shown in Figure 10-53. The same spacing, turned around, may be used for the left half of beam AB.

Where the loading is such that inelastic deformation may occur at intermediate points within the span (e.g., due to concentrated loads at or near mid-span), the spacing of hoops will have to be determined in a manner similar to that used above for regions near supports. In the present example, the maximum positive moment near mid-span (i.e., 100 ft-kips, see Table

10-6) is much less than the positive moment capacity provided by the three No. 7 continuous bars (172 ft-kips). **21.3.3.1**

(e) Negative-reinforcement cut-off points: For the purpose of determining cutoff points for the negative reinforcement, a moment diagram corresponding to plastic end moments and 0.9 times the dead load will be used. The cut-off point for two of the five No. 8 bars at the top, near support B of beam AB, will be determined.

With the negative moment capacity of a section with three No. 8 top bars equal to 218 ft-kips (calculated using $f_s = f_y = 60$ ksi and $\phi = 0.9$), the distance from the face of the right support B to where the moment under the loading considered equals 218 ft-kips is readily obtained by summing moments about section a—a in Figure 10-54 and equating these to -218 ft-kips. Thus,

$$51.8x - 477 - 3.2 \frac{x^3}{60} = -218$$

Solution of the above equation gives $x = 5.1$ ft. Hence, two of the five No. 8 bars near support *B* may be cut off (noting that $d = 21.5$ in. $> 12d_b = 12 \times 1.0 = 12$ in.) at

12.10.3

$$x + d = 5.1 + \frac{21.5}{12} = 6.9 \text{ ft say } 7.0 \text{ ft}$$

from the face of the right support *B*. With l_{dh} (see figure 10-35) for a No. 8 top bar equal to 14.6 in., the required development length for such a bar with respect to the tensile force associated with the negative moment at support *B* is $l_d = 3.5 l_{dh} = 3.5 \times 14.6/12 = 4.3$ ft < 7.0 ft. Thus, *the two No. 8 bars may be cut off 7.0 ft from the face of the interior support *B*.* **21.5.4.2**

At end *A*, one of the three No. 8 bars may also be cut off at a similarly computed distance of 4.5 ft from the (inner) face of the exterior support *A*. *Two bars are required to run continuously along the top of the beam.*

21.3.2.3

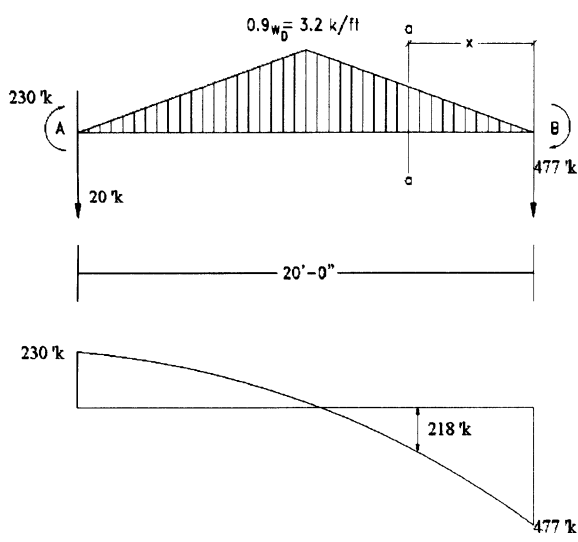


Figure 10-54. Moment diagram for beam AB

(f) Flexural reinforcement splices: Lap splices of flexural reinforcement should not be placed within a joint, within a distance $2d$ from faces of supports, or at locations of potential plastic hinging. Note that all lap

splices have to be confined by hoops or spirals with a maximum spacing or pitch of $d/4$, or 4 in., over the length of the lap. **21.3.2.3**

(1) Bottom bars, No. 7: The bottom bars along most of the length of the beam may be subjected to maximum stress. Steel area required to resist the maximum positive moment near midspan of 100 ft-kips (see Table 10-6), $A_s = 1.05$ in.² Area provided by the three No. 7 bars = 3 (0.60) = 1.80 in.², so that

$$\frac{A_{s(provided)}}{A_{s(required)}} = \frac{1.80}{1.05} = 1.71 < 2.0$$

Since all of the bottom bars will be spliced near midspan, use a class B splice. **12.15.2**

Required length of splice = $1.3 l_d \geq 12$ in. where

$$l_d = \frac{3}{40} \frac{d_b f_y}{\sqrt{f_c}} \frac{\alpha \beta \gamma \lambda}{c + k_{tr}} \quad \text{12.2.3}$$

where

$\alpha = 1.0$ (reinforcement location factor)

$\beta = 1.0$ (coating factor)

$\gamma = 1.0$ (reinforcement size factor)

$\lambda = 1.0$ (normal weight concrete)

$$c = 1.5 + 0.375 + \frac{0.875}{2} = 2.31 \quad (\text{governs})$$

(side cover, bottom bars)

or

$$c = \frac{1}{2} \left[\frac{20 - 2(1.5 + 0.375) - 0.875}{2} \right] = 3.84 \text{ in.}$$

(half the center to center spacing of bars)

$$k_{tr} = \frac{A_{tr} f_{yt}}{1500 s_n}$$

where

A_{tr} = total area of hoops within the spacing s and which crosses the potential plane of splitting through the reinforcement being developed (ie. for 3#3 bars)

f_y = specified yield strength of hoops
= 60,000 psi

s = maximum spacing of hoops
= 4 in.

n = number of bars being developed along the plane of splitting = 3

$$k_{tr} = \frac{(3 \times 0.11)60,000}{1500 \times 4.0 \times 3} = 1.1$$

$$\frac{c + k_{tr}}{d_b} = \left(\frac{2.31 + 1.1}{0.875} \right) = 3.90 > 2.5, \text{ use } 2.5$$

$$\therefore l_d = \frac{3}{40} \frac{0.875 \times 60,000}{\sqrt{4000}} \frac{1}{2.5} = 24.9 \text{ in.}$$

Required length of class B splice = $1.3 \times 24.9 = \underline{32.0 \text{ in.}}$

(2) Top bars, No. 8: Since the mid-span portion of the beam is always subject to a positive

bending moment (see Table 10-6), splices in the top bars should be located at or near midspan. Required length of class A splice = $1.0 l_d$.

For No. 8 bars,

$$l_d = \frac{3}{40} \frac{d_b f_y}{\sqrt{f'_c}} \frac{\alpha \beta \gamma \lambda}{\left(\frac{c + k_{tr}}{d_b} \right)}$$

where $\alpha = 1.3$ (top bars), $\beta = 1.0$, $\gamma = 1.0$, and $\lambda = 1.0$

$$c = 1.5 + 0.375 + \frac{1.0}{2} = 2.375 \text{ in. (governs)}$$

$$c = \frac{1}{2} \left[\frac{20 - 2(1.5 + 0.375) - 1.0}{2} \right] = 3.81 \text{ in.}$$

$$k_{tr} = 1.1$$

$$\frac{c + k_{tr}}{d_b} = \frac{2.375 + 1.1}{1.0} = 3.5 > 2.5 \text{ use } 2.5$$

$$\therefore l_d = \frac{3}{40} \frac{1.0 \times 60000}{\sqrt{4000}} \frac{1.3}{2.5} = 37.0 \text{ in.}$$

Required length of splice = $1.0 l_d = \underline{37.0 \text{ in.}}$

(g) Detail of beam. See Figure 10-55.

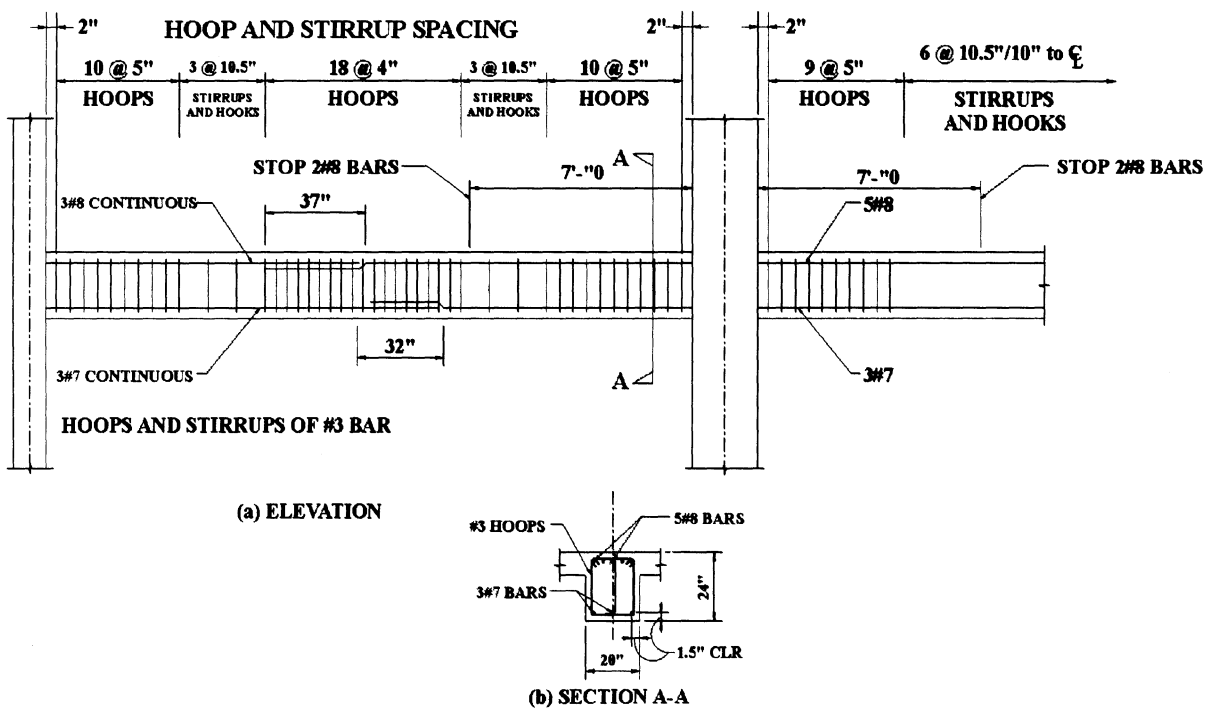


Figure 10-55. Detail of reinforcement for beam AB.

3. *Design of frame column A.* The aim here is to design the transverse reinforcement for the exterior tied column on the second floor of a typical transverse interior frame, that is, one of the frames in frame T-1 of Figure 10-48. The column dimension has been established as 22 in. square and, on the basis of the different combinations of axial load and bending moment corresponding to the three loading conditions listed in Table 10-7, *eight No. 9 bars arranged in a symmetrical pattern* have been found adequate.^(10-80,10-81) Assume the same beam section framing into the column as considered in the preceding section. $f_c' = 4000 \text{ lb/in.}^2$ and $f_y = 60,000 \text{ lb/in.}^2$

From Table 10-7, $P_u(\max) = 1076 \text{ kips}$:

$$P_u(\max) = 1076 \text{ kips} > \frac{A_g f_c'}{10} = \frac{(22)^2(4)}{10} = 194 \text{ kips}$$

Thus, ACI Chapter 21 provisions governing members subjected to bending and axial load apply. [21.4.1]

(a) Check satisfaction of vertical reinforcement limitations and moment capacity requirements:

(1) Reinforcement ratio:

$$0.01 \leq \rho \leq 0.06$$

$$\rho = \frac{A_{st}}{A_g} = \frac{8(1.0)}{(22)(22)} = 0.0165 \quad \text{O.K.}$$

[21.4.3.1]

(2) Moment strength of columns relative to that of framing beam in transverse direction (see Figure 10-56)

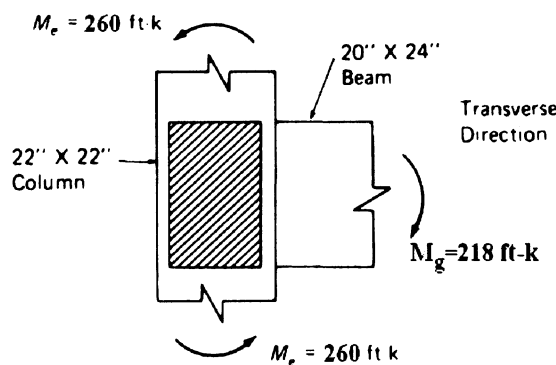


Figure 10-56. Relative flexural strength of beam and columns at exterior joint—transverse direction.

$$M_e(\text{columns}) \geq \frac{6}{5} M_g(\text{beams})$$

[21.4.2.2]

From Section 10.5.2, item 2, ϕM_n^- of the beam at A is 218 ft-kips, which may be mobilized during a sidesway to the left of the frame. From Table 10-7, the maximum axial load on column A at the second floor level for sidesway to the left is $P_u = 1070$ kips. Using the P - M interaction charts given in ACI SP-17A,⁽¹⁰⁻⁸¹⁾ the moment capacity of the column section corresponding to $P_u = \phi P_n = 1070$ kips, $f'_c = 4$ ksi, $f_y = 60$ ksi, $\gamma = 0.75$ (γ = ratio of distance between centroids of outer rows of bars to dimension of cross-section in the direction of bending), and $\rho = 0.0165$ is obtained as $\phi M_n = M_e = 260$ ft-kips. With the same size column above and below the beam, total moment capacity of columns = $2(260) = 520$ ft-kips. Thus,

$$\sum M_e = 520 > \frac{6}{5} M_g = \frac{(6)(218)}{5} = 262 \text{ ft-kips} \quad \text{O.K.}$$

(3) Moment strength of columns relative to that of framing beams in longitudinal direction (see Figure 10-57): Since the columns considered here are located in the center portion of the exterior longitudinal frames, the axial forces due to seismic loads in the longitudinal direction are negligible. (Analysis of the longitudinal frames under seismic loads indicated practically zero axial forces in the exterior columns of the four transverse frames represented by frame on line 1 in Figure 10-48) Under an axial load of $1.2 D + 1.6 L + 0.5 L_r = 1076$ kips, the moment capacity of the column section with eight No. 9 bars is obtained as $\phi M_n = M_e = 258$ ft-kips. If we assume a ratio for the negative moment reinforcement of about 0.0075 in the beams of the exterior longitudinal frames ($b_w = 20$ in., $d = 21.5$ in.), then

$$A_s = \rho b_w d \approx (0.0075)(20)(21.5) = 3.23 \text{ in.}^2$$

Assume four No. 8 bars, $A_s = 3.16$ in. Negative moment capacity of beam:

$$a = \frac{A_s f_y}{0.85 f_c b_w} = \frac{(3.16)(60)}{(0.85)(4)(20)} = 2.79 \text{ in}$$

$$\begin{aligned}\phi M_n &= M_g = \phi A_s f_y \left(d - \frac{a}{2} \right) \\ &= (0.90)(3.16)(60)(21.5 - 1.39)/12 \\ &= 286 \text{ ft-kips}\end{aligned}$$

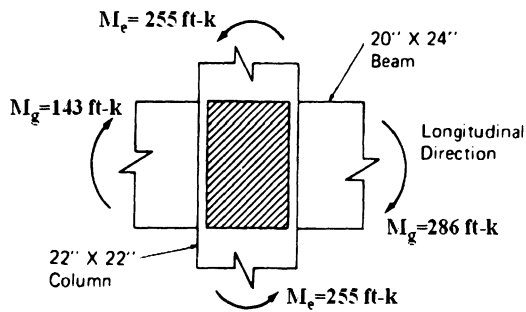


Figure 10-57. Relative flexural strength of beam and columns at exterior joint—longitudinal direction.

Assume a positive moment capacity of the beam on the opposite side of the column equal to one-half the negative moment capacity calculated above, or 143 ft-kips. Total moment capacity of beams framing into joint in longitudinal direction, for sidesway in either direction:

$$\sum M_g = 286 + 143 = 429 \text{ ft-kips}$$

$$\sum M_e = 2(258) = 516 \text{ ft-kips}$$

$$> \frac{6}{5} \sum M_g = \frac{6}{5}(429) = 515 \text{ ft-kips}$$

O.K. [21.4.2.2]

- (b) Orthogonal effects: According to IBC-2000, the design seismic forces are permitted to be applied separately in each of the two orthogonal directions and the orthogonal effects can be neglected.
- (c) Determine transverse reinforcement requirements:

(1) Confinement reinforcement (see Figure 10-38). Transverse reinforcement for confinement is required over a distance l_0 from column ends, where

$$l_0 \geq \begin{cases} \text{depth of member} = 22 \text{ in. (governs)} \\ \frac{1}{6}(\text{clear height}) = \frac{10 \times 12}{6} = 20 \text{ in.} \\ 18 \text{ in.} \end{cases} \quad [21.4.4.4]$$

Maximum allowable spacing of rectangular hoops:

$$s_{\max} = \begin{cases} \frac{1}{4}(\text{smallest dimension of column}) \\ = \frac{22}{4} = 5.5 \text{ in.} \\ 4 \text{ in. (governs)} \end{cases}$$

[21.4.4.2]

Required cross-sectional area of confinement reinforcement in the form of hoops:

$$A_{sh} \geq \begin{cases} 0.09 s h_c \frac{f_c}{f_{yh}} \\ 0.3 s h_c \left(\frac{A_g}{A_{ch}} - 1 \right) \frac{f_c}{f_{yh}} \end{cases}$$

[21.4.4.1]

where the terms are as defined for Equation 10-6 and 10-7. For a hoop spacing of 4 in., $f_{yh} = 60,000 \text{ lb/in.}^2$, and tentatively assuming No. 4 bar hoops (for the purpose of estimating h_c and A_{ch}), the required cross-sectional area is

$$A_{sh} \geq \begin{cases} \frac{(0.09)(4)(18.5)(4000)}{60,000} \\ = 0.44 \text{ in}^2 \\ (0.3)(4)(18.5) \left(\frac{484}{361} - 1 \right) \frac{4000}{60,000} \\ = 0.50 \text{ in}^2 \text{ (governs)} \end{cases} \quad [21.4.4.3]$$

No. 4 hoops with one crosstie, as shown in Figure 10-58, provide $A_{sh} = 3(0.20) = 0.60 \text{ in.}^2$

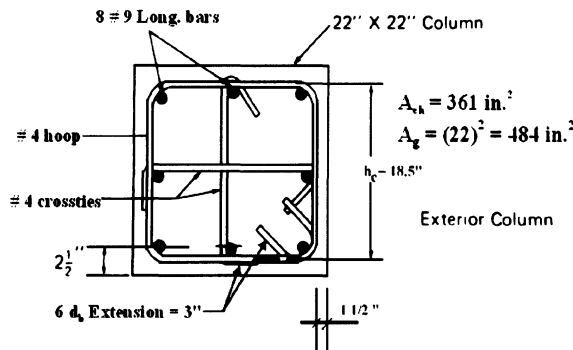


Figure 10-58. Detail of column transverse reinforcement.

(2) Transverse reinforcement for shear: As in the design of shear reinforcement for beams, the design shear in columns is based not on the factored shear forces obtained from a lateral-load analysis, but rather on the maximum probable flexural strength, M_{pr} (with $\phi = 1.0$ and $f_s = 1.25 f_y$), of the member associated with the range of factored axial loads on the member. However, the member shears need not exceed those associated with the probable moment strengths of the beams framing into the column.

If we assume that an axial force close to $P = 740$ kips ($\phi = 1.0$ and tensile reinforcement stress of $1.25 f_y$, corresponding to the "balanced point" on the P-M interaction diagram for the column section considered – which would yield close to if not the largest moment strength), then the corresponding $M_b = 601$ ft-kips. By comparison, the moment induced in the column by the beam framing into it in the transverse direction, with $M_{pr} = 299$ ft-kips, is $299/2 = 150$ ft-kips. In the longitudinal direction, with beams framing on opposite sides of the column, we have (using the same steel areas assumed earlier),

M_{pr} (beams) = M_{pr} (beam on one side) + M_{pr}^+ (beam on the other side) = $390 + 195 = 585$ ft-kips, with the moment induced at each end of the column = $585/2 = 293$ ft-kips. This is less than $M_b = 601$ ft-kips and will be used to

determine the design shear force on the column. Thus (see Figure 10-42),

$V_u = 2 M_u/l = 2(293)/10 = 59$ kips
using, for convenience,

$$V_c = 2\sqrt{f_c bd}$$

$$= \frac{2\sqrt{4000}(22)(19.5)}{1000} = 54 \text{ kips}$$

Required spacing of No. 4 hoops with $A_v = 2(0.20) = 0.40 \text{ in.}^2$ (neglecting crossties) and

$$V_s = (V_u - \phi V_c)/\phi = 14.8 \text{ kips} :$$

$$s = \frac{A_v f_y d}{V_s} = \frac{(2)(2.0)(60)(19.5)}{14.8} = 31.6 \text{ in.}$$

11.5.6.2

Thus, the transverse reinforcement spacing over the distance $l_0 = 22$ in. near the column ends is governed by the requirement for confinement rather than shear.

Maximum allowable spacing of shear reinforcement: $d/2 = 9.7$ in. 11.5.4.1

Use No. 4 hoops and crossties spaced at 4 in. within a distance of 24 in. from the column ends and No. 4 hoops spaced at 6 in. or less over the remainder of the column.

(d) Minimum length of lap splices for column vertical bars:

ACI Chapter 21 limits the location of lap splices in column bars within the middle portion of the member length, the splices to be designed as tension splices. 21.4.3.2

As in flexural members, transverse reinforcement in the form of hoops spaced at 4 in. ($d/4 = 19.5/4 = 4.9$ in.) is to be provided over the full length of the splice. 21.3.2.3

Since generally all of the column bars will be spliced at the same location, a Class B splice will be required. 12.15.2

The required length of splice is $1.3l_d$ where

$$l_d = \frac{3}{40} \frac{d_b f_y}{\sqrt{f'_c}} \left(\frac{\alpha \beta \gamma \lambda}{c + k_{tr}} \right)$$

where $\alpha = 1.0$, $\beta = 1.0$, $\gamma = 1.0$, and $\lambda = 1.0$

$$c = 1.5 + 0.5 + \frac{1.128}{2} = 2.6 \text{ in. (governs)}$$

$$\text{or } c = \frac{1}{2} \left[\frac{22 - 2(1.5 + 0.5) - 1.128}{2} \right] = 4.2 \text{ in.}$$

$$k_{tr} = \frac{A_{tr} f_{yt}}{1500 s_n} = \frac{(3 \times 0.2) \times 60,000}{1500 \times 4 \times 3} = 2.0$$

$$\frac{c + k_{tr}}{d_b} = \frac{2.6 + 2.0}{1.128} = 4.1 > 2.5 \text{ use } 2.5$$

$$\therefore l_d = \frac{3}{40} \frac{1.128 \times 60,000}{\sqrt{4000}} \frac{1.0}{2.5} = 32.1 \text{ in.}$$

Thus, required splice length = $1.3(32.1) = 42$ in. Use 44-in, lap splices.

(e) Detail of column. See Figure 10-59.

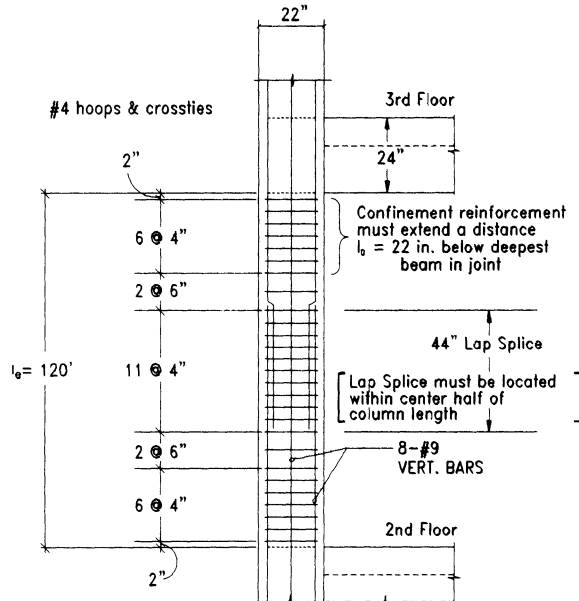


Figure 10-59. Column reinforcement details.

4. Design of exterior beam-column connection. The aim is to determine the transverse confinement and shear-reinforcement requirements for the exterior beam-column connection between the beam considered in item 2 above and the column in item 3. Assume the joint to be located at the sixth floor level.

(a) Transverse reinforcement for confinement: ACI Chapter 21 requires the same amount of confinement reinforcement within the joint as for the length l_0 at column ends, unless the joint is confined by beams framing into all vertical faces of the column. In the latter case, only one-half the transverse reinforcement required for unconfined joints need be provided. In addition, the maximum spacing of transverse reinforcement is (minimum dimension of column)/4 or 6 in. (instead of 4 in.).

21.5.2.1

21.5.2.2

In the case of the beam-column joint considered here, beams frame into only three sides of the column, so that the joint is considered unconfined.

In item 4 above, confinement requirements at column ends were satisfied by No. 4 hoops with crossties, spaced at 4 in.

(b) Check shear strength of joint: The shear across section x-x (see Figure 10-60) of the joint is obtained as the difference between the tensile force at the top flexural reinforcement of the framing beam (stressed to $1.25f_y$) and the horizontal shear from the column above. The tensile force from the beam (three No. 8 bars, $A_s = 2.37 \text{ in.}^2$) is $(2.37)(1.25)(60) = 178 \text{ kips}$

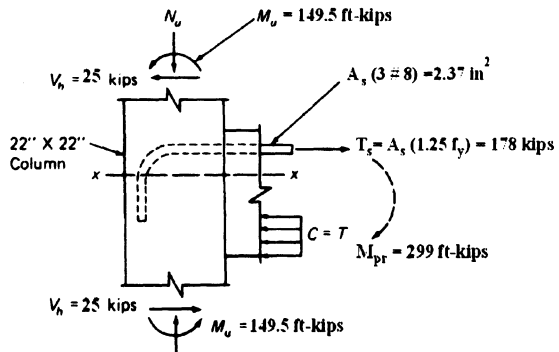


Figure 10-60. Horizontal shear in exterior beam-column joint.

An estimate of the horizontal shear from the column, V_h can be obtained by assuming that

the beams in the adjoining floors are also deformed so that plastic hinges form at their junctions with the column, with $M_p(\text{beam}) = 299 \text{ ft-kips}$ (see Table 10-9, for sidesway to left). By further assuming that the plastic moments in the beams are resisted equally by the columns above and below the joint, one obtains for the horizontal shear at the column ends

$$V_h = \frac{M_p(\text{beam})}{\text{story height}} = \frac{299}{12} = 25 \text{ kips}$$

Thus, the net shear at section x-x of joint is $178 - 25 = 153$ kips. ACI Chapter 21 gives the nominal shear strength of a joint as a function only of the gross area of the joint cross-section, A_j , and the degree of confinement provided by framing beams. For the joint considered here (with beams framing on three sides),

$$\begin{aligned} \phi V_c &= \phi 15 \sqrt{f_c A_j} \\ &= \frac{(0.85)(15)(\sqrt{4000})(22)^2}{1000} \\ &= 390 \text{ kips} > V_u = 153 \text{ kips O.K.} \end{aligned}$$

21.5.3.1
9.3.4.1

Note that if the shear strength of the concrete in the joint as calculated above were inadequate, any adjustment would have to take the form (since transverse reinforcement above the minimum required for confinement is considered not to have a significant effect on shear strength) of either an increase in the column cross-section (and hence A_j) or an increase in the beam depth (to reduce the amount of flexural reinforcement required and hence the tensile force T).

(c) Detail of joint. See Figure 10-61. (The design should be checked for adequacy in the longitudinal direction.)

Note: The use of crossties within the joint may cause some placement difficulties. To relieve the congestion, No. 6 hoops spaced at 4 in. but without crossties may be considered as an alternative. Although the cross-sectional area of confinement reinforcement provided by No. 6 hoops at 4 in. ($A_{sh} = 0.88 \text{ in.}^2$) exceeds the required amount (0.59 in.^2), the requirement of

section 21.4.4.3 of ACI Chapter 21 relating to a maximum spacing of 14 in. between crossties or legs of overlapping hoops (see Figure 10-41) will not be satisfied. However, it is believed that this will not be a serious shortcoming in this case, since the joint is restrained by beams on three sides.

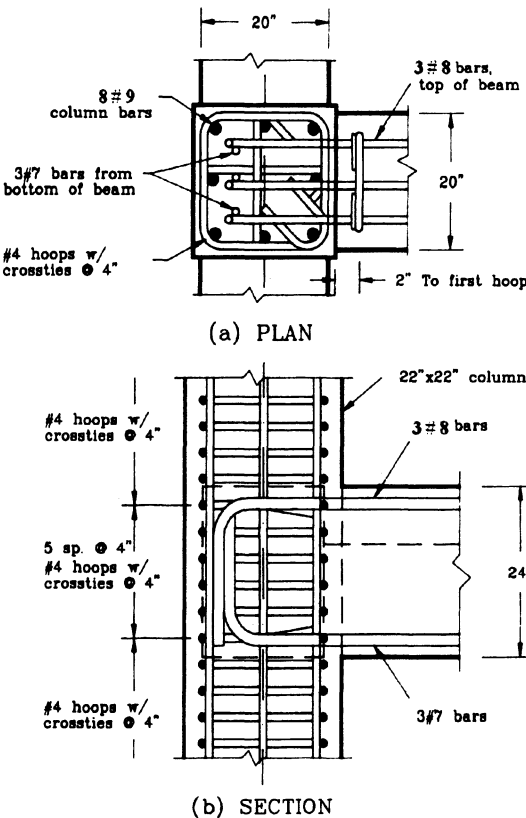


Figure 10-61. Detail of exterior beam-column connection.

5. Design of interior beam-column connection. The objective is to determine the transverse confinement and shear reinforcement requirements for the interior beam-column connection at the sixth floor of the interior transverse frame considered in previous examples. The column is 26 in. square and is reinforced with eight No. 11 bars.

The beams have dimensions $b = 20$ in. and $d = 21.5$ in. and are reinforced as noted in Section item 2 above (see Figure 10-55).

(a) Transverse reinforcement requirements (for confinement): Maximum allowable spacing of rectangular hoops,

$$s_{\max} = \begin{cases} \frac{1}{4}(\text{smallest dimension of column}) \\ = 26/4 = 6.5 \text{ in.} \\ 6 \text{ in. (governs)} \end{cases}$$

21.5.2.2
21.4.4.2

For the column cross-section considered and assuming No. 4 hoops, $h_c = 22.5$ in., $A_{ch} = (23)^2 = 529$ in.², and $A_g = (26)^2 = 676$ in.². With a hoop spacing of 6 in., the required cross-sectional area of confinement reinforcement in the form of hoops is

$$A_{sh} \geq \begin{cases} 0.09sh_c \frac{f_c}{f_{yh}} = \frac{(0.09)(6)(22.5)(4000)}{60,000} \\ = 0.81 \text{ in.}^2 \quad (\text{governs}) \\ 0.3sh_c \left(\frac{A_g}{A_{ch}} - 1 \right) \frac{f_c}{f_{yh}} \\ = (0.3)(6)(22.5) \left(\frac{676}{529} - 1 \right) \frac{4000}{60,000} \\ = 0.75 \text{ in.}^2 \end{cases}$$

21.4.4.1

Since the joint is framed by beams (having widths of 20 in., which is greater than $\frac{3}{4}$ of

the width of the column, 19.5 in.) on all four sides, it is considered confined, and a 50% reduction in the amount of confinement reinforcement indicated above is allowed. Thus, $A_{sh}(\text{required}) \geq 0.41$ in.².

No. 4 hoops with crossties spaced at 6 in. o.c. provide $A_{sh} = 0.60$ in.². (See Note at end of item 4.)

(b) Check shear strength of joint: Following the same procedure used in item 4, the forces affecting the horizontal shear across a section near mid-depth of the joint shown in Figure 10-62 are obtained:

$$\begin{aligned} (\text{Net shear across section x-x}) &= T_1 + C_2 - V_h \\ &= 296 + 135 - 59 \\ &= 372 \text{ kips} = V_u \end{aligned}$$

Shear strength of joint, noting that joint is confined:

$$\begin{aligned} \phi V_c &= \phi 20 \sqrt{f_c A_j} \\ &= \frac{(0.85)(20)\sqrt{4000}(26)^2}{1000} \quad \boxed{21.5.3.1} \\ &= 726 \text{ kips} \\ &> V_u = 372 \text{ kips} \quad \text{O.K.} \end{aligned}$$

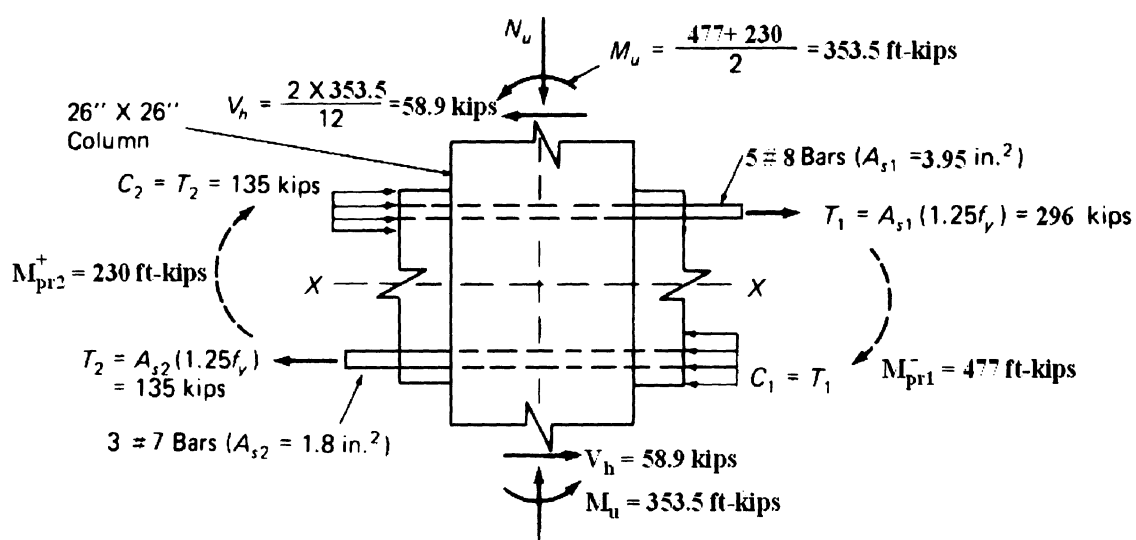


Figure 10-62. Forces acting on interior beam-column joint.

6. Design of structural wall (shear wall).

The aim is to design the structural wall section at the first floor of one of the identical frame-shear wall systems. The preliminary design, as shown in Figure 10-48, is based on a 14-in.-thick wall with 26-in. -square vertical boundary elements, each of the latter being reinforced with eight No. 11 bars.

Preliminary calculations indicated that the cross-section of the structural wall at the lower floor levels needed to be increased. In the following, a 14-in.-thick wall section with 32×50 -in. boundary elements reinforced with 24 No. 11 bars is investigated, and other reinforcement requirements determined.

The design forces on the structural wall at the first floor level are listed in Table 10-8. Note that because the axis of the shear wall coincides with the centerline of the transverse frame of which it is a part, lateral loads do not induce any vertical (axial) force on the wall.

The calculation of the maximum axial force on the boundary element corresponding to Equation 10-8b, $1.4 D + 0.5 L \pm 1.0 Q_E$, $P_u = 3963$ kips, shown in Table 10-8, involved the following steps: At base of the wall:

Moment due to seismic load (from lateral load analysis for the transverse frames), $M_b = 32,860$ ft-kips.

Referring to Figure 10-45, and noting the load factors used in Equation 10-8a of Table 10.8,

$$W = 1.2 D + 1.6 L + 0.5 L_r \\ = 5767 \text{ kips}$$

$$Ha = 30,469 \text{ ft-kips}$$

$$C_v = \frac{W}{2} + \frac{Ha}{d} \\ = \frac{5157}{2} + \frac{30,469}{22} = 3963 \text{ kips}$$

- (a) Check whether boundary elements are required: ACI Chapter 21 (Section 21.6.2.3) requires boundary elements to be provided if the maximum compressive extreme-fiber stress under factored forces exceeds $0.2 f_c'$, unless the entire wall is reinforced to satisfy Sections 21.4.4.1

through 21.4.4.3 (relating to confinement reinforcement).

It will be assumed that the wall will not be provided with confinement reinforcement over its entire height. For a homogeneous rectangular wall 26.17 ft long (horizontally) and 14 in. (1.17 ft) thick,

$$I_{n.a.} = \frac{(1.17)(26.17)^3}{12} = 1747 \text{ ft}^4$$

$$A_g = (1.17)(26.17) = 30.6 \text{ ft}^2$$

Extreme-fiber compressive stress under $M_u = 30,469$ ft-kips and $P_u = 5157$ kips (see Table 10-8):

$$f_c = \frac{P_u}{A_g} + \frac{M_u h_w / 2}{I_{n.a.}} = \frac{5157}{30.6} + \frac{(30,469)(26.17)/2}{1747} \\ = 397 \text{ ksf} = 2.76 \text{ ksi} > 0.2 f_c' = (0.2)(4) \\ = 0.8 \text{ ksi.}$$

Therefore, *boundary elements are required*, subject to the confinement and special loading requirements specified in ACI Chapter 21.

- (b) Determine minimum longitudinal and transverse reinforcement requirements for wall:

- (1) Check whether two curtains of reinforcement are required: ACI Chapter 21 requires that two curtains of reinforcement be provided in a wall if the in-plane factored shear force assigned to the wall exceeds $2A_{cv}\sqrt{f_c'}$, where A_{cv} is the cross-sectional area bounded by the web thickness and the length of section in the direction of the shear force considered. **21.6.2.2**

From Table 10-8, the maximum factored shear force on the wall at the first floor level is $V_u = 651$ kips:

$$2A_{cv}\sqrt{f_c'} = \frac{(2)(14)(26.17 \times 12)\sqrt{4000}}{1000} \\ = 556 \text{ kips} \\ < V_u = 651 \text{ kips}$$

Therefore, two curtains of reinforcement are required.

- (2) Required longitudinal and transverse reinforcement in wall:

Minimum required reinforcement ratio,

$$\rho_v = \frac{A_{sv}}{A_{cv}} = \rho_n \geq 0.0025 \quad (\text{max.})$$

spacing = 18 in.)

21.6.2.1

With $A_{cv} = (14)(12) = 168 \text{ in.}^2$, (per foot of wall) the required area of reinforcement in each direction per foot of wall is $(0.0025)(168) = 0.42 \text{ in.}^2/\text{ft}$. Required spacing of No. 5 bars [in two curtains, $A_s = 2(0.31) = 0.62 \text{ in.}^2$]:

$$s(\text{required}) = \frac{2(0.31)}{0.42}(12) = 17.7 \text{ in.} < 18 \text{ in.}$$

- (c) Determine reinforcement requirements for shear. [Refer to discussion of shear strength design for structural walls in Section 10.4.3, under "Code Provisions to Insure Ductility in Reinforced Concrete Members," item 5, paragraph (b).] Assume two curtains of No. 5 bars spaced at 17 in. o.c. both ways. Shear strength of wall ($h_w/l_w = 148/26.17 = 5.66 > 2$):

$$\phi V_n = \phi A_{cv} \left(2\sqrt{f_c} + \rho_n f_y \right)$$

where

$$\begin{aligned} \phi &= 0.60 \\ A_{cv} &= (14)(26.17 \times 12) = 4397 \text{ in.}^2 \\ \rho_n &= \frac{2(0.31)}{(14)(12)} = 0.0037 \end{aligned}$$

Thus,

$$\begin{aligned} \phi V_n &= \frac{(0.60)(4397)[2\sqrt{4000} + (0.0037)(60,000)]}{1000} \\ &= \frac{2638.2[126.5 + 222]}{1000} = 919 \text{ kips} \\ &> V_u = 651 \text{ kips} \quad \text{O.K.} \end{aligned}$$

Therefore, use two curtains of No. 5 bars spaced at 17 in. o. c. in both horizontal and vertical directions. **21.7.3.5**

- (d) Check adequacy of boundary element acting as a short column under factored vertical

forces due to gravity and lateral loads (see Figure 10-45): From Table 10-8, the maximum compressive axial load on boundary element is $P_u = 3963 \text{ kips}$.

21.5.3.3

With boundary elements having dimensions 32 in. \times 50 in. and reinforced with 24 No. 11 bars,

$$A_g = (32)(50) = 1600 \text{ in.}^2$$

$$A_{st} = (24)(1.56) = 37.4 \text{ in.}^2$$

$$\rho_{st} = 37.4/1600 = 0.0234$$

$$\rho_{min} = 0.01 < \rho_{st} < \rho_{max} = 0.06 \text{ O.K.}$$

21.4.3.1

Axial load capacity of a short column:

$$\phi P_n(\text{max}) = 0.80\phi[0.85f_c(A_g - A_{st}) + f_y A_{st}]$$

$$= (0.80)(0.70)[(0.85)(4)(1600 - 37.4)$$

$$+ (60)(37.4)]$$

$$= (0.56)[5313 + 2244] = 4232 \text{ kips} > P_u = 3963 \text{ kips} \quad \text{O.K.} \quad \boxed{10.3.5.2}$$

- (e) Check adequacy of structural wall section at base under combined axial load and bending in the plane of the wall: From Table 10-8, the following combinations of factored axial load and bending moment at the base of the wall are listed, corresponding to Eqs. 10-8a, b and c:

$$9-8a: P_u = 5767 \text{ kips}, M_u \text{ small}$$

$$9-8b: P_u = 5157 \text{ kips}, M_u = 30,469 \text{ ft-kips}$$

$$9-8c: P_u = 2293 \text{ kips}, M_u = 30,469 \text{ ft-kips}$$

Figure 10-63 shows the ϕP_n - ϕM_n interaction diagram (obtained using a computer program for generating P - M diagrams) for a structural wall section having a 14-in.-thick web reinforced with two curtains of No. 5 bars spaced at 17 in. o.c. both ways and 32 in. \times 50-in. boundary elements reinforced with 24 No. 11 vertical bars, with $f_c = 4000 \text{ lb/in.}^2$, and $f_y = 60,000 \text{ lb/in.}^2$ (see Figure 10-64). The design load combinations listed above are shown plotted in Figure 10-63. The point marked *a* represents the P - M combination corresponding to Equation 10-8a, with similar notation used for the other two load combinations.

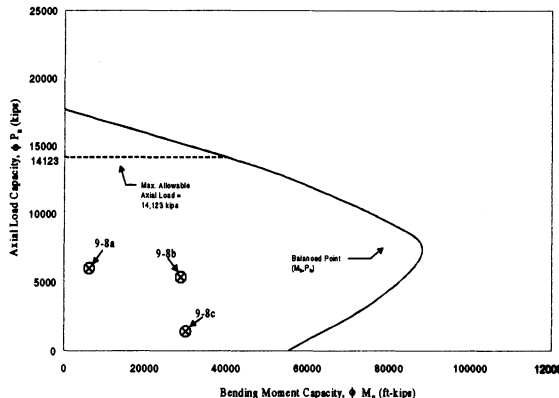


Figure 10-63. Axial load-moment interaction diagram for structural wall section.

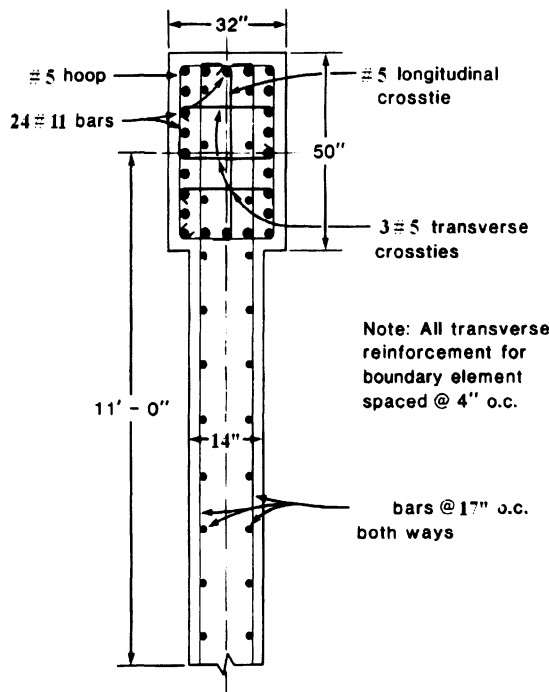


Figure 10-64. Half section of structural wall at base.

It is seen in Figure 10-63 that the three design loadings represent points inside the interaction diagram for the structural wall section considered. Therefore, *the section is adequate with respect to combined bending and axial load*.

Incidentally, the “balanced point” in Figure 10-63 corresponds to a condition where the compressive strain in the extreme concrete fiber is equal to $\epsilon_{cu} = 0.003$ and the tensile

strain in the row of vertical bars in the boundary element farthest from the neutral axis (see Figure 10-64) is equal to the initial yield strain, $\epsilon_y = 0.00207$.

- (f) Determine lateral (confinement) reinforcement required for boundary elements (see Figure 10-64): The maximum allowable spacing is

$$s_{max} = \begin{cases} 1/4(\text{smallest dimension of boundary element}) \\ = 32/4 = 8 \text{ in.} \\ 4 \text{ in. (governs)} \end{cases}$$

21.6.6.2
21.4.4.2

- (1) Required cross-sectional area of confinement reinforcement in short direction:

$$A_{sh} \geq \begin{cases} 0.09sh_c \frac{f_c'}{f_{yh}} \\ 0.3sh_c \left(\frac{A_g}{A_{ch}} - 1 \right) f_c' \end{cases} \quad 21.4.4.1$$

Assuming No. 5 hoops and crossties spaced at 4 in. o.c. and a distance of 3 in. from the center line of the No. 11 vertical bars to the face of the column, we have

$$h_c = 44 + 1.41 + 0.625 = 46.04 \text{ in. (for short direction)},$$

$$A_{ch} = (46.04 + 0.625)(26 + 1.41 + 1.25) \\ = 1337 \text{ in.}^2$$

$$A_{sh} > \begin{cases} (0.09)(4)(46.04)(4/60) \\ = 1.10 \text{ in.}^2 (\text{governs}) \\ (0.3)(4)(46.04) \left(\frac{(32)(50)}{1337} - 1 \right) \left(\frac{4}{60} \right) \\ = 0.72 \text{ in.}^2 \end{cases}$$

(required in short direction).

With three crossties (five legs, including outside hoops),

- A_{sh} (provided) = $5(0.31) = 1.55 \text{ in.}^2$ O.K.
 (2) Required cross-sectional area of confinement reinforcement in long direction:

$$h_c = 26 + 1.41 + 0.625 = 28.04 \text{ in.}$$

(for long direction),

$$A_{ch} = 1337 \text{ in.}^2$$

$$A_{sh} \geq \begin{cases} (0.09)(4)(28.04)(4/60) \\ = 0.67 \text{ in.}^2 \text{ (governs)} \\ (0.3)(4)(28.04)(1.196 - 1)(4/60) \\ = 0.44 \text{ in.}^2 \end{cases}$$

(required in long direction).

With one crosstie (i.e., three legs, including outside hoop),

$$A_{sh}$$
 (provided) = $3(0.31) = 0.93 \text{ in.}^2$ O.K.

- (g) Determine required development and splice lengths:

ACI Chapter 21 requires that all continuous reinforcement in structural walls be anchored or spliced in accordance with the provisions for reinforcement in tension. [21.6.2.4]

(1) Lap splice for No. 11 vertical bars in boundary elements (the use of mechanical connectors may be considered as an alternative to lap splices for these large bars): It may be reasonable to assume that 50% or less of the vertical bars are spliced at any one location. However, an examination of Figure 10-63 suggests that the amount of flexural reinforcement provided—mainly by the vertical bars in the boundary elements—does not represent twice that required by analysis, so that a class B splice will be required. [12.15.2]

Required length of splice = $1.3 l_d$ where $l_d = 2.5 l_{dh}$ [12.15.1]
 and

$$l_{dh} \geq \begin{cases} f_y d_b / 65\sqrt{f_c'} \\ = \frac{(60,000)(1.41)}{65\sqrt{4000}} = 21 \text{ in. (governs)} \\ 8 d_b = (8)(1.41) = 12 \text{ in.} \\ 6 \text{ in.} \end{cases}$$

21.5.4.2

Thus the required splice length is $(1.3)(2.5)(21) = 68 \text{ in.}$

- (2) Lap splice for No. 5 vertical bars in wall “web”: Here again a class B splice will be required. Required length of splice = $1.3 l_d$, where $l_d = 2.5 l_{dh}$, and

$$l_{dh} \geq \begin{cases} f_y d_b / 65\sqrt{f_c'} \\ = \frac{(60,000)(0.625)}{65\sqrt{4000}} = 9 \text{ in. (governs)} \\ 8 d_b = (8)(0.625) = 5.0 \text{ in.} \\ 6 \text{ in.} \end{cases}$$

Hence, the required length of splice is $(1.3)(2.5)(9) = 30 \text{ in.}$

Development length for No. 5 horizontal bars in wall, assuming no hooks are used within the boundary element: Since it is reasonable to assume that the depth of concrete cast in one lift beneath a horizontal bar will be greater than 12 in., the required factor of 3.5 to be applied to the development length, l_{dh} , required for a 90° hooked bar will be used [Section 10.4.3, under “Code Provisions Designed to Insure Ductility in Reinforced-Concrete Members”, item 2, paragraph (f)]:

21.5.4.2

$l_d = 3.5 l_{dh}$, where as indicated above, $l_{dh} = 9.0 \text{ in.}$ so that the required development length $l_d = 3.5(9) = 32 \text{ in.}$

This length can be accommodated within the confined core of the boundary element, so that no hooks are needed, as assumed. However, because of the likelihood of large horizontal cracks developing in the boundary elements, particularly in the potential hinging region near the base of the

wall, the horizontal bars will be provided with 90° hooks engaging a vertical bar, as recommended in the Commentary to ACI Chapter 21 and as shown in Figure 10-64. Required lap splice length for No. 5 horizontal bars, assuming (where necessary) $1.3 l_d = (1.3)(32) = 42$ in.

(h) Detail of structural wall: See Figure 10-64. It will be noted that the No. 5 vertical-wall "web" reinforcement, required for shear resistance, has been carried into the boundary element. The Commentary to ACI Section 21.6.5 specifically states that the concentrated reinforcement provided at wall edges (i.e. the boundary elements) for bending is not included in determining shear-reinforcement requirements. The area of vertical shear reinforcement located within the boundary element could, if desired, be considered as contributing to the axial load and bending capacity.

(i) Design of boundary zone using UBC-97 and IBC-2000 Provisions:

Using the procedure discussed in Section 10.4.3 item 5 (f), the boundary zone design and detailing requirements using these provisions will be determined.

(1) Determine if boundary zone details are required:

Shear wall boundary zone detail requirements to be provided unless $P_u \leq 0.1A_g f'_c$ and either $M_u/V_u l_u \leq 1.0$ or $V_u \leq 3 A_{cv} \sqrt{f'_c}$. Also, shear walls with $P_u > 0.35 P_0$ (where P_0 is the nominal axial load capacity of the wall at zero eccentricity) are not allowed to resist seismic forces.

Using 26 inch square columns; $0.1A_g f'_c = 0.1 \times (14 \times 19.83 \times 12 + 2 \times 26^2) \times 4 = 1873$ kips $< P_u = 3963$ kips. Using 32 × 50 columns also results in the value of $0.1A_g f'_c$ to be less than P_u . Therefore, boundary zone details are required.

Assume a 14 in. thick wall section with 32 × 50 in. boundary elements reinforced with 24 No. 11 bars as used previously. Also, it was determined that 2#5 bars at 17 in. spacing is needed as vertical reinforcement in the web. On this basis, the nominal axial load capacity of the wall (P_0) at zero eccentricity is:

$$\begin{aligned} P_0 &= 0.85 f'_c (A_g - A_{st}) + f_y A_{st} \\ &= 0.85 \times 4 \times (6195 - 82.68) + (60 \times 82.68) = 25,743 \text{ kips} \end{aligned}$$

Since $P_u = 3963$ kips = $0.15 P_0 < 0.35 P_0 = 9010$ kips, the wall can be considered to contribute to the calculated strength of the structure for resisting seismic forces.

Therefore, provide boundary zone at each end having a distance of $0.15 l_w = 0.15 \times 26.17 \times 12 = 47.1$ in. On this basis, a 32×50 boundary zone as assumed is adequate.

Alternatively, the requirements for boundary zone can be determined using the displacement based procedure. As such, boundary zone details are to be provided over the portion of the wall where compressive strains exceed 0.003. The procedure is as follows:

Determine the location of the neutral axis depth, c'_{u_0} .

From Table 10-8, $P'_u = 5767$ kips; the nominal moment strength, M'_{n_0} , corresponding to P'_u is 89,360 k-ft (see Figure 10-63). For 32 × 50 in. boundary elements reinforced with 24 #11 bars, c'_{u_0} is equal to 97.7 in. This value can be determined using the strain compatibility approach.

From the results of analysis, the elastic displacement at the top of the wall, Δ_E is equal to 1.55 in. using gross section properties and the corresponding moment, M'_{n_0} , at the base of the wall is 30,469 k-ft (see Table 10-8). From the analysis using the cracked section properties, the total deflection, Δ_t , at top

of the wall is 15.8 in. (see Table 10-3, $\Delta_t = 2.43 \times C_d = 2.43 \times 6.5 = 15.8$ in.), also $\Delta_y = \Delta_E M'_n / M'_E = 1.55 \times 89,360 / 30,469 = 4.55$ in.

The inelastic deflection at the top of the wall is:

$$\Delta_i = \Delta_t - \Delta_y = 15.8 - 4.55 = 11.25 \text{ in.}$$

Assume $l_p = 0.5$ $l_w = 0.5 \times 26.17 \times 12 = 157$ in., the total curvature demand is:

$$\phi_t = \frac{11.25}{(148 \times 12 - 157/2) \times 157} + \frac{0.003}{26.17 \times 12} \\ = 5.176 \times 10^{-5}$$

Since ϕ_t is greater than $0.003/c'_u = 0.003/97.7 = 3.07 \times 10^{-5}$, boundary zone details are required. The maximum compressive strain in the wall is equal to $\phi_t c'_u = 5.176 \times 10^{-5} \times 97.7 = 0.00506$ which is less than the maximum allowable value of 0.015. In this case, boundary zone details are required over the length,

$$\left(97.7 - \frac{0.003}{0.00506} \times 97.7 \right) = 39.8 \text{ in.}$$

This is less than the 50 in. length assumed. Therefore, the entire length of the boundary zone will be detailed for ductility.

(2) Detailing requirements:

Minimum thickness:

$$= l_w / 16 = \frac{(16 \times 12) - 24}{16} = 10.5 \text{ in.} < 32 \text{ in. O.K.}$$

Minimum length = 18 in. < 50 in. O.K.

The minimum area of confinement reinforcement is:

$$A_{sh} = \frac{0.09 s_h f'_c}{f_{yh}}$$

Using the maximum allowable spacing of $6d_b = 6 \times 1.41 = 8.46$ in. or 6 in. (governs), and assuming #5 hoops and crossties at a distance of 3 in. from the center line of #11 vertical bars to the face of the column, we have

$$h_c = 44 + 1.41 + 0.625 = 46.04$$

$$A_{sh} = \frac{0.09 \times 6 \times 46.04 \times 4}{60} = 1.66 \text{ in.}^2$$

With four crossties (six legs, including outside hoops), A_{sh} provided = 6 (0.31) = 1.86 in.² O.K.

Also, over the splice length of the vertical bars in the boundary zone, the spacing of hoops and crossties must not exceed 4 in. In addition, the minimum area of vertical bars in the boundary zone is $0.005 \times 32^2 = 5.12$ in.² which is much less than the area provided by 24#11 bars. The reinforcement detail in the boundary zone would be very similar to that shown previously in Figure 10-64.

REFERENCES

The following abbreviations will be used to denote commonly occurring reference sources:

- *Organizations and conferences:*

EBRI	Earthquake Engineering Research Institute
WCEE	World Conference on Earthquake Engineering
ASCE	American Society of Civil Engineers
ACI	American Concrete Institute
PCA	Portland Cement Association
PCI	Prestressed Concrete Institute

- *Publications:*

JEMD	Journal of Engineering Mechanics Division, ASCE
JSTR	Journal of the Structural Division, ASCE
JACI	Journal of the American Concrete Institute

- 10-1 International Conference of Building Officials, 5360 South Workman Mill Road, Whittier, CA 90601, *Uniform Building Code*. The latest edition of the Code is the 1997 Edition.
- 10-2 Clough, R. W. and Benuska, K. L., "FHA Study of Seismic Design Criteria for High-Rise Buildings," Report HUD TS-3. Federal Housing Administration, Washington, Aug. 1966.
- 10-3 Derecho, A. T., Ghosh, S. K., Iqbal, M., Freskakis, G. N., and Fintel, M., "Structural Walls in

- Earthquake-Resistant Buildings, Dynamic Analysis of Isolated Structural Walls—Parametric Studies,” Report to the National Science Foundation, RANN, Construction Technology Laboratories, PCA, Skokie, IL, Mar. 1978.
- 10-4 Derecho, A. T., Iqbal, M., Ghosh, S. K., Fintel, M., Corley, W. G., and Scanlon, A., “Structural Walls in Earthquake-Resistant Buildings, Dynamic Analysis of Isolated Structural Walls—Development of Design Procedure, Design Force Levels,” Final Report to the National Science Foundation, ASRA. Construction Technology Laboratories, PCA, Skokie, IL, July 1981.
- 10-5 Park, R. and Paulay, T., *Reinforced Concrete Structures*, John Wiley & Sons, New York, 1975.
- 10-6 Priestley, M.J.N. and Kowalsky, M.J., “Aspects of Drift and Ductility Capacity of Rectangular Cantilever Structural Walls”, Bulletin of the New Zealand National Society for Earthquake Engineering, Vol. 31, No. 2, 1998.
- 10-7 Paulay, T., “Earthquake-Resisting Walls—New Zealand Design Trends,” *JACI*, 144—152, May—June 1980.
- 10-8 Derecho, A. T., Iqbal, M., Fintel, M., and Corley, W. G., “Loading History for Use in Quasi-static Simulated Loading Test,” *Reinforced Concrete Structures Subjected to Wind and Earthquake Forces*, ACI Special Publication SP-63, 329—344, 1980.
- 10-9 Oesterle, R. G., Aristizabal-Ochoa, J. D., Fiorato, A. E., Russell, H. G., and Corley, W. G., “Earthquake-Resistant Structural Walls—Tests of Isolated Walls—Phase II,” Report to the National Science Foundation, ASRA, Construction Technology Laboratories, PCA, Skokie, IL, Oct. 1979.
- 10-10 American Concrete Institute, Detroit, Michigan, “Building Code Requirements for Reinforced Concrete—ACI 318-95.” The latest edition of the code is the 1995 Edition.
- 10-11 Iyengar, K. T. S. R., Desai, P., and Reddy, K. N., “Stress—Strain Characteristics of Concrete Confined in Steel Binders,” *Mag. Concrete Res.* 22, No. 72, Sept. 1970.
- 10-12 Sargin, M., Ghosh, S. K., and Handa, V. K., “Effects of Lateral Reinforcement upon the Strength and Deformation Properties of Concrete,” *Mag. Concrete Res.* 75—76, June—Sept. 1971.
- 10-13 Paulay, T. and Priestley, M.J.N., *Seismic Design of Reinforced Concrete and Masonry Buildings*, John Wiley & Sons, New York, 1992.
- 10-14 Sturman, G. M., Shah, S. P., and Winter, G., “Effects of Flexural Strain Gradients on Microcracking and Stress—Strain Behavior of Concrete,” Title No. 62-50, *JACI*, July 1965.
- 10-15 Clark, L. E., Gerstle, K. H., and Tulin, L. G., “Effect of Strain Gradient on the Stress—Strain Curve of Mortar and Concrete,” Title No. 64-50, *JACI*, Sept. 1967.
- 10-16 Mattock, A. H., “Rotational Capacity of Hinging Regions in Reinforced Concrete Beams,” *Proc. Intl. Symposium on Flexural Mechanics of Reinforced Concrete*, ASCE, 1965, 143—181, 1965. Also PCA Development Dept. Bulletin 101.
- 10-17 Corley, W. G., “Rotational Capacity of Reinforced Concrete Beams,” *JSTR Proc.* 92 (STS), 121—146, Oct. 1966. Also PCA Development Dept. Bulletin 108.
- 10-18 Naaman, A. E., Harajli, M. H., and Wight, J. K., “Analysis of Ductility in Partially Prestressed Concrete Flexural Members,” *PCIJ*, 64—87, May—June 1986.
- 10-19 Bertero, V. V. and Fellippa, C., “Discussion of ‘Ductility of Concrete,’ by Roy, H. E. H. and Sozen, M. A.,” *Proc. Intl. Svmp. on Flexural Mechanics of Reinforced Concrete*, ASCE, 227—234, 1965.
- 10-20 Standard Association of New Zealand, *Code of Practice for General Structural Design and Design Loadings for Buildings—NZS 4203:1 984*, Wellington, 1992.
- 10-21 Bertero, V. V., “Seismic Behavior of Structural Concrete Linear Elements (Beams and Columns) and Their Connections,” *Proc. of the A. IC. A. P-C. E. B. Symposium on Structural Concrete under Seismic Actions*, Rome, I, 123—212, 1979.
- 10-22 Popov, E. P., Bertero, V. V., and Krawinkler, H., “Cyclic Behavior of Three Reinforced Concrete Flexural Members with High Shear,” Report No. EERI 72-5, Univ. of California, Berkeley, Oct. 1972.
- 10-23 Brown, R. H. and Jirsa, J. O., “Shear Transfer of Reinforced Concrete Beams Under Reversed Loading,” Paper No. 16, *Shear in Reinforced Concrete*, Vol. 1, ACI Publication SP-42, 347—357, 1974.
- 10-24 Bertero, V. V. and Popov, E. P., “Hysteretic Behavior of R. C. Flexural Members with Special Web Reinforcement,” *Proc. U.S. National Conference on Earthquake Engineering—1975*, Ann Arbor, MI, 316-326, 1975.
- 10-25 Scribner, C. F. and Wight, J. K., “Delaying Shear Strength Decay in Reinforced Concrete Members under Large Load Reversals,” Report UMEE 78R2, Dept. of Civil Engineering, Univ. of Michigan, Ann Arbor, 1978.
- 10-26 Standards Association of New Zealand, *Code of Practice for the Design of Concrete Structures, NZS 3101, Part 1:1995*, Wellington, 1995.
- 10-27 Ehsani, M. R. and Wight, J. K., “Effect of Transverse Beams and Slab on Behavior of Reinforced Beam-to-Column Connections,” *JACI* 82, No. 2, 188—195, Mar.-Apr. 1985.

- 10-28 Leon, R. and Jirsa, J. O., "Bidirectional Loading of R. C. Beam—Column Joints," *EERI Earthquake Spectra* 2, No. 3, 537—564, May 1986.
- 10-29 ACI—ASCE Committee 352, "Recommendations for Design of Beam—Column Joints in Monolithic Reinforced Concrete Structures," *ACI J. Proc.* 82, No. 3, 266—283, May—June 1985.
- 10-30 Paulay, T., "Deterministic Design Procedure for Ductile Frames in Seismic Areas," Paper No. 15, *Reinforced Concrete Structures Subjected to Wind and Earthquake Forces*, ACI Publication SP-63, 357—381, 1980.
- 10-31 Paulay, T., "Developments in Seismic Design of Reinforced Concrete Frames in New Zealand," *Can. J. Civil Eng.* 8, No. 2, 91—113, June 1981.
- 10-32 Park, R., "Ductile Design Approach for Reinforced Concrete Frames," *EERI Earthquake Spectra* 2, No. 3, 565—619, May 1986.
- 10-33 CSA Standard A23.3-94, "Design of Concrete Structures", Canadian Standards Association, 1994.
- 10-34 Wight, I. K. and Sozen, M. A., "Strength Decay of RC Columns under Shear Reversals," *JSTR* 101, No. STS, 1053—1065, May 1975.
- 10-35 Sheikh, S. and Uzumeri, S. M., "Strength and Ductility of Tied Concrete Columns," *JSTR* 106, No. STS, 1079—1102, May 1980.
- 10-36 Park, R., Priestley, M. J. N., and Gill, W. D., "Ductility of Square-Confining Concrete Columns," *JSTR* 108, No. 5T4, 929—950, Apr. 1982.
- 10-37 Priestly, M. J. N. and Park, R., "Strength and Ductility of Concrete Bridge Columns under Seismic Loading," *A CI Strut'tural J.*, 61—76, Jan.—Feb. 1987.
- 10-38 Jennings, P. C. (ed.), "Engineering Features of the San Fernando Earthquake, February 9, 1971," Earthquake Engineering Research Laboratory, California Institute of Technology, Pasadena, June 1971.
- 10-39 Paulay, T., Park, R., and Priestley, M. J. N., "Reinforced Concrete Beam—Column Joints under Seismic Actions," *JA CI Proc.* 75, No. 11, 585—593, Nov. 1978.
- 10-40 Hanson, N. W. and Conner, H. W., "Seismic Resistance of Reinforced Concrete Beam—Column Joints," *JSTR* 93, 5T5, 533—560, Oct. 1967.
- 10-41 Meinheit, D. F. and Jirsa, J. O., "Shear Strength of R/C Beam—Column Connections," *JSTR* 107, 5Th, 2227—2244, Nov. 1982.
- 10-42 Abdel-Fattah, B. and Wight, J. K., "Study of Moving Beam Plastic Hinging Zones for Earthquake-Resistant Design of R/C Buildings," *ACI Structural J.*, 31—39, Jan—Feb. 1987.
- 10-43 Rosenblueth, E. and Meli, R., "The 1985 Earthquake: Causes and Effects in Mexico City," *ACI Concrete Int.* 8, No. 5, 23—34, May 1986.
- 10-44 Mitchell, D., Adams, J., DaVall, R. H., Lo, R. C., and Weichert, "Lessons from the 1985 Mexican Earthquake," *Can. J. Civil Eng.* 13, No. 5, 535—557, 1986.
- 10-45 Carpenter, J. E., Kaar, P. H., and Corley W. G., "Design of Ductile Flat Plate Structures to Resist Earthquakes," *Proc. 5th WCEE*, Rome, 1973.
- 10-46 Symonds, D. W., Mitchell, D., and Hawkins, N. M., "Slab—Column Connections Subjected to High Intensity Shears and Transferring Reversed Moments" SM 76-2, Division of Structures and Mechanics, Univ. of Washington, Oct. 1976.
- 10-47 Cardenas, A. E., Russell, H. G., and Corley, W. G., "Strength of Low-Rise Structural Walls," Paper No. 10, *Reinforced Concrete Structures Subjected to Wind and Earthquake Forces*, ACI Publication SP-63, 221—241, 1980.
- 10-48 Barda, F., Hanson, J. M., and Corley, W. G., "Shear Strength of Low-Rise Walls with Boundary Elements," *Reinforced Concrete Structures in Seismic Zones*, ACI Publication SP-53, 149—202, 1977.
- 10-49 Paulay, T., "Seismic Design Strategies for Ductile Reinforced Concrete Structural Wall", Proc. of International Conference on Buildings with Load Bearing Concrete Walls in Seismic Zones, Paris, 1991.
- 10-50 Oesterle, R. G., Fiorato, A. E., Johal, L. S., Carpenter, J. E., Russell, H. G., and Corley, W. G., "Earthquake-Resistant Structural Walls—Tests of Isolated Walls," Report to the National Science Foundation, Portland Cement Association, Nov. 1976.
- 10-51 Oesterle, R. G., Aristizabal-Ochoa, J. D., Fiorato, A. E., Russell, H. G. and Corley, W. G., "Earthquake Resistant Structural Walls—Tests of Isolated Walls—Phase II," Report to the National Science Foundation, Portland Cement Association, Oct. 1979.
- 10-52 Cardenas, A. and Magura, D. D., "Strength of High-Rise Shear Walls—Rectangular Cross Section," *Response of Multistory Concrete Structures to Lateral Forces*, ACI Publication SP-36, American Concrete Institute, 1973.
- 10-53 Corley, W. G., Fiorato, A. E., and Oesterle, R. G., "Structural Walls," Paper No. 4, *Significant Developments in Engineering Practice and Research*, Sozen, M. A. (ed.), ACI Publication SP-72, 77—130, 1981.
- 10-54 Oesterle, R. R., Fiorato, A. E., and Corley, W. G., "Reinforcement Details for Earthquake-Resistant Structural Walls," *ACI Concrete mt.*, 55—66, Dec. 1980.
- 10-55 Paulay, T., "The Design of Ductile Reinforced Concrete Structural Walls for Earthquake Resistance," *EERI Earthquake Spectra* 2, No. 4, 783—823, Oct. 1986.
- 10-56 Saatcioglu, M., Derecho, A. T., and Corley, W. G., "Dynamic Inelastic Response of Coupled Walls as

- Affected by Axial Forces," *Non-linear Design of Concrete Structures*, Proc. of CSCE—ASCE—ACI—CEB International Symposium, Univ. of Waterloo, Ontario, 639—670, Aug. 1979.
- 10-57 Shiu, K. N., Takayanagi, T., and Corley, W. G., "Seismic Behavior of Coupled Wall Systems," *JSTR* 110, No. 5, May 1051—1066, 1984.
- 10-58 Saatcioglu, M., Derecho, A. T., and Corley, W. G., "Parametric Study of Earthquake-Resistant Couple Walls," *JSTR* 113, No. 1, 141—157, Jan. 1987.
- 10-59 Paulay, T. and Binney, J. R., "Diagonally Reinforced Coupling Beams of Shear Walls," Paper No. 26, *Shear in Reinforced Concrete*, ACI Publication SP-42, Vol. 2, 579—598, 1974.
- 10-60 Barney, G. B., Shiu, K. N., Rabbat, B., Fiorato, A. E., Russell, HG and Corley, W. I., "Behavior of Coupling Beams under Load Reversal," PCA Res. & Dcv. Bulletin No. 68, 1980.
- 10-61 International Code Council (2000), *International Building Code 2000*, Virginia.
- 10-62 Vision 2000, "Performance Based Seismic Engineering of Buildings", Structural Engineers Association of California (SEOAC), Sacramento, California, 1995.
- 10-63 "Integrated Finite Element Analysis and Design of structures, SAP 2000", Computers and Structures, Inc. Berkeley, California, 1997.
- 10-64 "NASTRAN (NASA Structural Analysis Computer System)", Computer Software Management and Information System (COSMIC), Univ. of Georgia, Athens, Georgia.
- 10-65 "ANSYS—Engineering Analysis Systems," Swanson Analysis Systems, Inc., Houston, PA.
- 10-66 Habibullah, A., "Three Dimensional Analysis of Building Systems, ETABS", Version 6.2, Computers and Structures Inc., Berkeley, California, 1997.
- 10-67 Parkash, V. and Powell, G.H. "DRAIN-2DX: A General Purpose Computer program for Dynamic Analysis of Inelastic Plane Structures", Earthquake Engineering Research Center, University of California, Berkeley, CA, 1992.
- 10-68 Valles, R.E., Reinhorn, A.M., Kunnath, S.K., Li, C. and Madan, A., "IDARC Version 4.0: A Computer Program for the Inelastic Damage Analysis of Buildings", Report No. NCEER-96-0010, National Center for Earthquake Engineering Research, State University of New York at Buffalo, NY, 1996.
- 10-69 Clough, R. W., "Dynamic Effects of Earthquakes," *Trans. ASCE* 126, Part II, Paper No. 3252, 1961.
- 10-70 Blume, J. A., "Structural Dynamics in Earthquake-Resistant Design," *Trans. ASCE* 125, Part I, Paper No. 3054, 1960.
- 10-71 Berg, G. V., "Response of Multistory Structures to Earthquakes," Paper No. 2790, JEMD, Apr. 1961.
- 10-72 *Minimum Design Loads for Buildings and other Structures* (ASCE 7-95), a revision of ANSI/ASCE 7-93, American Society of Civil Engineers, New York, 1996.
- 10-73 Applied Technology Council, "Tentative Provisions for the Development of Seismic Regulations for Buildings," ATC Publication 3-06, U.S. Government Printing Office, Washington, 505 pp., 1978.
- 10-74 Seismology Committee, Structural Engineers Association of California (SEAOC), *Recommended Lateral Force Requirements and commentary*, Dec. 15, 1996.
- 10-75 Earthquake Engineering Research Institute, "Reducing Earthquake Hazards: Lessons Learned from Earthquakes," EERI Publication No. 86-02, Nov. 1986.
- 10-76 ACI Committee 315, "Details and Detailing of Concrete Reinforcement (ACI 315-80)," *JACI* 83, No. 3, 485—512, May—June 1986.
- 10-77 Fintel, M., "Ductile Shear Walls in Earthquake-Resistant Multistory Buildings," *JACI* 71, No. 6, 296—305, June 1974.
- 10-78 Derecho, A. T., Fintel, M., and Ghosh, S. K., "Earthquake-Resistant Structures," Chapter 12, *Handbook of Concrete Engineering*, 2nd Edition, M. Fintel (ed.), Van Nostrand Reinhold, 411—513, 1985.
- 10-79 ACI Committee 340, "Design Handbook in Accordance with the Strength Design Method of ACI 318- 89: Vol. 1—Beams, One-Way Slabs, Brackets, Footings, and Pile Caps" (ACI 340.1R-84), Publication SP-17(84), American Concrete Institute, 1984.
- 10-80 Concrete Reinforcing Steel Institute, *CRSI* Handbook, Schaumburg, IL. The latest edition of the handbook is the 1998 Edition.
- 10-81 ACI Committee 340, *Design Handbook in Accordance with the Strength Design Method of ACI 318-89: Vol. 2—Columns*, Publication SP-17A (90), American Concrete Institute, Detroit, Michigan, 1990.

Chapter 11

Seismic Design of Wood and Masonry Buildings

John G. Shipp, S.E., FASCE

Manager Design Services and Senior Technical Manager, EQE Engineering and Design, Costa Mesa, California

Gary C. Hart, Ph.D.

Professor of Engineering, University of California at Los Angeles, and President, Hart Consultant Group, Los Angeles, California

Key words: Wood Construction, Reinforced Masonry, ASD, LRFD, Limit States, Seismic Performance, Diaphragms, Subdiaphragms, Horizontal Diaphragms, Vertical Diaphragms, Connections, Tall Walls, Slender Walls, Serviceability, Drift, Diaphragm Flexibility.

Abstract: The purpose of this chapter is to present criteria and example problems of the current state of practice of seismic design of wood and reinforced masonry buildings. It is assumed that the reader is familiar with the provisions of either the Uniform Building Code (UBC), Building Officials and Code Administrators (BOCA), or Southern Building Code Congress International (SBCCI), or international code council, international building code (IBC). For consistency of presentation the primary reference, including notations and definitions, will be to the UBC 97. Included within the presentation on diaphragms are criteria and example problems for both rigid and flexible diaphragms. Also included is the UBC 97 criteria for the analytical definition of rigid versus flexible diaphragms. Wood shear walls and the distribution of lateral forces to a series of wood shear walls is presented using Allowable Stress Design (ASD). Masonry slender walls (out-of-plane loads) and masonry shear walls (in-plane loads) are presented using Load and Resistance Factor Design (LRFD).

11.1 INTRODUCTION

The design process can be separated into two basic efforts; the design for vertical loads and the design for lateral forces. The design for vertical loads for both wood and masonry is currently in transition from Allowable Stress Design (ASD) to Load and Resistance Factor Design (LRFD). The draft LRFD criteria for wood^(11-52, 11-53) is currently being reviewed by various industry committees prior to being submitted to the IBC codes for adoption.^(11-28, 11-36) The LRFD criteria for masonry walls for both in-plane and out-of-plane loads is currently in the Uniform Building Code - 1997.⁽¹¹⁻³⁸⁾

The current state of practice is to design wood members for vertical loads using ASD including all the unique Wood Design Modification Factors, see Table 11-1.^(11-35, 11-51) Masonry members are designed for vertical loads using Working Stress Design (WSD) with the standard linear stress - strain distribution assumptions. Wood members, both horizontal diaphragms and vertical diaphragms (shear walls), are designed for lateral forces using ASD; while masonry shear walls are designed for lateral forces using LRFD.

The purpose of this chapter is to present criteria and example problems of the current state of practice of seismic design of wood and reinforced masonry buildings. It is assumed that the reader is familiar with the provisions of either the Uniform Building Code (UBC), Building Officials and Code Administrators (BOCA), or Southern Building Code Congress International (SBCCI), or international code council, international building code (IBC). For consistency of presentation the primary reference, including notations and definitions, will be to the UBC 97. Included within the presentation on diaphragms are criteria and example problems for both rigid and flexible diaphragms. Also included is the UBC 97 criteria for the analytical definition of rigid versus flexible diaphragms.

Wood shear walls and the distribution of lateral forces to a series of wood shear walls is

presented using Allowable Stress Design (ASD). Masonry slender walls (out-of-plane loads) and masonry shear walls (in-plane loads) are presented using Load and Resistance Factor Design (LRFD).

11.2 LRFD/ Limit-State Design for Wood Construction

A United States and Canadian wood industry-sponsored effort to develop a reliability-based, load and resistance factor design (LRFD) Specification for engineered wood construction in the U.S. has been underway since 1988⁽¹¹⁻⁴⁹⁾. Far-reaching changes in design and material property assessment methodology have resulted. Not only has an LRFD Specification been developed using accepted principles of reliability-based design but many other up-to-the-minute applications of recent design and materials research have been incorporated. Now undergoing a Joint American Society of Civil Engineers (ASCE)/Industry Standards Committee review, the LRFD Specification for Wood Construction is expected to be presented in the international building code in the near future.

11.2.1 Design Methodology

Important advances in design methodology and in procedures for assessing the strength of components and connections have been made for the new LRFD Specification.^(11-42, 11-43, 11-46, 11-47, 11-50)

Load and resistance factor design (LRFD) methodology has become the standard procedure for practical application of the principles of reliability-based design. For the U.S. LRFD Specification, a simple format was chosen:

$$\lambda \phi R \geq \sum \gamma_i Q_i$$

where:

λ = time effect (duration of load) factor

Table II-1. Wood Matrix of Design Modification Coefficients, Ref NDS⁽¹¹⁻⁵¹⁾

Factor	NDS Section	Allowable Stresses						Mod	Bolts	Comment		
		F_b	F_c	F_{cp}	F_n	F_r	F_{rc}	F_t	F_v	E	p	q
C_e	5.3.4	X										Curvature (Gluelams Only)
C_F	4.3.2	X	X									Size Factor for Sawn Members Only
C_f	2.3.8	X						X				
C_R	2.3.6	X	X	X	X	X	X	X	X	X		Fire Retardant Treatment
C_b	2.3.10		X							X		Compression Perpendicular to Grain Form
C_D	2.3.2	X	X	X	X	X	X	X	X	X		Load Duration
C_M	2.3.3	X	X	X				X	X	X		Wet Service
C_p	2.3.93.7	X								X		Column Stability
C_L	2.3.7/3.3.3	X										Slenderness/Stability – Do not use with C_v
C_t	2.3.4	X	X	X	X	X	X	X	X	X		Temperature
C_T	4.4.3											Deflection Critical – Buckling Stiffness for 2x4 Truss
C_G	7.3.6									X	X	Group Action
C_{fu}	4.3.3/5.3.3	X										Flat Use (2" to 4" thick and Glulam only)
C_H	4.4.2							X				Horizontal Shear
C_V	5.3.2	X										Volume Factor GluLam Member Only
C_r	4.3.4	X										Repetitive Member
C_l	2.3.11	X	X	X	X			X	X			Incising to Increase Penetration of Preservatives

F_b = Bending
 F_c = Compression
 F_{cp} = Compression Perpendicular to Grain
 F_n = Hankinson Formula (3.10)
 F_r = Radial Stress
 F_{rc} = Radial Stress Compression (5.4.1)
 F_t = Tension

F_v = Horizontal Shear

E = Modules of Elasticity
 p = Parallel to Grain
 q = Perpendicular to Grain

Examples:

$$F'_x = F_x \times \text{sum } (C_i, \dots C_n)$$

$$F'_b = F_b(C_e)C_v, C_F \text{ or } C_L(C_f)(C_D)(C_M)(C_l)$$

$$\text{Defl}' = \frac{\text{Deflection} \times E}{E C_t C_m C_R}$$

ϕ = resistance factor
 R = reference resistance
 γ_i = load factors
 Q_i = effects of prescribed nominal loads

The reference resistance, R, includes all the necessary corrections for the effects of moisture and/or other end-use conditions. The load factors have been chosen to conform with U.S. practice for most engineered construction using values from ASCE 7-98⁽¹¹⁻⁵³⁾. Time effect factors, λ , have been completely reassessed. Using the latest stochastic load models and applying damage, the accumulation models of Gerhards and Link⁽¹¹⁻⁴⁵⁾, new time effect factors have been developed by Ellingwood and Rosowsky⁽¹¹⁻⁴³⁾. These time effect factors apply to the short term (5 minute) test strength of the wood member. The values resulting from these studies are summarized in Table 11-2.

Table 11-2. Time Effect Factors (λ)

Load Combination		Time Effect Factor
1.4 D		0.6
1.2 D+1.6L + 0.5 (L ₁ or S or R)	L _{storage}	0.7
	L _{occupancy}	0.8
	L _{impact}	1.25*
1.2D+1.6(L ₁ or S or R) + 0.5L		0.8
1.2D+1.6(L ₁ or S or R) + 0.8W		1.0
1.2D+1.3W+0.5L+0.5(L ₁ or S or R)		1.0
1.2D+1.5E+(0.5L or 0.2S)		1.0
0.9D-(1.3W or 1.5E)		1.0

*For connections, $\lambda = 1.0$ for L from impact.

Resistance factors, ϕ , have been assigned for each limit state, i.e., tension, compression, shear, etc. The following factors have been assigned for the current draft of the LRFD Specification:

ϕ_b (flexure)	= 0.85
ϕ_c (compression)	= 0.90
ϕ_s (stability)	= 0.85
ϕ_t (tension)	= 0.80
ϕ_v (shear)	= 0.75
ϕ_z (connections)	= 0.65

The use of simple factors for each limit state requires that the strength of components and connections include adjustment from a basic fifth percentile value (or average yield limit value for connections) to a level which will maintain prescribed levels of reliability. This method achieves designer simplicity and enables accurate strength assessment for each component, member and connection⁽¹¹⁻⁴⁷⁾.

As an example, the basic equation for moment design of bending members is

$$\lambda \phi_b M' = \lambda \phi_b F_b' S > M_u$$

Where

λ = The Effect Factor
 ϕ_b = 0.85
 F_b' = $F_b C_L C_f C_R C_D C_M C_t$
 S = Section Modulus
 M' = Adjusted Moment Resistance
 M_u = Factored Moment (i.e. 1.2D+1.6L)

11.2.2 Serviceability / Drift

Serviceability issues have long been recognized as an important consideration in the design of wood structures. Current specifications include limitations on deflection such as span/360 aimed at preventing cracking and providing protection from excessive deflection. While such restriction have proved to be adequate in many cases, they do not uniformly address problems of vibration and other serviceability issues⁽¹¹⁻⁵⁰⁾.

The U.S. LRFD Specification has taken a different approach which more nearly reflects practice regarding serviceability issues with other construction materials. The Specification requires structural engineers to address serviceability in design to ensure that "deflections of structural members and systems due to service loads shall not impair the serviceability of the structure." To assist the structural engineer in checking for serviceability, a comprehensive commentary is provided. Serviceability is defined broadly to include:

- Excessive deflections or rotation that may affect the appearance, functional use or

drainage of the structure, or may cause damaging transfer of load to non-load supporting elements and attachments.

- Excessive vibrations produced by the activities of building occupants or the wind, which may cause occupant discomfort or malfunction of building service equipment.
- Deterioration, including weathering, rotting, and discoloration."

It should be noted that checks on deflection and vibration should be made under service loads. The Specification defines service loads as follows:

"Service loads that may require consideration include static loads from the occupants and their possessions, snow on roofs, temperature fluctuations, and dynamic loads for human activities, wind-induced effects, or the operation of building service equipment. The service loads are those loads that act on the structures at an arbitrary point in time. In contrast, the nominal loads are loads with a small probability (in the range of 0.01 to 0.10) of being exceeded in 50 years (ASCE 7-98). Thus, appropriate service loads for checking serviceability limit states may be only a fraction of the nominal loads."

Detailed guidance is provided in the Specification Commentary for serviceability design for vertical deflections, drift of walls and frames, deflection compatibility, vibration prevention and for long-term deflection (creep). While this approach is not as prescriptive as in past codes, it is felt that by providing detailed guidance on methods for preventing serviceability problems, structural engineers will deal more realistically with these issues. In the past, structural engineers have often been misled into believing that by simply meeting a prescriptive requirement, SPAN/360 for example, that serviceability requirements would

automatically be satisfied. Of course, this has not always been the case.

11.3 LRFD/ LIMIT-STATE DESIGN FOR MASONRY CONSTRUCTION

The seismic design of masonry structures has made significant advances in the last decade. Initially the lead was provided by New Zealand and Canadian structural engineers and their contributions can be noted in the proceedings of the first three North American Masonry Conferences^(11-1, 11-2, 11-3) plus the third and forth Canadian Masonry Symposia^(11-4, 11-5). In the United States the work of the Masonry Society in the development of the 1985 Uniform Building Code⁽¹¹⁻⁶⁾ provided a point which marks a change in attitude and direction of seismic masonry design. While notable earlier masonry research efforts by Hegemier⁽¹¹⁻⁷⁾ and Mayes⁽¹¹⁻⁸⁾ were directed at seismic design considerations, it was the development of the 1985 UBC code, the Structural Engineers Association of California (SEAOC) review of the proposed code, and finally the adaptation in the 1985 by International Conference of Building Officials that started the new direction for seismic design of masonry structures.

The development of this new seismic design approach from the design implementation perspective is documented by approval by the International Conference of Building Officials (ICBO) of three design standards. They are:

1. The Strength Design Criteria for slender walls in section 2411 of the 1985/1991 UBC.
2. The Strength Design Criteria for one to four story buildings in ICBO Evaluation Services Inc., Evaluation Report Number 4115, first published in 1983⁽¹¹⁻⁹⁾
3. The Strength Design Criteria for shear walls in Section 2412 of the 1988/1991 UBC⁽¹¹⁻¹⁰⁾.

11.3.1 Behavior and Limit States

The behavior of a masonry component or system when subjected to loads can be described in terms of behavior and limit states. For illustrative purposes, we will use the slender wall shown in Figure 11-1.

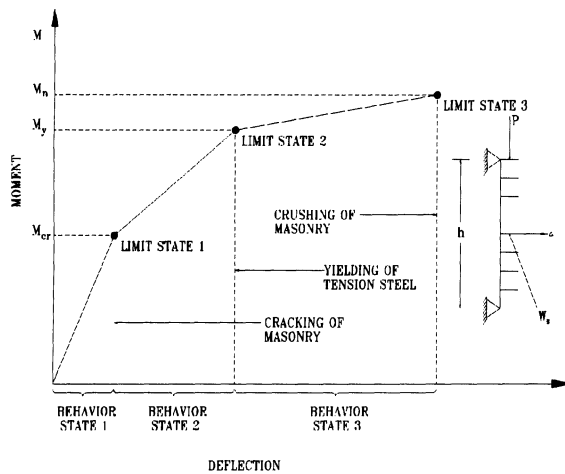


Figure 11-1. Moment-deflection curve for a typical slender wall

Table 11-3. Behavior and Limit States for a Ductile Slender Wall.

State	Description
Behavior state 1	Uncracked cross-section and $M < M_{cr}$
Limit state 1	$M = M_{cr}$ and stress in the masonry equal to the modulus of rupture.
Behavior state 2	Cracked cross-section with strain in the steel less than its yield strain and $M_{cr} < M < M_y$.
Limit state 2	$M = M_y$ and strain in the steel equal to its yield strain.
Behavior state 3	Cracked cross-section with strain in the steel greater than its yield strain but the maximum strain in the masonry less than its maximum usable strain and $M_y < M < M_u$.
Limit state 3	$M = M_u$ and strain in masonry equal to maximum usable strain.

As indicated in this figure the slender wall can be idealized for structural design as evolving through several identifiable states of behavior prior to reaching its final deformed position. We can define this evolution in terms

of "Behavior States". Table 11-3 defines the behavior states for the slender wall. For example, the first behavior state corresponds to the stress condition where the load-induced tensile stress is less than the modulus of rupture. In this behavior state, the wall cross section is uncracked and the load-induced moment is less than the cracking moment capacity of the wall cross section.

A "Limit State" exists at the end of each behavior state (see Table 11-3). For example, at the end of the first behavior state, we have the first limit state and it exists when the lateral load on the wall produces a tensile stress equal to the modulus of rupture.

The slender wall, goes through several behavior states prior to reaching its final or "Ultimate Limit State". For example, if we consider the load-induced moment as a measurable variable, it can be used to define the existence of the first limit state. In this case, the load-induced moment M will be equal to the cracking moment of the cross section (M_{cr}). The second limit state exists when the moment M is equal to the yield moment (M_y) and the third limit state exists when M is equal to the moment capacity of the wall (M_n). Therefore, we have identified three limit states whose existence can be numerically quantified as follows:

Limit State	Moment	Condition/Comment
1	M_{cr}	Serviceability/Cracking of Cross Section
2	M_y	Damage Control/ Permanent Steel Deformation
3	M_n	Ultimate/Nominal Moment Strength

Each of these limit states can be the focus of concern for the structural engineer according to different client or design criteria requirements. For example, the first limit state relates to the cracking of the cross section, and thus, possible water penetration. It can be viewed as a "Serviceability Limit State". The second limit state defines the start of permanent steel deformation or significant structural damage. It can be viewed as either a "Serviceability" or a

"Structural Damage Limit State". Finally, the third limit state defines the limit of our acceptable wall performance from a life safety perspective. Therefore, it is an "Ultimate" or "Strength" Limit State. Typically, it is this limit state that we are concerned with when we use the design approach called strength design. Limit state design can be thought of as a generalization of strength design where we leave open the possibility of addressing limit states other than the strength limit state.

The structural engineer must review the limit states that can exist for the structure he or she is designing. Then, a design criteria must be established that ensures, with an acceptable level of reliability, that the limit states that the structural engineer has identified as undesirable do not exist. For example, current slender wall design criteria adopted by the International Congress of Building Officials (ICBO) in the 1994 and 1997 Uniform Building Codes (UBC) identify an ultimate or strength design limit state that corresponds to limit state 3 in Table 11-3^(11-6, 11-10). For this example, the "Limit State Equation" is:

$$M_u \leq \phi M_n \quad (11-1)$$

where

M_u = Factored Moment or Load induced moment obtained from factored design loads.

M_n = nominal moment strength of the wall.

ϕ = capacity reduction factor that is intended to ensure that an acceptable level of reliability exists in the final design.

The design criteria must address both sides of Equation 11-1. The load-induced moment is obtained from a structural analysis using factored deterministic design loads. We calculate the nominal moment capacity of the wall using the nominal design values of the structural parameters, e.g., specified compressive strength, modulus of elasticity, etc., and the equations of structural engineering.

11.3.2 Limit States and Structural Reliability

One task in the United States-Japan coordinated research program under the direction of the Technical Coordinating Council for Masonry Research (TCCMAR) focused on the evaluation of available approaches whereby masonry design could incorporate the analytical method of structural reliability into "Limit State Design"⁽¹¹⁾. These reliability methods ranged from the very direct to the extremely sophisticated. It is the conclusion of the TCCMAR Category 8, Task 8.1 research that it is possible to significantly extend the rigor of today's masonry code to incorporate structural reliability. The new Steel Design Criteria accepted for the 1988 Uniform Building Code is Load and Resistance Factor Design (LRFD) and is based on structural reliability^(11-12,11-13,11-14,11-15). LRFD will, in all probability, be the basis of modern reinforced masonry design. The remainder of this section presents the basics of the LRFD approach and indicates why the identification and quantification of behavior and limit states is so important.

A limit state occurs when a load, Q , on a structural component equals the resistance, R , of the component. The occurrence of the limit state exists when $F=0$, where

$$F = R - Q \quad (11-2)$$

Consider our slender wall example and the third (or strength) limit state. We can consider R to be the moment capacity of the wall and Q to be the dead plus live plus seismic moment demand. If we denote the factored moment or "Moment Demand" as M_u , and the nominal moment strength or "Moment Capacity" as M_n , then Equation 11-2 can be written as

$$F = M_n - M_u \quad (11-3)$$

This equation is called the limit state design equation. The strength limit state exists when $M_u = M_n$ or, alternatively, $F = 0$. Stated differently, if F is greater than zero we know

that one of the first three behavior states exists and that the third limit state does not exist.

The economics of building design and construction requires us to have a balance between the safety that a limit state will not exist or be violated and construction costs. This, historically, has been attained by using a term called the factor of safety. In structural reliability, the parallel term is referred to as the "Reliability Index" associated with the limit state under consideration.

Because M_n and M_u are not known with certainty they are called random variables. F is a function of M_n and M_u . Hence, it is also a random variable with a mean F and standard deviation σ_F . The reliability index is defined in terms of the statistical moments of F . The reliability index β can be defined as

$$\beta = F/\sigma_F \quad (11-4)$$

Structural reliability theory and the associated mathematics is typically too complex for most design applications. Therefore, for design purposes, we must develop a more direct design criteria. Ideally, it is based on structural reliability concepts. This can be accomplished using the "First Order Second Moment" structural reliability theory. This theory first performs a Taylor's series expansion of F in terms of the random variables, for example R and Q . This expansion is done about the mean value of the random variables and only the first order partial derivatives are retained in the Taylor's series expansion, i.e., the name first order. Next, the mean and standard deviation of F in its Taylor's Series expanded form are calculated in terms of the mean and standard deviation (or, alternatively, coefficient of variation) of R and Q . Thus, the second term in the name "first order second moment" refers to second order statistical moments. With the mean and standard deviation of F so calculated, the reliability index can be expressed in terms of a constant α , the means (R and Q) and coefficient of variations (V_R and V_Q) of the random variables. So doing, we can write:

$$Q e^{\mu\beta V_Q} = R e^{-\mu\beta V_R} \quad (11-5)$$

Note that the right side of the equation relates to the resistance and the left side to the load effect. If we again consider the slender wall example, we can express this equation as:

$$M_u e^{\mu\beta V_{M_u}} = M_n e^{-\mu\beta V_{M_n}} \quad (11-6)$$

where

M_u and M_n = mean of M_u and M_n .
 V_{M_u} and V_{M_n} = coefficient of variation of M_u and M_n .

The left hand side of Equation 11-6 is the factored moment or "Design Moment Demand" and ideally is equal to the left hand side of Equation 11-1. The ASCE 7-88⁽¹¹⁻⁴¹⁾ load factors or similar reliability based factored loads define this design moment demand.

The right hand side of Equation 11-6 is the nominal moment strength or "Design Moment Capacity" that will have a level of structural reliability or safety β . This can be written as:

$$M_n = M_u e^{-\mu\beta V_{M_u}} \quad (11-7)$$

If we recall the right hand side of the limit state design equation for moment capacity given in Equation 11-1, it follows that:

$$M_u = \phi M_n = \phi M_u e^{-\mu\beta V_{M_u}} \quad (11-8)$$

Therefore, the capacity reduction factor ϕ , for this limit state is:

$$\phi = \frac{M_u}{M_n} e^{-\mu\beta V_{M_u}} \quad (11-9)$$

Equation 11-9 shows the dependence of the capacity reduction factor ϕ on: (i) the ratio of the factored moment to nominal design moment, (ii) the uncertainty or quality of construction and analytical modeling as manifested in the value of V_{M_u} , and (iii) the level of reliability, β value, that the design

criteria seeks to attain. These three items can and must be the focus of discussion among those involved in future masonry design criteria development.

11.4 SEISMIC LATERAL FORCES AND HORIZONTAL DIAPHRAGMS

11.4.1 Seismic Lateral Forces

Most wood and masonry buildings are one to three stories in height and qualify to be designed using a static lateral force procedure (SLFP). Thus the total design base shear in a given direction (V) is determined from the following Formula:

$$V = \frac{C_v I}{R T} W \quad (11-10A)$$

The total design base shear need not exceed the following:

$$V = \frac{2.5 C_a I}{R} W \quad (11-10B)$$

The total design base shear shall not be less than the following:

$$V = 0.11 C_a I W \quad (11-10C)$$

In addition, for seismic zone 4, the total base shear shall also not be less than the following:

$$V = \frac{0.8 Z N_v I}{R} W \quad (11-10D)$$

Where:

C_v = Seismic coefficient dependent upon soil profile type, as set forth in table 16-R of UBC 97⁽¹¹⁻³⁸⁾. C_v is a function of Z, seismic zone factor (effective

peak ground acceleration) and N_v , near-source factor in seismic zone 4.

- I = Importance factor.
- R = Numerical coefficient representative of the inherent over strength and global ductility capacity of lateral – force – Resisting systems, as set forth in table 16-N or 16-P of UBC 97⁽¹¹⁻³⁸⁾.
- T = Elastic fundamental period of vibration, in seconds, of the structure in the direction under consideration. The fundamental period T may be approximated from this following formula:

$$T = C_t (h_n)^{3/4} \quad (11-10E)$$

- Where:
- C_t = 0.035 for steel moment-resisting frames
- = 0.030 for reinforced concrete moment resisting frames
- = 0.020 for all other buildings
- W = The total seismic dead load including partition loads, snow loads, weight of permanent equipment and a minimum of 25 percent of storage live load (Note: Storage live load is defined as a uniform load of 125 PSf or greater).
- C_a = Seismic coefficient dependent upon soil profile type, as set forth in table 16-Q of UBC97⁽¹¹⁻³⁸⁾. C_a is a function of Z, seismic zone factor (effective peak ground acceleration) and N_a , near-source factor in seismic zone 4.
- N_a = Near-source factor used in the determination of C_a in seismic zone 4 related to both the proximity of the building or structure to known faults with magnitudes and slip rates as set forth in tables 16-S and 16-U of UBC97⁽¹¹⁻³⁸⁾. Note the magnitude of N_a (and thus the increase in base shear V) varies from 1.0 to 1.5.
- N_v = Near-source factor used in the determination of C_v in seismic zone 4 related to both the proximity of the

building or structure to known faults with magnitudes and slip rates as set forth in tables 16-T and 16-U of UBC97⁽¹¹⁻³⁸⁾. Note the magnitude of N_V (and thus the increase in base shear V) varies from 1.0 to 2.0.

A comparison of design base shear values for a 3-story wood building and a 3-story masonry building are presented in tables 11-10 and 11-11 (last chapter page). Note that for these types of buildings (relatively stiff/Rigid structural system with short period) The total design base shear is governed by Eq. 11-10B. Also note special provisions for near field effects in seismic zone 4 (i.e. N_V and N_a) and special minimum base shear equation 11-10D.

The vertical distribution of the design base shear over height of the structure is determined by the following formula:

$$F_x = \frac{(V - F_t)W_x h_x}{\sum_{i=1}^n W_i h_i} \quad (\text{Eq.11-11})$$

Where:

F_x = force applied at level n

w_x = that portion of W located at level x

h_i = height above base to level x

$F_t = 0.07TV$

= 0 for T of 0.7 seconds or less

= 0 for most wood or masonry buildings

The story force F_x at each level is applied to the diaphragm, then distributed through the diaphragm, collected by the drag or collector members, and delivered to the vertical lateral force resisting elements, such as shear walls, frames, braces, etc. The walls, frames or braces which resist these forces at each level, shall be analyzed and designed to meet stress and drift requirements.

Horizontal diaphragms (floor and roof diaphragms) shall be designed to resist forces determined in accordance with the following formula:

$$F_{px} = \frac{F_t + \sum_{i=x}^n F_i}{\sum_{i=x}^n W_i} W_{px} \quad (\text{Eq. 11-12})$$

Where:

F_{px} need not exceed $0.5C_aIW_{px}$ but shall not be less than $1.0C_aIW_{px}$.

The forces in both formulas are inertia forces at each level which represents the acceleration of the weight at each level. Formula (Eq. 11-11) produces the triangular distribution of forces for the overall analysis of the building which should fairly represent the distribution of forces from a dynamic analysis where the modes are combined. Formula (Eq. 11-12) represents a diaphragm design force which should represent the acceleration determined from the dynamic analysis for each diaphragm times the weight of the diaphragm. It is preferable to use the term "seismic coefficient" rather than acceleration/g since both formulas do not represent true earthquake acceleration but rather scaled design forces. Both formulas yield the same seismic coefficient for a one story building or at the roof of a multi-story building. The diaphragm design seismic coefficients are always larger than those for the story forces for the other levels.

The weight terms in Formula (Eq. 11-11) and (Eq. 11-12) are different. The term W_x in Formula (Eq. 11-11) is the total weight of each level of the building including all seismic resisting elements (walls, etc.) in both directions. The term W_{px} is the weight of the diaphragm and the seismic resisting elements which are being accelerated with the diaphragm and typically does not include the weight of the seismic resisting elements parallel to the direction of the forces (perpendicular to the span of the diaphragm)

Concrete or masonry walls shall be anchored to all floors and roofs which provide lateral support for the wall. The anchorage shall

provide positive direct connections between the wall and floor or roof construction capable of resisting the forces specified or a minimum force of 280 plf, whichever is greater. Walls shall be designed to resist bending between anchors when the anchor spacing exceeds 4 feet. Diaphragm deformations shall be considered in the design of the supported walls.

Diaphragms supporting concrete or masonry walls shall have continuous ties or struts between diaphragm chords to distribute the anchor forces. Added chords may be used to form sub-diaphragms to transmit the anchor forces to the main cross ties. A sub-diaphragm is a portion of a larger diaphragm designed to anchor and transfer local forces to primary diaphragm struts and the main diaphragm.

In Seismic Zones Nos. 2,3 and 4 anchorage shall not be accomplished by use of toenails or nails subject to withdrawal, nor shall wood ledgers or framing be used in cross-grain bending or cross-grain tension, and the continuous ties required shall be in addition to the diaphragm sheathing.

11.4.2 Horizontal Diaphragms

The total shear at any level will be distributed to the various vertical lateral force resisting elements (VLFR) of the lateral force resisting system (shear walls or moment-resisting frames) in proportion to their rigidities considering the rigidity of the diaphragm. The effect of diaphragm stiffness on the distribution of lateral forces is discussed below. For this purpose, diaphragms are classified into two groups rigid or flexible.

A rigid diaphragm (concrete) is assumed to distribute horizontal forces to the VLFR elements in proportion to their relative rigidities.^(11-29, 11-30, 11-31, 11-32) In other words, under symmetrical loading a rigid diaphragm will cause each VLFR element to deflect an equal amount with the result that a VLFR element with a high relative rigidity or stiffness will resist a greater proportion of the lateral force than an element with a lower rigidity factor.

A flexible diaphragm (maybe plywood) is analogous to a shear deflecting continuous beam or series of simply supported beams spanning between supports. The supports are considered non-yielding, as the relative stiffness of the vertical lateral force resisting elements compare to that of the diaphragm is great. Thus, a flexible diaphragm will be considered to distribute the lateral forces to the VLFR elements on a tributary area basis. A flexible diaphragm will not be considered capable of distributing torsional stresses, see Figure 11-2A & 11-2B.

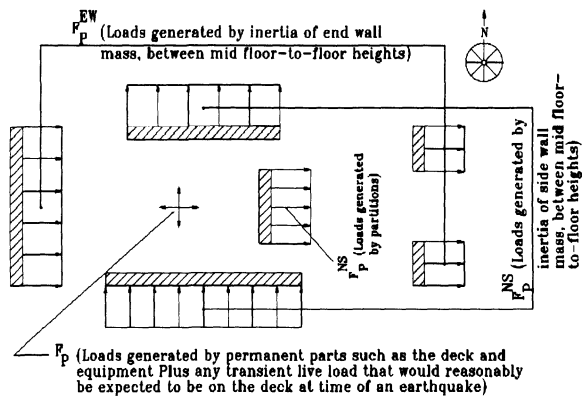


Figure 11-2A. Flexible/Plywood Diaphragm

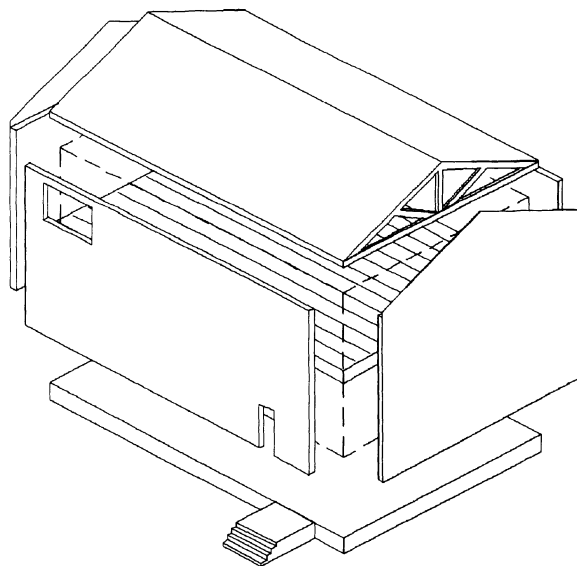


Figure 11-2B. Lateral Force Resisting System in all wood Building

Generally, it is assumed that the in-plane mass of a shear wall does not contribute to the diaphragm loading unless the shear wall is interrupted at the specific level. In case a shear wall does not extend below the floor level, both its horizontal and vertical loads must be distributed to the remaining walls. Of course, major difference in rigidities may be cause for redistribution.

A torsional moment is generated whenever the center of gravity (CG) of the lateral forces fails to coincide with the center of rigidity (CR) of the VLFR elements, providing the diaphragm is sufficiently rigid to transfer torsion. The magnitude of the torsional moment that is required to be distributed to the VLFR elements by a diaphragm is determined by the sum of the moments created by the physical eccentricity of the translational forces at the level of the diaphragm from the center of rigidity of the resisting elements ($M_T = F_p e$, where e = distance between CG and CR) plus the "accidental" torsion of 5%. The "accidental" torsion is an arbitrary code requirement intended to account for the uncertainties in the location of loads and stiffness of resisting elements. The accidental torsion is equivalent to the story shear acting with an eccentricity of not less than 5% of the building dimension at that level perpendicular to the direction of the force under consideration. The torsional distribution by rigid diaphragms to the resisting elements will be assigned to be in proportion to the stiffness of the elements and its distance from the center of rigidity.

The torsional design moment at a given story shall be the moment resulting from the eccentricities between applied design lateral forces at levels above that story and the VLFR elements in the story plus an accidental torsion. Negative torsional shear shall be neglected. Flexible diaphragms shall not be used for torsional distribution. Cantilever diaphragms on the other hand will distribute translational forces to VLFR elements, even if the diaphragm is flexible. In this case, the diaphragm and its chord act as a flexural beam

on supports (VLFR elements) whose resistance is in the same direction as the forces.

Diaphragms shall be considered flexible for the purposes of distributions of story shear and torsional moments when the maximum lateral deformation is more than two times the average story drift of the associated story. This may be determined by comparing the computed midpoint in-plane deflection of the diaphragm itself under lateral force with the story drift of adjoining vertical lateral force resisting elements under equivalent tributary lateral force.

The critical aspect of this new definition is that it may require that a given diaphragm be designed as rigid in one direction and flexible in the other orthogonal direction. For example, the plywood roof of a large and narrow masonry building with minimal shear walls in the long direction could qualify as a rigid diaphragm in the long direction and flexible in the narrow or short direction; which is probably closer to the actual behavior and observed performance of this type of building during an earthquake. See Tables 11-4 and 11-5 for equations for deflections of walls and diaphragms.

The general characteristics of motion of a flexible diaphragm is that the walls, being relatively rigid, respond to the accelerations of the ground, but a flexible (wood or metal deck) roof diaphragm, responds with an amplified motion. In seismic zones 3 and 4 with flexible diaphragms as defined above provide lateral support for walls, the values of F_p for anchorage shall be increased 50 percent.

11.5 FLEXIBLE HORIZONTAL DIAPHRAGM (PLYWOOD)

A horizontal plywood diaphragm acts in a manner analogous to a deep beam, where the plywood skin acts as a "web", resisting shear, while the diaphragm edge members perform the function of "flanges", resisting tension and compression induced by bending. These edge members are commonly called chords in diaphragm design.

Table 11-4. Concrete/CMU/Brick Wall Displacements

Fixed - Fixed $\beta = 1.2 \text{ & } G = E/2.2$	Fixed - Hinged $\beta = 1.2 \text{ & } G = E/2.2$	Comments
$\Delta = \frac{Ph^3}{12EI} + \frac{BPh}{GA}$ $= \frac{P}{E} \left[\frac{h^3}{12I} + \frac{1.2h(2.2)}{A} \right]$ $= \frac{P}{E} \left[\frac{h^3(12)}{12td^3} + \frac{2.64h}{td} \right]$ $= \frac{P}{Et} \left[\left(\frac{h}{d} \right)^3 + 2.64 \frac{h}{d} \right]$	$\Delta = \frac{Ph^3}{3EI} + \frac{BPh}{GA}$ $= \frac{P}{E} \left[\frac{h^3}{3I} + \frac{1.2h(2.2)}{A} \right]$ $= \frac{P}{E} \left[\frac{h^3(12)}{3td^3} + \frac{2.64h}{td} \right]$ $= \frac{P}{Et} \left[4 \left(\frac{h}{d} \right)^3 + 2.64 \frac{h}{d} \right]$	The Value for G as given in the literature varies from E/2.2 to E/2.5 $I = td^3/12$ $A = td$ Where: t = Wall Thickness d = Wall Depth h = Wall Height p = Load applied at top of Wall (lbs)
Fixed - Fixed $\beta = 1.2 \text{ & } G = E/2.5$	Fixed - Fixed $\beta = 1.2 \text{ & } G = E/2.5$	
$\Delta = \frac{P}{E} \left[\frac{h^3}{12I} + \frac{1.2h(2.5)}{A} \right]$ $= \frac{P}{Et} \left[\left(\frac{h}{d} \right)^3 + 3.0 \frac{h}{d} \right]$	$\Delta = \frac{P}{E} \left[\frac{h^3}{3I} + \frac{1.2h(2.5)}{A} \right]$ $= \frac{P}{Et} \left[4 \left(\frac{h}{d} \right)^3 + 3.0 \frac{h}{d} \right]$	

Table 11-5. Concrete Diaphragm Displacements

Hinged - Hinged $\beta = 1.2 \text{ & } G = E/2.2$	Hinged - Hinged $\beta = 1.2 \text{ & } G = E/2.2$	Comments
$\Delta = \frac{5Wl^4}{384EI} + \frac{\beta l^2 W}{8AG}$ $= \frac{5WL^4(12)}{384Et^3} + \frac{1.2l^2W(2.2)}{8btE}$ $= \frac{Wl^4}{6.4Et^3} + \frac{0.33l^2W}{btE}$ $= \frac{Wl}{Et} \left[\frac{1}{6.4} \left(\frac{l}{b} \right)^3 + 0.33 \left(\frac{l}{b} \right) \right]$ $= \frac{Wl}{6.4Et} \left[\left(\frac{l}{b} \right)^3 + 2.13 \left(\frac{l}{b} \right) \right]$	$\Delta = \frac{5Wl^4}{384EI} + \frac{\beta l^2 W}{8AG}$ $= \frac{5WL^4(12)}{384Et^3} + \frac{1.2(l^2)W(2.5)}{8btE}$ $= \frac{Wl^4}{6.4Et^3} + \frac{0.375l^2W}{btE}$ $= \frac{Wl}{Et} \left[\frac{1}{6.4} \left(\frac{l}{b} \right)^3 + 0.375 \left(\frac{l}{b} \right) \right]$ $= \frac{Wl}{6.4Et} \left[\left(\frac{l}{b} \right)^3 + 2.4 \left(\frac{l}{b} \right) \right]$	The Value for G as given in the literature varies from E/2.2 to E/2.5 $I = tb^3/12$ $A = tb$ Where: t = Diaphragm thickness b = Diaphragm Depth l = Diaphragm Length/Width w = Load applied along length of diaphragm (Plf)

Due to the great depth of most diaphragms in the direction parallel to application of force, and to their means of assembly, their behavior differs from that of the usual, relatively shallow, beam. Shear stresses have been proven to be essentially uniform across the depth of the diaphragm, rather than showing significant parabolic variation as in web of a beam. Similarly, chords, in a diaphragm are designed to carry all "flange" stresses, acting in simple tension or compression, rather than sharing these stresses significantly with the web. As in a beam, consideration must be given to bearing stiffeners, continuity of webs and chords, and web buckling.

Plywood diaphragms vary considerably in force-carrying capacity, depending on whether they are "blocked" or "unblocked". Blocking consist of lightweight nailers, usually 2 X 4's, framed between the joist, or other primary structural supports, for the specific purpose of connecting the edges of the plywood sheets. The reason for blocking the diaphragms is to allow nailing of the plywood sheets at all edges for better shear transfer. Design of unblocked diaphragms is controlled by buckling of unsupported plywood panel edges, with the result that such units reach a maximum load above which increased nailing will not increase capacity. For the same nail spacing, allowable design forces on blocked diaphragm are from 1½ to 2 times allowable design forces on its unblocked counter part. In addition, the maximum forces for which a blocked diaphragm can be designed are many times greater than those without blocking.

In a uniformly loaded floor or roof plywood diaphragm the shear normally decreases from a maximum at the exterior wall or boundary to zero at the centerline of a simple single diaphragm building. The four regions of diaphragm nailing are as follows: (1) Boundary - exterior perimeter of the diaphragm; (2) Continuous panel edges - based on the lay of the plywood, the continuous panel edges consist of multiple panel edges in a straight line parallel to the direction of diaphragm shear; (3) Other panel edges - including staggered (or

discontinuous) panel edges; and (4) field - interior of plywood panels. See UBC97 Table 23-11-H for diaphragm values and figures.

A common method of plywood diaphragm design is to vary the nail spacing of the boundary/continuous panel edges and the other panel edges based on the shear diagram. Using this procedure the engineer assigns regions of nail spacing. The transition areas between shear capacity regions are not considered boundary conditions. Boundary nailing only occurs at the perimeter of the plywood diaphragm (i.e. exterior wall). More complicated buildings may be comprised of two or more diaphragms which will require boundary nailing along interior walls and drag struts/collector elements.

The three major parts of a diaphragm are the web, the chords, and the connections. Since the individual pieces of the web must be connected to form a unit, and since the chord members in all probability are not single pieces; connections are critical to good diaphragm action. Their choice actually becomes a major part of the design procedure. Diaphragms are most commonly used for roofs and floors. They function usually as simple beams, and sometimes as cantilever beams. Shear walls or vertical diaphragms function as cantilevered beams. Each diaphragm serves, like a beam, only to transfer force. It must, therefore, be properly connected to resisting elements which can accommodate the force.

Horizontal and vertical diaphragms sheathed with plywood may be used to resist horizontal forces not exceeding those set forth in the code, or may be calculated by principles of mechanics without limitation by using values of nail strength and plywood shear values.⁽¹¹⁻³⁹⁾ Plywood for horizontal diaphragms should be at least ½ inch thick with joist spaced a maximum of 24 inches on center. It is not uncommon to specify 5/8 inch thick plywood with joist spaced a maximum of 24 inches on center for roof construction and 3/4 inch plywood with joist spaced a maximum of 16 inches on center for floor construction to minimize vertical load deflection and vibration concerns.

All boundary members shall be proportioned and spliced where necessary to transmit direction stresses. Framing members shall be at least 2-inch nominal in the dimension to which the plywood is attached. In general, panel edges shall bear on the framing members and butt along their center lines. Nails shall be placed not less than 3/8 inches from the panel edge, and spaced not more than 6 inches on center along panel edge bearings. Nails shall be firmly driven into the framing members. No unblocked panels less than 12 inches wide shall be used.

Lumber and plywood diaphragms may be used to resist horizontal forces in horizontal and vertical distributing or resisting elements, provided the deflection in the plane of the diaphragm as determined by calculations, test, or analogies drawn there from, does not exceed the permissible deflection of attached distributing or resisting elements.

Permissible deflection shall be that deflection up to which the diaphragm and any attached distributing or resisting element will maintain its structural integrity under assumed force/load conditions (i.e. continue to support design loads without danger to occupants of the structure).

Connections and anchorages capable of resisting the design forces shall be provided between the diaphragms and resisting elements. Openings in diaphragms which materially affect their strength shall be fully detailed on the plans, and shall have their edges adequately reinforced to transfer all shearing stresses. Flanges shall be provided at all boundaries of diaphragms and shear walls.

Additional restrictions are sometimes imposed by local jurisdictions. For example same cities limit the maximum distance between resisting elements of horizontal diaphragms to 200 feet for plywood with blocking, 150 feet for special double diagonal sheathing, 75 feet for plywood without blocking, and 75 feet for diagonal sheathing, unless evidence is submitted and approved by the Superintendent of Building illustrating that no hazard would result from deflections.

11.5.1 Deflections and Deflection Compatibility

Codes do not usually require deflection calculations if diaphragm length-width ratios are Restricted. The Uniform Building Code⁽¹¹⁻³⁸⁾ limits these ratios to 4:1 for horizontal diaphragms, and 2:1 for vertical diaphragms.

The deflection formula, taken from Douglas Fir Plywood Association Laboratory Report No. 55 by David Countryman - March 28, 1951, and Published in Uniform Building Code Standards 97,⁽¹¹⁻³⁸⁾ is

$$d = \frac{5vL^3}{8EA_b} + \frac{vL}{4Gt} + 0.188Le_n + \frac{\sum(\Delta_c X)}{2b} + EWD \quad (11-13)$$

Where:

d = mid-span deflection, inches

v = maximum shear, due to design loads in the direction under consideration, lb/ft.

L = length of diaphragm, feet

E = modulus of elasticity of chords, (Approximately 1,800,000 psi)

A = cross-sectional area of chords, inches²

b = width of diaphragm, feet

G = Shear modulus, psi (Approximately 90,000 psi)

t = effective thickness of plywood panels for shear,in

e_n = nail deformation/slippage inches, see Table 11-6

$\Sigma(\Delta_c X)$ = Sum of Individual chord-splice slip values each multiplied by its distance to nearest support

EWD = End wall deflection

$\Delta = L/480$ = Guideline allowable deflection

The first term represents deflection due to bending, the second term represents deflection due to panel shear, the third term represents the deflection from panel rotation caused by nail deformation/ slippage, the fourth represents

Table 11-6. "e_n" values (inches) for use in calculating diaphragm deflection due to nail deformation/slippage (structural 1 plywood)^{1,2,3,4}

Loads Per Nail (Pounds)	Nail Designation/Size		
	6d	8b	10d
60	0.012	0.008	0.006
80	0.020	0.012	0.010
100	0.030	0.018	0.013
120	0.045	0.023	0.018
140	0.068	0.031	0.023
160	0.102	0.041	0.029
180	----	0.056	0.037
200	----	0.074	0.047
220	----	0.096	0.060
240	----	----	0.077

1 Increase "e_n" values 20 Percent for plywood grades other than STRUCTURAL I.

2 Values apply to common wire nails.

3 Load per nail = maximum shear per foot divided by the number of nails per foot at interior panel edges.

4 Decrease values 50 percent for seasoned lumber.

deflections due to slip in chord splices, and the fifth accounts for end wall deflections.

Example: Calculate the deflection at the center of the long wall of a 200 foot by 400 foot building caused by a seismic force of 800 PLF, assuming all panel edges are blocked.

Thus:

$$v = 800 \text{ PLF}(400\text{ft})/2 (200\text{ft}) = 800 \text{ PLf}$$

$$L = 400 \text{ ft}$$

$$A = 25 \text{ in}^2 \text{ equivalent area of wood}$$

$$E = 1,800,000 \text{ Psi}$$

$$b = 200 \text{ ft}$$

$$G = 90,000 \text{ Psi}$$

$$t = 15/32 = 0.4653 \text{ in.}$$

$$e_n = 0.047 \text{ For 10d nails @ 3 inch on center (i.e. 200lb/nail)}$$

$$\Delta_c = 1/16 = 0.0625 \text{ at each splice (40 ft on center)}$$

Now:

$$d = \frac{5(800\text{PLF})(400\text{ft})^3}{8(1,800,000\text{PSI})25\text{in}^2(200\text{ft})} = 3.56\text{in}$$

$$+ \frac{800\text{PLF}(400\text{ft})}{4(90,000\text{PSI})(0.4683\text{in})} = 1.90\text{in}$$

$$- 0.188(400\text{ft})(0.047) = 3.53\text{in}$$

$$+ \frac{0.0625(200) + 2(0.0625)[40 + 80 + 120 + 160]}{2(200\text{ft})} = 0.16\text{in}$$

$$d = 9.15 \text{ inch}$$

Recall guideline allowable deflection (Δ)

$$\Delta = \frac{L}{480} = \frac{400\text{ft}(12\text{in}/\text{ft})}{480} = 10 \text{ inch}$$

Note calculated deflection (d) is less than guideline deflection (Δ).

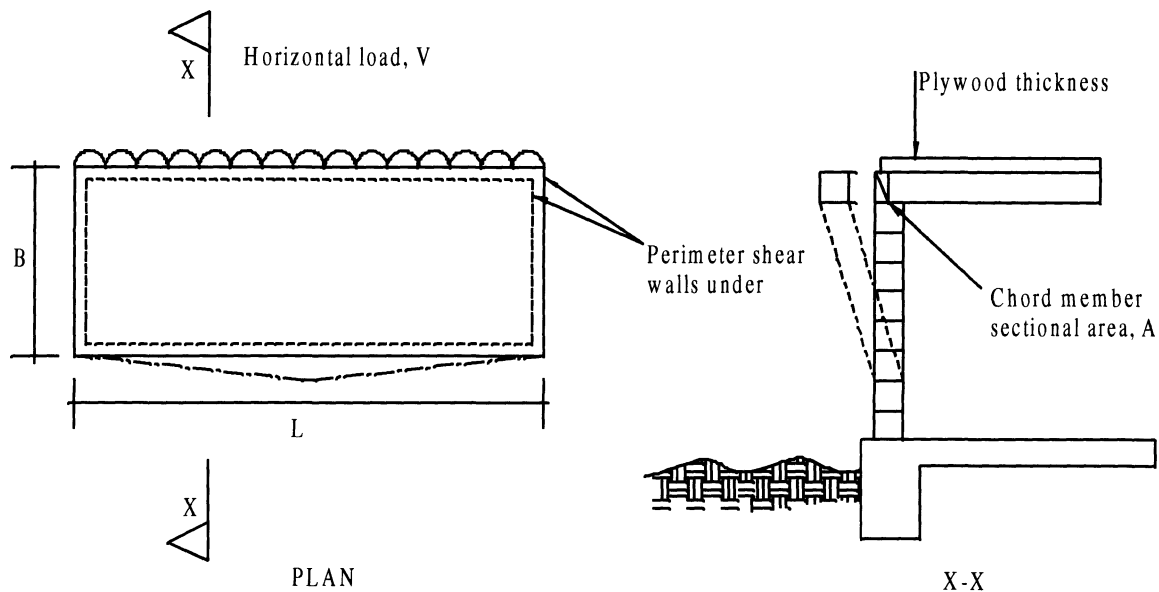
The calculated deflections obtained by the formula conservatively correspond with the results obtained from the full scale 20' x 40' blocked plywood diaphragm tests. The validity of this formula when applied to a span that is 10 times that of the test span is not known. However, the formula does represent the best available means for determining deflections of large spans. It is not applicable to unblocked plywood or diagonal sheathed diaphragm.

The formula for allowable deflection of concrete or masonry walls was developed by the "Horizontal Bracing Systems in Buildings having Masonry or Concrete Walls", Committee of the Structural Engineers Association of Southern California and was published in their Technical Bulletin No. 1, February, 1951. The formula is:

$$d = \frac{75H^2 f_b}{Eb} \quad (11-14)$$

Where:

d = maximum allowable deflection, inches



A typical horizontal timber diaphragm showing the effect on supporting walls of deflections under horizontal loading

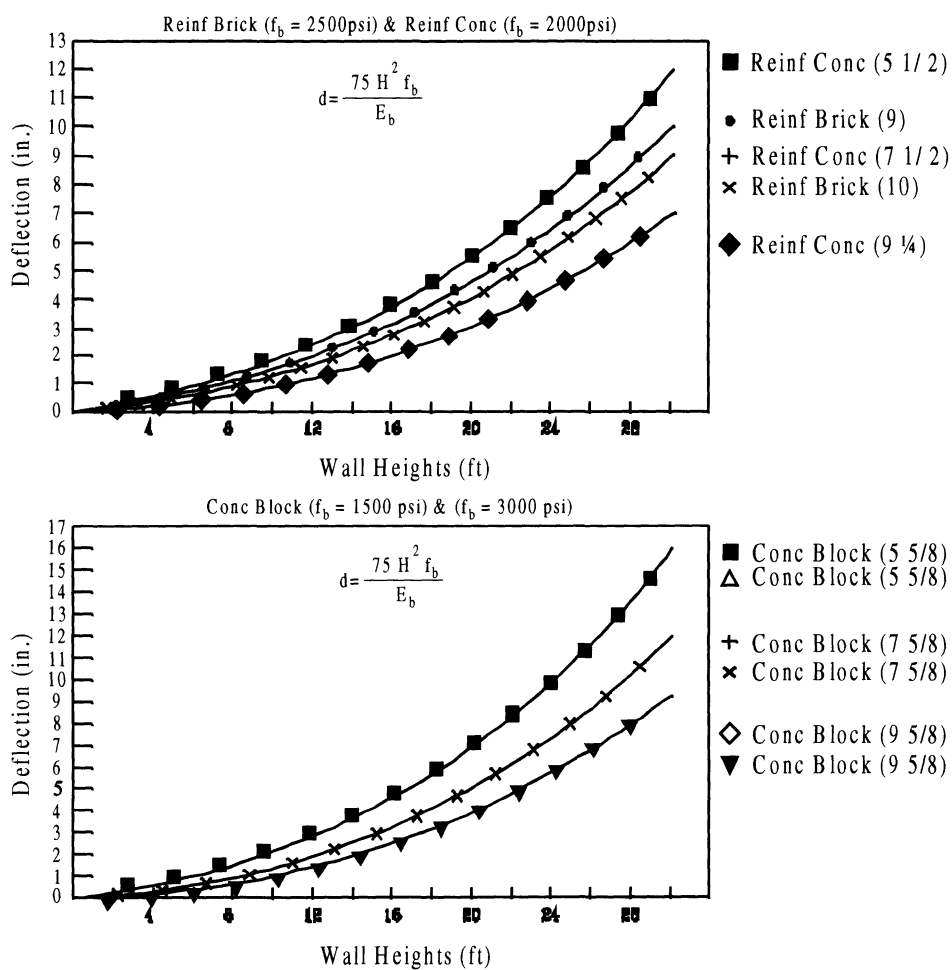


Figure 11-3. Permissive/Allowable Deflection of Concrete and Masonry Walls

H = wall height between horizontal support, feet
 f_b = allowable flexural compressive stress in psi
 E = modulus of elasticity in psi
 b = wall thickness, inches

See Figure 11-3 for plot of above formula and sketch of building and wall deflected shape.

11.5.2 Subdiaphragms

A subdiaphragm is unique to flexible diaphragms. Experience encountered in the San Fernando earthquake of February 1971, revealed that there was a basic weakness present in many of the modern industrial type buildings.

Over the years the practice of installing strap anchors between the walls and wood framing had been for the most part eliminated. The prevalent assumption was that as long as some of the ledger bolts were installed within 3½ to 4 inches of the top of the ledger, the cross grain bending of the ledger would be of a low enough magnitude that it would not result in a failure. This assumption was proven to be incorrect, also a split or crack at the upper ledger bolt might occur simply as a result of shrinkage of an unseasoned member. Especially where two rows of ledger bolts occurred, this split or crack would leave virtually no capacity of cross grain bending. Failures of predominantly tilt-up type buildings occurred at the roof to wall connections in this earthquake.

Much has been said about cross grain bending of wood ledgers which prior to 1972, were utilized for anchoring walls to roof or floor diaphragms. Many of the failures were attributed to cross grain bending, however, many of the failures occurred where the plywood connected to the ledger or in some cases at a point 4 to 8 feet and in some cases 20 feet away from the wall to roof joint. In other words, the wall fell over with a section of the roof still attached, or with the ledger completely attached.

This experience, like previous earthquakes, taught the engineering community an expensive

but important lesson in the behavior of structures. It is vital that we look at not just the building design as a whole, but that we must closely examine all the connections in the load path and make sure that they have the capacity to not only support the calculated load safely, but that they also have the reserve capacity to withstand the short term dynamic forces which may be several times the magnitude of the calculated force and where possible exhibit a yielding type failure rather than a brittle type failure.

The design methodology can be described simply as first calculating and designing the vertical load carrying system of the structure, followed by the lateral design for the structure as a whole establishing the diaphragm shears, nailing patterns and zones in the traditional manner. After this is complete, the members are selected for the required continuity ties across the building. For some framing systems the selection is quite obvious, however, for others it requires some judgment or possible investigation of alternate schemes.

The anchorage force shall be determined using the formula:

$$F_p = 4.0 C_a I_p W_p \quad (11-15A)$$

Alternatively, F_p may be calculated using the following formula:

$$F_p = \frac{a_p C_a I_p}{R_p} \left(1 + 3 \frac{h_x}{h_r} \right) W \quad (11-15B)$$

Except that:

F_p shall not be less than $0.7 C_a I_p W_p$ and need not be more than $4 C_a I_p W_p$.

Where:

h_x = Element or component attachment elevation with respect to grade. h_x shall not be taken less than 0.0.

h_r = Structure roof elevation with respect to grade.

a_p = In structure component amplification factor that varies from 1.0 to 2.5, as set forth in table 16-O

- of UBC97⁽¹¹⁻³⁸⁾; except $a_p = 1.5$ vs 1.0 for anchorage of walls to flexible diaphragms in seismic zones 3 and 4
- R_p = Component response modification factor as set forth in table 16-O of UBC97⁽¹¹⁻³⁸⁾; except that:
- $R_p = 1.5$ for shallow expansion anchor bolts, shallow chemical anchors or shallow cast-in-place anchors. Note shallow anchor bolts are those with an embedment length-to-diameter ratio of less than 8.
 - $R_p = 3.0$ for most other connection with anchor embedment length to diameter ratio equal to or greater than 8.

If the anchors are spaced greater than 4 feet apart, the wall must be designed to span between the anchors. This is generally not a problem for spacing up to 10 feet.

Next, if the members to which the walls are anchored are not continuously tied across the building, the subdiaphragms which carry and distribute these loads to the members and tie across the building, must be selected and analyzed both for shears, and chord forces. Note, the subdiaphragm length to width ratios must meet the 4 to 1 code requirements for plywood diaphragms regardless of the load levels. It is also possible and in some cases desirable to incorporate subdiaphragms into another larger subdiaphragm.

The methodology is probably best understood by the use of design examples.⁽¹¹⁻³⁵⁾ The following example problem will present the seismic design for lateral forces including the design of subdiaphragms for a one-story masonry building with a flexible plywood diaphragm.

11.6 EXAMPLE PROBLEM 1 - L-SHAPED BUILDING WITH CMU WALLS

A framing plan for a one story structure is shown on Figure 11-4. The structure is located in Seismic Zone 4. The importance factor is 1.0. Design for seismic forces only, neglect wind forces. Note walls along lines A,E and G contains 50% openings for truck doors which weighs 10 psf.

Required

- A) Design the roof diaphragm for N-S lateral forces so as to minimize nailing.
- B) Determine the chord forces at grid lines A and E.
- C) Design for the critical lateral forces along line E (3 locations). Indicate by detail how to nail, bolt, etc.
- D) Design the typical ledger bolting to wall along line A between 7 and 8.
- E) Analyze the subdiaphragms so as to minimize the number of cross ties based on the nailing determined in A.
- F) Check for flexible versus rigid diaphragm E-W direction only.

11.6.1 Part A

Lateral loads Seismic - Follow UBC 1997

$$V = \frac{C_v I}{R T} W = 0.763W \quad (11-10A)$$

$$V = \frac{2.5 C_a I}{R} W = 0.256W * \quad (11-10B)$$

$$V = 0.11 C_a I W = 0.051W \quad (11-10C)$$

$$V = \frac{0.80 Z N_v I}{R} W = 0.90W \quad (11-10D)$$

* Governs

Given:

Soil profile type S_D

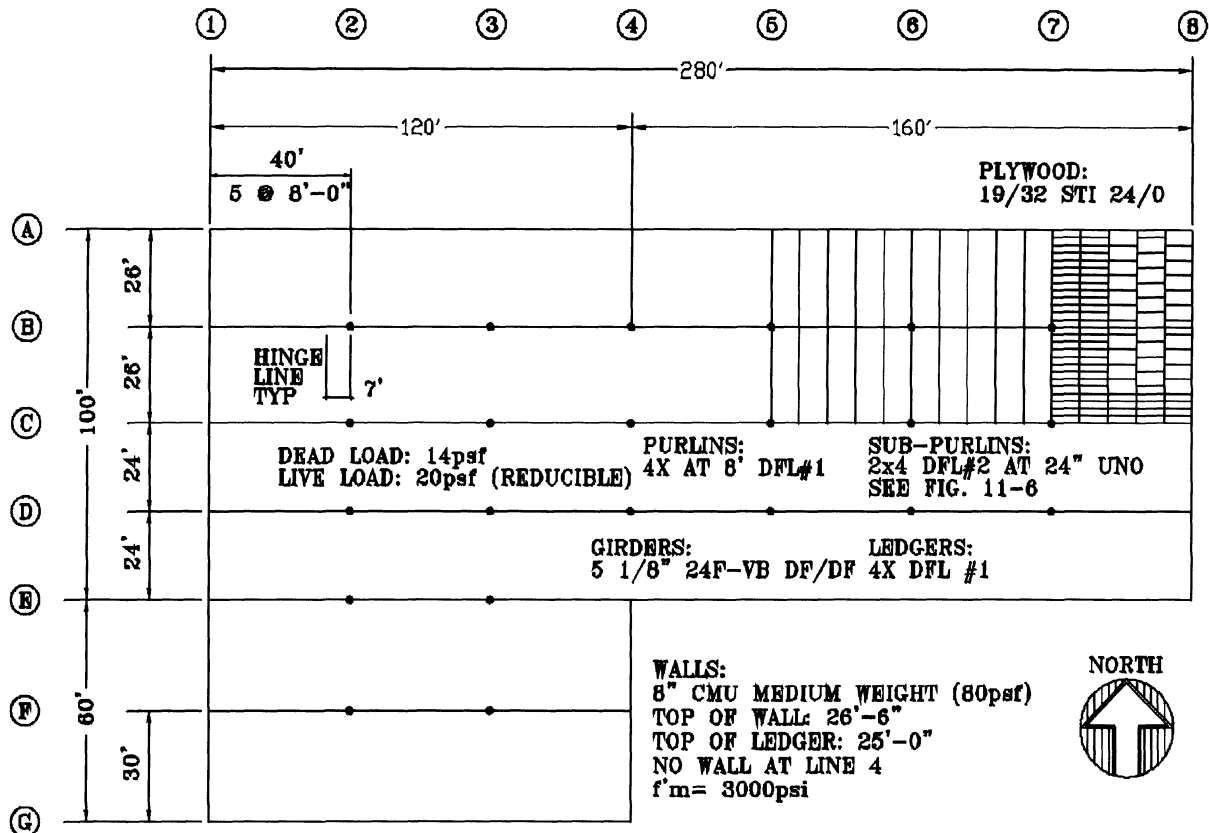


Figure 11-4. Roof Framing Plan

Closest distance to known seismic source =
4.5 km

$$N_a = 1.05$$

$$N_v = 1.27$$

Seismic Zone 4, Z = 0.40

$$C_a = 0.44(1.05) = 0.462$$

$$C_v = 0.64(1.27) = 0.81$$

$$T = 0.020(265)^{3/4} = 0.233 \text{ SEC}$$

$$R = 4.5$$

$$I = 1.0$$

Recall that UBC97 is a strength design code, thus to design wood elements using allowable stress design the seismic forces computed from strength design shall be divided by 1.4.

Therefore: for allowable stress design

$$V = \frac{0.256W}{1.4} = 0.183W$$

N-S Loads:

$$\begin{aligned} \text{Roof} & 14 \text{ PSF} \times 100 \text{ FT} = 1,400 \text{ lb/ft} \\ & 14 \text{ PSF} \times 160 \text{ FT} = 2,240 \text{ lb/ft} \end{aligned}$$

$$8 \text{ inch CMU wall} = 80 \text{ psf} \left[\frac{(26.5)^2}{2 \times 25} \right]$$

$$= 1,123.6 \text{ lb/ft}$$

Recall 50% openings for truck doors at walls A,E and G:

$$\begin{aligned} \text{Revised wall weight} & = 1123.6 \times 0.50 \\ & = 561.8 \text{ plf} \end{aligned}$$

$$\begin{aligned} \text{Weight of doors} & = 1123.6 \left[\frac{10 \text{ psf}}{80 \text{ psf}} \right] \\ & = 140.5 \text{ plf} \end{aligned}$$

$$\text{Total effective wall weight} = 561.8 + 140.5 = 702.3 \text{ plf}$$

Therefore:

$$W_1 = 0.183 [1,400 + 702.3 \times 2] = 513 \text{ lb/ft}$$

$$W_2 = 0.183 [2,240 + 702.3 \times 2] = 667 \text{ lb/ft}$$

$$\Sigma W = 513 \times 160 \text{ ft} + 667 \times 120 \text{ ft} = 162,120 \text{ lb}$$

$$\Sigma M_H = 0$$

Therefore : (See Figure 11-5)

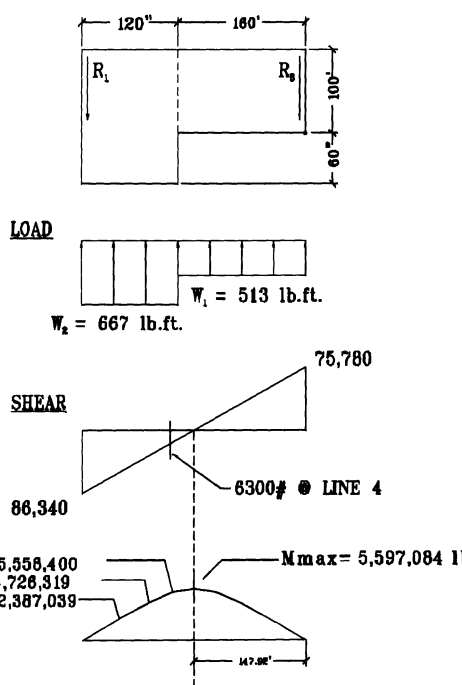


Figure 11-5. Diaphragm Loading

$$\begin{aligned} R_1 &= \frac{1}{280 \text{ ft}} [(513 \times 160 \text{ ft} \times 80 \text{ ft}) + 667 \times 120 \times (60 \text{ ft} + 160 \text{ ft})] \\ &= 86,340 \text{ lb} \\ R_8 &= 162,120 \text{ lb} - 86,340 \text{ lb} = 75,780 \text{ lb} \end{aligned}$$

N - S Roof diaphragm shear : (See Figure 11-6 and Table 11-7)

$$V_{r1} = \frac{86,340 \text{ lb}}{160 \text{ ft}} = 539.6 \text{ lb/ft} \quad \text{panel type B}$$

$$V_{r8} = \frac{75,780 \text{ lb}}{100 \text{ ft}} = 757.8 \text{ lb/ft} \quad \text{panel type A}$$

$$V_{r7} = \frac{75,780 - 513 \times 40 \text{ ft}}{100 \text{ ft}} = 552.6 \text{ lb/ft} \quad \text{panel type B}$$

$$V_{r3} = \frac{86,340 - 667 \times 80 \text{ ft}}{160 \text{ ft}} = 206.1 \text{ lb/ft} \quad \text{panel type C}$$

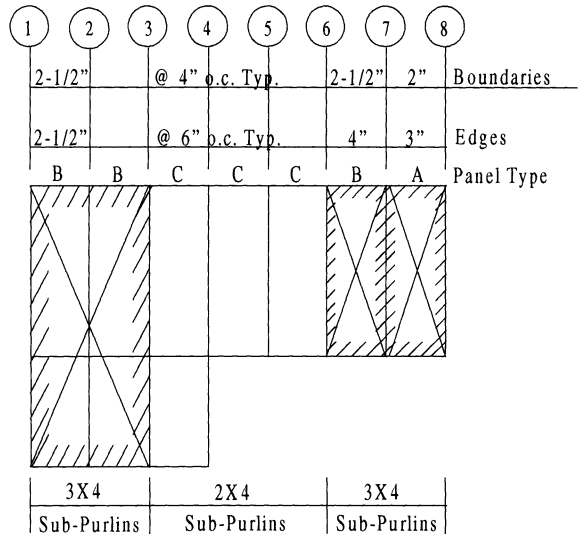


Figure 11-6. NS Loading - Diaphragm Boundaries

Table 11-7. NS Loading - Diaphragm Capacities

Diaphragm Capacity Table				
Type	Bound Nailing	Edge of Nailing	Width of Framing	Capacity Plf
A	2"	3"	3"	820
B	2 1/2"	4"	3"	720
C	4"	6"	2"	425
D ¹	2 1/2"	4"	2"	640

Ref. UBC 91 table 25-J-1

1. Framing at adjoining panel edge shall be 3-inch nominal in width with staggered nail spacing.

$$V_{r6} = \frac{75,780 - 513 \times 80 \text{ ft}}{100 \text{ ft}} = 347.4 \text{ lb/ft} \quad \text{panel type C}$$

Use 19/32 in. plywood str. I All edges blocked

Nailing schedule: Boundary: 10d (see Figure 11-6)

Edges: 10d (see Figure 11-

6)

Field: 10d @ 12 ft o.c.

Minimum allowable diaphragm shear = 425 lb/ft (See Table 11-7)

Note: Alternate use of panel type D instead of panel type B would require 3x4 sub purlins at adjoining panel edge versus all 3x4 members as shown.

11.6.2 Part B

Maximum moment in N-S direction:

$$x = \frac{75,780}{513} = 147.72 \text{ ft from } H$$

Therefore,

$$\begin{aligned} M_{\max} &= 75,780 (147.72) - 513 (147.72) \\ (147.72/2) &= 5,597,084 \text{ lb-ft} \end{aligned}$$

$$F = \frac{M}{D} = \frac{5,597,084}{100 \text{ ft}} = 55,971 \text{ lb}$$

cord stress @ lines A & E

11.6.3 Part C

Consider 3 locations at joints J,K & L on line E, see details on Figure 11-7

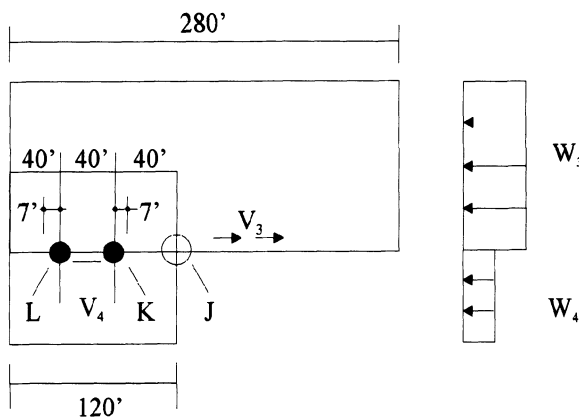


Figure 11-7. Diaphragm Splice Locations

Seismic force in E-W direction: Note to complete the design of joint "J" a similar drag strut connection is required for NS tension, reentrant forces along line 4.

Roof 14 psf x 280 ft = 3920 lb/ft

Roof 14 psf x 120 ft = 1620 lb/ft

$$\begin{aligned} \text{8 inch CMU wall} &= 80 \text{ psf} \left[\frac{(26.5)^2}{2 \times 25} \right] \\ &= 1123.6 \text{ lb/ft} \end{aligned}$$

Therefore

$$\begin{aligned} W_3 &= 0.183[3920 + 1123.6 \times 2] = 1128.6 \text{ lb} \\ / \text{ft} \end{aligned}$$

$$\begin{aligned} W_4 &= 0.183[1620 + 1123.6] = 502.1 \text{ lb/} \\ \text{ft} \end{aligned}$$

$$\begin{aligned} R_{E1} &= R_A = 1128.6 \text{ lb/ft} \frac{100 \text{ ft}}{2} \\ &= 56,430 \text{ lbs} \end{aligned}$$

$$\begin{aligned} R_{E2} &= R_G = 502.1 \text{ lb/ft} = \frac{60 \text{ ft}}{2} \\ &= 15,063 \text{ lbs} \end{aligned}$$

$$R_E = R_{E1} + R_{E2} = 71,493 \text{ lbs}$$

$$V_3 = 1128.6 \frac{100 \text{ ft}}{2 \times 280 \text{ ft}} = 201.5 \text{ lb/ft}$$

$$V_4 = 502.1 \left[\frac{60 \text{ ft}}{2 \times 120 \text{ ft}} \right] = 125.5 \text{ lb/ft}$$

11.6.3.1 @ joint J(see detail C on Figure 11-8)

$$\text{Chord stress} = [86,340 \times 120 \text{ ft} - 667 \times \frac{120^2}{2}] \left[\frac{1}{100 \text{ ft}} \right] = 55,584 \text{ lb}$$

$$\text{Drag force} = (201.5 \text{ plf} + 125.5 \text{ plf})(120 \text{ ft}) = 39,240 \text{ lb} < \text{chord stress}$$

Connections

a. To GLB Girder - Design using 1 in. diameter bolts in double shear with 2 bolts in a row (1.25 increase for metal side plates plus 1/3 for seismic). Allowable load parallel to grain for a 1" diameter bolt in a 5 1/8 member:

$$p = 5070 \text{ lbs/bolt.}$$

Therefore No. of bolts =

$$\frac{55,584 \text{ lbs}}{5,070 \text{ lbs/bolt} \times 1.25 \times 1.33} = 6.6$$

$$A_{\text{plate}} = \frac{55,584 \text{ lbs}}{22,000 \text{ psi} \times 1.33}$$

= 1.90 in.² required

$$A_{\text{provide}} = 0.25 \text{ in.} [18 - 4.2(2)] \times 2$$

= 5.00 in.² > 1.90 in.² OK

Use eight 1 inch diameter A307 bolts 1/4 in. x 18 in. A36 steel plate @ bolt side of beam

b. To concrete wall - design using #8 A706 reinforcing steel ($A_s = 0.79$)

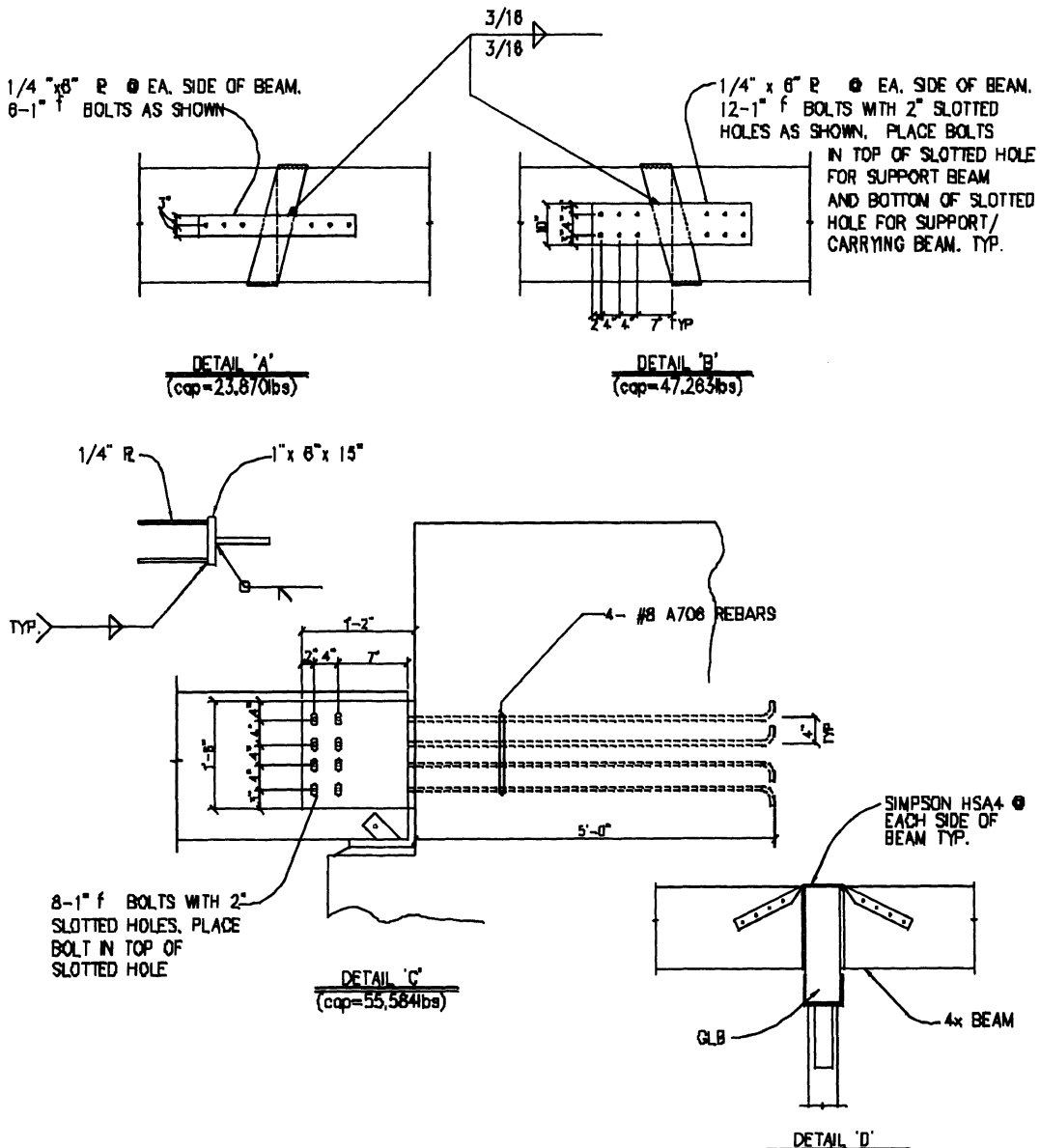


Figure 11-8. Details

Therefore No. of bars

$$= \frac{55,584 \text{ lbs}}{24,000 \text{ psi} \times 1.33 \times 0.79 \text{ in.}^2} = 2.20$$

$$\begin{aligned} \text{Development length } l_d &= 0.002 d_b f_s \\ &= 0.002(1.0 \text{ in.})(24,000 \text{ psi}) \\ &= 48 \text{ in.} \end{aligned}$$

Use: 4 - #8 A706 60 ksi
 $l = 5' - 0$

c. Back Plate (See Figure 11-9)

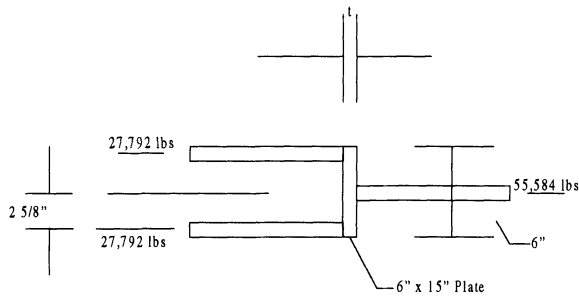


Figure 11-9. Loads on Back Plate - Detail C

Maximum moment on plate

$$M_e = 27,792 \text{ lb} \times 2.63 \text{ in.} = 73,093 \text{ in.-lb}$$

$$\begin{aligned} \text{Therefore } t &= \left[\frac{6M}{bF} \right]^{\frac{1}{2}} \\ &= \left[\frac{73,093 \text{ in.-lb} \times 6}{15 \text{ in.} \times 27,000 \times 1.33} \right]^{\frac{1}{2}} \\ &= 0.902 \text{ in.} \end{aligned}$$

Use 1 in. x 6 in. x 15 in. A36 steel back plate & 1/4 in. x 14 in. x 18 in. A36 steel side plates with eight 1 in. diameter A307 bolts to GLB and four #8 A706 reinforcing steel in CMU wall.

11.6.3.2@ Joint K(see detail B in Figure 11-8)

Chord Stress =

$$= \left[83,340 \times 87 \text{ ft} - 667 \times \frac{87^2}{2} \right] \left[\frac{1}{100 \text{ ft}} \right] = 47,263 \text{ lb}$$

Drag force = $(201.5 + 125.5)(87 \text{ ft}) = 28,449 \text{ lb}$ < Chord Stress

Try 1/4 in. plate @ each side of beam with 1 in. diameter bolts

$$\text{No. of bolts } \frac{47,263 \text{ lb}}{5,070 \text{ lb/bolt} \times 1.25 \times 1.33} = 5.61$$

$$\begin{aligned} A_{\text{plate}} &= \frac{47,263 \text{ lb}}{22,000 \text{ psi} \times 1.33} \\ &= 1.62 \text{ in.}^2 \quad \text{required} \end{aligned}$$

$$A_{\text{provided}} = 0.25 \text{ in.} [10-2(2)] \times 2$$

$$= 3.0 \text{ in.}^2 > 1.62 \text{ in.}^2 \text{ OK}$$

Use: Six 1 inch diameter A307 bolts 1/4 in. x 10 in. A36 steel plate @ each side of beam

11.6.3.3@Joint L(see detail A in Figure 11-8)

$$\begin{aligned} \text{Chord Stress} &= \left[83,349 \times 33 \text{ ft} - 667 \times \frac{33^2}{2} \right] \\ &\times \left[\frac{1}{100 \text{ ft}} \right] = 23,870 \text{ lb} \end{aligned}$$

Drag force = $(201.5 + 125.5)(33 \text{ ft}) = 10,791 \text{ lb}$ < Chord Stress

Try 1/4 in. plate @ each side of beam with 1 in. diameter bolts

Therefore No. of bolts

$$= \frac{23,870 \text{ lb}}{5,070 \text{ lb/bolt} \times 1.25 \times 1.33} = 2.83$$

$$A_{\text{pl}} = \frac{23,870 \text{ lb}}{22,000 \text{ psi} \times 1.33} = 0.82 \text{ in.}^2$$

$$A_{\text{provide}} = 0.25 \text{ in.} [6-2] \times 2 = 2.0 \text{ in.}^2 > 0.82 \text{ in.}^2 \text{ OK}$$

Use: Three 1 in. diameter bolts 1/4 in. x 6 in. steel plate @ each side of beam

Notes: 1. Capacity governed by bolts = $3(5070)(1.25)(1.33) = 25,287 \text{ lbs}$

2. Revise to use detail B as required by section 11.6.5, subdiaphragm "Y" below.

11.6.4 Part D

Loads along line A, between 7 and 8

Vertical loads:

$$w = 14 \text{ psf DL} + 20 \text{ psf LL} (26 \text{ ft}/2) = 442 \text{ lb/ft}$$

Allowable single shear load perpendicular to grain for a 3/4" diameter bolt in a 3 1/2 " member: $q = 630 \text{ lbs/bolt}$

Therefore bolt spacing

$$S = \frac{630 \text{ lbs/bolt} \times 1.25}{442 \text{ lb/ft}} \times 12 \text{ in.} = 21.4 \text{ inch}$$

Use: 3/4 inch diameter A307 anchor bolt with 4 x ledger with spacing of 18 in. o.c.

Therefore: load on bolt = $442 \times 1.5 \text{ ft.} = 663 \text{ lb/bolt}$

Recall: Lateral shear under seismic force:

$$V_3 = 201.5 \text{ lb/ft} \text{ (see item 11.6.3 above)}$$

$$\text{Load on bolt} = 201.5 \times 1.5 \text{ ft} = 302.3 \text{ lb/bolt}$$

Allowable single shear load parallel to grain for a 3/4" diameter bolt in a 3 1/2" member: $p = 1400 \text{ lb/bolt}$

Check stress in ledger with Hankinson formula

$$F_n = \frac{F_c F_{c\perp}}{F_c \sin^2 \theta + F_{c\perp} \cos^2 \theta}$$

Where:

$$\tan \theta = \frac{302.3}{663} = 0.456$$

Therefore:

$$\theta = 24.51 \quad \sin \theta = 0.415 \quad \cos \theta = 0.910$$

Therefore:

$$F_n = \frac{1,400 \times 630 \times 1.33}{1,400 \times (0.415)^2 + 630 \times (0.910)^2} \\ = 1537.8 \text{ lb/bolt}$$

Actual force: (Seismic + Dead Load)

$$\text{DL} = 663 (14/34) = 273.$$

$$P = [(273)^2 + (302.3)^2]^{1/2} \\ = 407.3 \text{ lb/bolt} < 1537.8 \text{ OK}$$

11.6.5 Part E

Subdiaphragms, see Figures 11-10 and 11-6 for panel types

1. Subdiaphragm "X": (Critical case between line E & G)

$$(\text{Span: depth}) = (30 \text{ ft}: 8 \text{ ft}) = (3.75: 1) < 4:1 \text{ OK}$$

Lateral force:

$$\text{Note for center 1/2 of diaphragm } F_p = 0.30(1.5) = 0.45 W_p$$

$$\text{Recall } F_p = ZIC_p W_p = 0.40(1.0)(0.75)W_p = 0.30 W_p(1.5) = 0.45 W_p$$

$$\text{Wall: } 80 \left[\frac{(26.5)^2}{2 \times 25 \text{ ft}} \right] 0.45 = 505.62 \text{ lb/ft} > 200 \text{ lb/ft}$$

Design wall anchors @ 4 ft o.c. (check for one Bay only)

$$V_x = \frac{505.62 \times 30 \text{ ft}}{2 \times 8 \text{ ft}} \\ = 948 \text{ lb/ft} > (720 \text{ lb/ft panel type B}) \text{ NG}$$

Expand subdiaphragm to 2 bays use continuity ties at each 2 x 4 at 2'-0 o/c similar to detail D, Figure 11-8.

$$V_x = \frac{505.62(30 \text{ ft})}{2(16)} = 474 \text{ lb/ft}$$

$< (720 \text{ lb/ft panel type B}) \quad OK$

$$\text{Chord load} = \frac{505.62 \text{ plf} \times 30^2 \text{ ft}^2}{8 \times 16 \text{ ft}} = 3555$$

$$\text{Required As} = \frac{3500 \text{ lbs}}{24000 \text{ psi}} = 0.146$$

Two #4 in CMU wall (As = 0.40)OK

Note: Purlins at first line from lines 1 and 8 require investigation for combined flexural and axial stresses due to dead loads plus chord forces.

Subdiaphragm "Y" Boundaries (5, 6, D & E)

(Span: depth) = (40 ft: 24 ft) = (1.67: 1) < 4:1 OK

Wall line E: = 505.62 lb/ft

$$V_y = \frac{505.62 \times 40 \text{ ft}}{2 \times 24 \text{ ft}} = 421.4 \text{ lb/ft} < 425 \text{ lb/ft}$$

(panel type C) OK

$$\text{Chord} = \frac{505.62 \times 40^2}{8(40)} = 2528.1 \text{ lb at midspan}$$

for girder on line - D and wall line - E

Only 6 wall panels (L=20 ft) available along line A and E to resist Seismic forces.

Only 4 wall panels (2 at L=24 ft and 2 at L=26 ft) available along lines 1 & 8

to resist seismic forces.

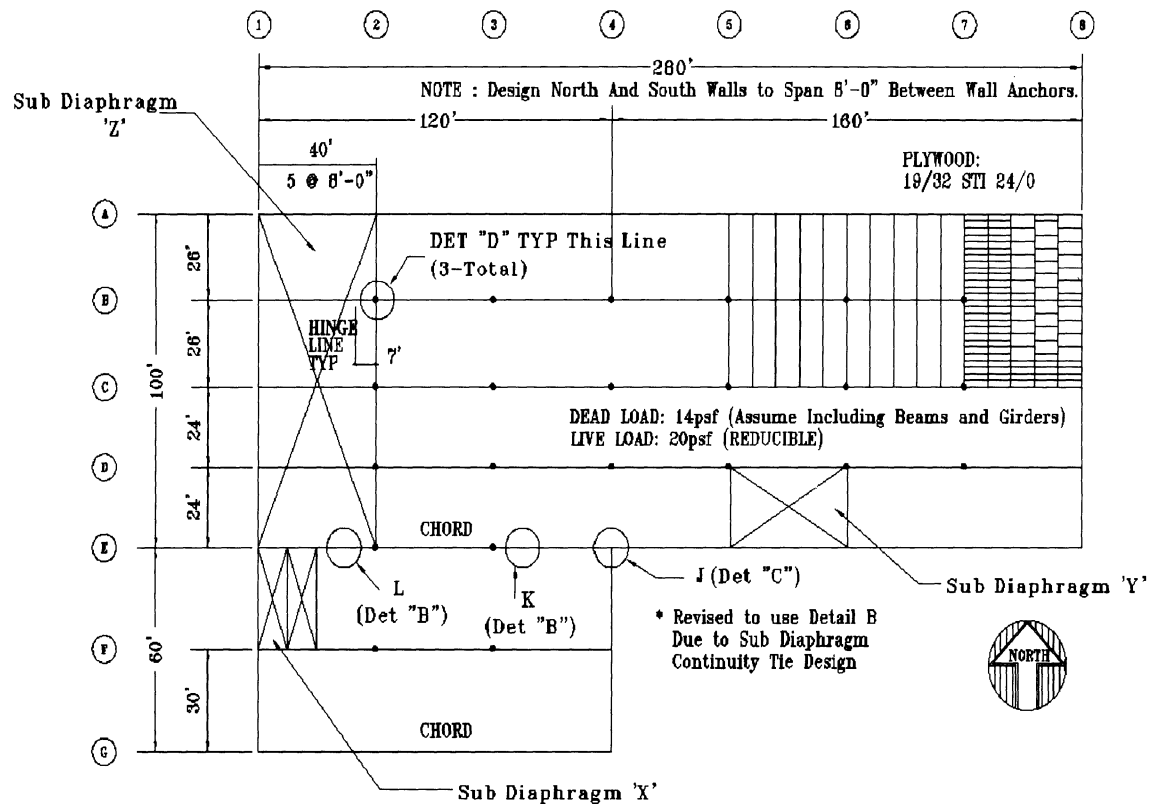


Figure 11-10. Subdiaphragms

Chord load @ girder support joint (7 ft from column)

$$V_y = 505.62 \times \frac{40 \text{ ft}}{2} = 10,112 \text{ lb}$$

Therefore:

$$\begin{aligned} M &= 10,112 \text{ lb} \times 7 \text{ ft} - 505.62 \text{ plf} (7^2/2) \\ &= 58,399 \text{ ft-lb} \end{aligned}$$

Therefore:

$$\text{Chord load} = \frac{58,399 \text{ ft-lb}}{24 \text{ ft}} = 2433 \text{ lbs}$$

Use: Simpson hinge connector HC3T, similar to Detail A Figure 11-8. Typ. @ all GLB to GLB connections

Girder tie across line D:

$$505.62 \text{ plf} \times 40 \text{ ft} = 20,225 \text{ lb}$$

Use: Simpson strap connectors HSA68 @ each side of beam, similar to Detail D, Figure 11-8

$$\text{Capacity} = 2 \times 11,000 \text{ lb} = 22,000 \text{ lb}$$

Typ. over all columns

See detail "D", Figure 11-8

Subdiaphragm "Z": @ boundaries (1, 2, A & E or 7, 8, A & E)

Span: depth = 100 ft = (2.5:1) < 4:1 OK

Wall load @ line 1 = 505.62 lb/ft

$$\begin{aligned} V_y &= \frac{505.62 \text{ plf} \times 100 \text{ ft}}{2(40 \text{ ft})} = 632 \text{ lb/ft} < 720 \text{ lb/ft panel type B} \quad \text{OK} \end{aligned}$$

$$\begin{aligned} \text{Chord} &= 505.62 \times \frac{100^2 \text{ ft}^2}{8 \times 40 \text{ ft}} \\ &= 15,801 \text{ lb} < 22,000 \text{ lb} \end{aligned}$$

(See girder tie across line D, above)

Drag force at line E for subdiaphragm:

$$\text{From Z: } 505.62 \text{ plf} \times \frac{100 \text{ ft}}{2} = 25,281 \text{ lb}$$

$$\text{From X: } 505.62 \text{ plf} \times \frac{30 \text{ ft}}{2} = 7,584 \text{ lb}$$

$$\text{Total} = 25,281 \text{ lb} + 7,584 \text{ lb} = 32,865 \text{ lb}$$

Recall: Capacity @ L = 25,287 < 32,865 NG

Use: Detail B @ Joint L (Revise from section 11.6.3.3 above)

11.6.6 Part F

Check for flexible versus rigid diaphragms
EW dir. only

Recall: d = mid-span deflections of diaphragm

$$= \frac{5VL^3}{8EAb} + \frac{VL}{4Gt} + 0.188Le_n + \text{chord splice slip (css)}$$

In the E-W direction between grid lines A + E:

$$V_3 = 201.5 \text{ lb/ft}$$

E = 29,000,000 psi for chord steel

A = 0.40 in.² (2 - #4 bars for chord steel)

L = 100 ft

b = 280 ft

G = 90,000 psi for plywood

$$t = 19/32 = 0.593$$

e_n = 0.029 (based on 160 lb/ft and 10d nails)

css = Zero. Bar elongation at splices is negligible for these loads

$$\begin{aligned} \Delta &= \text{Guideline allowable deflection} \\ &= L/480 = 100(\text{ft}) \times 12(\text{in./ft}) / 480 = 2.5 \text{ in.} \end{aligned}$$

Now:

$$\begin{aligned} d &= \frac{5(201.5)(100)^3}{8(29,000,000)(0.40)(280)} \\ &+ \frac{201.5(100)}{4(90,000)(0.593)} + 0.188(100)(0.029) \\ &= 0.0387 + 0.094 + 0.545 = 0.678 \text{ in.} \end{aligned}$$

Δ_A = Deflection of wall on line - A (see Table 11-4)

$$= \frac{P}{Et} \left[4\left(\frac{h}{d}\right)^3 + 3\left(\frac{h}{d}\right) \right]$$

Where:

$P = R_A = 56,430$ lbs total (Ref. Section 11.6.3)

$$P = P \text{ per panel} = P/6 = 56,430/6 = 9405 \text{ lbs}$$

$$f'_m = 3000 \text{ psi}$$

$$E = 750 f'_m = 2,250,000 \text{ psi}$$

$$t = 8 \text{ in}$$

$$h = 25 \text{ ft (top of ledger)}$$

$$d = 20 \text{ ft}$$

Now:

$$\Delta_A = \frac{9405 \text{ lb}}{2,250,000 \text{ psi} \times 7.625 \text{ in}} \left[4\left(\frac{25}{20}\right)^3 + 3\left(\frac{25}{20}\right) \right] \\ = 0.0064$$

For wall on line E we have:

$$P = R_E = 71,493 \text{ lb (Ref. Section 11.6.3)}$$

$$P = P \text{ per panel} = 71,493/6 = 11,915 \text{ lb}$$

$$\Delta_E = \frac{11915 \text{ lb}}{2,250,000 \text{ psi} \times 7.625 \text{ in}} \left[4\left(\frac{25}{20}\right)^3 + 3\left(\frac{25}{20}\right) \right] \\ = 0.008$$

Thus the average story drift = $(0.0064 + 0.0080)/2 = 0.0072$ in

Recall for flexible diaphragm behavior deflection of the diaphragm must be more than 2 times the average story drift:

$$0.678 > 2(0.0072)$$

Thus the E-W diaphragm is a flexible diaphragm and will behave consistent with the analysis presented herein.

From the above analysis and similar calculations it can be shown that most one story industrial/warehouse buildings with wood diaphragm and concrete or CMU walls will

qualify as flexible diaphragms. It can also be shown that one to three story apartment or office buildings with light weight concrete topping slab over a wood diaphragm and wood shear walls may very well qualify as a rigid diaphragm in one or both directions.

PLYWOOD SHEAR WALLS

Vertical diaphragms sheathed with plywood (plywood shear wall) may be used to resist horizontal forces not exceeding the values set forth in the code. Plywood shear walls are designed as a dual system; the overturning forces (compression/tension) are resisted by the boundary members while the shear forces are resisted by the web or plywood. As part of the consideration given to the design for uplift caused by seismic loads, the dead load shall be multiplied by 0.90 when used to reduce uplift. This criteria is required for materials which use working stress procedures and is intended to account for variations in dead load and the vertical component of an earthquake.

The deflection (d) of a blocked plywood shear wall uniformly nailed throughout may be calculated by use of the following formula:⁽¹¹⁻³⁸⁾

$$d = \frac{8vh^3}{EAh} + \frac{vh}{Gt} + 0.75he_n + \frac{h}{b}d_a \quad (11-16)$$

Where:

d = the calculated deflection, in inches.

v = maximum shear due to design loads at the top of the wall, in pounds per lineal foot.

A = area of boundary element cross section in square inches (vertical member at shear wall boundary)

h = wall height, in feet.

b = wall width, in feet.

d_a = deflection due to vertical displacement at anchorage details including slip in holdown, bolt elongation and crushing of sill plate.

E = elastic modulus of boundary element (vertical lateral force resisting member at

shear wall boundary), in pounds per square inch (approximately 1,800,000 psi).

G = modulus of rigidity of plywood, in pounds per square inch (approximately 90×10^3 ksi)

t = effective thickness of plywood for shear, in inches

e_n = nail deformation/slippage, in inches (see Table 11-6).

Δ = Allowable story drift = $0.005h$ for allowable stress loads.

For a typical plywood shear wall constructed of structural I plywood on 2 x 4 studs spaced at 16 inches on center with 4 x 4 boundary elements:

$$V = 500 \text{ plf}$$

$$A = 12.25 \text{ in}^2$$

$$h = 8'-0$$

$$b = 10'-0$$

$$d_a = 1/8 \text{ inch} = 0.125 \text{ inch}$$

$$E = 1.8 \times 10^6 \text{ psi}$$

$$G = 90 \times 10^3 \text{ psi}$$

$$t = 15/32 \text{ in}$$

$$e_n = 0.036$$

where:

10d nails at 4 inch on center load/nail

$$= 500 \text{ plf} (4/12) \text{ ft/nail}$$

$$= 167 \text{ lb/nail.}$$

Thus:

$$\begin{aligned} d &= \frac{8(500)(8)^3}{1.8 \times 10^6 (12.25)(10)} \\ &\quad + \frac{500(8)}{90 \times 10^3 (15/32)} + 0.75(8)(0.036) + 0 \\ &= 0.009 + 0.089 + 0.216 + 0.125 \left(\frac{8}{10} \right) \\ &= 0.0414 \end{aligned}$$

$$\Delta = 0.005(8 \text{ ft})(12 \text{ in}/\text{ft}) = 0.48 \text{ in.} > 0.414$$

OK.

More important than the magnitude of the displacement is the contributions of the components. The flexural component is negligible while the shear and nail deformation/slippage components are the dominate contributions. An evaluation of the deflection is that loads can be distributed to a series of wood shear walls based upon only the length of each wall when using the same plywood and nailing for walls of equal height.

Two example problems are presented. The first example problem presents a design procedure for an isolated plywood shear wall. The second example problem presents a design procedure for distribution of lateral seismic forces to a series of plywood shear walls.

EXAMPLE PROBLEM 5 - ISOLATED PLYWOOD SHEAR WALL

Isolated plywood shear wall is shown in Figure 11-11. Determine if the plywood shear wall is adequate.

Note: All shear in plywood web; all overturning moment loads in columns (boundary elements)

$$\text{Shear} = \frac{2400 \text{ lb}}{4 \text{ ft}} = 600 \text{ lbs/ft}$$

Use 15/32" plywood Structure I

Perimeter nails = 10d @ 3" with 1 5/8" penetration o/c for each panel edge

Field nails = 10d @ 12 in. o/c

4 x 4 post = boundary elements

Allowable shear = 665 lbs/ft > 600 lbs/ft OK

Check Bolts

Use 3/4 in. diameter at sill plate bolts ($P = 1420$ lbs for single shear in wood).

$$\text{No. required} = \frac{2400 \text{ lbs}}{1420 \text{ lb/bolt} \times 1.33} = 1.27$$

Use 2 bolts

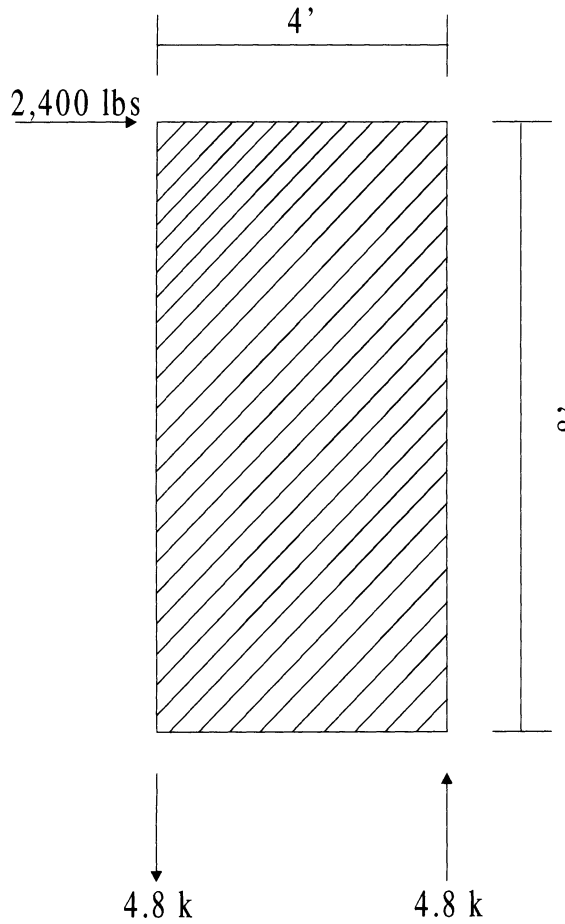


Figure 11-11. Isolated Plywood Shear Wall

$$\text{Overturning} = \frac{2400 \text{ lbs} \times 8 \text{ ft}}{4 \text{ ft}} = 4800 \text{ lbs}$$

Compression perpendicular to grain in sill plate: $= 4800 \text{ lb}/(3.5 \text{ in.})^2 = 392 \text{ psi} < 625 \text{ psi}$
OK

3/4" anchor bolt OK for $0.3 \times 20 = 6$ kips
Connection must resist 4.8 kips pull out

OK

Note: Net area of 3/4" dia. anchor bolt is 0.30 in^2 . with an allowable tension of 20 ksi.

Pull out of concrete for 3/4" ϕ :

$F = 2.25(2)(1.33) = 6$ kips; with special inspection and 1/3 seismic increase.

$$F = 6.0 > 4.8 \quad \text{OK}$$

Check End Stud
Check End Post for Compression
Recall: $F_c' = F_c * C_p$
Now:

$$C_p = \frac{1 + F_{CE}/F_c}{2c} - \left[\left[\frac{1 + F_{CE}/F_c}{2c} \right]^2 - \frac{F_{CE}/F_c}{c} \right]^{1/2}$$

Where:

$$F_{CE} = \frac{K_{CE} E'}{(l_e/d)^2} = 638$$

$K_{CE} = .30$ for visually graded lumber

$l_e = 96 \text{ in}$

$d = 3.5 \text{ in}$

$E = 1.6 \times 10^6 \text{ PSI}$

$C = 0.80$ For Sawn Lumber

$F_c' = F_c C_F C_R C_D C_N C_t = 1596 \text{ PSI}$

Where: $F_c = 1200 \text{ PSI}$

$C_F = 1.0$

$C_R = 1.0$

$C_D = 1.33$

$C_M = 1.0$

$C_t = 1.0$

Thus:

$$C_p = \frac{1 + 638/1596}{2(0.8)} - \left[\left[\frac{1 + 638/1596}{2(0.8)} \right]^2 - \frac{638/1596}{0.8} \right]^{1/2} = 0.262$$

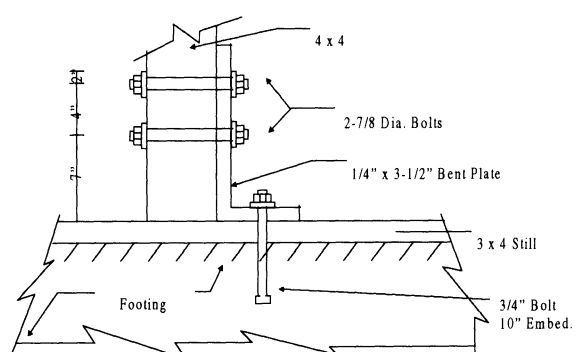


Figure 11-12. Shear Wall Post Connections

Therefore:

$$F_c' = 1596 (0.262) = 418 \text{ psi}$$

Now:

$$F_h = P/A = 4800 \text{ lbs}/12.25 \text{ in}^2 \\ = 392 \text{ psi} < 418 \quad \text{OK.}$$

Bolts to 4 x 4 post: (See Figure 11-12)

$$V_{\text{allow}} = 2(1790 \text{ lbs/bolt})(1.25)(1.33) \\ = 5.95 \text{ kips} > 4.8 \text{ kips...OK}$$

where

1.25 = increase for metal side plates

1.33 = increase for seismic (short term) force

Check Deflection:

$$V = 600 \text{ plf}$$

$$A = 12.25 \text{ in}^2$$

$$h = 8.0 \text{ ft}$$

$$b = 4.0 \text{ ft}$$

$$da = 0.1 \text{ in.}$$

$$E = 1.6 \times 10^6$$

$$G = 90 \times 10^3$$

$$t = 15/42 \text{ in.}$$

$$e_n = 0.029$$

$$d = \frac{8(600)(8)^3}{1.6 \times 10^6 (12.25)(4)} + \frac{600(8)}{90 \times 10^3 (15/32)} + \\ + 0.75(8)(0.029) + 0.1 \\ = 0.0313 + 0.107 + 0.174 + 0.10 \\ = 0.412 \text{ inch.}$$

$$\Delta = 0.005h = 0.005(8 \text{ ft})(12 \text{ in} / \text{ft}) \\ = 0.48 \text{ in.} > 0.412 \text{ in.} \quad \text{OK.}$$

Note that deflection/stiffness criteria will govern on short plywood walls with high shear load.

EXAMPLE PROBLEM 6 - DISTRIBUTION OF LATERAL SEISMIC FORCES TO A SERIES OF PLYWOOD SHEAR WALLS

Determine the distribution of lateral seismic force to series of plywood shear walls shown in Figure 11-13.

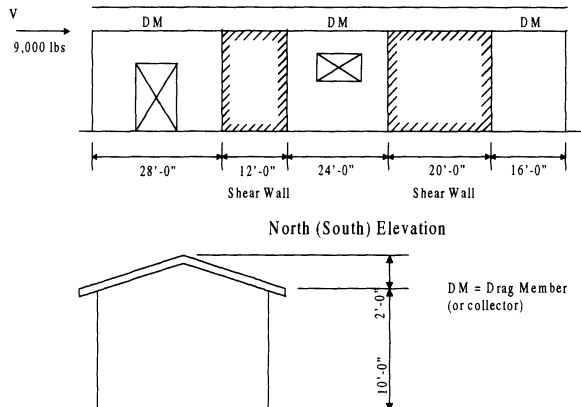


Figure 11-13. Building Elevations

Load to walls

$$\text{Total length of walls} = 12 + 20 = 32 \text{ ft}$$

$$\text{Load per foot of wall} = 9000 \text{ lbs}/32 \text{ ft} = 281.25 \text{ plf}$$

$$\text{Load to } 12 \text{ ft wall} = 281.25 \text{ plf} (12) = 3375 \text{ lbs}$$

$$\text{Load to } 20 \text{ ft wall} = 281.25 \text{ plf} (20) = 5625 \text{ lbs}$$

$$\text{Total} = 9000 \text{ lbs}$$

Load to drag struts/collectors

$$q = \text{load per foot at collector}$$

$$= 9000 \text{ lbs}/\text{ft}$$

$$= 90 \text{ plf}$$

Force diaphragm of collector/shear wall load

Thus:(See Figure 11-14)

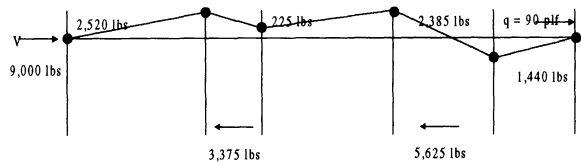


Figure 11-14. Collector/Drag Force Diagram

Drag strut at b: $F = 2520$ lbs compression
 Drag strut at c: $F = 225$ lbs compression
 Drag strut at d: $F = 2385$ lbs compression
 Drag strut at e: $F = 1440$ lbs tension

11.7 CMU SLENDER WALL (OUT-OF-PLANE FORCES)

The design of masonry walls can be divided into two separate procedures. The first procedure is the design of the wall for out-of-plane forces (forces perpendicular to the face of the wall). Walls designed using WSD are limited to an h'/b ratio of 30; where h' is the effective wall height and b is the effective wall thickness. Walls designed using LRFD are really slender walls and are not limited to an h'/b of 30 but must comply with strict reinforcement criteria and have special inspection. Walls designed as slender walls are becoming more prevalent and will be discussed in detail in the following chapter.

The second procedure is the design of the wall for in-plane forces (forces parallel to the length of the wall). Walls designed using WSD usually require a concentration of bars at the extreme ends of the wall to resist flexure stresses and overturning forces; and shear forces are carried either by the masonry or the steel. Walls designed using LRFD are called limit state or strength design shear walls and are allowed to account for the distributed vertical wall steel to resist flexure stresses and overturning forces; shear strength is proportioned to both the masonry and the steel. Strength design shear walls are a relatively new concept and will be discussed in detail following the section on slender walls.

Manual calculations are presented to demonstrate the procedure, but as the reader will quickly realize that for production design a computer software program is mandatory. A computer software program has been developed for both the slender wall computations and the shear wall computation and is available from the concrete masonry association of California and Nevada.⁽¹¹⁻³³⁾

11.7.1 Interaction Diagram

The appropriate method to model the capacity of a member subjected to both bending and axial loads is an interaction approach which accounts for the relationship between the stresses caused by bending and axial loads. An "Interaction Diagram", such as that shown in Figure 11-15, may be constructed by establishing the capacity of the member under various combinations of axial and flexural loads. Although an infinite number of points may be calculated, the critical points identified by numbers 1 through 6 on Figure 11-15 should be more than sufficient to construct an accurate interaction diagram. Each point is described by the axial capacity P_n and moment capacity M_n . Thus, M_n can be computed for a given P_n , or vice versa.

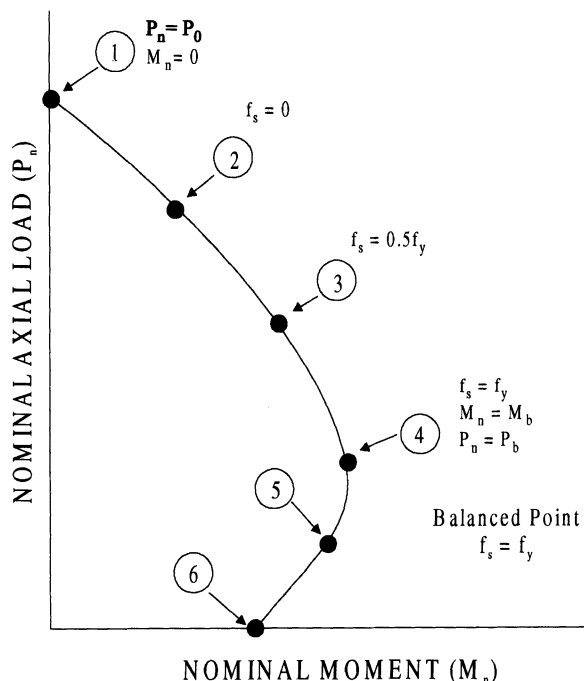


Figure 11-15. Interaction diagram for an eccentrically loaded member

For example, at one extreme, point 1, where no externally applied moment is imposed on the wall the nominal axial capacity of the wall, is:⁽¹¹⁻²⁰⁾

$$P_n = 0.85f_m'(A_n - A_s) + A_sF_y \quad (11-17)$$

The other extreme, point 6, is where the capacity of the member is the pure bending nominal flexural capacity of the wall, or:

$$M_n = 0.85f_m'ab[d - (a/2)] \quad (11-18)$$

The intermediate points may be established by choosing several condition of strain and, using the force-equilibrium and stress-strain relationships developed in Reference 11-16 for calculating P_n and M_n .

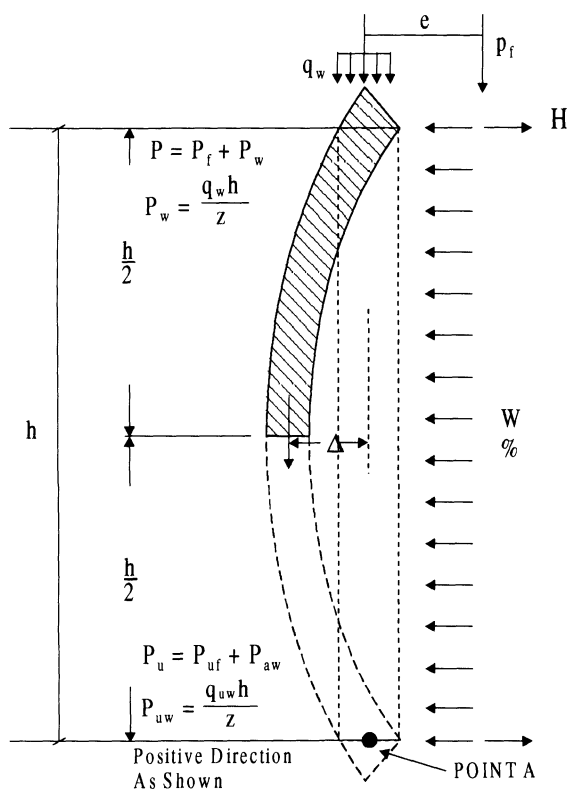


Figure 11-16. Loading geometry of slender wall

11.7.2 Structural Mechanics

The load-induced moment on a wall is a function of lateral wall deflection. If the wall is slender, usually a wall with height to thickness of 25 or more, herein referred to as a "Slender Wall", the lateral deflection can produce moments that are significant relative to the moment obtained using small deflection theory.

Figure 11-16 shows the forces acting on a slender wall with a pin connection at each end.

The summation of moments about the bottom of the wall, point A, gives the equation for the horizontal force at the upper wall support. That is:

$$P_f e + Hh - w(h^2/2) - q_w h(\Delta_a) = 0 \quad (11-19)$$

where

P = Design axial load = $P_f + P_w$

P_f = vertical load on wall per linear foot

e = eccentricity of vertical load

w = uniform lateral load on wall per linear foot

$P_w = q_w h/2$

q_w = weight of wall per linear foot

Δ_a = "effective" lateral deflection used to estimate dead load moment

If we assume that

$$\Delta_a = 2\Delta/3 \quad (11-20)$$

where Δ is the wall's mid-height lateral deflection, then

$$H = wh/2 - P_f e/h + 2q_w \Delta/3 \quad (11-21)$$

The first term corresponds to the classical small deflection reaction, the second term represents the change in the magnitude of the force due to an eccentric wall loading, and the third term incorporates the lateral wall deflection.

If we take the moment about the mid-height of the wall, the moment induced on the cross section from the external loads is

$$M = H(h/2) + P_f(\Delta + e) + (q_w h/2)\Delta_b - (wh/2)h/4 \quad (11-22)$$

where Δ_b is the "effective" lateral deflection used to estimate dead load moment. If we assume that

$$\Delta_b = \Delta/3 \quad (11-23)$$

which is consistent with Δ_a above and substitute H into the moment equation, it follows that

$$M = wh^2/8 + P_f e/2 + (P_f + q_w h/2)\Delta \quad (11-24)$$

The first term corresponds to the moment due to the classical small deflection moment from the uniform lateral load, the second term corresponds to the moment due to the eccentric vertical load on the wall, and the third term represents the moment due to large lateral deflections. This last term can be referred to as the P-Delta load.

The moment M and lateral force H are a function of Δ , which in turn is a function of the wall's cross-sectional properties and steel reinforcement as well as the moment M and the lateral load H . Therefore, the problem of calculating the moment M is iterative.

The ultimate axial load computed using the factored axial forces must be less than the evaluated nominal capacity:

$$\phi P_n \geq P_u \quad (11-25)$$

The slender wall must have a capacity equal to the sum of the superimposed factored axial dead and live loads, P_{uf} , factored wall dead load for the upper one-half, $q_u w H/2$, along with the factored lateral load from the wall and/or loading above (see Figure 11-16). The moment capacity of a wall section is calculated, assuming that axial strength does not govern the design, and it is checked against the moment generated under the applied lateral load and by the P-Delta effect.

Although most walls are loaded at a level which is considerably less than their axial load strength, a check can be made to determine if flexure controls the design, that is,

$$\phi P_b \geq P_u \quad (11-26)$$

in which

$$P_b = 0.85 f'_m b a_b - \sum A_s f_y$$

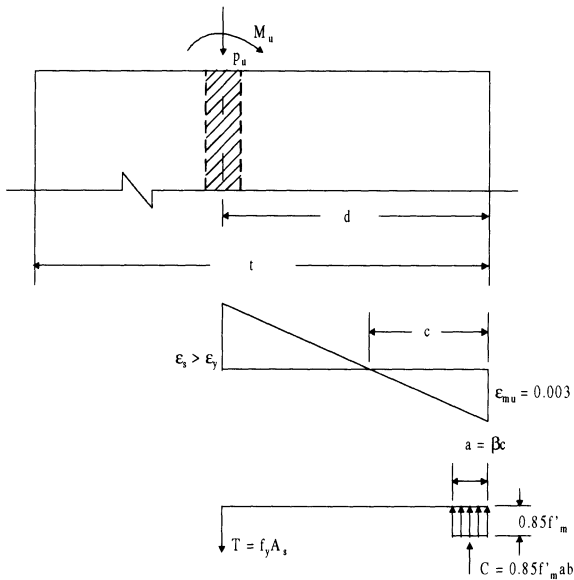


Figure 11-17. Stress and strain diagrams for steel at center of wall

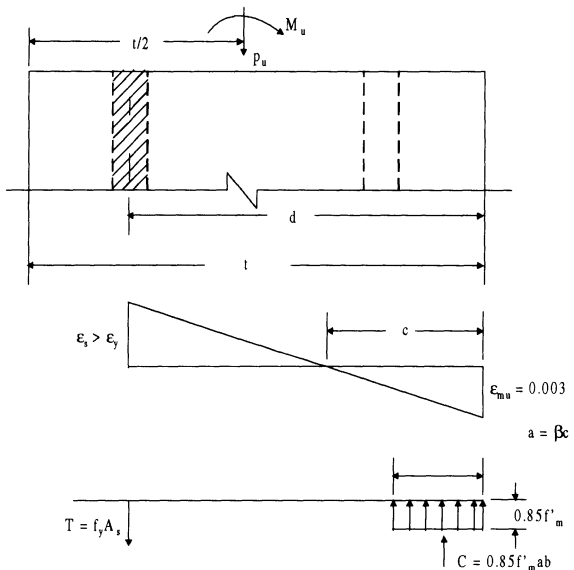


Figure 11-18. Stress and strain diagrams for steel at two faces (ignoring compression steel)

where

$$a_b = \left(\frac{87,000}{87,000 + f_y} \right) \beta d$$

The nominal moment capacity of the wall section loaded with a concentrically applied

load may be determined from force and moment equilibrium (see Figures 11-17 and 11-18). The axial load is

$$P_u = C - T$$

Thus:

$$C = P_u + T$$

$$0.85f'_m b a = P_u + A_s f_y \quad (11-27)$$

and solving for "a" yields

$$a = (P_u + A_s f_y) / (0.85f'_m b) \quad (11-28)$$

Summing the internal and external moments about the tension steel yields

$$M_u + P_u(d - t/2) - C(d - a/2) = 0$$

Substituting Equation 11-27 for C, and assuming $M_n = M_u$, the nominal moment capacity of a member with steel at two faces (Figure 11-18) is

$$M_n = (P_n + A_s f_y)(d - a/2) - P_n(d - t/2) \quad (11-29)$$

In the more typical case with steel in one layer of reinforcement at the centerline of the wall (Figure 11-17), the nominal moment capacity is

$$M_n = (P_n + A_s f_y)(d - a/2) \quad (11-30)$$

If the imposed moment, M_u , is less than the reduced moment capacity, ϕM_n , the wall section is acceptable.

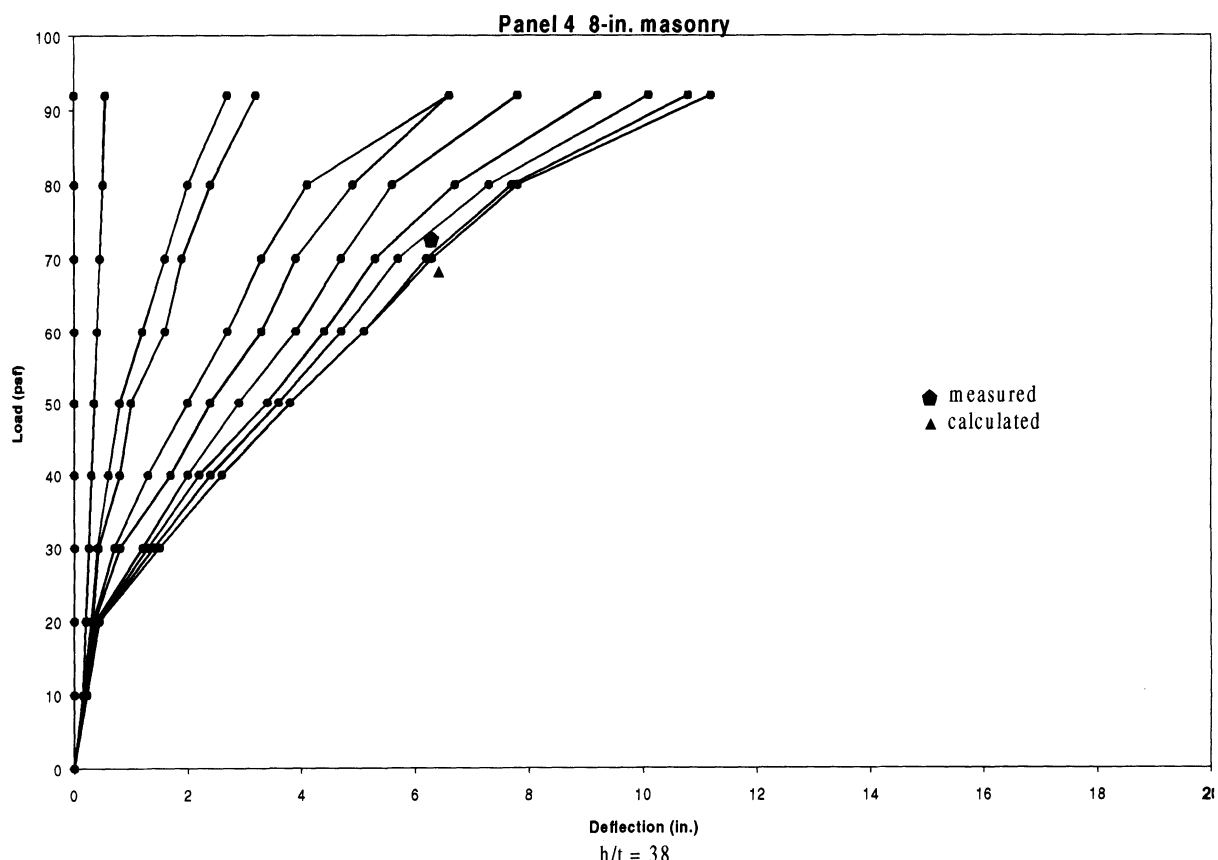


Figure 11-19. Load deflection curves (slender walls)

$$\phi M_n \geq M_u \quad (11-31)$$

This may be determined by comparing Equation 11-24 with Equation 11-29 or 11-30, multiplied by the appropriate ϕ factor.

In 1981, the Structural Engineers Association of Southern California (SEAOSC) tested 32 slender concrete, brick, and concrete masonry panels subjected to a constant axial and increasing lateral load⁽¹¹⁻¹⁷⁾. Panel capacities were predicted using the strength method developed by SEAOSC. The procedure for calculating ultimate moments and deflections is presented in Equations 11-30 and 11-31. Load deflection results of these tests for eight inches thick concrete masonry walls are presented in Figure 11-19. A close correlation was obtained between calculations and test data.

11.7.3 LRFD/Limit-State Design Criteria

The Limit State design procedure concerns reinforced hollow unit concrete masonry slender walls subjected to vertical and horizontal forces causing out-of-plane flexure.

A. Conditions for the design procedure:

1. The minimum nominal thickness of the masonry wall shall be six inches. Note : eight inch minimum wall is recommended.
2. The ratio of unsupported height to nominal wall thickness may not exceed 30 unless the axial stress at the location of maximum moment is equal to or less than 0.04 f_m' . (Same as concrete)
3. Minimum reinforcement ratio shall be 0.0007 in either direction and 0.002 total. (Title #4 requires a minimum of 0.003)
4. Maximum reinforcement shall not exceed 50 percent of the balanced steel ratio, ρ_b . Maximum steel in each cell shall not exceed 0.03 times the cell area unless the reinforcing steel is lap spliced and then it is 0.06 times the cell area. (see Table 11-8). Note: $\rho < 0.6 \rho_b$ for concrete

5. The principal wall reinforcement in the direction of span shall not be spliced within the middle third of the span.
6. All units shall be laid in running bond unless the wall is grouted solid. Note that running bond and solid grouting are recommended.
7. Masonry walls at corners and intersecting cross walls shall be effectively anchored to each other or separated to prevent seismic batter.
8. All grouts shall have a minimum compressive strength, f_c' , not less than of 2000 psi nor greater than 4,000 psi. f_c' shall be determined by prism tests. f_c' shall be greater than f_m' .
9. All grouts shall be consolidated by mechanically vibrating over the height of pour (vibration shall be performed after the initial loss of water and before initial set). Grout space shall be not less than the minimum necessary for mechanical vibration.
10. The specified compressive strength, f_m' , shall not be less than 1,500 psi nor greater than 3,000 psi. f_m' shall be determined by prism tests.
11. An inspector shall provide continuous inspection during all key phases of wall construction as identified on the structural plans.

Design Procedures:

Design of hollow unit reinforced concrete masonry shall be based on forces and moments determined from analysis. The analysis that considers slenderness of walls by representing effects of axial load and deflection in the calculation of required moments must be used. This design procedure must satisfy both strength and deflection limit states. The slender wall design procedures given herein shall be used when the ratio of unsupported height to nominal wall thickness is equal to or greater than 30 and when the vertical load stress at the location of the maximum moment does not exceed 0.04 f_m' .

$$(P_w + P_f)/A_g \leq 0.04 f_m' \quad (11-32)$$

where

P_f = Unfactored axial load from tributary floor and/or roof area, pounds.

P_w = Unfactored weight of the wall tributary to section under consideration, pounds.

f_m' = Specified compressive strength psi.

A_g = Gross area of wall, square inches.

Recall for working stress designs of CMU walls:

$$\begin{aligned} f_a &= 0.20 f_m [1 - (h'/42b)^3] \\ &= 0.20 f_m [1 - (30/42)^3] \\ &= 0.127 f_m @ (h'/b)_{\max} = 30 \\ &= 0.04 f_m' @ (h'/b) = 39 \text{ aside} \end{aligned}$$

Versus:

$f_a = 0.040 f_m$ without (h'/b) limit
For LRFD/limit-state design

Design Load Factors:

1. General: Strength required by a masonry wall shall be based on factored loads

2. Basic Load Combinations: Loading combinations shall be based on the selected loading criteria shown below:

Required strength, U, to resist factored loads

and forces shall be as follows:

$$U = 1.4D \quad (11-33a)$$

$$U = 1.2D + 1.6L + 0.5(L_r \text{ or } S) \quad (11-33b)$$

$$U = 0.9D \pm (1.0E \text{ or } 1.3W) \quad (11-33c)$$

$$U = 1.2D + 1.0E + (0.5L + 0.2S) \quad (11-33d)$$

Where:

D = Dead loads or related internal moments and forces.

L = Live loads or related internal moments and forces.

E = Load effects of earthquake or related internal moments and forces.

W = Wind loads or related internal moments and forces.

U = Required strength to resist factored loads or related internal moments and forces.

Design Assumptions for Nominal Strength:

1. Nominal strength of singly reinforced concrete masonry wall cross-sections subject to combined flexural and axial loads shall be based on applicable conditions of equilibrium

Table 11-8. Maximum Reinforcement for Masonry Slender Walls

Nominal Thickness inch	Actual Thickness inch	$f_m' = 1500 \text{ psi w/ } (\rho_u)_{\max} = 0.00535$		$f_m' = 3000 \text{ psi w/ } (\rho_u)_{\max} = 0.0107$	
		Reinforcement $(\rho_u)_{\max} bd$ As in ² /ft	Reinforcement As/b # in ² /ft	Reinforcement $(\rho_u)_{\max} bd$ As in ² /ft	Reinforcement As/b # in ² /ft
6	5.625	0.1805	# 4 @ 16 (0.15)	0.361	# 6 @ 16 (0.33)
8	7.625	0.2445	# 5 @ 16 (0.23)	0.489	# 7 @ 16 (0.45)
10	9.625	0.309	# 5 / # 6 @ 16 (0.28)	0.618	# 8 @ 16 (0.59)
12	11.625	0.373	# 6 @ 16 (0.33)	0.746	# 9 @ 16 (0.75)

$$(\rho_b)_{\max} = 0.00535$$

$$(\rho_b)_{\max} = 0.5 (\rho_b) \text{ masonry}$$

$$(\rho_b)_{\max} = 0.6 (\rho_b) \text{ concrete}$$

$$\rho_b = \frac{0.85 \beta f_m'}{f_y} \times \frac{87,000}{87,000 + f_y}$$

and compatibility of strains. Strain in reinforcement and masonry shall be assumed directly proportional to the distance from the neutral axis.

2. Maximum usable strain at extreme masonry compression fiber shall be assumed equal to 0.003 i.e at $0.85 f_m'$.

3. Maximum usable strain at extreme masonry compression for confinement limits e to 0.001 at $0.40 f_m'$

4. For steel strains less than the steel yield strain, the stress in reinforcement shall be taken as E_s times the steel strain. For steel strains greater than the steel yield strain the stress in the reinforcement shall be considered independent of strains and equal to f_y , where:

f_y = Specified yield strength of the reinforcement, psi

E_s = Modulus of Elasticity of reinforcement, = 29,000,000 psi

5. The tensile strength of masonry shall be neglected in flexural calculations of strength, except when computing the nominal cracking moment strength.

6. In the calculation of nominal moment strength the relationship between masonry compressive stress and masonry strain may be assumed to be rectangular. Masonry stress of $0.85 f_m'$ shall be assumed uniformly distributed over an equivalent compression zone bounded by the edges of the cross-section and a straight line located parallel to the neutral axis at a distance "a" from the fiber of maximum compressive strain.

Design Strength:

Required moment strength, M_u , shall be equal to or less than the nominal moment strength multiplied by a strength reduction factor.

$$M_u \leq \phi M_n \quad (11-34)$$

where:

M_n = Nominal moment strength.

ϕ = Strength reduction factor for nominal strength

= 0.80 for nominal wall thickness of 8 inches or greater

= 0.65 for nominal wall thickness of 6 inches or smaller

Modulus of Elasticity:

The nominal value of the modulus of Elasticity of the masonry, E_m shall be assumed as follows:

$$E_m = 750 f_m' \quad (11-35)$$

Modulus of Rupture:

The nominal value of the modulus of rupture (f_r) of the partially grouted or solid grouted hollow unit masonry wall system shall be assumed as follows:

$$f_r = 4.0 \sqrt{f_m'}, \text{ 235 maximum ... Fully grouted wall}$$

$$f_r = 2.5 \sqrt{f_m'}, \text{ 125 maximum ... Partially grouted wall}$$

Deflection Limitations:

The maximum wall deflection relative to the support, Δ_s , under unfactored lateral and vertical loads shall be $0.007h$ where h is the height of wall between supports. Note that $0.007h$ is approximately $l/142$ and may not be compatible with some non-structural elements such as doors and windows systems. One may want to use $l/240$ or 0.004 criteria to avoid possible conflicts.

Design Equations:

1. Deflections: The mid-height deflection for simple wall support conditions top and bottom due to the unfactored loads, Δ_s , shall be computed using either of the following equations:

$$M_s \leq M_{cr} \quad \Delta_s = \frac{5 M_s h^2}{48 E_m I_g} \quad (11-36)$$

$$\text{M}_{\text{cr}} < \text{M}_s < \text{M}_n \quad \Delta_s = \frac{5 \text{M}_{\text{cr}} h^2}{48 E_m I_g} + \frac{5(\text{M}_s - \text{M}_{\text{cr}})h^2}{48 E_m I_{\text{cr}}} \quad (11-37)$$

where:

I_g = Moment of inertia of the uncracked wall cross-section, in⁴.

I_{cr} = Moment of inertia of the cracked wall cross-section, in⁴.

M_{cr} = Cracking moment strength.

$$\text{M}_{\text{cr}} = S f_r \quad (11-38)$$

S = Section modulus of the uncracked wall cross-section, in³

M_s = Moment due to unfactored loads for a simple wall support condition top and bottom.

$$\text{M}_s = wh^2/8 + P_f(e/2) + (P_w + P_t)\Delta_s \quad (11-39)$$

where:

w = Distributed lateral load.

e = Eccentricity of the vertical load, P_f .

For other wall support conditions the maximum wall deflection shall be calculated using the equations of structural mechanics.

2. Required Moment Strength: The required moment strength or factored moment, M_u , for a simple wall support conditions top and bottom is the moment given by:

$$\text{M}_u = w_u h^2/8 + P_{uf}(e/2) + (P_u)\Delta_u \quad (11-40)$$

where:

w_u = Factored distributed lateral load.

Δ_u = Horizontal deflection at mid-height of wall calculated using Equation 11-40 for factored loads and $\text{M}_s = \text{M}_u$.

P_{uw} = Factored weight of the wall tributary to the section under consideration.

P_{uf} = Factored axial load on the wall from tributary floor and/or roof loads.

e = Eccentricity of the factored axial load, P_{uf} .

$$P_u = P_{uw} + P_{uf}$$

= Factored axial load at mid height of wall, including tributary wall weight.

3. Nominal Moment Strength: The nominal moment strength, M_n , of the wall is as follows:

$$\text{M}_n = A_{se} f_y [d - (a/2)] \quad (11-41)$$

where:

$$a = \frac{(P + A_s f_y)}{0.85 f_m b} \quad (11-42)$$

$$A_{se} = \frac{(P + A_s f_y)}{f_y} \quad (11-43)$$

b = Tributary width

d = Distance from extreme compression fiber to centroid of tension reinforcement.

11.7.4 Comments on the State of the Art Limit State Design Criteria

Reinforced hollow unit masonry that is constructed with good quality control and has its grout vibrated has been shown through experimental measurements to perform in flexure in a very similar fashion to reinforced concrete. The slender wall test conducted by the Structural Engineers Association of California and presented in Section 2411 of the 1985/1991 UBC is developed recognizing this similarity of basic engineering mechanics performance.

One basic assumption of the existing working stress design approach for axial load and flexure is that plane cross-sections remain plain during axial load and bending moment deformations. Alternatively stated, this means that the variation of strain is a linear function of the distance from the neutral axis. The proposed strength design approach for masonry shear walls makes the same assumption. This assumption is consistent with the assumption used in the strength design of reinforced concrete and is supported by experiments on masonry shear walls such as those presented for a six meter tall wall in Figure 11-20⁽¹¹⁻¹⁸⁾.

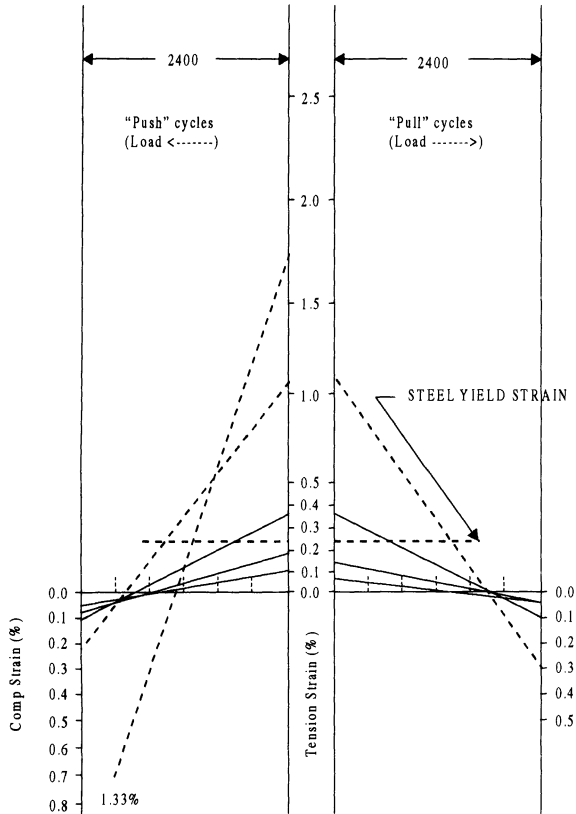


Figure 11-20. Strain profiles at 200 mm above base of a 6 m wall for different deformations

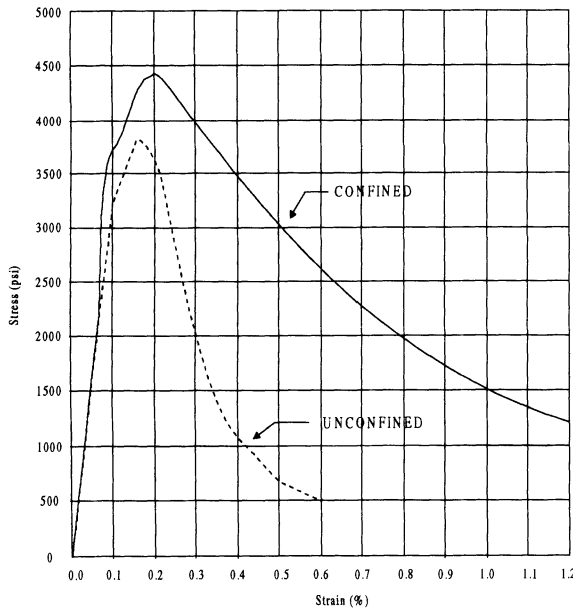


Figure 11-21. Priestly's stress-strain curves

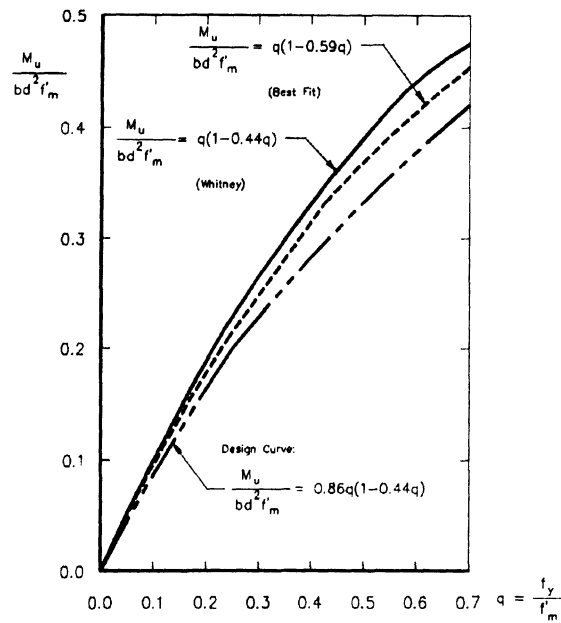


Figure 11-22. Tension controlled flexural test results

The assumption is made in the proposed design criteria that a rectangular stress block can be used to calculate the flexural capacity of shear walls. Stress-strain curves such as those presented in Figure 11-21 indicate that the stress-strain curve for masonry is not rectangular in shape but follows more closely a parabolic form. The reason for the selection of the rectangular stress block is one of convenience, and also, the recognition that the moment capacity of a section with a rectangular stress block closely approximates the moment capacity obtained using the more accurate representation of the stress strain curve.

Figure 11-22 shows the results of tests conducted in Canada for beams in flexure⁽¹¹⁻²¹⁾. The test results are compared with the estimated nominal moment capacity using a rectangular stress block and the design value using a strength reduction factor of 0.86.

Figure 11-23 shows an idealized stress strain curve with the parameters defined in Table 11-9 identified on the curve. Based on the TCCMAR data, the value of 0.003 for the maximum usable strain is slightly less the average value obtained from the test results.

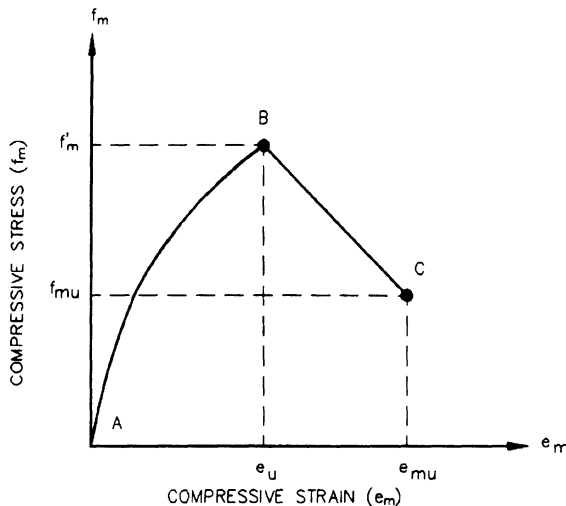


Figure 11-23. Unconfined concrete masonry stress-strain curve

The value of the maximum usable strain selected as part of this criteria is equal to the value most often cited for the design of reinforced concrete members. One might be inclined to be concerned with our selection of 0.003 because it is the same value as used for reinforced concrete. However, as indicated in Figure 11-24, the maximum usable strain value for concrete with maximum compressive value comparable to those values specified in the criteria for masonry far exceeds the 0.003 value. In particular, as reinforced concrete can obtain significantly higher maximum compressive values, it is only at these maximum compressive values where the 0.003 limitation is reasonable.

Table 11-9. Design Parameters for the Unconfined Concrete Masonry Stress-Strain Curve

Parameter	Comment
f'_m	Ultimate compressive stress. Nominal design value is specified by design engineer.
ϵ_u	Strain corresponding to f'_m . We recommend a nominal design value of 0.0020 to 0.0025.
f_{mu}	The minimum usable compressive stress in the strain region defined by strain values greater than the strain at ultimate compressive stress, ie., ϵ_{mu} . We recommend a nominal design value of 0.5 f'_m .

Parameter	Comment
ϵ_{mu}	Maximum usable unconfined strain. Alternately stated, it is the strain corresponding to the minimum usable compressive stress. We recommend a nominal design value of 0.0030.

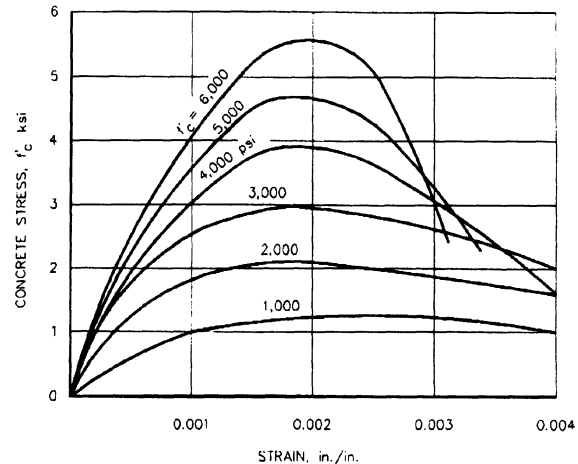


Figure 11-24. Typical stress-strain curves for concrete under short-time loading

The maximum strain can be increased where confinement is provided (see Figure 11-21). Experimental evidence indicates that confinement increases the maximum usable strain, and therefore, the component curvature ductility.^(11-19, 11-22)

11.7.5 Example Problem - Out of Plane loads on Reinforced Masonry Wall (Strength Design)

Determine if the fully grouted medium weight concrete masonry unit (CMU) slender wall (out-of-plane loads) shown in Figure 11-25 is adequate. Seismic Zone 4 ($C_a=0.44$), with special inspection.

Wall Properties:

Wall is fully grouted (medium wt.)	= 80 psf
Nominal block thickness	= 8 inch
Actual block thickness (b)	= 7.6 inch
Tributary width of roof	= 26 ft/2
Specified compressive stress (f_m')	= 3000 psi

Modulus of Rupture (f_r)	$= 4.0(f_m)^{1/2} = 219 \text{ psi}$
Modulus of elasticity of CMU (E_m)	$= 750 f_m'$
Specified yield str. of steel (F_y)	$= 60 \text{ ksi}$
Modulus of elasticity of steel (E_s)	$= 29 \times 10^6 \text{ psi}$
Area of vertical steel (A_s)	$= 0.33 \text{ in}^2/\text{ft}$
Eccentricity (e) ($(3.5/2 + 7.625/2)$)	$= 5.56 \text{ in}$
Depth to steel (d)	$= 3.81 \text{ in}$

Strength Reduction Factor for Flexure:
 $\phi = 0.80$

Unfactored Loads:

$$\text{Self Weight of Wall } (P_w) \text{ at mid-wall height} \\ P_w = [(25/2) + 1.5] 80 \text{ psf} = 1120 \text{ plf}$$

Roof Tributary Load (P_f)

$$P_f = (D+L_r)(26\text{ft}/2) = (14\text{psf}+20\text{psf})(13 \text{ ft}) \\ = 442 \text{ plf}$$

Seismic Lateral Load (w)

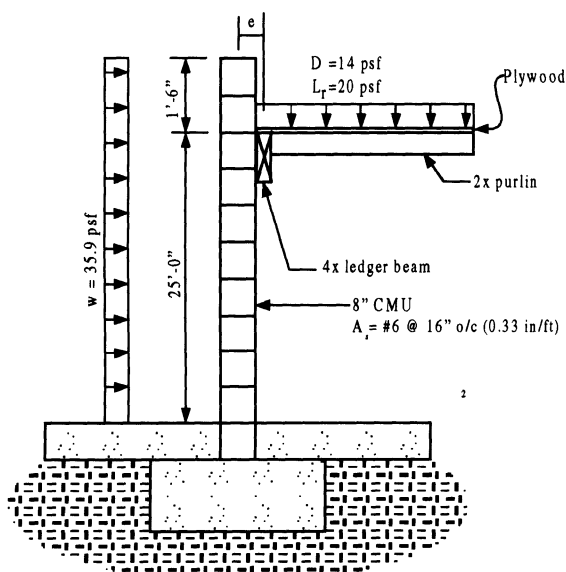


Figure 11-25. Cross-Section of Slender Wall

The wall is laterally supported at the base and roof. At the roof level, $h_x = h_r$, and so the lateral force is equal to:

$$F_p = \frac{(1.0)C_a I_p}{3.0} \left(1 + 3 \frac{h_x}{h_r} \right) W_p \\ = 1.33 C_a I_p W_p < 4 C_a I_p W_p$$

At the base of the wall, $h_x = 0$, and so the lateral force coefficient is equal to:

$$F_p = \frac{(1.0)C_a I_p}{3.0} \left(1 + 3 \frac{h_x}{h_r} \right) W_p \\ = 0.33 C_a I_p W_p < 0.7 C_a I_p W_p$$

Thus, use $0.7 C_a I_p W_p$ at the base. The design lateral forces are to be distributed in proportion to the mass distribution of the element. Therefore, the average force, which is uniformly distributed over the wall height, is given by:

$$F_p = \frac{(1.33+07)}{2} C_a I_p W_p = 1.02 C_a I_p W_p \\ = 1.02(0.44)(1.0)W_p \\ = (0.45)(80 \text{ psf}) = 35.9 \text{ psf}$$

SOLUTION OUTLINE:

- Vertical load stress check
- Maximum Reinforcement Check
- Cracking moment
- Moment of inertia (gross/cracked)
- Nominal moment strength (M_n)
- Unfactored service moments and displacements
- Factored moments and displacements.
- Design moment capacity

Vertical Load Stress Check

$$(P_w + P_f)/A_g \leq 0.04 f_m'$$

Where:

$$P_w = \text{Weight of wall} = 1120 \text{ plf} \\ P_f = \text{Tributary load} = 442 \text{ plf} \\ A_g = \text{Gross area of wall} = tb \\ = 7.625 \text{ in} (12 \text{ in}/\text{ft}) = 91.5 \text{ in}^2/\text{ft} \\ 0.04f_m' = 0.04(3000 \text{ psi}) = 120 \text{ psi}$$

Now

$$(1120+442)/91.5 = 17.07 \text{ psi} < 0.04f_m' \dots \text{OK}$$

Maximum Reinforcement Check

$$(\rho_b)_{\max} = 0.0107$$

$$(A_s)_{\max} = 0.489 \dots \text{Ref. Table 10-8}$$

$$(A_s)_{\text{actual}} = 0.33 < 0.489 \dots \text{OK}$$

Cracking Moment (M_{CR}): (w/o dead load)

$$M_{cr} = Sf_r$$

Where:

$$f_r = 4.0 (f_m')^{1/2} \dots 235 \text{ psi, max}$$

$$= 4.0 (3000)^{1/2}$$

$$= 219 \text{ psi}$$

$$S = Lb^2/6$$

$$= 12 \text{ in } (7.625)^2/6$$

$$= 116.3 \text{ in}^3/\text{ft}$$

Now:

$$M_{CR} = 116.3 \text{ in}^3 (219 \text{ psi})(1/1000 \text{ k/lb})$$

$$= 25.5 \text{ k-in/ft}$$

$$= 2.12 \text{ k-ft/ft}$$

Moment of Inertia (Gross/Cracked)**A. Gross Moment of Inertia (I_g)**

$$I_g = Lb^3/12$$

$$= 12 \text{ in } (7.6)^3/12$$

$$= 443.3 \text{ in}^3$$

B. Cracked Moment of Inertia (I_{cr})

$$I_{cr} = nA_{se}(d - c)^2 + (bc^3)/3$$

where:

$$A_{se} = (A_s f_y + P_u)/f_y = \text{effective area of steel}$$

$$A_s = 0.33 \text{ in}^2/\text{ft}$$

$$f_y = 60 \text{ ksi}$$

$$P_u = 1.2D + 0.5L_r$$

$$P_u = 1.2(1120 + 14(26/2)) +$$

$$0.5(20(26/2))$$

$$= 1.69 \text{ kips}$$

Now:

$$\begin{aligned} A_{se} &= [0.33 \text{ in}^2(60 \text{ ksi}) + 1.69]/60 \text{ ksi} \\ &= 0.36 \text{ in}^2/\text{ft} \end{aligned}$$

Next:

$$\begin{aligned} a &= (P_u + A_s f_y)/0.85 f_m b \\ &= [1.69 + 0.33(60)]/0.85(3.0)(12.0) \\ &= 0.71 \end{aligned}$$

Now:

$$\begin{aligned} c &= a/0.85 \\ &= 0.71/0.85 = 0.84 \text{ in.} \end{aligned}$$

Next:

$$b = 12.0 \text{ in.}$$

$$d = 3.8 \text{ in.}$$

$$\begin{aligned} n &= E_s/E_m = 29 \times 10^3 \text{ ksi}/750(3.0 \text{ ksi}) \\ &= 12.9 \end{aligned}$$

$$\begin{aligned} p &= A_s/bd \\ &= 0.33 \text{ in}^2/(12 \text{ in} \times 3.8 \text{ in}) = 0.0072 \end{aligned}$$

$$np = 12.9 (0.0072) = 0.093$$

Thus:

$$\begin{aligned} I_{cr} &= 12.9(0.36)[3.8 - 0.84]^2 \\ &\quad + 12 \text{ in}(0.84 \text{ in})^3/3 \\ &= 40.9 + 2.34 \\ &= 43.2 \text{ in}^4 \end{aligned}$$

Note : ratio of I_g to I_{cr} = $443.3/43.2 \approx 10:1$

Nominal moment strength (ϕM_n)

$$\begin{aligned} \phi M_n &= \phi A_{se} f_y [d - (a/2)] \\ &= 0.80(0.36 \text{ in}^2)(60 \text{ ksi})[3.81 - (0.71/2)] \\ &= 59.7 \text{ k-in.} \\ &= 4.98 \text{ k-ft.} \end{aligned}$$

Unfactored Service Moments and Displacements (Design for Deflection)

$$M_s = (wh^2/8) + P_f(e/2) + (P_w + P_f)\Delta_s$$

Where:

Δ_s = Midheight deflection under service lateral and vertical loads (without load factors

$[w=F_p/1.4]$). Maximum $\Delta_s = 0.007h = 0.007(25)(12) = 2.1$ in. Note that a deflection criteria used by some window systems is $l/240 = 0.004h$; thus $0.007 = l/143$ may be liberal for attached glazing.

$$\Delta_s = \begin{cases} \frac{5M_s h^2}{48E_m I_g} & (\text{For } M_s \leq M_{cr}) \\ \frac{5M_{cr} h^2}{48E_m I_g} + \frac{5(M_s - M_{cr})h^2}{48E_m I_{cr}} & (\text{For } M_{cr} < M_s < M_n) \end{cases}$$

Recall:

$$\begin{aligned} M_{cr} &= 25.5 \text{ k-in} = 2.12 \text{ k-ft} \\ \phi M_n &= 59.7 \text{ k-in} = 4.98 \text{ k-ft} \\ e &= 5.56 \text{ in.} \end{aligned}$$

Start: Try: $\Delta_1 = 0$

$$\text{Recall: } P_w + P_f = 1120 + 442 = 1562$$

$$\begin{aligned} M_1 &= [(35.9/1.4) \times (25)^2/8] \\ &\quad + 442 \times 5.56/(2 \times 12) + 1562(0) \\ &= 2003 + 102 \\ &= 2105 \\ &= 2.11 \text{ k-ft} < M_{cr} = 2.12 \text{ k-ft} \end{aligned}$$

Thus:

$$\begin{aligned} \Delta_2 &= \frac{5(2.11)(25)^2(1728)}{48(750)(3)(433)} \\ &= 0.24 \text{ in} \end{aligned}$$

Try: $\Delta_2 = 0.26$ in.

$$\begin{aligned} M_2 &= 2110 \text{ lb-ft} + 1562(0.26/12) \\ &= 2144 \text{ lb-ft} \\ &= 2.14 \text{ k-ft} \end{aligned}$$

$$\begin{aligned} \phi M_n &> 2.14 > M_{cr} \\ \Delta_3 &= \frac{5(2.12)(25)^2(1728)}{48(750)(3)(433)} \\ &\quad + \frac{5(2.14 - 2.12)(25)^2(1728)}{48(750)(3)(44.18)} \\ &= 0.26 \text{ in} \end{aligned}$$

$$\begin{aligned} \text{Use } M_s &= 2.14 \text{ k-ft} \\ &= 25.72 \text{ k-in} \\ \Delta_s &= 0.26 \text{ in.} < (.007h = 2.1 \text{ in}) \dots \text{OK} \end{aligned}$$

Factored (Ultimate) Moments and Displacements.

Load Case 1: $U = 0.9D + 1.0E$

Thus:

$$\begin{aligned} w_u &= 1.0(39.5 \text{ plf}) &= 39.5 \text{ plf} \\ P_{ufd} &= 0.9(14 \text{ psf} \times 26 \text{ ft}/2) &= 164 \text{ plf} \\ P_{ufl} &= 0 \\ P_{uw} &= 1.2(1120 \text{ plf}) &= 1344 \text{ plf} \\ P_{uf} &= P_{ufd} + P_{ufl} \\ &= 164 \text{ plf} + 0 \text{ plf} &= 164 \text{ plf} \\ P_u &= P_{uf} + P_{uw} \\ &= 164 \text{ plf} + 1344 \text{ plf} &= 1508 \text{ plf} \end{aligned}$$

Now:

$$M_u = (w_u h^2/8) + P_{uf}(e/2) + P_u \Delta_u$$

Where:

M_u = Factored moment at midheight of wall
 Δ_u = Midheight deflection under factored lateral and factored service loads

Try $\Delta_1 = 0$

$$\begin{aligned} M_1 &= 35.9(25)^2/8 \\ &\quad + 164 [5.56/(2 \times 12)] + 1508(0) \\ &= 2805 + 38.0 + 0 \\ &= 2843 \text{ lb-ft} = 2.84 \text{ k-ft} \end{aligned}$$

$$M_{cr} < 2.84 < \phi M_n$$

$$\begin{aligned}\Delta_2 &= \frac{5(2.12)(25)^2(1728)}{48(750)(3)(433)} \\ &\quad + \frac{5(2.84 - 2.12)(25)^2(1728)}{48(750)(3)(43.2)} \\ &= 0.245 + 1.157(2.84 - 2.12) = 1.08 \text{ in.}\end{aligned}$$

Try $\Delta_2 = 1.2$ in.

$$\begin{aligned}M_2 &= 2843 \text{ lb-ft} + 1508(1.2/12) \\ &= 2994 \text{ lb-ft} \\ &= 2.99 \text{ k-ft}\end{aligned}$$

$$M_{cr} < 2.99 \text{ k-ft} < M_n$$

$$\begin{aligned}\Delta_3 &= 0.245 + 1.157(2.99 - 2.12) \\ &= 0.245 + 1.01 \\ &= 1.25 \text{ in}\end{aligned}$$

Try $\Delta_3 = 1.27$

$$M_3 = 2843 \text{ lb-ft} + 1508 (1.27/12) = 3.00 \text{ k-ft}$$

$$\begin{aligned}\Delta_4 &= 0.245 + 1.157 (3.00 - 2.12) \\ &= 1.27 \text{ in}\end{aligned}$$

$$\begin{aligned}\text{Use } M_u &= 3.00 \text{ k-ft} \\ &= 36.0 \text{ k-in} \\ \Delta_u &= 1.27 \text{ inch}\end{aligned}$$

Load Case 2: $U = 1.2D + 1.0E$

The earthquake load on an element is given by:

$$E = \rho E_h + E_v$$

where E_h is the horizontal component and E_v is the vertical component of the earthquake load. The variable, ρ is the redundancy/reliability factor and is equal to 1.0 for elements of structures. For strength design, the vertical component is given by:

$$\begin{aligned}E_v &= 0.5C_a ID \\ &= 0.5(0.44)(1.0)D = 0.22D\end{aligned}$$

Thus, the load combination $U=1.2D + 1.0E$ becomes:

$$U = 1.2D + 1.0E$$

$$\begin{aligned}&= 1.2D + 0.22D + 1.0E_h \\ &= 1.42D + 1.0E_h \\ w_u &= 1.0(35.9 \text{ plf}) &= 35.9 \text{ plf} \\ P_{ufd} &= 1.42(14 \text{ psf} \times 26 \text{ ft}/2) &= 258.4 \text{ plf} \\ P_{ufl} &= 0 \\ P_{uw} &= 1.42(1120 \text{ plf}) &= 1590 \text{ plf} \\ P_{uf} &= P_{ufd} + P_{ufl} \\ &= 258.4 \text{ plf} + 0 \text{ plf} &= 258.4 \text{ plf} \\ P_u &= P_{uf} + P_{uw} \\ &= 258.4 \text{ plf} + 1590 \text{ plf} &= 1848.4 \text{ plf}\end{aligned}$$

Now:

$$M_u = (w_u h^2/8) + P_{uf}(e/2) + P_u \Delta_u$$

Where:

M_u = Factored moment at midheight of wall

Δ_u = Midheight deflection under factored lateral and factored service loads

Try $\Delta_1 = 0$

$$\begin{aligned}M_1 &= 35.9(25)^2/8 \\ &\quad + 258.4 \times 5.56/(2 \times 12) + 1848.8(0) \\ &= 2805 + 59.8 \\ &= 2864.8 \text{ lb-ft} = 2.86 \text{ k-ft}\end{aligned}$$

$$M_{cr} < 2.86 < \phi M_n$$

$$\begin{aligned}\Delta_2 &= \frac{5(2.12)(25)^2(1728)}{48(750)(3)(433)} \\ &\quad + \frac{5(2.86 - 2.12)(25)^2(1728)}{48(750)(3)(44.18)}\end{aligned}$$

$$= 0.245 + 1.157(2.86 - 2.12) = 1.1 \text{ in.}$$

Try $\Delta_2 = 1.2$ in.

$$\begin{aligned}M_2 &= 2864.8 \text{ lb-ft} + 1848.8 (1.2/12) \\ &= 3050 \text{ lb-ft} \\ &= 3.05 \text{ k-ft}\end{aligned}$$

$$M_{cr} < 3.05 \text{ k-ft} < M_n$$

$$\begin{aligned}\Delta_3 &= 0.245 + 1.157(3.05 - 2.12) \\ &= 0.245 + 1.076 \\ &= 1.32 \text{ in}\end{aligned}$$

Try $\Delta_3 = 1.34$

$$M_3 = 2864.8 \text{ lb-ft} + 1848.8(1.34/12) = 3.07 \text{ k-ft}$$

$$\begin{aligned}\Delta_4 &= 0.245 + 1.157 (3.07 - 2.12) \\ &= 1.34 \text{ in}\end{aligned}$$

$$\begin{aligned}\text{Use } M_u &= 3.07 \text{ k-ft} \\ &= 36.8 \text{ k-in...Controls} \\ \Delta_u &= 1.34 \text{ inch}\end{aligned}$$

Design moment capacity $M_u < \phi M_n$

$$\phi M_n = 59.7 \text{ k-in}$$

Where:

Strength Reduction Factor for Flexure

$$\phi = 0.80$$

$$M_u = 36.8 \text{ k-in} < 59.7 \text{ k-in ...OK}$$

Conclusion:

Slender wall is OK as shown

11.8 Shear Wall Design

11.8.1 General

Over 100 masonry shear walls with different steel ratios, axial load levels and sizes have been tested in the last decade. Therefore, it is possible to develop design criteria that are based on good quality, typically cyclic load reversal, test data. The design criteria for reinforced hollow unit concrete masonry shear walls in many respects follow the design criteria for reinforced concrete shear walls. However, as we shall later discuss, a major area of disagreement exists between many engineers who design concrete shear walls and many masonry designers over the use of highly reinforced boundary members. With that issue put aside it is possible, as this section will illustrate, to design ductile masonry shear walls that will perform well during seismic loading.

11.8.2 Structural Mechanics

The reader is referred to Volume two of the books entitled "Earthquake Design of Concrete Masonry Buildings" by Englekirk and Hart⁽¹¹⁻¹⁶⁾ and Design of Reinforced Masonry by Schneider and Dickey⁽¹¹⁻²³⁾ for excellent discussions of the structural mechanics of reinforced masonry design. In most respects it parallels the standard development of structural engineering design we are familiar with. For example, plane cross-sections are assumed to remain plane and a rectangular (Whitney) stress block replaces a more complex stress strain curve. The reader may wish to refer to these two references prior to reading the next subsection.

11.8.3 State-of-the-art Limit State Design Criteria

The following design criteria is very similar to the UBC design criteria. The reader is referred to Reference 11-24 for a history of that development.

A. Notations

A_e = effective area of masonry

A_n = net cross sectional area perpendicular to axial load square inches.

A_{mv} = net area of masonry section bounded by wall thickness and length of section in the direction of shear force considered, square inches.

A_s = area of tension reinforcement, square inches.

a_b = length of compressive stress block. inches.

b = effective width of wall, inches.

C_d = masonry shear strength coefficient as obtained from Figure 11-26.

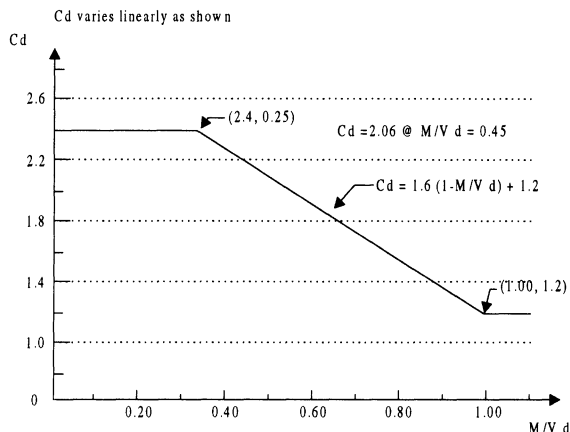


Figure 11-26. Nominal Shear Strength Coefficient (Cd)

d = distance from extreme compression fiber to centroid of tension reinforcement, inches.

D = dead loads, or related internal moments and forces.

E = load effects of earthquake, or related internal moments and forces.

E_s = modulus of elasticity of steel, 29,000,000 psi.

e_{mu} = maximum usable compressive strain of masonry.

F_s = allowable stress in reinforcement, psi.

f_s = computed stress in reinforcement, psi.

f_m' = specified compressive strength of masonry at the age of 28 days, psi

f_y = specified yield strength of reinforcement, psi.

L = live loads, or related internal moments and forces.

L_w = length of wall.

P_b = nominal balanced design axial strength.

P_o = nominal axial strength without bending loads.

P_u = required axial strength.

U = required strength to resist factored loads, or related internal moments and forces.

V_n = nominal shear strength.

V_m = nominal shear strength provided by masonry.

V_s = nominal shear strength provided by shear reinforcement.

ρ_n = ratio of distributed shear reinforcement on a plane perpendicular to plane of A_{mv} .

ϕ = strength reduction factor.

B. Quality Control Provision.

1. Special inspection during construction of the shear wall is required, especially after placement of the steel and prior to the pouring of the grout.

2. f_m' shall not be less than 1,500 psi nor greater than 4,000 psi. However, in concrete masonry a limit of 3,000 psi is recommended unless special quality control measures are taken or specified by the engineer.

3. f_m' shall be verified with prism testing.

C. Design Procedure

1. Required strength:

- For earthquake loading, the load factors shall be

$$U = 1.2D + 1.0E \quad (11-44)$$

$$U = 0.90D \pm 1.0E \quad (11-45)$$

- Required strength U to resist dead load D and live load L shall be at least equal to

$$U = 1.2D + 1.6L + 0.5(L_r + S) \quad (11-46)$$

2. Design Strength: Design strength provided by the shear wall cross section in terms of axial force, shear, and moment shall be computed as the nominal strength multiplied by the strength reduction factor, ϕ .

Shear walls shall be proportioned such that the design strength exceeds the required strength.

Strength reduction factor ϕ shall be as follows:

- Axial load and axial load with flexure: $\phi = 0.65$

For members in which f_y does not exceed 60,000 psi, with symmetrical reinforcement, ϕ may be increased linearly to 0.85 as ϕP_n decreases from 0.10 $f_m' A_e$ or 0.25 P_b to zero.

For solid grouted wall P_b may be calculated by Equation 11-47:

$$P_b = 0.85 f_m' b a_b \quad (11-47)$$

where

$$a_b = 0.85 \left[\frac{e_{mu}}{e_{mu} + \frac{f_y}{E_s}} \right] d \quad (11-48)$$

- Shear: $\phi=0.60$

The shear-strength reduction factor may be 0.80 for any shear wall when its nominal shear strength exceeds the shear corresponding to development of its nominal flexural strength for the factored-load combination

3. Design Assumptions for Nominal Strength: Nominal strength of shear wall cross sections shall be based on assumptions prescribed in Section 11.8.

The maximum usable strain, e_{mu} , at the extreme masonry compression fiber shall not exceed 0.003 unless compression tests on prisms indicate higher values are justified.

4. Reinforcement:

- Minimum reinforcement shall be 0.0007 in either direction and 0.002 total. (0.003 for California Hospitals and schools)

• When the shear wall failure mode is in flexure, the nominal flexural strength of the shear wall shall be at least three times the cracking moment strength of the wall from Equation 11-38.

• All continuous reinforcement shall be anchored or spliced in accordance with 1997 UBC Section.

• The minimum amount of vertical reinforcement shall not be less than one half the horizontal reinforcement.

• Maximum spacing of horizontal reinforcement within the region defined in Section 6C(i) below shall not exceed three times nominal wall thickness or 24 inches, whichever is less.

5. Axial strength: The nominal axial strength of the shear wall supporting axial loads only shall be calculated by Equation 11-49.

$$P_o = 0.85 f_m' (A_n - A_s) + f_y A_s \quad (11-49)$$

Axial design strength provided by the shear wall cross section shall satisfy the equation:

$$P_u \leq \phi(0.80)P_o \quad (11-50)$$

6. Shear strength:

a. The nominal shear strength shall be determined using either Section 6b or 6c. Figure 11-26 gives the values for C_d .

b. The nominal shear strength of the shear wall shall be determined from Equation 11-51, except as provided in Section 6c.

$$V_n = V_m + V_s \quad (11-51)$$

where

$$V_m = C_d A_{mv} \sqrt{f_m'} \quad (11-52)$$

and

$$V_s = A_{mv} \rho_n f_y \quad (11-53)$$

c. For a shear wall whose nominal shear strength exceeds the shear corresponding to development of its nominal flexural strength two shear regions exist.

(i) For all cross sections within the region defined by the base of the shear wall and a plane at a distance L_w above the base of the shear wall the nominal shear strength shall be determined from:

$$V_n = A_{mv} \rho_n f_y \quad (11-54)$$

The required shear strength for this region shall be calculated at a distance $L_w/2$ above the base of the shear wall but not to exceed one-half story height.

(ii) For the other region the nominal shear strength of the shear wall shall be determined from Eq 11-51.

7. Confinement of Vertical Steel: All vertical reinforcement whose corresponding masonry compressive stress, corresponding to factored forces, exceeds $0.75f_m'$ shall be confined when the failure mode is flexure. Vertical steel when it needs to be confined shall be done with a minimum of No.3 bars at a maximum of 8-inch spacing or equivalent within the grouted core and within the region defined as the base of the shear wall. When confinement is needed the vertical steel confined shall be at least from the end of the wall to a lateral distance three times the thickness of the wall.

11.8.4 Comments on State of the Art Design Criteria for Shear Walls

The design strength is obtained by multiplying the nominal strength by a strength reduction factor. The nominal strength is ideally the best professional estimate of the true strength of the member. The strength reduction factor is selected to account for the uncertainty of the value of the parameters in the nominal strength equation, the workmanship in the field, and the general confidence in the equation's

ability to predict the actual performance of the member.

For walls subjected to flexure and axial load the variation in the numerical value of the strength reduction factor is a function of the axial load on the shear wall. The primary reason for this is to insure that the walls performance is that of an under-reinforced flexural member. Therefore, we have divided the interaction diagram for the shear wall into two zone for the purpose of setting a value for the strength reduction factor. Zone 1 corresponds to sufficiently low axial loads to insure a very ductile shear wall performance. We have provided an axial load limit of less than 65% of an approximate calculation of the balance design axial load, P_b . This alternative approach, by being a function of the balance design axial load, places a stronger emphasis on the importance of quantifying the intensity of the axial load as a function of the balance design axial load in order to promote ductility. The value of 65% P_b is reasonable based on a reliability analysis which incorporated uncertainty in material properties and the design equation⁽¹¹⁻²⁵⁾. To provide a straightforward calculation of the balance design axial load, we have provided an equation which is a good approximation of the balance design axial load for purposes of the use here (i.e., typically less than 10% error). This approximation assumes that the forces from the positive tension steel and the negative compression steel balance each other in the equilibrium equation.

Zone 2 is for value of axial load greater than 65% of the balance design axial load. The numerical value of the strength reduction factor in Zone 2 is equal to 0.65. To ensure that the quality of the masonry is consistent with the engineering design assumptions, the minimum value of f_m' is set at 1500 psi. The maximum recommended value for f_m' is 3,000 psi unless a special level of quality control is used for concrete masonry. Unless the engineer has performed a check with his local block supplier it is reasonable to assume that 3,000 psi is a practical limit.

The strength reduction factor for shear walls where the mode of failure is shear is equal to 0.60. This typically represents shear walls that are long compared to their height.

For walls where flexure is a possible failure mode, the shear resistance that is provided is checked to ensure that the shear corresponding to the development of the full nominal flexural strength of the wall is provided. This approach is consistent with the approach taken for reinforced concrete in the 1997 UBC. In this situation, the strength reduction factor for shear is equal to 0.80.

The equation used to calculate the axial strength of the wall is equal to the specified compressive strength times the net area of the wall times an effective stress parameter value of 85% plus the yield stress of the steel times the area of the steel. This equation is directly consistent with the equation used in reinforced concrete design.

For pure axial load design, the strength reduction factor is equal to 0.65 and was discussed in Section 11-8. A further reduction is made to reduce the axial load by multiplying the nominal strength by 0.8 in order to account for accidental eccentricities.

The shear strength of shear walls can be determined using either of two alternative approaches. The first approach is used for shear walls where the failure mode is shear. In this situation, the strength reduction factor is equal to 0.60 and the nominal shear strength is obtained by adding two terms. The first term is the shear strength assumed to be provided by the masonry in a reinforced masonry wall. The second term is the shear strength provided by the shear reinforcement.

The second approach used to calculate the nominal shear strength of a wall is appropriate for shear walls where a flexural mode of failure is possible. The intent of this approach is to require that sufficient shear reinforcement is placed in the wall to insure a ductile flexural failure. In this situation, the strength reduction factor for shear is equal to 0.80. The flexural failure mode will result in a shear wall where the region near the base will be called upon to

undergo an inelastic moment curvature response. Therefore, we have identified two shear regions for such a shear wall. Shear region number one is a region defined from the base of the wall up to a distance equal to the length of the wall and is a plastic hinge region. In this region because of the inelastic cyclic response, only the shear resistance provided by the steel is considered in the design. In this region, the region above the plastic hinge, the masonry and the steel are both used to calculate the shear strength of the wall.

The use of boundary members in shear walls is a highly controversial topic in masonry design. The New Zealand Building code does not allow boundary members to be used in masonry shear walls⁽¹¹⁻²⁶⁾. The New Zealand approach is to encourage the structural engineer to uniformly distribute the vertical steel along the length of the wall. This, they argue, provides a more consistent distribution of shear stress between the wall and the foundation. The counter to this argument is the current approach taken by reinforced concrete design criteria. In essence, the current approach for reinforced concrete walls is to design the shear wall as if it were essentially a second class ductile frame and discount the concrete between the boundary members. The net result of this design is high axial loads at the ends of the wall.

The approach defined in UBC 97 for steel confinement determination specifies that the factored loads are applied to the shear wall and, using the principles of mechanics, the compressive stress in the masonry immediately adjacent to the vertical reinforcing bars is calculated. If this stress exceeds 75% of the maximum specified compressive stress, the vertical reinforcement must be confined. The 75% number is based on an approximate unconfined masonry prism strain value of 0.0015 for a stress strain curve that is parabolic between zero stress and maximum compressive stress (see Figure 11-21). If the strains are below 0.0015 then based on observations of prism tests we can expect no significant loss of strength or stiffness due to cyclic loading and small internal masonry cracking.

11.8.5 Example Problem – Reinforced Masonry Shear Wall (Strength Design)

This example problem is a variation of example 3K on page 95 of the book entitled "Reinforced Masonry Engineering Handbook - Clay and Concrete Masonry" by James Amrhein⁽¹¹⁻²⁷⁾. Determine if the CMU shear wall shown in Figure 11-27 is adequate for the following vertical and seismic loads. Use strength design UBC 97.

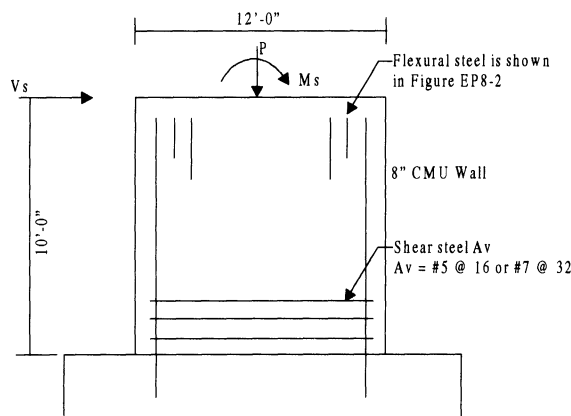


Figure 11-27. Elevation of Shear Wall

Loads: Dead Load = 30 kips

Live Load = 0 kips

Lateral Shear Force (V_E) = 75 kips

Seismic Moment (M_E) = 400 kip-ft

Load Factors: $U = 1.2D + 1.6L$

$$U = 1.2D + 0.5L + 1.0E$$

$$U = 0.9D \pm 1.0E$$

Reduction Factors: $\phi = 0.65$ Axial

$\phi = 0.65$ Axial plus flexure

$\phi = 0.80$ Flexure only

$\phi = 0.60$ Shear

Wall Properties:

Wall is fully grouted ($M_n \geq 1.8 M_{cr}$)

Normal block thickness = 8 inch

Actual block thickness (b) = 7.625 inch

Length of wall (L) = 12 ft

Specified compressive strength (f_m') = 1500 psi

Modulus of rupture (f_r) = $4.0\sqrt{f_m'}$

Maximum usable masonry strain (e_{mu}) = 0.003

Modulus of elasticity of CMU (E_m) = $750f_m'$

Shear modulus of masonry (G) = $0.4E_m$

Specified yield strength of steel (f_y) = 60 ksi

Modulus of elasticity of steel (E_s) = 29×10^6 psi

SOLUTION OUTLINE:

- Interaction diagram (generate/draw)
- Cracking moment strength (M_{cr})
- Load cases (axial plus flexure)
- Boundary members
- Shear

A. Interaction Diagram

1. Nominal axial load strength (P_o)

$$\begin{aligned} P_o &= 0.85 f_m'(A_e - A_s) + f_y A_s \\ &= 0.85(1.5\text{ksi})[12 \text{ ft} (12 \text{ in}/\text{ft})(7.625 \text{ in}) - \\ &\quad 10 \text{ bars} 0.31 \text{ in}^2/\text{bar}] + 60 \text{ ksi} (10 \text{ bars}) \\ &\quad (0.31 \text{ in}^2/\text{bar}) \\ &= 1581.99 \text{ kips} \end{aligned}$$

2. Design axial load strength (P_u)

$$\begin{aligned} P_u &= \phi(0.80)(P_o) \\ &= 0.65(0.80)(1581.99 \text{ kips}) \\ &= 822.64 \text{ kips} \end{aligned}$$

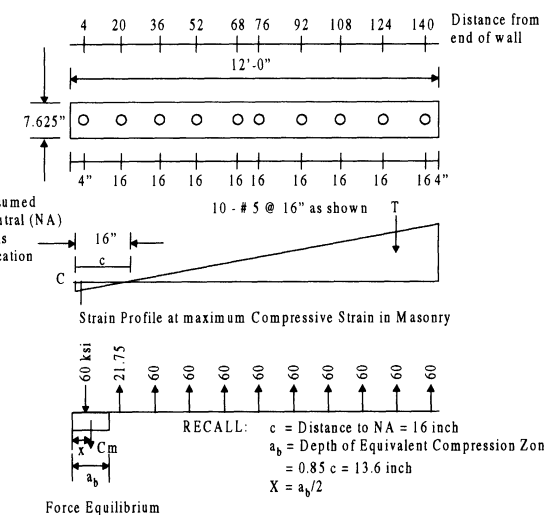


Figure 11-28. Steel locations, strain profile and force equilibrium diagrams

3. Nominal bending moment strength (M_o): See Figure 11-28.

Must solve for location of neutral axis (NA) such that sum of axial forces on cross section is zero.

- _ Assume location for NA; $c = 16$ inch.
- _ Use maximum allowable CMU strain of 0.003.
- _ Iterative solution.
- _ Take sum of moments about extreme compression fiber (end of wall).

$$T = A_s f_s = [21.75 \text{ ksi} + 8(60 \text{ ksi})](0.31 \text{ in}^2)$$

$$= 155 \text{ kips}$$

$$C = A_s f_s + \phi f_m' b a_b$$

$$= 0.31 \text{ in}^2 (60 \text{ ksi}) + 0.85 (1.5 \text{ ksi})(7.625 \text{ in})(13.6 \text{ in})$$

$$= 150.82 \text{ kips}$$

$T - C = 4$ kips close enough use $c = 16$ ".

$$M_o = A_s f_y - 0.85 f_m' b a_b$$

$$M_o = 0.31 \text{ in}^2 [21.75(20) + 60(36 + 52 + 68 + 76 + 92 + 108 + 124 + 140) - 0.31 \text{ in}^2 \times (60)(4)]$$

$$0.85(1.5)(13.6)^2(1/2)(7.625)$$

$$= 13080.4 - 74.4 - 899$$

$$= 12,107 \text{ k-in}$$

$$= 1009 \text{ k-ft}$$

4. Design bending moment strength (M_u)

$$M_u = 0.80 M_o$$

$$= 0.80(1009 \text{ k-ft})$$

$$= 807.2 \text{ k-ft}$$

5. Nominal balanced design axial strength (P_b): See Figure 11-29.

$$C_m = 0.85 f_m' b a_b$$

Where:

$$a_b = \left[\frac{\epsilon_{mu}}{\epsilon_{mu} + \frac{f_y}{E_s}} \right] d$$

$$= 0.85 \left[\frac{0.003}{0.003 + 60/29000} \right] d$$

$$= 0.85(0.5918)d$$

$$= 0.503(140 \text{ inch})$$

$$= 70.43 \text{ inch}$$

Recall:

$$c = \text{Distance to NA} = a_b/0.85$$

$$= 70.428/0.85$$

$$= 82.86 \text{ in}$$

$$T = \Sigma A_s f_y$$

$$= 0.31 \text{ in}^2 (9.6 + 26.4 + 43.2 + 60) \text{ ksi}$$

$$= 43.2 \text{ kips}$$

Now:

$$C = \Sigma A_s f_y + 0.85 f_m' b a_b$$

$$= 0.31 \text{ in}^2 (7.2 + 15.6 + 32.4 + 49.2 + 60 + 60) \text{ ksi} + 0.85(1.5)(7.625)(70.428)$$

$$= 69.56 + 684.69$$

$$= 754.25$$

Thus:

$$P_b = C - T$$

$$= 754.25 - 43.2$$

$$= 711 \text{ kips}$$

6. Design balanced design axial strength (P_{bu})

$$P_{bu} = \phi P_b$$

$$= 0.65 (711 \text{ kips})$$

$$= 462 \text{ kips}$$

7. Nominal balanced design moment strength (M_b): See Figure 11-29. Take sum of moments about plastic centroid (center of wall):

$$M_b = A_s f_y - 0.85 f_m' b X_b b$$

$$= 0.31[60(68) + 43.2(52) + 26.4(36) + 9.6(20) - 7.2(4) + 15.6(4) + 32.4(20) + 49.2(36) + 52(60) + 68(60)] + 0.85(1.5)(70.428)(36.76)(7.625)$$

$$= 5308 + 25169$$

$$= 30477 \text{ k-in}$$

$$= 2540 \text{ k-ft}$$

8. Design balanced design moment strength (M_{bu})

$$M_{bu} = \phi M_b$$

$$= 0.65(2540 \text{ k-ft})$$

$$= 1651 \text{ k-ft}$$

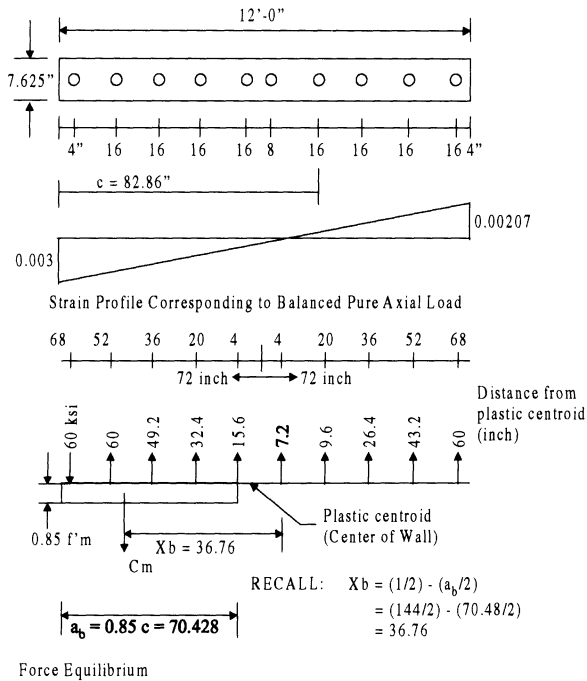


Figure 11-29. Balanced design load condition

B. Cracking moment strength

- Linearly elastic model
- Gross section properties

$$(P/A) + M_{cr}/S = f_r$$

Thus:

$$M_{cr} = S[(P/A) + f_r]$$

Where:

$$\begin{aligned} A &= bl = 7.625(144) = 1098 \text{ in}^2 \\ s &= bl^2/6 = 7.625 (144)^2/6 = 26,352 \text{ in}^3 \\ f_r &= 4.0 \sqrt{f_m} = 4.0(1500)^{1/2} = 155 \text{ psi} \\ P &= \text{Dead Load} = 30,000 \text{ lbs} \end{aligned}$$

Thus:

$$\begin{aligned} M_{cr} &= 26352[(30000/1098) + 155][(1/1000)(k/1b)] \\ &= 4804.6 \text{ k-in} \\ &= 400 \text{ k-ft} \end{aligned}$$

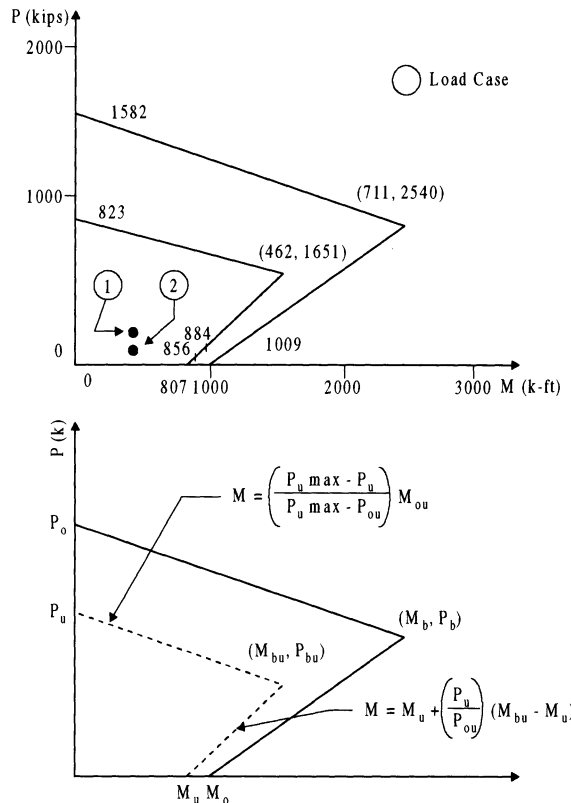


Figure 11-30. Interaction Diagram

C. Load Cases (See Figure 11-30)

Load Case 1:

$$\begin{aligned} U &= 12D + 1.0E \\ &= 1.42D + 1.0E_h \end{aligned}$$

Therefore;

$$\begin{aligned} U &= 1.42(30) + 1.0(400) \\ &= 42.6 \text{ kips} + 400 \text{ k-ft} \end{aligned}$$

From Figure 11-30:
 $P_u = 42.6 \text{ kips} < P_{bu} = 462 \text{ kips}$

Thus:

$$\begin{aligned} P_{bu}/(M_{bu} - M_u) &= P_u/M_x \\ M_x &= (P_u/P_{bu})(M_{bu} - M_u) \\ M_n &= M_u + M_x \\ &= M_u + (P_u/P_{bu})(M_{bu} - M_u) \\ &= 807 \text{ k-ft} + (42.6/462)(1651 - 807) \\ &= 884.8 \text{ k-ft Nominal Flexural Moment Strength} \end{aligned}$$

Note: $884.8 \text{ k-ft} > 400 \text{ k-ft} \quad \text{OK}$

Note: $M/M_{cr} = 884.8/400 = 2.2 > 1.8$ OK
(recall fully grouted wall)

Load Case 2:

$$\begin{aligned} U &= 0.90D + 1.0E \\ U &= 0.90(30) + 1.0(400) \\ &= 27 \text{ kips} + 400 \text{ k-ft} \end{aligned}$$

From Figure 11-30: $P_u = 27 \text{ kips} < P_{bu} = 462$

Thus:

$$\begin{aligned} M_n &= 807 + (27/462)(1651 - 807) \\ &= 856 \text{ k-ft} \end{aligned}$$

Note:

$$M_n/M_{cr} = 856/400 = 2.14 > 1.8 \dots \text{OK}$$

D. Boundary Elements

Section 2108.2.5.6 of the 1997 UBC states that:

"Boundary members shall be provided at the boundaries of shear walls when the compressive strains in the wall exceed 0.0015. The strain shall be determined using factored forces and R_w equal to 1.5"

Note that there is an error in the code since it refers to the obsolete R_w factor, which has been replaced by the R factor in the 1997 UBC. By comparing the values of the new R factor with the old R_w factor, one can conclude that the boundary member requirements should be calculated using an R of 1.1. Since the design forces for the bearing wall were calculated with an R factor of 4.5, the factored loads must be multiplied by $4.5/1.1 = 4.09$ in order to determine if the moment capacity of the wall at a maximum compressive strain of 0.0015 is less than that required for boundary members.

To calculate the moment capacity at a maximum compressive strain of 0.0015, we can assume a linear compressive stress-strain relationship for the masonry. So, using a linear strain model, $f_m = 0.75f'_m$ for a strain of 0.0015: See figure 11-31.

Must solve for neutral axis (c)

- _ Trial and error solution
- _ Take moments about plastic centroid

Load Case 1:

$$\begin{aligned} U &= 12D + 1.0E \\ &= 1.42D + 1.0E_h \\ (P_u &= 42.6 \text{ kips} \text{ and } M_u = 400 \text{ k-ft}) \end{aligned}$$

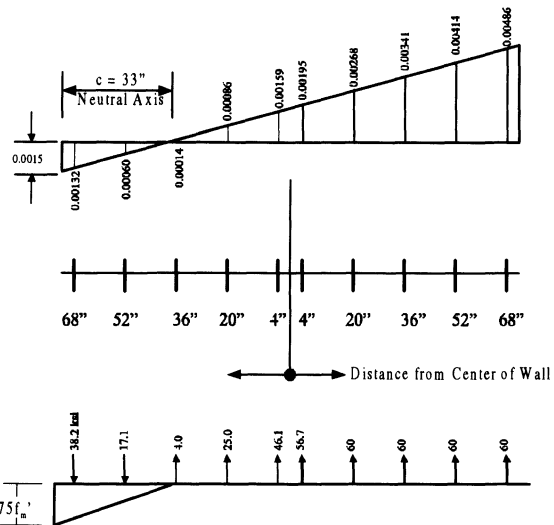


Figure 11-31. Stress/Strain relationship for determining boundary elements in masonry

By trial and error select depth to neutral axis, NA = 33.0 inches (See Figure 11-31 for stress and strain diagrams).

$$\begin{aligned} T &= A_s f_s \\ &= 0.31(4)(60) + 56.7 + 46.1 + 25 + 4 \\ &= 115.3 \text{ kips} \\ C &= A'_s f_s + 0.75 f'_m c b / 2 \\ &= 0.31(38.2 + 17.1) \\ &+ 0.75(1.5)(33)(7.625)(1/2) \\ &= 158.7 \text{ kips} \\ C-T &= 43.4 \text{ kips } (P_u = 42.6 \text{ kips}) \dots \text{OK} \end{aligned}$$

Use: NA = 33.0 inches

Take moments about the center of the wall centroid to determine moment corresponding to $0.75f'_m$. If $4.09M_u$ is less than M_n confinement of vertical steel is not required.

$$\begin{aligned} M_n &= A_s f_s (\text{dist. to Center of Wall}) \\ &+ 0.75 f'_m (c/2)(L/2 - c/3) \end{aligned}$$

$$\begin{aligned}
 &= 0.31[68(38.2) + 52(17.1) - 36(4.0) \\
 &\quad - 20(25) - 4(46.1) + 4(56.7) \\
 &\quad + 60(20+36+52+68)] \\
 &\quad + 0.75(1.5)(33/2)[(144/2) - (33/3)] \\
 &= 441.7 \text{ k-ft} < 4.09M_u = 1636 \text{ k-ft}
 \end{aligned}$$

Thus,

Boundary Elements Required.

E. Shear

1. Shear Demand

$$\begin{aligned}
 \text{Recall : } V_u &> \phi V_n \\
 V_u &> \phi (V_m + V_s) \\
 V_u &= 1.0V_E \\
 &= 1.0(75 \text{ kips}) \\
 &= 75 \text{ kips}
 \end{aligned}$$

2. Shear strength with only CMU (no shear steel)

$$\begin{aligned}
 V_n &= V_m (V_s = 0) \\
 &= C_d A_{mv} (f'_m)^{1/2}
 \end{aligned}$$

Where:

$$\begin{aligned}
 C_d &\propto M/Vd \\
 d &= 12 \text{ ft} - (4/12)\text{ft} = 11.67 \text{ ft} \\
 V &= 75 \text{ kips} \\
 M &= 400 \text{ k-ft} \\
 M/Vd &= 400/[75(11.67)] = 0.46 \text{ (from} \\
 \text{Figure 10-26: } C_d &= 2.06) \\
 A_{mv} &= l_w b = 144 \text{ in}(7.625 \text{ in}) = 1098 \text{ in}^2
 \end{aligned}$$

Now:

$$\begin{aligned}
 V_n &= C_d A_{mv} \sqrt{f'_m} ; C_d = 2.06 \\
 V_n &= 2.06 \times 1098 \text{ in}^2 (1500 \text{ psi})^{1/2} / 1000 \text{ lb/k} \\
 &= 87.6 \text{ kips} \\
 V_u &> \phi V_n \\
 \phi V_n &= 0.60(87.6 \text{ kips}) \\
 &= 52.6 \text{ kips} \\
 V_u &= 75 > 52.6 \dots \text{NG shear reinforcement required}
 \end{aligned}$$

3. Design shear reinforcement to carry total shear (at least majority, authors preference)

$$\begin{aligned}
 V_u &= \phi V_n = \phi V_s \dots (V_m = 0) \\
 V_u &= A_{mv} \rho_n f_y \phi
 \end{aligned}$$

Recall:

$$\begin{aligned}
 \rho_n &= V_u / A_{mv} f_y \phi \\
 &= 75 \text{ kips} / (1098 \text{ in}^2) (60 \text{ k/in}^2) (0.60) \\
 &= 0.0019
 \end{aligned}$$

Now:

$$\begin{aligned}
 A_v &= 0.0019(12 \text{ in})(7.625 \text{ in}) \\
 &= 0.174 \text{ in}^2/\text{ft} \\
 \text{USE: # 5 @ 16 in. o.c.} \\
 (A_v &= 0.23 \text{ in}^2/\text{ft} > 0.174 \text{ in}^2/\text{ft})
 \end{aligned}$$

Thus, the steel can carry all the shear

4. Shear strength of steel only:

$$\phi V_s = \rho_n A_{mv} f_y \phi$$

$$= \frac{0.23(1098 \text{ in}^2)(60 \text{ ksi})(0.60)}{(12 \frac{\text{in}}{\text{ft}})(7.625 \text{ in})} = 99.36 \text{ kips}$$

5. Bottom (L_w) of wall

Shear strength of steel only with $\phi=0.85$

$$\begin{aligned}
 V_s &= 99.36 \left(\frac{0.85}{0.60} \right) \\
 &= 140.76 \text{ kips} > 75 \text{ kips} \text{ OK}
 \end{aligned}$$

Table 11-10. Total Design Base Shear for 3-Story Building Wood Structural Panel Bearing Wall System

Notes	Item/Description	Total Design Base Shear (V) Seismic Zone and Factor				
		1 0.075	2A 0.15	2B 0.20	3 0.30	4 0.40
1	Cv	0.18	0.32	0.40	0.54	0.64Nv
	I	1.0	1.0	1.0	1.0	1.0
	R	5.5	5.5	5.5	5.5	5.5
2	T EQ. 10-10E	0.256	0.256	0.256	0.256	0.256
	Ca	0.12	0.22	0.28	0.36	0.44Na
3	Nv	-	-	-	-	1.2
3	Na	-	-	-	-	1.0
4	V EQ. 11-10A	0.128W	0.227W	0.284W	0.384W	0.545W
4	V EQ. 11-10B	0.055W*	0.10W*	0.127W*	0.164W*	0.20W*
4	V EQ. 11-10C	0.013W	0.024W	0.031W	0.039W	0.048W
4	V EQ. 11-10D	-	-	-	-	0.070W

Notes: 1. Soil profile type D
 2. $T = Ct (h_n)/3/4 = 0.256$ sec

For $Ct = 0.020$

$h_n = 30$ feet

3. Seismic source B
 Closest distance to seismic source = 5km

4. * = Governs

Table 11-11. Total Design Base Shear for 3- Story Building Masonry Shear Wall Bearing Wall System

Notes	Item/Description	Total Design Base Shear (V) Seismic Zone and Factor				
		1 0.075	2A 0.15	2B 0.20	3 0.30	4 0.40
1	Cv	0.18	0.32	0.40	0.54	0.64Nv
	I	1.0	1.0	1.0	1.0	1.0
	R	4.5	4.5	4.5	4.5	4.5
2	T EQ. 10-10E	0.256	0.256	0.256	0.256	0.256
	Ca	0.12	0.22	0.28	0.36	0.44Na
3	Nv	-	-	-	-	1.2
3	Na	-	-	-	-	1.0
4	V EQ. 11-10A	0.156W	0.278W	0.347W	0.469W	0.67W
4	V EQ. 11-10B	0.067W	0.122W*	0.156W*	0.20W*	0.244W*
4	V EQ. 11-10C	0.013	0.024W	0.031W	0.039W	0.048W
4	V EQ. 11-10D	-	-	-	-	0.085W

Notes: 1. Soil profile type D
 2. * = Governs

REFERENCES

- 11-1 First North American Masonry Conference, Univ. of Colorado, Boulder, CO, Aug. 1978
- 11-2 Second North American Masonry Conference, Univ of Maryland, College Park, MD, Aug. 1982
- 11-3 Third North American Masonry Conference, Univ. of Texas, Arlington, TX, June 1985
- 11-4 Third Canadian Masonry Symposium, Edmonton, Alberta, Canada, June 1982
- 11-5 Fourth Canadian Masonry Symposium, Univ. of New Brunswick, New Brunswick, Canada, June 1986
- 11-6 International Conference of Building Officials, *Uniform Building Code, 1985 Edition*, Whittier, CA, 1985
- 11-7 Hegemier, G., *Various Contributions to Second North American Masonry Conference*, Univ. Of Maryland, College Park, MD, Aug. 1982
- 11-8 Mayes, R., *Various Contributions to Second North American Masonry Conference*, Univ. Of Maryland, College Park, MD, Aug. 1982
- 11-9 International Conference of Building Officials, "Strength Design of One to four Story Concrete Masonry Building," Report No. 4115, ICBO, Whittier, CA, Feb. 1985.
- 11-10 International Conference of Building Officials, *Uniform Building Code, 1988 Edition*, Whittier, CA, 1988
- 11-11 Noland, J., *Various Contributions to Fourth North American Masonry Conference*, University of California at Los Angeles, Los Angeles, CA. Aug. 1987
- 11-12 Hart, G.V., *Uncertainty Analysis, Loads and Safety in Structural Engineering*, Prentice-Hall, Englewood Cliffs, NJ, 1982
- 11-13 Calambos, T. V., "Probability Based Load Criteria, Assessment of Current Design," *Proc. J. Structural Eng.*, ASCE 108, No. ST5, May 1982
- 11-14 Cornell, C.A., "Probability Based Load Criteria, Assessment of Current Design," *Proc. J. Structural Eng.*, ASCE 108, No. ST5, May 1982
- 11-15 Englekirk, R. E. and Hart, G. C., *Earthquake Design of Concrete Masonry buildings, Volume I*, Prentice-Hall, Englewood Cliffs, NJ, 1982
- 11-16 Englekirk, R. E. and Hart, G. C., *Earthquake Design of Concrete Masonry buildings, Volume II*, Prentice-Hall, Englewood Cliffs, NJ, 1984
- 11-17 ACI-SEAOSC Task Committee on Slender Walls, "Test Report on Slender Walls," Los Angeles CA, Feb. 1980-Sept. 1982.
- 11-18 Priestly, M. and Elder, D., "Seismic Behavior of Slender Concrete Masonry Shear Walls," *Bull. New Zealand Nat. Soc. Earthquake Eng.*, 15, No. 1, Mar. 1982
- 11-19 Priestly, M. and Elder, D., "Stress—Strain Curves for Unconfined and Confined Concrete Masonry," *ACI J. 80*, No. 7, May/June 1983
- 11-20 Wang, C. K. and Salmon, C. G., *Reinforced Concrete Design*, 3rd Edition, Harper and Row Publishers, Ney York, 1979.
- 11-21 Keller, G. R. and Sutler, G.T., "Variability of Reinforced Concrete Masonry Beam Strength in Fleure and Shear," Second North American Masonry Conference, College Park, MD, Aug. 1982
- 11-22 Kingsley, G. R. and Atkinson, R. H., "Stress-Strain Behavior of Grouted Hollow Unit Masonry," Fourth Canadian Masonry Symposium, Univ of New Bruswick, New Brunswick Canada, June 1986.
- 11-23 Schneider, R. R. and Dickey, W.L., *Reinforced Masonry Design*, 2nd Edition, Prentice-Hall, Englewood Cliffs, NJ, 1987.
- 11-24 Hart, G. C., Various Contributions to Fourth North American Masonry Conference, Univ. of California at Los Angeles, Los Angeles, CA, Aug 1987
- 11-25 Sajjad, N. A., "Reliability Analysis of Sleected Concrete Masonry Deisgn Equation," Masters Project, Univ. of California at Los Angeles, Los Angeles, CA 1987
- 11-26 Priestly, M., "New Zealand Seismic Design Philosophy for Masonry Structures," Fourth North American Masonry Conference, Los Angeles, CA, Aug. 1987
- 11-27 Amrheim, James E. "Reinforced Masonry Engiuneering Handbook – Clay and Concrete Masonry" 4th Edition, Masonry Institute of American, 2550 Beverly Boulevard Los Angeles, California 90057
- 11-28 ASCE Task Committee on LRFD for Engineered Wood Construction (1988), "Load and Resistance Factor Design for Engineered Wood Construction – A Pre-Standard Report" American Society of Civil Engineers, New York, N.Y. Contact Joseph F. Murphy P.O. Box 56164, Madison, WI 53705-9464
- 11-29 Benjamin, J.R., "Statically Indeterminate Structures", Mc Graw-Hill Book Company, Inc., New York, 1959
- 11-30 Briggs, L.A., Black, O.M., "Distribution of Lateral Loads in Small Buildings", Technical Book Company, Los Angeles, California, 1964
- 11-31 Brooks, Michael D., "Enercalc Engineering Software," 3070 Bristol Street, 6th floor, Costa Mesa, California 92626.
- 11-32 Derecho A. T., Schultz, D.M., Fintel M., "Analysis and Design of Small Reinforced Concrete Buildings for Earthquake Forces", Portland Cement Association, EB004.05, 1974
- 11-33 Hart, Gary C. and Basharkhah, Ali M., "Shear Wall Structural Engineering Analysis Computer Program" and "Slender Wall Structural Engineering Analysis Computer Program" available from Concrete Masonry Association of California and Nevada, 6060

- Sunrise Vista Drive, Suite 1875, Citrus Heights, California 95610
- 11-34 Map of EPA Contours prepared by U.S. Geological Survey for the 1988 edition of NEHRP Recommended Provision fro the Development of Seismic Regulations for New Buildings.
- 11-35 Shipp, John G., Structural Engineering License Review Manual – Timber Desgin” 2 Volumes – 1991, Professional Engineering Development Publication, Long Beach CA, 90815-0406 P.O. Box 15406
- 11-36 Structures Congress 91 Compact Papers, Ninth Structures Congress, Indianapolis, Indiana April 29-May 1 1991. Produced by ASCE 345 East 45th Street, New York, N.Y. 10017-2398
- 11-37 Timoshenko, S., “Strength of Materials – Part 1 Elementary Theory and Problems”, Third Edition, Van Nostrand Reinhold Company, New York.
- 11-38 Uniform Building Code and Uniform Building Standard 1997, International Conference of Building officials, 5360 South Walman Mill Road, Whittier, California, 90601.
- 11-39 Americna Plywood Association, “APA Design Construction Guide for Diaphragms”, American Plywood Association, P.O. Box 11700, Tacoma, Washington 98411-0700.
- 11-40 Computer and Structures, Inc. (CSI), “ETABS – Three Dimensional Analysis of building Systems”, 1918 University Ave., Berkeley, CA 94704.
- 11-41 American Society of Civil Engineers, “Minimum Design Loads for Buildsing and Other Structures,” (ASCE 7-98), ASCE, 1901 Alexander Bell Drive, Reston, Virginia 20191-4400
- 11-42 Criswell, M.E., “Design of Columns,” in “Wood: Engineering Design Concepts,” Volume IV, Clark C. Heritage Memorial Series on Wood, Forest Products Laboratory in Cooperation with the University of Wisconsin, published by the Pennsylvania State University 1986, 291-364.
- 11-43 Ellingwood, B/ and Rosowsky, D. “Duration of Load Effects in LRFD for Wood Construction,” Journal of Structural Engineering, ASCE, Vol. 117, No. 2, February 1991, 584-599.
- 11-44 Ellingwood, B/, Galambos, T.V., MacGregor, J.G. and Cornell, C.A. “Development of a Probability-Based Load Criteria for American National Standard A58.” U.S. Department of Commerce, National Bureau of Stndards. NBS SP577, June, 1980.
- 11-45 Gerhards, C. and Link, C., “Effect of Loading Rate on Bending Strength of Douglas-fir 2 by 4’s,” 1986, Forest Prod. J. 36(2):63-66.
- 11-46 Goodman, J.R., “Reliability-Based Design for Engineered Wood Construction—Update and Statu of U.S. Progress,” International Timber Engineering Conference, Tokyo, Kapan, 1990.
- 11-47 Gromala, D.S., Sharp, D.J. and moddy, R.C. “LRFD Concepts for Wood Systems,” ASCE Structures Congress, Indianapolis, IN, 1991.
- 11-48 McLain, T.E. and Thangjitham, S., “Bolted Wood Joint Yield Model,” Journal of the Structural Division,”American Society of Civil Engineers, 1983, New York, NY, 1988.
- 11-49 Murphy, J.F., ed., “Load and Resistance Factor Design for Engineered Wood Construction: A Pre-Standard Report,” Am. Soc. Of Civil Engrs., New York, NY, 1988.
- 11-50 Rosowsky, D. and Ellingwood, B., “System Reliability and Load-Sharing Effects in Light-Frame Wood Construction,” Journal of Structural Engineering, ASCE, Vol. 117, No. 4, April, 1991, 1096-1114.
- 11-51 American Forest and Paper Association, American Wood Council, “National Design Specifications – for Wood Construction” 1997 Edition ANSI/AF&PA NDS-1997, American National Standard
- 11-52 American Forest and Paper Association, American Wood Council “National Design Specification – for Wood Construction Supplement” 1997 Edition
- 11-53 American Forest and Paper Association, American Wood Council “LRFD Load and Resistance Factor Design – Manual for Engineered Wood Construction” 1996 Edition including supplements

Chapter 12

Seismic Upgrading of Existing Structures

Ronald O. Hamburger, S.E.

Senior Vice President, EQE International Inc., Oakland, California.

Craig A. Cole, S.E.

Project Manager, EQE International Inc., Oakland, California.

Key words: Structural Deficiencies, Structural Design, Seismic Rehabilitation, Reinforced Concrete, Steel, Wood, Performance Objectives, Prescriptive Requirements, Seismic Demand, Seismic Capacity, Strength, Stiffness, Flexibility, Drift, Deformation, Load Paths.

Abstract: This chapter presents important considerations for engineers upgrading the seismic resistance of existing structures including investigation of existing structural characteristics, identification of significant deficiencies, and selection of appropriate upgrade criteria and retrofit systems. In addition to all of the tasks required in design of a new structure, successful seismic upgrade of an existing structure requires development of a thorough understanding of the existing construction, research into its limiting strength and deformation characteristics, quantification of the owner's economic and performance objectives, and selection of an appropriate design criteria to meet these objectives, which is also acceptable to the building official. It also includes selection of retrofit systems and detailing which can be installed within the existing structure (which may have to remain open during the upgrade) at a practical cost and with minimum impact on building appearance, function and historic features. This chapter is organized into six sections. The differences between the seismic design philosophy for a new building and that for the upgrade for an existing building are discussed first followed by discussions on seismic deficiencies commonly found in buildings, the importance of establishing a rational seismic upgrade criteria, upgrade methods to mitigate common seismic deficiencies, and two example seismic upgrade projects. Since performance based design techniques are presented in a separate chapter of this handbook, we limit ourselves here to coverage of more traditional approaches to seismic rehabilitation.

12.1 INTRODUCTION

As compared to seismic upgrade of existing structures, design of a new structure for proper seismic performance is a relatively simple and straight-forward task. Modern building codes for new construction rigorously prescribe the design procedures to be employed based on intended building occupancy and performance and extensive research and data on seismic performance of the materials and detailing specified. The engineer designing a new structure has the opportunity to select the basic structural system and specify the materials and detailing incorporated. The engineer can participate in developing the structure's configuration and the placement of structural elements. Finally, the engineer for a new building has the opportunity to require inspection of important aspects of the construction and to confirm the quality of materials and workmanship incorporated. As a result, most structural characteristics important to seismic performance including ductility, strength, deformability, continuity, configuration and construction quality, can be controlled.

Seismic rehabilitation of existing structures presents a completely different problem. First, for most types of structures, up to very recently, there was no clear professional consensus on appropriate design criteria. That of course has changed substantially by publication of performance based design guidelines such as the FEMA 273/274^(12-1, 12-2) and the ATC-40⁽¹²⁻³⁾ guidelines (see Chapter 15 for application of these guidelines in seismic rehabilitation). The building codes for new construction are based on the use of modern materials and detailing, and are not directly applicable. Further, they incorporate levels of conservatism and performance objectives which may not be appropriate for use on existing structures due to economic limitations. The material strengths and ductility characteristics of an existing structure, will in general not be well defined. The configuration and materials of construction are predetermined. The details and quality of

construction are frequently unknown and because the structure has been in service for some time, deterioration and damage are often a concern.

In addition to all of the tasks required in design of a new structure, successful seismic upgrade of an existing structure requires development of a thorough understanding of the existing construction, research into its limiting strength and deformation characteristics, quantification of the owner's economic and performance objectives, and selection of an appropriate design criteria to meet these objectives, which is also acceptable to the building official. It also includes selection of retrofit systems and detailing which can be installed within the existing structure (which may have to remain open during the upgrade) at a practical cost and with minimum impact on building appearance, function and historic features.

This chapter presents important considerations for engineers upgrading the seismic resistance of existing structures including investigation of existing structural characteristics, identification of significant deficiencies, and selection of appropriate upgrade criteria and retrofit systems. The chapter is organized into six sections. The differences between the seismic design philosophy for a new building and that for the upgrade for an existing building are discussed in the following section, Section 12.2. Seismic deficiencies commonly found in buildings are then discussed in Section 12.3. The importance of establishing a rational seismic upgrade criteria is presented in Section 12.4. Upgrade methods to mitigate common seismic deficiencies are then discussed in Section 12.5. The last section, Section 12.6, contains two example seismic upgrade projects. Since performance based design techniques are presented in a separate chapter of this handbook, we limit ourselves here to coverage of more traditional approaches to seismic rehabilitation.

12.2 PURPOSE OF SEISMIC STRENGTHENING

Many structural engineers believe that the purpose of seismic strengthening is to upgrade the structure, to the maximum extent practical, into conformance with the lateral force requirements of the current building code. In reality this is not the purpose of seismic strengthening, but instead a method for achieving seismic upgrade, and often an inappropriate one.

As stated by the Structural Engineers Association of California⁽¹²⁻¹⁾ (SEAOC), the purpose of earthquake resistance provisions incorporated into the building codes is *to maintain public safety in extreme earthquakes likely to occur at the building's site*. Such provisions are intended to *safeguard against major failures and loss of life, not to limit damage, maintain functions, or provide for easy repair*. Specifically, it is expected that buildings designed to conform with the provisions of the building code would be able to:

- Resist a minor level of earthquake ground motion without damage;
- Resist a moderate level of earthquake ground motion without structural damage, but possibly experience some non-structural damage;
- Resist a major level of earthquake ground motion having an intensity equal to the strongest either experienced or forecast for the building site, without collapse, but possibly with some structural as well as non-structural damage.

These performance objectives were specifically formulated by SEAOC to apply to a broad range of structures and occupancies, based on trade-offs between public safety and economics. They were intended to apply to the general population of structures likely to be constructed and were specifically formulated under the influence of the seismicity of California, a region subject to frequent moderate magnitude earthquakes and occasional great earthquakes. These objectives can be reasonably attained in the design of new

structures by carefully conforming to four basic sets of provisions specified by the code: *strength, materials selection, structural detailing, and construction quality*.

12.2.1 Seismic Strengthening Considerations

Since current building codes do not in general apply to existing structures, the implicit performance objectives of these codes need not be rigidly adhered to for seismic upgrades. It is therefore extremely important that the structural engineer work with the building owner to carefully define the intended purpose of seismic strengthening based on specific safety and economic performance objectives. These are likely to vary considerably from one structure to another based on several key factors. These factors include:

- Economic value of the structure and remaining years of service life.
- Occupancy of the structure including the number of persons at risk within the structure, as well as the potential for structural failure to result in release of hazardous substances and injuries outside the structure.
- Function of the structure and the economic or societal cost which would result from loss of service due to earthquake induced damage.
- Historic significance of the structure and the effects of seismic upgrades on the cultural resource.
- The site-specific seismic hazard.
- The relative cost of achieving upgrades to various criteria.

As an example, most people would agree that it is not appropriate to upgrade an unoccupied warehouse to the same level of reliability as a building with high occupancy. Similarly, a building expected to remain in service for 10 years need not have the same level of reliability as a building expected to provide service for 100 years. Reconciliation of these complex issues requires both qualitative and quantitative evaluation. Selection of

appropriate design criteria cannot be made until these evaluations have been performed.

12.2.2 New Design Versus Retrofit Design Approaches

The basic design procedure for new structures consists of the selection of an appropriate level of lateral forces for design purposes, and then providing a complete, appropriately detailed, lateral force resisting system to carry these forces from the mass levels to the foundations. Deformations are checked as a secondary issue, and except for the design of flexible structures, they are not likely to control the design.

Deformation control can be relegated to a secondary consideration in the design of many new structures to code life-safety requirements because the modern materials and ductile detailing practices specified by present codes allow new structures to experience large deformations while experiencing limited damage. Older structures, however do not have the advantage of this inherent ductility. Therefore, control of deformations becomes an extremely important issue in the design of seismic retrofits. Given a ground motion criteria, and the desired performance level for that ground motion, the real task of seismic retrofit becomes one of controlling structural deformations, in response to that ground motion, to within acceptable levels. If the objective is to avoid collapse, then deformations must be controlled to an extent where stability of the vertical load carrying system is not lost. If post-earthquake functionality is the objective, then deformations must be controlled to an extent where unrecoverable cracking and bending of structural (and non-structural) elements is small enough to avoid the cosmetic appearance of an unsafe structure. This limited deformation level is necessary to ensure continued operation. Following a major earthquake, municipal building inspectors (with the assistance of local structural engineers) will perform a rapid screening assessment and make judgments as to

which buildings are obviously unsafe, which are obviously safe, and which require further evaluation to ascertain whether the buildings are safe or not. Unless the building is tagged as obviously safe the local government may limit the use of the building until it can be proven safe.

There are three primary types of deformations which must be considered and controlled in a seismic retrofit design. These are: global deformations, elemental deformations and inter-structural deformations.

Global deformations are the only type explicitly controlled by the building codes and are classically considered by reviewing inter-story drift (see Chapter 7). The basic concern is that large inter-story drifts can result in P-delta instabilities. Control of inter-story drift can also be used as a means of limiting damage to non-structural elements of a structure (fascia, partitions, ceilings, utilities, etc.). It is less effective as a means of limiting damage to individual structural elements.

Elemental deformations are the amount of distortion experienced by an individual element of a structure such as a beam, column, shear wall, or diaphragm. Building codes have very few provisions to directly control these deformations. They rely on ductility to ensure that individual elements will not adversely fail at the global deformation levels predicted for the structure. In existing structures, with questionable ductility, it is critical to evaluate the deformation of each element and to ensure that expected damage to the element, at the given deformation level, is acceptable. This requirement extends to elements normally considered to participate in the lateral force resisting system as well as those that do not. For example, a common mode of collapse for older concrete structures is a punching shear failure of flat slabs at interior columns (Figure 12-1). This results from excessive rotation plus vertical accelerations (and induced punching shear concentrations) at the slab-column joint. Often, the flat system is not considered to participate in the lateral force resisting system for a retrofitted structure. However, if the



Figure 12-1. Example of slab punching shear failure-January 17, 1994, Northridge earthquake

rotational deformation of these joints is not maintained below a damage threshold, the classic punching shear failure can still occur. Elemental deformations can sometimes be controlled by limiting calculated member stresses at realistic estimates of global structural deformation.

Inter-structural deformations are those that relate to the differential movement between elements of the structure. Failures which result from a lack of such control include classic failures of masonry walls which have not been anchored to diaphragms (Figure 12-2) or failures resulting from bearing connections slipping off beam seats. Building codes control these deformations by requiring interconnection of all portions of structures and the provision of continuity ties. These same "code" techniques can be effective as retrofits for an existing structure. However, in some cases provision of

continuity is not practical (for example at an expansion joint of a structure). In such cases, realistic estimate of expected deformations and ensuring that stability is maintained at these deformation levels is the most effective design procedure.

12.2.3 Realistic Seismic Deformations

Determination of the realistic deformation levels expected of a structure, when subjected to the design earthquake, is the most important and also most difficult task of seismic rehabilitation design. The seismic design provisions contained in modern American building codes including the UBC-97⁽¹²⁻⁵⁾ and IBC-2000⁽¹²⁻⁶⁾ are all based on analysis methodologies originally presented in ATC-3-06⁽¹²⁻⁷⁾.



Figure 12-2. Example of masonry wall separation – October 17, 1989, Loma Prieta earthquake

The ATC-3-06 methodologies rely on elastic dynamic analysis techniques with an input ground motion that has been substantially reduced from that actually expected to be experienced by the building. This reduction factor (R) used to be as large as 12 but currently it is as large as 8 (see Chapter 4). The forces obtained from the elastic dynamic analysis using this substantially reduced ground motion are then used to proportion the elements of the structure. However, it is explicitly recognized that the structural deformation levels predicted by such analyses are substantially smaller than what will be experienced by the real building. All codes, therefore, specify that deformation-critical aspects of the design, such as building separations and detailing of non-structural attachments, be evaluated at amplified deformation levels (see Chapters 4 and 7). It is

this amplified level of deformation rather than the deflections predicted by the code base shear forces that should be used for evaluating the adequacy of existing structural elements in a retrofitted structure.

It should be noted that even the use of amplified elastic deformations as an indication of real inelastic deformations of the structure is at best an approximation. The basis for this approach is founded in analytical research presented in a monograph by Newmark and Hall⁽¹²⁻⁸⁾. That research indicates that the maximum deflection (elastic plus inelastic deflection) of a structure can be predicted by the theoretical response of an elastic structure with the same initial dynamic properties.

The Newmark and Hall⁽¹²⁻⁸⁾ basic analytical research was conducted for very simple, single degree of freedom structures only, as opposed to the complex multi-story, multi-degree of

freedom structures commonly encountered in practice. Naeim and Anderson⁽¹²⁻⁹⁾ have shown that this assumption seems to be generally, but not always, valid for regular tall building structures. The profession seems to have reached a general consensus, however, that this assumption is also valid for other structures as a method of estimating inter-story drifts, providing that several limitations are observed:

1. The deformation levels are well under the range of overall stability of the structure.
2. The structure is reasonably regular with regard to stiffness and mass distribution. Soft and/or weak stories can result in substantially different inelastic deformation distributions from those predicted by elastic analyses. Inelastic torsional instabilities can have similar effects.
3. Throughout the range of deformations experienced, the structure does not experience a net loss of lateral force resisting capacity. Ductile structures will become softer as they are pushed into the range of inelastic response. However, they will continue to retain their plastic lateral force resisting capacity, and as they strain harden, will actually become somewhat stronger. Non-ductile structures, such as many older concrete and masonry structures will experience a loss of strength resulting from spalling of compressive material and slippage in tensile elements.

When designing new structures, the building codes provide prescriptive guidance to ensure that the above assumptions are valid. Global drifts are controlled to maximum levels to satisfy the first assumption. Severe soft and weak story conditions are specifically prohibited and torsional effects are carefully evaluated to cover the second. The use of ductile detailing ensures that the third assumption is valid. In designing seismic retrofits for existing structures, it is equally important to ensure that these same assumptions are valid for the combined system of the existing structure and retrofit system.

In addition to the above, the use of elastic estimates of real earthquake deformations also

has other limitations. Although the total deformation of the structure may be bounded by these techniques, it is feasible that the distribution of inelastic deformation throughout the structure is not well predicted by elastic analysis. As an example, elastic analysis of a cantilevered shear wall structure will indicate nearly uniform inter-story deformation over the height of the structure (Figure 12-3a). Direct application of the Newmark approach would lead the designer to believe that the inelastic response of the structure would also be distributed uniformly over the structure's height. In reality, however, properly designed shear wall structures become inelastic by developing a flexure hinge at the base of the wall, resulting in a concentration of inelastic behavior in the lower stories (Figure 12-3b). For such structures, the distribution of inelastic deformation is poorly predicted by this approach.

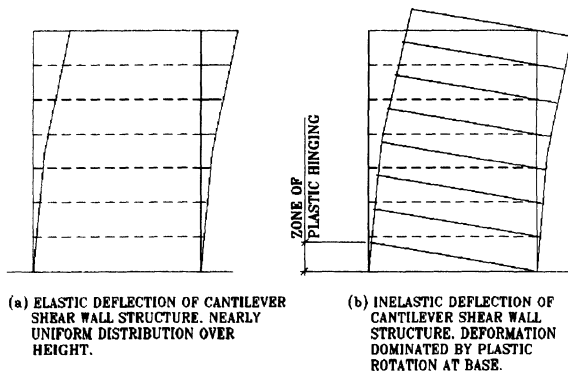


Figure 12-3. Comparison of elastic and inelastic deflections distributions

Nonlinear Analysis Techniques - As an alternative to using the code approach of amplified elastic response for estimating maximum expected deformations, direct calculation of these deformations through the use of non-linear dynamic analysis techniques is also possible and has become increasingly popular (see Chapter 15). Software systems for nonlinear static and dynamic analysis of structures are becoming increasingly available in the design office environment (see Chapter 16). Use of such techniques is required for

design of certain types of seismic force resisting systems including certain classes of base isolation and energy dissipation systems and may also be appropriate for some conventional structures.

The principal advantage of nonlinear analysis techniques is that they allow direct calculation of inelastic response including the effects of any inherent hysteretic damping of the structure. To the extent that assumptions with regard to the non-linear force-deformation characteristics of the elements incorporated in the model are correct, the deformation pattern calculated by these techniques are more consistent with the real structural behavior, and can indicate the "real" distribution of inelastic deformations within the structure. However, the validity of results obtained from this approach is highly dependent on the assumptions of element properties, and in the case of time-history analysis, the appropriateness of the ground motion time histories used. Most designers using this technique attempt to conservatively estimate responses, by altering the assumptions used on element properties, and by evaluating the response to multiple time histories.

Quasi-inelastic analysis approaches are also available which permit evaluation of complex structures. The most common of these is the so-called "progressive yield" or "static pushover" analysis. A simple way to use this approach is to start with an elastic model of the structure which is analyzed for a static distribution of lateral forces. Stresses within the structure are evaluated and zones of yielding identified. The elastic model is then modified by placing "hinges" and "reduced stiffness" elements at locations of computed yielding. The revised model is then re-analyzed statically for additional static lateral forces. This process is repeated until the total structural deformation required by design criteria is attained or the structure is found to become unstable (see Chapter 15 for more information).

Regardless of the technique utilized, in order to properly understand the seismic behavior of an existing structure, it is critically

important to understand the likely distribution of deformations throughout the structure under the criteria earthquake ground motion. One should recognize that deformations are likely to be substantially larger and differently distributed than is predicted by a direct elastic analysis to code specified forces.

12.3 COMMON DEFICIENCIES

This section describes typical deficiencies found in existing construction which can lead to poor earthquake performance. For the purposes of this section, poor earthquake performance is defined as endangerment of life safety through either partial or total collapse. As previously discussed, for some types of structures and occupancies it may be desirable to obtain better performance than merely protection of life safety. To obtain such performance, it is necessary to mitigate each of the deficiencies discussed in this section, as well as to ensure that expected earthquake induced deformations are kept small enough to prevent significant damage to key elements of the structure.

Until recently, there has been little consensus in the engineering profession as to appropriate methods for determining if an existing structure is seismically hazardous. Some engineers have attempted to apply the current building codes as evaluation tools for existing structures. The problem with this approach is that since the codes are revised every few years, most existing buildings will not meet the current code to some extent, a few years down the road. This would result in a finding that nearly every building is hazardous and requires upgrade. Such a finding is obviously both technically incorrect and economically not feasible to manage.

One of the most seismically hazardous class of buildings common throughout the world are structures constructed with load bearing walls of unreinforced masonry. A significant amount of research has been performed in recent years on the performance of these buildings and effective methods of improving their seismic performance. Much of this research was

published as the ABK Methodology⁽¹²⁻¹⁰⁾. Portions of these documents have since been adapted and placed into a code form as an appendix to the Uniform Code for Building Conservation⁽¹²⁻¹¹⁾. The procedures of these documents can be a useful guideline for the rehabilitation of masonry bearing wall structures.

A number of more general-purpose evaluation guidelines have also been recently published on the subject of seismic evaluation. These include, Rapid Visual Screening of Buildings for Potential Seismic Hazards⁽¹²⁻¹²⁾ and the NEHRP Handbook for Seismic Evaluation of Existing Buildings⁽¹²⁻¹³⁾. The first of these is a method of rapidly determining the probability of earthquake induced failure of a building, based on identification of building type, age, configuration, condition and local site characteristics. Few calculations are performed in this method and it should be used only to obtain a preliminary indication as to whether more detailed evaluation of a structure is justified. The second publication is intended to provide detailed evaluation guidelines. It provides in-depth checklists and calculation procedures developed for different building types, which may be used to identify key seismic deficiencies present in an existing building.

Both the rapid screening and detailed evaluation methodologies are based on the observation that most earthquake induced building collapses can be attributed to several fundamental flaws. These are briefly identified in this section. The reader is referred to the references 12 and 13 for more detailed procedural guidance. The reader is also cautioned, that both references 12 and 13 are keyed to a specific ground motion criteria, (a median estimate of the strongest level of ground shaking likely to effect a site in any 500 year period). In addition, the NEHRP document is intended to identify life safety hazards only. In many cases, depending on the performance desired of a particular structure, it may be necessary to modify the evaluation criteria contained in these documents to utilize more (or

less) severe ground motions and to incorporate more (or less) restrictive deformation limits.

Incomplete Lateral Force Resisting System: One of the most common causes of earthquake-induced collapse is the lack of a complete lateral force resisting system. In order to successfully resist collapse, each element of a structure must be positively connected to the whole in such a manner that inertial loads generated by the element from motion in any direction can be transmitted back to the ground in a stable manner.

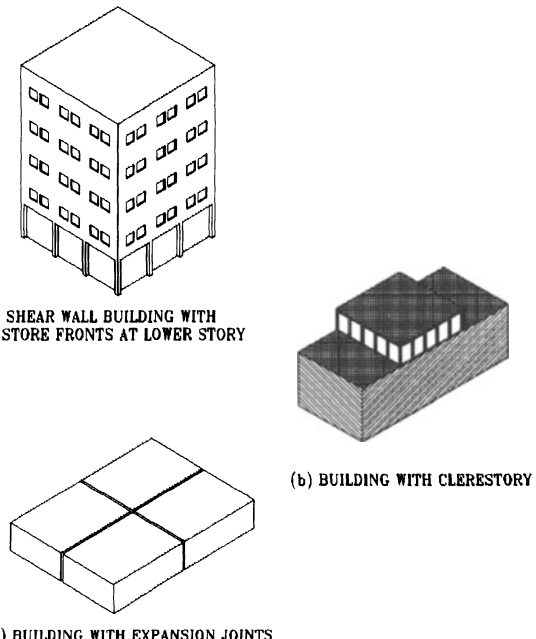


Figure 12-4. Building types in which incomplete lateral force resisting systems are common

As a minimum, a complete lateral force resisting system will include at least three non-concurrent vertical lines of lateral force resisting elements (moment frames, braced frames or shear walls) and at each level of significant mass a horizontal diaphragm to interconnect these vertical elements. Together, this assemblage of elements must provide adequate rigidity to control structural deformations to tolerable levels.

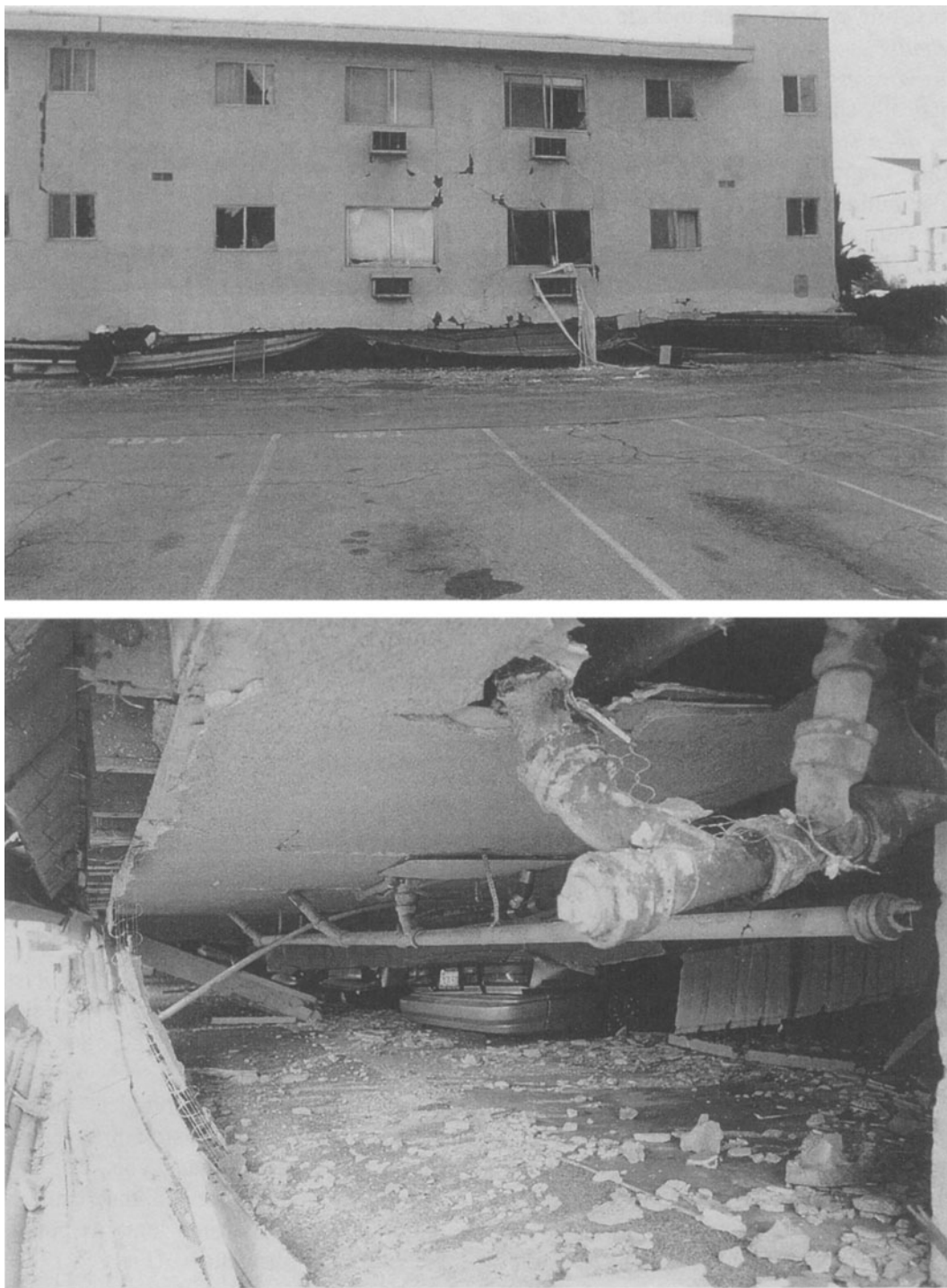


Figure 12-5. Example of building over garage collapse – January 17, 1994, Northridge earthquake

There are a number of common building configuration and design features which often result in a building without a complete lateral force resisting system. These include *open store fronts/house over garage, clerestory conditions, and expansion joint conditions*. These are schematically shown in Figure 12-4.

The *open store front or house over garage* condition, common in urban construction and for older buildings, has often lead to building collapse during strong ground motion. In older mid- and high-rise construction, the primary vertical elements of the lateral force resisting system are often the perimeter concrete or masonry walls which act as perforated shear walls. A similar condition to the open storefront is the building or house over garage. When such buildings have store-front systems or open garage fronts at the lower story, the vertical shear resistance provided by the walls of the upper stories is not present. This results in a discontinuous lateral force resisting system. Such a condition is most severe for buildings with openings on two of four sides, as the building becomes torsionally or laterally unstable at the lower story (Figure 12-5).

The *clerestory* condition is common in many low- and mid-rise buildings in either commercial or residential occupancy. The problem is that the clerestory is a major discontinuity in the horizontal roof diaphragm, which requires the structure on either side of the clerestory plus the clerestory roof to behave as independent elements. If the structure on opposite sides of the clerestory or the clerestory roof is not by itself stable, then collapse can occur. Figure 12-6 depicts damage of the column supporting a clerestory, as well as significant window damage. If the structure on both sides of the joint is stable, then differential movement of the structure on opposite sides can result in severe damage. Long narrow buildings with one end having an open store-front are also a common configuration that have a high degree of torsional instability.

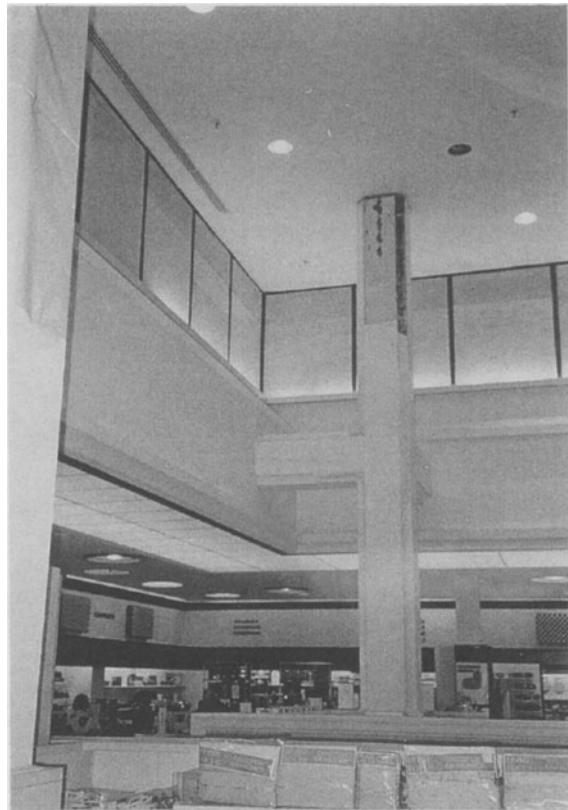


Figure 12-6. Top of column and window damage due to inadequate lateral system at clerestory

Expansion joints are a common feature of many large buildings of low- and mid-rise construction, particularly in areas with significant seasonal temperature variation. They are placed in buildings to relieve stresses induced by thermal expansion of the building frame as well as to provide relief in exterior finishes (particularly roofing). The system of expansion joints placed in a building will effectively divide it into separate structural units. Some buildings with such joints have not been designed with a complete lateral force resisting system for the structural segments on each side of the joints. This can result in collapse. Another problem that can occur in buildings with expansion joints is pounding of the adjacent structures (Figure 12-7). The severity of this problem is minimized somewhat if the diaphragm levels on each side of the joint align so that the slabs of one structure do not

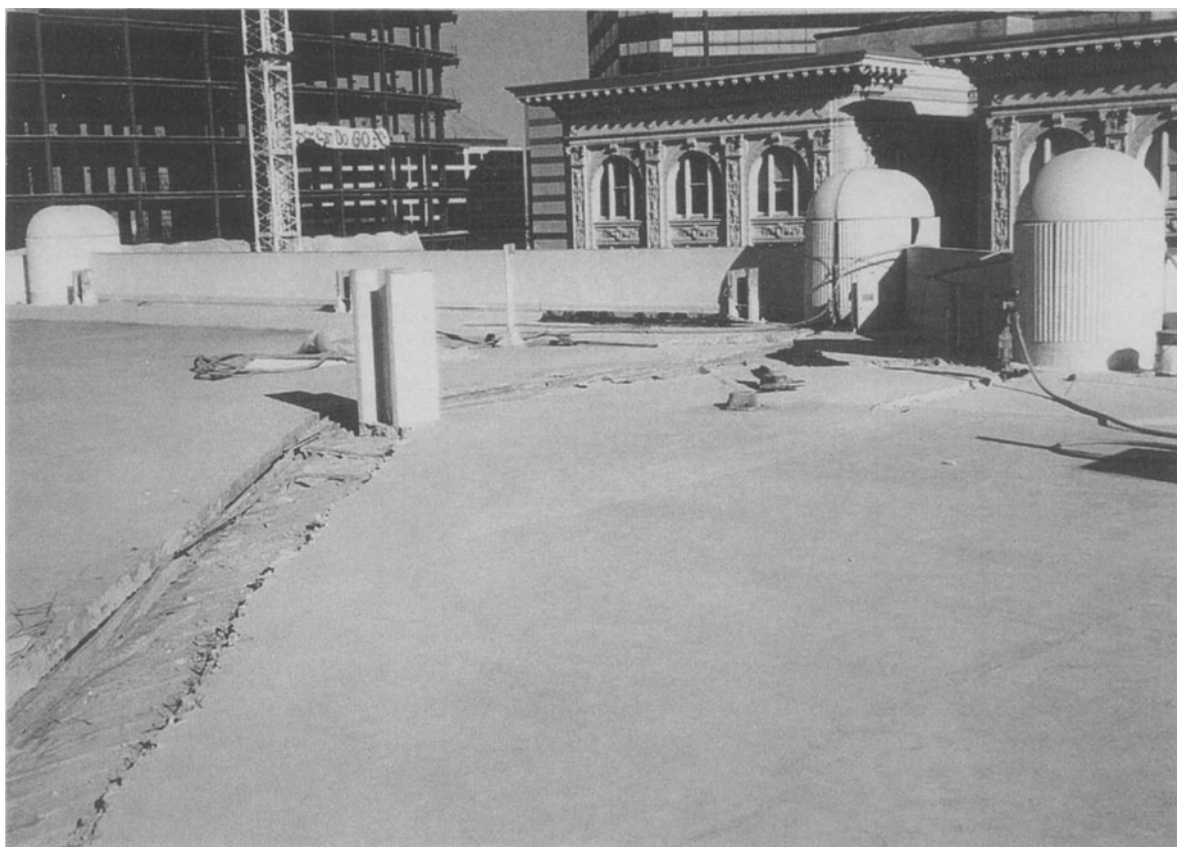


Figure 12-7. Example of pounding damage at a building expansion joint – October 17, 1989, Loma Prieta earthquake

act as knife edges against the columns of the adjacent structure.

Light wood framed structures are another type, which often does not have a complete lateral force resisting system. Typically, the perimeter walls, interior partitions, ceilings, floors and roofs will provide an informal but effective lateral force resisting system above the lowest floor level. However, the entire assemblage is frequently not attached to the foundations with positive connections. Failures resulting from entire residential structures sliding off their foundations have been common in past earthquakes. Even more common are failures which originate due to inadequately sheathed or braced cripple walls beneath the occupied areas of the structure.

Structural Continuity and Inter-element deformations: Structural continuity is an important factor for good seismic performance.

If all of the various components of a structure are not adequately tied together, the pieces can move independently and in different directions. This can result in dislodging elements from structures and the loss of bearing support for vertical load carrying elements. Modern codes require that all elements of a structure be tied together or that sufficient accommodation be made for the real displacements such that failure does not occur. These considerations were often overlooked in older structures. Common deficiencies include: inadequate anchorage of walls to diaphragms for out-of-plane and in-plane deformations (Figure 12-8); use of sliding type beam bearing connections with undersized bearing dimensions; inadequate attachment of architectural elements including cladding, ceilings, and partitions to the structure; inadequate attachment of equipment and utilities to the structure.



Figure 12-8. Out-of-plane wall failure of tilt-up building – January 17, 1994, Northridge earthquake

Excessive Lateral Flexibility: Buildings with complete lateral force resisting systems but excessive flexibility in the elements of their lateral force resisting systems have occasionally collapsed. Such buildings can experience very large lateral displacements when subjected to ground shaking. Structures with significant gravity loading can become unstable under large lateral deformation, as a result of P-delta effects. Since flexible structures tend to have relatively long fundamental periods of vibration, such structures tend to perform adequately when located on sites with firm soils, as the energy content of ground shaking transmitted by such sites to the structures is relatively limited. However, flexible structures located on sites with deep soft soils can experience very large demands. Typically, structures with inter-story drift ratios of 1% or

less at real deformation levels (as discussed in Section 12.2.3) behave acceptably.

Brittle elements: Modern design practice for buildings expected to withstand strong ground shaking requires the incorporation of ductile materials and detailing in the design of structures, such that deformations substantially larger than those expected at normal service levels can be tolerated without loss of structural capacity. Older construction rarely was provided with this ductility. As a result, elements tend to be brittle, and can rapidly lose strength when strained beyond their elastic or nominal capacities. Examples of common non-ductile construction include: unreinforced masonry walls, certain classes of concrete frames, and reinforced concrete and masonry walls, and some braced steel frame construction.

Unreinforced masonry walls can be composed of common clay brick, stone, hollow clay tile, adobe, or concrete masonry materials. Walls of these materials have limited strength, and very little ductility for in-plane demands. Slender walls, with large ratios of unsupported length to thickness have often failed due to out-of-plane demands. Inadequate anchorage of these walls to diaphragms is a common deficiency which contributes to poor out-of-plane performance.

Non-ductile Concrete Frames. If adequately designed, moment resisting frames of reinforced concrete can provide excellent behavior in strong earthquake shaking. However, many earthquake induced collapses of structures relying on non-ductile concrete frames for their lateral resistance have occurred. A number of problems can result in poor earthquake performance of concrete frames.

These include deficiencies in: shear capacity, joint shear capacity, placement of reinforcement for load reversals, development of reinforcement, confinement of the concrete and lateral support for reinforcing steel.

Shear failure of reinforced concrete columns and beams is a brittle failure mode and can result in sudden loss of load carrying capacity and collapse (Figure 12-9). In frames with adequate strength to remain elastic under real deformation levels (see Section 12.2.3), the beams and columns should have greater shear capacity than required at these deformation levels. In frames which experience flexural yielding at the joints under real deformation levels, the shear strength of the elements must be greater than their flexural capacity or failure can result. The shear strength capacity of members with relatively low axial compressive stress levels should be limited to that provided



Figure 12-9. Collapse of concrete parking garage structure - October 17, 1989, Loma Prieta earthquake

by the reinforcing steel as the shear strength of the concrete in such members quickly degrades under cyclic loading.

Shear failure of joints in moment resisting frames can also occur. The beam column joint of a moment resisting frame can be subjected to very large shears, resulting from the transfer of flexural stresses between the elements. Failure has occurred at such joints, particularly when the lateral confinement reinforcement in the columns does not run continuously through the joint zone. Frames with eccentric beam column joints or relatively slender beams tend to be weaker than those without such features.

Moment resisting frames subjected to strong ground shaking will typically experience large flexural load reversals at their joints. Some concrete frames designed primarily for gravity load resistance have little if any positive beam reinforcing steel (located at the bottom face of the beam) continuous through the beam column joint. As a result, the frames do not have

capacity to resist load reversals. For good performance, frames must have a minimum percentage of the beam positive reinforcing developed continuously through the beam column joints.

Inadequate development of reinforcing steel is another common problem. In frames with inadequate strength to remain elastic at real deformation levels, the flexural reinforcing steel will yield. Repeated cyclic loading of the bars into the yield range results in a breakdown of the bond between the reinforcing steel and concrete, which can result in a loss of flexural strength and frame instability.

Inadequate Concrete Confinement - Normal weight concrete elements with nominal lateral reinforcement can withstand compressive strains on the order of 0.003 to 0.004. Compressive strains in excess of this amount will result in crushing and spalling of the concrete and degradation of the element's capacity to carry load. Strong ground shaking

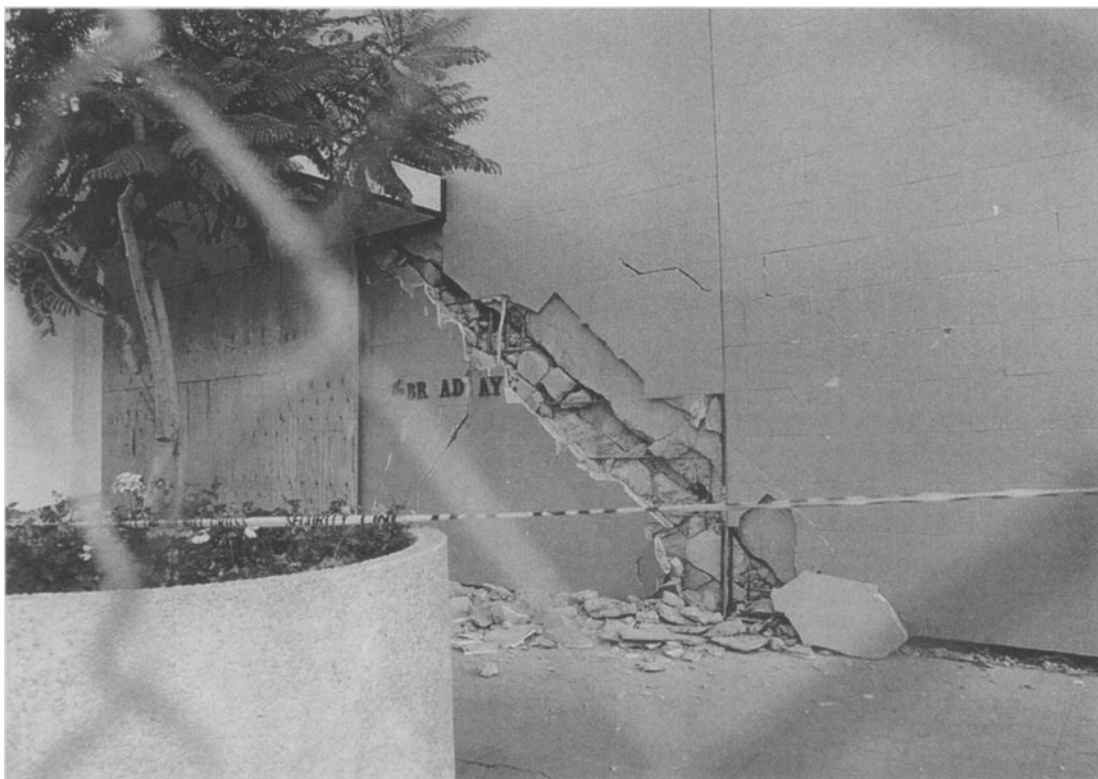


Figure 12-10. Shear failure of concrete wall – January 17, 1994, Northridge earthquake

can induce large compressive strains in concrete at flexural hinge regions of beam column joints. Large compressive strains resulting from large overturning demands can also occur in columns. Unless closely spaced lateral confinement reinforcing is provided, compressive strains at real deformation levels in excess of about 0.004% in normal weight concrete and 0.002% in lightweight concrete can result in structural failure. This is not a concern for members with low strain demands at real deformation levels.

Large tensile strains, particularly at flexural hinge regions of frames can also result in member failure, unless closely spaced lateral reinforcement is provided. When a flexural hinge forms, large tensile strains and elongation will occur in the longitudinal reinforcing steel. When structural response reverses, under cyclic motion, the elongated steel is forced into compression, and if not provided with adequate lateral support, will buckle. In addition to causing premature spalling of cover concrete, this can lead to low-cycle fatigue failure of the reinforcing and loss of structural capacity.

Reinforced concrete and masonry walls can have many of the same problems described for reinforced concrete frames, particularly if they are highly perforated by openings, or are tall and slender. Generally, walls with relatively low levels of axial load, moderate quantities of vertical reinforcing steel and shear capacities greater than their flexural capacities behave in a ductile manner, while those without these features can be quite brittle. Wall failures can occur as a result of excessive shear demands (Figure 12-10), as a result of crushing at the edges under extreme flexural strains, or as a result of failure of the reinforcement, as previously described for concrete frames. The most common wall failures occur in the spandrel beams present over door and window openings. Very large stress concentrations occur in these elements, often resulting in damage at relatively low levels of lateral load. Once the spandrels have failed, overturning demands on individual piers can increase

substantially, and the stiffness and strength of the structure decrease.

Braced steel frame structures have been commonly damaged in earthquakes, but collapses have been rare. The most common damage is to the bracing itself. Light rod braces often fracture, as a result of a concentration of inelastic strain demands at the threaded portion of the rods. In heavier structures, inelastic buckling of compression braces is also common (Figure 12-11). Compression braces of intermediate slenderness, and non-compact section properties can experience brittle fracture as a result of low-cycle fatigue induced by large secondary stresses at buckled sections. Failure of bracing connections is also common, particularly when the strength of the connection is less than the strength of the brace itself. Highly eccentric brace connections tend to fail prematurely due to the large secondary stresses induced by the eccentricities.



Figure 12-11. Example of brace buckling – October 1, 1987 Whittier earthquake

Although failure of braces is one mode of common failure (Figure 12-11), other failure modes can also occur in these structures. One of the more common failure modes occurs in structures with "chevron" type bracing, where the beam at the apex of the chevrons can be severely deformed by large unbalanced force in the "tension" brace following buckling of the "compression" brace. Some structural collapses have occurred as a result of braces which were designed too strong, relative to other portions of the structure. Over-strength bracing can place very large overturning demands on columns, resulting in buckling of these critical gravity load carrying elements. Knee braced frames, in which the braces induce flexural demands on columns can also result in premature column failure.

Inadequate diaphragms - Reliance on inadequate diaphragms can be another cause of earthquake-induced collapse. Although the floors and roofs of most structures provide diaphragm capacity, unless the structures were specifically designed to resist seismic loads, these features are often grossly inadequate. Common diaphragm deficiencies in buildings include *inadequate shear capacity, inadequate flexural capacity, extreme flexibility, poor connectivity to vertical elements of the lateral force resisting system, and lack of continuity*.

Diaphragms of differing materials have widely different shear strengths. Systems consisting of cast-in-place concrete, composite systems of concrete filled metal deck, and horizontal steel braced systems tend to have very large capacities and excellent ductility. Diaphragms constructed of timber sheathing and certain metal decks have very limited capacity but intermediate ductility. Diaphragms consisting of poorly bonded precast concrete planks or of poured gypsum slabs tend to have very low shear capacity and negligible ductility.

Flexural capacity of diaphragms should also be considered. Classic engineering evaluation techniques of flexible diaphragms treat these elements as simply supported horizontal beams, spanning between the various vertical elements of the lateral force resisting systems. The

diaphragm material itself (timber sheathing, metal deck, diagonal braces, etc.) are considered to act as the web of this beam while discrete continuous chord elements at the edges of the member are provided to resist flexural demands. The presence of walls around the perimeter of a diaphragm may alter the pattern of flexural demands. In such structures, the walls themselves may directly resist the shear stresses at the boundaries of the diaphragm such that the classic "simple beam" analogy is not valid. Regardless, a rational stress path must exist such that the diaphragm remains in internal as well as external equilibrium. A common deficiency in diaphragms is an absence of local flexural chords around openings. This can greatly reduce the effectiveness of otherwise competent diaphragms.

The basic functions of the diaphragm is to tie the elements of a structure together at a given level and distribute inertial loads to the various vertical elements of the lateral force resisting system. Diaphragms which are *extremely flexible* can result in very large inter-story drifts for supported elements such as walls subjected to out-of-plane loads. It is important that the diaphragm have adequate stiffness to prevent excessive inter-story drifts from developing. This problem tends to be most pronounced with diaphragms of timber construction or those of unfilled metal deck construction. The ABK methodology⁽¹²⁻¹⁰⁾ provides a good procedure for estimating the deformability of timber diaphragms. Other methods for calculating diaphragm deformability are presented in the Tri-Services Manual for seismic design⁽¹²⁻¹⁴⁾.

Poor connectivity of the diaphragm to the vertical lateral force resisting elements is also common, particularly in structures with relatively large diaphragms and isolated vertical shear resisting elements. It is important that collectors be provided in such diaphragms to transfer shears into the frames and walls. Another common deficiency with regard to shear transfer is a physical separation between the diaphragm web and the top of the vertical

lateral force resisting elements. Examples include timber diaphragms which lack blocking of the joists at shear walls and metal deck diaphragms supported by purlins or open web joists which frame above the girders of frames. In such diaphragms the joists or purlins can roll-over at the edges under the influence of diaphragm shear demands.

Continuity is an important consideration for diaphragms constructed of materials with limited tensile capacity including plywood, gypsum and concrete. Under the influence of large concentrated inertial loads, such as generated by heavy masonry or concrete walls supported at a diaphragm edge, diaphragms with limited tensile capacity can rip apart unless directly provided with continuous elements to tie the structure together. In timber diaphragms, continuity can best be provided through the framing members. In concrete diaphragms, reinforcement must provide the required continuity.

Non-structural elements. Non-structural elements are those pieces of a structure which are not intended by the designer to act as structural load carrying elements. Common non-structural elements include non-load bearing walls, cladding, ceilings, ornamentation, and mechanical and electrical services and utilities.

Non-load bearing walls including construction of hollow clay tile, concrete masonry, concrete, and other materials are a common problem in structures. Often not directly considered by the original structural designer of the building, these elements can have substantial influence on the performance of a structure. They can alter its stiffness, deformation patterns, lateral force resisting capacity and failure modes. Common problems include partial height walls which can induce shear failures where they bear against the mid-height of columns, and irregular placement of walls in a building which can create torsional problems and soft stories. In addition to their effect on the behavior of the structure, partition walls can fail either due to in-plane deformations or out-of-plane accelerations

resulting in potential personnel hazards as well as substantial architectural damage.

Buildings of recent construction often have curtain wall type *cladding systems*. A common deficiency of such systems is an inability to withstand the large lateral deformations the building experiences under strong ground motion. If the cladding has not be provided with adequate deformation capacity, panels can crush or connections can fail, creating a substantial falling hazard.

Ceilings are a frequent source of damage in earthquakes. Suspended plaster ceilings which are not adequately braced to a nearby diaphragm are a particular problem. These heavy ceiling systems can sway independently, much like a pendulum, and batter adjacent structural elements including walls. This is a common mode of failure initiation in unreinforced masonry buildings.

Exterior ornamentation on structures including parapets, statuary, balustrades, balconies and similar items can also be problem areas. Often, these decorative elements have limited capacity to resist earthquake induced lateral accelerations. Failure typically results in a falling hazard.

Mechanical and Electrical Utilities must be maintained in a serviceable condition for structures which are expected to remain functional following an earthquake. Even in less critical facilities, shaking induced damage to these elements can result in substantial consequential damage to architectural elements. For example failed mechanical and electrical systems can result in fire initiation as well as in flooding. Unfortunately, most mechanical and electrical systems in existing structures are not adequately installed to prevent earthquake induced damage. Major equipment items are not adequately anchored to the structure to prevent sliding or overturning. Piping and conduit systems typically are not adequately braced and provisions have often not been made for earthquake induced building deformation.

Poor construction quality has contributed to the earthquake induced failure of many properly designed structures. Masonry

structures tend to be particularly vulnerable. A number of failures have occurred in reinforced masonry walls because grout had not been placed in reinforced cells. Poor quality mortar is also common. In concrete structures, under-strength concrete has occasionally resulted in failures. Welded reinforcing steel splices are often quite brittle and can prematurely fail if proper procedures were not followed during construction. Similar problems can occur at welded connections of steel structures. Timber buildings are also susceptible to problems arising from poor construction quality, including such basic errors as framing the structure differently than intended, or failing to provide the connectors specified.

Deteriorated condition also contributes to earthquake induced failures. Common problems include dry-rot and infestation damage to wood structures, rusting of steel and spalling of concrete on marine structures, and weather deteriorated mortar in masonry structures.

Site characteristics are also too often overlooked by structural engineers with regard to building performance. Unstable sites with propensities for liquefaction, lateral spreading, land sliding or large earthquake induced differential settlements can lead to extensive damage to structures which are otherwise adequately designed. It is critically important to assess the nature and likely stability of the local geotechnical conditions as a first step in the evaluation and retrofit of any existing structure.

12.4 UPGRADE CRITERIA

Up to very recently, there were no consensus documents defining seismic upgrade criteria and provisions with the exception of unreinforced masonry buildings⁽¹²⁻¹¹⁾ structures. A multi-year two-phase project of the National Earthquake Hazard Reduction Program (NEHRP) which was underway for this purpose came to fruition in 1997 by publication of the FEMA-273/274 documents (see Chapter 15).

It is very important to establish a clear statement spelling out the desired performance objectives for the upgrade, and that the design

criteria to achieve these objectives be identified. The identification of the design criteria is particularly important. Even if an upgrade is required by an ordinance, it is still important that a clear understanding exists between the engineer and the owner as to what the objectives and the seismic performance of the upgraded building is likely to be.

The performance objectives, as stated earlier, are likely to vary considerably from one building to another based on several factors. These factors include: economic value of the structure, occupancy, function of the structure, historic significance, site specific seismic hazard, and the relative cost of achieving upgrades to various criteria.

A building-specific design criteria should be established that defines how the designer will accomplish the specified performance objectives. As a minimum the design criteria should address the following issues.

1. Testing program to determine existing materials properties

Existing documentation, including original drawings and specifications, material test reports, and geotechnical reports are likely to be lacking for many buildings being upgraded. Important structural elements may often be concealed, requiring destructive investigations to determine element sizes and locations.

The extent, type and location of exploration/testing for each building should be established to determine material properties of the lateral force resisting elements and other structural and non-structural elements that are to be assessed or strengthened to accomplish the performance objectives. The material testing program should provide not only material force capacity data but also deformation capacity data where practical.

2. Design force levels

A design demand level has to be established, compatible with the performance objectives to be achieved. In selecting a design demand level, one should consider the performance objectives, the importance, the size, and type of lateral force resisting system of the structure, its ability to sustain damage without collapse and

the consequences of varying levels of damage, as well as the available resources. There are two common methods to establish the design demand levels (1) code based approach, in which minimum inertial lateral forces are defined; and (2) a probabilistic method, in which ground motion characteristics with a defined probability of occurring are determined, and then used to measure structure response.

The most common bases of design use the force method, with design of new elements (and check for adequacy of existing elements) to a factored percentage of the minimum lateral forces specified by the building code. Commonly, the factor is taken less than one in order to account for the reduced expected life of an existing structure as well as to control construction costs to reasonable levels.

The probabilistic approach is most commonly used for large projects, projects with restrictive performance criteria such as Emergency Operations Centers or Hazardous Materials containing facilities, and for structures in near fault regions. The probabilistic approach commonly uses a two level earthquake criteria, most commonly specifying a design level event (DBE) and a maximum credible event (MCE). The DBE is typically taken as an event in which serviceability of the structure is intended to be maintained. The MCE is an event at which collapse is to be avoided. The probability of each of these events can be adjusted depending on the importance and goals for the structure. For base isolated structures, the UBC currently specifies the DBE as an event with a 10% chance of exceedance in 50 years and an MCE as an event with a 10% chance of exceedance in 100 years. The lower the probability of exceedance of an earthquake, the more severe it is. For some structures, it may be more appropriate to take the DBE as a 10% in 100 years event and the MCE as a 10% in 500 years earthquake. Regardless, the ground motion is typically characterized as response spectra curves, which can then be utilized to determine deformations of the structure.

3. Drift limitations

As has been previously discussed drift control is much more important in the upgrade design of an existing building than in the design of a new building. Hence global and/or element drift control parameters need to be established that will provide adequate assurance that the upgraded building will meet the performance objectives.

4. Detailing criteria for existing and new elements

Detailing in existing buildings frequently does not meet the requirements of new construction and will therefore perform in a less ductile manner. Consideration for this less than desirable performance needs to be incorporated in the design criteria. This can be accomplished by not relying on existing members to participate in the lateral force resisting system or by controlling deformations in existing elements to levels where adequate participation is provided. The former is frequently not practical.

5. Compatibility of new and old construction

The stiffness and strength of existing elements may not be compatible with new upgrade elements. A steel moment frame or even a braced frame added to resist the forces of an existing unreinforced brick masonry wall with inadequate capacity is such an example. The brick wall may resist the lateral load until its capacity is reached. The wall will then fail and the entire load would be redistributed to the steel frame. Assuming the wall participates in parallel with the frame may lead to a poor performing structure unless the capacity of the masonry wall is ignored or the steel frame is designed to control wall deformations.

Deformation and strength criteria that will provide adequate compatibility of old and new elements should therefore be specified.

6. Construction quality control

Adequate connection of new elements to existing elements is both critical and highly dependent upon existing material properties, sizes, locations and contractor accessibility. The likelihood of encountering unexpected field conditions is much greater in retrofitting existing buildings than in the construction of

new buildings. It is therefore important that a quality control program involving frequent inspection, testing, and observation by the design engineer, be established and accepted by the owner.

7. Criteria for non-structural elements

Adequate performance of certain non-structural elements may be required to ensure performance objectives are achieved. Non-structural elements such as hollow clay tile partition walls around exit corridors, heavy ornamentation, light fixtures, building cladding, etc. may require supplemental anchorage reinforcement or other upgrade measures may provide for adequate life-safety. Adequate performance of essential systems, such as power and telephone service may also be required for facilities where post-earthquake functionality is required. Design force and deformation criteria for selected non-structural components therefore need to be established.

12.5 COMMON UPGRADE METHODS

Structural rehabilitation or strengthening of a building in general can be accomplished through a variety of approaches, each with its merits and limitations. The specific considerations and their relative importance in the selection of the most appropriate upgrade method are unique to each building.

The following paragraphs present methods that are commonly used to correct or improve the building deficiencies previously discussed. The structural considerations of alternate upgrade methods are presented along with their advantages and disadvantages. It should be kept in mind, however, that other factors may influence, or even dictate, the selection of a particular method for a particular building. These other factors include cost, function, and aesthetics.

Alternate upgrade approaches can generally be utilized to correct building deficiencies, each with a different impact on cost, function and aesthetics. Cost will always be a major

consideration when evaluating methods to upgrade a building. Seismic upgrade costs can range greatly depending upon the deficiencies present, the performance objectives of the upgrade, the function and aesthetic constraints, and whether the building will be occupied during construction. Costs may range from as low as one dollar a square foot, to as high as one hundred dollars a square foot.

Most buildings are intended to serve one or more functional purposes (e.g. to provide housing or to enclose a commercial or industrial activity). Since the functional requirements are essential to the effective use of the building, extreme care must be exercised in the planning and design of the structural modification to an existing building to assure that the modifications will not seriously impair the functional use. For example, in a building to be utilized for leasing office space, a minimum of fixed walls or partitions is important to allow flexibility in the office layout for accommodating the space requirements of different tenants. The addition of steel braces or shear walls across the open office space may significantly decrease the flexibility and hence the value of the office space.

The preservation of existing aesthetic features may, in some cases, have a significant impact on the selection of an upgrade method. Historical buildings, for example, may require special upgrade techniques to preserve historical features. In some cases, when permissible, removal and replication of these features during the upgrade process may be more cost-effective than preservation or restoration.

12.5.1 Incomplete Lateral Force Resisting System

Three building features that commonly result in an incomplete lateral force resisting system were presented previously. These are open store-fronts, clerestory conditions, and expansion joint conditions. Lack of adequate foundation anchorage is another common example. Common methods to correct these deficiencies are presented below.

Open store-front - The deficiency in a building with an open store front is the lack of a vertical line of resistance along one or two sides of a building. This results in a lateral system that is excessively soft at one end of the building causing a significant torsional response and potential instability.

The most effective method of correcting this deficiency is to install a new stiff vertical element in the line of the open front side or sides (Figure 12-12). Should the owner desire to maintain the open front appearance braced steel frames located directly behind storefront windows are a common method utilized to provide the necessary stiffness and strength. The braces have some aesthetic impact but are commonly located to minimize functional impact. Shear walls may also be utilized to provide adequate strength. In both cases collectors are required to adequately distribute the loads into the diaphragm. Adequate anchorage of vertical elements into the foundation is also required to resist overturning forces.

Steel moment frames can also be utilized to provide adequate strength, provided that inelastic deformations of the frame under severe seismic loads are carefully considered to ensure that displacements are controlled.

Clerestory - A clerestory can result in a significant discontinuity of a horizontal diaphragm. As with all upgrades the function of the structure must be an important consideration. Clerestories are typically designed in a building to provide an open airy feeling.

A common method to address the resulting diaphragm discontinuity is the addition of a horizontal steel truss (Figure 12-13a). Light-weight steel members can be designed to transfer diaphragm shears while minimizing visual obstructions to the clerestory.

An alternate approach to correcting a clerestory deficiency is to reduce the demands on the diaphragm through the addition of new vertical lateral force resisting elements such as shear walls or braced frames (Figure 12-13b). By reducing the demands, diaphragm

deformations and stresses can be controlled to within acceptable limits. Impact on space utilization must be considered in locating the vertical elements.

Expansion Joints are installed in structures for a variety of reasons including: (1) to control the effect of deformations caused by temperature changes during and after construction; (2) to control the effects of construction shrinkage or creep; or (3) merely to simplify the lateral analysis of different portions of a building, particularly when the addition to a structure is designed.

Structural members exposed to the elements (i.e. large temperature changes) prior to the installation of exterior walls, finishes, and building climate control systems, may be protected through the use of expansion joints. After the building systems are installed differential temperatures are kept to a minimum rendering the expansion joints no longer necessary.

Another common reason for the presence of an expansion joint in a building is to accommodate post-tension concrete shrinkage and creep deformations. After shrinkage and creep has stabilized (nearly all movement will have occurred within months of the construction) there is no longer any need for the expansion joint. Expansion joints are also frequently installed to control deformations of the roof membrane to prolong their life.

Once reason for the existence of the expansion joint is clearly understood intelligent decisions can be made regarding the future need of the joints. Expansion joints can present similar concerns to a building as open store fronts, i.e. lack of lateral resistance along one side of the structure. Common methods of correcting this deficiency include: (1) installing vertical lateral load resisting elements along both sides of the joint; (2) modifications to the connection such that horizontal shear can be transferred across the joint, but not axial forces; and (3) elimination of the joint.

If the expansion joint needs to be maintained, installation of new vertical lateral load resisting elements on each side of the joint

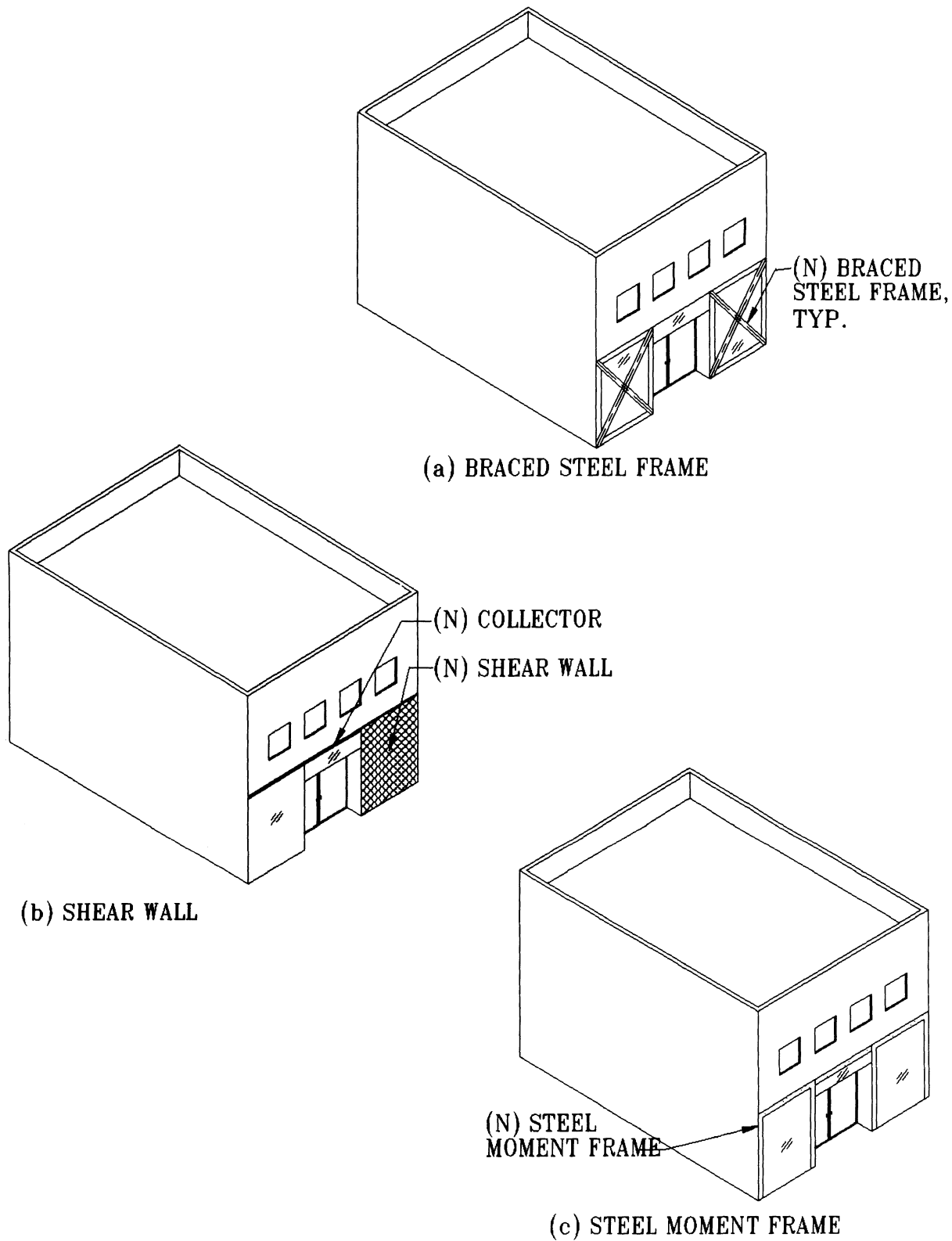


Figure 12-12. Common methods for upgrading a building with an open store front

will provide two complete lateral load resisting systems (Figure 12-14a). This method does cause a significant impact to the flexibility of the building space.

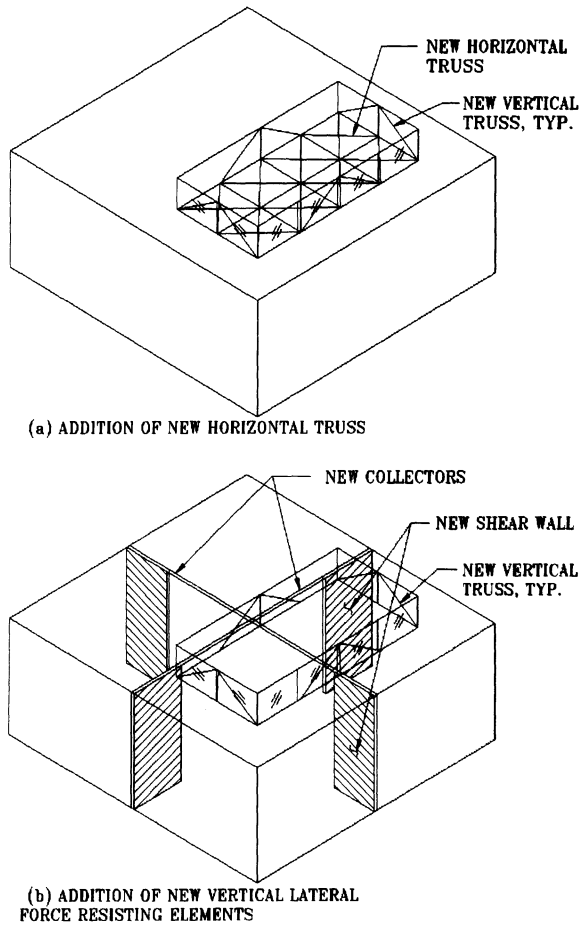
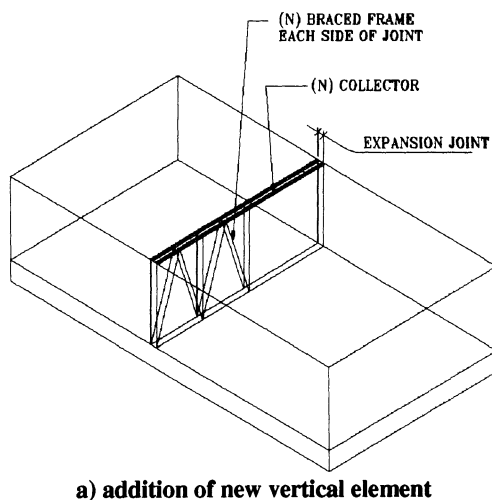


Figure 12-13. Common methods for upgrading a building with a clerestory.



a) addition of new vertical element

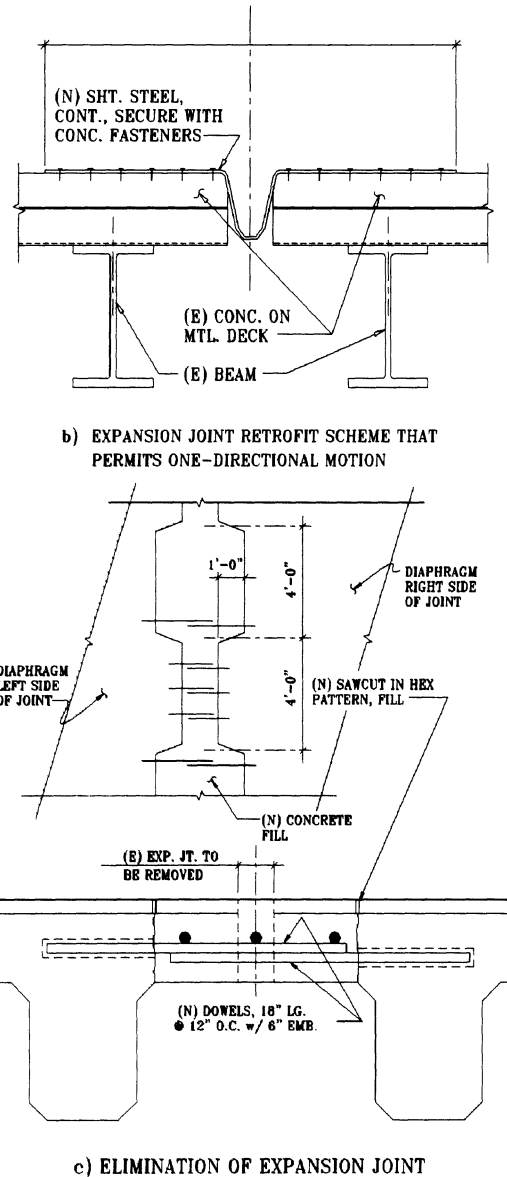


Figure 12-14. Common methods for upgrading a building with an expansion joints.

Should the vertical lateral load resisting elements on one side of the diaphragm have sufficient stiffness and strength to resist rotation, the deficiency can be corrected by modifying the connection to resist horizontal shear only. Figure 12-14b presents one option used on a metal deck with concrete fill diaphragm. The connection resists shear parallel to the joint but permits expansion in the perpendicular direction.

Elimination of the joint may be the best solution from a cost and a performance point of

view if the original intent of the joint is no longer necessary. Figure 12-14c presents a common detail utilized to connect a new slab, in this case fill for an existing expansion joint, to an existing slab, thereby eliminating the joint. It is important that continuous members capable of resisting chord forces be installed at the perimeter of the diaphragm.

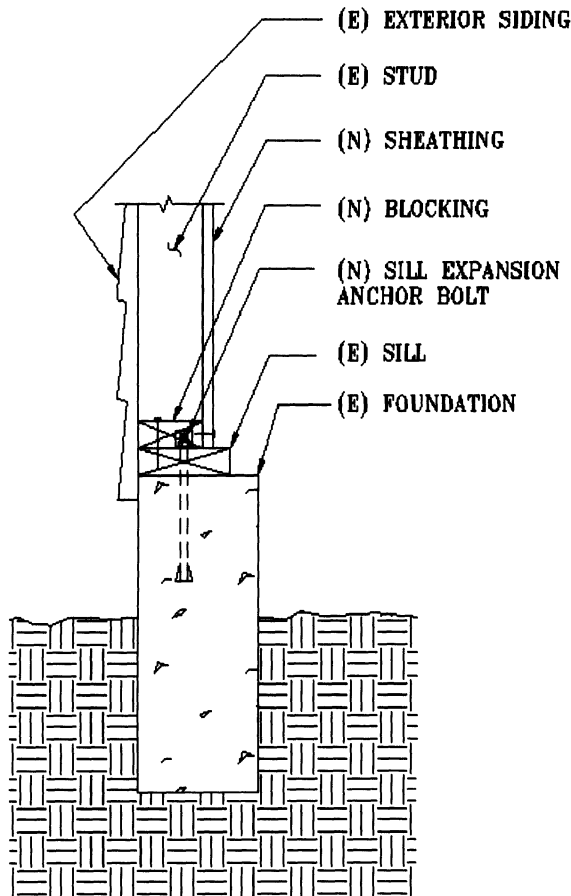


Figure 12-15. Providing wall to foundation anchors

Lack of Foundation Anchorage - Light wood-framed structures without positive connection to the foundation is another common problem where a complete load path is lacking. Providing a positive connection, (i.e. expansion anchors through the sill plate into the foundation) will correct this problem (Figure 12-15).

Light wood-framed structures also commonly have cripple stud walls above the foundation. The lack of stiffness and strength of the cripple walls can lead to failure in an

earthquake. Adding plywood sheathing on the inside of the cripple wall as shown in Figure 12-16 is a common method used to correct this deficiency. Proper nailing is required to provide a continuous and adequate load path from the floor diaphragm and walls above the floor to the foundation.

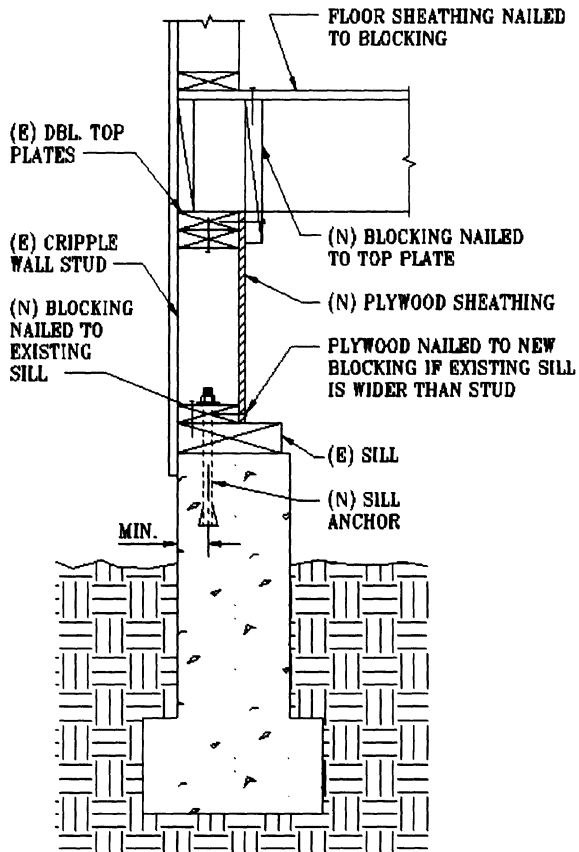


Figure 12-16. Strengthening of a cripple stud wall

12.5.2 Lack of Structural Continuity and Inter-element Deformation

Common structural continuity and inter-element deformation deficiencies were identified previously. These include: inadequate anchorage of walls to diaphragms, use of sliding type beam bearing connections with undersized bearing dimensions, and inadequate attachment of various architectural, equipment and utility elements to the structure.

Inadequate wall-to-diaphragm anchorage - In existing buildings reentrant corners are typical locations where the connection of floor

and roof diaphragms to existing walls may be inadequate to accommodate real earthquake induced displacements. This problem is particularly acute with flexible diaphragm systems. Walls adjacent to the reentrant corner will keep local diaphragm deformations to a minimum, e.g. below 1/4 inch (Figure 12-17). However, global diaphragm deformations may be large, e.g. greater than 2 inches. The resulting deformation incompatibility will likely lead to a connection failure at the reentrant corner.

The common method for correcting this deficiency is to install a diaphragm collector. The collector will distribute the stresses into the diaphragm eliminating the stress concentration and deformation incompatibility at the reentrant

corner. Existing roof framing members may be utilized as collectors provided the members can accommodate dead plus seismic loads. Figure 12-18 presents a common method for installing a collector in a wood diaphragm.

Structures with heavy walls and wood diaphragms may cause excessive out-of-plane stresses on the diaphragm when subjected to strong ground motions. These excessive stresses may occur at the diaphragm to wall connection or they may occur in the diaphragm if the roof or floor system is not designed for these forces. Correction of this deficiency is commonly accomplished through the installation of out-of-plane tension connections at the perimeter wall (Figure 12-17) and continuity ties across the diaphragm (Figure 12-

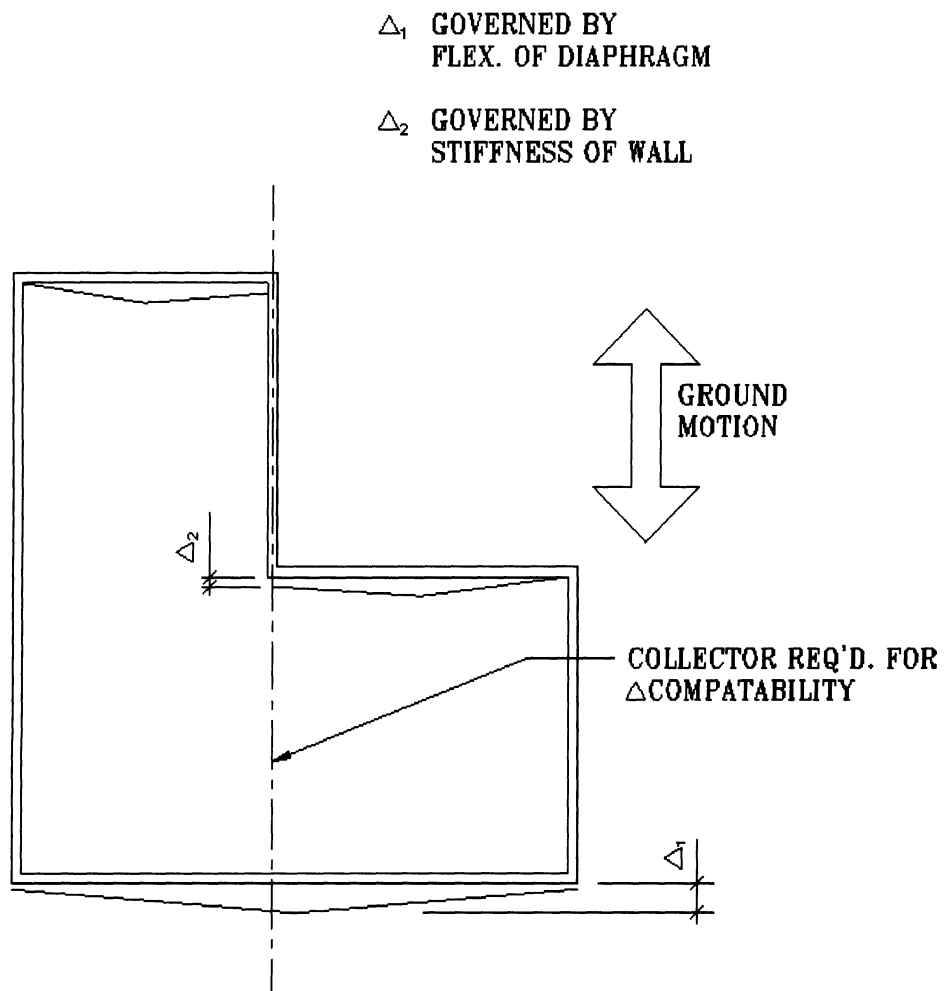


Figure 12-17. Deformation incompatibility at reentrant corner

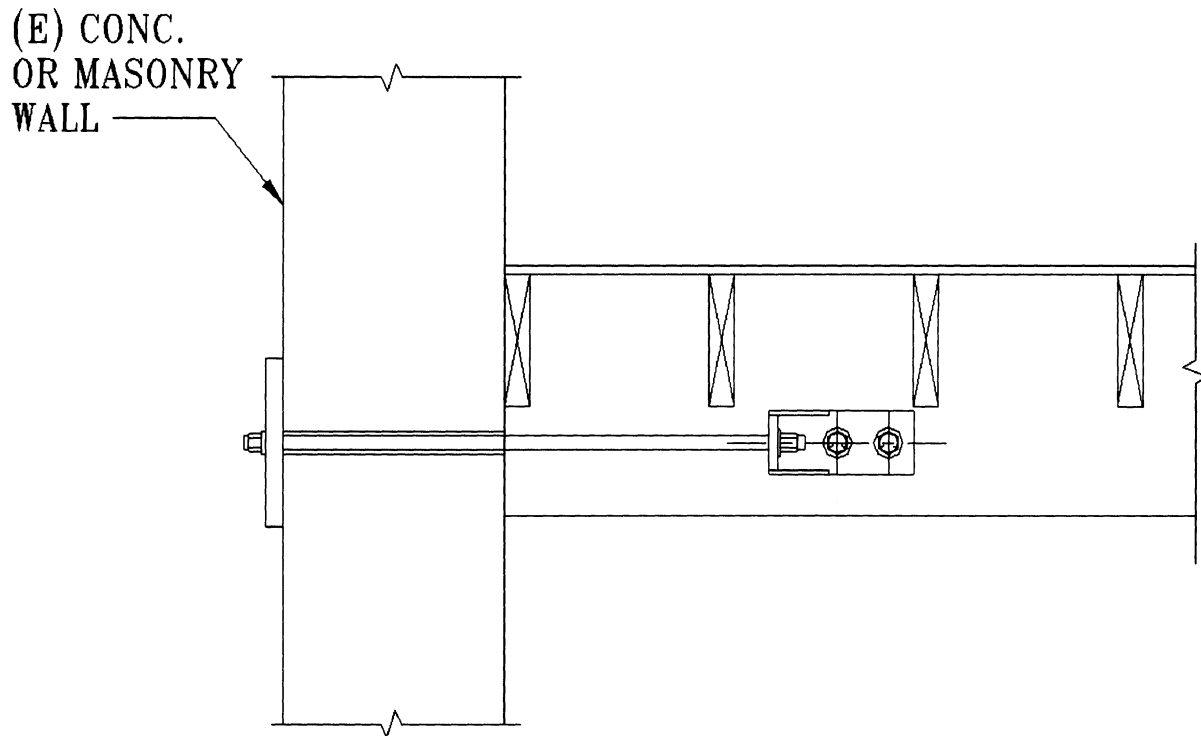


Figure 12-18. Out-of-plane wall anchor

26). With the installation of these elements the walls and diaphragms will respond as a unit, keeping inter-element deformations to a minimum.

Insufficient Bearing at Sliding Connections - Another common deficiency in existing buildings is insufficient bearing area for sliding type beam bearing connections. Floor and roof beams have slid off their bearing supports in past earthquakes and resulted in local collapse. There are four common methods for mitigating this deficiency. The first is to enlarge the beam bearing area, to accommodate the large deformations. Second, the potential for excessive differential deformations can be reduced by stiffening the lateral systems on one or both sides of the connection. Third, elimination of the sliding connection may be possible as previously discussed for expansion joints. A fourth alternative is to provide a redundant vertical support under the beam such that if the beam becomes dislodged from its support, a local collapse will not result. The first alternative is commonly the most cost

effective, however, the second and third alternatives may be less expensive if strengthening of partitions of the building are required to address other deficiencies.

12.5.3 Excessive Flexibility

Buildings with a complete lateral force resisting system but with excessive flexibility can be upgraded by introducing elements to increase stiffness and hence reduce deformations. Care needs to be taken, however, as increased stiffness is likely to result in increased amplification of seismic demands.

12.5.4 Brittle Structural Systems

The following paragraphs discuss common methods to upgrade deficiencies in buildings with brittle structural systems including unreinforced masonry (URM) buildings, non-ductile concrete frame buildings, reinforced concrete and masonry wall buildings and braced steel frame construction.

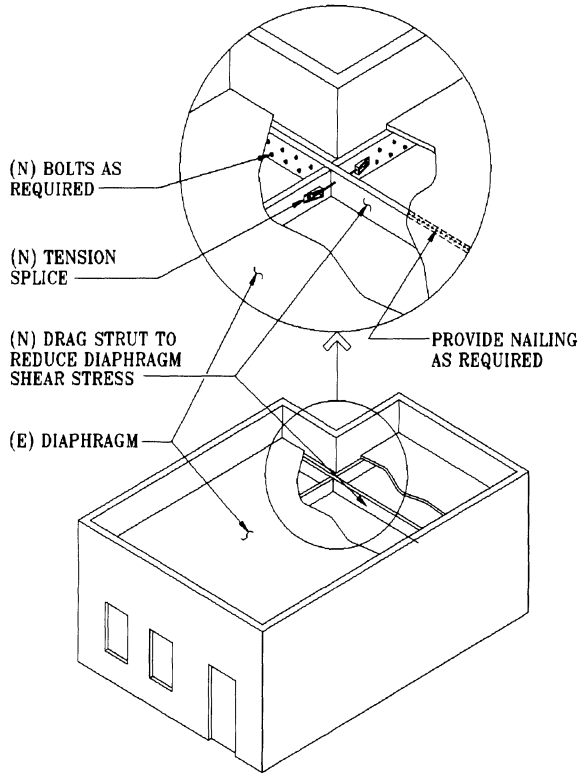


Figure 12-19. New drag strut in wood diaphragm

URM buildings - The most severe deficiency of a URM building is commonly inadequate connection of the walls to the diaphragms. URM building walls may also have limited strength and ductility, both in- and out-of-plane. Common methods for upgrading URM buildings include providing attachments between the walls and the diaphragms (Figure 12-19), and increasing the strength and ductility of the walls. In-plane deficiencies can be corrected by: (1) adding shotcrete to one face of the wall (Figure 12-20), (2) infilling existing windows, or (3) reducing the demand on existing walls through the introduction of supplemental walls.

Out-of-plane deficiencies can be corrected by: adding shotcrete, center coring the wall and installing reinforcing dowels (Figure 12-21), and adding steel "strongbacks" to stiffen and strengthen the walls (Figure 12-22). Adding strongbacks is typically the most cost effective, if out-of-plane capacity is the only consideration. Strongbacks can be installed to span either vertically or horizontally. If increased in-plane capacity is also required,

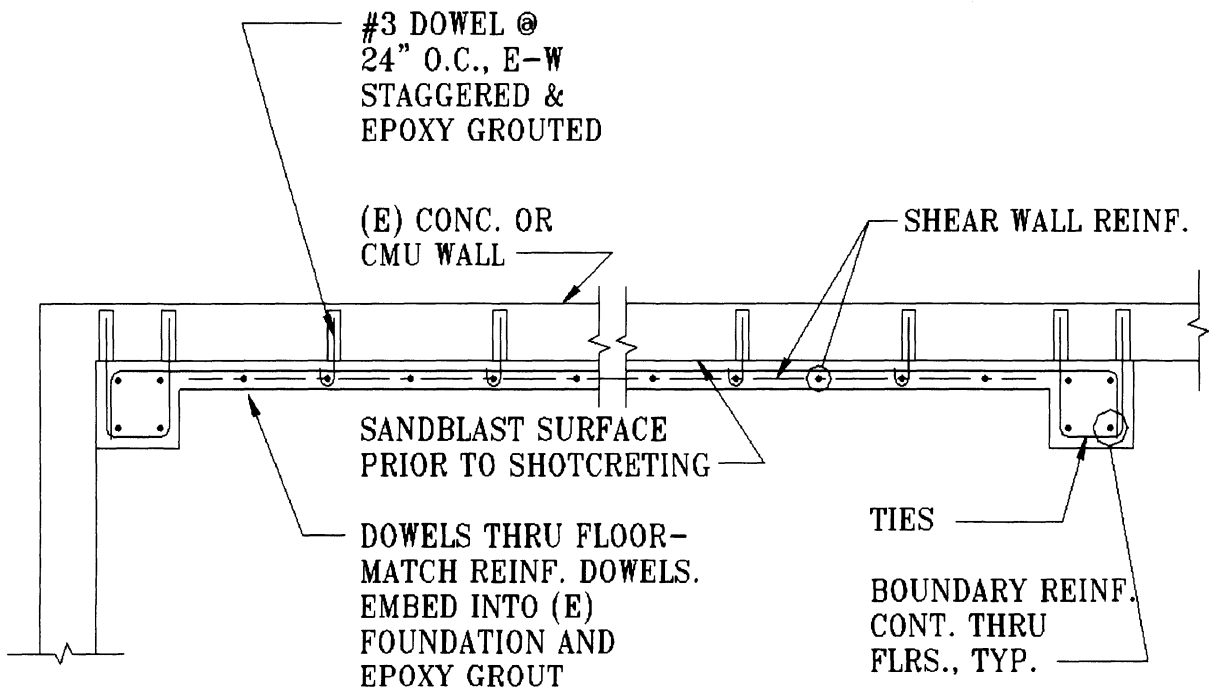


Figure 12-20. Upgrade of existing concrete or CMU wall utilizing shotcrete-Plan view

adding shotcrete may be found to be more efficient. Center coring is typically utilized when preserving the architectural appearance of both sides of the wall is desired.

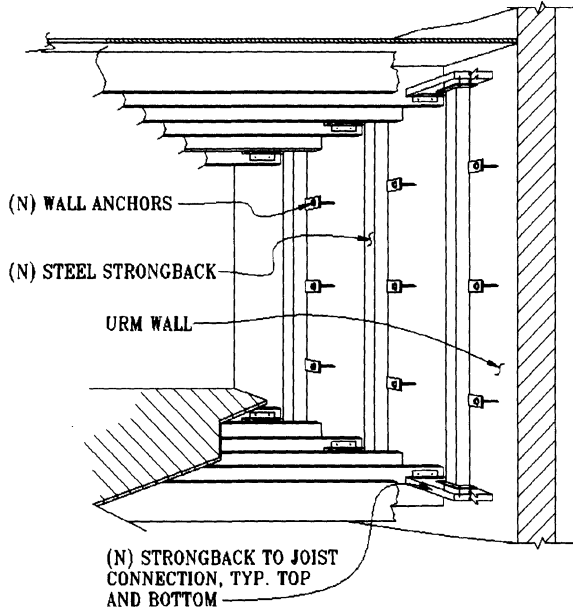


Figure 12-21. Out of plane strengthening of a URM wall using steel strongbacks.

Nonductile concrete frames - Non-ductile concrete structures have limited capability to accommodate building and element deformations. Hence, correcting the deficiencies of non-ductile concrete frame structures requires a good understanding of the behavior existing materials. This usually requires testing concrete cylinders to determine post-yield stress-strain relationships. This testing requires special equipment to monitor displacements as the load decreases. Inelastic beam and column moment-curvature relationships can then be determined using the results of the post-yield tests and estimates of available element ductility can be made.

Once available element ductilities are understood deformation limits can be defined and various upgrade methods evaluated. Common upgrade methods include: (1) reducing the drift demands by adding supplemental resisting elements, such as shear walls, braced frames or additional moment frames; (2) increasing the available ductility of

(N) 4" DIA. CORE DRILLED AND GROUTED WITH A POLYESTER-SAND MIXTURE WITH STEEL REINFORCEMENT

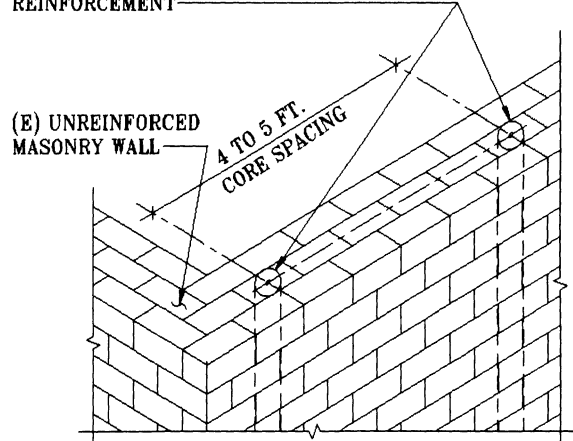


Figure 12-22. Example of center coring technique

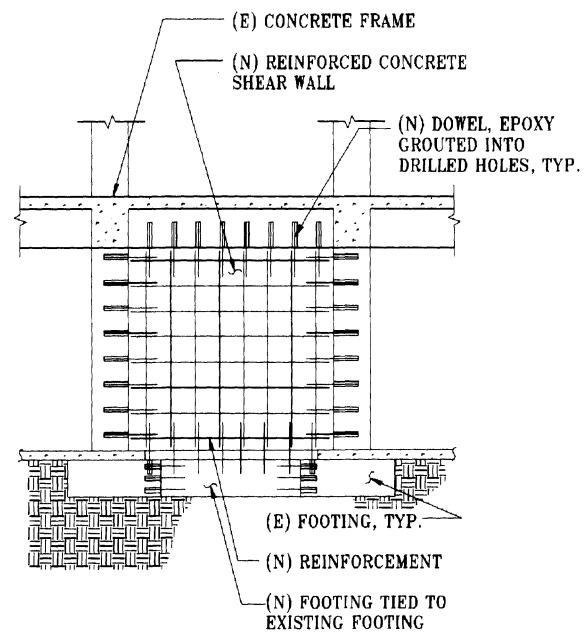


Figure 12-23. Strengthening an existing concrete frame building with a reinforced concrete shear wall.

the elements such as increasing confinement of reinforcing steel; or (3) changing the system to a shear wall system by infilling the concrete frames with reinforced concrete as indicated in Figure 12-23.

Upgrading a non-ductile concrete frame building may involve a significant amount of retrofit work. Both the first alternative, adding supplemental elements, and the third

alternative, changing to a shear wall system, will likely result in the existing frames becoming ineffectual in resisting lateral loads due to the differential stiffness between new and existing elements. A significant amount of foundation work may also be required as lateral loads will be resisted at discrete locations as opposed to every foundation in an original distributed frame design. Should supplemental elements be added to control drifts, the elastic and inelastic stiffness compatibility of the new and existing members need to be evaluated.

Increasing element ductility through added confinement steel can be accomplished, however, at significant expense. New rectangular column ties added around existing members have been shown to be ineffectual in providing confinement. Concrete jackets with circular ties or round steel pipe jackets with infilled concrete provide much more effective confinement, however, this may require a significant increase in the final dimensions of the beams or columns. Details to provide adequate confinement at beam-column joints are difficult to develop and install.

Reinforced Concrete and Masonry Walls - Brittle reinforced concrete and masonry wall buildings can be upgraded by installing elements to control inelastic deformations. This can be accomplished by increasing the wall strength and stiffness through: (1) placement of reinforcing steel and shotcrete on the inside or outside of existing walls; (2) infilling window or door openings; or (3) by reducing the demands on existing walls by providing new supplemental walls.

Adding shotcrete to existing walls is the most common method to upgrade existing inadequate masonry or concrete walls. It is most cost effective to shotcrete the exterior of a building due to the ease of construction access for shotcrete and new foundation installation (if required), as well as the simplicity of providing shear and tension continuity across floor levels.

Exterior shotcrete is not always possible due to property line restrictions, access, or aesthetic reasons. Hence shotcreting of interior walls is also commonly performed. Adequate continuity

of boundary elements and shear transfer across floors is required for inside applications. As shotcrete wall thickness can be as small as 3 inches, little floor space is lost. Figure 12-20 presents a typical detail of a shotcrete application to the inside of an existing concrete or CMU wall.

Infilling windows is a viable alternative if the elimination of a sufficient number of windows can be tolerated. Loss of a considerable number of windows may affect the natural air circulation in the building, will impact the amount of natural light, as well as the aesthetic appearance of the structure. When improving the capacity of shear walls by infilling windows care should be taken to ensure that adequate bond is provided between new and existing materials. This can be provided through the use of dowels. An infill material with a modulus of elasticity similar to the existing structure should be utilized so that wall deformations will be uniform.

Braced steel frames structures - Common deficiencies of braced steel frame structures include: (1) weak connections, (2) non-compact members experiencing low-cycle fatigue failures; (3) beam failures in chevron braced systems; (4) column failures due to overstrength bracing; or (5) column failure of knee-braced frames.

Weak connections are common problems in existing braced frame systems as seismic codes have only recently required that braced frame connections be designed to have greater capacity than the tension capacity of the attached brace. Strengthening the capacity of the existing connection can be accomplished by the addition of new bolts or welds provided the gussets are adequate for the higher loads. Alternatively the connections can be cut out and replaced with stronger connections. If the existing brace members require strengthening or replacement with members of greater capacity, it is probable that new connections should also be designed.

Non-compact braces with intermediate slenderness can experience brittle fracture as a result of low-cycle fatigue induced by large

secondary stresses at buckled sections. This deficiency can be mitigated by reducing the slenderness of the member by providing lateral bracing at intermediate locations or by increasing the capacity of the brace by increasing the area of the brace.

Beam failures may occur in chevron systems should large unbalanced forces in the "tension" brace occur following the buckling of the "compression" brace. This deficiency can be mitigated by increasing the bending capacity of the beam or by designing the braces (and their connections) to remain elastic. Increasing the beam capacity is typically the most cost effective approach. Designing the braces to remain elastic is usually not recommended as realistic design forces can not be accurately estimated.

Column failure in a braced frame system can lead to a local collapse. Where overstrength braces cause the weak link of the structure to occur in the column, design modifications are required. The existing brace could be removed and an adequately designed brace could be installed. Alternatively, the column and brace connections could be strengthened.

12.5.5 Inadequate diaphragms

Common deficiencies for diaphragms include *inadequate shear capacity*, *inadequate flexural capacity*, *extreme flexibility*, *poor connectivity to vertical elements of the lateral force resisting system*, and *lack of continuity*. The method for addressing these deficiencies is dependent upon the construction of the existing diaphragm. There are five common types of roof or floor diaphragm construction: timber, concrete, metal deck, precast, and horizontal steel bracing.

Timber Diaphragms - Timber diaphragms can be constructed of straight-laid or diagonal plank sheathing, or of plywood. Common deficiencies include *inadequate shear capacity*, *inadequate chord capacity*, *inadequate stiffness*, *inadequate continuity*, and *poor connectivity to vertical elements*.

Strengthening timber diaphragms with inadequate *shear capacity* can be accomplished by additional nailing, overlaying with plywood, or reducing the span of the diaphragm through the introduction of supplemental vertical lateral force resisting elements. Adding nails to existing plywood (with the addition of blocking) can cost effectively increase the capacity of existing plywood, however, this is not true for straight or diagonal plank sheathing. For these systems added nailing is not practical due to the large number of nails required and the propensity for existing planking to split when nailed.

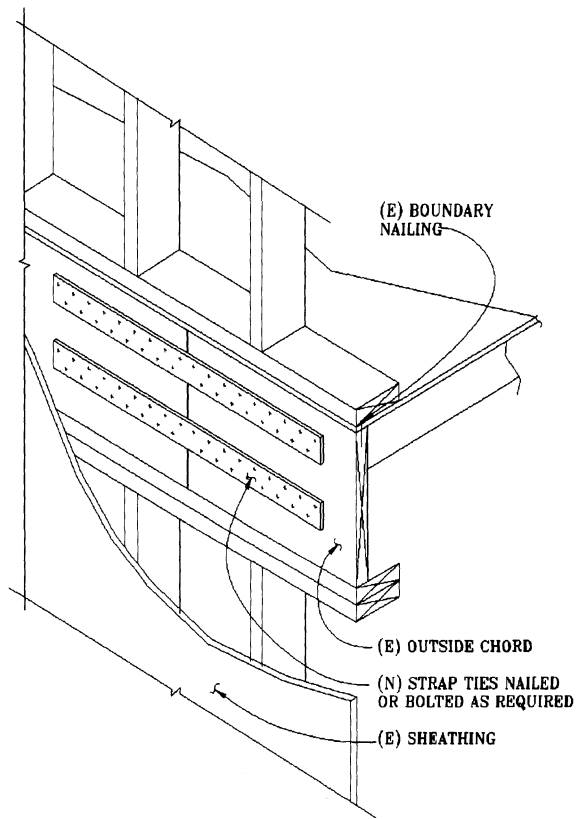


Figure 12-24. Chord splice of wood diaphragm.

The most common approach for increasing the shear capacity of plank sheathed systems is to provide a plywood overlayment. The existing planking can then be used in lieu of new blocking. Plywood should be configured such that new panel edges do not align with existing plank edges. Typically staples at close spacing on either side of the plywood joints are

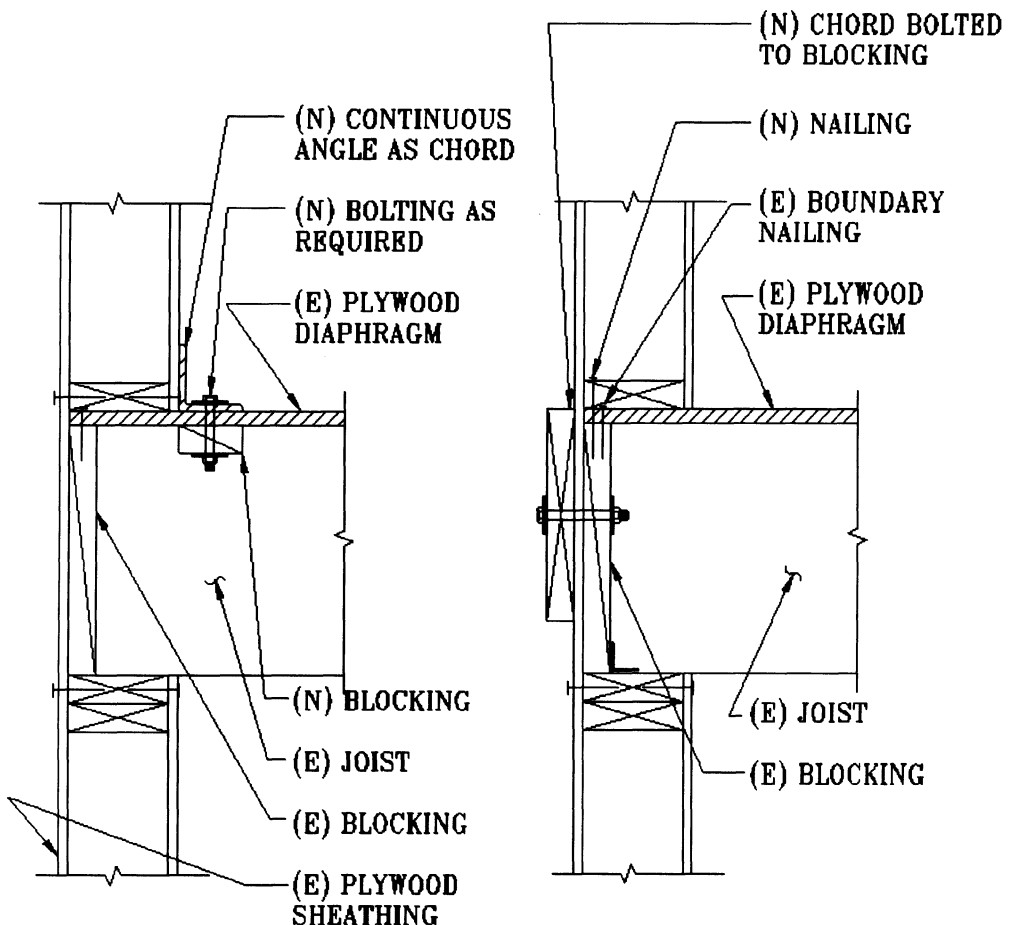


Figure 12-25. New chord member for wood diaphragm

specified as the planking provides insufficient wood depth for adequate nail penetration. The capacity of the combined plywood plus plank sheathing must be determined through a rational analysis. In addition to increasing the shear capacity of the diaphragms the plywood overlayment will also significantly increase the stiffness.

The shear capacity of existing plywood diaphragms can also be increased through the use of sheet metal strips placed over the plywood edges and securing the sheet metal to the plywood on both sides of the joints with staples. This approach is described in Reference 16.

Timber diaphragms with *inadequate chord capacity* can be upgraded by providing adequate connections to existing perimeter framing or through the addition of new

continuous members. Figure 12-24 presents a detail where continuity across the connections of the existing rim joists are provided with the use of metal hardware. Figure 12-25 presents two examples where new chord members have been added to the existing diaphragm. In all cases adequate shear transfer connection capacity is required between the diaphragm and the chord member.

Drift limits frequently control member design on multi-story buildings with flexible lateral systems. *Excessive drifts* can also be expected on long span timber diaphragms, particularly when they are used with heavy walled structures. Diaphragm drifts need to be checked for these types of structures. Several alternatives can be implemented should drifts exceed acceptable levels, including: reducing the span by adding supplemental vertical lateral

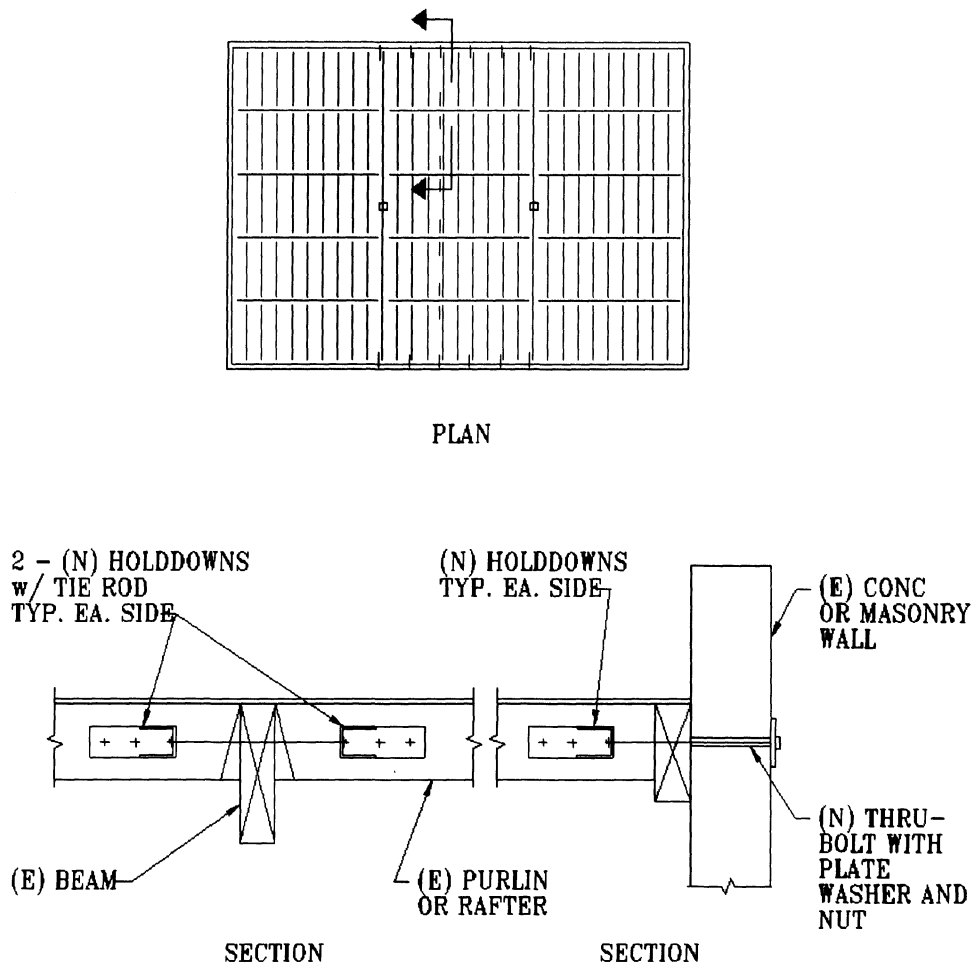


Figure 12-26. Adding continuity to an existing timber diaphragm

force-resisting members; increasing the stiffness of the diaphragm; or modifying internal structural and non-structural elements such that the excessive drifts can be tolerated.

Poor connectivity of timber diaphragms to walls is also a common problem. Timber diaphragms that lack blocking of joists at shear walls can roll-over at the edges. Adding blocking and ensuring adequate nails or metal connectors are provided to resist shears and local overturning or rolling of the blocking will address this deficiency.

Lack of continuity across diaphragms constructed of materials with limited tensile capacity, such as timber diaphragms, can lead to significant damage, particularly in structures constructed with heavy walls. Under the influence of large inertial loads at the edge of

the diaphragm, diaphragms with limited tensile capacity can rip apart unless directly provided with continuous ductile elements to tie the structure together. This continuity is best provided by the timber framing members, however, timber framing connections typically have little tensile capacity. Metal hardware such as hold-downs can be installed across joints to remedy this deficiency. Figure 12-26 presents a common method for providing adequate continuity in an existing timber diaphragm. Symmetrical connectors should be utilized where possible to minimize eccentric loads on existing framing.

The number of continuity ties, their location, and capacity is dependent upon a number of factors including flexibility and tensile capacity of the diaphragm, tributary mass of walls, and

dynamic response of the diaphragm. The structural community has developed a simplified method of providing for attachment of heavy walled structures to timber diaphragms and providing continuity across the diaphragm through the use of sub-diaphragms. This method can be used for new construction or retrofitting existing buildings. For more information on wood sub-diaphragms see ATC-7⁽¹²⁻¹⁴⁾ or Beyers⁽¹²⁻¹⁵⁾.

Concrete Diaphragms - Common deficiencies of concrete diaphragms include inadequate shear capacity, inadequate chord capacity and excessive shear stresses at diaphragm openings or plan irregularities.

Inadequate shear capacity of concrete diaphragms is commonly addressed by reducing the shear demand on the diaphragm by providing supplemental vertical lateral force resisting elements or by increasing the diaphragm capacity by adding a concrete overlayment. The addition of a concrete overlayment is usually quite expensive as this requires the complete removal of all existing partitions and floor finishes and may require the strengthening of existing beams and columns such that they can resist the added dead load demands due to the weight of the new concrete.

Adding supplemental vertical lateral force resisting elements may be more cost effective depending upon the amount of foundation work required. This approach will also reduce demands on other elements that have deficiencies.

Increasing the *chord capacity* of existing concrete diaphragms can be accomplished by adding new concrete or steel members or by improving the continuity of existing members. Figure 12-27 presents a common method for increasing the chord capacity of a concrete diaphragm with the addition of a new concrete member. This member can be placed above or below the diaphragm. Locating the chord below the diaphragm will typically have less impact on floor-space, however, details to ensure continuity of the chord as it traverses past intersecting beams can be costly. The addition of a steel strap to the outside of the building,

dowled into the wall can also provide adequate chord capacity. Sufficient dowels must be provided to transfer the shears from the diaphragm to the walls.

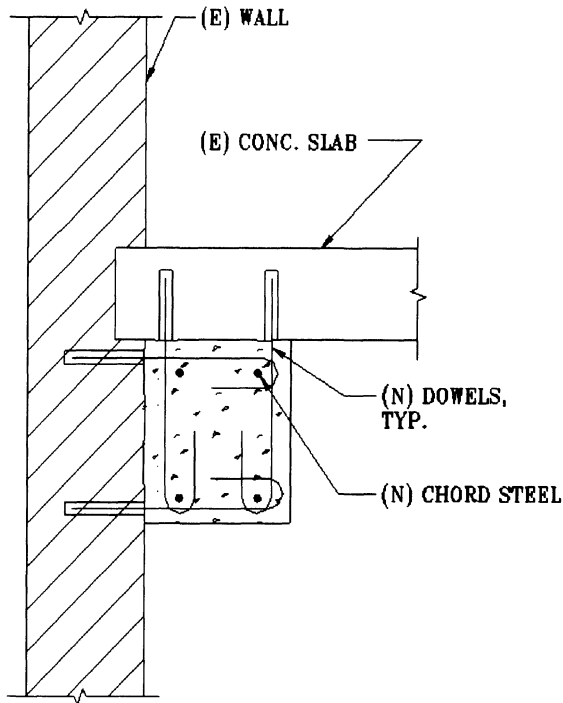


Figure 12-27. Adding a new chord member to an existing concrete diaphragm.

Existing steel frame buildings with concrete floor slabs are frequently constructed with simple or semi-rigid beam-to-column connections. The beams may have adequate capacity to resist vertical demands as well as diaphragm chord demands, however, the connections may have inadequate strength or stiffness to transmit chord forces. Figure 12-28 presents an example of a common approach used to increase the strength and stiffness of an existing steel frame connection to provide adequate chord capacity for the concrete diaphragm.

Excessive shear stresses at diaphragm openings or plan irregularities can be mitigated by distributing the forces in the diaphragm by means of reinforced concrete drag struts cast beneath the slab and made integral through the use of drilled and grouted dowels (Figure 12-29).

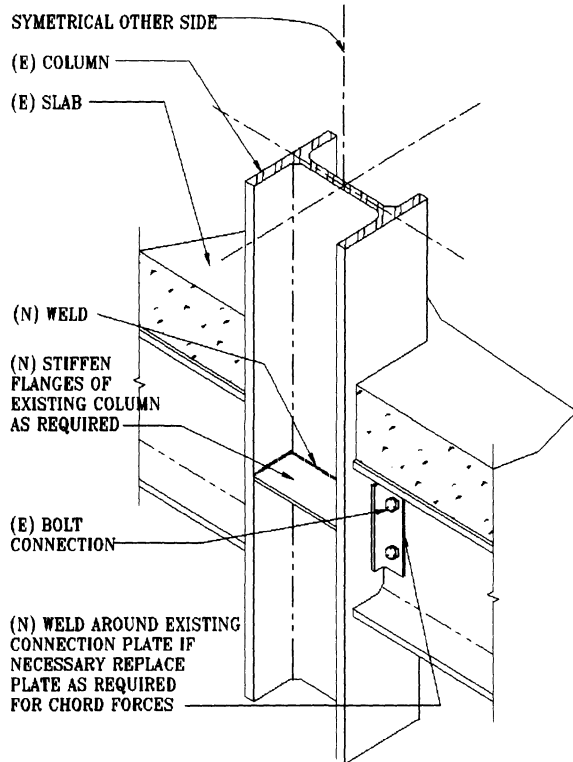


Figure 12-28. Example of details to modify simple connection to provide chord tension capacity

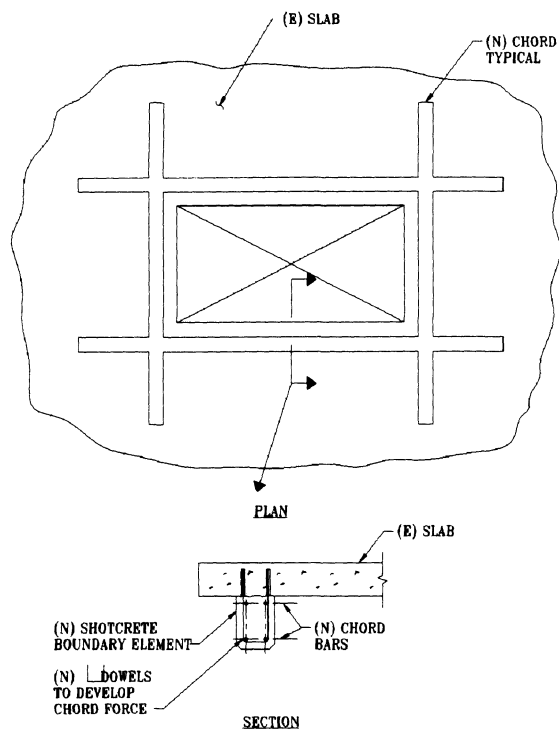


Figure 12-29. Example of diaphragm opening reinforcement.

Alternately, if the opening can be eliminated, the stress concentration can be removed by infilling the opening.

Excessive local diaphragm stresses at a reentrant corner can also be reduced through the introduction of drag struts as shown in Figure 12-30.

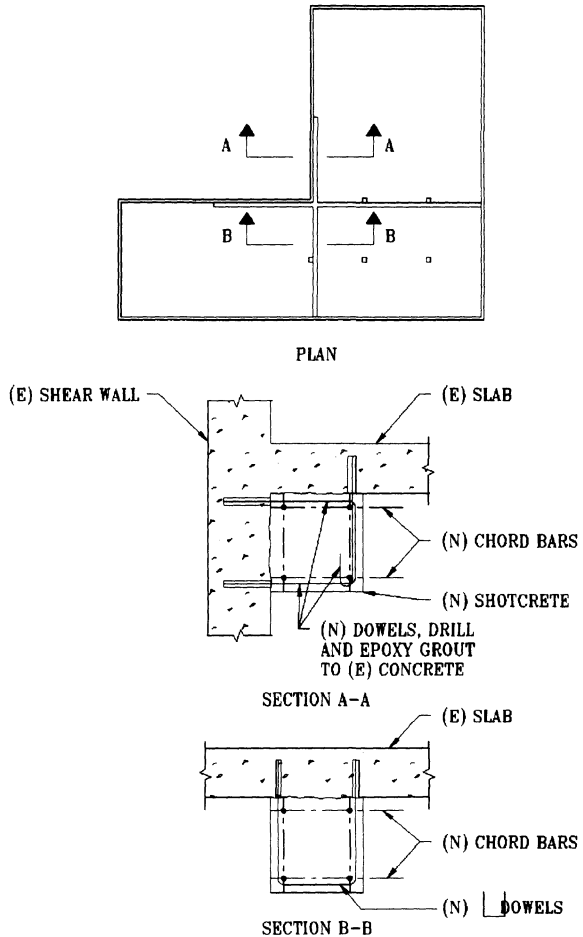


Figure 12-30. Addition of drag struts at concrete reentrant corner

Precast Concrete Diaphragms - Common deficiencies of precast concrete diaphragms include inadequate shear capacity, inadequate chord capacity and excessive shear stresses at diaphragm openings or plan irregularities.

Existing precast concrete slabs (typically constructed using precast tees or cored planks) commonly have *inadequate shear capacity*. Frequently, limited shear connectors are provided between adjacent units and a minimal topping slab with steel mesh reinforcement is

placed over the planks to provide an even surface to compensate for the irregularities in precast elements. The composite diaphragm may have limited shear capacity.

Strengthening the existing diaphragm is generally not cost effective. Adding a reinforced topping slab is generally prohibitive because of the added weight. Adding mechanical connectors between units is generally not practical, because the added connectors are unlikely to have sufficient stiffness, compared to the topping slab, to resist an appreciable load. The connectors would therefore need to be designed for the entire shear load assuming the topping slab fails. The number of fasteners, combined with edge distance concerns typically makes this impractical.

The most cost effective approach is generally to reduce the diaphragm shear forces through the addition of supplemental shear walls or braced frames.

Inadequate chord capacity on a precast concrete deck can be mitigated in a similar fashion as discussed earlier for a cast-in-place concrete diaphragm. A new chord member can be added above or below the precast concrete deck as shown in Figure 12-27.

Excessive stresses at diaphragm openings or plan irregularities in precast concrete diaphragms can also be mitigated in a similar manner as described earlier for cast-in-place concrete diaphragms (as shown in Figures 12-29 and 30).

Steel Deck Diaphragms - Inadequate diaphragm shear and chord capacities, and excessive diaphragm stresses at diaphragm openings or plan irregularities are common deficiencies in steel deck diaphragms.

Steel deck diaphragm *shear capacity* is limited by the shear capacity of the corrugated sheet steel and the fastener capacity connecting adjacent deck sheets (typically through crimping of the seams or seam welding). The capacity is also controlled by the spacing of deck-to-beam connections which prevent out-of-plane buckling.

A modest amount of increased shear capacity can be achieved through additional welding at sheet seams. Removal of insulation fill on roof decks is required to provide access for the welding.

Should added welding be insufficient or impractical, reducing the demands to below the shear capacity of the diaphragm can be accomplished by adding supplemental vertical lateral force-resisting elements. New steel braced frames or shear walls can be added to cut down the diaphragm span. Drag struts connecting to the new braced frame or shear wall will be required to distribute the loads into the diaphragm.

Inadequate flexural capacity of steel deck diaphragms may occur due to incomplete or inadequate chord members. Perimeter steel beams or ledgers need to be continuous to act as chords. Beam-to-column connections at the perimeter may have inadequate stiffness or strength in the axial direction of the beams to adequately act as chords. Increasing the strength and stiffness of these connections similar to the method shown in Figure 12-31 can address this deficiency.

Excessive local diaphragm stresses at a reentrant corner in a steel deck diaphragm may be the result of an inadequate load path between girders (or beams) and the steel deck, particularly where open-web steel joist (OWSJ) construction is utilized. In this type of construction the joists span between girders with the top chord of the joist being placed on top of the top chord of the girder. The top of the joist and the girder are therefore not at the same elevation. Hence, the steel deck is not directly connected to the girder. Shear transfer between the girder and deck must therefore occur through the joist-to-girder connection. Figure 12-32 presents a common situation where this condition occurs and a typical method that is utilized to correct the deficiency.

Excessive stresses will occur in the diaphragm at the reentrant corner shown in Figure 12-32 unless adequate drag struts exist to distribute these stresses along an extended length of the diaphragm. The joist and girder at

the reentrant corner may provide this drag strut function provided the joist is adequately connected to the shear wall at the reentrant corner. Frequently the framing is constructed as shown in Figure 12-32 (b), without the cap plate. The OWSJ support connection may have inadequate capacity and stiffness to transfer lateral loads from the deck to the girder, and hence the OWSJ connection may fail and/or the diaphragm may fail adjacent to the reentrant corner. The addition of a cap plate with adequate connection capacity to both the metal deck and truss will provide the necessary load path and distribute forces into the diaphragm.

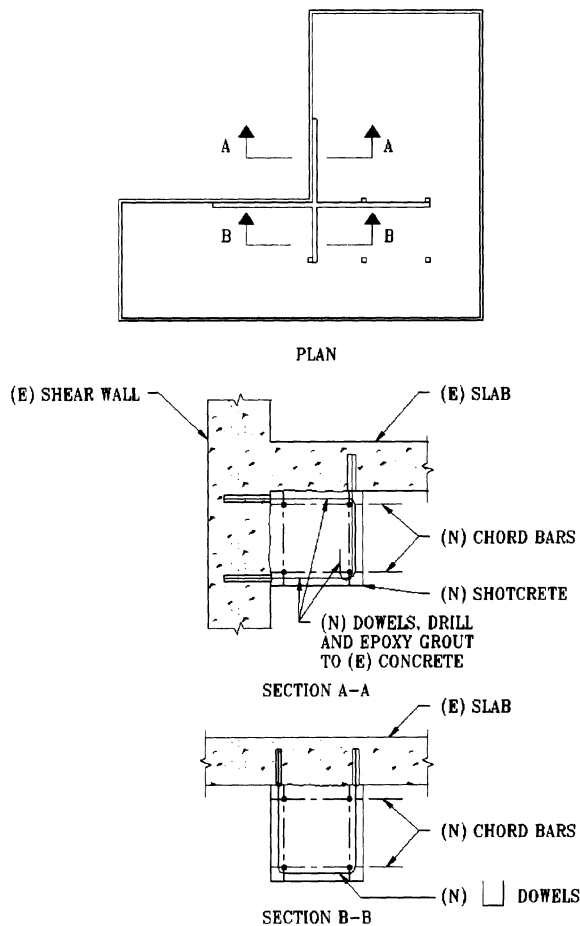


Figure 12-31. New chords at reentrant diaphragm corner.

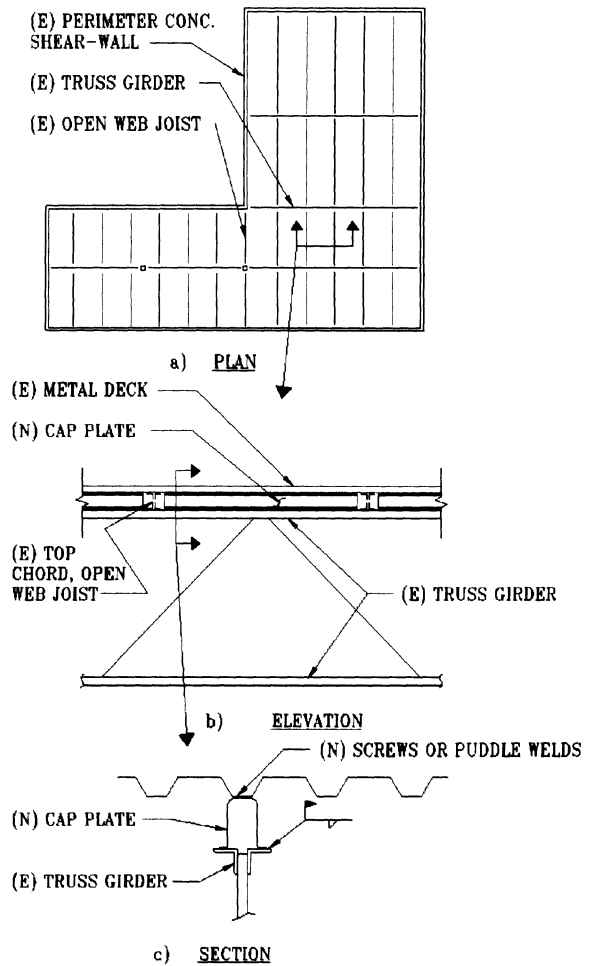


Figure 12-32. Strengthening of the steel deck-to-girder connection, (a) plan view, (b) elevation of truss girder, (c) section of metal deck and top chord of truss girder.

12.5.6 Non-structural Elements

Common non-structural elements include non-load bearing walls, cladding, ceilings, ornamentation, and mechanical and electrical services and utilities.

Non-load bearing walls - Common upgrade techniques for improving the performance of buildings with non-structural walls which adversely affect the seismic response of a building include: removing the walls; removing the walls and replacing them with walls constructed of relatively flexible materials (e.g. gypsum board sheathing); or modifying the wall connections such that they will not participate in resisting lateral loads. The first

two alternatives are the most commonly utilized.

Removal and replacement of existing hollow clay tile, concrete, or brick masonry partitions is the preferred method of addressing the inadequate out-of-plane capacity of non-structural partitions. Replacement may not be practical, however, due to cost or the desire to preserve architectural finishes.

Alternatively, steel strongbacks can provide out-of-plane support. Steel members are installed at regular intervals and secured to the masonry with drilled and grouted anchors. The masonry spans between the steel members and the steel members either span vertically between floor diaphragms or horizontally between building columns. An example of a strongback installation detail is shown in Figure 12-21.

A third method for mitigating masonry walls with inadequate out-of-plane capacity is to provide a structural overlay. The overlay may be constructed of plaster with welded wire mesh reinforcement, or concrete with reinforcing steel or welded wire mesh. This approach is used at times merely to provide containment of the masonry. Non-structural masonry walls are frequently used as firewalls around means of egress. Egress walls with deficient out-of-plane capacity can fail or result in rubble blocking the egress. Containment of the masonry with a plaster or concrete overlay can maintain free means of egress, although the walls may have to be replaced following a major seismic event.

Architectural Elements - Building cladding, veneers, ceilings, and partitions were frequently not designed or installed to safely accommodate seismic deformations in a building.

Precast concrete cladding panels were installed in many buildings with nearly rigid connections. The connections may not have the flexibility or ductility to accommodate large building deformations. Failure of the connection may result in heavy panels falling away from the building. Complete correction of this deficiency is likely to be costly as numerous panel connections would need to be

modified to accommodate anticipated building drifts. This may require removal and reinstallation or replacement of the panels. A more economical solution is to install redundant flexible/ductile connections that will hold the panels from falling should the existing connections fail.

Improper design and installation of precast concrete cladding may also be more than just a cladding connection problem. The cladding may act as an unintended lateral load resisting element should the connections be rigid and insufficient gaps be present between panels. Correcting this deficiency can be accomplished by installing occasional seismic joints in the panels to minimize the stiffness of the cladding or by stiffening the existing lateral force resisting system.

Stone or masonry veneers on buildings may be inadequately secured. During strong ground shaking the wall to which veneers are attached may deform causing the veneer layer to separate from the wall. The veneers may become falling hazards unless their anchorages can accommodate this deformation. Remediying this situation may be expensive. Removal and replacement of the veneer with adequate anchorage is one option. A second option is to decrease the deformation of the supporting wall by adding supplemental stiffness to the structure.

Building ornamentation such as parapets, cornices, signs and other appendages are another potential falling hazard during strong ground shaking. Unreinforced masonry parapets with heights at least 1-1/2 times their width are particularly vulnerable to damage. Parapets are commonly retrofit by providing bracing back to the roof framing (Figure 12-33). Providing adequate flashing details at the roof connections is an important part of the upgrade details.

Some cornices or other stone or masonry appendages are retrofit by installing drilled and grouted anchors at regular intervals. Others are retrofit by removal and replacement in kind with adequate anchorage or replacement with a lightweight substitute material such as plastic, fiberglass, or metal.

The most common failure observed in a moderate earthquake occurs to *suspended acoustical tile ceilings*. Failure typically occurs at the perimeter of the building. Unbraced ceilings are significantly more flexible than the floors or roofs to which they are attached. The ceilings therefore will sway independent from the floor or roof, typically resulting in the runners at the walls breaking their connections. This deficiency can be reduced by stiffening the suspended ceiling system through the installation of diagonal wires at regular spacing between the ceiling grid and structural floor or roof members. Vertical compression struts are also required at the location of the diagonal wires to resist the upward component of force caused by the lateral loads. A typical installation detail is shown in Figure 12-34. Current code standards such as those contained in UBC-97 and IBC-2000 provide standards for the installation of new suspended ceiling systems that can also be utilized for the upgrade of existing ceiling systems (see Chapter 13 for more information on design of non-structural systems and components).

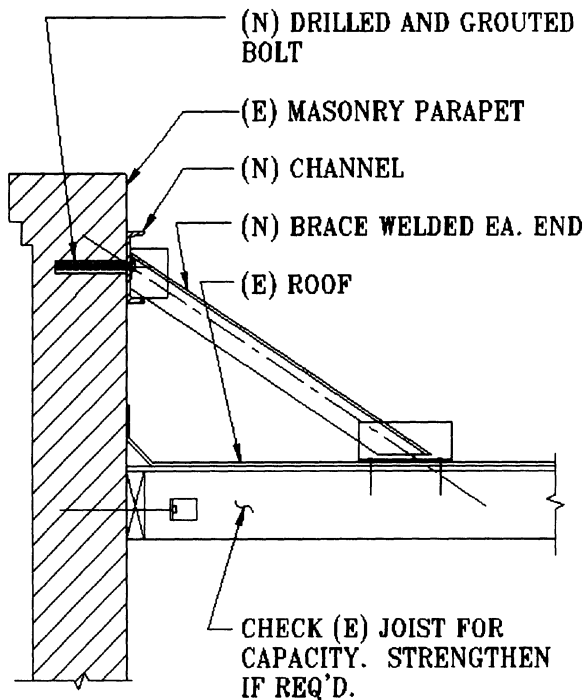


Figure 12-33. strengthening of a masonry parapet with steel braces.

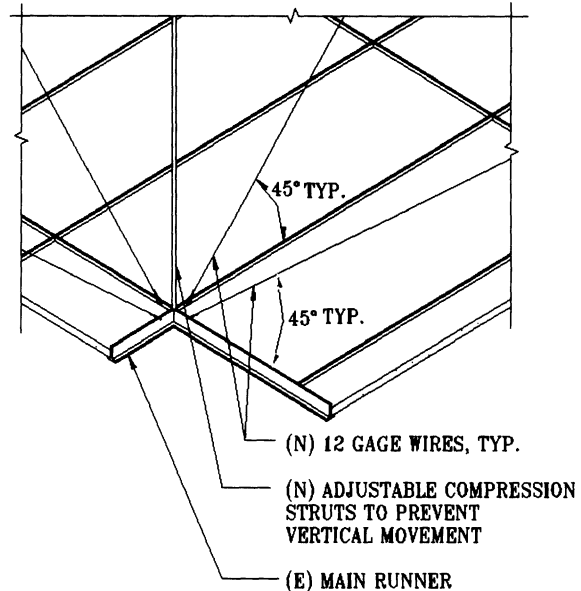


Figure 12-34. Lateral bracing of a suspended ceiling.

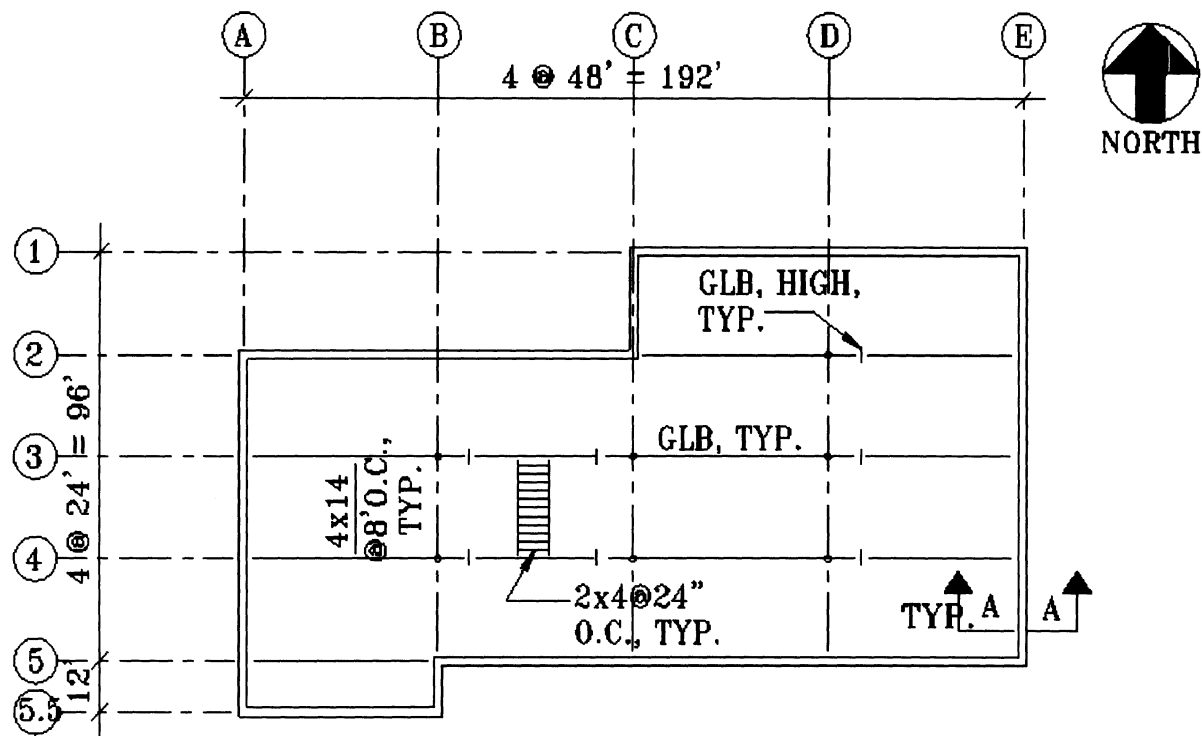
12.6 Examples

12.6.1 Tilt-Up Building Seismic Upgrade

A large number of precast low-rise concrete buildings with wood diaphragms were constructed in the U.S. beginning in the 1950's. This economical mode of construction was used for many office, warehouse, and light manufacturing buildings. The 1971 San Fernando earthquake, however, exposed a number of deficient conditions in typical tilt-up construction buildings. The tilt-up building shown in plan in Figure 12-35 contains many of these deficiencies. The following describes one method to upgrade the building.

The existing building has the following parameters:

- 1/2 inch C-D, Structural II roof plywood, unblocked with 8d nails at 6 inches on center.
- 3x14 wood ledgers 2x4 joists at 2 foot on center 4x14 purlins at 8-ft. on center glulam beams (GLB) at 24 feet on center, GLB are constructed with cantilever hinges.
- Total roof load including roofing and framing is $12 \text{ lb}/\text{ft}^2$.



ROOF PLAN - EXAMPLE 1

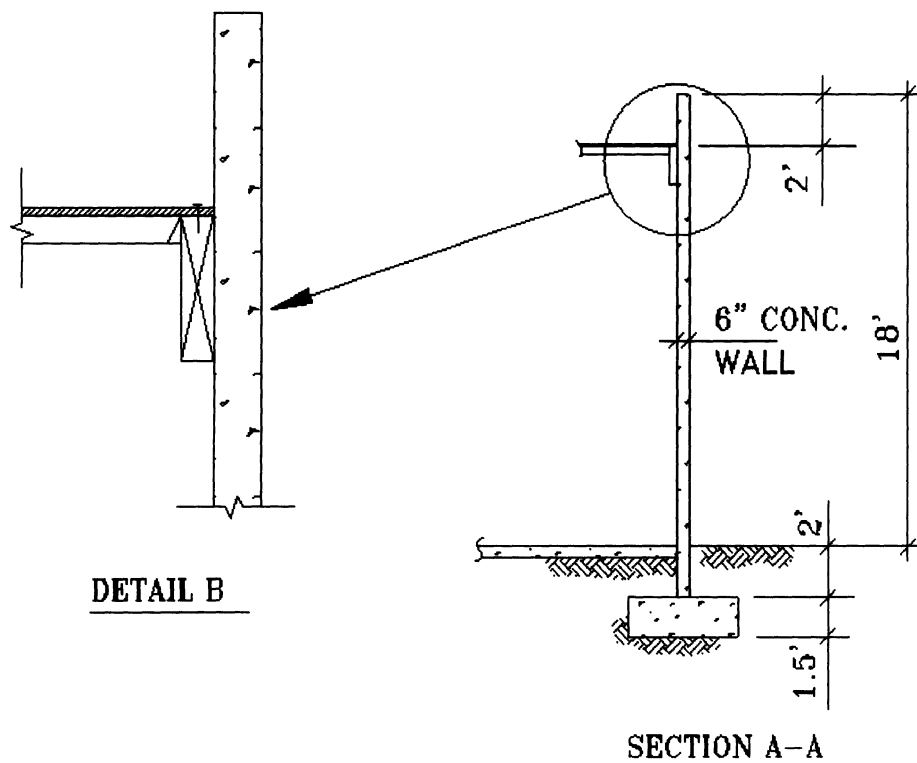


Figure 12-35. Example tilt-up building , plan and wall elevation

- Walls are 6-in. thick precast concrete panels, 18 feet high. The roof is connected 16 feet above grade.
- The wall panels are connected to the floor slab via #4 dowels at 24 inches on center.

The general upgrade objective is to bring the building up to the design provisions of the UBC-9^a Uniform Building Code pursuant to discussions and a written understanding between the owner and the engineer. Therefore the building base shear is calculated as follows:

$$V = ZICW/R_w \text{ where:}$$

$$Z=0.4, \text{ zone 4}$$

$$I=1.0$$

$$C=2.75 \text{ (maximum)}$$

$$R_w = 6 \text{ concrete shear wall, bearing}$$

$$\text{Therefore: } V = 0.183W$$

The weight of the wall tributary to the roof diaphragm = $0.5 \text{ ft}(150 \text{pcf})(18 \text{ ft})^2/(2 \times 16 \text{ ft}) = 760 \text{ plf}$. The roof demands are therefore:

$$W_1 = 0.183 \times (12 \text{ psf} \times 84 \text{ ft} + 760 \text{ plf} \times 2 \text{ walls}) = 463 \text{ plf}$$

Similarly:

$$w_2 = 436 \text{ plf}$$

$$w_3 = 489 \text{ plf}$$

$$w_4 = 384 \text{ plf}$$

$$w_5 = 700 \text{ plf}$$

$$w_6 = 489 \text{ plf}$$

^a Since performance based design methods are presented in Chapter 15, in the examples presented in this chapter we utilize the more traditional way of upgrading buildings. That is, to bring the structure up to one of the previous editions of the building code used to design new buildings. Rather arbitrarily, we have selected UBC-91 provisions as the objective criteria for examples of this Chapter. Obviously, other editions of this or other applicable codes may have been used.

Figure 12-36 depicts the seismic demand on the roof diaphragm in both the north-south and east-west directions and the wall reactions and diaphragm shears assuming a tributary distribution of loads (flexible diaphragm).

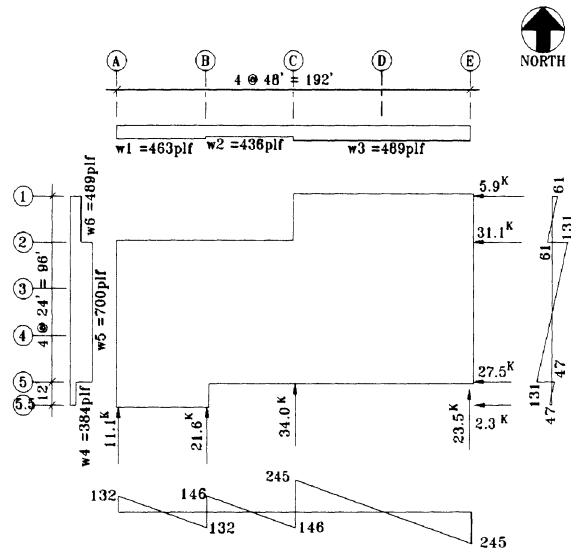


Figure 12-36. Example tilt-up building. - Seismic demands, reactions and shear diagrams.

The plywood is unblocked and configured according to UBC-91 Table No. 25-J-1, case 2 in the north-south direction and case 4 in the east-west direction. The allowable shear capacity for the diaphragm per Table 25-J-1 is 180 plf.

Deficiencies

The example building has the following obvious deficiencies:

1. The diaphragm has inadequate shear capacity at lines C and E (245 plf demand > 180 plf capacity).
2. Out-of-plane wall anchorage is provided via cross-grain bending in the ledgers, which is not permitted per UBC-91 2337(b)9D.
3. No continuity ties exist per UBC-91 2337(b)9C.
4. Inadequate collector connections are provided at the reentrant corners, i.e., at lines B and C in the north-south direction and lines 2 and 5 in the east-west direction.

5. Overturning of wall panels at lines B between 5 and 5.5 and at line C between 1 and 2 are potential deficiencies based on observation of the lateral load resisting system. Therefore the wall overturning at line B between 5 and 5.5 is checked as follows:
- Weight of the wall above ground equals 16,200 lbs and the weight below ground including the footing equals 7,200 lbs. Therefore, the total gravity load for the wall is 23,400 lbs.
 - The tributary lateral load from the wall equals $0.183W = 0.183 \times 16,200 = 2,965$ lbs.
 - The wall overturning forces and resisting forces are shown in Figure 12-37.

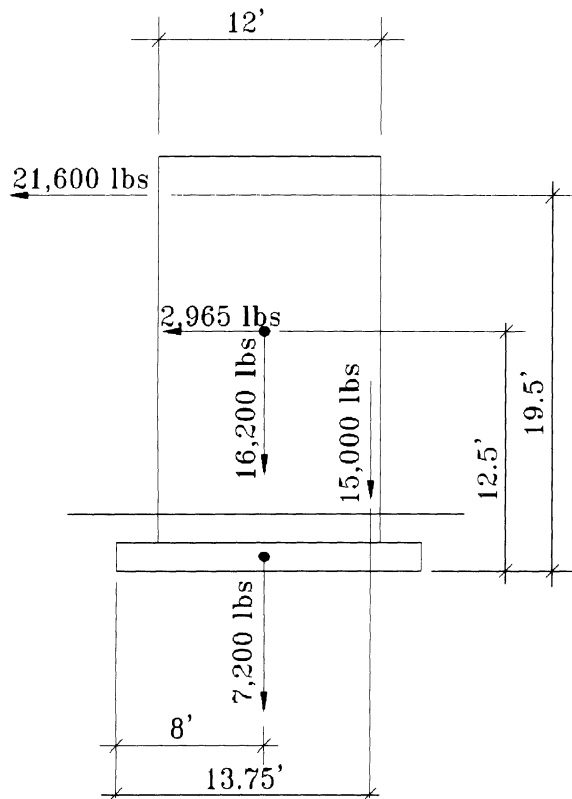


Figure 12-37. Example tilt-up - building ,Wall Reaction at line B between 5 and 5.5

The overturning moment and the resisting moment is calculated as follows (assuming rotation occurs at the toe of the footing and that a 15,000 pound dead load of the return wall will be mobilized):

$$\begin{aligned} M_{\text{or}} &= 21,600 \text{ lbs} \times 19.5 \text{ ft} + 2,965 \text{ lbs} \times 12.5 \text{ ft} \\ &= 458,263 \text{ lb-ft.} \end{aligned}$$

$$\begin{aligned} M_{\text{R}} &= (16,200 \text{ lbs} + 7,200 \text{ lbs}) \times 0.85 \times 8 \text{ ft} \\ &+ 15,000 \text{ lbs} \times 0.85 \times 13.75 \text{ ft} \\ &= 334,432 \text{ lb-ft.} \end{aligned}$$

Note: Dead loads are reduced by 0.85 when used to resist uplift [UBC-91 2337(a)].

$M_{\text{ot}} > M_{\text{R}}$, therefore not acceptable

The wall at line C between lines 1 and 2 was checked in a similar manner and the restoring moment was found to exceed the overturning moment and hence was determined to be adequate. Therefore, the fifth deficiency is that the wall at line B between 5 and 5.5 has inadequate capacity to resist overturning.

Strengthening Options

The following options are considered for addressing the above described deficiencies:

1. Correcting the inadequate roof diaphragm shear capacity can be accomplished by:
 - a. Reducing the diaphragm shear by introducing a new lateral force resisting element (e.g. shear wall or braced frame) between lines C and E, or
 - b. Strengthening the roof diaphragm, where demands exceed capacity by adding blocking and nailing.

Option 1b is selected for this building. A new lateral force-resisting element (option 1a) would reduce the open space layout of the building and would require costly foundation work. Removal of roofing would be required for both options. Removal would be required for option 1a to permit nailing between the plywood and roof joist collectors required to correct deficiency number 4. Roofing removal would be required for option 1b in designated areas such that new blocking and nailing may be installed.

2. New hardware is required between the roof framing and the concrete walls to provide direct out-of-plane connection capacity.

3. New hardware is required at GLB hinge connections, and subframing intersections at main framing to provide adequate continuity.
4. New hardware is required at GLB hinge connections, and subframing intersections with main framing to provide adequate collector capacity at framing attached to reentrant corner walls.
5. Two options were considered to address the inadequate overturning capacity of the wall at line B between 5 and 5.5:
 - a. Improving the foundation to resist the overturning force, or
 - b. Permitting the wall to rock.

Option 5b is selected as the least costly alternative of the two. Permitting the wall to rock will result in a redistribution of diaphragm shears to the west of line C. A diaphragm shear check (shown below) demonstrates no adverse conditions result because of this redistribution.

The lateral roof load the wall is capable of resisting is determined by summing the moments about the toe of the wall (see Figure 12-37):

The sum of the moments about the toe of the wall = 0.0, therefore:

$$(16,200 \text{ lbs} + 7,200 \text{ lbs}) \times 0.85 \times 8 \text{ ft} + 15,000 \text{ lbs} \times 85 \times 13.75 \text{ ft} - 2,965 \text{ lbs} \times 12.5 \text{ ft} - P \times 19.5 \text{ ft} = 0.0$$

Solving for P, we have

$$P = 15,250 \text{ lbs.}$$

Figure 12-38 depicts the new distribution of diaphragm shears in the north-south direction. The shear stress, 188 plf at the west side of Line C exceeds the capacity of 180 plf by less than 5%, hence is deemed acceptable.

Strengthening Provisions

1. Diaphragm Shear

Increasing the capacity of the roof diaphragm is accomplished by adding blocking with 8d nailing at 6 inches on center. The new capacity equals 270 plf (UBC-91 Table 25-J-1, blocked diaphragm for 15/32 C-D structural II

sheathing). The blocking is to be added in the areas shown in Figure 12-39.

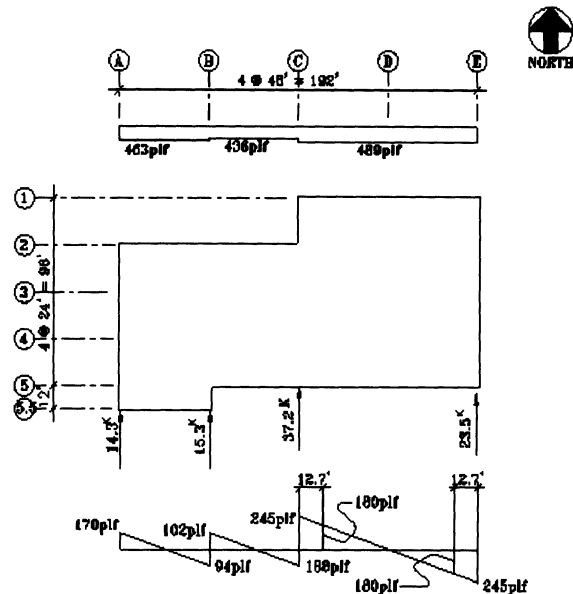


Figure 12-38. Example tilt-up building - Roof plan – Revised shear distribution assuming wall at line B resists a maximum of 15.3 kips.

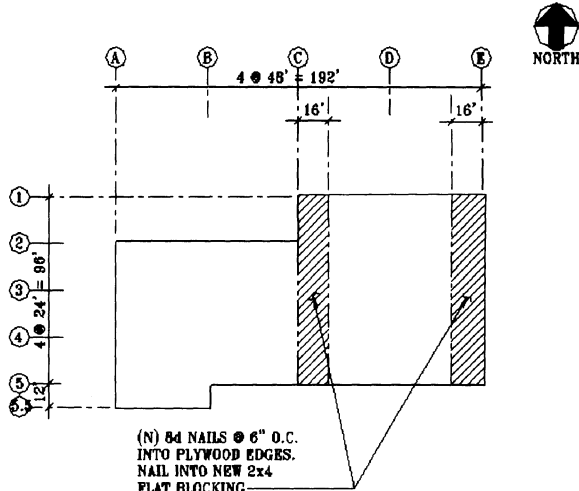


Figure 12-39. Example tilt-up building - Roof plan - Areas requiring blocking with added nailing.

2. Out-of-Plane Anchorage

Positive direct connections between the wall panels and the roof construction is required per UBC-91 2337(b)⁽¹²⁻¹⁹⁾. The demands for the out-of-plane anchorage are calculated per UBC-91 equation 36-1:

$$F_p = ZIC_p W_p$$

where: $C_p = 0.75$ for the outer quarters of the diaphragm, and $C_p = 1.125$ for center half of the diaphragm (UBC-91 Table 23-P, note 3)

The cost of the installation in a retrofit design is primarily labor not hardware. Therefore all out-of-plane anchorage is designed utilizing $C_p = 1.125$. The out-of-plane anchor demand is therefore:

$$\begin{aligned} F_p &= ZIC_p W_p = 0.4 \times 1.0 \times 1.125 W_p \\ &= 0.45 W_p \end{aligned}$$

The tributary weight of the wall is

$$W_p = 0.5(150 \text{pcf})(18 \text{ft})^2 / (2 \times 16 \text{ft}) = 759 \text{plf}$$

The wall was checked and determined to be capable of spanning 8 feet. Hence, the new out-of-plane wall anchors are to be located at 8 ft on center. The connection demand is therefore

$$F_p = 0.45 \times 759 \text{ plf} \times 8 \text{ ft}$$

$$F_p = 341 \text{ plf} \times 8 \text{ ft} = 2,732 \text{ lbs/anchor}$$

The joists are checked for the DL + EQ load and are found to be adequate.

3. Continuity Ties

The use of subdiaphragms is permitted to meet the continuity tie provisions of UBC-91 2337(b)9.C. The subdiaphragm configuration selected for providing continuity across the building is depicted in Figure 12-40. Alternate configurations could also be utilized.

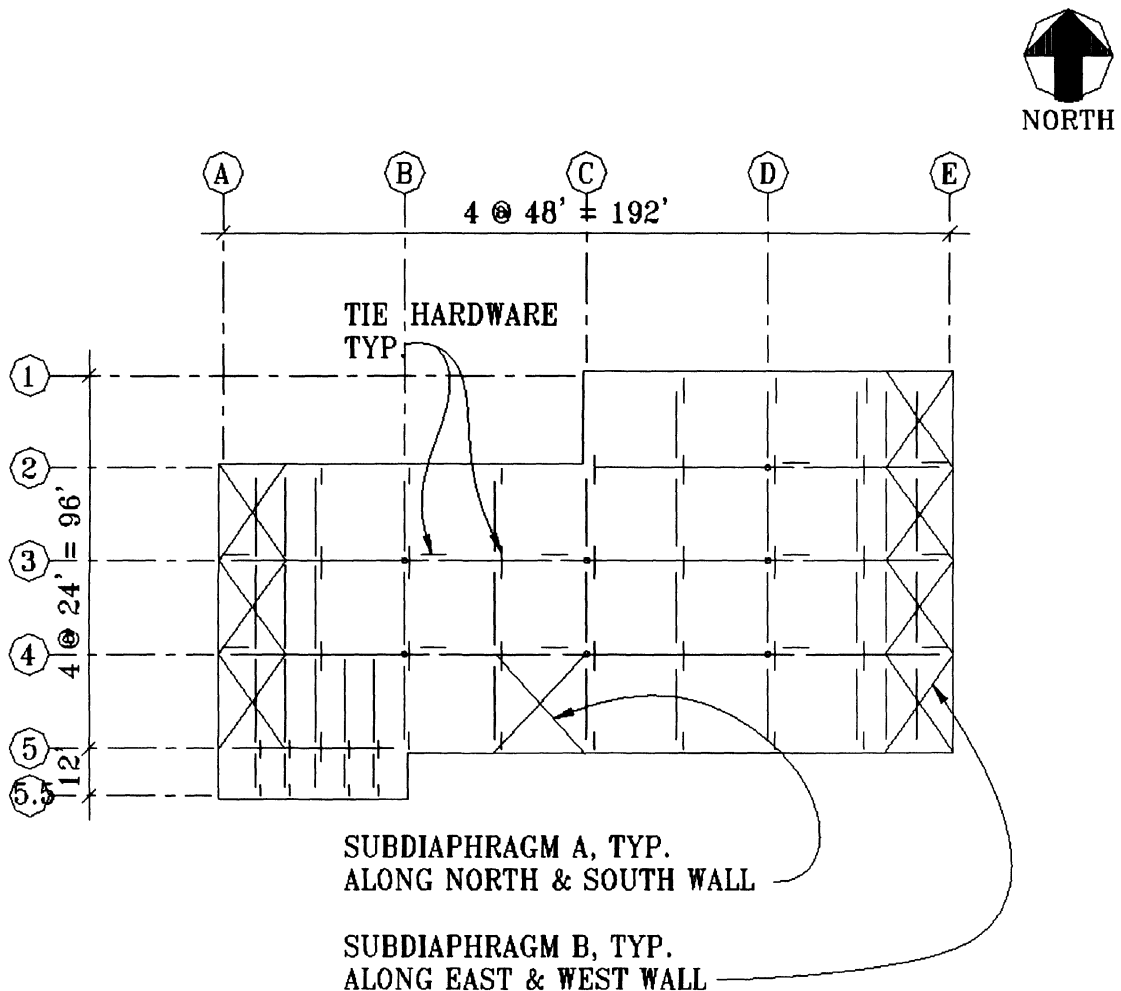


Figure 12-40. Example tilt-up building - Roof plan – Sub diaphragms

North-south direction

Continuity ties shall transfer the wall weight of

$$\begin{aligned} F_p &= ZICW_p = 0.4 \times 1.0 \times 0.7 \times W_p = 0.3W_p \\ &= 0.3 \times 759 = 228 \text{ plf} (> 200 \text{ plf min per UBC-91 Section 2310}) \end{aligned}$$

24 foot square subdiaphragms, designated "A" are provided in the north-south direction. 24 feet wide by 16 feet deep diaphragms would provide adequate shear capacity $228 \text{ plf} \times 12 \text{ ft}/16 \text{ ft} = 171 \text{ plf}$ demand $< 180 \text{ plf}$ capacity), however connections would have to be added across the subpurlins to provide a subdiaphragm chord. The GLBs serve as the chord members when a 24 foot subdiaphragm is utilized.

Therefore, the continuity tie demand across the GLBs = $228 \text{ plf} \times 24 \text{ ft} = 5,472 \text{ lbs}$

East-west direction

Subdiaphragms B are 24 feet wide and 16 feet deep in the east-west direction.

The diaphragm shear demand as calculated previously is 171 plf. The continuity demand = $228 \text{ plf} \times 24 \text{ ft} = 5472 \text{ lbs}$.

4. Collectors

The collector forces at the reentrant corners are shown in Figure 12-41. Detailing of the collector connections at the reentrant corner at line C-2 must provide for significant capacity (30,700 lbs and 18,300 lbs in the N-S and E-W directions respectively). The connection shown in Figure 12-42 is symmetrical, with respect to the wall and the roof framing in both directions, as significant additional strengthening would be required to resist moments induced by an unsymmetrical connection.

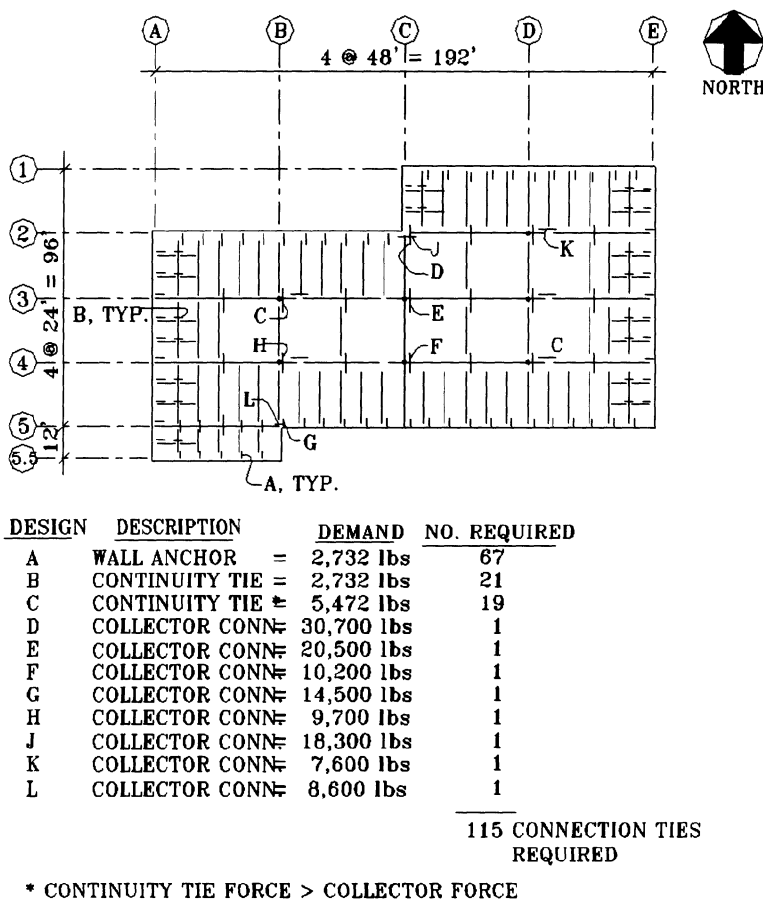


Figure 12-41. Example tilt-up building -Roof plan – Summary connection upgrade

Strengthening Summary

The new blocking and nailing shown in Figure 12-39 and the new connections shown in Figures 12-41 and 42 present the recommended upgrade requirements for the example tilt-up.

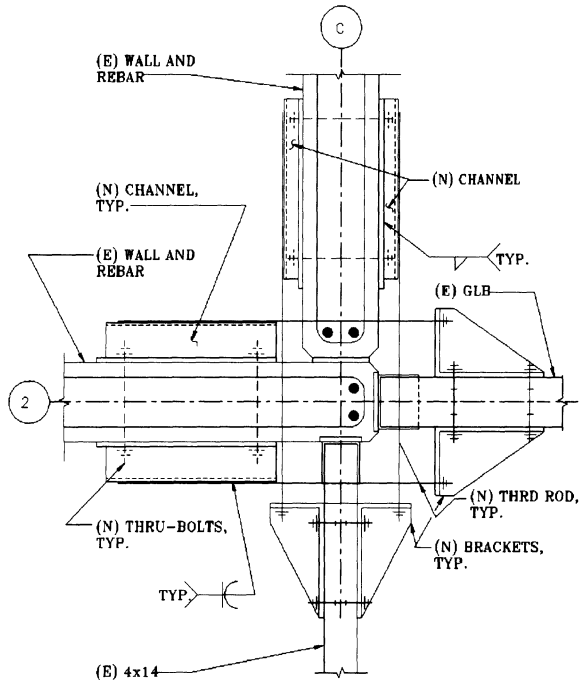


Figure 12-42. Example tilt-up building - Plan view – Collector connections at column line C-2

12.6.2 Unreinforced Brick Masonry Bearing Wall Building Upgrade

The type of building that has experienced the most severe damage in past earthquakes is the unreinforced brick masonry (URM) bearing wall building. This type of construction is prevalent throughout the United States, and is used for commercial, institutional, industrial, low-rise office, and residential occupancies. The URM bearing wall building, shown in plan in Figure 12-43 and an interior elevation in Figure 12-44, is a typical two-story URM structure. The following describes one method to upgrade the building.

The existing building has the following parameters:

Roof framing consists of:

1 by straight sheathing
2×10 joists at 2 foot on center
8×16 purlins at 20 foot on center
8×8 post columns
Total roof dead load including roofing and framing is 13 psf.
The roof is located 26 feet above the ground level first floor.

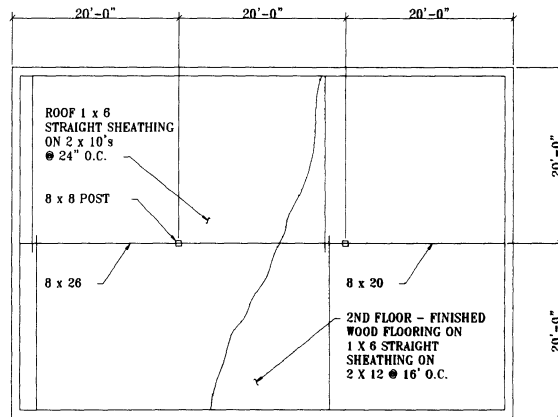


Figure 12-43. Example URM building, Plan layout – Typical URM bearing wall building.

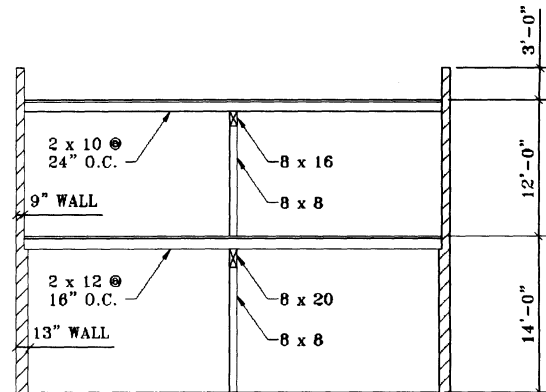


Figure 12-44. Example URM building, Interior elevation.

The second floor is located 14 feet above the ground level first floor.

A three foot tall brick parapet extends above the roof around the entire building.

Second floor framing consists of:

- 1 by straight sheathing with perpendicular finished flooring
- 2×12 joists at 16 inches on center
- 8×20 beams
- 8×8 post columns

- Total second floor dead load framing weight is 12 psf.
 - Some partitions exist at the second floor and none at the first, assume 10 psf.
 - The second floor walls are comprised of two wythes of brick masonry with a total thickness of 9 inches.
- The first floor walls are comprised of three wythes of brick masonry with a total thickness of 13 inches.
- A 16 by 8 foot stairway opening is located in the southwest corner of the second floor diaphragm.

Criteria

The upgrade criteria selected is that specified in the 1991 Uniform Code for Building Conservation (UCBC)^b "Special Procedure" pursuant to discussions and a written understanding between the owner and the engineer.

Dead Load Distribution

Following is the assumed distribution of roof DL's:

$$\text{Roof } 60' \times 40' \times 13 \text{ psf} = 31,200 \text{ lbs}$$

E&W Walls:

$$90 \text{ psf} \times (12'/2+3') \times 2(40') \times .80^* = 51,800 \text{ lbs}$$

N&S Walls:

$$90 \text{ psf} \times (12'/2+3') \times 2(60') = 97,200 \text{ lbs}$$

Partitions tributary to roof:

$$(10 \text{ psf}/2) \times 40' \times 60' = 12,000 \text{ lbs}$$

$$\text{Total Roof} = \underline{192,200 \text{ lbs}}$$

Following is the assumed distribution of 2nd floor DL's:

$$\text{Floor } 60' \times 40' \times 12 \text{ psf} = 28,800 \text{ lbs}$$

^b Since performance based design methods are presented in Chapter 15, in the examples presented in this chapter we utilize the more traditional way of upgrading buildings. That is, to bring the structure up to one of the previous editions of the building code used to design new buildings. Rather arbitrarily, we have selected UCBC-91 provisions as the objective criteria for examples of this Chapter. Obviously, other editions of this or other applicable codes may have been used.

E&W Walls

$$[90\text{psf} \times (12'/2)(2)(40') + 130(14/2)(2)(40')] \times .80^* = 92,800 \text{ lbs}$$

N&S Walls

$$[130\text{psf} \times (14'/2) + 90\text{psf} \times (12'/2)] \times 2(60') = 174,000 \text{ lbs}$$

Partitions trib to roof

$$(10 \text{ psf}/2) \times 40' \times 60' = 12,000 \text{ lbs}$$

$$\text{Total 2nd Floor} = \underline{307,600 \text{ lbs}}$$

$$\text{Total Building} = 499,800 \text{ lbs}$$

- window area in east and west walls is assumed equivalent to 20 percent of the wall area

Seismic Demand Loads

The building base shear is calculated as follows:

$$V = .33ZW \quad \text{where: } Z = 0.4, \text{ Zone 4}$$

$$\text{Therefore: } V = 0.13W$$

The weight of the building has been calculated as 499.8 kips. Hence

$$V = 0.13 \times 499.8 = 65.0 \text{ kips}$$

Demand Vs. Capacity of the Diaphragms

Check the demand versus capacity of the diaphragms using the special procedure outline UCBC-91 Section A109(d).

Roof Diaphragm

Per UCBC-91 A109(d)4.B(i) for a diaphragm without qualifying cross-walls at levels immediately above or below:

$$\text{DCR} = 0.833ZW_a / [(\text{Sum}(v_u \times D))]$$

where:

$$\begin{aligned} W_{a(N-S)} &= \text{total tributary dead load in N-S direction} \\ &= 31,200 \text{ lbs} + 97,200 \text{ lbs} + 12,000 \text{ lbs} \\ &= 140,400 \text{ lbs} \end{aligned}$$

$$\begin{aligned} W_{a(E-W)} &= \text{total tributary dead load in E-W direction} \\ &= 31,200 \text{ lbs} + 51,800 \text{ lbs} + 12,000 \text{ lbs} \\ &= 95,000 \text{ lbs} \end{aligned}$$

$v_u = 100 \text{ plf}$ (for straight sheathing per UCBC-91 Table No. A-1-C)

$$D_{N-S} = 40' \\ D_{E-W} = 60'$$

$$\Sigma(v_u \times D_{N-S}) = 100 \text{ plf} \times 2 \times 40' = 8,000 \text{ lbs}$$

$$\Sigma(v_u \times D_{E-W}) = 100 \text{ plf} \times 2 \times 60' = 12,000 \text{ lbs}$$

Therefore:

$$DCR_{N-S} = 0.833 \times 4 \times 140,400 / 8,000 = 5.8$$

$$DCR_{E-W} = 0.833 \times 4 \times 95,000 / 12,000 = 2.6$$

From UCBC-91 Figure A-1-1 at $DCR_{N-S} = 5.8$ a diaphragm span of 60' is unacceptable. However at $DCR_{E-W} = 2.6$ the shorter diaphragm span is acceptable.

Second Floor Diaphragm

The 2nd floor diaphragm shear demands are calculated as follows:

$$W_{N-S} = (28.8^k + 174.0^k + 12^k) \times 0.13 / 60' = \\ = 215^k \times 0.13 / 60' = 0.4 \text{ k/ft}$$

$$W_{E-W} = (28.8^k + 92.8^k + 12^k) \times 0.13 / 40' = \\ = 134^k \times 0.13 / 40' = 0.4 \text{ k/ft}$$

$$DCR = 0.833 Z W_a / [(\Sigma(v_u \times D))]$$

where:

$W_{a(N-S)}$ = total tributary dead load in N-S direction = 215,000 lbs

$W_{a(E-W)}$ = total tributary dead load in E-W direction = 134,000 lbs

$v_u = 500 \text{ plf}$ (for straight sheathing with perpendicular wood flooring per UCBC-91 Table No. A-1-C)

$$D_{N-S} = 40' + 24' = 64'$$

$$D_{E-W} = 60' + 52' = 112'$$

$$\Sigma(v_u \times D_{N-S}) = 500 \text{ plf} \times (64') = 32,000 \text{ lbs}$$

$$\Sigma(v_u \times D_{E-W}) = 500 \text{ plf} \times (112') = 56,000 \text{ lbs}$$

$$DCR_{N-S} = 0.833 \times 4 \times 215,000 / 32,000 = 2.2$$

$$DCR_{E-W} = 0.833 \times 4 \times 134,000 / 56,000 = 0.80$$

Therefore the second floor diaphragm meets the UCBC-91 special procedure criteria.

Mitigate Roof Diaphragm Deficiencies

The owner of the building does not want walls in the first floor. Hence crosswalls can not be continuous from the roof to the ground. By adding a crosswall in the north-south direction between the roof and second floor diaphragms the roof diaphragm would be acceptable. Try 3/8" C-D plywood on two sides secured with 8d nails @ 6 inches on center (capacity per UBC-91 Table 25-K-1 is 264 plf). Check UCBC A109(d)4.B.(iv)

$$DCR = 0.833 Z W_a / [(\Sigma(v_u \times D))]$$

where:

$$W_{a(N-S)} = 140,400 + 215,000 \text{ lbs} = 355,400 \text{ lbs}$$

$$\Sigma(v_u \times D) = 100 \times 2 \times 40 + 500 \times (64') = 40,000 \text{ lbs}$$

Therefore:

$$DCR = 0.833 \times 4 \times 355,400 \text{ lbs} / 40,000 \text{ lbs} = 3.0$$

From Figure A-1-1 at $DCR_{N-S} = 3.0$ the 60' diaphragm is acceptable. Therefore the only upgrade required to address the deficient roof diaphragm is to add a crosswall in the north-south direction. Try one 12' crosswall. Recheck A109(d)4.B.(ii):

$$DCR = 0.833 Z W_a / [(\Sigma(v_u \times D)) + v_{cb}]$$

where:

$$W_{a(N-S)} = 140,400 \text{ lbs}$$

$$\Sigma(v_u \times D) = 100 \text{ plf} \times 2 \times 40' = 8,000 \text{ lbs}$$

$$v_{cb} = 12' \times 2 \times 264 \text{ plf} = 6,336 \text{ lbs}$$

Therefore:

$$DCR = 0.833 \times 4 \times 140,400 \text{ lbs} / (8,000 + 6,336 \text{ lbs})$$

$$= 3.26$$

and

$$v_{cb} = 6,336 \text{ lbs} > 0.3 \text{Sum}(v_u \times D) = .3(8,000)$$

$$= 2,400 \text{ lbs} \text{ (per UCBC-91 A109(d).3.B)}$$

∴ The diaphragm/wall assembly is acceptable

Address Cross-wall Overturning

The cross-wall will impart large vertical loads on the existing beams due to overturning moments. Therefore additional framing will be needed to address these loads.

Design the floor framing to support the capacity of the wall. For a 12' long wall 12' high, the lateral and vertical load will equal = $12 \text{ ft} \times 2 \times 264 \text{ lbs/ft} = 6,336 \text{ lbs}$.

$$\text{The moment} = 6,336 \text{ lbs} \times 12 \text{ ft} / (20 \text{ ft}) \times 8 \text{ ft} =$$

$$= 30,413 \text{ lb-ft}$$

Two wood beams, a 4×16 in the roof framing and 4×12 beam in the second floor framing is adequate to resist this moment. The addition of these beams and the connection of the new plywood to the framing is shown in Figures 12-45. The beams on the north side of the column are utilized as collectors via the connections to the new beams shown in Figure 12-45.

Diaphragm-To-Wall Shear Connection

Check the shear transfer between the diaphragms and the wall per UCBC A109(d).5.

Roof

$$V = \text{lesser of: } \frac{1}{2} Z C_p W_d \text{ or } V = V_u D$$

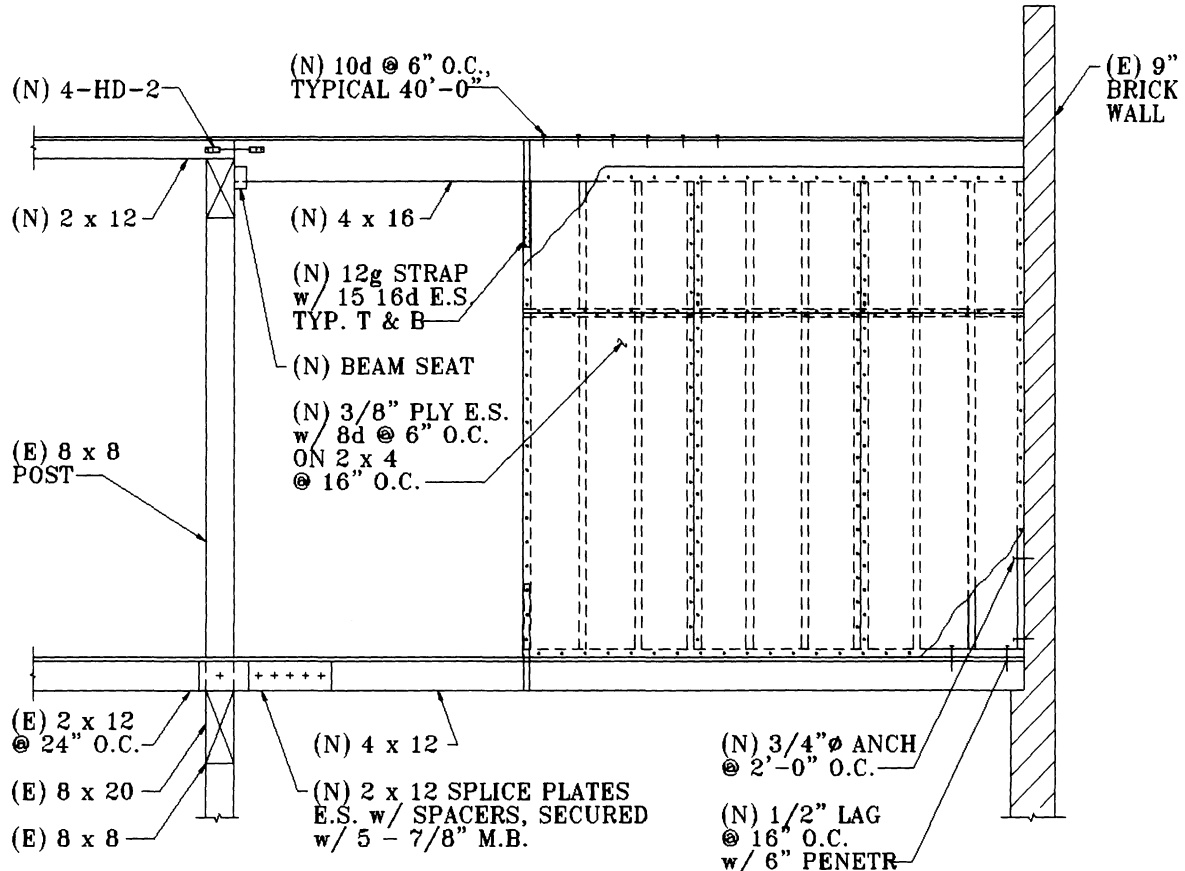


Figure 12-45. Example URM building, New cross wall

N-S

$$\frac{1}{2}ZC_p W_d = 0.5 \times 0.4 \times 0.5(140.4^k) = 14.0^k$$

$$V=V_u D = 0.1 \text{ klf} \times 2 \times 40' = 8.0^k \quad \text{controls}$$

Therefore,

$$v = 8,000 \text{ lbs}/(2 \times 40') = 100 \text{ plf}$$

E-W

$$\frac{1}{2}ZC_p W_d = 0.5 \times 0.4 \times 0.5(95.0^k) = 9.5^k$$

controls

$$V=V_u D = 0.1 \text{ klf} \times 2 \times 60' = 12.0^k$$

Therefore

$$v = 9,500 \text{ lbs}/(2 \times 60') = 79 \text{ plf}$$

Per UCBC-91 Table No. A-1-D and UBC-91 Table 24M the allowable shear capacity per bolt = 1 k/bolt. Therefore required spacing = 10' o.c., use 4' minimum spacing, capacity = 250 plf.

2nd Floor

$$V = \text{lesser of } \frac{1}{2}ZC_p W_d \text{ or } V=V_u D$$

N-S

$$\frac{1}{2}ZC_p W_d = 0.5 \times 0.4 \times 0.75(215^k) = 32^k$$

$$V=V_u D = 0.5 \text{ klf} \times (40'+24') = 32^k \text{ controls}$$

Therefore

$$v = 32,000/(40'+24') = 500 \text{ plf}$$

Use 3/4 bolt at 2'-0" o.c (cap=500 plf)

E-W

$$\frac{1}{2}ZC_p W_d = 0.5 \times 0.4 \times 0.75(134^k) = 20.1^k$$

$$V=V_u D = 0.5 \text{ klf} \times 2 \times 60' = 60.0^k$$

Therefore 20.1^k controls and

$$v = 20,100/(2 \times 60') = 168 \text{ plf}$$

use 4' o.c. along E-W walls (cap = 250 plf)

Out Of Plane Anchors

H/t of 2nd story = 144"/9" = 16.0 > 14 therefore unacceptable

H/t of 1st story = 168"/13" = 12.9 < 16 therefore acceptable

Spacing per UCBC-91 A110(e)3 of wall bracing is lesser of $\frac{1}{2}$ wall height or 10' therefore minimum spacing at second floor = 6'.

$$F_p = ZIC_p w_p$$

$$= 0.4 \times 1.0 \times 0.75 \times w_p = 0.3 w_p$$

$$\text{Strength } M = w l^2 / 8$$

where:

$$w = 0.3 \times 90 \text{ psf} \times 6' = 162 \text{ plf or 13.5 pli}$$

therefore:

$$M = 162 \text{ plf} \times (12')^2 / 8 = 2,916 \text{ lb-ft.}$$

$$S_{\text{req}} = M / (1.33 F_b) =$$

$$= 2,916 \times 12 / (1.33 \times 6 \times 46,000) = 1.0 \text{ in}^3$$

Select

$$TS \ 3 \times 3 \times 3/16, S = 1.14 \text{ in}^3, I = 2.60 \text{ in}^4$$

Maximum deflection per UCBC A110(e)2.= $1/10 \times 9" = 0.9 \text{ inch}$

$$\text{Defl} = 5wl^4 / (384EI)$$

$$= 5 \times 13.5(12 \times 12)^4 / (384 \times 29,000,000 \times 2.60)$$

$$= 1.0 \text{ in} > 0.9,$$

therefore

$$\text{use TS } 4 \times 4 \times 3/16, I = 6.59 \text{ in}^4, S = 3.30 \text{ in}^3$$

Connection of Strongbacks to Roof

The strongback-to-roof connection load = 162 plf $\times (12'/2) = 972 \text{ lbs}$

Therefore:

The length of diaphragm required to transfer the load = $972 \text{ lbs} / (2 \times 100 \text{ plf}) = 4.9 \text{ ft.}$, use 6 feet.

In the direction parallel to the roof framing this can be accomplished by connecting the strongbacks to the joists and connecting the joists to the diaphragm. A typical detail showing this connection is shown in Figure 12-46.

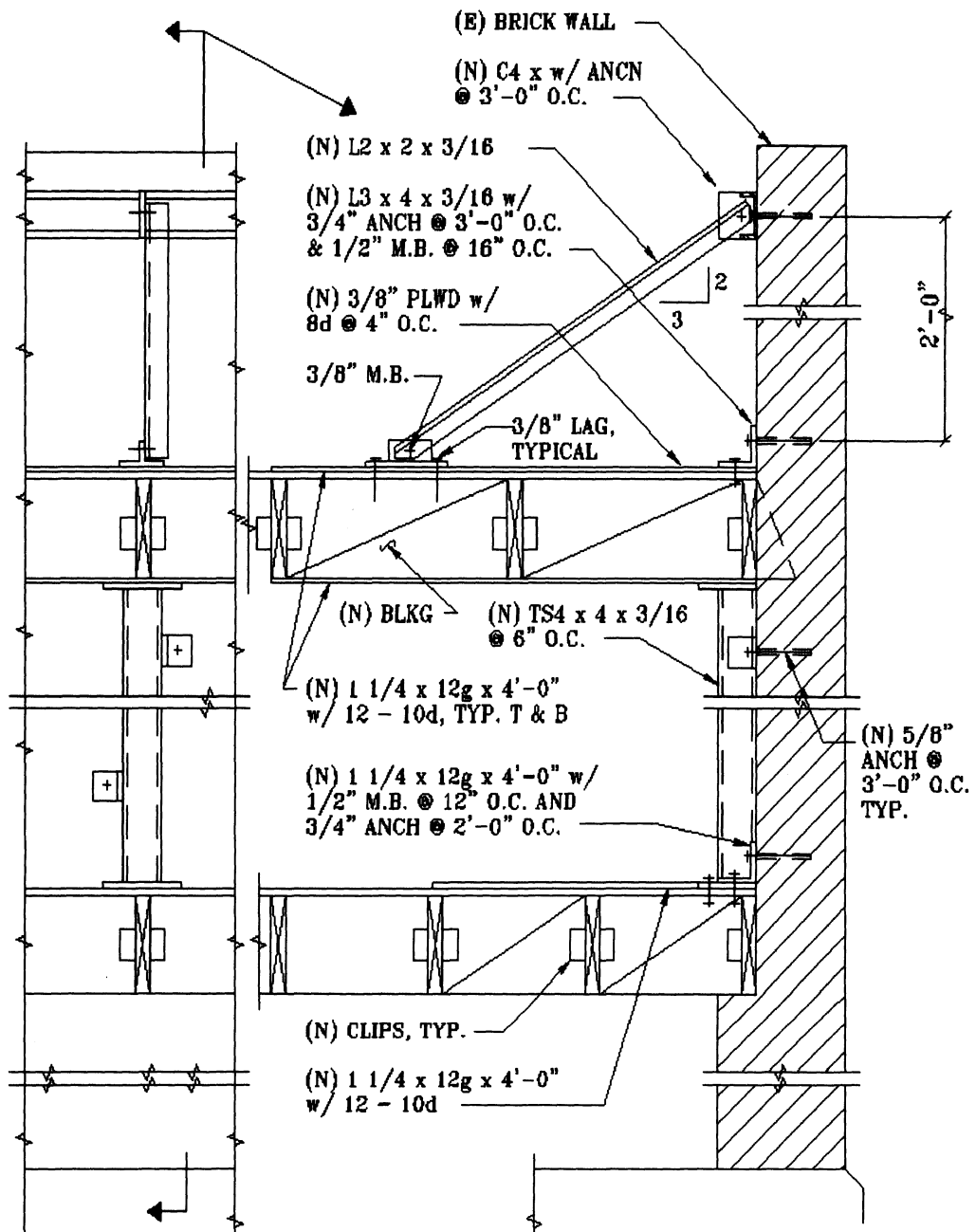


Figure 12-46. Example URM building, Strong backs on east and west walls

In the direction perpendicular to the framing blocking needs to be added such that 8 feet of diaphragm becomes engaged. Alternately plywood can be added at the end of the building reinforcing the diaphragm and permitting a reduction in the required length of the blocking. This latter option is selected as the roofing at the edge of the diaphragm needs to be removed

to install new shear connections. Figure 12-47 shows a typical detail of this connection.

Connection of Strongbacks to 2nd floor

$$\text{Connection load} = 162 \text{ psf}(12)/2 = 972 \text{ lbs}$$

The length of diaphragm required to transfer the load therefore
 $= 972 \text{ lbs}/(2 \times 500 \text{ plf}) = 1.0 \text{ ft. use } 2 \text{ ft } 8 \text{ inches.}$

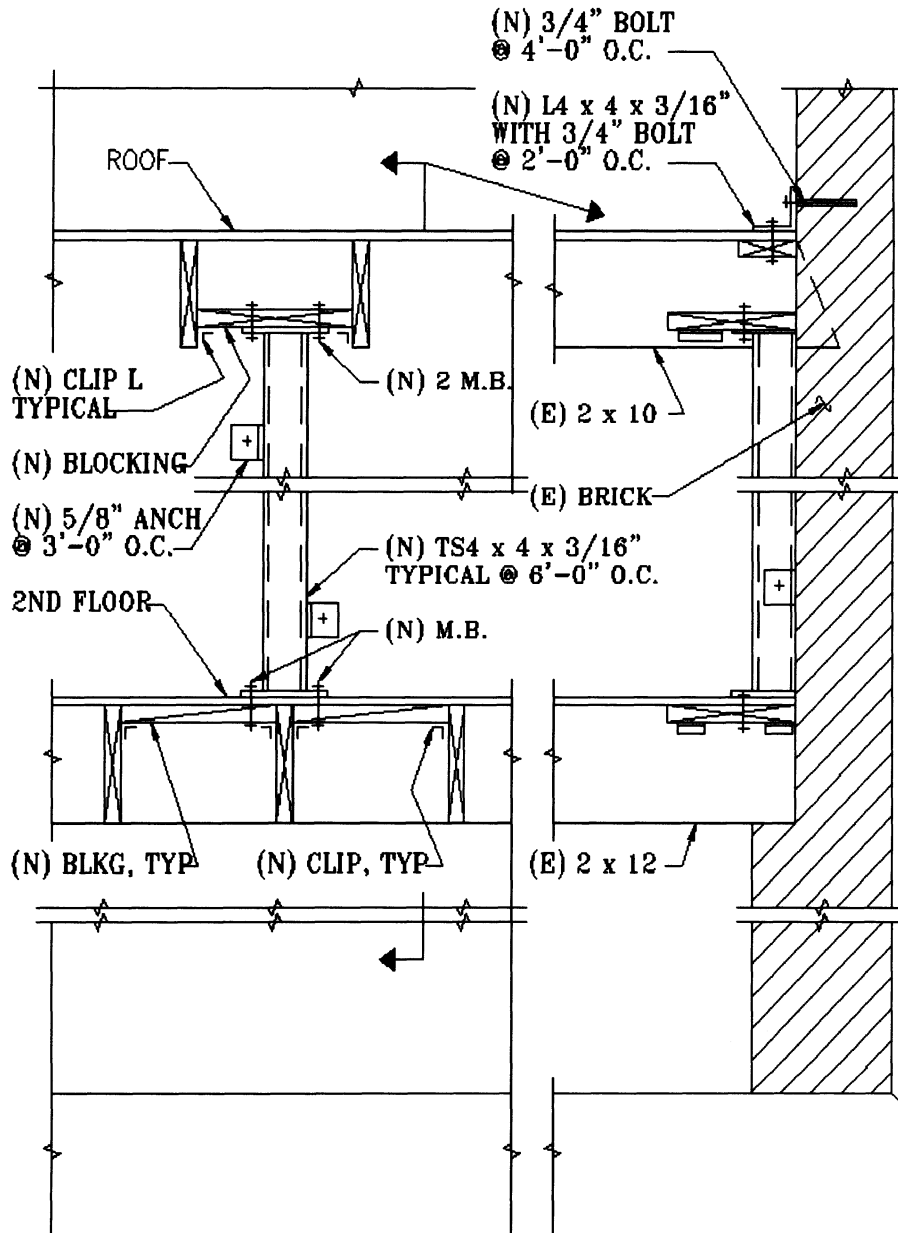


Figure 12-47. Example URM building, Strong backs on north and south walls

Parapet

Brace the parapet at 4 feet on center.

$$F_p = ZIC_p w_p,$$

$$= 0.4 \times 1.0 \times 0.75 \times w_p = 0.3 \times w_p$$

where

$C_p = 0.75$ for braced parapet per UBC-91
Table 23-P.

$$w_p = 90 \text{ psf} \times 3 \text{ ft} \times 4 \text{ ft} = 1080 \text{ lbs at 4' o.c.}$$

Therefore:

$$F_p = 0.3 \times 1080 \text{ lbs} = 324 \text{ lbs at 4' o.c.}$$

Connect the parapet to the braces with a channel spanning 4'.

$$M = w l^2 / 8 = .03 \times 90 \text{ psf} \times 2'(4')^2 / 8 = 108 \text{ lb-ft.}$$

$$S_{\text{req}} = M / (1.33 F_b) =$$

$$= 108 \times 12 / (1.33 \times .6 \times 36,000) = 0.05 \text{ in}^3$$

Check deflection

$$\begin{aligned}\text{Max Defl.} &= 0.9'' = 5wl^4/(384EI), \text{ therefore} \\ I_{\text{req}} &= 5wl^4/(.9 \times 384E) \\ &= 5 \times (.3 \times 90 \times 2/12)(4 \times 12)^4 / (0.9 \times 384 \times 29 \times 10,000,000) \\ &= 0.01 \text{ in}^4\end{aligned}$$

$$\text{use C3x4.1, } S_y = .20 \text{ in}^3, I_y = .20 \text{ in}^4$$

A typical detail of the parapet bracing is shown in Figure 12-48.

Wall Shear

An interior elevation of the west wall is shown in Figure 12-48. The wall piers will be checked for in-plane shear in accordance with UCBC Section A109(d)6.

Second Floor Piers

The wall story force distributed to the east and west walls is:

Smaller of:

$$V_R = 0.33Z(W_{wx} + W_d/2) \text{ or}$$

$$\begin{aligned}0.33ZW_{wx} + v_uD \\ W_{wx} = 51,800 \text{ lbs}/2 = 25,900 \text{ lbs}\end{aligned}$$

$$W_d = (31,200 + 12,000 + 97,200)/2 = 70,200 \text{ lbs}$$

Therefore

$$V_R = 0.33 \times 0.4 \times (25,900 + 140,200/2) = 12,700 \text{ lbs}$$

and

$$\begin{aligned}V_R = 0.33 \times 0.4 \times (25,900 + 100(40)) = 7,400 \text{ lbs} \\ \text{controls}\end{aligned}$$

In-place shear tests of the wall were performed in accordance with the provisions of UCBC-91 A106(c)3. The test shears, v_t , were determined to be 100 psi. Therefore, the allowable shear per UCBC-91 A103(b) is:

$$v_a = 0.1v_t + 0.15P_D/A$$

Pier 1

$$H_1 = 4', D_1 = 1.67'$$

$$P_{D1} = 2(1.67' + 2.5')(7')(90 \text{ psf}) = 5,254 \text{ lbs}$$

Pier 2

$$H_2 = 4', D_2 = 3.33'$$

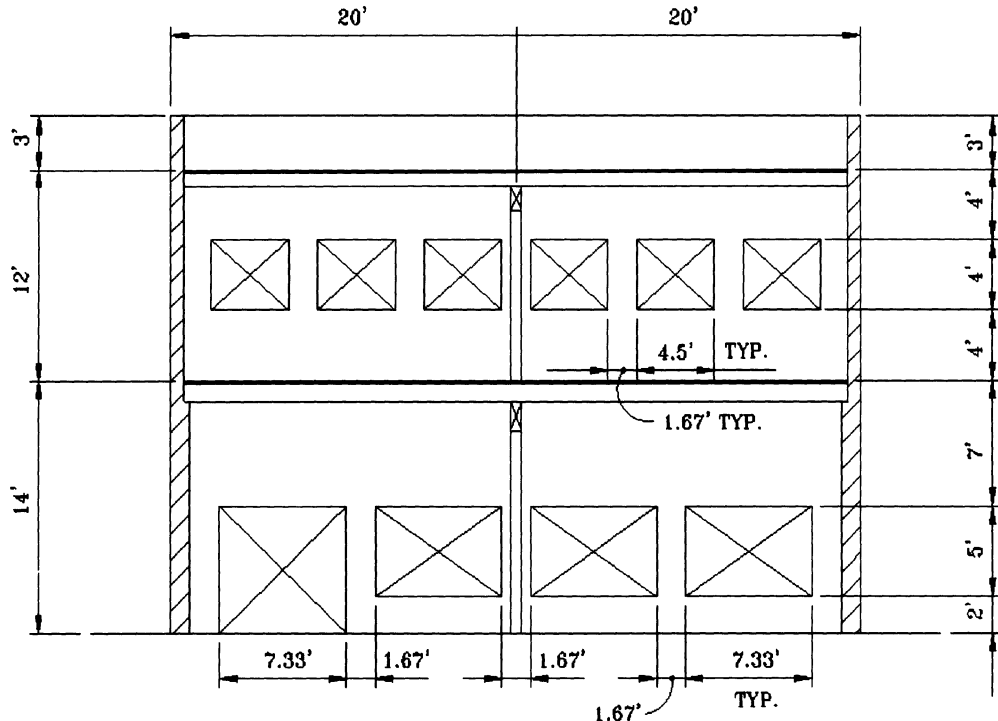


Figure 12-48. Example URM building, Interior elevation of west wall

$$P_{D2} = 2(5'+1.67')(7')(90\text{psf}) = 8,404 \text{ lbs}$$

$$\begin{aligned} v_{a1} &= 0.1(100) + (0.15)(5,254)/(1.67 \times 12 \times 9) = \\ &= 10 + 2.2 = 14.4 \text{ psi} \end{aligned}$$

$$\begin{aligned} v_{a2} &= 0.1(100) + (0.15)(8,404)/(1.67 \times 12 \times 9) = \\ &= 10 + 7.0 = 17.0 \text{ psi} \end{aligned}$$

The shear capacity V_a , and the rocking shear capacity V_r are calculated:

$$\begin{aligned} V_{a1} &= v_{a1} \times D_1 \times t = 14.4 \text{ psi} \times (1.67' \times 12 \times 9) = \\ &= 2,597 \text{ lbs} \end{aligned}$$

$$\begin{aligned} V_{a2} &= v_{a2} \times D_2 \times t = 17.0 \text{ psi} \times (1.67' \times 12 \times 9) = \\ &= 3,066 \text{ lbs} \end{aligned}$$

$$\begin{aligned} V_{r1} &= 0.5 P_{D1} \times D_1 / H_1 = 0.5 \times 5,254 \text{ lbs} \times (1.67'/4') = \\ &= 1,097 \text{ lbs} \end{aligned}$$

$$\begin{aligned} V_{r2} &= 0.5 P_{D2} \times D_2 / H_2 = 0.5 \times 8,404 \text{ lbs} \times (1.67'/4') = \\ &= 1,754 \text{ lbs} \end{aligned}$$

Therefore, rocking capacity controls for both piers and the total wall capacity =

$$\begin{aligned} 2 \times V_{r1} + 5 \times V_{r2} &= 2(1,097 \text{ lbs}) + 5(1,754 \text{ lbs}) \\ &= 10,964 \text{ lbs} > 7,400 \text{ lbs wall demand,} \\ &< 7,200 \text{ lbs wall demand,} \\ \therefore \text{the wall is adequate} \end{aligned}$$

The first floor is checked in a similar manner and the west wall was found inadequate. The north, south and east walls at

both stories were also evaluated and found to be adequate.

Add Braced Frame at West Wall

A braced steel frame is to be added behind the west wall to transfer the shear from the roof and second floor diaphragms to the foundation. A chevron braced frame and a concentric braced frame configuration were considered. The chevron braced frame required two very large 70 lbs/ft beams spanning 20 feet across the top of the chevrons (one at the roof and one at the second floor) to resist the vertical load component of the tension brace should the compression brace buckle. The concentric braced frame was therefore selected as the center post required a modest TS 5×5 center post (at 12 lbs per foot). Details of the braced frame are shown in Figure 12-49.

The dead weight of the end wall and tributary floor loads were checked and found sufficient to resist the overturning of the braced frame. Column elements were added at the south east wall and center pilaster and connected to the masonry to mobilized the dead load. The columns were designed continuous from the foundation through the second floor framing to below the roof. Steel angles were utilized as column elements at the center pilaster with the outstanding legs passing around the existing 8 by 20 in. beam to provide continuity of the column through the second floor.

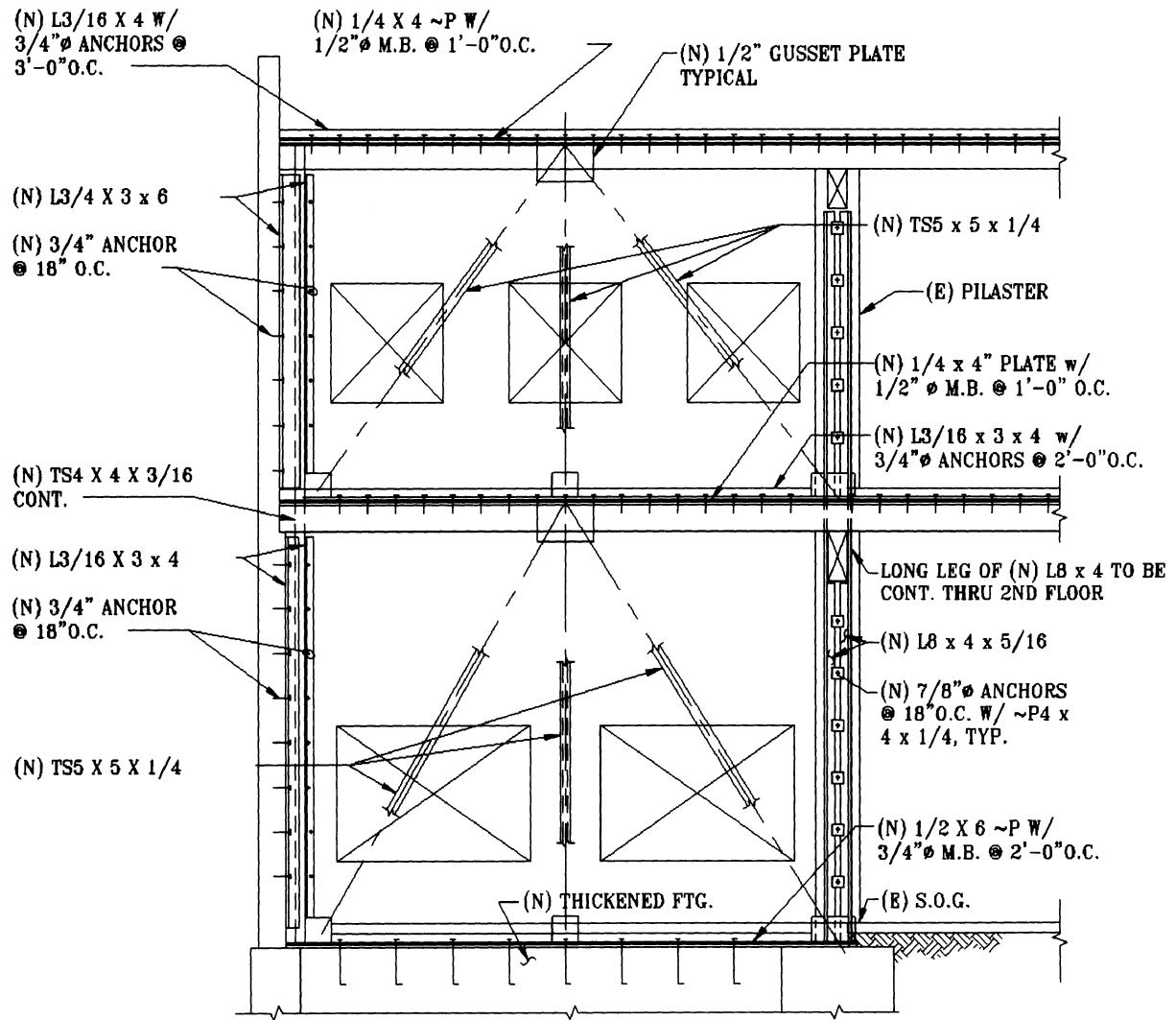


Figure 12-49. Example URM building, steel braced frame

REFERENCES

- for Buildings". TM 5-809-10, NAVFAC P-355, AFM88-3 Chap. 13.
- 12-1 Federal Emergency Management Agency (1997), *NEHRP Guidelines for the Seismic Rehabilitation of Buildings*, FEMA-273, Washington, D.C.
- 12-2 Federal Emergency Management Agency (1997), *NEHRP Commentary on the Guidelines for the Seismic Rehabilitation of Buildings*, FEMA-274, Washington, D.C. Seismology Committee, Structural Engineers Association of California. 1990. "Recommended Lateral Force Requirements and Commentary." Sacramento, CA 95819-0440
- 12-3 Applied Technology Council (1996), *Seismic Evaluation and Retrofit of Concrete Buildings*, ATC-40, Volume 1 and 2, Report No. SSC 96-01, Seismic Safety Commission, Redwood City, CA.
- 12-4 Seismology Committee, Structural Engineers Association of California. 1990. "Recommended Lateral Force Requirements and Commentary." Sacramento, CA 95819-0440
- 12-5 International Conference of Building Officials (1997), *Uniform Building Code*, Whittier, CA.
- 12-6 International Code Council, *International Building Code 2000*, Falls Church, Virginia, 2000.
- 12-7 Applied Technology Council. 1978. "Tentative Provisions for the Development of Seismic Regulations for Buildings." NBS SP-510. Palo Alto, CA.
- 12-8 Naeim, F. and Anderson, J.C. (1985), "Ground Motion Effects on the Seismic Response of Tall Buildings," *Second Century of the Skyscraper Workshop on Earthquake Loading and Response*, Chicago, Illinois, Jan.
- 12-9 Newmark N.M. and Hall W.J. 1982. "Earthquake Spectra and Design." Earthquake Engineering Research Institute. Oakland, CA.
- 12-10 ABK Joint Venture. 1984. "Methodology for Mitigation of Seismic Hazards in Existing Unreinforced Masonry Buildings. The Methodology." Topical Report 08. National Science Foundation. Washington, D.C.
- 12-11 International Conference of Building Officials. 1991. "Uniform Code for Building Conservation. Appendix Chapter 1." Whittier, CA.
- 12-12 Applied Technology Council. 1988. "Rapid Visual Screening of Buildings for Potential Seismic Hazards." Federal Emergency Management Agency. Washington, D.C.
- 12-13 Building Seismic Safety Council. 1992. "NERHP Handbook for the Seismic Evaluation of Existing Buildings." Federal Emergency Management Agency. Washington, D.C.
- 12-14 Departments of the Army, the Navy and the Air Force. 1982. "Technical Manual Seismic Design
- for Buildings". TM 5-809-10, NAVFAC P-355, AFM88-3 Chap. 13.
- 12-15 Applied Technology Council. 1991. "Development of Recommended Guidelines for Seismic Strengthening of Existing Buildings: Phase I, Issue Identification and Resolution", ATC-28 Interim Report.
- 12-16 American Plywood Association, February 5 1985 *Stapled Sheet Metal Blocking*, John R. Tissel,
- 12-17 Applied Technology Council. 1981. "Guidelines for the Design of Horizontal Wood Diaphragms", ATC-7.
- 12-18 Beyer, Donald E., 1988. *Design of Wood Structures*, McGraw Hill, Second Edition.

Chapter 13

Design of Nonstructural Systems and Components

John D. Gillengerten, S.E.

Senior Structural Engineer, Office of Statewide Health Planning and Development, State of California.

Key words: Nonstructural Components, Bracing, Seismic Restraint, Architectural Components, Mechanical And Electrical Component Bracing, Bracing Of Pipes, Ducts, Conduits, Nonstructural Performance Objectives

Abstract: For the majority of buildings, the nonstructural components represent a high percentage of the total capital investment. Failure of these components in an earthquake can disrupt the function of a building as surely as structural damage, and can pose a significant safety risk to building occupants as well. Past earthquakes have dramatically illustrated the vulnerabilities of the nonstructural components. Apart from the falling hazard posed by the light fixtures, non-structural failures can create debris that can block egress from the building, and hamper rescue efforts. In this Chapter, we deal chiefly with those components and systems that are installed in the structure during construction or remodel, for which design details are provided on the construction documents. We will touch briefly on the contents and equipment items that the owner or occupants may place in the building. The failure of these items may pose a significant risk to the occupants of the structure. However, these items are diverse, and the designer should address their anchorage and bracing on a case-by-case basis. Nonstructural elements can generally be divided into architectural, mechanical, and electrical systems and components. Architectural components include items such as exterior curtain walls and cladding, non-load bearing partitions, ceiling systems, and ornaments such as marquees and signs. Mechanical components and systems include boilers, fans, air conditioning equipment, elevators and escalators, tanks and pumps, as well as distributed systems such as HVAC (Heating, Ventilation, and Air Conditioning) ductwork and piping systems. Electrical components include transformers, panels, switchgear, conduit, and cable tray systems. Components may be mounted at grade (on the ground floor or basement of a building) or installed on the upper levels or roof of the structure. Our focus is on "nonstructural components" as opposed to "nonbuilding structures". Nonstructural components consist of equipment and systems that are supported vertically and laterally by a structural framework independent of the component itself -- a piece of equipment supported by a building frame, for example. In addition, we will consider the anchorage and bracing of moderately sized components at or below grade, such as chillers, pumps, and fans.

13.1 INTRODUCTION

For the majority of buildings, the nonstructural components represent a high percentage of the total capital investment. Failure of these components in an earthquake can disrupt the function of a building as surely as structural damage, and can pose a significant safety risk to building occupants as well. Past earthquakes have dramatically illustrated the vulnerabilities of the nonstructural components. Figure 13-1 illustrates the collapse of a suspending ceiling system in the 1971 San Fernando Earthquake. Apart from the falling hazard posed by the light fixtures, failures of this nature create debris that can block egress from the building, and hamper rescue efforts. Figure 13-2 shows a heavy rooftop tank that fell from its saddle mounts in 1994 Northridge Earthquake. Failure of this tank flooded the lower levels of the building.

In this Chapter, we deal chiefly with those components and systems that are installed in the structure during construction or remodel, for which design details are provided on the construction documents. We will touch briefly on the contents and equipment items that the owner or occupants may place in the building. The failure of these items may pose a significant risk to the occupants of the structure, as illustrated in Figure 13-3. However, these items are diverse, and the designer should address their anchorage and bracing on a case-by-case basis.

Nonstructural elements can generally be divided into architectural, mechanical, and electrical systems and components. Architectural components include items such as exterior curtain walls and cladding, non-load bearing partitions, ceiling systems, and ornaments such as marquees and signs. Mechanical components and systems include



Figure 13-1. Damaged suspended ceiling and light fixtures, Olive View Hospital, San Fernando Valley Earthquake of 1971 (Steinbrugge Collection, Earthquake Engineering Research Center, University of California, Berkeley.)

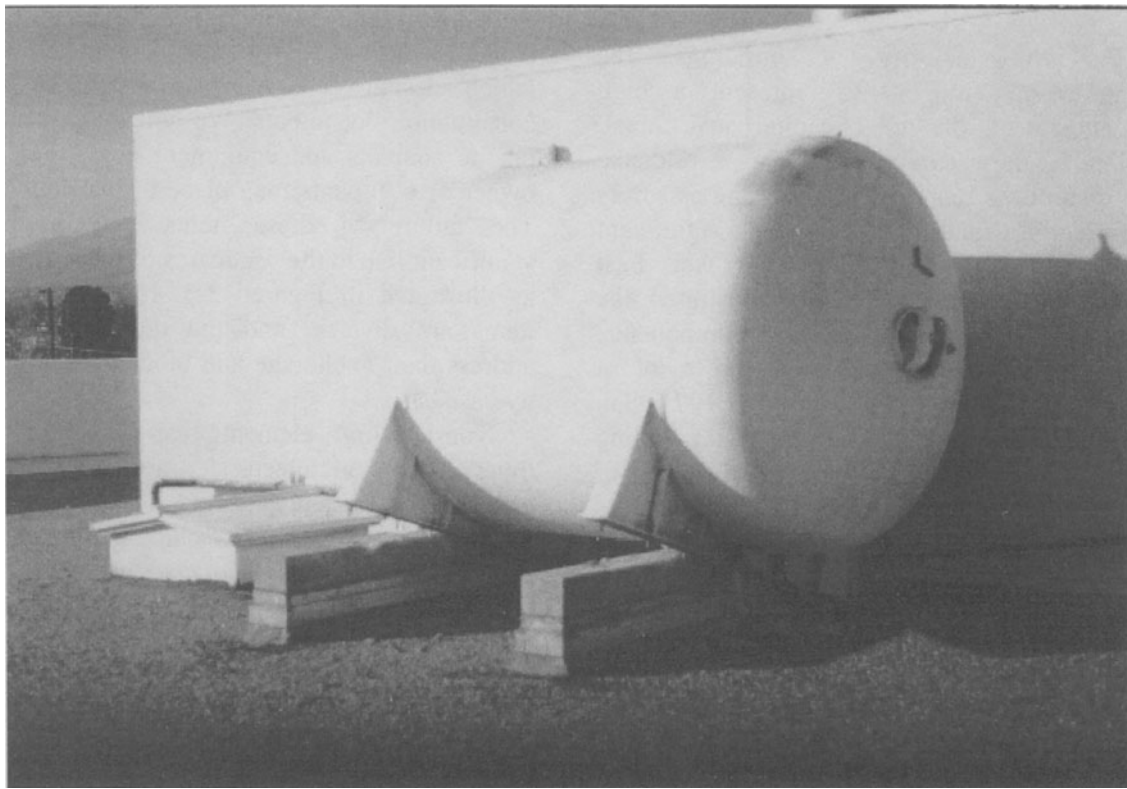


Figure 13-2. Rooftop tank failure, 1994 Northridge Earthquake

boilers, fans, air conditioning equipment, elevators and escalators, tanks and pumps, as well as distributed systems such as HVAC (Heating, Ventilation, and Air Conditioning) ductwork and piping systems. Electrical components include transformers, panels, switchgear, conduit, and cable tray systems. Components may be mounted at grade (on the ground floor or basement of a building) or installed on the upper levels or roof of the structure.

Our focus is on “nonstructural components” as opposed to “nonbuilding structures”. Nonstructural components consist of equipment and systems that are supported vertically and laterally by a structural framework independent of the component itself -- a piece of equipment supported by a building frame, for example. In addition, we will consider the anchorage and bracing of moderately sized components at or below grade, such as chillers, pumps, and fans.



Figure 13-3. Overturned library shelves

Nonbuilding structures are supported on or below grade, and do not rely on another structure for vertical and lateral stability. Examples of nonbuilding structures include large industrial boilers and machinery, cooling

towers, industrial storage rack systems, pressure vessels, and tanks. There are wide variations in the construction and dynamic properties of nonbuilding structures. Components such as pressure vessels, boilers, and chillers may be rigid structures, massively constructed with little inherent ductility. Seismic response of these components is often characterized by sliding or overturning at the level of connection to the ground. When damage occurs to these components, it is often concentrated in the connections or anchor bolts. At the opposite end of the spectrum are structures such as cooling towers, which are often flexible and highly redundant, with behavior quite similar to that for buildings.

The development of seismic design provisions for nonstructural components has lagged behind that of primary structural system. Until the advent of seismic codes, there was no clear distinction between structural and nonstructural components. Buildings had no dedicated lateral force resisting system, relying on plaster or brick walls and partitions for lateral strength. Earthquakes in the early part of the 20th century demonstrated the vulnerability of architectural features such as unreinforced brick parapets and exterior walls. Few observations were made regarding the seismic performance of mechanical and electrical systems, which existed in rudimentary forms.

In the 1933 Long Beach Earthquake, failure of fire sprinkler piping led to some of the earliest seismic provisions for piping systems. Lateral bracing provisions were added to the 1961 Uniform Building Code, dealing chiefly with the design and attachment of architectural components. However, it was not until the 1964 Alaska and 1971 San Fernando Earthquakes that the vulnerabilities of nonstructural components and systems in modern buildings were exposed. Earthquake reconnaissance reports from these and subsequent earthquakes identified many conditions and practices that caused extensive property damage and put building occupants at risk during strong ground shaking. Building code provisions have undergone continual development,

incorporating lessons learned in these earthquakes. For example, the 1964 Alaska Earthquake demonstrated the vulnerabilities of precast concrete cladding systems. There were widespread failures of ceiling systems and mechanical equipment in the 1971 San Fernando Earthquake, and failures in piping systems in the 1994 Northridge Earthquake. After each of these events, building codes have been modified in an effort to address these vulnerabilities.

Structures that must continue in uninterrupted operation during and after an earthquake will require nonstructural component designs that exceed the levels in most building codes. In general, building codes treat equipment and systems as "black boxes", in that while the seismic design for the item is limited to anchorage and bracing, the integrity of the component itself is not expressly considered. For example, seismic design of an electrical transformer typically consists of design of the anchor bolts connecting the unit to the structure, and perhaps a check of the mounting brackets on the transformer enclosure. However, checks of the integrity of the internal components of the unit are much less common, and are not required by building codes, even though the internal components may be acceleration sensitive and vulnerable to damage at acceleration levels significantly lower than the design anchorage force. For piping systems, bracing designed to prevent a collapse of the piping system may not be sufficient to prevent leaks or occasional breaks. The next generation of building codes will apply performance-based design to the anchorage and bracing of nonstructural components. In performance based-design, the design of a components or system is controlled by the level of seismic performance desired by the owner of the structure, or mandated by the governing building official.

Section 13.2 discusses performance objectives for different nonstructural components and systems. Section 13.3 examines different aspects of the seismic behavior of nonstructural components. Section

13.4 reviews the analytical approaches in different design standards. Sections 13-5 and 13-6 discuss some of the design characteristics of architectural and mechanical components and systems that have performed well in past earthquakes.

13.2 PERFORMANCE OBJECTIVES

The basic objective of seismic design is to provide an adequate level of safety, supplying protection that is appropriate for the seismic hazard and the importance of the component or system. Beyond this basic level of safety, which protects occupants from life threatening injury or death, higher levels of performance may be demanded, to limit damage or protect against loss of function. Tables 13-1 and 13-2 from FEMA 274 provide, for a range of architectural, mechanical, electrical, and plumbing systems and components, descriptions of damage states at different performance objectives. These descriptions depict the condition of the component or system following a design level earthquake.

For new construction, the minimum design objective should be Life Safety. Nonstructural components and systems in buildings constructed to this performance objective do not pose a significant threat to life, although the building may close for repairs following a strong earthquake. The emphasis is on elimination of falling hazards, but the nonstructural elements may not be functional or repairable following a strong earthquake.

Essential facilities, such as hospitals, police and fire stations, and emergency command centers may be designed with the intent that they meet the Immediate Occupancy or Operational performance objectives. Structures designed to these performance objectives are expected to be functional during or shortly after an earthquake. Interruption of lifeline services (public utilities such as electricity, water, and sewer) may disrupt the function of buildings designed to the Immediate Occupancy objective. Structures designed to the

Operational performance objective generally have independent or back-up lifeline systems, and are not dependent on public utilities. When rehabilitating an existing structure, financial or physical constraints may limit the designer to the Hazards Reduced performance level, an objective somewhat below Life Safety.

Acceptance criteria for nonstructural components depend on the consequences of failure, and the performance level desired. For example, a water piping system may meet acceptance criteria for Life Safety if anchorage failures do not result in collapse of the system. The same installation will not meet the criteria for Immediate Occupancy, if the piping system develops leaks that will render the system inoperable. Components or systems containing significant amounts of hazardous materials require special care, since a breach may have catastrophic consequences.

Current building codes approach performance objectives indirectly. Buildings constructed to the minimum code provisions are expected to meet the Life Safety objective. Essential facilities are designed to more stringent standards. Component anchorage is designed for higher force levels, and a broader range of components may be subject to anchorage and bracing requirements. However, the desired performance objectives for essential facilities are sometimes unclear, and the relationship between the code provisions and performance objectives may not be defined.

Seismic design of nonstructural components is a balance between the potential losses versus the cost of damage mitigation measures. There are many cases where significant damage can be prevented by simply anchoring components to the floor or walls, at little cost. However, limiting damage to low levels in some components can be extremely costly. With the exception of essential facilities, economics should drive the selection of the design performance objective. An economic analysis should consider not only the direct cost of earthquake damage, but also indirect losses such as business interruption.

Table 13-1. Nonstructural Performance Levels and Damage – Architectural Components⁽¹³⁻²⁾

Component	Nonstructural Performance Levels			
	Hazards Reduced Level	Life Safety	Immediate Occupancy	Operational
Cladding	Severe damage to connections and cladding. Many panels loosened.	Severe distortion in connections. Distributed cracking, bending, crushing, and spalling of cladding elements. Some fracturing of cladding, but panels do not fall.	Connections yield; minor cracks (< 1/16" width) or bending in cladding.	Connections yield; minor cracks (< 1/16" width) or bending in cladding.
Glazing	General shattered glass and distorted frames. Widespread falling hazards.	Extensive cracked glass; little broken glass.	Some cracked panes; none broken.	Some cracked panes; none broken.
Partitions	Severe racking and damage in many cases.	Distributed damage; some severe cracking, crushing, and racking in some areas.	Cracking to about 1/16" width at openings. Minor crushing and cracking at corners.	Cracking to about 1/16" width at openings. Minor crushing and cracking at corners.
Ceilings	Most ceilings damaged. Light suspended ceilings dropped. Severe cracking in hard ceilings.	Extensive damage. Dropped suspended ceiling tiles. Moderate cracking in hard ceilings.	Minor damage. Some suspended ceiling tiles disrupted. A few panels dropped. Minor cracking in hard ceilings.	Generally negligible damage. Isolated suspended panel dislocations, or cracks in hard ceilings.
Parapets and Ornamentation	Extensive damage; some fall in nonoccupied areas.	Extensive damage; some fall in nonoccupied areas.	Minor damage.	Minor damage.
Canopies & Marquees	Extensive distortion.	Moderate distortion.	Minor damage.	Minor damage.
Chimneys & Stacks	Extensive damage. No collapse.	Extensive damage. No collapse.	Minor cracking.	Negligible damage.
Stairs & Fire Escapes	Extensive racking. Loss of use.	Some racking and cracking of slabs, usable.	Minor damage.	Negligible damage
Light Fixtures	Extensive damage. Falling hazards occur.	Many broken light fixtures. Falling hazards generally avoided in heavier fixtures (> 20 pounds)	Minor damage. Some pendant lights broken.	Negligible damage
Doors	Distributed damage. Many racked and jammed doors.	Distributed damage. Some racked and jammed doors.	Minor damage. Doors operable.	Minor damage. Doors operable.

Table 13-2. Nonstructural Performance Levels and Damage, Mechincal, Electrical, and Plumbing Systems/Components⁽¹³⁻²⁾

Nonstructural Performance Levels				
System/ Component	Elevators out of service; counterweights off rails.	Elevators out of service; counterweights do no dislodge.	Elevators operable; can be started when power available.	Elevators operate.
HVAC Equipment	Most units do not operate; many slide or overturn; some suspended units fall.	Units shift on supports, rupturing attached ducting, piping and conduit, but do not fall.	Units are secure and most operate if power and other required utilities are available.	Negligible damage.
Ducts	Ducts break loose of equipment and louvers; some supports fail; some ducts fall.	Minor damage at joints, with some leakage. Some supports damaged, but systems remain suspended	Minor damage at joints, but ducts remain serviceable.	Negligible damage.
Piping	Some lines rupture. Some supports fail. Some piping falls.	Minor damage at joints, with some leakage. Some supports damaged, but systems remain suspended.	Minor leaks develop at a few joints.	Negligible damage.
Fire Sprinkler Systems	Many sprinkler heads damaged by collapsing ceilings. Leaks develop at couplings. Some branch lines fail.	Some sprinkler heads damaged by swaying ceilings. Leaks develop at some couplings.	Minor leakage at a few heads or pipe joints. System remains operable.	Negligible damage.
Fire Alarm Systems	Ceiling mounted sensors damaged. System nonfunctional	May not function.	System is functional	System is functional
Emergency Lighting	Some lights fall. Power may not be available.	System is functional	System is functional	System is functional
Electrical Distribution Equipment	Units slide and/or overturn, rupturing attached conduit. UPS systems short out. Diesel generators do not start.	Units shift on supports and may not operate. Generators provided for emergency power start; utility service lost.	Units are secure and generally operable. Emergency generators start, but may not be adequate to service all power requirements.	Units are functional. Emergency power is provided, as needed.
Plumbing	Some fixtures broken; lines broken mains disrupted at source.	Some fixtures broken; lines broken mains disrupted at source.	Fixtures and lines serviceable; however, utility service may not be available.	System is functional. On-site water supply provided, if required.

13.3 NONSTRUCTURAL COMPONENT BEHAVIOR

Nonstructural components can be classified as deformation or acceleration sensitive. If the performance of a component is controlled by the supporting structure's deformation (typically measured by inter-story drift), it is deformation sensitive. Examples of deformation sensitive components include partitions, curtain walls, and piping systems running floor to floor. These components are often rigidly connected to the structure and span from floor to floor. Since they are vulnerable to racking and damage due to story drift, they are deformation sensitive.

When a component is not vulnerable to damage from inter-story displacements, such as a mechanical unit anchored to the floor of a structure, the component is acceleration sensitive. Acceleration sensitive components are vulnerable to shifting or overturning, if their

anchorage or bracing is inadequate. The force provisions of building codes generally produce design forces high enough to prevent sliding, toppling, or collapse of acceleration sensitive components. Many components are both deformation and acceleration sensitive, although a primary mode of behavior can generally be identified. Table 13-3, taken from FEMA 274, identifies typical nonstructural components and whether they are acceleration or deformation sensitive.

Good seismic performance of deformation sensitive components can be obtained in two ways, by limiting the inter-story drift of the supporting structure, or by designing the component or system to accommodate the expected lateral displacements without damage. For higher structural performance objectives, the drift limit criteria for deformation sensitive components may govern the design of the primary lateral force-resisting system. In addition to considering the effects of lateral

Table 13-3. Nonstructural Components: Response Sensitivity⁽¹³⁻²⁾

Component		Sensitivity		Component		Sensitivity	
		Acc.	Def.			Acc.	Def.
A. Architectural				B. Mechanical Equipment			
1.	Exterior Skin			1	Mechanical Equipment		
	Adhered Veneer	S	P		Boilers and Furnaces	P	
	Anchored Veneer	S	P		General Mfg. And Process Machinery	P	
	Glass Blocks	S	P		HVAC Equipment, Vibration Isolated	P	
	Prefabricated Panels	S	P		HVAC Equipment, Nonvibration Isolated	P	
2.	Partitions			2.	HVAC Equipment, Mounted In-line with Ductwork	P	
	Heavy	S	P		Storage Vessels and Water Heaters		
	Light	S	P		Structural Supported Vessels (Category 1)	P	
3.	Interior Veneers			3.	Flat Bottom Vessels (Category 2)	P	
	Stone, Including Marble	S	P		Pressure Piping	P	S
	Ceramic Tile	S	P		Fire Suppression Piping	P	S
4.	Ceilings			4.	Fluid Piping, not Fire Suppression		
	a. Directly Applied to Structure	P			Hazardous Materials	P	S
	b. Dropped, Furred, Gypsum Board	P			Nonhazardous Materials	P	S
	c. Suspended Lath and Plaster	S	P		Ductwork	P	S
5.	d. Suspended Integrated Ceiling	S	P				
	Parapets and Appendages	P					
6.	Canopies and Marquees	P					
7.	Chimneys and Stacks	P					
8.	Stairs	P	S				

Acc. = Acceleration-Sensitive

Def. = Deformation-Sensitive

P = Primary Response

S = Secondary Response

displacement of the primary structure, care must be taken that components and systems do not impact each other during the earthquake. Impact has been the source of widespread damage in past earthquakes. Interaction between components can be avoided by maintaining adequate clearances between flexibly supported equipment and systems. In addition, flexible couplings should be provided between rigid or braced components and those that are flexibly mounted or free to displace. Finally, displacement sensitive components and their connections must be designed to withstand their own inertial forces, generated by the earthquake.

Approximate median drift values that can be tolerated by different components are summarized in Table 13-4. The values given are median values based on recommendations in FEMA 273. These drift values are expected to generate severe damage to the nonstructural component at the Life Safety Performance Level, and moderate damage at the Immediate Occupancy Performance Level. The drifts are actual expected (unreduced) values. These deformations can be accommodated through flexible couplings, sliding joints, or through deformation of ductile elements in the component or system. The proximity of components to structural members and other systems must be considered. Distribution systems, such ducts, pipes, and conduits will “swing” between bracing points during ground shaking. Impacts between systems should be avoided, since they can cause support failures, and in piping systems, loss of contents.

Table 13-4. Drift Limits for Deformation Sensitive Components⁽¹³⁻¹⁾

Component	Performance Objective	
	Life Safety	Immediate Occupancy
Adhered Veneer	0.03	0.01
Anchored Veneer	0.02	0.01
Nonstructural Masonry	0.02	0.01
Prefabricated Wall Panels	0.02	0.01
Glazing Systems	0.02	0.01
Heavy Partitions	0.01	0.005
Light Partitions	Not required	0.01
Interior Veneers	0.02	0.01

The amount of separation between components needed to prevent interaction should be determined. When determining the amount of separation needed, both the deformations of the bracing system and the deformations of the component between bracing points need to be considered. For example, the total displacement in a piping system should consider the deformation of the pipe braces and the deformations of the pipe itself between support points under the design seismic loading.

Design standards treat various types of nonstructural components individually, but interrelationships exist between components that must be considered. Failure of one component can precipitate failure of entire systems. For example, a pipe suffering a support failure may drop on to a suspended ceiling system, which in turn could fall into an exit corridor. Conversely, a well-braced pipe rigidly attached to a flexibly mounted pump can produce undesirable performance (Figure 13-4).

Acceleration sensitive components should be anchored or braced to the structure to prevent movement under the design loading. Care must be taken that these components are not anchored in such a way as to inadvertently affect the structural system. For example, if the base of a component with significant strength and stiffness is anchored to the floor and the top of the component is rigidly braced to the floor above, it can have the unintended effect of altering the response of the structural system. An example of this type of unintended interaction between a nonstructural component and the structural system is illustrated in Figure 13-5. The nonstructural masonry partition acts as a shear wall, which can lead to an unintended redistribution of lateral load. This condition could be avoided by providing isolation joints between the masonry wall and the structural columns wide enough to prevent interaction between the two elements, while providing a sliding connection at the top of the wall, which provides out-of-plane support but allows in-plane movement.

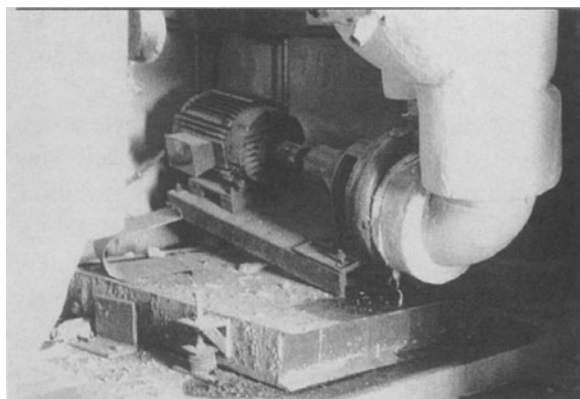


Figure 13-4. Failure of a flexibly mounted pump connected to a braced piping system, 1994 Northridge Earthquake

Components and systems mounted at or below grade respond to ground shaking in a fashion similar to buildings. The dynamic properties of the component (mass and

stiffness) and the characteristics of the ground motion (frequency content, duration, etc.) govern their response. Behavior of components on the upper floors of buildings is complicated by the interaction of the dynamic characteristics of the structure and component. In cases where the mass of the nonstructural component is large in comparison with the overall mass of the structure, the techniques presented in this Chapter should be used with great caution. Large components may have a significant effect on the overall response of the structure. Depending on the dynamic properties of the component and the supporting structure, their dynamic response may be closely coupled. In general, if the component weight exceeds 20% of the total dead weight of the floor, or exceeds 10% of the total weight of the structure, the procedures discussed in this section should not be used. In such cases, the component and the

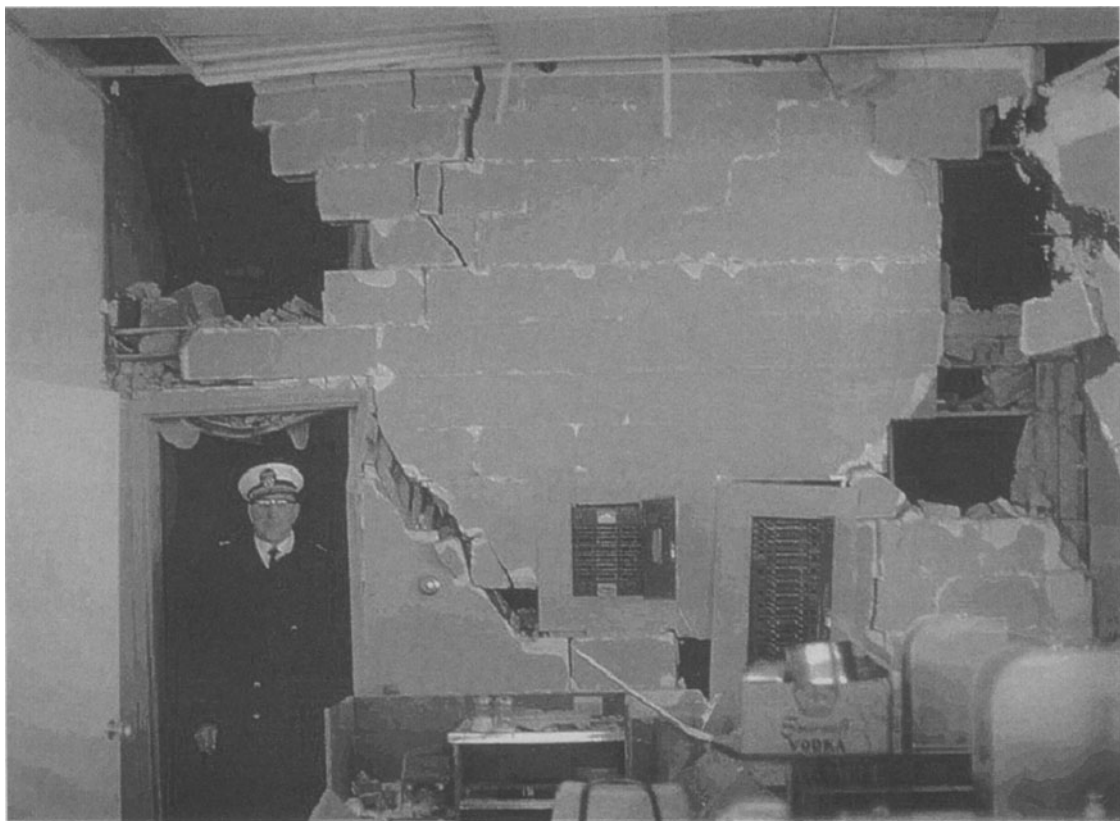


Figure 13-5. Nonstructural partition acting as a shear wall, 1964 Alaskan Earthquake. (Steinbrugge Collection, Earthquake Engineering Research Center, University of California, Berkeley.)

structure should be analyzed together, including proper representation of the flexibility of the component and its supports.

Mechanical components with rotating or reciprocating components are often isolated from the structure with vibration isolation mounts. The isolation mounts may use either rubber-in-shear, springs, or air cushions to prevent transmission of vibrations to the structure. Vibration isolation mounts can dramatically alter the dynamic properties of components, by increasing their flexibility. Seismic inertial forces on isolated components are amplified. Improperly designed vibration isolation installations can fail under the increased dynamic and impact loads. Isolation mounts must be specifically designed to resist these effects. Housekeeping pads used to support equipment should be cast monolithically with the structural slab, or be adequately reinforced and doweled to the structural slab.

The ability to survive the earthquake physically intact does not guarantee the performance objective for the component or system has been met. As noted in Tables 13-1 and 13-2, a component or system may need to be functional following an earthquake in order to meet higher performance objectives. This requires seismic design of the operating parts of mechanical and electrical components, either through dynamic testing or through analysis. Systems relying on lifelines may require on-site back-up sources of water, emergency electrical power, and waste water storage to meet the Operational objective.

13.4 DESIGN STANDARDS

The development of analytical techniques for nonstructural components has mirrored that for the primary structure of buildings. Most of these techniques use equivalent lateral force methods, where the component is designed for a lateral seismic force that is expressed as a fraction of the component weight. Deformation sensitive components are designed to accommodate the design story drifts, amplified

to the levels expected in the design earthquake. The objective of these approaches is to produce an anchorage or bracing scheme for the components that can withstand the accelerations generated by the earthquake, without allowing the component to shift or topple. In addition, the component must be able to tolerate the actual deformations of the primary structure without becoming dislodged, or adversely affecting the primary structure.

In this section we will examine the provisions of four design standards, the 1994 and 1997 editions of the *Uniform Building Code* (UBC), the *Tri-Services Manual*, and the 1997 *National Earthquake Hazards Reduction Program (NEHRP) Recommended Provisions for Seismic Regulations for New Buildings and Other Structures*, FEMA 302. These provisions provide the designer with guidance on typical nonstructural seismic issues, and may be used as resources on more complex or unusual projects.

Building codes may exempt components from anchorage and bracing requirements, depending on the level of seismic risk at the site, the occupancy of the structure, and the importance of the components. In regions of low seismicity, all components are typically exempt from seismic bracing requirements. In regions of moderate seismicity, bracing requirements are often limited to critical systems or hazardous components, such as cantilever parapets. In areas of high seismicity, furniture and components that are floor mounted and weigh less than 400 pounds are generally exempt from anchorage and bracing requirements. Items that are suspended from the wall or ceiling and weigh less than 20 pounds are also typically exempt. However, exempt unanchored components may pose a risk, and consideration should be given to restraining items that could shift or topple, both for safety reasons and to limit property loss.

All components requiring anchorage should be designed for a minimum seismic force. Seismic forces are dependent on the following factors: component weight; flexibility or stiffness of the component and/or supports;

input acceleration at the point of attachment to the structure; an importance factor based on functionality requirements or the hazard posed by the item; and the ductility, redundancy and energy absorption capability of the component and its attachments to the structure. Positive restraints must be provided, and friction forces that are induced by gravity should be ignored, because vertical ground motions may reduce the effects of gravity. The effects of prying action and connection eccentricities on anchor loads should be accounted for in the design.

13.4.1 1994 UBC/Tri-Services Manual Static Analysis

Both the 1994 UBC and the Tri-Services Manual are based on procedures presented in the 1990 edition of the Structural Engineers Association of California Seismology Committee Recommendations. In the 1994 UBC, the design lateral force for components is given by the basic formula:

$$F_p = ZI_p C_p W_p \quad (13-1)$$

where:

F_p = lateral force applied to the center of mass of the component

Z = seismic coefficient that varies depending on the seismic zone in which the structure is located, and varies from 0.075 and 0.4

I_p = component importance factor, which depends on the occupancy of the structure and varies from 1.0 to 1.5

C_p = horizontal force factor, typically equal to 0.75 for most components, 2.0 for cantilever parapets and appendages,

W_p = weight of the component.

Components are classified as flexible or rigid, depending upon their dynamic characteristics. Rigid components are those with a fundamental period of vibration less than 0.06 seconds. Flexible components are those with higher fundamental periods. The values for

C_p are amplified by a factor of 2 for flexible components, and may be reduced by 2/3 for components mounted at or below grade.

The response of components located on the upper levels is complicated by the dynamic response of the structure in the ground shaking. Seismic input motion to the nonstructural component is filtered and amplified by the structure. This can produce dramatic amplifications of lateral force demands on the component, especially if the fundamental period of vibration of the component approaches a predominant mode of vibration of the supporting structure. In the Tri-Services Manual, an effort is made to more precisely consider the amplification of the seismic response experienced by flexible equipment on the upper levels of structures.

In the Tri-Services Manual, the force equation is modified to:

$$F_p = ZI_p A_p C_p W_p \quad (13-2)$$

where

A_p = magnification factor, dependent upon the ratio of the fundamental period of the component, T_a , and the period of the building T .

The component period may be determined by

$$T_a = 0.32 \sqrt{\frac{W_p}{k}} \quad (13-3)$$

where

k = Stiffness of the equipment and/or the component supports, measured as kips per inch deflection of the center of gravity of the component, and

W_p = weight of the component, in kips.

The values of A_p vary from 1.0 to 5.0, depending on the relationship of the dynamic characteristics of the component and the supporting structure. If the dynamic properties of either the equipment or the structure are unknown, then a default value of $A_p = 5.0$ is used. For rigid components ($T_a \leq 0.06$ seconds), $A_p = 1.0$. When the period of non-rigid or

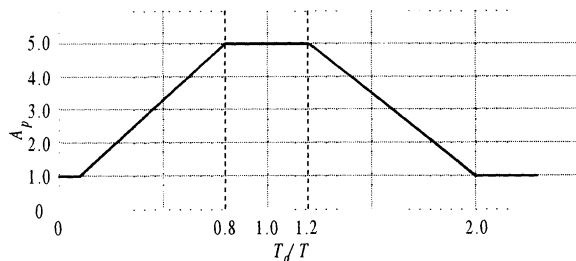
flexibly mounted equipment is not known, but the fundamental period of the building is known, estimated values of A_p may be taken from Table 13-5, taken from Freeman, (1998).

Table 13-5. Estimated Amplification Factors, A_p Nonrigid and Flexibly Supported Equipment (Reference 13-3)

Builing Period T (seconds)	< 0.5	0.75	1.0	2.0	> 3.0
A_p	5.0	4.75	4	3.3	2.7

Where the dynamic properties of the structure and the equipment are known, then the value of A_p may be computed by first determining the fundamental period of the component, T_a using Equation 13-3. Then the ratio of T_a / T is determined, and the amplification factor A_p found from the appropriate curves from Figure 13-6, taken from the Tri-Services Manual.

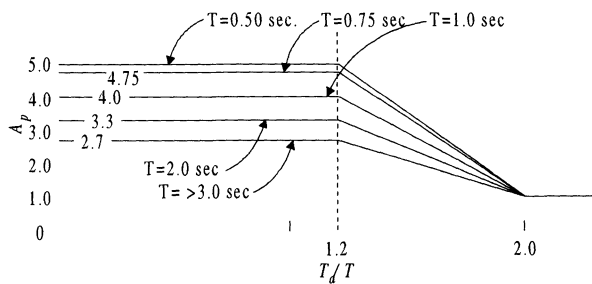
Figure 13-6 shows the relationship between A_p and the ratio of the component to structure period. For a given component, the computation of the A_p factor can be somewhat involved, since higher modes of vibration of the structure must be considered. For structures with fundamental periods less than 2 seconds, Freeman recommends that A_p factors for the first, second, and third modes of vibration be computed. For structures with periods of greater than 2 seconds, the fourth and fifth modes should also be considered. The largest value of A_p governs. The product of $I_p A_p C_p$ need not exceed 3.75.



(a) When the fundamental period of the building is equal or less than 0.5 seconds ($T \leq 0.5$)

13.4.2 1997 UBC Analysis

The 1997 UBC provisions introduced significant changes in the design procedures for nonstructural components. These changes were driven by analysis of instrument records obtained from buildings that have experienced earthquake shaking. An examination of these records indicated that buildings experience a trapezoidal distribution of floor accelerations, varying linearly from the ground acceleration at the base to 3 or 4 times the ground acceleration at the roof. Figures 13-7 and 13-8, taken from FEMA 303, plot the amplification of peak acceleration versus height in the building based on data obtained from 405 building strong motion instrument records. Figure 13-7 shows the variation of the ratio of peak structural acceleration A to peak ground acceleration A_g versus height in the building for all records. Figure 13-8 shows the variation of the ratio of peak structural acceleration A to peak ground acceleration A_g versus height in the building for records where A_g exceeded 0.10g. The accelerations in both figures are mean values plus one standard deviation. The amplification of shaking as a function of height in the building is clearly shown. Other concepts introduced in the 1997 UBC include consideration of "near fault" and soils effects, use of Strength Design level loads, and introduction of an in-structure amplification factor, a_p , which accounts for the force amplification effects experienced by flexible components.



(b) When the fundamental period of the building is greater than 0.5 seconds ($T > 0.5$). (Note: If $T_a / T < 1.2$, A_p is equal to value obtained from Table 13-5)

Figure 13-6. Amplification factor, A_p for nonrigid and flexibly supported equipment⁽¹³⁻⁵⁾

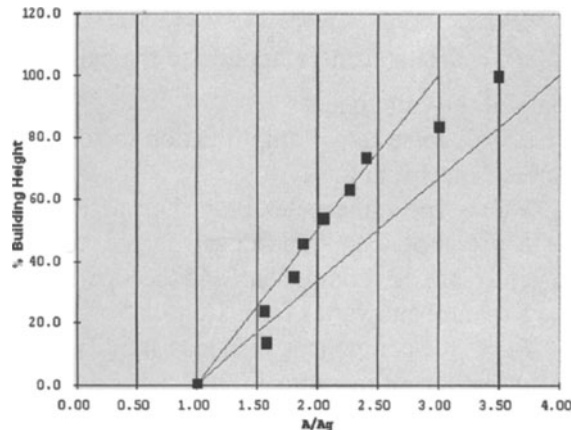


Figure 13-7. Amplification of peak ground acceleration (mean + 1 σ) vs. building height⁽¹³⁻⁷⁾

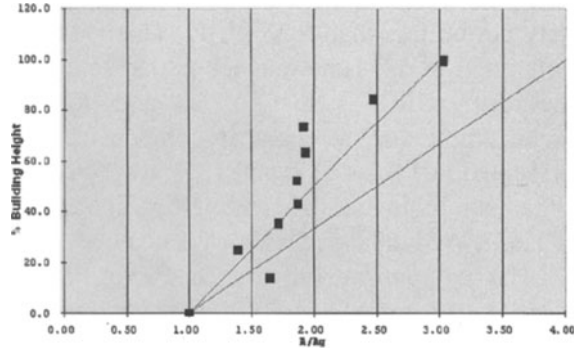


Figure 13-8. Amplification of peak ground acceleration (mean + 1 σ) vs. building height, Ag > 0.10g⁽¹³⁻⁷⁾

The design lateral force for nonstructural components in the 1997 UBC is given by

$$F_p = \frac{a_p C_a I_p}{R_p} \left(1 + 3 \frac{h_x}{h_r} \right) W_p \quad (13-4)$$

where

F_p = lateral force applied to the center of mass of the component

a_p = in-structure amplification factor, that varies from 1.0 to 2.5

C_a = seismic coefficient that varies depending on the seismic zone in which the structure is located and the proximity to active earthquake faults. C_a varies from 0.075 to 0.66

I_p = component importance factor, which depends on the occupancy of the structure and varies from 1.0 to 1.5

R_p = component response modification factor, which varies from 1.5 to 3.0

h_x = element or attachment elevation with respect to grade, h_x shall not be taken as less than 0.

h_r = the structure roof elevation, with respect to grade

F_p shall not be less than $0.7 C_a I_p W_p$, and need not exceed $4 C_a I_p W_p$.

The a_p factor accounts for the dynamic amplification of force levels for flexible equipment. Rigid components, defined as components including attachments which have a period less than 0.06 seconds, are assigned an $a_p = 1.0$. Flexible components, which are defined as components including attachments which have a period greater than 0.06 seconds, are assigned an $a_p = 2.5$. Values of R_p are assigned based on the nature of the connections to the structure, as well as the properties of the component. Components fabricated of ductile materials and attachments may be assigned a R_p of 3. Components fabricated of nonductile materials or attachments are assigned a R_p of 1.5. Where connection of the component to concrete or masonry is made with shallow expansion, chemical, or cast-in-place anchors, R_p is taken as 1.5. Shallow anchors are defined as those anchors with an embedment length to diameter ratio of less than 8. If the anchors are constructed of brittle materials (such as ceramic elements in electrical components), or when anchorage is provided by adhesive, R_p is taken as 1.0. The term "adhesive" in this case refers to connections made using surface application of a bonding agent, and not anchor bolts embedded using epoxy or other adhesives. An example of anchorage made with adhesive would be post base plates glued to the surface of the structural floor in a raised access floor system. The design forces for equipment mounted on vibration isolation mounts must be computed using an a_p of 2.5 and a R_p of 1.5. If the isolation mount is attached to the structure using shallow or

expansion-type anchors, the design forces for the anchors must be doubled.

In addition to lateral force requirements, the 1997 UBC specifies that for essential or hazardous facilities components must be designed for the effects of relative motion, if the component is attached to the structure at several points. An example would be a vertical riser in a piping system that runs from floor to floor. The component must accommodate the Maximum Inelastic Response Displacement, Δ_M , defined as:

$$\Delta_M = 0.7R\Delta_s \quad (13-5)$$

13.4.3 1997 NEHRP Analysis

The 1997 NEHRP provisions are similar in form to those in the 1997 UBC, although there are several significant differences. Many of these differences arise from the way ground shaking intensity is expressed. Rather than expressing ground shaking intensity through coefficients which are related to earthquake zones, the 1997 NEHRP expresses shaking intensity through peak spectral accelerations, which are mapped for long and short period structures. Because contour maps are used to present spectral accelerations, the increase in ground shaking intensity due to near-fault effects are directly accounted for, without the need for an additional factor in the force equation. As with the 1997 UBC, design loads are expressed at Strength Design (or Load and Resistance Factor Design) levels. Based on study of the records of instrumented buildings in areas of higher ground shaking intensity (Figure 13-8), the amplification of motion from the ground to roof levels was reduced from 4 to 3.

The design lateral force for nonstructural components in the 1997 NEHRP is given by:

$$F_p = \frac{0.4a_p S_{DS} W_p}{I_p} \left(1 + 2 \frac{z}{h} \right) \quad (13-6)$$

where

F_p = lateral force applied to the center of mass of the component

a_p = in-structure amplification factor, that varies from 1.0 to 2.5

S_{DS} = spectral acceleration, short period

I_p = component importance factor, which depends on the component and occupancy of the structure and varies from 1.0 to 1.5

R_p = component response modification factor, which varies from 1.0 to 3.5.

z = element or attachment elevation with respect to grade. z shall not be taken as less than 0.

h = the average roof height of the structure relative to grade

F_p need not be greater than $1.6S_{DS}I_pW_p$, and may not be less than $0.3S_{DS}I_pW_p$. The a_p factor is defined in the same manner as that found in the 1997 UBC. Values of a_p and R_p for architectural and mechanical components are presented in Tables 13-6 and 13-7, respectively. When combining seismic and vertical loads, the reliability/redundancy factor, ρ , is taken as 1.0.

The component Importance Factor, I_p , is taken as 1.5 for life-safety components which must function after an earthquake, components with hazardous contents, storage racks in occupancies open to the public, and all components that could effect continued operation in essential (Seismic Use Group III) structures. For all other components, I_p , is taken as 1.0.

Values of R_p in the 1997 NEHRP are assigned based on the over-strength and deformability of the component's structure and attachments. Deformability is defined as the ratio of ultimate deformation to limit deformation. Ultimate deformation is the deformation at which failure occurs, and which is deemed to occur if the sustainable load reduces to 80 percent or less of the maximum strength. Limit deformation is defined as twice the initial deformation that occurs at a load equal to 40 percent of the maximum strength. Low deformability components have deformability of 1.5 or less, and are assigned a $R_p = 1.25$. High Deformability components

Table 13-6. Architectural Component Coefficients (FEMA 302)

Architectural Component or Element	a_p^a	R_p^b
Interior Nonstructural Walls and Partitions		
Plain (unreinforced) masonry walls	1.0	1.25
All other walls and partitions	1.0	2.5
Cantilever Elements (unbraced or braced to structural frames below its center of mass)		
Parapets and cantilever interior nonstructural walls	2.5	2.5
Chimneys and stacks where laterally supported by structures	2.5	2.5
Cantilever Elements (Braced to a structural frame above its center of mass)		
Parapets	1.0	2.5
Chimneys and Stacks	1.0	2.5
Exterior nonstructural walls	1.0	2.5
Exterior Nonstructural Wall Elements and Connections		
Wall Element	1.0	2.5
Body of wall panel connections	1.0	2.5
Fasteners of the connecting system	1.25	1
Veneer		
High deformability elements and attachments	1.0	2.5
Low deformability elements and attachments	1.0	1.25
Penthouses (except when framed by an extension of the building frame)	2.5	3.5
Ceilings		
All	1.0	2.5
Cabinets		
Storage cabinets and laboratory equipment	1.0	2.5
Access floors		
Special access floors	1.0	2.5
All other	1.0	1.25
Appendages and Ornamentations	2.5	2.5
Signs and Billboards	2.5	2.5
Other Rigid Components		
High deformability elements and attachments	1.0	3.5
Limited deformability elements and attachments	1.0	2.5
Low deformability elements and attachments	1.0	1.25
Other flexible components		
High deformability elements and attachments	2.5	3.5
Limited deformability elements and attachments	2.5	2.5
Low deformability elements and attachments	2.5	1.25

^aA lower value for a_p may be justified by detailed dynamic analysis. The value for a_p shall not be less than 1.00. The value of $a_p = 1$ is for equipment generally regarded as rigid and rigidly attached. The value of $a_p = 2.5$ is for flexible components of flexibly attached components and flexible components including attachments.

^b $R_p = 1.25$ for anchorage design when component anchorage is provided by expansion anchor bolts, shallow chemical anchors, or shallow (nonductile) cast-in-place anchors or when the component is constructed of nonductile materials. Power-actuated fasteners (shot pins) shall not be used for component anchorage in tension applications in Seismic Design Categories D, E or F. Shallow anchors are those with an embedment length-to-diameter ratio of less than 8.

have deformability greater than 3.5 when subjected to four fully reversed cycles at the limit deformation, and are assigned an $R_p = 3.5$. Limited deformability components, defined as components that have neither high nor low deformability, are assigned a $R_p = 2.5$. The design force F_p for vibration isolated components must be doubled.

Component anchorage to concrete and masonry are subject to additional requirements. Anchors embedded in concrete or masonry must be proportioned to carry the least of the following:

- The design strength of the connected part, or
- Two times the force in the connected part due to the prescribed forces, or

Table 13-7. Mechanical and Electrical Component Coefficients (FEMA 302)

Mechanical and Electrical Component or Element ^c	a_p^a	R_p^b
General Mechanical		
Boilers and furnaces	1.0	2.5
Pressure vessels on skirts and free-standing	2.5	2.5
Stacks	2.5	2.5
Cantilevered chimneys	2.5	2.5
Other	1.0	2.5
Manufacturing and Process Machinery		
General	1.0	2.5
Conveyors (nonpersonnel)	2.5	2.5
Piping Systems		
<i>High deformability elements and attachments</i>	1.0	3.5
<i>Limited deformability elements and attachments</i>	1.0	2.5
<i>Low deformability elements and attachments</i>	1.0	1.25
HVAC System Equipment		
Vibration isolated	2.5	2.5
Nonvibration isolated	1.0	2.5
Mounted in-line with ductwork	1.0	2.5
Other	1.0	2.5
Elevator Components	1.0	2.5
Escalator Components	1.0	2.5
Trussed Towers (free-standing or guyed)	2.5	2.5
General Electrical		
Distributed systems (bus ducts, conduit, cable tray)	2.5	3.5
Equipment	1.0	2.5
Lighting Fixtures	1.0	1.25

^aA lower value for a_p is permitted provided a detailed dynamic analysis is performed which justifies a lower limit. The value for a_p shall not be less than 1.00. The value of $a_p = 1$ is for equipment generally regarded as rigid or rigidly attached. The value of $a_p = 2.5$ is for flexible components or flexibly attached components.

^b $R_p = 1.25$ for anchorage design when component anchorage is provided by expansion anchor bolts, shallow chemical anchors, or shallow (nonductile) cast-in-place anchors or when the component is constructed of nonductile materials. Power-actuated fasteners (shot pins) shall not be used for component anchorage in tension applications in Seismic Design Categories D, E or F. Shallow anchors are those with an embedment length-to-diameter ratio of less than 8.

^cComponents mounted on vibration isolation systems shall have a bumper restraint or snubber in each horizontal direction. The design force shall be taken as $2F_p$.

- The maximum force that can be transferred to the connected part by the component structural system.

Components must also meet requirements for relative displacements. Seismic relative displacement, D_p , is defined as

$$D_p = \delta_{xA} - \delta_{yA} \quad (13-7)$$

Where

δ_{xA} = deflection at building level x of the structure, determined by elastic analysis and multiplied by the C_d factor

δ_{yA} = deflection at building level y of the structure, determined by elastic analysis and multiplied by the C_d factor

D_p need not exceed

$$D_p = (X - Y) \frac{\Delta_{aa}}{h_{sx}} \quad (13-8)$$

Where

X = height of upper support attachment at level x as measured from the base.

Y = height of upper support attachment at level y as measured from the base.

h_{sx} = story height used in the definition of the allowable drift

Δ_{aa} = allowable story drift of for the structure

The provisions for cases where the connection points are on two separate structures are developed in a similar manner.

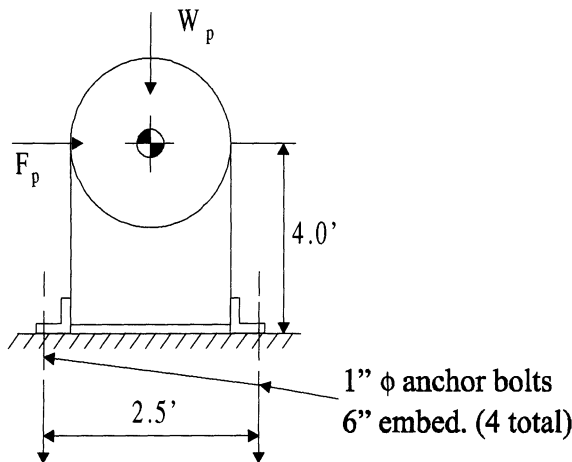


Figure 13-9. Boiler Example

Example 13-1

A steam boiler will be installed in the mechanical penthouse on the roof of a 4-story building. The dimensions of the unit are shown in Figure 13-9. The fundamental period of the boiler is 0.04 seconds. There are 4 one-inch diameter anchor bolts, one at each corner of the boiler, embedded in a concrete slab. The bolts have an embedment length of 6 inches. The building is in a region of high seismicity, UBC Seismic Zone 4. Per the 1997 UBC, the site is within 5 kilometers of a "Type B" seismic source, and located on Soil Profile Type S_D . Per the 1997 NEHRP, the 0.2 second spectral response acceleration is $S_s = 175\text{ g}$.

1. Using the 1994 UBC provisions, determine the shear and tension demands on the anchor bolts.

$$Z = 0.4 \text{ (Seismic Zone 4)}$$

$$I_p = 1.0 \text{ (Standard occupancy structure)}$$

$$C_p = 0.75$$

$$W_p = 20.0 \text{ kips}$$

The period of the component is less than 0.06 seconds, so the equipment is considered rigid. The design lateral force for the component, determined by Equation 13-1 is

$$\begin{aligned} F_p &= Z I_p C_p W_p \\ &= 0.4(1.0)(0.75)(20.0 \text{ kips}) \\ &= 0.3(20.0 \text{ kips}) = 6.0 \text{ kips} \end{aligned}$$

The shear per anchor bolt is

$$V = F_p/4 = (6.0 \text{ kips})/4 = 1.5 \text{ kips per anchor bolt.}$$

The overturning moment is

$$M_{ot} = (6.0 \text{ kips})(4.0 \text{ ft}) = 24.0 \text{ kip-ft}$$

and the resisting moment is

$$M_r = (0.85)(20.0 \text{ kips})(1.25 \text{ ft}) = 21.3 \text{ kip-ft.}$$

Note that the resisting moment is reduced 15%, to take into account the effects of vertical acceleration. Taking the sum of the moments about a corner of the base, the uplift force F_t in the anchors equals

$$F_t = \frac{24.0 - 21.3}{(2.5)(2 \text{ anchor bolts / side})} = 0.54 \text{ kips}$$

Note that the Tri-Services Manual will produce identical results, since for this case $A_p = 1.0$.

2. Using the 1997 UBC provisions, determine the shear and tension demands on the anchor bolts, assuming the bolts will be designed using Allowable Stress procedures.

$$h_x = h_r = 40 \text{ feet (roof top installation)}$$

$$I_p = 1.0 \text{ (Standard occupancy structure)}$$

$$a_p = 1.0 \text{ (rigid component)}$$

$$W_p = 20.0 \text{ kips}$$

$$l_e/d_b = 6.0/1.0 = 6 \text{ (the ratio of anchor bolt embedment length/bolt diameter)}$$

For Soil Profile Type S_D , $C_a = 0.44N_a$, where N_a is the near source factor. Our site is within 5 kilometers of a "Type B" seismic source, so $N_a = 1.0$. Therefore $C_a = 0.44$. $R_p = 1.5$, because the ratio of anchor bolt embedment depth to diameter of 6 is less than 8.

The design lateral force for the component determined by Equation 13-4 is

$$F_p = \frac{a_p C_a I_p}{R_p} \left(1 + 3 \frac{h_x}{h_r} \right) W_p$$

$$F_p = \frac{(1.0)(0.44)(1.0)}{15} \left(1 + (3) \frac{40}{40} \right) W_p$$

$$= 1.17(20.0 \text{ kips}) = 23.4 \text{ kips}$$

The shear per anchor bolt, is

$$V = F_p/4 = (23.4 \text{ kips})/4 = 5.9 \text{ kips per anchor bolt.}$$

The overturning moment is

$$M_{ot} = (23.4 \text{ kips})(4.0 \text{ ft}) = 93.6 \text{ kip-ft}$$

and the resisting moment is

$$M_r = (0.9)(20.0 \text{ kips})(1.25 \text{ ft}) = 22.5 \text{ kip-ft.}$$

Note that in this case, the resisting moment is reduced 10%, to take into account vertical accelerations. Taking the sum of the moments about a corner of the base, the uplift force F_t in the anchors equals

$$F_t = \frac{93.6 - 22.5}{(2.5)(2 \text{ anchors / side})} = 14.2 \text{ kips}$$

To convert these shear and tension forces to Allowable Stress Design levels, we divide by a factor of 1.4, to obtain

$$V = 5.9 \text{ kips}/1.4 = 4.2 \text{ kips}$$

$$F_t = 14.2 \text{ kips}/1.4 = 10.1 \text{ kips}$$

3. Using the 1997 NEHRP, determine the shear and tension demands on the anchor bolts, assuming the bolts will be designed using Allowable Stress procedures.

$$z = h = 40 \text{ feet (roof top installation)}$$

$$I_p = 1.0 \text{ (Standard occupancy structure)}$$

$$a_p = 1.0 \text{ (rigid component)}$$

$R_p = 1.25$, because the ratio of anchor bolt embedment depth to diameter is less than 8. For Soil Profile Type S_D , $S_{MS} = 1.0S_S$, and $S_{DS} = (2/3)S_{MS}$. Therefore,

$$S_{DS} = (2/3)(1.75 \text{ g}) = 1.17 \text{ g}$$

The design lateral force for the component determined by Equation 13-6 is

$$F_p = \frac{0.4a_p S_{DS} W_p}{\frac{R_p}{I_p}} \left(1 + 2 \frac{z}{h} \right)$$

$$F_p = \frac{(0.4)(1.0)(1.17)}{\frac{1.25}{1.0}} \left(1 + (2) \frac{40}{40} \right) W_p$$

$$= 1.12(20.0 \text{ kips}) = 22.5 \text{ kips}$$

The shear per anchor bolt is

$$V = F_p/4 = (22.5 \text{ kips})/4 = 5.6 \text{ kips per anchor bolt.}$$

The overturning moment is

$$M_{ot} = (22.5 \text{ kips})(4.0 \text{ ft}) = 90.0 \text{ kip-ft}$$

and the tension per bolt from overturning is

$$F_t = \frac{90.0}{(2.5)(2 \text{ anchors / side})} = 18.0 \text{ kips}$$

and the dead load tributary to each anchor bolt is

$$F_D = 20.0 \text{ kips}/4 \text{ bolts} = 5.0 \text{ kips}$$

The gravity load is reduced by $0.2S_{DS}D$ to account for the effects of vertical seismic accelerations. The net tension per bolt is

$$T = 18.0 - [5.0 - (0.2)(1.17)(5.0)] = 14.2 \text{ kips per bolt.}$$

To convert these shear and tension forces to Allowable Stress Design levels, we divide by a factor of 1.4, to obtain

$$V = 5.6 \text{ kips}/1.4 = 4.0 \text{ kips}$$

$$F_t = 14.2 \text{ kips}/1.4 = 10.1 \text{ kips}$$

The design shear and tension demands on the bolt must be doubled unless the design strength of the connected part or the maximum force that can be delivered by the component structural system limits the load to anchor bolts. An example of a mechanism that could limit the force to the bolt would be yielding of a steel base plate or bracket. For the purposes of comparison, we assume that the base plate yields at the design load.

The results obtained from the four methods are summarized in Table 13-8. Clearly, the design of rigid, acceleration sensitive components has become significantly more conservative in the 1997 UBC and NEHRP provisions. Design bolt shears in our example increase by 126% and 180% respectively, using the 1997 NEHRP and 1997 UBC. Increases in

the design uplift demands on the anchor bolts increase even more dramatically, over 18 times the 1994 UBC provisions using the 1997 UBC.

A portion of these increases can be attributed to changes in the characterization of ground shaking in regions of high seismic risk. In addition, the 1997 UBC and NEHRP provisions include factors to account for amplification of ground motion in the upper portions of structures. Finally, the 1997 provisions attempt to refine and rationalize the reduction factors (R_p). Individually, each of these changes can be justified, but collectively, they produce very conservative results, that are difficult to justify in the light of experience in recent earthquakes.

Table 13-8. Summary, Example 1 Results

Method	Bolt Shear	Bolt Tension
1994 UBC	1.5 kips	0.54 kips
Tri-Services Manual	1.5 kips	0.54 kips
1997 UBC	4.2 kips	10.1 kips
1997 NEHRP	4.0 kips	10.1 kips

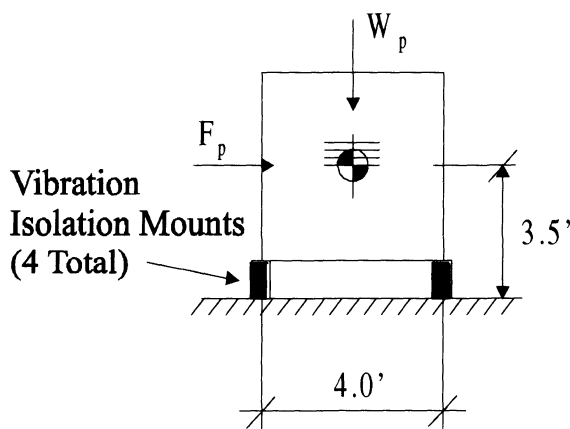


Figure 13-10. Emergency Generator Example

Example 13-2

An electrical generator is installed on the third floor of a 5-story emergency command center. The dimensions of the unit are shown in Figure 13-10. The generator is mounted on four vibration isolation mounts (one at each corner of the unit), with a lateral stiffness of 3 kips/inch each. The building floor-to-floor height is 12 feet, and the fundamental period of the building is 0.5 seconds. The building is in

UBC Seismic Zone 3, a region of moderately high seismicity, and is not in the proximity of an active fault.. Per the 1997 NEHRP, the 0.2 second spectral response acceleration is $S_s = 100\% g$. The site has been identified as Soil Profile Type S_D

1. Using the 1994 UBC provisions, determine the shear and tension demands on the vibration isolation mounts.

$$Z = 0.3 \text{ (Seismic Zone 3)}$$

$$I_p = 1.5 \text{ (essential occupancy structure)}$$

$$C_p = 0.75$$

$$W_p = 15.0 \text{ kips}$$

The period of the equipment can be estimated using equation (13-3):

$$T_a = 0.32 \sqrt{\frac{W_p}{k}}$$

$$T_a = 0.32 \sqrt{\frac{15.0 \text{ kips}}{(3.0 \text{ kips/inch})(4 \text{ mounts})}}$$

$$T_a = 0.36 \text{ seconds}$$

The period of the component is greater than 0.06 seconds, so the equipment is considered flexible and the value of C_p must be multiplied by a factor of 2. The design lateral force for the component using Equation 13-1 is

$$\begin{aligned} F_p &= Z I_p C_p W_p \\ &= 0.3(1.5)(2 \times 0.75)(15.0 \text{ kips}) \\ &= 10.2 \text{ kips} \end{aligned}$$

The shear per vibration isolation mount is

$$V = F_p / 4 = (10.2 \text{ kips})/4 = 2.6 \text{ kips per mount.}$$

The overturning moment is

$$M_{ot} = (10.2 \text{ kips})(3.5 \text{ ft}) = 35.7 \text{ kip-ft}$$

and the resisting moment is

$$M_r = (0.85)(15.0 \text{ kips})(2.0 \text{ ft}) = 25.5 \text{ kip-ft.}$$

Taking the sum of the moments about a corner of the base, the uplift force F_t in the vibration isolation mount equals

$$\begin{aligned} F_t &= \frac{35.7 - 25.5}{(4.0)(2 \text{ mounts/side})} \\ &= 1.3 \text{ kips per mount} \end{aligned}$$

2. Using the provisions of the Tri-Services Manual, determine the shear and tension demands on the vibration isolation mounts.

Since $T_a = 0.36$ seconds, the equipment is considered flexibly mounted. The ratio of component period to fundamental period of the structure is

$$\frac{T_a}{T} = \frac{0.36}{0.5} = 0.72$$

Entering the graph in Figure 13-6, we obtain a value for $A_p = 4.5$. It is unlikely that the higher modes of vibration of the building will produce a greater value of A_p . Then the design lateral force using Equation 13-2 is

$$\begin{aligned} F_p &= ZI_p A_p C_p W_p \\ &= (0.3)(1.5)(4.5)(0.75)W_p \\ &= 1.52 W_p \end{aligned}$$

However, $I_p A_p C_p$ need not exceed 3.75, which in this example governs. Substituting these values into Equation 13-2, we find

$$F_p = (0.3)(3.75)W_p = 1.13 W_p = 16.9 \text{ kips}$$

The shear per vibration isolation mount is

$$V = F_p/4 = (16.9 \text{ kips})/4 = 4.2 \text{ kips per mount.}$$

The overturning moment is

$$M_{ot} = (16.9 \text{ kips})(3.5 \text{ ft}) = 59.2 \text{ kip-ft}$$

and the resisting moment is

$$M_r = (0.85)(15.0 \text{ kips})(2.0 \text{ ft}) = 25.5 \text{ kip-ft.}$$

Summing moments about a corner of the base, the uplift force F_t in the vibration isolation mount equals

$$\begin{aligned} F_t &= \frac{59.2 - 25.5}{(4.0)(2 \text{ mounts/side})} \\ &= 4.2 \text{ kips per mount} \end{aligned}$$

3. Using the 1997 UBC provisions, determine the shear and tension demands on the vibration isolation mounts, assuming they will be designed using Allowable Stress procedures.

$$h_x = (3 \text{ floors})(12 \text{ feet/floor}) = 36 \text{ feet}$$

$$h_r = (5 \text{ floors})(12 \text{ feet/floor}) = 60 \text{ feet}$$

$$I_p = 1.5 \text{ (essential occupancy structure)}$$

$$a_p = 2.5 \text{ (flexible component)}$$

$$R_p = 1.5 \text{ (vibration isolated component)}$$

$$W_p = 15.0 \text{ kips}$$

$$N_a = 1.0 \text{ (no nearby faults)}$$

For Soil Profile Type S_D , $C_a = 0.36N_a = 0.36$. Substituting these variables into Equation (13-4), the design lateral force for the component using Equation 13-4 is

$$F_p = \frac{a_p C_a I_p}{R_p} \left(1 + 3 \frac{h_x}{h_r} \right) W_p$$

$$\begin{aligned} F_p &= \frac{(2.5)(0.36)(1.5)}{1.5} \left(1 + (3) \frac{36}{60} \right) W_p \\ &= 2.52 W_p \end{aligned}$$

However, F_p need not exceed $4C_a I_p W_p$, so

$$F_p = 4(0.36)(1.5) W_p = 2.16 W_p = 32.4 \text{ kips}$$

The shear per isolation mount is

$$V = F_p/4 = (32.4 \text{ kips})/4 = 8.1 \text{ kips per isolation mount.}$$

The overturning moment is

$$M_{ot} = (32.4 \text{ kips})(3.5 \text{ ft}) = 113.4 \text{ kip-ft}$$

and the resisting moment is

$$M_r = (0.9)(15.0 \text{ kips})(2.0 \text{ ft}) = 27.0 \text{ kip-ft.}$$

Summing the moments about a corner of the base, the uplift force F_t in the vibration isolation mount equals

$$F_t = \frac{113.4 - 27.0}{(4.0)(2 \text{ anchors / side})} = 10.8 \text{ kips}$$

To convert these shear and tension forces to Allowable Stress Design levels, we divide by a factor of 1.4, to obtain

$$V = 8.1 \text{ kips}/1.4 = 5.8 \text{ kips}$$

$$F_t = 10.8 \text{ kips}/1.4 = 7.7 \text{ kips}$$

4. Using the 1997 NEHRP/FEMA 273, determine the shear and tension demands on the vibration isolation mounts, assuming the mounts will be designed using Allowable Stress procedures.

$$z = 36 \text{ feet}$$

$$h = 60 \text{ feet}$$

$$I_p = 1.5 \text{ (essential component)}$$

$$a_p = 2.5 \text{ (flexible component)}$$

$$R_p = 2.5$$

$$W_p = 15.0 \text{ kips}$$

For Soil Profile Type S_D , $S_{MS} = 1.1S_S$, and $S_{DS} = (2/3)S_{MS}$. Therefore,

$$S_{DS} = (2/3)(1.1)(1.00 \text{ g}) = 0.73 \text{ g}$$

The design lateral force for the component from Equation 13-6 is

$$F_p = \frac{0.4a_p S_{DS} W_p}{R_p} \left(1 + 2 \frac{z}{h} \right)$$

$$F_p = \frac{(0.4)(2.5)(0.73)}{2.5} \left(1 + (2) \frac{36}{60} \right) W_p$$

$$= 0.96(15.0 \text{ kips}) = 14.4 \text{ kips}$$

Since the component is mounted on vibration isolators, the design force is doubled, so

$$F_p = (2)(14.4 \text{ kips}) = 28.8 \text{ kips}$$

The shear per isolation mount is

$$V = F_p/4 = (28.8 \text{ kips})/4 = 7.2 \text{ kips per isolation mount.}$$

The overturning moment is

$$M_{ol} = (28.8 \text{ kips})(3.5 \text{ ft}) = 100.8 \text{ kip-ft}$$

and the tension per mount from overturning is

$$F_t = \frac{100.8}{(4.0 \text{ feet})(2 \text{ mounts/side})} = 12.8 \text{ kips}$$

The dead load tributary to each isolation mount is

$$F_D = 15.0 \text{ kips}/4 \text{ mounts} = 3.8 \text{ kips}$$

The gravity load is reduced by $0.2S_{DS}D$, and the net tension per isolation mount is

$$T = 12.6 - [3.8 - (0.2)(0.73)(3.8)] = 9.4 \text{ kips per mount.}$$

To convert these shear and tension forces to Allowable Stress Design levels, we divide by a factor of 1.4, to obtain

$$V = 7.2 \text{ kips}/1.4 = 5.1 \text{ kips}$$

$$F_t = 9.4 \text{ kips}/1.4 = 6.6 \text{ kips}$$

The results obtained from the four methods for this example are summarized in Table 13-9. Again, this example shows the four methods can produce results that differ significantly. The 1994 UBC is by far the simplest method, and yields the lowest design forces. The other three methods add significant complexity, and produce higher design forces. In this example,

the higher design forces may be justified, since there have been a number of failures of vibration isolated equipment in recent earthquakes. As with Example 13-1, a portion of the increase in design force using the 1997 UBC and the 1997 NEHRP can be attributed to changes in the design ground shaking intensities. The amplification of design forces in the upper levels of the structure is in keeping with strong motion data obtained from recent earthquakes. Figure 13-8 shows that a linear amplification of ground acceleration by a factor of three from the ground to roof levels (as used in the 1997 NEHRP) bounds instrument records well, while the amplification factor of 4 used in the 1997 UBC is conservative. The 1994 UBC and Tri-Services approaches ignore this phenomenon.

Table 13-9. Summary, Example 2 Results

Method	Bolt Shear	Bolt Tension
1994 UBC	2.6 kips	1.3 kips
Tri-Services Manual	4.2 kips	4.2 kips
1997 UBC	5.8 kips	7.7 kips
1997 NEHRP	5.1 kips	6.6 kips

13.5 DESIGN CONSIDERATIONS FOR ARCHITECTURAL COMPONENTS

13.5.1 General

Architectural nonstructural components include items such as exterior curtain walls and cladding; non-load bearing partitions; ceiling systems; and ornaments such as marquees and signs. In addition, they can include a wide array of shelving, cabinets, workstations, and equipment that are installed by the building occupant.

For life safety, the objective of the design should be to limit the severity of damage to the architectural components so that they do not topple, or detach themselves from the structure and fall. For higher performance objectives, it may be necessary to control damage to the

components so that functionality is not impaired. For example, a curtain wall system that does not fall from the building or block egress may be considered to have met a life safety performance objective. For immediate occupancy, it may be necessary to limit damage of the system so that it continues to be weather-tight.

Much of the information in the following sections has been adopted from the excellent discussion of nonstructural components found in FEMA 273 and FEMA 274.

Some architectural components are inherently vulnerable to earthquake damage. For example, cracking will occur in stucco and plaster at relatively low levels of ground shaking. Limiting building drift, or providing component anchorage to protect these materials from damage, is generally not cost-effective. Much damage can be minimized through careful detailing of the components. The objective is to minimize the amount of distortion experienced by the element due story drift, and for acceleration-sensitive items, provide adequate anchorage to prevent shifting or toppling. With proper attention to detailing, damage in moderate ground shaking can be limited to a level that is easily and inexpensively repaired.

Damage to building contents outside the scope of the designer, such as furniture, countertop items (for example, computers), cabinets, and shelving can be limited by providing adequate anchorage for these items. The contents of cabinets and shelving can be restrained. However, most items that are portable are difficult to anchor effectively for seismic forces. People using these items will often prefer not to employ the seismic latches, tethers, or other restraint devices provided, since they generally make the use of the item less convenient.

13.5.2 Architectural Finishes

Plaster and stucco are common finish materials that are very brittle. At relatively low displacements, plaster begins to crack. As

displacements increase and the finish is further distorted, the material spalls, and can separate from the supporting lath. Plaster directly applied over structural elements that form part of the lateral force-resisting system is especially vulnerable. In a large earthquake, the structural elements are expected to experience inelastic behavior, and the distortions of the elements associated with this behavior will usually cause significant damage to the plaster finish. Generally, repairs to the plaster finishes are inexpensive, and the damage does not represent a significant hazard. However, failure of a large plaster or gypsum board surface, such as a ceiling, can pose both a falling hazard and block the path of egress. Ceiling systems should be designed to accommodate the expected distortions of the supporting structure without collapse. Where significant diaphragm distortions are expected, consideration should be given to isolating the furring for plaster ceilings from the diaphragm.

Shear cracking of surface finishes near doors and windows is a common form of earthquake damage, and is probably unavoidable. Although this type of damage is most common in plaster surfaces, other wall finishing materials are vulnerable. Post-earthquake repairs are relatively inexpensive, provided matching materials are available. For tile finishes, finding a suitable matching tile for repairs can be difficult.

Adhered veneer refers to thin surface materials, such as tile, thin set brick, or stone, which rely on adhesive attachment to a backing or substrate for support. This includes tile, masonry, stone, terra cotta and similar materials not over 1 inch in thickness, as well as ceramic tile and exterior plaster (stucco). These materials are supported by adhesive (not mechanical) attachment to a supporting substrate, which may be masonry, concrete, cement plaster, or a structural framework. Adhered veneers are deformation sensitive, and their seismic performance depends on the performance of the supporting substrate. Adhered veneer materials are often inherently brittle. Deformation of the substrate leads to

cracking, which can result in the veneer separating from the substrate. The key to good seismic performance is to detail the substrate so as to isolate it from the effects of story drift. The materials are most vulnerable at discontinuities, such as corners and openings.

The threat to life safety posed by adhered veneers depends on the height of the veneer, the size and weight of the fragments likely to become dislodged, and the nature of the occupancy. It is important to distinguish between falling of individual units such as tiles, which typically would not be considered a life-safety issue, and large areas of the veneer separating from the substrate and falling.

Anchored veneer consists of masonry units that are attached to the supporting structure by mechanical means. This type of veneer is both acceleration and deformation sensitive. The masonry units can be dislodged by accelerations which distorts or fail the mechanical connectors. Deformations of the supporting structure may displace or dislodge the units by racking. Damage to anchored veneers can be controlled by limiting the drift ratios of the supporting structure, isolating units from story drift through slip connections or joints, and by anchoring the veneers for an adequate force level that includes consideration of the vertical component of ground shaking. Special attention should be paid at locations likely to experience large deformations, especially at corners and around openings.

Masonry veneer facades on steel frame buildings should be avoided unless the veneer is securely tied to a separate wall or framework that is independent of the primary (gravity and lateral load carrying) steel frame. Otherwise, adequate provisions for the large expected lateral deformation of the steel frame must be made. Wire or straight rod ties should not be used to anchor face brick to a wall, especially when a layer of insulation or an air gap separates the two elements. Large masonry facades may be designed as part of the structural system.

13.5.3 Exterior Ornaments and Appendages

Exterior ornaments and appendages are nonstructural components that project above or away from the building. They include marquees, canopies, signs, sculptures, and ornaments, as well as concrete and masonry parapets. These components are acceleration sensitive, and if not properly braced or anchored can become disengaged from the structure and topple. Building codes require consideration of vertical accelerations for cantilever components. Features such as balconies are typically an extension of the floor structure, and should be designed as part of the structure. Parapets and cornices, unless well braced, are flexible components and design forces for these components should be amplified accordingly.

Heavy roof tiles pose a significant falling hazard, unless the tiles are securely attached to the roof diaphragm. One method of securing mission tiles is shown in Figure 13-11. The tie wires used to secure the tiles should be corrosion resistant.

13.5.4 Partitions

Partitions are vertical non-load bearing elements that are used to divide spaces. They may span vertically floor to floor or horizontally between cross walls. In some cases, partitions span to a hard ceiling (plaster or gypsum board), or may extend to the ceiling, and stop, with lateral bracing extending to the floor or roof structure above. Partitions may be classified as heavy or light. Heavy partitions are generally constructed of masonry materials including glass block masonry. They are self-supporting for gravity, isolated from the structural framework, and weigh in excess of 10 pounds per square foot (note that if these partitions are not isolated from the structural framework, they may behave as part of the building's lateral force resisting system). Light partitions consist of wood or metal studs covered with gypsum board, lath and plaster, or wood. Light partitions typically weigh less than 10 pounds per square foot.

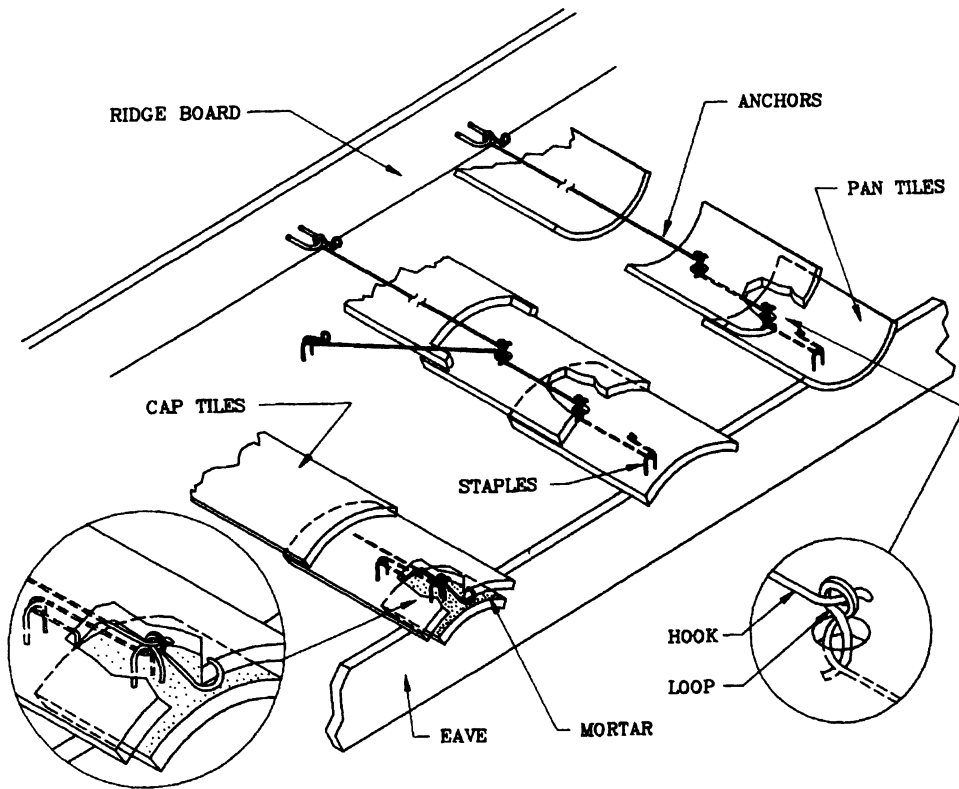


Figure 13-11. Roof tile anchor details

Partitions are acceleration and deformation sensitive. Partitions spanning floor to floor will suffer shear cracking and distortion due to story drift, unless detailed to accommodate drifts without racking. If the partitions undergo significant distortions, adhered veneers can fall off. In the out-of-plane direction, high accelerations can cause flexural cracking and if the top or bottom connections to the structure fail, collapse. If partitions are isolated from the supporting structure or are free standing, they become acceleration sensitive.

Seismic performance of partitions is controlled by attachment of the finish materials, and the support conditions at the floor or roof structure and ceiling system. The top connection should allow for vertical movement of the floor or roof structure and horizontal in-plane motion, but resist out of plane forces. Partitions in buildings with flexible structural frames should be anchored to only one structural element, such as a floor slab, and separated by a physical gap from all other

structural elements. Reinforced masonry partitions tied to more than one structural element should be considered part of the structural system. Unreinforced masonry should not be used for partitions or filler walls.

Connections at the top of the partition should accommodate in plane movement, but provide out of plane support. A gap, with an adequately sized resilient filler (if necessary for sound or fire separation), should isolate the structural frame from the nonstructural partition walls. Figure 13-12 illustrates one method of providing this separation for heavy partitions, while at the same time bracing the wall against out-of-plane motion. Figures 13-13 and 13-14 illustrate methods of bracing full and partial height light partitions. Partial height partitions should never be laterally supported by suspended T-bar ceiling systems. Partitions that cross building seismic joints are particularly susceptible to damage due to differential structural movement across the joints.

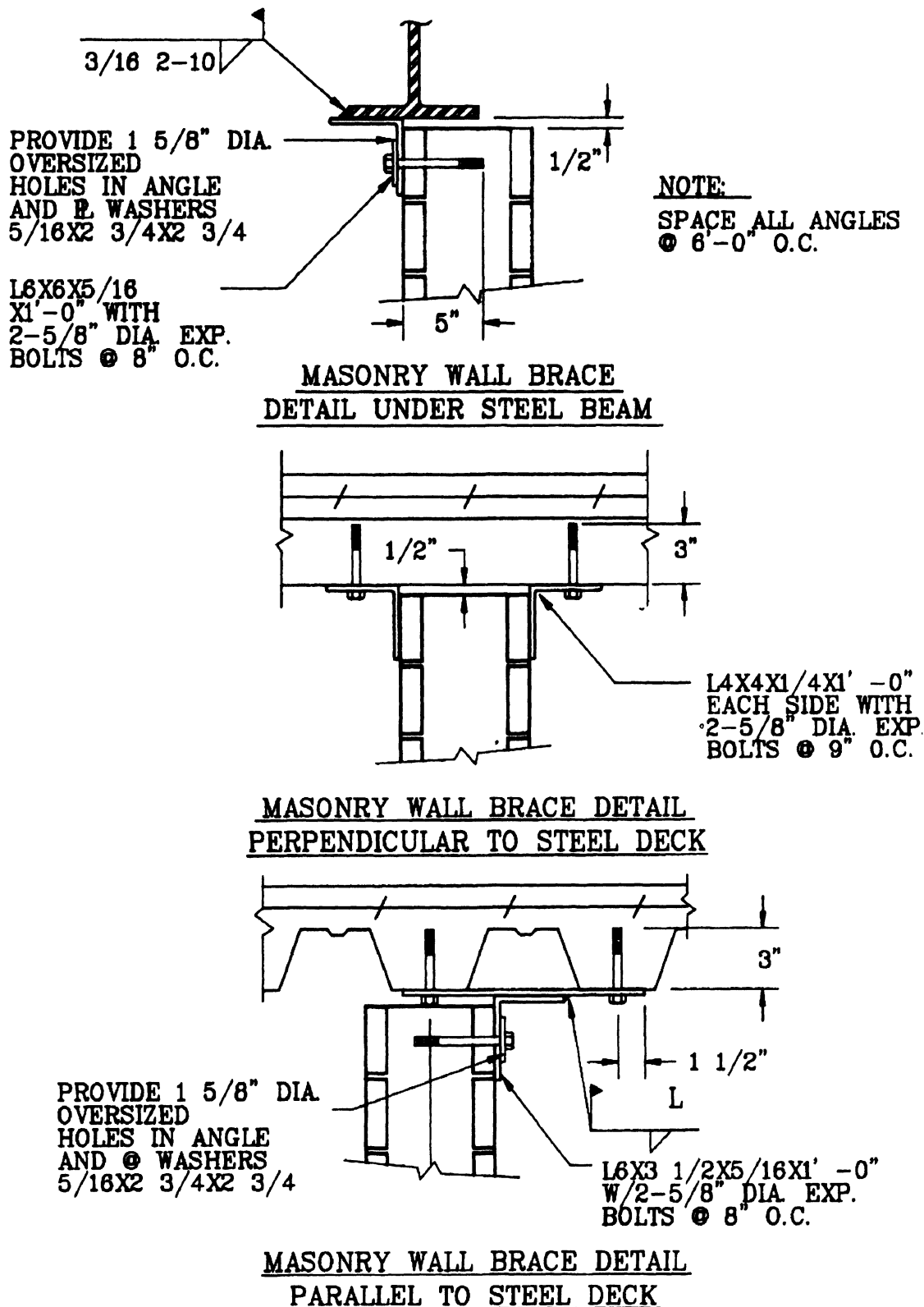


Figure 13-12. Nonbearing masonry wall details

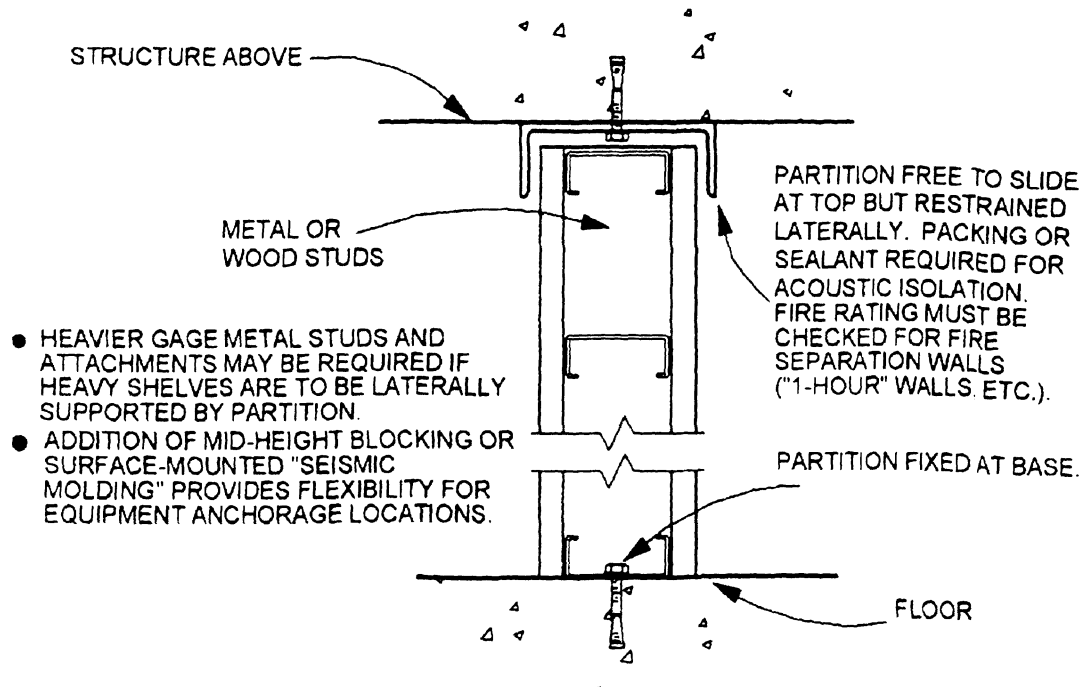


Figure 13-13. Seismic bracing for light partitions ⁽¹³⁻¹⁰⁾

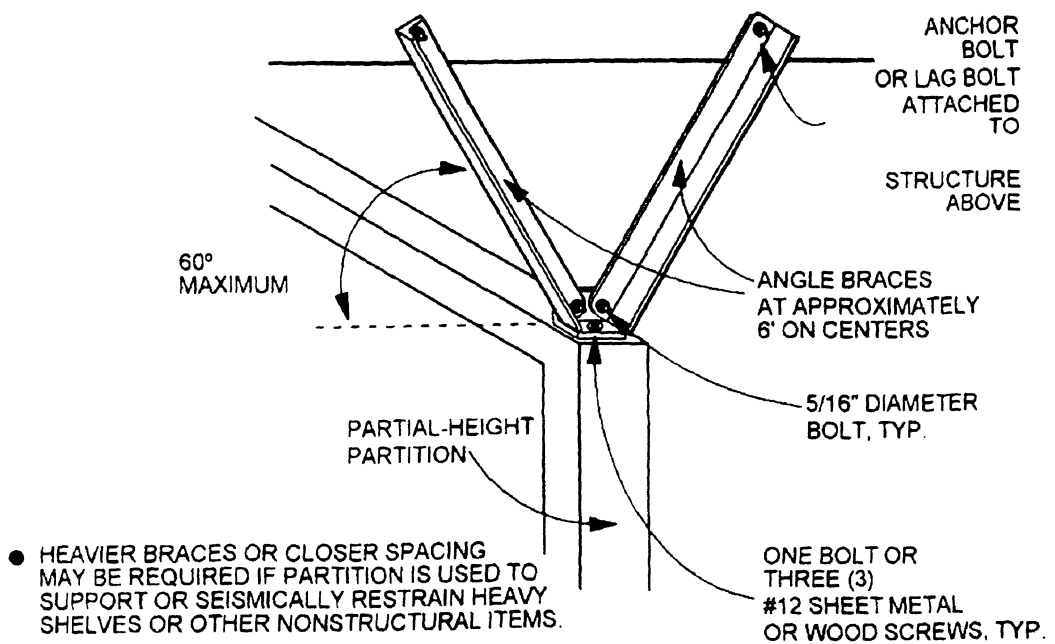


Figure 13-14. Seismic bracing for light partitions

Some modern interior planning approaches utilize nonanchored partition systems that rely upon the self-weight of the partitions, corners, or spread bases to supply stability. When subjected to seismic forces, these partitions are more susceptible to overturning than anchored systems. Decisions on their use should take into account the flexibility of such systems and their ease of installation, as opposed to the possible danger of overturning during an earthquake. Of particular importance in this regard are those systems that utilize hanging furniture or storage systems as part of the partition system. Some partitions are lightweight screens and may not necessarily cause injury or significant damage if overturned. However, other systems are more dense and heavier than full-height stud and gypsum board walls. The weight and stability of these systems must be given careful consideration in areas of high seismic risk.

13.5.5 Curtain Wall Systems

Curtain wall systems consist of prefabricated wall units and a variety of glass wall systems. Prefabricated wall systems include precast units (including units faced with an adhered or attached veneer), laminated metal faced insulating panels, unitized curtain wall systems, and steel framed panels with mechanically attached masonry, Glass Fiber Reinforced Concrete (GFRC), metal, or stone facing. These units may span vertically, from floor-to-floor or horizontally. Glass curtain wall systems include stick-framed systems assembled on site, sloped glazing and skylights, storefront systems, and structural glazing. Curtain wall systems are both acceleration and deformation sensitive, and can be dislodged by direct acceleration or failure of connections due to story drift.

Cladding units should have a minimum of four anchors per unit. Because of thermal movement and shrinkage considerations, the cladding unit connection system is generally statically determinate. Therefore, failure of a single connection can result in the cladding unit becoming unstable and falling from the

building. The consequences of an anchorage failure are potentially grave, since large precast cladding units can weigh in excess of 20 kips. Therefore, building codes require that the connections for prefabricated panels be designed for the unreduced expected story drift of the structure, and be able to resist high inertial loads in such a manner as to preclude failure. For precast concrete panels, connections are designed to ensure ductile behavior. The body of the connection, made up of steel plate or shapes, is designed for 1.33 times the design force for the panel skin. Elements of the connection that may behave in a brittle manner, such as welds, bolts, and items embedded in the concrete such as inserts and anchor bolts, are designed for 4 times the panel design force.

For panelized cladding systems, the units must be detailed in such a manner so as to permit lateral story drift of the structural frame. Units that span from floor to floor must accommodate drift through sliding or bending connections, or by rocking. Sliding connections may be detailed using bolts that slide in slotted holes. The length of the slot should equal twice the expected story drift, plus the diameter of the fastener, plus an allowance for construction tolerances. For sliding connections to be effective, the fastener should be centered in the slot, because if the bolt "bottoms out" at the end of the slot in an earthquake, extremely high shearing forces will be developed in the fastener. Connections that rely on bending in ductile elements can provide excellent performance, provided that the bending element is long enough to accommodate the expected story drifts without inelastic bending in the strain hardening range. Connections using threaded rods should be carefully designed, since the rod may suffer a low-cycle fatigue failure if subject to even moderate inelastic bending. The rocking mechanism permits cladding units to accommodate story drift by allowing vertical motions in the gravity load-bearing connections, through the use of vertical slots or oversize holes.

Special consideration should be given to the layout of joints in prefabricated wall systems.

At building corners, and when adjacent units utilize different methods for accommodating story drift, adjacent cladding units may not move in a uniform manner. Joints between cladding units may close causing adjacent panels to come into contact, imposing high loads on the panels and their anchors.

Glass curtain wall systems are typically assemblies of structural subframes attached to the main structure. They may be prefabricated or assembled on site, and include stick framed curtain walls assembled on site, prefabricated unitized curtain wall systems, storefronts, and skylights. Glazing systems are predominantly deformation sensitive, but can be damaged by high accelerations. Glazing in "dry" installations (where the glass is held in place by putty, a rubber/vinyl bead, or wood or metal stops) can shatter due to a combination of racking of the frame due to story drift coupled with out of plane forces. Failures of glazing systems in past earthquakes have been attributed to number of causes. Deficiencies in the design of the supporting frame and the cutting and placement of the glass can result in poor performance. A lack of sufficient support around the edges of the glass pane (edge bite), due to an oversized opening in the frame, or an undersized glass pane, may allow the glass to fall out. A lack of edge blocking can also allow the glass panes to shift and fall from the frame. If the glass panes are cut large, there may be insufficient clearance between pane and frame to permit racking. Frames that are attached to the structure that are not detailed to accommodate story drift will flex and twist. When frame racks due to story drift, the pane comes into contact with the frame and the glass, which cannot distort in-plane, will shatter. If the gasket around a glass pane loosens and falls from the opening, it may allow the glass to fall out, or move and shatter in the frame.

The type of glass used also affects safety. Ordinary annealed glass produces sharp-edged shards when broken. Safety (or tempered) glass is required when glass extends to within 18 inches of the ground or floor. Tempered glass fractures into small round-edged pieces, which

pose a lower hazard. Laminated glass generally remains intact, even if it cracks. Tempered or laminated glass should be used in exits or where large glazed areas front public walks.

13.5.6 Ceiling systems

Ceiling systems are horizontal and sloping assemblies attached to or suspended from the structure. At exterior locations, ceiling systems may be referred to as soffits. While there are many different architectural treatments for ceilings, structurally, they can be classified into two main categories of systems, those that are attached directly to the building structure (surface applied materials), and those that are suspended from the structure by wires or other means.

Surface applied materials consist of wood, acoustical tile, gypsum board, plaster, or metal panels applied directly to wood or steel joists, concrete slabs, or metal deck. The surface materials may be attached with mechanical fasteners or adhesive. This class of ceiling systems also includes gypsum board ceilings attached to wood or steel furring supported by a supplemental framework, braced back to the primary structure. Surface applied materials typically perform well in earthquakes, provided the structural elements supporting this system perform reasonably well.

Suspended ceilings include T-bar systems with integrated lighting and mechanical components, and suspended lath and plaster or gypsum board systems. There are a variety of suspended T-bar systems available. Most common are exposed spline systems (where the supporting T-bar frame is visible), concealed spline systems (hidden supporting frame), and luminous systems (lighting diffused through opaque panels). Suspended ceiling systems are acceleration and deformation sensitive. Seismic performance of suspended ceiling systems is controlled by the behavior of the support system, and historically concealed spline systems have performed better than exposed spline systems.

Suspended T-bar systems consist of a lightweight grid, which supports ceiling panels, light fixtures, and HVAC diffusers. These systems are highly vulnerable to damage unless the grid is securely braced with splay wires or other bracing devices and vertical compression struts (Figure 13-15). In an earthquake, the ceiling is subject to forces from light fixtures and ceiling ventilation diffusers. Sprinkler heads projecting through the ceiling may damage the panels and supports. Suspended ceiling systems in buildings with long spans and flexible structural systems are at greater risk.

Distortion of the grid can result in a loss of panels and may cause light fixtures and diffusers to drop. However, light ceiling panels that weigh less than 2 pounds per square foot do not pose a life safety risk, and are generally more of a nuisance than a hazard. Heavy items such as light fixtures and HVAC diffusers should have an independent supporting system, unless the ceiling suspension system is

designed to carry the added weight of the fixtures during an earthquake. Positive, mechanical connections should be provided to keep the object attached to the grid. In addition, heavy items supported by the ceiling system should be provided with safety wires, to prevent the items from dropping should they become detached from the supporting grid.

Standards for seismic bracing of ceiling systems have been developed⁽¹³⁻¹¹⁾. In general, a seismic bracing strategy for suspended ceiling system should provide bracing against lateral and vertical movements. The disposition of bracing should account for concentrations of mass, such as light fixtures and diffusers. The ceiling system should be rigidly attached to two adjacent walls, and permitted to "float" along the walls directly opposite those where the system is attached. This permits the walls to distort and "rack" in plan without buckling the grid or pulling it apart. Along the "floating" edges, a shelf angle provides vertical support to the ceiling. The angle must be wide enough to

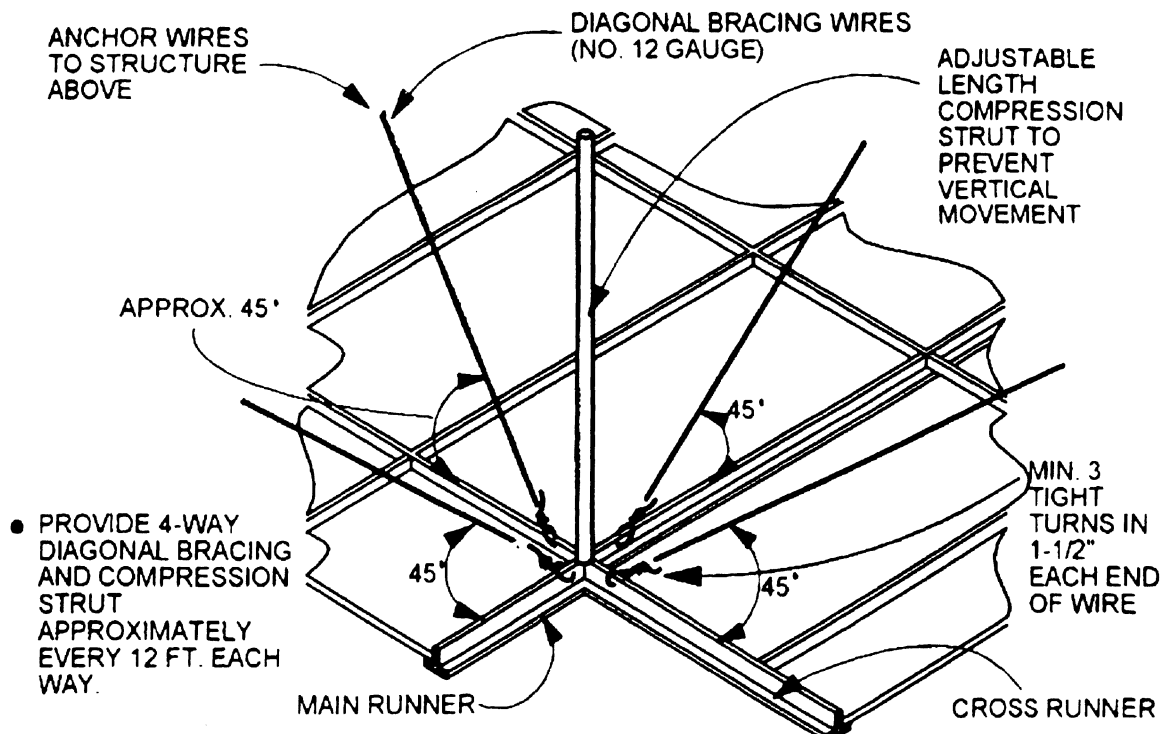


Figure 13-15. Seismic bracing for suspended T-bar ceiling systems⁽¹³⁻¹⁰⁾

allow for differential movement between opposing walls. Care must be taken to ensure that the grid is not inadvertently connected to the walls at the “floating” edge. At the perimeter of the ceiling, the main and cross runners of the ceiling grid should be supported by hangers.

The connection between the main runners and cross runners should positive, using locking clips or screws, to prevent the ceiling grid from coming apart during an earthquake. Friction-type connections should be avoided.

Suspended lath and plaster and gypsum board systems can perform well, being inherently rigid in the plane of the ceiling. However, if the ceiling system is heavy and large, careful consideration of the design and detailing is needed, because the ceiling can pose significant risk to life if it drops. Reference 13-12 outlines the seismic design requirements for rigid suspended ceiling systems. Complex installations will require special engineering.

The hanger wires supporting the ceiling must be securely attached to the structure above, and the lath properly wired to the furring channels. Proper installation of these wires is crucial to satisfactory performance. Hanger wires may unwind, break, or fail at the connection to the structure in a strong earthquake. Isolation joints must be provided at building seismic separations. Without these joints, relative movements between the structures will damage the ceiling, and in some cases, collapse of the ceiling.

Rigid ceiling systems should be braced against vertical and lateral movement at regular intervals. Where gypsum board is used, seismic performance can be enhanced by the use of steel nailing strips. If the ceiling is irregular (with changes in elevation, reentrant corners, etc.), the supporting channels should be mechanically connected with bolts, screws, or welds. Corners should be rigidly braced. The arrangement of lateral bracing should consider discontinuities in the ceiling created by rows of light fixtures or HVAC diffusers. It may be desirable to add bracing members at these discontinuities, to tie the ceiling together. Light

fixtures and diffusers should be securely fastened to the ceiling supports. The use of toggle bolts in the plaster or gypsum board for attachment of these items should be avoided.

13.5.7 Exitways, Stair, and Elevator Enclosures

Exitways, stair, and elevator enclosures include treads, risers, landings, and surrounding shafts that make up the enclosures. These enclosures can be either acceleration or deformation sensitive. If integral with the structure, stairs and enclosures must be considered in the overall design and analysis, including their contribution to overall structural stiffness and response due to bracing action. Failure of the enclosure can render the stairs or elevator unusable.

Following an earthquake, building occupants will attempt to leave the building through the exitways. Care should be used, to ensure that design features of the exitways do not impede safe egress. The doors should be designed to accommodate seismic drift, so they will not jam open or closed in an earthquake. The use of veneer or ceiling treatments that could become dislodged and fall should be avoided. The covers over seismic joints should be designed to accommodate the expected story drifts without significant damage. Light fixtures should be adequately braced for seismic loads. Stone veneers should be properly anchored to the supporting frames, and the frames should be designed to accommodate story drift without racking.

13.5.8 Building Contents

Building contents can pose a significant risk during a strong earthquake. The following section provides general information on improving the seismic performance of building contents. However, since the contents are generally furnished and installed by the owner, anchorage of these items is typically outside the scope of the design professional.

Storage racks, such as those found in warehouse stores, can pose a significant hazard. Storage racks installations should be engineered. Storage racks designed and installed in accordance with the standard of the Rack Manufacturers Institute⁽¹³⁻¹⁵⁾ have been proportioned to withstand seismic forces. Special care should be taken to protect the legs of the racks, which are vulnerable to damage from forklifts. Adequate clearance between the rack and structural elements, such as walls and columns, should be provided to prevent interaction between the rack and the building structure.

Storage cabinets, bookshelves, filing cabinets, and display cases come in a myriad of shapes and sizes. In general, items that are tall and slender should be anchored to the wall to prevent tipping. Tall furniture, and items that have glass shelves should not be placed in the path of egress. Items that may shift or topple should not be placed where they could block exit doors. Providing latches on cabinet doors, and shelf lips or face bars on open shelving, can prevent loss of contents during ground shaking.

13.6 MECHANICAL/ ELECTRICAL COMPONENTS

13.6.1 General

Mechanical and electrical components consist of equipment such as pumps, boilers, chillers, fans, transformers, and electrical switchgear, as well as distribution systems such as piping, ducts, conduits, and cable trays. Most electrical and mechanical equipment are pre-manufactured, "off the shelf" items. The characteristics of each component are developed based upon functional needs. These characteristics – such as the presence of internal spring isolators or ceramic components, determine damage potential.

When discussing seismic performance of mechanical components, it is important to

differentiate between Life Safety and Immediate Occupancy performance objectives. Functionality of the component following an earthquake is not generally a life safety issue. For the Life Safety objective, it is usually sufficient if the component does not shift or topple during an earthquake. For Immediate Occupancy, the component or system may be required to function following the earthquake. For the higher performance objectives, the component manufacturer must show through analysis or by shake-table test that the component remains functional following the prescribed level of ground shaking.

Much of the information in the following sections has been adopted from the discussion of mechanical and electrical components found in FEMA 273 and FEMA 274.

Mechanical and electrical equipment is generally acceleration sensitive. Failure modes include sliding, overturning, or tilting of items mounted on the floor or roof. Items suspended from or attached to walls or ceilings may suffer loss of support and fall. Distribution systems, such as piping, ducts or wiring connected to the unit can fail. Most equipment items are fairly robust, since they must survive the rigors of transportation and installation at the job site. However, the internal components of equipment may be blocked or restrained to prevent damage during transit. Upon removal of these restraints, the internal components of the item may be much more vulnerable to shaking damage.

Mechanical equipment and systems are either rigidly anchored to the primary structure, or installed on flexible mounts (to control vibration or permit thermal movements). The lateral capacity of rigidly mounted equipment is often governed by the capacity of the anchor bolt or fastener. Failures can also occur at the connection between the component and pipes, ducts, or conduits that connect to the component.

Vibrating mechanical equipment (typically equipment with rotating components, such as chillers, pumps or emergency generators) is often installed on resilient mounting systems,

particularly when the equipment is on the upper floors of a structure. The most common vibration isolation mounts rely on springs or elastomeric devices to limit the transmission of vibration and sound to the rest of the structure. Unless specifically designed to resist seismic forces, isolated components are vulnerable to damage at low levels of ground shaking.

13.6.2 Rigidly Mounted Components

The primary aim of seismic design for rigidly mounted components is that they remain in place. The effects of shaking on internal parts are generally not considered. If functionality of the component is critical, then a special evaluation is required. This may include seismic qualification of the internal components of the equipment through shake table testing, detailed analysis, or experience data from past

earthquakes. In this section, our focus is on anchorage issues, and the design of structural components of the equipment, such as base plates, anchor bolts, legs, braces, etc. Most equipment is not a life safety threat unless it can overturn or fall, or if failure of the component results in the interruption of a critical function or the release of hazardous materials.

The lateral capacity of rigidly mounted components can be governed by the capacity of the anchor bolts, the capacity of the unit frame or body, or by the capacity of a yielding element, such as a base plate or mounting tab. Installations with capacity governed by the anchor bolt capacity are the least desirable, but are often unavoidable. An example of a tank installation governed by anchor bolt capacity is illustrated in Figures 13-2 and 13-16. This rooftop saddle mounted tank displaced in the Northridge Earthquake. The tank itself was

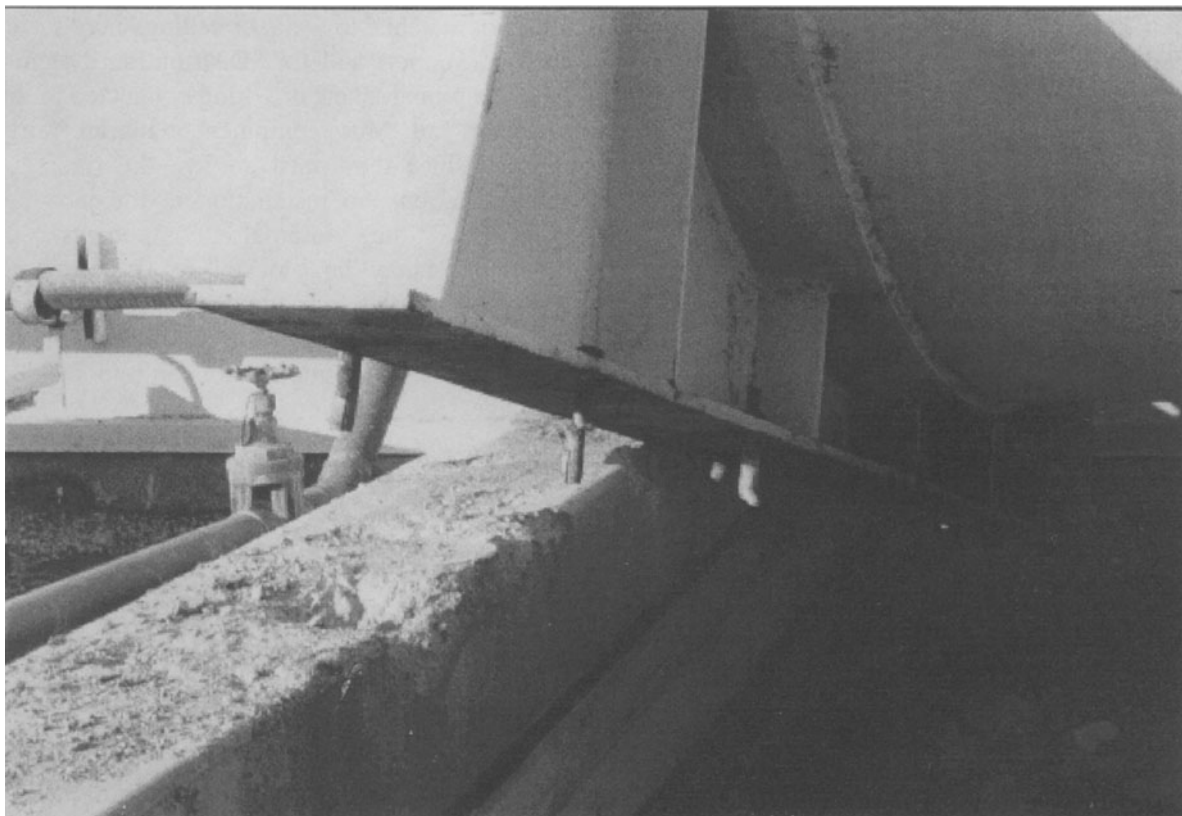


Figure 13-16. Tank in figure 13-2, expansion anchor failure

undamaged. Introduction of a yielding element in the connection could have limited the loads delivered to the anchor bolts, precluding this failure. By introducing a yielding element, such as a steel plate in weak axis bending, the designer can introduce a yielding element, providing a mechanism for the dissipation of energy and limiting the amount load that can be delivered to the anchor bolts. Where this cannot be done, the design forces for the anchor bolts should be increased, to preclude a brittle failure of the installation.

The designer should consider the load path for the seismic forces of the component. The design anchorage forces will generally be significantly higher than the design lateral forces for the primary structure or framing supporting the component. For example, a heavy air conditioning unit may be mounted on a roof diaphragm of untopped steel deck. At the point of attachment, the air conditioning unit may deliver design lateral forces to the steel deck that exceed the design shears for the roof diaphragm. The designer should check the load path – in this case, the diaphragm capacity in the immediate vicinity of the unit – for the component vertical and lateral loads. Local elements of the supporting structure should be designed and constructed for the component forces, where they control the design of the elements or their connections. When checking the supporting structure, the design forces should not be modified due to anchorage conditions. For example, using the 1997 NEHRP provisions, it would not be necessary to reduce the R_p factor due to shallow anchor bolt embedment.

In general, installations that rely on threaded pipe connections, for example, a vertical tank supported on pipe legs, should be avoided. Threaded connections are subject to low-cycle fatigue failures. Saddle mounted tanks should be restrained by straps or lugs to the supporting frame. Pipe and conduit connections to equipment should be designed to accommodate differential movement, through the use of braided or flexible connections.

13.6.3 Vibration Isolated Components

A vibration-isolated component can experience much higher seismic accelerations than the same component, rigidly mounted. This is due to the amplification effects of the vibration mounts. The dynamic characteristics of vibration-isolated equipment are dominated by the properties of the isolation mount. The fundamental period of isolated components can lengthen to the point where a resonance condition with one or more modes of the primary structure is possible. This can result in amplifications in lateral force by a factor of five or more. The key to controlling these effects is through the use of snubbers.

Isolated components can either be internally snubbed (the snubber is an integral part of the vibration isolation device) or externally snubbed (through the use of separate snubbers, installed independent of the isolation device). Regardless of the type of snubber used, it is vital that an elastomeric pad be provided to reduce the impact force generated when the component strikes the snubber. Selection of the proper elastomeric pad can be crucial, and the manufacturers' recommendations for the material should be closely followed. Research and experience has shown that the degree of force amplification due to impact can be reduced if the clearance between the component and the snubber (air gap) is limited to $\frac{1}{4}$ inch or less. The use of inertia pads above the vibration isolators should be carefully considered in the design of the system, since they can add a great deal of mass. As with fixed components, it is vital that a load path of adequate strength be provided for vibration-isolated components. Special attention should be given to the reinforcement of housekeeping slabs, and to their connection to the structural slab. Ideally, the housekeeping slabs should be cast monolithically with the structural slab. If this is not possible, sufficient dowels should be provided to transfer the lateral forces from the component to the diaphragm. The design lateral force should include any amplification effects

due to the vibration isolators, and friction due to gravity forces should be neglected.

When suspended components are mounted with vibration isolation devices, care must be taken to ensure that the bracing elements do not “short out” the vibration isolators. For example, the benefits of vibration isolation may be lost if the unit is laterally braced with steel angles to the structure. The hangers and braces must be designed for the amplified forces, and if hanger rods are used, they may need to be stiffened to prevent buckling under the compressive loads generated by the vertical component of the brace force. If the body of the component does not have sufficient strength and rigidity, a supplemental structural frame around the item may be necessary.

Flexible couplings should be provided where pipes, ducts, or conduits meet vibration-isolated systems. Figure 13-4 illustrates the results of vibration-isolated component rigidly attached to a braced pipe.

13.6.4 Piping Systems

Piping systems are predominantly acceleration sensitive, but runs between floors or buildings are deformation sensitive. Joint failures caused by inadequate support or bracing, with accompanying loss of contents under pressure, are the most common failures. Most pressure piping systems (defined as piping systems carrying fluids which, in their vapor stage, exhibit a gage pressure greater than 15 psi) are inherently ductile and have sufficient inherent flexibility to accommodate seismic motions. Attachments and braces for seismic loading are needed, particularly for large diameter pipes. Bracing in most installations is performed to prescriptive standards, such as the SMACNA and NFPA-13 guidelines^(13-13,13-14).

Flexible couplings to accommodate building movements should be provided at structural separations, as well as at the base of the structure where pipes pass from the ground into the structure. Figure 13-17 illustrates such an

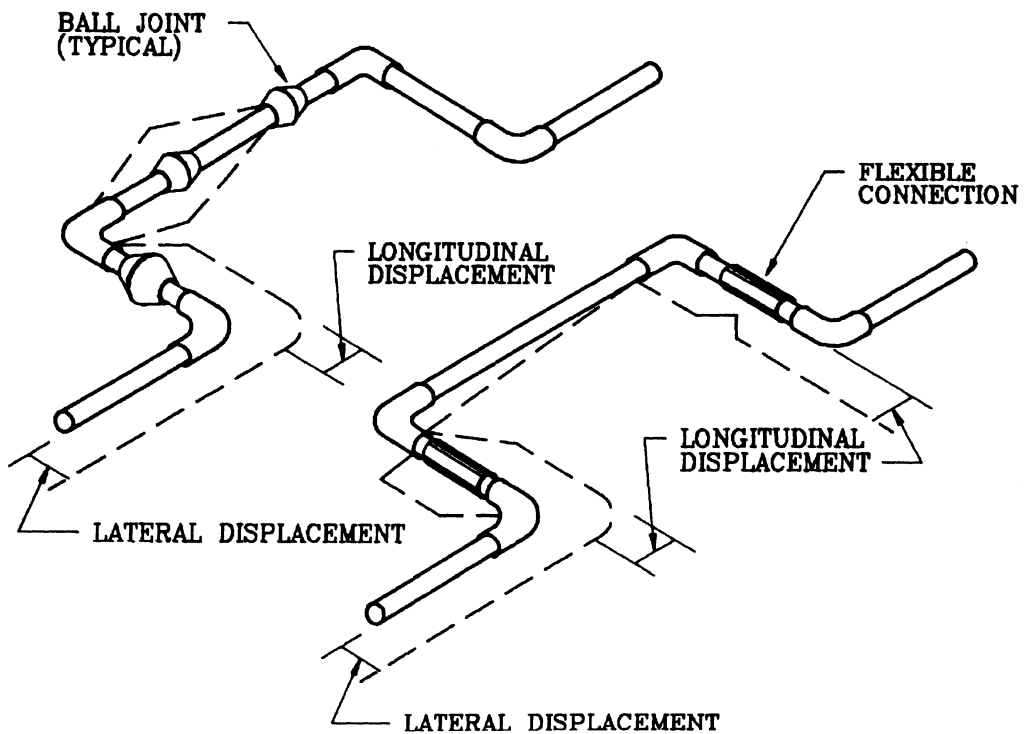


Figure 13-17. Piping details at a seismic gap

arrangement.

Damage to fire suppression piping has generally been the result of joint failures and differential movement between the piping and portions of structure. Failures have been caused by impact of branch lines and sprinkler heads on adjacent elements, such as hard ceilings. Providing sway bracing at fire sprinkler branch lines and long sprinkler drops can reduce this type of damage. Providing larger openings for the sprinkler heads in hard ceiling surfaces can prevent the ceiling from fracturing the sprinkler heads due to movement of the piping.

Sway bracing requirements for piping are specified in building codes and bracing is generally required at specified intervals, based on the size of the pipe. A typical pipe brace

installation is shown in Figure 13-18. Additional bracing should be provided at bends and elbows. Flexible couplings should be provided where piping crosses seismic separation joints, and where the piping is connected to vibration isolated equipment. Small diameter pipes that are allowed to sway should have flexible couplings installed at equipment connections. Where piping penetrates walls or floors, the pipe sleeves should be large enough to accommodate any anticipated relative movements.

The designer should note that in general, the sway bracing specified in the prescriptive standard may not prevent local leaks. If the contents of the piping system are hazardous, a more detailed analysis is warranted.

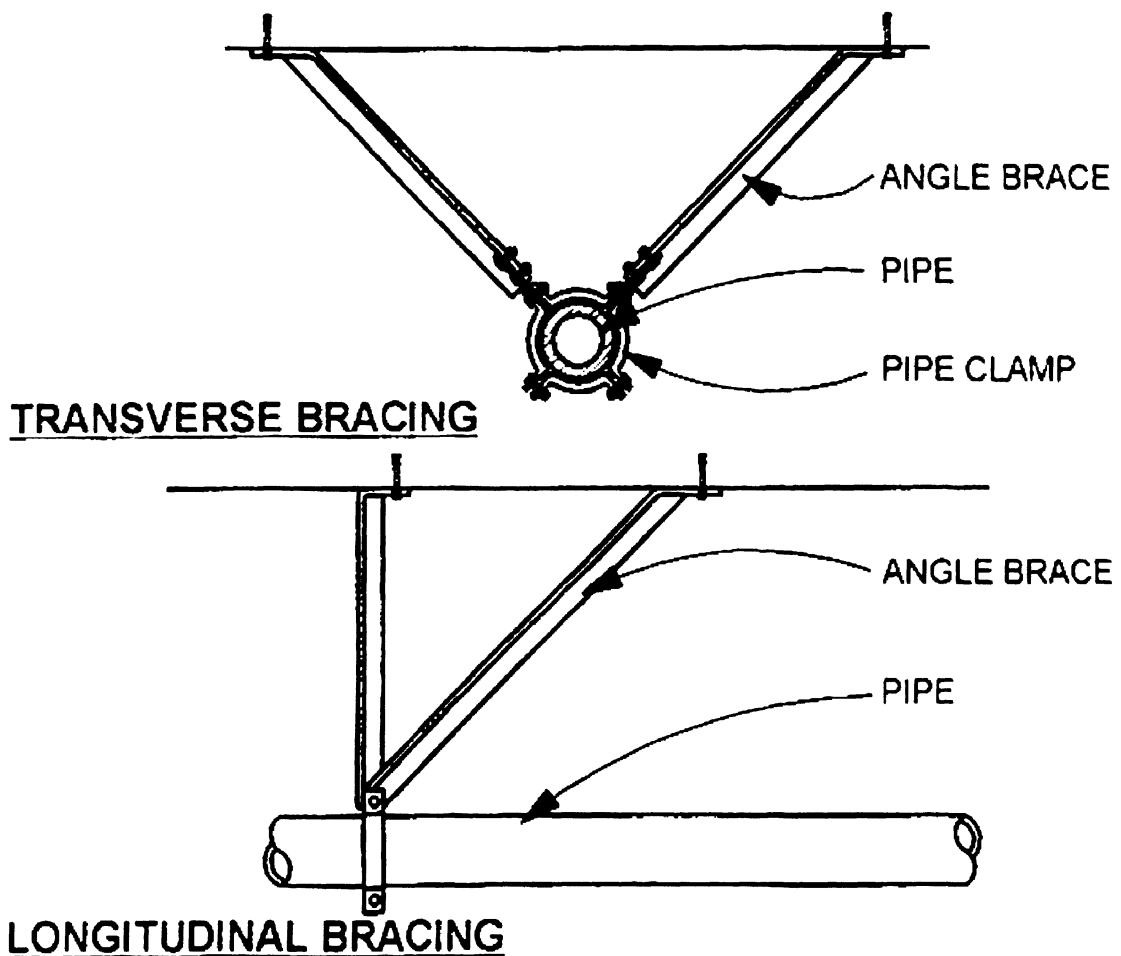


Figure 13-18. Seismic sway bracing for piping systems⁽¹³⁻¹⁰⁾

13.6.5 Air Distribution Systems

Sheet metal ducts can tolerate large distortions and generate low inertial loads, but have little inherent strength. Ducts rarely collapse, but the joints are particularly vulnerable. Joint failures result in a loss of air pressure. In line equipment such as axial flow fans should be braced independent of the duct system.

Air distribution systems are predominantly acceleration sensitive, but runs between floors or buildings are deformation sensitive. Large ducts (over six square feet in area or 24 inches in diameter) should be braced to the structure. Figure 13-19 illustrates a method of providing this bracing. Flexible duct connections should be installed with enough slack material to allow for the expected differential movement between fans and the ductwork. Duct openings through walls or floors must be large enough to accommodate the anticipated movement of the ducts. Ceiling diffusers and registers should be secured to ductwork with sheet metal screws, to prevent them from falling should they become dislodged. Diffusers connected to flexible ducts should be provided with safety wires to the floor or roof above, and should be securely fastened to the ductwork.

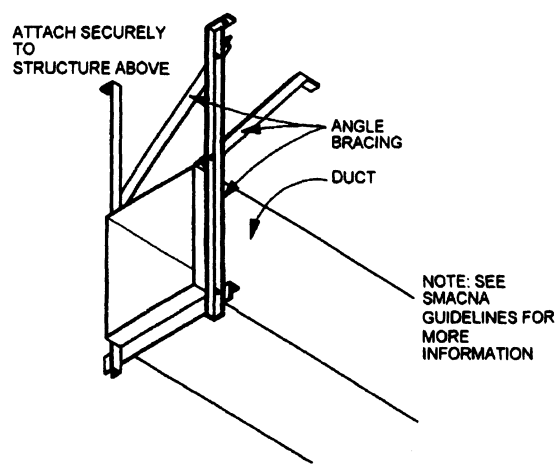


Figure 13-19. Seismic sway bracing for HVAC duct systems⁽¹³⁻¹⁰⁾

13.6.6 Elevators:

Elevator equipment includes the mechanical equipment such as motor generators and sheaves, electrical controllers, as well as the car and counterweight frames and guide rails. Elevator machinery behaves in the same manner as other heavy floor-mounted equipment. Mechanical and electrical components should be anchored to resist inertial forces.

Experience in past earthquakes has shown that the counterweight rails in elevators are vulnerable to damage. During the shaking, the rails can bend, allowing the counterweights to displace into the elevator shaft. Unless a careful post-earthquake survey of the shaft is made, it may not be apparent that this has occurred. The danger is that the displaced counterweights may strike the car if the elevator is operated. Recent editions of the building codes have required that the heavier counterweight guide rails be used, to limit distortions in an earthquake. Elevators should be equipped with a seismic switch, that senses significant ground shaking and shuts the elevator down, or forces it to operate in a "go slow" mode. The seismic switch should only be reset after an inspection by a qualified technician.

13.6.7 Electrical Equipment

Electrical equipment includes electrical and communication equipment, electrical panels, motor control centers, switch gear, transformers, emergency generators, battery racks, light fixtures, and other fixed components, as well as distribution systems such as conduit and cable trays. These components are generally acceleration sensitive, except for conduit and cable trays crossing building separations or running from floor to floor, which may be deformation sensitive.

Electrical panels may be flush or surface mounted. Flush mounted panels generally perform well, providing the panel is attached to the wall studs that frame the opening for the panel. Surface mounted panels should be

screwed or bolted into the supporting wall studs or into a steel backing plate that spans between the studs. Toggle bolts in plaster or gypsum board should be avoided.

Motor control centers and switchgear should be anchored to the floor, and for tall units, braced or anchored at the top. If structural bracing at the top is omitted at tall units, conduit running into the upper portions of the unit may be damaged while acting as bracing. Where relative movement between units could occur, flexible braided connections should be used in lieu of copper bus.

Emergency generators are generally installed on vibration isolation mounts. In order to function after an earthquake, all components of the system should be anchored for seismic forces. These components include the prime mover and generator, starting equipment including batteries, day tank, main fuel tank, radiators, exhaust silencers/mufflers, as well as the motor control and switchgear. If the

generator is mounted on vibration isolators, the line from the main fuel tank to the generator should be flexible enough to accommodate the expected lateral displacements of the isolated components. Emergency generators that rely upon the municipal water supply for engine cooling should be avoided, since utility lifelines generally fail following a strong earthquake. Batteries should be restrained in adequately anchored racks or boxes.

Transformers come in a variety of sizes, and can be floor mounted, or suspended from the walls or ceiling. If wall or ceiling mounted, the transformers should be adequately attached to the supporting frame, and the frame proportioned to resist seismic forces. In some cases, floor mounted transformers are stacked, to conserve space. If the units are stacked, the upper unit should be bolted to the lower unit, and the adequacy of the lower unit frame or enclosure should be verified for the anchorage forces at the connection between the two units.

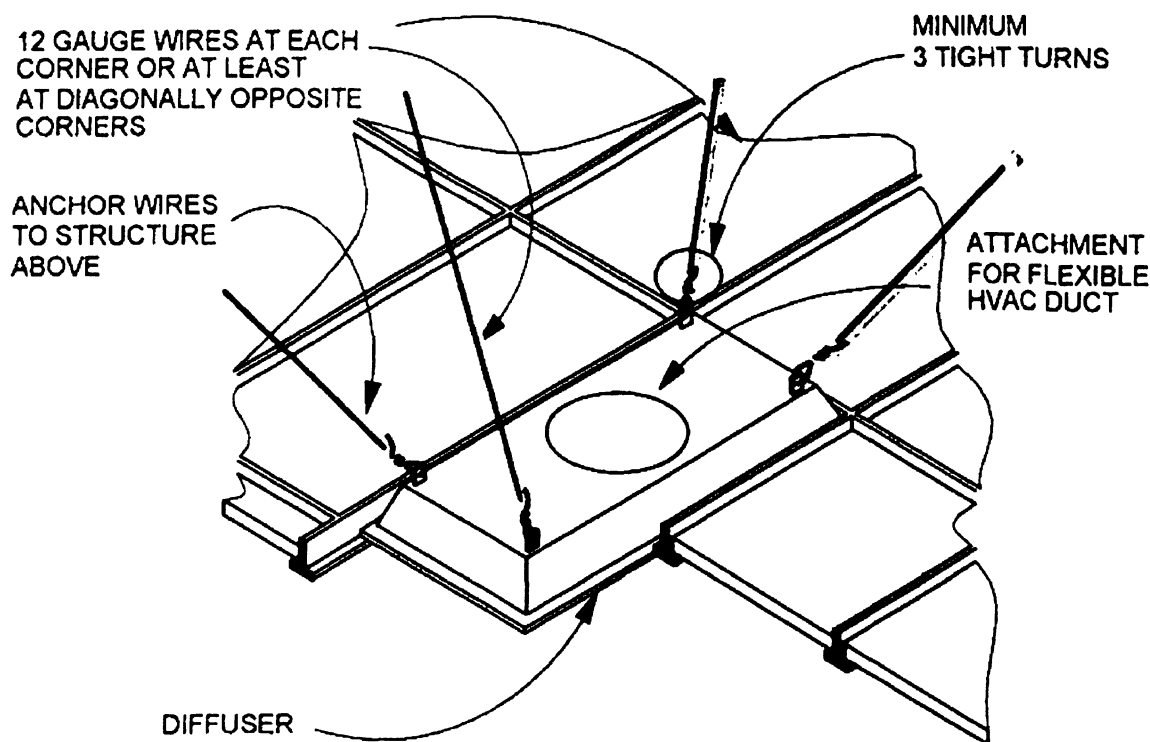


Figure 13-20. Seismic safety wires for HVAC diffusers, light fixtures

Lighting fixtures come in a number of types, and may be recessed and surface mounted in ceilings or walls, supported within a suspended ceiling, and suspended from the ceiling or structure (pendant fixtures). Lighting fixture support failures are generally due to failure of the attachment of the fixture to the wall or ceiling, or failure of the wall or ceiling. Distortions of T-bar system may allow fixtures to fall. Providing slack safety wires at opposing corners of light fixtures in T-bar ceilings will prevent them from falling, should the grid distort and the fixtures become detached. Excessive swing of pendant fixtures should be avoided, since it may result in impact with other building components or the support attachment may pull out of the ceiling. Recessed lighting fixtures should be secured to the ceiling suspension system. The suspension system should be of intermediate or heavy grade construction, and be designed to carry the weight of the ceiling fixtures. In addition, the fixtures should be provided with independent safety supports (Figure 13-20). Auxiliary support framing is required where the alignment of the lighting fixtures concentrates significant mass in a portion of the ceiling grid.

Conduits and cable trays should be braced at regular intervals. Where conduit and bus ducts pass across seismic joints, flexible connections that can accommodate the expected relative displacements should be provided. Separate ground connectors should be provided in conduit runs that pass across seismic joints.

REFERENCES

- 13-1 FEMA, 1997, *NEHRP Guidelines for the Seismic Rehabilitation of Buildings*, Federal Emergency Management Agency (Report No. FEMA 273), Washington, D.C.
- 13-2 FEMA, 1997, *NEHRP Commentary on the Guidelines for the Seismic Rehabilitation of Buildings*, Federal Emergency Management Agency (Report No. FEMA 274), Washington, D.C.
- 13-3 Freeman, S., "Design Criteria for Nonstructural Components Based on the Tri-Services Manuals", Proceedings of Seminar on Seismic Design, Retrofit, and Performance of Nonstructural Components, ATC 29-1, 1998
- 13-4 International Conference of Building Officials, "Uniform Building Code," 1994 Edition, Whittier, California, 1994.
- 13-5 Departments of Navy, Army, and Air Force, 1992, "Tri-Services Manual: Seismic Design of Buildings," Navy NAVFAC-355, Army TM 5-809-10, Air Force AFM 88-3, Chap. 13, Washington, D.C.
- 13-6 International Conference of Building Officials, "Uniform Building Code," 1997 Edition, Whittier, California, 1997.
- 13-7 BSSC, 1997, "NEHRP Recommended Provisions for Seismic Regulations for New Buildings and Other Structures, Part 1: Provisions and Part 2: Commentary," prepared by the Building Seismic Safety Council for the Federal Emergency Management Agency (Report No. FEMA 302 and 303), Washington, D.C..
- 13-8 Singh, M.P., "Generation of Seismic Floor Spectra," Journal of the Engineering Mechanics Division, ASCE, Vol. 101, No. EM5, October, 1975.
- 13-9 Biggs, J.M. and Roessel, J.M., "Seismic Analysis of Equipment Mounted on a Massive Structure," In Seismic Design of Nuclear Power Plants, R.J. Hanson, editor, M.I.T. Press, Cambridge, MA, 1970.
- 13-10 FEMA, 1994, *Reducing the Risks of Nonstructural Earthquake Damage, A Practical Guide*, Federal Emergency Management Agency, (Report No. FEMA 74), Washington, D.C.
- 13-11 OSA, 1990, "Metal Suspension Systems for Lay-In Panel Ceilings, IR 47-4" California Office of the State Architect, Structural Safety Section, March 1990.
- 13-12 OSA, 1990, "Drywall Ceiling Suspension - Conventional Construction - One Layer, IR 47-5" California Office of the State Architect, Structural Safety Section, March 1990.
- 13-13 SMACNA, 1992, *Guidelines for Seismic Restraint of Mechanical Systems and Plumbing Piping Systems*, Sheet Metal Industry Fund of Los Angeles and Plumbing and Piping Industry Council, Sheet

- Metal and Air Conditioning Contractors National Association, Chantilly, Virginia.
- 13-14 NFPA, 1996, *Standard for the Installation of Sprinkler Systems, NFPA-13*, National Fire Protection Association, Quincy, Massachusetts.
- 13-15 RMI, 1990, *Specification for the Design, Testing, and Utilization of Industrial Steel Storage Racks*, Rack Manufacturers Institute.

Chapter 14

Design of Structures with Seismic Isolation

Ronald L Mayes, Ph.D.
Consulting Engineer, Berkeley, California

Farzad Naeim, Ph.D., S.E.
Vice President and Director of Research and Development, John A. Martin and Associates, Inc., Los Angeles, California

Key words: Base Isolation, Damage Control, Design Examples, Damping, Earthquake Engineering, Energy Dissipation, Feasibility of Isolation, Friction Devices, High-Damping rubber bearings, IBC-2000, Lead-Rubber Bearings, New Construction, Preliminary Design, Response Spectrum Analysis, Seismic Isolation, Seismic Rehabilitation, Static Analysis, Time-History Analysis.

Abstract: This chapter surveys the principles, benefits, and the feasibility of seismic isolation. The basic principles of seismic isolation are introduced first. Contrary to a perception held by many engineers, neither the concept of seismic isolation is new nor its application is necessarily complex. What is new is the availability of relatively new materials and devices worked to perfection over the last two decades and advances in computational techniques now commonly in use by practicing engineers. Force-deflection characteristics of commonly used isolation devices are introduced next followed by guidelines for evaluation of the feasibility of seismic isolation as an alternative for a given project. The differences in approach to new construction and rehabilitation of existing structures are highlighted. The building code provisions for seismic isolation are covered next. The very recently released year 2000 edition of the International Building Code (IBC-2000) takes a much more simple approach to seismic isolation than did its direct predecessor, the 1997 edition of the Uniform Building Code (UBC-97). This is true even though the theory and objectives implemented in both of these codes are the same. The simplification is largely due to incorporation of spectral hazard maps in IBC-2000. A very practical side-effect of this incorporation is elimination of near-fault factors from the design process simply because now they are explicitly contained in the map. In many cases, design according to the new IBC-2000 requirements will result in smaller displacement and force demands on the isolation system and the structure above the isolation plane. This in terms mean that seismic isolation can be implemented much more economically than it was possible under UBC-97. The IBC-2000 design provisions for seismic isolation are discussed in detail. A simple preliminary design procedure is provided to aid engineers in initial sizing of the isolation devices. Several examples are provided to illustrate the practical application of the material covered in this chapter.

14.1 INTRODUCTION

Because of today's concern for liability, engineering innovations must be exhaustively tested and analytically proven to a degree unknown in the past. Early engineers were respected for their ability to design from first principles and produce designs that were conceptually right even though analytical or laboratory methods did not exist that would remove all doubt. For the most part, the great early engineers removed doubt by force of their personality and confidence. They took risks that would be unthinkable today.

The field of seismic design is, as perhaps benefits a subject directly concerned with both life safety and uncertainty, cautious and slow to innovate. In practice, improved seismic design does not represent a market opportunity because seismic safety is generally taken for granted. Like other code-dominated issues, and like airplane safety, seismic safety has never been much of a selling point. Money diverted to improve seismic resistance is often seen as a detraction from more visible and enjoyable attributes.

Improvements in seismic safety, since about the time of the San Francisco earthquake of 1906, have been due primarily to acceptance of ever-increasing force levels to which buildings must be designed. Innovation has been confirmed to the development and acceptance of economical structural systems that perform reasonably well, accommodate architectural demands such as open exteriors and the absence of interior walls, and enable materials such as steel and reinforced concrete to compete in the marketplace on near-equal terms.

The vocabulary of seismic design is limited. The choices for lateral resistance lie among shear walls, braced frames, and moment-resistant frames. Over the years, these have been refined and their details developed, and methods of analysis and modeling have improved and reduced uncertainty. But the basic approach has not changed: construct a ductile and/or strong building and attach it securely to the ground. This approach of arm

wrestling with nature is neither clever nor subtle, and it involves considerable compromise.

Although codes have mandated steadily increasing force levels, in a severe earthquake a building, if it were to remain elastic, would still encounter forces several times above its designed capacity. This situation is quite different from that for vertical forces, in which safety factors insure that actual forces will not exceed 50% of designed capacity unless a serious mistake has been made. For vertical forces, this is easy to do. But to achieve similar performance for seismic forces, the structure would be unacceptably expensive and its architectural impact would be extreme. This discrepancy between seismic demand and capacity is traditionally accommodated by reserve capacity, which includes uncalculated additional strength in the structure and often the contribution of portions and exterior cladding to the strength and stiffness of the building. In addition, the ability of materials such as steel to dissipate energy by permanent deformation—which is called ductility—greatly reduces the likelihood of total collapse.

Modern buildings contain extremely sensitive and costly equipment that have become vital in business, commerce, education and health care. Electronically kept records are essential to the proper functioning of our society. These building contents frequently are more costly and valuable than the buildings themselves. Furthermore, hospitals, communication and emergency centres, and police and fire stations must be operational when needed most: immediately after an earthquake.

Conventional construction can cause very high floor accelerations in stiff buildings and large interstory drifts in flexible structures. These two factors cause difficulties in insuring the safety of the building components and contents (Figure 14-1).

In the past decade, an alternative to the brute-force to nature has finally reached the stage of more widespread application. This approach is obvious and easily explainable at

the cocktail-party level: why not detach the building from the ground in such a way that the earthquake motions are not transmitted up through the building, or are at least greatly reduced? This conceptually simple idea has required much research to make it feasible, and only with modern computerized analysis has become possible. Application has depended on very sophisticated materials research into both natural and composite materials in order to provide the necessary performance.

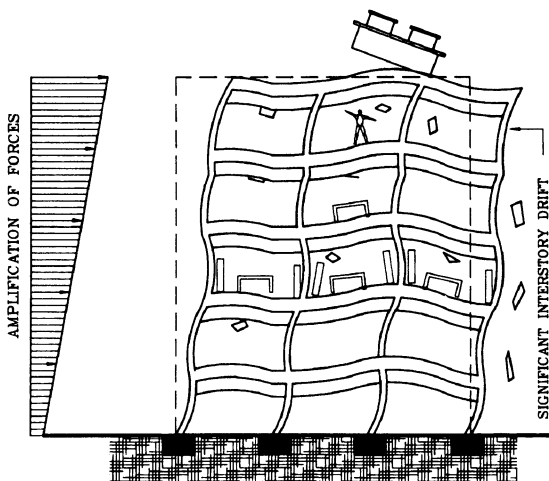


Figure 14-1. Conventional Structure

This new concept, now generally termed seismic isolation, meets all the criteria for a classic modern technological innovation. Imaginative advances in conceptual thinking were necessary, as were materials new to the industry, and ideas have developed simultaneously on a worldwide basis. But the method threatens conventional and established design procedures, so the road to seismic-isolation innovation is paved with argument, head shaking, and bureaucratic caution—all, to some extent, well-intentioned and necessary, given our litigious society.

Mounting buildings on an isolation system will prevent most of the horizontal movement of the ground from being transmitted to the buildings. This results in a significant reduction in floor accelerations and interstory drifts,

thereby providing protection to the building contents and components (Figure 14-2).

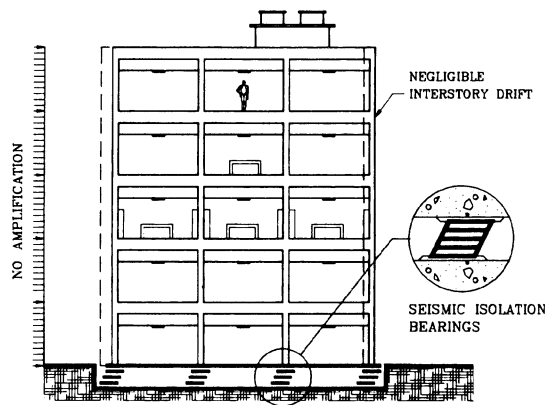


Figure 14-2. Base Isolated Structure

The principle of seismic isolation is to introduce flexibility at the base of a structure in the horizontal plane, while at the same time introducing damping elements to restrict the amplitude of the motion caused by the earthquake. The concept of isolating structures from the damaging effects of earthquakes is not new. The first patent for a seismic isolation scheme was taken out in 1909⁽¹⁴⁻¹⁾ and since that time several proposals with similar objectives have been made (see References 14-2 to 14-8). Nevertheless, until the last two decades, few structures have been designed and built using these principles.

However, new impetus was given to the concept of seismic isolation by the successful development of mechanical-energy dissipaters and elastomers with high damping properties (see References 14-8 to 14-15). Mechanical-energy dissipaters, when used in combination with a flexible isolation device, can control the response of the structure by limiting displacements and forces, thereby significantly improving seismic performance. The seismic energy is dissipated in components specifically designed for that purpose, relieving structural elements, such as beams and columns, from energy-dissipation roles (and thus damage). There are over two hundred civil engineering structures that have now been constructed using

the principles of seismic isolation. Kelly⁽¹⁴⁻⁶⁾, Buckle and Mayes⁽¹⁴⁻⁷⁾ and Naeim and Kelly⁽¹⁴⁻⁸⁾ provide an excellent history of world overview. Other references containing overview material are given in references 14-25 and 14-41.

The advantages of seismic isolation include the ability to eliminate or very significantly reduce structural and nonstructural damage, to enhance the safety of the building contents and architectural facades, and to reduce seismic design forces. These potential benefits are greatest for stiff structures fixed rigidly to the ground, such as low- and medium-rise buildings, nuclear power plants, bridges, and many types of equipment. Some tectonic and soil-foundation conditions may, however, preclude the use of seismic isolation.

14.1.1 An Idea Whose Time Has Come

The elastomeric bearing and the mechanical damper are fundamental components in many seismic isolation schemes. But it is not just the invention of the elastomeric bearing and the energy dissipater which has made seismic isolation a practical reality. Three other parallel, but independent, developments have also contributed to its success.

The first of these was the development of reliable software for the computer analysis of structures so as to predict their performance and determine design parameters. Work has been in progress for more than 25 years on the software for inelastic analysis of structural systems, and there are many available programs. Application to seismically isolated structures is straightforward, and correlation studies with model tests show many software systems to be soundly based.

The second development was the use of shaking tables which are able to simulate the effects of real recorded earthquake ground motions on different types of structures. The results of shaking-table tests over the last 20 years (see Reference 14-16 to 14-22 and 14-31 to 14-40) have provided another mechanism to enhance confidence in the way buildings respond during real earthquakes. In addition,

the results provide an opportunity to validate computer modeling techniques which are then used on full-size structures.

A third important development is in the skill of the engineering seismologist in estimating ground motions at a particular site. Recent advances in seismology have given more confidence in site-specific ground motions which take into account fault distances, local and global geology, and return periods. These design motions are basic input to the computer modeling of seismically isolated systems and are a vital step in the estimation of system performance.

In summary then, five recent developments are together responsible for elevating seismic isolation from fantasy to practical reality:

The design and manufacture of high-quality elastomeric (rubber) pads, frequently called bearings, that are used to support the weight of the structure but at the same time protect it from earthquake-induced forces.

The design and manufacture of mechanical-energy dissipaters (absorbers) and high-damping elastomers that are used to reduce the movement across the bearings to practical and acceptable levels and to resist wind loads.

The development and acceptance of computer software for the analysis of seismically isolated structures which includes nonlinear material properties and the time-varying nature of the earthquake loads.

The ability to perform shaking-table tests using real recorded earthquake ground motions to evaluate the performance of structures and provide results to validate computer modeling techniques.

The development and acceptance of procedures for estimating site-specific earthquake ground motions for different return periods.

14.2 CONSIDERATIONS FOR SEISMIC ISOLATION

The need for seismic isolation of a structure may arise if any of the following situations apply:

- Increased building safety and post-earthquake operability are desired.
- Reduced lateral design forces are desired.
- Alternate forms of construction with limited ductility capacity (such as precast concrete) are desired in an earthquake region.
- An existing structure is not currently safe for earthquake loads.

For new structures current building codes apply in all seismic zones, and therefore many designers may feel that the need for seismic isolation does not exist because the code requirements can be satisfied by current designs. Code designs, however, are generally controlled by a design philosophy which produces structures which are much more prone to damage than their seismic isolated counterparts. A typical building code statement of philosophy⁽¹⁴⁻²³⁾ states that buildings designed in accordance with its provisions will

- resist minor earthquakes without damage,
- resist moderate earthquakes without structural damage but with some nonstructural damage,
- resist major earthquakes without collapse but with structural and nonstructural damage.

These principles of performance also apply to conventional buildings that are rehabilitated to code-level design forces.

Seismic isolation promises the capability of providing a building with better performance characteristics than our current code approach towards conventional buildings and thus represents a major step forward in the seismic design of civil engineering structures. In the case of a building retrofit, the need for isolation may be obvious: the structure may simply not be safe in its present condition should an earthquake occur. In such cases, if seismic isolation is suitable, its effectiveness compared with alternative solutions such as strengthening should be examined.

14.2.1 Solutions for Nonstructural Damage

One of the more difficult issues to address from a conventional design viewpoint is that of reducing nonstructural and building-content damage. This is very often ignored, and when addressed, can be very expensive to incorporate in conventional design. In fact, the cost of satisfying the more stringent bracing requirements of nonstructural elements in a California hospital is on the order of \$2 to \$4 per square foot more than for ordinary commercial buildings.

There are two primary mechanisms that cause nonstructural damage. The first is related to interstory drift between floors, and the second to floor accelerations. Interstory drift is defined as the relative displacement that occurs between two floors divided by the story height. Floor accelerations are the absolute accelerations that occur as a result of the earthquake, and in conventional construction they generally increase up the height of the building. Together, these two components cause damage to the building contents, architectural facades, partitions, piping and ductwork, ceilings, building equipment, and elevators (Figure 14-1).

Clearly, a design concept that reduces both interstory drifts and floor accelerations combines the best aspects of these two current design philosophies. Seismic isolation is such a concept (Figure 14-2), since it can significantly reduce both floor accelerations and interstory drift and thus provide a viable economic solution to the difficult problem of reducing nonstructural earthquake damage.

14.3 BASIC ELEMENTS OF SEISMIC ISOLATION SYSTEMS

There are three basic elements in any practical seismic isolation system. These are:

1. a flexible mounting so that the period of vibration of the total system is lengthened sufficiently to reduce the force response;
2. a damper or energy dissipater so that the relative deflections between building and ground can be controlled to a practical design level; and
3. a means of providing rigidity under low (service) load levels such as wind and minor earthquakes.

Bridge structures have for a number of years been supported on elastomeric bearings⁽¹⁴⁻²⁴⁾, and as a consequence have already been designed with a flexible mount. It is equally possible to support buildings on elastomeric bearings, and numerous examples exist where buildings have been successfully mounted on pads. To date this has been done more for vertical-vibration isolation rather than seismic protection. Over 100 buildings in Europe and Australia have been built on rubber bearings to isolate them from vertical vibrations from subway systems below, and are performing well more than 40 years after construction. By increasing the thickness of the bearing, additional flexibility and period shift can be attained.

While the introduction of lateral flexibility may be highly desirable, additional vertical flexibility is not. Vertical rigidity is maintained by constructing the rubber bearing in layers and sandwiching steel shims between layers. The steel shims, which are bonded to each layer of rubber, constrain lateral deformation of the rubber under vertical load. This results in vertical stiffness and of a similar order of magnitude to conventional building columns.

An elastomeric bearing is not the only means of introducing flexibility into a structure, but it appears to be one of the most practical approaches. Other possible devices include rollers, friction slip plates, capable suspension, sleeved piles, and rocking (stepping) foundations (Figures 14-3 to 14-7). The most popular devices for seismic isolation of buildings in the United States are the lead-rubber bearings, high-damping rubber bearings and the friction pendulum system (Figure 14-8).

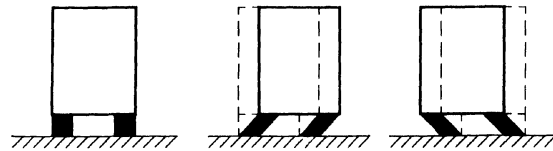


Figure 14-3. Elastomeric bearings

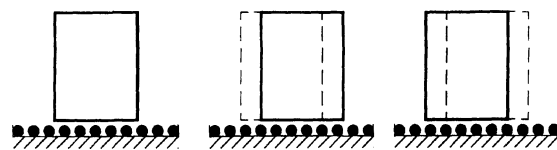


Figure 14-4. Rollers

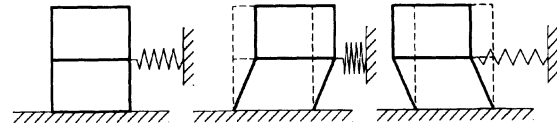


Figure 14-5. Sleeved Piles

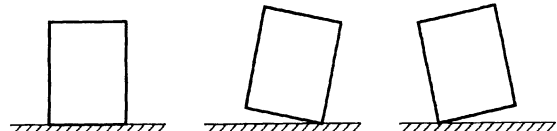


Figure 14-6. Rocking

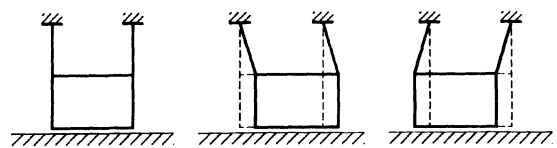


Figure 14-7. Cable Suspension

The reduction in force with increasing period (flexibility) is shown schematically in the force-response curve of Figure 14-9. Substantial reductions in base shear are possible if the period of vibration of the structure is significantly lengthened.

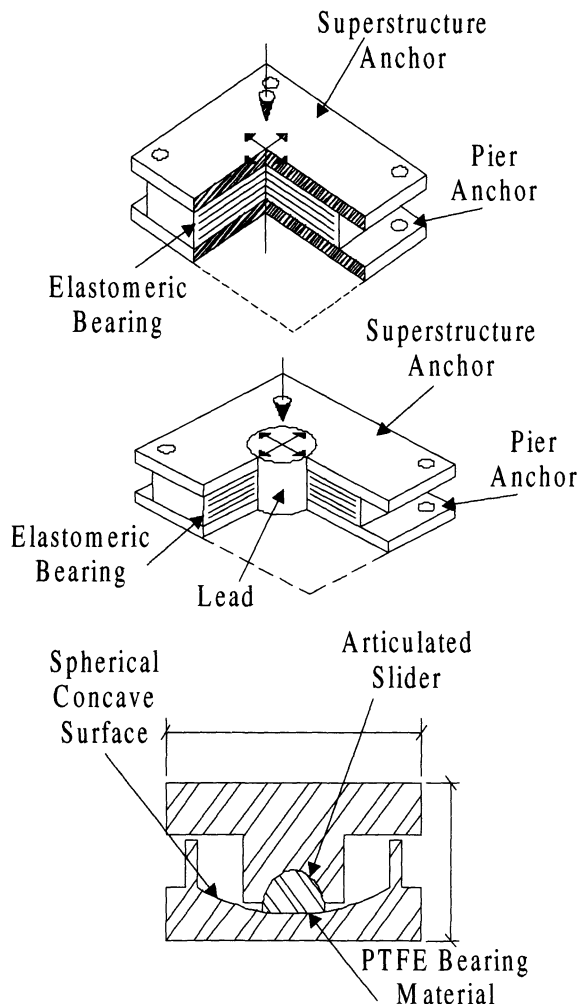


Figure 14-8. Most popular building isolation devices (Top: the high damping rubber device; Middle: the lead-rubber device; Bottom: the friction pendulum device).

The reduction in force response illustrated in Figure 14-9 is primarily dependent on the nature of the earthquake ground motion and the period of the fixed-base structure. Further, the additional flexibility needed to lengthen the period of the structure will give rise to large relative displacements across the flexible mount. Figure 14-10 shows an idealized displacement response curve from which displacements are seen to increase with increasing period (flexibility). However, as shown in Figure 14-11, if substantial additional damping can be introduced into the structure, the displacement problem can be controlled. It is also seen that increasing the damping reduces the forces at a given period and removes much

of the sensitivity to variations in ground motion characteristics, as indicated by the smoother force response curves at higher damping levels. Care must be taken, however, not to induce excessive damping into the system because that could produce story accelerations difficult to pin down in an ordinary dynamic analysis.

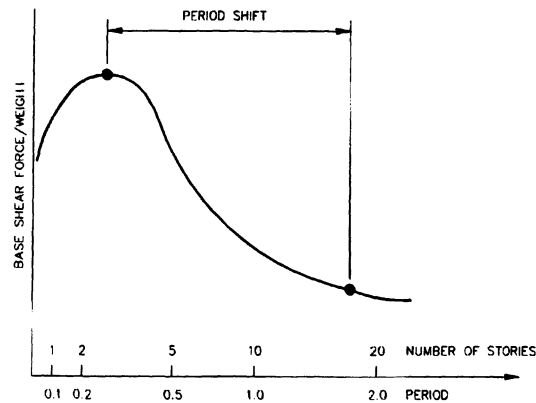


Figure 14-9. Idealized force response spectrum

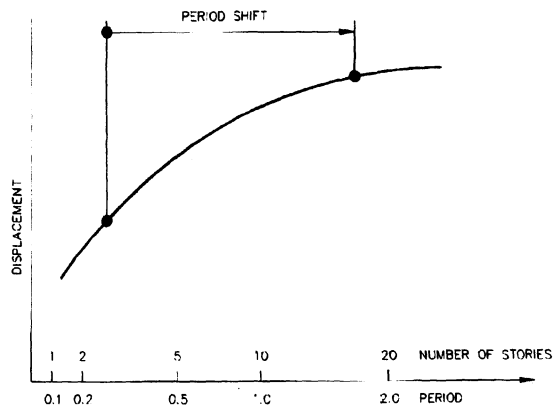


Figure 14-10. Idealized displacement response spectrum

Energy Dissipation One of the most effective means of providing a substantial level of damping is through hysteretic energy dissipation. The term "hysteretic" refers to the offset in the loading and unloading curves under cyclic loading. Work done during loading is not completely recovered during unloading, and the difference is lost (dissipated) as heat. Figure 14-12 shows an idealized force-displacement loop, where the enclosed area is a

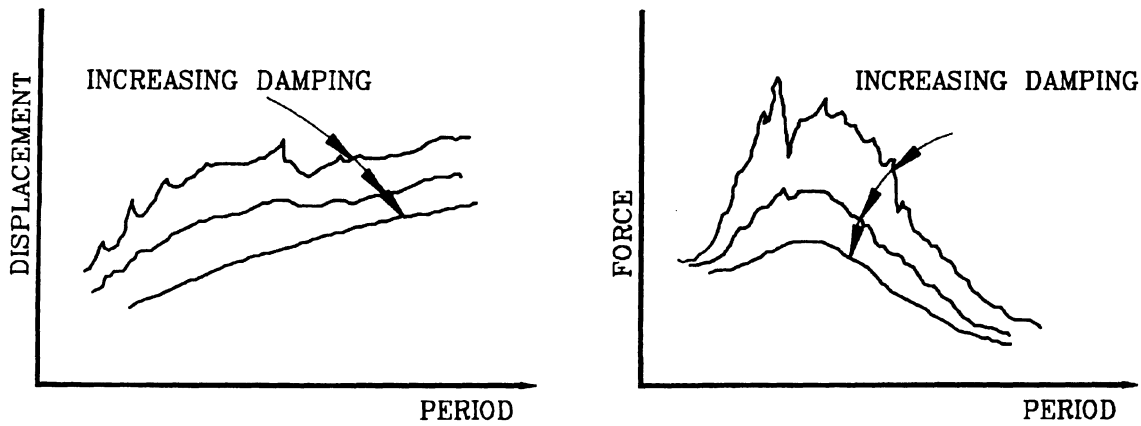


Figure 14-11. Response spectra for increasing damping

measure of the energy dissipated during one cycle of motion. Mechanical devices which use friction or the plastic deformation of either mild steel or lead to achieve this behavior have been developed^(14-9 to 14-14), and several mechanical-energy dissipation devices developed in New Zealand are shown in Figure 14-13.

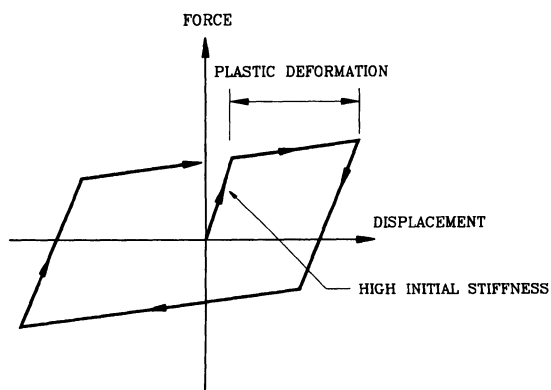


Figure 14-12. Hysteretic force-deflection curve

Many engineering materials are hysteretic by nature, and all elastomers exhibit this property to some extent. By the addition of special-purpose fillers to elastomers, it is possible to increase their natural hysteresis without unduly affecting their mechanical properties⁽¹⁴⁻¹⁰⁾. Such a technique gives a useful source of damping, but so far it has not been possible to achieve the same level of energy dissipation as is possible

with, say, a lead-rubber elastomeric bearing or supplemental viscous dampers.

Friction is another source of energy dissipation which is used to limit deflections. However, with the exception of the friction pendulum system, it can be a difficult source to quantify. A further disadvantage is that most frictional devices are not self-centering, and a permanent offset between the sliding parts may result after an earthquake. The friction pendulum system overcomes this problem by using a curved rather than flat surface on which the friction occurs. In proportioning a lead-rubber system or a friction pendulum system care must be exercised in design to ensure that the restoring force during expected seismic events would overcome the resistance of the device to self-centering. In practice it is common to compliment lead-rubber bearings with ones without a lead core and this approach has proved to be very successful.

Hydraulic damping has been used successfully in some bridges and a few special-purpose structures⁽¹⁴⁻⁷⁾. Potentially high damping forces are possible from viscous fluid flow, but maintenance requirements and high initial cost have restricted the use of such devices.

Rigidity for low lateral loads and flexibility for high seismic loads is very desirable. It is clearly undesirable to have a structural system

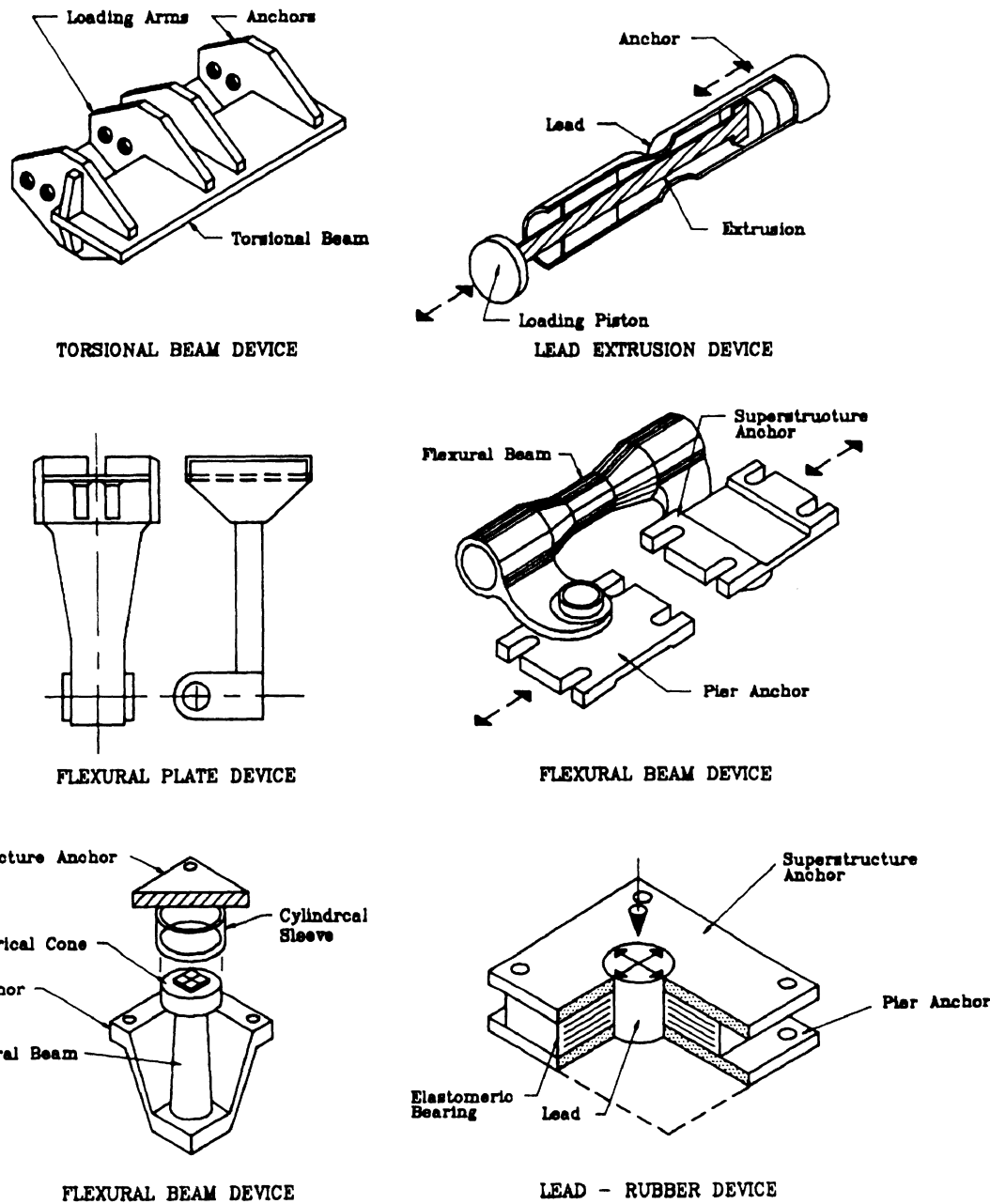


Figure 14-13. Various mechanical energy dissipaters

which will vibrate perceptibly under frequently occurring loads such as minor earthquakes or wind loads.

Lead-rubber bearings, well designed high damping rubber bearings, as well as other mechanical-energy dissipaters provide the desired low load rigidity by virtue of their high elastic stiffness (Figure 14-14). Some other

seismic isolation systems require a wind restraint device for this purpose—typically a rigid component designed to fail under a given level of lateral load. This can result in a shock loading being transferred to the structure due to the sudden loss of load in the restraint. Nonsymmetrical failure of such devices can also introduce undesirable torsional effects in a

building. Further, such devices will need to be replaced after each failure.

Table 14-1 summarizes the sources of flexibility that have been discussed above. A more detailed explanation of these concepts can be found in the proceedings of two workshops on base Isolation and Passive Energy Dissipation that have been conducted by Applied Technology Council^(14-25 and 14-41) as well as a recent textbook by Naeim and Kelly⁽¹⁴⁻⁸⁾.

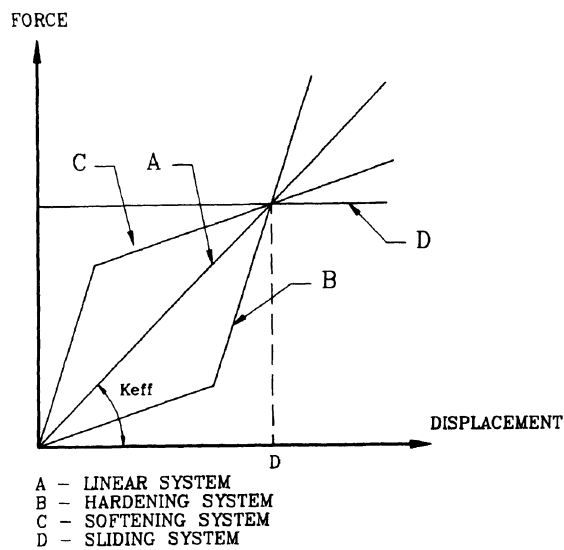


Figure 14-14. Idealized force-displacement relationships for isolation systems

Table 14-1. Alternative Sources of Flexibility and Energy Dissipation

Flexible Mounting Systems

- Unreinforced rubber blocks
- Elastomeric bearings
(reinforced rubber blocks)
- Sliding plates
- Roller and / or ball bearings
- Sleeved piles
- Rocking systems
- Suspended floors
- Air cushions
- Slinky springs

Damping Devices/ Mechanisms

- Plastic deformation of a metal
- Friction
- High-damping elastomers
- Viscous fluid damping
- Tuned mass damping

14.4 FORCE-DEFLECTION CHARACTERISTICS

Conceptually, there are four basic types of force-deflection relationships for isolation systems. These idealized relationships are shown in Figure 14-15, with each idealized curve having the same design displacement D for the design-level earthquake.

A linear isolation system is represented by curve A and has the same isolated period for all earthquake load levels. In addition, the force generated in the superstructure is directly proportional to the displacement across the isolation system. A linear isolation system will require some form of wind-restraining mechanism to be added to the system.

A hardening isolation system is represented by curve B. This system is soft initially (long effective period) and then stiffness (effective period shortens) as the earthquake load level increases. When the earthquake load level induces displacements in excess of the design displacement in a hardening system, the superstructure is subjected to higher forces and the isolation system to lower displacements than in a comparable linear system. Like a linear system, a hardening system will also require some form of additional wind-restraining mechanism.

A softening isolation system is represented by curve C. This system is stiff initially (short effective period) and softens (effective period lengthens) as the earthquake load level induces displacements in excess of the design displacement in a softening system, the superstructure is subjected to lower forces and the isolation system to higher displacements than in a comparable linear system. The high initial stiffness of a softening system is the wind-restraining mechanism.

A flat sliding isolation system is represented by curve D. This system is governed by the friction force of the isolation system. As in the softening system, the effective period lengthens as the earthquake load level increases, and the loads of the superstructure remain constant. The displacement of the sliding isolation system

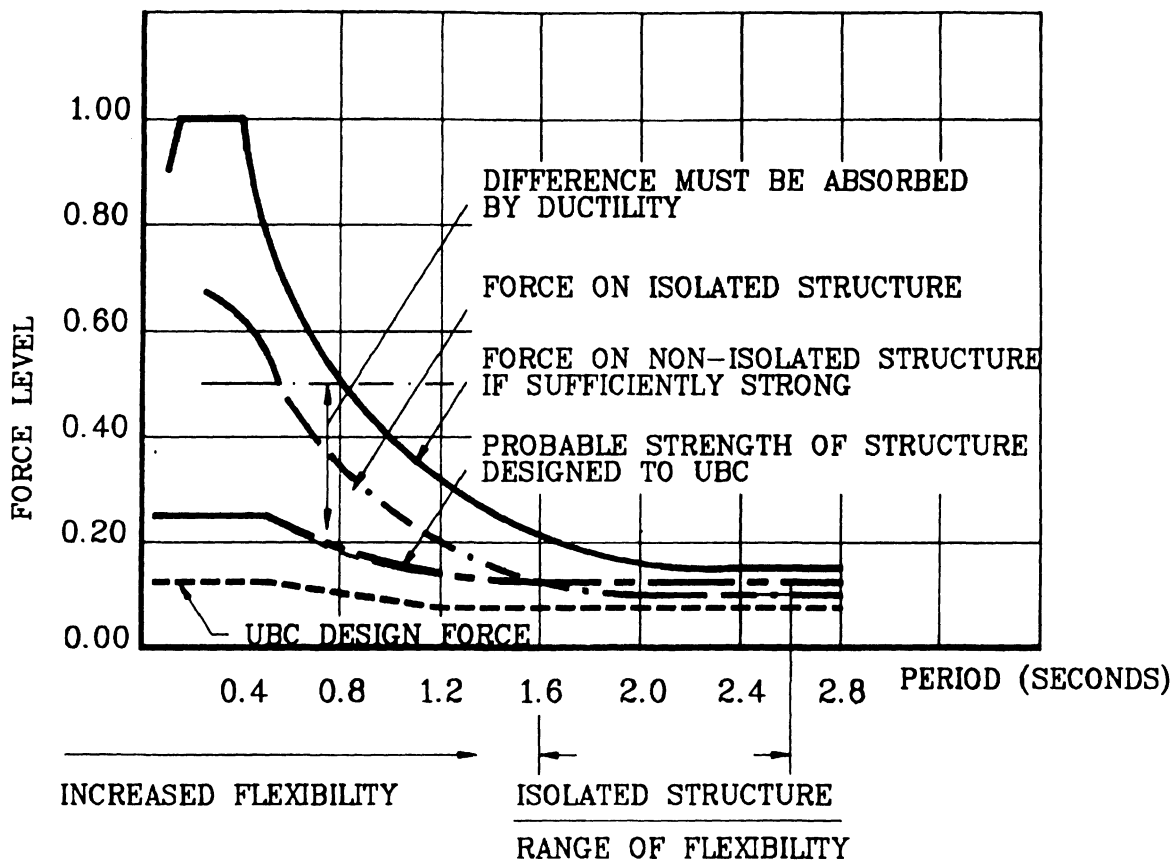


Figure 14-15. Design principles of seismic isolation

after repeated earthquake cycles is highly dependent on the vibratory characteristics of the ground motion and may exceed the design displacement. Consequently, minimum design requirements do not adequately define the peak seismic displacement for seismic isolation systems governed solely by friction forces. The value of the coefficient must be high enough to resist the wind forces.

14.5 SEISMIC-ISOLATION DESIGN PRINCIPLES

The design principles for seismic isolation are illustrated in Figure 14-16. The top curve of this figure shows the realistic forces based on a 5% ground response spectrum which will be imposed on a non-isolated structure from typical code forces⁽¹⁴⁻²⁸⁾. The spectrum shown is

for a rock site if the structure has sufficient elastic strength to resist this level of load. The lowest curve shows the forces which a typical code⁽¹⁴⁻²⁸⁾ requires a structure to be designed for, and the second-lowest curve shows the probable strength assuming the structure is designed for the corresponding code forces. The probable strength is typically about 1.5 to 2.0 times higher than the design strength because of the design load factors, actual material strengths which are greater in practice than those assumed for design, conservatism in structural design, and other factors. The difference between the maximum elastic force and the probable yield strength is an approximate indication of the energy which must be absorbed by ductility in the structural elements.

When a building is isolated, the maximum elastic forces are reduced considerably due to period shift and energy dissipation, as shown in

Figures 14-10 and 14-12. The elastic forces on a seismically isolated structure are shown by the dashed curve in Figure 14-16. This curve corresponds to a system with as high as 30% equivalent viscous damping.⁽¹⁴⁻²⁹⁾

If a stiff building, with a fixed-base fundamental period of 1.0 sec or less, is isolated, then its fundamental period will be increased into the 1.5- to 2.5-sec range (Figure 14-10). This results in a reduced code design force (Figure 14-16), but more importantly in the 1.5- to 2.5-sec range the probable yield strength of the isolated building is approximately the same as the maximum forces to which it will be subjected. Therefore, there will be little or no ductility demand on the structural system, and the lateral design forces can be theoretically reduced by approximately 50%, if the building code permits such a reduction.

14.6 FEASIBILITY OF SEISMIC ISOLATION

Structures are generally suitable for seismic isolation if the following conditions exist:

- The subsoil does not produce a predominance of long period ground motion such as that obtained in Mexico City.
- The structure has two stories or more (or is unusually heavy).
- The site permits horizontal displacements at the base of the order of 8 in. or more.
- The structure is fairly squat.
- Wind lateral loads and other non-earthquake load are less than approximately 10% of the weight of the structure.

Each project must be assessed individually and early in the design phase to determine its suitability for seismic isolation. For this assessment, there are differences between new construction and the retrofit of the existing structures. The following sections provide some guidelines for each of the situations.

14.6.1 New Construction

Structure The first consideration in assessing the suitability of a new project is the structure itself. Seismic isolation achieves a reduction in earthquake forces by lengthening the period of vibration at which the structure responds to the earthquake motions. The most significant benefits obtained from isolation are in structures for which the fundamental period of vibration without base isolation is short—less than 1 sec. The natural period of a building generally increases with increasing height. Taller buildings reach a limit at which the natural period is long enough to attract low earthquake forces without isolation.

Therefore seismic isolation is most applicable to low-rise and medium-rise buildings and becomes less effective for high-rise ones. The cut-off depends mainly on the type of framing system. Shear-wall structures and braced-frame structures are generally stiffer than moment frames of equivalent height, and so, for shear walls and braced frames isolation may be effective up to 12 to 15 stories, whereas with moment frames the cut-off is generally about 8 to 10 stories. These numbers are only generalizations and there are, of course, exceptions, as discussed to the retrofits of the 19-story Oakland City Hall and the 28-story Los Angeles City Hall. The isolation system must also resist maximum lateral loads from other sources without yielding in order to avoid unacceptable displacements and vibrations under service loads, such as wind. Therefore, if these service lateral loads exceed about 10% of the structure's weight, the building should not be isolated.

Soil Conditions The second consideration when assessing the suitability of a structure for seismic isolation is the soil condition and the geology of the site. Generally, the stiffer the soil, the more effective the isolation.

The flexibility of the structure determines how it will respond to a given earthquake motion. However, the form of the earthquake motion as it arrives at the base of a structure may be modified by the properties of the soil

through which the earthquake waves travel. If the soil underlying the structure is very soft, the high frequency content of the motion may be filtered out, and the soil may produce long-period motions. An extreme example of this was seen in the 1985 Mexico City earthquake. Lengthening the period of a stiff structure in these lake-bed soil conditions will amplify rather than reduce the ground motions, and hence for sites such as Mexico City seismic isolation should not be considered.

Another geologic consideration is the distance from a major fault. For near-fault situations, generally the design forces and displacements are amplified to allow for the recently observed fling or pulse effect of near-fault ground motions.

Adjacent Structures A third consideration in assessing suitability is any constraints imposed by adjacent structures at the proposed site. As discussed earlier, the basic concept of seismic isolation systems minimize these displacements, but nevertheless base displacements of the order of 8 to 20 in. generally occur. If the site is very confined due to neighbouring buildings built on the boundary, it may not be possible to accommodate these displacements.

14.6.2 Retrofit of Existing Structures

Retrofit of existing structures to improve their earthquake safety involves additional considerations, compared with new construction, because of the constraints already present. Some structures are inherently more suitable for retrofit using seismic isolation than others. For example, bridge superstructures are generally supported on steel bearings. Replacement of these bearings with elastomeric ones is a fairly simple, low-cost operation that will lead to a reduction in earthquake forces and allow the option of redistributing forces away from the weak substructures into abutments more capable of sustaining them⁽¹⁴⁻³⁰⁾.

Buildings are often more difficult to retrofit than bridges. However, seismic isolation may often be an effective solution for increasing the

earthquake safety of existing buildings without the addition of new structural elements which detract from the features which originally make the building worth preserving. Although seismic isolation reduces earthquake forces, it does not eliminate them. Consequently, the strength and ductility of an existing structure must at least be sufficient to resist the reduced forces that result from isolation. If the strength of the existing structure is extremely low (less than 0.05 of the weight of the building), then additional strengthening versus some strengthening and the provision of isolation will need to be studied.

In addition to the conditions discussed above from new buildings, the issues to be addressed in the seismic isolation retrofit of an existing structure are:

- Is there sufficient clearance with adjacent buildings to permit a movement of 6 to 24 inches?
- Do the building and its existing foundations have sufficient strength and ductility to resist the reduced seismic forces?
- What is the appropriate level for the plane of isolation—foundation level, basement level, ground level, or the top, bottom, or mid-height of the columns?
- The pros and cons with regard to the plane of isolation are:
 - Any structure with a full subbasement or basement that can be temporarily disrupted is a good isolation candidate, since the work can be confined to that area.
 - A structure with piled foundations can be more easily retrofitted at the foundation level than one with spread footings.
 - Provisions for the zone of isolation at the top, bottom, or mid-height of the basement-, first-, or second-level columns requires a detailed evaluation of the column capacities. If the strength of the column is not sufficient to resist the reduced isolation forces, three potential options exist. First, the column may be strengthened and act as a cantilever. Second, a new framing system with stiff beams may be developed at the plane of isolation to reduce the column forces. Third,

the mid-height column solution may be considered, since it reduces the column moments significantly.

In summary, seismic rehabilitation of an existing structure provides the ability to confine most of the construction work to the level where the plane of isolation is to be provided, whereas conventional methods generally require the addition of structural elements to all levels of the building. This trade-off can be very important if continued use of the facility is desired, as in hospitals or command and control centers.

14.6.3 Uplift and Overturning

In many types of structural systems increasing lateral forces will induce net tensions in elements once the axial loads caused by the overturning moment exceeds the gravity loads. This may occur for example at the edges of shear walls or the columns in braced or moment-resisting frames.

In conventional design this tension is resisted in the base connections and foundations, although only if it occurs under the code levels of the earthquake lateral loads. The more severe loading occurring under actual maximum earthquakes will produce overturning moments much greater than the design value, and therefore tension forces will be induced even where none are indicated under code loading. In this case, it is assumed that the structural detailing and redundancies are sufficient to prevent failure due to the uplift.

More recent studies⁽¹⁴⁻¹⁶⁾ have indicated that uplift may in fact be beneficial in reducing earthquake forces in conventional structures. In Fact, at least two actual structures in New Zealand have been explicitly designed for uplift as a form of seismic isolation: a stepping bridge and a chimney stack.

For a structure isolated on elastomeric bearings, the effects of uplift must be examined more carefully, since the elastomeric bearing is not suitable for resisting large tensile loads. For a fully bolted connection, an elastomeric bearing can resist 250 to 300 psi in tension

before significant softening of the bearing occurs.

Therefore, if uplift is indicated in an isolated structure, detailed analysis must be performed to quantify the vertical displacements for connection design. This involves a nonlinear analysis with realistic maximum credible earthquake records and requires significant analytical effort.

To avoid this, the optimum strategy is to avoid or minimize uplift. This is done by careful configuration of the lateral load-resisting elements. The important parameters are the height-to-width ratio of the lateral load-resisting system and the amount of gravity load carried by these elements. Another alternative is to utilize the "loose-bolt" connections which permit certain amount of isolator uplift without subjecting the bearing to net tension. Such connections have been successfully implemented in several major buildings in southern California such as the Los Angeles City Hall seismic retrofit and the Lake Arrowhead and Saint John new hospital buildings.

14.7 DESIGN CODE REQUIREMENTS

By the time this book reaches the market the design of new seismically isolated buildings in United States will be probably governed by the International Building Code 2000 (IBC-2000)⁽¹⁴⁻⁴²⁾. It is likely, however, that design in some jurisdictions will be still controlled by the provisions of the IBC-2000 predecessor, (UBC-97)⁽¹⁴⁻⁴³⁾. As documented by Naeim and Kelly⁽¹⁴⁻⁸⁾ UBC-97 is an unnecessarily complicated and conservative as far as seismic isolation design is concerned. Therefore, in this section we limit our discussion to the provisions of IBC-2000. Readers who are interested in learning more about UBC-97 and its predecessors are referred to the referenced textbook by Naeim and Kelly.

Primarily intended to regulate the design of new buildings, the IBC-2000 does not really cover the retrofit of existing buildings using

isolation, although most retrofit projects do follow either the IBC or UBC regulations closely. IBC-2000 regulations are written in such a way as to be nonspecific with respect to isolation systems. No particular isolation systems are identified as being acceptable, but the regulations require that any isolation system should be stable for the required displacement, provide increasing resistance with increasing displacement, and have properties that do not degrade under repeated cyclic loading.

The underlying philosophy is that an isolated building designed using IBC-2000 will out-perform fixed-base construction in moderate and large earthquakes. It is not the intent of the code to reduce the construction cost but to minimize damage to isolated structures and their contents.

Increasingly, the seismic upgrade design of existing structures is influenced by the NEHRP Guidelines for the Seismic Rehabilitation of Buildings (FEMA-273) and its commentary (FEMA- 274), which are published by the Federal Emergency Management Agency^(14-44, 14-45). FEMA-273 provisions are very similar to those of the IBC-2000 with one exception: FEMA-273 permits a new analysis approach called *Static Nonlinear Analysis* or the “Pushover” method (see Chapter 15).

A 1986 document published by a subcommittee of the Structural Engineers Association of Northern California (SEAONC) and generally referred to as the *Yellow Book*⁽¹⁴⁻²⁶⁾ has served as the backbone of all new code provisions.

The seismic criteria adopted by current model codes involve a two-level approach to seismic hazard, which are as follows:

- The Design Basis Earthquake (DBE): That level of ground shaking that has a 10% probability of being exceeded in 50 years (475 year-return period earthquake)
- The Maximum Considered Earthquake (MCE): The maximum level of ground shaking that may ever be expected at the building site. MCE is taken as 2% probability of being exceeded in 50 years (2500-year return period earthquake).

Notice that this is different from UBC-97 definition of MCE which was 10% probability of being exceeded in 100 years (1000-year return period earthquake)

14.7.1 Design Methods

Static Analysis: For all seismic isolation designs it is necessary to perform a static analysis. This establishes a minimum level for design displacements and forces. The static analysis is also useful both for preliminary design of the isolation system and the structure when dynamic analysis is required and for design review; under certain circumstances it may be the only design method used.

Static analysis alone will suffice if:

1. The structure is located at a site with $S_I \leq 0.60g$. S_I is determined using the spectral acceleration maps published as a part of IBC-2000.
2. The site soil is classified as Class A, B, C, or D (see Chapter 3).
3. The structure above the isolation plane is not more than four stories or 65 feet in height.
4. The effective period at maximum displacement of the isolated system, T_M , does not exceed 3.0 seconds.
5. The effective period at design displacement, T_D , is greater than three times the elastic, fixed-base period of the structure.
6. The structural system above the isolation plane is regular.
7. The effective stiffness of the isolation system at design displacement is greater than one third of the effective stiffness at 20% of design displacement.
8. The isolation system can produce the restoring force requirements mandated by the code (IBC-2000 Sec. 1623.5.1.4).
9. The force deflection characteristics of isolation system are independent of rate of loading, vertical load, and bilateral load.
10. The isolation system does not limit MCE displacements to less than S_{MI}/S_{DI} times the total design displacements.

Dynamic Analysis: Dynamic analysis may be used in all cases and must be used if the requirements mentioned for adequacy of static analysis are not satisfied. Dynamic analysis may take the form of response spectrum analysis or time-history analysis.

Response spectrum analysis would suffice if requirements number 2 and 7-10 as mentioned for static analysis, are satisfied. Otherwise, a time-history analysis will be required. Use of more than 30% critical damping is not permitted in response spectrum analysis even if the system is designed to provide for more.

Regardless of the type of dynamic analysis to be performed a site-specific design spectra corresponding to DBE and MCE events must be developed and used (instead of the code published default spectra) if:

- The structure is located on a Class E or F site, or
- The structure is located at a site with $S_1 \leq 0.60g$.

If time history analysis is to be performed, then a suite of representative earthquake ground motions must be selected that satisfy the following requirements:

1. At least three pairs of recorded horizontal ground motion time-history components should be selected and used.
2. The time histories should be consistent with the magnitude, fault distance, and source mechanisms that control the DBE and/or MCE events.
3. If appropriate recorded time-histories are not available, appropriate simulated time-histories may be used to make up the total number of required records.
4. For each pair of horizontal ground motion components, the square root sum of the squares (SRSS) of the 5 percent-damped spectrum of the scaled horizontal components is to be constructed.
5. The time-histories are to be scaled such that the average value of the SRSS spectra does not fall below 1.3 times the 5 percent-damped design spectrum (DBE or MCE) by more than 10 percent over a range of $0.5T_D$ to $1.25T_M$ where T_D and T_M are effective

isolated periods at design displacement and maximum displacement, respectively.

6. Each pair of time histories is to be applied simultaneously to the model considering the most disadvantageous location of mass eccentricity. The maximum displacement of the isolation system is to be calculated from the vectorial sum of the two orthogonal components at each time step.
7. The parameters of interest are calculated for each time-history analysis. If three time history analyses are performed, then the maximum response of the parameter of interest is to be used for design. If seven or more time histories are used, then the average value of the response parameter of interest may be used.

As Naeim and Kelly have pointed out ⁽¹⁴⁻⁸⁾, this formulations contains implicit recognition of the crucially important fact that design spectra are definitions of a criteria for structural analysis and design and are not meant to represent characteristics of a single event.

14.7.2 Minimum Design Displacements

Four distinct displacements calculated using simple formulas and used for static analysis, also serve as the code permitted lower bound values (subject to some qualification) for dynamic analysis results. These are:

- D_D : the design displacement, being the displacement at the center of rigidity of the isolation system at the DBE;
 - D_M : the displacement, at the center of rigidity of the isolation system at the MCE;
 - D_{TD} : the total design displacement, being the displacement of a bearing at a corner of the building and includes the component of the torsional displacement in the direction of D_D
 - D_{TM} : same as D_{TD} but calculated for MCE.
- DD and DM are simply spectral displacement values calculated assuming constant spectral velocity from code published spectral maps and adjusted for damping.

$$D_D = \left(\frac{g}{4\pi^2} \right) \frac{S_{D1} T_D}{B_D} \quad (14-1)$$

$$D_M = \left(\frac{g}{4\pi^2} \right) \frac{S_{M1} T_M}{B_M} \quad (14-2)$$

where g is the gravitational acceleration, S_{D1} and S_{M1} are spectral coefficients, T_D and T_M are isolated periods, and B_D and B_M are damping coefficients corresponding to the DBE and MCE level responses, respectively.

S_{D1} and S_{M1} are functions of two parameters:

- S_1 , the MCE 5% damped spectral acceleration for the site available from the maps accompanying the IBC-2000 and also available on Internet via the USGS and CDMG web sites, and
- F_v , the site coefficient defined for various site classes and acceleration levels (see Chapter 3).

Such that

$$S_{M1} = F_v S_1 \quad (14-3)$$

$$S_{D1} = \frac{2}{3} S_{M1} \quad (14-4)$$

The effective damping in the system, β , at the DBE and MCE response levels (referred to as β_D and β_M) are computed from

$$\beta_D = \frac{1}{2\pi} \left(\frac{\text{total area of hysteresis loop}}{K_{D,\max} D_D^2} \right) \quad (14-5)$$

$$\beta_M = \frac{1}{2\pi} \left(\frac{\text{total area of hysteresis loop}}{K_{M,\max} D_M^2} \right) \quad (14-6)$$

$K_{D,\max}$ and $K_{M,\max}$ are effective stiffness terms defined in Section 14.7.3. The damping reduction factors B_D for the DBE and B_M for the MCE are given in a tabular form (IBC-2000,

Table 1623.2.2.1), with linear interpolation to be used for intermediate values. A very close approximation to the table values is given by Naeim and Kelly⁽¹⁴⁻⁸⁾ as

$$\frac{1}{B} = 0.25(1 - \ln \beta) \quad (14-7)$$

where β is given as the fraction of critical damping (not as a percentage).

14.7.3 Effective Isolated System Periods

The effective isolated periods T_D and T_M corresponding to the DBE and MCE response are computed from

$$T_D = 2\pi \sqrt{\frac{W}{K_{D,\min} g}} \quad (14-8)$$

$$T_M = 2\pi \sqrt{\frac{W}{K_{M,\min} g}} \quad (14-9)$$

where

W = the weight of the building

g = gravity

$K_{D,\min}$ = minimum effective horizontal stiffness of the isolation system at the design displacement (DBE).

$K_{M,\min}$ = minimum effective horizontal stiffness of the isolation system at the maximum displacement (MCE).

The values of $K_{D,\min}$ and $K_{M,\min}$ are not known to the engineer during the preliminary design phase. The design procedure will begin with an assumed value which is obtained from previous tests on similar components or by using the material characteristics and a schematic of the proposed isolator. After the preliminary design is satisfactorily completed, prototype isolators will be ordered and tested, and the values of $K_{D,\min}$, $K_{D,\max}$, $K_{M,\min}$, and $K_{M,\max}$ will be obtained from the results of the prescribed program of tests on the prototypes.

The total design displacements, D_{TD} and D_{TM} (which include torsion), are

$$D_{TD} = D_D \left(1 + y \frac{12e}{b^2 + d^2} \right) \quad (14-10)$$

$$D_{TM} = D_M \left(1 + y \frac{12e}{b^2 + d^2} \right) \quad (14-11)$$

where b and d are plan dimensions at the isolation plane, e is the actual eccentricity plus 5% accidental eccentricity, and y is the distance to a corner perpendicular to the direction of seismic loading.

14.7.4 Design Forces

The superstructure and the elements below the isolation interface are designed for forces based on the DBE design displacement, D_D . The isolation system, the foundation and structural elements below the isolation system must be designed to withstand the following minimum lateral seismic force

$$V_b = K_{D_{max}} D_D \quad (14-12)$$

If other displacements rather than D_D generate larger forces, then those forces should be used in design rather than the force obtained from Equation 14-12.

The structure above the isolation plane should withstand a minimum shear force, V_s , as if it was fixed base where:

$$V_s = \frac{K_{D_{max}} D_D}{R_I} \quad (14-13)$$

In above equations $K_{D_{max}}$ is the maximum effective stiffness of the isolation system at the design displacement (DBE) in the horizontal direction and R_I is a reduction factor analogous to the R factor that would have been used for the superstructure if it was not isolated (see Chapter 5). IBC-2000 defines RI as

$$1.0 \leq R_I = \frac{3}{8} R \leq 2.0 \quad (14-14)$$

If dynamic analysis is performed, it is possible to have design displacements and design forces that are less than those given by Equations 14-12 and 14-13. In such cases, The total design displacement, D_{TD} , for the isolation system can be reduced to not less than 90% of that given by the static formula, and the total maximum displacement, D_{TM} , can be reduced to not less than 80% of the static formula result. Furthermore, the code permits a further reduction by replacing D_D and D_M in the static formulas by D'_D and D'_M , where

$$D'_D = \frac{D_D}{\sqrt{1 + \left(\frac{T}{T_D}\right)^2}} \quad (4-14)$$

$$D'_M = \frac{D_M}{\sqrt{1 + \left(\frac{T}{T_M}\right)^2}} \quad (4-15)$$

In all cases the value of V_s should not be less than

- the seismic force required by the code provisions for a fixed-base structure;
- the base shear corresponding to the factored design wind load
- one and a half times the lateral force required to fully activate the isolation system, i.e., the yield load of a lead-plug rubber bearing or slip threshold of a sliding bearing system

14.7.5 Vertical Distribution of Design Force

In order to conservatively consider participation of higher modes in response, the vertical distribution of the force on the superstructure of an isolated building is similar to that prescribed for fixed-base construction.

This is so, although the seismic isolation theory suggests a uniform distribution of forces over the height of the superstructure. Therefore, the lateral force at level x , denoted by F_x , is computed from the base shear, V_s , by

$$F_x = V_s \frac{h_x w_x}{\sum_{i=1}^N w_i h_i} \quad (14-15)$$

where w_x and w_i are the weights at level i or x and h_x and h_i are the respective heights of structure above isolation level.

14.7.6 Drift Limitations

The maximum interstory drift (relative displacement of adjacent floors) permitted by the IBC-2000 is a function of method of analysis in that more drift is permitted when more sophisticated analyses are performed.

Static Analysis: The drift at any level x is calculated from Equation 14-16 and should not exceed $0.015h_{sx}$ (h_{sx} is the story height below level x).

$$\delta_x = \frac{R_I \delta_{se}}{I_E} \quad (14-16)$$

where δ_{se} is the drift determined by an elastic analysis and I_E is the occupancy importance factor for the building as defined in Chapter 5.

Response Spectrum Analysis: The drift at any level x calculated from response spectrum analysis should not exceed $0.015h_{sx}$.

Time-History Analysis: The drift at any level x calculated from a time-history analysis considering the nonlinear behavior of the isolators should not exceed $0.020h_{sx}$. The code has an additional paragraph stating that this drift should be calculated using Equation 14-16. However, the relevance of such a provision to nonlinear time-history analysis is not clear and this may be just a printing error in the very first edition of the IBC that has just been released at the time of this writing. P-Δ effects must be

considered whenever the interstory drift ratio exceeds $0.010/R_I$.

14.7.7 Peer Review

IBC-2000 similar to its predecessors requires the design of the isolation system and the related test programs to be reviewed by an independent team of registered design professionals and others experienced in seismic analysis methods and theory and application of seismic isolation. The scope of this review includes, but is not limited to the following items:

1. Review of site-specific design ground motion criteria such as design spectrum and time-histories as well as other project-specific information.
2. Review of the design criteria and the preliminary design procedures and results.
3. Overview and observation of the prototype testing program.
4. Review of the final design of the entire structural system and supporting analyses and calculations.
5. Review of the isolation system quality control and production testing program.

14.7.8 Testing Requirements for Isolators

Code testing requirements of the isolator units before they can be accepted are contained in Section 16.23.8 of IBC-2000. The code requires that at least two full-sized specimens of each type of isolator be tested. The sequence and the necessary number of cycles of testing vary with the amount of deformation the isolators are subjected to. For example, twenty fully reversed cycles of loading is to be performed at a displacement corresponding to the wind design force.

The tests required are a specified sequence of horizontal cycles under $D + 0.5L$ from small horizontal displacements up to D_{TM} . The maximum vertical load used during testing is $1.2DL + 0.5LL + E_{max}$, and the minimum is $0.8DL - E_{min}$ where E_{max} and E_{min} are the

maximum downward and upward load on the isolator that can be generated by an earthquake.

14.7.9 Design Example

Consider a small building with a plan dimension of 150 feet by 70 feet. The total weight of the structure is estimated at 4200 kips. The lateral load resisting system consists of ordinary steel concentrically braced frames ($R=5$). The building is regular in both the plan and the elevation. The actual distance between the center of mass and the center of rigidity of each floor is 80 inches.

The project site is located in downtown Los Angeles on a site with soil Class C. Evaluation of IBC-2000 seismic hazard maps (see Chapter 3) has produced values of $S_S=1.5g$ and $S_I=0.60g$. The fixed base period of the building is 0.40 secs. The isolation system should provide effective isolated periods in the vicinity of $T_D = 2.0$ and $T_M = 2.3$ seconds, respectively. The anticipated damping is about 15% critical. A margin of $\pm 10\%$ variation in stiffness from the mean stiffness values of the isolators is considered acceptable. Estimate the minimum design displacements, minimum lateral forces, and maximum permitted interstory drift ratios according to the IBC-2000 requirements.

SOLUTION:

T_D and T_M are given. Therefore, from Equations 14-8 and 14-9:

$$2.0 = 2\pi \sqrt{\frac{4200}{386.4 K_{D_{\min}}}}$$

$$\Rightarrow K_{D_{\min}} = 107 \text{ kips/in.}$$

$$2.3 = 2\pi \sqrt{\frac{4200}{386.4 K_{M_{\min}}}}$$

$$\Rightarrow K_{M_{\min}} = 81 \text{ kips/in.}$$

As specified in the problem, we assume a +10% variation about the mean stiffness values. Therefore,

$$K_{D_{\max}} = (1.10) \frac{107}{0.90} = 131 \text{ k/in.}$$

$$K_{M_{\max}} = (1.10) \frac{81}{0.90} = 99 \text{ k/in.}$$

A Linear interpolation of values of 1.2 and 1.5 given in IBC-2000 Table 1623.2.2.1 for 10% and 20% damping results in $B = 1.35$. Alternatively, From Equation 14-7:

$$\frac{1}{B} = 0.25(1 - \ln \beta) = 0.25(1 - \ln 0.15) = 0.7243$$

$$B = 1.38$$

The same level of damping is assigned to both DBE and MCE events for preliminary design purposes. The value of $F_v = 1.3$ is obtained from IBC-2000 Table 1615.1.2 (see Chapter 3) for site Class C and $S_I = 0.60 > 0.50$. The Spectral coefficients needed for calculation of minimum displacements are obtained from Equations 14-3 and 14-4:

$$S_{M_1} = F_v S_1 = (1.3)(0.60) = 0.78g$$

$$S_{D_1} = \frac{2}{3} S_{M_1} = \frac{2}{3}(0.78) = 0.52g$$

The minimum design displacements now may be obtained from Equations 14-1 and 14-2 as:

$$D_D = \left(\frac{386.4}{4\pi^2} \right) \frac{(0.52)(2.0)}{1.35} = 7.55 \text{ in.}$$

$$D_M = \left(\frac{386.4}{4\pi^2} \right) \frac{(0.78)(2.3)}{1.35} = 13.02 \text{ in.}$$

The eccentricity needed to calculate total displacements is

$$e = 80 + (0.05)(150)(12) = 170 \text{ in.}$$

and from Equations 14-10 and 14-11 noting that the same multiplier applies to both equations

$$\left(1 + y \frac{12e}{b^2 + d^2}\right) =$$

$$\left(1 + \frac{150}{2} \frac{(170)}{150^2 + 70^2}\right) = 1.47 \text{ and}$$

$$D_{TD} = (7.55)(1.47) = 11.1 \text{ in.}$$

$$D_{TM} = (13.02)(1.47) = 19.1 \text{ in.}$$

The minimum design shear force for the isolation system and structural elements below the isolation plane is obtained from Equation 14-12:

$$V_b = K_{D_{\max}} D_D = (131)(7.55) = 989 \text{ kips}$$

which corresponds to a seismic base shear coefficient of 0.24. The reduction factor from Equation 14-14 is:

$$R_I = \frac{3}{8} R = \frac{3}{8}(5) = 1.875 \leq 2.0$$

The design base shear for design of the superstructure (Equation 14-13) is:

$$V_s = \frac{K_{D_{\max}} D_D}{R_I} = \frac{V_b}{R_I} = \frac{989}{1.875} = 527 \text{ kips}$$

which in turn translates to a seismic base shear coefficient of 0.126. Remember that this force has to be larger than the base shear obtained for a similarly situated fixed-base building with a period of 2.0 sec. The procedure for calculating base shear force for conventional buildings is explained in Chapter 5 and therefore not repeated here.

14.8 SEISMIC-ISOLATION CONFIGURATIONS

The seismic-isolation configuration, including the layout and the installation details for the isolation system, depends on the site constraints, type of structure, construction, and other related factors. The following details are

provided as an aid in determining appropriate layouts for particular projects and are not intended to restrict the designer in individual cases.

14.8.1 Bearing Location

Figures 14-16 to 14-19 provide typical planes of isolation for elastomeric bearings in buildings both with and without separate basement levels. Some of the advantages and disadvantages associated with each layout are listed in the figures. The following general guidelines are considerations for determining a suitable layout:

- The bearing location should permit access for inspection and replacement, should this become necessary.

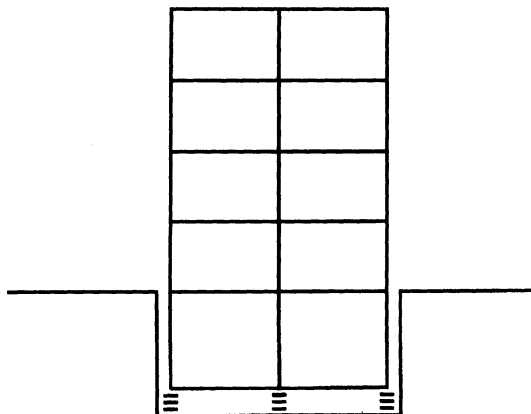
A full diaphragm above or below the isolators to distribute lateral loads uniformly to each bearing is preferable. If distribution is by tie beams only, the bearings should be arranged in proportion to the lateral load taken by each element, i.e., larger bearings under stiffer elements.

- Free movement for the maximum predicted horizontal displacement must be available.
- A layout which allows stub walls or columns as a backup system for vertical loads should be used wherever possible.
- Consideration must be given to the continuity of services, stairways, and elevators at the plane of isolation.
- Consideration must be given to details for cladding if it will extend below the plane of isolation.

14.8.2 Connection Details

Although connection details vary from each project, the design principles remain the same:

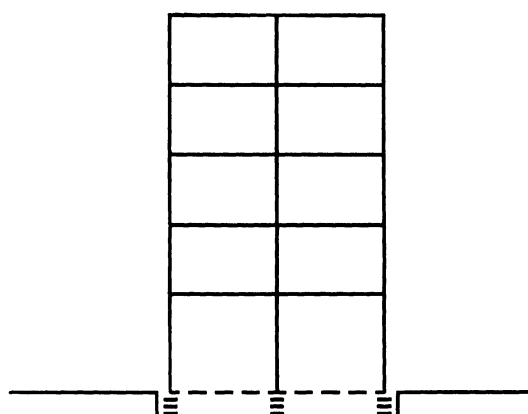
1. The bearing must be free to deform in shear between the outer shims; i.e., the upper surface of the bearing must be able to move freely horizontally.

**ADVANTAGES**

- No special detailing required for separation of internal services such as elevator and stairways.
- No special cladding separation details.
- Base of columns connected by diaphragm at isolation level.
- Simple to incorporate back-up system for vertical loads.

DISADVANTAGES

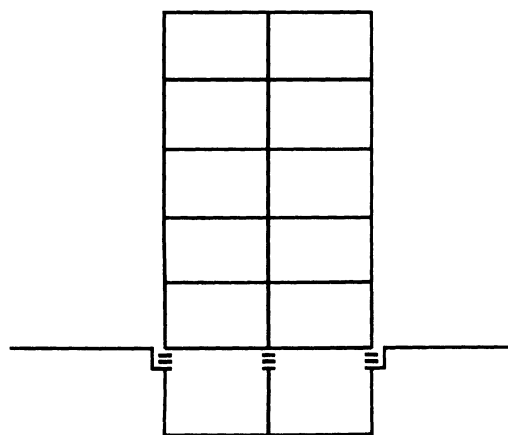
- Added structural costs unless sub-basement required for other purposes.
- Requires a separate (independent) retaining wall.

Figure 14-16. Bearings located in sub-basement**ADVANTAGES**

- Minimal added structural costs.
- Separation at level of base isolation is simple to incorporate.
- Base of columns may be connected by diaphragm.
- Easy to incorporate back-up system for vertical loads.

DISADVANTAGES

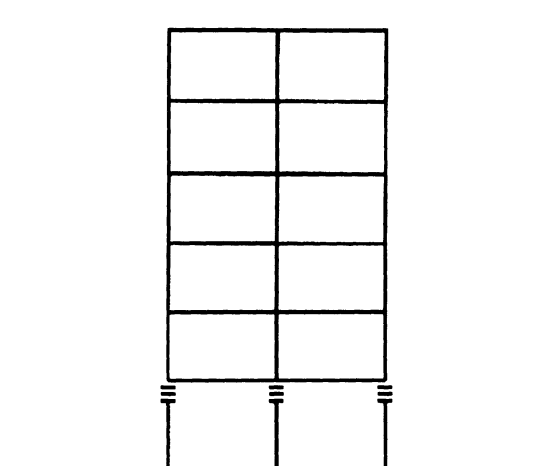
- May require cantilever pit.

Figure 14-18. Bearings located at bottom of first story columns**ADVANTAGES**

- No Sub-basement Requirement.
- Minimal added structural costs.
- Base of columns connected by diaphragm at isolation level.
- Backup system for vertical loads provided by columns.

DISADVANTAGES

- May require cantilevered elevator shaft below first floor level.
- Special treatment required for internal stairways below first floor level.

Figure 14-17. Bearings located at top of basement columns**ADVANTAGES**

- Minimal added structural costs.
- Economic if first level is for parking.
- Backup system for vertical loads provided by columns.

DISADVANTAGES

- Special detail required for elevators and stairs.
- Special cladding details required if first level is not open.
- Special details required for vertical services.

Figure 14-19. Bearings located at top of first story columns

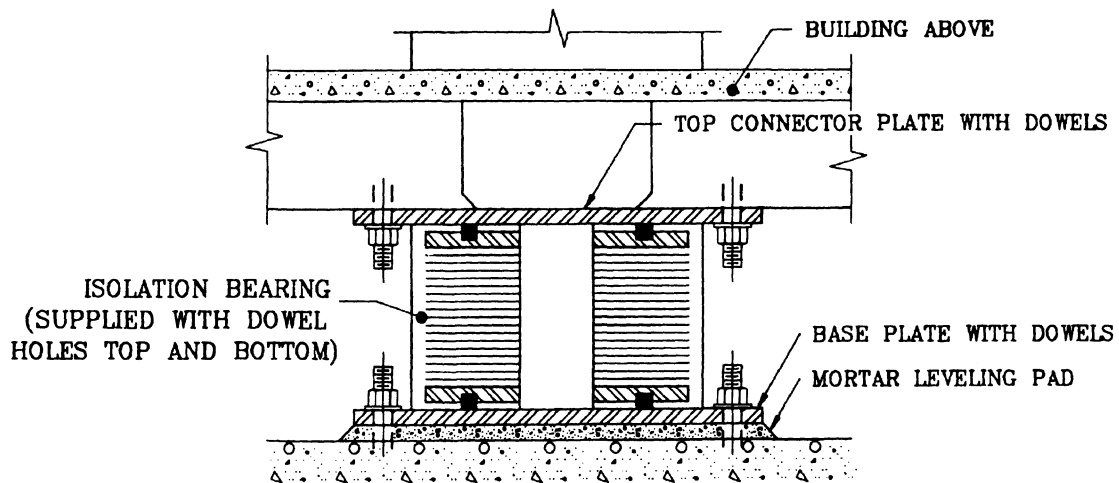


Figure 14-20. Installation using dowels

2. The connections must have the capacity for transferring maximum seismic forces between the substructure and the superstructure.
3. Ease of construction must be kept in mind to insure access for installation and, in the case of a retrofit, temporary support for the superstructure.

The most common bearing construction has outer load plates of $\frac{3}{4}$ - $1\frac{1}{2}$ in. steel covered by $\frac{1}{8}$ in. rubber layers. During the manufacture, holes for bolts or dowels are formed through the outer rubber layers and load plates. Exterior cover plates with bolts or dowels are then added to the bearing prior to installation. These exterior plates may be either welded or bolted to the structure. It is important to insure that the bolts or dowels do not intrude into the internal rubber layers. Figure 14-20 is an example of a connection detail using dowels. The more common trend is to use fully bolted rather than dowelled connections.

14.8.3 Provision for Bearing Removal

Where practical, provision should be made to ease removal and replacement of the bearings should this ever be necessary. This requires two things: (i) a means of supporting the building

weight while the bearing is removed, and (ii) a means of removing the bearing without undue damage to the connections.

The ease of meeting this first requirement will depend on the location of the bearings and type of backup safety system used. In a subbasement, jacks can generally be used between the foundation and basement floor to support the bearing load. If a backup safety system is used (as described in the following section), provision for jacking may be incorporated into the design. Bearing locations at the top of columns will require shoring to be erected around columns to provide a jacking platform if a backup system has not been provided.

The removal of the bearing once the load is removed will be simplified if bolted connections are used to connect to the structure. For example, the connection detail shown in Figure 14-20 could be modified to simplify bearing removal. In this modification, double plates would be added at the bottom of the bearing as shown in Figure 14-21. The bearing complete with dowel plates could then be removed. For a welded connection, removal would entail cutting the welds.

A combination of a removal and backup safety-system detail is shown in Figure 14-22.

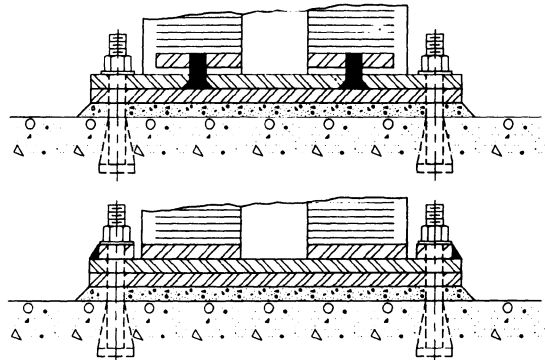


Figure 14-21. Details for replacement bearings

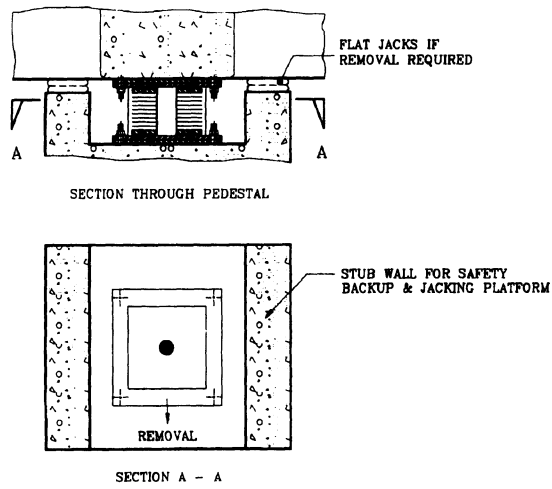


Figure 14-22. Backup and removal detail

14.8.4 Backup Safety System

Depending on the importance of the building, it may be considered desirable to incorporate such a system depends on the bearing location and configuration. For bearing locations at the top of columns a layout is shown schematically in Figure 14-23. This provides a means of supporting the vertical load, and a lateral displacement limiter. An alternate to the scheme of location bearings at the top of columns is to locate them at the base of the columns as shown in Figure 14-24.

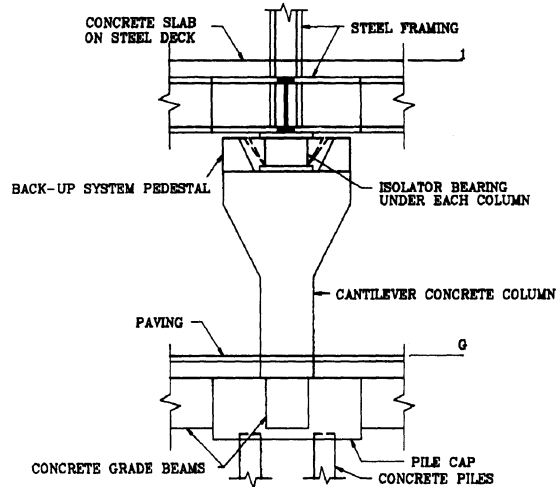


Figure 14-23. Bearings at top of columns

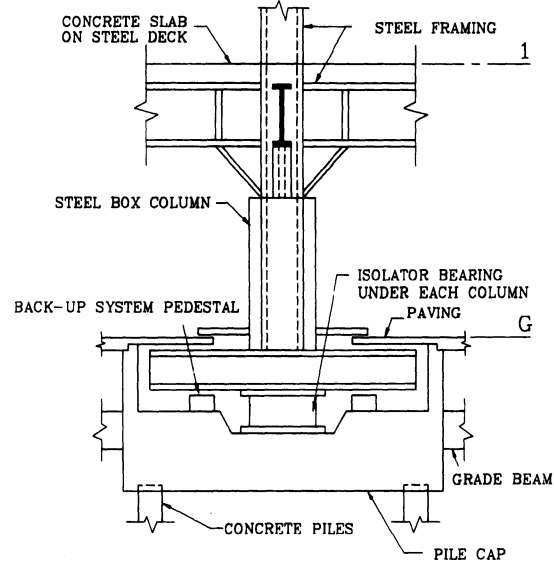


Figure 14-24. Bearings at base of columns

14.9 ISOLATOR DESIGN PROCEDURES

Basic procedures for design of the high damping and low damping rubber isolators (HDR, LDR), lead-rubber isolators (LRB), and the friction pendulum isolators (FPS) are presented in this section. The primary purpose of this information is to aid design engineer in preliminary sizing of the isolators needed for a

given project. For information The reader is encouraged to read the recent textbook by Kelly⁽¹⁴⁻⁴⁶⁾ for a very detailed coverage of mechanical characteristics and modeling of HDR and LRB isolators. A less exhaustive but more practical coverage of the same topics may be found in a recent textbook by Naeim and Kelly⁽¹⁴⁻⁸⁾. Further instructions and details for design of FPS isolators may be obtained from the patent-holder, Earthquake Protection Systems of Berkeley, California and from Reference 14-40.

The need for an isolation system which is stiff under low levels of lateral load (e.g. wind) but flexible under higher levels (i.e. earthquakes) necessarily leads to a nonlinear system. The properties of most isolator systems are characterized as bilinear. Although a trilinear model with stiffening at large horizontal displacements better represents the performance of HDR isolators.

Any complete design procedure should insure that (i) the bearings will safely support the maximum gravity service loads throughout the life of the structure and (ii) the bearings will provide a period shift and hysteretic damping during one or more design earthquakes. The steps to achieve these aims are:

1. The minimum required plan size is determined for the maximum gravity loads at each bearing location.
2. The total rubber thickness or dimensions of the FPS isolator is computed to give the period shift during earthquake loadings.
3. The damping characteristics of the isolator system is calculated to ensure proper value of the hysteretic damping and wind resistance required.
4. The performance of the bearings as designed is checked under gravity, wind, thermal, earthquake, and any other load conditions.

14.9.1 Elastomeric Isolators

One of the most important parameters in design of elastomeric bearings is the shape factor, S , defined as

$$S = \frac{\text{loaded area}}{\text{force - free area}}$$

For a circular pad with a diameter of Φ and a single layer rubber thickness, t

$$S = \frac{\Phi}{4t} \quad (14-17)$$

Generally a good design tries to keep the value of S to somewhere between 10 and 20.

The horizontal stiffness of a single isolator is given by

$$K_H = \frac{GA}{t_r} \quad (14-18)$$

where G is the shear modulus of the rubber, A is the full cross-sectional area of the pad, and t_r is the total thickness of rubber. The maximum shear strain, γ , experienced by the isolator is the maximum horizontal displacement, D , divided by the total rubber thickness, t_r .

$$\gamma = \frac{D}{t_r} \quad (14-19)$$

The vertical stiffness of a rubber bearing is given by

$$K_V = \frac{E_c A_s}{t_r} \quad (14-20)$$

where E_c is the compression modulus of the rubber-steel composite and A_s is the area of a steel shim plate. For a circular pad without any holes in the center

$$E_c = 6GS^2 \quad (14-21)$$

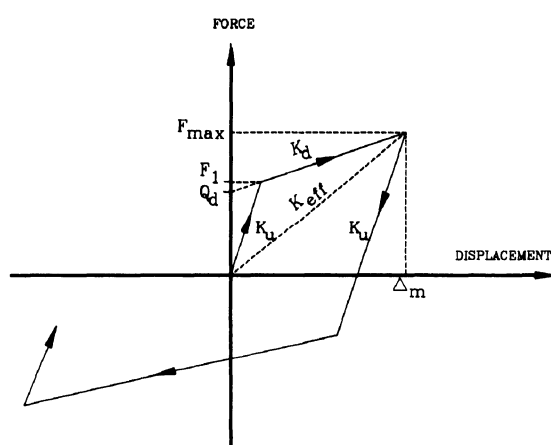
For bearings with very large shape factors the compressibility of rubber affects the value of E_c . In such cases a more accurate estimate of E_c may be obtained from

$$E_c = \frac{6GS^2 K}{6GS^2 + K} \quad (14-22)$$

where K is the bulk modulus of rubber and generally varies from 145,000 psi to 360,000 psi depending on the type of rubber being used. The value of 290,000 psi is most commonly used.

14.9.2 Lead-Rubber Isolators (LRB)

The lead-rubber bearing is a nonlinear system which may be very effectively idealized in terms of a bilinear force—deflection curve with constant values throughout many cycles of loading (Figure 14-25). Formulas developed in the previous section are also applicable here with some additional equations that model the lead core properties.



Q_d = Characteristic strength (kips)
 F_1 = Yield force (kips)
 F_{max} = Maximum force (kips)
 K_d = Post-elastic stiffness (kip/inch)
 K_u = Elastic (unloading) stiffness (kip/inch)
 K_{eff} = Effective stiffness
 Δ_m = Maximum bearing displacement

Figure 14-25. Typical bilinear hysteresis loop

The characteristic strength, Q_d , can be accurately estimated as being equal to the yield force of the lead plug. The yield stress of lead is about 1,500 psi. The effective stiffness of the lead-plug bearing, K_{eff} , at a horizontal

displacement D larger than the yield displacement D_y , may be defined in terms of the post-elastic stiffness, K_d , and characteristic strength, Q_d , as

$$K_{eff} = K_d + \frac{Q_d}{D} \quad D \geq D_y \quad (14-23)$$

The natural period is given as

$$T = 2\pi \sqrt{\frac{W}{K_{eff} g}} \quad (14-24)$$

As a rule of thumb for lead-rubber isolators K_u is taken as $10K_d$. Kelly⁽¹⁴⁻⁴⁶⁾ has shown that with this assumption, the effective percentage of critical damping provided by the isolator, β_{eff} , can be obtained from

$$\beta_{eff} = \frac{4Q_d(D - Q_d/9K_u)}{2\pi(K_u D + Q_d)D} \quad (14-25)$$

14.9.3 Friction Pendulum System

If the load on an FPS isolator is W , and the radius of curvature of the FPS dish is R , then the horizontal stiffness of the isolator may be defined for design purposes as

$$K_H = \frac{W}{R} \quad (14-26)$$

The natural period of an FPS isolated system is only a function of R

$$T = 2\pi \sqrt{\frac{R}{g}} \quad (14-27)$$

The effective (peak-to-peak) stiffness of the isolator is given by

$$K_{eff} = \frac{W}{R} + \frac{\mu W}{D} \quad (14-27)$$

where μ is the friction coefficient and all other terms are defined previously. The friction coefficient has been shown to be independent of velocity for pressures of 20 ksi or more on the articulated slider⁽¹⁴⁻⁸⁾. The damping provided by the system, β , is a function of horizontal displacement and may be obtained from

$$\beta = \frac{2}{\pi} \frac{\mu}{\mu + D/R} \quad (14-28)$$

An estimate of the rise of the structure (vertical displacement) as a result of movement along the curved surface of the isolator may be obtained from

$$\delta_v \equiv \frac{1}{2} \frac{D^2}{R} \quad (14-29)$$

14.9.4 Design Example

Assume you are in charge of designing a four story isolated building. The owner, a public entity, requires that the design accommodate competing isolation systems to bid on the job. The architect needs to know the maximum dimensions of the isolators so that she can complete her schematic design. Your engineering team needs to know the design base shears for proportioning the structural system above and the elements below the isolation surface. You would like to estimate these values for three alternative isolation systems:

- a) a high damping rubber system
- b) a lead-rubber system which may or may not be complimented by ordinary low-damping isolators, and
- c) a friction pendulum system.

The following information is also available to you at this time.

- The structural system above the isolation plane is a shear wall system with $R = 6$.
- The total weight of the building is 14,120 kips.
- There are a total of 60 support points (i.e., 60 isolators).

- The average sustained load on an interior isolator is 500 kips.
- The fixed-base period of the super-structure is estimated to be about 0.70 seconds.
- From IBC-2000 for this site, $S_{DI}=0.56$

Estimate the size of isolators needed for each of the three alternatives and the corresponding seismic design base shears so that the architect and engineers could make substantial progress while you are performing your final design of the isolators and preparing for procurement and prototype testing process.

SOLUTION

$$T_D \geq 3T_{fixed-base} = 3(0.7) = 2.1 \text{ sec.}$$

To be on the safe side, take $T_D=2.5$ sec for preliminary design. The reduction fact, RI for the superstructure is calculated from Eq. 14-14 as

$$1.0 \leq R_I = \frac{3}{8}(6) = 2.25 \leq 2.0 \Rightarrow R_I = 2.0$$

a) High-Damping Rubber Isolators

To be conservative we size the isolator under largest sustained load. That is an interior isolator under 500 kips of load. We take damping to be 10% subject to verification. Therefore, from Eq. 14-17 or from Table 1623.2.2.1 of IBC-2000, $B_D=1.20$.

We take a typical high damping rubber compound with $G=145$ psi and $K=300$ ksi. Therefore, our first estimate for the horizontal stiffness of the isolator is obtained from Eq. 14-8 as

$$K_H = \frac{W}{g} \left(\frac{2\pi}{T} \right)^2 = \frac{500}{386} \left(\frac{2\pi}{2.5} \right)^2 = 7.35 \text{ k/in.}$$

The design displacement is obtained from Eq. 14-1

$$D_D = \left(\frac{g}{4\pi^2} \right) \frac{(0.56)(2.5)}{1.20} = 11.43 \text{ in.}$$

Usually we want to achieve this displacement at about 150% shear strain. From Eq. 14-19, we can estimate the total rubber thickness required

$$\gamma = \frac{D}{t_r} \Rightarrow t_r = \frac{11.43}{1.50} = 7.6 \text{ in.}$$

Now we calculate the cross-sectional area and the required diameter of the bearing from Eq. 14-18

$$A = \frac{K_H t_r}{G} = \frac{7.33(7.6)}{0.145} = 384 \text{ in}^2$$

$$\Phi = \sqrt{\frac{4A}{\pi}} = \sqrt{\frac{4(384)}{\pi}} = 22.12 \text{ in}$$

Use $\Phi = 24$ in.

Now we re-calculate A , K_H and T_D based on this bearing diameter:

$$A = \frac{\pi\Phi^2}{4} = \frac{\pi(24)^2}{4} = 452 \text{ in}^2$$

$$K_H = 7.35(452/384) = 8.65 \text{ k/in}$$

$$T_D = 2.50\sqrt{(7.33/8.65)} = 2.3 \text{ sec} > 2.1 \text{ sec}$$

Selecting a shape factor of $S=10$, from Eq. 14-17 we can calculate the thickness of individual rubber layers, t

$$t = \frac{\Phi}{4S} = \frac{24}{4(10)} = 0.6 \text{ in, say } 5/8"$$

$$\text{number of layers} = \frac{7.6}{5/8} = 12.1, \text{ say } 12$$

$$t_r = 12(5/8) = 7.5 \text{ in}$$

Using 0.1 in thick steel shim plates and one inch top and bottom end plates, the total height of the bearing is

$$h = 7.5 + 2(1.0) + 11(0.1) = 10.6 \text{ in}$$

Let us now estimate the base shear coefficient for design of the superstructure, C_s , and the corresponding value for the base, C_b .

$$C_b = \frac{V_b}{W} \cong \frac{K_H D}{W} = \frac{8.65(11.43)}{500} = 0.20$$

$$C_s = \frac{C_b}{R_I} \cong 0.10$$

b) Lead-Rubber Isolators

It is usually more beneficial to begin designing isolation systems using LRB isolators as a system and then assign individual isolator properties. The reason is that often the best solution is a combination of LRB isolators and low damping rubber isolators (i.e., isolators without the lead plug).

In LRB isolators since damping comes from the lead core, usually there is no need to use high damping rubber and therefore ordinary rubber is generally used. Given the solution in Part (a) of this problem, it is obvious that we do not need a large amount of damping here. Therefore, we use 15% critical damping subject to verification and a rubber compound with a shear modulus of $G=60$ psi.

The same target period of 2.5 seconds is maintained. Either from Eq. 14-17 or from Table 1623.2.2.1 of IBC-2000, for $\beta=15\%$, $B_D=1.35$ and from Eq. 14-1

$$D_D = \left(\frac{g}{4\pi^2} \right) \frac{(0.56)(2.5)}{1.35} = 10.16 \text{ in.}$$

Treating the entire isolation system as a unit, the required stiffness corresponding to this period is

$$K_H = \frac{W}{g} \left(\frac{2\pi}{T} \right)^2 = \frac{14,120}{386} \left(\frac{2\pi}{2.5} \right)^2 = 231 \text{ k/in.}$$

The energy dissipated per cycle is

$$W_D = 2\pi K_{eff} D^2 \beta_{eff} = 2\pi(231)(10.16)^2(0.15) \\ = 22,462 \text{ k-in}$$

The area of the hysteresis loop, however, is also given by

$$W_D = 4Q_d(D - D_y)$$

and if ignore D_y because of its relatively small size

$$Q_d \approx \frac{W_D}{4D} = \frac{22,462}{4(10.16)} = 552 \text{ kips}$$

Now, we can estimate K_d from Eq. 14-23:

$$K_d = K_{eff} - \frac{Q_d}{D} = 231 - \frac{552}{10.16} \\ = 176 \text{ kips/in}$$

and since

$$D_y = \frac{Q_d}{K_u - K_d} \text{ and } K_u \approx 10K_d, \text{ then}$$

$$D_y \approx \frac{Q_d}{9K_d} = \frac{552}{9(176)} = 0.35 \text{ in.}$$

The total cross sectional area of the lead plug area needed for the entire isolation system is

$$A_{pb}^{total} = \frac{Q_d}{F_y^{pb}} = \frac{552}{1.5} = 368 \text{ in}^2$$

For the sake of simplicity, we keep the diameter of all isolators the same at $\Phi=24$ in. Using 3.5 inch diameter lead cores in 40 of the 60 isolators provides a lead cross sectional area of slightly more than 385 square inches. Now we have to recalculate Q_d based on this new area of lead

$$Q_d = 385(1.5) = 578 \text{ kips}$$

The stiffness provided by lead plugs is

$$K_{pb} = \frac{Q_d}{D} = \frac{578}{10.16} = 57 \text{ k-in}$$

and the remainder of required stiffness has to be provided by rubber. Therefore,

$$K_{rubber} = K_H - \frac{Q_d}{D} = 231 - \frac{552}{10.16} = 176 \text{ k-in}$$

The total cross sectional area of the rubber is

$$A_{rubber} = 60 \frac{\pi(24)^2}{4} - 385 = 26,744 \text{ in}^2$$

and from Eq. 14-18, we can now establish the required total rubber thickness, t_r , as

$$t_r = \frac{GA}{K_{rubber}} = \frac{(60 \times 10^{-3})(26,744)}{176} \\ = 9.1 \text{ in}$$

Therefore, assuming 1.0 inch thick top and bottom end plates and steel shims, our isolators will have a height of less than 12 inches.

The seismic shear coefficients are calculated as in Part (a):

$$C_b = \frac{231(10.16)}{14,120} = 0.167$$

$$C_s = \frac{0.17}{2} = 0.083$$

c) Friction Pendulum System

Using the same target period of 2.5 seconds, from Eq. 14-27

$$2.5 = 2\pi \sqrt{\frac{R}{386}} \Rightarrow R = 61.23 \text{ in}$$

Eq. 14-28 indicates that effective damping and maximum displacement are inter-related. For example, assuming a coefficient of friction

of $\mu=0.06$ and a design displacement of $D=12$ inches, we get

$$\beta_{eff} = \frac{2}{\pi} \frac{0.06}{0.06 + 12.0/61.23} = 15\%$$

The selected value of $D=12$ inches satisfies the minimum code prescribed displacement of 10.16 inches which was calculated for the same basic parameters ($T=2.5$ sec., $\beta=15\%$, $B=1.35$) in Part (b).

From Eq. 14-27 the effective total stiffness of the FPS isolation system consisting of 60 identical isolators will be

$$K_{eff} = \frac{14,120}{61.23} + \frac{0.06(14,120)}{12.0} = 301 \text{ k/in}$$

and the seismic base shear coefficients are calculated as before:

$$C_b = \frac{K_{eff} D}{W} = \frac{301(12.0)}{14,120} = 0.25$$

$$C_s = \frac{C_b}{R_I} = \frac{0.25}{2} = 0.125$$

14.10 CONCLUSIONS

Several practical systems of seismic isolation have been developed and implemented in recent years, and interest in the application of this technique continues to grow. Although seismic isolation offers significant benefits, it is by no means a panacea. Feasibility studies are required early in the design phase of a project to evaluate both the technical and the economic issues. If its inclusion is appropriate from a technical and first-cost perspective, then significant life-cycle cost advantages can be achieved. Thus, seismic isolation represents an important step forward in the continuity search for improved seismic safety.

The construction costs of incorporating seismic isolation in new buildings in the United

States indicates that it depends on two primary variables: the design force level of the conventional building and the location of the plane of isolation. The theory of seismic isolation permits substantial cost savings for isolated buildings compared to convention construction. However, given the current code regulations, the initial cost for seismic isolated structures can be equal to or exceed the cost for a similarly situated fixed base building by as much as 5%. However, one should keep in mind that this is a very minor price to pay for achieving a structures which will have a substantially better seismic performance during major earthquakes. Simply stated, achieving the level of performance provided by seismic isolation is virtually impossible through conventional construction.

For the retrofit of existing buildings, seismic isolation may only be technically applicable in one out of approximately eight buildings. When it is technically feasible it has the attractive feature that most of the construction work is confined to the basement area. Retrofit construction costs, when compared to a conventional code force level upgrade, have been shown to be comparable. In addition, disruption to the operation of the facility may be avoided during construction with the use of seismic isolation.

One of the major difficulties in comparing the costs and benefits of a conventional and an isolated structure is the significant difference in their performance characteristics. In the only such design performed to date, a critical Fire Command and Control Facility for Los Angeles County required both a conventional and an isolated two story structure to meet the same stringent performance criteria. In this case the isolated design was shown to be 6% less expensive.

If equivalent performance designs are not performed then the costs and benefits of different structural design schemes can only be assessed by calculating and comparing the four principal cost impact factors: 1) construction cost; 2) earthquake insurance premium; 3) physical damage that must be repaired and 4)

disruption costs, loss of market share and potential liability to occupants for their losses. Earthquake damage studies have shown that seismic isolation can reduce the cost of earthquake damage factors of 4 to 7. Furthermore, the estimated dollar value of earthquake damage in an isolated building has been shown to be less than the currently available 10% earthquake insurance deductible.

REFERENCES

- 14-1 Calantarians, J. A., "Improvements in and Connected with Building and Other Works and Appurtenances to Resist the Action of Earthquakes and the Like," Paper No. 325371, Engineering Library, Stanford University, CA, 1909.
- 14-2 deMontalk, Robert Wladislas, Shock Absorbing or Minimizing Means for Buildings," U.S. Patent No. 1,847,820, 1932.
- 14-3 Bechtold, Jacob, "Earthquake-Proof Building," US Patent No. 845,046, 1907.
- 14-4 Wright, F.L., An Autobiography: Frank Lloyd Wright, Horizon Press, New York, 1977.
- 14-5 Green, N.B., "Flexible First Story Construction for Earthquake Resistance," Trans. Amer. Soc. Civil Eng. 100, 645, 1935.
- 14-6 Kelly, J.M. "Aseismic Base Isolation: Its History and Prospects," Joint Sealing and Bearing Systems for Concrete Structures, Publication SP-70, American Concrete Institute, 1982.
- 14-7 Buckle, I.G. and Mayes, R.L., "Seismic Isolation: History, Application and Performance - A World View," Earthquake Spectra Journal, Theme Issue: Seismic Isolation, EERI, Vol. 6, No. 2, May 1990; and Buckle, I.G., "Development and Application of Base Isolation and Passive Energy Dissipation: A World Overview," Applied Technology Council Report 17, Palo Alto, CA, Mar. 1986.
- 14-8 Naeim, F. and Kelly, J.M., *Design of Seismic Isolated Structures: From Theory to Practice*, John Wiley and Sons, Inc., New York, 1999.
- 14-9 Skinner, R.E., Tyler, R.G., Heine, A.J., and Robinson, W.J., "Hysteretic Dampers for the Protection of Structures from Earthquakes," Bull. New Zealand Nat. Soc. Earthquake Eng. 13, No. 1, Mar. 1980.
- 14-10 Way, D. and Lew, M., "Design and Analysis of a High Damping Rubber Isolation System," Applied Technology Council Report No. 17, Palo Alto, CA, 1986.
- 14-11 Jolivet, F. and Richli, M., "Aseismic Foundation System for Nuclear Power Stations," Transactions of the Fourth Conference on Structural Mechanics in Reactor Technology, San Francisco, Vol. K, No. 9/2, 1977
- 14-12 Castiglinoni, A., Urbano, C., and Stupazzini, B., "Seismic Design of Bridges in High Activity Region," Proceedings of the Seventh European Conference on Earthquake Engineering, Athens, Vol. 6, 186-203, 1982.
- 14-13 Ikonomou, A.S., "Seismic Isolation of Bridges with the Alexismon," Proceedings of the Conference on Short an Medium Span Bridges, Toronto, 141-153, 1982.
- 14-14 Robinson, W.H., "Lead-Rubber Hysteretic Bearings Suitable for Protecting Structures During Earthquakes," J. Earthquake Eng. And Structural Dynamics 10, 593-604, 1982.
- 14-15 Blakeley, R. W. G., et al., "Recommendations for the Design and Construction of Base Isolated Structures," Bull. New Zealand Nat. Soc. Earthquake Eng. 12, No. 2, 1979.
- 14-16 Kelly, J. M. and Tsztroo, D., "Earthquake Simulation Testing of a Stepping Fram with Energy-Absorbing Devices," Report No. UCB/EERC-77/17, Earthquake Engineering Research Center, Univ. of California, Berkeley, 1977.
- 14-17 "Earthquake Simulator Tests of a Nine-Story Steel Frame with Columns Allowed to Uplift," report No. UCB/EERC-77/23, Earthquake Engineering Research Center, Univ. of California, Berkeley, 1977.
- 14-18 Kelly, J. M., Eidinger, J. M., and Derham, C. J., "A Practical Soft Story System," Report No. UCB/EERC-77/27, Earthquake Engineering Research Center, Univ. of California, Berkeley, 1977.
- 14-19 Kelly, J. M., Beucke, K. E., and Skinner, M. S., "Experimental Testing of a Friction Damped Aseismic Base Isolation System with Fail-Safe Characteristics," Report No. UCB/EERC-80/18, Earthquake Engineering Research Center, Univ. of California, Berkeley, 1980.
- 14-20 Kelly, J. M., Beucke, K. E., and Skinner, M. S., "Experimental Testing of an Energy-Absorbing Base Isolation System," Report No. UCB/EERC-80/35, Earthquake Engineering Research Center, University of California, Berkeley, 1980.
- 14-21 Kelly, J. M., and Hodder, S. B., "Experimental Study of Lead and Elastomeric Dampers for Base Isolation Systems," Report No. UCB/EERC-81/16, Earthquake Engineering Research Center, Univ. of California, Berkeley, 1981.
- 14-22 Kelly, J. M., Buckle, I. G., and Tsai, H. C., "Earthquake Simulator Testing of a Base Isolated Bridge Deck," Report No. UCB/EERC-85/09, Earthquake Engineering Research Center, Univ. of California, Berkeley, 1985.
- 14-23 Structural Engineers Association of California, Recommended Lateral Force Requirements and Commentary, San Francisco, 1983.

- 14-24 Stanton, J. F. and Roeder, C. W., "Elastomeric Bearings: Design, Construction and Materials," NCHRP Report 248, Transportation Research Board, Washington, 1982.
- 14-25 Applied Technology Council, "Proceedings of a Seminar and Workshop on Base Isolation and Passive Energy Dissipation," ATC Report No. 17, Palo Alto, CA, 1986.
- 14-26 Structural Engineers Association of Northern California (1986), *Tentative Seismic Isolation Design Requirements*, San Francisco, 1986.
- 14-27 Structural Engineers Association of Northern California, Tentative Lateral Force Requirements, San Francisco, 1985.
- 14-28 International Conference of Building Officials, *Uniform Building Code*, Whittier, CA 1994.
- 14-29 Kelly, T. E., Mayes, R. L., and Jones, L. R., "Preliminary Design Procedures for Seismically Isolated Structures," Proceedings of a Seminar on Base Isolation and Passive Energy Dissipation, Report No. 17, Applied Technology Council, Palo Alto, CA, 1986.
- 14-30 Buckle, I.G. and mayes, R.L. (1990), "The Application of Seismic Isolation to Bridges," Proceedings ASCE Structures Congress: Seismic Engineering - Research and Practice, pp 633-642, May, 1990.
- 14-31 Chalhoub, M.S., and Kelly, J.M., (1989) "Earthquake Simulator Evaluation of a Combined Sliding Bearing and Tension Controlled Rubber Bearing Isolation System." Proceeding, 1989 ASME Pressure Vessels and Piping Conference, American Society of Mechanical Engineers, Hawaii, Vol. 181, pp 59-64.
- 14-32 Constantinou, M.C., Mokha, A., and Reinhorn, A.M., (1990) "Teflon Bearings in Base Isolation II: Modeling," *Journal of Structural Engineering*, ASCE, Vol. 116, No. 2 pp. 455-474.
- 14-33 Griffith, M.C., Aiken, T.D., and Kelly, J.M. (1988) "Experimental Evaluation of Seismic Isolation of a Nine-Story Braced Steel Frame Subject to Uplift." Report No. UCB/EERC-88/05, Earthquake Engineering Research Center, University of California, Berkeley.
- 14-34 Kelly, J.M., Eidenger, J.M. and Derham, C.J. (1977) "A Practical Soft Story System," Report No. UCB/EERC-77/27, Earthquake Engineering Research Center, University of California, Berkeley.
- 14-35 Kelly, J.M., Beucke, K.E. and Skinner, M.S. (1980), "Experimental Testing of an Energy-Absorbing Base Isolation System," Report No. UCB/EERC-80/35, Earthquake Engineering Research Center, University of California, Berkley.
- 14-36 Kelly, J.M. and Hodder, S.B. (1981), "Experimental Study of Elastomeric Dampers for Base Isolation Systems," Report No. UCB.EERC-81/16, Earthquake Engineering Research Center, University of California, Berkeley.
- 14-37 Kell, J.M., Buckle, I.G. and Tsai, H.C. (1985), "Earthquake Simulator Testing of Base Isolated Bridge Deck," Report Bo UCB/EERC-85/09, Earthquake Engineering Research Center, University of California, Berkley.
- 14-38 Mokha, A., Constantinou, M.C., and Reinhorn, A.M., (1990), "Teflon Bearings in Base Isolation I: Testing," *Journal of Structural Engineering*, ASCE, Vol. 116, No. 2, pp. 438-454.
- 14-39 Mohka, A., Constantinou, M.C., and Reinhorn, A.M., (1990), "Teflon Bearings in a Seismic Base Isolation. Experimental Studies and mathematical Modeling." Report No. NCEER-88-0038, National Center for Earthquake Engineering Research, State University of New York, Buffalo.
- 14-40 Zayas, V., Low, S.S., and Mahin, S.A., (1987) "The FPS Earthquake resisting System, Experimental Report." Report No. UCB/EERC-87/01, Earth Engineering Research Center, University of California, Berkeley.
- 14-41 Applied Technology Council, "proceedings of a Workshop on Seismic Isolation, Passive Energy
- 14-42 International Code Council (2000), *International Building Code*, March.
- 14-43 International Conference of Building Officials, *Uniform Building Code*, Whittier, CA 1997.
- 14-44 Federal Emergency Management Agency (1997), *NEHRP Guidelines for the Seismic Rehabilitation of Buildings*, FEMA-273, Washington, D.C., October.
- 14-45 Federal Emergency Management Agency (1997), *NEHRP Commentary on the Guidelines for the Seismic Rehabilitation of Buildings*, FEMA-274, Washington, D.C., October.
- 14-46 Kelly, J.M. (1996), *Earthquake-Resistant Design with Rubber*, 2nd Edition, Springer-Verlag, London.

Chapter 15

Performance Based Seismic Engineering

Farzad Naeim, Ph.D., S.E.

Vice President and Director of Research and Development, John A. Martin & Associates, Inc., Los Angeles, California

Hussain Bhatia, Ph.D., P.E.

Senior Research Engineer, John A. Martin & Associates, Inc., Los Angeles, California

Roy M. Lobo, Ph.D., P.E.

Senior Research Engineer, John A. Martin & Associates, Inc., Los Angeles, California

Key words: Seismic Performance; Performance Based Design; Seismic Demand; Capacity; ADRS Spectrum; Target Displacement; Performance Objectives; Push-over Analysis; Capacity Spectrum; Static Analysis; Nonlinear Analysis; Damage Control; Life safety, Collapse Prevention; Immediate Occupancy

Abstract: Performance based seismic engineering is the modern approach to earthquake resistant design. Rather than being based on prescriptive mostly empirical code formulations, performance based design is an attempt to predict buildings with predictable seismic performance. Therefore, performance objectives such as life-safety, collapse prevention, or immediate occupancy are used to define the state of the building following a design earthquake. In one sense, performance based seismic design is limit-states design extended to cover the complex range of issues faced by earthquake engineers. This chapter provides a basic understanding of the promises and limitations of performance based seismic engineering. The state-of-the-art methodologies and techniques embodied in the two leading guidelines on this subject (ATC-40 and FEMA 273/274) are introduced and discussed. Numerical examples are provided to illustrate the practical applications of the methods discussed.

15.1 INTRODUCTION

The promise of performance-based seismic engineering (PBSE) is to produce structures with predictable seismic performance. To turn this promise into a reality, a comprehensive and well-coordinated effort by professionals from several disciplines is required.

Performance based engineering is not new. Automobiles, airplanes, and turbines have been designed and manufactured using this approach for many decades. Generally in such applications one or more full-scale prototypes of the structure are built and subjected to extensive testing. The design and manufacturing process is then revised to incorporate the lessons learned from the experimental evaluations. Once the cycle of design, prototype manufacturing, testing and redesign is successfully completed, the product is manufactured in a massive scale. In the automotive industry, for example, millions of automobiles which are virtually identical in their mechanical characteristics are produced following each performance-based design exercise.

What makes PBSE different and more complicated is that in general this massive payoff of performance-based design is not available. That is, except for large-scale developments of identical buildings, each building designed by this process is virtually unique and the experience obtained is not directly transferable to buildings of other types, sizes, and performance objectives. Therefore, up to now PBSE has not been an economically feasible alternative to conventional prescriptive code design practices. Due to the recent advances in seismic hazard assessment, PBSE methodologies, experimental facilities, and computer applications, PBSE has become increasing more attractive to developers and engineers of buildings in seismic regions. It is safe to say that within just a few years PBSE will become the standard method for design and delivery of earthquake resistant structures.

In order to utilize PBSE effectively and intelligently, one need to be aware of the

uncertainties involved in both structural performance and seismic hazard estimations. We discuss these issues first before exploring the philosophies and detailed requirements of the two most prominent PBSE guidelines available today. These guidelines are generally referred to by their short names: ATC-40⁽¹⁵⁻¹⁾ and FEMA-273/274^(15-2,15-3).

15.2 UNCERTAINTIES IN SEISMIC DESIGN AND PERFORMANCE

Every structural system is designed to have a seismic capacity that exceeds the anticipated seismic demand. Capacity is a complex function of strength, stiffness and deformability conjectured by the system configuration and material properties of the structure.

A key requirement of any meaningful PBSE exercise is the ability to assess seismic demands and capacities with a reasonable degree of certainty. The recent popularity of PBSE has brought many state-of-the-art analysis and design techniques into the mainstream of earthquake engineering practice. Furthermore, it has opened the door for a multi-disciplinary approach to seismic design which involves developers and building officials as well as engineers and earth-scientists. These are very positive developments which are bound to improve the quality of earthquake resistant construction.

The mere desire to produce structures with predictable seismic performance does not by itself, however, turn PBSE into a reality. Many uncertainties and gaps of knowledge have to be dealt with before PBSE turns from a promise into a reality. Structural engineering practice has been able to produce structures which with a few notable exceptions (i.e., welded steel moment frame structures during the 1994 Northridge earthquake) generally exceed performance expectations postulated by routine design analysis. Our capability to estimate the ultimate seismic capacities and failure loads associated with a structure, however, at least

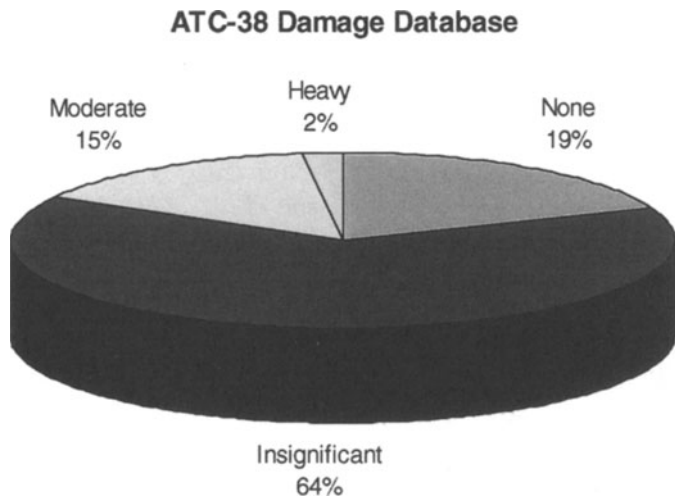


Figure 15-1. Damage State in 530 Buildings within 15 km of epicenter Surveyed After the 1994 Northridge Earthquake

outside the academic research settings is fairly limited and not up to the standards needed for a reliable prediction of seismic performance.

For example, following the Northridge earthquake, the Applied Technology Council conducted a survey of 530 buildings which were located within 300 meters of strong-motion recording sites⁽¹⁵⁻⁴⁾. From the total of 530 buildings which were located in the areas of strong shaking (San Fernando Valley, Santa Monica, and West Los Angeles) with peak ground acceleration in their vicinity ranging from 0.15g to 1.78g, only 10 (less than two-percent) showed heavy damage, a total of 78 buildings (about 15-percent) showed moderate damage and 340 (64-percent) were marked by insignificant damage (Figure 15-1). If response of these buildings were predicted by standard design analysis techniques, a far worse picture would have been predicted.

Crandell⁽¹⁵⁻⁵⁾ performed a similar statistically-based study of the seismic performance of residential buildings located within a 10-mile radius of the Northridge earthquake epicenter (Figure 15-2). Three hundred forty one of the 375 randomly selected

homes were surveyed and although more than 90 percent of the homes in the sample were old and built prior to the 1971 San Fernando Valley earthquake the cases of moderate to high damage were infrequent (less than 2-percent). Most occurrences of serious damage were located in foundation systems and were associated with localized site conditions such as liquefaction, fissuring, and hillside slope failures. Here again, design analysis would have predicted much larger damage percentage than the 2-percent number reported by Crandell.

Large uncertainties also exist in our estimates of design ground motion. For example, median estimates of spectral accelerations for a magnitude 7.0 event at rupture distance of 10 km obtained from various attenuation relations can vary by as much as 50 percent⁽¹⁵⁻⁶⁾. If the uncertainties associated with other source and regional variables are also considered, the variance could be significantly larger. Most attenuation relations are updated every few years (Figure 15-3), indicating that there are still many things to be learned about the generation and propagation of earthquake ground motion.

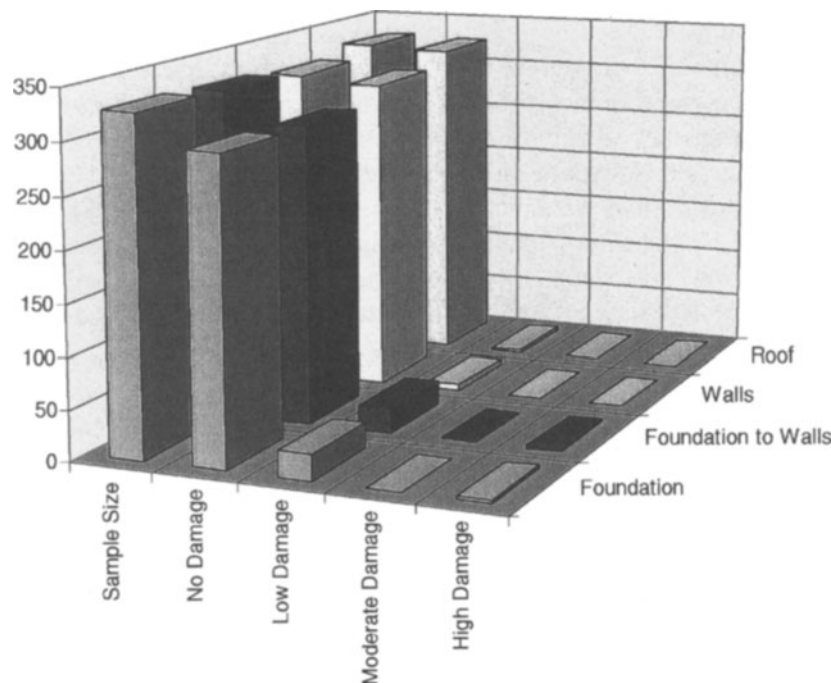


Figure 15-2. Description of Damage During the 1994 Northridge Earthquake to Single Family Dwellings Within a 10 Miles Radius of the Epicenter (data from Crandell, 1997)

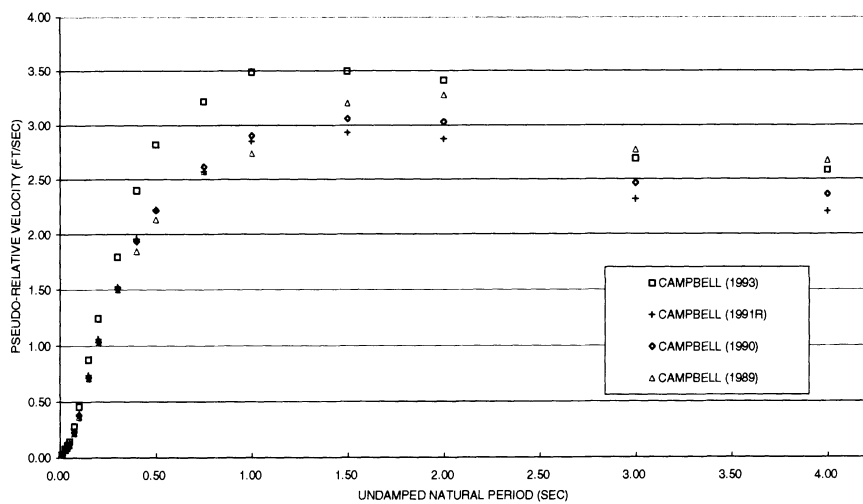


Figure 15-3. Evolution of a Typical Attenuation Relation (Spectral velocity estimates are shown for a magnitude 7.0 event at 5.0 km for a strike-slip fault)

Another source of uncertainty is critical shortage of recorded earthquake ground motion where they are needed most. Despite the tremendous growth in the number of earthquake records during the past decade, the number of recordings from large earthquakes close by. Figure 15-3⁽¹⁵⁻⁷⁾ shows a bivariate histogram of horizontal components recorded in north and central America categorized by magnitude and epicentral distance, indicating practically no record of $M > 7.5$ at distances less than 20 km. All of the data for $M > 8$ records come from a

single event (Mexico, 1985). Clearly, this is one of the areas where more information is needed for performance based design

Since PBSE is inherently multi-disciplinary in nature, further educational efforts are also of vital importance in bringing PBSE to fruition by developing a common understanding of issues and a common PBSE language and vocabulary. Only a broad multi-disciplinary approach can succeed in reduction of uncertainties, knowledge gaps, and common misunderstandings.

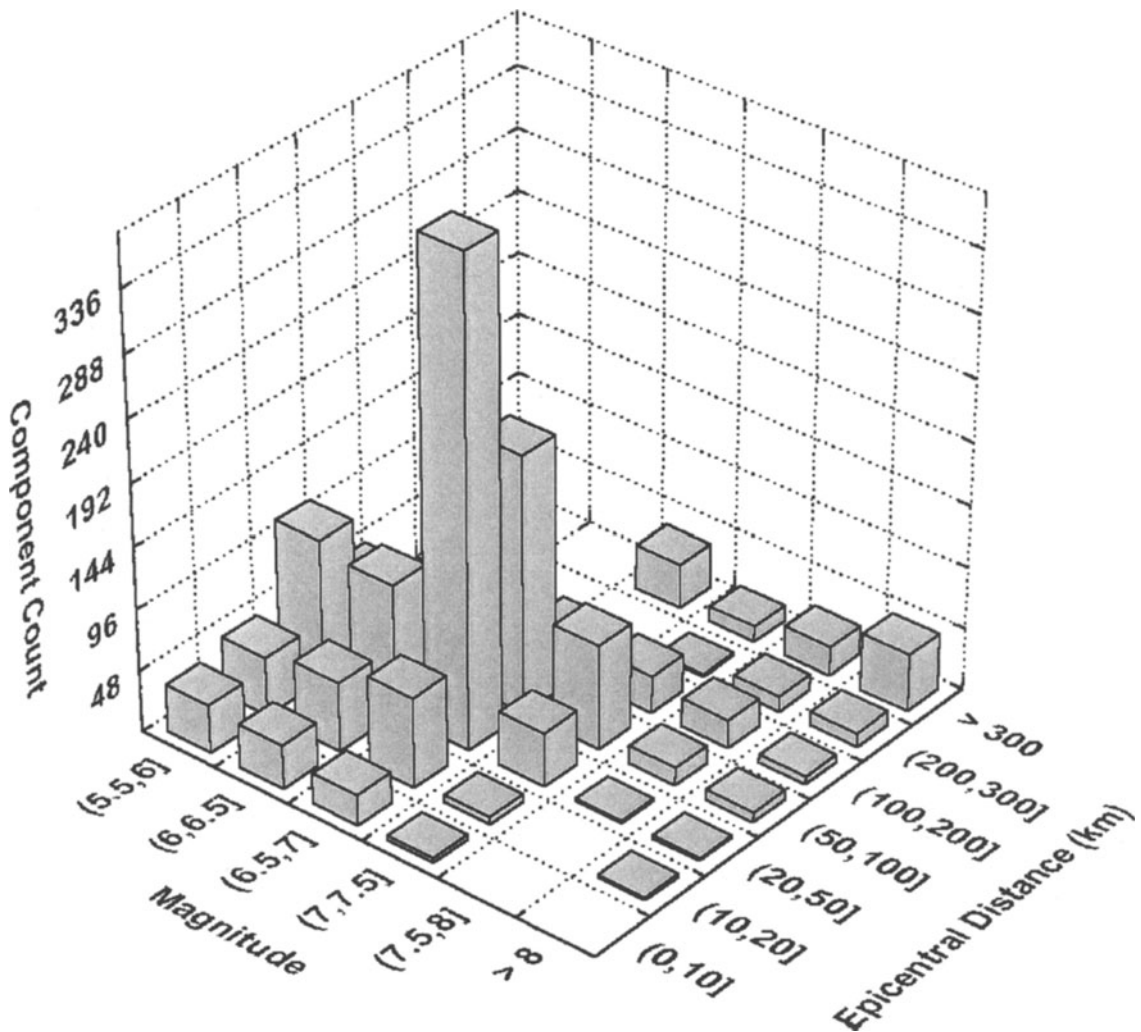


Figure 15-4. Distribution of Magnitude and Distance among Available Earthquake Records for North and Central America, 1933-1994 ($M > 5.5$; $PGA > 0.05g$)

15.3ATC-40

15.3.1 Introduction

Seismic Evaluation and Retrofit of Concrete Buildings⁽¹⁵⁻¹⁾ commonly referred to as ATC-40 was developed by the Applied Technology Council (ATC) with funding from the California Safety Commission. Although the procedures recommended in this document are for concrete buildings, they are applicable to most building types. This document provides a practical guide to the entire evaluation and retrofit process using performance-based objectives. Although it is not intended for the design of new buildings, the analytical procedures described in this document are certainly applicable.

ATC-40 recommends the following steps for the entire process of evaluation and retrofit:

1. Initiation of a Project: Determine the primary goal and potential scope of the project.
2. Selection of Qualified Professionals: Select engineering professionals with a demonstrated experience in the analysis, design and retrofit of buildings in seismically hazardous regions. Experience with PBSE and non-linear procedures is also needed.
3. Performance Objective: Choose a performance objective from the options provided for a specific level of seismic hazard.
4. Review of Building Conditions: Perform a site visit and review drawings.
5. Alternatives for Mitigation: Check to see if the non-linear procedure is appropriate or relevant for the building under consideration.
6. Peer Review and Approval Process: Check with building officials and consider other quality control measures appropriate to seismic evaluation and retrofit.
7. Detailed Investigations: Perform a non-linear static analysis if appropriate.

8. Seismic Capacity: Determine the inelastic capacity curve also known to pushover curve. Convert to capacity spectrum.
9. Seismic Hazard: Obtain a site specific response spectrum for the chosen hazard level and convert to spectral ordinates (ADRS)^(15-8,15-9,15-10), see Section 15.3.6) format.
10. Verify Performance: Obtain performance point as the intersection of the capacity spectrum and the reduced seismic demand in spectral ordinates (ADRS) format. Check all primary and secondary elements against acceptability limits based on the global performance goal.
11. Prepare Construction Documents: Detail retrofit to conform to code requirements and get analysis and design peer-reviewed and submit for plan check.
12. Monitor Construction Quality.

The performance-based roots of ATC-40 are essentially the same as FEMA-273 and FEMA-274, *NEHRP Guidelines for the Seismic Rehabilitation of Building*^(15-2, 15-3) and SEAOC's *Vision 2000: Performance-Based Seismic Engineering of Buildings* (1995)⁽¹⁵⁻¹¹⁾.

15.3.2 Performance Objectives

A performance objective has two essential parts – a damage state and a level of seismic hazard. Seismic performance is described by designating the maximum allowable damage state (performance level) for an identified seismic hazard (earthquake ground motion). A performance objective may include consideration of damage states for several levels of ground motion and would then be termed a dual or multiple-level performance objective.

The target performance objective is split into Structural Performance Level (SP-n, where n is the designated number) and Non-structural Performance Level (NP-n, where n is the designated letter). These may be specified independently, however, the combination of the two determines the overall Building Performance level.

Structural Performance Levels are defined as:

- **Immediate Occupancy (SP-1):** Limited structural damage with the basic vertical and lateral force resisting system retaining most of their pre-earthquake characteristics and capacities.
- **Damage Control (SP-2):** A placeholder for a state of damage somewhere between Immediate Occupancy and Life Safety.
- **Life Safety (SP-3):** Significant damage with some margin against total or partial collapse. Injuries may occur with the risk of life-threatening injury being low. Repair may not be economically feasible.
- **Limited Safety (SP-4):** A placeholder for a state of damage somewhere between Life Safety and Structural Stability.
- **Structural Stability (SP-5):** Substantial Structural damage in which the structural system is on the verge of experiencing partial or total collapse. Significant risk of injury exists. Repair may not be technically or economically feasible.
- **Not Considered (SP-6):** Placeholder for situations where only non-structural seismic evaluation or retrofit is performed.

Non-structural Performance Levels are defined as:

- **Operational (NP-A):** Non-structural elements are generally in place and functional. Back-up systems for failure of external utilities, communications and transportation have been provided.
- **Immediate Occupancy (NP-B):** Non-structural elements are generally in place but may not be functional. No back-up systems for failure of external utilities are provided.
- **Life Safety (NP-C):** Considerable damage to non-structural components and systems but no collapse of heavy items. Secondary hazards such as breaks in high-pressure, toxic or fire suppression piping should not be present.

- **Reduced Hazards (NP-D):** Extensive damage to non-structural components but should not include collapse of large and heavy items that can cause significant injury to groups of people..
- **Not Considered (NP-E):** Non-structural elements, other than those that have an effect on structural response, are not evaluated.

Combinations of Structural and Non-structural Performance Levels to obtain a Building Performance Level are shown in Table 15-1.

15.3.3 Nonlinear Static Procedures

In Nonlinear Static Procedure, the basic demand and capacity parameter for the analysis is the lateral displacement of the building. The generation of a capacity curve (base shear vs roof displacement Figure 15-5) defines the capacity of the building uniquely for an assumed force distribution and displacement pattern. It is independent of any specific seismic shaking demand and replaces the base shear capacity of conventional design procedures. If the building displaces laterally, its response must lie on this capacity curve. A point on the curve defines a specific damage state for the structure, since the deformation for all components can be related to the global displacement of the structure. By correlating this capacity curve to the seismic demand generated by a specific earthquake or ground shaking intensity, a point can be found on the capacity curve that estimates the maximum displacement of the building the earthquake will cause. This defines the performance point or target displacement. The location of this performance point relative to the performance levels defined by the capacity curve indicates whether or not the performance objective is met.

Table 15-1. Combinations of Structural and Non-structural Levels to form Building Performance Levels⁽¹⁵⁻¹⁾

Non-structural Performance Levels	Building Performance Levels					
	SP-1 Immediate Occupancy	SP-2 Damage Control (Range)	SP-3 Life Safety	SP-4 Limited Safety (Range)	SP-5 Structural Stability	SP-6 Not Considered
NP-A Operational	1-A Operational	2-A	NR	NR	NR	NR
NP-B Immediate Occupancy	1-B Immediate Occupancy	2-B	3-B	NR	NR	NR
NP-C Life Safety	1-C	2-C	3-C Life Safety	4-C	5-C	6-C
NP-D Reduced Hazards	NR	2-D	3-D	4-D	5-D	6-D
NP-E Not Considered	NR	NR	3-E	4-E	5-E Structural Stability	Not Applicable

Legend

White	Commonly referenced Building Performance Levels (SP-NP)
Light Gray	Other possible combinations of SP-NP
Dark Gray	Not recommended combinations of SP-NP

Thus, for the Nonlinear Static Procedure, a static pushover analysis is performed using a nonlinear analysis program for an increasing monotonic lateral load pattern. An alternative is to perform a step by step analysis using a linear program. The base shear at each step is plotted again roof displacement. The performance point is found using the Capacity Spectrum Procedure^[15-8,15-9,15-10] described in subsequent sections. The individual structural components are checked against acceptability limits that depend on the global performance goals. The nature of the acceptability limits depends on specific components. Inelastic rotation is typically one of acceptability parameters for beam and column hinges. The limits on inelastic rotation are based on observation from tests and the collective judgement of the development team.

15.3.4 Inelastic Component Behavior

The key step for the entire analysis is identification of the primary structural

elements, which should be completely modeled in the non-linear analysis. Secondary elements, which do not significantly contribute to the building's lateral force resisting system, do not need to be included in the analysis.

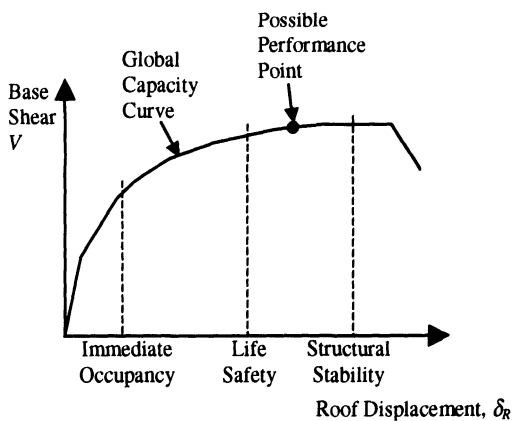


Figure 15-5. Building Capacity Curve

In concrete buildings, the effects of earthquake shaking are resisted by vertical frame elements or wall elements that are

connected to horizontal elements (diaphragms) at the roof and floor levels. The structural elements may themselves comprise of an assembly of elements such as columns, beam, wall piers, wall spandrels etc. It is important to identify the failure mechanism for these primary structural elements and define their non-linear properties accordingly. The properties of interest of such elements are relationships between the forces (axial, bending and shear) and the corresponding inelastic displacements (displacements, rotations, drifts). Earthquakes usually load these elements in a cyclic manner as shown in Figure 15-6a. For modeling and analysis purposes, these relationship can be idealized as shown in Figure 15-6b using a combination of empirical data, theoretical strength and strain compatibility.

Using the component load-deformation data and the geometric relationships among components and elements, a global model of the structure relates the total seismic forces on a building to its overall lateral displacement to generate the capacity curve. During the pushover process of developing the capacity curve as brittle elements degrade, ductile elements take over the resistance and the result is a saw tooth shape that helps visualize the performance. Once the global displacement demand is estimated for a specific seismic hazard, the model is used to predict the resulting deformation in each component. The ATC 40 document provides acceptability limits for component deformations depending on the specified performance level.

15.3.5 Geotechnical effects

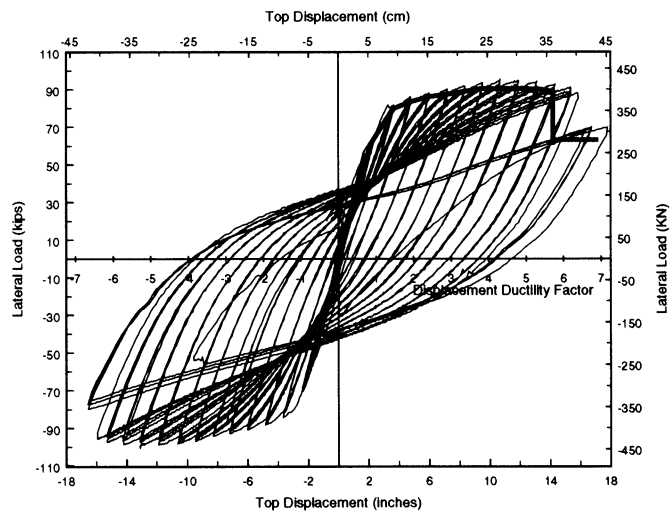
The deformation and movement of the foundations of a building can significantly affect the seismic response and performance of structures. As the structural components are represented by non-linear load-displacement relationships, analogous techniques compatible

and consistent with the general methodology should be used for the effects of the foundations.

The response parameters of foundation elements are dependent on structural as well as geotechnical components. Spread footings elements, for example, might consist of a rigid structural plate component model of the concrete footing bearing on soil represented by geotechnical components with appropriate force-displacement properties. Some generic models for typical foundation elements and acceptance criterion for structural components of the foundations are provided in ATC-40.

There is a large degree of uncertainty associated with both strength and stiffness of the geotechnical components. Thus, ATC-40 recommends enveloping analysis to determine the sensitivity of seismic performance to foundation behavior (See Figure 15-8). Guidance is provided for representative properties of normally encountered soil materials that are based on limited initial investigations in ATC-40. If the analysis shows sensitivity to foundation behavior than more detailed investigations and tests of geotechnical properties may be warranted.

Geotechnical properties are very ductile and failure is rarely encountered. Thus, deformation limits of geotechnical components are not explicitly defined. However, deformation of geotechnical components may affect the deformation and acceptability of components in the superstructure. It should also be noted that geotechnical components tend to accumulate residual displacements. This tendency may affect the acceptability of a structure for higher performance objectives such as Immediate Occupancy. Soil structure interaction also has beneficial affects such as lower demands on structural members due to base rotation, lower forces due to uplift and damping effects that reduce demand on the superstructure.



(a) Backbone curve from actual hysteretic behavior

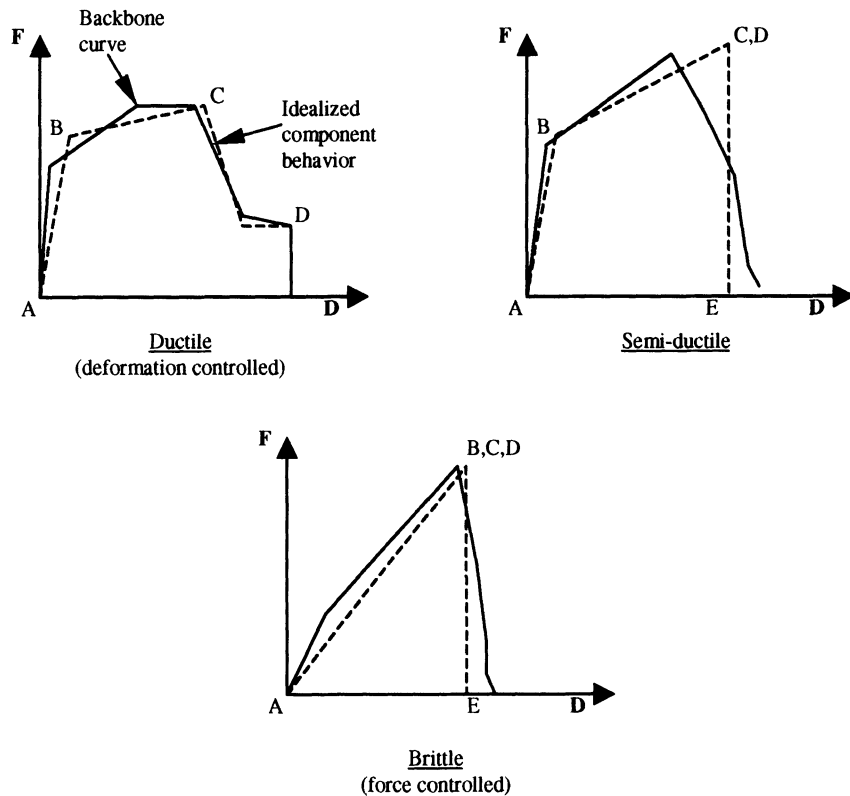
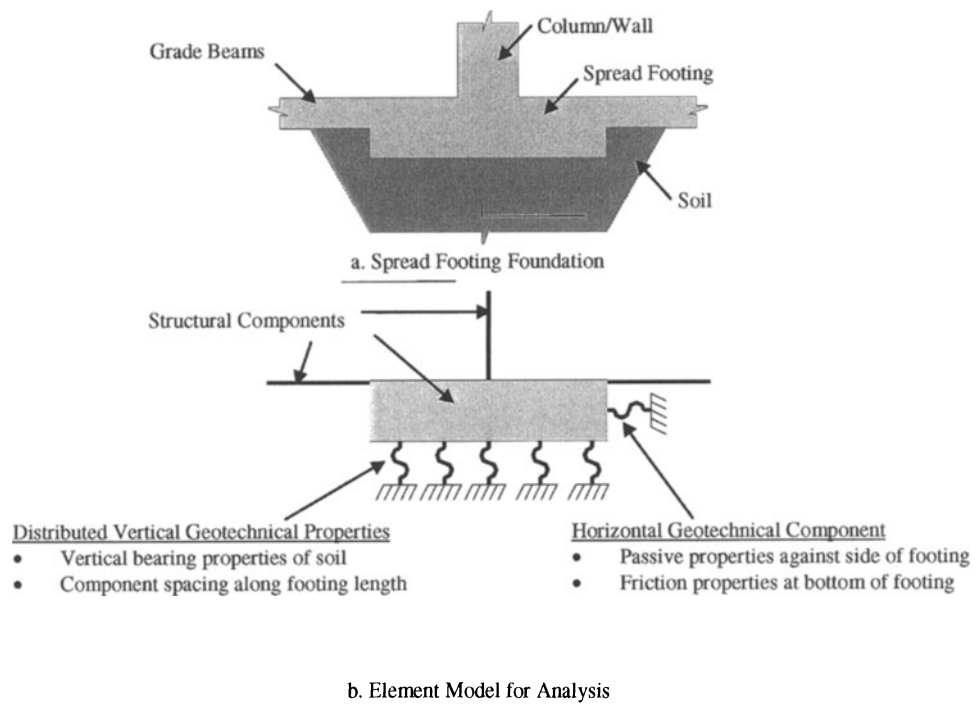
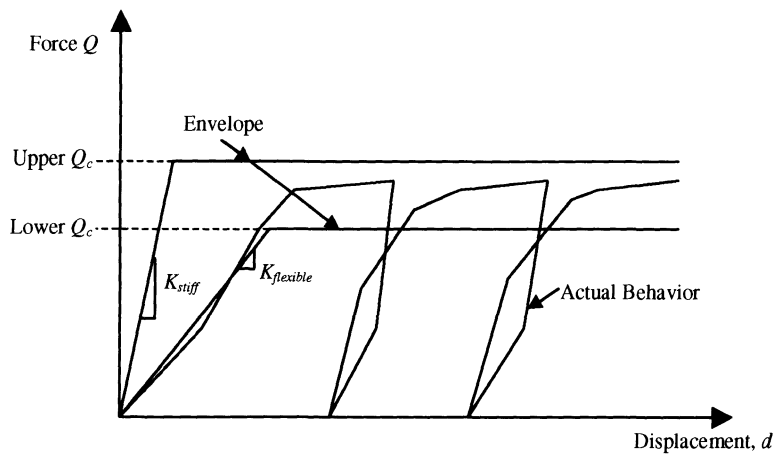
(b) Idealized component behavior from backbone curves⁽¹⁵⁻¹⁾

Figure 15-6. Idealized Component Force-Deformation Relationships

Figure 15-7. Shallow Foundation Model⁽¹⁵⁻¹⁾Figure 15-8. Basic Force-Displacement Envelope for Geotechnical Components⁽¹⁵⁻¹⁾

15.3.6 Capacity Spectrum Method

One of the methods used to determine the performance point is the Capacity Spectrum Method^(15-8,15-9,15-10), also known as the Acceleration-Displacement Response Spectra method (ADRS). The Capacity Spectrum Method requires that both the capacity curve and the demand curve be represented in response spectral ordinates. It characterizes the seismic demand initially using a 5% damped linear-elastic response spectrum and reduces the spectrum to reflect the effects of energy dissipation to estimate the inelastic displacement demand. The point at which the capacity curve intersects the reduced demand curve represents the performance point at which capacity and demand are equal.

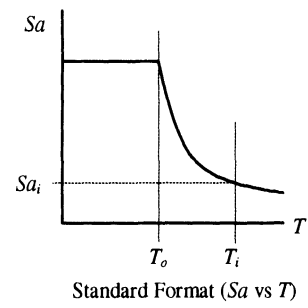
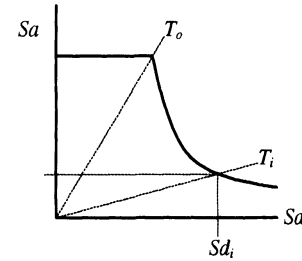
To convert a spectrum from the standard Sa (Spectra Acceleration) vs T (Period) format found in the building codes⁽¹⁵⁻¹³⁾ to ADRS format, it is necessary to determine the value of Sd_i (Spectral Displacement) for each point on the curve, Sa_i, T_i . This can be done with the equation:

$$Sd_i = \frac{T_i^2}{4\pi^2} Sa_i g \quad (15-1)$$

Standard demand response spectra contain a range of constant spectral acceleration and a second range of constant spectral velocity, S_v . Spectral acceleration and displacement at period T_i are given by:

$$Sa_i g = \frac{2\pi}{T_i} S_v, \quad Sd_i = \frac{T_i}{2\pi} S_v \quad (15-2)$$

The capacity spectrum can be developed from the pushover curve by a point by point conversion to the first mode spectral coordinates. Any point V_i (Base Shear), δ_i (Roof Displacement) on the capacity (pushover) curve is converted to the corresponding point Sa_i, Sd_i on the capacity spectrum using the equations:

Standard Format (Sa vs T)ADRS Format (Sa vs Sd)Figure 15-9. Response Spectrum Conversion⁽¹⁵⁻¹⁾

$$Sa_i = \frac{V_i / W}{\alpha_1} \quad (15-3)$$

$$Sd_i = \frac{\delta_i}{(PF_1 \times \phi_{1,roof})} \quad (15-4)$$

Where α_1 and PF_1 are the modal mass coefficient and participation factors for the first natural mode of the structure respectively. $\phi_{1,roof}$ is the roof level amplitude of the first mode. The modal participation factors and modal coefficient are calculated as:

$$PF_1 = \left[\frac{\sum_{i=1}^n (w_i \phi_{i1}) / g}{\sum_{i=1}^n (w_i \phi_{i1}^2) / g} \right] \quad (15-5)$$

$$\alpha_i = \frac{\left[\sum_{i=1}^n (w_i \phi_{ii}) / g \right]^2}{\left[\sum_{i=1}^n w_i / g \right] \left[\sum_{i=1}^n (w_i \phi_{ii}^2) / g \right]} \quad (15-6)$$

Where w_i is the weight at any level i .

As displacement increase, the period of the structure lengthens. This is reflected directly in the capacity spectrum. Inelastic displacements increase damping and reduce demand. The Capacity Spectrum Method reduces the demand to find an intersection with the capacity spectrum, where the displacement is consistent with the implied damping.

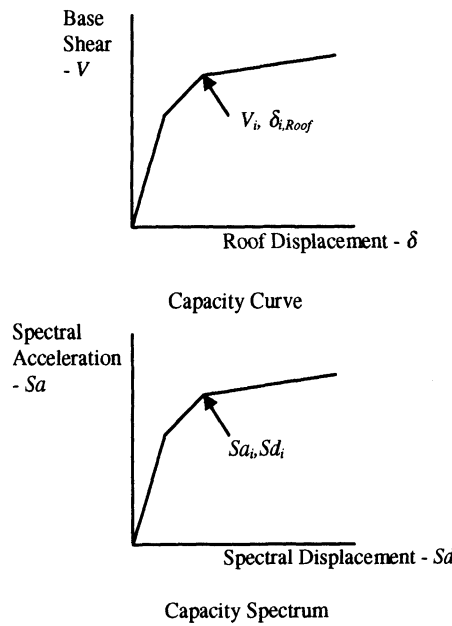


Figure 15-10. Capacity Spectrum Conversion⁽¹⁵⁻¹⁾

The damping that occurs when the structure is pushed into the inelastic range can be viewed as a combination of viscous and hysteretic damping. Hysteretic damping can be represented as equivalent viscous damping. Thus, the total effective damping can be estimated as:

$$\beta_{eff} = \lambda \beta_o + 0.05 \quad (15-7)$$

Where β_o is the hysteretic damping and 0.05 is the assumed 5% viscous damping inherent in

the structure. The λ -factor (called κ -factor in ATC-40) is a modification factor to account for the extent to which the actual building hysteresis is well represented by the bilinear representation of the capacity spectrum (See Table 15-3 and Figure 15-11).

The term β_o can be calculated using:

$$\beta_o = \frac{1}{4\pi} \frac{E_D}{E_{So}} \quad (15-8)$$

Where E_D is the energy dissipated by damping and E_{So} is the maximum strain energy. The physical significance is explained in Figure 15-11.

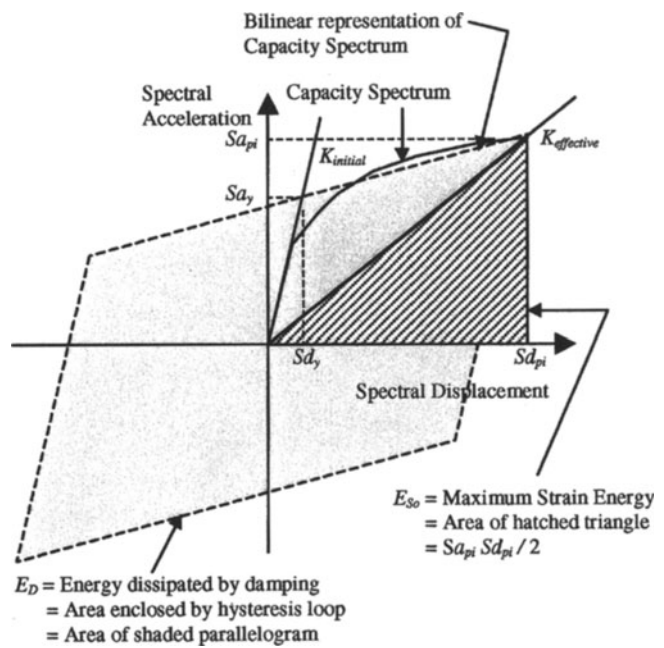


Figure 15-11. Derivation of Energy dissipated by Damping⁽¹⁵⁻¹⁾

To account for the damping, the response spectrum is reduced by reduction factors SR_A and SR_V which are given by

$$SR_A = \frac{1}{B_s} = \frac{3.21 - 0.68 \ln(\beta_{eff})}{2.12} \quad (15-9)$$

$$SR_V = \frac{1}{B_L} = \frac{2.31 - 0.41 \ln(\beta_{eff})}{1.65} \quad (15-10)$$

Both SR_A and SR_V must be greater than or equal to allowable values in Table 15-4.

The elastic response spectrum (5% damped) is thus reduced to a response spectrum with damping values greater than 5% critically damped (See Figure 15-12). Note, the limits of the spectral reduction factors are arbitrary and need further study.

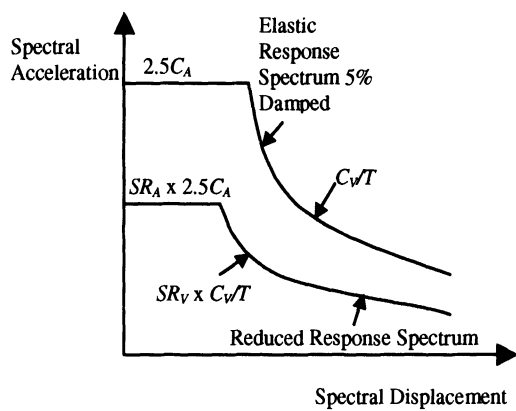


Figure 15-12. Reduced Response Spectrum⁽¹⁵⁻¹⁾

Table 15-2. Structural Behavior Types⁽¹⁵⁻¹⁾

Shaking Duration ¹	Essentially New Building ²	Average Existing Building ³	Poor Existing Building ⁴
Short	Type A	Type B	Type C
Long	Type B	Type C	Type C

1. See Section 4.5.2 of ATC-40 for criterion.
2. Buildings whose primary elements make up an essentially new lateral system and little strength or stiffness is contributed by non-complying elements.
3. Building whose primary elements are combination of existing and new elements, or better than average existing systems.
4. Buildings, whose primary elements make up non-complying lateral force systems with poor and unreliable hysteretic behavior.

Table 15-3. Values for Damping Modification Value, λ

Structural Behavior Type	β_o (percent)	λ
Type A	≤ 16.25	1.0
	≥ 16.25	$1.13 - 0.51 \frac{(S_{a_y} S_{d_{pi}} - S_{d_y}}{S_{a_{pi}}/S_{a_{pi}} S_{d_{pi}}}$
Type B	≤ 25	0.67
	≥ 25	$0.845 - 0.446 \frac{(S_{a_y} S_{d_{pi}} - S_{d_y}}{S_{a_{pi}}/S_{a_{pi}} S_{d_{pi}}}$
Type C	Any Value	0.33

Table 15-4. Minimum Allowable Value for SR_A and SR_V ⁽¹⁵⁻¹⁾

Structural Behavior Type	SR_A	SR_V
Type A	0.33	0.50
Type B	0.44	0.56
Type C	0.56	0.67

There are three procedures described in ATC-40 to find the performance point. The most transparent and most convenient for programming is Procedure A. To find the performance point using Procedure A the following steps are used:

1. A 5% damped response spectrum appropriate for the site for the hazard level required for the performance objective is developed and converted to ADRS format.
2. The capacity curve obtained from the non-linear analysis is converted to a capacity spectrum using Equations 15-3 and 15-4.
3. A trial performance point $S_{a_{pi}}$, $S_{d_{pi}}$ is selected. This may be done using the equal displacement approximation (See Figure 15-13) or on the basis of engineering judgement.
4. A bilinear representation of the capacity spectrum is developed such that the area under the capacity spectrum and the bilinear representation is the same. In the case of a saw-tooth capacity spectrum, the bilinear representation must be based on the capacity spectrum that makes up the portion of the composite capacity spectrum where the performance point $S_{a_{pi}}$, $S_{d_{pi}}$ occurs.
5. The spectral reduction factors SR_A and SR_V are computed using Equations 15-9 and 15-10 and the demand spectrum is reduced as shown in Figure 15-12. The reduced demand spectrum is plotted together with the capacity spectrum.

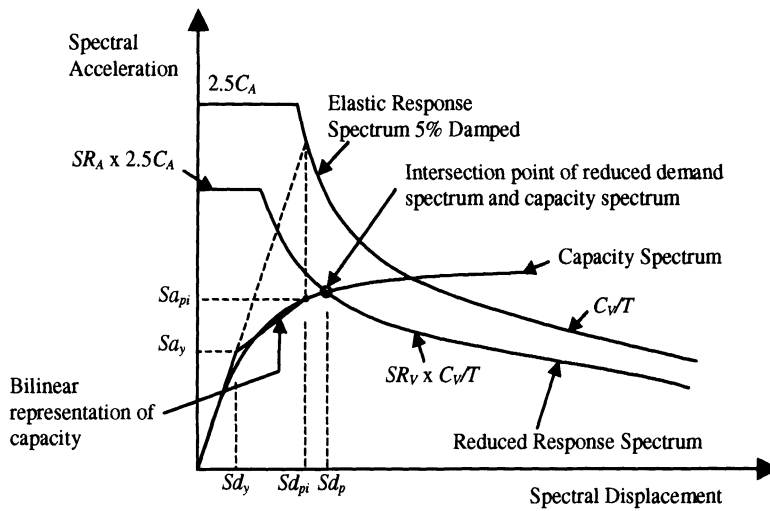


Figure 15-13. Capacity Spectrum Procedure A to Determine Performance Point

6. If the reduced demand spectrum intersects the capacity spectrum at Sa_{pi} , Sd_{pi} or if the intersection point Sd_p is within 5% of Sd_{pi} , then this point represents the performance point.
7. If the intersection point does not lie within acceptable tolerance (5% of Sd_{pi} or other) then select another point and repeat Steps 4 to 7. The intersection point obtained in Step 6 can be used as the starting point for the next iteration.

Procedure B is also an iterative method to find the performance point, which uses the assumption that the yield point and the post yield slope of the bilinear representation, remains constant. This is adequate for most cases, however, in some cases this assumption may not be valid. Procedure C is graphical method that is convenient for hand analysis.

15.3.7 Checking Performance at Expected Maximum Displacement

Once the performance point Sa_p , Sd_p (which are in spectral ordinates) is found, the base shear (V_p) and roof displacement (δ_p) at the performance point are found using Equation 15-3 and 15-4. The following steps should be used in the performance check:

1. For the global building response, verify
 - a. The lateral force resistance has not degraded by more than 20% of the peak resistance.
 - b. The lateral drift limits satisfy the limits given in the Table 15-5.
2. Identify and classify the different elements in the building in the following types: beam-column frames, slab-column frames, solid walls, coupled walls, perforated walls, punched walls, floor diaphragms and foundations.
3. Identify all primary and secondary elements.
4. For each element type, identify the critical components and actions to check as detailed in Chapter 11 of ATC-40.
5. The strength and deformation demands at the performance point should be equal to or less than the capacities detailed in Chapter 11 of ATC-40.
6. The performance of secondary elements (such as gravity load carrying members not part of the lateral load resisting system) are reviewed for acceptability for the specified performance level.
7. Non-structural elements are checked for the specified performance level.

15.3.8 Other Considerations

Other considerations that should be noted are

1. Torsion: For 3D models, the lateral load should be applied at the center of mass of each floor and the displacement plotted on the capacity curve should be for the center of mass for the roof. Use of 2D models should be limited to building where the torsional effects are sufficiently small such that the maximum displacement at any point is not more than 120% of the displacement at the center of mass.
2. For structure with long fundamental modes, higher mode effects may be more critical. Pushover analysis should be performed for additional mode shapes using corresponding force distributions.

Table 15-5. Deformation Limits⁽¹⁵⁻¹⁾

Performance Limit				
Interstory Drift Limit	Immediate Occupancy	Damage Control	Life Safety	Structural Stability
Maximum Total Drift	0.01 0.002	0.01 – 0.002	0.02	0.03 V_i/P_i
Maximum inelastic Drift	0.005	0.005 – 0.015	No Limit	No Limit

15.3.9 Example

An example is provided of the procedure to determine the performance point using the Capacity Spectrum Method. This example reworked from numbers provided in the ATC-40 document.

15.3.9.1 Building Description

The example building is a seven-story reinforced concrete building. The total weight

Table 15-6. Conversion of Pushover Curve to Capacity Spectrum⁽¹⁵⁻¹⁾

Point	V (kips)	δ_R (in)	V/W	$PF_1 \cdot \phi_{1,roof}$	α_1	Sa (g)	Sd (g)	T (sec)
A	2200	2.51	0.209	1.31	0.828	0.254	1.92	0.88
B	2600	3.60	0.247	1.28	0.800	0.309	2.81	0.96
C	2800	5.10	0.266	1.35	0.770	0.346	3.78	1.06
D	3000	10.90	0.285	1.39	0.750	0.380	7.84	1.45

PF_1 and α_1 change because the mode shape is changing as yielding occurs

of the building is 10,540 kips. The pushover curve determined for the building is given in Table 15-6. The pushover (capacity) curve is converted into a capacity spectrum using Equation 15-3 and 15-4. The demand for the building for the performance level desired is determined to be Soil Type S_D with C_A and C_V being 0.44 and 0.64 respectively. The demand spectrum is converted to ADRS format using Equation 15-1.

The demand and capacity spectrum are plotted together as shown in Figure 15-14. Using an equal displacement approximation, the first trial performance point Sa_{p1} , Sd_{p1} is selected. A bilinear representation is developed such that the area under the capacity spectrum is the same as the area under the bilinear curve. Thus:

$$\begin{aligned} Sa_{p1} &= 0.36g & Sd_{p1} &= 5.5 \text{ in} \\ Sa_y &= 0.31g & Sd_y &= 2.35 \text{ in} \end{aligned}$$

$$\begin{aligned} \beta_{eff} &= \frac{63.7\lambda(Sa_y Sd_{p1} - Sd_y Sa_{p1})}{Sa_{p1} Sd_{p1}} + 5 \\ &= 14.11\% \end{aligned}$$

A λ of 0.33 is used for structural behavior type C from Table 15-3. Thus, the spectral reduction factors are calculated from Equations 15-9 and 15-10 as:

$$SR_A = \frac{3.21 - 0.68\ln(14.11)}{2.12} = 0.665$$

$$SR_V = \frac{2.31 - 0.41\ln(14.11)}{1.65} = 0.742$$

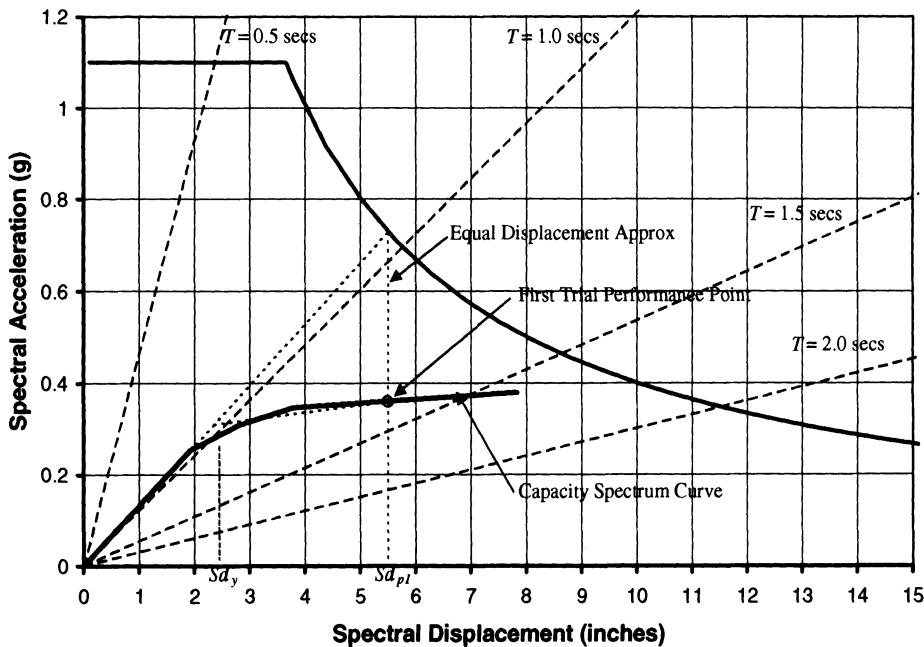


Figure 15-14. Determination of the First Trial Performance Point

Using the spectral reduction factors, the demand spectrum is reduced as per Figure 15-12. The reduced spectrum is plotted together with the capacity spectrum and the intersection point is found (See Figure 15-15). The demand spectrum intersects the capacity spectrum at a spectral displacement of 6.1 inches. As this displacement is not within 5% of the first trial displacement of 5.5 inches.

A new trial performance point must be chosen and the process repeated. The second trial point may be chosen as the intersection from the previous iteration. However, in this example, the second trial performance point is chosen by engineering judgement at a spectral displacement of 5.9 inches. A new bilinear representation is constructed and the process repeated:

$$\begin{aligned} Sa_{p2} &= 0.365g & Sd_{p2} &= 5.9 \text{ in} \\ Sa_y &= 0.305g & Sd_y &= 2.3 \text{ in} \end{aligned}$$

$$\begin{aligned} \beta_{eff} &= \frac{63.7\lambda(Sa_y Sd_{p2} - Sd_y Sa_{p2})}{Sa_{p2} Sd_{p2}} + 5 \\ &= 14.37\% \end{aligned}$$

The new spectral reduction factors are calculated from Equations 15-9 and 15-10 as:

$$SR_A = \frac{3.21 - 0.68 \ln(14.37)}{2.12} = 0.659$$

$$SR_V = \frac{2.31 - 0.41 \ln(14.37)}{1.65} = 0.738$$

A new reduced demand spectrum is plotted and a new intersection point is obtained. As seen in Figure 15-17, the intersection point is at a spectral displacement of 6.0 inches. As this intersection is within 5% of the second trial point, the demand spectral displacement is 6.0 inches.

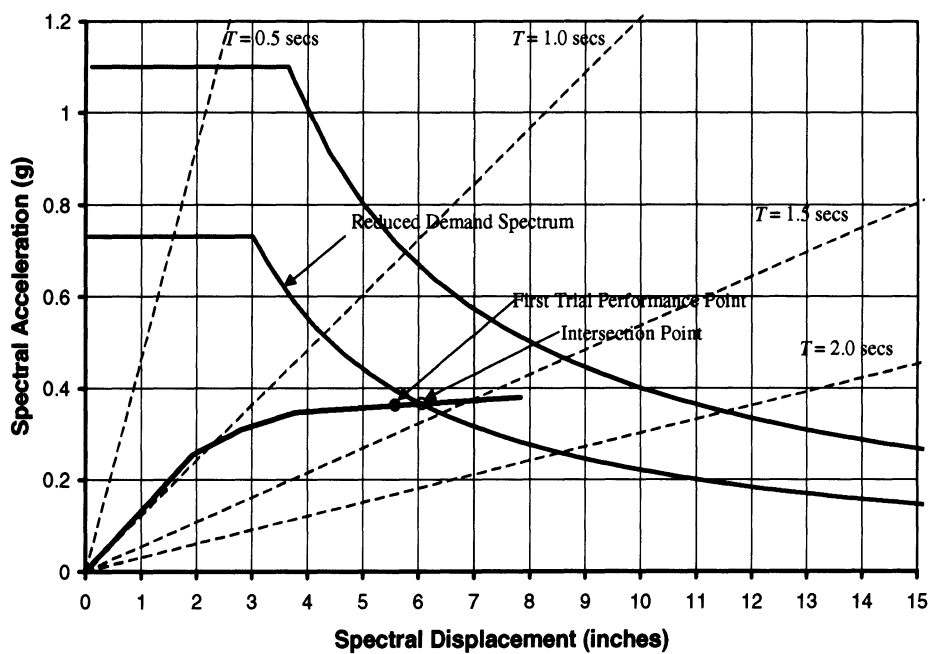


Figure 15-15. Determination of Intersection Point and Comparison with the First Trial Performance Point

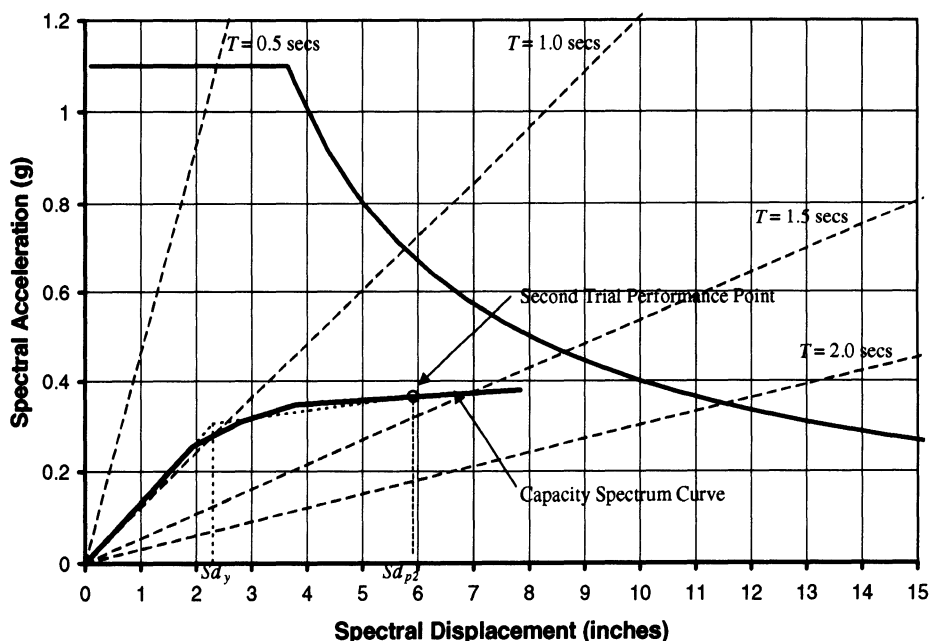


Figure 15-16. Determination of Second Performance Point

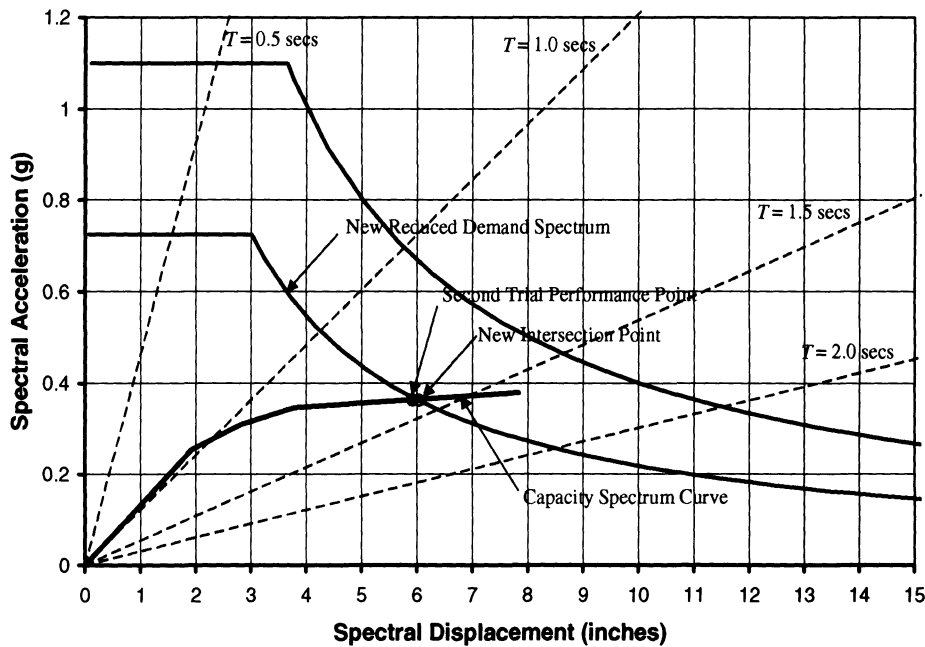


Figure 15-17. Determination of Final Performance Point

The actual roof displacement at the performance point is calculated from Equation 15-4. The modal participation factor is used by linear interpolation from Table 15-6.

$$\delta_r = PF_1 \cdot \phi_{roof,1} \times Sd_p \\ = 1.35 \times 6.0 = 8.1 \text{ inches}$$

Similarly, the base shear can be found from the spectral acceleration at the performance point by using Equation 15-3. The modal mass coefficient can be found by linear interpolation from Table 15-6.

$$V_p / W = \alpha_1 \times Sa_p \\ = 0.76 \times 0.365 = 0.277$$

The element capacities are checked for the building at this performance point as detailed in Section 15.3.7.

15.3.10 Recent Advances in the Capacity Spectrum Method

In recent publications it has been reported by Chopra and Goel^(15-14,15-15) that the Capacity Spectrum Method as described in ATC-40 does not produce conservative estimates of inelastic peak displacements when compared to inelastic response spectrum analysis. It has also been reported that the ATC-40 procedures are deficient relative to even the elastic design spectrum in the velocity and displacement sensitive regions of the spectrum. An improved method has been suggested by Chopra and Goel⁽¹⁵⁻¹⁵⁾ which makes use of inelastic spectra using any of three $R_y\mu-T$ equations (Newmark and Hall⁽¹⁵⁻¹⁶⁾, Krawinkler and Nassar⁽¹⁵⁻¹⁷⁾ and Vidic, Fajfar and Fischinger⁽¹⁵⁻¹⁸⁾). In this improved Capacity Spectrum Method, the capacity and the constant ductility design spectra are plotted in ADRS format. The capacity spectrum intersects the demand spectrum for several values of ductility μ . The

deformation at the performance point is given by the one intersection point where the ductility factor calculated from the capacity spectrum matches the value associated with the intersected demand spectrum.

Another method for determining the performance point is suggested by Fajfar⁽¹⁵⁻¹⁹⁾. Here the ductility demand is determined using the equal displacement rule and the inelastic design spectra. Another variant of the Capacity Spectrum method called the Yield Point Spectra⁽¹⁵⁻²⁰⁾ has recently been suggested. Here the yield displacement is plotted on the abscissa instead of the spectral displacement and $R_y-\mu-T$ relations or exact computations are used instead of equivalent viscous damping.

15.4 FEMA 273 and 274

15.4.1 Introduction

NEHRP Guidelines for the Seismic Rehabilitation of Buildings (FEMA-273)⁽¹⁵⁻²⁾ and the associated commentary (FEMA-274)⁽¹⁵⁻³⁾ was developed by the Building Seismic Safety Council (BSSC) with subcontractors American Society of Civil Engineering (ASCE) and the Applied Technology Council (ATC) with the funding provided by the Federal Emergency Management Agency (FEMA). The primary purpose of FEMA-273 was to provide technically sound and nationally acceptable guidelines for the seismic rehabilitation of buildings. Although the document was written with the objective of performance based retrofit of existing structures, the procedures described therein are equally applicable for new design. Unlike the ATC-40 document, these recommendations are applicable to all building materials and define acceptability limits for linear as well as non-linear analysis.

The basic procedure is similar to that recommended in ATC-40. The owner decides the performance object that needs to be achieved. The engineer then designs the retrofit or new structure to achieve the performance objective. The definitions of the basic

performance levels are similar to those defined in ATC 40 (See Section 15.3.2).

FEMA-273 defines ground motion hazard levels in a probabilistic basis. Four ground motion hazard levels are defined

Earthquake Probability of Exceedence	Mean Return Period (years)
50% in 50 years	72
20% in 50 years	225
BSE-1 10% in 50 years	474
BSE-2 2% in 50 years	2,475

Where BSE is the Basic Safety Earthquake. The broad range of performance objectives recommended for a given earthquake hazard levels are shown in Table 15-7

Table 15-7. Rehabilitation Objectives⁽¹⁵⁻²⁾

Building Performance Levels					
	Operational Level (1-A)	Immediate Occupancy Level (1-B)	Life Safety Performance Level (3-C)	Collapse Prevention Performance Level	
Earthquake Hazard Level	50%/50 yrs	a	b	c	d
	20%/50 yrs	e	f	g	h
	BSE-1 10%/50 yrs	i	j	k	l
	BSE-2 2%/50 yrs	m	n	o	p

k+p = Basic Safety Objective

k+p+any of a, e, i or m; or b, f, j, or n = Enhanced Objectives

o = Enhanced Objectives

k alone or p alone = Limited Objective

c, g, d, h = Limited Objectives

From Table 15-7, it is clear that FEMA-273 specifies a two-level design to achieve the Basic Safety Objective (BSO), Life Safety Performance Level for BSE-1 demands and Collapse Prevention Level for BSE-2 demands. However, for new structures it is possible to control ductility and configuration of the design

to an extent that will permit those structures designed to achieve Life Safety Performance Level for a BSE-1 level earthquake to also avoid collapse for much larger events.

Two sets of earthquake hazard maps are distributed with FEMA-273 and 274. One set provide key response acceleration for the Maximum Considered Earthquake (MCE) which in most areas represents a 2%/50 years exceedence level. The other uses 10%/50 years exceedence probability. Thus, it is possible to obtain a BSE-1 and BSE-2 level spectra from these maps.

15.4.2 Mathematical Modeling

FEMA-273 provides four analysis procedures for systematic design and rehabilitation of buildings. The Linear Static (LSP) and Linear Dynamic Procedures (LDP) are linearly elastic analysis, which may include geometric non-linearity. Also some material non-linearity is also introduced by use of cracked properties for concrete and masonry components even though the analysis is linear. In the Nonlinear Static (NSP) and Nonlinear Dynamic Procedures (NDP) material non-linearity is included in the analysis.

15.4.2.1 Basic Assumptions

In general, a three dimensional analysis consisting of an assembly of elements and components is recommended. Three-dimensional analysis is required when the building has plan irregularities and when torsional effects cannot be ignored or indirectly captured.

For buildings with flexible diaphragms, the diaphragms may be individually modeled and analyzed as two-dimensional assemblies of components and elements or three-dimensional models with flexible elements.

Explicit modeling of connections is not required if the connection is stronger than the connected components or when the deflection of the connection does not cause a significant

increase in the relative deformation between the connected components.

15.4.2.2 Horizontal Torsion

In addition to the actual eccentricities between the centers of mass and centers of rigidity, a additional accidental torsional moment should be included which may be produced by including a horizontal offset in the centers of mass equal to a minimum of 5% of the horizontal dimension at a given floor level.

For buildings with rigid diaphragms, the effects of torsion must be included when the maximum displacement at any point in a diaphragm exceeds the average displacement in that diaphragm by more than 10%. For linear analysis, the effect of accidental torsion is amplified by a factor A_x :

$$A_x = \left(\frac{\delta_{\max}}{1.2\delta_{\text{avg}}} \right)^2 \quad (15-11)$$

Where δ_{\max} and δ_{avg} are the maximum and average displacements in a diaphragm. A_x is greater than 1 and not greater than 3.

If $\eta = \delta_{\max}/\delta_{\text{avg}}$ is greater than 1.5, then a three-dimensional analysis is required. For two-dimensional analysis subject to this limitation, the effect of torsion can be included for LSP and LDP by increasing the design forces and displacement by η . For NSP, the target displacement is increased by η and for NDP the amplitude of the ground acceleration record is increased by η .

15.4.2.3 Primary and Secondary Elements

Primary elements are key parts of the seismic framing system required in the design to resist earthquake effects. These must be evaluated to resist earthquake forces as well as gravity loads if required. Secondary elements are not designed to be part of the lateral force resisting system but must be evaluated to ensure they can simultaneously sustain earthquake induced deformation and gravity loads.

For linear analysis procedures, the secondary elements must not constitute more

than 25% of the total stiffness of the primary elements at any level and may not be included in the analysis. For nonlinear procedures, the stiffness of the primary as well as the secondary elements must be included in the model. Additionally, the stiffness of non-structural elements must not exceed 10% of the total lateral stiffness of any story. If this is exceeded, then the non-structural elements must be included in the model.

15.4.2.4 Deformation and Force Controlled Elements

Elements can be classified as either deformation controlled or force controlled. A deformation controlled element is one that has an associated deformation that is allowed to exceed yield value, that is, the maximum associated deformation of the element is limited by the ductility of the element. A force controlled element is one where the maximum associated displacement is not allowed to exceed yield value. Elements with limited ductility shall be considered to be force controlled. See Table 15-8 for calculation of element capacities used to compare with demands.

15.4.2.5 Stiffness and Strength Assumptions

Element and component stiffness properties and strength assumptions for most material types are provided in FEMA-273. Guidelines for structural and foundation elements are also provided. These are similar to those provided in ATC-40.

15.4.2.6 Foundation Modeling

Foundation modeling assumptions are similar to ATC-40 (See Section 15.3.5). The foundation system may be included in the model for analysis with stiffness and damping properties as defined in Chapter 4 of FEMA-273. Otherwise, unless specifically prohibited, the foundation may be assumed to rigid and not included in the model.

Table 15-8. Calculation of Element Capacities⁽¹⁵⁻²⁾

Parameter	Deformation Controlled	Force Controlled
Linear Procedures		
Existing Material Strength	Mean value with allowance for strain hardening	Lower bound (Mean – Std Dev)
Existing Capacity	$m\kappa Q_{CE}$	κQ_{CE}
New Material Strength	Mean value	Specified value
New Capacity	Q_{CE}	Q_{CE}
Nonlinear Procedures		
Deformation Capacity – Existing Element	$\kappa \times$ Deformation limit	N/A
Deformation Capacity – New Element	Deformation limit	N/A
Strength Capacity – Existing Element	N/A	κQ_{CL}
Strength Capacity – New Element	N/A	κQ_{CL}

κ = Knowledge factor

m = Demand Modifier for expected ductility

Q_{CE} = Expected Strength

Q_{CL} = Lower Bound Estimate of Strength

15.4.2.7 Diaphragms

Diaphragms transfer earthquake induced inertial loads to the vertical elements of the seismic framing system. Connection between the diaphragms and the vertical elements of the lateral load resisting system must have sufficient strength to transfer the maximum calculated inertial loads. Diaphragms may be flexible, stiff or rigid. Flexible diaphragms are those where the maximum lateral deformation of the diaphragm is more than twice the average inter-story drift of the story below the diaphragm. Rigid diaphragms are those where the maximum lateral deformation of the diaphragm is less than half the average inter-story drift of the associated story. Diaphragms that are neither rigid nor flexible can be considered to be stiff.

Mathematical models of buildings with stiff or flexible diaphragms must consider the effect of diaphragm flexibility. For buildings with flexible diaphragms at each floor level, the

vertical lines seismic framing may be designed independently with seismic masses assigned on the basis of tributary areas.

15.4.2.8 P-Delta Effects

For linear procedures, at each story the quantity θ_i shall be computed for each direction of response as follows:

$$\theta_i = \frac{P_i \delta_i}{V_i h_i} \quad (15-12)$$

Where P_i is the portion of the total weight of the structure including dead, permanent live and 25% of the transient live loads acting on the columns and load bearing walls. V_i is the total calculated shear force, h_i is the story height and δ_i is the lateral drift in the direction under consideration at story i .

For linear procedures, the story drifts δ_i must be increased by $1/(1 - \theta_i)$ for evaluation of the stability coefficient, θ_i . Therefore, the process is iterative. If the stability coefficient, θ_i is less than 0.1, the static P-Delta effects are small and can be ignored. If the stability coefficient, θ_i is greater than 0.33, the structure is unstable. If it lies between 0.1 and 0.33 than the seismic forces at level i must be increased by $1/(1 - \theta_i)$.

For non-linear procedures, these second order effects must be directly included in the model by use of geometric stiffness of all elements subject to axial loads. Dynamic P-Delta effects are included in the LSP and NSP by use of Coefficient C_3 (See Section 15.4.3.1 and 15.4.3.3).

15.4.2.9 Soil Structure Interaction

Soil Structure Interaction (SSI) may modify the seismic demand on the structure. To include SSI, one may use the effective fundamental period and effective damping ratios of the foundation-structure system to compute seismic demand or explicitly model SSI. SSI effects shall not be used to reduce component and element actions by more than 25%.

15.4.2.10 Multidirectional Effects

Buildings should be designed for seismic forces in any horizontal direction. For regular buildings, seismic displacements and forces may be assumed to act non-concurrently in the direction of each principle axis of the building. For buildings with plan irregularities and buildings with intersecting elements, multidirectional effects must be considered. An acceptable procedure is use of 100% of the seismic force in one horizontal direction and 30% of the seismic force in the perpendicular direction. Alternately SRSS may be used to combine forces in orthogonal directions.

Vertical excitation of horizontal cantilevers and pre-stressed elements must be considered. Vertical shaking characterized by a spectrum with ordinates equal to 67% of those of the horizontal spectrum is acceptable where site-specific data is not available.

15.4.2.11 Load Combinations

The component gravity loads to be considered for combination with seismic loads are:

When effects of gravity and seismic loads are additive:

$$Q_G = 1.1(Q_D + Q_L + Q_S) \quad (15-13)$$

When the effects of gravity counteract seismic loads

$$Q_G = 0.9Q_D \quad (15-14)$$

Where Q_D , Q_L and Q_S are dead, live and snow loads respectively. Effective live loads may be assumed to be 25% of the unreduced live load but not less than measured live loads. Effective snow loads are 70% of the full design snow loads or an approved percentage by a regulatory agency.

Combination with earthquake loads is discussed in subsequent sections. Note such load combinations are relevant for linear analysis. Non-linear analysis is not conducive to checking both of the above load

combinations and therefore only the critical load combination (by inspection) may be used.

15.4.3 Analysis Procedures

15.4.3.1 Linear Static Procedure

In this procedure a linear elastic model is used in the analysis with an equivalent damping that approximates values expected for loading near the yield point. A pseudo-lateral load is computed as shown in the following section and applied to the model. The resulting forces and displacements in the elements are then checked against capacities modified to account for inelastic response demands.

15.4.3.1.1 Pseudo Lateral Load

To compute the pseudo lateral load, the fundamental period must be first determined. The period may be determined by one of the following methods:

1. Eigenvalue value analysis of the building. For buildings with flexible diaphragms, the model must consider representation of diaphragm flexibility unless it can be shown that the effects of the omission will not be significant.
2. Use of the following equation

$$T = C_t h_n^{3/4} \quad (15-15)$$

Where T is the fundamental period in seconds under the direction under consideration and h_n is the height above the base to the roof.

$C_t = 0.035$ for steel moment resisting frames.

$C_t = 0.030$ for moment resisting frame system of concrete and eccentrically braced steel frames.

$C_t = 0.020$ for all other framing systems.

$C_t = 0.060$ for wood buildings.

3. For one-story buildings with flexible diaphragms:

$$T = (0.1\Delta_w + 0.078\Delta_d)^{0.5} \quad (15-16)$$

Where Δ_w and Δ_d are in-plane wall and diaphragm displacements in inches due to a lateral loads in the direction under consideration equal to the weight tributary to the diaphragm. For multiple span diaphragms, a lateral load equal to the gravity weight tributary to the span under consideration can be applied to each span to calculate a separate period for each diaphragm span. The period so calculated that maximizes the pseudo lateral load is to be used for the design of all walls and diaphragm spans in the building.

The total pseudo lateral load, V in a given horizontal direction is determined as

$$V = C_1 C_2 C_3 S_a W \quad (15-17)$$

Where

C_1 = Modification factor to relate expected maximum inelastic displacements to displacements calculated for the linear elastic response. C_1 can be calculated as in Section 15.4.3.3.4 with the elastic base shear substituted for V_y . Alternatively C_1 may be calculated as follows

$C_1=1.5$ for $T < 0.10$ secs

$C_1=1.0$ for $T \geq T_0$ secs

Linear interpolation can be used to calculate C_1 for intermediate value of T .

T = Fundamental period of the building in the direction under consideration. For SSI, the effective fundamental period should be used.

T_0 = Characteristic period of the response spectrum, defined as the period associated with the transition from the constant acceleration segment of the spectrum to the constant velocity segment of the spectrum

C_2 = Modification factor to represent the effect of stiffness degradation and strength deterioration on the maximum displacement response. Values for different framing for different performance levels are listed in Table 15-9. Linear interpolation can be used to calculate C_2 for intermediate value of T .

C_3 = Modification factor to represent the increased displacement due to dynamic P-Delta effect. This effect is in addition to P-Delta

described in Section 15.4.2.8. For values of θ less than 0.1, C_3 may be set equal 1.0. For values of θ greater than 0.1, C_3 shall be calculated as $1+5(\theta-0.1)/T$. The maximum value of θ for all stories shall be used to calculate C_3 .

S_a = Response spectrum acceleration at the fundamental period and damping ratio of the building in the direction under consideration.

W = Total dead load and anticipated live load as indicated below:

- In storage and warehouse occupancies, a minimum of 25% of the floor live load,
- The actual partition weight or minimum weight of 10 psf of floor area, whichever is greater,
- The applicable snow load,
- The total weight of permanent equipment and furnishings.

Vertical distribution of the base shear V is done by the following:

$$F_x = C_{vx} V \quad (15-18)$$

Table 15-9. Values of Modification Factor $C_2^{(15-2)}$

Performance Level	$T=0.1$ second		$T \geq T_0$ seconds	
	Framing Type 1	Framing Type 2	Framing Type 1	Framing Type 2
Immediate Occupancy	1.0	1.0	1.0	1.0
Life Safety	1.3	1.0	1.1	1.0
Collapse Prevention	1.5	1.0	1.2	1.0

Framing Type 1 = Structures in which more than 30% of the story shear any level is resisted by components or elements whose strength and stiffness deteriorate during the design earthquake. Such elements and components include: ordinary moment-resisting frames, concentrically braced frames, frames with partially restrained connections, tension only braced frames, unreinforced masonry walls, shear-critical walls and piers, or any combination of the above.

Framing Type 2 = All frames not assigned to Framing Type 1

$$C_{vx} = \frac{w_x h_x^k}{\sum_{i=1}^n w_i h_i^k} \quad (15-19)$$

$k = 1.0$ for $T \leq 0.5$ second

$= 2.0$ for $T \geq 2.5$ second

Linear interpolation is used to estimate values of k for intermediate values of T . C_{vx} is the vertical distribution factor, V is the pseudo lateral load from Equation 15-17, w_i is the weight of level i , w_x is the weight of the building of any level x , h_i is height from the base to floor level i and h_x is height from the base to floor level x .

Floor diaphragms are designed to resist the inertial forces developed at the level under considerations and the horizontal forces resulting from offsets or changes in stiffness in the vertical seismic framing elements above and below the diaphragm. The diaphragm inertial force F_{px} at level x is given by

$$F_{px} = \frac{1}{C_1 C_2 C_3} \sum_{i=x}^n F_i \frac{\frac{w_x}{n}}{\sum_{i=x}^n w_i} \quad (15-20)$$

Where F_i is the lateral load applied at floor level i as given by Equation 15-18.

The base shear, vertical distribution and forces on the diaphragms for the LSP is not unlike current codes, however force levels and acceptance criterion for the elements in the lateral load resisting systems depend on the desired performance level.

15.4.3.1.2 Acceptance Criteria to satisfy Performance Point requirements

The design forces shall be calculated as per the following:

For Deformation-Controlled Elements -

$$Q_{UD} = Q_G \pm Q_E \quad (15-21)$$

For Force-Controlled Elements -

$$Q_{UF} = Q_G \pm \frac{Q_E}{C_1 C_2 C_3 J} \quad (15-22)$$

$$Q_{UF} = Q_G \pm \frac{Q_E}{C_1 C_2 C_3} \quad (15-23)$$

Where Q_{UD} and Q_{UF} are the demands due to gravity and earthquake forces for deformation and force controlled elements respectively. Q_E is the demand due to the earthquake forces described in the previous section and J is the force delivery reduction factor given by:

$$J = 1.0 + S_{xs} \quad (15-24)$$

J cannot exceed 2 and S_{xs} is the short period spectral acceleration parameter for the design spectrum. Alternately, J can be taken as the smallest demand capacity ratio of the components in the load path delivering force to the component in question.

The capacities of elements must be checked against the demands as follows:

For Deformation-Controlled elements -

$$m\kappa Q_{CE} \geq Q_{UD} \quad (15-25)$$

For Force-Controlled elements -

$$\kappa Q_{CL} \geq Q_{UF} \quad (15-26)$$

Where Q_{CE} and Q_{CL} are the expected and lower bound strength of the element or component respectively. m is the demand modifier to account for the deformation associated with demand at the selected performance level. κ is the knowledge factor to account for uncertainty in capacity evaluations. A value of 0.75 is used for κ when only a minimum knowledge is available and a value of 1.0 can be used when comprehensive knowledge is available for the element or component in question.

The capacities that need to be checked against demands for each element type and material are listed in Chapters 5 to 8 in FEMA-

273 together with the demand modifiers, m , for each performance level.

15.4.3.2 Linear Dynamic Procedure

The basis, modeling approaches and acceptance criterion for the Linear Dynamic Procedure (LDP) is similar to those described for LSP. The main exception is that the response is obtained from either a linearly elastic response spectrum or a time-history analysis. As with LSP, LDP will produce displacements that are approximately correct, but will produce inertial forces that exceed those that would be obtained in a yielding building.

The response spectrum method uses peak modal responses calculated from an eigenvalue analysis of a mathematical model. The time history method involves a time-step by time-step evaluation of the building response using a discretized record or synthetic record as base motion input. In both the methods, only modes contributing significantly to the response need to be considered. In the response spectrum analysis, modal responses are combined using rational methods to estimate total building response quantities.

15.4.3.2.1 Ground Motion

The ground motion can be characterized by either a linearly elastic response spectrum which may be site specific or a ground acceleration time history which may be recorded or synthesized. In both cases, the ground motion must be appropriately scaled to reflect the hazard level that is associated with the performance level desired (See Table 15-7)

15.4.3.2.2 Response Spectrum Method

All significant modes must be included in the response spectrum analysis such that at least 90% seismic mass participation is achieved in each of the building's principle directions. Modal damping must reflect the damping inherent in the building at the deformation levels less than yield deformation.

The peak member forces, displacements, story forces, shears and base reactions for each

mode should be combined using SRSS (square root sum of squares) or CQC (complete quadratic combination). It should also be noted that the directivity of the forces is lost in the response spectrum analysis and therefore the combination of forces must reflect this loss.

Multidirectional effects should also be investigated when using the response spectrum analysis.

15.4.3.2.3 Time History Method

All the requirements for response spectrum analysis are also identical for the time history analysis. Response parameters are computed for each time history analysis. If 3 pairs of time histories are used, the maximum response of the parameter of interest shall be used for the design. If seven or more pairs of time histories are used, the average response (of the maximum of each analysis) of the parameter of interest is to be used.

Multidirectional effects can be accounted by using a three dimensional mathematical model and using simultaneously imposed pairs of earthquake ground motions along each of the horizontal axes of the building.

15.4.3.2.4 Acceptance Criteria to satisfy Performance Point requirements

The acceptance criterion for LDP is similar to that described for LSP. However, all deformations and force demands obtained from either the response spectrum or the time history analysis must be multiplied by the product of the modification factors C_1 , C_2 and C_3 . Force demands on elements of the floor diaphragm need not be increased by these factors. The seismic forces on the diaphragm obtained in the analysis must not be less than 85% than those obtained in LSP (See Equation 15-20).

15.4.3.3 Nonlinear Static Procedure

In the Nonlinear Static Procedure (NSP) the nonlinear load-deformation characteristics of individual elements and components are modeled directly. The mathematical model of the building is subjected to monotonically increasing lateral load until a target

displacement is reached or the building collapses. The target displacement is intended to represent the maximum displacement likely to be experienced during the design earthquake. The nonlinear effects are directly included in the model and therefore the calculated inertial forces are reasonable approximations of those expected during the design earthquake.

The target displacement can be calculated by any procedure that accounts for nonlinear response on displacement amplitude as well as damping effects at the performance point. One such procedure called the Displacement Coefficient Method is described in FEMA 273. ATC-40 also includes this method as an alternative method of finding the performance point. The advantage of this method over the Capacity Spectrum procedure is its simplicity.

The modeling requirements for NSP are similar to those described in ATC-40. The pushover analysis is performed and a curve relating the base shear force and the lateral displacement of the control node are established between 0 and 150% of the target displacement, δ_t . Acceptance criterion is based on the forces and deformation corresponding to the displacement of the control node equal to δ_t .

The analysis model must be sufficiently discretized to represent the load-deformation response of each element or component. Particular attention needs to be paid to identifying locations of inelastic action along the length of element or component. Thus, local models of elements or assemblages of elements need to be studied before embarking on the global models.

15.4.3.3.1 Control Node

The control node is usually the center of mass of the roof of the building. The top of the penthouse should not be considered to be the roof. As the displacement of the control node is compared with the target displacement, the choice of the control node is very important.

15.4.3.3.2 Lateral Load Patterns

The lateral load should be applied to building in profiles that approximately bound

the likely vertical and horizontal distribution of the inertial force in an earthquake. At least two vertical distributions of lateral loads must be considered with NSP. Note use of only one load pattern may not identify potential deficiencies in the building.

The two lateral load patterns that are recommended are

1. Uniform Load Pattern: Here the lateral load may be represented by values of C_{vx} as given by Equation 15-19.
2. Modal Pattern: Here the lateral load pattern is consistent with story shear distribution in a response spectrum analysis where there is at least 90% mass participation and the appropriate ground motion is used.

Other appropriate load patterns substantiated by rational analysis may be substituted for the above.

15.4.3.3.3 Period Determination

The effective fundamental period, T_e in the direction considered can be computed using the pushover curve obtained in the NSP. A bilinear representation of the pushover curve is constructed to estimate the effective lateral stiffness, K_e , and the yield strength of the building, V_y . The effective lateral stiffness can be taken as the secant stiffness calculated at a base shear force equal to 60% of the yield strength (See Figure 15-18).

The effective fundamental period, T_e is computed as:

$$T_e = T_i \sqrt{\frac{K_i}{K_e}} \quad (15-27)$$

Where T_i and K_i are the initial elastic fundamental period in seconds and initial stiffness of the building in the direction under considered.

It is obvious that to determine the effective fundamental period, T_e , and the target displacement, δ_t , the pushover curve for the building is needed.

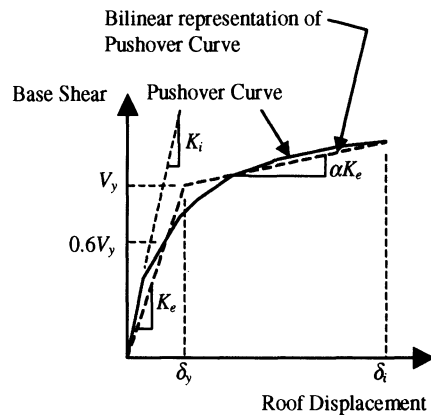


Figure 15-18. Calculation of Effective Stiffness K_e ⁽¹⁵⁻²⁾

15.4.3.3.4 Target Displacement

Using the Displacement Coefficient Method the target displacement can be computed as:

$$\delta_t = C_0 C_1 C_2 C_3 S_a \frac{T_e^2}{4\pi^2} g \quad (15-28)$$

Where

C_0 = Modification factor to relate the spectral displacement and likely building roof displacement. C_0 can be calculated using one of the following

1. The first modal participation factor at the level of the control node.
2. The modal participation factor at the level of the control node calculated using a shape vector corresponding to deflected shape of the building at the target displacement.
3. The appropriate value from Table 15-10.

C_1 = Modification factor to relate maximum inelastic displacements to displacements calculated for linear elastic response. C_1 may be calculated as follows:

Table 15-10. Values for Modification Factor C_0 ⁽¹⁵⁻²⁾

Number of Stories	Modification Factor ¹
1	1.0
2	1.2
3	1.3
5	1.4
10+	1.5

1. Linear interpolation should be used to calculate intermediate values

$$C_1 = 1.0 \text{ for } T_e \geq T_0 \\ C_1 = [1.0 + (R-1) T_0/T_e]/R \text{ for } T_e < T_0$$

Values for C_1 need not exceed those given for LSP (See Section 15.4.3.1.1) and in no case is C_1 taken less than 1.0.

T_0 = Characteristic period of the response spectrum, defined as the period associated with the transition from the constant acceleration segment of the spectrum to the constant velocity segment of the spectrum.

R = Ratio of the elastic strength demand to calculated yield strength coefficient. R can be computed as

$$R = \frac{S_a}{V_y/W} \frac{1}{C_0} \quad (15-29)$$

Where W is the dead weight and anticipated live as computed for LSP (See Section 15.4.3.1.1) and V_y is the yield strength determined from the bilinear representation of the pushover curve (See Figure 15-18).

C_2 = Modification factor to represent the effect of hysteresis shape on the maximum displacement response. Values of C_2 can be obtained from Table 15-9.

C_3 = Modification factor to represent increased displacements due to dynamic P-Delta effects. For buildings with positive post-yield stiffness, C_3 can be set equal to 1.0. For buildings with negative post yield stiffness C_3 is given as

$$C_3 = 1.0 + \frac{|\alpha|(R-1)^{3/2}}{T_e} \quad (15-30)$$

Where α is the ratio of post-yield stiffness to effective elastic stiffness (See Figure 15-18). C_3 need not exceed values calculated for LSP (See Section 15.4.3.1.1).

S_a = Response spectrum acceleration at the effective fundamental period, T_e and damping ratio for the building in the direction under consideration.

For buildings with flexible diaphragms at each floor level, a target displacement can be calculated for each line of vertical framing.

Equation 15-28 can be used to determine this target displacement using the effective fundamental period of the line of vertical framing. The general procedures described for NSP are to be used for each line of vertical framing with masses assigned to the mathematical model on the basis of tributary area.

For stiff diaphragms, which are neither rigid nor flexible, any rational procedure can be used to determine target displacements. An acceptable procedure is to multiply the target displacement obtained from Equation 15-28 by the ratio of the maximum displacements at any point on the roof to the displacements of the center of mass of the roof, both computed by a response spectrum analysis of a 3-D model of the building using a design response spectrum. The target displacement thus computed may not be less than those obtained from Equation 15-28 assuming rigid diaphragms. No vertical line of framing can have displacements less than the target displacement. The target displacement should also be modified as per Section 15.4.2.2 to account for system torsion.

Diaphragms are designed for forces computed in LSP (See Section 15.4.3.1.1) or LDP (See Section 15.4.3.2.4)

15.4.3.3.5 Acceptance Criteria to satisfy Performance Point requirements

For deformation-controlled elements, the maximum deformation demand must be less than expected deformation capacity. Procedures for computing expected deformation capacity are specified in Chapters 5 to 8 of FEMA-273 for various elements and materials.

For force-controlled elements, the maximum design forces must be less than the lower bound strengths Q_{CL} . Procedures for computing the lower bound strengths are also specified in Chapters 5 to 8 of FEMA-273 for various elements and materials.

15.4.3.4 Nonlinear Dynamic Procedure

The Nonlinear Dynamic Procedure (NDP) uses a dynamic time history analysis of a nonlinear mathematical model. The basis,

modeling approaches and acceptance criterion for the NDP are similar to those of the NSP. With the NDP the design displacements are not established using a target displacement, but determined directly through the dynamic time history analysis. As the analysis can be very sensitive to characteristics of individual ground motions, it is advisable to perform the analysis with more than one ground motion. Ground motions used for the analysis and the analysis procedure should be similar to those used in LDP (See Section 15.4.3.2).

It should be noted that the volume of data generated in NDP is enormous and it is difficult to condense the data to useful performance based design information. Sensitivity analysis to various parameters is also a prerequisite for NDP analysis. Thus, NDP must only be used with caution for very important, irregular and unusual structures.

15.4.4 Example

An example is provided of an analysis of existing building using NSP.

15.4.4.1 Building Description

The example building is a reinforced concrete structure located in California. The building was constructed circa 1962. The structure is irregular in plan, with a footprint similar to a compressed "H". The structure has been divided into the East, West, and Central Wings, as illustrated in Figure 15-19.

The building is situated on a site that slopes to the west. The structure has a total of seven levels, plus two small penthouses. The sloping site introduces significant complexities to the structure. The upper five levels are essentially above grade. The West Wing is a total of seven levels tall, two of which are partially below or below grade, depending on the slope of the site. The East Wing is five levels tall, with a partial basement. A portion of the first level is below grade, due to the sloping site.

Vertical loads are resisted by one-way concrete slabs spanning to reinforced concrete beams and girders. Thicker slabs are used in

some areas, including a 17-inch thick "sonovoid" slab, a cast-in-place concrete slab with voids. The sonovoid slabs are located at the ground and first floor. The slabs, beams, and girders are supported by tied and spirally reinforced concrete columns and concrete bearing walls. The columns rest on spread footings, with continuous footings under the perimeter and interior walls.

There are some unusual features in the vertical load-carrying system. Along the north and south exterior walls and the Central Wing, vertical loads are carried by concrete columns outside the building envelope. At the second level, columns are discontinuous and are supported by transfer girders. At the First Floor, the Central Wing relies on massive concrete frames to resist vertical loads.

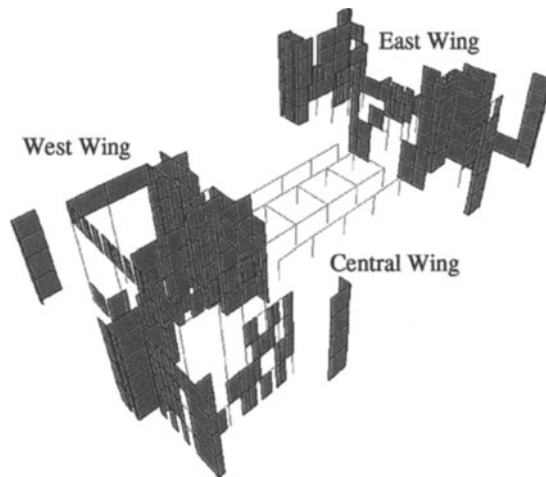


Figure 15-19. 3-D Linear Model of Example Building

The lateral force-resisting system of the example building consists of the concrete floor and roof slabs, acting as rigid diaphragms and reinforced concrete shear walls. The majority of the shear walls are concentrated around the elevator shafts and stair wells, with additional walls internally and on the building exterior. There are numerous vertical discontinuities in the interior shear walls, especially below the first floor. Most of the shear walls are in the East and West Wings.

15.4.4.2 Performance Objective

In keeping with project requirements, the linear as well as nonlinear analysis and rehabilitation design focused on the Basic Safety Objective. In the nonlinear static analysis, the building is pushed to the target displacement for the BSE-1 and BSE-2 level earthquakes.

15.4.4.3 Mathematical Modeling

The nonlinear analysis of the example building was performed using NLPUSH, the nonlinear module to SAP2000. The concrete shear walls were modeled using column elements. P-M interaction diagrams were generated for each column element. The column elements have stiffness in the strong axis computed based on the stiffness of the actual wall. Weak axis stiffness was assumed to be negligible. As NLPUSH requires the interaction surface to be input for both directions of bending, the wall is assumed to have the same moment capacity in both directions of strong axis bending. The gravity frames have been identified as secondary elements, and representative frames have been explicitly modeled to monitor the demands on the gravity load-carrying system. The diaphragms have been assumed to be rigid.

Potential failures in shear and flexure are considered in the analytical model. The wall and column elements have flexural hinges input at the top and bottom of the element at a distance of 0.05 times the element length from each end. Shear hinges are input at mid-height of the element. Because of numerical convergence problems, the column and wall elements had to be split into three segments with one hinge per segment. The flexure hinges are assigned to the top and bottom segments, and the shear hinge to the central segment. Wall elements with flanges are uncoupled and treated as separate walls, with the effective flange width assigned individually to the two walls.

Beams and coupling beams are modeled as frame elements with flexure or shear hinges depending which is the governing mode of failure. Full height walls spanning between

walls or columns are connected by stiff unyielding elements.

Values for effective stiffness of the structural elements for the initial analysis are taken from Table 6-4 of FEMA 273. The stiffness for walls is the cracked stiffness, with a flexural rigidity of $0.5E_cI_g$. The columns are assumed to be in compression with a flexural stiffness $0.7E_cI_g$. The beams are non-prestressed and have an initial stiffness of $0.5E_cI_g$. The shear stiffness is included for columns, beams and walls as $0.4E_cA_w$.

The mathematical model of the building was subjected to monotonically increasing lateral forces until either the target displacement is reached or until the model became unstable. Because the building is not symmetric about any plane, the lateral loads were independently applied in both positive and negative directions.

The relationship between the base shear and lateral force was established for displacements ranging between 0 and 150% of δ_t , where δ_t corresponds to the target displacement for the BSE-1 earthquake. Two lateral load patterns were applied to the structure. The uniform load pattern was applied using lateral loads that are proportional to the mass at each floor. The dynamic load pattern was applied, using a lateral load pattern similar to the story shear distribution calculated by combining the modal responses from a response spectrum analysis with sufficient number of modes to capture 90% of the mass. Foundation flexibility was not expected to be a significant factor in the nonlinear analysis of the building.

15.4.4.4 Target Displacement

The mapped short period response acceleration parameter, S_s and the modified mapped response acceleration parameter at one second period, S_1 , for the given site are obtained from the maps provided with FEMA 273. These maps are the Probabilistic Earthquake Ground Motion maps for California/Nevada for the 0.2 seconds and 1.0 second Spectral Response Acceleration (5% of Critical Damping) with 10% probability of exceedence in 50 years. The values obtained for the example site are:

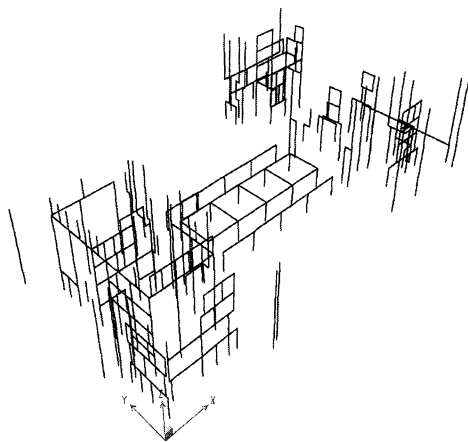


Figure 15-20. 3-D Nonlinear Model of Example Building

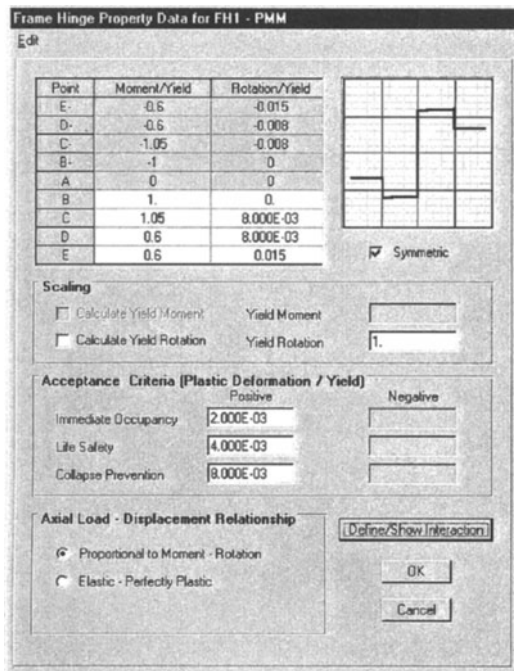


Figure 15-21. Typical Force Deformation Curve for Members Controlled by Flexure

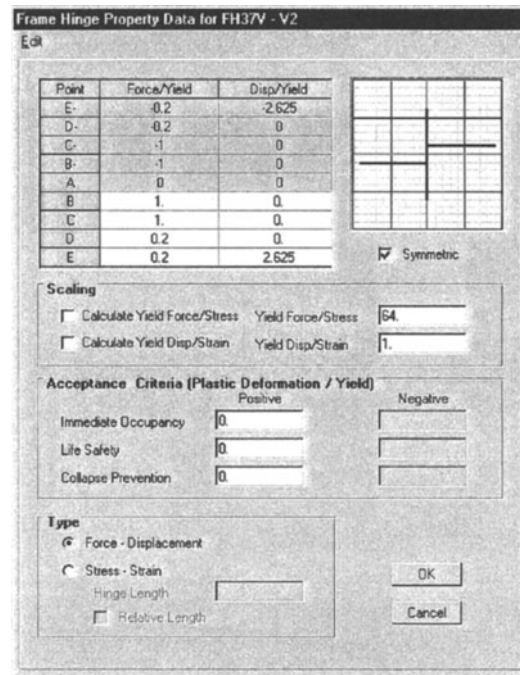


Figure 15-22. Typical Force Deformation Curve for Columns Controlled by Shear

$$S_S = 1.5g \text{ and } S_1 = 0.75g$$

These values adjusted for Site Class C from Tables 2-13 and 2-14 of FEMA-273 give the design short period spectral response acceleration parameter, S_{xs} and design spectral response acceleration parameter, S_{x1} as:

$$S_{xs} = 1.5 \times 1.0 = 1.5g$$

$$S_{x1} = 0.75 \times 1.0 = 0.975g$$

The period T_0 of the general response spectrum curve at an effective damping of 5% is:

$$T_0 = \frac{S_{x1} B_s}{S_{xs} B_1} = \frac{0.975}{1.5} = 0.65 \text{ seconds}$$

Where B_s and B_1 are 1.0 from Table 2-15 of FEMA-273.

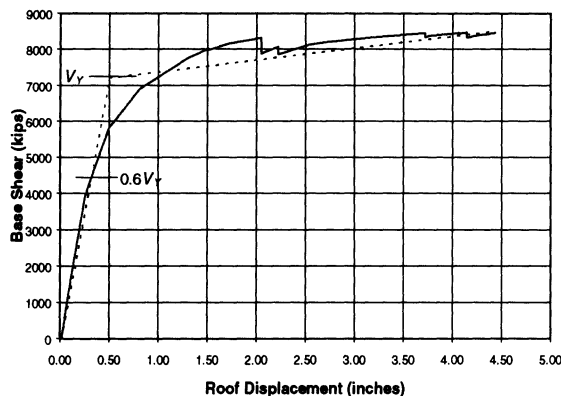


Figure 15-23. Pushover Curve for the Positive East-West Direction Loading (Uniform Pattern)

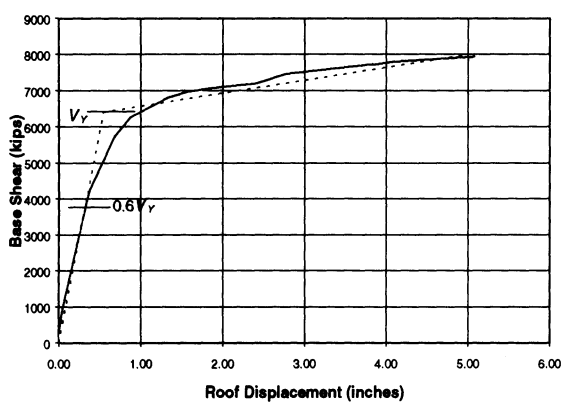


Figure 15-24. Pushover Curve for the Positive North-South Direction Loading (Uniform Pattern)

The period of the building is less than 0.65, thus the spectral acceleration, S_a for the site falls in the constant acceleration part of the spectrum, and is equal to 1.5g.

The target displacement is calculated using:

$C_0 = 1.3$ from Table 15-10, as the lower level is very stiff compared with the rest of the structure.

$C_2 = 1.0$ from Table 15-9 for framing Type 2.

$C_3 = 1.0$ for positive post yield stiffness assumed.

$W = 38,064$ kips

$T_i = 0.65$ seconds

$T_e = 0.41$ seconds in East-West direction

= 0.46 seconds in North-South direction

For the East-West Direction for $V_y = 7,200$ lbs from Figure 15-23:

$$R = \frac{S_a}{V_y/W C_0} = \frac{1.5}{7,200/38,064} \times \frac{1}{1.3} \\ = 6.1$$

$$C_1 = \left[1 + (R - 1) \frac{T_0}{T_e} \right] \frac{1}{R} \\ = \left[1 + (6.1 - 1) \frac{0.65}{0.41} \right] \frac{1}{6.1} \\ = 1.49$$

This value is reduced to the maximum value of C_1 in Section 15.4.3.1.1, which is 1.28 (interpolated for $T_e = 0.41$ seconds). Thus:

$$\delta_t = C_0 C_1 C_2 C_3 S_a \frac{T_e^2}{4\pi^2} g \\ = 1.3 \times 1.28 \times 1 \times 1 \times 1.5 \times \frac{0.41^2}{4\pi^2} g \\ = 4.11 \text{ inches}$$

Similarly for the North-South direction:

$V_y = 6,400$ lbs from Figure 15-24

$R = 6.86$

$C_1 = 1.33$

$\delta_t = 5.37$ inches

Thus, using Equation 15-28, the target displacements for the North-South and East-West directions was determined to be 4.11 inches, and 5.37 inches respectively. The pushover analysis has been continued for 1.5 times the target displacements for collapse prevention

15.4.4.5 Analysis Results

Pushover analyses were performed for the positive and negative North-South and East-West directions of the building. The pushover curves were not able to achieve the target displacement even for the Life Safety

acceptance criteria for BSE-1 in the East-West and North-South directions.

The maximum displacement reached and the type and number of hinges formed for the various pushover analyses performed was recovered. From the results of the pushover analyses, it was seen that the Modal pattern is more detrimental to this building as more number of hinges were formed for a given displacement level compared to the Uniform pattern. This also goes to show that the lower floors of this building are relatively stronger than the upper floors. However this building in its existing configuration was unable to achieve its target displacement. The building could only be pushed to a displacement of 2.8" in the negative East-West direction and 4.34" in the negative North-South direction.

The analyses also revealed a number of columns supporting walls above to have rotations beyond collapse. Many of the walls and beams also had plastic rotations beyond the Life Safety requirement at the target displacement. Some of the columns in the central wing had shear failures under the uniform pattern for push in the East-West direction. Clearly, this building does not meet the acceptance criteria of the basic safety objective, and therefore needs retrofit.

15.5 Conclusions

The principal advantage of PBSE is that the choice of performance goals lies with the owner who can decide the acceptable damage state. The engineer can also convey to the owner a better understanding of the expected damage state. PBSE does not eliminate the risks associated with uncertainties in ground motions, material properties, element behavior or geotechnical properties. However, it provides a new technique to remove unnecessary conservatism for some parameters and discover unidentified deficiencies for others. If implemented correctly and competently, PBSE can produce a design that is more reliable than traditional procedures.

One very useful characteristic of the ATC-40 and FEMA 273/274 documents is that they provide a step-by-step approach for PBSE. This is an important first step towards a building code implementations of performance based design.

There are some weaknesses that need to be addressed with additional research. Three broad areas need work:

1. A more reliable and conservative methodology, which is widely accepted, needs to be developed for establishing the performance point. More accurate equations need to be developed to find the effective damping or equivalent ductility used to reduce the design response spectra to levels consistent with observed structural behavior.
2. More sophisticated computer analysis programs are needed which can do nonlinear analysis of concrete/masonry/plywood shear walls, concrete and steel joints, confined concrete sections, etc. There is also a need to reduce the data to a finite number of parameters than can be used for design.
3. The element capacities and deformations limits for various performance levels are currently based on engineering judgment or relatively small number of experiments. More experimental and theoretical work is needed to establish reliable element capacities and deformation limits for given performance objectives.

REFERENCES

- 15-1 Applied Technology Council (1996), *Seismic Evaluation and Retrofit of Concrete Buildings*, ATC-40, Volume 1 and 2, Report No. SSC 96-01, Seismic Safety Commission, Redwood City, CA.
- 15-2 Federal Emergency Management Agency (1997), *NEHRP Guidelines for the Seismic Rehabilitation of Buildings*, FEMA-273, Washington, D.C.
- 15-3 Federal Emergency Management Agency (1997), *NEHRP Commentary on the Guidelines for the Seismic Rehabilitation of Buildings*, FEMA-274, Washington, D.C.

- 15-4 King, S.A. and Rojhan, C. (1997), "ATC-38 Database on the Performance of Buildings Near Strong-Motion Recordings," *Proceedings of Northridge Earthquake Research Conference*, CUREe, Los Angeles, August.
- 15-5 Crandell, J.H. (1997), "Statistical assessment of Residential Construction Damage by the Northridge Earthquake," *Proceedings of Northridge Earthquake Research Conference*, CUREe, Los Angeles, August.
- 15-6 Naeim, F. and Kelly, J.M. (1999), *Design of Seismic Isolated Structures – From Theory to Practice*, John Wiley & Sons, New York.
- 15-7 Naeim, F. (1998), "Earthquake Ground Motions and Performance Based Design", *Performance Based Seismic Engineering Invitational Workshop*, Earthquake Engineering Research Institute, San Diego, California.
- 15-8 Freeman, S.A., Nicoletti, J.P. and Tyrell, J.V., 1975, "Evaluation of Existing Buildings for Seismic Risk: A Case Study of Pudget Sound Naval Shipyard, Bremerton, Washington," *Proceedings of U.S. National Conference of Earthquake Engineers*, Berkeley, Earthquake Engineering Research Institute.
- 15-9 Freeman, S.A., 1998, "Development and use of Capacity Spectrum Method," Paper No. 269, *Proceedings of the 6th U.S. National Conference of Earthquake Engineering*, Seattle, Washington.
- 15-10 U.S. Army, 1986, *Seismic Design Guidelines for Essential Buildings*, Departments of the Army (TM5-809-10-1), Navy (NAVFAC P355.1), and the Air Force (AFM88-3), Washington, DC.
- 15-11 Structural Engineers Association of California (SEAOC), 1995, *Vision 2000: Performance-Based Seismic Engineering of Buildings*, Sacramento, California.
- 15-12 International Code Council, 2000, *International Building Code 2000*.
- 15-13 International Conference of Building Officials, 1997, *Uniform Building Code*, Whittier, CA.
- 15-14 Chopra, A.K. and Goel R.K., 1999, *Capacity-Demand-Diagram Methods for Estimating Seismic Deformation of Inelastic Structures: SDF Systems*, Pacific Earthquake Engineering Research Center, PEER-1999/02, University of California, Berkeley, California.
- 15-15 Chopra, A.K. and Goel R.K., 2000, "Capacity-Demand-Diagram Methods Based on Inelastic Design Spectrum," *Earthquake Spectra*, Volume 15, Number 4, EERI, Oakland, California.
- 15-16 Newmark, N.M., and Hall,W.J., 1982, *Earthquake Spectra and Design*, Earthquake Engineering Research Institute, Berkeley, California.
- 15-17 Krawinkler, H. and Nassar, A.A., 1992, "Seismic Design based on Ductilities and Cumulative Damage Demands and Capacities," in *Nonlinear Seismic Analysis and Design of Reinforced Concrete Buildings*, P. Fajfar and J. Krawinkler, Editors., Elsevier Applied Science, New York.
- 15-18 Vidic, T., Fajfar, P. and Fischinger, M., 1994, "Consistent Inelastic Design Spectra: Strength and Displacement," *Earthquake Engineering and Structural Dynamics* 23(5).
- 15-19 Fajfar, P., 2000, "A Nonlinear Analysis Method for Performance Based Seismic Design," Accepted for Publication in *Earthquake Spectra*, EERI, Oakland, California.
- 15-20 Aschheim M., Black, E.F., 2000, "Yield Point Spectra for Seismic Design and Rehabilitation," *Earthquake Spectra*, Volume 16, Number 2, EERI, Oakland, California.
- 15-21 Cormartin, C.D., Niewiarowski, Freeman, S.A. and Turner, F.M., 2000, "Seismic Evaluation and Retrofit of Concrete Buildings; A Practical Overview of the ATC-40 Document," *Earthquake Spectra*, Volume 16, Number 1, EERI, Oakland, California.
- 15-22 Chai, W. and Guh, J., 1999, "Performance-Based Design of Concrete Shear Wall Buildings," *Proceedings of 1999 SEAOC Convention, Structural Engineers Association of California*, Santa Barbara, California.

Chapter 16

Computer Applications in Seismic Design

Farzad Naeim, Ph.D., S.E.

Vice President and Director of Research and Development, John A. Martin & Associates, Inc., Los Angeles, California.

Roy F. Lobo, Ph.D., P.E.

Senior Research Engineer, John A. Martin & Associates, Inc., Los Angeles, California.

Hussain Bhatia, Ph.D., P.E.

Senior Research Engineer, John A. Martin & Associates, Inc., Los Angeles, California.

Key words: Computer Applications, Earthquake Engineering, Earthquake Ground Motion, Engineering Judgment, General-Purpose Software, Loss Estimation, Instrumented Building Response, Seismic Design, Special-Purpose Software

Abstract: This chapter surveys the state-of-the-art in computer applications in seismic design. The field of computer applications is rapidly changing. Therefore, a general overview of contemporary applications is provided with references to the relevant worldwide web site addresses. The ever-increasing reliance on computer applications requires a re-doubling of emphasis on sound engineering judgment by practicing professionals. Computers can enable us to perform engineering tasks we did not dream to be possible just a few years ago. Blind faith in computers, however, may produce results that are far less reliable than back of the envelope calculations by a seasoned engineer.

16.1 INTRODUCTION

This chapter provides a sampling of computer applications in seismic design at the time of this writing. No other field of science and technology moves forward faster than computer and communication technologies. Therefore, it is vital for the reader to examine the state of knowledge and practice at the time of his/her reading because significant advances may have occurred in between the time of writing this chapter and the time it is being read. To assist the reader in this task, we will point to relevant Internet resources in different parts of this chapter.

The builder's need for computational devices predates ancient Babylonian, Persian, and Greek empires. Over the ages, as the complexity of engineering concepts grew, it initially created *master craftsmen*: people who could design and build magnificent structures without an exact understanding of underlying mathematical principles but a fantastic ability to apply structural proportions found workable in nature. For example, it is said that the slenderness of the Pantheon columns were derived from studying the proportions of the human female leg-bones. The curves of many magnificent ancient domes were derived from the shape of wild mushroom crowns⁽¹⁶⁻¹⁾. Over many centuries, remarkable structures were built –without any precise mathematical formulation– that withstood the test of the time. These designs were based on what we now refer to as *sound engineering judgment*. The design-build practice that is now becoming prevalent in the United States and other advanced countries, was the only form of construction known for many centuries.

The next stage in engineering evolution brought about the *multidisciplinary masters*. People like Leonardo Davinci who was an

artist, architect and engineer at the same time exemplify this category. The growth of science and engineering knowledge in the 20th century made high degrees of specialization necessary and made multidisciplinary masters extinct. Today, not only we distinguish structural engineers from civil engineers but we further break down each field of expertise: structural designers, structural analysts, earthquake engineers, wind design engineers, cladding specialists, seismic isolation specialists, design ground motion specialists, etc. Therefore, we live in the era of *specialists*.

Specialization increases the depth of the knowledge but unfortunately reduces the breadth of it. The grand vision common to master builders and multidisciplinary masters are very difficult to find. At the same time the growth of computing hardware and software over the past two decades have been monumental. It is safe to say that all specialists now rely on computing facilities to the extent that was imaginable just a few years ago. The combined effect of reduction in the scope of knowledge (brought about by specialization) and heavy reliance on computational devices (caused by rapid growth of computing facilities) can be dangerous. Engineering has never been, or can be, a pure game of numbers. Engineering judgment is simply too important to be lost to blind faith in computing devices. There is a need for balance. We have to find ways of maximizing our use of computer technology without leaving our engineering judgment behind. Seismic design students must be trained to develop and to value a physical feeling for how buildings resist earthquake forces, why they survive them, and the cause of their failure. The best use of computer technology is only possible if respect for engineering judgment is nurtured and preserved.

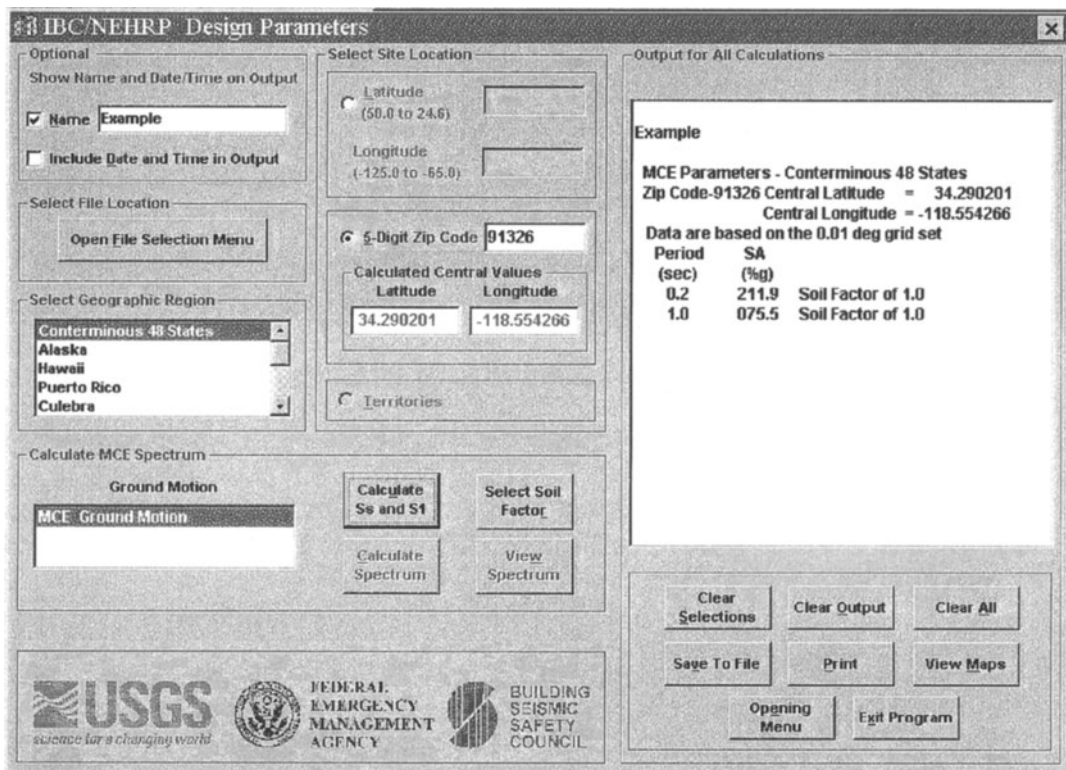


Figure 16-1. Seismic Hazard Map CD-ROM Supplement to IBC-2000

The computer revolution that started in the last quarter of the 20th century and is still accelerating today, has the potential of impacting human civilization more than the advent of printing by Gutenberg⁽¹⁶⁻²⁾. As will be noticed from reading this chapter, earthquake engineers are now achieving objectives that could not have been even imagined a short few years ago. A few examples would be illustrative. The probabilistic seismic hazard map of the entire United States for default site soil conditions is now readily available on the Internet and distributed as a part of the 2000 International Building Code (IBC-2000)⁽¹⁶⁻³⁾ as well as FEMA Guidelines for Seismic Rehabilitation of Existing Buildings^(16-4, 16-5). A companion CD-ROM to these documents allows the user to identify design spectral ordinates of any site by providing its latitude and longitude. For more approximate applications, providing a postal zip code also suffices! (Figure 16-1).

Instrumental Intensity maps for significant earthquakes in the southern California region are automatically produced by the *Trinet* and *Cube* networks. The *Cube* maps are instantaneously sent via e-mail to subscribers. *Trinet* shake maps may be viewed on the Internet (<http://www.Trinet.org>) within a few minutes after earthquakes (Figure 16-2). A clickable map for Southern California faults available at a web site (<http://www.scecdc.scec.org/faultmap.html>) permits users to point to any fault and obtain all relevant information (Figure 16-3).

In the field of loss estimation, emergency management and post-earthquake response, the GIS based HAZUS-99 software system⁽¹⁶⁻⁶⁾ developed under a grant from the Federal Emergency Management Agency (FEMA) has provided a new horizon to various casualty loss scenario and probabilistic analysis (Figures 16-4 and 16-5).

In seismic analysis and design of very complex structures, automotive and airplane proportioning and design software have been utilized to accommodate the sophisticated curvatures in the architectural and structural systems (Figure 16-6)⁽¹⁶⁻⁷⁾.

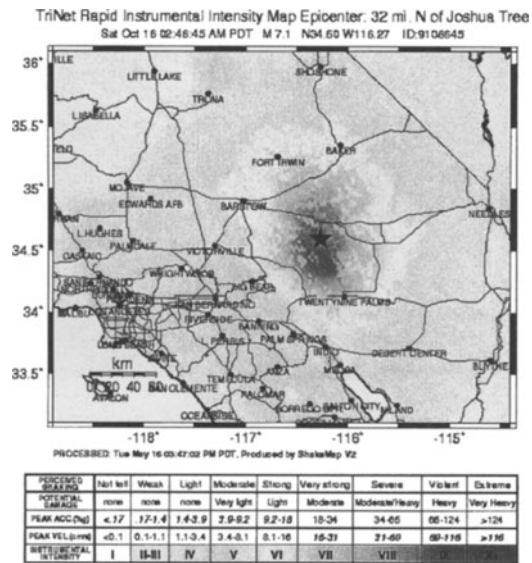


Figure 16-2. A TriNet Shake Map for the 1999 Hector Mines Earthquake in southern California (www.trinet.org).

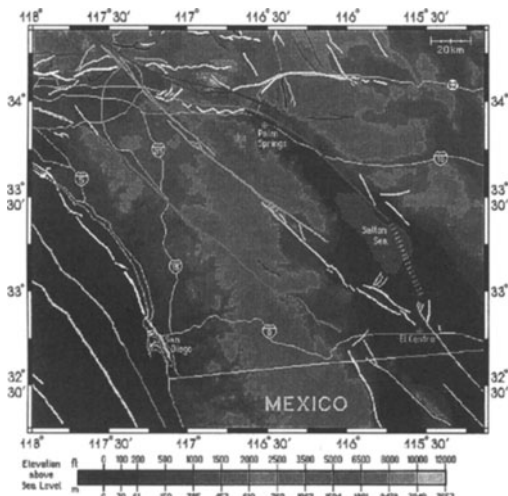


Figure 16-3. A clickable Fault Map Available on the Internet (www.scec.org).

Detailed nonlinear finite element analysis techniques have been successfully utilized to predict the experimental behavior of proposed structural connections (Figures 16-7 and 16-8)⁽¹⁶⁻⁸⁾.

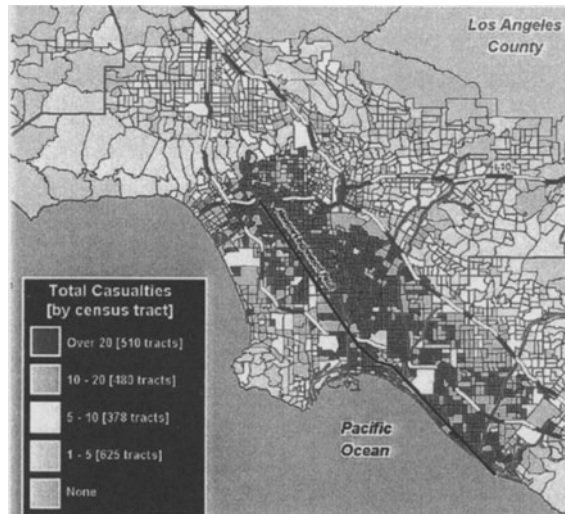


Figure 16-4. A HAZUS-99 casualty loss estimate for a scenario event in southern California.

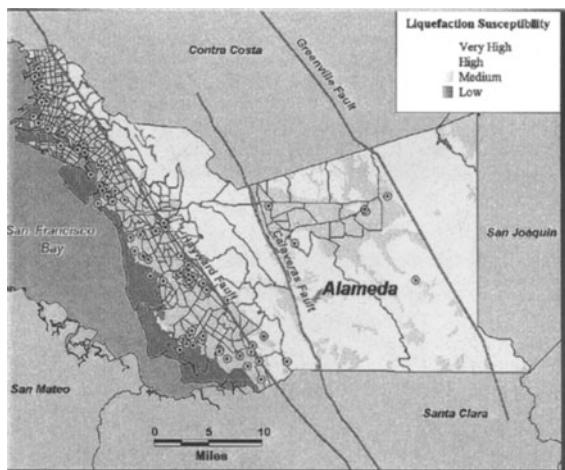


Figure 16-5. A HAZUS-99 analysis of liquefaction potential and dangers posed by hazardous material storage sites in Alameda county of California.

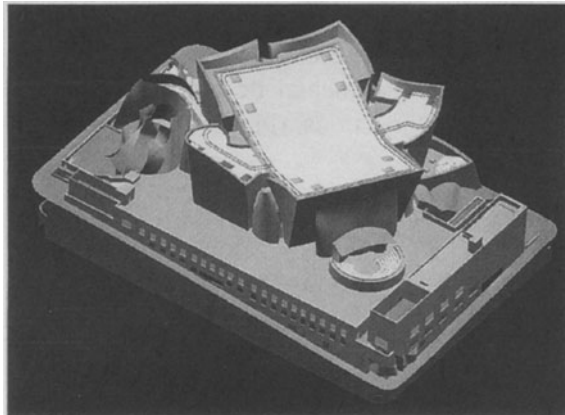


Figure 16-6. The Disney Concert Hall, under construction in Los Angeles, California was designed using CATIA, a software primarily used in automotive and airplane design applications.

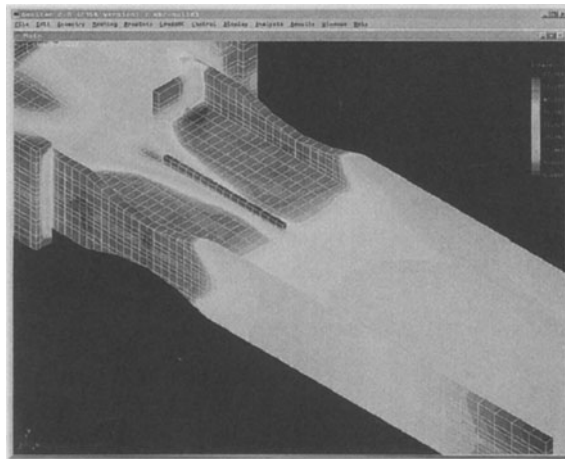


Figure 16-7. Nonlinear finite element analyses were instrumental in shaping a new SMRF connection for the UCLA Replacement Hospital under construction in Los Angeles, California.

Last, but not least, up-to-date literature searches can be conducted online. Therefore, seismic design engineers rarely need to “re-invent the wheel”. Now, it is not only always possible, but a necessity, to check the relevant information on the Internet before one starts to embark on an unfamiliar path. A few web sites of particular significance in this regard are listed in Table 16-1.

In short, computer applications have tremendously enhanced our capabilities in all facets of seismic design and construction. At

the same time, computer applications has to be balanced with sound engineering judgment and a true physical sense of seismic performance, for it to benefit –and not adversely affect– the safety and quality of the end product.

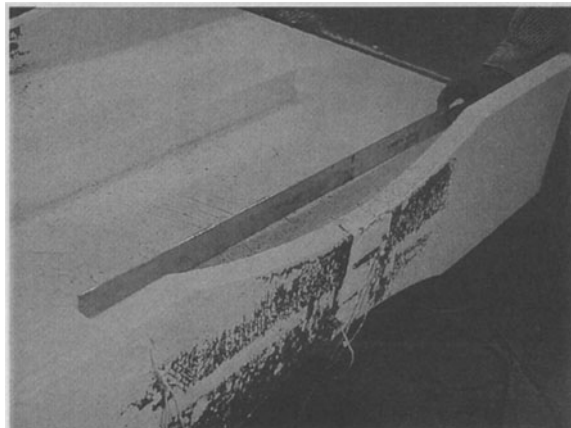


Figure 16-8. Full-scale testing confirms the findings of the compute model shown in Fig. 16-7.

Table 16-1. Important World-Wide-Web sites

Organization	Web Site Address
Earthquake Engineering Research Institute	http://www.eeri.org
Multidisciplinary Center for Earthquake Engineering Research	http://mceer.buffalo.edu
Mid-America Earthquake Center	http://mae.ce.uiuc.edu
Pacific Earthquake Engineering Research Center	http://peer.berkeley.edu
The Earthquake Hazards Mitigation Information Network	http://www.eqnet.org
Applied Technology Council	http://www.atcouncil.org
Trinet	http://www.trinet.org
Southern California Earthquake Center	http://www.scec.org
California Strong Motion Instrumentation Program (CSMIP)	http://www.consrv.ca.gov
USGS National Earthquake Information System	http://wwwneic.cr.usgs.gov
HAZUS User Group	http://www.hazus.org
Federal Emergency Management Agency	http://www.fema.gov

16.2 EARTHQUAKE RECORDS

A few short years ago, it was very difficult to get hold of a good collection of earthquake records for design. That is no longer the case. Naeim and Anderson⁽¹⁶⁻⁹⁾ have compiled a comprehensive list of design attributes of horizontal and vertical components of available ground motion for North and Central America as well as Hawaii. Once the desired design attributes are determined, it takes only a short visit to various web sites that contain large databases of earthquake records for various regions of the world. For example, for California records, the CSMIP web site provides time series as well as spectral ordinates of a variety of recorded ground motions (Figures 16-9 to 16-11).

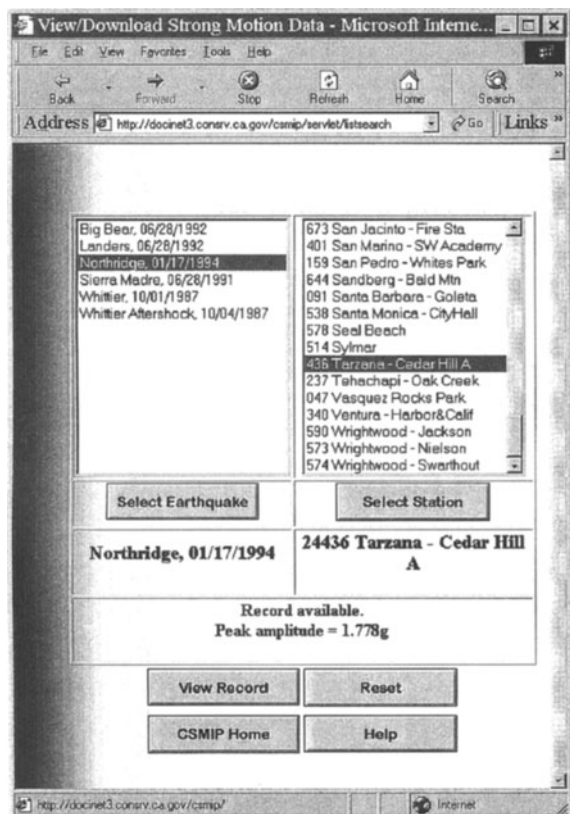


Figure 16-9. Selecting an earthquake record from the CSMIP web site.

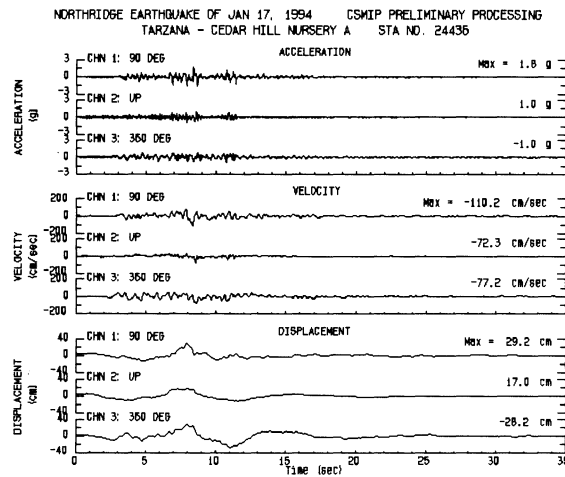


Figure 16-10. Time series for the earthquake record selected in Fig. 16-9 as displayed on the CSMIP web site.

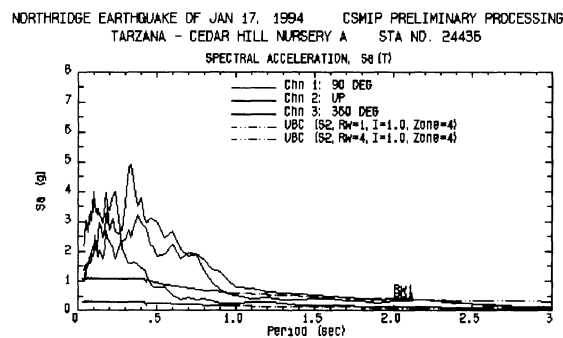


Figure 16-11. Response spectra for the earthquake record selected in Fig. 16-9 as displayed on the CSMIP web site.

16.3 MONITORING SEISMIC ACTIVITY

Besides click-able fault maps, seismocams (worldwide web pages connected directly to seismograms or to cameras focused on them) can be found in abundance on the Internet, some very serious work is being conducted in this area that could not possibly been performed without computer assistance. Perhaps the most significant of these experiments is being conducted by TriNet in Southern California.

TriNet is a multifunctional seismic network for earthquake research, monitoring and computerized alerts. TriNet is a cooperative

project between US Geological Survey, California Institute of Technology, and the Strong Motion Instrumentation Program of the California Division of Mines and Geology. The goals of TriNet are to provide data for research in engineering and earth sciences, emergency response applications and development of a seismic computerized alert network. The TriNet network features a dense recording of ground motions in all frequency bands, dense strong motion instrumentation with 150 broadband and 600 strong motion sensors all connected to a central processing system. The network can issue automatic post-earthquake intensity maps very quickly after an earthquake (see Figure 16-2).

16.4 SEISMIC HAZARD ANALYSIS

There are a variety of software systems with different levels of sophistication available in the marketplace. Arguably, the computer programs developed by the California geologist Dr. Thomas F. Blake (are among the most widely used at least in the western United States (<http://www.thomasfblake.com>). We will highlight Blake's programs as representative applications in this field.

The *EQSEARCH* program⁽¹⁶⁻¹⁰⁾ contains a searchable catalog of significant earthquakes in western United States dating back to 1880. Given a site latitude and longitude, soil conditions and the choice of attenuation relationship, the program reports historical events that have occurred within a given radius (or rectangle) around the site. The program then uses this information to estimate the peak ground accelerations observed at the site as well as a Gutenberg-Richter recurrence relationship for the site (see Figures 16-12 to 16-14).

The *EQFAULT* program⁽¹⁶⁻¹¹⁾ can be used to perform a deterministic seismic hazard analysis for a given site. The input information is similar to that of the previous program. *EQFAULT*, however, searches a three-dimensional database of earthquake faults and reports maximum magnitude associated with each fault and an

estimate of the corresponding maximum accelerations experienced at the site (Figures 16-15 and 16-16).

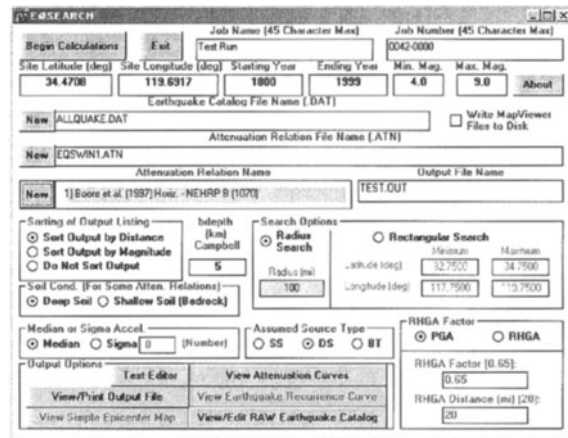


Figure 16-12. A typical *EQSEARCH* input screen

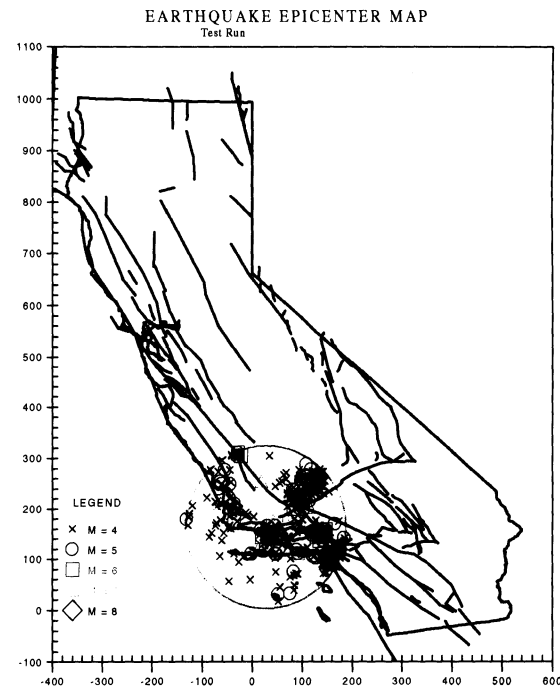


Figure 16-13. A typical epicenter map generated by *EQSEARCH*

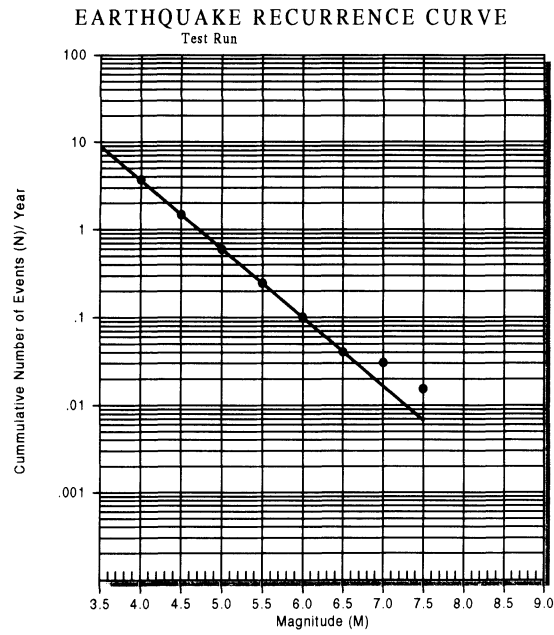


Figure 16-14. An earthquake recurrence curve generated by application of *EQSEARCH*

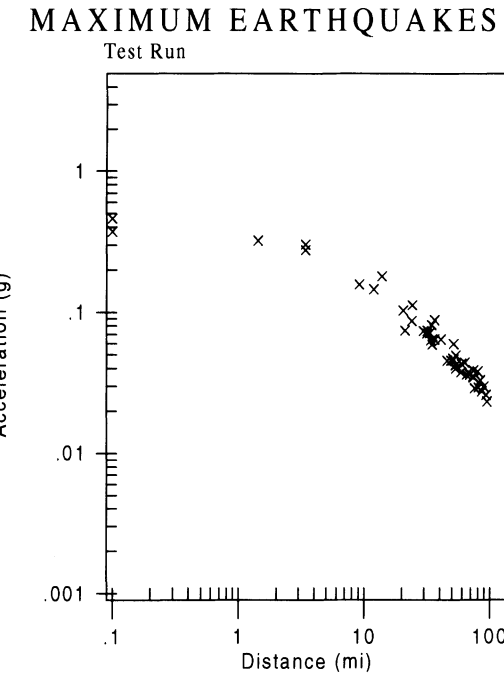


Figure 16-16. A site acceleration versus distance chart generated by *EQFAULT*

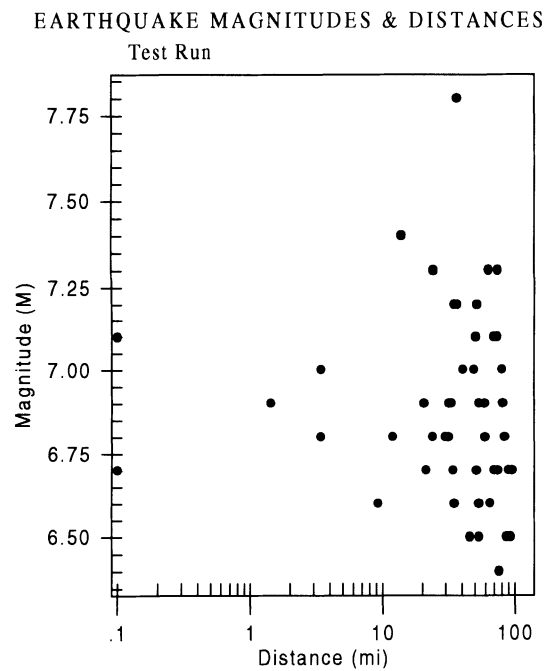


Figure 16-15. A plot of earthquake magnitudes and their corresponding distances from a given site generated by the *EQFAULT* program



Figure 16-17. A typical input screen for the *FRISKSP* computer program

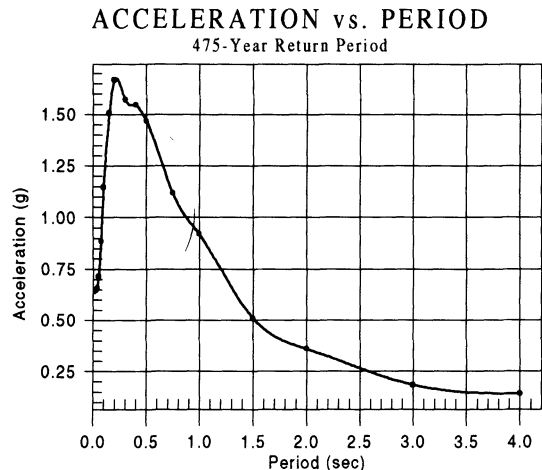


Figure 16-18. A probabilistic design spectrum generated by the FRISKSP computer program

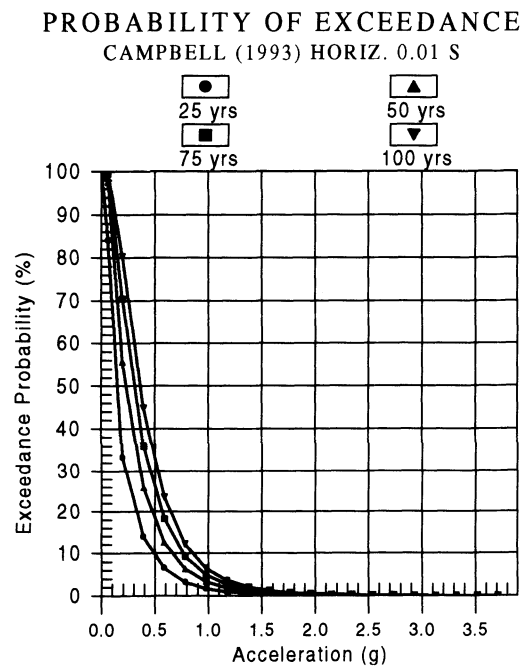


Figure 16-19. A typical probability of exceedance chart for peak ground acceleration generated by FRISKSP computer program

FRISKSP program⁽¹⁶⁻¹²⁾ is a more complicated software than the previous two and performs a probabilistic seismic hazard analysis for a given site and is capable of generating a set of probabilistic design spectra corresponding to the desired average return periods and dispersions (Figures 16-17 to 16-19). It is also capable of hazard de-aggregation

16.5 LOSS ESTIMATION, SCENARIO ANALYSIS AND PLANNING

The loss estimation methodology and application was revolutionized by release of the HAZUS-99 software system⁽¹⁶⁻⁶⁾, development of which was made possible through a concentrated and prolonged funding by the Federal Emergency Management Agency (FEMA).

HAZUS-99 was intended to provide local, state and regional officials with the tools necessary to plan and stimulate efforts to reduce risk from earthquakes and to prepare for emergency response and recovery from an earthquake. The program was also intended to provide the basis for assessment of nationwide risks of earthquake loss. HAZUS-99 can be used by a variety of users with needs ranging from simplified estimates that require minimal input to refined calculations of earthquake loss. Since it is totally built around a geographical information system (GIS) technology, its application and enhancement are rather straightforward.

The vision of earthquake loss estimation requires a methodology that is both flexible, accommodating the needs of a variety of different users and applications, and able to provide the uniformity of a standardized approach. The framework implemented in HAZUS-99 includes each of the components shown in Figure 16-20:

- Potential Earth Science Hazard (PESH)
- Inventory
- Direct Physical Damage
- Induced Physical Damage
- Direct Economic/Social Loss, and
- Indirect Economic Loss.

As indicated by arrows in Figure 16-20, HAZUS-99 modules are interdependent with output of some modules acting as input to others. In general, each of the components will be required for loss estimation. However, the degree of sophistication and associated cost will vary greatly by user and application.

Framing the earthquake loss estimation methodology as a collection of modules permits adding new modules (or improving models/data of existing modules) without reworking the entire methodology. Improvements may be made to adapt modules to local or regional needs or to incorporate new models and data.

The modular nature of the HAZUS-99 methodology permits a logical evolution of the methodology as research progresses and the state-of-the-art advances.

HAZUS-99 incorporates state-of-the-art models in the earthquake loss estimation methodology. For example, ground shaking

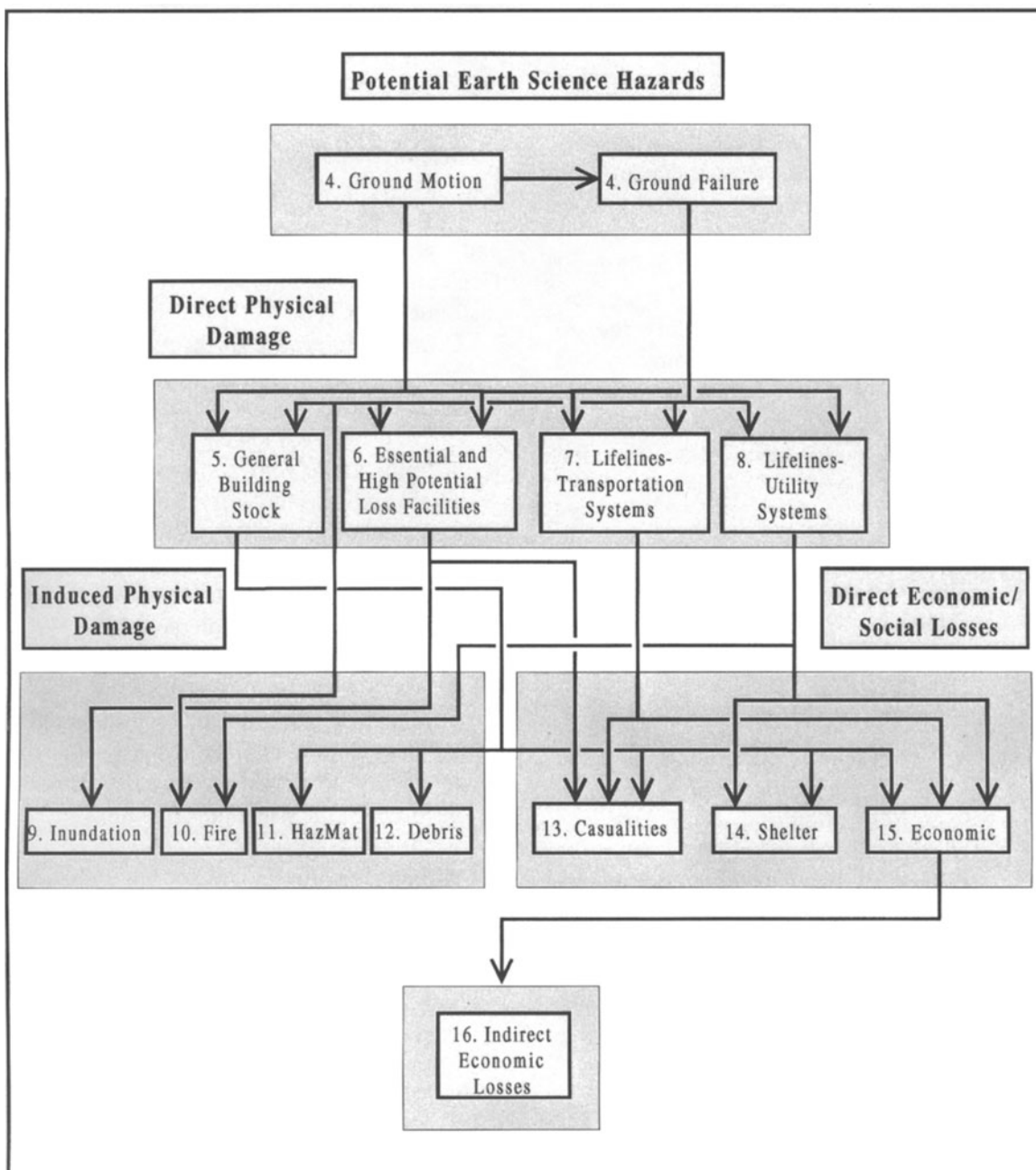


Figure 16-20. Flowchart of HAZUS-99 loss estimation methodology⁽¹⁶⁻⁶⁾

hazard and related damage functions are described in terms of spectral response rather than MMI. Modules include damage loss estimators not previously found in most studies, such as induced damage due to fire following earthquake and indirect economic losses. A nationally applicable scheme is developed for classifying buildings, structures and facilities.

HAZUS-99 incorporates both deterministic (scenario earthquake) and probabilistic descriptions of spectral response. Alternatively, it accepts user-supplied maps of earthquake demand. The software also accepts externally supplied maps of earthquake ground shaking. The uncertainty in earthquake demand due to spatial variability of ground motion is addressed implicitly by the variability of damage probability matrices or fragility curves. Uncertainty in earthquake demand due to temporal variability (i.e., earthquake recurrence rate) or uncertainty in the magnitude of earthquake selected for scenario events may be readily evaluated by the users. Loss estimation using HAZUS-99 may be conducted on a regional or a national scale.

16.6 EERI/IAEE WORLDWIDE HOUSING ENCYCLOPEDIA PROJECT

Under the joint leadership of the Earthquake Engineering Research Institute (*EERI*) and the International Association of Earthquake Engineers (*IAEE*) and cooperation of engineers from over 70 countries an online encyclopedia of earthquake vulnerability of worldwide housing is under progress. This is a monumental task of immense practical consequences. By collecting and comparing various types of housing vulnerability across the globe and local techniques currently deployed for hazard mitigation, for the first time the sharing of experience and expertise may be exercised in a truly universal scale. The online version to be developed and published on the Internet can be of immense value to

governmental as well as nongovernmental agencies. It could be also used by funding agencies such as the World Bank in rational prioritization of investments in earthquake hazard reduction projects. The interested reader is referred to the *EERI* web site (<http://www.eeri.org>) for more information.

16.7 INSTRUMENTED BUILDING RESPONSE ANALYSIS

Seismic performance of instrumented buildings provide a vital link for critical evaluation of various theories, code provisions, and practices utilized in seismic design. Generally, there are two types of seismic instrumentation:

1. *Code Instrumentation* whereby according to mandates of the applicable building code, some significant structures are instrumented. Codes usually mandate a minimal level of instrumentation for buildings of certain height and/or complexity. The requirements are usually satisfied by installation of a tri-channel accelerometer at the base, mid-height, and roof of the building. Generally, in this type of application the various sensors are not time-synchronized.
2. *Extensive Instrumentation* whereby buildings are instrumented by installation of a relatively large number of sensors (usually between 10 to 30) throughout the plan and elevation of the structure. The sensor locations are designed to maximize post-earthquake understanding of building response. Dozens of buildings have been extensively instrumented by CSMIP and USGS agencies in California. The records of instrumented response may be downloaded from the Internet (see Table 16-1).

To illustrate the lessons that can be learned from studying seismic performance of instrumented structures, Naeim developed an interactive CD-ROM based information system (Figure 16-21)⁽¹⁶⁻¹³⁾. This information system

contains detailed information regarding performance of 20 extensively instrumented buildings during the 1994 Northridge earthquake. However, the database organization and the overall structure of the information system are readily expandable to include other buildings and/or other earthquakes. It provides facilities for manipulating instrument records in either frequency or time domain, combining and contrasting them, identification of predominant building frequencies, and generation of moving windows fast Fourier transform (FFT) functions to track possible structural damage by identifying significant shifts in predominate building periods.



Figure 16- 21. The main folder for one of the 20 buildings contained in the information system CD-ROM



Figure 16-22. A buckled penthouse brace documented for the building shown in Figure 16-21.



Figure 16-23. One of the damaged columns for a severely damaged building documented in the information system CD-ROM

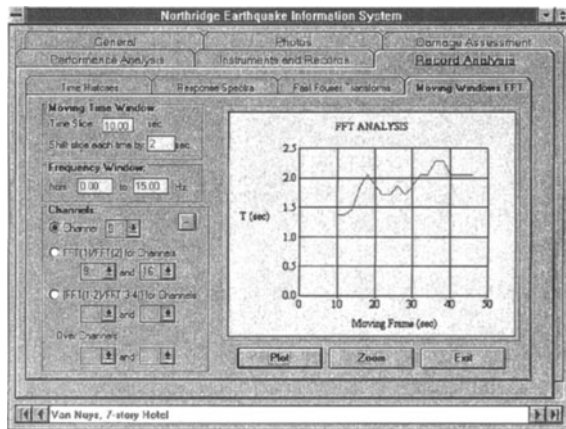


Figure 16-24. A moving-windows FFT plot generated for the building shown in Figure 16-23 using the information system utilities indicating a significant softening of the building due to damage. Horizontal axis in the plot shows the time and the vertical axis shows predominant building period as a function of time.

16.8 STRUCTURAL ANALYSIS AND DESIGN

Structural engineers have always been at the forefront of computer applications. The advancement of computer technology in terms of both hardware and software has vastly broadened the use of computers in seismic analysis and design. The advent of personal computers and availability of very sophisticated analysis software on this platform has further integrated computers into routine seismic analysis and design practices. The large scale finite element analysis programs that were available only on mainframe computers are now readily accessible on ordinary personal computers. As a matter of fact, interactive finite element analysis software has been even successfully ported on to some pocket calculators⁽¹⁶⁻¹⁴⁾.

Two and three-dimensional linear static analysis of structures has become so routine that it is hardly worth extended review in this chapter. It is fair to say, that the generally available competent software systems for performing these tasks could be primarily

distinguished based on their user interface, ease of use, and the extent to which graphical modeling of the structure has been made possible. The same observation is not necessarily true for linear dynamic analysis where the number of robust software systems that can properly model untypical cases without ill-conditioning and other similar problems is fairly limited.

Nonlinear analysis software systems, on the other hand, are in a revolutionary stage. They are undergoing rapid changes to accommodate the various practical needs that have become critical because of the rise in popularity of performance based design techniques (see Chapter 15) and application of technologies such as seismic isolation and energy dissipation devices (see Chapter 14).

A structure is said to exhibit nonlinear behavior when its response is not directly proportional to the applied load. Generally, three distinct types of nonlinearity may be distinguished:

1. *Material nonlinearities* account for the hysteretic behavior of the material. Their characteristics are derived from the constitutive stress-strain properties of the material. Commonly utilized material nonlinearity models include elastic-plastic, hyper-elastic, visco-elastic, or visco-plastic behaviors. The onset of nonlinear behavior (yielding) is governed by various yield criteria and their associated flow and hardening rules such as the Tresca and Von-Mises criteria. Depending on the material used in the structure, different yield criteria surfaces and yield to choose from. Examples and surfaces are selected. Examples include the Hill's criterion for anisotropic materials and the Mohr-Coulomb, Drucker Prager, and Cam-clay criteria for soils and rock.
2. *Geometric nonlinearities* are the effects of large displacements on basic structural assumptions or on the equilibrium state. They include large deflections, P-Δ effects, and buckling.
3. *Boundary nonlinearities* model the behavior of elements in contact, but not connected to

each other. These are specified either by *gap* (compression only), *hook* (tension only), *sliders* (friction at point of contact) or *slide-line* (friction over line of contact) elements.

Generally speaking, computer programs used in seismic analysis and design can be classified into two main categories: *general-purpose* and the *special-purpose* structural analysis software.

General-purpose analysis programs are not specifically designed for seismic analysis and design but can certainly be used for this purpose. There are many general-purpose analysis programs that can analyze structures with any or all of the above mentioned non-linearities. The example⁽¹⁶⁻¹⁵⁾ presented in Figure 16-25 shows the analysis of an anchored cylindrical storage tank under reversed seismic loading. As the walls of the storage tank are made of very thin plates of steel, the deformations of the walls due to hydrodynamic loads are large. Also in many cases, the buckling of the walls of such tanks are preceded by yielding of the steel. Thus, both material and geometric non-linearities are involved in the analysis. For unanchored tanks⁽¹⁶⁻¹⁵⁾, the problem becomes more complex with participation of the uplifting of the base plate from the foundation in dissipating energy during an earthquake. In such cases, the analysis program must also include contact non-linearities as shown in Figure 16-26. Thus, for such seismic analyses, a general-purpose program is needed.

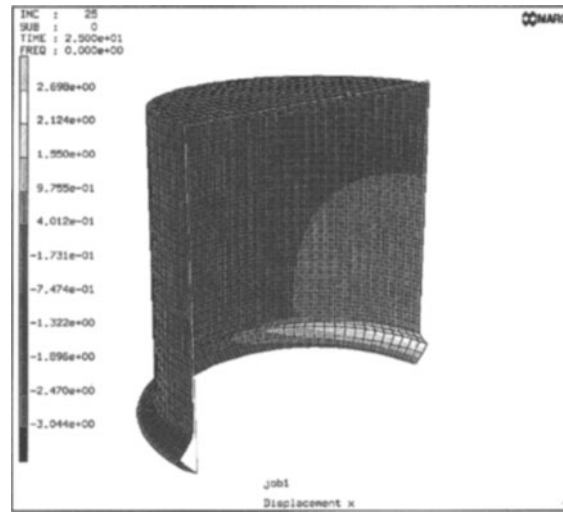
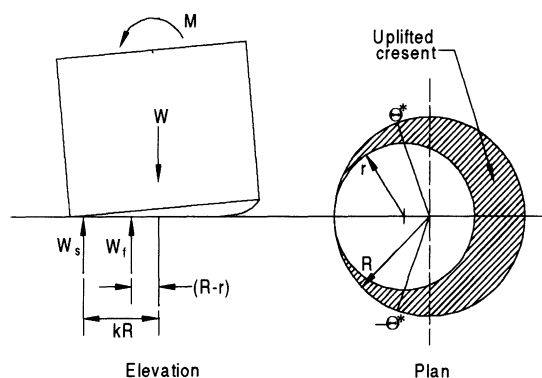


Figure 16-25. Buckling of an anchored cylindrical storage tank subject to reversed hydrodynamic pressures during an earthquake. MARC⁽¹⁶⁻¹⁶⁾ was used in the analysis.

Because of the practical utility that special purpose software systems provide, their use is more widespread than the general-purpose software. A practicing engineer is usually better served by using a special purpose software tailored to handle the specific type of project at hand rather than using a general purpose software to tackle all kinds of projects. In addition general-purpose programs by their nature are more complex and difficult to master. Therefore, training engineering staff on the use of specialty software tends to be less burdensome. General-purpose programs also tend to be more costly in terms of initial purchase and subsequent maintenance.



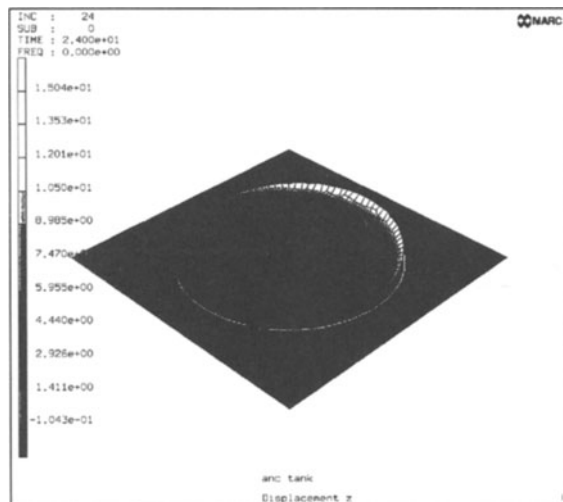
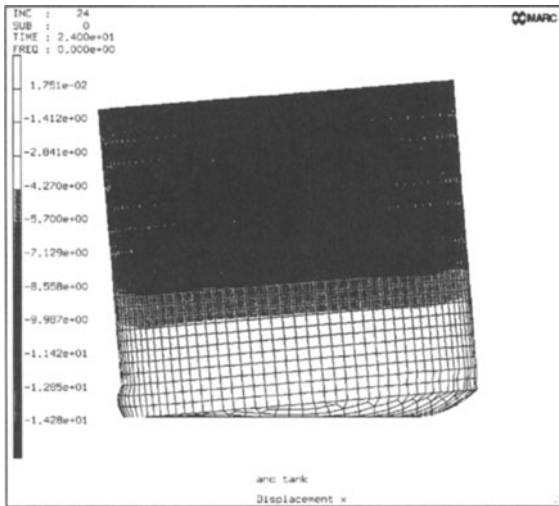


Figure 16-26. Buckling and uplifting of an unanchored cylindrical storage tank under seismic loads. Shown at the bottom is the base plate of the tank uplifting from its rigid foundation due to the hydrodynamic pressures on the vertical walls of the tank. The resisting moment is due to fluid pressure causes the unique crescent shape of the uplifted portion of the base plate of the tank. MARC was used in the analysis.

Seismic design of complex projects often involves application of both general purpose and special purpose software. For example, the design of the Staples Center sports arena in Los Angeles⁽¹⁶⁻¹⁷⁾, The Eiffel Tower II in Las Vegas⁽¹⁶⁻¹⁸⁾ and seismic correction of the Royce Hall⁽¹⁶⁻¹⁹⁾ all necessitated application of a variety of software from both groups of computer programs (see Figures 16-27, 16-28, and 16-29).

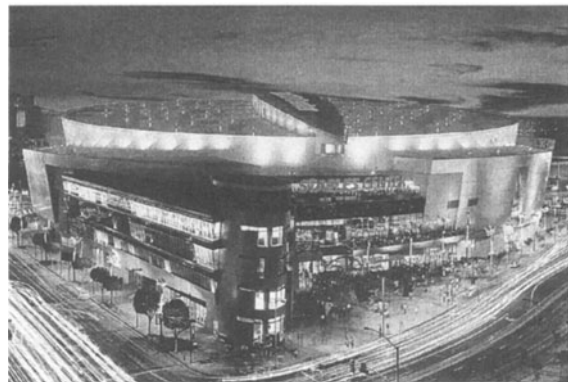


Figure 16-27. The roof truss of the Staples Center was analyzed using the RISA-3D computer program. Shear walls were analyzed using SAP-2000. Special software was developed to pass information from various programs to each other.

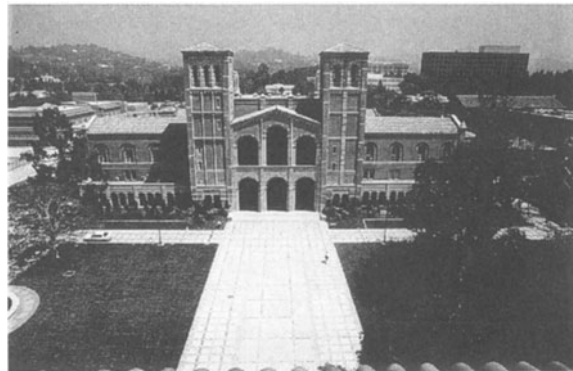


Figure 16-28. Royce Hall seismic rehabilitation design utilized SAP-90 computer program in conjunction with BIAx and other nonlinear analysis software. Specialty software was developed for cross-platforms communications.

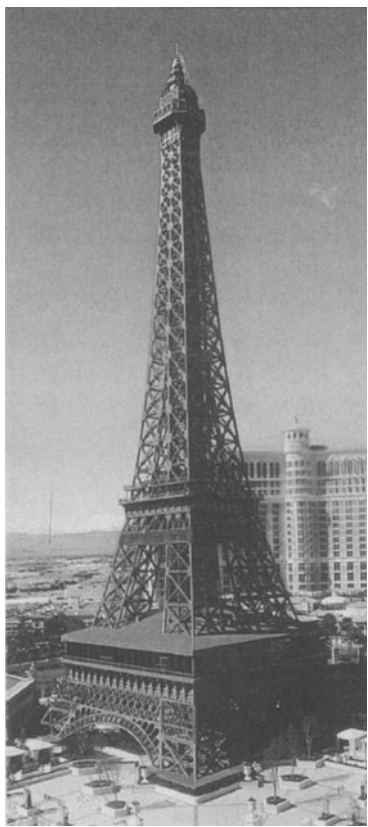


Figure 16-29. Eiffel Tower II in Las Vegas was analyzed and designed using SAP-2000. Nonlinear buckling analyses for temperature effects and fire scenarios were conducted using the ROBOT software system

Commonly used general-purpose analysis software include SAP-2000⁽¹⁶⁻²⁰⁾, ADINA⁽¹⁶⁻²¹⁾, NASTRAN⁽¹⁶⁻²²⁾, ALGOR⁽¹⁶⁻²³⁾, ABAQUS⁽¹⁶⁻²⁴⁾, COSMOS/M⁽¹⁶⁻²⁵⁾, ANSYS⁽¹⁶⁻²⁶⁾ and MARC⁽¹⁶⁻¹⁶⁾. The features and capabilities of these systems are so rapidly changing that a comparative discussion of their feature in a textbook like this could be counterproductive.

In addition to the above-named proprietary software systems, there are a variety of programs available in the public domain. These are generally programs motivated by academic research and are made available by various universities and research institutions. NONSAP⁽¹⁶⁻²⁷⁾ and ANSR⁽¹⁶⁻²⁸⁾ are examples of public domain general purpose computer programs.

Special-purpose programs, developed for analysis and design of building structures, are

often used in seismic analysis and design of buildings. They are generally faster and provide information that could be more readily applied to design purposes. Perhaps the most popular building seismic analysis software is ETABS⁽¹⁶⁻²⁹⁾. Currently a commercial software developed and maintained by Computers and Structures, Inc. of Berkeley, California, ETABS has its roots in public-domain versions of TABS, TABS-80 and ETABS developed at the University of California at Berkeley, during the 1970s. The current commercial version of the program, however, is a very powerful and user-friendly program and has little in common with its old university developed predecessors.

A handful of public-domain programs are used extensively in nonlinear seismic analysis of structures. Perhaps the most widely used among this class of programs is DRAIN-2DX⁽¹⁶⁻³⁰⁾ which is widely used in both professional and research applications (Figure 16-30).

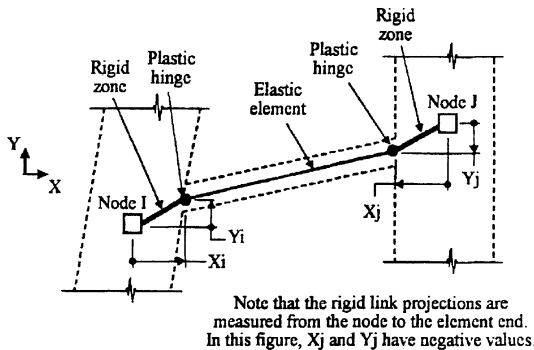


Figure 16-30. A DRAIN-2D nonlinear beam element

The success of DRAIN-2DX has resulted in the development of an entire family of DRAIN programs such as DRAIN-3DX⁽¹⁶⁻³¹⁾, and DRAIN-BUILDING⁽¹⁶⁻³²⁾. Various hysteretic models are implemented in the DRAIN family of programs (Figure 16-31) where the slope of the unloading branch is based on the previous maximum plastic hinge rotation. All plastic deformation effects including the effects of degrading stiffness can now be modeled.

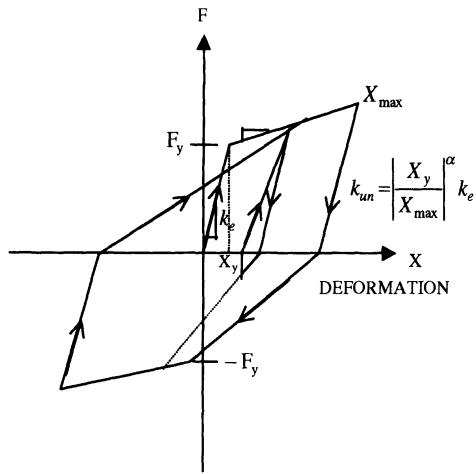


Figure 16-31. Modified Takeda Model⁽¹⁶⁻³³⁾ is one of the hysteretic behavior models implemented in the DRAIN and IDARC family of programs

A very promising development recently incorporated in the DRAIN family of programs is the incorporation of fiber elements (Figure 16-32) that allow modeling of various behavior states occurring at the same cross section of a beam or column element.

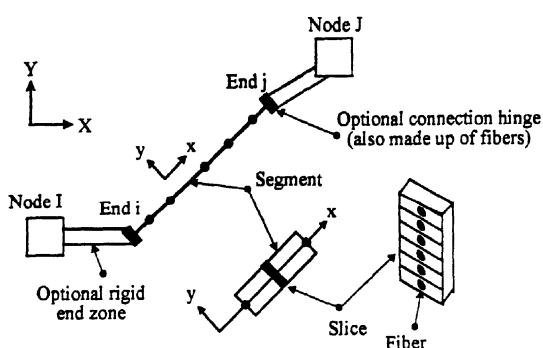


Figure 16-32. A typical beam modeled by fiber elements

IDARC is another family of very powerful public-domain computer programs developed and maintained at the University of Buffalo. The original IDARC⁽¹⁶⁻³⁴⁾ was developed for damage analysis of reinforced concrete structures. The IDARC family of programs^(16-35) to 6-37), however, can now be used for nonlinear analysis of steel structures as well⁽¹⁶⁻³⁹⁾.

A major difference between IDARC and DRAIN families of programs, is in the

construction of the inelastic element stiffness matrices. DRAIN programs use a concentrated plasticity model where the inelastic deformation is concentrated at the locations of plastic joints. The individual member stiffness matrix in IDARC is constructed based on a flexibility approach. This permits modeling of plasticity distributed along the length of the member. Concentrated plasticity models are generally better for modeling steel structures while distributed plasticity models (Figure 16-33) more accurately represent the response of reinforced concrete members (Figure 16-34).

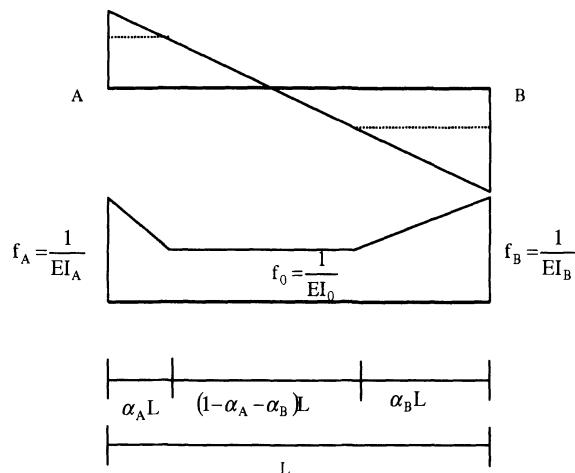


Figure 16-33. A distributed plasticity/flexibility model

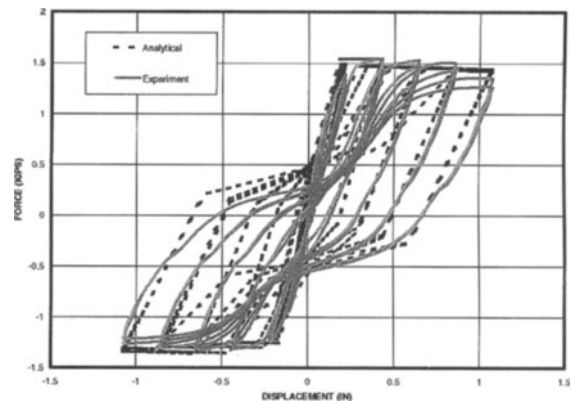


Figure 16-34. Analytical (using the distributed flexibility model) and experimental results compared for cyclic tests on a cantilever concrete column

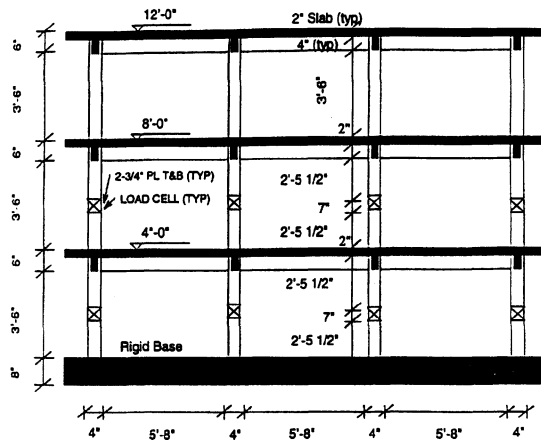


Figure 16-35. Model of a three-story building

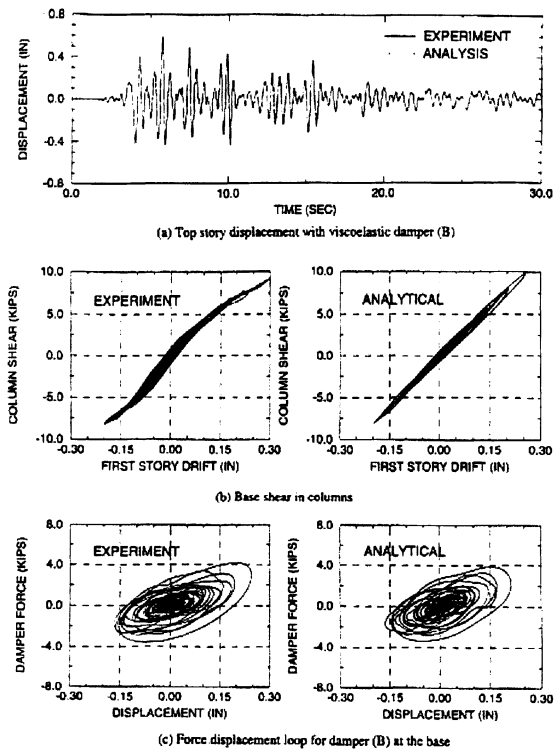


Figure 16-36. Comparison of Analytical Responses with Experiment for model shown in Fig. 16-33⁽¹⁶⁻³⁸⁾.

The correlation among the analytical predictions and observed performance has been continuously improving. For example, Figure 16-35 shows the model of a three story building tested at the University at Buffalo. Diagonal brace dampers were added between floors as a retrofit alternative. As indicated by Figure 16-

36 the analytical and experimental results are in good agreement. Blind predictions of actual seismic response by analytical means, however, have not generally been as successful.

16.9 CONCLUSION

Computers are inseparable from contemporary seismic design. While advances in computer technology have broadened the range of problems that can be handled by earthquake engineers, they have had the unfortunate side-effect of downplaying the importance of sound engineering judgment.

Although vital to current seismic design practice, computer use if not subordinated to design experience and engineering judgment, is nothing but a recipe for disaster.

REFERENCES

- 16-1 Pearce, P. (1980), *Structure in Nature Is a Strategy for Design*, The MIT Press, Massachusetts Institute of Technology, Cambridge, MA.
- 16-2 Naeim, F. (1998), "Internet Frontiers for Earthquake Engineering Design and Education", *Proceedings of the 6th National Conference on Earthquake Engineering*, Earthquake Engineering Research Institute, Seattle, WA.
- 16-3 International Code Council (2000), *International Building Code*, March.
- 16-4 Federal Emergency Management Agency (1997), *NEHRP Guidelines for the Seismic Rehabilitation of Buildings*, FEMA-273, Washington, D.C.
- 16-5 Federal Emergency Management Agency (1997), *NEHRP Commentary on the Guidelines for the Seismic Rehabilitation of Buildings*, FEMA-274, Washington, D.C.
- 16-6 Federal Emergency Management Agency (1999), *HAZUS – FEMA's Tool for Estimating Potential Losses from Natural Disasters*, CD-ROM set, Washington, DC.
- 16-7 Naeim, F., Martin, J.A., Jr., Gong, V., Norton, G., Schindler, B.S., Scambelurri, M. and Rahman, M.A. (1999), "Structural Analysis and Design of the Walt Disney Concert Hall, Los Angeles," *Proceedings of the 1999 SEOAC Annual Convention*, Santa Barbara, CA.
- 16-8 Naeim, F., Patel, K., Tu, K.C., Saiidi, M., Itani, A., and Anderson, J.C. (2000), "A New Rigid Connection for Heavy Beams and Columns in Steel

- Moment Resisting Frames," *Proceedings of the 5th Conference on Tall Buildings in Seismic Regions*, Los Angeles, CA.
- 16-9 Naeim, F. and Anderson, J.C. (1996), *Design Classification of Horizontal and Vertical Earthquake Ground Motion (1933-1994)*, Report No. 7738-96, John A. Martin & Associates, Inc., Los Angeles, CA.
- 16-10 Blake, T.F. (2000), *EQSEARCH: A Computer Program for the Estimation of Peak Acceleration from California Historical Earthquake Catalogs*, Version 3.0, Thomas F. Blake Computer Services and Software, Thousand Oaks, CA. (<http://www.thomasblake.com>)
- 16-11 Blake, T.F. (2000), *EQFAULT: A Computer Program for the Deterministic Estimation of Peak Acceleration using Three-Dimensional California Faults as Earthquake Sources*, Version 3.0, Thomas F. Blake Computer Services and Software, Thousand Oaks, CA.
- 16-12 Blake, T.F. (2000), *FRISKSP: A Computer Program for the Probabilistic Estimation of Peak Acceleration and Uniform Hazard Spectra using Three-Dimensional California Faults as Earthquake Sources*, Version 4.0, Thomas F. Blake Computer Services and Software, Thousand Oaks, CA.
- 16-13 Naeim, F. (1997), *Performance of Instrumented Buildings During the January 17, 1994 Northridge Earthquake -- An Interactive Information System --*, Report No. 97-7530.68, John A. Martin & Associates, Inc., Los Angeles.
- 16-14 Naeim, F. (1991), "Interactive Finite Element Analysis on a Pocket Calculator," *Computers and Structures*, Pergamon Press, Vol. 41, No. 2, Oxford.
- 16-15 Bhatia, H. (1997), *Seismic Analysis and Retrofit of Cylindrical Liquid Storage Tanks*, Ph.D. Dissertation, University of California, Irvine.
- 16-16 MARC Analysis Research Corporation (2000), *The MSC/MARC Software System*, (<http://www.marc.com>)
- 16-17 Martin, J.A., Jr. and Naeim, F. (2000), *Structural analysis and Design of the Staples Center*, ASG-ASCE 6th Annual Symposium, University of Southern California, Los Angeles, January.
- 16-18 Naeim, F. (2000), *Eiffel Tower II: Re-engineering a Landmark*, Invited Lecture, North American Steel Construction Conference, Las Vegas, February.
- 16-19 Naeim, F. (1997), *UCLA Royce Hall: Anatomy of An Award Winning Seismic Correction*, Annual Convention, American Concrete Institute, April.
- 16-20 Computers and Structures, Inc. (2000), *SAP2000 Integrated Finite Element Analysis and Design of Structures*, Berkeley, CA. (<http://www.csiberkeley.com>)
- 16-21 ADINA R&D, Inc. (2000), *The ADINA System*, (<http://www.adina.com>)
- 16-22 MSC Software Corporation (2000), *The MSC/NASTRAN Software System*, (<http://www.mscsoftware.com>).
- 16-23 ALGOR Corporation (2000), *ALGOR Virtual Prototyping Solutions for Mechanical Engineers*, (<http://www.algor.com>).
- 16-24 Hibbitt, Karlsson & Sorensen, Inc. (2000), *The ABACUS Software System*, (<http://www.hks.com>).
- 16-25 Structural Analysis and Research Corporation (2000), *The COSMOS/M Software System*, (<http://www.srac.com>).
- 16-26 ANSYS Inc. (2000), *The ANSYS/Structural Software System*, (<http://www.ansys.com>).
- 16-27 Bathe, K.J., E.L. Wilson and R.H. Iding (1974), *NONSAP - A Structural Analysis Program for Static and Dynamic Response of Nonlinear Systems*, Structural Engineering Lab, Report No. UCB/SESM-74/3, Department of Civil Engineering, University of California, Berkeley, California.
- 16-28 Mondkar, D.P. and Powell, G.H., (1975), *ANSR-I General Purpose Program for Analysis of Nonlinear Structural Response*, EERC report No. 75-37.
- 16-29 Computers and Structures, Inc. (2000), *ETABS Linear & Nonlinear Static & Dynamic Analysis & Design of Building Systems*, (<http://www.csiberkeley.com>)
- 16-30 Prakash, V., Powell, G.H., and Filippou, F.C. (1992), *DRAIN-2DX: Base Program User Guide*, Report NO. UCB/SEMM-92/29 Department of Civil Engineering, University of California, Berkeley.
- 16-31 Prakash, V., Powell G.H., Campbell S.D., and Filippou F.C. (1992), *DRAIN-3DX Preliminary Element User Guide*, Report, Department of Civil Engineering, University of California, Berkeley, CA. December.
- 16-32 Prakash, V., Powell G.H., and Filippou F.C. (1992) *DRAIN-BUILDING Base Program User Guide*, Report No. UCB/SEMM-92/31.
- 16-33 Takeda, T., Sozen, M.A., and Nielsen, N.N., (1970), "Reinforced Concrete Response to Simulated Earthquakes," *Proceedings*, ASCE, Vol. 96, No. ST12.
- 16-34 Park, Y.J., Reinhorn, A.M., and Kunath, S.K., (1987), *IDARC: Inelastic damage analysis of reinforced concrete frame -- shear-wall structures*, Tech. Report NCEER-87-0008, State Univ. of New York at Buffalo, N.Y.
- 16-35 Valles, R.E., Reinhorn, A.M., Kunath, S.K., Li, C., and Madan, A. (1996), *IDARC2D: A Computer Program for the Inelastic Damage Analysis of Buildings*, Tech. Report NCEER-96-0010, State Univ. of New York at Buffalo. (<http://civil.eng.buffalo.edu/idarc2d50/>)

- 16-36 Lobo, R.F., (1994), *Inelastic Dynamic Analysis of Reinforced Concrete Structures in Three Dimensions*, Ph.D. Dissertation. University at Buffalo, NY.
- 16-37 Lobo, R.F. and Naeim, F. (1998), *JAMA-IDARC-3D: A Computer Program for the Three Dimensional Inelastic Analysis of Building Structures*, John A. Martin and Associates, Inc., Los Angeles, CA.
- 16-38 Lobo, R.F., Bracci, J.M., Shen, K.L., Reinhorn, A.M., Soong, T.T., (1993), *Inelastic Response of Reinforced Concrete Structures with Viscoelastic Braces*, Technical Report NCEER-93-0006, National Center for Earthquake Engineering Research, SUNY/Buffalo.
- 16-39 Naeim, F., Skliros, K., Reinhorn, A.M., and Sivaselvan, M.V. (2000), *Effects of Hysteretic Deterioration Characteristics on Seismic Response of Moment Resisting Steel Structures*, A report to the SAC Joint Venture, Report No. 2000/8428, John A. Martin and Associates, Inc., Los Angeles, CA.

Appendix

Conversion Factors

LENGTH

To Convert from	To	Multiply by	To Convert from	To	Multiply by
Inches	feet	0.083333	Meters	millimeters	10
	angstrom units	2.54×10^8		meters	1×10^{-2}
	micrometers	25400		inches	39.370079
	millimeters	25.4		feet	3.2808399
	centimeters	2.54		angstrom units	1×10^{10}
	meters	0.0254		micrometers	1×10^6
Feet	inches	12.0	Yard	millimeters	1×10^3
	angstrom units	3.048×10^9		centimeters	1×10^2
	micrometers	304800		feet	3
	millimeters	304.80		centimeter	91.44
	centimeters	30.48		meter	0.9144
	meters	0.3048		Angstrom units	inches
Millimeters	inches	3.9370079×10^{-2}		feet	3.28084×10^{-10}
	feet	3.2808399×10^{-3}		micrometers	0.0001
	angstrom units	1×10^7		millimeters	1×10^{-7}
	micrometers	1×10^3		centimeters	1×10^{-8}
	centimeters	1×10^{-1}		meters	1×10^{-10}
	meters	1×10^{-3}	Micrometers	inches	3.9370079×10^{-5}
Centimeters	inches	0.39370079		feet	3.2808399×10^{-6}
	feet	0.032808399		angstrom units	1×10^4
	angstrom units	1×10^8		millimeters	1×10^{-3}
	micrometers	1×10^4		centimeters	1×10^{-4}
				meters	1×10^{-6}

* For additional information, see American Society for Testing and Materials, *Metric Practice Guide*, ASTM E 380-72, 34 pp., 1973; International Organization of Standardization "International Stardt, SI Units, and Recommendations for the Use of their Multiples and Certain Other Units, "Ref. No. ISO 1000-1973(E), 21 pp., 1973; National Bureau of Standards, *Engineering Standards, U.S. Metric Study*, NBS SP 345-11, 250 pp., 1971.

AREA

To Convert from	To	Multiply by
Square meters	square feet	10.76387
	square centimeters	1×10^4
	square inches	1550.0031
Square feet	square meters	9.290304×10^{-2}
	square centimeters	929.0304
	square inches	144
Square centimeters	square meters	1×10^{-4}
	square feet	1.076387×10^{-3}
	square inches	0.155
Square inches	square meters	6.4516×10^{-4}
	square feet	6.9444×10^{-3}
	square centimeters	6.4516
Square yard	acres	2.066×10^{-4}
	square feet	0
	square centimeters	8361.273
	square miles	3.228×10^{-7}
Acres	square meters	4046.849
	square feet	43560
	yards	4840

VOLUME

To Convert from	To	Multiply by
Cubic centimeters	cubic meters	1×10^{-6}
	cubic feet	3.5314667×10^{-5}
	cubic inches	0.061023744
Cubic meters	cubic feet	35.314667
	cubic centimeters	1×10^6
	cubic inches	61023.74
Cubic inches	cubic meters	1.6387064×10^{-5}
	cubic feet	5.7870370×10^{-4}
	cubic centimeters	16.387064
Cubic feet	cubic meters	0.028316847
	cubic centimeters	28316.847
	cubic inches	1728
U.S. gallons (gal)	cubic centimeters	3785
	cubic meters	3.785×10^{-3}
	cubic feet	0.133680
	cubic inches	231
	cubic yards	4951×10^{-3}
	British Imperial gallons	0.833
	liters	3.785

FORCE

To Convert from	To	Multiply by
Pounds	dynes	4.44822×10^5
	grams	453.59243
	kilograms	0.45359243
	tons (long)	4.464286×10^{-4}
	tons (short)	5×10^{-4}
	kips	1×10^{-3}
	tons (metric)	4.5359243×10^{-4}
	Kips	
	pounds	1000
Kilograms	tons (short)	0.500
	kilograms	453.59243
	tons (metric)	0.45359243
	dynes	980665
Tons (short)	grams	1000
	pounds	2.2046223
	tons (long)	9.8420653×10^{-4}
	tons (short)	11.023113×10^{-4}
	kips	2.2046223×10^{-3}
	tons (metric)	0.001
	Tons (short)	
	kilograms	907.18474
	pounds	2000
Tons (metric)	kips	2
	tons (metric)	0.907185
	grams	1×10^6
	kilograms	1000
Pound force (lbf)	pounds	2204.6223
	kips	2.2046223
	tons (short)	1.1023112
	newtons	4.45
Kilogram force (kgf)	newtons	9.81
	(kgf)	

VELOCITY

To Convert from	To	Multiply by
Centimeters/sec	microns/second	10,000
	meters/minute	0.600
	feet/minute	1.9685
	miles/hour	0.022369
	feet/year	1034643.6
	Microns/second	
Microns/second	centimeters/second	0.0001
	meters/minute	0.000060
	feet/minute	0.00019685
	miles/hour	0.0000022369
	feet/year	103.46436

To Convert from	To	Multiply by	To Convert from	To	Multiply by
Feet/minute	centimeters/second	0.508001	Months	minutes	1440
	microns/second	5080.01		hours	24
	meters/minute	0.3048		months	3.28767×10^{-2}
	miles/hour	9,91136363		years	0.0027397260
	feet/year	5256000		milliseconds	2.6283×10^9
Feet/year	microns/second	0.009665164		seconds	2.6283×10^6
	centimeters/second	0.0000009665164		minutes	43800
	meters/minute	5.79882×10^{-7}		hours	730
	feet/minute	1.9025×10^{-6}		days	30.416666
	miles/hour	2.16203×10^{-8}		years	0.08333333
Miles/hour	centimeters/second	44.7041	Years	milliseconds	3.1536×10^{10}
	meters/minute	26.82		seconds	3.1536×10^7
	feet/hour	52.80		minutes	525600
	feet/minute	88		hours (mean solar)	8760
	feet/second	1.467		days (mean solar)	365
	miles/second	2.778×10^{-4}		months	12

TIME

To Convert from	To	Multiply by
Milliseconds	seconds	10^3
	minutes	1.66666×10^{-5}
	hours	2.777777×10^{-7}
	days	1.1574074×10^{-8}
	months	3.8057×10^{-10}
	years	3.171416×10^{-11}
Seconds	milliseconds	1000
	minutes	1.66666×10^{-2}
	hours	2.777777×10^{-4}
	days	1.1574074×10^{-5}
	months	3.8057×10^{-7}
	years	3.171416×10^{-8}
Minutes	milliseconds	60000
	seconds	60
	hours	0.0166666
	days	6.944444×10^{-4}
	months	2.283104×10^{-5}
	years	1.902586×10^{-6}
Hours	milliseconds	3600000
	seconds	3600
	minutes	60
	days	0.0416666
	months	1.369860×10^{-3}
	years	1.14155×10^{-4}
Days	milliseconds	86400000
	seconds	86400

STRESS

To Convert from	To	Multiply by
Pounds/square inch	pound/square foot	144
	feet of water	2.3066
	kips/square foot	0.144
	kilograms/square centimeter	0.070307
	tons/square meter	0.70307
	atmospheres	0.068046
Pounds/square foot	kilopascals	6.9
	pounds/square inch	0.0069445
	feet of water	0.016018
	kips/square foot	1×10^{-3}
	kilograms/square centimeter	0.000488243
	tons/square meter	0.004882
Feet of water (at 39.2 °F)	atmospheres	4.72541×10^{-4}
	pascals	47.9
	pounds/square inch	0.43352
	pounds/square foot	62.427
	kilograms/square centimeter	0.0304791
Inches of Hg	tons/square meter	0.304791
	atmospheres	0.029499
	inches of Hg	0.88265

To Convert from	To	Multiply by	To Convert from	To	Multiply by
Kips/square foot	pounds/square inch	6.94445	Newton's/square meter	pounds/square inch	14.696
	pounds/square foot	1000		tons(short)/square foot	1.0581
	tons(short)/square foot	0.5000		pascals	1.00
	kilograms/square centimeter	0.488244			
	tons(metric)/square meter	4.88244			
	Kilograms/square centimeter	14.223			
	pounds/square foot	2048.1614			
	feet of water (39.2 °F)	32.8093			
	kips/square foot	2.0481614			
	tons/square meter	10			
Tons (short)/square foot	atmospheres	0.96784	Pounds/cubic meter	pounds/cubic inch	0.036127292
	atmospheres	0.945082		pounds/cubic foot	62.427961
	kilograms/square centimeter	9764.86		grams/cubic centimeter	0.001
	tons(metric)/square meter	9.76487		tons(metric)/cubic meter	0.001
	pounds/square inch	13.8888		pounds/cubic inch	3.6127292 × 10 ⁻⁵
Tons (metric)/square meter	pounds/square foot	2000		pounds/cubic foot	0.062427961
	kips/square foot	2.0		grams/cubic centimeter	27.679905
	kilograms/square centimeter	0.10		tons (metric)/cubic meter	27.679905
	pounds/square foot	204.81614		kilograms /cubic meter	27679.905
	kips/square foot	0.20481614		pounds/cubic foot	1728
Atmospheres	tons (short)/square foot	0.102408	Pounds/cubic foot	grams/cubic centimeter	0.016018463
	feet of water at 39.2 °F	33.899		tons(metric)/cubic meter	0.016018463
	kilograms/square centimeter	1.03323		kilograms/cubic meter	16.018463
	grams/square centimeter	1033.23		pounds/cubic inch	5.78703704 × 10 ⁻⁴
	kilograms/square meter	10332.3		grams/cubic centimeter	1.00
tons (metric) /square meter	tons (metric) /square meter	10.3323		kilograms/cubic meter	1000.00
	pounds/square foot	2116.22		pounds/cubic inch	0.03612772
				pounds/cubic foot	62.427961

UNIT WEIGHT

COEFFICIENT OF CONSOLIDATION, C_v

To Convert from	To	Multiply by
Square centimeters/second	square centimeters/year	3.1536×10^7
	square meters/year	3.1536×10^3
	square inches/second	0.155
	square inches/year	4.8881×10^6
	square feet/ year	3.39447×10^4
Square inches/second	square inches/year	3.15368×10^7
	square feet/year	2.1900×10^5
	square centimeters/second	6.4516
	square centimeters/year	2.0346×10^8
	square meters/year	2.0346×10^4

COEFFICIENT OF THERMAL CONDUCTIVITY, k

To Convert from	To	Multiply by
Btu/hr-ft ² -(°F/ft)	cal/sec-cm ² -(°C/cm)	4.134×10^{-3}
W/cm ² -(°C/cm)	Btu/hr-ft ² -(°F/ft)	57.780
W/cm ² -(°C/cm)	cal/sec-cm ² -(°C/cm)	0.239

TEMPERATURE

$$T(^{\circ}C) = \frac{5}{9}[T(^{\circ}F) - 32]$$

$$T(^{\circ}F) = \frac{9}{5}T(^{\circ}C) + 32$$

$$T(K) = T(^{\circ}C) + 273.18$$

Index

- ABAQUS program, 809
Accelerograms, 50–51, 54, 117
ACI, *see* American Concrete Institute
Active seismic earth pressures, 178–180
ADINA program, 809
Adjacency problems, 315–319, 736
Aftershocks, 6
Agadir, Morocco earthquake, 312
Air distribution systems, 718
AISC, *see* American Institute of Steel Construction
ALGOR program, 809
Allowable Stress Design (ASD), 565
Alquist-Priolo Earthquake Fault Zoning Act, 178
American Concrete Institute (ACI), 503–528
on beam-column connections, 486–487
on beams, 480–481
on columns, 482, 483–484, 547
on confinement reinforcement, 474, 524, 550
on ductility, 506–528
on floor diaphragms, 384
on frame-shear wall systems, 531, 532, 543
on lap splices, 549
on load combinations, 504–506
on load factors, 504–506
on shear strength, 551
on slab-column connections, 488
on strength reduction factors, 504–506
on structural walls, 496, 553, 556, 557
American Institute of Steel Construction (AISC), 411, 412, 413, 445, 454–455
on concentrically braced frames, 426, 427, 431, 433, 435, 436
on eccentrically braced frames, 440, 441, 442, 443, 444, 456
on moment-resisting frames, 415, 416, 417, 422, 423, 424
American Society of Civil Engineers (ASCE)
on floor diaphragms, 382–384
on masonry buildings, 565, 567, 571
on reinforced concrete structures, 503–528, 536
Anatolian fault, 5
Anchorage, Alaska earthquake, 9, 24, 156, 170, 171, 172f, 280, 296, 318, 380–381, 465, 488, 685
Anchorage Westward Hotel, 318
ANSYS program, 809
Appendages, exterior, 705
Applied Technology Council (ATC)
on deformations, 628–629
on performance-based seismic engineering, 759, 760, 763–777
Approximate buckling analysis, 336–337
Approximate P-Delta analysis, 340–344
modified version of, 345–346
Architect/engineer relationship, 319–320
Architectural considerations, 275–325
adjacency problems, 315–319
architect/engineer relationship, 319–320
configuration, 277–282
general building characteristics, 289–294
methods of analysis, 282–289
structurally restrictive detailing, 313–315
Architectural finishes, 704–705
Architectural integrity, 330
Architectural nonstructural components, 687t, 697t, 703–713
Area (conversion factors), 816
Armenian earthquake, 290
Arvin High School Administrative Building, 378, 379f
ASCE, *see* American Society of Civil Engineers
ATC, *see* Applied Technology Council
Attenuation, 63–69
Axial force, 440–441
Axial load, 512–517, 554–555, 613
Axial strength, 611, 613
Bachman blind thrust fault, 139
Base shear, 217, 228, 250, 254–255, 258, 265
Basic Safety Earthquake 1 (BSE-1), 85, 777–778
Basic Safety Earthquake 2 (BSE-2), 85, 777–778
Basic Safety Objective (BSO), 777, 788
Beam outside of link, 443, 457
Beams, *see also* Strong column-weak beam criterion;
Weak column-strong beam problem
of concentrically braced frames, 435
coupling, 522
failure of, 654
reduced sections, 418–421
of reinforced concrete structures, 478–481, 508–512, 540–546
shear failure of, 637–638
of special concentrically braced frames, 455
of steel moment-resisting frames, 416
Beam-to-column connections
in eccentrically braced frames, 443
in reinforced concrete structures, 484–488, 518–519, 550–552
in special moment frames, 449–450
in steel moment-resisting frames, 416–421
Bearing capacity loss, 156, 158
Bearings, 746, *see also* Elastomeric bearings; Lead-rubber bearings
Becker Penetration Test (BPT), 154
Behavior states, 569–570
Bent action, 349–351, 356–357

- Blind thrust faults, 16, 139
 Body wave magnitude, 28, 29
 Boundary nonlinearities, 806–807
 Bow action, 378
 Braced frames, 360–361, 362t, 363f
 Braced steel frame structures, 639–640, 653
 Bridge building form, 322–323
 Brittle structural systems, 636, 650–654
 Buckling, 427, 432, 433, 435, 436
 Building contents, 712–713
 Building Performance Level, 763
 Building period, 251, 266–267
 Building proportion, 290–291
 Building symmetry, 291–292
- Calaveras fault, 79
 Canadian Concrete Code of Practice, 483, 499
 Cantilever displacements, 351–353
 Cantilever walls, 471–472
 Capacity design, 482, 498
 Capacity estimates, 466
 Capacity Spectrum Method, 765, 769–772, 773–777
 Caracas, Venezuela earthquake, 128, 488
 Ceiling systems, 710–712
 Center of rigidity, 369
 Chartres Cathedral, 293
 Chemical stabilization of soil, 165
 Chi-Chi, Taiwan earthquake, 4, 24f, 33, 43, 44, 147, 176, 177f
 Chilean earthquake, 9, 24, 29, 43, 307
 Chord action, 352, 356, 357, 361
 Chord capacity, 655, 657, 659
 Cladding systems, 641, 661
 Clay soils, 154–155
 Clerestory, 634, 645
 Code instrumentation, 804
 Coefficient of consolidation (conversion factors), 819
 Coefficient of thermal conductivity (conversion factors), 819
 Collapse earthquakes, 10
 Collapse Prevention Level, 777
 Collectors, 664, 668
 Columns, 307–309, *see also* Beam-to-column connections; Link-to-column connections; Panel zones; Slab-column connections; Strong column-weak beam criterion; Weak column-strong beam problem
 of concentrically braced frames, 435
 of eccentrically braced frames, 443–444, 458–459
 failure of, 654
 of reinforced concrete structures, 481–484, 517, 547–550
 shear failure of, 637–638
 of special concentrically braced frames, 454–455
 of steel moment-resisting frames, 424–425
 Compaction grouting, 163
 Compaction piling, 162
 Complete quadratic combination (CQC), 116, 229, 230, 784
 Compression wall, 499
 Computer applications, 793–811
 earthquake records, 799
- EERI/IAEE housing encyclopedia project, 804
 instrumented building response analysis, 804–805
 loss estimation, 802–804
 scenario analysis, 802–804
 seismic activity monitoring, 799–800
 seismic hazard analysis, 800–802
 seismic isolation, 727
 structural analysis and design, 806–811
 Concentrically braced frames (CBFs), 425–436, *see also*
 Ordinary concentrically braced frames; Special concentrically braced frames
 Concrete diaphragms, 657–659
 Concrete masonry unit (CMU) slender walls, 595–609
 Concrete masonry unit (CMU) walls, 582–595
 Concrete slabs, 441
 Cone penetration test (CPT), 152–153, 154
 Configuration, 277–282, *see also* Irregular configurations
 Confinement reinforcement, 474–475, 524, 548, 550, 552, 555–556, 638–639
 Connections
 for CMU walls, 585–588
 for concentrically braced frames, 433–435
 for seismic isolators, 744–746
 for special concentrically braced frames, 454
 for steel-moment resisting frames, 417–418
 weak, 653
 Construction quality, 641–642
 Continent-to-continent collisions, 7
 Continuity ties, 667–668
 Control node, 784
 Conversion factors, 815–819
 COSMOS/M program, 809
 Coupled walls, 498–500
 Coupling beams, 522
 Cracking moment strength, 606, 616
 Crescent City earthquake, 24
 Cross-wall overturning, 672–677
 Cube network, 796
 Curtain wall systems, 709–710
- Dallas City Hall, 312f
 Damage Control Performance Level, 764
 Damped single-degree-of-freedom (SDOF) systems, 193–195
 Dashte-e-Bayaz, Iran, earthquake, 8
 Dead load distribution, 670
 De-amplification factors, 109–110
 Deconstructed building form, 323
 Deep-focus earthquakes, 6
 Deep soil mixing, 165
 Deflection, 578–581, 606–607
 Deflection amplification factor, 411–412
 Deflection compatibility, 578–581
 Deflection limitations, 601
 Deformations, 627–631, 635, 648–650, 696–697, 779
 elemental, 627–628
 global, 627
 inter-structural, 627, 628
 link, 437–438
 Demand
 estimates of, 465–466
 vs. capacity of diaphragm, 670–671

- Design Basis Earthquake (DBE), 738, 739, 740, 741, 743
Design earthquakes, 36
Design forces, 741–742
Design level event (DBE), 643
Design spectra, 98–106
Design spectral response accelerations, 265
Design strength, 601, 611, 614–618
Diagonal brace, of EBFs, 442, 457–458
Diaphragms, 664, 666, 779–780
 concrete, 657–659
 configuration of, 302–303
 demand vs. capacity of, 670–671
 flexible, 376–377, 574, 575–582, 590–591
 floor, *see* Floor diaphragms
 horizontal, 573, 574–575
 inadequate, 640, 654–660
 plywood, 574, 575–582
 poor connectivity of, 640–641
 rigid, 376–377, 574, 590–591
 roof, 670–672
 semi-rigid, 376–377
 steel deck, 659–660
 sub, 581–582, 588–590
 timber, 654–657
 vertical, 591
Differential compaction, 167–169
Dilatancy theory of earthquakes, 8–9
Dip-slip faults, 16, 24, 31
Directivity, 75–76
Direct P-Delta method, 342–344, 356
Disney Concert Hall, 798f
Displacement, 606–609
 expected maximum, 772
 lateral, *see* Lateral displacement
 minimum, 739–741
 shear leak, 353–354, 356, 357
 spectral, 202, 217, 739
Displacement attenuation, 69
Displacement Coefficient Method, 784, 785
Displacement ductility, 111, 471
Displacement ductility ratio, 197
Displacement functions, 211–213
Distance from source of energy, 63–71, 96
Drainage, 166
DRAIN family of programs, 809–810
Drift, 327–370
 in braced frames, 360–361, 362t, 363f
 choice of member stiffness for, 348–349
 defined, 329
 in frame-shear wall systems, 364f, 365f, 366f, 367–368, 536
 in linear static force procedures, 256–257, 268–269
 in moment frames and framed tubes, 349–360
 pounding and, 316
 second-order analysis techniques for, 334
 seismic code requirements for, 369–370
 seismic isolation and, 742
 seismic upgrading and, 643
 in steel structures, 412
 in timber diaphragms, 655–656
 torsional effects and, 368–369
 in wood buildings, 567–568
Drift index, 329
Ductility, 468–472, 474–477, 530
 code provisions, 506–528
 displacement, 111, 471
 sectional, 475–477
 yield level vs., 468–470
Ductility ratio, 470
Dynamic amplification, 197
Dynamic analysis, 173–174, 271, 739, 741
Dynamic compaction, 163–164
Dynamic equilibrium, 185–186
Dynamic lateral force procedure, 258
Dynamic loading, 195–210
Dynamic response, 183–245
 of elastic structures, 201–205, 216–219
 generalized coordinate approach, 210–219
 of MDOF systems, 222–231
 of nonlinear MDOF systems, 231–242
 of nonlinear SDOF systems, 219–222
 of SDOF systems, 186–195
 verification of, 243–245
Dynamic tests, 473
Earthquake ground motion, 1–44, 47–87, 188–189, 783,
 see also Design spectra; Earthquakes; Response spectra
 artificially generated, 39–41, 116–117
 characteristics of, 51–61
 estimating, 86–87
 factors influencing, 61–76
 IBC guidelines for determining, 145–146
 prediction of, 37–43
 recorded, 49–51
 seismic risk evaluation, 35–37, 76–86
 seismic waves in, 17–21
 world distribution of, 4–6
Earthquake records, 799
Earthquakes
 causes of, 6–10
 collapse, 10
 damage mechanisms of, 21–24
 deep-focus, 6
 intermediate-focus, 6
 intraplate, 7–8
 plate-edge, 7
 prediction of, 37–43
 quantification of, 26–30
 reservoir-induced, 10
 shallow-focus, 6, 13
 tectonic, 6–8
Earthquake source models, 30–35
Earthquake-type loading, 472–500
 pseudo-dynamic tests, 473
 rate of, 474
 sequence of large-amplitude, 496
 slowly reversed cyclic (quasistatic), 472–473, 493
 static monotonic, 472, 493
Eccentrically braced frames (EBFs), 436–444, 445
Economical containers, 278
Effective isolated system periods, 740–741
Effective length factor method, 334–335
Effective peak ground acceleration (EPA), 130–131

- Eiffel Tower II, 808, 809f
 El Asnam, Algeria earthquake, 308
 Elastic analysis, 235
 Elastic design response spectra, 130–135, 206–210
 Elastic stiffness, of ECBs, 437
 Elastic structures, 201–205, 216–219
 Elastomeric bearings, 727, 729, 736, 737, 744, 748–749
 Electrical systems/components, 641, 688t, 698t, 718–720
 Elemental deformations, 627–628
 Elevators, 712, 718
 El Faro building, 299
 Empirical Green's functions, 41–42
 Energy content of earthquakes, 112–116
 Energy dissipation, 727, 729, 730–733
 Epicenter of earthquake, 6
 EQFAULT program, 800, 801f
 EQSEARCH program, 800, 801f
 Equations of motion, 219–220, 225–227
 Equivalent lateral force (ELF) method, 282–283, 285, 287, 288, 313
 Erzincan, Turkey earthquake, 5
 ETABS program, 224–225, 235, 237f, 238f, 243, 532, 809
 Exact P-Delta analysis, 346–348
 Excavation of liquefiable soils, 162
 Exitways, 712
 Expansion joints, 634–635, 645–648
 Expected maximum displacement, 772
 Explosions, 9
 Extensive instrumentation, 804
 Factored moments, 607–609
 Far-field effects, 20, 63, 66
 Fault gouge, 16
 Fault ruptures, 32, 176–178
 Faults
 Anatolian, 5
 Bachman blind thrust, 139
 blind thrust, 16, 139
 Calaveras, 79
 dip-slip, 16, 24, 31
 Hayward, 16, 79
 Newport-Inglewood, 138
 normal, 16
 oblique, 16
 reverse, 16, 75
 reverse-slip, 94, 96–97
 San Andreas, 11, 13, 16, 21, 30, 37, 76, 79, 138
 source characteristics, 75, 96–97
 sources of, 11–16
 strike-slip, 15, 24, 31, 75, 94, 96–97, 176
 thrust, 16, 176
 transform, 7
 FEMA-273, 85–86, 106
 on nonstructural systems and components, 690, 702, 713
 on performance-based seismic engineering, 759, 763, 777–791
 on seismic isolation, 738
 on seismic upgrading, 625, 642
 FEMA-274
 on nonstructural systems and components, 689, 713
 on performance-based seismic engineering, 759, 763, 777–791
 on seismic isolation, 738
 on seismic upgrading, 625, 642
 FEMA-302, 247, 692, 697t
 FEMA-303, 247, 694
 Flat sliding isolation systems, 733–734
 Flexibility, excessive, 636, 650
 Flexible diaphragms, 376–377, 574, 575–582, 590–591
 Flexural cantilevers, 337–338
 Flexural capacity, 640, 659
 Flexural members, 508–512, 540–546
 Flexural reinforcement splices, 545–546
 Fling, 41
 Floods, 171
 Floor diaphragms, 373–406
 classification of behavior, 376–377
 code provisions, 382–384
 design examples, 384–406
 determination of rigidity, 377–378
 factors affecting behavior, 378
 Flow failures, 156
 Focus of earthquake, 6, 31
 Force (conversion factors), 816
 Force-controlled elements, 779
 Force deflection, 733–734
 Foreshocks, 6
 Foundation anchorage, lack of, 648
 Foundation modeling assumptions, 779
 Fourier amplitude spectrum, 54, 55–57
 Framed tubes, 349–360
 Frame-shear wall systems
 design examples, 528–558
 drift design of, 364f, 365f, 366f, 367–368, 536
 Free-face conditions, 159, 160–161
 Free vibration, 191–195
 Frequency content of ground motion, 54–61
 Frequency paper, 202
 Friction pendulum systems (FPS), 731, 747–748, 749–750, 752–753
 FRISKSP program, 802
 Garage, house over, 634
 Generalized coordinate approach, 210–219
 Generalized properties/parameters, 211–214
 General-purpose analysis programs, 807–809
 Geology, 35–36, 71–74, 92–95
 Geometric nonlinearities, 806
 Geometric stiffness matrix, 346–348
 Geotechnical design, 125–181
 differential compaction and, 167–169
 fault rupture and, 176–178
 flooding and, 171
 landslides and, 169–170
 lateral seismic earth pressures and, 178–180
 lurching and, 171
 performance-based seismic engineering and, 766
 seiches and, 173
 seismic settlement and, 167–169
 site effects and, 127, 128–146
 soil liquefaction and, 146–166
 soil-structure interaction and, 173–176
 subsidence and, 167–169
 tsunamis and, 171–173

- Global deformations, 627
Grand Arch of the Defense, 322
Grant Hotel, 318
Great pyramid of Gizeh, 281
Ground motion, *see* Earthquake ground motion
Guam earthquake, 308–309
Guggenheim Museum, 323, 324f
Gutenberg-Richter relationship, 76, 77
- Haicheng, China earthquake, 37
Hardening isolation systems, 733
Harmonic loading, 195–196
Harzards Reduced Performance Level, 686
Hayward fault, 16, 79
HAZUS-99 software system, 796, 797f, 802–804
High-damping rubber (HDR) isolators, 747–748, 750–751
Hilo, Hawaii earthquake, 24, 25f
Hong Kong and Shanghai Bank, 321
Horizontal diaphragms, 573, 574–575, *see also* Flexible diaphragms
Horizontal reinforcement, 524
Human comfort, 330
Hydraulic damping, 731
Hysteretic energy dissipation, 427–430, 730–733
- IBC, *see* International Building Code
IDARC family of programs, 810
Immediate Occupancy Performance Level, 686, 690, 713, 764
Imperial County Services Building, 305, 306f, 315
Imperial Hotel, 290
Imperial Valley earthquake, 33, 49, 50, 51, 53f, 56, 57, 65, 71, 107f, 108, 117
 architectural characteristics and, 305
 response spectra in, 89f, 90f, 91, 204f
 soil liquefaction and, 154
Impulse base acceleration, 198–199
Impulse loading, 195, 196–198, 200
Incoherency of ground motion, 41
Inelastic component behavior, 765–766
Inelastic response spectra, 106–112
Inertial effects, 465
In-situ densification, 162–164
Instrumented building response analysis, 804–805
Intensity of earthquake, 26–29
Interaction diagram, 595–596, 614–616
Inter-element deformations, 635, 648–650
Intermediate-focus earthquakes, 6
Intermediate moment frames (IMFs), 415
Intermediate strength panel zones, 423
International Building Code 2000 (IBC-2000)
 on deformations, 628
 on drift and P-Delta, 369–370
 on floor diaphragms, 382–384
 on linear static force procedures, 262–273
 on reinforced concrete structures, 482, 501, 503–528, 531, 532, 536, 538, 539, 548, 557–558
 on seismic isolation, 737–738, 740, 741, 742, 743
 seismic requirements, 140–146
International Style, 279–280, 321–322
Interstory drift index (IDI), 234, 242
Inter-structural deformations, 627, 628
- Intraplate earthquakes, 7–8
Inverted setbacks, 311
Irregular configurations, 247, 257–258, 270, 281
 codes and analysis methods, 283–289
 seismic significance of, 294–319
Iterative P-Delta method, 340–342
- J.C. Penney Department Store, 299
Jet grouting, 165
Joint shear failure, 638
- Kanto, Japan earthquake, 290, 296
Kern County earthquake, 378
Kobe, Japan earthquake, 33, 76, 130–131, 312, 316, 318, 320
Kocaeli, Turkey earthquake, 147
- Landers earthquake, 13, 14f, 42, 71, 176
Landslides, 169–170
Lap splices, 509, 511, 513, 524, 545, 549–550, 556–557
Lateral bracing, of ECBs, 458
Lateral displacement, 159–161, 356, 357, 360, 361, 367, 535–536, 537t
Lateral flexibility, excessive, 636
Lateral force resisting systems, incomplete, 632–634, 644–648
Lateral forces
 distribution of, 254–255
 plywood shear walls and, 594–595
 reinforced concrete structures and, 501–502, 531, 533t, 534t
 wood and masonry buildings and, 572–574
Lateral load patterns, 784–785
Lateral-load-resisting elements, 528–530
Lateral seismic earth pressures, 178–180
Lateral spread displacement, 160–161
Lateral spreading, 156, 157f
Lateral stability, 329, 330–334
Lead-rubber bearings (LRB), 731, 732, 749, 751–752
Length (conversion factors), 815
Life Safety Performance Level, 686, 690, 713, 764, 777–778, 790–791
Limited Safety Performance Level, 764
Limit states
 for CMU slender walls, 599–604
 for masonry buildings, 569–572
 for shear walls, 609–612
 for wood buildings, 565–568
Linear Dynamic Procedure (LDP), 778, 783–784
Linear isolation systems, 733
Linear Static Procedure (LSP), 778, 781–783
Linear static seismic lateral force procedures, 247–273
 IBC-2000 on, 262–273
 UBC-97 on, 250–262
Link behavior, 439–442
Link deformation, 437–438
Link design, 456–457
Link rotation, 458
Link stiffeners, 458
Link strength, 438–439
Link-to-column connections, 443
Lloyds building, 321

- Load and Resistance Factor Design (LRFD)
 for CMU slender walls, 595
 for masonry buildings, 568–572
 for wood buildings, 565–568
- Load combinations, 504–506, 536–540, 780–781
- Load factors, 504–506
- Loma Prieta earthquake, 4, 21, 39f, 41, 42, 43, 67, 72, 87, 96, 97f, 104, 243
 architectural characteristics and, 319
 soil liquefaction in, 156, 157f, 158, 162, 166
- Long Beach earthquake, 685
- Los Angeles City Hall, 735, 737
- Los Angeles Rapid Transport District Headquarters, 323, 324f
- Loss estimation, 802–804
- Love waves, 18
- Low damping rubber (LDR) isolators, 747–748
- LRFD, *see* Load and Resistance Factor Design
- Lurching, 171
- Magnitude of earthquake, 27–30, 74, 95
- Magnitude saturation, 28–29
- Managua, Nicaragua earthquake, 22f, 23, 318
- MARC program, 807f, 808f, 809
- Masonry buildings, 563–619
 with CMU slender walls, 595–609
 with CMU walls, 582–595
 lateral forces in, 572–574
 limit states for, 569–572
 LRFD for, 568–572
 with shear walls, 609–619
- Masonry veneers, 661
- Mass properties, 189–191, 222–223
- Material nonlinearities, 806
- Maximum Considered Earthquake (MCE), 140, 145–146, 262, 738, 739, 740, 743, 778
- Maximum considered earthquake response spectral acceleration, 141–142, 143f, 144f
- Maximum credible event (MCE), 643
- Maximum reinforcement check, 606
- Mechanical systems/components, 641, 688t, 698t, 713–718
- Messina, Italy earthquake, 5
- Mexico City earthquakes, 43, 72, 103, 128, 196, 290, 292, 296, 301, 316, 318–319, 736
- MGM Grand Hotel, 297
- Mine burst, 10
- Minimum strength panel zones, 423
- Miyagi-ken-oki, Japan earthquake, 308, 309f
- Modulus of elasticity, 601
- Modulus of rupture, 601
- Moment-area method, 352, 353, 361
- Moment magnitude, 28, 29
- Moment of inertia, 606
- Moment resistant frames, 349–360, *see also* Steel moment-resisting frames
- Monadnock Building, 293
- Mononobe-Okabe formulation, 179, 180
- Moving window Fourier amplitude spectra (MWFAS), 244–245
- Multiple-degree-of-freedom (MDOF) systems, 222–242
 mass and stiffness properties, 222–223
 mode shapes and frequencies, 223–225
- nonlinear response, 231–242
- NASTRAN program, 809
- National Earthquake Hazard Reduction Program (NEHRP), 85, 140, 247
 on irregular structures, 285, 286f
 on nonstructural systems, 692, 696–699, 700–701, 702, 703, 715
 on regular buildings, 283
 on seismic isolation, 738
 on steel structures, 411–413, 415, 445
- Near-source effects, 20, 63, 130–135, 254, 255t
 description of, 70–71
 examples, 138–139
- Negative bracing member method, 344–345
- Negative moment reinforcement, 541
- Negative-reinforcement cut-off points, 544–545
- NEHRP, *see* National Earthquake Harzard Reduction Program
- Neopolitan, Italy earthquake, 3
- Newhall Fire Station, 198
- New Madrid earthquakes, 167
- Newmark-Hall design spectrum, 207, 208f, 209
- Newport-Inglewood fault, 138
- New Zealand Code, 481, 482, 483, 490, 498, 568, 613, 731, 737
- Niigata, Japan earthquake, 21f, 22–23, 37, 158, 465
- Nominal strength, 600–601, 606, 611
- Non-compact braces, 653–654
- Nonductile concrete frames, 637, 652–653
- Non-lateral-load resisting elements, 526–527
- Nonlinear analysis software systems, 806–807
- Nonlinear analysis techniques, 235–242, 630–631
- Nonlinear Dynamic Procedure (NDP), 778, 786–787
- Nonlinear multiple-degree-of-freedom (MDOF) systems, 231–242
- Nonlinear single-degree-of-freedom (SDOF) systems, 219–222
- Nonlinear Static Procedure (NSP), 764–765, 778, 784–787
- NONLIN program, 199
- Non-load bearing walls, 641, 660–661
- Nonparallel systems, 285, 300–302
- Non-structural Performance Levels, 763, 764
- Nonstructural systems and components, 681–720
 architectural, 687t, 697t, 703–713
 behavior of, 689–692
 design standards, 692–703
 electrical, 688t, 698t, 718–720
 mechanical, 688t, 698t, 713–718
 performance objectives, 686
 plumbing, 688t
 seismic isolation and, 728
 seismic upgrading of, 641, 644, 660–662
- Normal faults, 16
- Northridge earthquake, 4, 6, 33, 43, 70, 76, 104, 235, 306, 320, 759–760, 761f
 impulse base acceleration in, 198
 instrumented building response analysis in, 805
 near-source effects, 130–131
 nonstructural systems and components in, 683, 685, 714
 reinforced concrete structures in, 526
 steel structures in, 416–417, 418, 443

- Numerical integration, 220–222
- Oakland City Hall, 735
- Oblique faults, 16
- Occupancy Importance Factor, 262, 412
- Olive View Hospital, 305, 314, 315f, 484, 485f, 683f
- Open store front, 634, 645, 646f
- Operational Performance Level, 764
- Ordinary concentrically braced frames (OCBFs), 427, 431, 432–433, 436
- Ordinary moment frames (OMFs), 415
- Ornamentation, exterior, 641, 661, 705
- Oroville dam earthquake, 13
- Out-of-plane forces, 285, 595, 604–609, 651–652, 664, 666–667
- Overturning moment, 256, 268, 737
- Panel zones, 354–355, 421–424, 451
- Partitions, 705–709
- Passive seismic earth pressures, 180
- P-Delta analysis, 329, 332–333
- approximate, 340–344
 - choice of member stiffness for, 348–349
 - direct, 342–344, 356
 - exact, 346–348
 - iterative, 340–342
 - modified version of approximate, 345–346
 - seismic code requirements for, 369–370
- P-Delta effects, 256, 257, 269–270, 627, 780
- Peak ground acceleration (PGA), 130
- Peak ground motion, 51, 52t
- Peer review, 742
- Performance-based seismic engineering (PBSE), 757–791
- deformation and force-controlled elements, 779
 - examples of, 773–776, 787–791
 - at expected maximum displacement, 772
 - foundation modeling assumptions, 779
 - geotechnical effects in, 766
 - inelastic component behavior in, 765–766
 - load combinations in, 780–781
 - mathematical modeling in, 778, 788
 - multidirectional effects in, 780
 - P-Delta effects in, 780
 - performance objectives, 763–764, 788
 - period determination, 785
 - primary and secondary elements in, 778–779
 - soil-structure interaction in, 780
 - stiffness and strength assumptions, 779
 - target displacement, 785–786, 788–790
- Perimeter resistance, 292–294
- Perimeter strength/stiffness variations, 297–300
- Period paper, 202
- Peruvian earthquake, 23, 170
- Piping systems, 716–717
- Plan density, 292–294
- Plan structural irregularities, 257t, 258, 269t, 270, 287
- specific problems, 294–319
- Plate-edge earthquakes, 7
- Plumbing systems/components, 688t
- Plywood diaphragms, 574, 575–582
- Plywood shear walls, 591–595
- Pompidou Center, 321
- Positive moment reinforcement, 542
- Post-modern architecture, 321–322
- Pounding, 315–319
- Power spectral density, 54, 58–61
- Precast concrete cladding, 661
- Precast concrete diaphragms, 658–659
- Prestigious/high-style image, 278–279
- Primary elements, 498, 778–779
- Probabilistic approach, 643
- Probable flexural strength, 480, 510
- Problem solving/functional facilities, 278
- Pseudo-dynamic tests, 473
- Pseudo lateral load, 781–782
- Pushover analysis, 231, 235, 631, 738, 765
- P waves, 17–20, 28
- Quality control, 610, 643–644
- Quasi-inelastic analysis techniques, 631
- Rat Island earthquake, 6
- Rayleigh's method, 214–216, 251
- Rayleigh waves, 18
- Reduced beam sections, 418–421
- Reduced Hazards Performance Level, 764
- Reduction factors, 629
- Redundancy, 256, 292–294, 433
- Reentrant corners, 285, 291–292, 294–297, 659–660
- Regular buildings, 281, 282–283
- Reinforced concrete structures, 463–555
- axial load and bending, 512–517, 554–555
 - beams, 478–481, 508–512, 540–546
 - beam-to-column connections, 484–488, 518–519, 550–552
 - behavior under earthquake-type loading, 472–500
 - code provisions, 500–528
 - columns, 481–484, 517, 547–550
 - confinement reinforcement, 474–475, 524, 548, 550, 552, 555–556
 - coupled walls, 498–500
 - design concept and detailing, 467–468
 - design examples, 528–558
 - design for inertial effects, 465
 - design for strong earthquakes, 468
 - ductility in, 468–472, 474–477, 506–528, 530
 - estimates of capacity, 466
 - estimates of demand, 465–466
 - flexural members, 508–512
 - frames in regions of moderate seismic risk, 527–528
 - limitations on material strengths, 507
 - load combinations, 504–506, 536–540
 - load factors, 504–506
 - natural periods of vibration, 532–558
 - non-lateral-load resisting elements, 526–527
 - performance criteria, 500–501
 - strength reduction factors, 504–506
 - structural walls, 488–498, 522, 524–525, 553–558
- Reinforced concrete walls, 639, 653
- Reinforced masonry shear walls, 609–619
- Reinforced masonry walls, 639, 653
- Reinforcing steel, inadequate development, 638
- Reliability factor, 256, 270
- Reservoir-induced earthquakes, 10

- Response modification factors (*R*-factors), 111–112, 118, 130, 267, 411
- Response spectra, 49, 87–98, 117–118, 145, 202, 203f, 204f
design spectra distinguished from, 98
elastic, 130–135, 206–210
energy content and, 112–116
factors influencing, 92–98
inelastic, 106–112
- Response-spectrum analysis, 228–229, 230–231
of elastic structures, 217–219
in performance-based seismic engineering, 783–784
in seismic isolation, 739, 742
- Reverse faults, 16, 75
- Reverse-slip faults, 94, 96–97
- Richter scale, 27–29
- Rigid diaphragms, 376–377, 574, 590–591
- Rigidly mounted equipment, 713, 714–715
- Roof diaphragms, 670–672
- Royce Hall, 808
- St. Peter's Cathedral, 293
- San Andreas fault, 11, 13, 16, 21, 30, 37, 76, 79, 138
- San Fernando earthquake, 9, 13, 33, 63, 86, 92, 280, 305, 314, 760
landslides and, 170
nonstructural systems and components in, 683, 685
reinforced concrete structures in, 484, 485f
subdiaphragms in, 581
tilt-up buildings in, 662
- San Francisco earthquake, 13, 22, 29, 156, 725
- San Salvador earthquake, 168
- Santa Barbara earthquake, 296, 305
- SAP-2000 program, 809
- Scenario analysis, 802–804
- SEAOC, *see* Structural Engineers Association of California
- Secondary elements, 498, 778–779
- Second-order analysis techniques, 334
- Sectional ductility, 475–477
- Seiches, 173
- Seismic activity monitoring, 799–800
- Seismic base shear equation, 140–141
- Seismic coefficients, 133, 141, 251, 254t
- Seismic dead load, 251
- Seismic demand loads, 670
- Seismic design category, 265
- Seismic hazard analysis, 800–802
- Seismic importance factor, 250, 252t
- Seismic isolation, 723–754
backup safety system, 747
basic elements of systems, 728–733
configurations, 744–747
design code requirements, 737–744
design examples, 743–744, 750–753
design principles for systems, 734–735
design procedures, 747–748
feasibility of, 735–737
flat sliding systems, 733–734
hardening systems, 733
linear systems, 733
for new construction, 735–736
- retrofit of existing structures, 736–737
- softening systems, 733
- testing requirements for isolators, 742–743
- Seismic maps, 79–86
- Seismic response analysis, 234–235
- Seismic response coefficient, 266
- Seismic risk evaluation, 35–37, 76–86
- Seismic Sea Wave Warning System, 24
- Seismic settlement, 167–169
- Seismic source type, 254, 255t
- Seismic upgrading, 623–678
for brittle structural systems, 636, 650–654
common deficiencies, 631–642
criteria for, 642–644
examples, 662–678
for excessive flexibility, 650
for inadequate diaphragms, 640, 654–660
for inter-element deformations, 635, 648–650
for lateral force resisting systems, 632–634, 644–648
nonlinear analysis techniques, 630–631
for nonstructural elements, 641, 644, 660–662
purpose of, 626–631
quasi-inelastic analysis techniques, 631
for structural continuity, 635, 648–650
tilt-up, 662–669
for URM bearing wall buildings, 669–677
- Seismic use group, 262
- Seismic waves, 17–21
- Seismic Zone Factors, 128, 130, 250
- Semi-rigid diaphragms, 376–377
- Serviceability, 567–568
- Serviceability limit state, 569–570
- Service loads, 502
- Settlement, 155–156
seismic, 167–169
- Shaking tables, 473, 727
- Shallow-focus earthquakes, 6, 13
- Shear, 477, 543–544, 549, *see also* Base shear; Story shear
- Shear cantilevers, 337, 338–340
- Shear capacity, 654–655, 657, 658–659, 659, 664, 666
- Shear failure, 637–638
- Shear leak displacements, 353–354, 356, 357
- Shear link critical length, 439–440
- Shear strength
of beam-column connection, 550–551, 552
of panel zones, 422–423
of reinforced masonry shear walls, 611–612, 613, 618
of shear walls, 521–522, 524–525
undrained, 136
- Shear stress, 493, 657–658
- Shear walls, 519–526
boundary elements, 521, 553, 554, 555–556
boundary zones, 523–524, 557–558
coupling beams, 522
design of, 553–558
frame-, *see* Frame-shear wall systems
plywood, 591–595
reinforced masonry, 609–619
strength of, 521–522
- Shear wave velocity, 135, 153–154
- Short columns, 307–309
- SH waves, 21, 33

- Single-degree-of-freedom (SDOF) systems, 49, 56, 87, 88, 98, 113, 114, 185, 186–195, 202, 207
damped, 193–195
free vibration, 191–195
generalized, 210, 217, 218–219, 222, 226, 230–231
mass and stiffness properties, 189–191
nonlinear, 219–222
time-dependent force in, 186–188
undamped, 192–193
- Site class, 262
- Site coefficients, 128, 262–265
- Site effects, 127, 128–146, 289–290
average shear wave velocity in, 135
average standard penetration resistance in, 135–136
average undrained shear strength in, 136
examples, 136–138
seismic upgrading and, 642
- Site modification, 162–165
- Slab-column connections, 488
- Slenderness ratio, 430–431
- Sliding connections, insufficient, 650
- Sloping site, 159–160, 161
- Slowly reversed cyclic (quasistatic) loading, 472–473, 493
- Softening isolation systems, 733
- Soft story structures, 287, 303–307
- Soil alteration, 164–165
- Soil conditions, 22–23, 127, 128, 735–736
- Soil grouting, 165
- Soil liquefaction, 146–166
causes of, 146–147
cone penetration test for, 152–153, 154
drainage and, 166
ground failures induced by, 156–159
lateral displacement due to, 159–161
settlement induced by, 155–156
shear wave velocity in, 153–154
site modification and, 162–165
structural design and, 165–166
- Soil profiles, 128, 129, 131, 135, 251–254, 255t
- Soils engineering input, 36–37
- Soil-structure interaction, 173–176, 780
- Special concentrically braced frames (SCBFs), 426, 431, 432, 435, 436, 445, 451–455
- Special moment frames (SMFs), 415–416, 445, 446–451
- Special purpose software systems, 807–809
- Spectral displacement, 202, 217, 739
- Spectral pseudo-acceleration, 202, 217
- Spectral pseudovelocity, 202
- Spectrum analysis, 218–219
- Square root of the sum of the squares (SRSS), 229, 230, 530, 739, 784
- Stability index, 343
- Stairs, 712
- Standard penetration resistance, 135–136
- Standard Penetration Test (SPT), 147–150, 154
- Staples Center, 808
- Static analysis, 738, 742
- Static monotonic loading, 472, 493
- Static nonlinear analysis, 232–234
- Steel deck diaphragms, 659–660
- STEELER program, 235
- Steel moment-resisting frames (SMFs), 415–425
imtermediate, 415
ordinary, 415
special, 415–416, 445, 446–451
- Steel structures, 409–459
concentrically braced frames for, 425–436
design examples, 444–459
eccentrically braced frames for, 436–444, 445, 455–459
materials, 413
moment-resisting frames for, 415–425, 445
- Stiffness
for drift and P-Delta analysis, 348–349
in MDOF systems, 222–223
in performance-based seismic engineering, 779
perimeter variations in, 297–300
in SDOF systems, 189–191
- Stone veneers, 661
- Story shear, 256, 446–447
- Stress (conversion factors), 817–818
- Strike-slip faults, 15, 24, 31, 75, 94, 96–97, 176
- Strong column-weak beam criterion, 450–451, 481, 507, 513, 517
- Strong motion duration, 54, 55t, 69–70, 73–74, 97–98, 110
- Strong panel zones, 423
- Structural analysis and design, 806–811
- Structural continuity, 635, 648–650
- Structural damage limit state, 570
- Structural Engineers Association of California (SEAOC), 283–285, 500, 503, 568, 579, 599, 602, 626
- Structurally restrictive detailing, 313–315
- Structural Performance Levels, 763, 764
- Structural reliability, 570–572
- Structural stability, 330
- Structural Stability Performance Level, 764
- Structural system coefficient, 251
- Structural walls, 488–498, 522, 524–525
design of, 553–558
monotonic vs. reversed cyclic loading, 493
reinforcement detailing, 496–498
section shape, 493–496
sequence of large-amplitude load cycles, 496
shear stress, 493
- Subdiaphragms, 581–582, 588–590
- Subsidence, 167–169
- Sum of the absolute values (SAV), 229, 230
- Surface wave magnitude, 28, 29
- Surface waves, 18, 20
- Suspended acoustical tile ceilings, 662
- SV waves, 21
- S waves, 17–21
- TABS program, 809
- Taft earthquake, 53f, 99, 114
- Tag Mail, 293
- Tectonic creep, 16
- Tectonic earthquakes, 6–8
- Temperature (conversion factors), 819
- Tension wall, 499
- Thrust faults, 16, 176
- Tilt-up building seismic upgrade, 662–669
- Timber diaphragms, 654–657
- Time (conversion factors), 817
- Time-dependent force, 186–188

- Time-history analysis, 4, 195, 227–228, 245
 of elastic structure response, 201–202, 216–217
 of performance-based seismic engineering, 784
 of seismic isolation, 739, 742
- Tokai-oki, Japan earthquake, 308
- Tokyo, Japan earthquake, 22
- Torsion, 256, 269–270, 368–369, 528, 773, 778
- Torsional irregularity structures, 287–288
- Torsional stability index, 343
- Total dead load, 265–266
- Transform faults, 7
- TriNet network, 796, 799–800
- Tripartite log paper, 202
- Tri-Services Manual, 692, 693–694, 699, 702
- Tsunamis, 4–5, 23–24, 25f, 171–173
- Turnagain Heights landslide, 169–170
- UBC, *see* Uniform Building Code
- UCLA Replacement Hospital, 798f
- Ultimate limit state, 569, 570
- Umeda Sky Building, 322
- Undamped natural periods of vibration, 532–558
- Undamped single-degree-of-freedom (SDOF) systems, 192–193
- Undrained shear strength, 136
- Unfactored service moments, 606–607
- Uniform Building Code 94 (UBC-94), 128–129
 on elastic response spectra, 134
 on masonry buildings, 570
 on near-source effects, 131
 on nonstructural systems and components, 692, 693–694, 699, 701
 site profile examples, 136–137
- Uniform Building Code 97 (UBC-97), 105, 249
 on deformations, 628
 on drift and P-Delta, 369
 on elastic response spectra, 134
 on floor diaphragms, 382–384
 on horizontal diaphragms, 577, 578, 582
 on lateral forces, 572, 573
 on linear static force procedures, 250–262
 on masonry buildings, 565, 570
 on near-source effects, 131, 132t, 138–139
 on nonstructural systems and components, 692, 694–696, 699, 700–701, 703
 overview, 129–130
 on reinforced concrete structures, 482, 503–528, 557–558
 on seismic isolation, 737
 on shear walls, 613
 site profile examples, 137–138
 on soil profiles, 135
- Unit weight (conversion factors), 818
- Unreinforced brick masonry (URM) bearing wall buildings, 669–677
- Unreinforced masonry (URM) buildings, 650, 651–652
- Unreinforced masonry (URM) walls, 637
- Uplift, 737
- Valdivia, Chile earthquake, 167
- Velocity (conversion factors), 816–817
- Velocity attenuation, 68
- Vertical diaphragms, 591
- Vertical distribution of force, 268
- Vertical lateral force resisting element (VLFR), 574–575
- Vertical lateral load resisting elements (VLLR), 375, 376, 378, 383, 384
- Vertical load stress check, 605
- Vertical reinforcement, 524
- Vertical setbacks, 309–313
- Vertical structural irregularities, 257t, 258, 270, 287
 specific problems, 303–313
- Vibration, undamped (elastic) natural periods, 532–558
- Vibration isolated components, 713–714, 715–716
- Vibratory probes, 162–163
- Vibroflotation, 163
- Vibro-replacement, 165, 166
- Volcanic earthquakes, 9
- Volume (conversion factors), 816
- Vrancea, Romania earthquake, 196
- Walls
- CMU, 582–595
 - CMU slender, 595–609
 - coupled, 498–500
 - non-load bearing, 641, 660–661
 - reinforced masonry, 639, 653
 - shear, *see* Shear walls
 - structural, *see* Structural walls
 - URM, 637
- Wall-to-diaphragm anchorage, inadequate, 648–650
- Warped building form, 323
- Weak column-strong beam problem, 307–309
- Weak story structures, 287, 303–307
- West Anchorage High School Building, 380–381
- Width-to-thickness ratio, 431–434
- Wood buildings, 563–619
 with CMU slender walls, 595–609
 with CMU walls, 582–595
 drift and, 567–568
 lateral forces in, 572–574
 limit states for, 565–568
 LRFD for, 565–568
 serviceability and, 567–568
 with shear walls, 609–619
- Working Stress Design (WSD), 565, 595
- Wright, Frank Lloyd, 290
- Yellow Book*, 738
- Yield level vs. ductility, 468–470